

A Study on Hydrodynamic Processes in Channel Bifurcations

Tan Cha Yao

18023253

June 2026

A thesis submitted in part consideration of the degrees of

PhD in Civil Engineering

Acknowledgement

Many challenges are encountered in this study including physical constraints and mentally issue, this study will not be accomplished without any assistance from my supervisors, friends, and families.

Prof. Ir. Dr. Teo Fang Yenn

I would like to give the most appreciation to all my main supervisor: Prof. Ir. Dr. Teo Fang Yenn, an excellent and insightful mentor during my study. Prof. Ir. Dr. Teo is the cornerstone of this study as the whole journey of this study is fully supported by him.

Prof. Ir. Dr. Lai Sai Hin

I would like to appreciate my co-supervisor: Prof. Ir. Dr. Lai Sai Hin. His supporting on physical modelling and machine learning enhances the research quality of this study.

Assoc. Ir. Dr. Lee Min Lee

I would like to appreciate my second co-supervisor is Dr. Lee, his guidance on PhD's research and writing is very useful to me on this study.

Ms. Rozita

Graceful appreciation to the lab technician, Ms. Rozita. She provides a lot of assistance during the physical modelling stage.

Abstract

Bifurcation flow is a hydrodynamic separation processes into two or more tributaries that can be commonly observed in various environments. It can naturally occur in a river system; it can also be found in engineering projects for flow control to achieve flood mitigation or water supply. The flow discharge can be manipulated by the downstream hydraulic structures, such as weirs, gates, and barrages. Among all types of hydraulic structures for flow control, the weir is considered a passive type of structure for flow regulation. The bifurcated flow will be affected by the dimensions of weirs at both tributaries; therefore, in this study, the discharge partitioning of channel bifurcation flow is investigated with various height combinations of downstream weirs. The discharge partitioning and height combination of weir are quantified as discharge ratio and weir height ratio in this study.

This study also identifies the impact of bifurcation angle and slope on the hydrodynamic processes of bifurcation flow. The findings show that the flow behaves differently under different conditions. The bifurcation angle does not alter the water depth and velocity in both tributaries; in contrast, the slope has an impact on the water depth and velocity. However, experiment observations in this study shows a completely different trend when ratios are considered. The bifurcation angle certainly has an impact on both water depth ratio and flow velocity ratio; in contrast, no influence on these ratios is observed when the slope is changed.

Another finding is that the secondary flow may be completely stagnated when the flow is small, with 100% of the flow divided into the primary tributary. Therefore, the threshold effect of weir height combination is identified and found to be related to the upstream discharge. The discharge ratio becomes dynamic when the upstream discharge is unsteady.

The last part of this study involves the training of a machine learning model for predicting discharge partitioning under different conditions, especially upstream discharge. It shows the potential application of machine learning models for predicting flow and discharge partitioning in channel bifurcation flow.

Overall, the hydrodynamic processes of channel bifurcation flow can be controlled using various weir height combinations, and the weir height combination should be carefully considered, as the discharge partitioning changes dynamically with upstream discharge. With the assistance of machine learning models, prediction of the hydrodynamic processes of channel bifurcation can support decision-making in design and flow control, which is an essential part of engineering for flood mitigation.

Table of Contents

Acknowledgement ..... **i**

Abstract ..... **ii**

Table of Contents ..... **iv**

List of Figures ..... **vii**

List of Tables ..... **xiv**

Chapter 1 Introduction **1**

1.1 Background of Study 1

1.2 Problem Statement 5

1.3 Research Questions 6

1.4 Aim and Objectives 7

1.5 Significance of Study 8

1.6 Chapter Outline 9

Chapter 2 Literature Review **10**

2.1 Classification of River Bifurcation 10

2.2 Classification of Physical Model 11

2.3 Modelling of Branch Flow 13

2.3.1 Physical Model 13

2.3.2 Analytical Model 15

2.3.3 Numerical Model 17

2.4 Modelling of Bifurcation Flow 19

2.4.1 Nodal Point Relation 19

2.4.2 Physical Model 21

2.4.3 Sediment Transport in Bifurcation 26

2.4.4 Analytical Model 26

2.4.5 Numerical Model 28

2.5 Field Study of River Bifurcation 30

2.6 Machine Learning of River Bifurcation 32

2.7 Potential Research Gap 38

Chapter 3 Methodology.....39
3.1 Physical Model 39
3.1.1 Experiment Setup 39
3.1.2 Data Collection 50
3.1.3 Data Analysis 55
3.2 Numerical Model 70
3.2.1 Simulation Setup 70
3.2.2 Data Analysis 79
3.3 Machine Learning Model 83
3.3.1 Machine Learning Model Training Data Set 83
3.3.2 Machine Learning Model Setup 84
3.3.3 Machine Learning Model Prediction 86
Chapter 4 Physical Modelling of Channel Bifurcation 88
4.1 Introduction 88
4.2 Experiment Test of Channel Bifurcation 89
4.2.1 Water Depth 89
4.2.2 Superelevation of Water Depth 94
4.2.3 Average Water Depth 103
4.2.4 Water Surface Level 106
4.2.5 Flow Velocity 110
4.2.6 Average Flow Velocity 111
4.2.7 Flow Discharge 116
4.2.8 Head above Weir Crest 119
4.2.9 Froude Number and Reynolds Number 122
4.3 Dimensionless Factor Analysis 124
4.3.1 Water Depth Ratio 124
4.3.2 Flow Velocity Ratio 132
4.3.3 Discharge Ratio 144
4.3.4 Threshold of Weir Height Ratio 155
4.4 Summary of Findings 160

Chapter 5 Numerical Modelling of Channel Bifurcation 162
5.1 Introduction 162
5.2 Simulation of Channel Bifurcation 163
5.3 Dimensionless Factor Analysis 165
5.3.1 Multiple Linear Regression Analysis 165
5.3.2 Simple Linear Regression Analysis..... 166
5.3.3 Threshold of Weir Height Ratio 170
5.4 Comparisons of Physical Modelling and Numerical Modelling 170
Chapter 6 Machine Learning Model of Channel Bifurcation 172
6.1 Model Training Performance..... 172
6.2 Machine Learning Model Prediction 182
6.2.1 Discharge at Upstream 182
6.2.2 Bifurcation Angle 186
6.2.3 Slope 190
6.2.4 Minimum Weir Height 194
6.3 Summary of Findings 198
Chapter 7 Conclusions and Recommendations.....199
7.1 Conclusions..... 199
7.1.1 Physical Model 199
7.1.2 Numerical Model 201
7.1.3 Machine Learning Model..... 202
7.2 Recommendations..... 203
7.2.1 Physical Model 203
7.2.2 Numerical Model 203
7.2.3 Machine Learning Model..... 204
References R-1

List of Figures

Figure 1.1: Illustration of neck cut-off and chute cut-off (Source: Crosato, 2008) 2

Figure 1.2: Longitudinal training wall (Source: Le, et al., 2018) 2

Figure 1.3: Sri Johor Pond (Source: Department of Irrigation and Drainage Malaysia, 2008) 3

Figure 2.1: Proposed classification of river bifurcation 11

Figure 2.2: Classification of physical model 12

Figure 2.3: Water surface profile in the main channel (Source: Shettar and Murthy, 1996) 18

Figure 2.4: Graph of discharge ratio versus water depth ratio (Source: Bolla Pittaluga et al., 2003) 20

Figure 2.5: Model Setup by Roosjen & Zwanenburg (1995) 21

Figure 2.6: Graph of bifurcation angle and deposit angle (Source: Federici and Paola, 2003) 22

Figure 2.7: Graph of comparing between experiment result and BRT model (Source: Bertoldi et al., 2007) 23

Figure 2.8: Definition of bifurcation angle (δA) and internal angle/deposit angle (δB). (Source: Thomas et al., 2011) 24

Figure 2.9: Comparison of discharge ratio of two geometries. (Source: Thomas et al., 2011) 25

Figure 2.10: Discharge ratio against inverse weir height ratio for Geometry A and B. (Source: Thomas et al., 2011) 25

Figure 2.11: Graph of flow depth of equal weir height (left) and unequal weir height (right) (Source: Thomas et al., 2011) 25

Figure 2.12: Graph of flow rate ratio (Source: Zawawi, et al., 2019) 27

Figure 2.13: The numerical model of bifurcation (Source: Kleinhans, et al., 2008) 28

Figure 2.14: Discharge ratio against upstream discharge (Source: Zolezzi, et al., 2006) 31

Figure 2.15: Longitudinal profile of water surface and bed elevation (Source: Zolezzi, et al., 2006) 32

Figure 2.16: Deep neural network (Stryker et al., 2026) 33

Figure 2.17: Architecture framework of ANN (Source: www.analyticsvidhya.com) 33
Figure 2.18: Architecture framework of CNN (Source: www.analyticsvidhya.com) 34
Figure 2.19: Architecture framework of RNN (Source: www.analyticsvidhya.com) 34
Figure 2.20: Architecture of DeepRiver (Source: Isikdogen, et al., 2018) 36
Figure 2.21: Visualisation of automatically extracted channel (Source: Isikdogen, et al., 2018)..... 37
Figure 3.1: MICRO RIVER MODEL-FM 59 40
Figure 3.2: Plan view of 30° bifurcation physical model..... 41
Figure 3.3: Plan view of 40° bifurcation physical model..... 42
Figure 3.4: Plan view of 50° bifurcation physical model..... 43
Figure 3.5: Typical cross-section of channel..... 44
Figure 3.6: Definition of bifurcation angle and internal angle 45
Figure 3.7: Definition of point of bifurcation and wedge-shaped channel wall 45
Figure 3.8: Section view of suppressed rectangular sharp-crested weir 47
Figure 3.9: Location of weir in the experiment 47
Figure 3.10: Picture of ACM2-RS and ACM3-RS 50
Figure 3.11: The direction of measured velocity 51
Figure 3.12:Illustration of cross section for data collection..... 52
Figure 3.13: Point of velocity measurement for upstream channel..... 53
Figure 3.14: Point of velocity measurement for downstream channel..... 53
Figure 3.15: Water depth measurement..... 54
Figure 3.16: Water depth measurement (Plan)..... 56
Figure 3.17: Water depth and percentage difference (Section)..... 56
Figure 3.18: Superelevation of water depth (Plan)..... 57

Figure 3.19: Average water depth (Plan and profile) 58
Figure 3.20: Water surface level (Plan and profile) 60
Figure 3.21: Water depth and flow velocity (Section) 61
Figure 3.22: Average flow velocity (Plan and profile) 62
Figure 3.23: Flow discharge of section (Plan and profile) 64
Figure 3.24: Calculation sheet (Part 1) 67
Figure 3.25: Calculation sheet (Part 2) 68
Figure 3.26: Definition of H and P of sharp-crested weir 69
Figure 3.27: Example of 3D Geometry in FLOW-3D 71
Figure 3.28: The direction of flow and space 76
Figure 3.29: Mesh size for model setup 77
Figure 3.30: Example of recorded discharge in time series 80
Figure 3.31: Example of discharge ratio in time series 82
Figure 3.32: Feeding data set preparation for machine learning model 84
Figure 3.33: Deep neural network (IBM Cloud Education, 2020) 85
Figure 3.34: Example of epoch in machine learning training 86
Figure 3.35: Illustration of overfitting of training-validation gap 87
Figure 4.1: Measured water depth 90
Figure 4.2: Water depth and percentage difference – 30_03_5050 91
Figure 4.3: Water depth and percentage difference – 30_03_5560 92
Figure 4.4: Water depth and percentage difference – 30_03_5055 93
Figure 4.5: Superelevation of water depth (different WH_r) 95
Figure 4.6: Superelevation of water depth (different slope) 96
Figure 4.7: Peak superelevation of water depth (Graphical) 97

Figure 4.8: Example of superelevation of water depth (50_05_5050) 99

Figure 4.9: Plan and profile of average water depth (different slope with 30°bifurcation angle and WH_r) 103

Figure 4.10: Comparison between water surface level with different slope 107

Figure 4.11: Comparison between water surface level with different bifurcation angle 108

Figure 4.12: Comparison between water surface level with different weir height ratio 109

Figure 4.13: High flow velocity near inner bank..... 110

Figure 4.14: Relationship of flow velocity (near surface) and slope 114

Figure 4.15: Relationship of flow velocity (near bed) and slope .. 115

Figure 4.16: Discharge comparison between different weir height ratio (A: left tributary; B: right tributary) 120

Figure 4.17: Relationship of water depth ratio and weir height ratio (Bifurcation Angle) 127

Figure 4.18: Relationship of water depth ratio and weir height ratio (Slope) 128

Figure 4.19: Relationship of linear coefficient and bifurcation angle (Water depth ratio) 129

Figure 4.20: Plotting of developed equation (Water depth ratio) 131

Figure 4.21: Relationship of flow velocity ratio near surface and weir height ratio (Bifurcation angle) 135

Figure 4.22: Relationship of flow velocity ratio near surface and weir height ratio (Slope) 136

Figure 4.23: Relationship of flow velocity ratio near bed and weir height ratio (Bifurcation angle)..... 137

Figure 4.24: Relationship of flow velocity ratio near bed and weir height ratio (Slope) 138

Figure 4.25: Relationship of linear coefficient and bifurcation angle (Flow velocity ratio near surface flow) 139

Figure 4.26: Relationship of linear coefficient and bifurcation angle (Flow velocity ratio near bed flow) 140

Figure 4.27: Plotting of developed equation (Flow velocity ratio near surface) 142

Figure 4.28: Plotting of developed equation (Flow velocity ratio near bed) 143

Figure 4.29: Relationship of discharge ratio and weir height ratio (Bifurcation angle) 147

Figure 4.30: Relationship of discharge ratio and weir height ratio (Slope) 148

Figure 4.31: Relationship of linear coefficient and bifurcation angle (Discharge ratio) 149

Figure 4.32: Plotting of developed equation (Discharge ratio) 151

Figure 4.33: Relationship between discharge ratio and weir height ratio (Comparison) 153

Figure 4.34: Threshold of weir height ratio summary 157

Figure 4.35: Threshold of weir height ratio summary (Zoom in) 158

Figure 4.36: Relationship of ratio and parameters 161

Figure 5.1: Example of numerical simulation result (A: summary of result; B: simulated discharge; C: discharge ratio) 164

Figure 5.2: Relationship of discharge ratio and weir height ratio (1) 168

Figure 5.3: Relationship of discharge ratio and weir height ratio (2) 169

Figure 5.4: Relationship of discharge ratio and weir height ratio 171

Figure 6.1: Model Performance of N10L1 173

Figure 6.2: Model Performance of N20L1 174

Figure 6.3: Model Performance of N30L1 175

Figure 6.4: Model Performance of N10L2 176

Figure 6.5: Model Performance of N10L3 177

Figure 6.6: Model Performance of N30L3 178
Figure 6.7: The spike in Model N10L2 179
Figure 6.8: The bottleneck effect in Model N10L2 180
Figure 6.9: Relationship of discharge ratio and discharge at upstream (Model N10L1)..... 183
Figure 6.10: Relationship of discharge ratio and discharge at upstream (Model N20L1)..... 183
Figure 6.11: Relationship of discharge ratio and discharge at upstream (Model N30L1)..... 184
Figure 6.12: Relationship of discharge ratio and discharge at upstream (Model N10L2)..... 184
Figure 6.13: Relationship of discharge ratio and discharge at upstream (Model N10L3)..... 185
Figure 6.14: Relationship of discharge ratio and discharge at upstream (Model N30L3)..... 185
Figure 6.15: Relationship of discharge ratio and bifurcation angle (Model N10L1) 187
Figure 6.16: Relationship of discharge ratio and bifurcation angle (Model N20L1) 187
Figure 6.17: Relationship of discharge ratio and bifurcation angle (Model N30L1) 188
Figure 6.18: Relationship of discharge ratio and bifurcation angle (Model N10L2) 188
Figure 6.19: Relationship of discharge ratio and bifurcation angle (Model N10L3) 189
Figure 6.20: Relationship of discharge ratio and bifurcation angle (Model N30L3) 189
Figure 6.21: Relationship of discharge ratio and Slope (Model N10L1) 191
Figure 6.22: Relationship of discharge ratio and Slope (Model N20L1) 191
Figure 6.23: Relationship of discharge ratio and Slope (Model N30L1) 192

Figure 6.24: Relationship of discharge ratio and Slope (Model N10L2) 192
Figure 6.25: Relationship of discharge ratio and Slope (Model N10L3) 193
Figure 6.26: Relationship of discharge ratio and Slope (Model N30L3) 193
Figure 6.27: Relationship of discharge ratio and minimum weir height (Model N10L1) 195
Figure 6.28: Relationship of discharge ratio and minimum weir height (Model N20L1) 195
Figure 6.29: Relationship of discharge ratio and minimum weir height (Model N30L1) 196
Figure 6.30: Relationship of discharge ratio and minimum weir height (Model N10L2) 196
Figure 6.31: Relationship of discharge ratio and minimum weir height (Model N10L3) 197
Figure 6.32: Relationship of discharge ratio and minimum weir height (Model N30L3) 197

List of Tables

Table 2.1: List of previous study focus area 10

Table 2.2: Quantitative evaluation of DeepRiver and RivaMap (Source: Isikdogen, et al., 2018)..... 37

Table 3.1: Weir height combination..... 48

Table 3.2: List of experiment runs. 49

Table 3.3: Weir height combination..... 71

Table 3.4: List of experiment runs 72

Table 3.5: Vertical layer's name 76

Table 3.6: Gravitational acceleration constant 78

Table 3.7: Machine learning model setup (Neurons and layers) 85

Table 4.1: Peak superelevation of water depth (Tabulated) 98

Table 4.2: Summary of percentage difference for water depth near inner bank at Section D 100

Table 4.3: Summary of percentage difference for water depth near inner bank at Section E..... 101

Table 4.4: Summary of percentage difference for water depth near inner bank at Section F..... 102

Table 4.5: Summary of average water depth 104

Table 4.6: Reduction of average water depth by slope..... 105

Table 4.7: Summary of average flow velocity (Near surface)..... 112

Table 4.8: Summary of average flow velocity (Near bed)..... 113

Table 4.9: Example of flow discharge calculation 116

Table 4.10: Summary of flow discharge of section 117

Table 4.11: Discharge in each experiment runs 118

Table 4.12: Measured head above weir crest (H) 119

Table 4.13: Comparison of dimensionless parameter with Thomas et al. (2011)..... 123

Table 4.14: Result of MLR analysis (Water depth ratio)..... 124

Table 4.15: Coefficient of linear regression (Water depth ratio) .. 125

Table 4.16: Comparison of coefficient of developed equation with experiment data (Water depth ratio)..... 129

Table 4.17: Result of MLR analysis (Flow velocity ratio) 132

Table 4.18: Coefficient of linear regression (Flow velocity ratio) . 134

Table 4.19: Comparison of coefficient of developed equation with experiment data (Flow velocity ratio near surface flow) 139

Table 4.20: Comparison of coefficient of developed equation with experiment data (Flow velocity ratio near bed flow) 140

Table 4.21: Result of MLR analysis (Discharge ratio) 144

Table 4.22: Coefficient of linear regression (Discharge ratio)..... 145

Table 4.23: Comparison of coefficient of developed equation with experiment data (Discharge ratio) 149

Table 4.24: Comparison of discharge ratio with Thomas et al. (2011) 154

Table 4.25: Summary of threshold of weir height ratio 156

Table 5.1: Result of MLR analysis (Discharge ratio) 165

Table 5.2: Summary of threshold of weir height ratio 170

Table 6.1: Summary of training performance 181

Table 6.2: Comparison of model performance and prediction 198

Chapter 1 Introduction

1.1 Background of Study

Bifurcation is a hydraulic phenomenon in which a single stream of flow divides into two or more distributaries. Bifurcation can be commonly observed in natural river system, across a range of geomorphological environments, including river deltas, braided river systems, and meandering channels. It plays an important role in natural river system such as landscape evolution, sediment distribution, and the long-term morphology of river networks.

Formation of river bifurcation can be observed at meandering river; it is generated or eliminated by a long-term process named fluvial geomorphology, which is caused by sediment transport and erosion of riverbank. At each river bend, the outer bank is eroded due to its high flow velocity; the inner bank is accreted due to low flow velocity (Crosato, 2008). When both outer bank chute meet each other, chute cut-off or neck cut-off is formed (Figure 1.1). Consequently, the stream is bifurcated into two streams which are new flow path (neck cut-off or chute cut-off) and original flow path (bend part). The discharge rate of new flow path will gradually increase since it is a shorter path for stream to flow, in contrast, the flow rate and velocity of original path will slowly decrease. Due to the lower kinetic energy in the original path, the sediment from upstream is likely to be deposited and further slow down the flow. This bifurcation will exist until the complete formation of oxbow lake or avulsion.

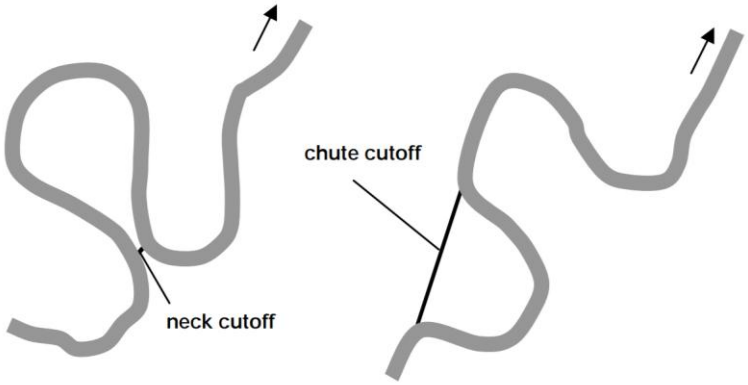


Figure 1.1: Illustration of neck cut-off and chute cut-off (Source: Crosato, 2008)

Unlike natural bifurcation, artificial river bifurcation is more maintainable and manageable. The geometry of river bifurcation is more maintainable with vegetated riverbank protection or artificial riverbank protection such as concrete wall. One of the applications of river bifurcation is longitudinal training wall, a replacement design for traditional transverse groynes. Compared to traditional transverse groynes, this design does not reduce the usable width of the river and ensures the low flow condition for the navigation purpose (Le, et al., 2018).



Figure 1.2: Longitudinal training wall (Source: Le, et al., 2018)

Branching is a type of artificial river bifurcation that is designed to diverge flow from mainstream for irrigation, stormwater diversion and restoration of wetland. One example is the Sri Johor Pond (flood detention pond) as presented in Figure 1.3. It is located at Bandar Sri Permaisuri, Kuala Lumpur (Department of Irrigation and Drainage Malaysia, 2008). A weir is constructed at the entrance of the diverging channel for flow regulation during normal flow period. During a heavy rain event, when the water level is higher than the weir, excessive flow will be diverged from Kerayong River to Sri Johor Pond for temporary storage. After the heavy rain event, the stored water will be released back to the river to restore the storage capacity of Sri Johor Pond for the next flood event. This weir plays a key role in controlling the discharge partitioning.

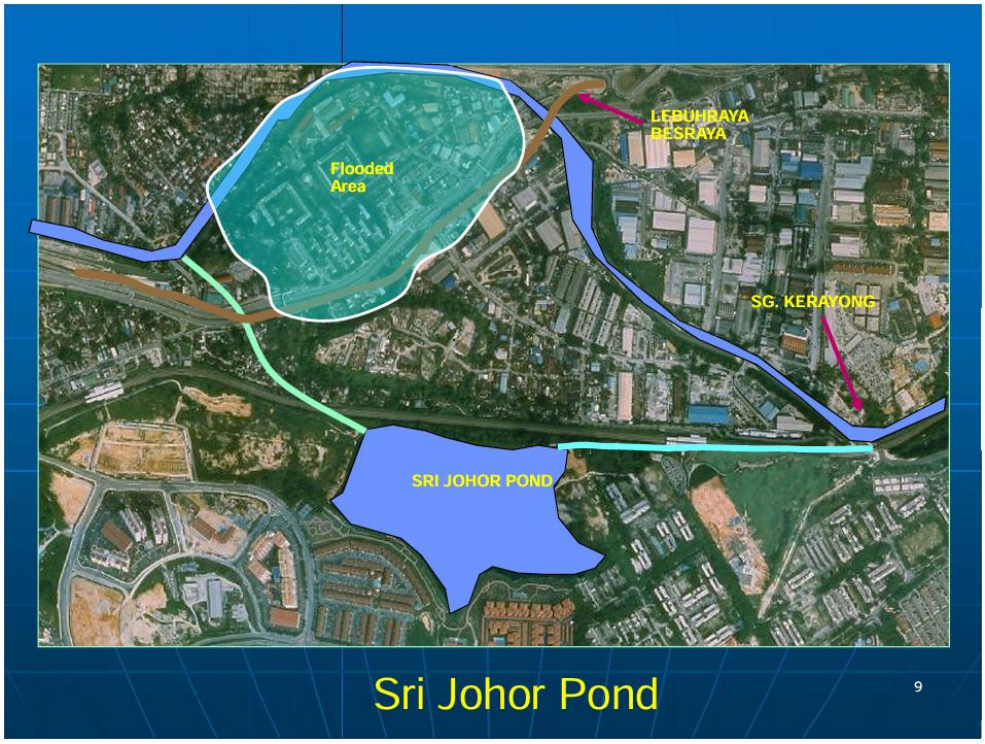


Figure 1.3: Sri Johor Pond
(Source: Department of Irrigation and Drainage Malaysia, 2008)

One of the hydraulic characteristics of a bifurcation system is the discharge partitioning. This discharge partitioning is governed by a complex interaction of factors including but not limited to slope, dimensions of tributaries, grain size, and the downstream boundary conditions (Bertoldi & Tubino, 2007 and Thomas, et al., 2011).

In natural river system, where the downstream boundary condition is uncontrolled, the partitioning evolves dynamically over time as a function of sediment transport and river morphology. Some past studies such as Bolla Pittaluga, et al. (2004) and Bertoldi (2004) have been conducted on the bifurcation flow of a river system under natural conditions with no interference of hydraulic structures at the downstream boundary condition of its tributaries.

In engineered systems, the downstream boundary condition is often regulated by hydraulic structures, such as weirs, sluice gates, and barrages. These hydraulic structures serve as a tool for engineers to manipulate the discharge partitioning. Some studies focused on the impact of hydraulic structures on the hydrodynamic processes of bifurcation flow, for example: Thomas, et al. (2011), Marra, et al. (2014), and Salter et al. (2019).

Among the hydraulic structures that are used for flow regulation at bifurcation, the weir has widely been applied due to its simplicity, passive operation, relatively low cost of construction, and low maintenance requirements (Ahsan, 2020). A weir installed at the outlet of a tributary raises the water surface level of upstream, thereby increasing flow resistance and reducing the discharge through that branch. By varying the height of weirs installed at the outlets of both tributaries, one can theoretically achieve a desired ratio of discharge between the two tributaries.

1.2 Problem Statement

The cost of hydraulic structure construction and its environmental impact is expensive and significant. Unjustified design of hydraulic structure usually comes with risk and damage, which is typically catastrophic and irreversible. To study the impact of hydraulic structure on the hydrodynamic of bifurcation, scaled down physical modelling is typically selected for studying the hydrodynamic processes. The cost of physical modelling and its time consumption are relatively high compared with other methods of study, such as numerical modelling. However, physical modelling generally provides more representative result as physical model is "alive" in the physical world.

Comprehensive study was conducted by Thomas, et al. (2011), Marra, et al. (2014), and Salter et al. (2019) for the impact of weir on the hydrodynamic of bifurcation. These studies introduced the weir as the control hydraulic structure to manipulate the discharge partitioning and examine its impact on the hydrodynamic flow pattern at the bifurcation section. However, these past studies only covered a limited range of control parameters, such as internal angle, slope, weir height, and inlet discharge. A study with a wider range of these parameters helps to reinforce the understanding of the impact of these parameters on the hydrodynamic processes. However, study on the impact of bifurcation angle on the hydrodynamic processes was absent.

As conducting a physical model is too costly, conventionally, modern engineers design the hydraulic structure and study its impact on bifurcation partitioning by numerical model, which is a simulation to replicate the real-life condition. Numerical model is certainly accurate, and its result is generally acceptable by the industry.

Engineers may encounter some issues during the decision stage, a reference on the relationship between the hydraulic structure's dimension and hydrodynamic processes will certainly be helpful for the decision.

Therefore, a study that focuses on describing the discharge partitioning with various hydraulic structure design may bridge the knowledge gap and serve as some idea for decision on engineering design. In this study, weir was selected as the hydraulic structure for the comprehensive study of its impact on hydrodynamic processes of bifurcation.

1.3 Research Questions

The main research questions for this study are listed below:

> *How does the hydraulic structure affect the hydrodynamic processes of a symmetrical bifurcation with a variety of channel properties?*

To answer this question, three sub-questions are expressed as below:

1. How do the weir height combinations affect the hydrodynamic processes of symmetrical bifurcation?

2. How do the channel properties such as bifurcation angle and slope affect the hydrodynamic processes of symmetrical bifurcation?

3. What relationship can be developed to describe the discharge partitioning?

1.4 Aim and Objectives

The study aims to investigate the hydrodynamic processes on channel bifurcations with sharp-crested weir for manipulating discharge partitioning. The study on the bifurcation behaviours of flow with different conditions is essential for controlling the discharge downstream of the tributaries' weir for flood risk management.

A comprehensive analysis and discussion of the results is reported to highlight the bifurcation behaviour under various bifurcation angles, slopes, and weir heights in the physical model. A numerical model is simulated as the extension of physical model to investigate the effects of hydraulic structures on the bifurcation of an idealised channel. The results will be compared with the experimental results. Artificial intelligence with machine learning will be trained by using the physical and numerical modelling results for prediction of bifurcation behaviours for understanding the trends of channel bifurcation flow under various conditions.

In accordance with the main aim, the primary objectives of this study are listed below:

1. To develop a fundamental understanding of the hydrodynamic processes and interactions between a variety of flow conditions and a wide range of hydraulic structures for bifurcation channels.

2. To investigate the relationships between discharge ratio and weir height ratio over a variety of flow conditions and bifurcation geometries with physical modelling.

3. To identify other hydraulic parameters for correctly ascertaining the hydrodynamic processes of bifurcation channel flows for numerical modelling.

4. To predict the bifurcation behaviour with machine learning model.

1.5 Significance of Study

This study focuses on manipulating the discharge partitioning of bifurcation flow by bifurcation angle, slope, and the weir height at both tributaries' ends. Physical model and numerical model were conducted to investigate the relationship. Results show that the flow in channel bifurcation can be manipulated by the mentioned control variables. However, only bifurcation angle and weir height ratio have impact on the discharge ratio. This indicates the weir height ratio is not the only main factor for discharge partitioning, bifurcation angle shall be considered carefully during the design stage. Second part of this study shows the potential of prediction on discharge partitioning by training machine learning model.

1.6 Chapter Outline

Chapter 1 is an introduction to the channel bifurcation in this study; the problem statement, aim, and objectives are presented in this chapter.

Chapter 2 presents the literature review on bifurcation flow in various aspects. A main key is to understand the differences between bifurcation flow and branch flow.

Chapter 3 describes the methodology adopted by this study in 3 approaches: physical modelling, numerical modelling, and machine learning model training. Each approach has its own strengths and weaknesses; the 3 approaches used in this study are to provide a better understanding of bifurcation flow in overall aspect.

Chapter 4 demonstrates the results and findings based on physical modelling. All results are further analysed with dimensionless factors to study the relationship between each factor and parameter. Equations are developed in this chapter to describe the relationship.

Chapter 5 is the extension of Chapter 4, same bifurcation setup with different control parameters is simulated in Flow-3D. To understand the bifurcation flow with different conditions, the numerical model result is compared with the result from physical model.

Chapter 6 covers machine learning model development based on the results from physical modelling and numerical modelling. The trained machine learning model is used to predict the bifurcation flow in various conditions.

Chapter 7 concludes the key findings in this study with recommendations for further reference.

Chapter 2 Literature Review

2.1 Classification of River Bifurcation

This study performed an observation on the title of previous studies. Two general terms had been used which were branch flow (sometimes called dividing flow) and bifurcation flow. There is no clear definition or quantitative method to distinguish branch flow and bifurcation flow. Table 2.1 shows some examples of previous studies with the title name includes either branch/dividing or bifurcation.

Table 2.1: List of previous study focus area

Branch / Dividing	Bifurcation
A new method to predict flow in a branch channel (Pattabhiramiah & Rajaratnam, 1960)	Channel bifurcation in braided rivers: Equilibrium configurations and stability (Pittaluga et al., 2003)
A new method of predicting the flow in a 90° branch channel (Krishnappa & Seetharamiah, 1963)	River bifurcation analysis by physical and numerical modelling (Zanichelli, et al., 2004)
Approximate treatment of flow in branches and bends (Hager, 1984)	Bifurcation dynamics and avulsion duration in meandering rivers by one-dimensional and three-dimensional models (Kleinhans et al., 2008)
Division of flow in short open (Ramamurthy & Satish, 1988)	Bifurcation modelling in a meandering gravel-sand bed river (Sloff & Mosselman, 2012)
Dividing flow in open channels (Ramamurthy et al., 1990)	A reduced complexity model of gravel sand river bifurcation (Schielen & Blom, 2018)
A numerical study of division of flow (Shettar & Murthy, 1996)	Mathematical modeling for flood mitigation: Effect of bifurcation angles in river flowrates (Zawawi et al., 2019)

To simplify and clarify the issue above, in this study, river bifurcation is classified into bifurcation flow and branch flow. Figure 2.1 shows an illustration of the classification of river bifurcation.

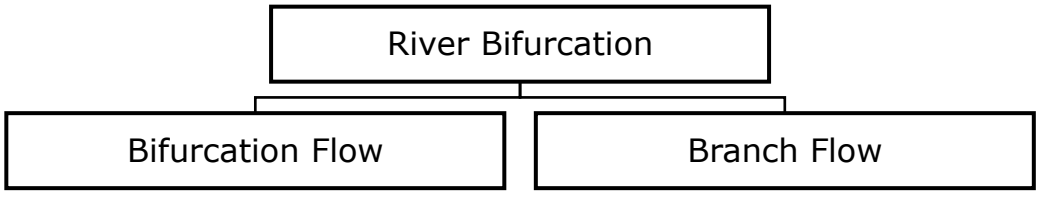


Figure 2.1: Proposed classification of river bifurcation

Bifurcation flow is defined as a split of flow without a predetermined major or minor stream; the flow properties of both downstream may not have a huge difference from the quantitative perspective. However, natural bifurcation may be morphed and the difference in flow properties between the two downstream becomes significant over time, such as the formation of an oxbow lake. Branch flow is defined as split of flow with a major and a minor stream, usually the minor downstream is a smaller stream which diverges a relatively small portion of flow from the major stream. In some cases, a river originally has one stream when the discharge is small. When the discharge is slightly higher, a small branch may appear and a bar is formed between the two downstream; if a heavy rain event happens, the water level may be higher than the elevation of the bar, thus, becoming one stream until the water level drops back.

2.2 Classification of Physical Model

Physical model for river bifurcation experiment can be further classified into two types, which are freely formed bifurcation and forced bifurcation. A freely formed bifurcation experiment is designed so that the water flows through an erodible bed without an obstruction installed at the point of bifurcation; this allows the stream to evolve naturally to form a natural bifurcation. Federici and Paola (2003) and Bertoldi and Tubino (2005) performed freely formed bifurcation experiments to determine the bifurcation angle and deposit angle of a stable bifurcation. The relationship between Shields stress, width ratio, and the stability of bifurcation was investigated.

A forced bifurcation experiment, by contrast, is designed to split the streamflow intentionally by constructing a partition board as the indestructible bifurcation point. The forced bifurcation with soil as river bed is named an erodible bed model; in contrast, without soil is named a non-erodible bed model. Zanichelli, et al. (2004), Bertoldi

et al. (2007) and Thomas et al. (2011) performed forced bifurcation experiments to determine the discharge distribution under different conditions such as weir height, width-height ratio, slope of bed, and internal angle.

Both types of experiment are designed to develop a hydrodynamic model for river bifurcation, freely formed is for natural bifurcation such as river delta, braided river and anabranching river; forced bifurcation is for artificial bifurcation such as irrigation canal, reinforced riverbank of natural bifurcation and diverging channel for detention pond. Figure 2.2 illustrates the further classification for physical model.

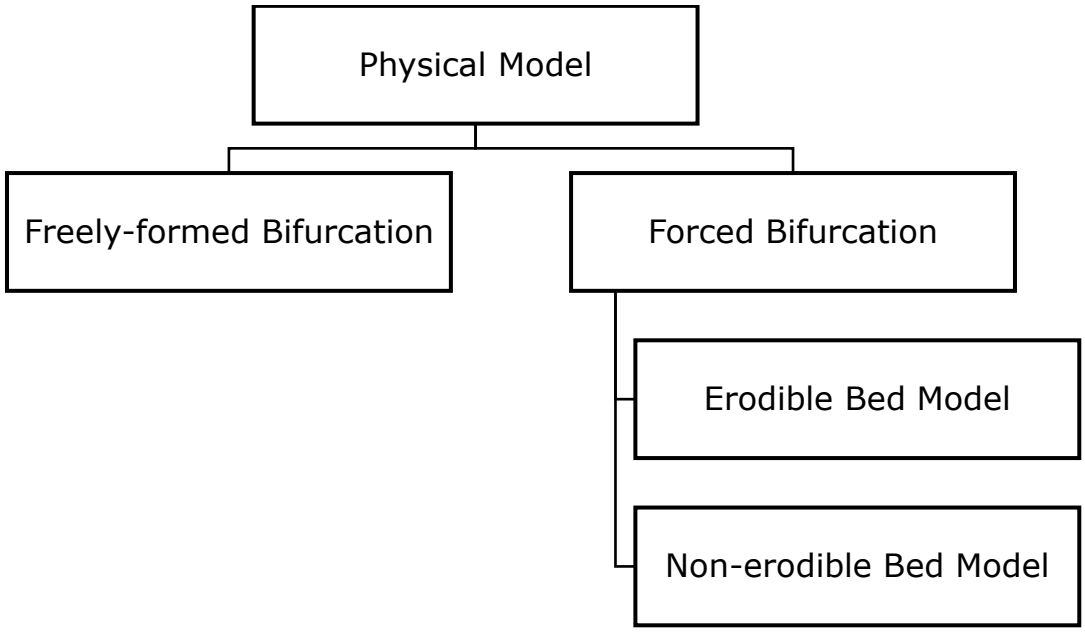


Figure 2.2: Classification of physical model

2.3 Modelling of Branch Flow

At the early stage of river bifurcation research timeline, branch flow was the focus of study, which is defined as a relatively minor flow that diverges from the main streamflow; the discharge rate of branching flow is relatively smaller than the discharge rate of main streamflow. Most of these previous studies were designed for investigation of open channel flow of artificial structure, thus, sediment was not considered in these previous studies.

Alomari & Yusuf et al. (2016) conducted a review on branch flow into three main properties based on flow characteristics, physical characteristics, and modelling of the branching flow. This study concluded that the study on the effect of various branching geometries on the flow properties is important.

2.3.1 Physical Model

According to Ramamurthy & Satish (1988), the first detailed experimental study of open channel branch flow was done by Taylor (1944). It was a physical model which was designed as a right-angled branch with a subcritical flow condition. The width of main channel and branch channel was equal. This study proposed an empirical graphical solution by a trial-and-error process.

Grace and Priest (1958) published an article on branch flow experiments with different width ratios and branch angles. The study showed that a regime with waves occurred when the Froude number of the branch channel (lower section) was relatively small. The regime with waves occurred when free overfall condition existed at the end section of the junction (Beginning of branch channel and downstream of main channel).

Law (1965) experimented with dividing flow under subcritical flow with a right-angled branch. This experiment was compared with the result from Grace and Priest (1958). The study concluded the contraction coefficient is a function of the Froude number of the flow in the main channel and branch channel.

Lakshmana Rao, et al. (1968) conducted an experiment for right-angled branch flow, the flow condition was manipulated by tail-gate which was installed at the end of downstream of main channel and branch channel. This study concluded the discharge distribution of the branch channel is dependent on few parameters, which were branch angle, ratio of width of branch channel to width of main channel, Froude number of downstream of main channel and Froude number of branch channel. The effect of Froude number of branch channel on the discharge distribution was negligible when the downstream of the main channel was supercritical flow (Froude number > 1).

Physical experiments were conducted by various studies on the hydrodynamics of branch flow and discharge partitioning in a right-angled branch flow (Krishnappa and Seetharamiah 1963, Cheong 1991, Neary and Odgaard 1993, Barkdoll et al. 1998, Hsu et al. 2002, Abderrezzak et al. 2011, Rivière et al. 2014, Herrero et al. 2015, Sayed 2019, Alfatlawi & Hussein 2024b, and Shen et al., 2024).

Other than right-angled branch flow, the bifurcation dynamics were studied by Lama et al. (2002), Lama et al. (2003), and Moghadam et al. (2014) with different branching angles.

2.3.2 Analytical Model

Krishnappa & Seetharamiah (1963) performed a dimensional analysis for right-angled branch flow with condition of subcritical flow at the main channel and supercritical flow at the branch channel. This setup was similar to constructing a side weir with zero height. Two parameters were used to determine the discharge distribution (discharge of branch/discharge of inlet). A linear relationship was found between discharge distribution and width ratio:

$$\frac{Q_B}{Q_U} = (1.545 - 1.45\ Fr_U) = \frac{W_B}{W_U} + 0.16(1 - 2\ Fr_U) \qquad \text{Equation 2.1}$$

where, Q_B is discharge of branch, Q_U is discharge of inlet, W_B is width of branch channel, W_U is width of inlet channel and Fr_U is Froude number of upstream main channel.

Hager (1984) proposed a simplified loss coefficient for the downstream and branch channel by using pressure, energy head, and momentum equations with approximate treatment. The theoretical function was applicable to the branching angle between 0° and 105°.

$$\xi_t = q\left(q - \frac{1}{2}\right) \qquad \text{Equation 2.2}$$

$$\xi_l = 1 - 2q\cos\left(\frac{3\delta}{4}\right) + q^2 \qquad \text{Equation 2.3}$$

where, ξ_t is loss coefficient of through branch, ξ_l is loss coefficient of lateral branch, q is discharge distribution and δ is branching angle.

A study about the effect of water withdrawal on sedimentation was conducted by Kerssens & Urk (1986). RIVMOR was the one-dimensional mathematical model that was used to evaluate the bed and water level; it was further calibrated and validated by experimental data from a sand flume constructed at Delft Hydraulics. The water was withdrawn from both sides of the flume and the opening was located at around one-third of the flume length. Water discharge was measured by the V-notch weir. In general, RIVMOR had a reasonable result for the prediction of long-term aggradation and degradation, also resulting changes in stage and depth.

Ramamurthy, et al. (1988) developed an analytical model based on the principle of momentum, energy, and continuity. The model was a right-angled branch flow with different bed width ratio; the flow condition was subcritical flow. The model was validated by experiments, and it matched well with the experiment data. However, the analytical model was limited for three cases, which were the width of branch channel is shorter than the main channel, main channel downstream Froude number less than 0.7 and branch channel Froude number more than 0.35. The discharge ratio was found to be related to Froude number in the downstream of main channel.

Ramamurthy, et al. (1990) further developed the analytical model by applying a momentum transfer equation to determine the relationship between depth ratio, Froude number, and discharge ratio. This analytical model was applicable for all branch flow conditions.

2.3.3 Numerical Model

A two-dimensional numerical model (Shettar and Murthy, 1996) was developed to simulate open channel division flow which was based on the two-dimensional depth-averaged form of continuity and momentum equations, assuming a hydrostatic pressure distribution. This study showed effective stress tensor was contributed by three elements which were viscous stress, turbulent stress, and momentum dispersion. Viscous stress and momentum dispersion were considered as negligible for effective stress tensor, and the turbulent stress was modelled by adopting depth-averaged version of k-ε turbulence. The study region of this model was divided into elementary quadrilateral cells and solved through Pseudo-transient method using Mac-Cormack Explicit Scheme. Right-angled junction experiment was conducted to verify the numerical model prediction. Figure 2.3. shows that the numerical model result matched the experimental data for the relationship between discharge ratio and Froude number, but high inlet Froude number was not applicable ($F>0.65$). For water surface profile along main and branch channel, the agreement between the numerical model and experiment was considered as good. However, the prediction was slightly unmatched at the beginning of the branch channel as shown in Figure 2.3. The difference between the numerical model and experimental data was generally low for the depth-averaged velocity profile. The size of separation zone from numerical model as shown in the figure was matched to the observation from experiment. Energy losses were calculated from the result of numerical model; there is a similarity compared to close conduit flow. Generally, this numerical model was adequate for open channel branching flow analysis.

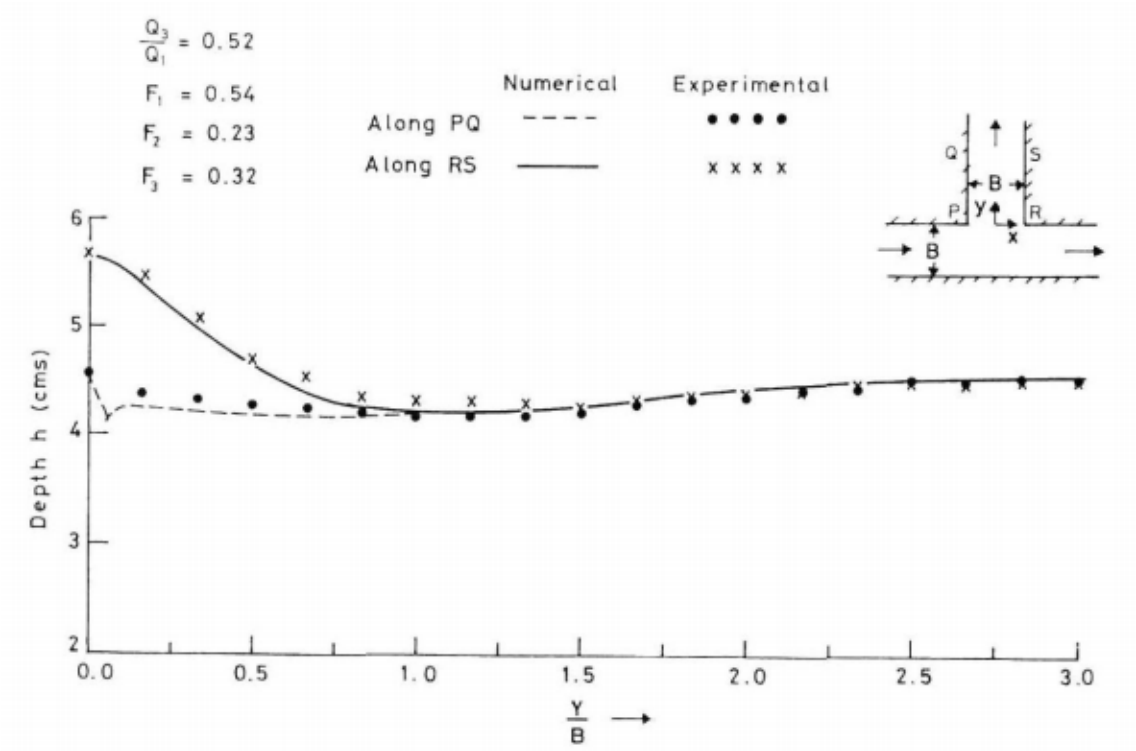


Figure 2.3: Water surface profile in the main channel (Source: Shettar and Murthy, 1996)

Pirzadeh & Shamloo (2007) conducted simulation for detail application of lateral intake inflow with 2D and 3D FLUENT (CFD solver). The channel geometry and boundary conditions of this simulation were setup corresponding to Shettar & Murthy (1996) with result comparison (physical modelling result). The study showed FLUENT is an effective tool for the prediction of lateral intake flow pattern with 3D better than 2D.

Quoted from Ramamurthy et al. (2007) "past experimental studies were mostly limited to the collection of test data on the assumption that the flow was 1D or 2D". Thus, this past study conducted a 3D physical modelling study and 3D numerical modelling study. A comprehensive understanding of velocity profile in 3D was discussed by this past study. A result of the comparison by this past study was that the flow depth ratio matched the proposed theoretical relation by Hsu et al. (2002).

Alfatlawi & Hussein (2024a) studied the optimum flow system in open channel branch flow by using FLOW-3D. The key findings show the maximum discharge ratio happened at branch angle of 15° to 25°. The maximum contraction zone was observed at 25° with minimal energy loss, thus, the optimal branch angle was 25°.

2.4 Modelling of Bifurcation Flow

2.4.1 Nodal Point Relation

In the past, many studies have attempted to provide an analytical model to describe the behaviour of river bifurcation with consideration of sediment transport. One of the cornerstones is Wang et al. (1995), one-dimensional nodal point relation for the model with the relation between sediment transport, discharge rate and width of channel:

$$\frac{\mathrm{S_b}}{\mathrm{S_c}} = \mathrm{f}\left(\frac{\mathrm{Q_b}}{\mathrm{Q_c}}\right) \qquad \text{Equation 2.4}$$

$$\frac{\mathrm{S_b}}{\mathrm{S_c}} = \mathrm{f}\left(\frac{\mathrm{B_b}}{\mathrm{B_c}}\right) \qquad \text{Equation 2.5}$$

This study assumed a dimensionless quantities nodal point relation as below:

$$\frac{\mathrm{S}_b}{\mathrm{S}_c} = \mathrm{f}\left(\frac{B_b}{B_c}, \frac{Q_b}{Q_c}, \frac{\mathrm{C}_b}{\mathrm{C}_c}, \frac{\mathrm{a}_b}{\mathrm{a}_c}, \dots\right) \frac{\mathrm{S_b}}{\mathrm{S_c}} = \mathrm{f}\left(\frac{\mathrm{Q_b}}{\mathrm{Q_c}}\right) \qquad \text{Equation 2.6}$$

Finally, the following empirical equation was considered in their study when k > 0:

$$\frac{S_b}{S_c} = \left(\frac{Q_b}{Q_c}\right)^k \left(\frac{B_b}{B_c}\right)^{(1-k)} \qquad \text{Equation 2.7}$$

Chezy water motion and mass-balance for sediment are estimated as following:

$$Q_j = B_j C_j {a_j}^{3/2} {i_j}^{1/2}, \qquad j = b, c \qquad \text{Equation 2.8}$$

$$S_j = B_j m \left(\frac{Q_j}{B_j a_j} \right)^n, \qquad j = b, c$$ Equation 2.9

Three equilibrium states were found which both branches are open and either branch a or branch b is closed. When k > n/3, the equilibrium is stable, but it becomes unstable when k <n/3. The equation is strongly affected by the empirical factor k, which is hardly define and do not have relation to the bifurcation geometry or the flow condition.

To overcome the issue, Bolla Pittaluga et al. (2003) proposed an alternative formulation for the nodal point condition with a quasi-two-dimensional method. For a relatively high Shield stress, υ, the discharge ratio of subdivision channel and the water depth ratio (water depth of the two subdivision channels) were plotted versus the ratio of channel length and shown in Figure 2.4. The transverse sediment exchange equation and transverse discharge rate were proposed as:

$$S_y = Q_{sy} = S_a \left[\frac{Q_y D_a}{Q_a \propto D_{abc}} - \frac{r}{\sqrt{\vartheta_a}} \frac{\partial \eta}{\partial y} \right]$$ Equation 2.10

$$Q_y = \frac{1}{2} \left[Q_b - Q_c - Q_a \frac{b_b - b_c}{b_b + b_c} \right]$$ Equation 2.11

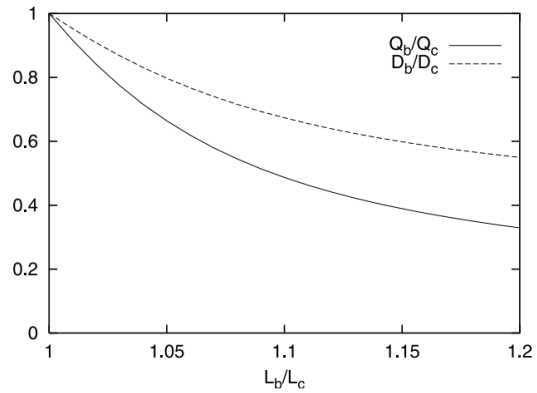


Figure 2.4: Graph of discharge ratio versus water depth ratio (Source: Bolla Pittaluga et al., 2003)

2.4.2 Physical Model

den Dekker & van Voorthuizen (1994) and Roosjen & Zwanenburg (1995) conducted experiments as shown in Figure 2.5. The aim of the study by den Dekker & van Voorthuizen (1994) was to relate the local three-dimensional configuration of bifurcation to the relevant parameters of the different general nodal-point relations. Roosjen & Zwanenburg (1995) studied the relation between the ratio of discharge and the sediment transport at the point of bifurcation.

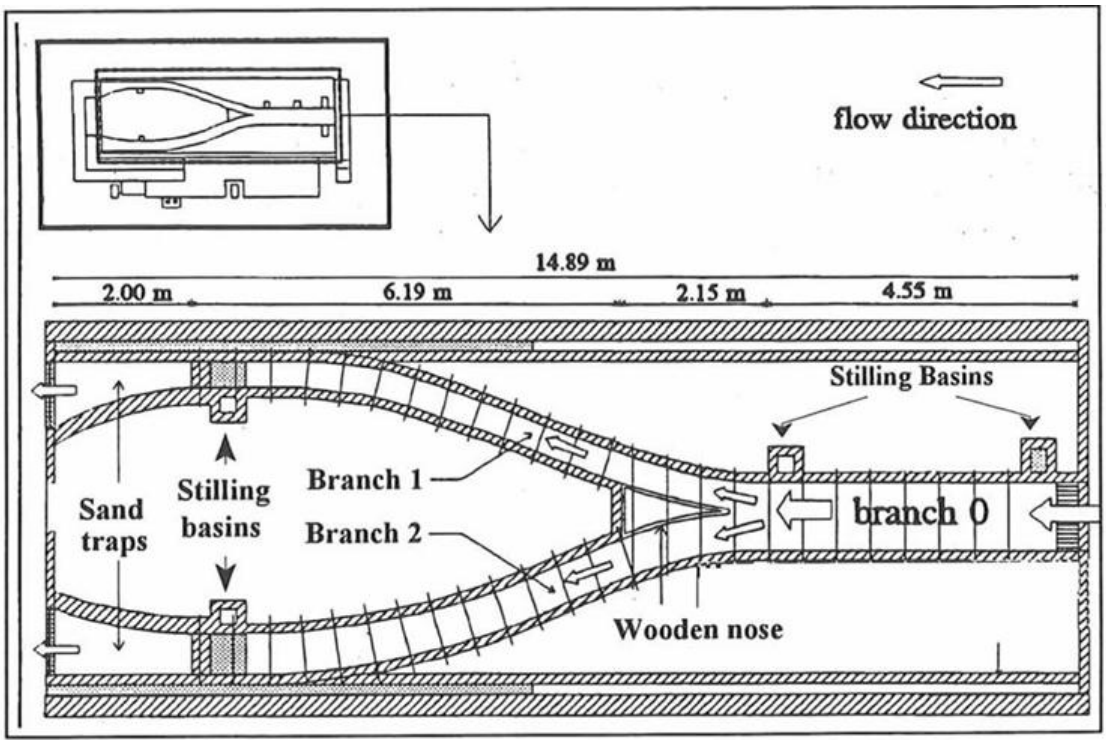


Figure 2.5: Model Setup by Roosjen & Zwanenburg (1995)

Federici and Paola (2003) conducted an experiment for observing the formation of braided network. An observation showed a "stable" bifurcation was formed when Shields stress was more than 0.15, and a "switch" bifurcation was observed when Shields stress was less than 0.15. Figure 2.6 shows that the bifurcation angle ranged from 60° to 90°, and the deposit angle was about 1.5 times the bifurcation angle.

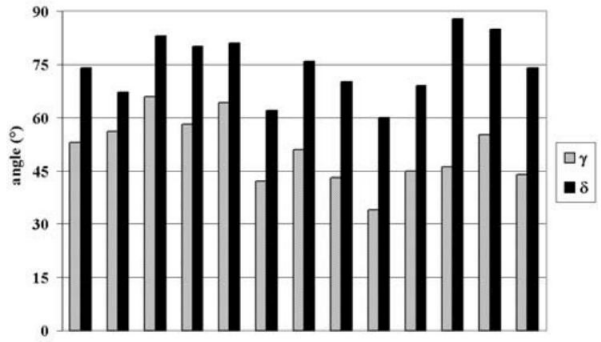


Figure 2.6: Graph of bifurcation angle and deposit angle (Source: Federici and Paola, 2003)

A physical model of bifurcation Po di Goro-po, Venezia, was constructed by Zanichelli, et al. (2004) for determining the discharge distribution. A two-dimensional depth averaged numerical model of the river bifurcation was verified with the result from physical model. The physical model was designed with 1:100 scale, the Reynolds number was scaled from 13 X 10^3 to 28 X 10^3. A scale effect was observed during the experiment, in which the non-major channel discharge had a 10% difference. However, the eddy viscosity coefficient scale ($\lambda^{-3/2}$) was matched with the result from the physical model experiment. The numerical model in this study, FESWMS-2DH, was concluded that there was an acceptable result for engineering purpose, but calibration was required.

The observation in freely formed braided river experiment (Bertoldi and Tubino, 2005) showed the naturally formed bifurcation angle fell between 35° and 55° and the deposit angle between 40° and 60°. There was a relationship between shields stress and width ratio for the condition of uniform sediment, which was the higher value of Shields stress, the higher value of width ratio. The diameter of sediment had no effect on this relationship. However, the experiment with graded sediment did not match the behaviour above, which the width ratio was lower. Analysis on bifurcation points showed it was more scattered. These results concluded that the fixed and graded sediment had different mechanisms.

Bertoldi et al. (2007) performed a physical experiment with Y-shaped forced bifurcation with 0.3%, 0.5% and 0.7% slope. Width ratio (aspect ratio) was designed in the range of 4 to 25 and Shields stress in the range of 0.045 to 0.11, this arrangement was trying to simulate the typical condition of natural gravel bed, braided network. The main finding was that the smaller the inlet discharge, the larger the observed imbalance at the node of bifurcation. The node was balanced when there was a large value of Shields stress or a small value of width ratio.

A strong relationship was found between discharge ratio and inlet step for the experiment with slopes of 0.3% and 0.5%, in contrast, this was not for the case of 0.7% slope due to influence of migrating alternate bars near the point of bifurcation. A linear regression was plotted and produced a simple equation:

$$\Delta_\eta = 1 - r_Q \qquad \text{Equation 2.12}$$

The experiment data was used to test the accuracy of BRT model (Bolla Pittaluga et al., 2003) and concluded that the BRT model was able to produce the relationship between local bed topography and discharge partition at the bifurcation node. Figure 2.7 showed a comparison between the experiment result and the BRT model.

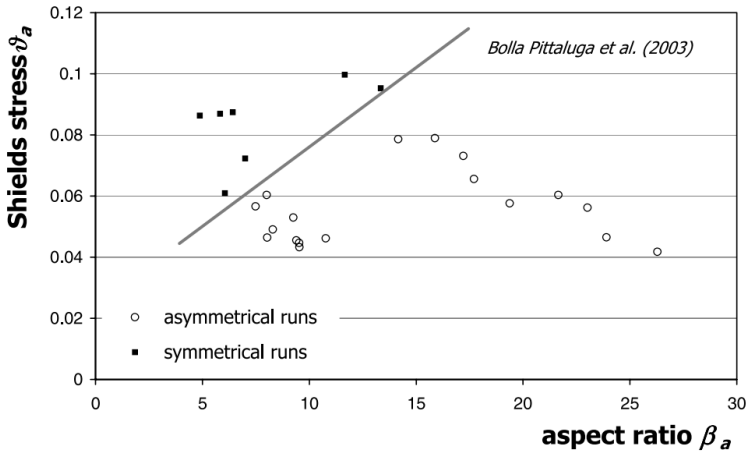


Figure 2.7: Graph of comparing between experiment result and BRT model (Source: Bertoldi et al., 2007)

Thomas et al. (2011) conducted a non-erodible bed symmetrical bifurcation experiment with different combination of bifurcation angle and deposit angle (deposit angle is renamed as internal angle), the definition is shown in Figure 2.8.

The experimental combinations were Geometry A (54° for both angle) and Geometry B (bifurcation 54° and internal angle 81°), the result in Figure 2.9 shows the discharge ratio of both geometries had a similar result with no statistically significant difference (95% confidence interval). Other than that, the weir height was the main factor for discharge ratio (Figure 2.10), the experiment found that the discharge ratio (right divide left) was inversely proportional to weir height (right divide left). The lower the height of weir of the subdivision, the lesser the water flows through.

An observation from the experiment was the super-elevated water surface with a peak at the point of bifurcation head as shown in Figure 2.11. The case of unequal weir height had higher peak super-elevation compared with equal weir height.

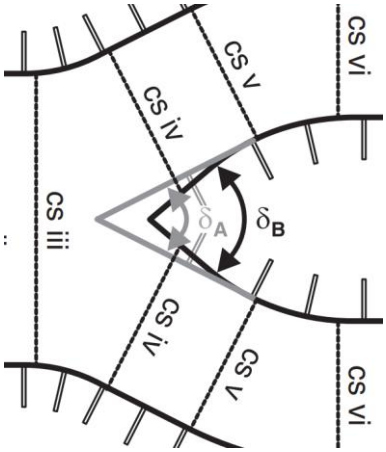


Figure 2.8: Definition of bifurcation angle (δA) and internal angle/deposit angle (δB). (Source: Thomas et al., 2011)

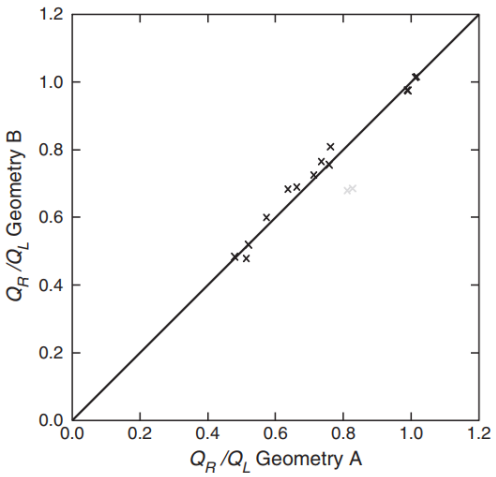


Figure 2.9: Comparison of discharge ratio of two geometries. (Source: Thomas et al., 2011)

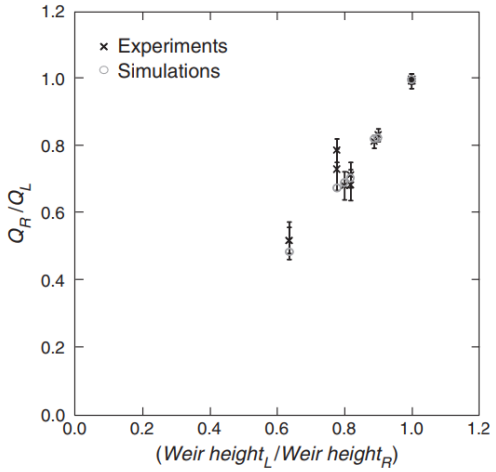


Figure 2.10: Discharge ratio against inverse weir height ratio for Geometry A and B. (Source: Thomas et al., 2011)

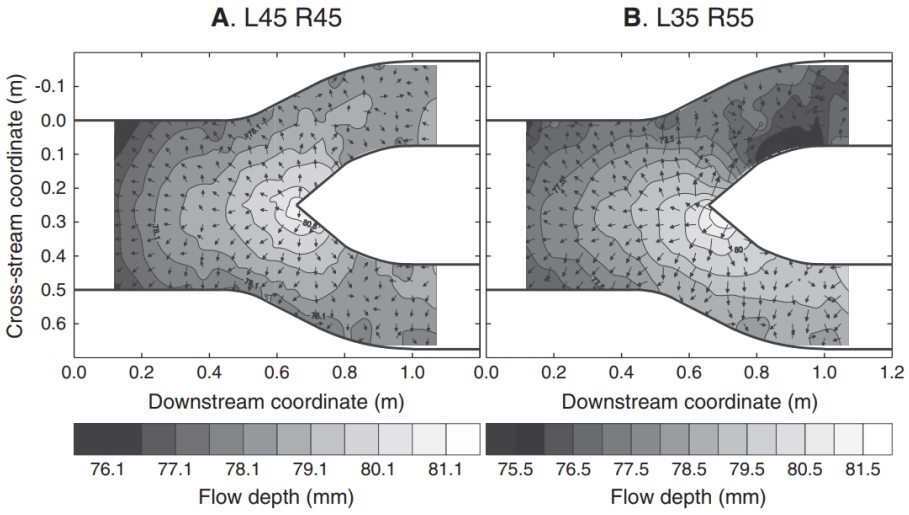


Figure 2.11: Graph of flow depth of equal weir height (left) and unequal weir height (right) (Source: Thomas et al., 2011)

2.4.3 Sediment Transport in Bifurcation

Szewczyk, et al. (2020) studied the bedload transport of channel bifurcation for the condition of channel abandonment (disconnection of tributary due to formation of sand plugs: sedimentation at the inlet of tributary) by manipulating bifurcation angle, flow incidence angle, and bed slope. The experiment was conducted with symmetrical bifurcation (equal incidence angle) and asymmetrical bifurcation (unequal incidence angle). According to the findings, under the constant discharge and sediment loading rate, channel disconnection occurred in highly asymmetrical bifurcation; in contrast, no disconnection was observed in symmetrical bifurcation. Under the asymmetrical bifurcation configuration, discharge partitioning became unequal when the diversion angle was higher than 22.5°. Disconnection of the channel was found to happen when the diversion angle was higher than or equal to 30°.

Das et al. (2023) studied the physical process of discharge and sediment distribution of channel bifurcation with 3 different sizes of sediment (0.190mm, 0.260mm, and 0.275mm) and various inflow discharge.

Calderón et al. (2025) conducted an experimental analysis to determine the relationship between flow velocity and sediment transport in a lateral bifurcation that features sand bar.

2.4.4 Analytical Model

Zawawi, et al. (2019) developed an analytical model for trapezoidal cross section channel open channel bifurcation flow. It was derived from continuity equation, momentum principle and algebraic manipulation. This analytical model was used to predict the bifurcation discharge rate with various parameters, for example, Froude number, deflect angle, width of channel and depth of flow. The generation equation of bifurcation flow can be described as below:

$$(1+2k_o)\left[\frac{1}{2}(1-{y_r}^2-Br_1{y_r}^2\cos\theta_1)+\frac{k_o}{3}(1-{y_r}^3-{y_r}^3\cos\theta_1)\right] = {F_o}^2(1+k_o)^2\left[\frac{1+k_o}{y_r}\left(\frac{(1+q_r)^2}{(Br_2+k_oy_r)}\cos\theta_2+\frac{{q_r}^2}{(Br_1+k_oy_r)}\cos\theta_1\right)-1+C\big((1-q_r)\sin\theta_2+q_r\sin\theta_1\big)\right]$$

Equation 2.13

where, k_o is side slope ratio, y_r is depth of flow ratio, q_r is flowrate ratio, Br_1 is width ratio of channel 1, Br_2 is width ratio of channel 2, θ_1 is deflect angle of channel 1, θ_2 is deflect angle of channel 2, F_o is Froude number of upstream channel.

Based on this model, the study applied 2 sets of geometry and flow properties into the derived equation. Upstream main channel was same as channel 1 and downstream channel 2 was smaller than channel 1, thus, the flowrate ratio should be more than 0.5. The result in Figure 2.12 showed the flowrate ratio was quite consistent within the range of 0° and 45° (deflect angle of channel 1 and channel 2), with a minimum value of 0.787 and maximum value of 0.841 (approximately 7% difference). For deflect angle lower than 45°, the effect of deflect angle on flowrate ratio was small, but there was a significant impact for the case of deflect angle larger than 45°.

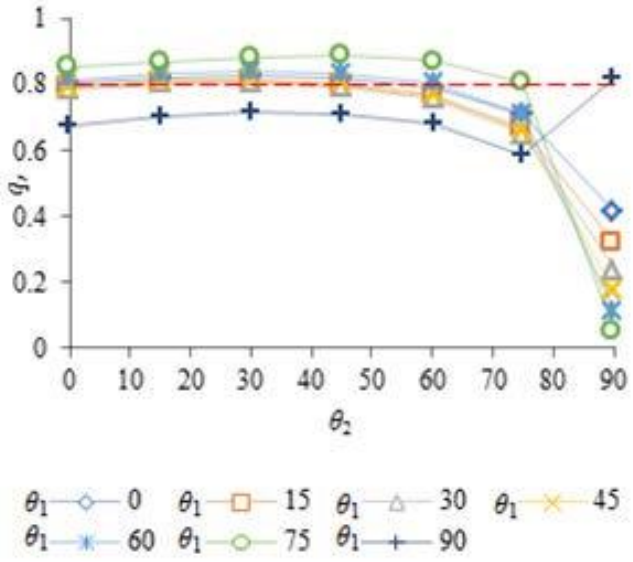


Figure 2.12: Graph of flow rate ratio (Source: Zawawi, et al., 2019)

Durante et al. (2024) introduced a revised analytical model based on BRT model to predict the stability of river bifurcation. This revised analytical model was incorporated with downstream effects into the examination of river bifurcation. The formula by this study allows the river bifurcation to be described in different behaviour of bifurcation flow in sand-bed and gravel bed.

A new analytical model was proposed by Barile et al. (2024) to reproduce the equilibrium configuration of a bifurcation under partial avulsion conditions. This analytical model was developed based on 1D numerical modelling result by coupling the latter model with BRT model. This study provided a tool to determine the long-term evolution of bifurcation with controlling factors such as flow variability, sea level rise, and bank erosion.

2.4.5 Numerical Model

Kleinhans, et al. (2008) applied Delft three-dimensional morphodynamic model system for the study on bifurcation morphology with different set of scenarios (Figure 2.13). Nodal point relation was used for predicting the sediment distribution which the input was the result of flow distribution from three-dimensional model. It was further compared with the sediment distribution result from three-dimensional model. Morphodynamic evolution of both nodal point relation one-dimensional model and three-dimensional model were compared.

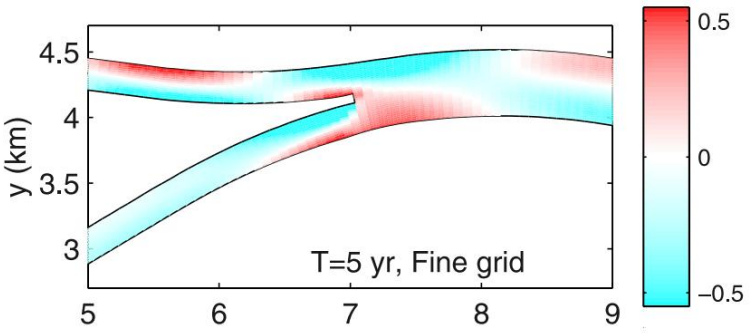


Figure 2.13: The numerical model of bifurcation (Source: Kleinhans, et al., 2008)

Various findings were determined from the result of numerical model. The upstream bend radius was found to be related to discharge distribution. A sharp bend had a faster development of fixed bar. The discharge distribution with all bend radius was highly becoming imbalance after long period of time. The sediment division fluctuated initially and showed a similar asymmetrical distribution after a long term. Due to the asymmetrical discharge and sediment distribution, the downstream channel on the side of the inner bend of upstream was slowly “disappeared” and stabilised with a non-zero discharge and sediment transport value. An inner-bend downstream with larger gradient was found to encounter the effect of bend radius, which the dominant discharge channel became the inner-bend downstream channel when the gradient was increased by 30%. When the backwater adaption length (bifurcation point to downstream water body which can cause backwater effect) was longer than the previous model, the deposition of sediment in the inner bend downstream becomes slower. A sudden flood was simulated in the model to study the effect of flood on the bifurcation evolution. Result showed the flood had no significant effect with the assumption of no bank erosion due to the flood. The previous simulation had 504m width and the dominant channel is inner-bend, but the dominant bifurcation changed to outer-bend when the width was between 228 and 378m.

The comparison between the numerical finding and the previously published nodal point relation showed the nodal point relation did not consider the effect of upstream bend. The numerical finding behaved like the nodal point relation but had a huge difference in the initial stage.

Thollibon & Ariffin (2013) conducted a review on bifurcation numerical model with 4 types of models, which are CCHE2D model, CAESAR Model, DELFT3D model and RIVER2D Model. The study concluded that CAESAR is the most adequate model for bifurcation study and some enhancements to the algorithm are encouraged for improvement.

A study by Fang et al. (2025) investigated how streamflow, tidal amplitude, and channel length affecting the flow division at the Tianhe/Nanhua bifurcation in the Pearl River Delta by using Delf3D. The key findings show that the flow division is dynamically governed by different conditions. During the dry season with low upstream discharge, tidal at the downstream outlets dominantly control the flow division ratio. Whereas during wet season, specifically during flood event, the upstream inflow and channel length becomes the primary determinants of flow distribution.

2.5 Field Study of River Bifurcation

Zolezzi, et al. (2006) conducted field measurement on two locations, which were Ridanna Creek and Sunwapta River. From the direct measurement, the relationship between discharge and free-water surface elevation was derived as below:

$$h = 0.3129Q^{0.39} \quad \text{Eq. 2.14}$$

$$h = 1.62 - 0.028Q \quad \text{Eq. 2.15}$$

The data analysed from the field measurement showed a quasi-linear relationship between the discharge ratio and the upstream discharge, imbalance may be observed when the upstream discharge was low enough. In Figure 2.14, the angular coefficient represents the tendency in the stage of unbalanced configuration, the lower the value, the higher the likelihood of becoming unbalanced.

Figure 2.15 showed the aggradation occurred near the bifurcation, the observation resulted from the enchanted tendency towards deposition induced by backwater effect due to local flow divergence.

Inlet step phenomena were commonly observed in this field study; the size of inlet step was mainly affected by the asymmetric water distribution and scaled with mean upstream flow depth. The degree of transverse asymmetry between both sides of the inlet step changed along the longitudinal direction. This study recommended to develop a method to define its value for bifurcation. There were another two phenomena which related to inlet step. Firstly, the inlet step corresponding to transverse bed inclination usually extended over a few channel widths. Secondly, the outer bank of larger downstream was invariably eroded over few channel widths.

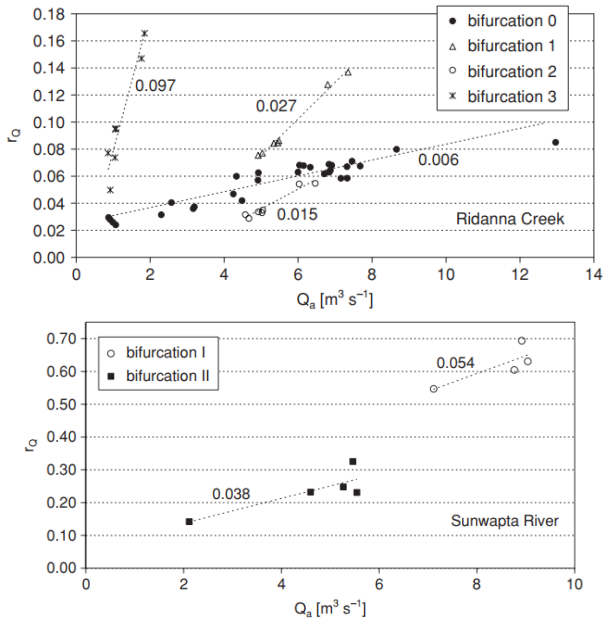


Figure 2.14: Discharge ratio against upstream discharge (Source: Zolezzi, et al., 2006)

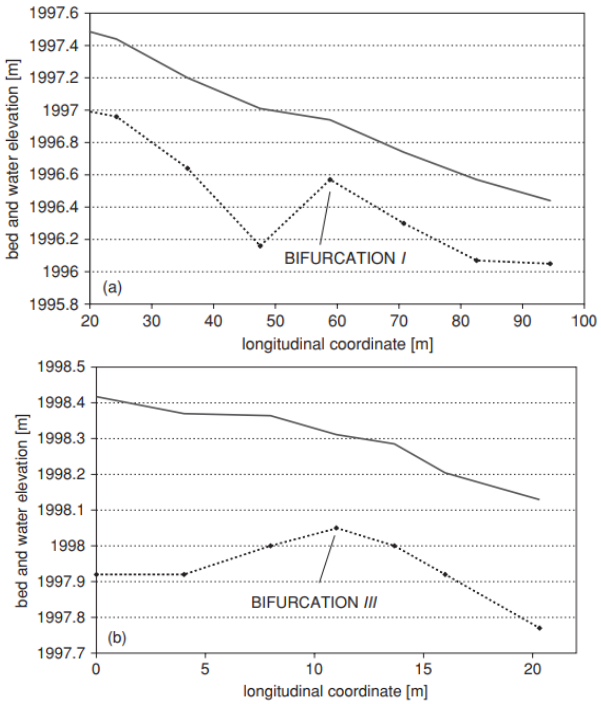


Figure 2.15: Longitudinal profile of water surface and bed elevation (Source: Zolezzi, et al., 2006)

2.6 Machine Learning of River Bifurcation

Artificial intelligence (AI) usually refers to a machine that can mimic human intelligence (Science, 2025). Machine learning (ML) is an algorithm that has the ability of self-learning through a huge amount of data, which requires a deep learning algorithm. Machine Learning can be classified into Supervised, Unsupervised, and Reinforcement machine learning algorithms (Stryker et al., 2026).

The deep learning is a learning system with multilayer deep neural network architecture (Figure 2.16), which requires a large amount of training data, is limited to a specific application, and is hardly interpretable. The fundamental of the neural network is the nodes with a linear regression model, which is shown below:

$$\sum_{i=1}^{m} w_i x_i + bias = w_1 x_1 + w_2 x_2 + \ldots + w_m x_m + bias \qquad \text{Equation 2.16}$$

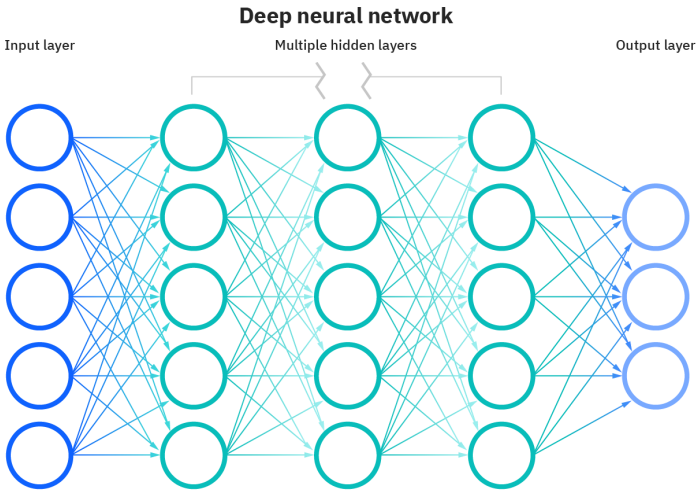


Figure 2.16: Deep neural network (Stryker et al., 2026)

There are 3 major types of neural network, which are Artificial Neural Network (ANN), Convolution Neural Network (CNN), and Recurrent Neural Network (RNN). ANN is a simple feed-forward neural network, which is illustrated in Figure 2.17. Machine learning requires large amount of computing power due to the multi-layer, using high resolution image for machine learning is computationally expensive, therefore, CNN is a specialised neural network for image-based machine learning, which the image will be convolved with filter and slowly reduce the resolution of the image for each convolution step. Figure 2.18 and Figure 2.19 show the architecture framework of CNN and RNN respectively.

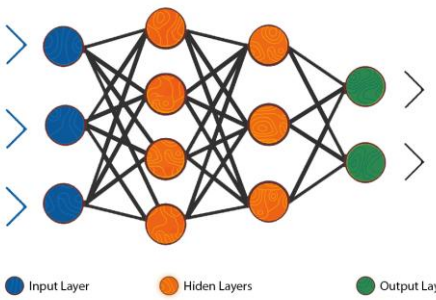


Figure 2.17: Architecture framework of ANN (Source: www.analyticsvidhya.com)

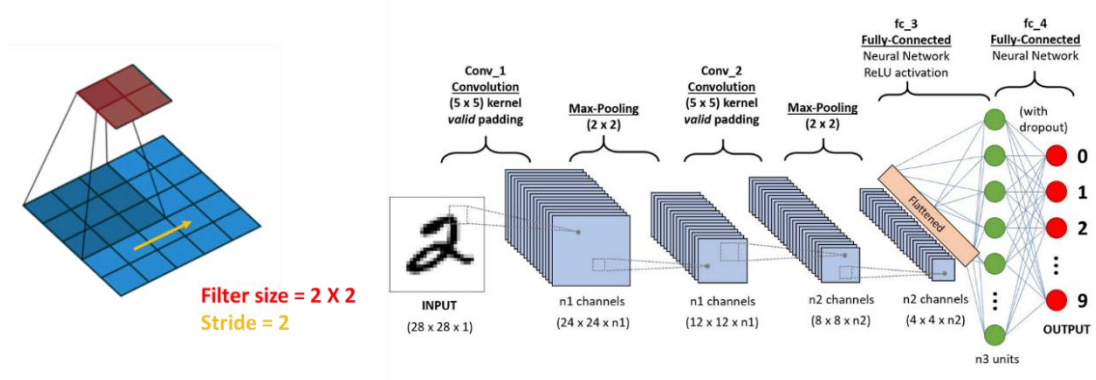


Figure 2.18: Architecture framework of CNN (Source: www.analyticsvidhya.com)

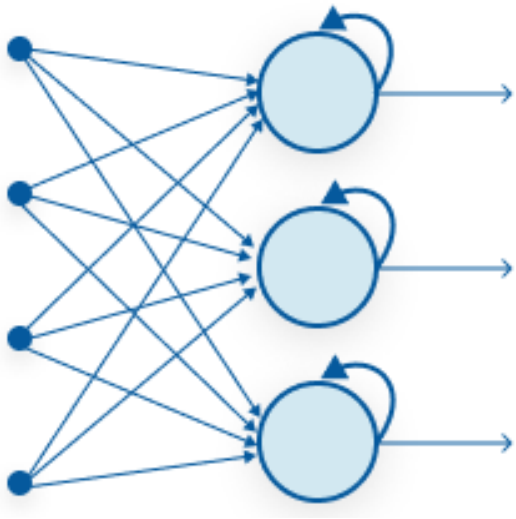


Figure 2.19: Architecture framework of RNN (Source: www.analyticsvidhya.com)

A deep learning-based surface water mapping was developed by Isikdogan, et al. (2017a) named as DeepWaterMap, convolutional neural network (CNN) was proposed as the framework for the machine learning. It was able to separate water from land, snow, ice, cloud, and shadow by only using Landsat as input. The result showed DeepWaterMap could perform significantly better than the modified normalised difference water index. The next step was to develop a machine learning model to determine the river network, which presented in next paragraph.

A deep-learning-based river network extraction model named DeepRiver (Figure 2.20) was developed by Isikdogen, et al. (2018) to learn the properties of rivers from synthetic data and identify the river centreline at the bifurcation. DeepRiver was able to differentiate the river and ocean, which was useful for extracting the shape of a river near the sea, especially a river delta. Firstly, a random generator produced unlimited synthetic input images of rivers for training the machine. The model was designed to consist of a 10-scale convolutional module with an adaptive loss function. The adaptive function was designed to apply a spatial max pooling to the pixelwise loss value, instead of calculating the average loss over all pixels.

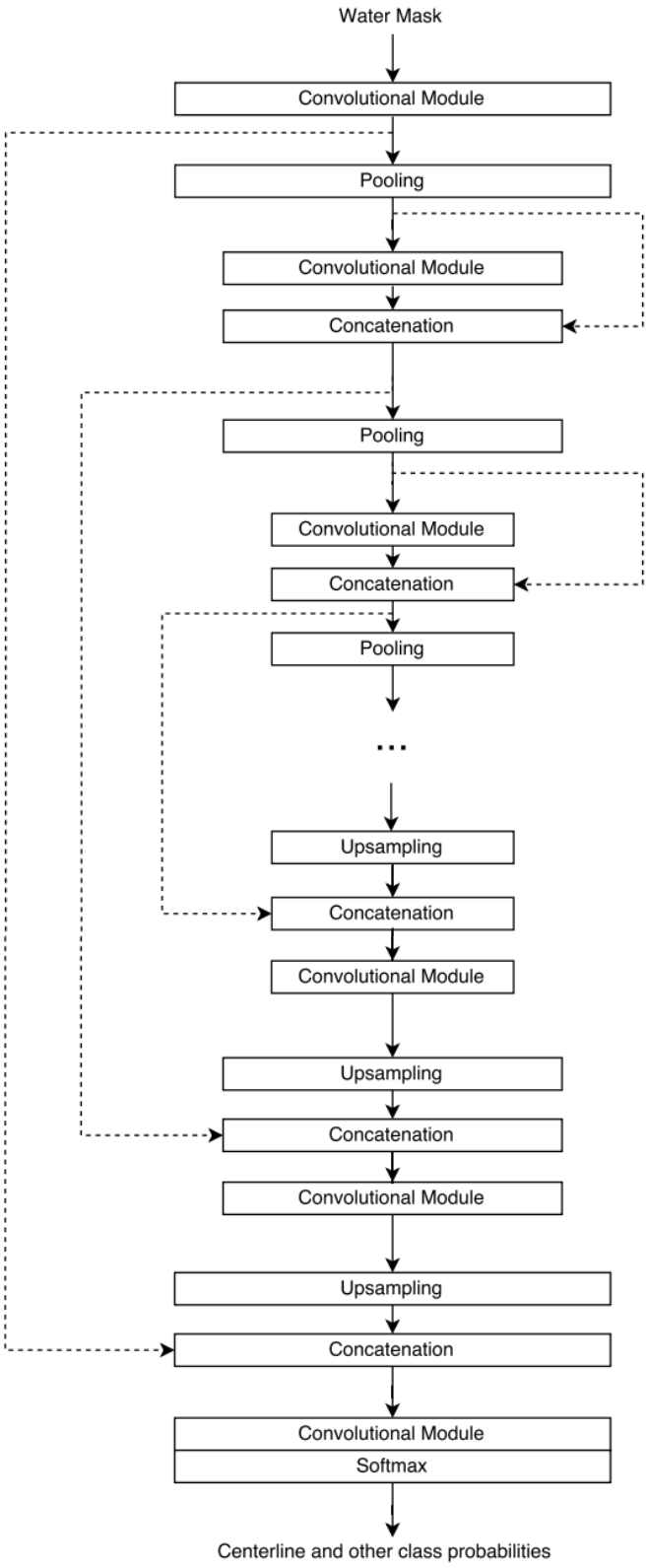


Figure 2.20: Architecture of DeepRiver (Source: Isikdogen, et al., 2018)

Isikdogen, et al. (2018) evaluated the learning model by comparing it to the result generated from RivaMap (a numerical-based software for automated river analysis and a mapping engine). Table 2.2 and Figure 2.21 showed the quantitative evaluation of DeepRiver and RivaMap (Isikdogan, et al., 2017b), both could extract the river network quite well; generally, DeepRiver had better performance than RivaMap. Even though DeepRiver was able to extract the river network from noisy water masks, the accuracy was still affected by the poor-quality input water masks.

Table 2.2: Quantitative evaluation of DeepRiver and RivaMap (Source: Isikdogen, et al., 2018)

Metric	RivaMap	DeepRiver
Precision	0.87	0.97
Recall	0.85	0.88
Commission Error	0.13	0.03
Omission Error	0.15	0.12
F1 Score	0.86	0.92
Width Correlation	0.83	0.92

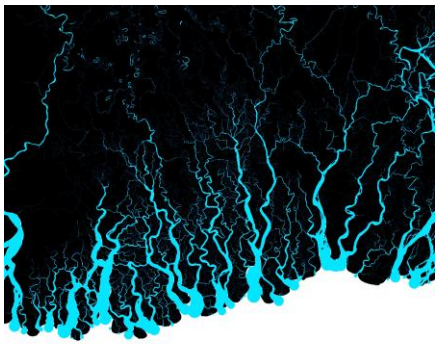


Figure 2.21: Visualisation of automatically extracted channel (Source: Isikdogen, et al., 2018)

2.7 Potential Research Gap

Many of the past studies about physical modelling of branch flow (Section 2.3.1) or bifurcation flow (Section 2.4.2) did not focus on the impact of hydraulic structures on the hydrodynamic processes of bifurcation flow, except for Bertoldi & Tubino, 2007 and Thomas et al. (2011). Another knowledge gap in past studies is the impact of bifurcation angle and bed slope on the hydrodynamic processes of bifurcation flow.

Another part of the research gap is the application of machine learning model on prediction of bifurcation flow. Study like Isikdogen, et al. (2017a), Isikdogen, et al. (2017b), and Isikdogen, et al. (2018) focus on river bifurcation pattern detection, visualisation, and extraction with CNN model. The physics behind the hydrodynamic processes of bifurcation flow have yet to be discovered with machine learning model such as ANN model.

Chapter 3 Methodology

3.1 Physical Model

3.1.1 Experiment Setup

To study the impact of different weir height combinations on the hydrodynamic processes of channel bifurcation, an idealised channel bifurcation was designed and fabricated for experiment.

The study of channel bifurcation was conducted in a 6.0m long and 1.9m wide stainless-steel flume (MICRO RIVER MODEL-FM 59 in Figure 3.1) at the River Engineering Lab, University of Malaya. This flume was originally designed for micro river simulation with sand as the surface material to simulate the natural river flow. However, the flume was modified to fit in a channel bifurcation model with a redesigned piping system.

The model was designed as a modular type with 3 major sections. The first section was a 1.9m-length inlet channel for receiving water from the pump and stabilising the flow, the second section was a 2.0m-length bifurcation section for bifurcating flow into two distributaries, and the last section was two identical 1.5m-length distributaries for collecting water back to the water tank. The advantage of modular type model was flexibility, allowing the bifurcation section to be easily replaced with different bifurcation angles without replacing the other two sections. The distributaries were relocated to connect both ends whenever the bifurcation angle was changed. Refer to Figure 3.2, Figure 3.3, and Figure 3.4 for complete plan view of physical model with different bifurcation angles.



Figure 3.1: MICRO RIVER MODEL-FM 59

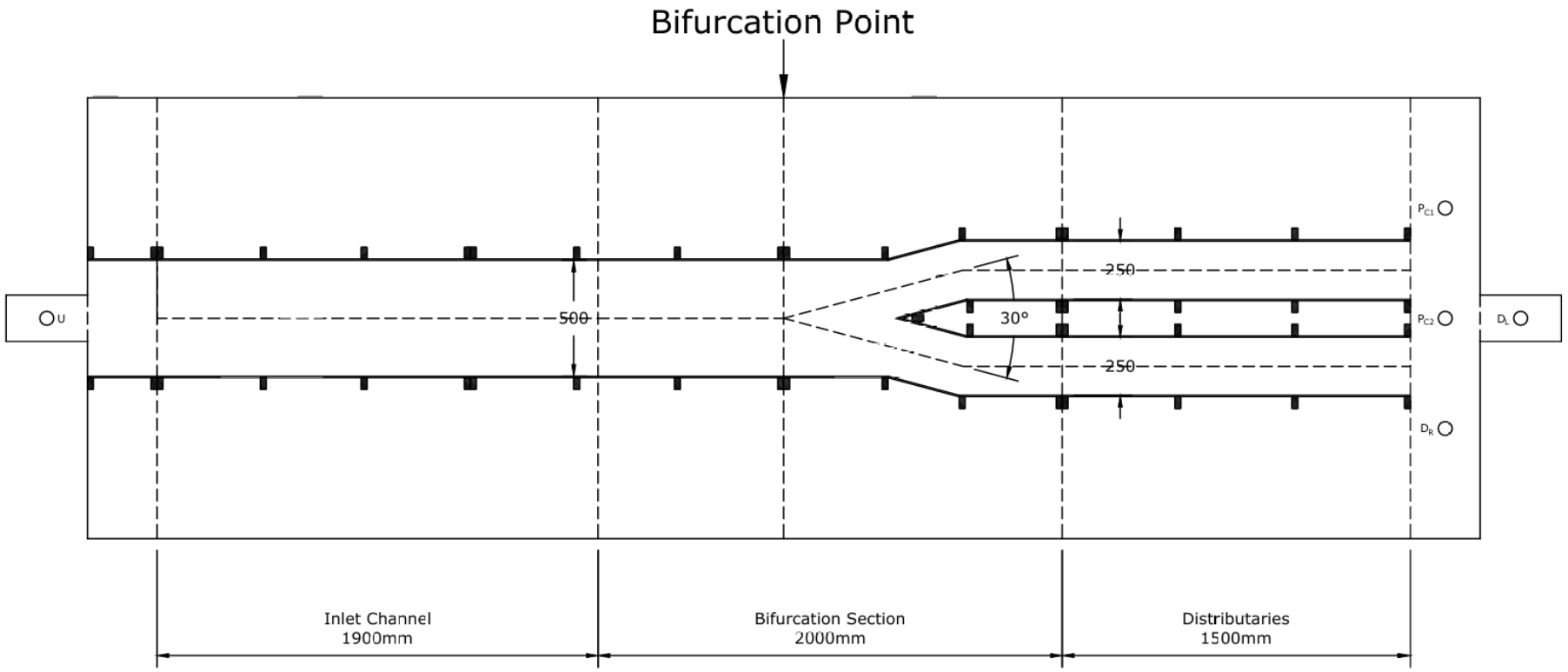


Figure 3.2: Plan view of 30° bifurcation physical model

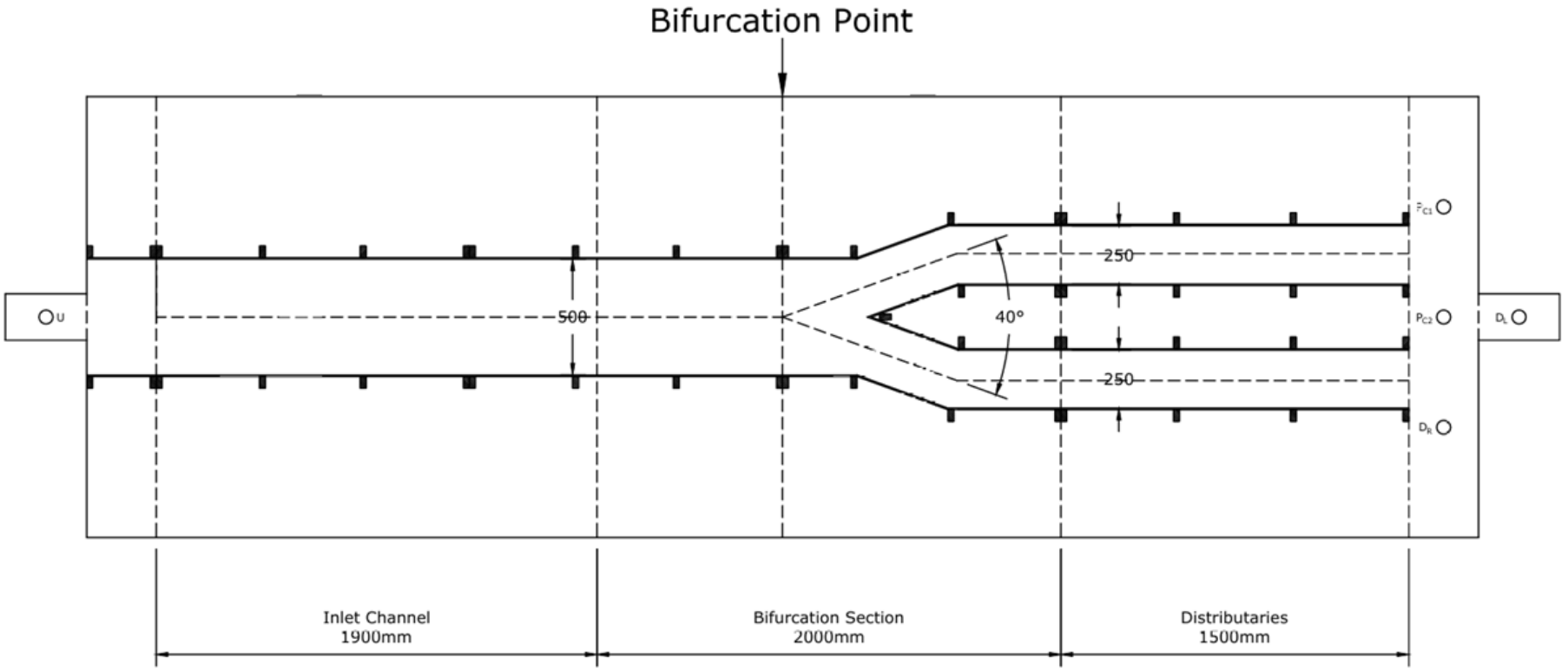


Figure 3.3: Plan view of 40° bifurcation physical model

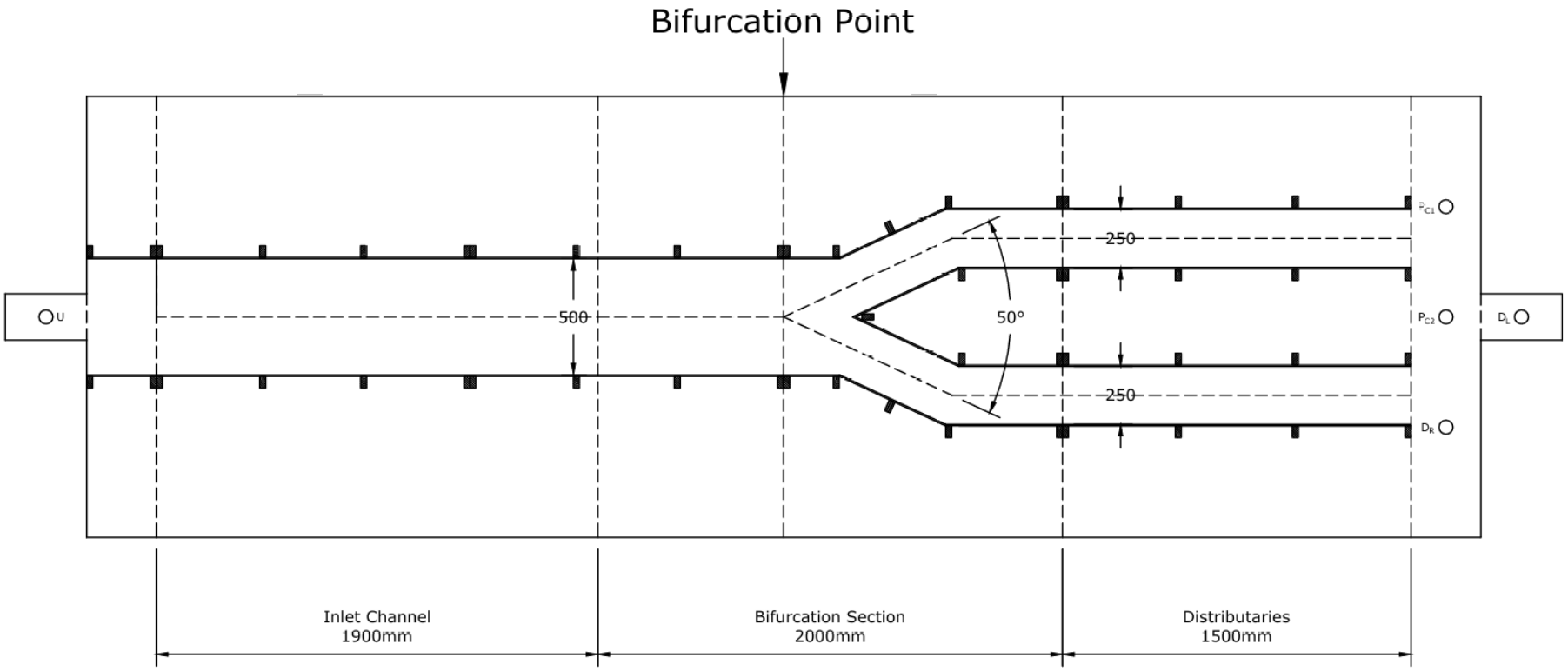


Figure 3.4: Plan view of 50° bifurcation physical model

The channels were constructed of plywood and wood strip to form its structural support; waterproof plastic was applied on the inner surface of channel to avoid leakage of water.

The cross section of both upstream and downstream channels was designed as a 250mm-height rectangular channel. The effective height of the channel was limited to 200mm due to the presence of lateral bracing at the top of channel for stability purposes.

To avoid energy losses due to contraction and expansion of the channel, the width of the downstream channel was designed as 250mm, which was half of the upstream channel (500mm). The width of both types of channels was designed the same as the setup in Thomas et al. (2011) and Marra et al. (2014) to ensure the experiment was conducted under similar conditions for better comparison.

Figure 3.5 shows the cross-section of upstream and downstream.

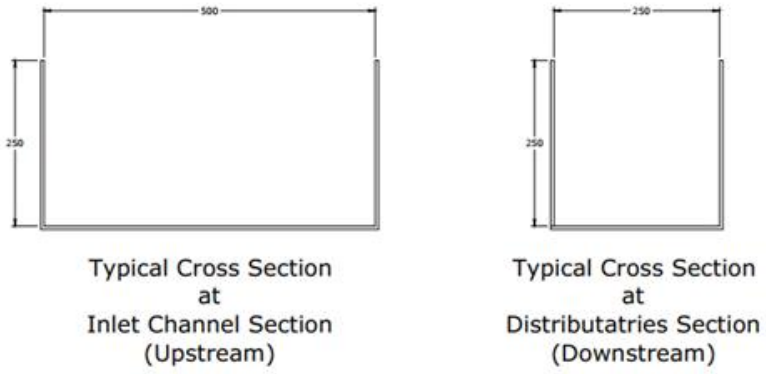


Figure 3.5: Typical cross-section of channel

According to the experiment conducted by Thomas et al. (2011), the internal angle has a minor effect on the discharge ratio. Therefore, the internal angle of bifurcation section was designed and fabricated equal to the bifurcation angle. Figure 3.6 illustrates the definition of bifurcation angle and internal angle. The bifurcation angle and internal angle are defined based on point of bifurcation and wedge-shaped channel wall as illustrated in Figure 3.7.

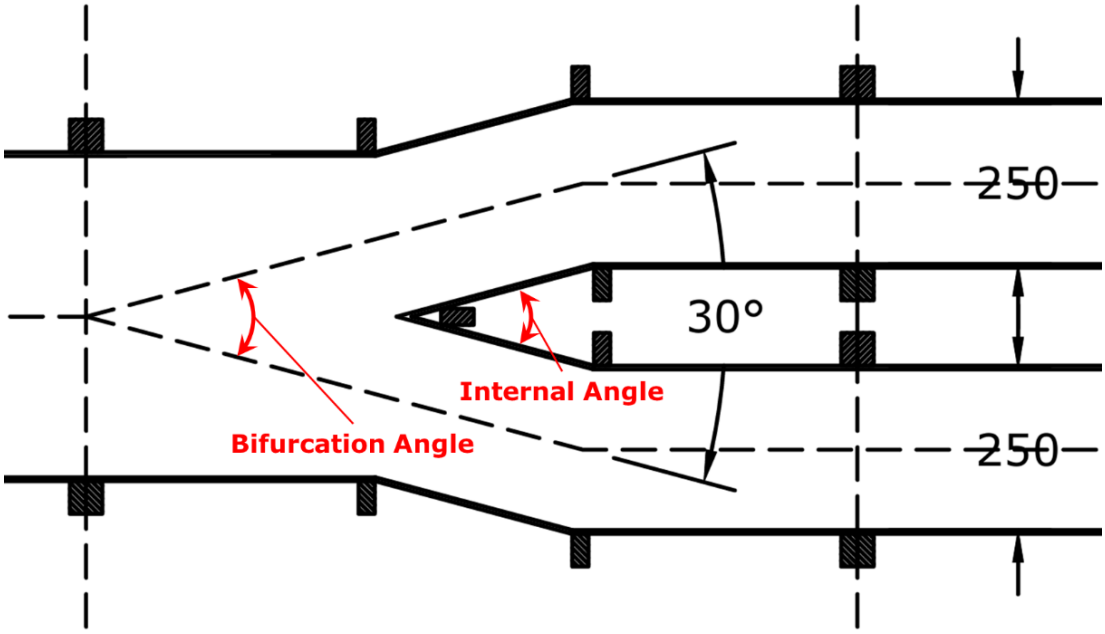


Figure 3.6: Definition of bifurcation angle and internal angle

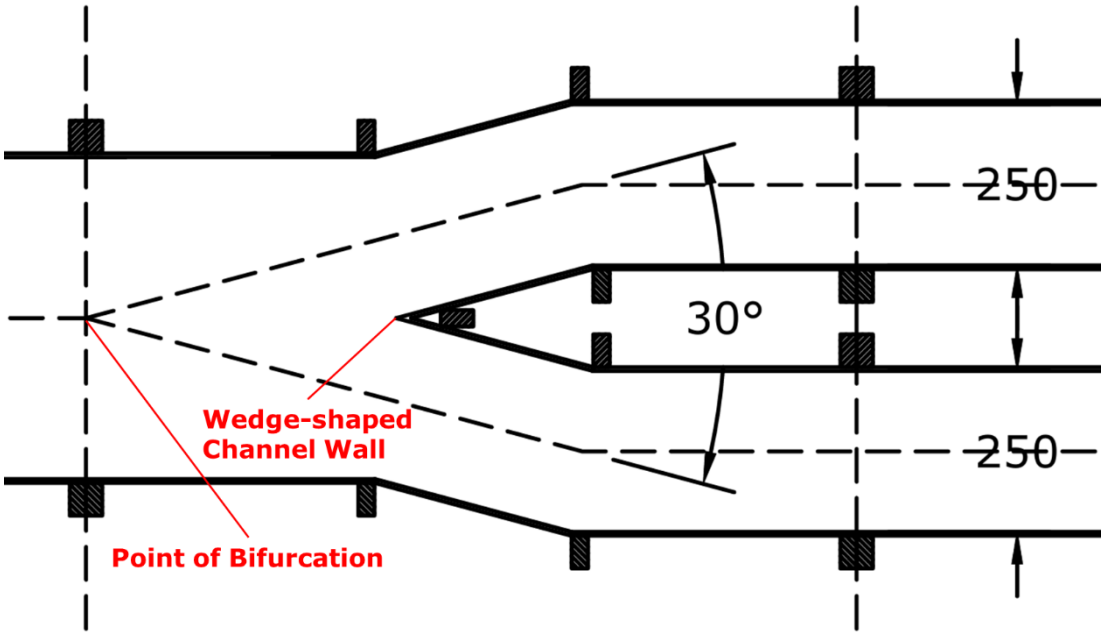


Figure 3.7: Definition of point of bifurcation and wedge-shaped channel wall

In the experimental design, three control parameters were considered, which were bifurcation angle (Θ), overall channel bed slope (hereinafter referred to as slope, Δ), and weir height (WH).

The 54° bifurcation angle that adopted by Thomas et al. (2011) for the experiment was informed by the findings from Bertoldi and Tubino (2005); the bifurcation angle of natural bifurcation was observed to range between 35° and 55°. Another past study by Szewczyk et al. (2020) experimented with 30°, 45°, 60°, and 90°, but the width of the tributaries was same as inlet channel, which was 40mm wide. With the basis of Thomas et al. (2011) and to further extend the range of bifurcation angle, three different bifurcation angles were selected for this study which were 30°, 40°, and 50°.

The slope introduced from previous studies such as Bertoldi and Tubino (2005), Salter et al. (2019), and Szewczyk et al. (2020) was higher than 1%. The slope in this experiment was achieved by elevating one end of the flume with a hydraulic jack. Due to the site constraint, the maximum slope by the flume was about 1%. The high slope of the flume caused significant vibration on the platform. Therefore, each bifurcation angle was experimented with 0.3%, 0.5%, and 0.7%.

To simplify the experiment, suppressed rectangular sharp-crested weir was selected for the experiment (Figure 3.8). The weirs were installed at the end of both tributaries as shown in Figure 3.9.

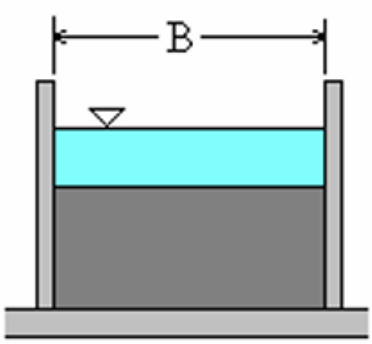


Figure 3.8: Section view of suppressed rectangular sharp-crested weir

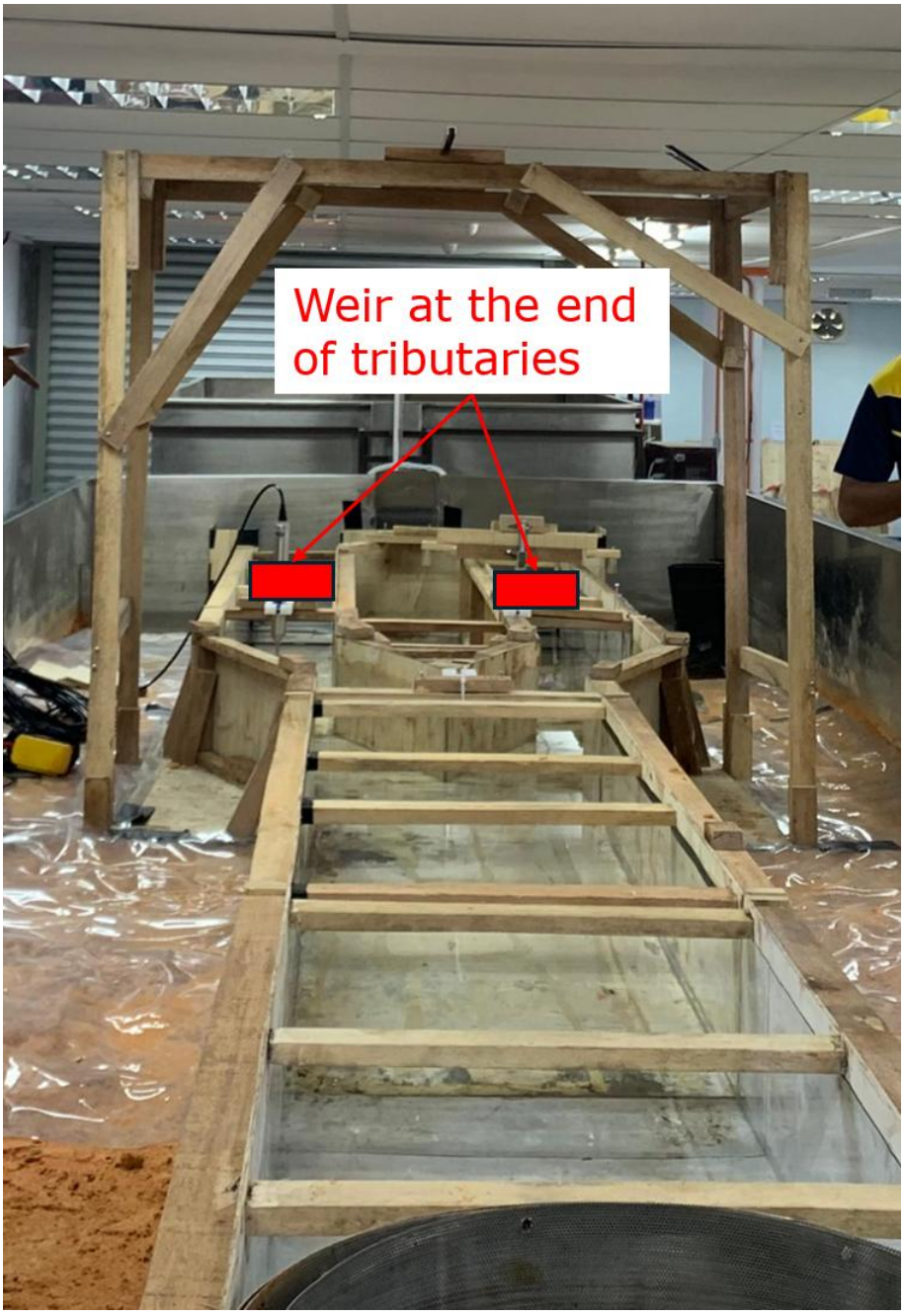


Figure 3.9: Location of weir in the experiment

The weir heights used by Thomas et al. (2011) were 35mm, 40mm, 45mm, 50mm, and 55mm. 7 combinations of weir were selected in this past study with a range of 0.636 to 1.000 as its weir height ratio. The weir height in this study referred to the experiment by Thomas et al. (2011). To explore the impact of a weir with a higher weir height compared to the past study, the height of weirs in this study was selected as 50mm, 55mm, and 60mm. With 50mm as the base weir height, 4 combinations listed in Table 3.1 were selected as the experiment setup. The first 3 weir combinations were conducted successfully with flow observed on both tributaries; however, no flow was observed at the right tributary during the last set of weir combination (Weir height combination = 50:60) regardless of bifurcation angle and slope. Therefore, the last set of weir combination was removed from the list of experiments.

Table 3.1: Weir height combination

Left Weir Height (mm)	Right Weir Height (mm)	Weir Height Ratio
50	50	1.000
55	60	0.917
50	55	0.909
50	60	0.833

The equation of weir height ratio is listed as Equation 3.1:

$$WH_r = \frac{\mathrm{WH}_L}{\mathrm{WH}_R}, dimensionless \qquad \text{Equation 3.1}$$

where, WH_r is weir height ratio

WH_L and WH_R is weir height on left and right tributary

To simplify the calculation and analysis, the left weir height was set as always lower than the right weir height. This ensures the value of WHr always lower than 1.

With consideration of all proposed parameters above, 27 experiments were conducted in this study which are listed in Table 3.2.

Table 3.2: List of experiment runs.

Bifurcation Angle (°)	Slope (%)	Left Weir Height (mm)	Right Weir Height (mm)	Weir Height Ratio	Name of Run
30	0.3	50	50	1.000	30_03_5050
		55	60	0.917	30_03_5560
		50	55	0.909	30_03_5055
	0.5	50	50	1.000	30_05_5050
		55	60	0.917	30_05_5560
		50	55	0.909	30_05_5055
	0.7	50	50	1.000	30_07_5050
		55	60	0.917	30_07_5560
		50	55	0.909	30_07_5055
40	0.3	50	50	1.000	40_03_5050
		55	60	0.917	40_03_5560
		50	55	0.909	40_03_5055
	0.5	50	50	1.000	40_05_5050
		55	60	0.917	40_05_5560
		50	55	0.909	40_05_5055
	0.7	50	50	1.000	40_07_5050
		55	60	0.917	40_07_5560
		50	55	0.909	40_07_5055
50	0.3	50	50	1.000	50_03_5050
		55	60	0.917	50_03_5560
		50	55	0.909	50_03_5055
	0.5	50	50	1.000	50_05_5050
		55	60	0.917	50_05_5560
		50	55	0.909	50_05_5055
	0.7	50	50	1.000	50_07_5050
		55	60	0.917	50_07_5560
		50	55	0.909	50_07_5055

3.1.2 Data Collection

Velocity of flow and water depth were measured in each experiment run. Further calculation and analysis in Section 3.1.3 were calculated based on these two hydraulic properties.

The velocity was measured by Electromagnetic Current Velocity Meter, a single-point current measurement tool which was manufactured by JFE Advantech Co., Ltd. Two types of instruments were available for measurement: ACM2-RS and ACM3-RS. ACM2-RS can measure velocity of flow in 2 directions (x & y), its sensor was a black cylindrical shape as shown in Figure 3.10. ACM3-RS can measure velocity of flow in 3 directions (x, y & z), its sensor was a black spherical shape as shown in Figure 3.10. The size of the sensor of ACM3-RS was relatively bigger than the sensor of ACM2-RS, with the consideration of the turbulence effect caused by the ACM3-RS's sensor and relatively low water depth. ACM2-RS was selected for the measurement throughout all experiments. ACM2-RS was a directional velocity sensor; therefore, the sensor should be placed with the red-dot face oriented against the direction of flow (direction of negative y as shown in Figure 3.11).



Figure 3.10: Picture of ACM2-RS and ACM3-RS

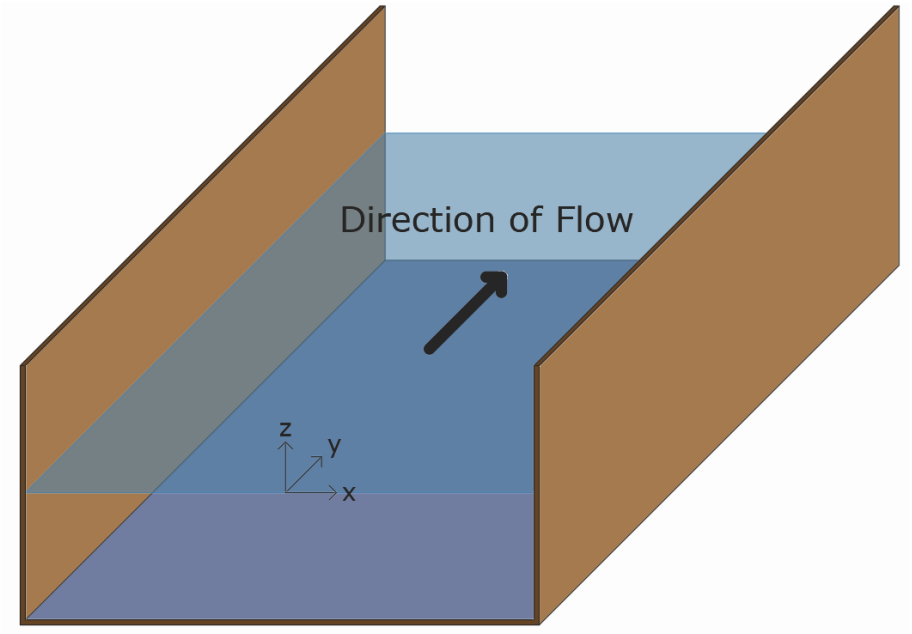


Figure 3.11: The direction of measured velocity

For each experiment run, 6 sections were designated as the cross section for data collection as shown in Figure 3.12. Upstream channel consisted of 3 sections: Section A, B, and C. Downstream channel consisted of 3 sections: Section D, E, and F. Each section in the downstream channel was further separated into 2 sub-sections with prefix of L and R that indicate Left and Right. 2 sets of ACM2-RS sensors were positioned to measure data at the same time. Sensor with series number of 101 was assigned to Section A, B, and C; sensor with series number of 107 was assigned to Section D, E, and F.

The sensor of both ACM2-RS and ACM3-RS has a range of ±250cm/s with accuracy of ±0.5cm/s or ±2%. The velocity measurement in the experiment of this study range between 0.4cm/s and 4.0cm/s, thus, the measurement error by the device can be as low as 0.008cm/s, and as high as 0.5cm/s.

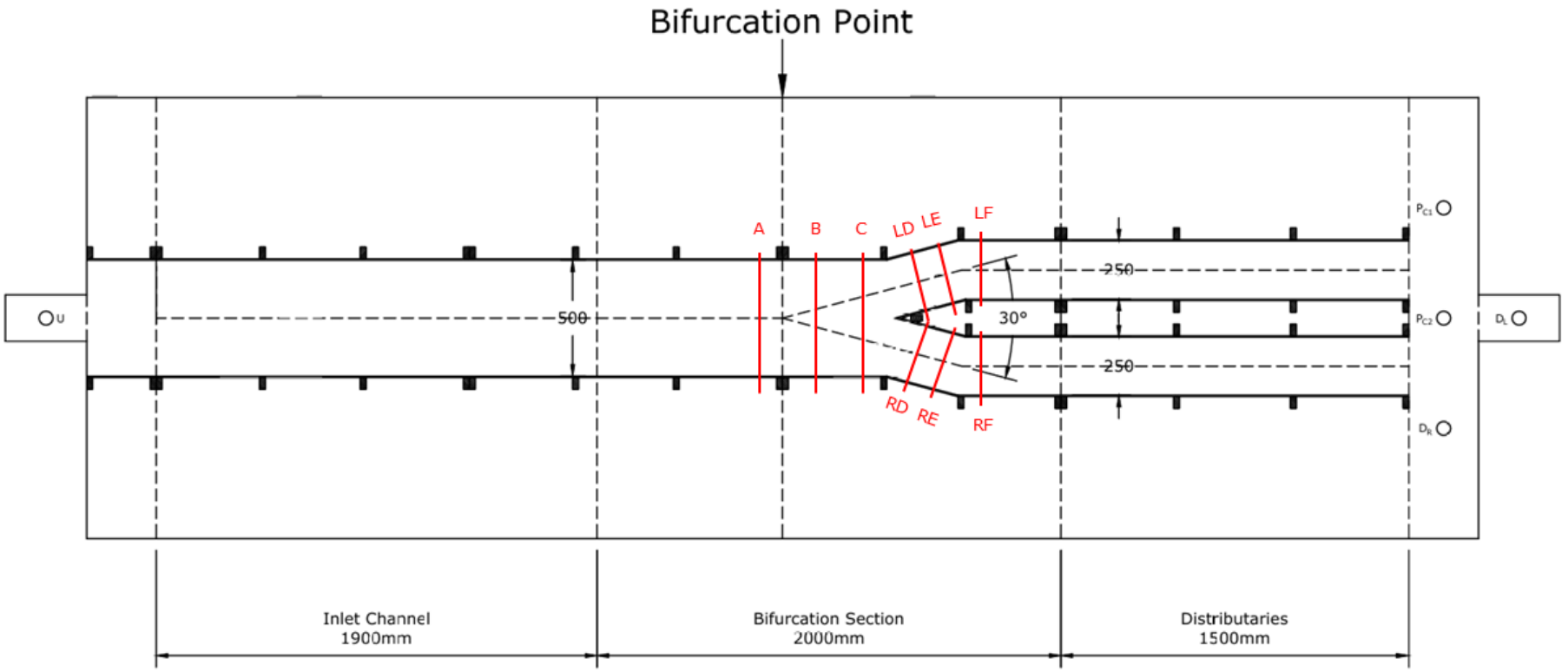


Figure 3.12:Illustration of cross section for data collection

For both upstream and downstream channel, the ACM2-RS was positioned to measure near surface flow and near bed flow. Upstream channel consisted of 9 measurement points for near surface flow and near bed flow with 50mm interval (total 18 subsections). Downstream channel consisted of 4 measurement points for near surface flow and near bed flow at 50mm interval (total 8 subsections). Figure 3.13 and Figure 3.14 show the position of measured points in a cross-section view. Each point was measured for a duration of 1 to 2 minutes; the frequency of data collection was set to 3Hz (3 data collections per second).

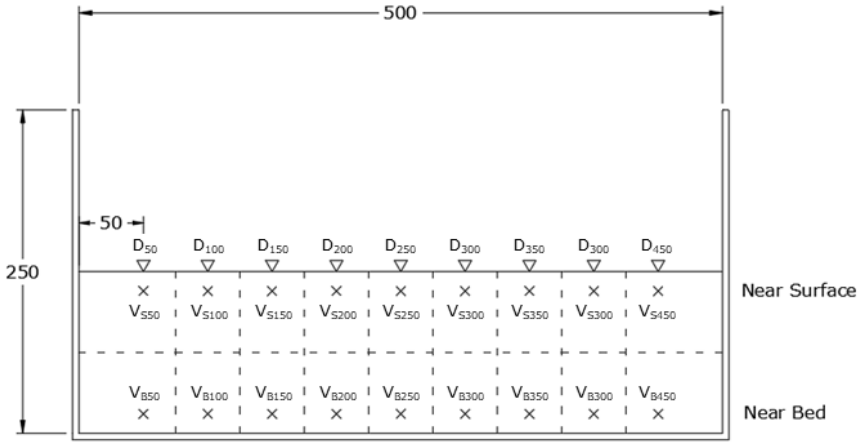


Figure 3.13: Point of velocity measurement for upstream channel

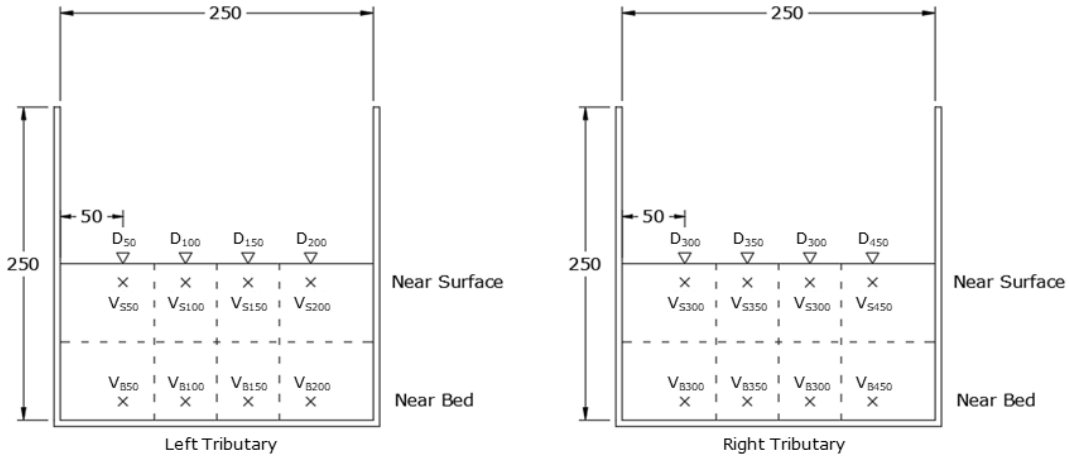


Figure 3.14: Point of velocity measurement for downstream channel

The water depth was determined by measuring the level of water surface and channel bed. The level of water surface measurement may be affected by the small vibration from the pump. To minimise this impact, 3 measurements were taken for the level of water surface and average value was calculated accordingly. Due to incompatibility between the experimental setup and existing commercial point gauges, the water level was measured by a DIY point gauge which was made of a digital vernier calliper (±0.05mm) and wood strip (Figure 3.15). In each experiment run, the head above weir crest on both tributaries was measured with the DIY point gauge.

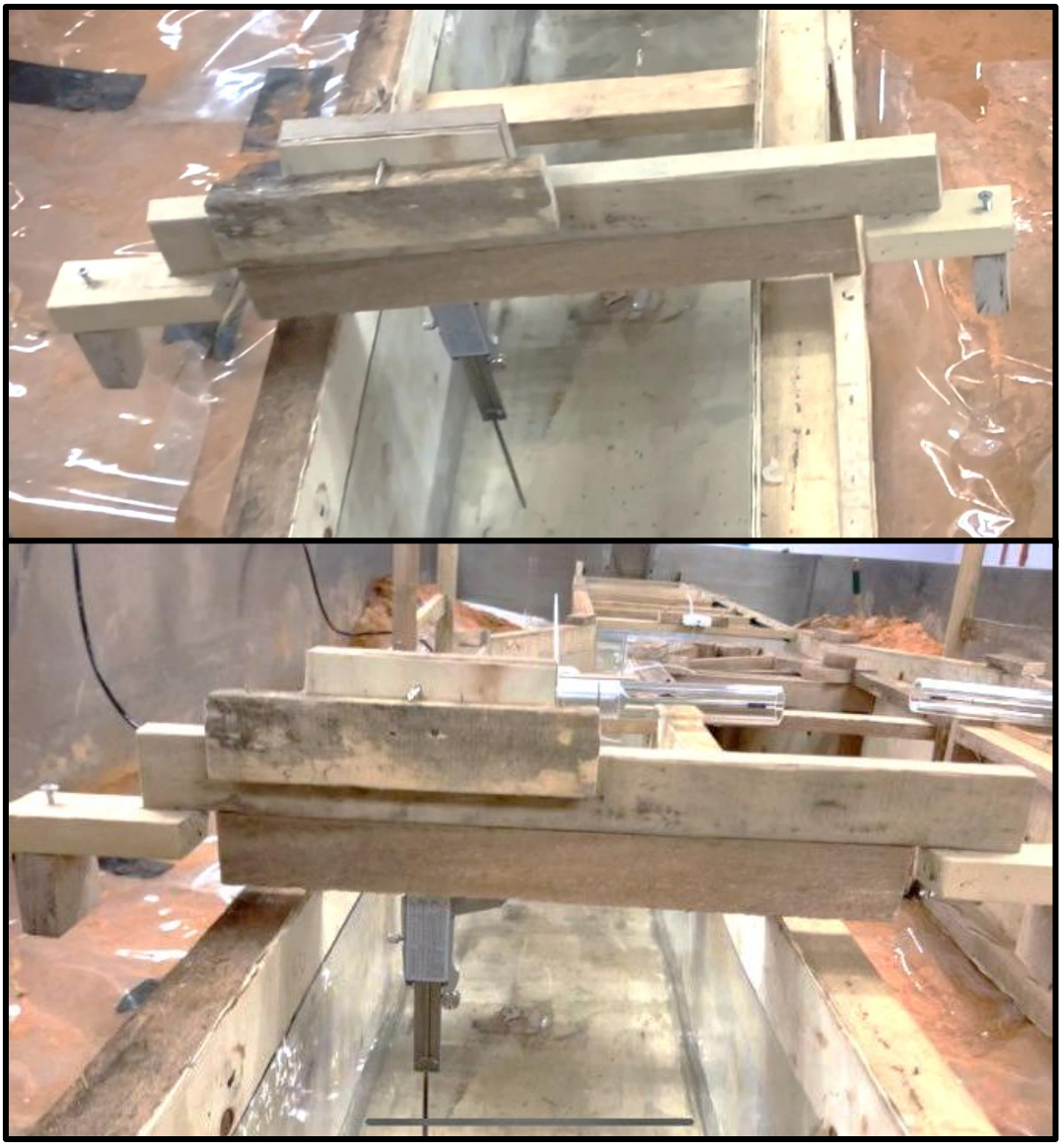


Figure 3.15: Water depth measurement

3.1.3 Data Analysis

Water Depth

For each experiment run, the measured water depth of each location was recorded and illustrated in the format of plan and cross-section view. An example is shown in Figure 3.16 and Figure 3.17 for experimental run 30_03_5050. Figure 3.16 indicates measured water depth at each location; these values are plotted in the cross-section view (Figure 3.17) as dark blue dots (primary vertical axis). The grey dots and lines (secondary vertical axis) indicate the percentage difference in comparing to the lowest value in the same cross-section. As the measured water depth differs by only a few mm in the same cross-section, the grey line provides a better graphical illustration to highlight the relationship between each measured water depth in the same section.

The cross-sections in upstream and downstream channel are implemented with Equation 3.2 and Equation 3.3 respectively for the percentage difference calculation. The equation of percentage difference is shown as Equation 3.2 (Section A, B and C) and Equation 3.3 (Section D, E and F):

$$\Delta D_n = \frac{D_n}{min\{D_{50}, D_{100}, \dots D_{450}\}} \times 100, \% \qquad \text{Equation 3.2}$$

$$\Delta D_n = \frac{D_n}{min\{D_{50}, \dots D_{200}, D_{300} \dots D_{450}\}} \times 100, \% \qquad \text{Equation 3.3}$$

where, ΔD_Δ is percentage difference of water depth at location n

D_n is water depth at location n

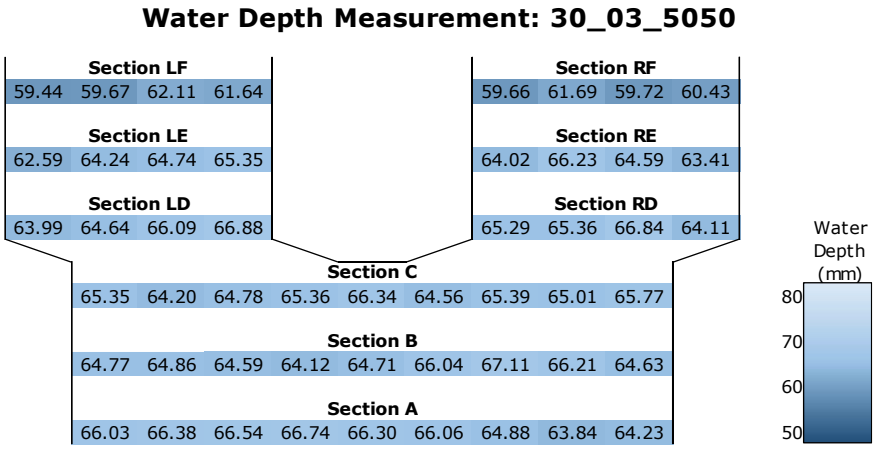


Figure 3.16: Water depth measurement (Plan)

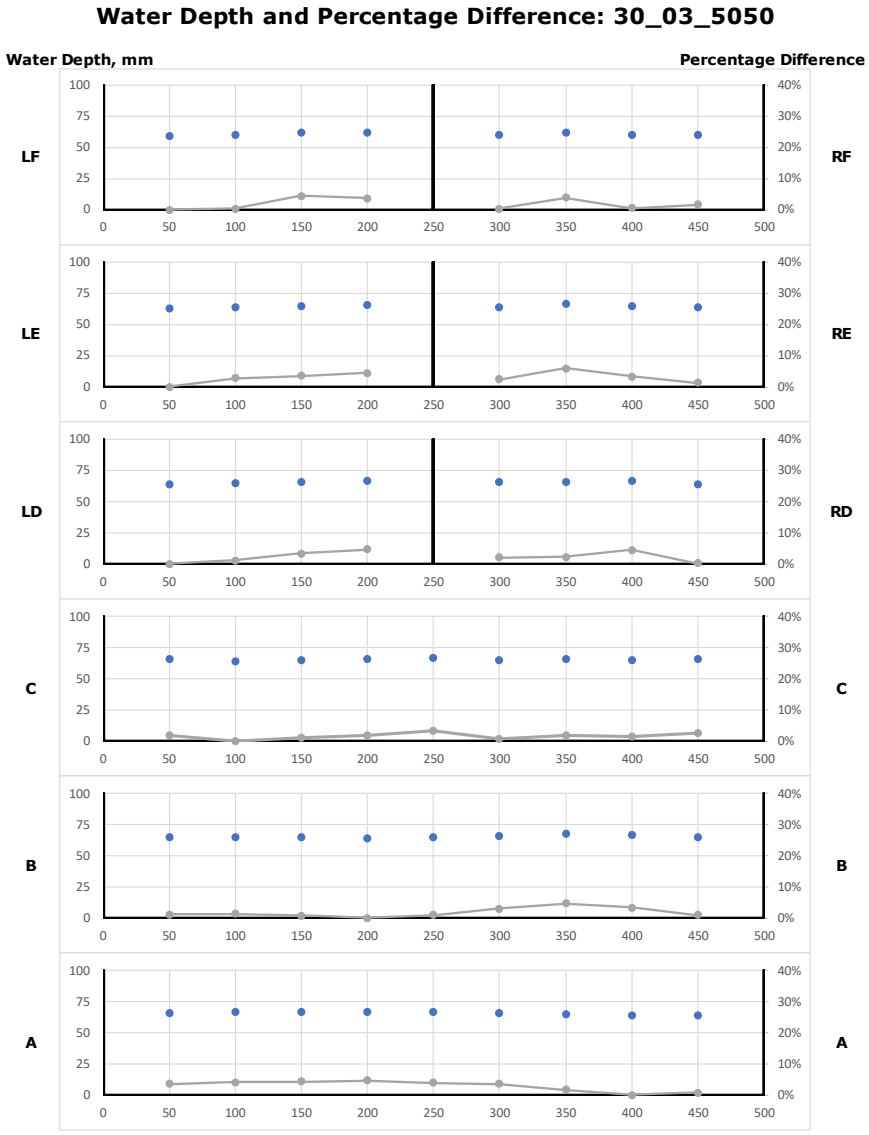


Figure 3.17: Water depth and percentage difference (Section)

Superelevation of Water Depth

Figure 3.18 shows the effect of superelevation of water depth (SeWD). This study proposed a method to quantify the degree of water depth superelevation: each water depth was compared with the lowest water depth within the upstream channels (Section A, B and C). The equation of superelevation of water depth (SeWD) is listed as Equation 3.4:

$$\text{SeWD} = \frac{D_n}{min\begin{Bmatrix} Section\ A: D_{50}, D_{100}, \dots D_{450} \\ Section\ B: D_{50}, D_{100}, \dots D_{450} \\ Section\ C: D_{50}, D_{100}, \dots D_{450} \end{Bmatrix}} \times 100\ , \% \qquad \text{Equation 3.4}$$

where, $SeWD$ is superelevation of water depth

D_n is water depth at location n

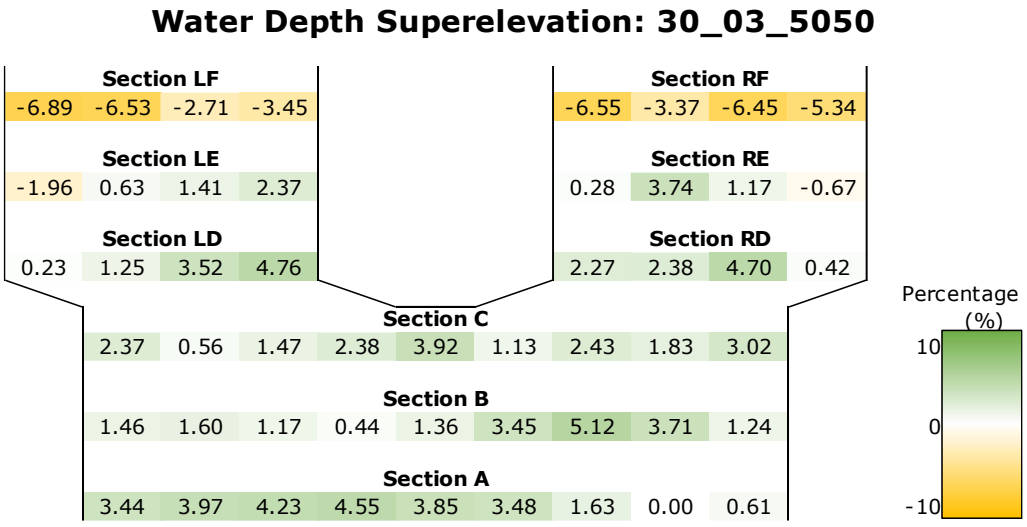


Figure 3.18: Superelevation of water depth (Plan)

Average Water Depth

Average value of water depth in each cross-section is calculated according to the measured water depth in Figure 3.16 and presented in the Figure 3.19. In the figure, upstream channel and right distributary are plotted as orange series and left distributary as dark blue series.

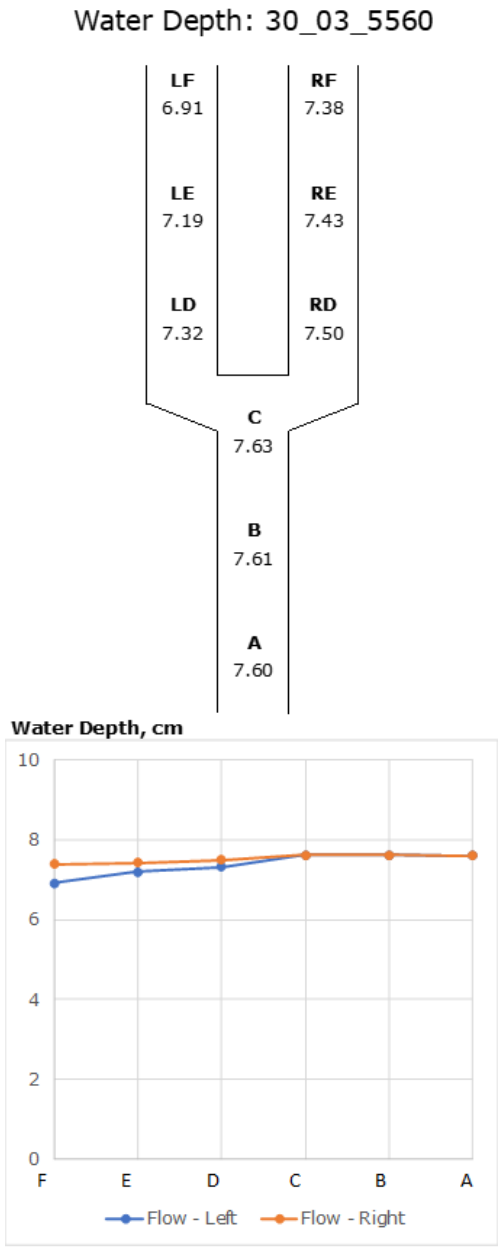


Figure 3.19: Average water depth (Plan and profile)

Water Depth Ratio

Water depth ratio is a comparison of water depth between left and right tributary. For any weir height ratio less than 1.00, water depth in the right tributary is always larger and is always assigned as the denominator in the equation. The equation of water depth ratio is listed as Equation 3.5:

$$D_r = \frac{\min(\overline{D}_L, \overline{D}_R)}{\max(\overline{D}_L, \overline{D}_R)}, dimensionless \quad \text{Equation 3.5}$$

where, D_r is water depth ratio

$\overline{D}_L$ and $\overline{D}_R$ is average water depth of left and right tributary

Water Surface Level

As the experiment was conducted in a flume with slope, the measured water depth was not equal to water surface level. To simplify this issue, the datum (+0.00cm) in this study was referred to the channel bed of the weir, where the weir was installed at the elevation of zero. The water surface level is an average value of the cross-section. The water surface level at each cross-section and at the weir is plotted in Figure 3.20 (plan and profile), the black line in the figure is the channel bed.

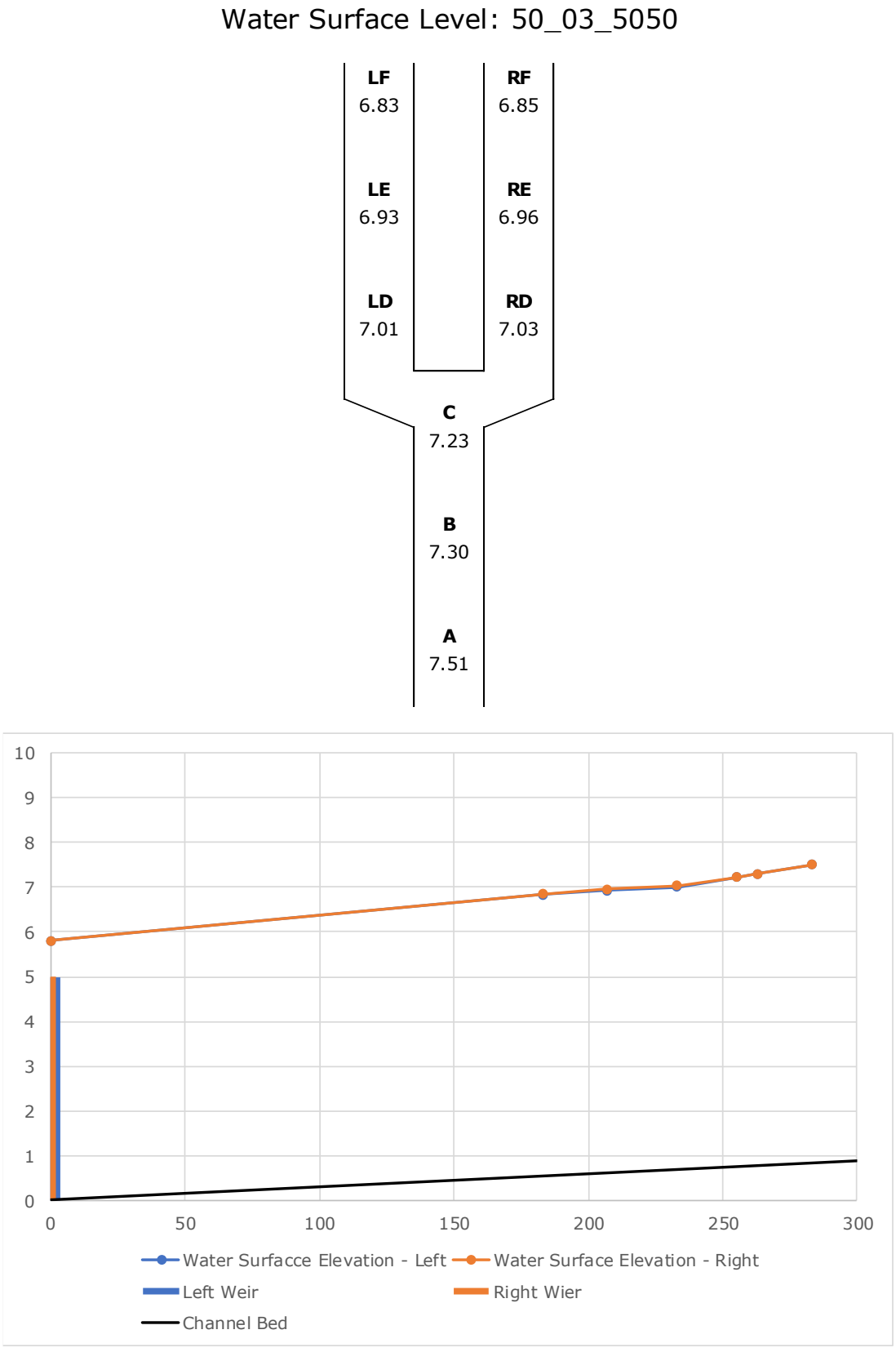


Figure 3.20: Water surface level (Plan and profile)

Flow Velocity

The velocity of each sub-section at near surface (NS) and near bed (NB) is recorded and presented in plan and section (Figure 3.21).

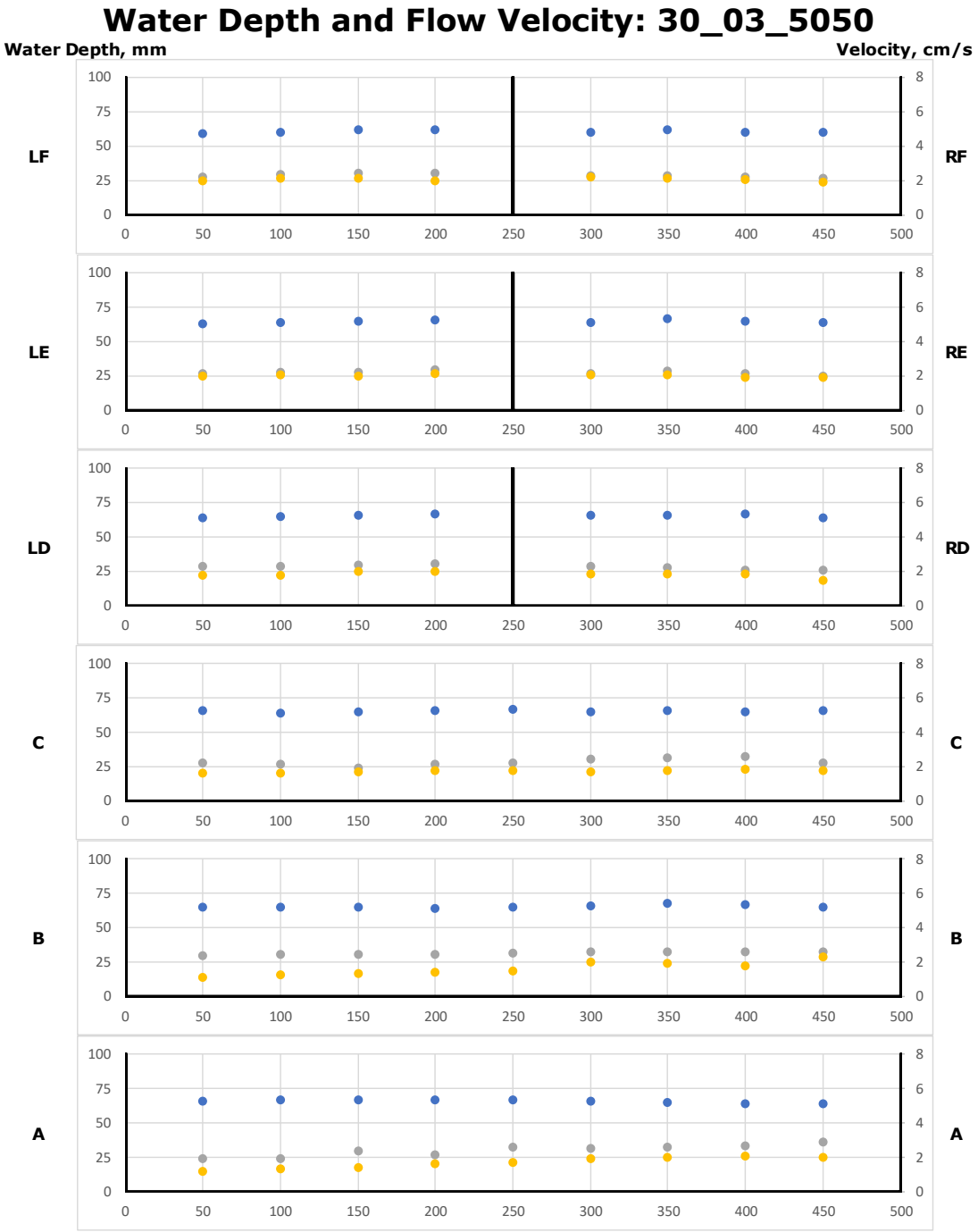


Figure 3.21: Water depth and flow velocity (Section)

Average Flow Velocity

Average flow velocity was calculated by averaging the flow velocity in the same section. The average value is plotted in plan and profile (Figure 3.22). The equation of average flow velocity is listed as Equation 3.6:

$$\bar{V}_\phi = \frac{\sum V_n}{N}, cm/s \qquad \text{Equation 3.6}$$

where, $\bar{V}_\phi$ is average flow velocity of section (applied for NS and NB)

V_n is flow velocity of subsection

N is number of subsections

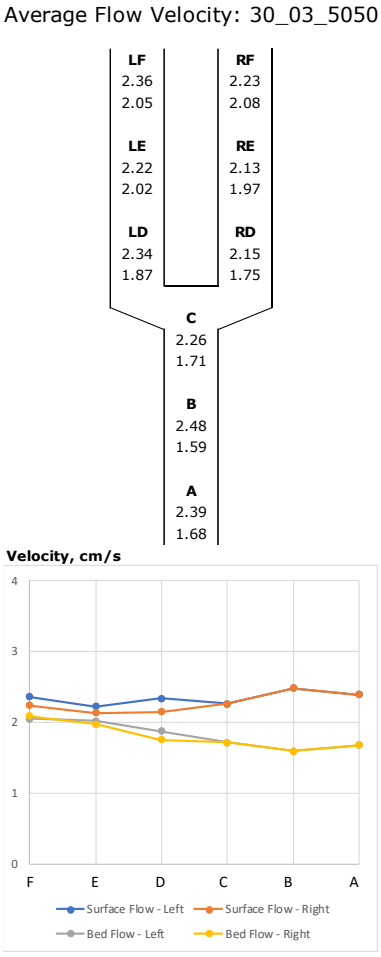


Figure 3.22: Average flow velocity (Plan and profile)

Flow Velocity Ratio

Flow velocity ratio is a comparison of flow velocity between left and right tributary. For any weir height ratio less than 1.00, flow velocity in the left tributary is always larger and is always assigned as the denominator in the equation. The equation of flow velocity ratio is listed as Equation 3.7:

$$V_r = \frac{\min(\bar{V}_L, \bar{V}_R)}{\max(\bar{V}_L, \bar{V}_R)}, dimensionless \quad \text{Equation 3.7}$$

where, V_r is flow velocity ratio

$\bar{V}_L$ and $\bar{V}_R$ is average flow velocity of left and right tributary

Flow Discharge of Subsection

The velocity-area method from the Water Measurement Manual 3rd Edition (2001) is adopted to calculate the flow discharge of a cross-section, each subsection is calculated with its flow velocity, water depth, and subsection width. The equation of flow discharge of subsection is listed as Equation 3.8**:**

$$Q_n = V_n \times \frac{1}{2} D_n \times W_n, cm^3/s \quad \text{Equation 3.8}$$

where, Q_n is flow discharge of subsection

V_n is flow velocity of subsection

D_n is water depth of subsection

W_n is flow width of subsection (refer to Figure 3.14)

Flow Discharge of Section

The flow discharge of each section is the summation of all subsections, where upstream section consists of 18 subsections and each tributary section consists of 8 subsections. The flow discharge of each section is plotted in plan and profile (Figure 3.23). The equation of flow discharge of cross-section is listed as Equation 3.9:

$$Q_{\phi} = \sum Q_{\phi,n} \ , cm^3/s \qquad \text{Equation 3.9}$$

where, Q_{ϕ} is flow discharge of section

$Q_{\phi,n}$ is flow discharge of subsection for section ϕ

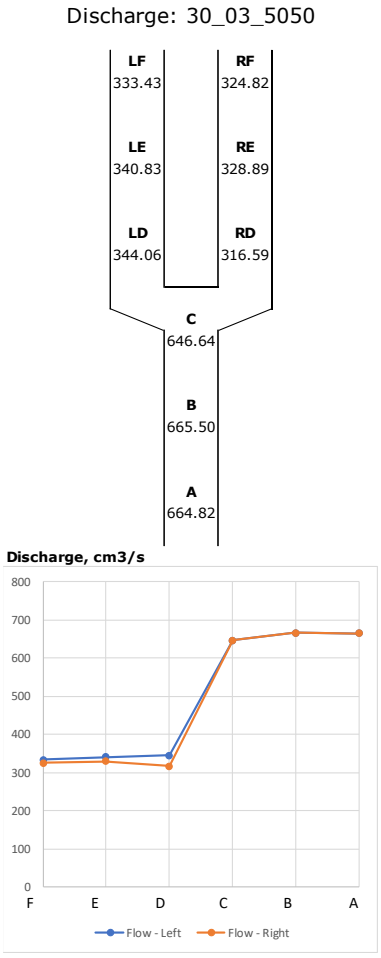


Figure 3.23: Flow discharge of section (Plan and profile)

Discharge Ratio

Discharge ratio is a comparison of flow discharge between left and right tributary. For any weir height ratio less than 1.00, flow discharge in the left tributary is always larger and is always assigned as the denominator in the equation. The equation of discharge ratio is listed as Equation 3.10:

$$Q_r = \frac{Q_R}{Q_L}, dimensionless \qquad \text{Equation 3.10}$$

where, Q_r is discharge ratio

Q_R and $Q_L$is discharge of left and right tributary

Froude Number and Reynolds Number

The characteristics of flow in the experiment were determined by Froude number and Reynolds number. The formula of Froude number and Reynolds number of each section are listed as Equation 3.11 and Equation 3.12:

$$Fr_\phi = \frac{\bar{V}_\phi}{\sqrt{g\bar{D}_\phi}}, dimensionless \qquad \text{Equation 3.11}$$

where, Fr_ϕ is Froude number of section

$\bar{V}_\phi$ is average flow velocity of section

g is gravitational acceleration constant

$\bar{D}_\phi$ is average water depth of section

$$Re_\phi = \frac{\bar{V}_\phi H_\phi}{\nu}, dimensionless$$ Equation 3.12

where, Re_ϕ is Reynolds number of section

$\bar{V}_\phi$ is average flow velocity of section

H_ϕ is wetted perimeter

ν is kinematic viscosity of water

Summary of Calculation

Figure 3.24 and Figure 3.25 show a comprehensive calculation sheet including:

1. Water Depth (Measured, average, and ratio)
2. Flow Velocity (Measured, average, and ratio)
3. Flow Discharge (Sub-section, section, and ratio)
4. Froude Number and Reynolds Number

Downstream

	Subsection Name		L50	L100	L150	L200		R50	R100	R150	R200
	Subsection Width	(mm)	75	50	50	75		75	50	50	75
	A	Velocity	(cm/s)								
	A1	Near Surface Flow		2.22	2.38	2.43	2.42		2.29	2.28	2.23	2.14
	A2	Near Bed Flow		2.01	2.10	2.09	2.00		2.19	2.16	2.03	1.94
Section F	B	Water Depth	(mm)	59.44	59.67	62.11	61.64		59.66	61.69	59.72	60.43
	C	Discharge	(cm3/s)									
	C1	Near Surface Flow		49.38	35.43	37.68	56.05		51.19	35.15	33.36	48.41
	C2	Near Bed Flow		44.85	31.29	32.51	46.23		49.03	33.38	30.31	43.99
	C3	Total Discharge		**94.23**	**66.73**	**70.19**	**102.29**		**100.22**	**68.53**	**63.68**	**92.40**
	A	Velocity	(cm/s)									
	A1	Near Surface Flow		2.15	2.22	2.21	2.31		2.11	2.25	2.15	2.01
	A2	Near Bed Flow		1.95	2.02	2.00	2.11		2.06	2.03	1.91	1.88
Section E	B	Water Depth	(mm)	62.59	64.24	64.74	65.35		64.02	66.23	64.59	63.41
	C	Discharge	(cm3/s)									
	C1	Near Surface Flow		50.53	35.64	35.70	56.71		50.55	37.22	34.67	47.85
	C2	Near Bed Flow		45.65	32.49	32.41	51.69		49.39	33.60	30.87	44.74
	C3	Total Discharge		**96.18**	**68.13**	**68.11**	**108.41**		**99.94**	**70.82**	**65.54**	**92.59**
	A	Velocity	(cm/s)									
	A1	Near Surface Flow		2.26	2.28	2.38	2.42		2.25	2.23	2.07	2.03
	A2	Near Bed Flow		1.77	1.78	1.98	1.95		1.82	1.84	1.87	1.49
Section D	B	Water Depth	(mm)	63.99	64.64	66.09	66.88		65.29	65.36	66.84	64.11
	C	Discharge	(cm3/s)									
	C1	Near Surface Flow		54.32	36.82	39.26	60.76		55.06	36.48	34.57	48.90
	C2	Near Bed Flow		42.55	28.74	32.70	48.90		44.64	30.01	31.17	35.77
	C3	Total Discharge		**96.87**	**65.56**	**71.96**	**109.67**		**99.70**	**66.49**	**65.74**	**84.66**

Figure 3.24: Calculation sheet (Part 1)

Water Depth

Average Water Depth, cm

LF	RF
6.07	6.04

Depth Ratio

RF/LF
0.99

Average Water Depth, cm

LE	RE
6.42	6.46

Depth Ratio

RE/LE
0.99

Average Water Depth, cm

LD	RD
6.54	6.54

Depth Ratio

RD/LD
1.00

Velocity

Average Velocity, cm/s

LF	RF
2.36	2.23
2.05	2.08

Velocity Ratio

RF/LF
0.95
0.99

Average Velocity, cm/s

LE	RE
2.22	2.13
2.02	1.97

Velocity Ratio

RF/LF
0.96
0.98

Average Velocity, cm/s

LD	RD
2.34	2.15
1.87	1.75

Velocity Ratio

RF/LF
0.92
0.94

Discharge

Sum of Discharge, cm3/s

LF	RF	LF+RF
333.4	324.8	658.3

Discharge Ratio

RF/LF
0.97

Sum of Discharge, cm3/s

LE	RE	LE+RE
340.8	328.9	669.7

Discharge Ratio

RE/LE
0.96

Sum of Discharge, cm3/s

LD	RD	LD+RD
344.1	316.6	660.6

Discharge Ratio

RD/LD
0.92

Froude

Froude Number

LF	RF
0.0286	0.0280

Froude Number

LE	RE
0.0267	0.0257

Froude Number

LD	RD
0.0263	0.0243

Reynold

Reynold Number

LF	RF
5782	5656

Reynold Number

LE	RE
5576	5387

Reynold Number

LD	RD
5532	5129

Figure 3.25: Calculation sheet (Part 2)

Head above Weir Crest

The head above weir crest was measured and calculated with the Kindsvater-Carter method to verify the calculated discharge by velocity-area method (Water Measurement Manual 3rd Edition, 2001). The Kindsvater-Carter method discharge equation is listed as Equation 3.13, this equation is simplified for a 250mm width suppressed rectangular sharp-crested weir. Keep in mind that the equation by Kindsvater-Carter method is in imperial units; however, the outcome of the calculation was converted back to metric units for better comparison. Figure 3.26 shows the definition of H and P of sharp-crested weir in the simplified equation.

$$Q_{Weir} = (0.4\frac{H}{P} + 0.322)(0.81721)(H + 0.003)^{1.5}, ft^3/s \quad \text{Equation 3.13}$$

where, Q_{Weir} is flow discharge at weir (Kindsvater-Carter method)

H is head above weir crest

P is weir height (50mm, 55mm & 60mm)

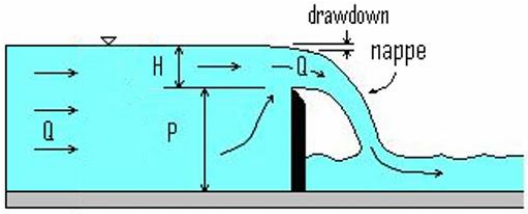


Figure 3.26: Definition of H and P of sharp-crested weir

3.2 Numerical Model

3.2.1 Simulation Setup

In Section 3.1, 50mm was selected as the base height for weir, the height was increased by 5mm to create multiple options of weir. One of the weaknesses of physical modelling is the lack of precision on small dimension during fabrication and experiment stage. Fabrication had a measurement error of 1 to 2mm; 5mm interval ensured that substantial differences could be observed and measured during experiment even if the weir height was fabricated with few mm of error.

To study the impact of different weir height combinations on the hydrodynamic processes of channel bifurcation with smaller interval of weir height, a numerical model was simulated in software named FLOW-3D, a computational fluid dynamic (CFD) software for complex 3-dimensional (3D) fluid dynamic flow simulation.

The geometry of the numerical model was set up identically to the physical model; an example of 3D geometry is shown in Figure 3.27. The three control parameters in numerical simulation were bifurcation angle (Θ), slope (Δ), and weir height (WH). Four different bifurcation angles were selected for this study which were 30°, 40°, 50°, and 60°. Each bifurcation angle was simulated with 0.3%, 0.5%, 0.7%, 0.9% slope. The height of weirs was 50mm, 53mm, 55mm, 57mm, 60mm, 62mm, and 65mm. 2 sets of weir height (50mm and 55mm) were selected as the base weir to investigate the effect of base weir height on the discharge ratio. 8 combinations listed in Table 3.3 were chosen. With consideration of all proposed parameters above, 128 simulations were conducted in this study which are listed in Table 3.4.

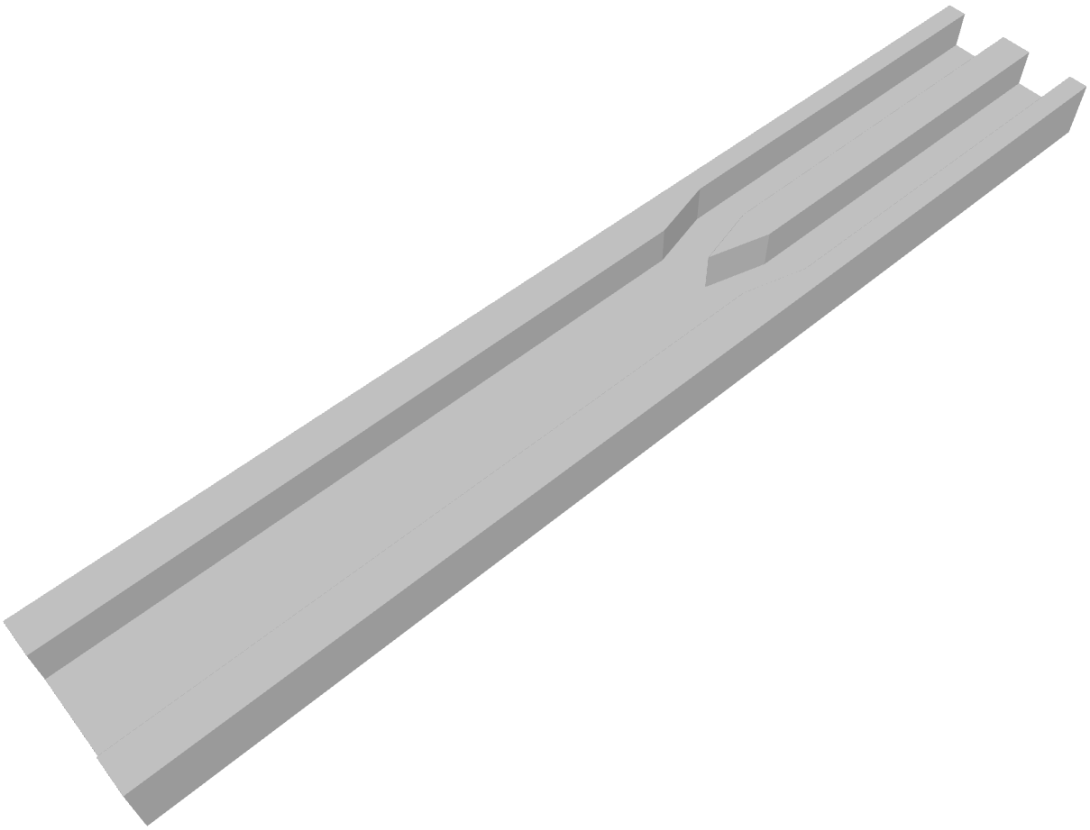


Figure 3.27: Example of 3D Geometry in FLOW-3D

Table 3.3: Weir height combination

Base Weir Height (mm)	Left Weir Height (mm)	Right Weir Height (mm)	Weir Height Ratio
50	50	50	1.000
		53	0.943
		55	0.909
		57	0.877
		60	0.833
55	55	60	0.917
		62	0.887
		65	0.846

Table 3.4: List of experiment runs

Bifurcation Angle (°)	Slope (%)	Left Weir Height (mm)	Right Weir Height (mm)	Weir Height Ratio	Name of Run
30	0.3	50	50	1.000	30_03_5050
			53	0.943	30_03_5053
			55	0.909	30_03_5055
			57	0.877	30_03_5057
			60	0.833	30_03_5060
		55	60	0.917	30_03_5560
			62	0.887	30_03_5562
			65	0.846	30_03_5565
	0.5	50	50	1.000	30_05_5050
			53	0.943	30_05_5053
			55	0.909	30_05_5055
			57	0.877	30_05_5057
			60	0.833	30_05_5060
		55	60	0.917	30_05_5560
			62	0.887	30_05_5562
			65	0.846	30_05_5565
	0.7	50	50	1.000	30_07_5050
			53	0.943	30_07_5053
			55	0.909	30_07_5055
			57	0.877	30_07_5057
			60	0.833	30_07_5060
		55	60	0.917	30_07_5560
			62	0.887	30_07_5562
			65	0.846	30_07_5565
	0.9	50	50	1.000	30_09_5050
			53	0.943	30_09_5053
			55	0.909	30_09_5055
			57	0.877	30_09_5057
			60	0.833	30_09_5060
		55	60	0.917	30_09_5560
			62	0.887	30_09_5562
			65	0.846	30_09_5565

Table 3.4: List of experiment runs [Cont.]

Bifurcation Angle (°)	Slope (%)	Left Weir Height (mm)	Right Weir Height (mm)	Weir Height Ratio	Name of Run
40	0.3	50	50	1.000	40_03_5050
			53	0.943	40_03_5053
			55	0.909	40_03_5055
			57	0.877	40_03_5057
			60	0.833	40_03_5060
		55	60	0.917	40_03_5560
			62	0.887	40_03_5562
			65	0.846	40_03_5565
	0.5	50	50	1.000	40_05_5050
			53	0.943	40_05_5053
			55	0.909	40_05_5055
			57	0.877	40_05_5057
			60	0.833	40_05_5060
		55	60	0.917	40_05_5560
			62	0.887	40_05_5562
			65	0.846	40_05_5565
	0.7	50	50	1.000	40_07_5050
			53	0.943	40_07_5053
			55	0.909	40_07_5055
			57	0.877	40_07_5057
			60	0.833	40_07_5060
		55	60	0.917	40_07_5560
			62	0.887	40_07_5562
			65	0.846	40_07_5565
	0.9	50	50	1.000	40_09_5050
			53	0.943	40_09_5053
			55	0.909	40_09_5055
			57	0.877	40_09_5057
			60	0.833	40_09_5060
		55	60	0.917	40_09_5560
			62	0.887	40_09_5562
			65	0.846	40_09_5565

Table 3.4: List of experiment runs [Cont.]

Bifurcation Angle (°)	Slope (%)	Left Weir Height (mm)	Right Weir Height (mm)	Weir Height Ratio	Name of Run
50	0.3	50	50	1.000	50_03_5050
			53	0.943	50_03_5053
			55	0.909	50_03_5055
			57	0.877	50_03_5057
			60	0.833	50_03_5060
		55	60	0.917	50_03_5560
			62	0.887	50_03_5562
			65	0.846	50_03_5565
	0.5	50	50	1.000	50_05_5050
			53	0.943	50_05_5053
			55	0.909	50_05_5055
			57	0.877	50_05_5057
			60	0.833	50_05_5060
		55	60	0.917	50_05_5560
			62	0.887	50_05_5562
			65	0.846	50_05_5565
	0.7	50	50	1.000	50_07_5050
			53	0.943	50_07_5053
			55	0.909	50_07_5055
			57	0.877	50_07_5057
			60	0.833	50_07_5060
		55	60	0.917	50_07_5560
			62	0.887	50_07_5562
			65	0.846	50_07_5565
	0.9	50	50	1.000	50_09_5050
			53	0.943	50_09_5053
			55	0.909	50_09_5055
			57	0.877	50_09_5057
			60	0.833	50_09_5060
		55	60	0.917	50_09_5560
			62	0.887	50_09_5562
			65	0.846	50_09_5565

Table 3.4: List of experiment runs [Cont.]

Bifurcation Angle (°)	Slope (%)	Left Weir Height (mm)	Right Weir Height (mm)	Weir Height Ratio	Name of Run
60	0.3	50	50	1.000	60_03_5050
			53	0.943	60_03_5053
			55	0.909	60_03_5055
			57	0.877	60_03_5057
			60	0.833	60_03_5060
		55	60	0.917	60_03_5560
			62	0.887	60_03_5562
			65	0.846	60_03_5565
	0.5	50	50	1.000	60_05_5050
			53	0.943	60_05_5053
			55	0.909	60_05_5055
			57	0.877	60_05_5057
			60	0.833	60_05_5060
		55	60	0.917	60_05_5560
			62	0.887	60_05_5562
			65	0.846	60_05_5565
	0.7	50	50	1.000	60_07_5050
			53	0.943	60_07_5053
			55	0.909	60_07_5055
			57	0.877	60_07_5057
			60	0.833	60_07_5060
		55	60	0.917	60_07_5560
			62	0.887	60_07_5562
			65	0.846	60_07_5565
	0.9	50	50	1.000	60_09_5050
			53	0.943	60_09_5053
			55	0.909	60_09_5055
			57	0.877	60_09_5057
			60	0.833	60_09_5060
		55	60	0.917	60_09_5560
			62	0.887	60_09_5562
			65	0.846	60_09_5565

Meshing is one of the important components in numerical modelling. Theoretically, a smaller meshing size generates a higher degree of detail and a more accurate result; however, the consequence is a much longer simulation time. To balance the model accuracy, model representation, and computation time, the mesh size of the x- and y-axes was assigned as 50mm. The vertical axis, which is the z-axis, was separated into 4 layers; counting from the bottom, these were near bed flow, near surface flow below weir, near surface flow above weir, and surface flow. The details of vertical layer are summarised in Table 3.5. The direction of flow and space is illustrated in Figure 3.28. The meshing's size for model setup is illustrated in Figure 3.29.

Table 3.5: Vertical layer's name

Vertical Layer's Name	Size
Near Surface Flow	10mm
Near Surface Flow above Weir	Weir Height different between Left Tributary and Right Tributary
Near Surface Flow below Weir	½ Base Weir Height
Near Bed Flow	½ Base Weir Height

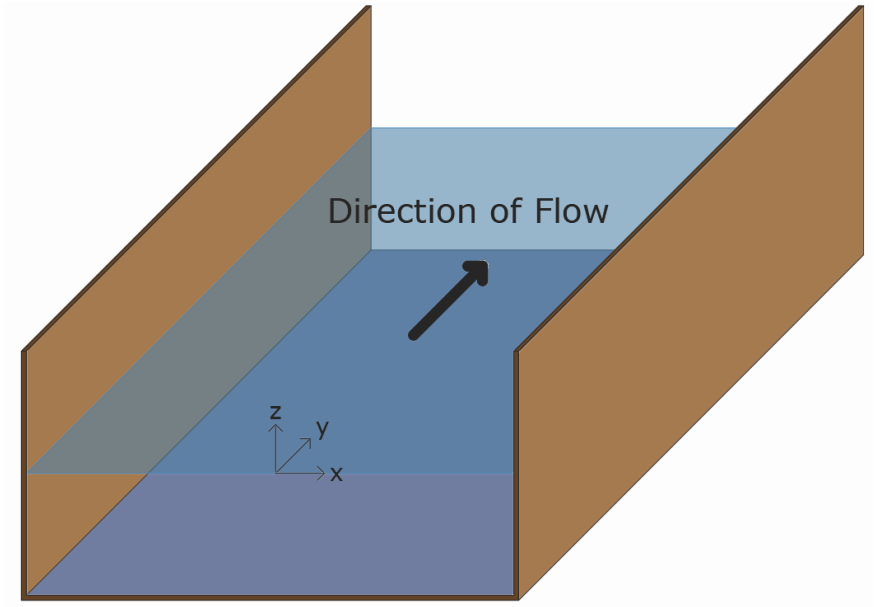


Figure 3.28: The direction of flow and space

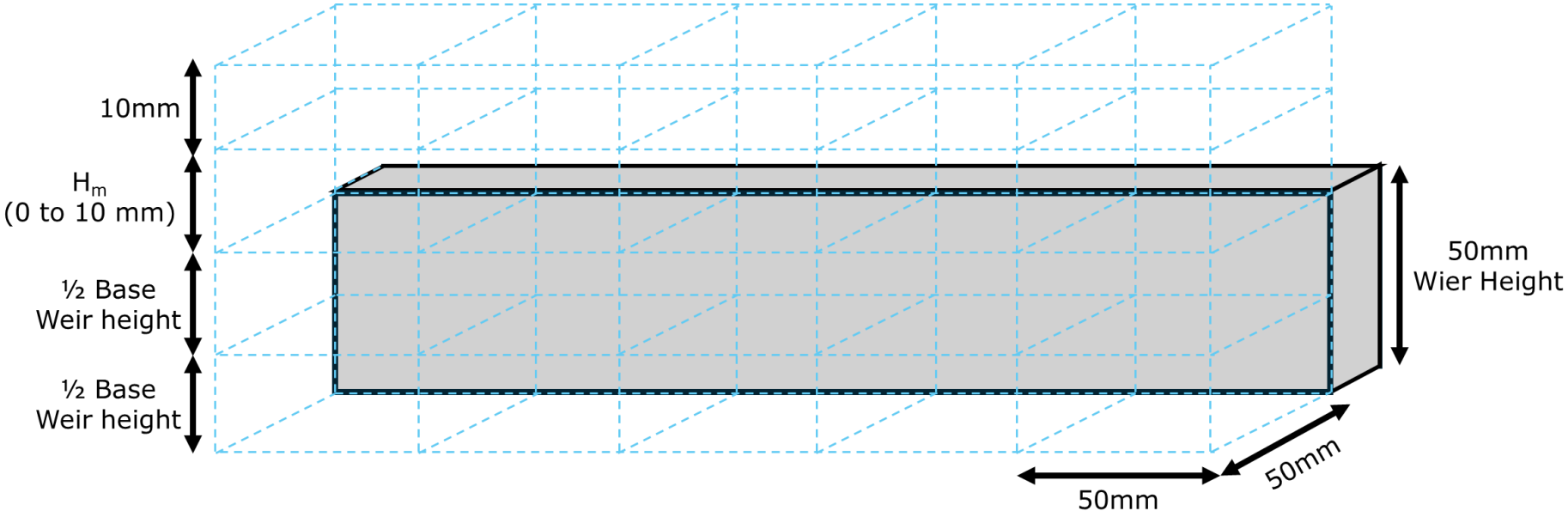


Figure 3.29: Mesh size for model setup

The mesh building mechanism in FLOW-3D is a formation of multiple groups of Cartesian non-uniform rectangular blocks on a x-y global plane. To simulate the slope effect, the channel bed is required to be inclined and overlapped with each contacted mesh block. FLOW-3D provides a method to calculate the actual block properties whenever it interacts with the channel bed; this is named the Fractional Area-Volume Obstacle Representation (FAVOR™). This approach of creating an environment with slope is time-consuming and more computationally intensive. Therefore, this study proposed a method to simulate the slope effect by adjusting the global gravitational acceleration in y and z-axis. By default, the gravitational acceleration is negative g value in z-axis and y-axis is zero. Both axes were adjusted according to Table 3.6, this applied gravitational acceleration to the fluid in both the y- and z-axes to simulate the slope effect.

Table 3.6: Gravitational acceleration constant

Slope, %	Gravitational Acceleration Constant, $m^3/kg\ s^2$	
	Y-axis	Z-axis
0.0	0.000000	-9.810000
0.1	0.009810	-9.809995
0.2	0.019620	-9.809980
0.3	0.029430	-9.809956
0.4	0.039240	-9.809922
0.5	0.049049	-9.809877
0.6	0.058859	-9.809823
0.7	0.068668	-9.809760
0.8	0.078477	-9.809686
0.9	0.088286	-9.809603
1.0	0.098095	-9.809510

The upstream boundary condition was assigned a 1000cm3/s steady-state flow for all simulations. All simulations were run for a 120sec duration with a 0.2sec time step; the results were recorded at 1sec intervals.

3.2.2 Data Analysis

An example of simulation run 30_03_5565 is plotted in Figure 3.30 with discharge and time. In the figure, discharge of left and right tributary was coloured with blue and orange respectively. If the discharge fluctuated excessively, the stencil value of discharge (sQ) will be calculated. The stencil of discharge at time t refers to averaging the discharge over a range of S_n (S_n is set as 9 or 11 in this study). The equation is listed as Equation 3.14:

$$\mathrm{sQ}_n = Average\ [Q_{t=n-5} \cdots Q_{t=n} \cdots Q_{t=n+5}], m^3/s \qquad \text{Equation 3.14}$$

where, sQ_n is stencil value of discharge at t=n

$Q_{t=n}$ is discharge at t=n

Bold lines in Figure 3.30 indicate the average value of discharge of left and right tributary. Discharge ratio is calculated based on the average discharge; it is listed as Equation 3.15:

$$\mathrm{Q}_r = \frac{\bar{Q}_L}{\bar{Q}_R}, dimensionless \qquad \text{Equation 3.15}$$

where, Q_r is discharge ratio

$\bar{Q}_L$ and $\bar{Q}_R$is average discharge of left and right tributary

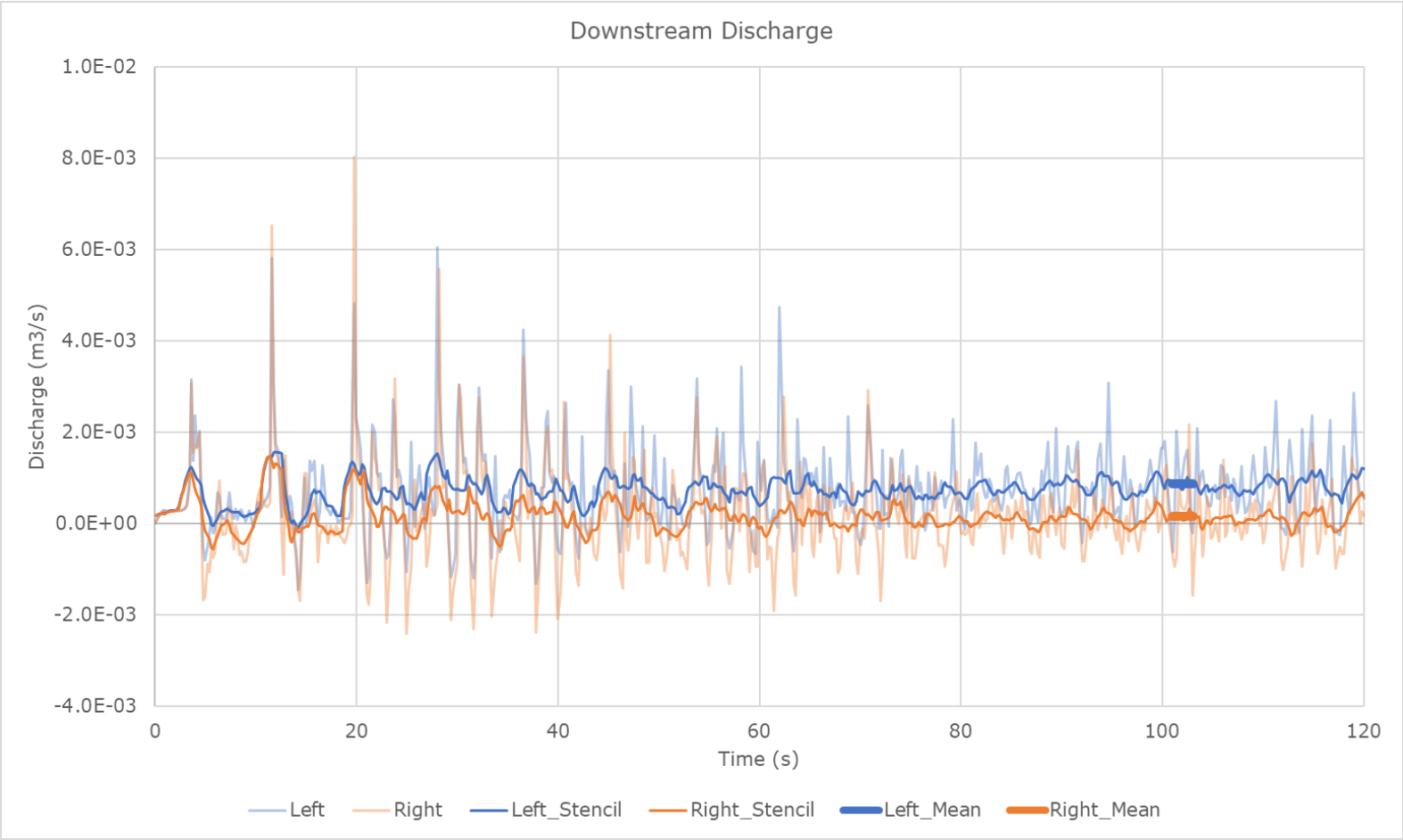


Figure 3.30: Example of recorded discharge in time series

The discharge ratio in each recorded time step in Figure 3.31 was calculated based on discharge of left and right tributary. The time step discharge ratio at time = n is listed as Equation 3.16:

$$\mathrm{Q}_{r,t=n} = \frac{Q_{L,t=n}}{Q_{R,t=n}}, dimensionless \quad \text{Equation 3.16}$$

where, $\mathrm{Q}_{r,t=n}$ is time step discharge ratio when t=n

$Q_{L,t=n}$ and $Q_{R,t=n}$is discharge of left and right tributary when t=n

The time step discharge ratio was calculated by averaging the value over the duration N; it is listed as Equation 3.17:

$$\mathrm{Q}_{r,t} = Average\left[\mathrm{Q}_{r,t=n} \cdots \mathrm{Q}_{r,t=n+N}\right], dimensionless \quad \text{Equation 3.17}$$

where, $\mathrm{Q}_{r,t}$ is time step discharge ratio

$\mathrm{Q}_{r,t=n}$ is time step discharge ratio when t=n

The selected time shall be located at a relatively stable stage without negative time step discharge ratio. To ensure the consistency of calculation and minimise the difference in value between discharge ratio and time step discharge ratio, equal duration with same start time shall be chosen for both ratios. Discharge ratio was selected for further analysis.

All simulation results are recorded in Appendix B1.

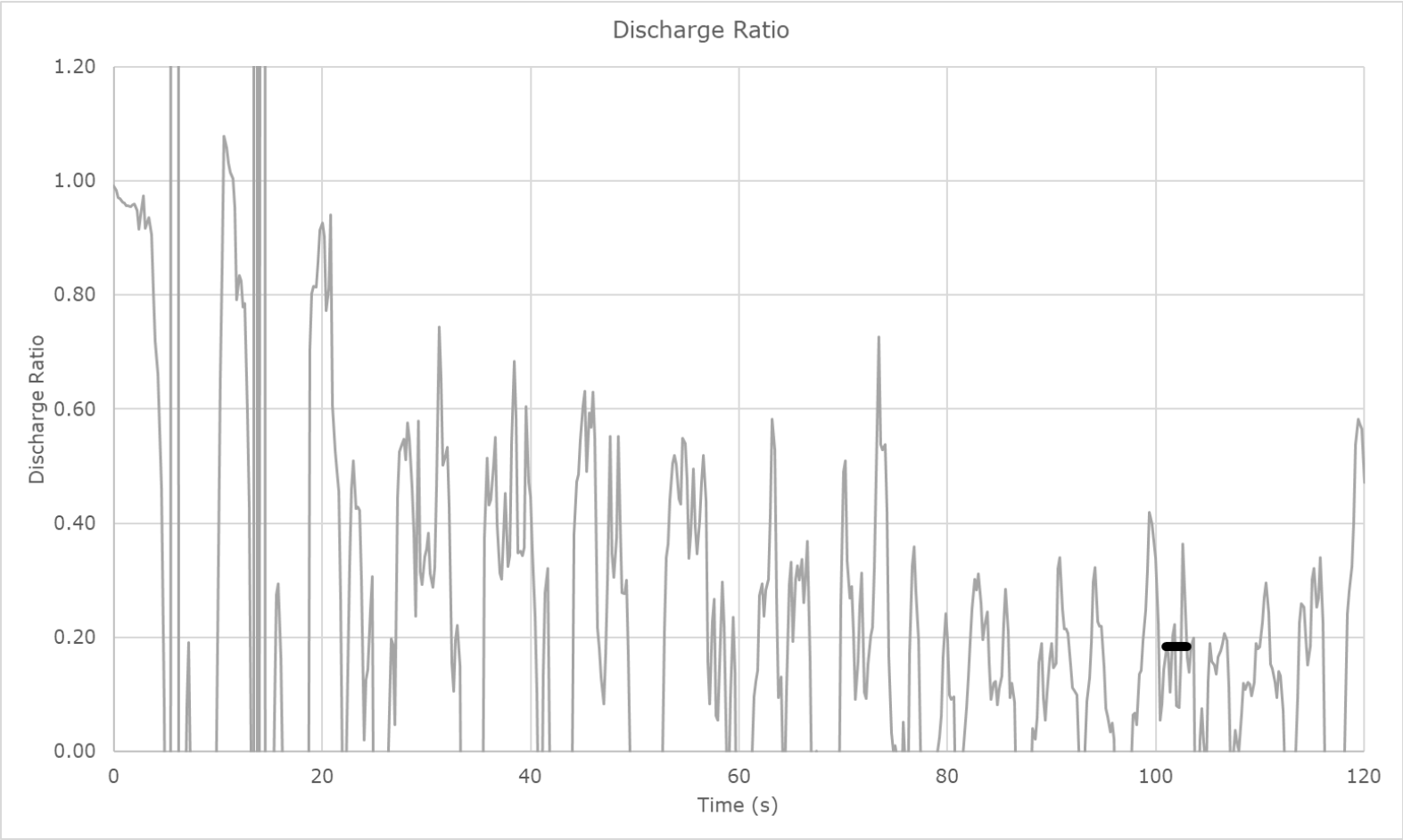


Figure 3.31: Example of discharge ratio in time series

3.3 Machine Learning Model

3.3.1 Machine Learning Model Training Data Set

To train an artificial intelligence model with machine learning ability, data are required to feed the model with a certain degree of pre-processing. The discharge of upstream, bifurcation angle, slope, left weir height, right weir height, and weir height ratio were selected as the variables (labelled as input) in the model, its corresponding results were labelled as output for training. Afterward, a supervised learning model was set up with these organised data.

3 sources of data were applied, which were from physical model result in this study (27 data), numerical model result in this study (128 data), and results from Thomas et al. (2011) (11 data). The feeding data is listed in Appendix C1. As mentioned in Section 3.1, the conducted experiment in this study has the same geometry as Thomas et al. (2011), but the inflow discharge was different. Therefore, the results from Thomas et al. (2011) were pre-processed as part of the feeding data for this machine learning model.

From the feeding data set, 70% of the data were used for training, 15% were reserved as test data, and the remaining 15% were used for validation. The selection of data for training, testing and validation was randomly assigned by the algorithm to prevent order bias and ensure accurate generalisation of the machine learning model.

The feeding data set preparation is illustrated in Figure 3.32.

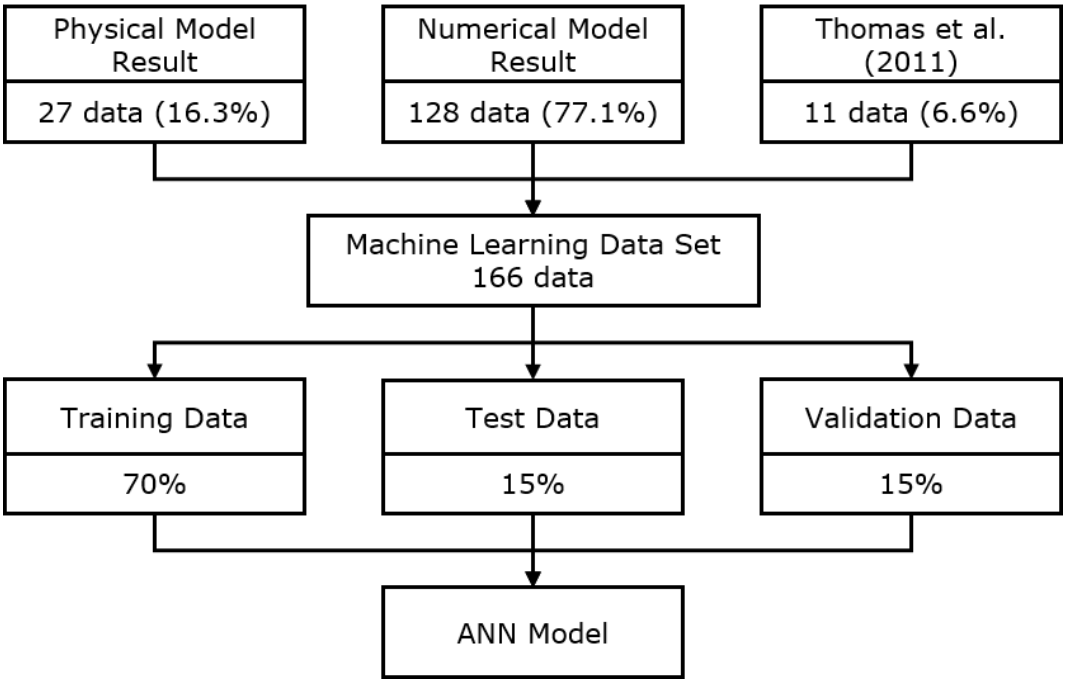


Figure 3.32: Feeding data set preparation for machine learning model

3.3.2 Machine Learning Model Setup

The algorithm of the machine learning model was set up using MATLAB, specifically the Neural Net Fitting module. The computational method of the Neural Net Fitting module was the Artificial Neural Network (ANN), a type of computational method with artificial neurons.

To study the impact of different ANN settings on the prediction accuracy of bifurcation flow, 6 models were set up with different numbers of hidden layers and numbers of neurons in a single hidden layer. The model architecture in this study was classified as single layer model (N10L1, N20L1, and N30L1) and multi-layer model (N10L2, N10L3, and N30L3). Figure 3.33 demonstrates the illustrative definition of hidden layer and number of neurons. The model's setup is listed in Table 3.7.

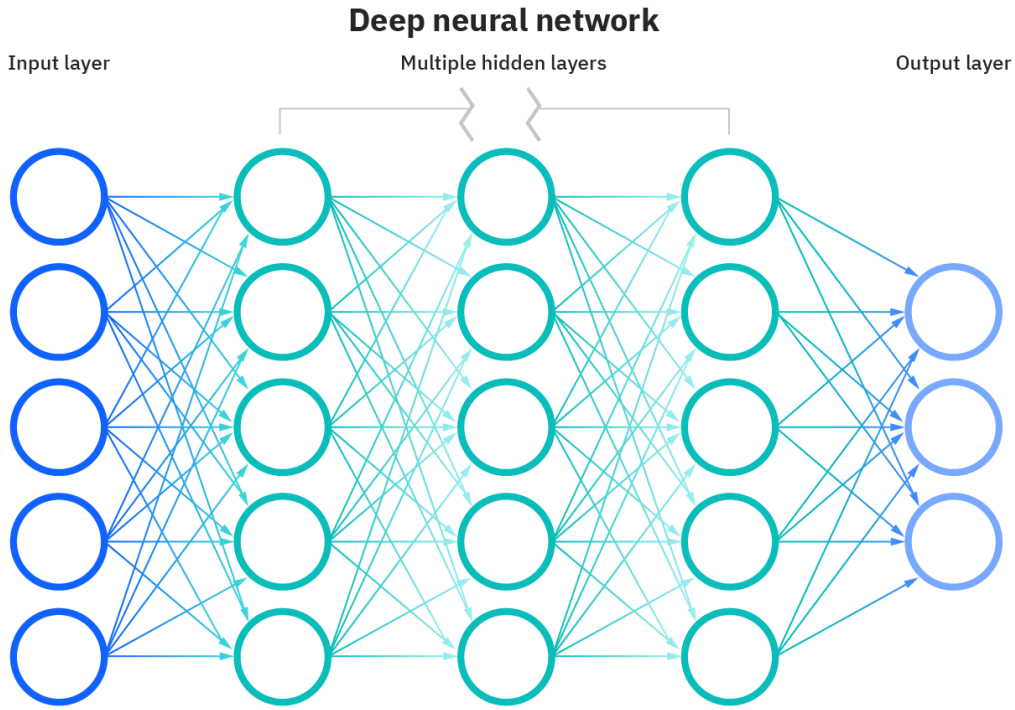


Figure 3.33: Deep neural network (IBM Cloud Education, 2020)

Table 3.7: Machine learning model setup (Neurons and layers)

Model Name	Model Setup	
	Number of Neurons	Number of Hidden Layers
N10L1	10	1
N20L1	20	1
N30L1	30	1
N10L2	10	2
N10L3	10	3
N30L3	30	3

3.3.3 Machine Learning Model Prediction

Different variables were designed to test the 6 trained models for their accuracy of prediction and reliability. Appendix C2 shows the data used for testing the ability of the trained model in prediction.

The number of epochs was used to determine the convergence, overfitting point, and generalisation ability of the machine learning model. The explanation of these determinations is listed below:

- Convergence: Does the model learn generalisable patterns?
- Overfitting point: When does memorisation begin?
- Generalisation ability: How does the model work on new data?

Generally, a short training (few epochs) means insufficient learning. However, there is no standard to limit boundary of sufficient and insufficient learning. Sufficient learning of the model is also affected by other factors such as the total number of feeding data and the type of model. Epochs do not reflect the prediction accuracy of the model. An example is shown in Figure 3.34.

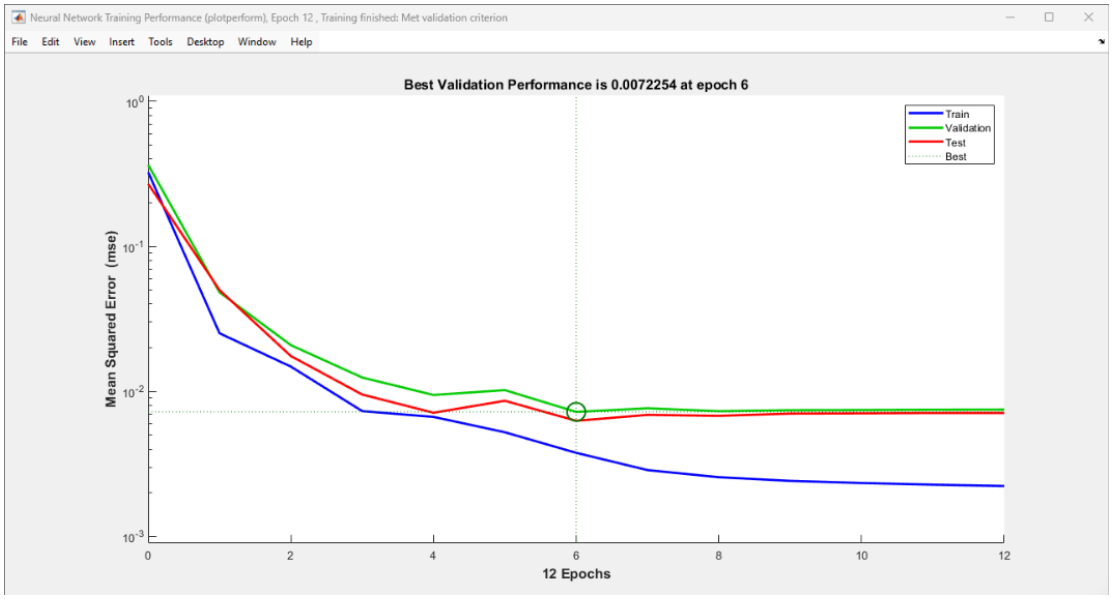


Figure 3.34: Example of epoch in machine learning training

A small training-validation gap indicates a good generalisation of model; in contrast, a large training-validation gap represents overfitting (Figure 3.35). Like epochs, the training-validation gap does not equal to the accuracy of prediction. The formula of training-validation gap is listed as Equation 3.18.

$$Gap = \frac{{R_V}^2 - {R_T}^2}{{R_V}^2} \times 100, \% \qquad \text{Equation 3.18}$$

where, ${R_V}^2$ is validation loss

${R_T}^2$ is training loss

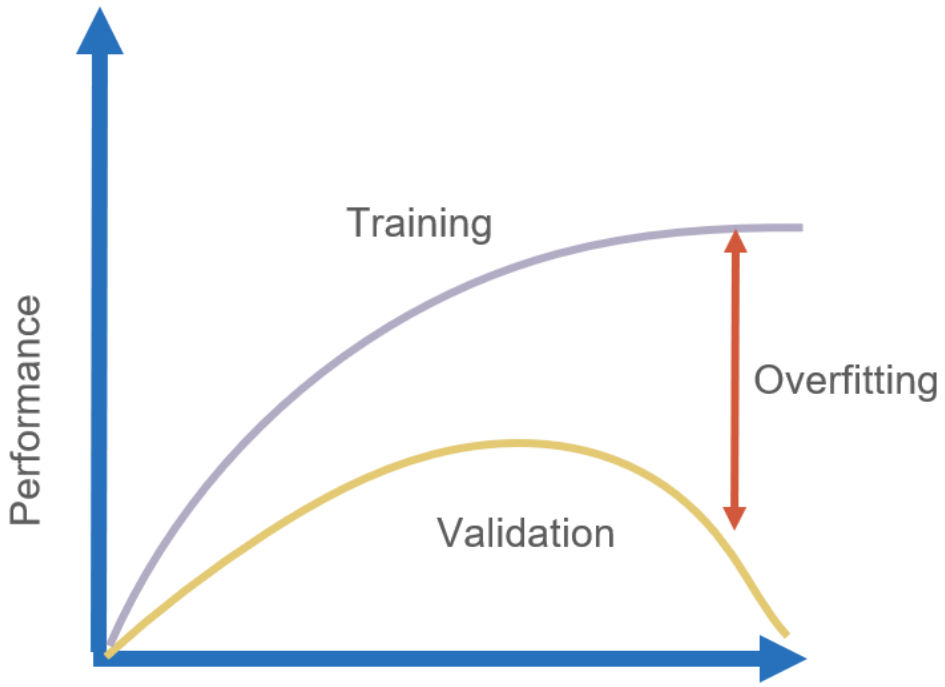


Figure 3.35: Illustration of overfitting of training-validation gap

Chapter 4 Physical Modelling of Channel Bifurcation

4.1 Introduction

In this study, an idealised symmetrical bifurcation channel was designed to demonstrate the hydrodynamic processes of channel bifurcation with interference of downstream hydraulic structures. Multiple dimensionless factors (Ratios) are adopted for further analysis such as water depth ratio (D_r), flow velocity ratio (V_r), and discharge ratio (Q_r). Objectively, an equation is derived for each dimensionless factor according to the experimental parameters, which are bifurcation angle (Θ), slope (Δ), and weir height ratio (WH_r). Furthermore, threshold of weir height ratio is another key finding in this study.

Section 4.2 presents the results from physical modelling with discussion in 6 aspects, which are water depth, water surface level, flow velocity, discharge, head above weir crest, and Froude and Reynolds numbers. All preliminary results are analysed with dimensionless factors in Section 4.3, a summary of findings with an infographic is presented at the end of this section. All findings in Chapter 4 are concluded and summarised in Section 4.4.

4.2 Experiment Test of Channel Bifurcation

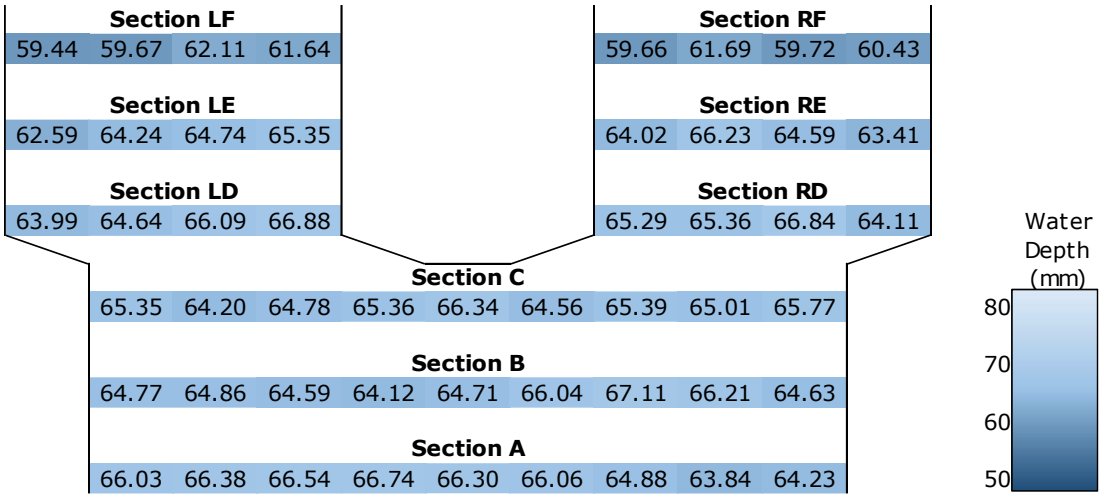
4.2.1 Water Depth

All measured water depth data are recorded in Appendix A1. It is plotted in section view with percentage difference in Appendix A2.

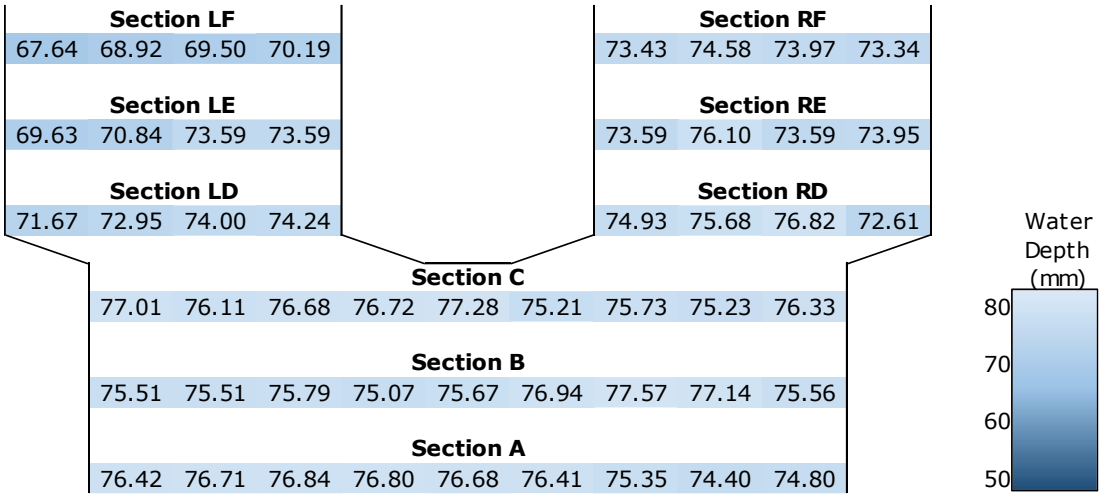
Figure 4.1 shows the measured water depth for 3 experiment runs, which are 30_03_5050, 30_03_5560, and 30_03_5055 respectively. Figure 4.2, Figure 4.3, and Figure 4.4 show the measured water depth in section view with percentage difference for experiment runs 30_03_5050, 30_03_5560, and 30_03_5055.

Percentage difference (secondary vertical axis) shows that the left part of Section A and the right part of Section B are relatively higher than other parts of the section with a peak value of about 5%. This bump phenomenon can be observed through all the experiment runs. Ideally, the water depth at Section A and Section B should be flat or left-right symmetrical. The little bumpy curve shows the potential of uneven channel bed or flow turbulence. Nevertheless, within the same section, the highest water depth is only 2 to 5mm higher than the lowest water depth; this is relatively small compared to the actual water depth, which is at least 50mm. In conclusion, this minor error due to experiment setup is acceptable and can be ignored for further analysis.

Water Depth Measurement: 30_03_5050



Water Depth Measurement: 30_03_5560



Water Depth Measurement: 30_03_5055

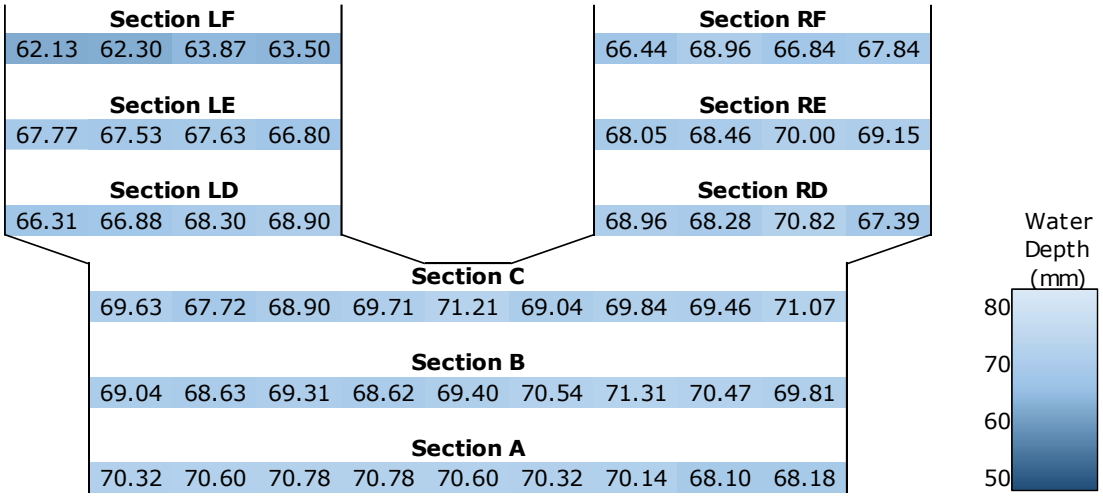


Figure 4.1: Measured water depth

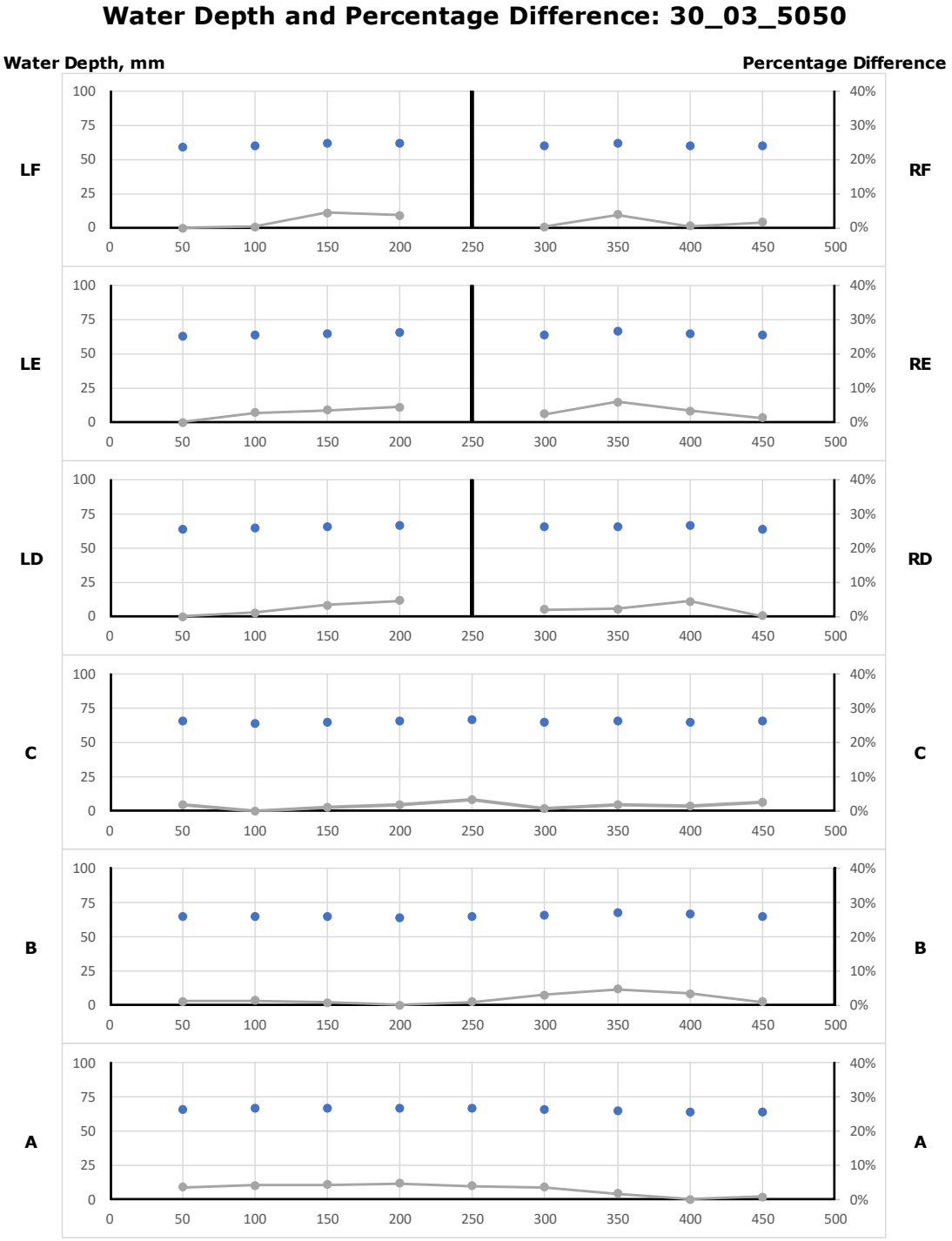


Figure 4.2: Water depth and percentage difference – 30_03_5050

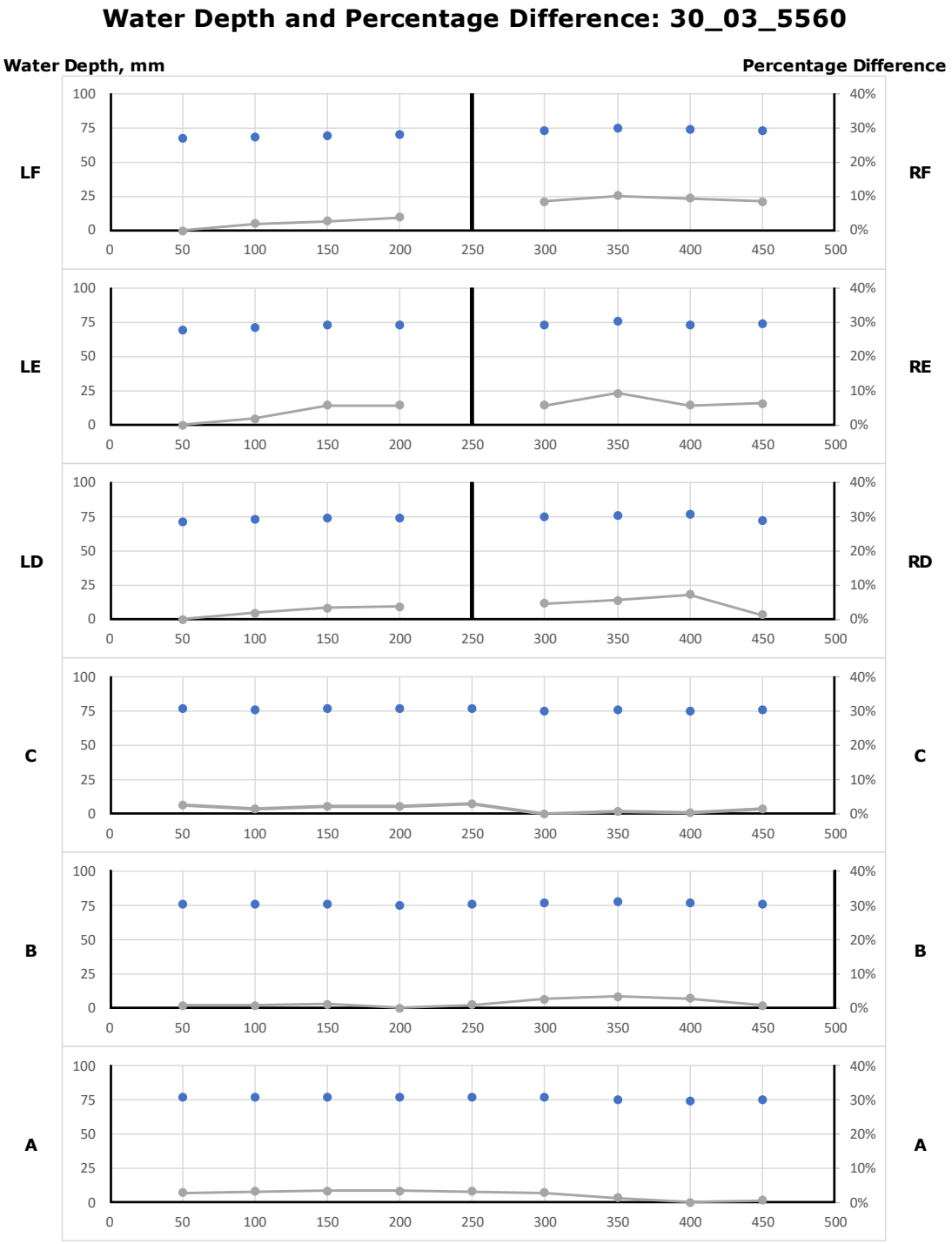


Figure 4.3: Water depth and percentage difference – 30_03_5560

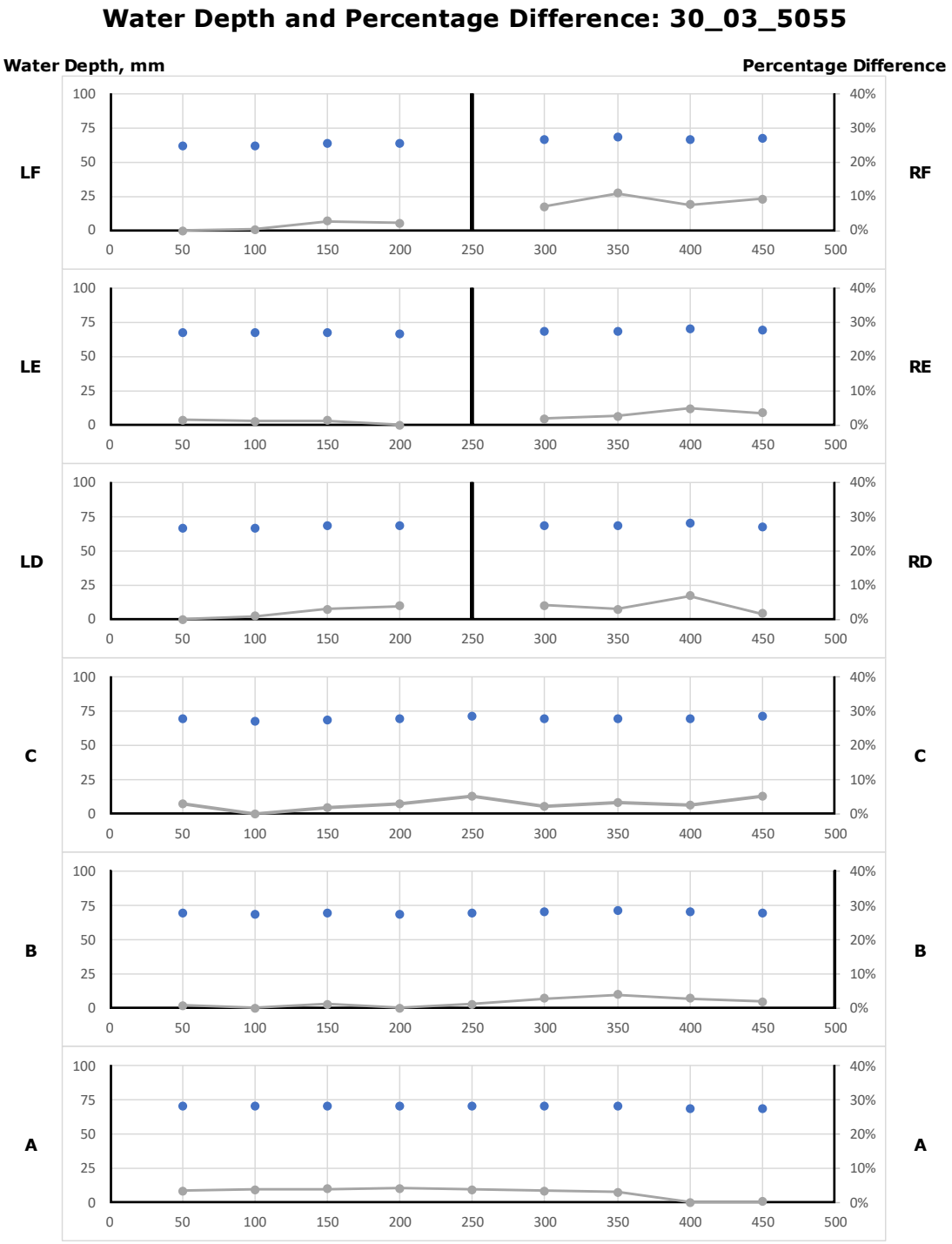


Figure 4.4: Water depth and percentage difference – 30_03_5055

4.2.2 Superelevation of Water Depth

A comparison between each water depth and the lowest value of water depth in the upstream channel is conducted to represent the superelevation of water depth (SeWD) at the bifurcation section. Zero value indicates the lowest water depth. Any water depth higher than upstream lowest water depth is labelled with green colour (positive); any water depth lower than upstream lowest water depth is labelled with orange colour (negative).

Figure 4.5 shows SeWD for experiment runs with different WH_r: 30_03_5050, 30_03_5560, and 30_03_5055. The water depth within the red line is superelevated compared to its surroundings; this can be observed through all the experiment runs. Water depth is superelevated around the bifurcation section near wedge-shaped channel wall and inner bank of tributaries. Symmetrical weir height (WH_r = 1.00) has a more symmetrical pattern of superelevation than asymmetrical weir height; the SeWD propagates further downstream toward the right tributary as the WH_r lowers in value.

Figure 4.6 shows SeWD for experiment runs with different slope: 30_03_5050, 30_05_5050, and 30_07_5050. The SeWD tends to propagate towards downstream as the slope increases with different WH_r.

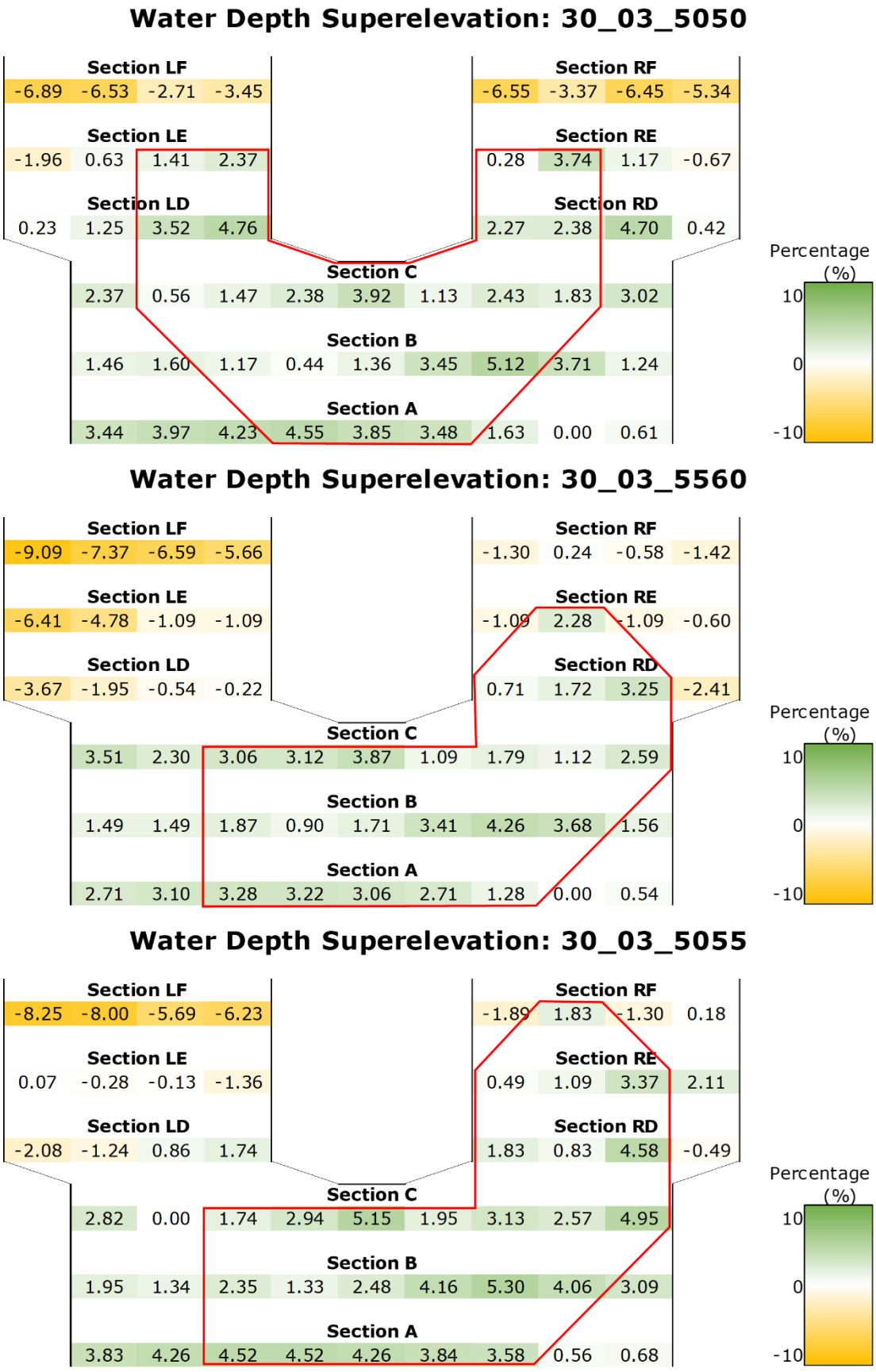


Figure 4.5: Superelevation of water depth (different WH_r)

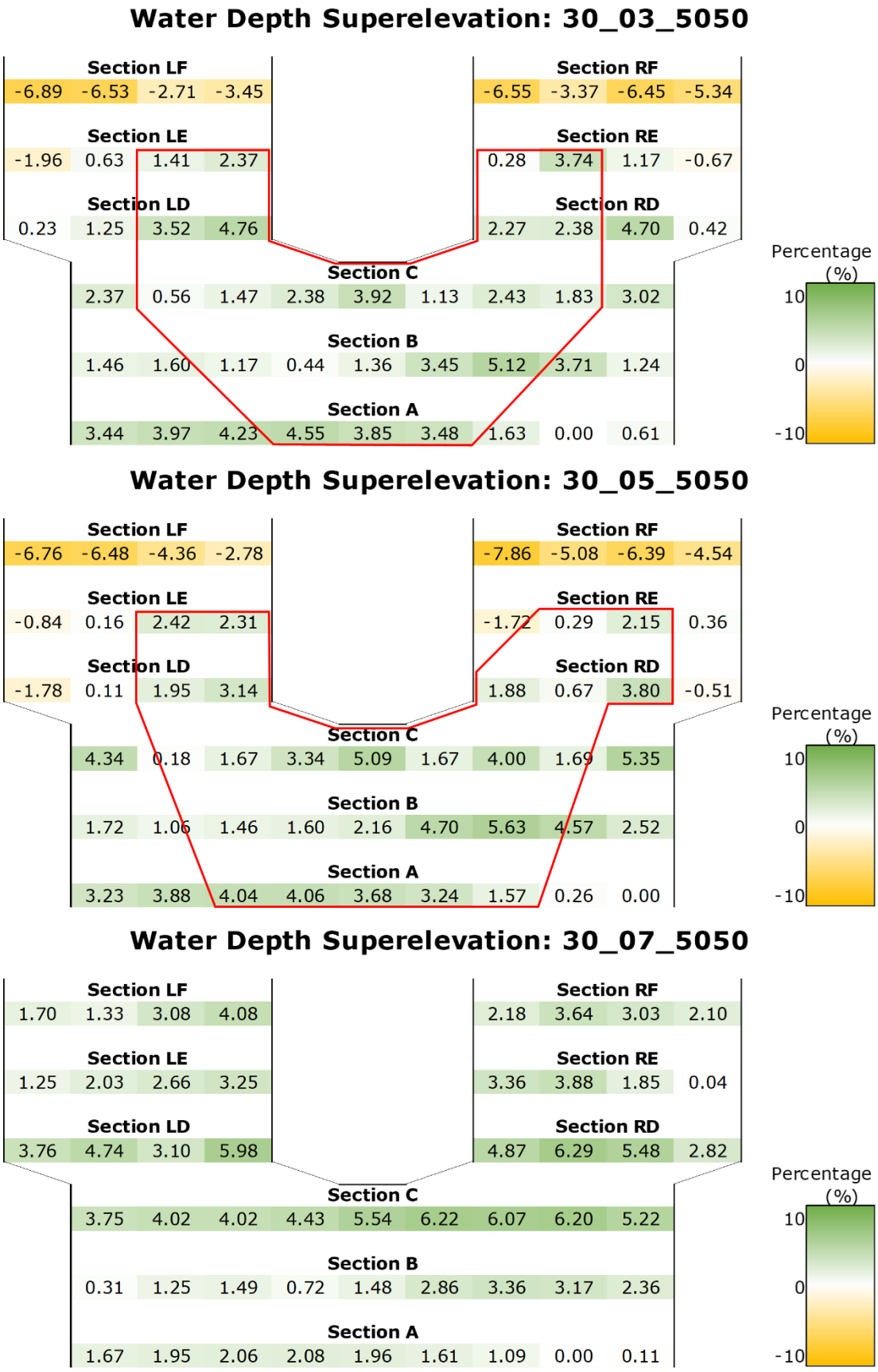


Figure 4.6: Superelevation of water depth (different slope)

According to a study conducted by Thomas et al. (2011), the SeWD is about a 5.0% rise in elevation for equal weir height (WH_L:WH_R = 45:45, WH_r = 1.00); about a 5.9% rise in elevation for unequal weir height (WH_L:WH_R = 35:55, WH_r = 0.636).

In this study, the peak value of SeWD is presented in Figure 4.7 and summarised in Table 4.1. Generally, the peak SeWD ranges from 3.8% to 9.7%. By comparing equal and unequal weir height, no significant trend is observed to indicate that the peak SeWD is affected by WH_r and bifurcation angle. However, an increment of slope generally leads to a larger value in peak SeWD.

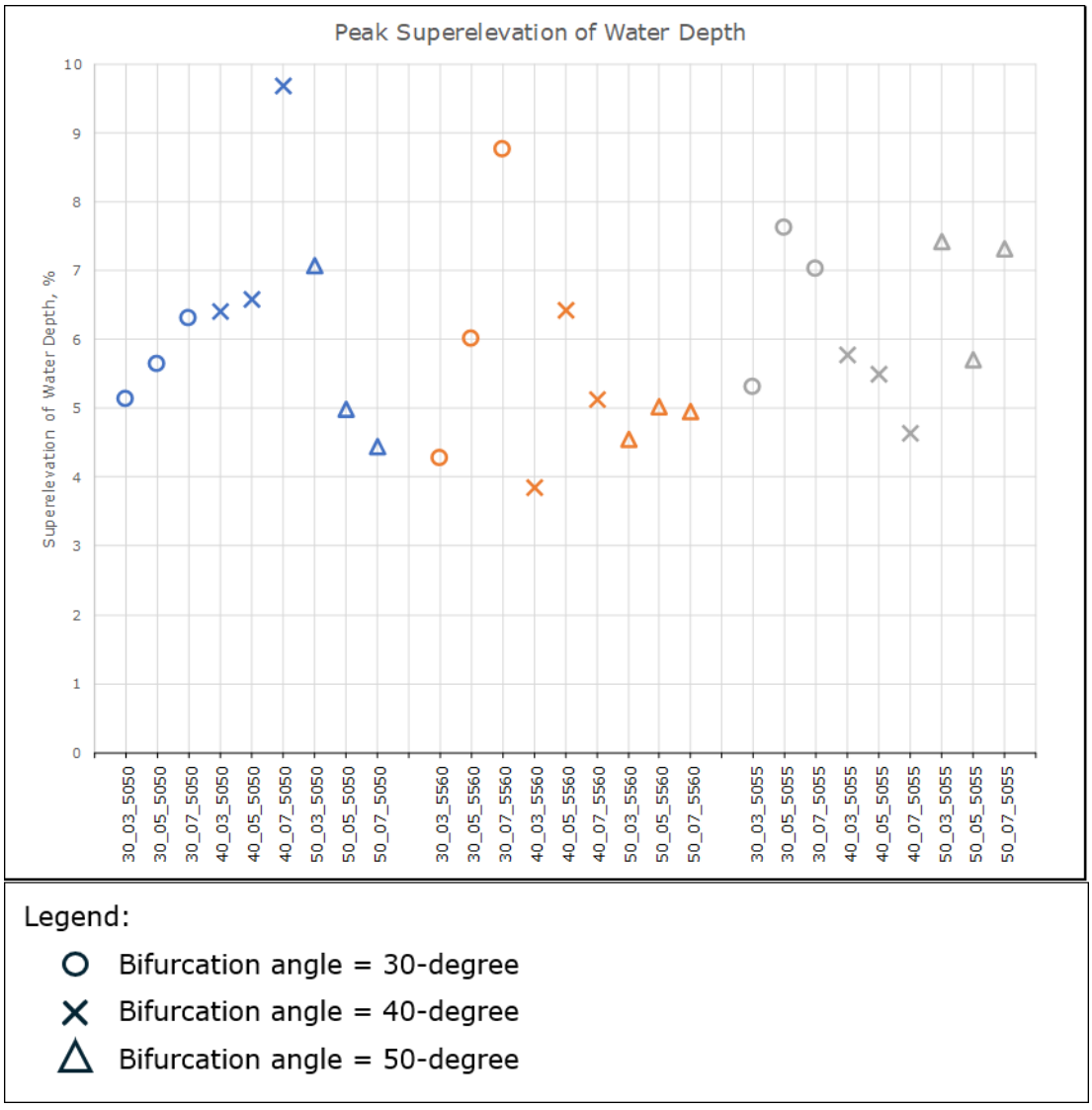


Figure 4.7: Peak superelevation of water depth (Graphical)

Table 4.1: Peak superelevation of water depth (Tabulated)

Weir Height Combination	Experiment Run	Peak Water Depth Superelevation, %
50:50	30_03_5050	5.1
	30_05_5050	5.6
	30_07_5050	6.3
	40_03_5050	6.4
	40_05_5050	6.6
	40_07_5050	9.7
	50_03_5050	7.1
	50_05_5050	5.0
	50_07_5050	4.4
	Average	6.2
55:60	30_03_5560	4.3
	30_05_5560	6.0
	30_07_5560	8.7
	40_03_5560	3.8
	40_05_5560	6.4
	40_07_5560	5.1
	50_03_5560	4.6
	50_05_5560	5.0
	50_07_5560	4.9
	Average	5.4
50:55	30_03_5055	5.3
	30_05_5055	7.6
	30_07_5055	7.0
	40_03_5055	5.8
	40_05_5055	5.5
	40_07_5055	4.6
	50_03_5055	7.4
	50_05_5055	5.7
	50_07_5055	7.3
	Average	6.3

Due to the SeWD, for all types of weir height combinations, the inner bank of both left and right tributaries has higher water depth than their outer banks. Figure 4.8 shows an example of SeWD in section view (50_05_5050); the red arrow indicates the direction of water depth gradient (from high towards low).

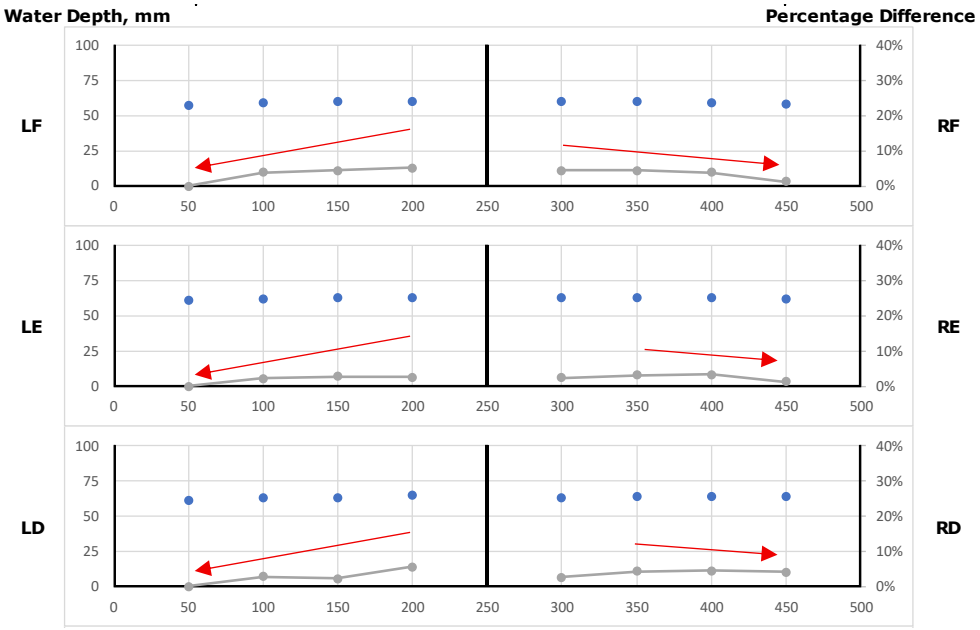


Figure 4.8: Example of superelevation of water depth (50_05_5050)

For the tributaries (Section D, E, and F), the percentage difference in Appendix A2 was calculated according to the whole section without separating it into left and right. To analyse SeWD in the tributaries, the left and right tributaries are separately analysed. Percentage difference was calculated to represent the degree of SeWD. These are summarised and tabulated in Table 4.2, Table 4.3, and Table 4.4 for Section D, E, and F respectively.

For all types of weir height combinations, the percentage difference of the right tributary is always smaller than that of the left tributary, regardless of the bifurcation angle and slope; this is because the setup was not 100% left-right symmetrical. However, the water depth between the left and right tributaries differs only slightly for weir height combination 50:50. Hence, the measured water depth is acceptable. The maximum percentage difference is 4.2% at Section D, where Sections E and F are lower than Section D as both sections are further away from the point of bifurcation. According to percentage difference analysis from Table 4.2, Table 4.3, and Table 4.4, the weir height combination has minor impact on the percentage difference.

Table 4.2: Summary of percentage difference for water depth near inner bank at Section D

Weir Height Combination	Experiment Run	Percentage Difference, %	
		Left Tributary $\left(\frac{D_{200}-D_{50}}{D_{50}}\right)$	Right Tributary $\left(\frac{D_{300}-D_{450}}{D_{450}}\right)$
50:50	30_03_5050	4.5	1.8
	30_05_5050	5.0	2.4
	30_07_5050	2.1	2.0
	40_03_5050	4.3	3.7
	40_05_5050	2.5	1.6
	40_07_5050	6.6	3.2
	50_03_5050	4.8	-1.4
	50_05_5050	5.5	-1.6
	50_07_5050	1.6	0.5
	Average	4.1	1.4
55:60	30_03_5560	3.6	3.2
	30_05_5560	2.1	2.6
	30_07_5560	6.4	2.6
	40_03_5560	5.2	2.6
	40_05_5560	4.4	1.6
	40_07_5560	4.1	3.1
	50_03_5560	5.3	-3.1
	50_05_5560	5.2	-0.2
	50_07_5560	1.8	1.4
	Average	4.2	1.5
50:55	30_03_5055	3.9	2.3
	30_05_5055	3.7	2.5
	30_07_5055	3.6	5.4
	40_03_5055	3.4	4.0
	40_05_5055	7.8	2.0
	40_07_5055	5.4	3.3
	50_03_5055	3.9	-2.6
	50_05_5055	2.0	-1.3
	50_07_5055	2.4	0.0
	Average	4.0	1.7

Table 4.3: Summary of percentage difference for water depth near inner bank at Section E

Weir Height Combination	Experiment Run	Percentage Difference, %	
		Left Tributary $\left(\frac{D_{200}-D_{50}}{D_{50}}\right)$	Right Tributary $\left(\frac{D_{300}-D_{450}}{D_{450}}\right)$
50:50	30_03_5050	4.4	1.0
	30_05_5050	3.2	-2.1
	30_07_5050	2.0	3.3
	40_03_5050	1.0	0.3
	40_05_5050	2.5	-0.7
	40_07_5050	4.2	-0.7
	50_03_5050	2.7	3.5
	50_05_5050	2.5	1.1
	50_07_5050	2.8	0.6
	Average	2.8	0.7
55:60	30_03_5560	5.7	-0.5
	30_05_5560	1.0	-0.9
	30_07_5560	5.6	0.8
	40_03_5560	1.7	0.1
	40_05_5560	4.2	-0.7
	40_07_5560	4.0	-0.2
	50_03_5560	5.3	-0.3
	50_05_5560	2.4	1.3
	50_07_5560	2.9	-1.5
	Average	3.6	-0.2
50:55	30_03_5055	-1.4	-1.6
	30_05_5055	1.8	-1.1
	30_07_5055	3.2	4.8
	40_03_5055	2.3	0.0
	40_05_5055	2.1	-0.3
	40_07_5055	4.3	-0.6
	50_03_5055	4.7	0.5
	50_05_5055	2.7	-1.3
	50_07_5055	3.3	1.2
	Average	2.6	0.2

Table 4.4: Summary of percentage difference for water depth near inner bank at Section F

Weir Height Combination	Experiment Run	Percentage Difference, %	
		Left Tributary $\left(\frac{D_{200}-D_{50}}{D_{50}}\right)$	Right Tributary $\left(\frac{D_{300}-D_{450}}{D_{450}}\right)$
50:50	30_03_5050	3.7	-1.3
	30_05_5050	4.3	-3.5
	30_07_5050	2.3	0.1
	40_03_5050	-0.2	-0.4
	40_05_5050	1.0	-0.4
	40_07_5050	-0.4	1.0
	50_03_5050	4.8	3.7
	50_05_5050	5.2	3.1
	50_07_5050	5.3	3.6
	Average	2.9	0.7
55:60	30_03_5560	3.8	0.1
	30_05_5560	3.3	-2.8
	30_07_5560	3.7	-0.9
	40_03_5560	0.7	-0.8
	40_05_5560	1.0	-1.0
	40_07_5560	-0.5	-0.5
	50_03_5560	3.8	3.3
	50_05_5560	4.6	3.5
	50_07_5560	4.7	3.0
	Average	2.8	0.4
50:55	30_03_5055	2.2	-2.1
	30_05_5055	3.7	-2.4
	30_07_5055	1.9	1.2
	40_03_5055	-0.5	-0.1
	40_05_5055	0.2	-1.4
	40_07_5055	-0.6	0.0
	50_03_5055	4.8	4.2
	50_05_5055	6.0	3.4
	50_07_5055	5.3	4.2
	Average	2.6	0.8

4.2.3 Average Water Depth

The measured water depth data in each cross-section are averaged and summarised in Table 4.5. In Appendix A4, plan and profile of average water depth are plotted accordingly, an example is presented in Figure 4.9.

In Figure 4.9, the average water depth is reduced when slope is increased. To study this relationship, the reduction of average water depth between each slope is calculated and listed in Table 4.6, for example: average water depth of 30_05_5050 minus average water depth of 30_03_5050 is 0.28 (cell is highlighted with light green). Red cells indicate the possibility of an outlier in the data, where a decrement of average water depth is observed when slope is increased.

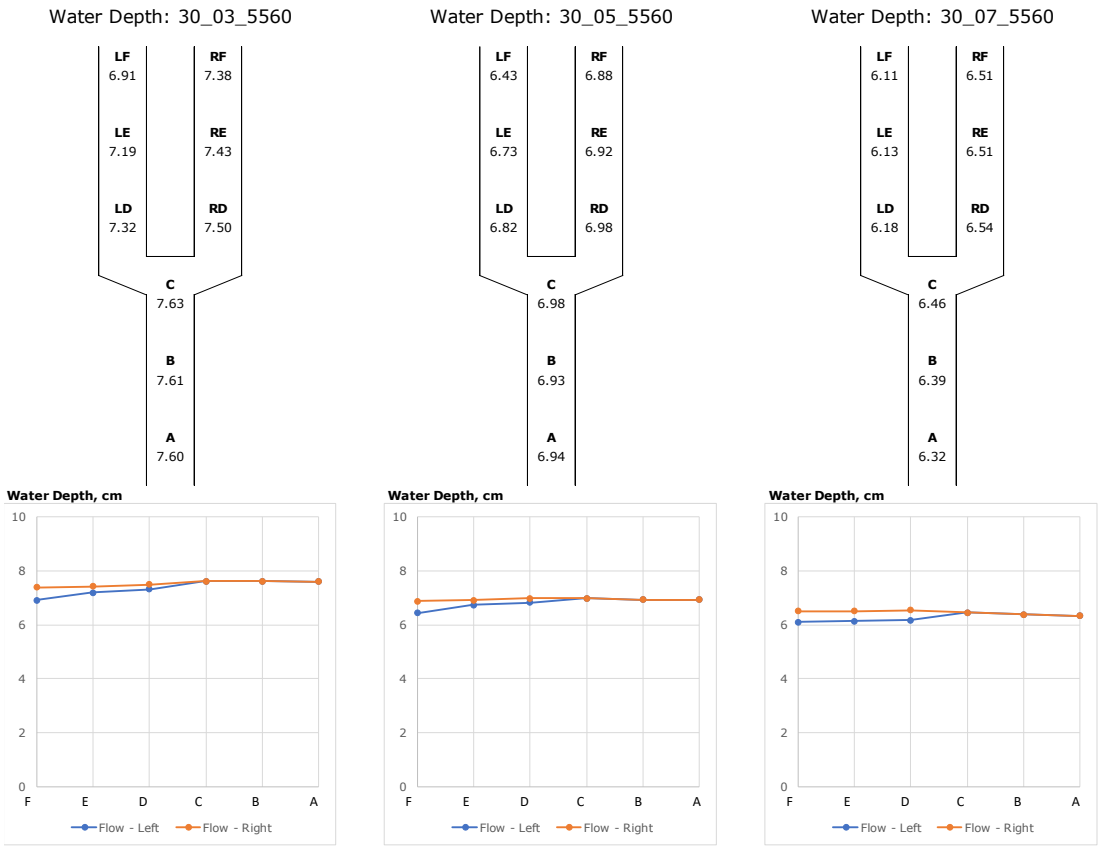


Figure 4.9: Plan and profile of average water depth (different slope with 30°bifurcation angle and WH_r)

Table 4.5: Summary of average water depth

Experiment Run	Average Water Depth, cm (Left Tributary)			Average Water Depth, cm (Right Tributary)			Average Water Depth, cm (Upstream)		
	F	E	D	F	E	D	C	B	A
30_03_5050	6.07	6.42	6.54	6.04	6.46	6.54	6.52	6.52	6.57
30_05_5050	5.80	6.17	6.16	5.74	6.12	6.20	6.29	6.28	6.27
30_07_5050	5.56	5.54	5.66	5.57	5.54	5.68	5.69	5.52	5.49
40_03_5050	6.29	6.24	6.25	6.26	6.25	6.31	6.27	6.31	6.26
40_05_5050	5.93	5.84	5.92	5.93	5.89	5.96	5.91	5.91	5.94
40_07_5050	5.85	5.72	5.64	5.88	5.75	5.74	5.69	5.61	5.63
50_03_5050	6.29	6.31	6.31	6.30	6.34	6.33	6.46	6.51	6.66
50_05_5050	5.91	6.21	6.28	5.92	6.26	6.35	6.34	6.43	6.43
50_07_5050	5.71	5.76	6.02	5.68	5.78	5.97	6.10	6.19	6.09
30_03_5560	6.91	7.19	7.32	7.38	7.43	7.50	7.63	7.61	7.60
30_05_5560	6.43	6.73	6.82	6.88	6.92	6.98	6.98	6.93	6.94
30_07_5560	6.11	6.13	6.18	6.51	6.51	6.54	6.46	6.39	6.32
40_03_5560	7.05	7.02	7.02	7.55	7.48	7.63	7.74	7.77	7.76
40_05_5560	6.72	6.65	6.79	6.96	6.95	7.05	7.03	7.10	7.01
40_07_5560	6.61	6.50	6.50	6.92	6.83	6.83	6.85	6.90	6.91
50_03_5560	7.05	7.02	7.02	7.55	7.48	7.63	7.74	7.77	7.76
50_05_5560	6.41	6.85	6.92	7.28	7.40	7.41	7.40	7.43	7.34
50_07_5560	6.27	6.62	6.63	6.97	6.93	6.88	6.89	6.89	6.80
30_03_5055	6.30	6.74	6.76	6.75	6.89	6.89	6.96	6.97	7.00
30_05_5055	5.88	6.38	6.38	6.43	6.52	6.59	6.54	6.43	6.44
30_07_5055	5.40	5.52	5.52	5.90	5.88	5.97	5.92	5.99	5.87
40_03_5055	6.50	6.43	6.47	7.00	6.97	7.11	7.07	7.04	7.04
40_05_5055	6.22	6.15	6.11	6.49	6.43	6.59	6.56	6.57	6.55
40_07_5055	5.94	5.92	5.86	6.29	6.21	6.26	6.30	6.34	6.38
50_03_5055	6.23	6.54	6.64	6.82	6.86	6.84	6.91	6.97	6.95
50_05_5055	6.10	6.39	6.52	6.76	6.93	6.88	6.97	6.95	6.91
50_07_5055	5.47	5.83	5.76	6.15	6.09	6.04	5.92	5.89	5.92

Table 4.6: Reduction of average water depth by slope

Experiment Run	Average Water Depth, cm (Left Tributary)			Average Water Depth, cm (Right Tributary)			Average Water Depth, cm (Upstream)		
	F	E	D	F	E	D	C	B	A
30_03_5050	-	-	-	-	-	-	-	-	-
30_05_5050	0.28	0.25	0.38	0.29	0.33	0.34	0.23	0.24	0.30
30_07_5050	0.24	0.63	0.50	0.18	0.58	0.51	0.60	0.76	0.78
40_03_5050	-	-	-	-	-	-	-	-	-
40_05_5050	0.36	0.40	0.34	0.33	0.36	0.35	0.36	0.40	0.32
40_07_5050	0.08	0.12	0.28	0.06	0.15	0.23	0.23	0.30	0.31
50_03_5050	-	-	-	-	-	-	-	-	-
50_05_5050	0.37	0.09	0.03	0.38	0.08	-0.03	0.13	0.08	0.23
50_07_5050	0.20	0.46	0.26	0.24	0.47	0.39	0.23	0.23	0.34
30_03_5560	-	-	-	-	-	-	-	-	-
30_05_5560	0.47	0.46	0.50	0.51	0.51	0.52	0.65	0.68	0.67
30_07_5560	0.33	0.60	0.64	0.36	0.40	0.44	0.52	0.54	0.62
40_03_5560	-	-	-	-	-	-	-	-	-
40_05_5560	0.33	0.37	0.24	0.59	0.53	0.58	0.71	0.68	0.74
40_07_5560	0.11	0.14	0.28	0.04	0.12	0.23	0.19	0.20	0.10
50_03_5560	-	-	-	-	-	-	-	-	-
50_05_5560	0.63	0.16	0.10	0.26	0.08	0.22	0.35	0.34	0.41
50_07_5560	0.15	0.23	0.29	0.31	0.47	0.53	0.51	0.54	0.54
30_03_5055	-	-	-	-	-	-	-	-	-
30_05_5055	0.41	0.37	0.38	0.32	0.37	0.30	0.42	0.54	0.56
30_07_5055	0.48	0.86	0.86	0.53	0.64	0.62	0.62	0.44	0.57
40_03_5055	-	-	-	-	-	-	-	-	-
40_05_5055	0.29	0.28	0.36	0.51	0.54	0.52	0.51	0.47	0.49
40_07_5055	0.28	0.23	0.24	0.20	0.22	0.33	0.26	0.23	0.17
50_03_5055	-	-	-	-	-	-	-	-	-
50_05_5055	0.14	0.15	0.13	0.05	-0.07	-0.04	-0.06	0.02	0.05
50_07_5055	0.62	0.56	0.76	0.62	0.84	0.84	1.05	1.06	0.99

4.2.4 Water Surface Level

Several observations can be discovered from the results of water surface level plotting. Complete results in plan and profile view of water surface elevation are plotted in Appendix A5.

By comparing the result with different slope in Figure 4.10, the water surface elevation within the bifurcation section is raised with steeper slope. Noticeable result in Section 4.2.3 shows water depth is reduced with steeper slope. Both results are not contradictory as the experiment is set up in a flume with slope. Another observation from Figure 4.10 is that the measured points at the bifurcation section are slightly higher in gradient compared to the points at the weir. This shows the energy loss at the bifurcation section with significant turbulent flow properties.

Water surface level with different bifurcation angle is plotted in Figure 4.11, the water surface level within both tributaries generally rose by 0.2cm when the bifurcation angle changed from 30° to 40°. When the bifurcation angle changed from 40° to 50°, the water surface level at the upstream channel rose by approximately 0.2cm.

The water surface level at the weir section of both tributaries is at about the same level (Figure 4.12). This phenomenon can be found in all experiment runs, including different weir height combinations. This may be due to the small dimension of the experiment setup. Significant differences in water surface level may be found in a larger-scale experiment.

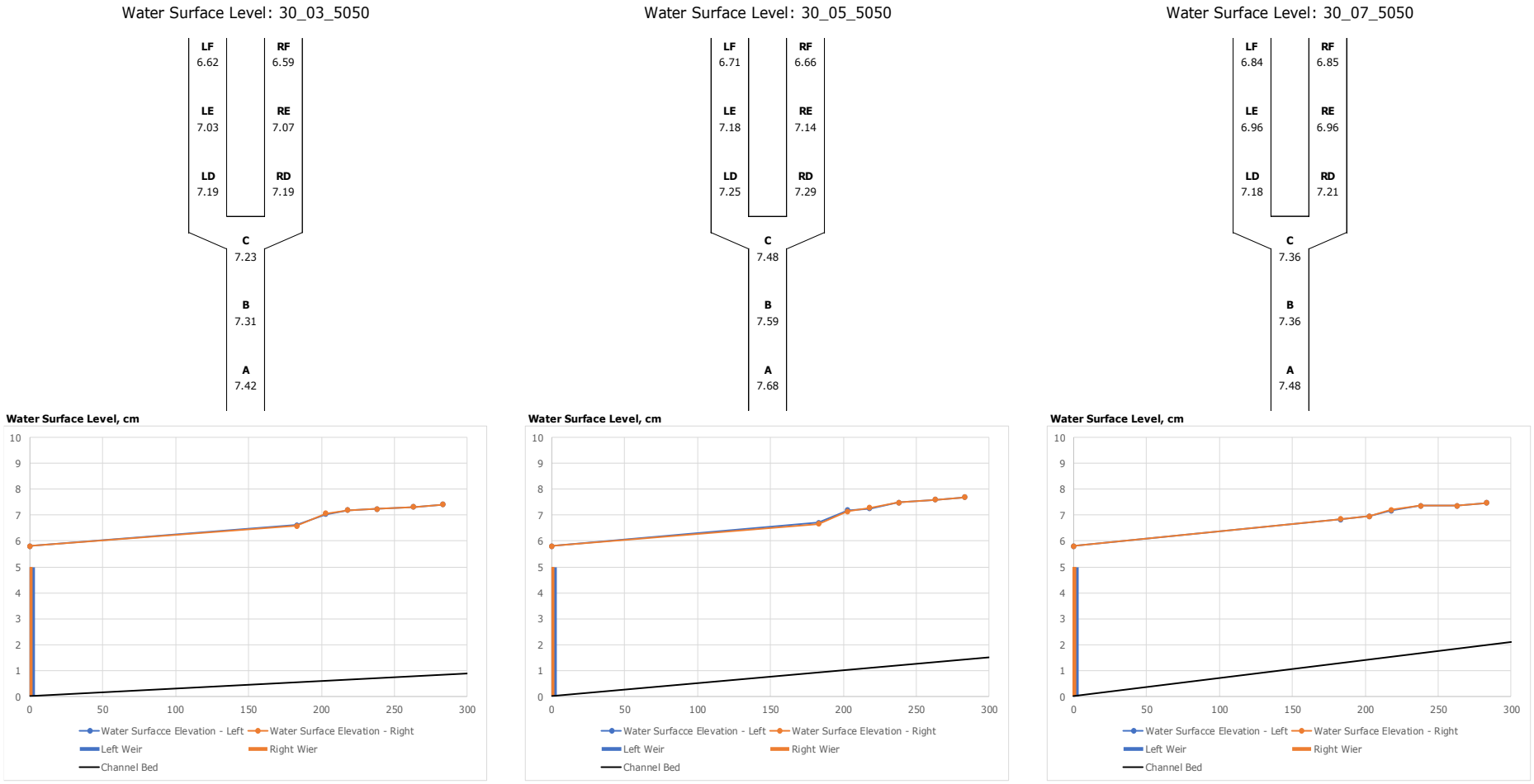


Figure 4.10: Comparison between water surface level with different slope

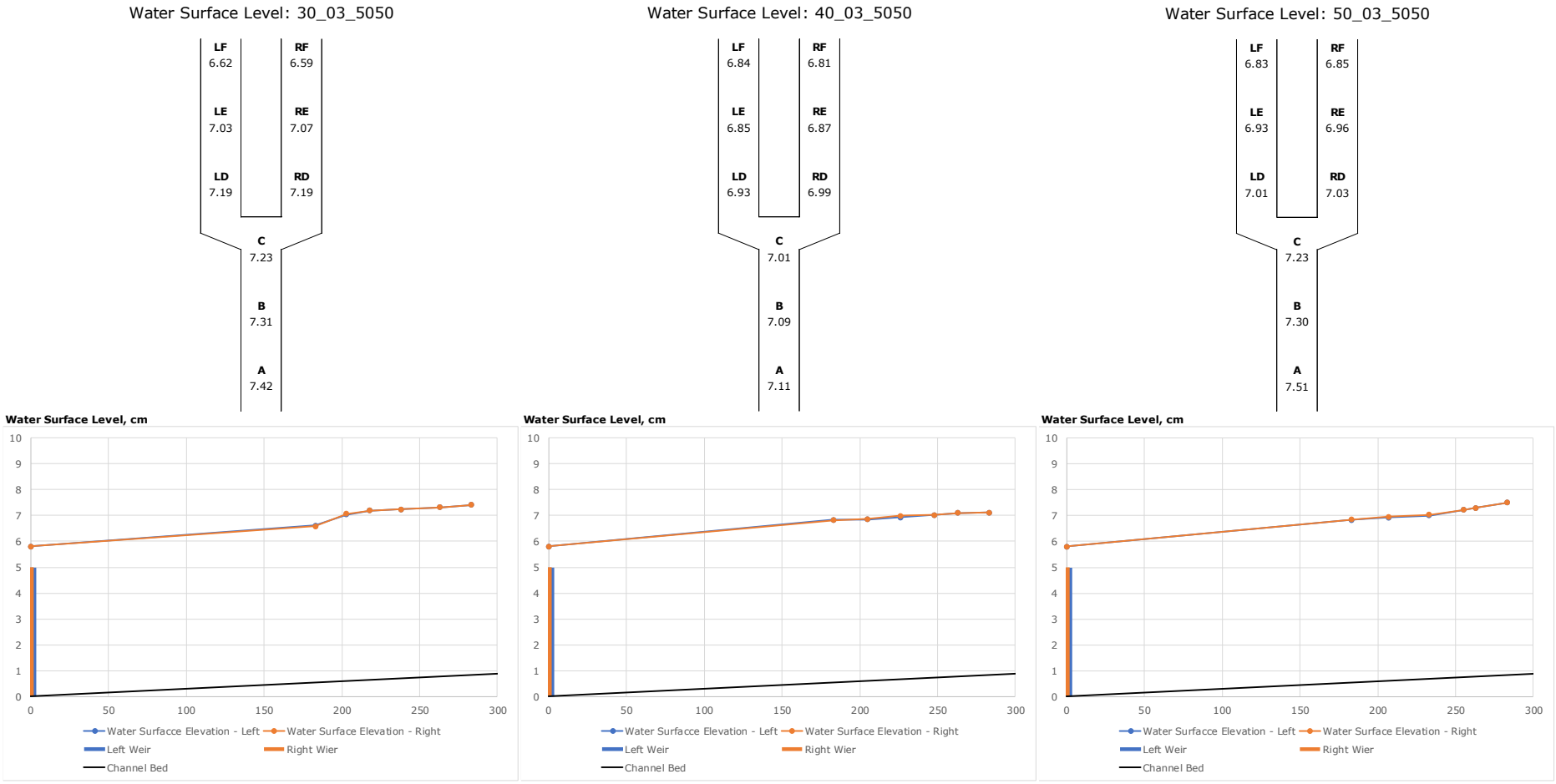


Figure 4.11: Comparison between water surface level with different bifurcation angle

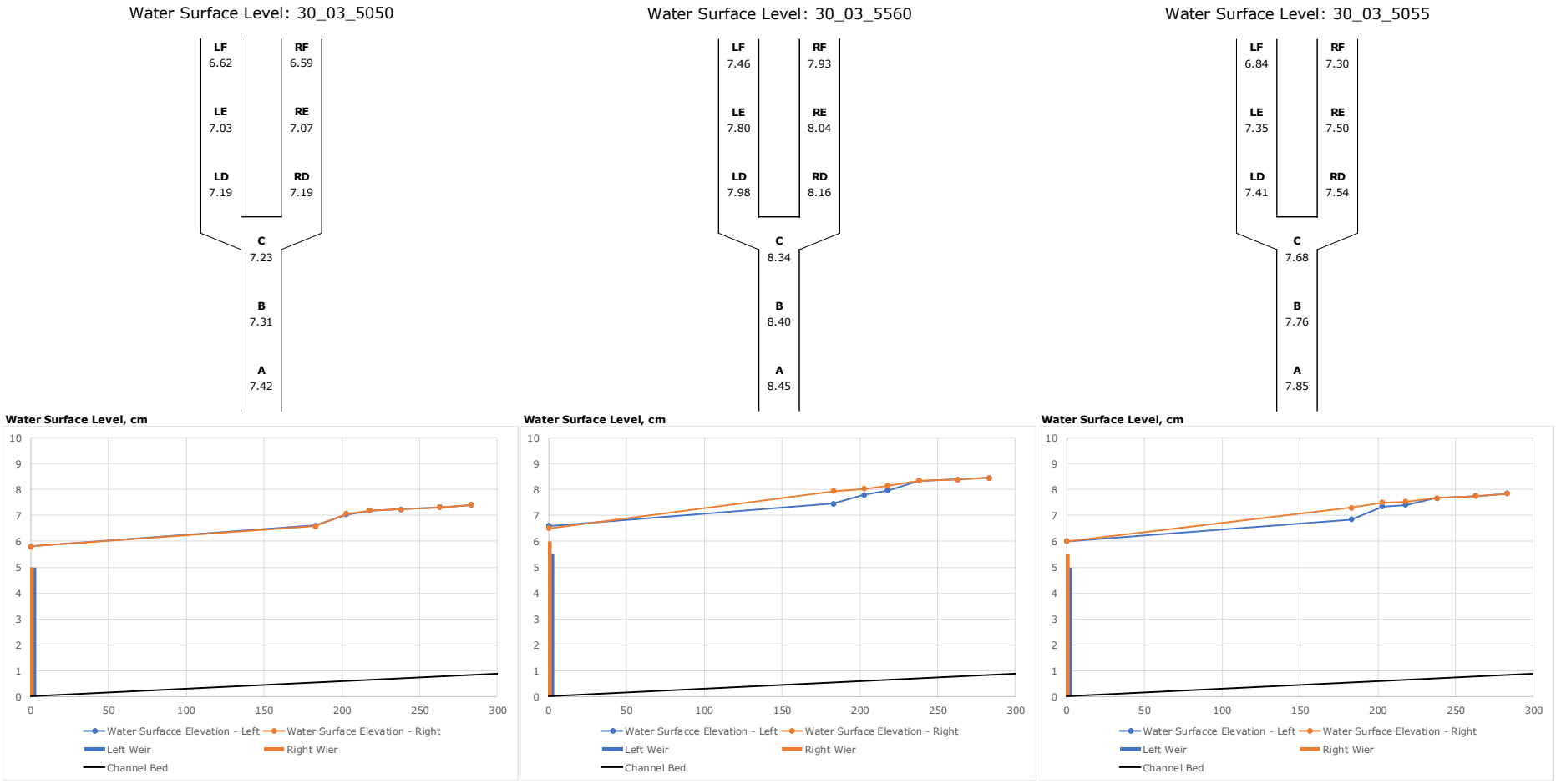


Figure 4.12: Comparison between water surface level with different weir height ratio

4.2.5 Flow Velocity

All flow velocity data are plotted in Appendix A3 (Section) and recorded in Appendix A10. Regardless of bifurcation angle, slope, and weir height combination, the flow velocity near surface is always larger than near bed.

Like water depth, for all types of weir height combinations, the inner bank of both left and right tributaries has higher flow velocity than their outer banks. Figure 4.8 shows an example of superelevation of flow velocity (50_05_5050); the red arrow indicates the direction of velocity gradient (from high towards low). Findings from Thomas et al. (2011) showed similar behaviour of velocity at the downstream of the tributaries; however, the upstream of both tributaries was reversed, in which the outer bank had higher velocity than the inner bank. One hypothesis is introduced to explain the differences: the discharge used in both experiments was different, and a larger discharge may lead to a curved velocity profile.

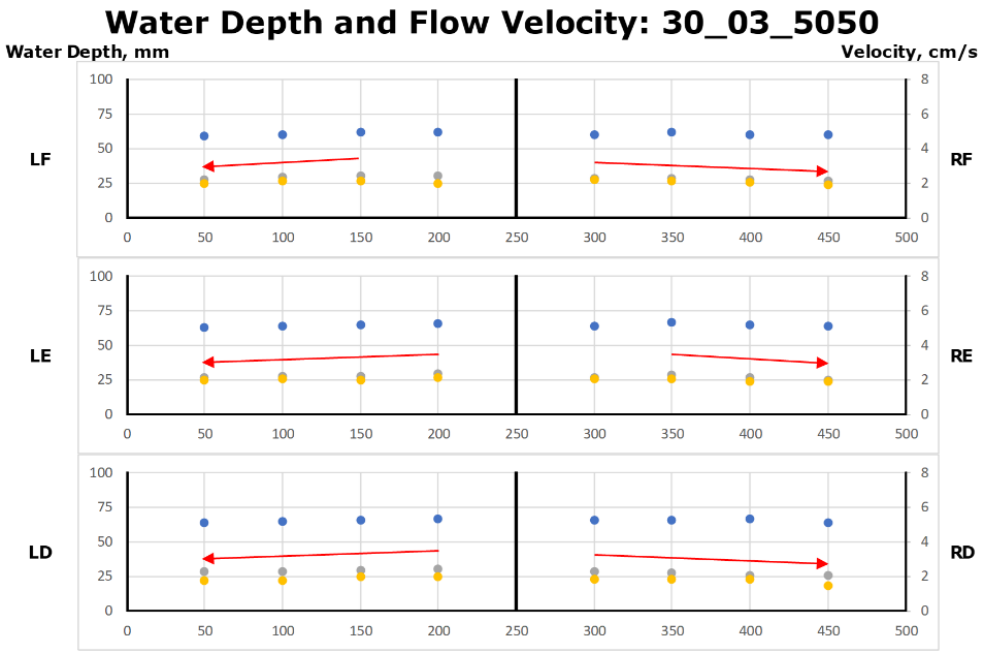


Figure 4.13: High flow velocity near inner bank

4.2.6 Average Flow Velocity

The measured flow velocity data in each cross-section are averaged and summarised in Table 4.7 for near surface flow and

Table 4.8 for near bed flow. In Appendix A6, plan and profile of average flow velocity are plotted accordingly.

Figure 4.14 and Figure 4.15 show the relationship between flow velocity and slope. According to the figures, the following relationships can be observed:

1. Average flow velocity is increased when slope is steeper.
2. Average flow velocity is affected by its lowest weir height and weir height ratio.
3. No relation is found between average flow velocity and bifurcation angle.

Table 4.7: Summary of average flow velocity (Near surface)

Experiment Run	Average Flow Velocity, cm/s (Left Tributary)			Average Flow Velocity, cm/s (Right Tributary)			Average Flow Velocity, cm/s (Upstream)		
	F	E	D	F	E	D	C	B	A
30_03_5050	2.36	2.22	2.34	2.23	2.13	2.15	2.26	2.48	2.39
30_05_5050	2.56	2.13	2.40	2.25	2.22	2.36	2.18	2.30	2.46
30_07_5050	2.70	2.52	2.37	2.39	2.45	2.41	2.80	2.81	2.64
40_03_5050	2.58	2.42	2.31	2.19	2.23	2.38	2.53	2.51	2.63
40_05_5050	2.67	2.58	2.54	2.68	2.38	2.54	2.52	2.51	2.69
40_07_5050	2.61	2.55	2.70	2.54	2.42	2.54	2.76	2.77	2.67
50_03_5050	2.68	2.50	2.46	2.42	2.56	2.55	2.63	2.63	2.58
50_05_5050	2.44	2.42	2.42	2.16	2.30	2.39	2.79	2.59	2.55
50_07_5050	2.67	2.71	2.63	2.53	2.63	2.54	2.69	2.59	2.49
30_03_5560	3.45	3.18	3.25	0.84	0.90	0.73	1.88	2.15	2.14
30_05_5560	3.61	3.26	3.51	0.87	0.72	0.91	2.05	2.11	2.48
30_07_5560	3.89	3.79	3.64	1.29	0.94	0.83	2.21	2.39	2.28
40_03_5560	3.31	3.32	3.31	0.65	0.69	0.72	2.20	2.05	1.90
40_05_5560	3.41	3.59	3.63	1.00	0.66	0.75	2.41	2.16	2.37
40_07_5560	3.53	3.24	3.45	1.02	0.74	1.06	2.25	2.35	2.27
50_03_5560	3.20	3.05	3.15	0.74	0.86	0.80	1.85	1.78	1.82
50_05_5560	3.53	3.25	3.25	0.95	0.77	0.97	2.05	1.96	2.06
50_07_5560	3.88	3.71	3.72	0.86	0.71	0.90	2.48	2.12	1.90
30_03_5055	3.39	3.12	2.77	1.18	1.02	1.05	2.09	2.43	2.17
30_05_5055	3.77	3.34	3.39	1.12	1.31	1.42	2.31	2.54	2.23
30_07_5055	3.80	3.66	3.69	1.32	1.23	1.18	2.56	2.50	2.57
40_03_5055	3.54	3.34	3.29	1.05	1.13	1.26	2.04	2.21	2.06
40_05_5055	3.40	3.31	3.23	1.04	0.89	1.27	2.20	2.08	2.02
40_07_5055	3.51	3.54	3.62	1.30	1.07	1.33	2.43	2.44	2.31
50_03_5055	3.36	3.24	3.22	1.12	0.96	1.18	2.54	2.38	2.30
50_05_5055	3.24	3.50	3.23	0.99	0.98	1.09	2.08	1.96	2.04
50_07_5055	3.99	3.92	3.42	1.40	1.04	1.64	2.73	2.64	2.58

Table 4.8: Summary of average flow velocity (Near bed)

Experiment Run	Average Flow Velocity, cm/s (Left Tributary)			Average Flow Velocity, cm/s (Right Tributary)			Average Flow Velocity, cm/s (Upstream)		
	F	E	D	F	E	D	C	B	A
30_03_5050	2.05	2.02	1.87	2.08	1.97	1.75	1.71	1.59	1.68
30_05_5050	1.91	1.99	1.95	1.97	1.96	1.84	2.01	1.90	1.77
30_07_5050	2.15	2.31	2.29	2.20	2.11	2.21	1.87	1.84	2.06
40_03_5050	1.87	2.14	1.95	1.87	2.04	1.74	1.68	1.61	1.66
40_05_5050	1.98	2.12	2.15	1.67	2.14	1.80	2.07	2.01	1.90
40_07_5050	2.20	2.31	2.11	2.01	2.15	1.95	1.93	1.89	2.13
50_03_5050	1.78	1.84	1.91	1.73	1.66	1.64	1.59	1.41	1.44
50_05_5050	2.07	1.98	2.12	1.89	2.00	1.85	1.50	1.56	1.60
50_07_5050	2.20	2.13	2.15	2.25	2.17	2.04	1.74	1.75	1.84
30_03_5560	2.69	2.84	2.79	0.60	0.37	0.44	1.58	1.34	1.27
30_05_5560	2.96	3.06	2.77	0.69	0.71	0.45	1.66	1.62	1.45
30_07_5560	3.02	3.35	3.33	0.24	0.43	0.41	1.77	1.63	1.78
40_03_5560	2.71	3.09	3.08	0.47	0.56	0.58	1.28	1.35	1.56
40_05_5560	2.93	3.33	3.21	0.34	0.50	0.49	1.40	1.56	1.54
40_07_5560	3.05	3.18	3.37	0.34	0.58	0.16	1.69	1.59	1.65
50_03_5560	3.02	2.85	2.81	0.51	0.57	0.53	1.70	1.59	1.57
50_05_5560	3.02	2.84	2.84	0.46	0.43	0.63	1.69	1.74	1.65
50_07_5560	2.93	2.85	2.61	0.56	0.51	0.77	1.44	1.69	1.81
30_03_5055	2.78	2.74	2.90	0.86	0.95	1.02	1.66	1.33	1.64
30_05_5055	3.16	2.83	2.85	0.96	0.84	0.67	1.75	1.55	1.80
30_07_5055	3.35	3.35	3.45	1.04	1.12	0.95	1.90	1.83	1.83
40_03_5055	2.70	3.00	2.98	0.65	0.65	0.62	1.70	1.58	1.63
40_05_5055	2.82	2.88	2.88	0.62	0.67	0.60	1.46	1.66	1.79
40_07_5055	3.19	3.39	3.33	0.65	0.96	0.77	1.86	1.83	1.91
50_03_5055	3.17	3.02	2.95	0.72	0.84	0.77	1.35	1.35	1.40
50_05_5055	3.09	2.70	3.17	0.71	0.88	0.88	1.72	1.80	1.69
50_07_5055	3.22	2.96	3.27	0.82	0.56	0.83	1.88	1.91	1.74

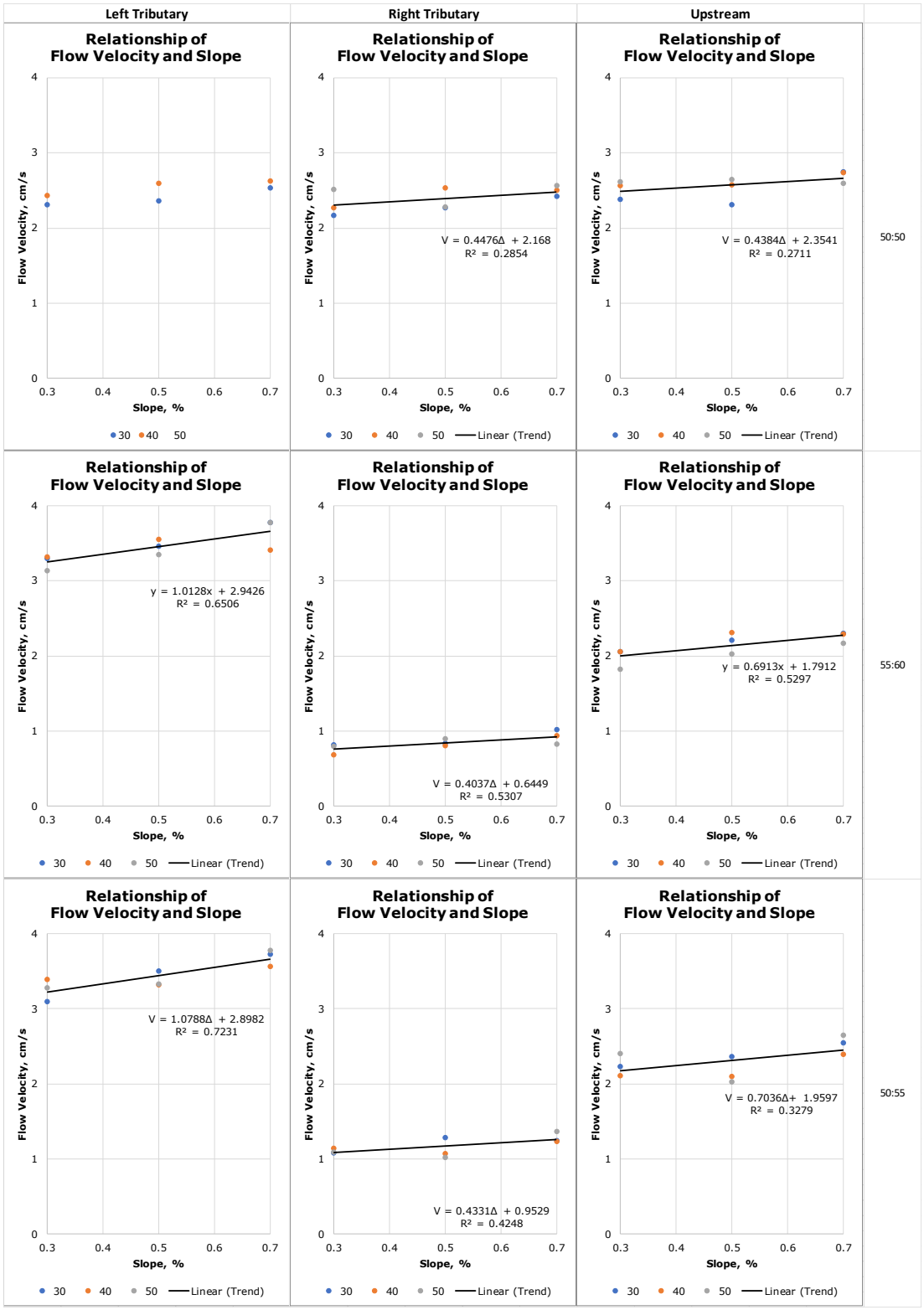


Figure 4.14: Relationship of flow velocity (near surface) and slope

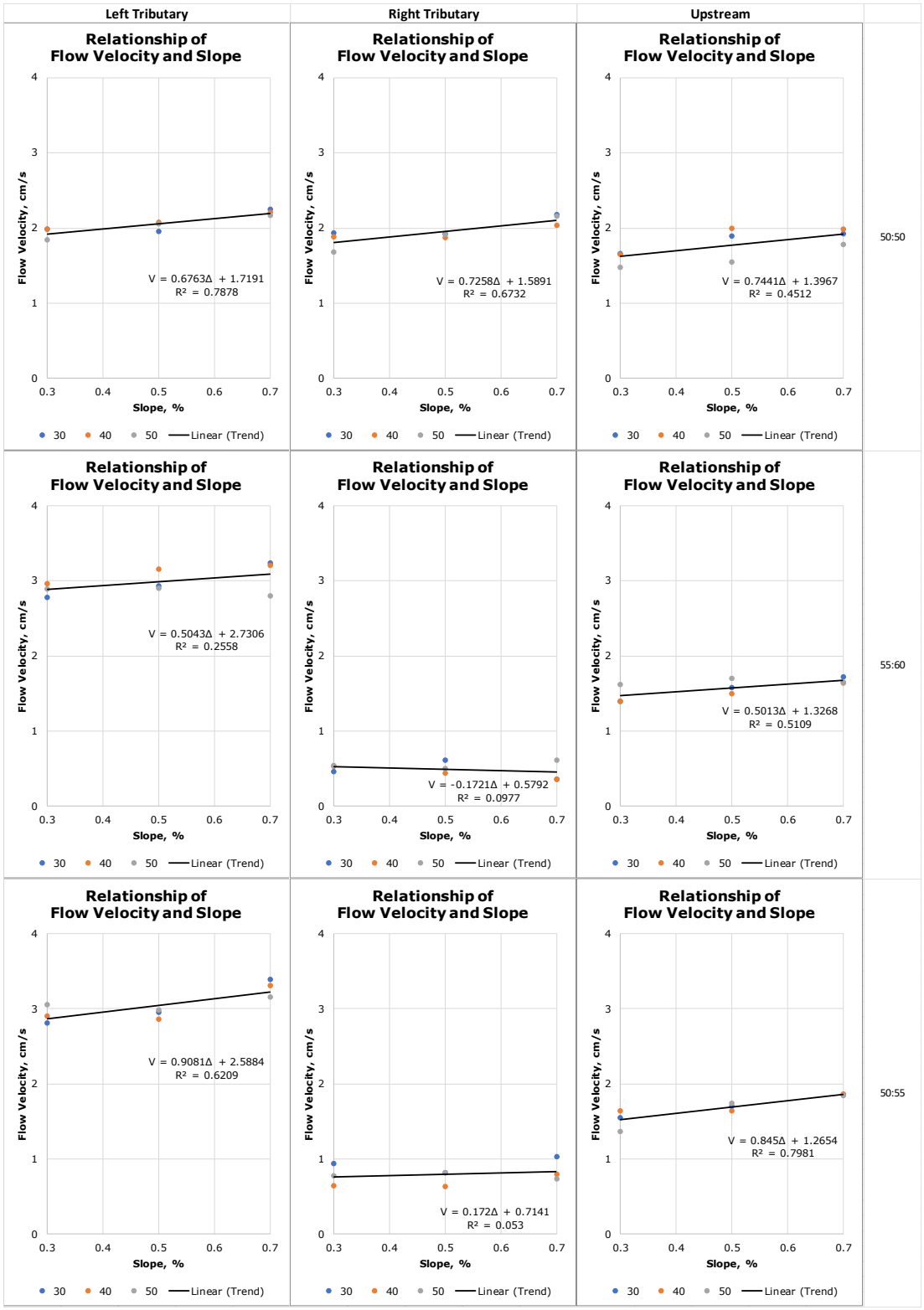


Figure 4.15: Relationship of flow velocity (near bed) and slope

4.2.7 Flow Discharge

Flow discharge of each subsection calculations are recorded and presented in Appendix A10, an example is shown in Table 4.9. All the subsection flow discharge in the same section are summed and summarised in Table 4.10. In Appendix A7, plan and profile of flow discharge of each section are plotted accordingly. The average discharge in each experiment run is summarised in

Table 4.11. In this study, the flow discharge ranges from 610.7 to 680.8 cm^3/s with mean of 659.4 cm^3/s and standard deviation of 12.7 cm^3/s.

Table 4.9: Example of flow discharge calculation

Downstream

	Subsection Name		L50	L100	L150	L200		R50	R100	R150	R200
	Subsection Width	(mm)	75	50	50	75		75	50	50	75
Section F	A Velocity	(cm/s)									
	A1 Near Surface Flow		2.22	2.38	2.43	2.42		2.29	2.28	2.23	2.14
	A2 Near Bed Flow		2.01	2.10	2.09	2.00		2.19	2.16	2.03	1.94
	B Water Depth	(mm)	59.44	59.67	62.11	61.64		59.66	61.69	59.72	60.43
	C Discharge	(cm3/s)									
	C1 Near Surface Flow		49.38	35.43	37.68	56.05		51.19	35.15	33.36	48.41
	C2 Near Bed Flow		44.85	31.29	32.51	46.23		49.03	33.38	30.31	43.99
	C3 Total Discharge		**94.23**	**66.73**	**70.19**	**102.29**		**100.22**	**68.53**	**63.68**	**92.40**
Section E	A Velocity	(cm/s)									
	A1 Near Surface Flow		2.15	2.22	2.21	2.31		2.11	2.25	2.15	2.01
	A2 Near Bed Flow		1.95	2.02	2.00	2.11		2.06	2.03	1.91	1.88
	B Water Depth	(mm)	62.59	64.24	64.74	65.35		64.02	66.23	64.59	63.41
	C Discharge	(cm3/s)									
	C1 Near Surface Flow		50.53	35.64	35.70	56.71		50.55	37.22	34.67	47.85
	C2 Near Bed Flow		45.65	32.49	32.41	51.69		49.39	33.60	30.87	44.74
	C3 Total Discharge		**96.18**	**68.13**	**68.11**	**108.41**		**99.94**	**70.82**	**65.54**	**92.59**
Section D	A Velocity	(cm/s)									
	A1 Near Surface Flow		2.26	2.28	2.38	2.42		2.25	2.23	2.07	2.03
	A2 Near Bed Flow		1.77	1.78	1.98	1.95		1.82	1.84	1.87	1.49
	B Water Depth	(mm)	63.99	64.64	66.09	66.88		65.29	65.36	66.84	64.11
	C Discharge	(cm3/s)									
	C1 Near Surface Flow		54.32	36.82	39.26	60.76		55.06	36.48	34.57	48.90
	C2 Near Bed Flow		42.55	28.74	32.70	48.90		44.64	30.01	31.17	35.77
	C3 Total Discharge		**96.87**	**65.56**	**71.96**	**109.67**		**99.70**	**66.49**	**65.74**	**84.66**

Upstream

	Subsection Name		U50	U100	U150	U200	U250	U300	U350	U400	U450
	Subsection Width	(mm)	75	50	50	50	50	50	50	50	75
Section C	A Velocity	(cm/s)									
	A1 Near Surface Flow		2.21	2.16	1.87	2.12	2.22	2.44	2.48	2.57	2.23
	A2 Near Bed Flow		1.62	1.63	1.66	1.74	1.78	1.69	1.73	1.82	1.75
	B Water Depth	(mm)	65.35	64.2	64.78	65.36	66.34	64.56	65.39	65.01	65.77
	C Discharge	(cm3/s)									
	C1 Near Surface Flow		54.21	34.72	30.27	34.67	36.75	39.46	40.57	41.83	55.07
	C2 Near Bed Flow		39.67	26.09	26.88	28.38	29.52	27.33	28.30	29.65	43.28
	C3 Total Discharge		**93.88**	**60.81**	**57.15**	**63.05**	**66.27**	**66.79**	**68.86**	**71.47**	**98.35**
Section B	A Velocity	(cm/s)									
	A1 Near Surface Flow		2.33	2.40	2.41	2.40	2.48	2.55	2.60	2.60	2.58
	A2 Near Bed Flow		1.06	1.26	1.32	1.38	1.48	1.95	1.91	1.73	2.26
	B Water Depth	(mm)	64.77	64.86	64.59	64.12	64.71	66.04	67.11	66.21	64.63
	C Discharge	(cm3/s)									
	C1 Near Surface Flow		56.67	38.94	38.88	38.43	40.10	42.03	43.70	42.96	62.46
	C2 Near Bed Flow		25.85	20.40	21.33	22.16	23.91	32.16	32.12	28.58	54.80
	C3 Total Discharge		**82.52**	**59.34**	**60.22**	**60.59**	**64.01**	**74.19**	**75.82**	**71.54**	**117.27**
Section A	A Velocity	(cm/s)									
	A1 Near Surface Flow		1.89	1.90	2.38	2.15	2.54	2.51	2.60	2.66	2.90
	A2 Near Bed Flow		1.19	1.31	1.41	1.58	1.70	1.90	1.94	2.05	2.00
	B Water Depth	(mm)	66.03	66.38	66.54	66.74	66.30	66.06	64.88	63.84	64.23
	C Discharge	(cm3/s)									
	C1 Near Surface Flow		46.88	31.45	39.53	35.81	42.13	41.38	42.23	42.46	69.78
	C2 Near Bed Flow		29.54	21.70	23.52	26.32	28.12	31.44	31.52	32.77	48.25
	C3 Total Discharge		**76.42**	**53.16**	**63.05**	**62.13**	**70.25**	**72.82**	**73.74**	**75.23**	**118.03**

Table 4.10: Summary of flow discharge of section

Experiment Run	Flow Discharge of Section, cm^3/s (Left Tributary)			Flow Discharge of Section, cm^3/s (Right Tributary)			Flow Discharge of Section, cm^3/s (Upstream)		
	F	E	D	F	E	D	C	B	A
30_03_5050	333.4	340.8	344.1	324.8	328.9	316.6	646.6	665.5	664.8
30_05_5050	323.0	316.9	333.7	301.4	318.7	324.0	659.9	657.6	661.8
30_07_5050	336.2	335.3	328.9	318.9	316.0	326.4	659.6	643.0	646.7
40_03_5050	348.9	355.1	334.4	317.2	332.6	324.2	651.4	648.5	676.5
40_05_5050	343.3	342.2	348.6	322.6	332.0	322.0	675.2	666.5	677.8
40_07_5050	351.6	347.0	338.8	332.2	324.9	322.1	665.6	651.5	672.7
50_03_5050	349.9	341.9	344.7	325.1	335.8	327.7	682.0	656.2	669.7
50_05_5050	332.6	341.0	355.9	299.1	336.3	335.0	674.0	663.9	664.6
50_07_5050	346.4	347.3	356.7	338.7	346.6	339.2	676.1	672.1	661.5
30_03_5560	528.1	539.7	552.0	131.6	117.4	108.4	659.9	661.8	649.3
30_05_5560	526.7	527.9	534.0	132.9	125.1	118.7	645.3	645.6	677.0
30_07_5560	525.4	545.9	538.2	124.0	112.2	101.6	641.5	639.8	640.5
40_03_5560	529.7	561.6	559.8	105.8	116.9	123.4	670.9	659.4	667.1
40_05_5560	531.9	574.6	578.9	117.0	101.4	109.5	663.9	658.3	682.3
40_07_5560	543.9	520.4	553.0	116.6	111.3	103.2	672.1	677.0	673.9
50_03_5560	547.1	516.4	521.5	117.4	133.6	127.2	685.8	652.9	656.4
50_05_5560	525.0	520.8	528.9	128.0	110.3	146.0	689.1	687.2	678.4
50_07_5560	532.7	541.2	522.4	124.2	105.6	143.2	672.9	653.6	630.8
30_03_5055	483.1	492.1	478.3	171.7	169.5	170.2	651.3	651.5	662.2
30_05_5055	507.4	489.7	496.4	166.9	174.6	170.1	660.1	653.5	648.5
30_07_5055	481.7	482.3	492.3	173.9	172.5	156.9	656.6	647.8	642.7
40_03_5055	505.8	509.8	507.5	148.9	155.0	166.5	656.1	665.9	650.5
40_05_5055	482.3	475.2	467.4	134.9	125.2	154.0	595.5	609.8	619.8
40_07_5055	497.2	511.5	509.3	152.4	156.7	164.9	673.3	669.7	672.5
50_03_5055	507.9	511.0	511.9	156.5	153.7	165.1	666.3	648.6	640.1
50_05_5055	481.1	495.0	520.5	144.0	161.1	169.3	656.0	650.5	641.5
50_07_5055	491.5	500.2	479.1	170.5	127.8	186.3	680.7	670.5	639.2

Table 4.11: Discharge in each experiment runs

Run	Bifurcation Angle (°)	Slope (%)	Left Weir Height (mm)	Right Weir Height (mm)	Weir Height Ratio	Discharge (cm^3/s)
30_03_5050	30	0.3	50	50	1.000	660.9
30_03_5560	30	0.3	55	60	0.917	658.0
30_03_5055	30	0.3	50	55	0.909	655.0
30_05_5050	30	0.5	50	50	1.000	649.5
30_05_5560	30	0.5	55	60	0.917	655.6
30_05_5055	30	0.5	50	55	0.909	661.2
30_07_5050	30	0.7	50	50	1.000	651.8
30_07_5560	30	0.7	55	60	0.917	644.8
30_07_5055	30	0.7	50	55	0.909	651.1
40_03_5050	40	0.3	50	50	1.000	664.8
40_03_5560	40	0.3	55	60	0.917	665.7
40_03_5055	40	0.3	50	55	0.909	661.0
40_05_5050	40	0.5	50	50	1.000	671.7
40_05_5560	40	0.5	55	60	0.917	669.6
40_05_5055	40	0.5	50	55	0.909	610.7
40_07_5050	40	0.7	50	50	1.000	667.7
40_07_5560	40	0.7	55	60	0.917	661.9
40_07_5055	40	0.7	50	55	0.909	667.9
50_03_5050	50	0.3	50	50	1.000	672.2
50_03_5560	50	0.3	55	60	0.917	659.7
50_03_5055	50	0.3	50	55	0.909	660.2
50_05_5050	50	0.5	50	50	1.000	667.1
50_05_5560	50	0.5	55	60	0.917	668.9
50_05_5055	50	0.5	50	55	0.909	653.2
50_07_5050	50	0.7	50	50	1.000	680.8
50_07_5560	50	0.7	55	60	0.917	654.4
50_07_5055	50	0.7	50	55	0.909	657.6

4.2.8 Head above Weir Crest

A consistent pattern of head above weir crest (H) was found during the experiment; the water surface was relatively consistent at higher H values compared to lower H values. Fluctuation of water surface is significant for the right tributary with 55mm and 60mm height weir. The measured H is listed in Table 4.12. The H value is the same for different experimental setups of bifurcation angle and slope. Unlike water depth (>50mm), the H was relatively small, therefore, the measured H was recorded as a range due to the small value and limitation of the tool.

Table 4.12: Measured head above weir crest (H)

Weir Height Combination	Left Tributary			Right Tributary		
	Weir Height	H, mm	Q_{Weir}, cm^3/s	Weir Height	H, mm	Q_{Weir}, cm^3/s
50:50	50	7 to 9	317 to 380	50	7 to 9	317 to 380
55:60	55	11 to 12	590 to 667	60	4 to 6	153 to 258
50:55	50	10 to 11	517 to 590	55	4 to 6	153 to 258

Theoretically, based on conservation of momentum, the calculated discharge at weir (Q_{Weir}) by the Kindsvater-Carter method should be the same as the calculated discharge (QCal) by the velocity-area method. Practically the discharge is expected to be different due to the error of measurement, small dimension of experiment setup, imperfection of experiment setup, and other factors. In addition, the equation for both discharge calculation is an approximate approach; thus, minor differences are predicted and acceptable.

To compare these 2 methods of discharge calculation, Figure 4.16 is plotted for both tributaries (A: left tributary; B: right tributary). Bold lines indicate the Q_{Weir} (range) as the measured H value was too small (refer to Table 4.12 for the range); Q_{Cal} is plotted as solid dot. The colour specifies the group of experiment runs with different weir height ratio.

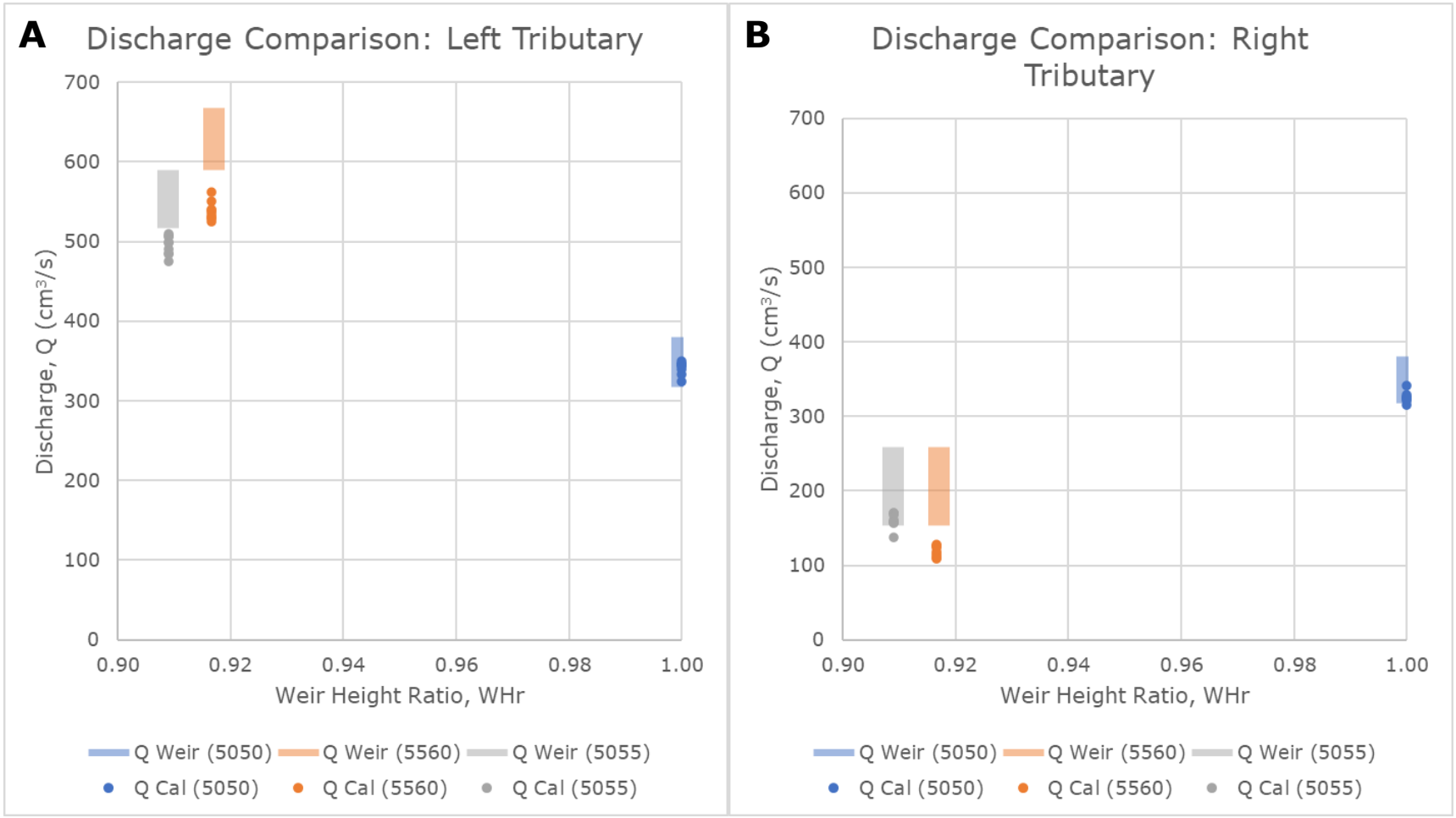


Figure 4.16: Discharge comparison between different weir height ratio (A: left tributary; B: right tributary)

The comparison shows the Q_{Cal} falls within the range of Q_{Weir} when the weir height ratio is equal to 1 (weir height combination is 50:50). 1 experiment run for right tributary was out of the range. Based on the experiment setup ideology, the weir height of left tributary was always smaller than right tributary whenever any weir height ratio less than 1 is selected. Therefore, the discharge in left tributary is higher than right tributary as presented in Figure 4.16. For the low discharge at right tributary, 8 out of 9 Q_{Cal} fall within the range of Q_{Weir} for weir height combination 50:55. All Q_{Cal} are not within the range of Q_{Weir} for weir height combination 55:60. None of the experiment runs for high discharge at left tributary are within its range of Q_{Weir}.

The calculated discharge differences between the 2 methods are much more significant for the high discharge. 3 possible explanations are suggested to explain this observation:

1. Kindsvater-Carter method reflected the accurate discharge; however, Velocity-area method may not be suitable for flow measurement at the bifurcation section.

2. Velocity-area method reflected the accurate discharge; however, Kindsvater-Carter method may not be accurately measured as the head above weir crest is too small or the weir is located too near to the point of bifurcation or both.

3. Velocity-area method reflected the accurate discharge; however, Kindsvater-Carter method may not be suitable for bifurcation flow within a certain range of distance from bifurcation point, especially weir height ratio is too small.

4.2.9 Froude Number and Reynolds Number

For each experiment run, the Froude number and Reynolds number at the upstream channel are averaged and tabulated in Table 4.13. The complete details of Froude number and Reynolds number are recorded in Appendix A8 and Appendix A9. Based on the result, the flow in all experiment runs at the upstream channel is subcritical and turbulent.

The upstream average Froude number ranges from 0.0197 to 0.0317 with mean of 0.0251 and standard deviation of 0.0034. The mean value of Froude number from experiment by Thomas et al. (2011) is 0.2. The threshold value is inversely proportional to Froude number at upstream. Without additional data, no specific type of equation can be used to describe the relationship. Froude number is calculated based on 2 factors: flow velocity and square root of water depth. Square root of water depth has an insignificant difference between the left and right tributaries for any weir height ratio less than 1.00, thus, the dominant factor is the flow velocity. Therefore, the comparison of Froude number between left and right tributary has a similar pattern to the flow velocity comparison (Appendix A6 vs Appendix A8).

The upstream average Reynolds number ranges from 11256 to 14459 with mean of 12691 and standard deviation of 918. By comparing the Reynolds number at the tributaries to the upstream channel, one observation is the reduction of Reynolds number at the tributaries when the weir height combination is 50:50. When weir height combination is 50:55, the Reynolds number of the main flow in the left tributary is slightly reduced and the secondary flow in the right tributary drops significantly. More reduction of Reynolds number can be found at the right tributary when weir height combination is 55:60, the main flow in the left tributary becomes higher than its upstream.

Table 4.13: Comparison of dimensionless parameter with Thomas et al. (2011)

Study	Experiment Run	Weir Height Ratio	Discharge Ratio	Froude Number	Reynolds Number
Current Study	30_03_5050	1.000	0.953	0.0252	12737
	30_05_5050	1.000	0.966	0.0268	13163
	30_07_5050	1.000	0.961	0.0316	14291
	40_03_5050	1.000	0.938	0.0268	13169
	40_05_5050	1.000	0.945	0.0300	14135
	40_07_5050	1.000	0.944	0.0317	14459
	50_03_5050	1.000	0.954	0.0256	12913
	50_05_5050	1.000	0.942	0.0265	13164
	50_07_5050	1.000	0.976	0.0282	13599
	30_03_5560	0.917	0.221	0.0200	11263
	30_05_5560	0.917	0.237	0.0229	12100
	30_07_5560	0.917	0.210	0.0254	12629
	40_03_5560	0.917	0.209	0.0198	11299
	40_05_5560	0.917	0.195	0.0229	12215
	40_07_5560	0.917	0.205	0.0239	12549
	50_03_5560	0.917	0.239	0.0197	11256
	50_05_5560	0.917	0.244	0.0218	12047
	50_07_5560	0.917	0.234	0.0232	12144
	30_03_5055	0.909	0.352	0.0228	12069
	30_05_5055	0.909	0.343	0.0255	12784
	30_07_5055	0.909	0.346	0.0288	13596
	40_03_5055	0.909	0.309	0.0225	11997
	40_05_5055	0.909	0.291	0.0233	11784
	40_07_5055	0.909	0.312	0.0270	13353
	50_03_5055	0.909	0.310	0.0229	12051
	50_05_5055	0.909	0.317	0.0228	12011
	50_07_5055	0.909	0.330	0.0295	13882
Thomas et al. (2011)	A-L35R45	0.778	0.79	0.21	10200
	A-L35R55	0.636	0.52	0.20	10400
	A-L40R45	0.889	0.81	0.21	10800
	A-L40R50	0.800	0.68	0.20	10600
	A-L45R45	1.000	1.00	0.20	10400
	A-L45R50	0.900	0.83	0.19	10300
	A-L45R55	0.818	0.69	0.19	10000
	B-L35R45	0.778	0.73	0.21	10500
	B-L35R55	0.636	0.52	0.20	10500
	B-L45R45	1.000	0.99	0.20	10500
	B-L45R55	0.818	0.72	0.18	9900

4.3 Dimensionless Factor Analysis

4.3.1 Water Depth Ratio

Multiple Linear Regression Analysis

Multiple linear regression (MLR) analysis is conducted in this section to study the linear relationship between dependent variable (water depth ratio) and independent variables (bifurcation angle, slope, and weir height ratio).

Table 4.14 shows the P-value of slope is higher than 0.05, thus, its relationship with water depth ratio is statistically non-significant. With this approach, a multi-linear equation can be written as Equation 4.1:

$$D_r = -0.0512 \sin \Theta + 0.6039 WH_r + 0.4256, dimensionless \quad \text{Equation 4.1}$$

where, D_r is water depth ratio

WH_r is weir height ratio

Θ is bifurcation angle

Table 4.14: Result of MLR analysis (Water depth ratio)

	Coefficients	Standard Error	t Stat	P-value
Intercept	0.425596442	0.054168293	7.85692918	5.83747E-08
Sin Θ	-0.051162316	0.020913532	-2.446373812	0.022493465
Δ	-0.005074933	0.013922311	-0.364518012	0.718801282 (P>0.05)
WH_r	0.603932639	0.055201395	10.94053222	1.36585E-10

Linear Regression Analysis by Grouping

Other than MLR analysis, another approach which is linear regression analysis by grouping with graph plotting is conducted in this section with weir height ratio as the primary independent variable.

To study the relationship between water depth ratio and weir height ratio, linear regression line is plotted to fit with 3 groups of bifurcation angle in **Figure 4.17** and 3 groups of slope in Figure 4.18, both linear regressions are calculated with intersection at coordinate {1,1}, as the line should theoretically pass through the coordinate {1,1}.

Coefficient of determination (R^2) in Figure 4.17 and Figure 4.18 show the weir height ratio is partly correlated ($0.90 < R^2 < 0.95$) with water depth ratio as an independent variable in linear regression. The 3 linear equations in Figure 4.17 show bifurcation angle is associated with some trigonometric properties. In contrast, the 3 linear regressions in Figure 4.18 show similar coefficient of linear regression, thus, no tendency can be determined for slope as an independent variable, a similar finding to MLR analysis. All linear regression coefficients are summarised in Table 4.15.

Table 4.15: Coefficient of linear regression (Water depth ratio)

Bifurcation Angle	Figure 4.17	
	M	C
30	0.5608	0.4392
40	0.6553	0.3447
50	0.7868	0.2132
Slope	Figure 4.18	
	M	C
0.3	0.6628	0.3372
0.5	0.6483	0.3517
0.7	0.6918	0.3082

In the linear equation (grouped by bifurcation angle) with weir height ratio as the primary independent variable, the gradient and constant coefficient are correlated to the secondary independent variable which is bifurcation angle. The gradient coefficient is related to the square of the sine function, and the constant coefficient is related to the square of the cosine function. Generally, an equation can be written to describe the relation, which is listed as Equation 4.2:

$$D_r = (0.6 \sin^2 \Theta + 0.4)\, WH_r + 0.6 \cos^2 \Theta\,, dimensionless \quad \text{Equation 4.2}$$

where, D_r is water depth ratio

WH_r is weir height ratio

Θ is bifurcation angle

Noticeably, the coefficient of determination (R^2) of linear regression in Figure 4.17 is generally less than 0.95. Since Equation 4.2 is fully developed based on experimental result, this equation may not be fully accurate, and further verification is required.

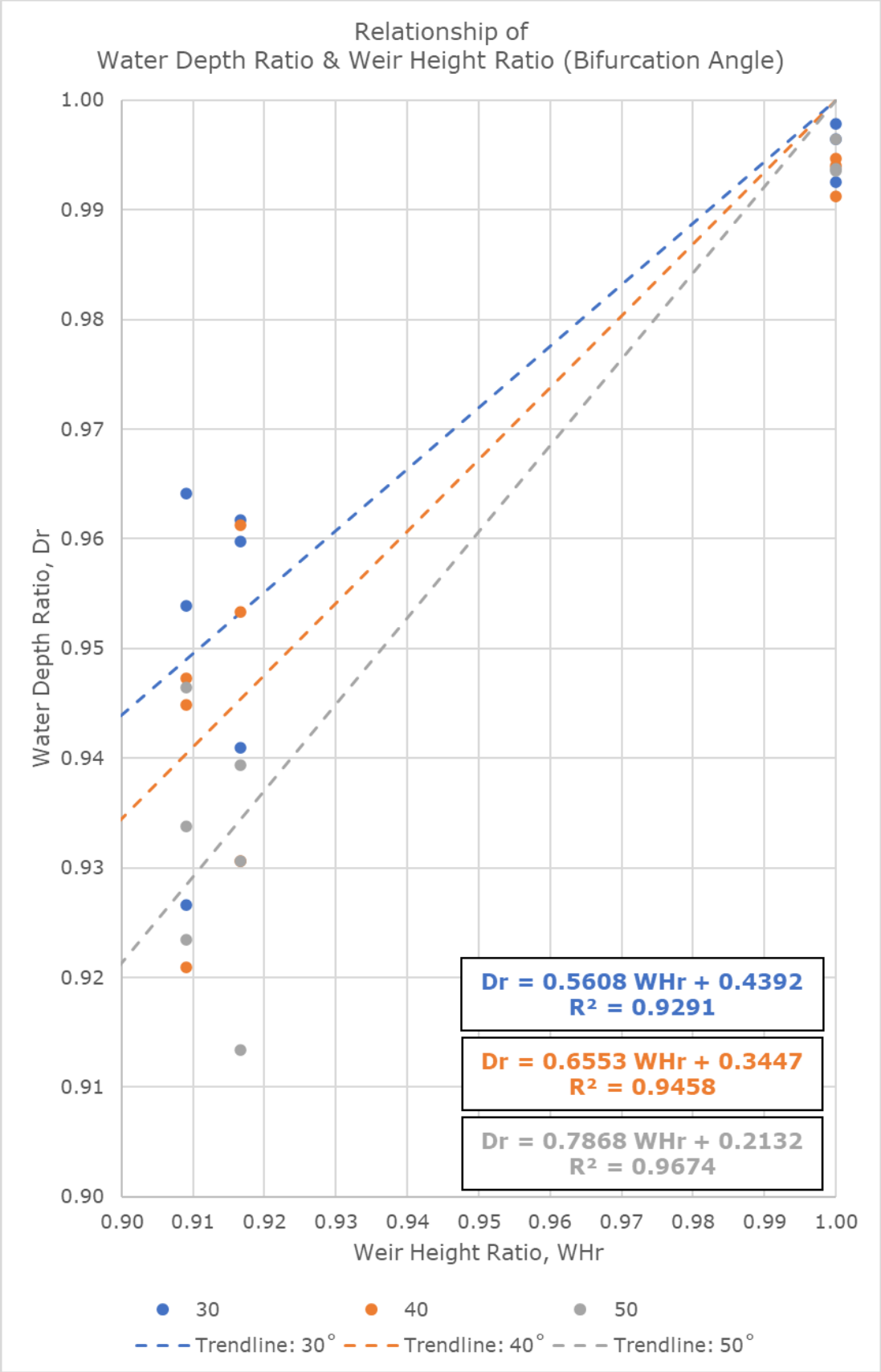


Figure 4.17: Relationship of water depth ratio and weir height ratio (Bifurcation Angle)

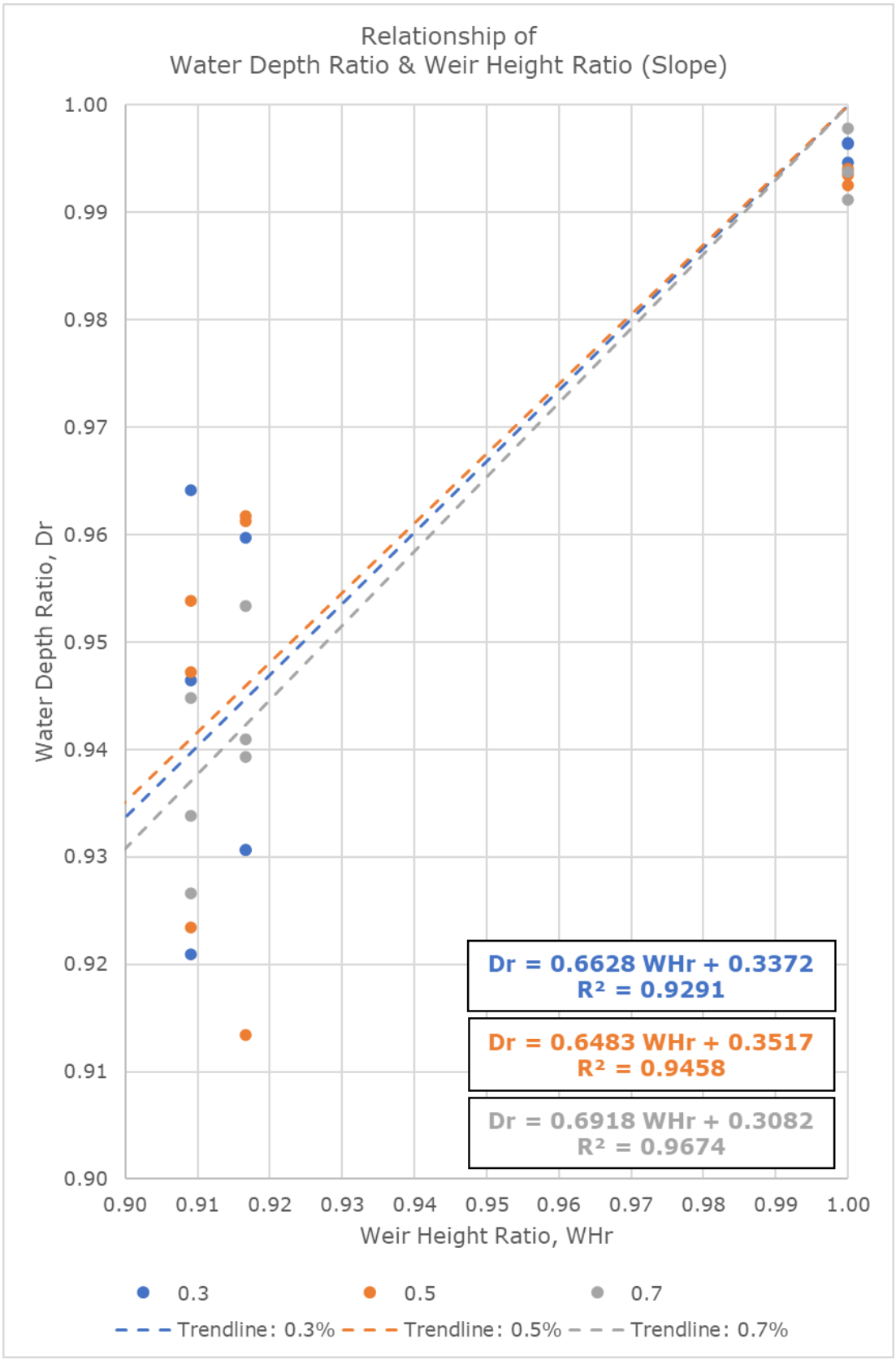


Figure 4.18: Relationship of water depth ratio and weir height ratio (Slope)

The coefficient of linear regression is compared between Equation 4.2 and the linear equation in Figure 4.17. A comparison with various bifurcation angles is summarised in Table 4.16 and plotted in Figure 4.19. Since the relationship of coefficient between developed equation and experiment data is non-linear, R^2 is not suitable to quantify the relationship, thus, P-value is applied which 1.18E-04 and 9.95E-04 for coefficient M and C respectively. Equation 4.2 with lower P-value is a more accurate model than the Equation 4.1 (P-value = 0.0225).

Table 4.16: Comparison of coefficient of developed equation with experiment data (Water depth ratio)

Bifurcation Angle	Developed Equation (Equation 4.2)		Experiment Data (Figure 4.17)	
	$M = 0.6 \times \sin^2 \Theta - 0.4$	$C = 0.6 \times \cos^2 \Theta$	M	C
0	0.4000	0.6000	NA	NA
10	0.4181	0.5819	NA	NA
20	0.4702	0.5298	NA	NA
30	0.5500	0.4500	0.5608	0.4392
40	0.6479	0.3521	0.6553	0.3447
50	0.7521	0.2479	0.7868	0.2132
60	0.8500	0.1500	NA	NA
70	0.9298	0.0702	NA	NA
80	0.9819	0.0181	NA	NA
90	1.0000	0.0000	NA	NA

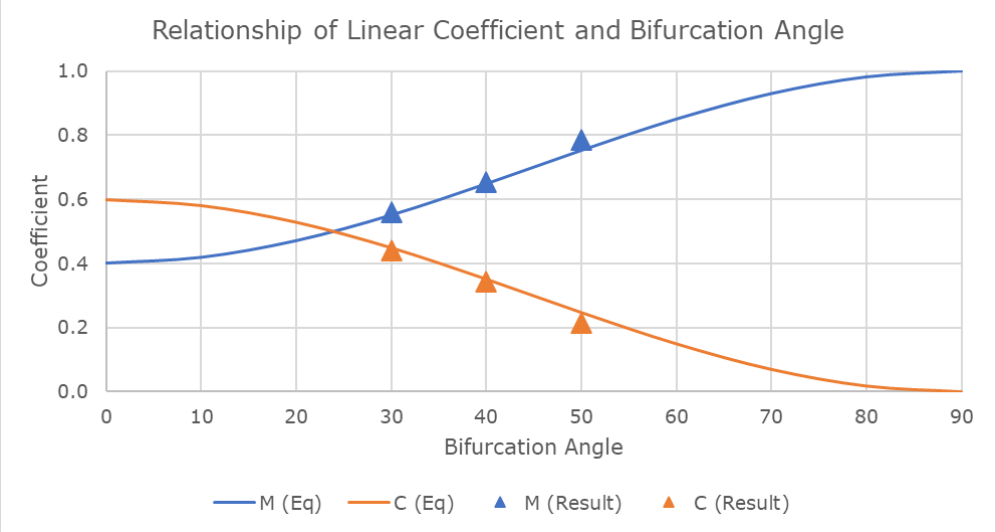


Figure 4.19: Relationship of linear coefficient and bifurcation angle (Water depth ratio)

According to the developed equation, the impact of WH_r on D_r is less impactful when bifurcation angle is decreased. At the condition of 90°bifurcation, D_r is directly proportional to WH_r ($D_r = WH_r$).

When bifurcation angle is close to zero (theoretical assumption), the D_r will be at the minimum value of 0.6 when WH_r is close to zero, this shows that the developed equation has significant limitations. Few assumptions are listed to discuss about this issue:

1. The developed equation is not suitable for all range of weir height ratio.
2. Trigonometric function may not be suitable to describe the relationship between bifurcation and weir height ratio.
3. Linear function may not be suitable to describe the relationship between water depth ratio and weir height ratio

Lastly, the Equation 4.2 is plotted in Figure 4.20 with the bifurcation angle that range from 0° to 90°. In Figure 4.20, any plotted line on the left of red dotted line is predicted and shall be further verified.

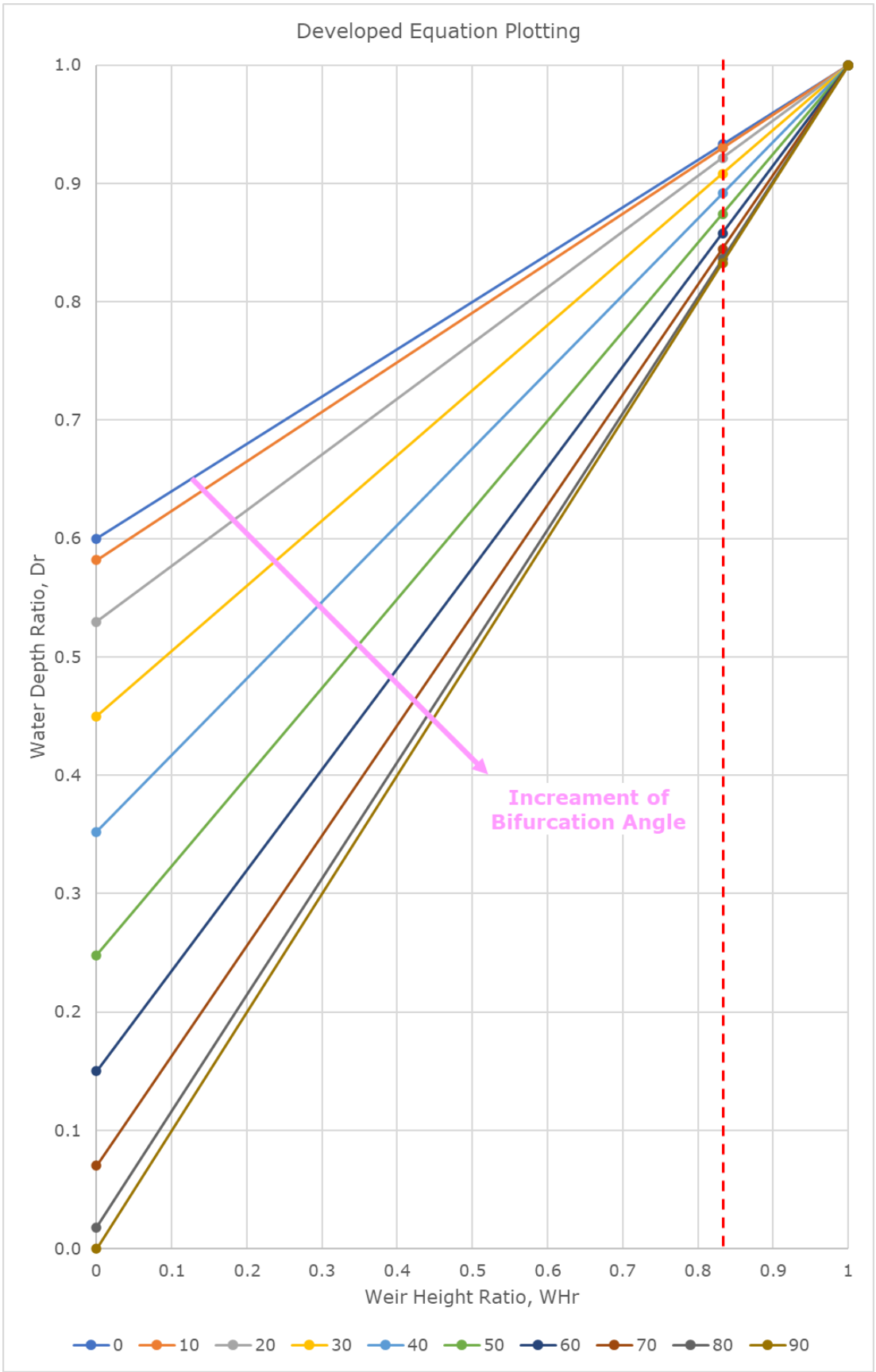


Figure 4.20: Plotting of developed equation (Water depth ratio)

4.3.2 Flow Velocity Ratio

Multiple Linear Regression Analysis

MLR analysis is conducted in this section to study the linear relationship between dependent variable (flow velocity ratio) and independent variables (bifurcation angle, slope, and weir height ratio).

Table 4.17 shows the P-value of bifurcation angle and slope is higher than 0.05, thus, their relationship with flow velocity ratio (near surface) is statistically non-significant. This applies to both near surface and near bed flow. With this approach, a multi-linear equation can be written as Equation 4.3 and Equation 4.4:

$$V_{r,NS} = 7.3886\, WH_r - 6.4548, dimensionless \quad \text{Equation 4.3}$$

$$V_{r,NB} = 8.1948\, WH_r - 7.2070, dimensionless \quad \text{Equation 4.4}$$

where, $V_{r,NS}$ and $V_{r,NB}$ are flow velocity ratio for near surface flow and near bed flow

WH_r is weir height ratio

Table 4.17: Result of MLR analysis (Flow velocity ratio)

	Coefficients	Standard Error	t Stat	P-value
	Near Surface			
Intercept	-6.454761797	0.320712514	-20.12631721	4.21535E-16
Sin 2Θ	-0.019289088	0.123822091	-0.155780665	0.877565093 (P>0.05)
Slope	0.037431447	0.082429388	0.454103173	0.654010839 (P>0.05)
Weir Height Ratio	7.388626491	0.326829168	22.60699841	3.29282E-17
	Near Bed			
Intercept	-7.207047175	0.359870394	-20.02678548	4.69664E-16
Sin 2Θ	-0.063756199	0.138940337	-0.458874653	0.650631208 (P>0.05)
Slope	-0.029357752	0.092493729	-0.317402619	0.753801607 (P>0.05)
Weir Height Ratio	8.194810456	0.36673387	22.34538757	4.25572E-17

Linear Regression Analysis by Grouping

Like water depth ratio, linear regression analysis by grouping is conducted in this section with weir height ratio as the primary independent variable in linear regression analysis.

To study the relationship between flow velocity ratio and weir height ratio, linear regression line is plotted to fit with 3 groups of bifurcation angle in Figure 4.21 and Figure 4.23 for near surface flow and near bed flow respectively. Similarly, the 3 groups of slopes for the 2layersr of flows are plotted in Figure 4.22 and Figure 4.24. All linear regressions are calculated with intersection at coordinate {1,1}, as the line should theoretically pass through the coordinate {1,1}.

All linear regressions coefficient in Figure 4.21, Figure 4.22, Figure 4.23, and Figure 4.24 are summarised and plotted in Table 4.18. Coefficient of determination (R^2) in the figures show the flow velocity ratio is strongly correlated ($R^2 > 0.95$) with weir height ratio as an independent variable in linear regression. The 3 linear equations in both Figure 4.21 and Figure 4.23 show bifurcation angle is associated with some trigonometric properties. In contrast, the linear regression in both Figure 4.21 and Figure 4.23 show similar coefficient of linear regression, thus, no tendency can be determined for slope as an independent variable, a similar finding to MLR analysis.

Table 4.18: Coefficient of linear regression (Flow velocity ratio)

Bifurcation Angle	Near Surface Flow (Figure 4.21)		Near Bed Flow (Figure 4.23)	
	M	C	M	C
30	7.9690	-6.9690	8.7325	-7.7325
40	8.1505	-7.1505	9.3057	-8.3057
50	8.0980	-7.0980	8.8655	-7.8655
Slope	Near Surface Flow (Figure 4.22)		Near Bed Flow (Figure 4.24)	
	M	C	M	C
0.3	8.1200	-7.1200	8.8567	-7.8567
0.5	8.1188	-7.1188	8.9565	-7.9565
0.7	7.9787	-6.9787	9.0906	-8.0906

In the linear equation (grouped by bifurcation angle) with weir height ratio as the primary independent variable, the gradient coefficient and constant coefficient are correlated to the secondary independent variable which is bifurcation angle. Generally, an equation can be written to describe the relation for both near surface flow and near bed flow, which is listed as Equation 4.5 and Equation 4.6:

$$V_{r,NS} = (7.5 \sin 2\theta + 1)\, WH_r - 7.5 \sin 2\theta\,, dimensionless \quad \text{Equation 4.5}$$

$$V_{r,NB} = (8.5 \sin 2\theta + 1)\, WH_r - 8.5 \sin 2\theta\,, dimensionless \quad \text{Equation 4.6}$$

where, $V_{r,NS}$ and $V_{r,NB}$ are flow velocity ratio for near surface flow and near bed flow

WH_r is weir height ratio

Θ is bifurcation angle

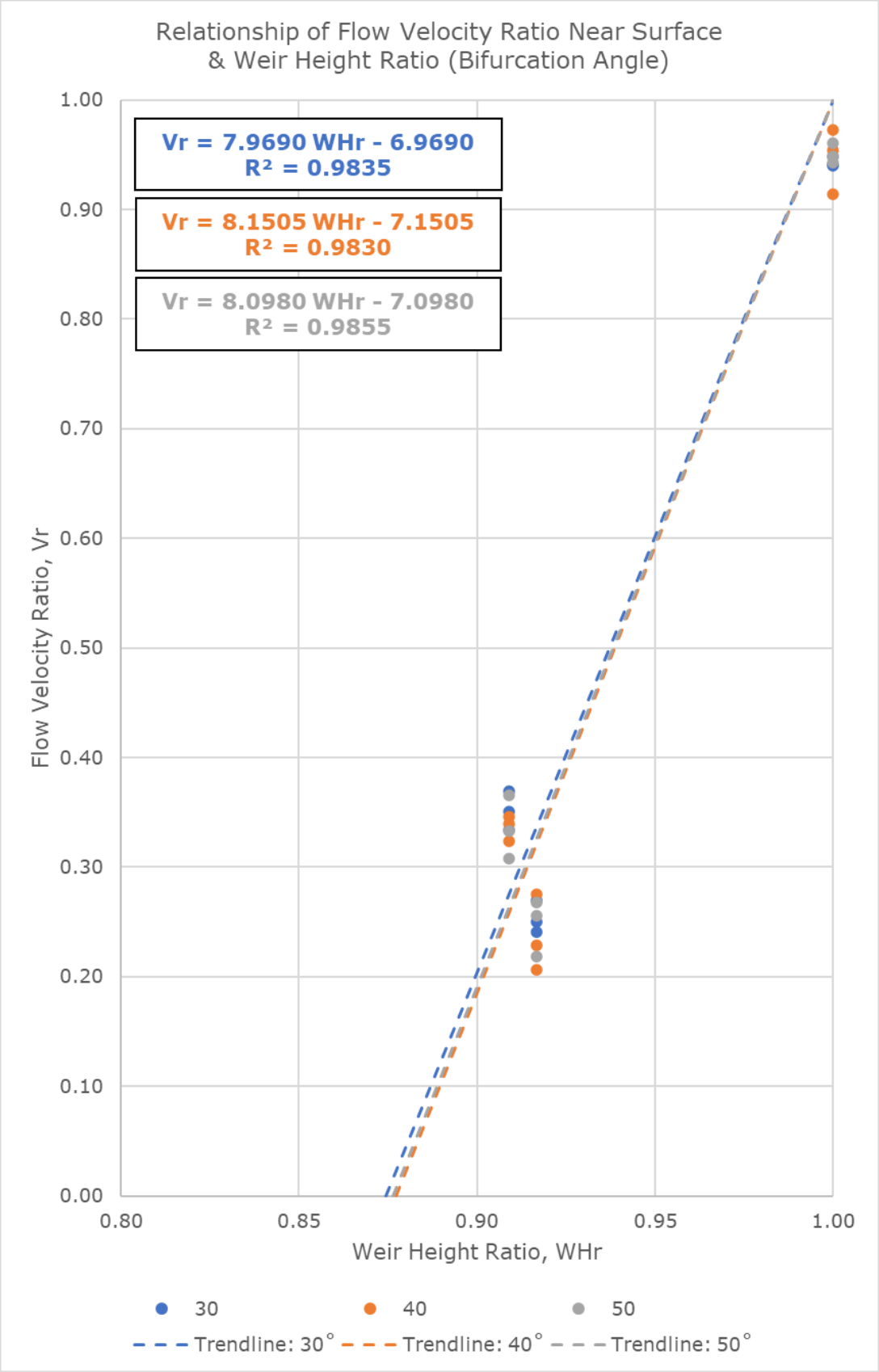


Figure 4.21: Relationship of flow velocity ratio near surface and weir height ratio (Bifurcation angle)

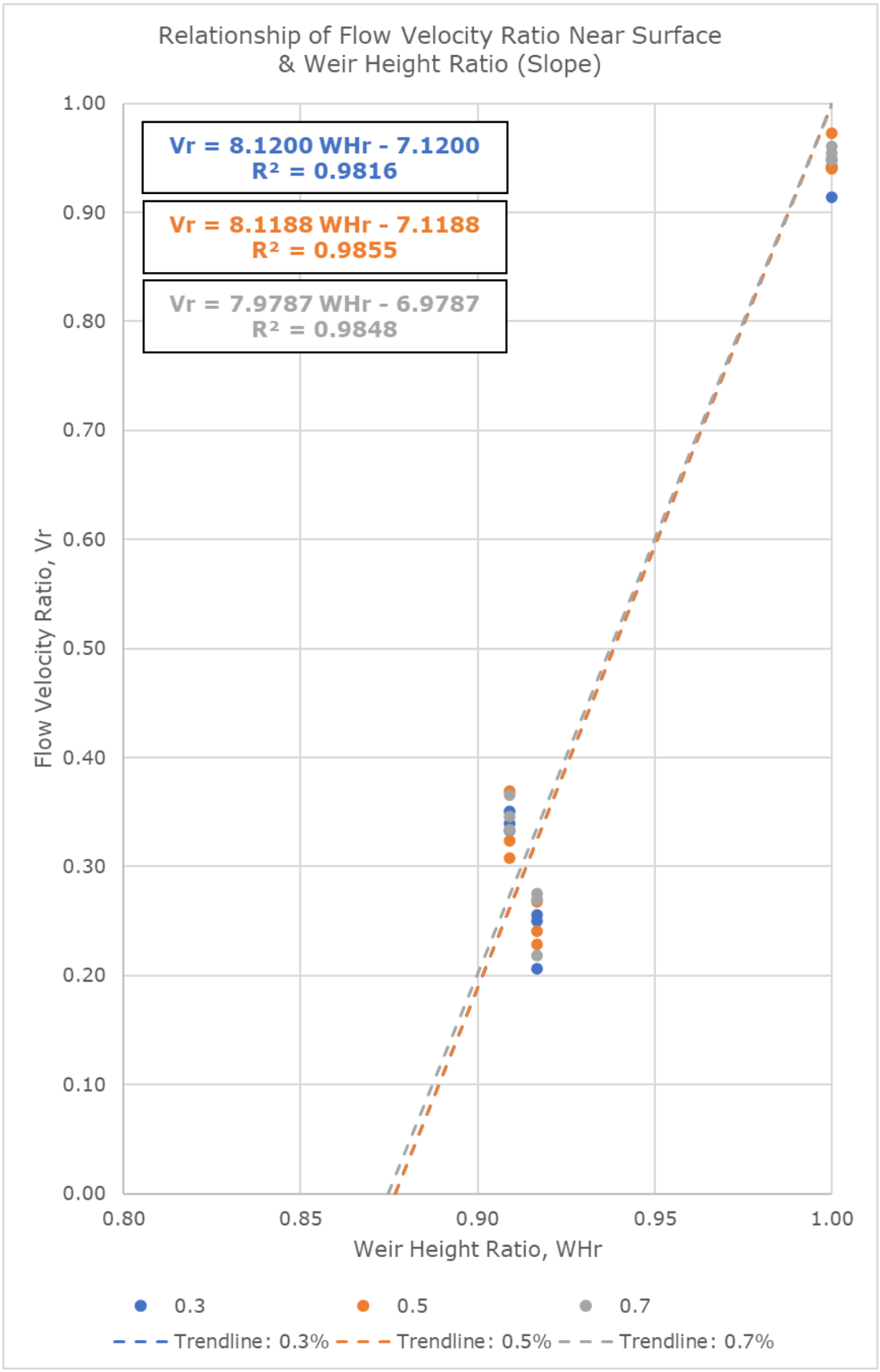


Figure 4.22: Relationship of flow velocity ratio near surface and weir height ratio (Slope)

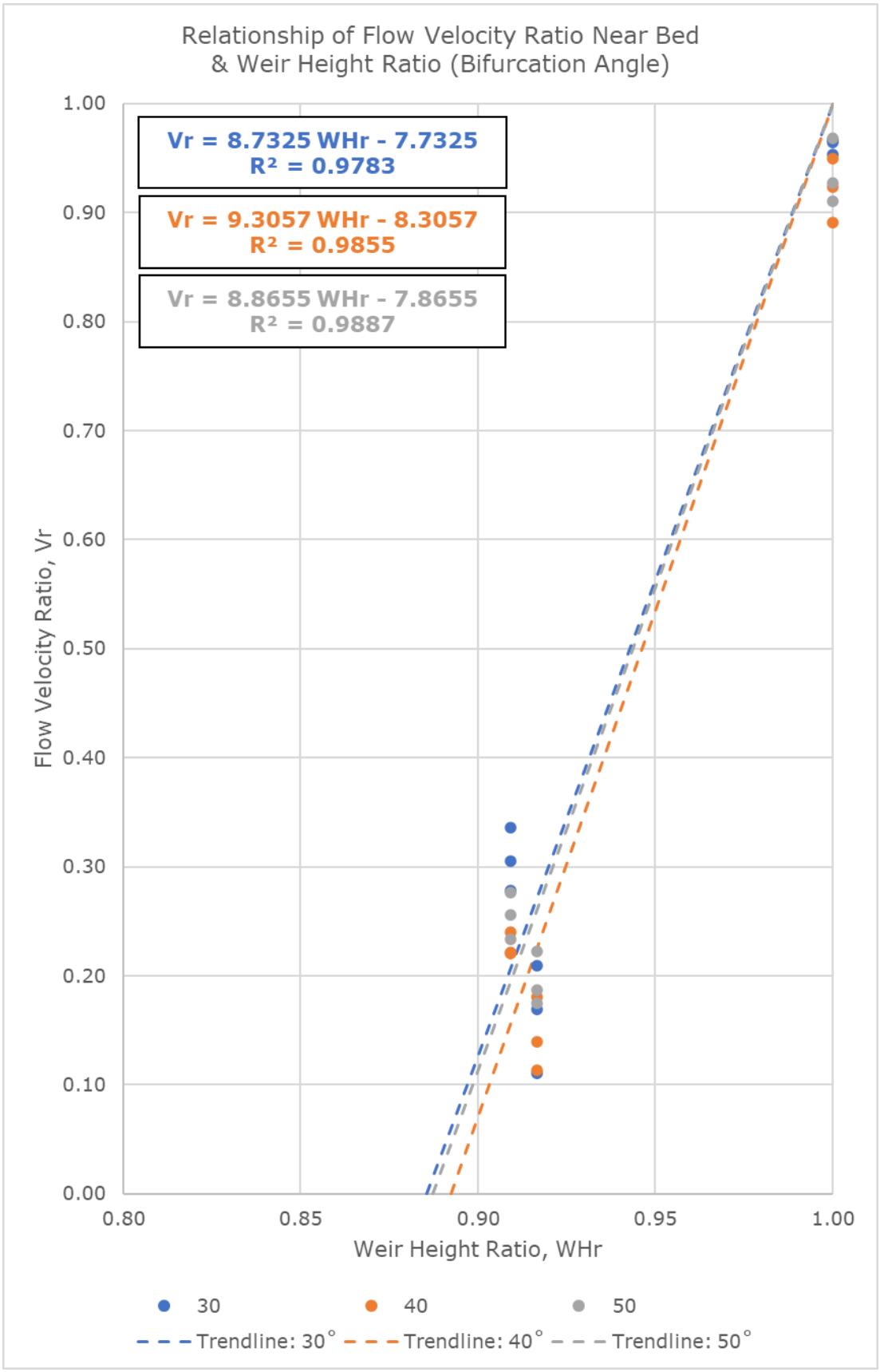


Figure 4.23: Relationship of flow velocity ratio near bed and weir height ratio (Bifurcation angle)

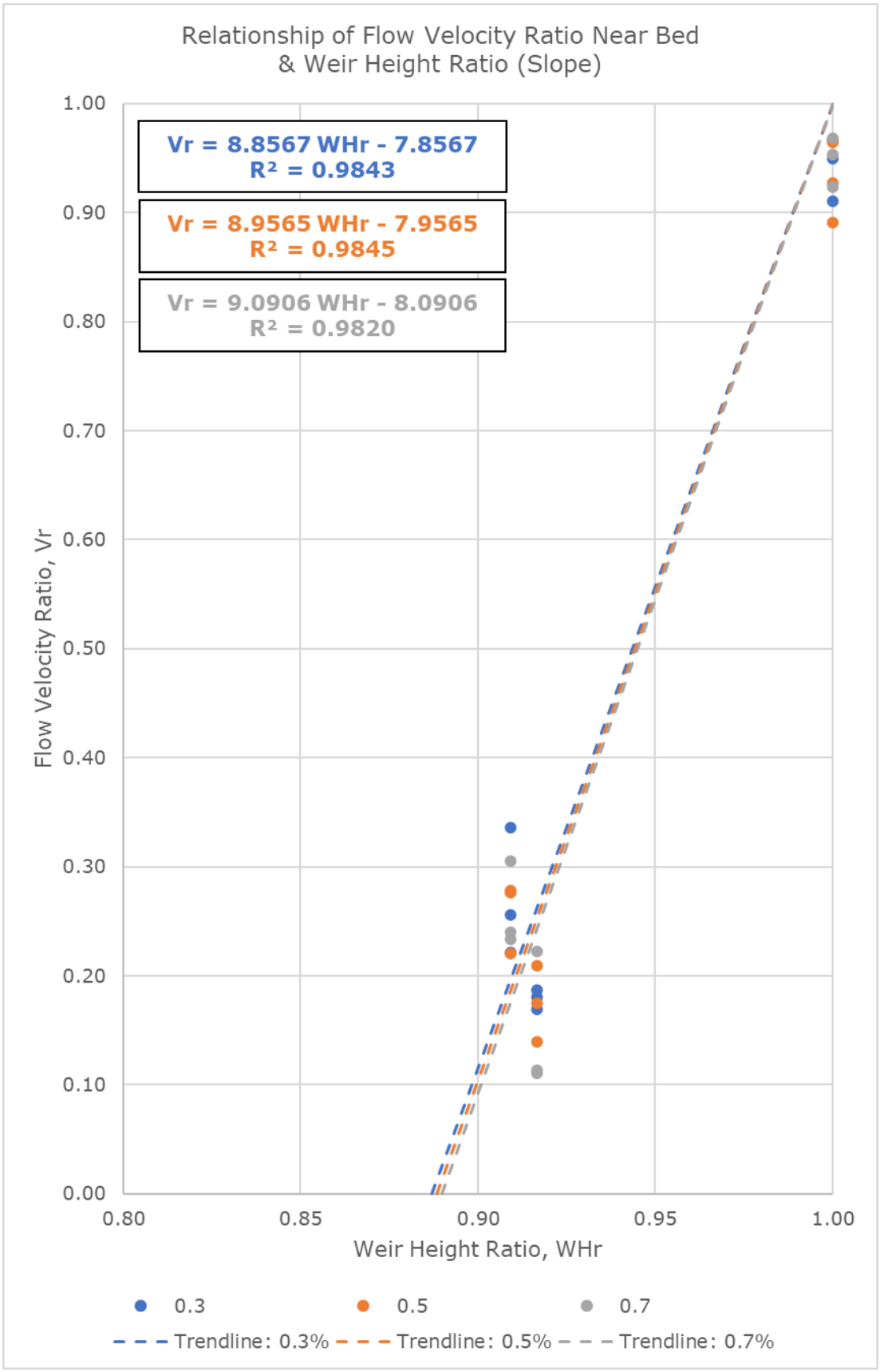


Figure 4.24: Relationship of flow velocity ratio near bed and weir height ratio (Slope)

The coefficient of linear regression is compared between Equation 4.5 and the linear equation in Figure 4.21 for near surface flow. The comparison with various bifurcation angle is summarised in Table 4.19 and plotted in Figure 4.25. As mentioned before, P-value is applied for nonlinear comparison, which is 9.19E-04 and 1.20E-03 for coefficient M and C respectively. Equation 4.5 with lower P-value is a more reflective model than Equation 4.3 (P-value = 0.8776).

Table 4.19: Comparison of coefficient of developed equation with experiment data (Flow velocity ratio near surface flow)

Bifurcation Angle	Developed Equation (Equation 4.5)		Experiment Data (Figure 4.21)	
	M = 7.5 x sin 2Θ + 1	C = -7.5 x sin 2Θ	M	C
0	1.0000	0.0000	NA	NA
10	3.5652	-2.5652	NA	NA
20	5.8209	-4.8209	NA	NA
30	7.4952	-6.4952	7.9690	-6.9690
40	8.3861	-7.3861	8.1505	-7.1505
45	8.5000	-7.5000	NA	NA
50	8.3861	-7.3861	8.0980	-7.0980
60	7.4952	-6.4952	NA	NA
70	5.8209	-4.8209	NA	NA
80	3.5652	-2.5652	NA	NA
90	1.0000	0.0000	NA	NA

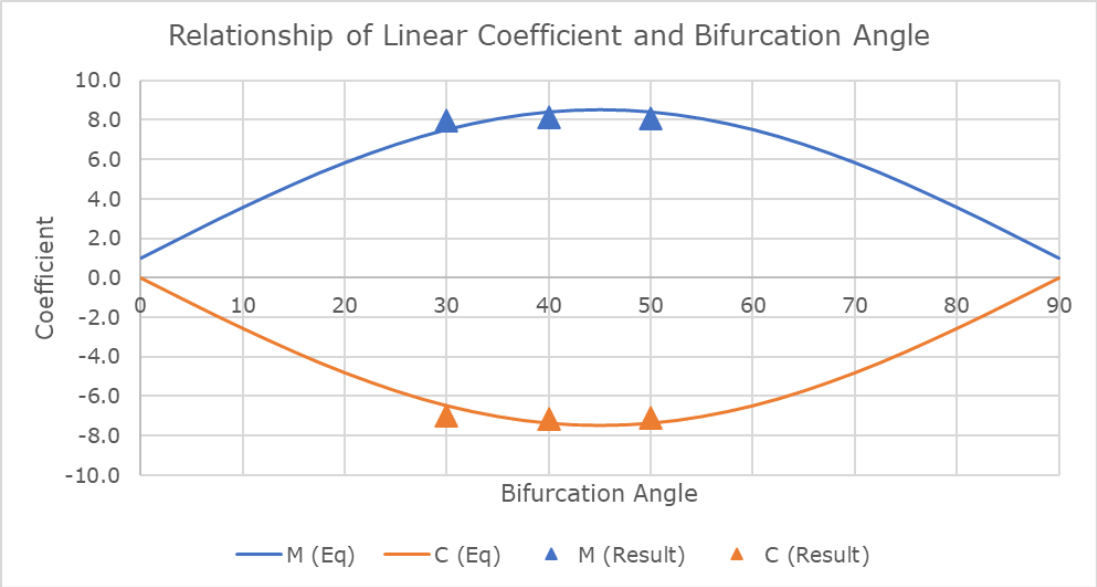


Figure 4.25: Relationship of linear coefficient and bifurcation angle (Flow velocity ratio near surface flow)

Comparison of linear regression for near bed flow is also conducted between Equation 4.6 and Figure 4.23. The comparison with various bifurcation angle is summarised in Table 4.20 and plotted in Figure 4.26. As mentioned before, P-value is applied for nonlinear comparison, which is 7.81E-04 and 9.87E-04 for coefficient M and C respectively. Equation 4.6 with lower P-value is a more reflective model than Equation 4.4 (P-value = 0.6506).

Table 4.20: Comparison of coefficient of developed equation with experiment data (Flow velocity ratio near bed flow)

Bifurcation Angle	Developed Equation (Equation 4.6)		Experiment Data (Figure 4.23)	
	M = 8.5 x sin 2Θ + 1	C = -8.5 x sin 2Θ	M	C
0	1.0000	0.0000	NA	NA
10	3.9072	-2.9072	NA	NA
20	6.4637	-5.4637	NA	NA
30	8.3612	-7.3612	8.7325	-7.7325
40	9.3709	-8.3709	9.3057	-8.3057
45	9.5000	-8.5000	NA	NA
50	9.3709	-8.3709	8.8655	-7.8655
60	8.3612	-7.3612	NA	NA
70	6.4637	-5.4637	NA	NA
80	3.9072	-2.9072	NA	NA
90	1.0000	0.0000	NA	NA

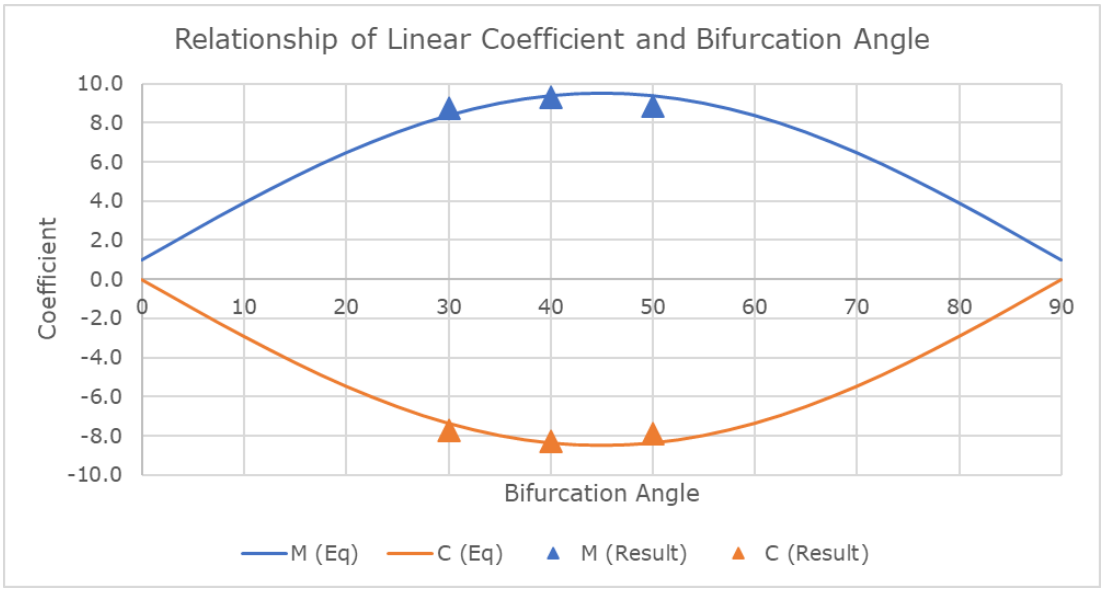


Figure 4.26: Relationship of linear coefficient and bifurcation angle (Flow velocity ratio near bed flow)

According to both developed equations, the impact of WH_r on V_r is less impactful when bifurcation angle is at 0° and 90°, V_r is also directly proportional to WH_r at this moment. The impact of WH_r on V_r is maximum at the condition of 45° bifurcation.

When bifurcation angle is at 45°, the V_r will be -7.5 (NS) and -8.5 (NB) when WH_r is close to zero, this negative shows that the developed equation has significant limitations. Few assumptions are listed to discuss about this issue:

1. The developed equation is not suitable for all range of weir height ratio.
2. Trigonometric function may not be suitable to describe the relationship between bifurcation and weir height ratio.
3. Linear function may not be suitable to describe the relationship between flow velocity ratio and weir height ratio

The Equation 4.5 is plotted in Figure 4.27 (NS) and the Equation 4.6 is plotted Figure 4.28 (NB) with the bifurcation angle that range from 0° to 90°. For both figures, any plotted line on the left of red dotted line is predicted and shall be further verified.

Under the same weir height ratio, the developed equations show the $V_{r,NS}$ is always larger than $V_{r,NB}$ with any bifurcation angle. The Equation 4.5 and Equation 4.6 are further analysed and its relationship can be represented by the Equation 4.7:

$$V_{r,NS} = \frac{7.5 \sin 2\theta + 1}{8.5 \sin 2\theta + 1} V_{r,NB} - \frac{\sin 2\theta}{8.5 \sin 2\theta + 1}, dimensionless \quad \text{Equation 4.7}$$

where, $V_{r,NS}$ and $V_{r,NB}$ are flow velocity ratio for near surface flow and near bed flow

θ is bifurcation angle

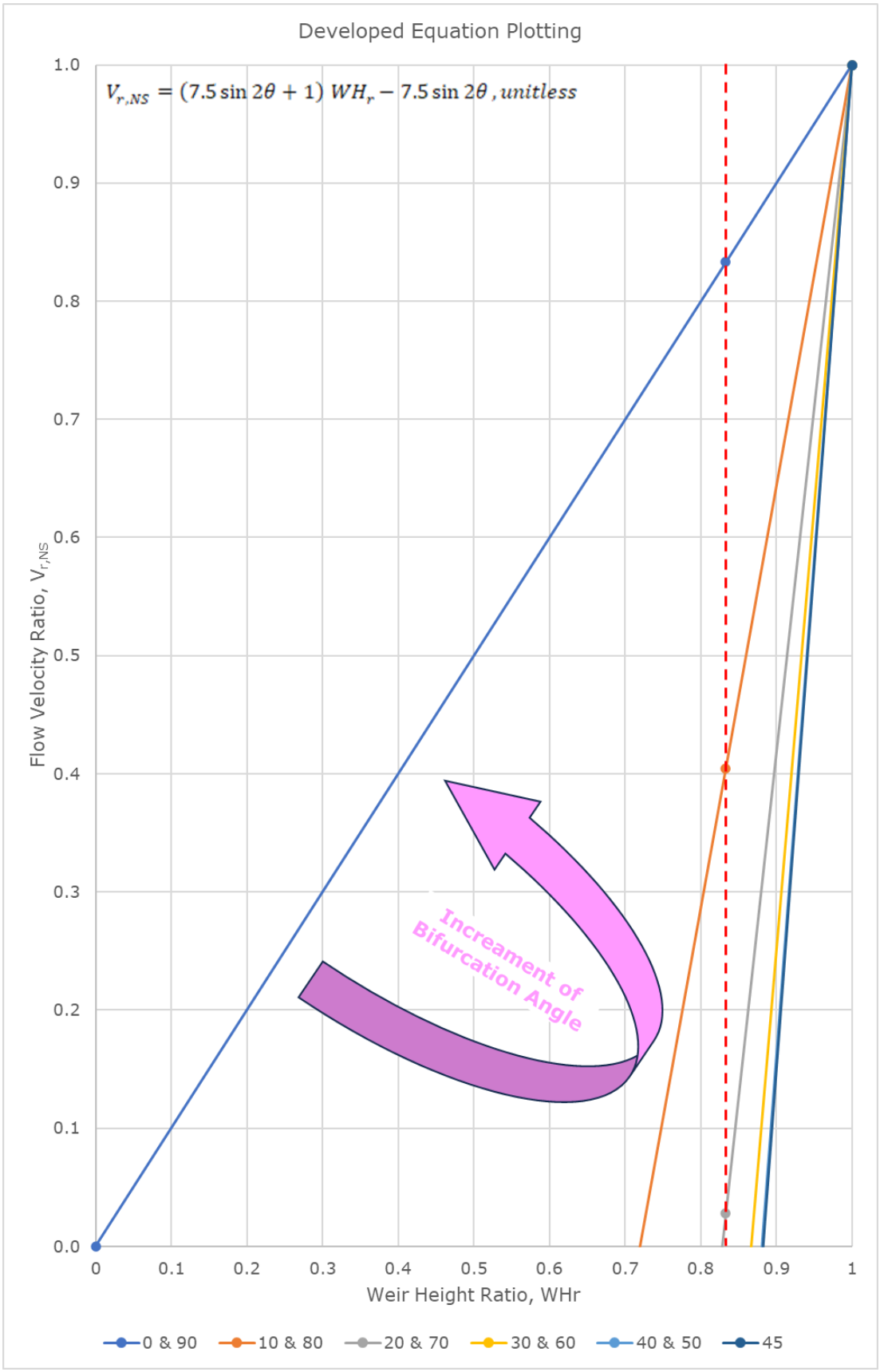


Figure 4.27: Plotting of developed equation (Flow velocity ratio near surface)

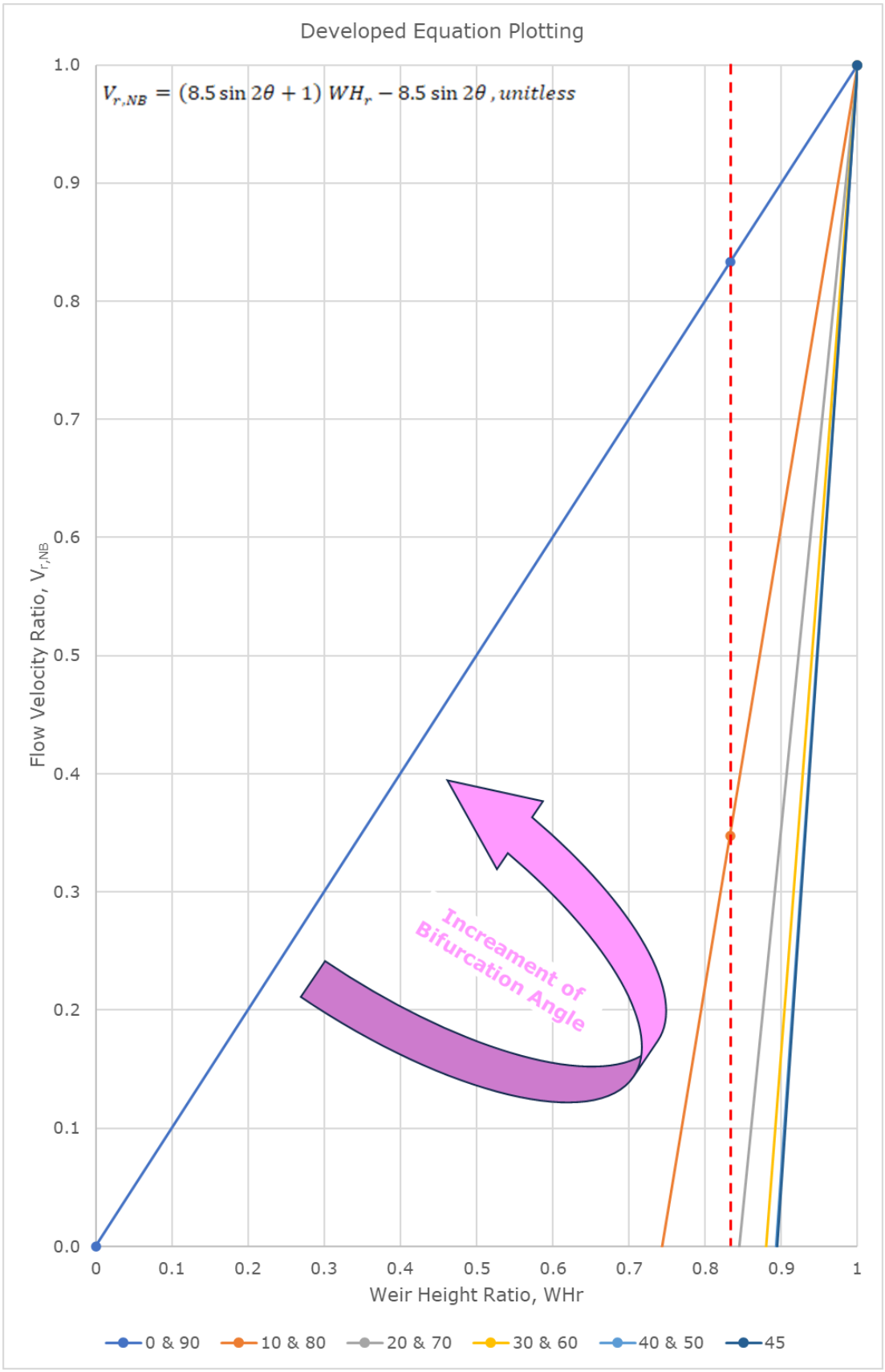


Figure 4.28: Plotting of developed equation (Flow velocity ratio near bed)

4.3.3 Discharge Ratio

Multiple Linear Regression Analysis

MLR analysis is conducted in this section to study the linear relationship between dependent variable (discharge ratio) and independent variables (bifurcation angle, slope, and weir height ratio).

Table 4.21 shows the P-value of bifurcation angle and slope is higher than 0.05, thus, its relationship with discharge ratio is statistically non-significant. With this approach, a multi-linear equation can be written as Equation 4.8:

$$Q_r = 7.6942\, WH_r - 6.7382, dimensionless \quad \text{Equation 4.8}$$

where, Q_r is discharge ratio

WH_r is weir height ratio

Table 4.21: Result of MLR analysis (Discharge ratio)

	Coefficients	Standard Error	t Stat	P-value
Intercept	-6.738193606	0.334710006	-20.13143762	4.19203E-16
Sin Θ	-0.022287142	0.129226304	-0.172465982	0.86457984 (P>0.05)
Slope	0.008916819	0.086027017	0.103651384	0.918344523 (P>0.05)
Weir Height Ratio	7.694228314	0.341093621	22.55752624	3.45577E-17

Linear Regression Analysis by Grouping

Similarly, linear regression analysis by grouping with graph plotting is conducted in this section with weir height ratio as the primary independent variable.

To study the relationship between discharge ratio and weir height ratio, linear regression line is plotted to fit with 3 groups of bifurcation angle in Figure 4.29 and 3 groups of slope in Figure 4.30, both linear regressions are calculated with intersection at coordinate {1,1}, as the line should theoretically pass through the coordinate {1,1}.

Coefficient of determination (R^2) in Figure 4.29 and Figure 4.30 show the weir height ratio is strongly correlated ($R^2 > 0.95$) with discharge ratio as an independent variable in linear regression. The 3 linear equations in Figure 4.29 show bifurcation angle is associated with some trigonometry properties. In contrast, the 3 linear regressions in Figure 4.30 show similar coefficient of linear regression, thus, no tendency can be determined for slope as an independent variable, a similar finding to MLR analysis. All linear regression coefficients are summarised in Table 4.22.

Table 4.22: Coefficient of linear regression (Discharge ratio)

Bifurcation Angle	Figure 4.29	
	M	C
30	8.1627	-7.1627
40	8.5263	-7.5263
50	8.2389	-7.2389
Slope	Figure 4.30	
	M	C
0.3	8.2986	-7.2986
0.5	8.3281	-7.3281
0.7	8.3013	-7.3013

In the linear equation (grouped by bifurcation angle) with weir height ratio as the primary independent variable, the gradient and constant coefficient are correlated to the secondary independent variable which is bifurcation angle. The gradient coefficient is related to the sine function, and the constant coefficient is related to the cosine function. Generally, an equation can be written to describe the relation, which is listed as Equation 4.9:

$$Q_r = (8.0 \sin 2\theta + 1)\, WH_r - 8.0 \sin 2\theta \,, dimensionless \quad \text{Equation 4.9}$$

where, Q_r is discharge ratio

WH_r is weir height ratio

Θ is bifurcation angle

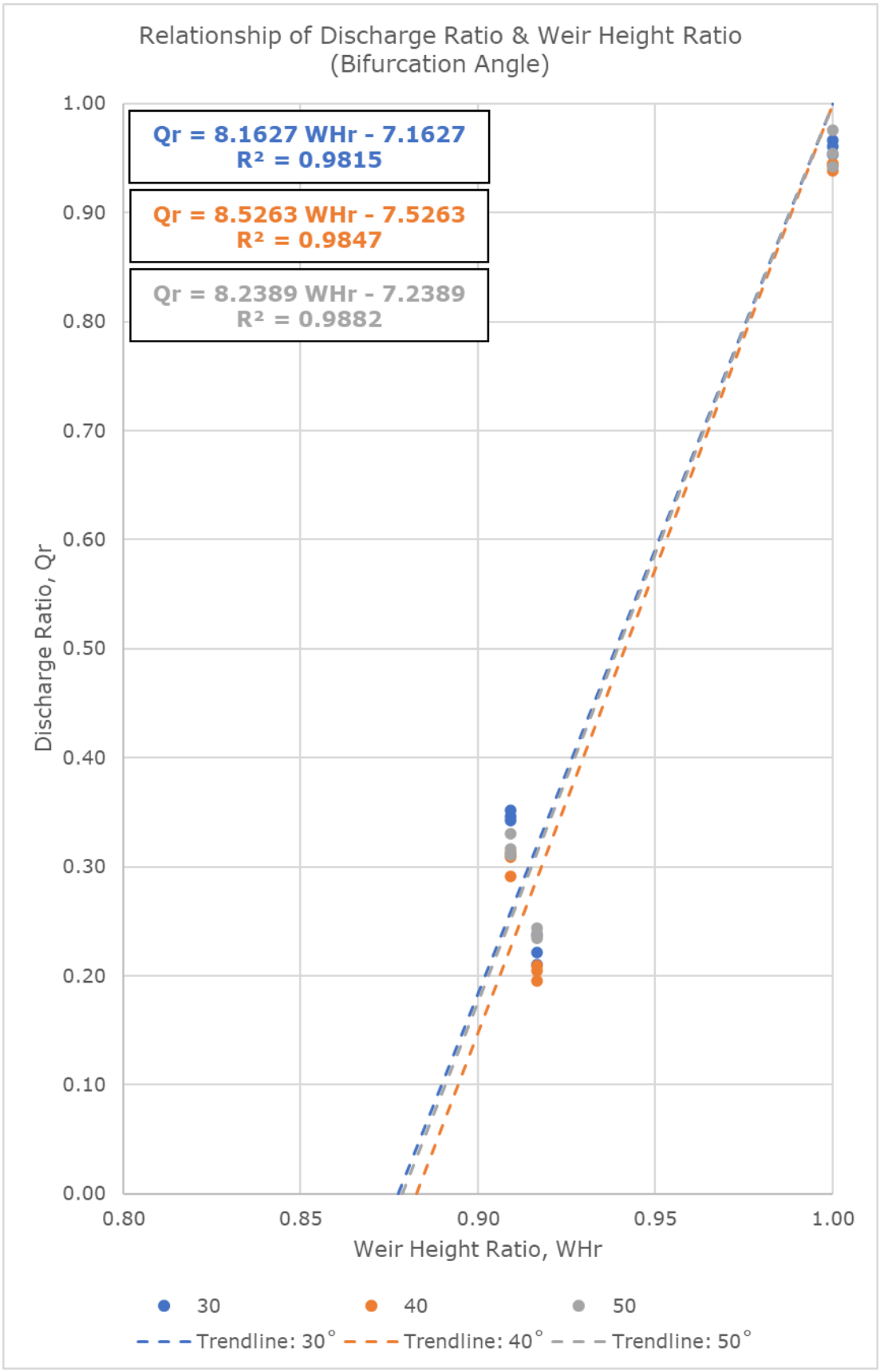


Figure 4.29: Relationship of discharge ratio and weir height ratio (Bifurcation angle)

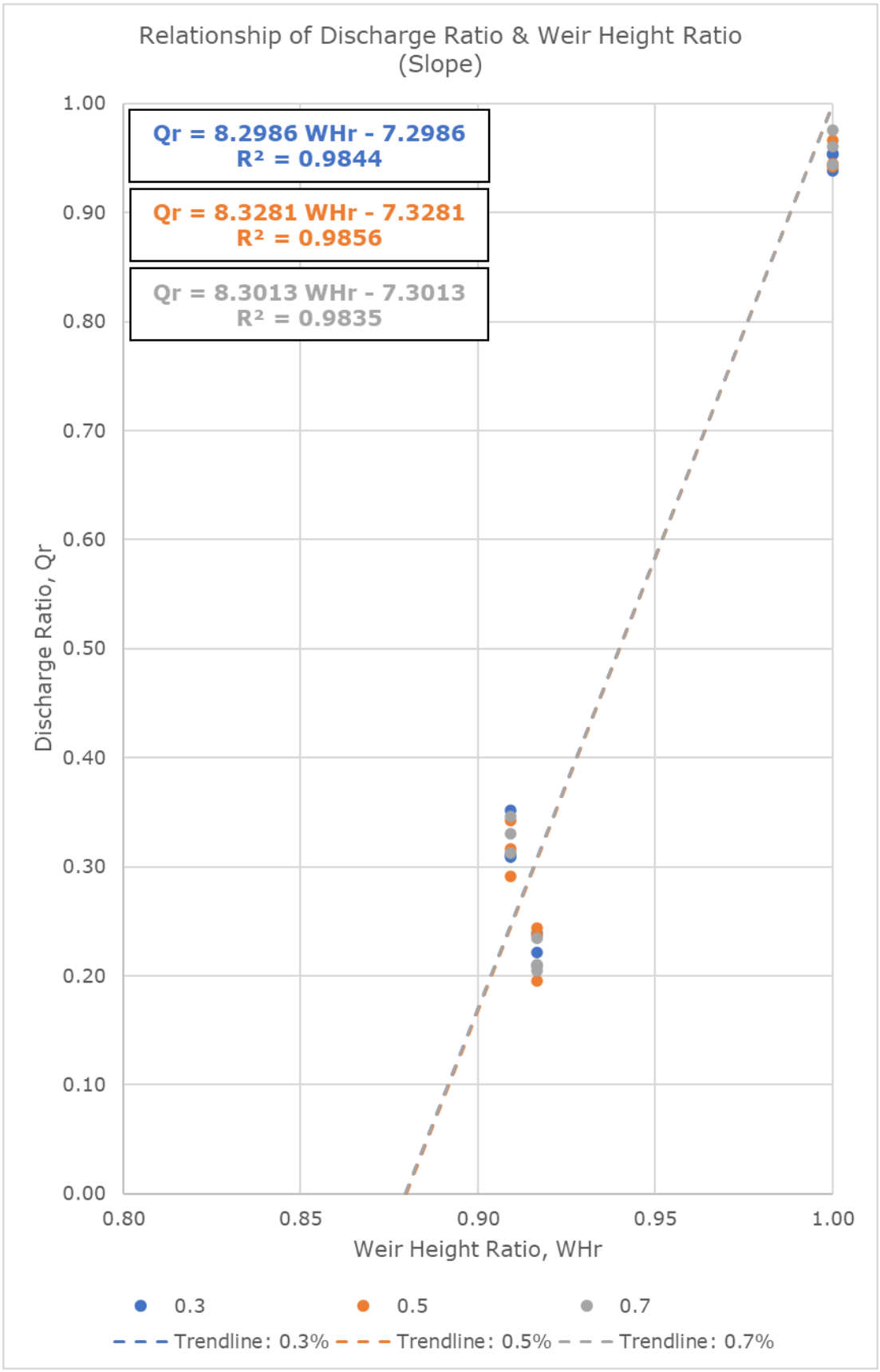


Figure 4.30: Relationship of discharge ratio and weir height ratio (Slope)

The coefficient of linear regression is compared between Equation 4.9 and the linear equation in Figure 4.29. The comparison with various bifurcation angle is summarised in Table 4.23 and plotted in Figure 4.31. As mentioned before, P-value is applied for nonlinear comparison, which is 8.91E-04 and 1.14E-03 for coefficient M and C respectively. Equation 4.9 with lower P-value is a more reflective model than Equation 4.8 (P-value = 0.8646).

Table 4.23: Comparison of coefficient of developed equation with experiment data (Discharge ratio)

Bifurcation Angle	Developed Equation (Equation 4.9)		Experiment Data (Figure 4.29)	
	M = 8.0 x sin 2Θ + 1	C = -8.0 x sin 2Θ	M	C
0	1.0000	0.0000	NA	NA
10	3.7362	-2.7362	NA	NA
20	6.1423	-5.1423	NA	NA
30	7.9282	-6.9282	8.1627	-7.1627
40	8.8785	-7.8785	8.5263	-7.5263
45	9.0000	-8.0000	NA	NA
50	8.8785	-7.8785	8.2389	-7.2389
60	7.9282	-6.9282	NA	NA
70	6.1423	-5.1423	NA	NA
80	3.7362	-2.7362	NA	NA
90	1.0000	0.0000	NA	NA

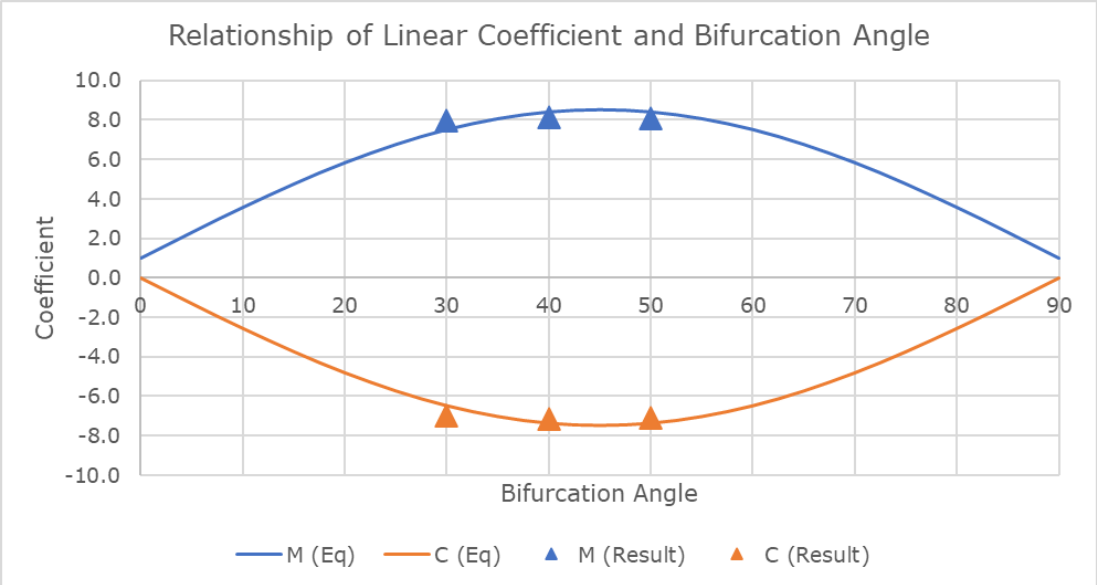


Figure 4.31: Relationship of linear coefficient and bifurcation angle (Discharge ratio)

According to the developed equation, the impact of WH_r on Q_r is less impactful when bifurcation angle is at 0° and 90°, Q_r is also directly proportional to WH_r at this moment. The impact of WH_r on Q_r is maximum at the condition of 45° bifurcation.

When bifurcation angle is at 45°, the V_r will be -8.0 (NS) when WH_r is close to zero, this negative shows that the developed equation has significant limitations. Few assumptions are listed to discuss about this issue:

1. The developed equation is not suitable for all range of weir height ratio.
2. Trigonometric function may not be suitable to describe the relationship between bifurcation and weir height ratio.
3. Linear function may not be suitable to describe the relationship between discharge ratio and weir height ratio

The Equation 4.9 is plotted in Figure 4.32 with the bifurcation angle that range from 0° to 90°. Any plotted line on the left of red dotted line is predicted and shall be further verified.

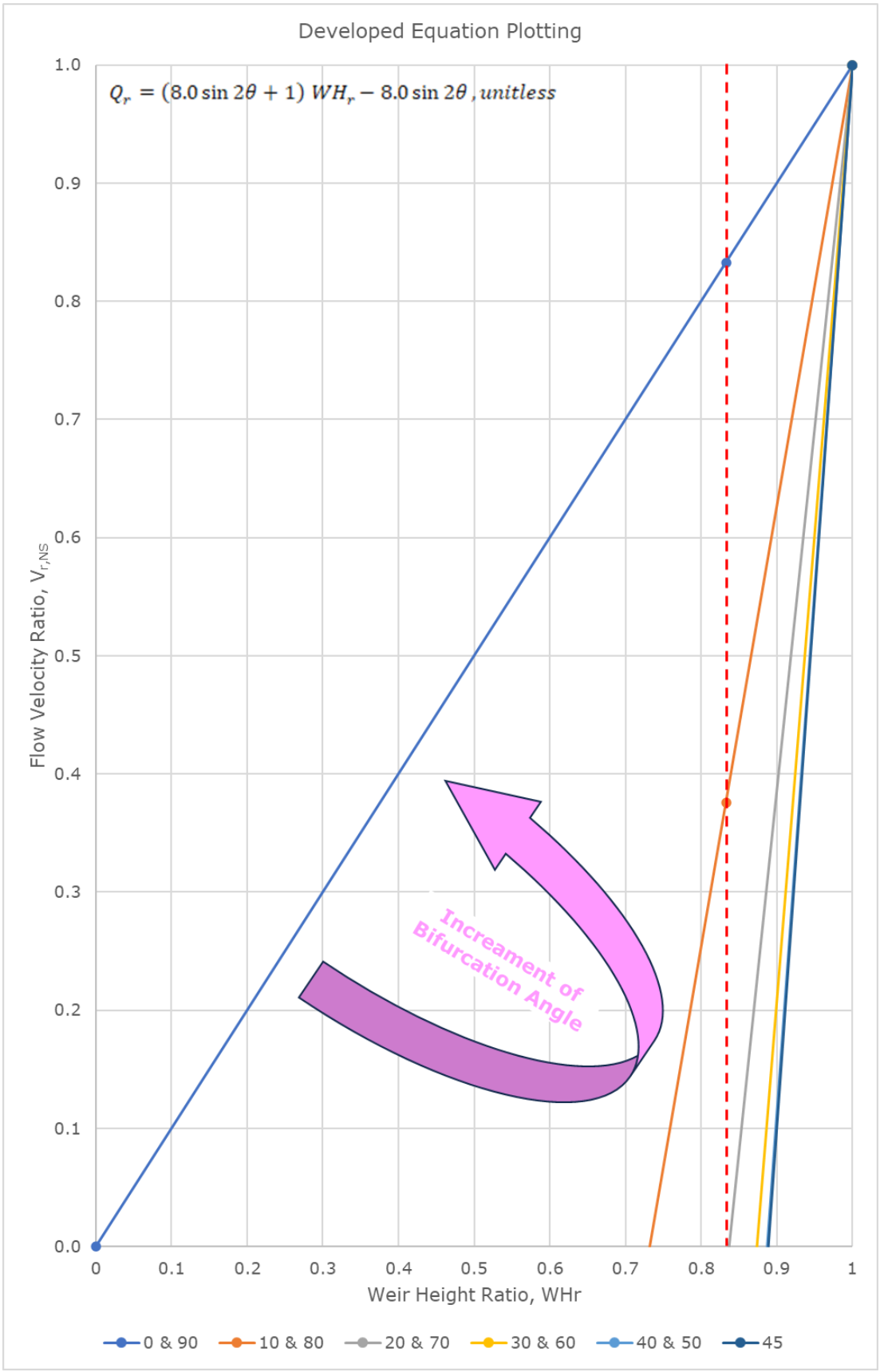


Figure 4.32: Plotting of developed equation (Discharge ratio)

Similar experiment setup was conducted by Thomas et al. (2011) with more flow discharge. The value is converted to cm^3/s for easier comparison, which is 5970 to 7190 cm^3/s with mean of 6680 cm^3/s and standard deviation of 263 cm^3/s. This is about 10 times more discharge than the experiment in this study. The weir height ratio and discharge ratio from this study and Thomas et al. (2011) are tabulated in Table 4.24.

To conduct a comparison between two set of data, both data are plotted in Figure 4.33 and linear regression analysis is conducted for both data. The linear equation which calculated based on Thomas et al. (2011) is listed as Equation 4.10. However, Thomas et al. (2011) proposed a function of best fit at power of 1.38 to represent the relationship, this is listed as Equation 4.11.

$$Q_r = 1.25WH_r - 0.27, dimensionless \quad \text{Equation 4.10}$$

$$Q_r = {WH_r}^{1.38}, dimensionless \quad \text{Equation 4.11}$$

where, Q_r is discharge ratio

WH_r is weir height ratio

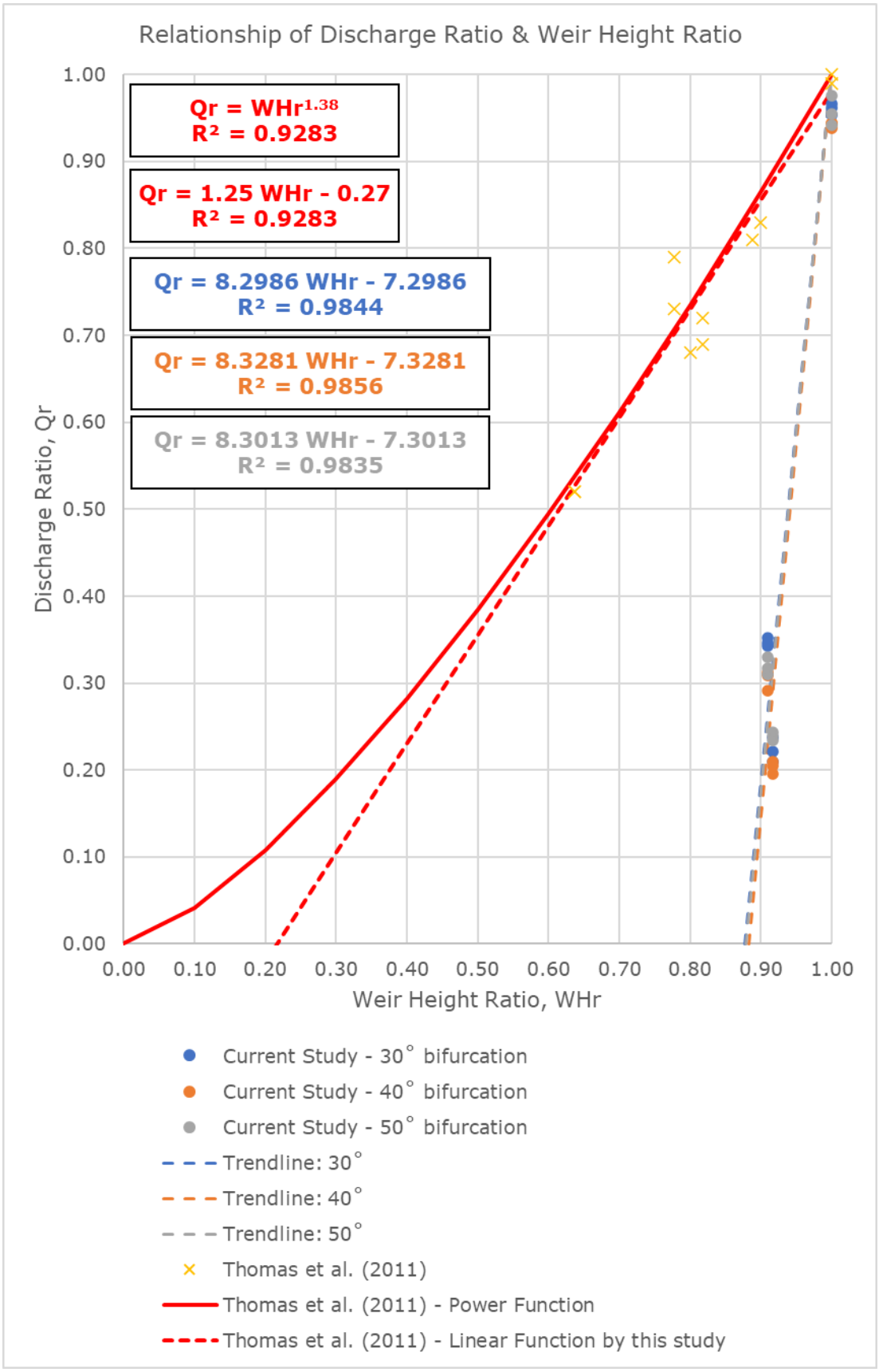


Figure 4.33: Relationship between discharge ratio and weir height ratio (Comparison)

Table 4.24: Comparison of discharge ratio with Thomas et al. (2011)

Study	Experiment Run	Left Weir Height, mm	Right Weir Height, mm	Weir Height Ratio	Discharge Ratio
Current Study	30_03_5050	50	50	1.000	0.953
	30_05_5050	50	50	1.000	0.966
	30_07_5050	50	50	1.000	0.961
	40_03_5050	50	50	1.000	0.938
	40_05_5050	50	50	1.000	0.945
	40_07_5050	50	50	1.000	0.944
	50_03_5050	50	50	1.000	0.954
	50_05_5050	50	50	1.000	0.942
	50_07_5050	50	50	1.000	0.976
	30_03_5560	55	60	0.917	0.221
	30_05_5560	55	60	0.917	0.237
	30_07_5560	55	60	0.917	0.210
	40_03_5560	55	60	0.917	0.209
	40_05_5560	55	60	0.917	0.195
	40_07_5560	55	60	0.917	0.205
	50_03_5560	55	60	0.917	0.239
	50_05_5560	55	60	0.917	0.244
	50_07_5560	55	60	0.917	0.234
	30_03_5055	50	55	0.909	0.352
	30_05_5055	50	55	0.909	0.343
	30_07_5055	50	55	0.909	0.346
	40_03_5055	50	55	0.909	0.309
	40_05_5055	50	55	0.909	0.291
	40_07_5055	50	55	0.909	0.312
	50_03_5055	50	55	0.909	0.310
	50_05_5055	50	55	0.909	0.317
	50_07_5055	50	55	0.909	0.330
Thomas et al. (2011)	A-L35R45	35	45	0.778	0.79
	A-L35R55	35	55	0.636	0.52
	A-L40R45	40	45	0.889	0.81
	A-L40R50	40	50	0.800	0.68
	A-L45R45	45	45	1.000	1.00
	A-L45R50	45	50	0.900	0.83
	A-L45R55	45	55	0.818	0.69
	B-L35R45	35	45	0.778	0.73
	B-L35R55	35	55	0.636	0.52
	B-L45R45	45	45	1.000	0.99
	B-L45R55	45	55	0.818	0.72

4.3.4 Threshold of Weir Height Ratio

During the experiment, flow was fully conveyed to left tributary when weir height combination is 50:60 (WH_r = 0.833), discharge was zero at the right tributary. This had occurred at each experiment run regardless of bifurcation angle and slope. For simplification of discussion, this effect is named as threshold of weir height ratio (T_{WHR}), which is defined as the bottom limit of weir height ratio when all flow conveys to main channel and the flow in secondary channel is completely stagnated.

By observation during the experiment setup stage, the range of threshold value in this study shall be between 0.833 and 0.909, and not equal to 0.909.

In theoretical aspect, T_{WHR} can be determined by calculating the WH_r when V_r or Q_r is zero. Thus, any developed equations from Section 4.3.2 and Section 4.3.3 are studied for T_{WHR}.

The MLR analysis on flow velocity ratio from Section 4.3.2 shows the threshold value of 0.874 (Equation 4.3) and 0.879 (Equation 4.4) for near surface and near bed flow respectively. In the linear regression analysis by grouping section, the analysis shows the T_{WHR} has different value with different bifurcation angle. T_{WHR} can be graphically determined from Figure 4.27 (NS) and Figure 4.28 (NB) when the line intersects with V_r =0.

Like flow velocity, the T_{WHR} that is based on MLR analysis on discharge ratio is 0.876 (Equation 4.8). The equation of discharge ratio (Equation 4.9) has the same properties as velocity ratio (Equation 4.5 and Equation 4.6), similarly, T_{WHR} can be graphically determined from Figure 4.32 with any bifurcation angle setup at Q_r =0.

The TWHR calculated by flow velocity ratio and discharge ratio are summarised in Table 4.25 and illustrated in Figure 4.34 and Figure 4.35 for comparison.

Table 4.25: Summary of threshold of weir height ratio

Bifurcation Angle, °	From Flow Velocity Ratio		From Discharge Ratio
	Near Surface	Near Bed	
Multiple Linear Regression Analysis			
For bifurcation angle between 30 to 50	0.874	0.879	0.876
Linear Regression Analysis by Grouping			
0	0.000	0.000	0.000
10	0.720	0.720	0.732
20	0.828	0.828	0.837
30	0.867	0.867	0.874
40	0.881	0.881	0.887
45	0.882	0.895	0.889
50	0.881	0.881	0.887
60	0.867	0.867	0.874
70	0.828	0.828	0.837
80	0.720	0.720	0.732
90	0.000	0.000	0.000

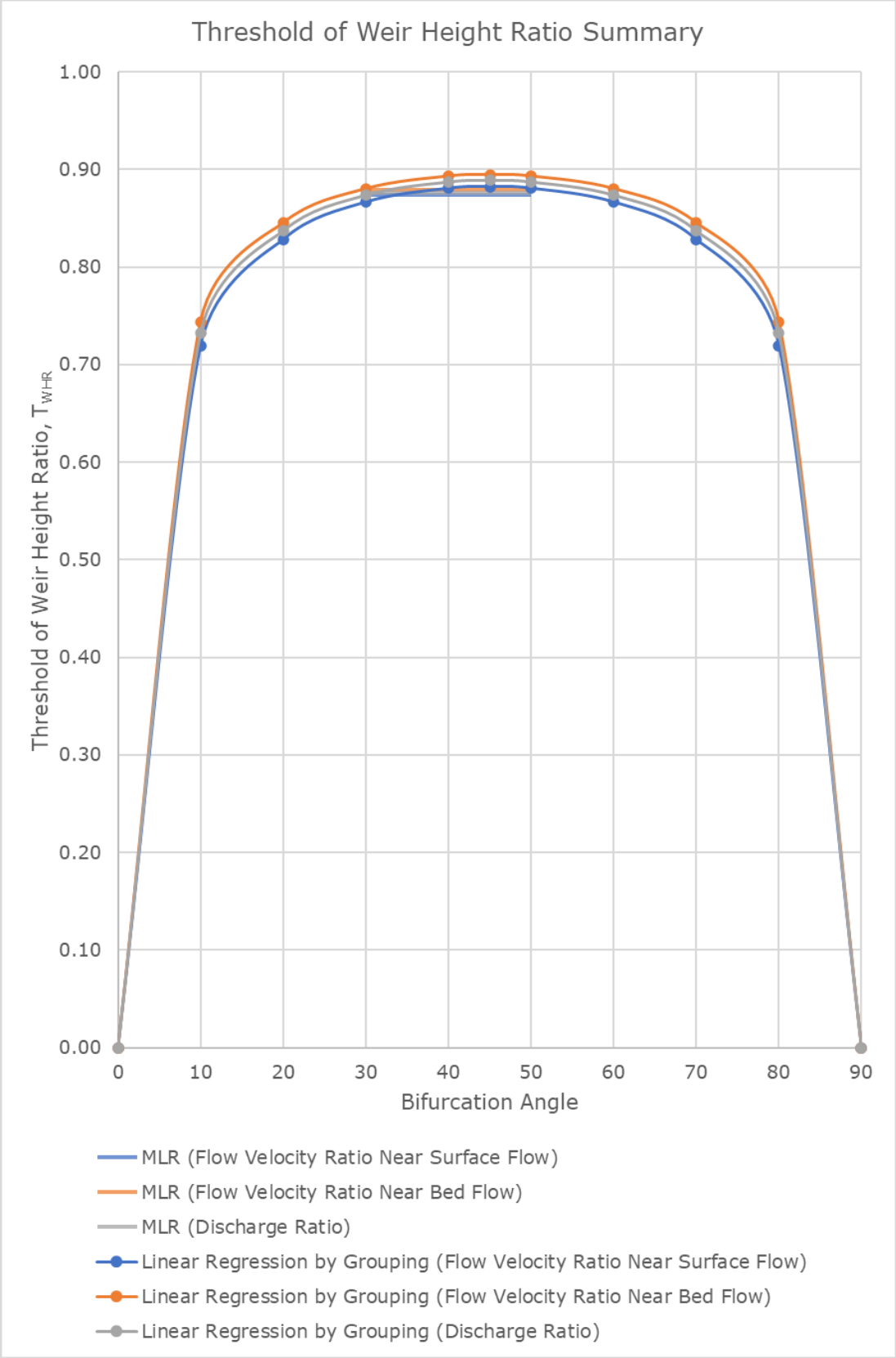


Figure 4.34: Threshold of weir height ratio summary

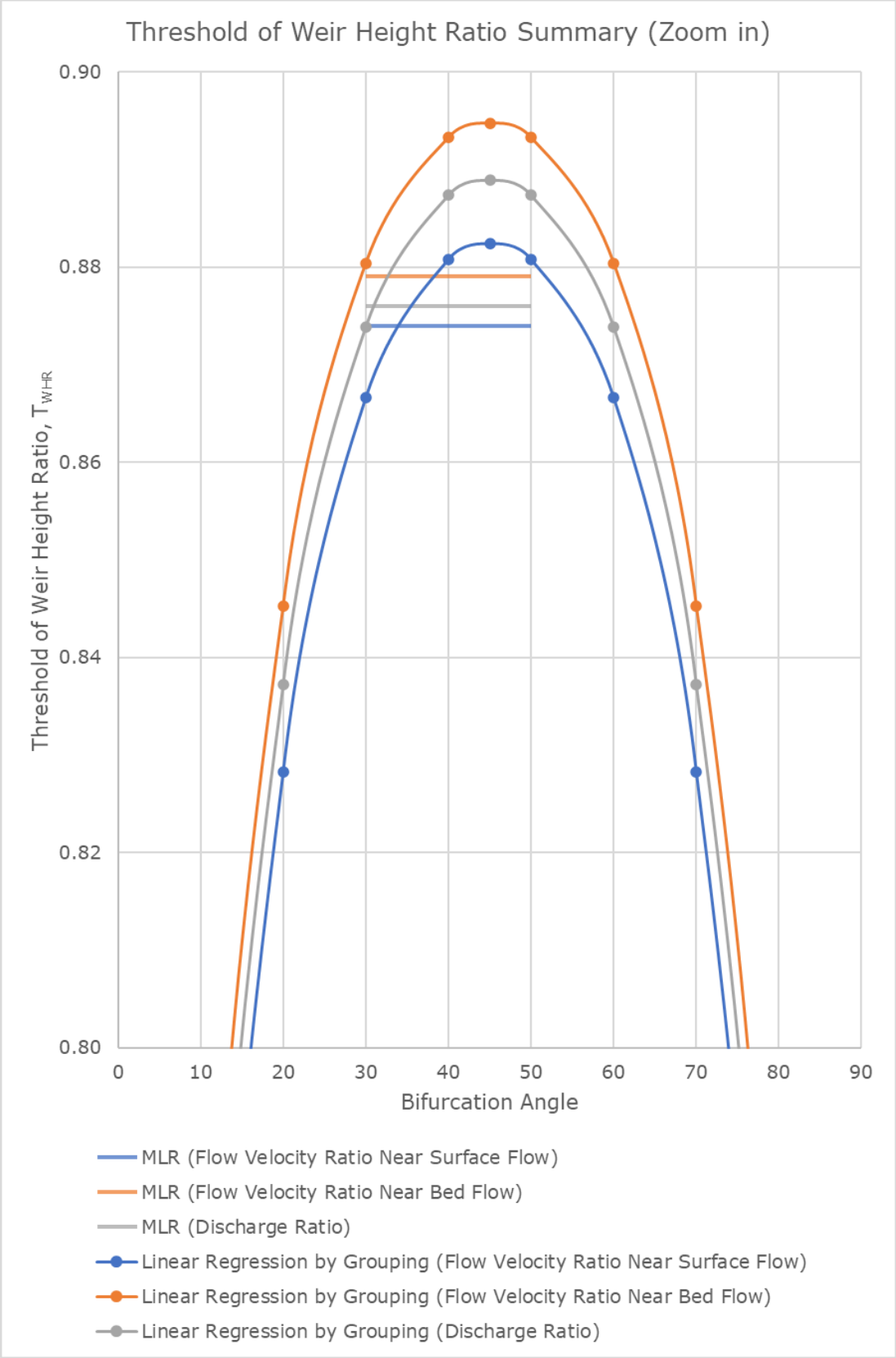


Figure 4.35: Threshold of weir height ratio summary (Zoom in)

Equation 4.11 is the proposed equation (power function) from Thomas et al. (2011). One mathematical property of power function with coefficient value of 1 is the y-axis interception is located at origin, which represents the discharge ratio is zero whenever weir height ratio is zero. The linear equation (Equation 4.10) which based on Thomas et al. (2011) shows a threshold value of 0.216, while the threshold value of this study is ranged from 0.867 to 0.895.

The finding of threshold effect from this study contradicts the proposed equation by Thomas et al. (2011) and proposed equation by this study which is based on result from Thomas et al. (2011).

Compared to Thomas et al. (2011), this study was conducted with 10 times lower flow discharge, and the length of distributary is slightly shorter. The width of upstream and tributary channel is the same for both experiments. Without further experiment, 3 hypotheses are suggested to explain this contradiction**:**

1. Threshold effect may be happening below certain discharge or Froude number.
2. Threshold effect may be happening if the weir is located too close to the point of bifurcation.
3. Discharge at upstream is suspected as the key factor on the threshold of weir height ratio, discharge at upstream is inversely proportional to threshold value.

Froude number is a dimensionless parameter related to discharge. To analyse the relationship between discharge, discharge ratio, and weir height ratio, Froude number may be another option, as it is a dimensionless parameter like discharge ratio and weir height ratio.

4.4 Summary of Findings

In summary, water depth ratio (D_r), flow velocity ratio (V_r), and discharge ratio (Q_r) are correlated to bifurcation angle (Θ) and weir height ratio (WH_r). Slope (Δ) is not the main factor for any ratio, however, it does affect the flow water depth, flow velocity, and discharge. The threshold of weir height ratio (T_{WHR}) is suspected to be influenced by discharge and Froude number of upstream in an inversely proportional relationship.

The relationship between each ratio and parameters are illustrated in Figure 4.36. Control variable (light pink box) is the fundamental compartment to manipulate the experiment with different setup. The light blue box is the measured parameter from the experiment runs. The dark blue which are weir height ratio, discharge and Froude number, these are calculated from the control variables and measured parameters. Dimensionless factors (light green) are the designed factors to study the hydraulic dynamic processes of symmetrical bifurcation with various control variables. Threshold (orange) is the limit of weir height ratio; this value varies with different conditions.

The arrow lines in Figure 4.36 are demonstrating the relationship, which the colour indicates:

1. Blue arrow: A calculation with standard formula.
2. Orange arrow: Relationship can be observed without developed equation.
3. Green arrow: Relationship and equation are discovered.
4. Red arrow: Hypothetically related with insufficient data to support.

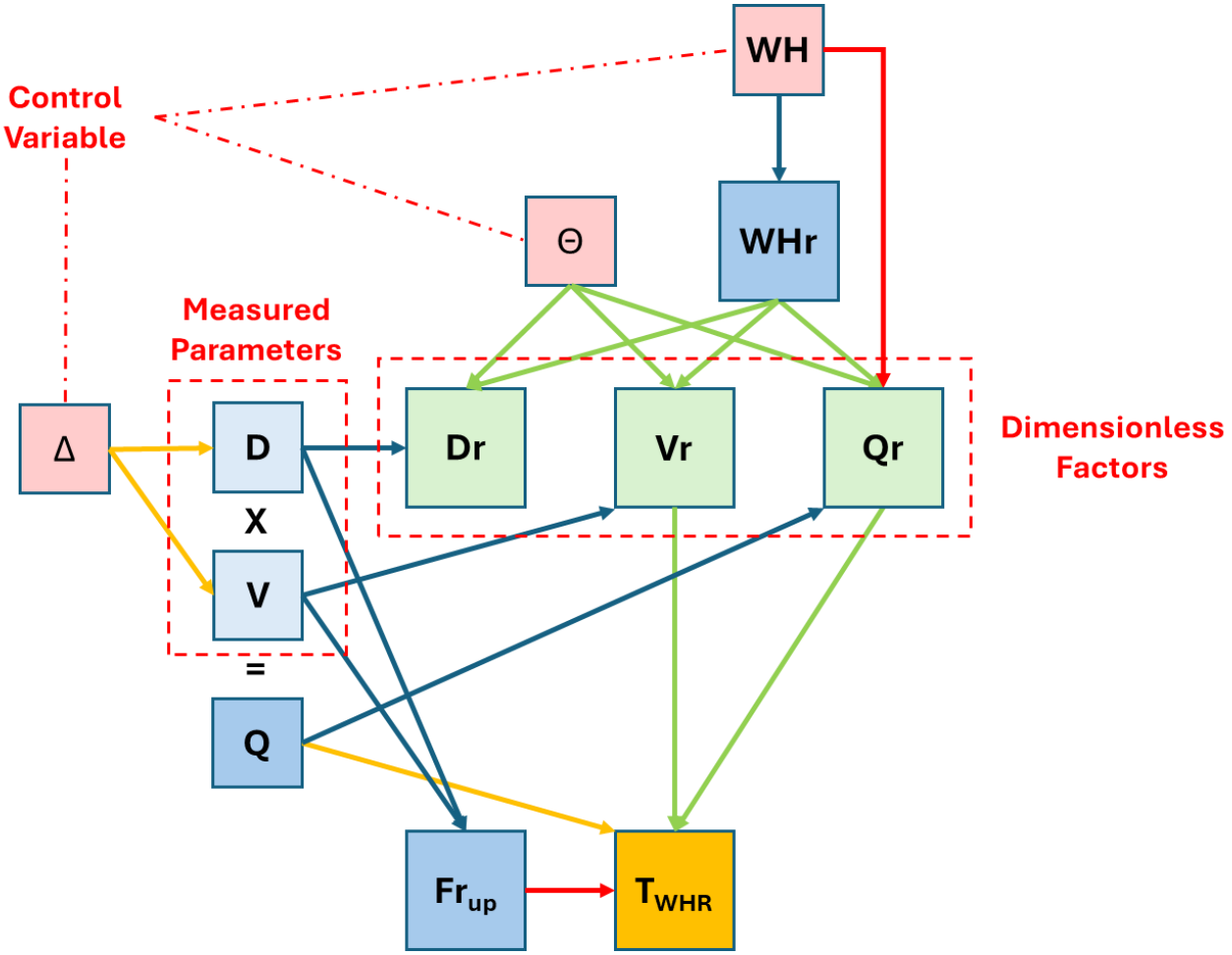


Figure 4.36: Relationship of ratio and parameters

Chapter 5 Numerical Modelling of Channel Bifurcation

5.1 Introduction

To extend the range of control parameters designated in the physical modelling study (Chapter 4), a numerical model was developed to simulate the channel bifurcation with different conditions. In this chapter, discharge ratio (Q_r) is the primary dimensionless factor with 3 control parameters: bifurcation angle (Θ), slope (Δ), and weir height ratio (WH_r). This chapter is mainly a discussion of the findings based on discharge ratio. Furthermore, threshold of weir height ratio is analysed as the key finding in this study. Further comparison between physical modelling and numerical modelling is conducted in this study.

Section 5.2 summarises the result outcome of discharge from numerical simulation. Section 5.3 presents the dimensionless factor analysis in 3 aspects, which are MLR analysis, simple linear regression analysis by grouping of weir height, and threshold of weir height ratio. The comparison of dimensionless factor analysis between physical modelling and numerical modelling is conducted in Section 5.4.

5.2 Simulation of Channel Bifurcation

Discharge of left and right tributary was extracted from the result file of numerical modelling. These results are summarised and plotted in Appendix B. Figure 5.1 (A: summary of result; B: simulated discharge; C: discharge ratio) shows an example of numerical simulation result.

A general observation on the extracted discharge is fluctuation in the discharge value; this can be found in both the left and right tributaries. During the first 40 seconds, the fluctuation is expected as all numerical modelling requires some time to stabilise from the initial condition. The fluctuation after the 40th second is generally smaller compared to the first 40 seconds. However, this is an indicator of the slight instability of the numerical model, which can be further improved.

Overall, relatively significant instability can be observed from the simulations when the smallest slope (0.3%) is adopted.

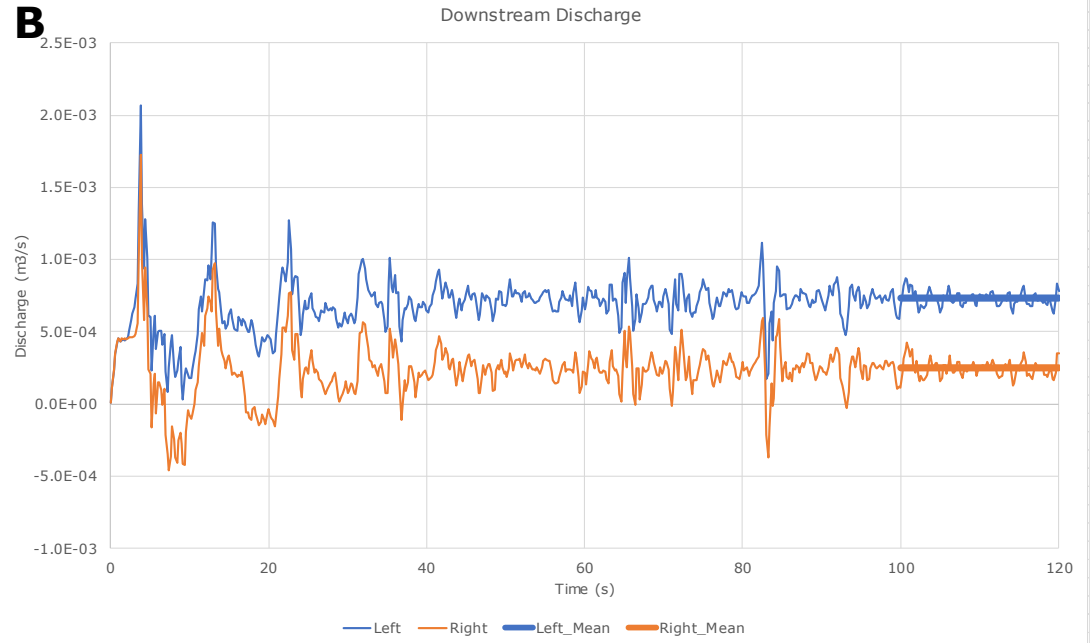
A

30_05_5057

Name	Symbol	Left	Right	Unit
Weir Height	WH	50	57	mm
Initial Time	Ti	100	100	s
End Time	Te	120	120	s
Initial Number	Ni	500	500	unitless
End Number	Ne	600	600	unitless
Average Discharge	$\bar{Q}$	7.305E-04	2.479E-04	m3/s

Name	Symbol	Equation	Result	Unit
Weir Height Ratio	WHr	WHL/WHR	0.877	dimensionless
Discharge Ratio	Qr	$\bar{Q}$_L/$\bar{Q}$_R	0.339	dimensionless
Time Step Discharge Ratio	Qr,t	Average[Q_(r,t=n)···Q_(r,t=n+N)]	0.336	dimensionless

B



C

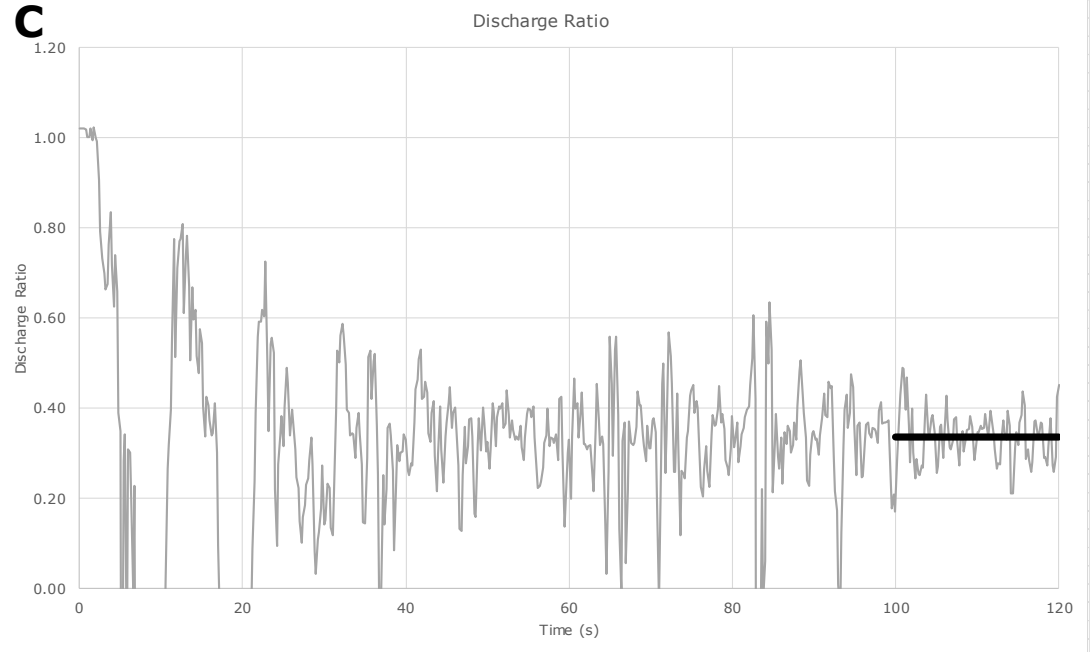


Figure 5.1: Example of numerical simulation result (A: summary of result; B: simulated discharge; C: discharge ratio)

5.3 Dimensionless Factor Analysis

5.3.1 Multiple Linear Regression Analysis

Multiple linear regression (MLR) analysis is conducted in this section to study the linear relationship between dependent variable (discharge ratio) and independent variables (bifurcation angle, slope, and weir height ratio).

Table 5.1 shows the P-value of slope is higher than 0.05; thus, its relationship with discharge ratio is statistically non-significant. With this approach, a multi-linear equation can be written as Equation 5.1:

$$Q_r = -0.4849 \sin \Theta + 4.8851\, WH_r - 3.6026, dimensionless \quad \text{Equation 5.1}$$

where, Q_r is discharge ratio

WH_r is weir height ratio

Θ is bifurcation angle

Table 5.1: Result of MLR analysis (Discharge ratio)

	Coefficients	Standard Error	t Stat	P-value
Intercept	-3.602646034	0.216118365	-16.66978199	4.2209E-27
Sin Θ	-0.484905318	0.092350986	-5.250678277	1.33469E-06
Δ	-0.029035709	0.056568852	-0.513280861	0.609243778 (P>0.05)
WH_r	4.885138088	0.222661338	21.93976796	1.28533E-34

5.3.2 Simple Linear Regression Analysis

Various trends can be observed from the result; therefore, data grouping is conducted for a better illustration of the results. Figure 5.2 and Figure 5.3 show the plotted result by 2 groups, it is based on the smallest weir height which are 50 mm (Group 50) and 55mm (Group 55). In both figures, Group 50 includes all slope and all bifurcation angles from 30° to 50°. Bifurcation angle 60° is separately presented in Figure 5.2 and Figure 5.3 by group to avoid poor visualisation of data due to overlapping.

The discharge ratio is found to be proportional to weir height ratio. There is insufficient evidence to prove that bifurcation angle and slope strongly affect the discharge ratio. This contradicts the finding from Section 4.3.3 in which bifurcation angle is related to discharge ratio in a sine function.

Result also proves the discharge ratio is affected by the smallest weir height, the data (Blue vs Orange) in Figure 5.2 and Figure 5.3 show their distinctiveness. Hypothetically, the threshold of weir height ratio is inversely proportional to the smallest weir height. Due to the limited number of simulations and limited range of control parameters, no equation is predicted to describe its relationship.

To study the relationship between discharge ratio and weir height ratio, 2 linear regression lines are plotted to fit with Group 50 and Group 55 in Figure 5.2 and Figure 5.3. Both linear regression lines are calculated with intersection at coordinate {1,1}, as the line should theoretically pass through the coordinate {1,1}. The relationship can be written as Equation 5.2 and Equation 5.3 for Group 50 and Group 55 respectively.

$$\mathrm{Q}_r = 5.0128\, WH_r - 4.0128, dimensionless \qquad \text{Equation 5.2}$$

$$\mathrm{Q}_r = 5.5408\, WH_r - 4.5408, dimensionless \qquad \text{Equation 5.3}$$

where, Q_r is discharge ratio

WH_r is weir height ratio

The threshold of weir height ratio can be predicted from Equation 5.2 and Equation 5.3 which are 0.801 and 0.820 for Group 50 and Group 55 respectively. This finding shows the threshold of weir height ratio is inversely proportional to the smallest weir height.

The special case in this study is the data set with bifurcation angle of 60°. No tendency is observed due to the chaotic nature of the results. In Group 50 (Figure 5.2), the result shows a curvy trend for all slopes except 0.3%. In Group 55, the coefficient of determination of the linear regression is very small due to the deviation of data between each discharge ratio. In conclusion, 60° angle results are excluded from the analysis.

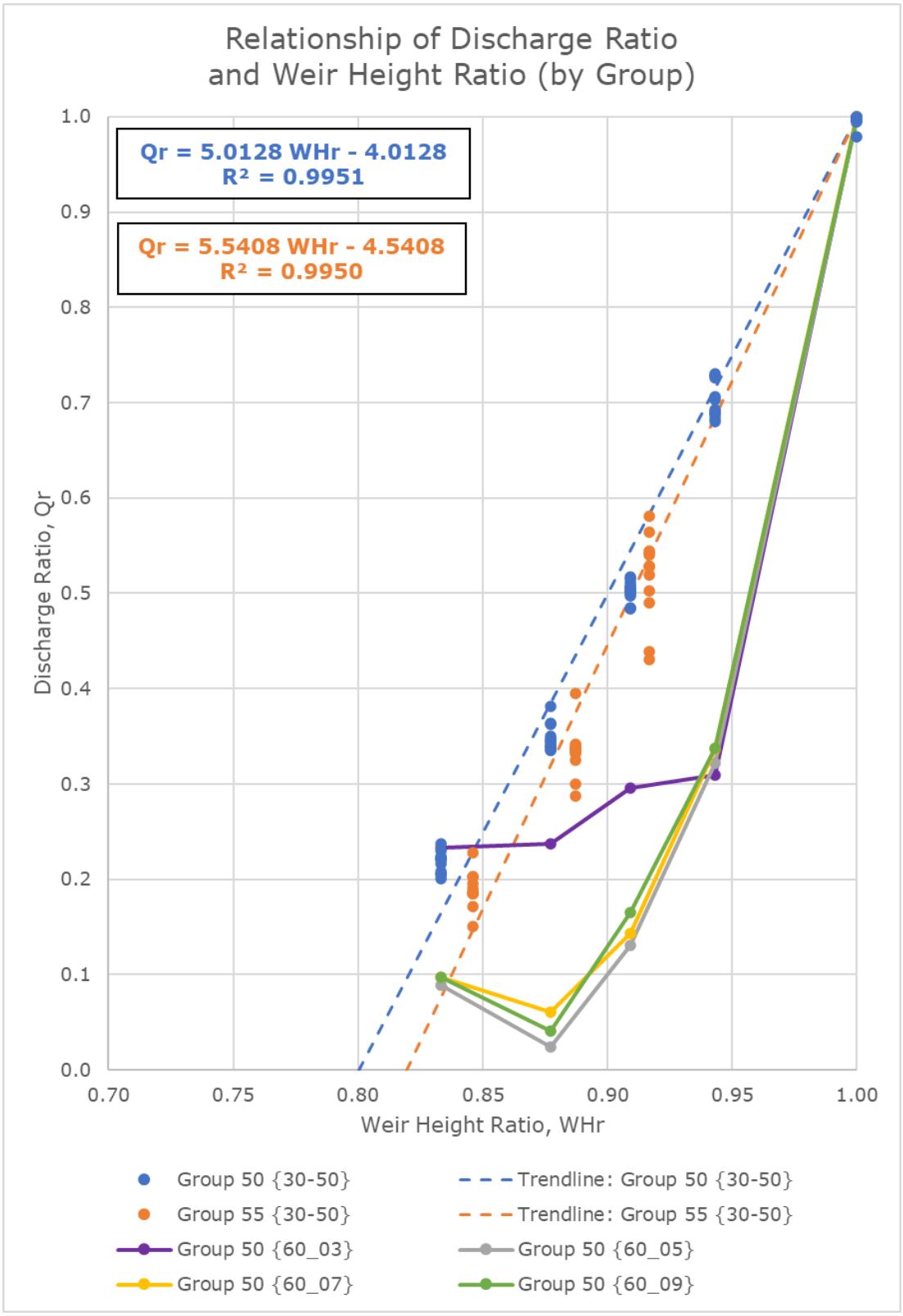


Figure 5.2: Relationship of discharge ratio and weir height ratio (1)

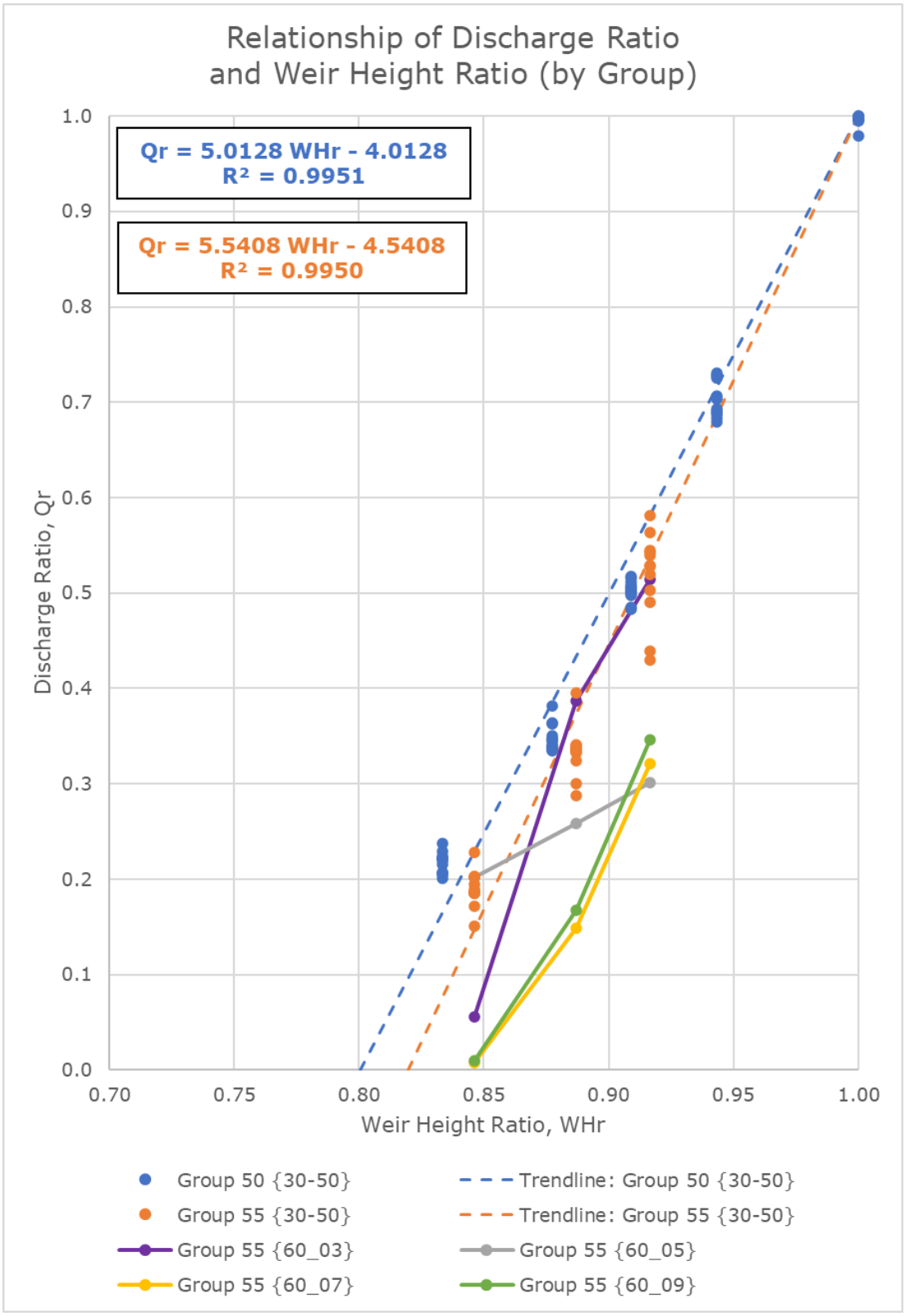


Figure 5.3: Relationship of discharge ratio and weir height ratio (2)

5.3.3 Threshold of Weir Height Ratio

The threshold of weir height ratio calculated from the discharge ratio from Section 5.3.1 and Section 5.3.2 are summarised in Table 5.2. The dimensionless factors analysis shows that the smallest weir height is found to be impactful on the threshold of weir height ratio.

Table 5.2: Summary of threshold of weir height ratio

Smallest Weir Height	Threshold of Weir Height Ratio
Section 5.3.1	
50 & 55 Data	0.737
Section 5.3.2	
50	0.801
55	0.820

5.4 Comparisons of Physical Modelling and Numerical Modelling

As noted in Chapter 4, the upstream discharge is hypothesised to affect the threshold of weir height ratio; this can be observed when the results of physical modelling, numerical modelling, and Thomas et al. (2011) are compared in Figure 5.4. The inlet discharge of numerical modelling was higher than physical modelling but lower than the inlet discharge in Thomas et al. (2011). Therefore, the value of the threshold of weir height ratio (x-axis intercept in Figure 5.4) ranges between the value from physical modelling and Thomas et al. (2011).

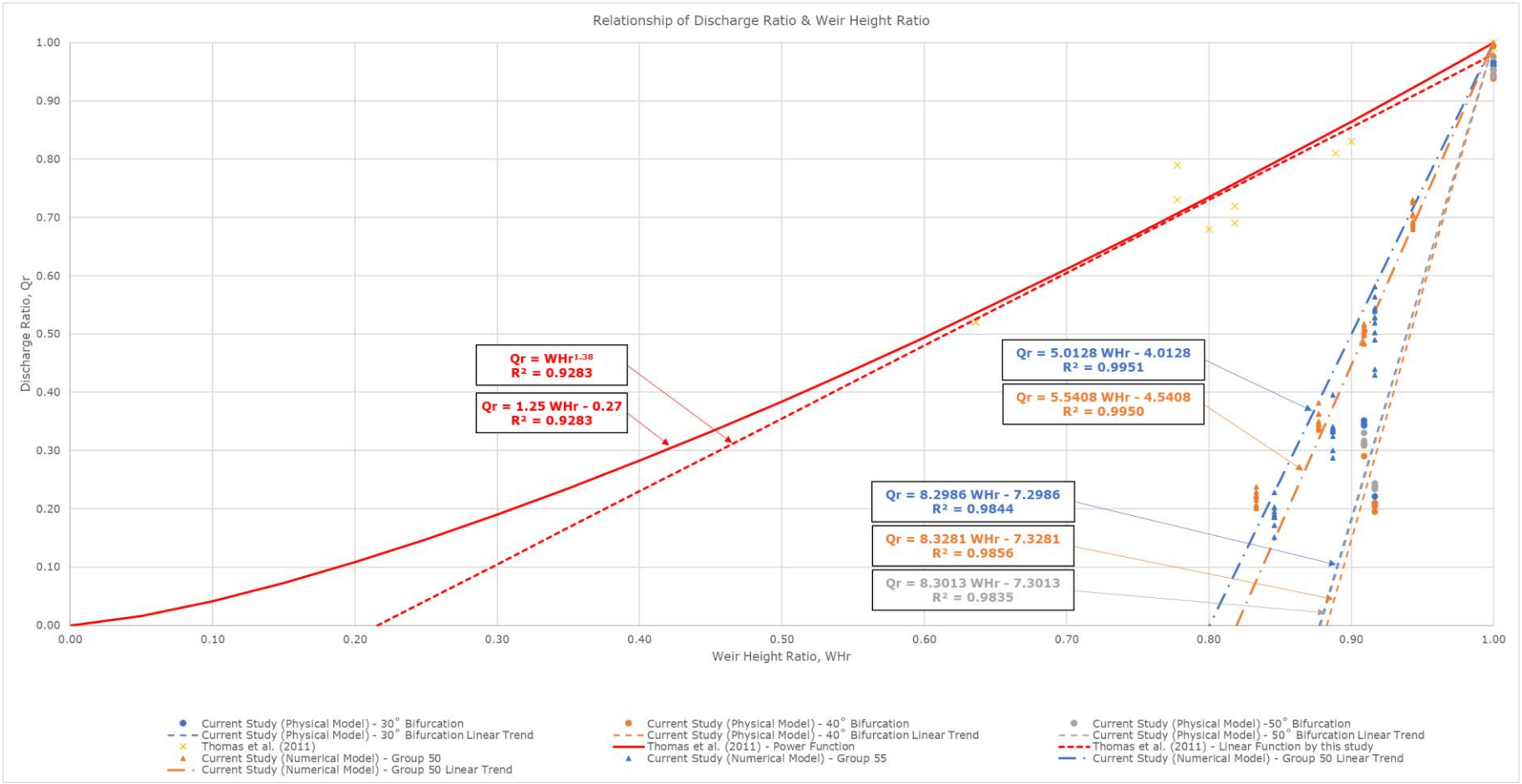


Figure 5.4: Relationship of discharge ratio and weir height ratio

Chapter 6 Machine Learning Model of Channel Bifurcation

6.1 Model Training Performance

The training performances of the 6 models are shown in Figure 6.1, Figure 6.2, Figure 6.3, Figure 6.4, Figure 6.5, and Figure 6.6.

The epoch for best validation performance ranges from 6 to 21; this indicates the machine learning model can easily reach the acceptable range of accuracy (small mean squared error) with the provided data for training.

The coefficient of determination in most of the trained models is more than 0.95, except the testing stage in the Model N30L3 (R^2 = 0.87178) and the validation stage in the Model N10L2 (R^2 = 0.94017). The coefficient of determination from validation and testing show that the predicted results from the trained model are correlated to the provided labelled data. Due to the limitation of data range, the prediction from the model may be inaccurate for any data that is out of the range of labelled data.

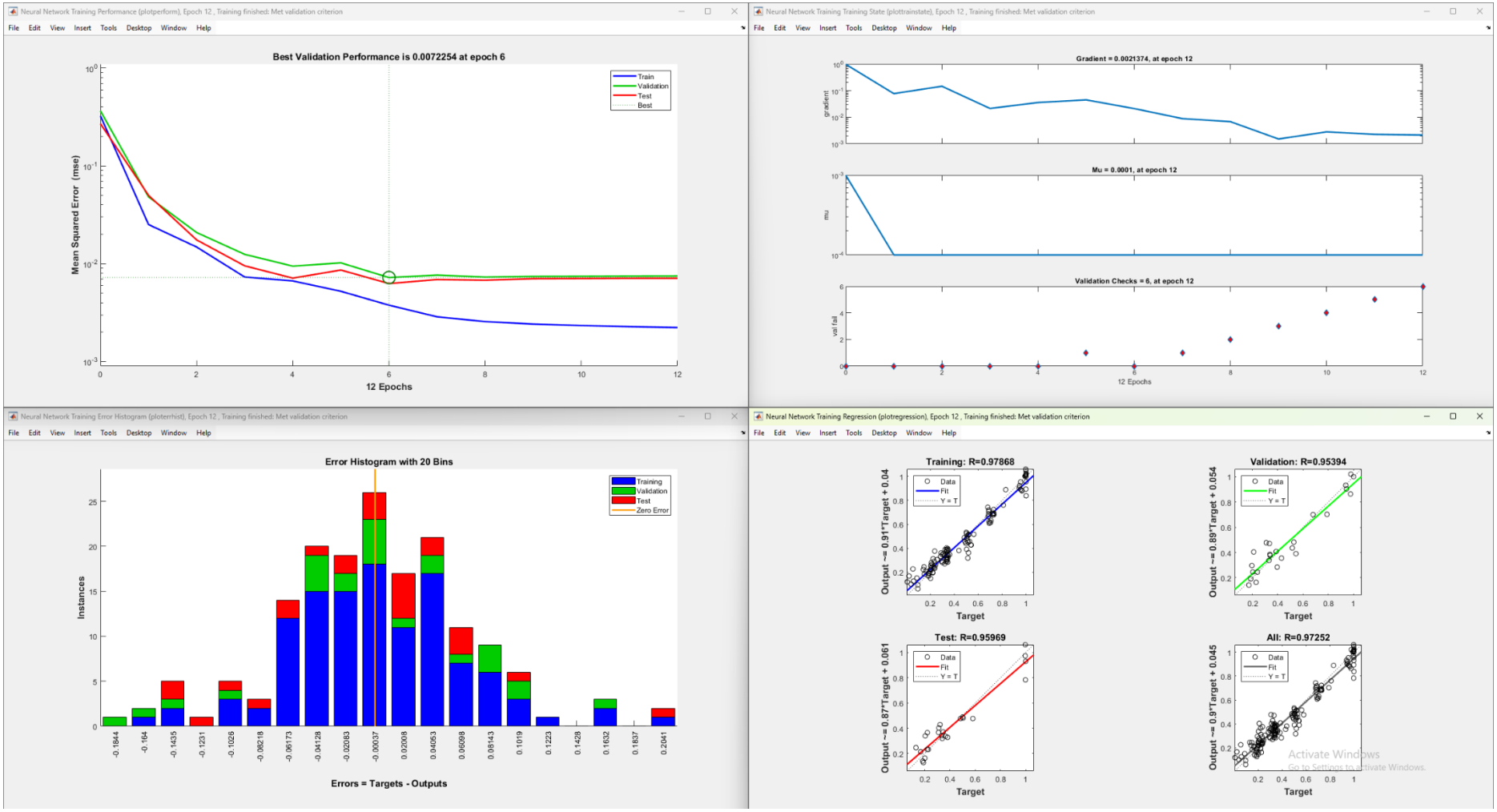


Figure 6.1: Model Performance of N10L1

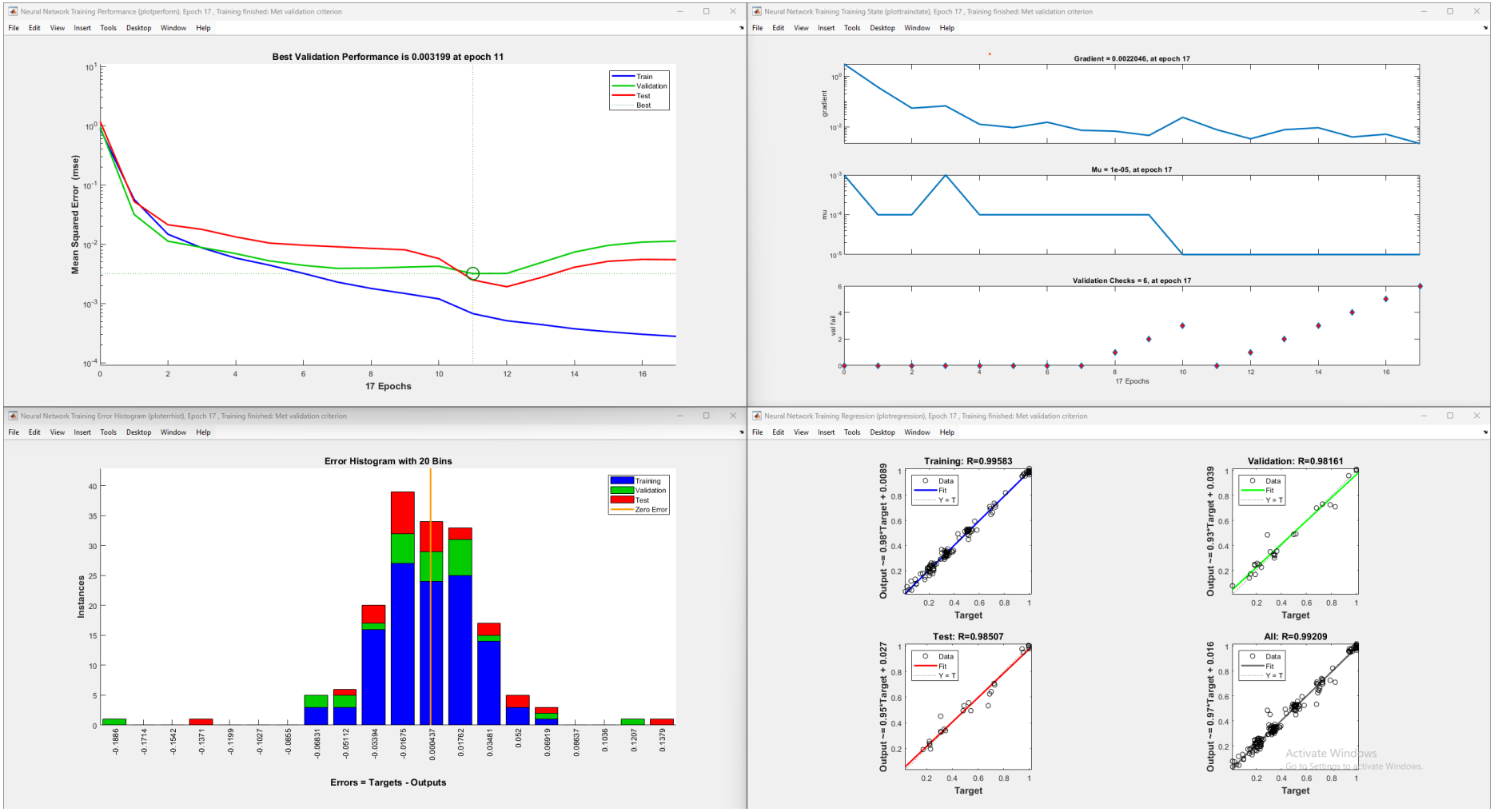


Figure 6.2: Model Performance of N20L1

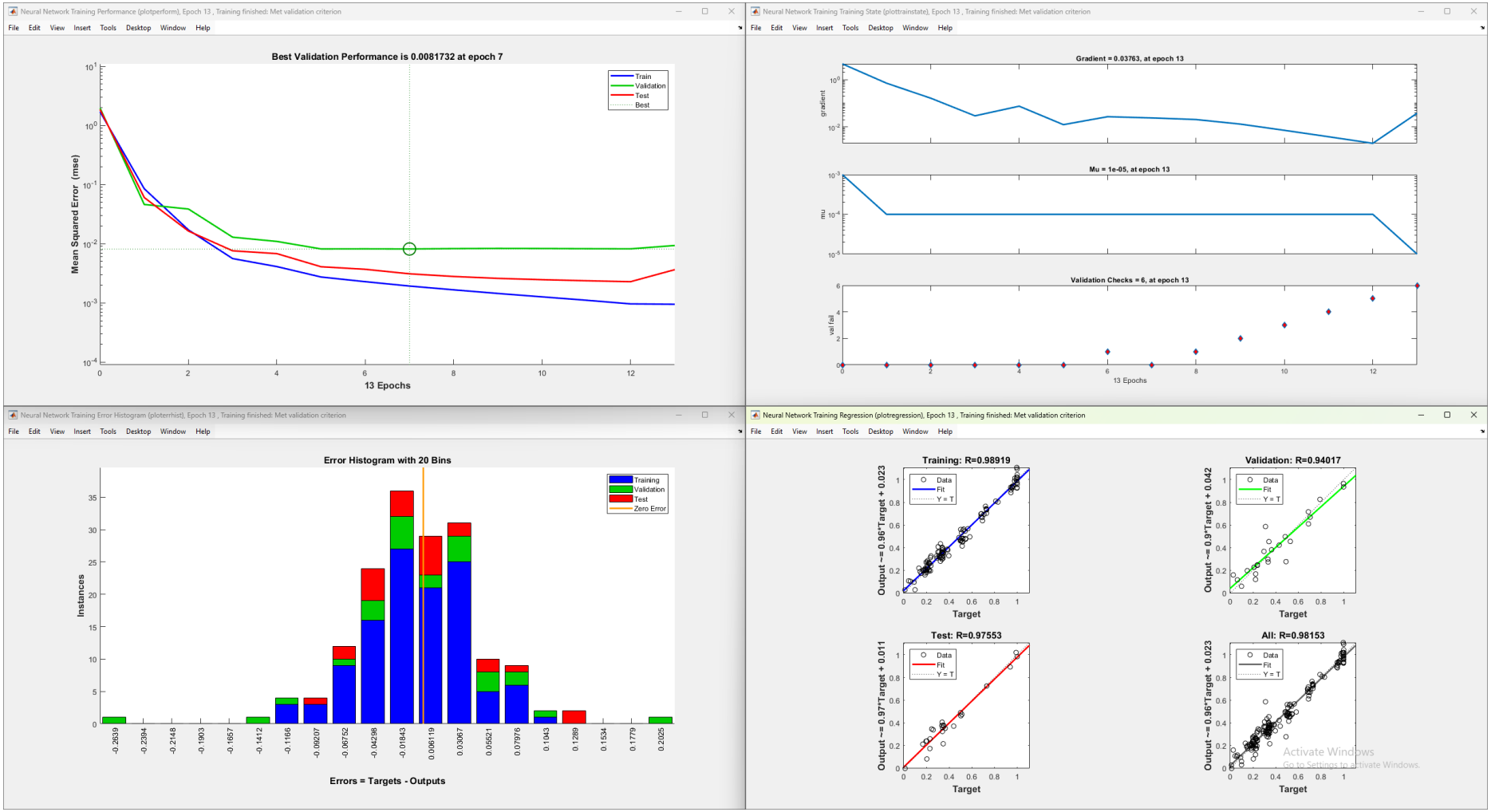


Figure 6.3: Model Performance of N30L1

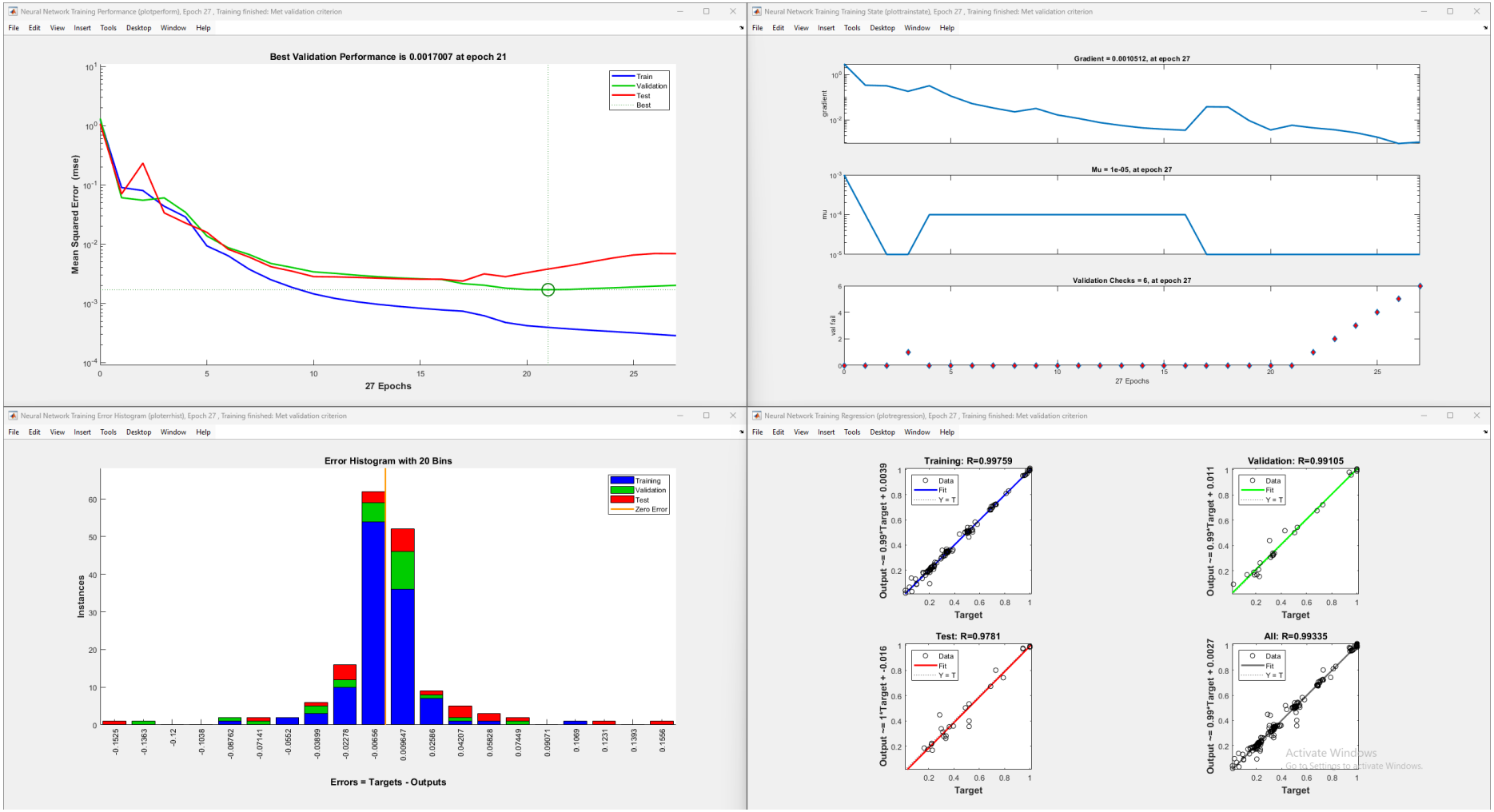


Figure 6.4: Model Performance of N10L2

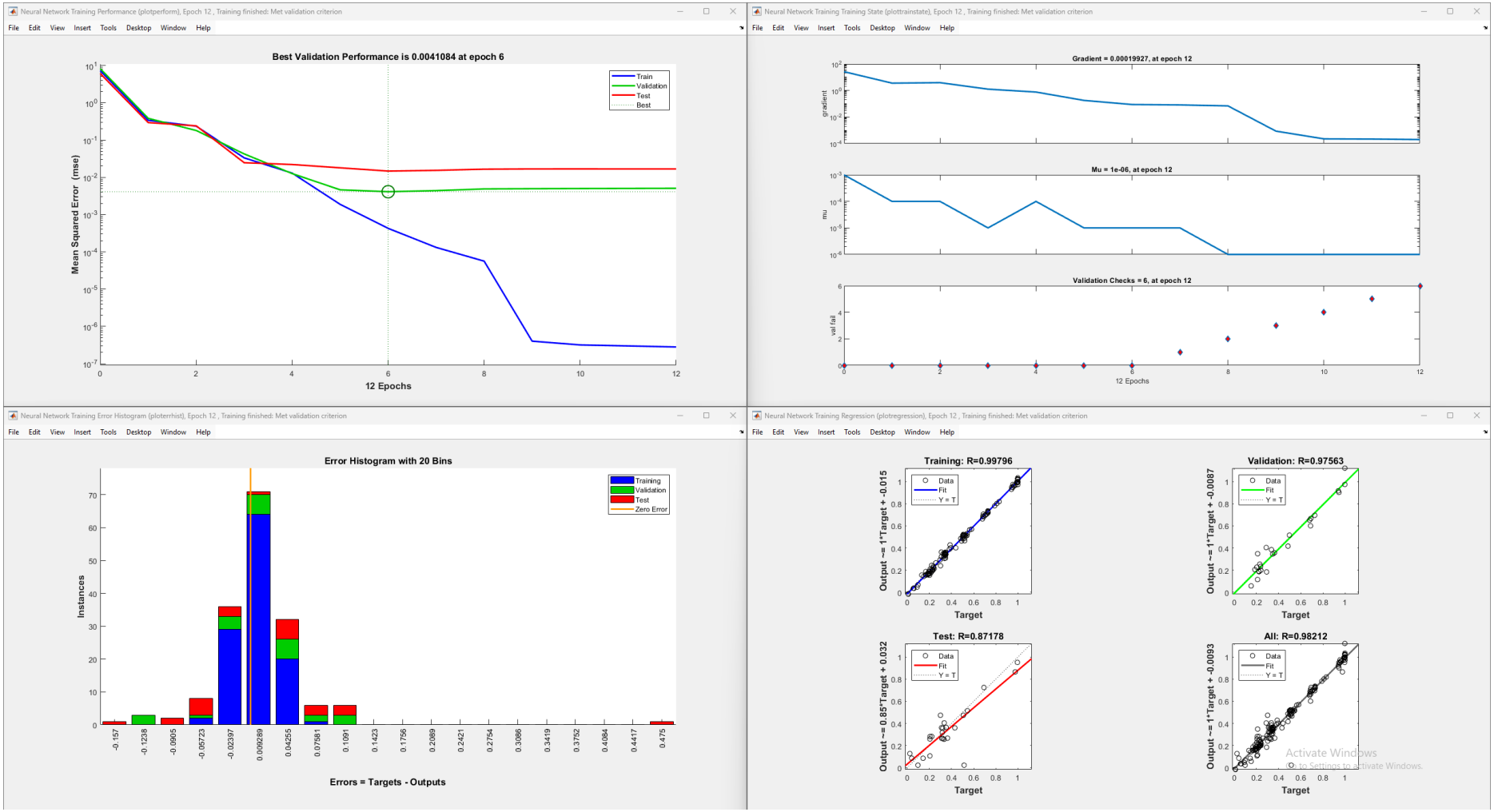


Figure 6.5: Model Performance of N10L3

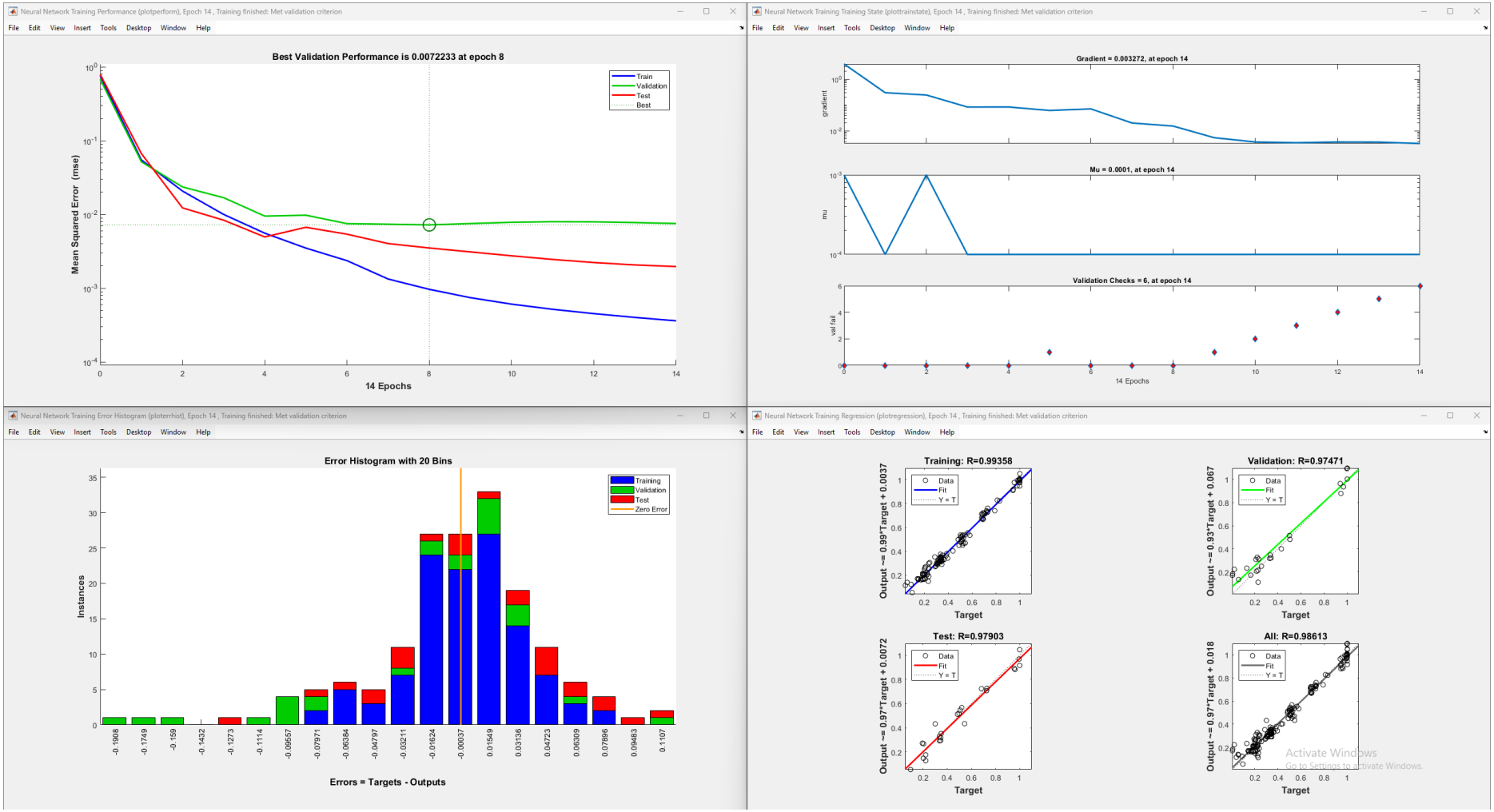


Figure 6.6: Model Performance of N30L3

Table 6.1 summarises the training performance of the models with ranking based on the overall performance.

The best-performing model was N20L1 with the highest validation and test R^2, and its training R^2 was ranked as the second best. This model also performed well in Training-Validation Gap and Validation-Test Gap.

Significant spike (Figure 6.7) was observed in Model N10L2 (epoch 2), this indicates the model is unstable during the training stage, thus, this model is the least reliable. One hypothesised cause is the bottleneck effect from the multiple layers of neurons. With multiple layers, the information flows through the subsequent layer without expansion of the number of neurons, which could be the bottleneck. This bottleneck may cause gradient instability and inefficient learning path for the machine learning model. Figure 6.8 demonstrates the bottleneck in the layer under the Model N10L2 architecture. A better architecture framework for ANN in bifurcation can be setting up higher number of neurons to form a pyramid structure.

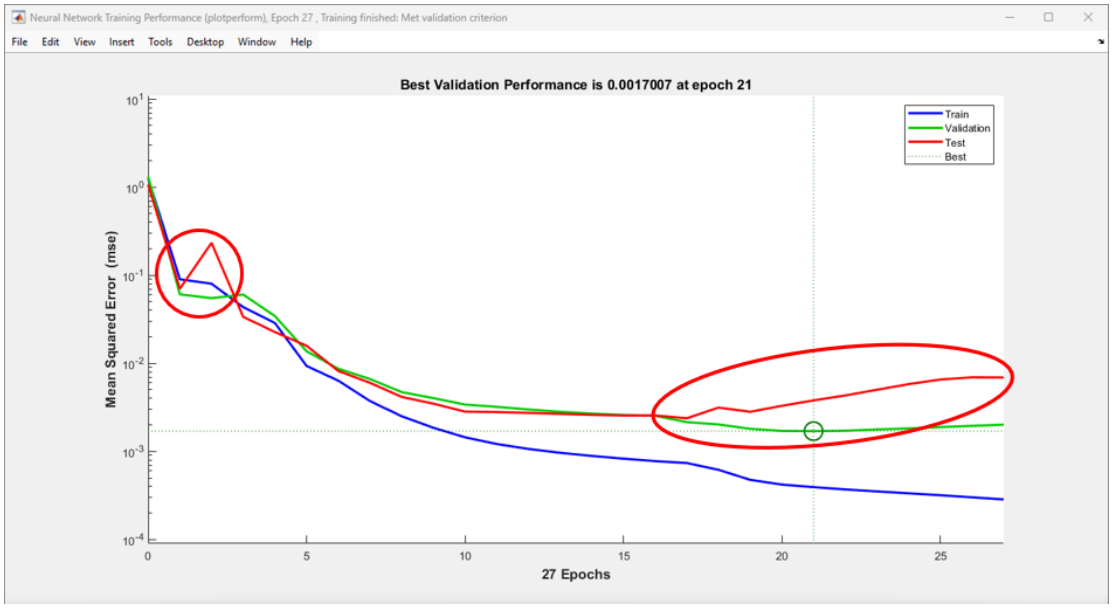


Figure 6.7: The spike in Model N10L2

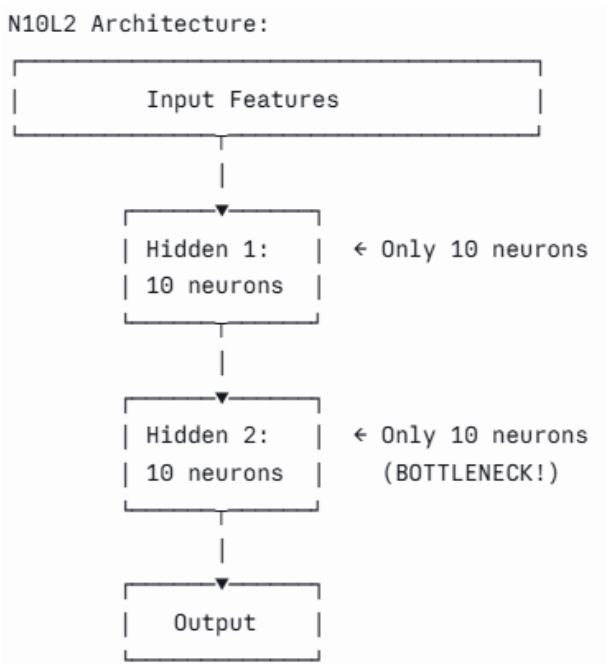


Figure 6.8: The bottleneck effect in Model N10L2

Table 6.1: Summary of training performance

Model	Stopping epoch	Spikes Observed	Best Validation MSE	Validation R^2	Test R^2	Training R^2	Training-Validation Gap (Overfitting Indicator)	Validation-Test Gap (Generalization Indicator)	Ranking
N10L1	6	Minor	0.00722	95.39%	95.97%	**97.87%**	2.48%	0.58%	3
N20L1	11	Minor	0.00320	**98.16%**	**98.51%**	99.58%	1.42%	**0.33%**	1
N30L1	13	Minor	**0.00817**	**94.02%**	97.55%	98.92%	**4.90% (Severe Overfitting)**	3.47%	4
N10L2	21	**Significant**	**0.00170**	99.11%	97.78%	99.76%	**0.65%**	1.33%	6
N10L3	6	Minor	0.00411	97.56%	**87.18%**	**99.80%**	2.24%	**10.38% (Poor)**	5
N30L3	8	Minor	0.00722	97.47%	97.90%	99.36%	1.46%	0.43%	2
Best	-	-	N10L2	N20L1	N20L1	N10L3	N10L2	N20L1	-

6.2 Machine Learning Model Prediction

6.2.1 Discharge at Upstream

As discussed, the discharge at upstream may be one of the factors that affect the discharge ratio. To study the potential of machine learning model prediction on this hypothesis, various discharges at upstream are tested with the trained models. All predictions from the 6 models are plotted in Figure 6.9, Figure 6.10, Figure 6.11, Figure 6.12, Figure 6.13, and Figure 6.14. The feeding data range was labelled with red text in these figures.

Under the training without specific constraint, the N10L3 (Figure 6.13) shows the most acceptable prediction among the 6 trained models. By definition, the discharge ratio must not be more than 1, however, all the trained models are predicting the discharge ratio more than 1 under certain conditions. Surprisingly, the Model N10L3 shows the potential of self-constraining the discharge ratio to below 1. Other than that, the threshold of weir height ratio can be observed when the discharge at upstream is too low. A smaller weir height ratio requires higher discharge at upstream to break its threshold. These trends are consistent with the findings from physical modelling and numerical modelling.

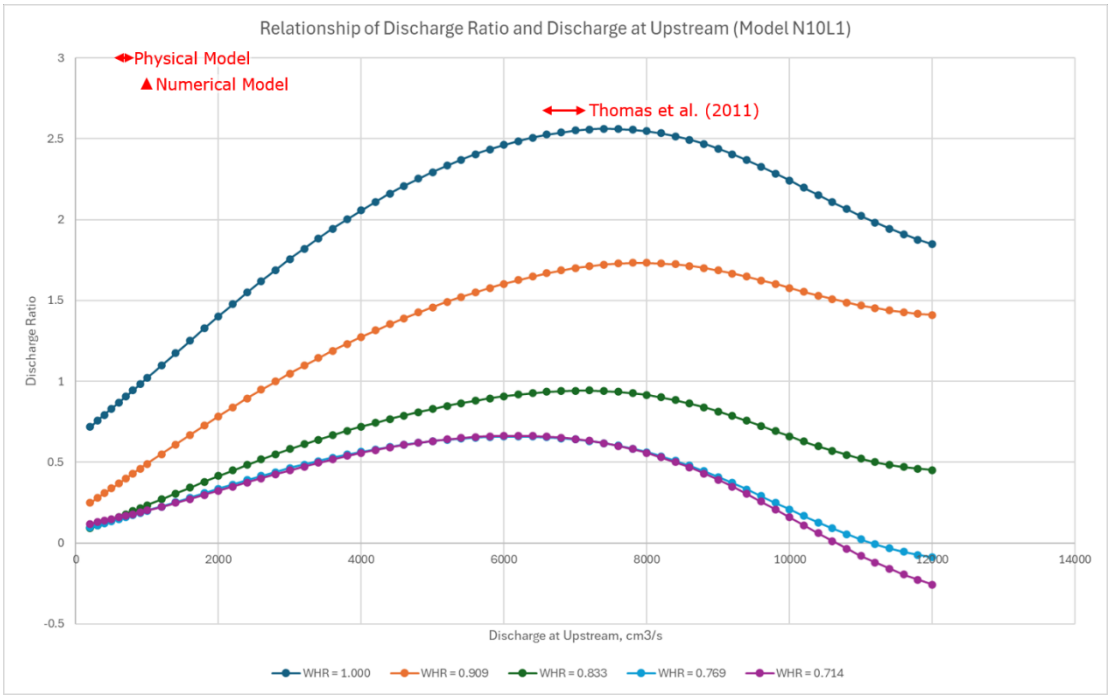


Figure 6.9: Relationship of discharge ratio and discharge at upstream (Model N10L1)

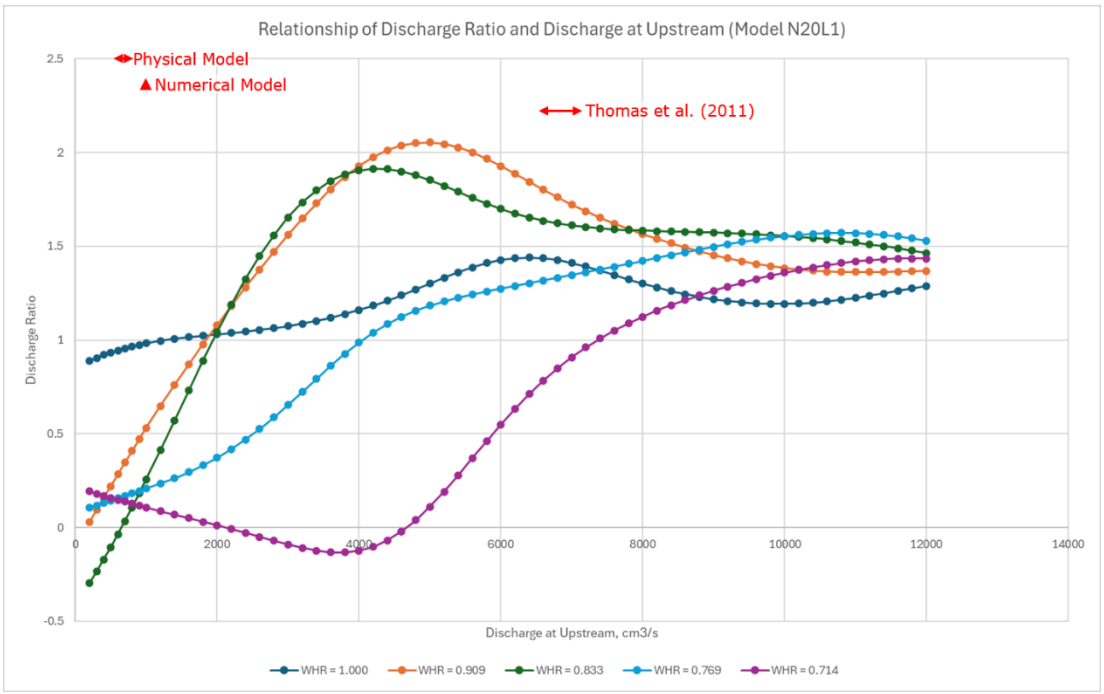


Figure 6.10: Relationship of discharge ratio and discharge at upstream (Model N20L1)

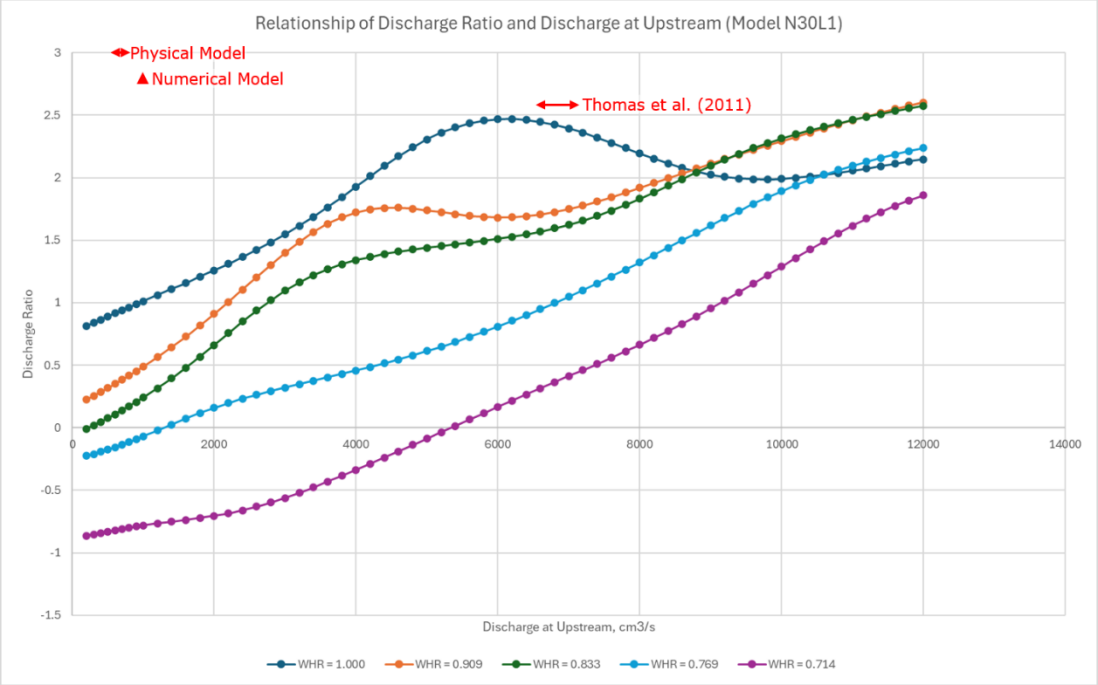


Figure 6.11: Relationship of discharge ratio and discharge at upstream (Model N30L1)

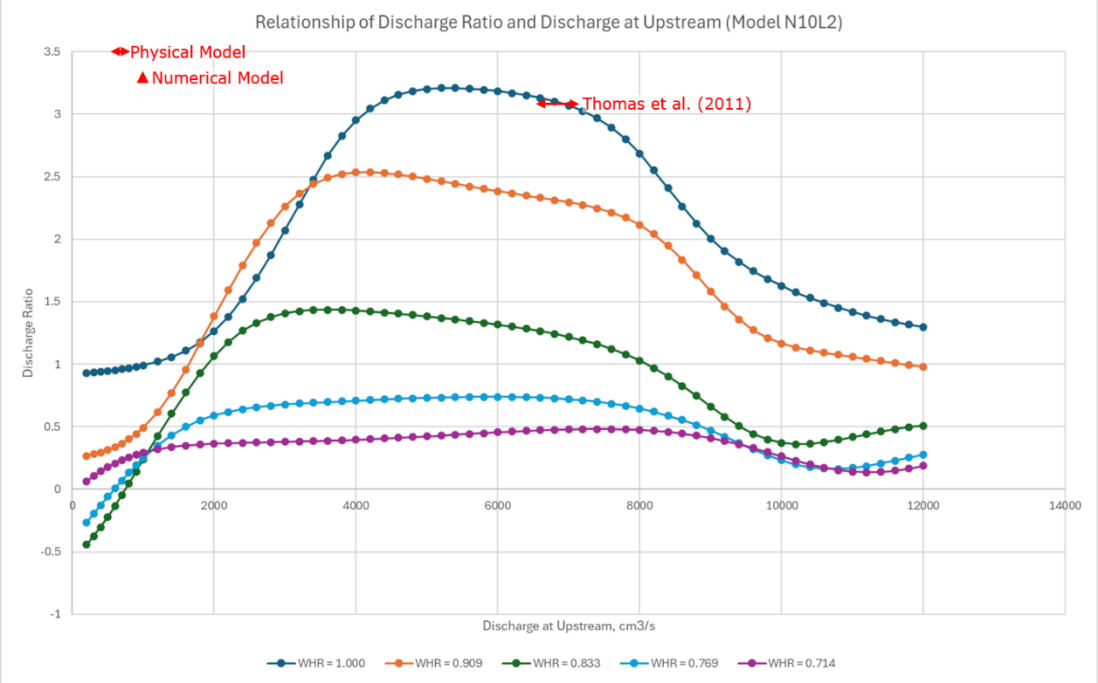


Figure 6.12: Relationship of discharge ratio and discharge at upstream (Model N10L2)

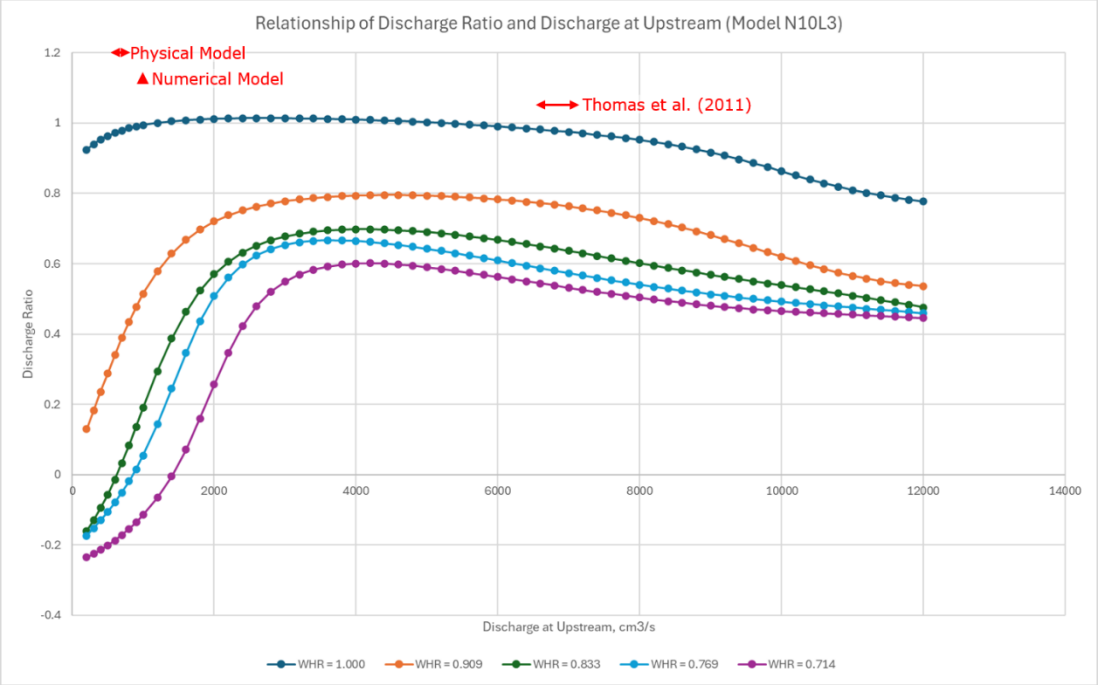


Figure 6.13: Relationship of discharge ratio and discharge at upstream (Model N10L3)

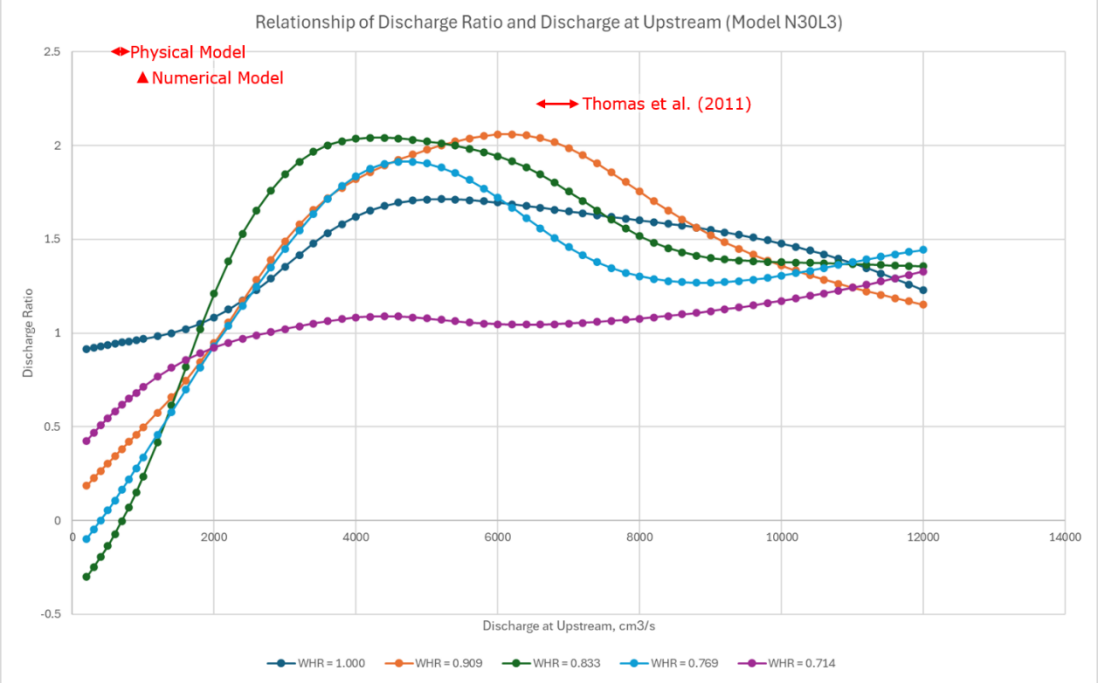


Figure 6.14: Relationship of discharge ratio and discharge at upstream (Model N30L3)

6.2.2 Bifurcation Angle

Similarly, various bifurcation angles were designed as input for the trained model prediction with constant discharge at upstream. All predictions are plotted in Figure 6.15, Figure 6.16, Figure 6.17, Figure 6.18, Figure 6.19, and Figure 6.20. The feeding data range was labelled with red text in these figures.

The most stable prediction among the 6 trained models is Model N10L1, which is plotted in Figure 6.15. It shows a curvy reduction of discharge ratio as the bifurcation angle is increased. The discharge ratio value becomes negative as the bifurcation angle increased; this prediction is not reliable after 70°. The finding from physical modelling shows the discharge ratio is correlated with bifurcation angle in a sine function relationship. However, the prediction from Model N10L1 is unrelated to any sine function. 3 possible assumptions can be used for explaining this contradiction:

1. The relationship between discharge ratio and bifurcation angle may not be sine function.
2. Bifurcation angle in sine function (sin Θ) may be more suitable for model training than the angle itself (Θ).
3. Both assumptions mentioned above.

The Model N30L1 in Figure 6.17 shows a smoother curve, but the discharge ratio is negative when WHR is equal to 0.714 and 0.769. The prediction curve in other models either fluctuates or shows a negative discharge ratio, or both.

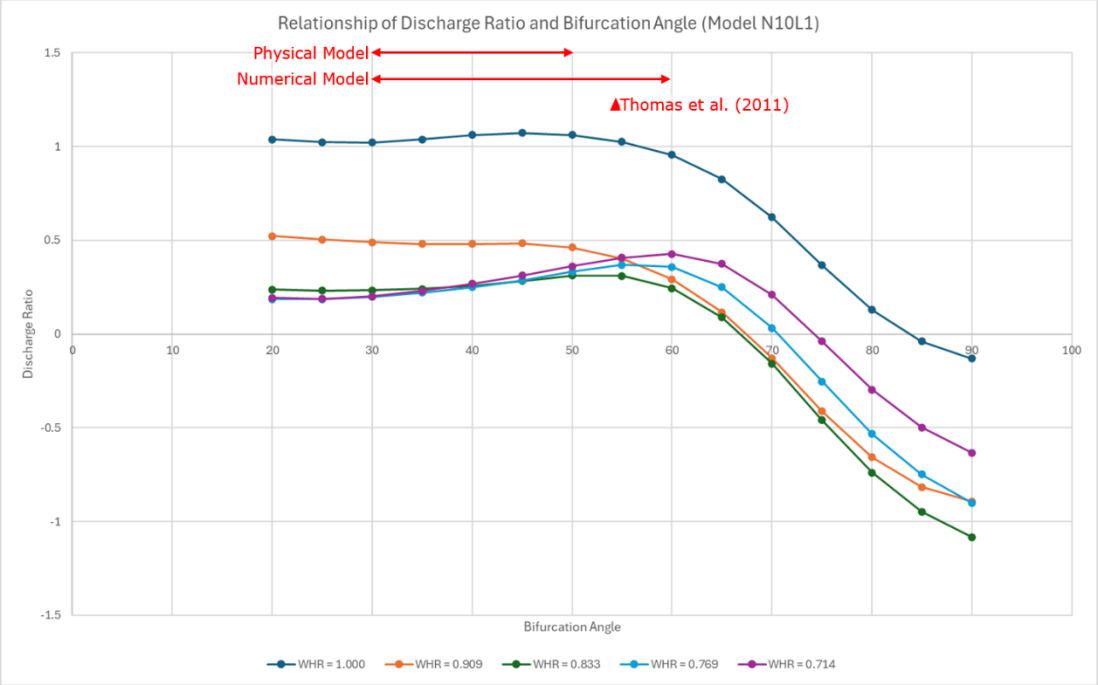


Figure 6.15: Relationship of discharge ratio and bifurcation angle (Model N10L1)

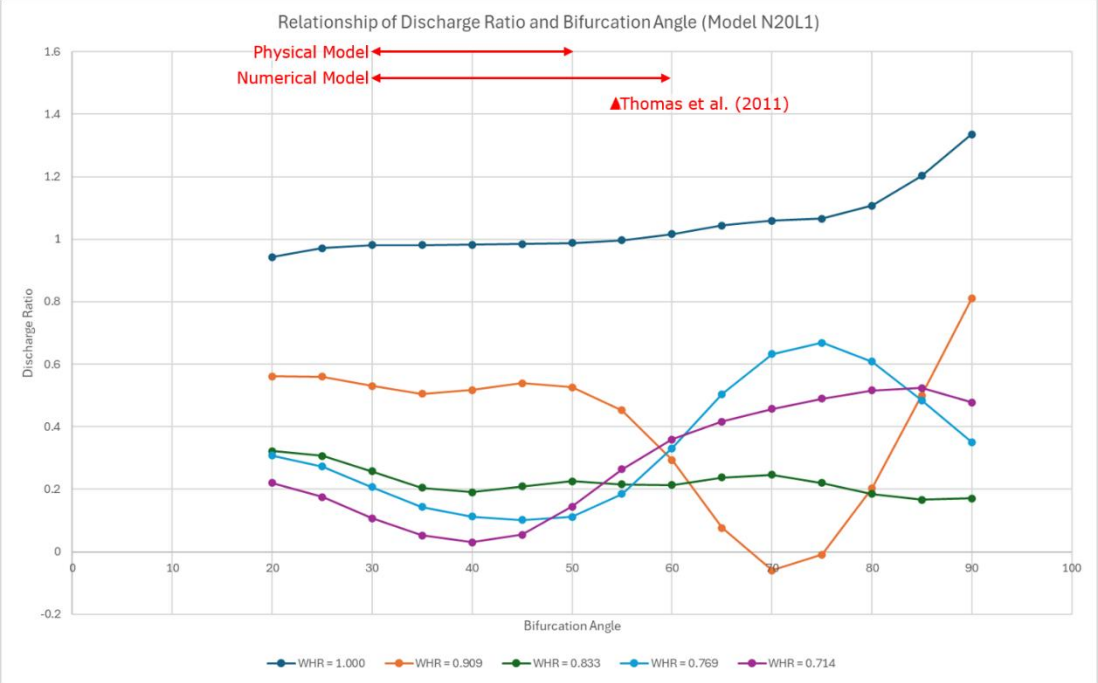


Figure 6.16: Relationship of discharge ratio and bifurcation angle (Model N20L1)

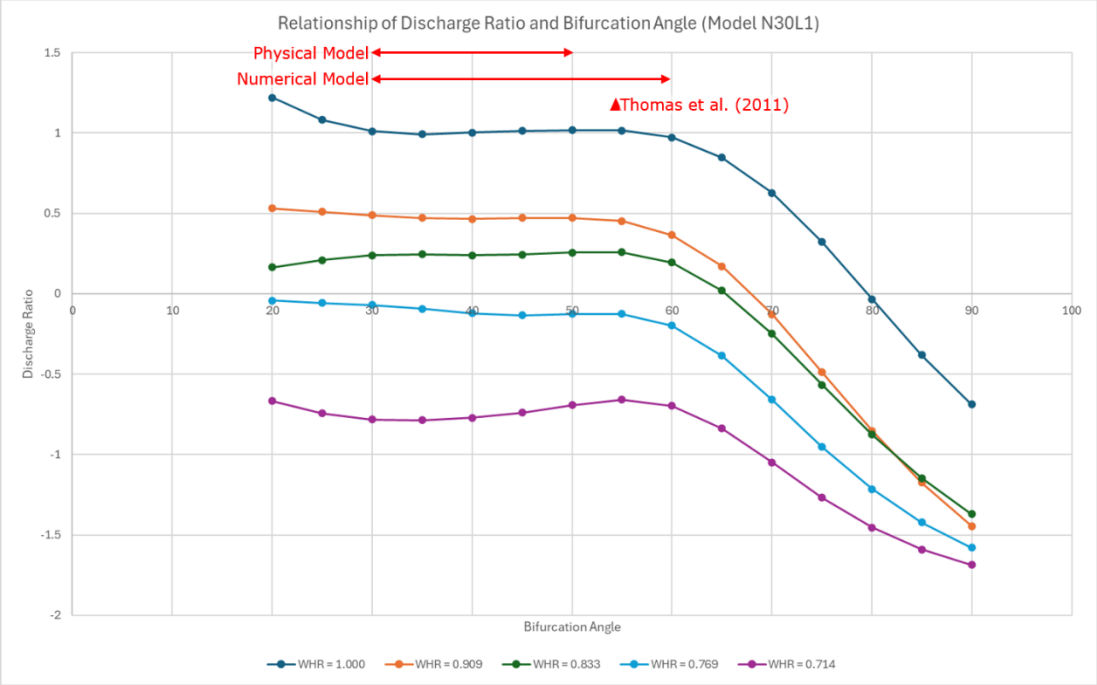


Figure 6.17: Relationship of discharge ratio and bifurcation angle (Model N30L1)

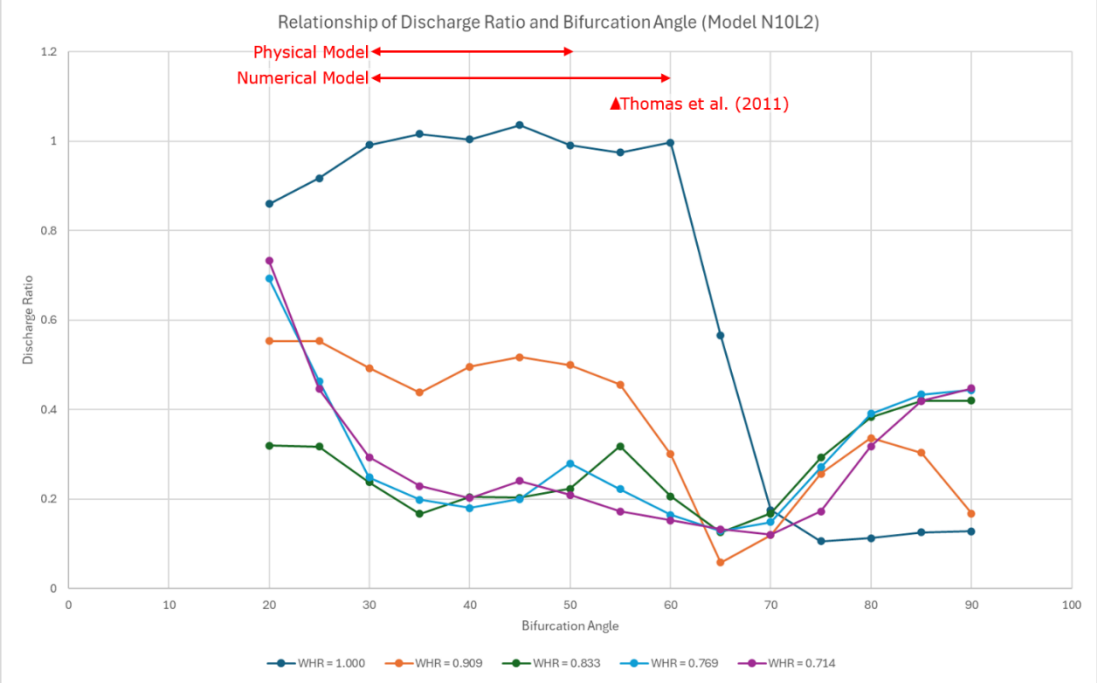


Figure 6.18: Relationship of discharge ratio and bifurcation angle (Model N10L2)

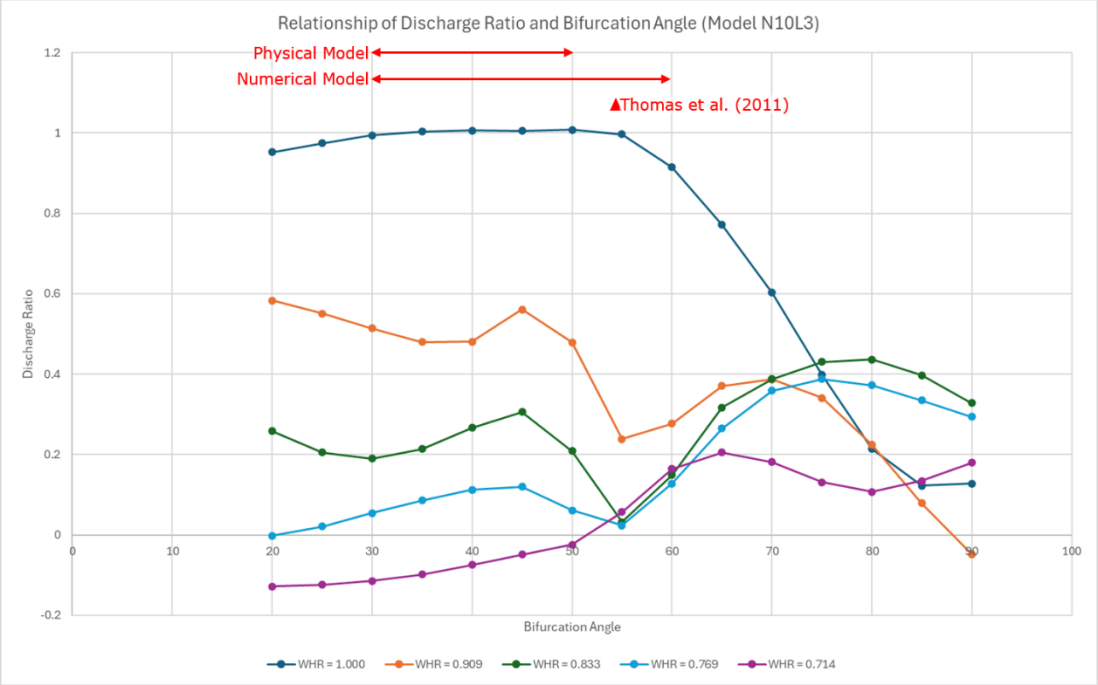


Figure 6.19: Relationship of discharge ratio and bifurcation angle (Model N10L3)

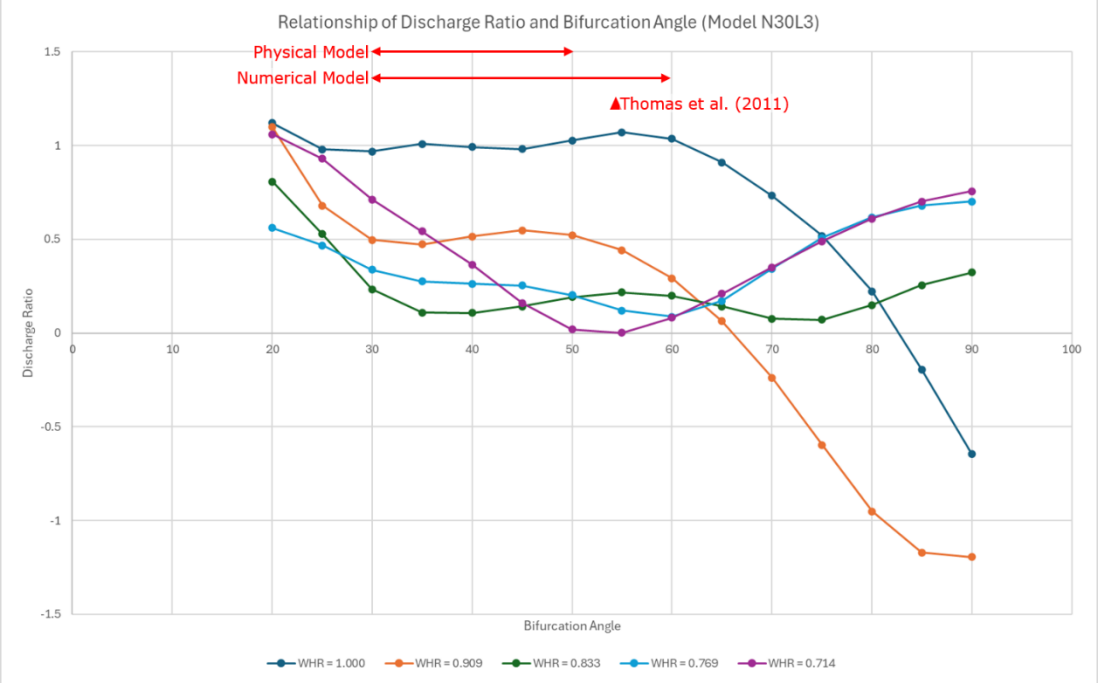


Figure 6.20: Relationship of discharge ratio and bifurcation angle (Model N30L3)

6.2.3 Slope

The findings from physical modelling show no correlation between discharge ratio and slope. However, the prediction in Figure 6.21, Figure 6.22, Figure 6.23, Figure 6.24, Figure 6.25, and Figure 6.26 show that slope does affect the discharge ratio. The feeding data range was labelled with red text in these figures.

The prediction curves of these models are relatively chaotic, and no trend can be observed. In conclusion, these models are not suitable for predicting discharge ratio by slope. Other than Model N10L1, other models showed a negative prediction of discharge ratio, which is incorrectly predicted.

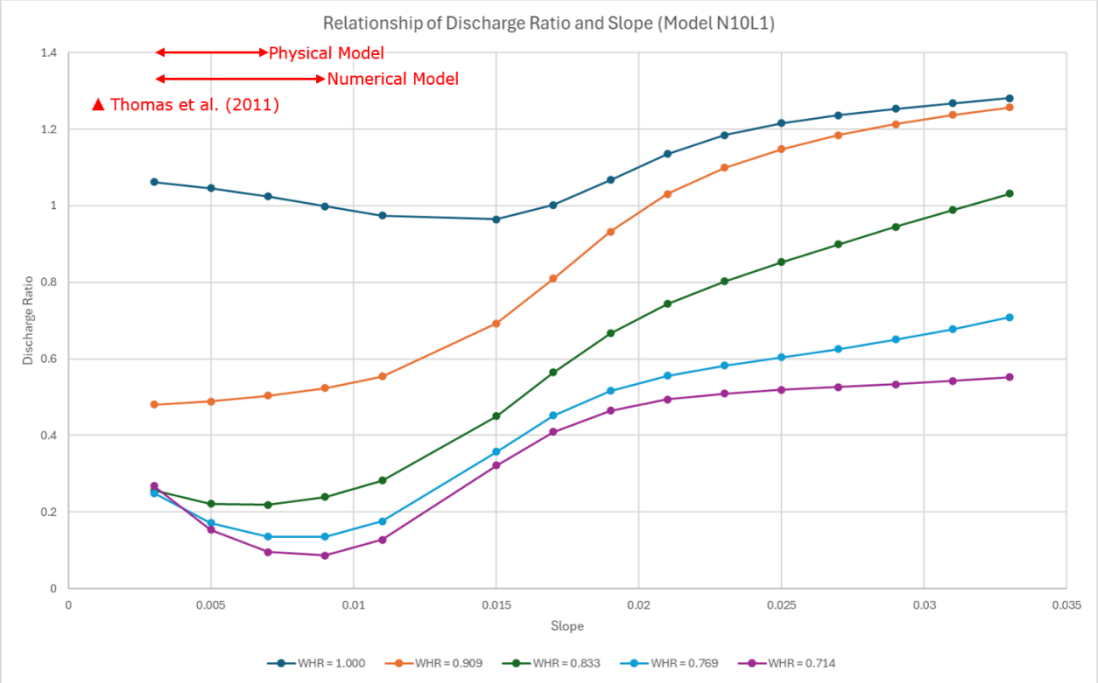


Figure 6.21: Relationship of discharge ratio and Slope (Model N10L1)

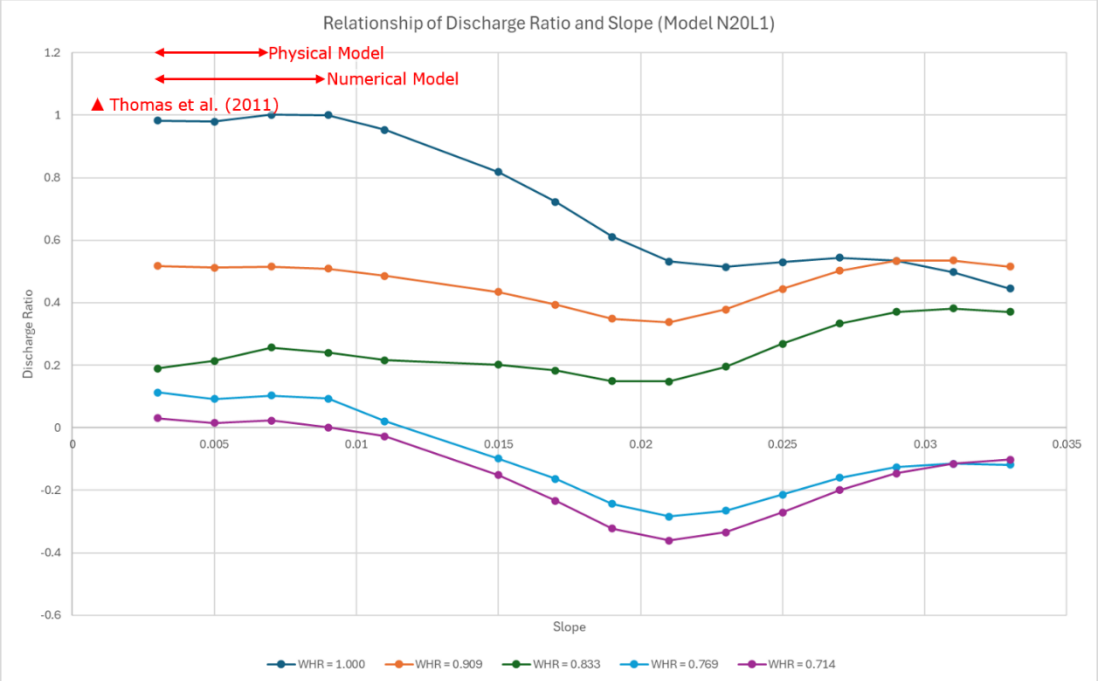


Figure 6.22: Relationship of discharge ratio and Slope (Model N20L1)

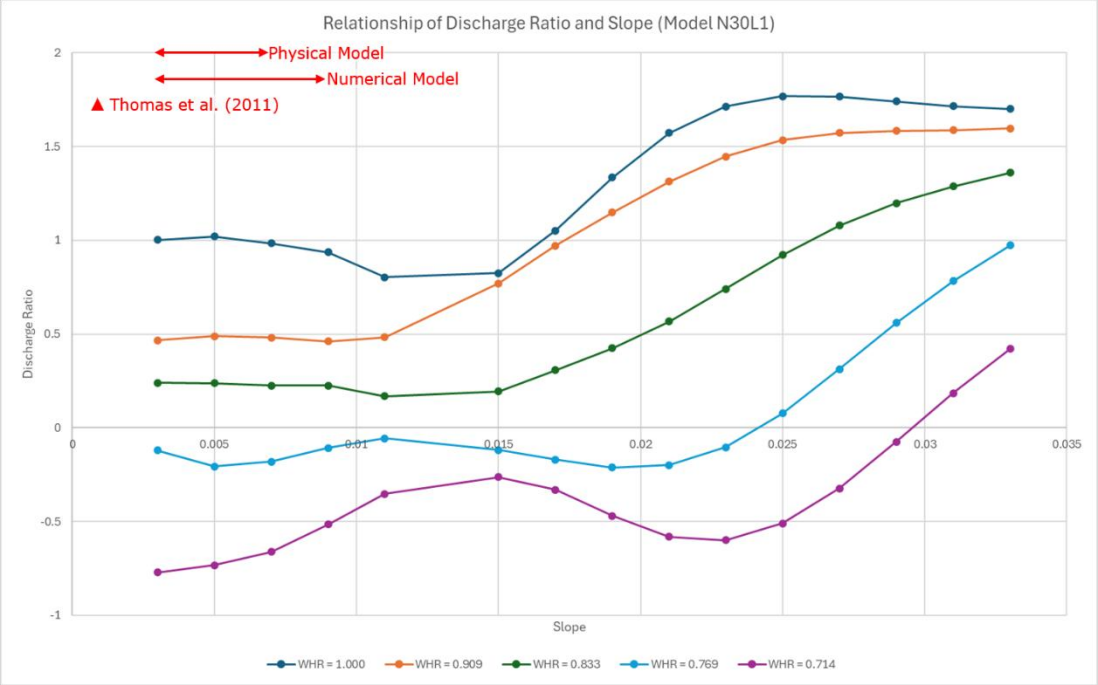


Figure 6.23: Relationship of discharge ratio and Slope (Model N30L1)

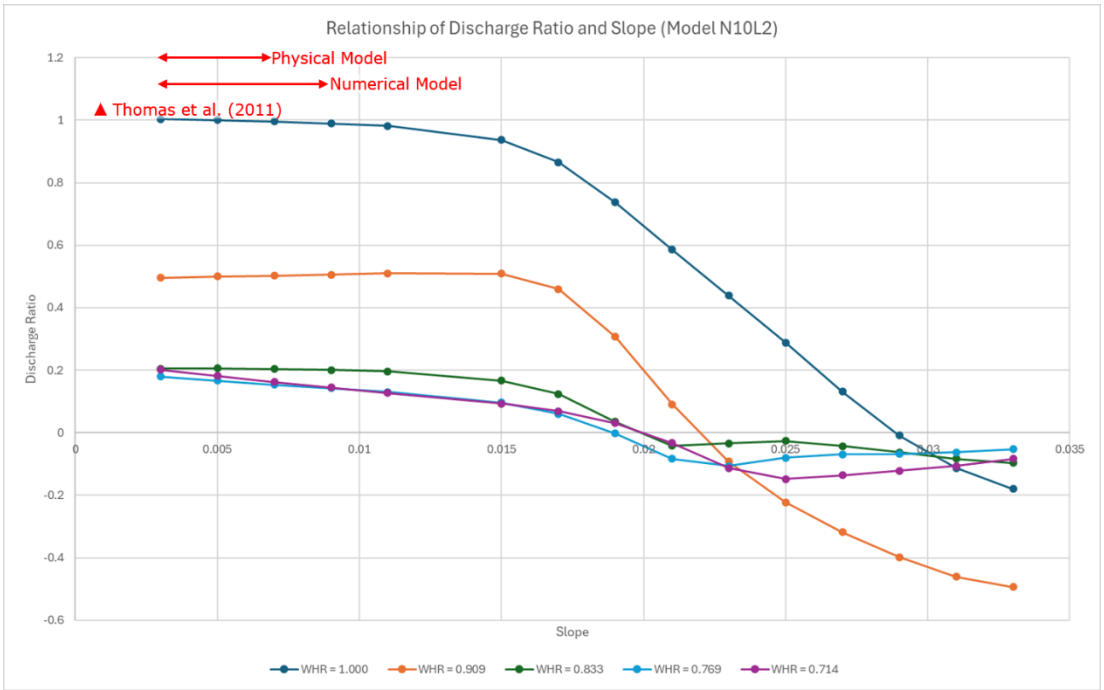


Figure 6.24: Relationship of discharge ratio and Slope (Model N10L2)

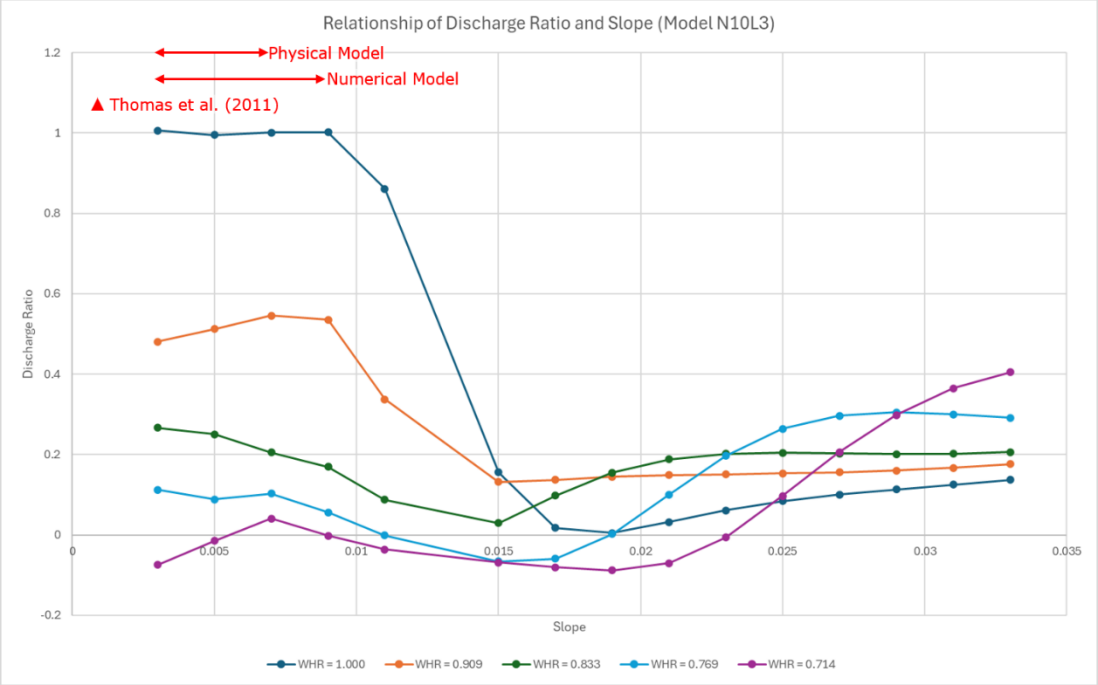


Figure 6.25: Relationship of discharge ratio and Slope (Model N10L3)

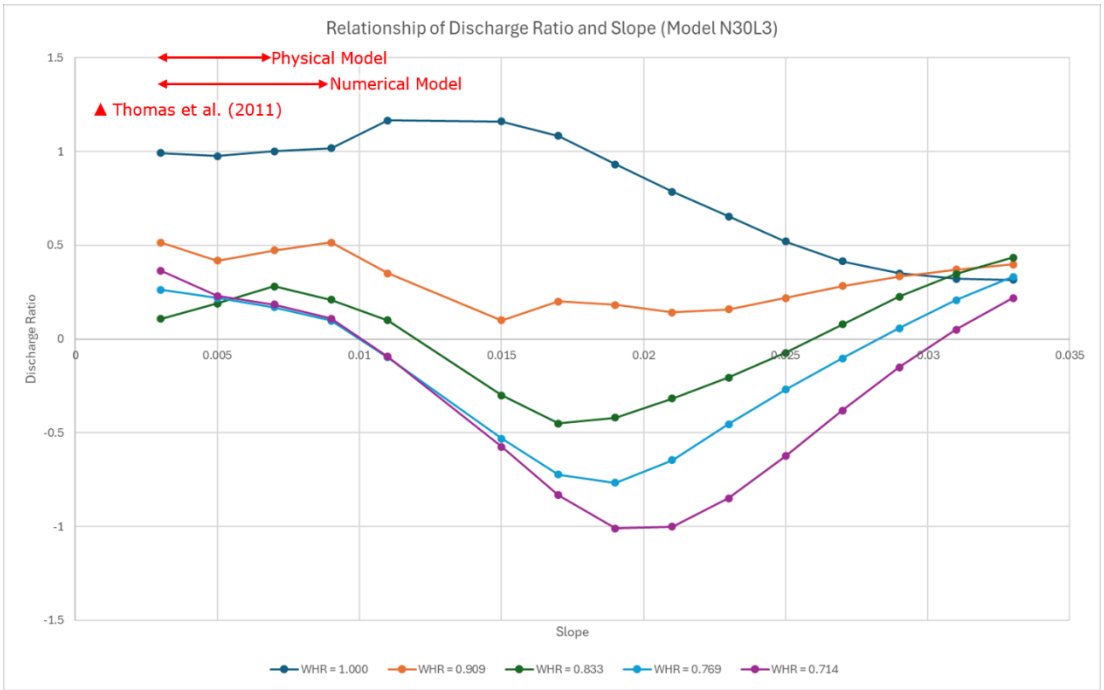


Figure 6.26: Relationship of discharge ratio and Slope (Model N30L3)

6.2.4 Minimum Weir Height

To study the relationship between discharge ratio and minimum weir height, various weir heights in the left tributary with a 0.8 weir height ratio are tested with the trained models. The predictions are plotted in Figure 6.27, Figure 6.28, Figure 6.29, Figure 6.30, Figure 6.31, and Figure 6.32.

Like slope, no trend can be observed among the predictions from the 6 trained models. However, the grouping method in numerical modelling shows the discharge ratio is affected by the minimum weir height. Without further data, this relationship cannot be predicted with only physical modelling and numerical modelling results. The predictions in the machine learning model may be accurate within a certain range or partially correct, further study is required to determine its properties.

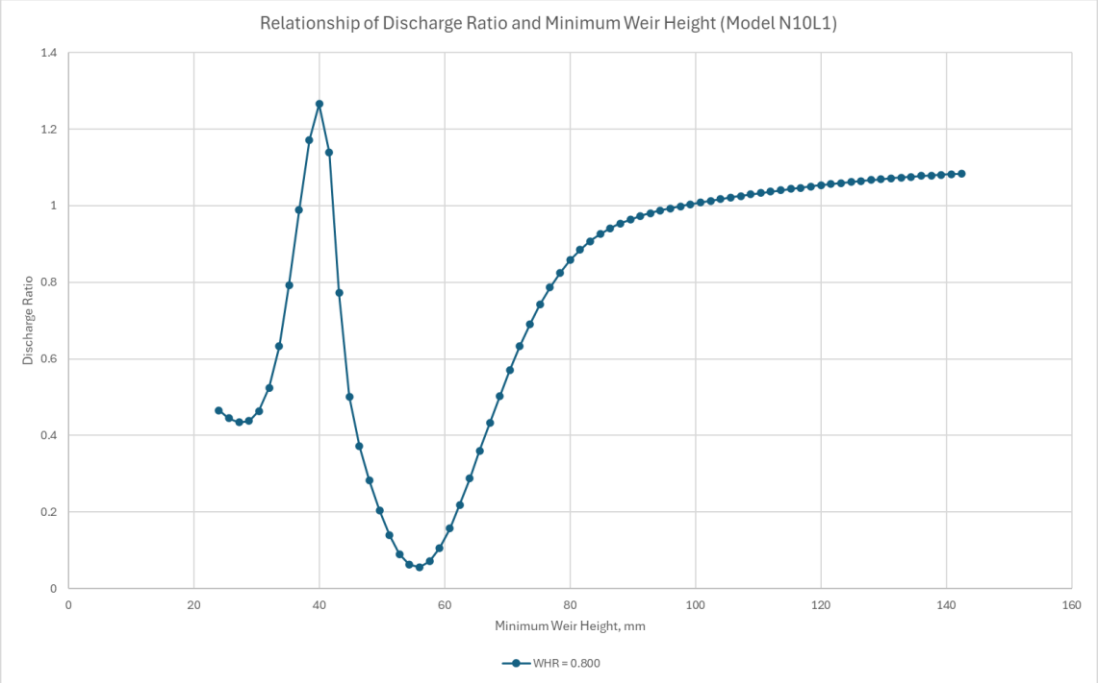


Figure 6.27: Relationship of discharge ratio and minimum weir height (Model N10L1)

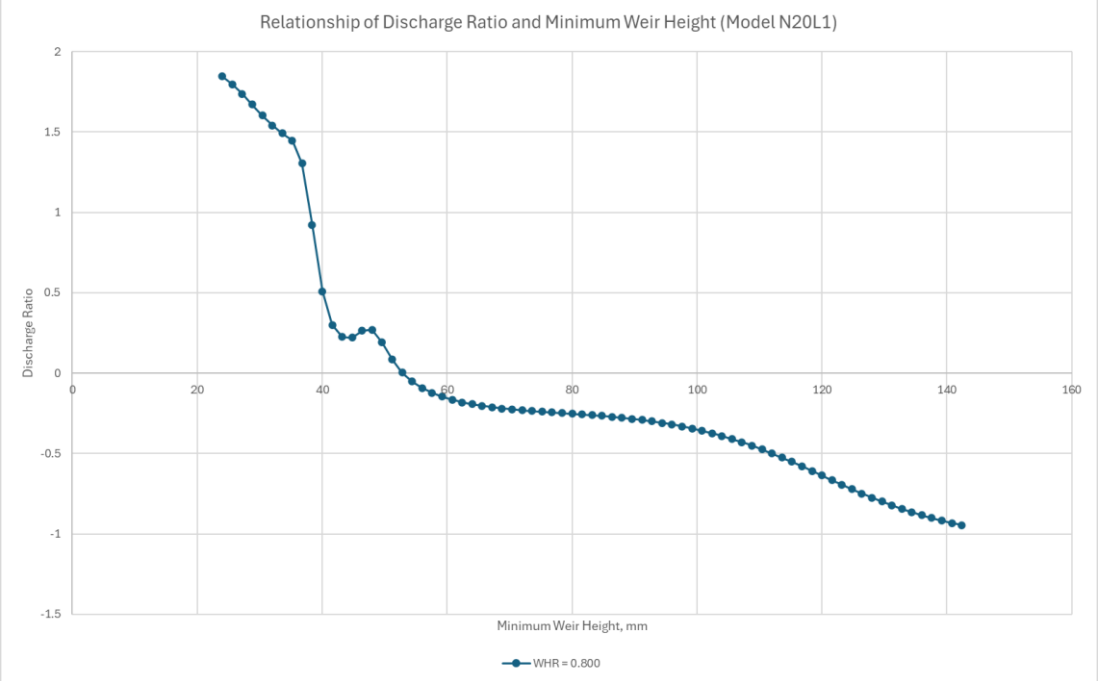


Figure 6.28: Relationship of discharge ratio and minimum weir height (Model N20L1)

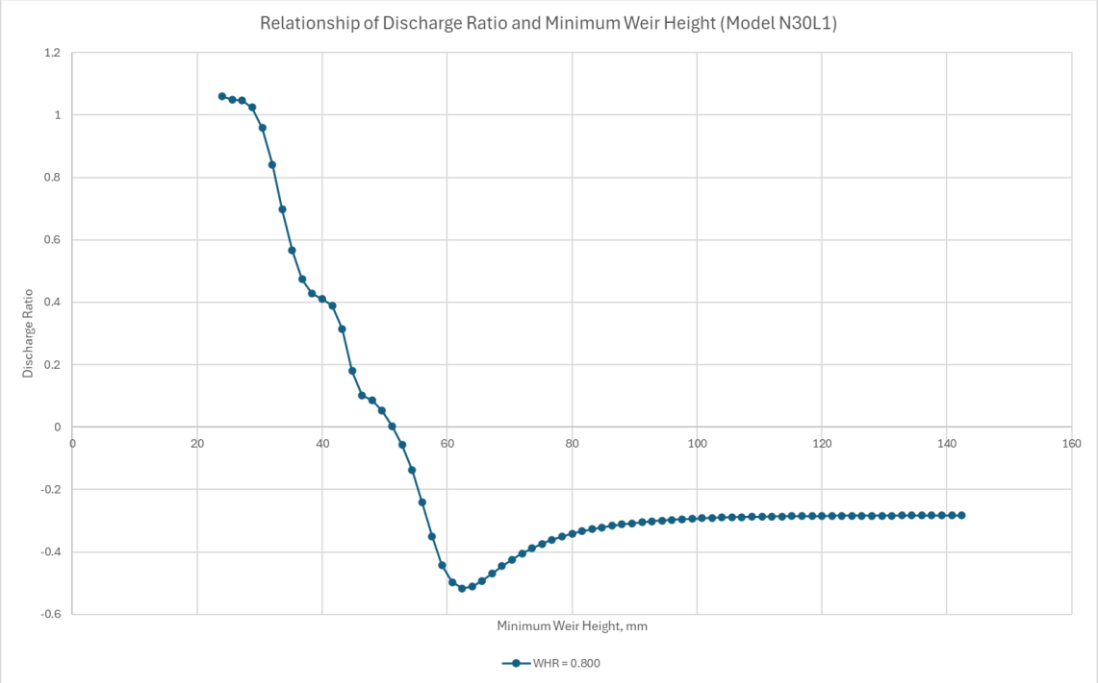


Figure 6.29: Relationship of discharge ratio and minimum weir height (Model N30L1)

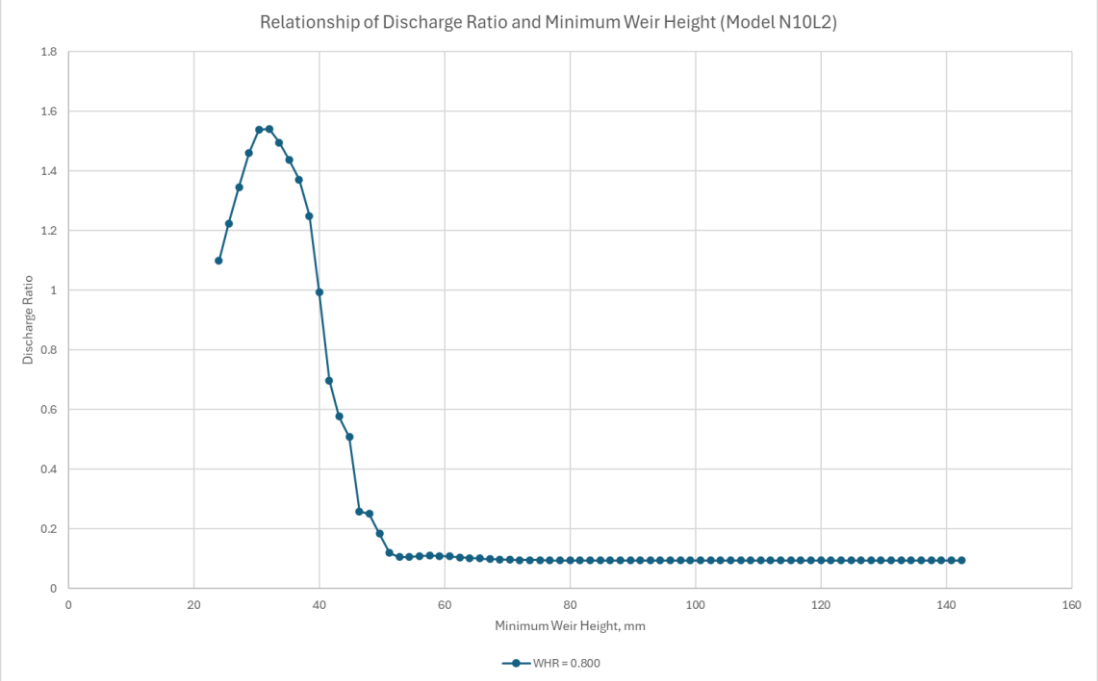


Figure 6.30: Relationship of discharge ratio and minimum weir height (Model N10L2)

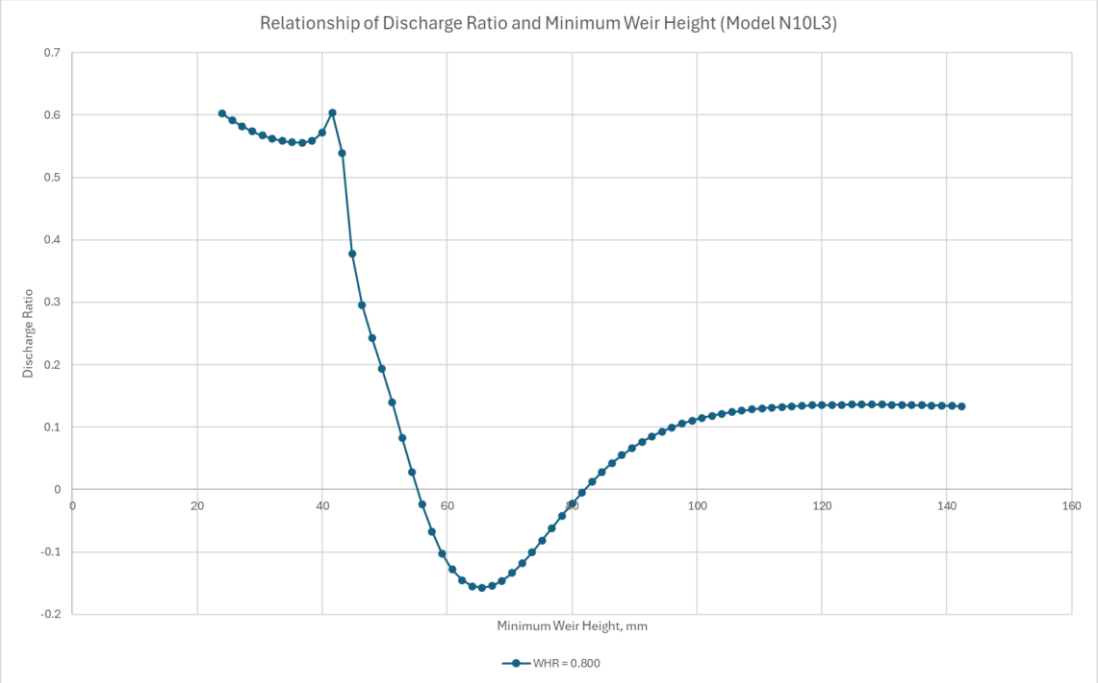


Figure 6.31: Relationship of discharge ratio and minimum weir height (Model N10L3)

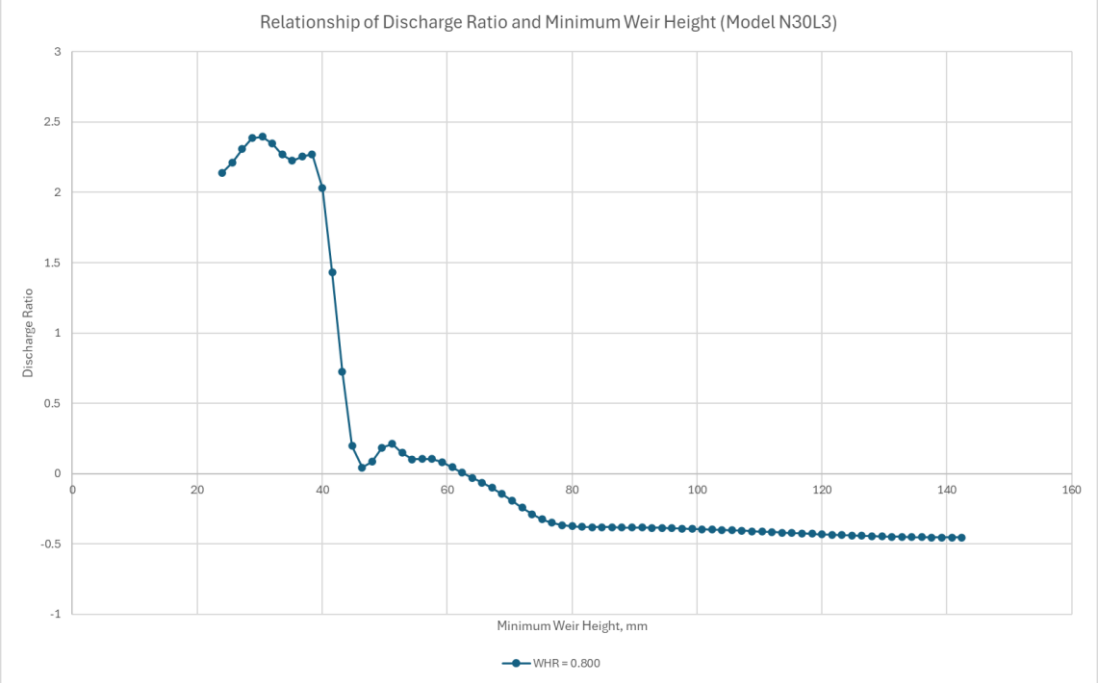


Figure 6.32: Relationship of discharge ratio and minimum weir height (Model N30L3)

6.3 Summary of Findings

Based on the ranking in training performance (Section 6.1), the best-performing model is N20L1, and the worst-performing model is N10L2. Overall, multi-layer models performed poorly compared with single-layer models. One hypothesis for these poorly performing models is that the architecture of the multiple-layer model may generate a bottleneck effect, as explained in Section 6.1.

Based on the prediction from these models, only 2 models (N10L1 and N10L3) showed the reasonable prediction by discharge at upstream and bifurcation angle.

Table 6.2 summarises the model performance and prediction. Comparison shows the best model in training performance does not have the ability to make a reasonable prediction on discharge ratio for any of the 4 factors. These results indicate that the models are not well trained. The prediction is not accurate when the discharge ratio is predicted based on bifurcation angle, slope, and minimum weir height under the current models. With future modifications, the ability of prediction by machine learning model may be accurate enough, however, further study and validation are required.

Table 6.2: Comparison of model performance and prediction

Model	Training Performance Ranking	Model Prediction			
		Discharge at Upstream	Bifurcation Angle	Slope	Minimum Weir Height
N10L1	3		✓		
N20L1	1				
N30L1	4				
N10L2	6				
N10L3	5	✓			
N30L3	2				

Chapter 7 Conclusions and Recommendations

7.1 Conclusions

7.1.1 Physical Model

The superelevation of water depth effect is formed around the bifurcation section near the wedge-shaped channel wall and the inner bank of the tributaries. The water depth gradient in asymmetrical weir height tends to be propagated towards the tributary with higher weir height when weir height ratio is smaller. The water depth gradient propagates further downstream when slope is steeper. There is insufficient evidence to prove that the peak value of superelevation of water depth has any correlation with weir height ratio and bifurcation angle. For superelevation of water depth near inner bank of tributary, the analysis by percentage difference shows minor impact of weir height ratio on the value of percentage difference.

Overall, the average water depth is inversely proportional to slope regardless of any bifurcation angle and weir height ratio, however, the water depth ratio is not affected by slope. In contrast, water depth ratio is found to be related to bifurcation angle and weir height ratio: weir height ratio is the variable of the linear function while bifurcation angle is the factor of the coefficients in the linear function. As the equation is drafted according to the experimental data, any value out of the range of the experiment is a prediction.

Unlike average water depth, water surface level is raised when slope is increased. Water surface level is found to be related to bifurcation angle. The water surface level at the weir section is approximately the same on both tributaries regardless of bifurcation angle, slope and weir height ratio.

This fundamental understanding of the hydrodynamic processes for bifurcation channels matches the first objective of this study, which includes interactions between a variety of flow conditions and a wide range of hydraulic structures.

The velocity of near surface flow is higher than near bed flow regardless of bifurcation angle, slope and weir height ratio. Like superelevation of water depth, flow velocity near inner bank is relatively higher than outer bank at the same section. Curvy velocity outline was discovered by Thomas et al. (2011), but no similar observation is found in this study, the low discharge in this experiment may be the main reason. Water naturally moves towards lower energy states through the path with least resistance. The tributary with higher weir height induces a "higher resistance", thus its flow velocity is relatively lower than the tributary with lower weir height.

The average flow velocity at each section is proportional to slope but not affected by bifurcation angle. The average flow velocity is found to be affected by weir height ratio, especially the height of the lowest weir height. Flow velocity ratio is not correlated with bifurcation angle and slope, but it is mainly manipulated by weir height ratio. The velocity ratio of both near surface flow and near bed flow are introduced using linear functions. Based on the two linear functions, the threshold of weir height ratio is determined, which are 0.873 from near surface flow and 0.886 from near bed flow.

All results show the discharge ratio is proportional to weir height ratio and correlated with bifurcation angle in a sine function; in contrast, it is not correlated with slope.

Comparison with Thomas et al. (2011) shows the threshold of weir height ratio may be affected by discharge or Froude number at upstream. From the experiment, the threshold of weir height ratio is found to range from 0.833 to 0.909. The threshold of weir height ratio is inversely proportional to discharge and Froude number at upstream.

The study in physical modelling of channel bifurcation with dimensionless factor analysis helps to understand the relationships between discharge ratio and weir height ratio over a variety of flow conditions and bifurcation geometries (Second Objective).

7.1.2 Numerical Model

All results from the numerical model show the discharge ratio is proportional to weir height ratio but not correlated with bifurcation angle and slope. As the bifurcation angle is one of the control variables of discharge ratio in physical modelling, this contradicts the physical model findings. One of the suspicions regarding this contradiction was the inlet discharge, as the discharge in the numerical model was higher than in the physical model. The impact of bifurcation angle on the discharge partitioning may be dissipated as the inlet discharge increased. The lowest weir height in the tributary is also affecting the discharge ratio in an inversely proportional relationship.

Comparison with Thomas et al. (2011) and physical model shows the threshold of weir height ratio is affected by the discharge at upstream. From the simulation, the threshold of weir height ratio with 1000cm^3/s is found to range from 0.737 to 0.820. The threshold of weir height ratio is inversely proportional to discharge at upstream. Other than discharge at upstream, the lowest weir height in the tributary is also affecting the threshold of weir height ratio.

The results of the numerical model further identify the effect of hydraulic parameters on the hydrodynamic processes of bifurcation channel flows (Third Objective).

7.1.3 Machine Learning Model

The performance and coefficient of determination of the trained machine learning model show the high reliability of the machine learning model in the application of predicting the bifurcation flow. However, this prediction may be constrained within a range of input as the data for feeding is limited. Another suspicion regarding the poor performance is the architecture of the model; multiple layers model may generate bottleneck to further reduce the performance of model.

The current trained model also shows illogical value of discharge ratio as the ANN model in this study is a purely mathematical approach without additional constraint settings on values based on physics. Alternative setup on the ANN model may improve its ability of prediction, especially the discharge ratio must be constrained to less than 1 during the ANN model training stage. In conclusion, the model for discharge ratio with discharge at upstream is partially correct; this shows the capability of application in bifurcation prediction by ANN model.

Finally, the machine learning model is trained and applied for predicting the bifurcation behaviour (Fourth Objective).

7.2 Recommendations

7.2.1 Physical Model

Due to the limitation of flume, the inlet discharge is relatively low. A recommended improvement to the experimental setup would be to increase the inlet discharge. Additional range of control parameters (bifurcation angle, slope, and weir height) allows better understanding on the effect of these control parameters, specifically regarding the impact on hydrodynamic processes of channel bifurcation and dimensionless factors such as discharge ratio.

The velocity measurement is manually measured at each point, as the inlet discharge of the physical model will never be consistent throughout the whole experiment, multiple sets of ADCP can be implemented in the experiment to avoid the lag time effect and provide an instantaneous measurement for all measurement points.

7.2.2 Numerical Model

As the discharge in the physical model does not match that in the numerical model, the comparison between the two models is not feasible. A constant rate of inlet discharge for both models will improve the validation of the model. The inlet discharge in the numerical model was assumed to be a fixed value. To enlarge the database for machine learning model training, simulation with wide range of inlet discharge is recommended.

7.2.3 Machine Learning Model

To develop a better machine learning model for prediction of channel bifurcation, the architecture of the ANN may adopt different numbers of neurons in multiple layers to avoid the bottleneck effect. Different basic architecture types, such as Long Short-Term Memory (LSTM), can be implemented as the model type for training. As the feeding data in this study is very limited, and a significant improvement to the machine learning model would be to provide more data based on physical model experiments or numerical model simulations.

Physics-informed neural networks (PINNs) could be another alternative option for machine learning model. This architecture integrates the physics of hydraulics or fluid mechanics that govern a given dataset in the machine learning process. The advantage of PINNs is quoted “the additional physics knowledge regularizes the predicted solution in the presence of noisy measurement data, enabling PINNs to learn the true underlying signal rather than overfitting the noisy data” (MathWorks, no date).

The complete 3D result from numerical model may be used for machine learning model training, a comprehensive model can be developed to predict the channel bifurcation behaviour in a dynamic aspect. Hence, CNN- and RNN-type models are recommended for learning the hydrodynamic processes of bifurcation.

References

Abderrezzak, K.E.K., Lewicki, L., Paquier, A., Rivière, N., & Travin, G, 2011. Division of critical flow at three-branch open channel intersection. *Journal of Hydraulic Research*, 49(2), pp. 231-238.

Ahsan, A., 2020. *Hydraulic structures - theory and applications*, IntechOpen, London.

Alfatlawi, T.J.M. & Hussein, A.M., 2024a. A numerical study of diversion flow to determine the optimum flow system in open channels. *Water Practice & Technology*, 19(4), pp. 1330-1347.

Alfatlawi, T.J.M. & Hussein, A.M., 2024b. Probing the complexities of optimal flow in open channels: experimental and numerical validation with diversion flow. *Journal of Hydroinformatics*, 26(10), pp. 2618.

Alomari, N.K., Yusuf, B., & Ali, T.A.M., 2016. Flow in a branching open channel: a review. *Pertanika Journal of Scholarly Research Reviews,* 2(2), pp. 40-56.

Barile, G., 2025. *River bifurcations: key processes, timescales and evolutionary trajectories*. Ph.D. Thesis. University of Trento

Barile, G., Redolfi, M., & Tubino, M., 2024. Analysis of autogenic bifurcation processes resulting in river avulsion. *Earth Surface Dynamics*, 12, pp. 87-103.

Barkdoll, B.D., & Odgaard, A.J., 1998. Experimental comparison of dividing open-channel with duct flow in T-junction. *Journal of Hydraulic Engineering*, 124(1), pp. 92-95.

Bertoldi, W. & Tubino, M., 2005. Bed and bank evolution of bifurcating channels. *Water Resources Research,* 41(7), W07001.

Bertoldi, W. & Tubino, M., 2007. River bifurcations: Experimental observations on equilibrium configurations. *Water Resources Research,* 43(10), pp. W10437.

Bertoldi, W., 2004. *River bifurcations*. Ph.D. Thesis. University of Trento.

Bolla Pittaluga, M., Repetto, R. & Tubino, M., 2003. Channel bifurcation in braided rivers: Equilibrium configurations and stability. *Water Resources Research,* 39(3), 1046.

Calderón, D., Mohamed K., & Oriz, J., 2025. Experimental analysis of the relationship between flow velocities and sediment transport in a laboratory channel featuring a lateral bifurcation and sand bed. *Enfoque UTE*, 16(3), pp. 1-15.

Cheong, H., 1991. Discharge coefficient of lateral; diversion from trapezoidal channel. *Journal of Irrigation and Drainage Engineering*, 117(4), pp. 461-475.

Crosato, A., 2008. Analysis and modelling of river meandering.PhD. Thesis. Delft University of Technology.

Das, A., Barman, B.C., & Nandi, N., 2023. On some aspects of flow characteristics of the bifurcated channel – An experimental approach. *ISH Journal of Hydraulic Engineering*, *29*(2), pp. 147–153.

den Dekker, P. & van Voorthuizen, J., 1994. *Research on the morphological behaviour of bifurcatios in rivers*. M.Sc. Thesis, Delft University of Technology.

Department of Irrigation and Drainage Malaysia, 2008. Flood mitigation – structure and non structural measures and flood response. *Malaysian Technical Cooperation Program*, pp 9.

Durante, L., Bolla Pittaluga, M., Porcile, G., & Tambroni, N., 2024. Downstream control on the stability of river bifurcations. *Journal of Geophysical Research: Earth Surface*, 129(10), pp. e2023JF007548.

Fang, Y. et al., 2025. Varying flow division forced by streamflow and tidal force in bifurcation channels in the Pearl River Delta, South China. *Geomatics, Natural Hazards and Risk*, 16(1), pp. 2501736

Federici, B. & Paola, C., 2003. Dynamics of channel bifurcations in noncohesive sediments. *Water Resources Research,* 39(6), pp. 1162.

Foh, Z.X., Tan, C.Y., Haniffah, M.R.M.H., Kasiman, E.H., & Teo, F.Y., 2021. Numerical analysis of flow characteristics for idealised y-shaped channels. *The 5th International Conference on Water Resources (ICWR2021)*, Malaysia, 26-27 November 2021.

Grace, J.L. & Priest, M.S., 1958. Division of Flow in Open Channel Junctions. *Auburn University Bulletin*, 31.

Hager, W.H., 1984. An approximate treatment of flow in branches and bends. *Journal of Mechanical Engineering Science,* 198(63), pp. 63-69.

Herrero, A., Bateman, A., & Medina, V., 2015. Water flow and sediment transport in a 90° channel diversion: an experimental study. *Journal of Hydraulic Research*, 53(2), pp. 253-263.

Hsu, C., Tang, C., Lee, W., & Shieh. M., 2002. Subcritical 90° equal-width open-channel dividing flow. *Journal of Hydraulic Engineering*, 128(7), pp. 716-720.

Isikdogan, F., Bovik, A., & Passalacqua, P., 2017a. RivaMap: An automated river analysis and mapping engine. *Remote Sensing of Environment,* 202(1), pp. 88-97.

Isikdogan, F., Bovik, A., & Passalacqua, P., 2017b. Surface water mapping by deep learning. *IEEE Journal of Selected Topics in Applied Earth Observations and Remote Sensing,* 10(11), pp. 4909-4918.

Isikdogen, F., Bovik, A., & Passsalacqua, P., 2018. Learning a river network extractor using an adaptive loss function. *IEEE Geoscience and Remote Sensing Letters,* 15(6), pp. 813-817.

Julien, P.Y., 2018. *River Mechanics.* 2nd Edition ed. s.l.:Cambridge University Press.

Kerssens, P.J.M. & van Urk, A., 1986. Experiemntal studies on sedimentation due to water withdrawal. *Journal of Hydraulic Engineering,* 112(7), pp. 641-651.

Kleinhans, M.G., Jagers, H.R.A., Mosselman, E., & Sloff, C.J., 2008. Bifurcation dynamics and avulsion duration in meandering rivers by one-dimensional and three-dimensional models. *Water Resources Research,* 44(8).

Krishnappa, G. & Seetharamiah, K., 1963. A New Method of Predicting the Flow in a 90° branch channel. *La Houille Blanche, International Water Journal,* 49(7), pp. 775-778.

Kuang, H., 2011. *Physical and numerical modelling study of meandering in fluvial rivers*. Ph.D. Thesis. Cardiff University.

Lakshmana Rao, N.S., Sridharan, K., & Baig, M.A., 1968. *Experimental Study of Division of Fow in Open Channel.* Sydney, The Institution of Engineers, Australia, pp. 139-142.

Lama, S.K., Kudoh, K., & Kuroki, M., 2003. Study of flow characteristics of junction flow with free flow condition at branch channel. *Annual Journal of Hydraulic Engineering*, 47, pp. 601-606.

Lama, S.K., Kuroki, M., and Hasegawa, K. (2002). Study of flow bifurcation at the 30° open channel junction when the width ratio of branch channel to main channel is large. *Annual Journal of Hydraulic Engineering*, 46, 583-588.

Law, S.W., 1965. *Dividing flow*. M.Sc. Thesis. McGill University.

Le, T., Crosato, A., Mosselman, E., & Uijttewaal, W., 2018. On the stability of river bifurcations created by longitudunal training walls. Numerical investigation. *Advances in Water Resources,* 113, pp. 112-125.

Marra, W.A., Parsons, D.R., Kleinhans, M.G., Keevil, G.M. & Thomas, R.E., 2014. Near-bed and surface flow division patterns in experimental river bifurcations. *Water Resources Research,* 50(2), pp. 1506-1530.

MathWorks, no date. *What Are Physics-Informed Neural Networks (PINNs)?* Accessed 2023 https://www.mathworks.com/discovery/physics-informed-neural-networks.html

Moghadam, M.K., Bajestan, M.S., Sedghi, H., & Seyedian, M., 2014. An experimental and numerical study of flow patterns at a 30 degree water intake from trapezoidal and rectangular channels. *Transactions of Civil Engineering*, 38(C1), pp. 85-97.

Neary, V.S. & Odgaard, A.J., 1993. Three-dimensional flow structure at open channel diversion. *Journal of Irrigation and Drainage Engineering*, 119(11), pp. 1223-1230.

Ng, K.J., Tan, C.Y., Selvarajoo A., Haniffah M.R.M., Kasiman E.H., LAI S.H., YUAN D., & TEO F.Y., 2022, Simulating channel bifurcation flows with weirs for flood risk reduction. Larhyss Journal, 49, pp. 181-196.

Oga, T. et al., 2020. River state classification combining patchbased processing and CNN. *PLoS ONE,* 15(12).

Pattabhiramiah, K.R. & Rajaratnam, N., 1960. A new method to predict flow in a branch channel. *Irrigation & Power Journal, New Delhi*, 17(1), pp. 48-51.

Pirzadeh, B. & Shamloo, H., 2007. Numerical investigation of velocity field in dividing open-channel flow. *12th WSEAS International Conference on Applied Mathematics*, Cairo, Egypt, 29-31 2007.

Ramamurthy, A.S. & Satish, M.G., 1988. Division of Flow in Short Open Channel Branches. *Journal of Hydraulic Engineering,* 114(4), pp. 428-438.

Ramamurthy, A.S., Qu, J., & Vo, D., 2007. Numerical and experimental study of dividing open-channel flows. *Journal of Hydraulic Engineering*, 133(10), pp. 1135-1144.

Ramamurthy, A.S., Tran, D.M., & Carballada, L.B., 1990. Dividing Flow in Open Channels. *Journal of Hydraulic Engineerig,* 116(3), pp. 449-455.

REFORM (2022). REFORM: REstoring rivers FOR effective catchment Management | REFORM. [online] Available at: https://www.reformrivers.eu/start.html [Accessed 2022]

Rivière, N., Travin, G., & Perkins, R.J., 2014. Transcritical flows in three and four branch open-channel intersections. *Journal of Hydraulic Engineering*, 140(4).

Roosjen, R. & Zwanenburg, C., 1995. *Research on bifurcations in rivers*. M.Sc. Thesis. Delft University of Technology.

Salter, G., Voller, V.R. & Paola, C., 2019. How does the downstream boundary affect avulsion dynamics in a laboratory bifurcation?. *Earth Surface Dynamics*, 7(4), pp. 911-927.

Sayed, T., 2019. An experimental study of branching flow in open channels. Limnological Review, 19(2). pp. 93-101.

Schielen, R.M.J. & Blom, A., 2018. A reduced complexity model of gravel sand river bifurcation. *Advances in Water Resources*, 121, pp. 9-21.

Science, 2025. *Researchers claim their AI model simulates the human mind. Others are skeptical*. Accessed 2025. https://www.science.org/content/article/researchers-claim-their-ai-model-simulates-human-mind-others-are-skeptical

Shen, Y. et al., 2024. Initial experimental investigation of hydraulic characteristics at right-angle diversion in a combined canal and pipe water conveyance system. *Water*, 16(22), pp. 3174.

Shettar, A.S. & Murthy, K.K., 1996. A numerical study of division of flow in open channels. *Journal of Hydraulic Reserach,* Volume 34:5, pp. 651-675.

Sloff, K. & Mosselman, E., 2012. Bifurcation modelling in a meandering gravel–sand bed river, *Earth Surface Processes and Landforms,* 37(14), pp. 1556-1566.

Stryker, C., Lee, F., Bergmann, D., & Scapicchio, M., 2026. *The 2026 Guide to Machine Learning*. Accessed 2026. https://www.ibm.com/think/machine-learning#605511093

Szewczyk, L., Grimaud, J., & Cojan, I., 2020. Experimental evidence for bifurcation angles control on abandoned channel fill geometry. *Earth Surface Dynamics*, 8(2), pp. 275-288.

Taylor, E. H., 1944. Flow Characteristics at Rectangular Open-Channel Junction. *Transactions of the American Society of Civil Engineers,* 109(1).

Tholibon, D.A. & Ariffin, J., 2013. *International Journal of Sciences: Basic and Applied Research (IJSBAR)*, 8(1), pp. 45-50.

Thomas, R.E., Parsons, D.R., Sandbach, S.D., Keevil, G.M., Marra, W.A., Hardy, R.J., Best, J.L, Lane, S.N., & Ross, J.A., 2011. An experiment study of discharge partitioning and flow structure at symmetrical bifurcations. *Earth Surface Processes and Landforms,* 36(15), pp. 2069-2082.

United States Department of the Interior Bureau of Reclamation, 2001. Water Measurement Manual 3rd Edition.

van Leeuwe, G., 2018. *Approximating river bed level at river bifurcation if data is scarce*. M.Sc. Thesis. University of Twente.

Wang, Z.B., Vries, M.D., Fokkink, R.J., & Langerak, A., 1995. Stability of river bifurcations in 1D morphodynamic models. *Journal of Hydraulic Research,* 33(6), pp. 739-750.

Zanichelli, G., Caroni, E. & Fiorotto, V., 2004. River bifurcation analysis by physical and numerical modeling. *Journal of Hydraulic Engineering,* 130(3), pp. 237-242.

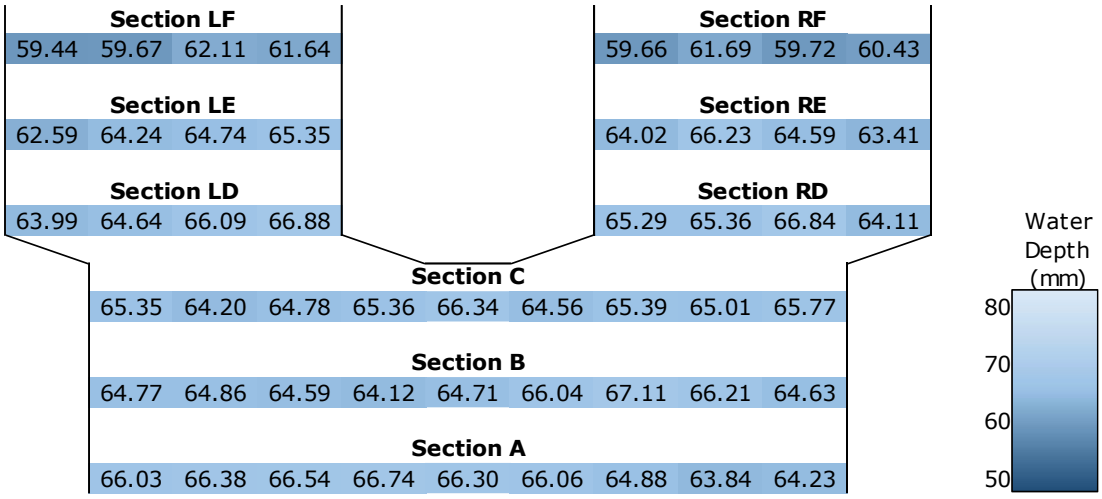
Zawawi, I.S.M. et al., 2019. Mathematical modeling for flood mitigation: Effect of bifurcatioin angles in river flowrates. *Civil Engineering and Architecture,* 7(6A), pp. 50-57.

Zolezzi, G., Bertoldi, W., & Tubino, M., 2006. Morphological analysis and prediction of river bifurcations. *Braided Rivers: Process, Deposits, Ecology and Management*, pp. 233-256.

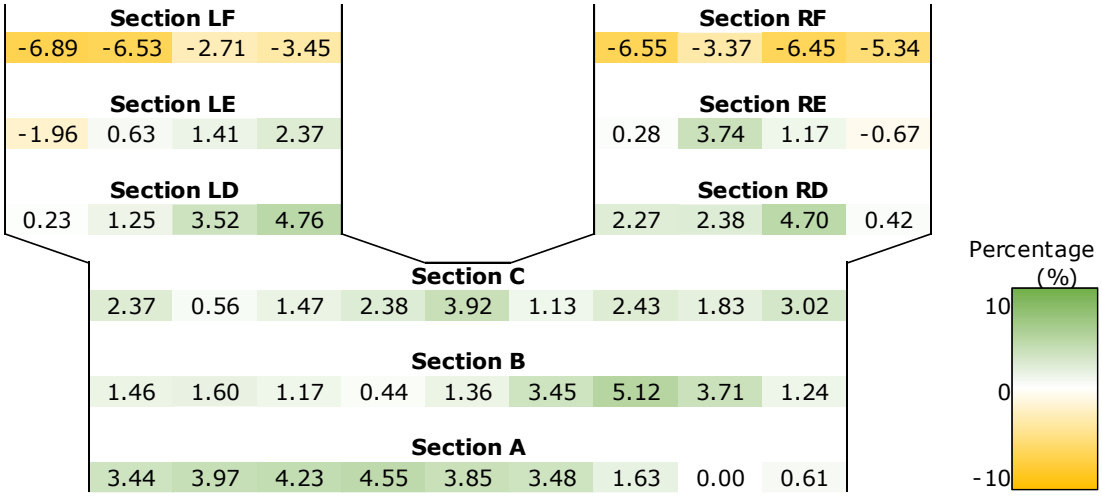
Appendix A1 Measured Water Depth and Superelevation of Water Depth (Plan)

Bifurcation Angle, °	Slope, %	Left Weir Height, mm	Right Weir Height, mm	Name of Run	Page Number
30	0.3	50	50	30_03_5050	A-2
		55	60	30_03_5560	A-3
		50	55	30_03_5055	A-4
	0.5	50	50	30_05_5050	A-5
		55	60	30_05_5560	A-6
		50	55	30_05_5055	A-7
	0.7	50	50	30_07_5050	A-8
		55	60	30_07_5560	A-9
		50	55	30_07_5055	A-10
40	0.3	50	50	40_03_5050	A-11
		55	60	40_03_5560	A-12
		50	55	40_03_5055	A-13
	0.5	50	50	40_05_5050	A-14
		55	60	40_05_5560	A-15
		50	55	40_05_5055	A-16
	0.7	50	50	40_07_5050	A-17
		55	60	40_07_5560	A-18
		50	55	40_07_5055	A-19
50	0.3	50	50	50_03_5050	A-20
		55	60	50_03_5560	A-21
		50	55	50_03_5055	A-22
	0.5	50	50	50_05_5050	A-23
		55	60	50_05_5560	A-24
		50	55	50_05_5055	A-25
	0.7	50	50	50_07_5050	A-26
		55	60	50_07_5560	A-27
		50	55	50_07_5055	A-28

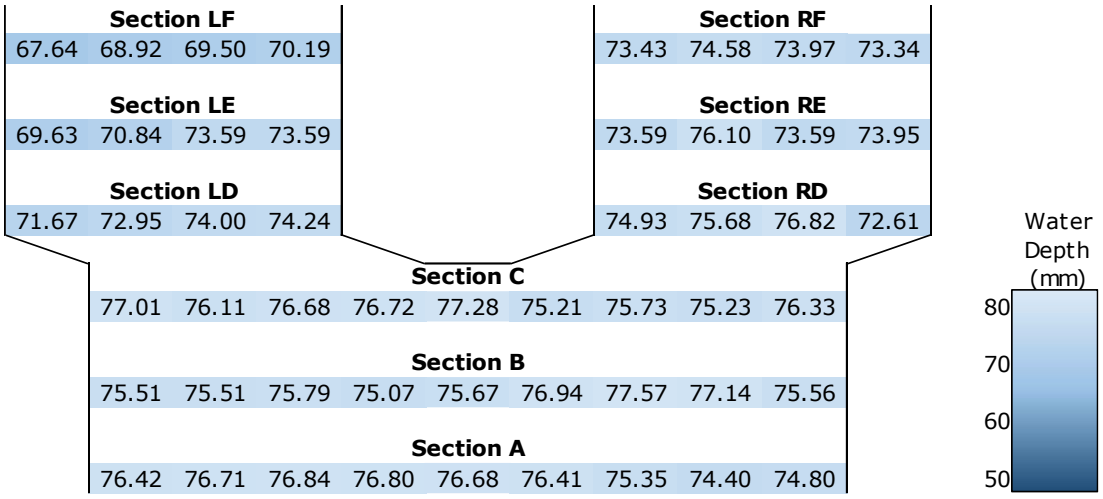
Water Depth Measurement: 30_03_5050



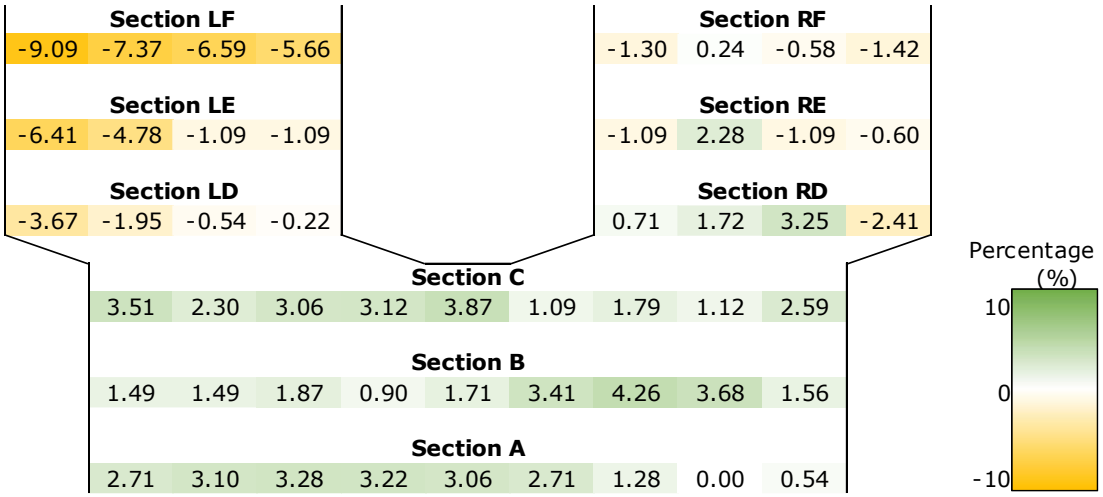
Water Depth Superelevation: 30_03_5050



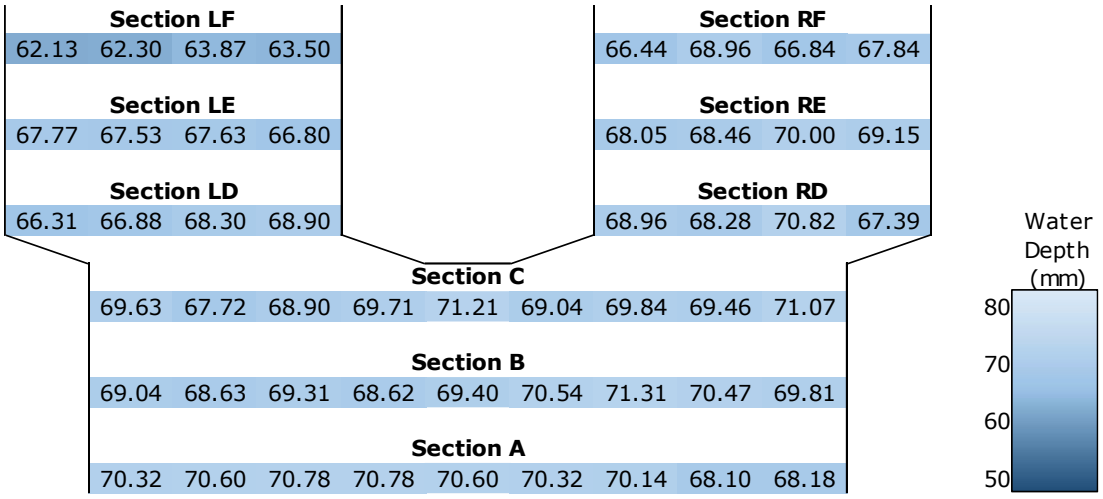
Water Depth Measurement: 30_03_5560



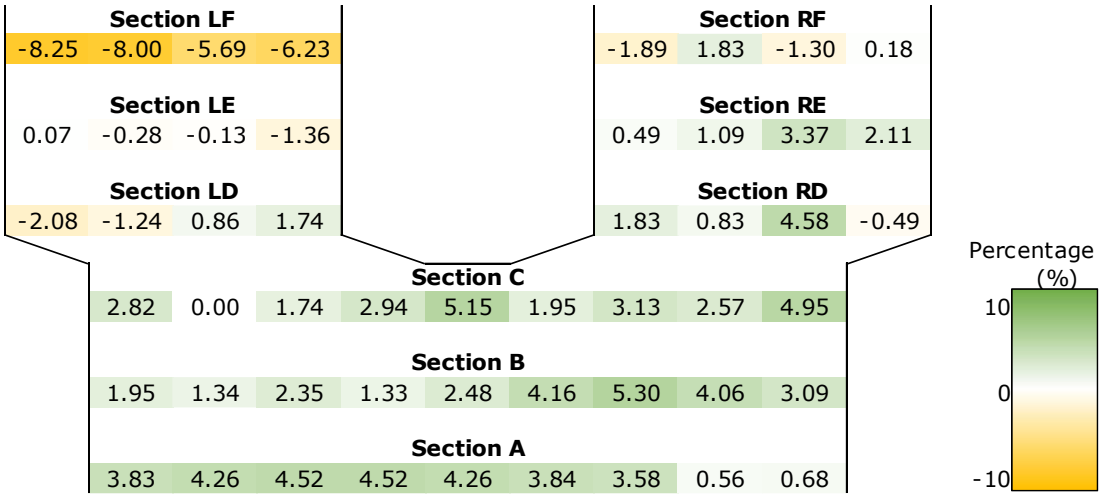
Water Depth Superelevation: 30_03_5560



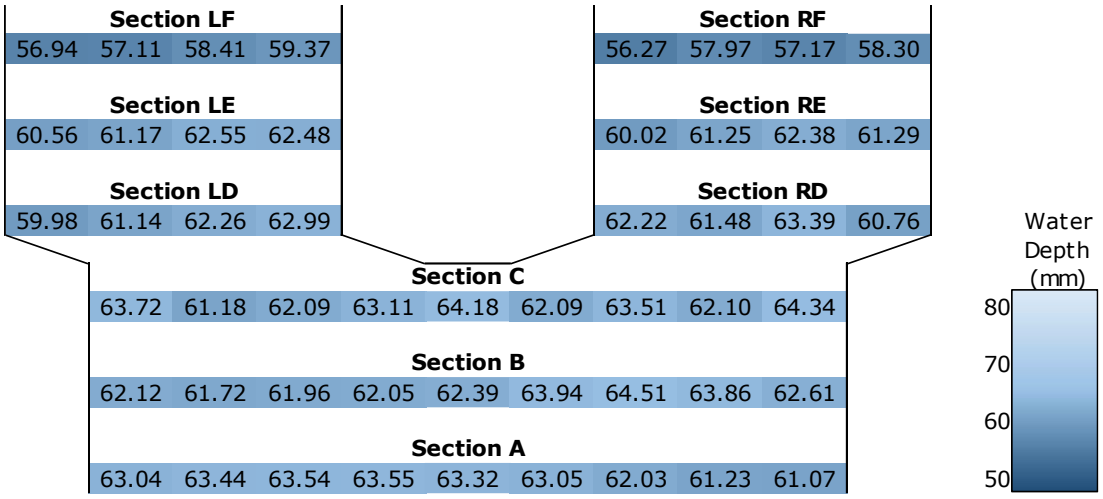
Water Depth Measurement: 30_03_5055



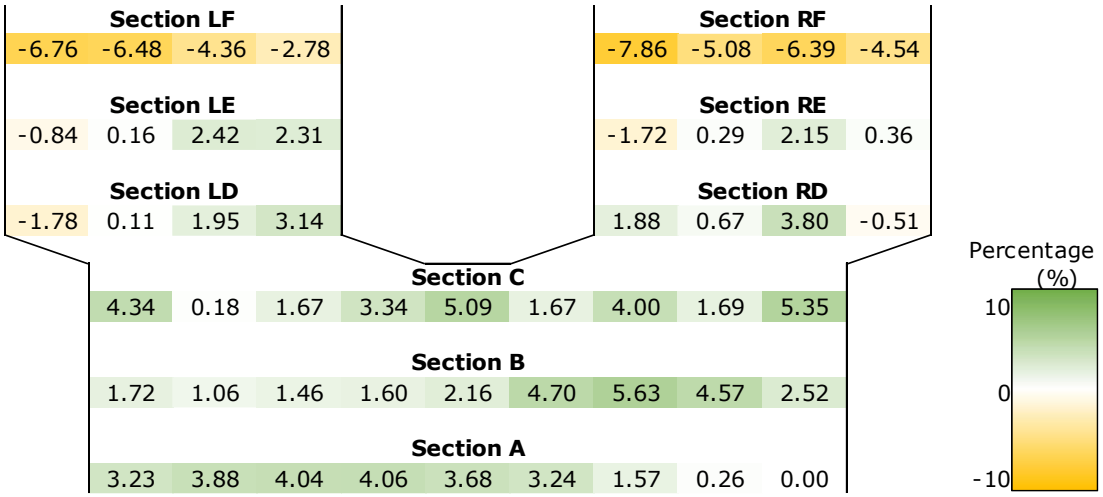
Water Depth Superelevation: 30_03_5055



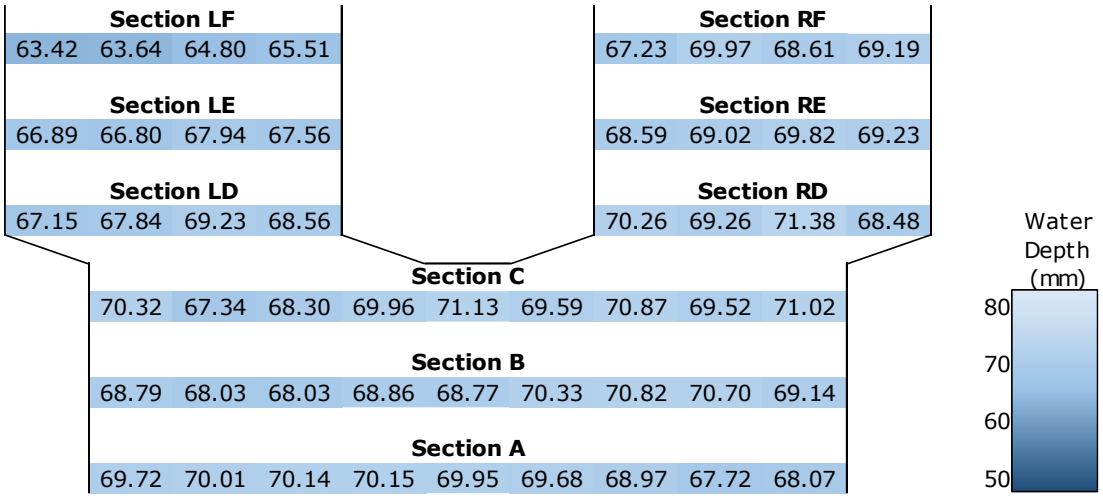
Water Depth Measurement: 30_05_5050



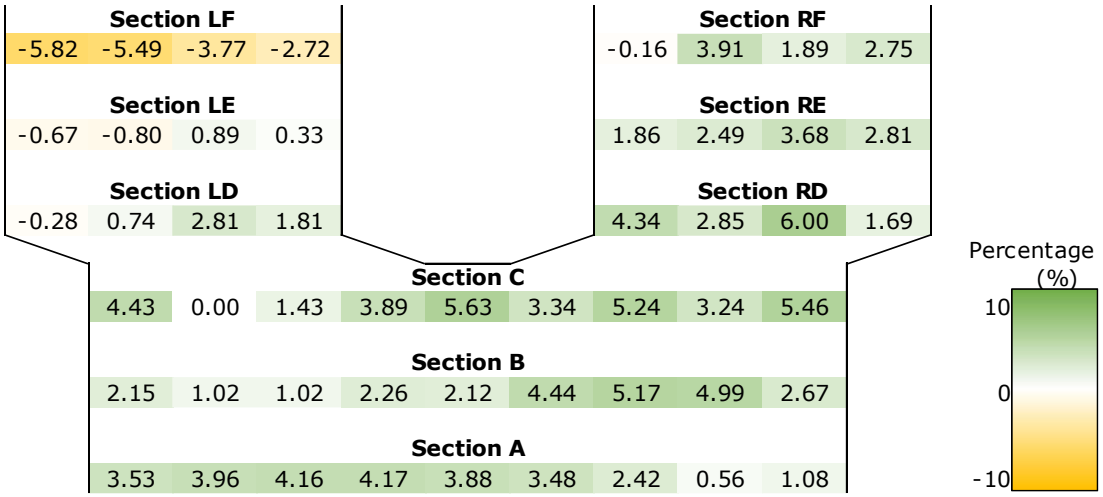
Water Depth Superelevation: 30_05_5050



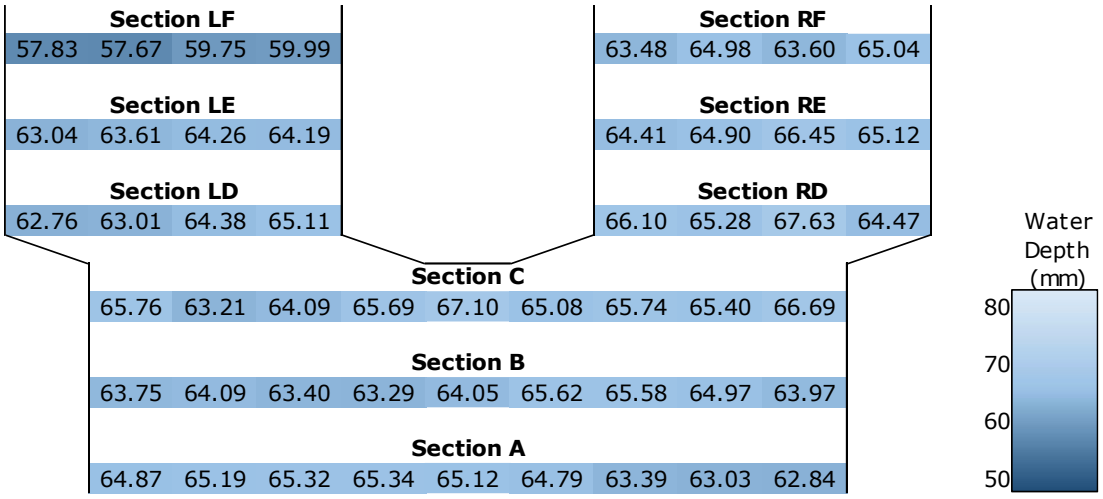
Water Depth Measurement: 30_05_5560



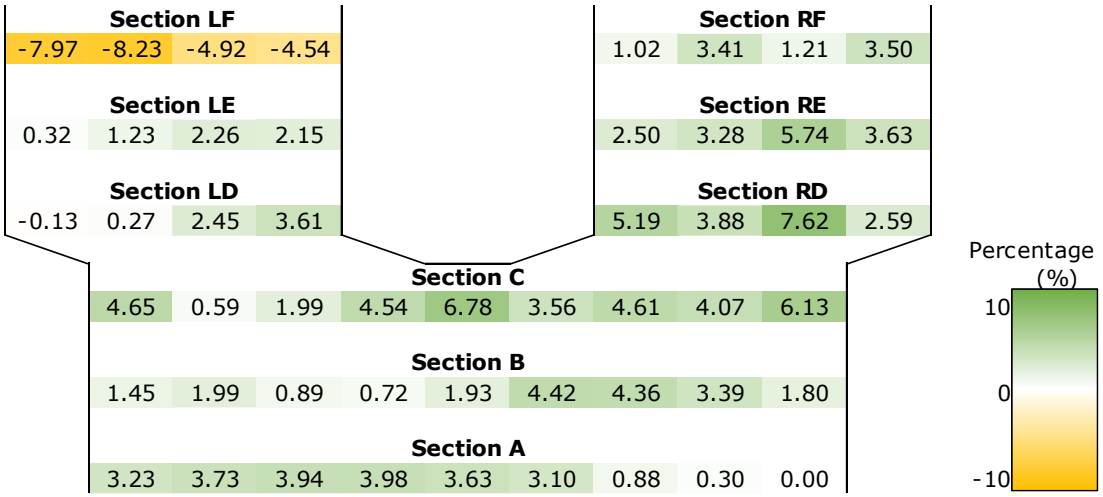
Water Depth Superelevation: 30_05_5560



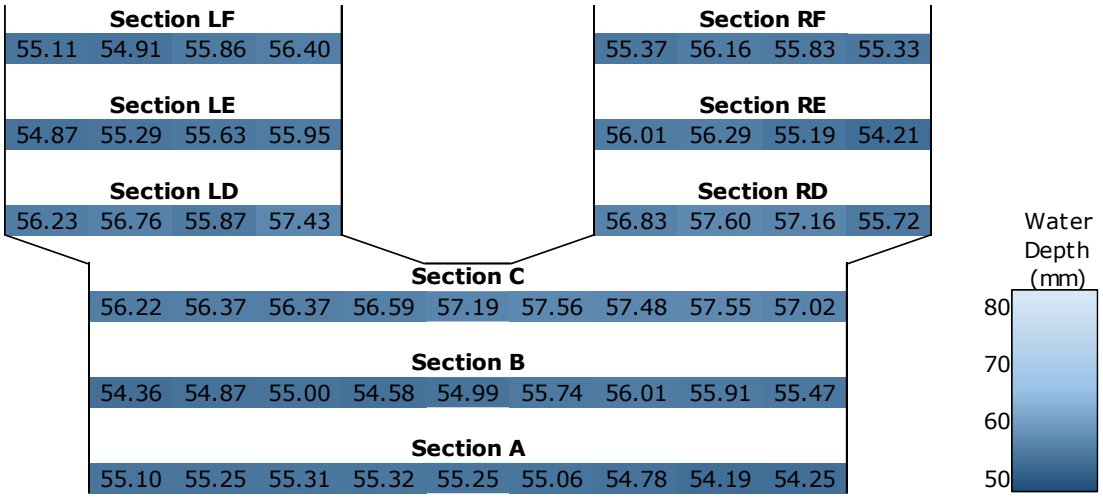
Water Depth Measurement: 30_05_5055



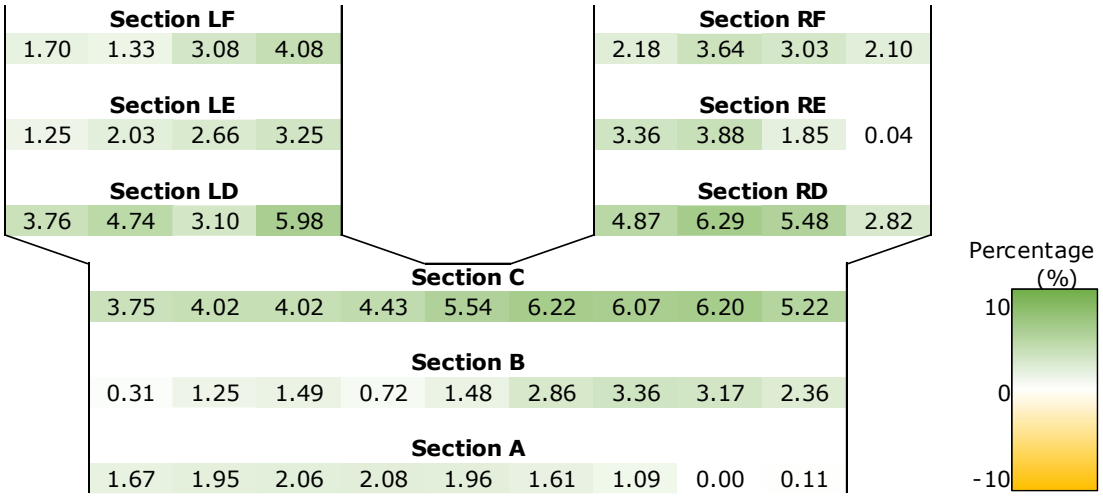
Water Depth Superelevation: 30_05_5055



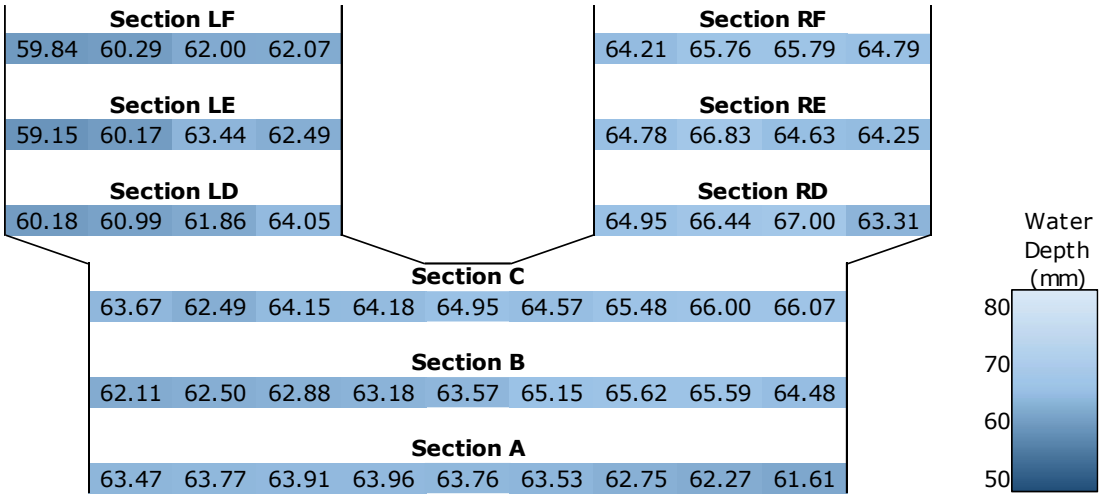
Water Depth Measurement: 30_07_5050



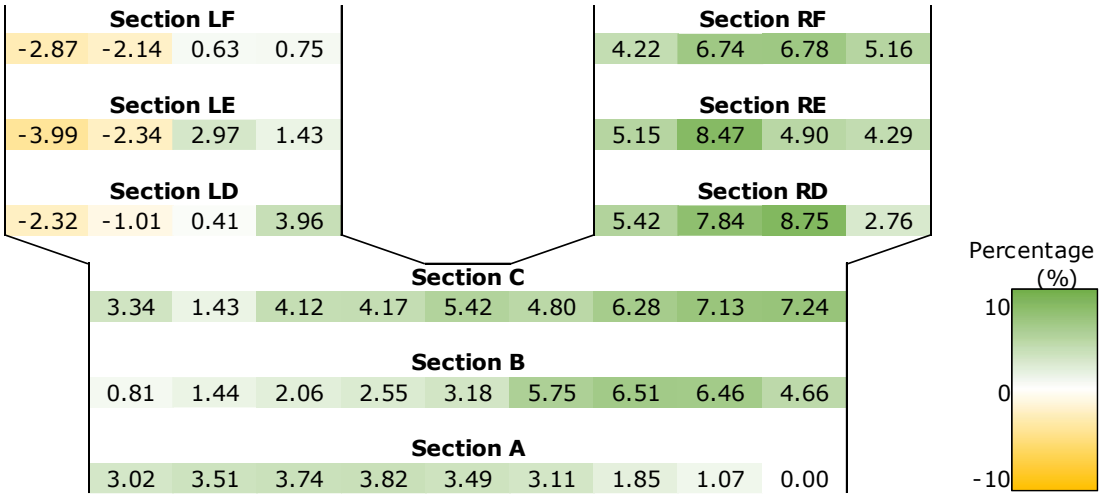
Water Depth Superelevation: 30_07_5050



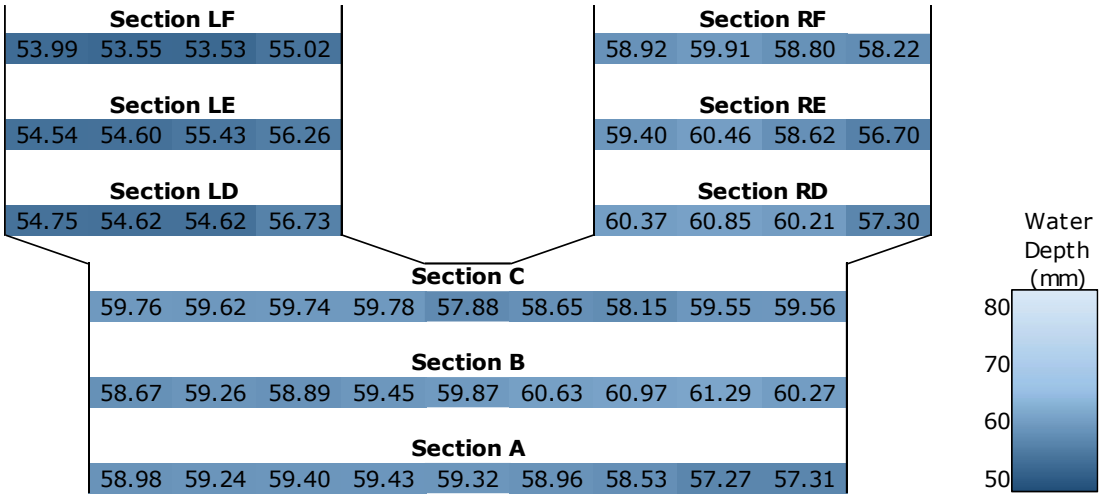
Water Depth Measurement: 30_07_5560



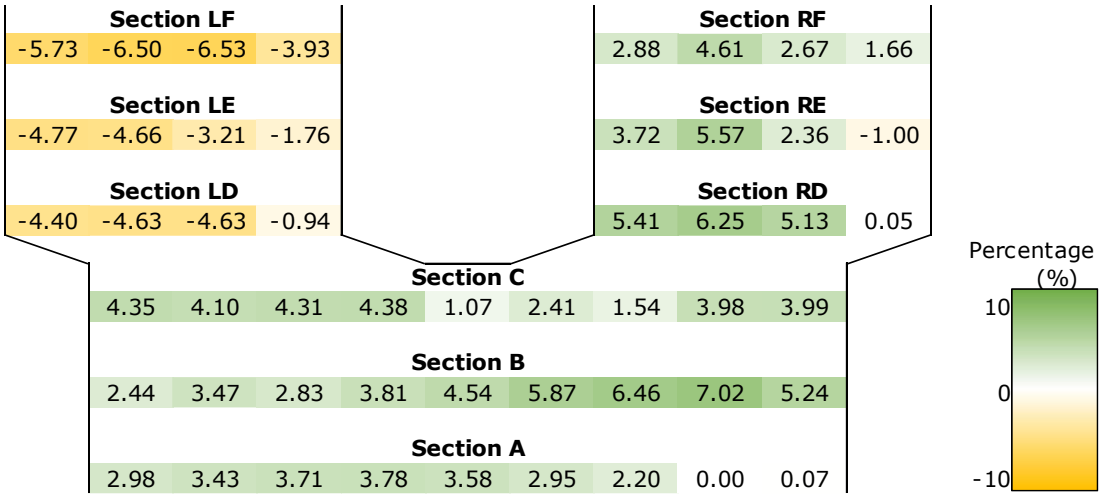
Water Depth Superelevation: 30_07_5560



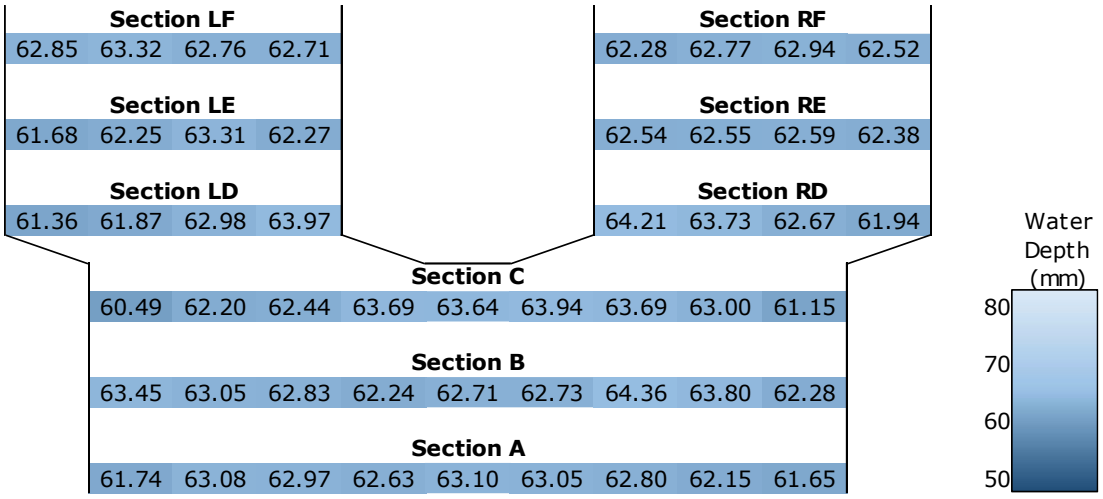
Water Depth Measurement: 30_07_5055



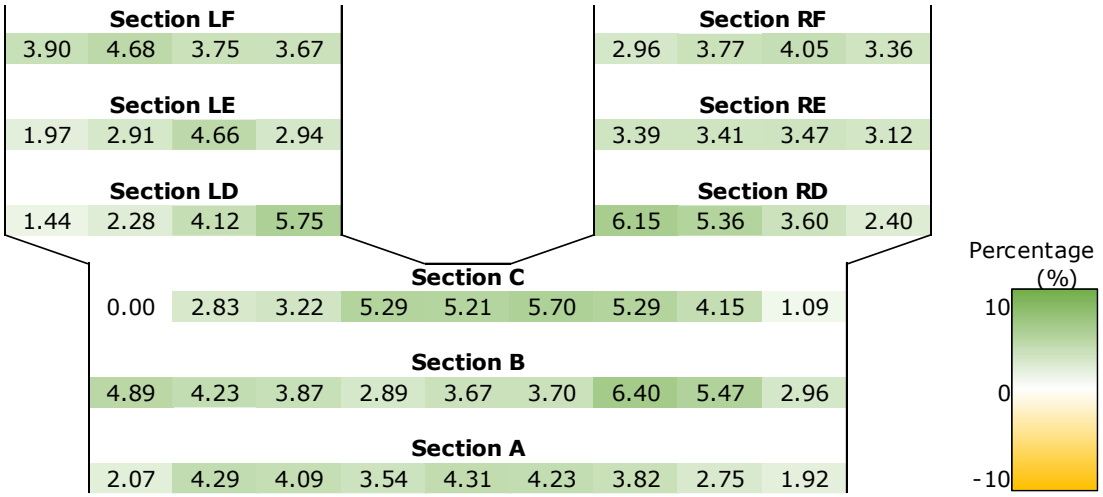
Water Depth Superelevation: 30_07_5055



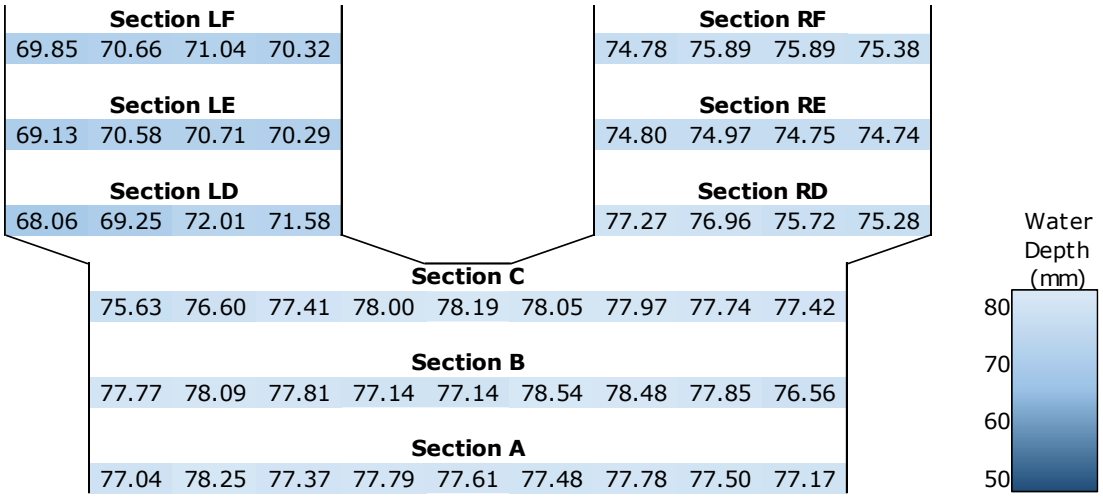
Water Depth Measurement: 40_03_5050



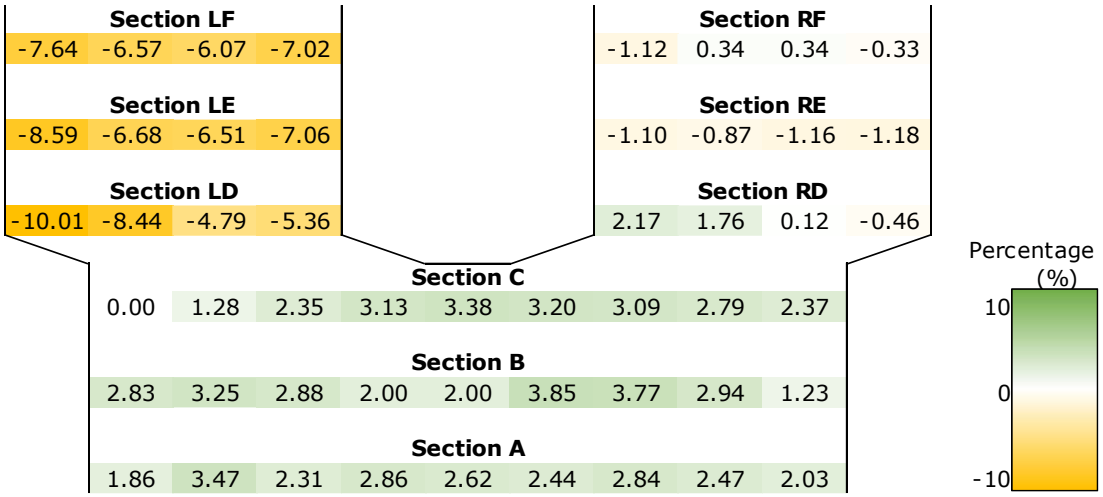
Water Depth Superelevation: 40_03_5050



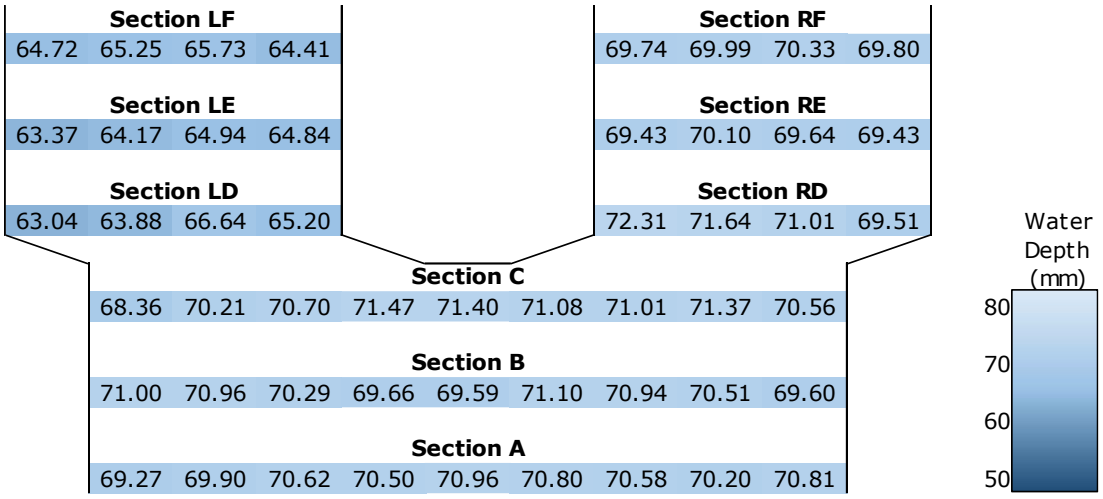
Water Depth Measurement: 40_03_5560



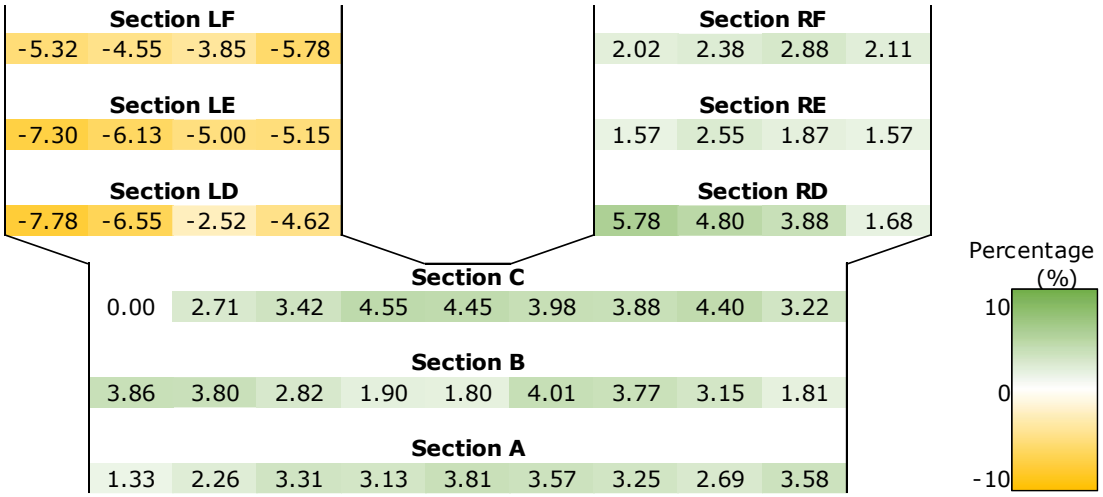
Water Depth Superelevation: 40_03_5560



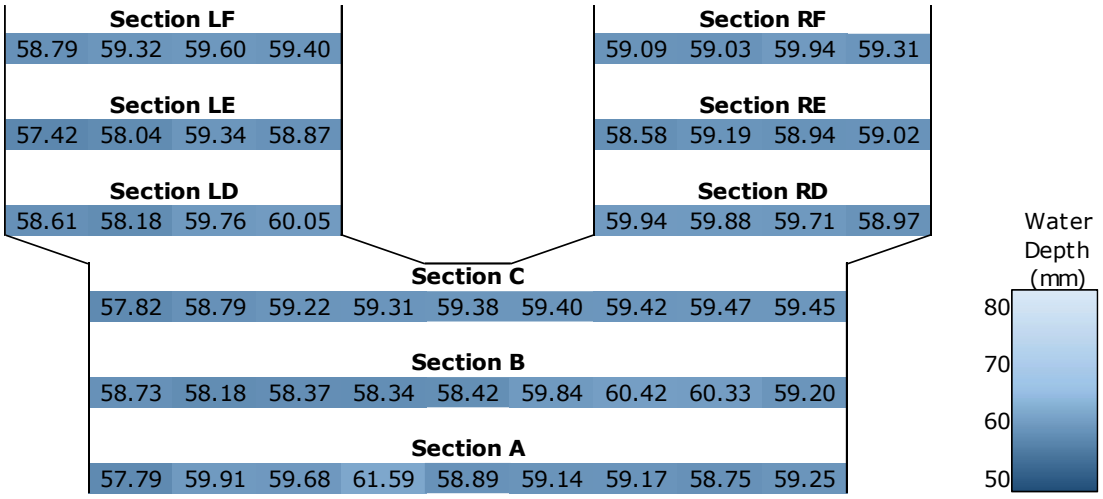
Water Depth Measurement: 40_03_5055



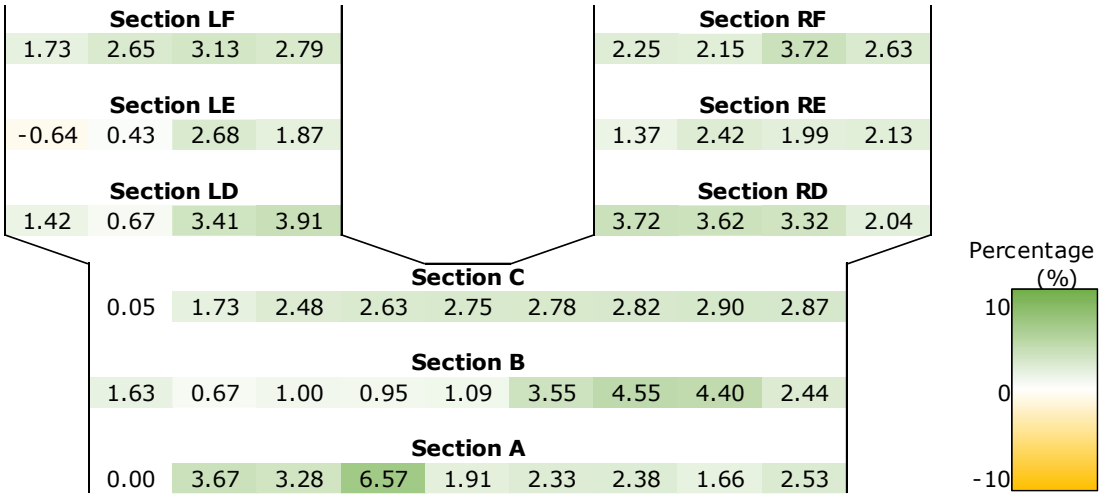
Water Depth Superelevation: 40_03_5055



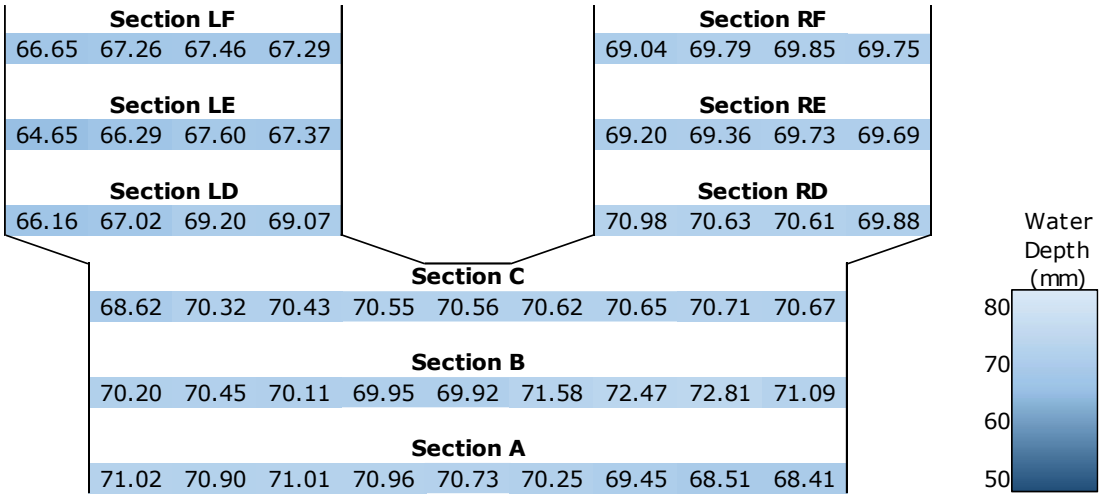
Water Depth Measurement: 40_05_5050



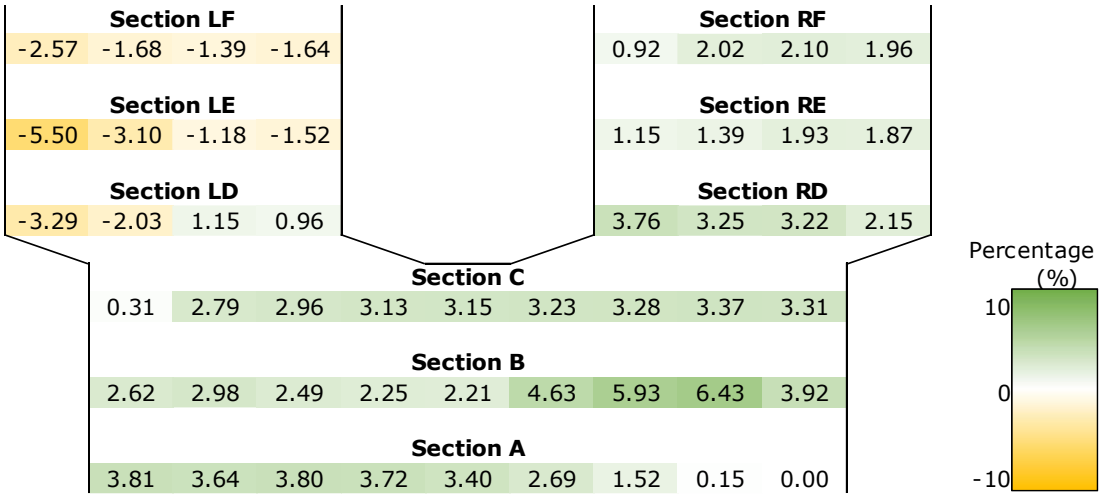
Water Depth Superelevation: 40_05_5050



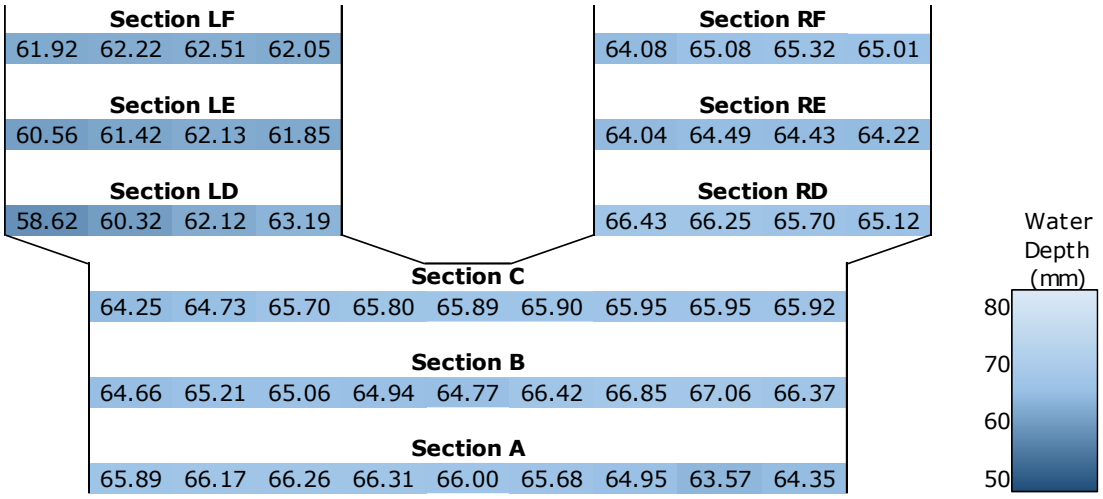
Water Depth Measurement: 40_05_5560



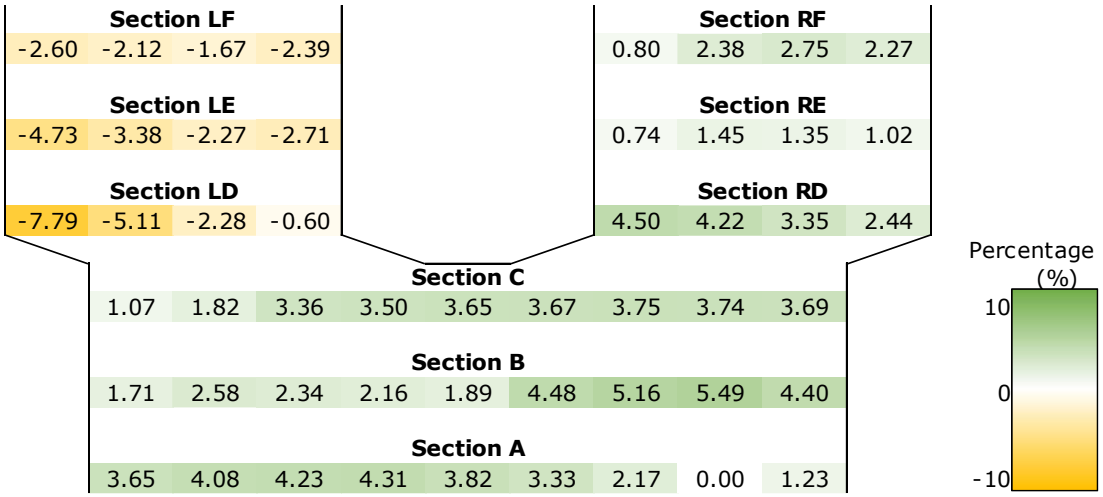
Water Depth Superelevation: 40_05_5560



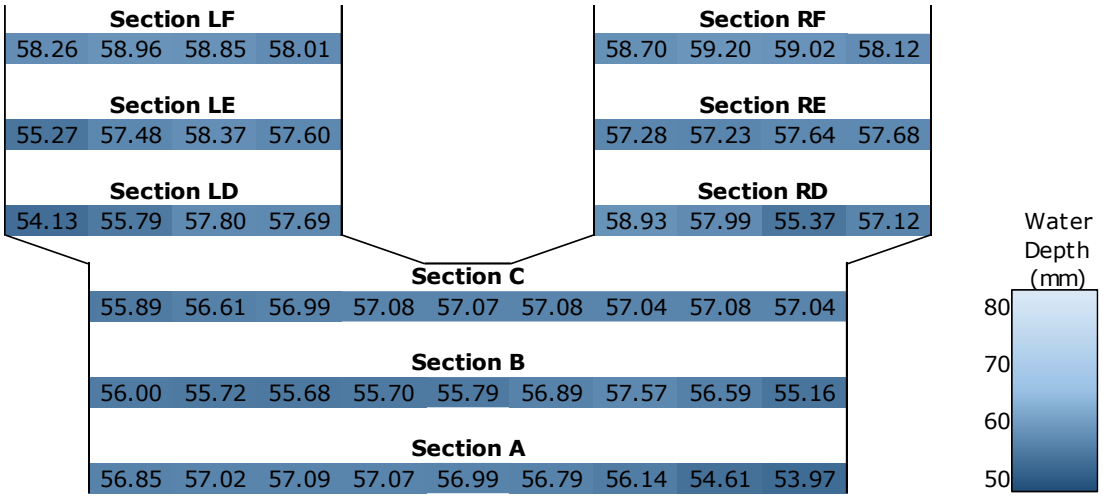
Water Depth Measurement: 40_05_5055



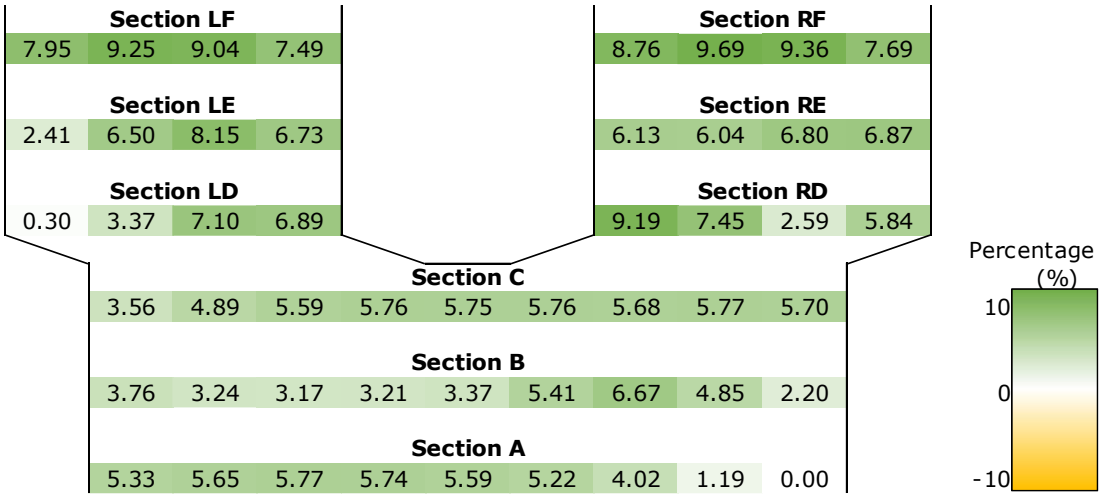
Water Depth Superelevation: 40_05_5055



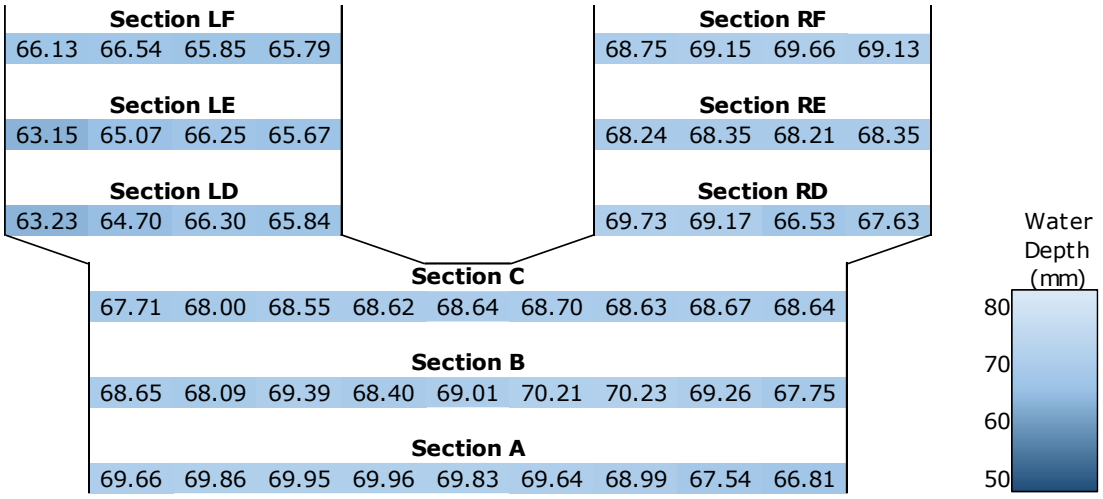
Water Depth Measurement: 40_07_5050



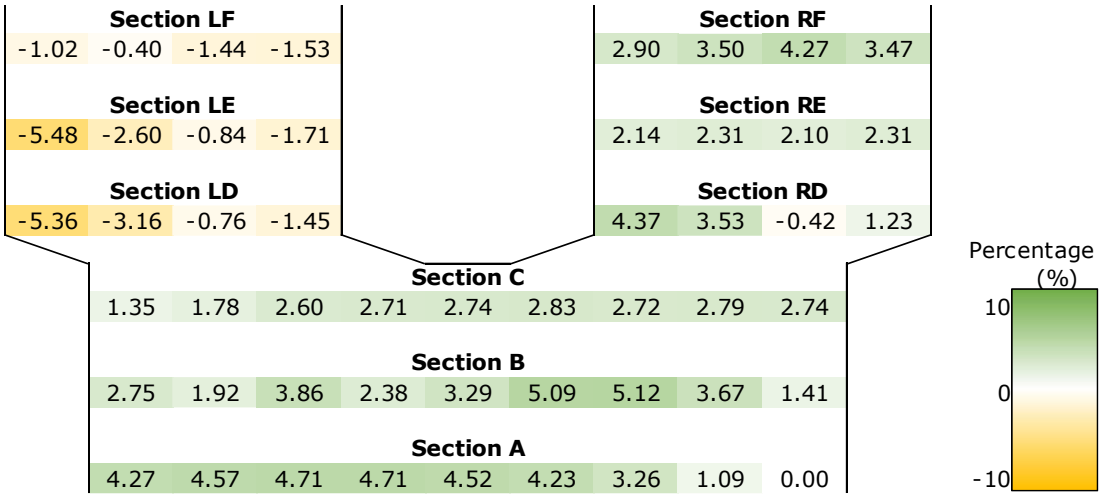
Water Depth Superelevation: 40_07_5050



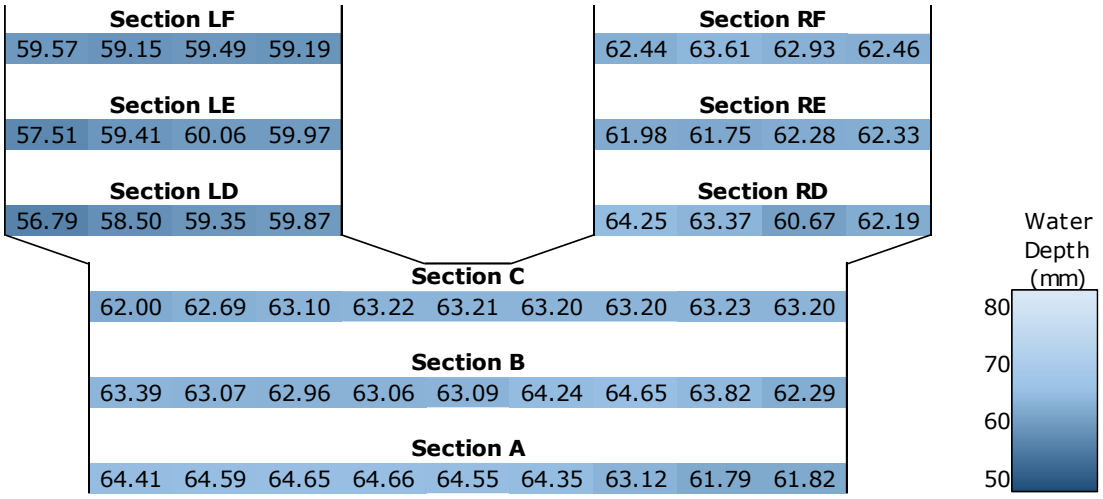
Water Depth Measurement: 40_07_5560



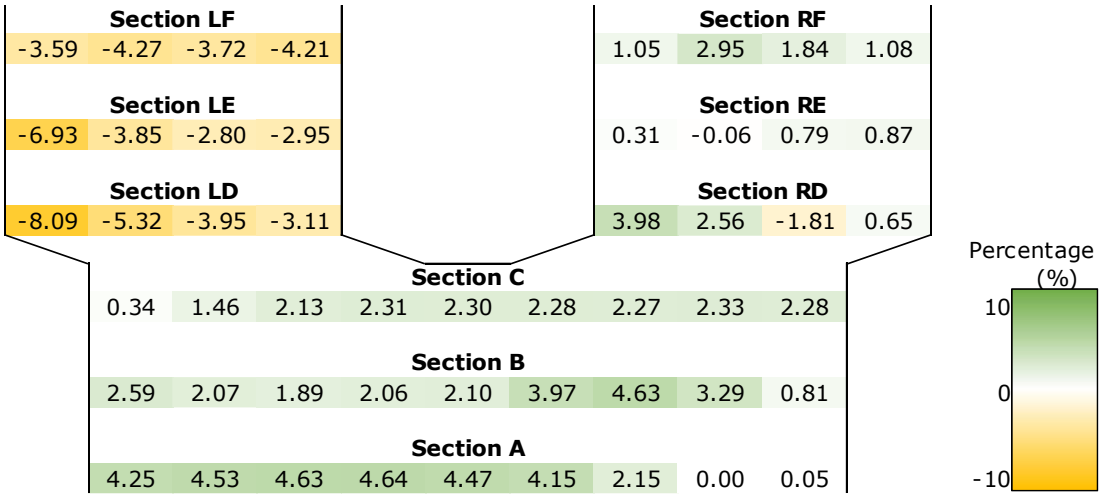
Water Depth Superelevation: 40_07_5560



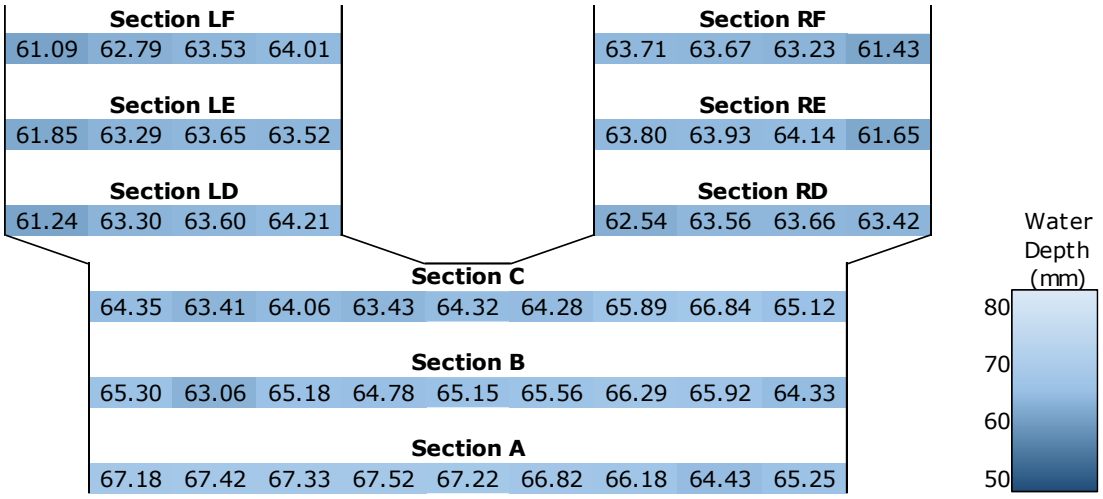
Water Depth Measurement: 40_07_5055



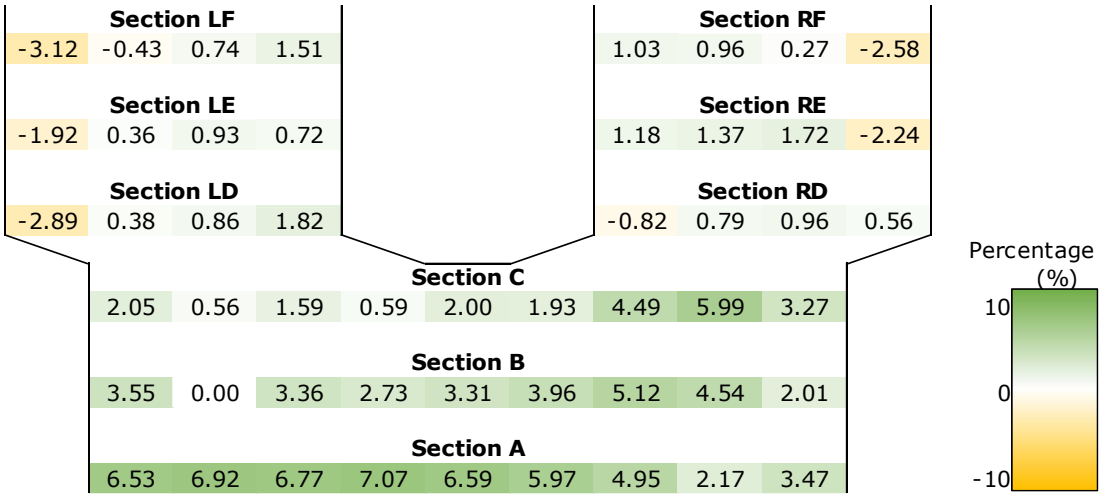
Water Depth Superelevation: 40_07_5055



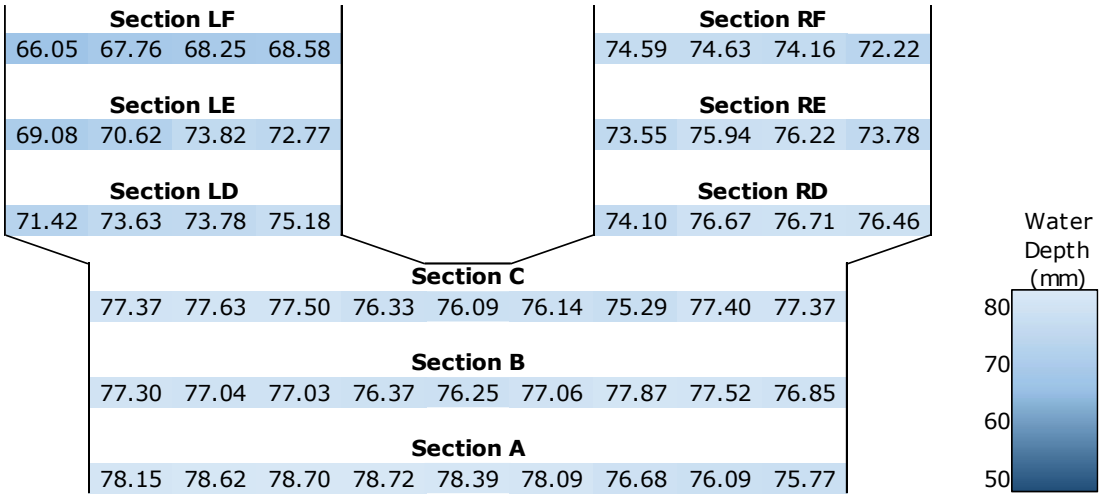
Water Depth Measurement: 50_03_5050



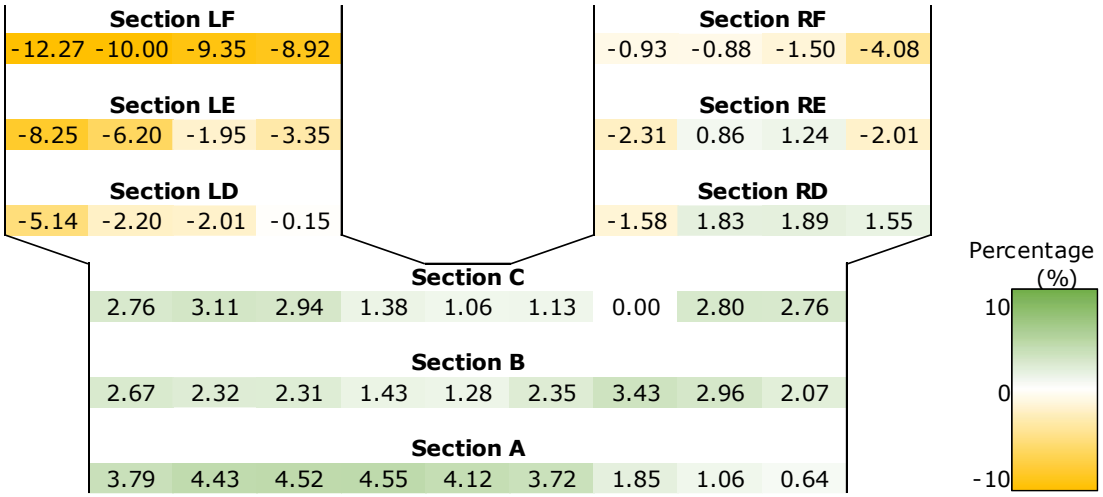
Water Depth Superelevation: 50_03_5050



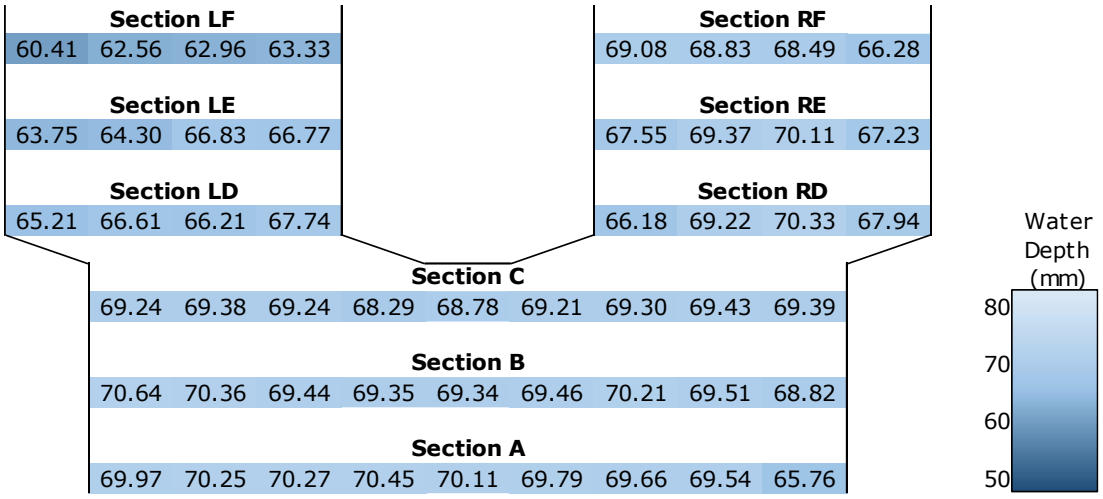
Water Depth Measurement: 50_03_5560



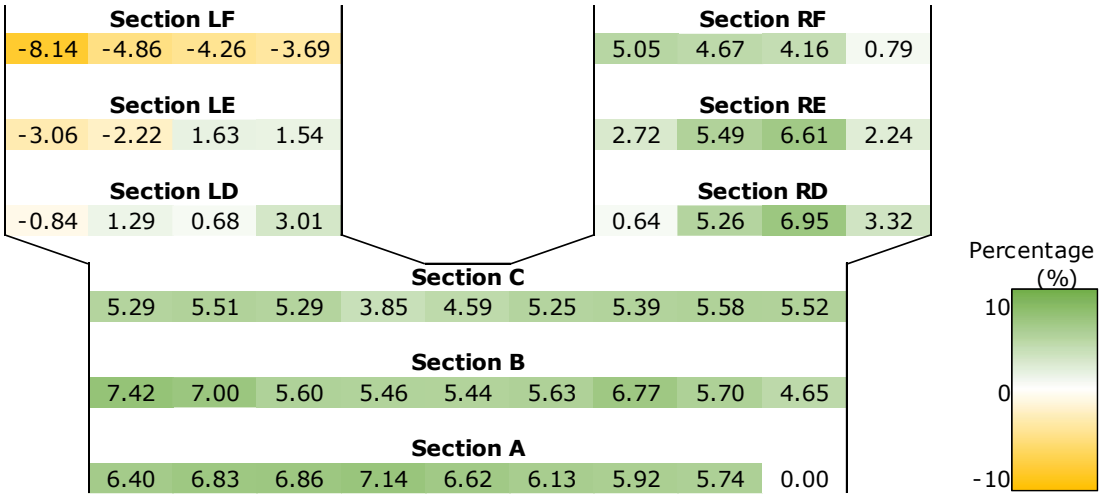
Water Depth Superelevation: 50_03_5560



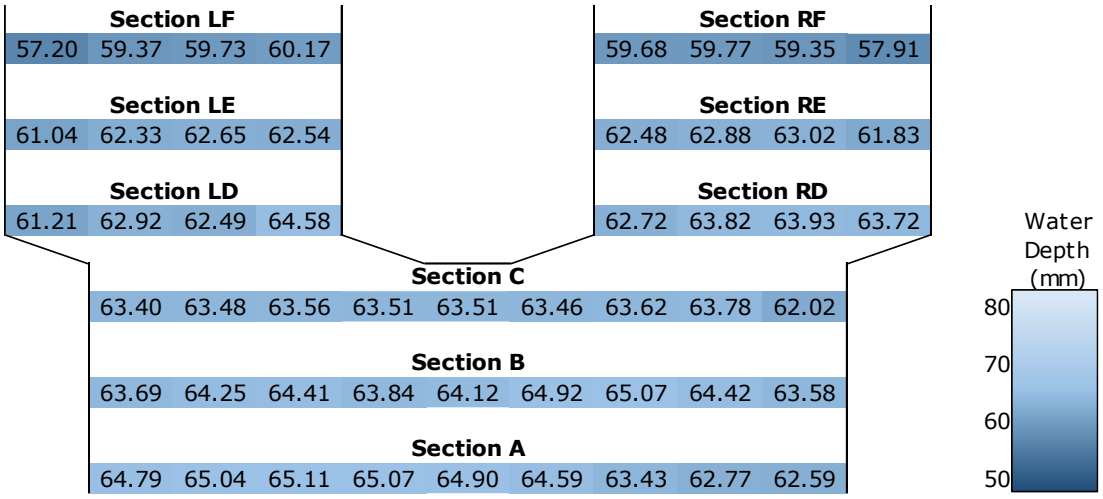
Water Depth Measurement: 50_03_5055



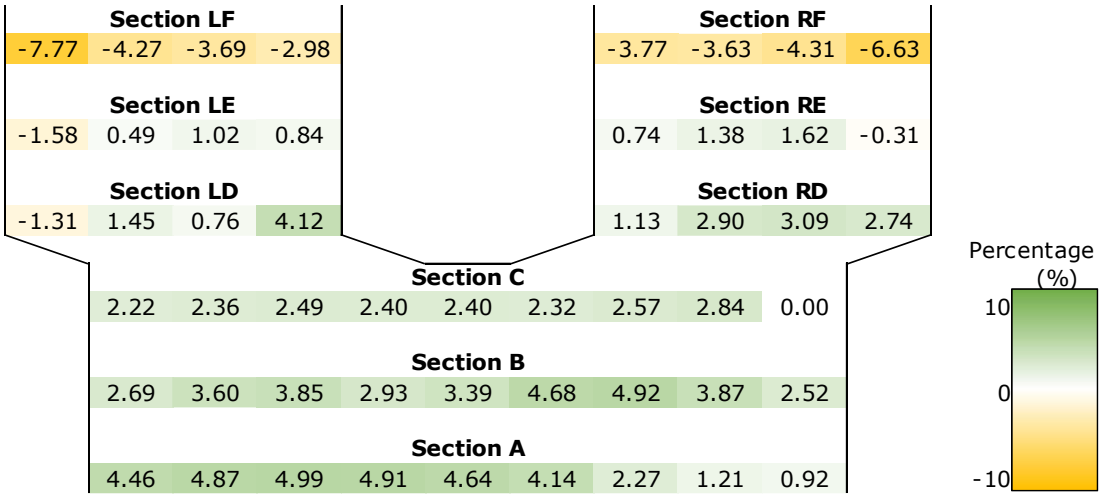
Water Depth Superelevation: 50_03_5055



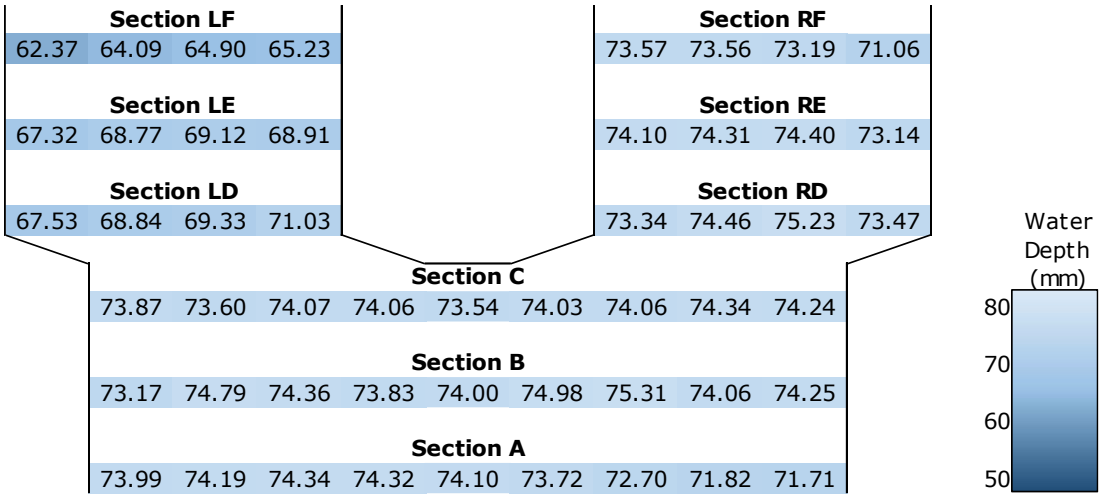
Water Depth Measurement: 50_05_5050



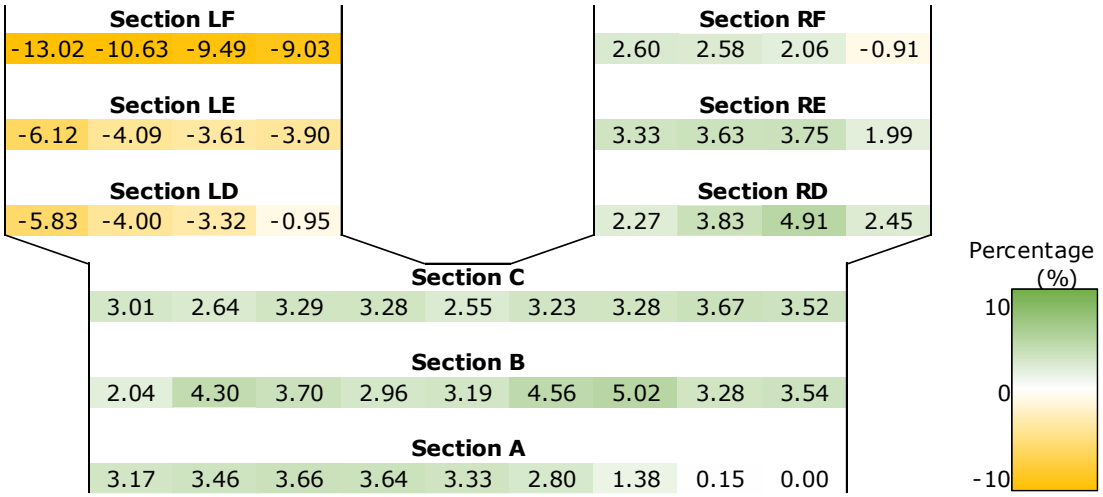
Water Depth Superelevation: 50_05_5050



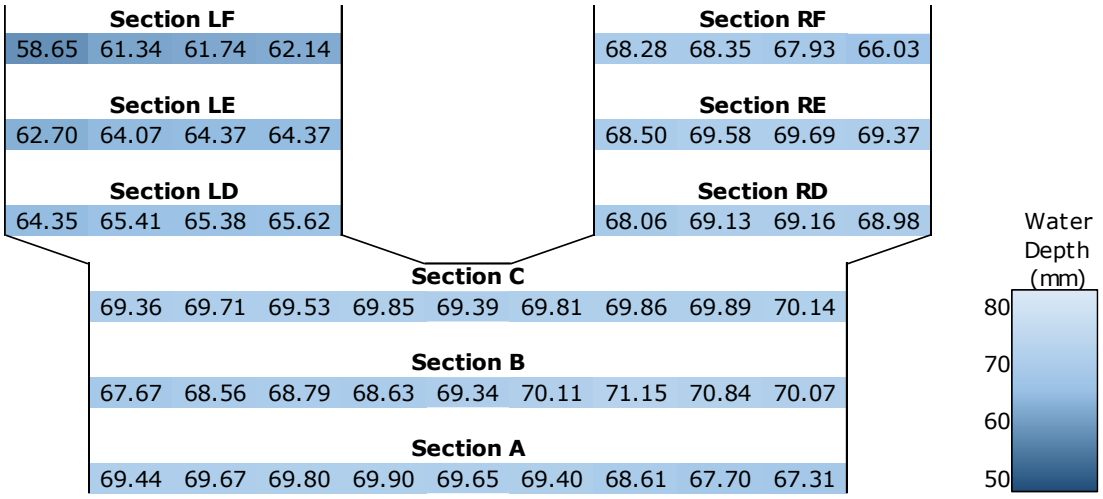
Water Depth Measurement: 50_05_5560



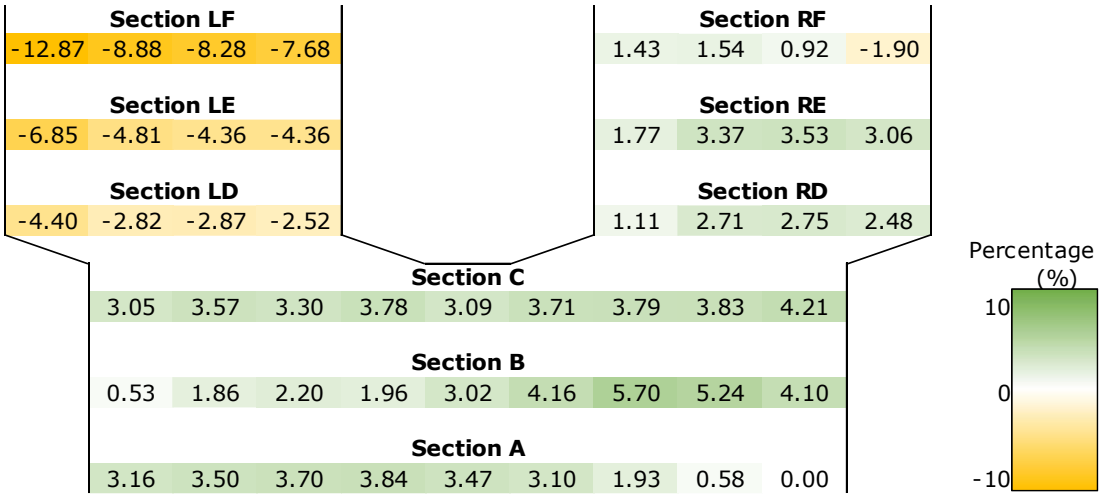
Water Depth Superelevation: 50_05_5560



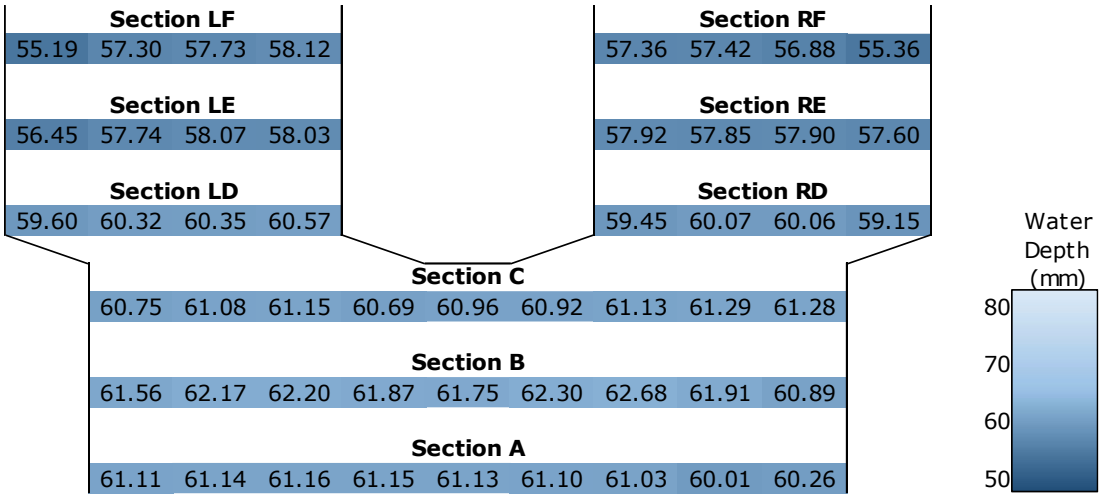
Water Depth Measurement: 50_05_5055



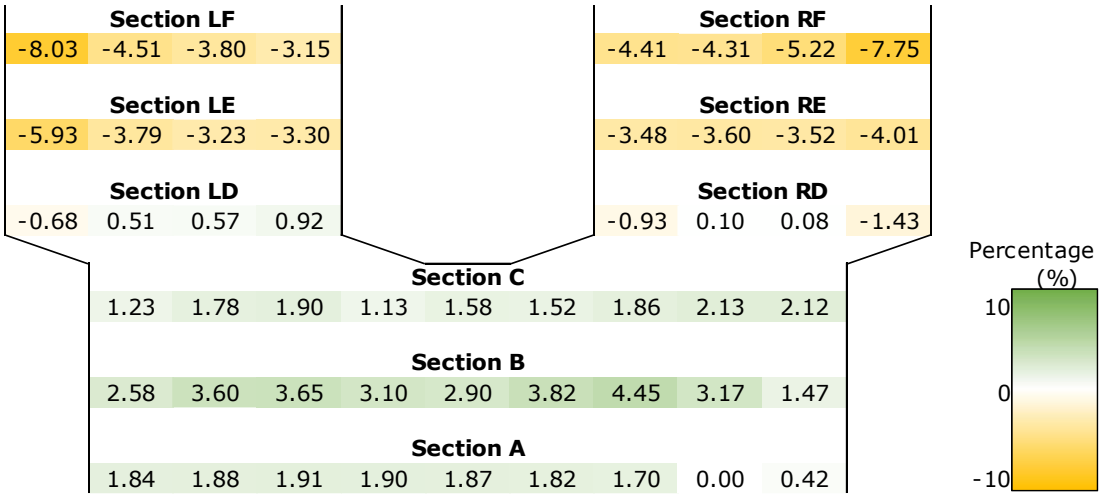
Water Depth Superelevation: 50_05_5055



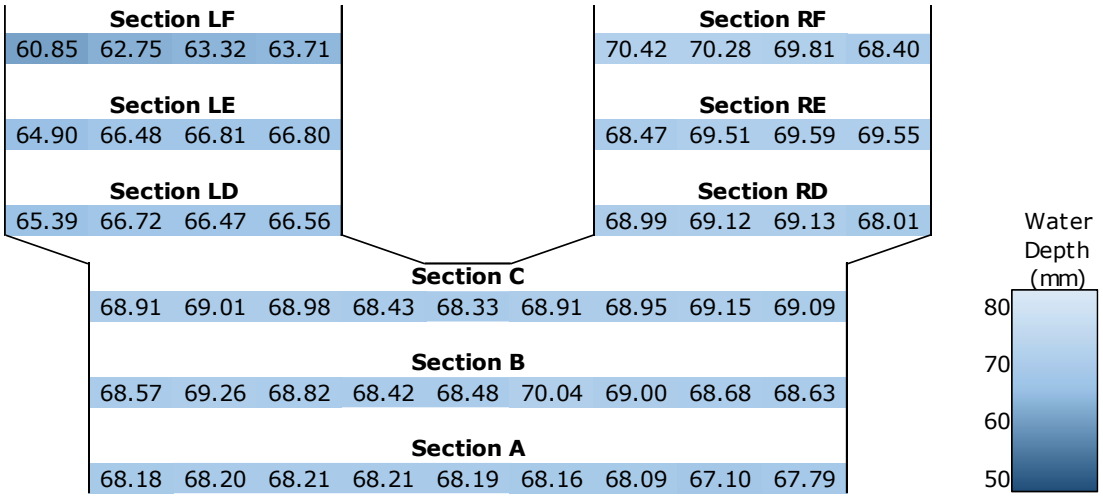
Water Depth Measurement: 50_07_5050



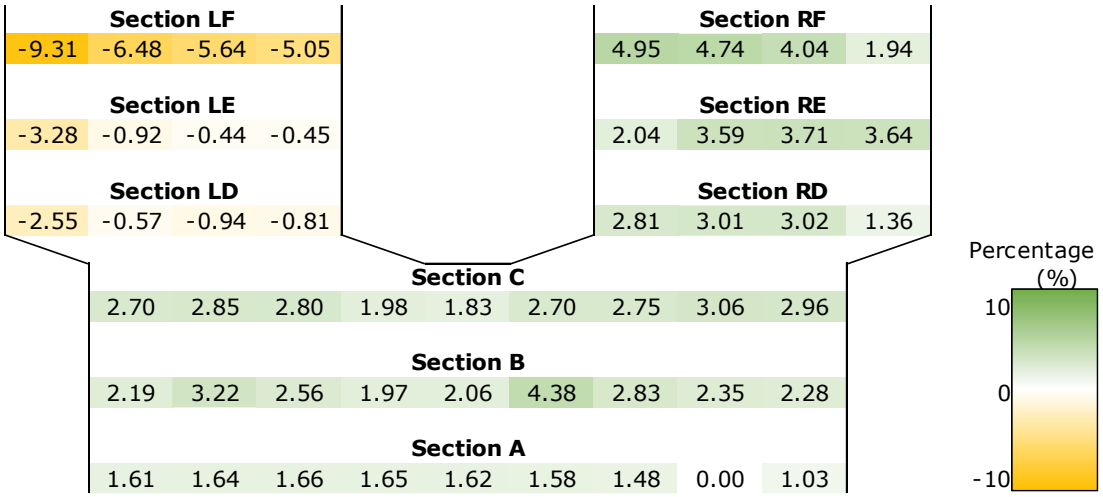
Water Depth Superelevation: 50_07_5050



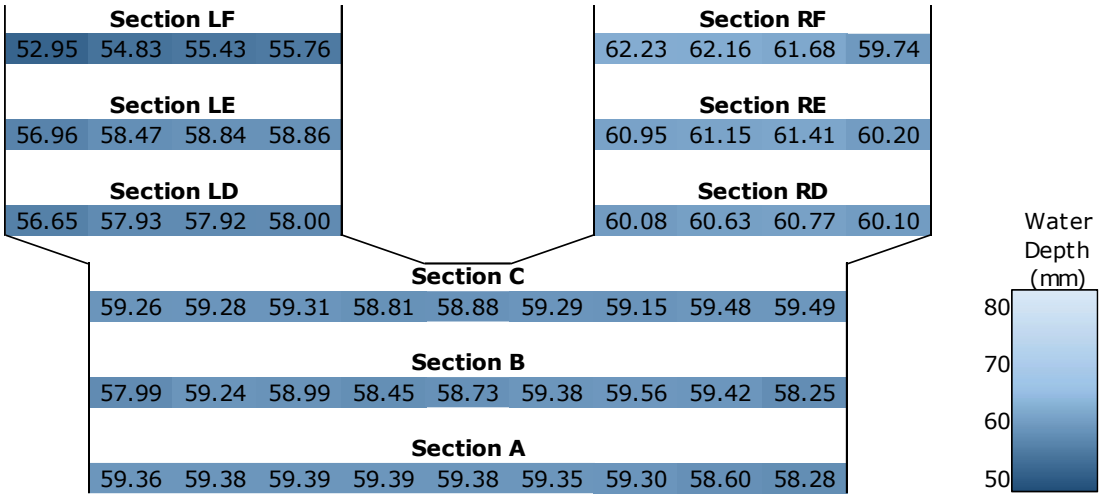
Water Depth Measurement: 50_07_5560



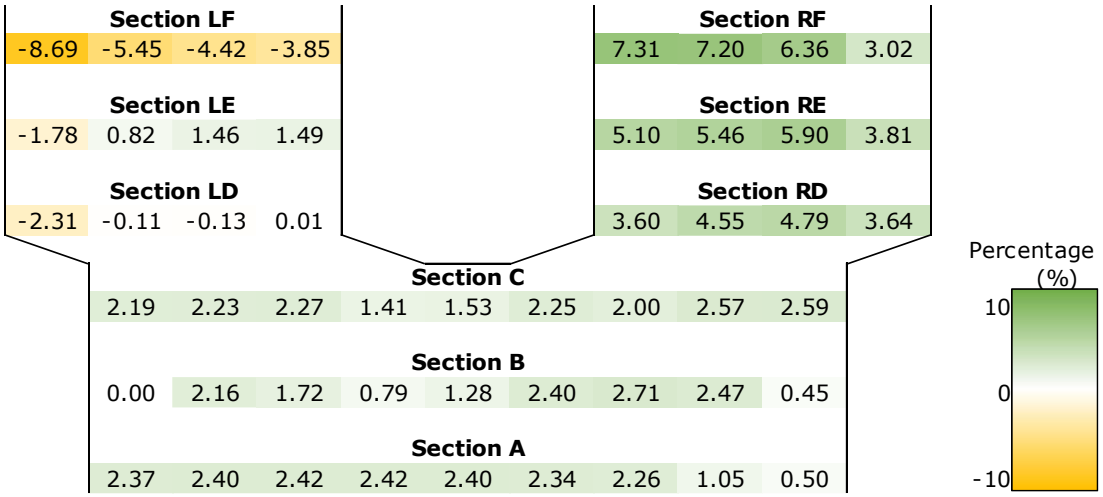
Water Depth Superelevation: 50_07_5560



Water Depth Measurement: 50_07_5055



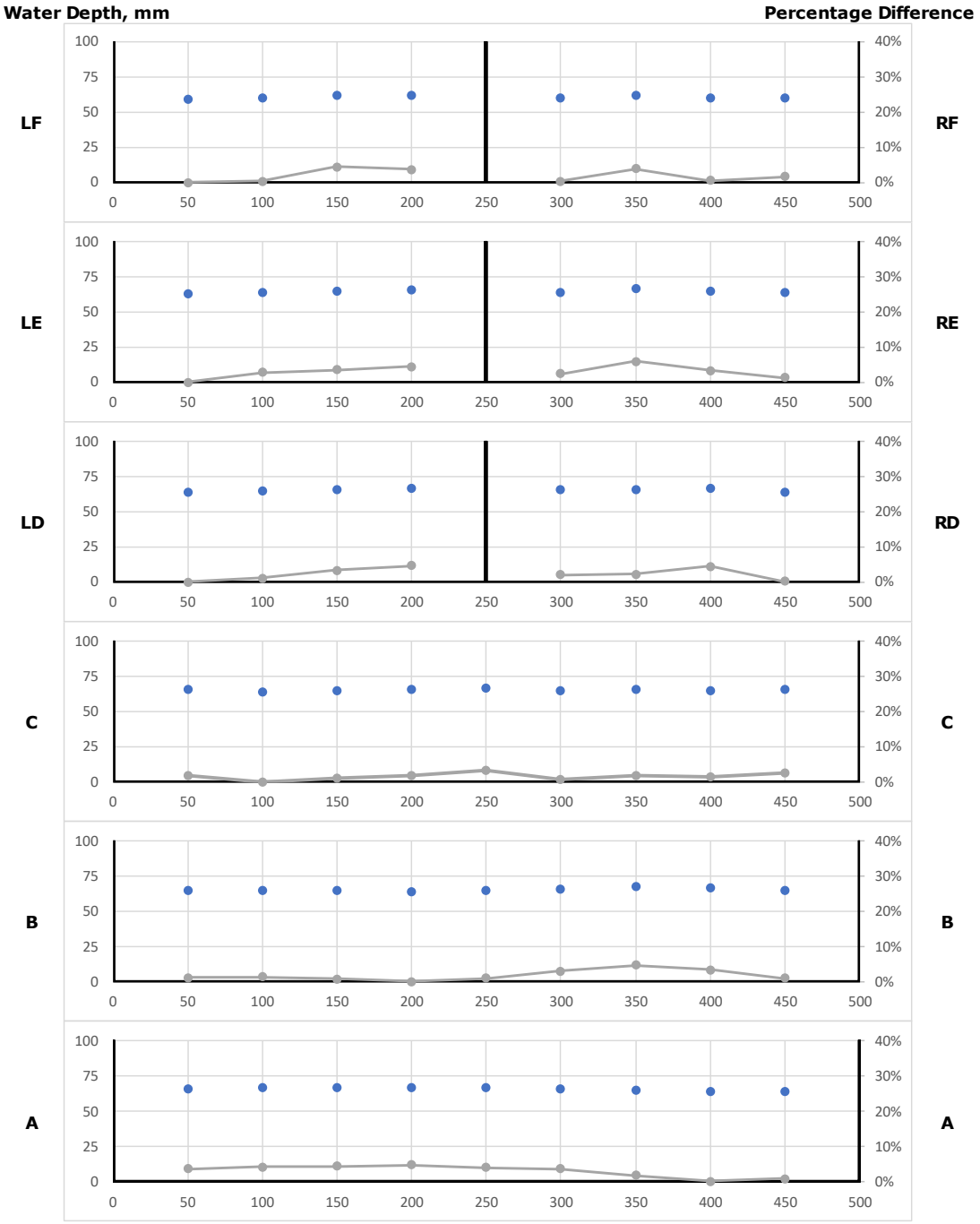
Water Depth Superelevation: 50_07_5055



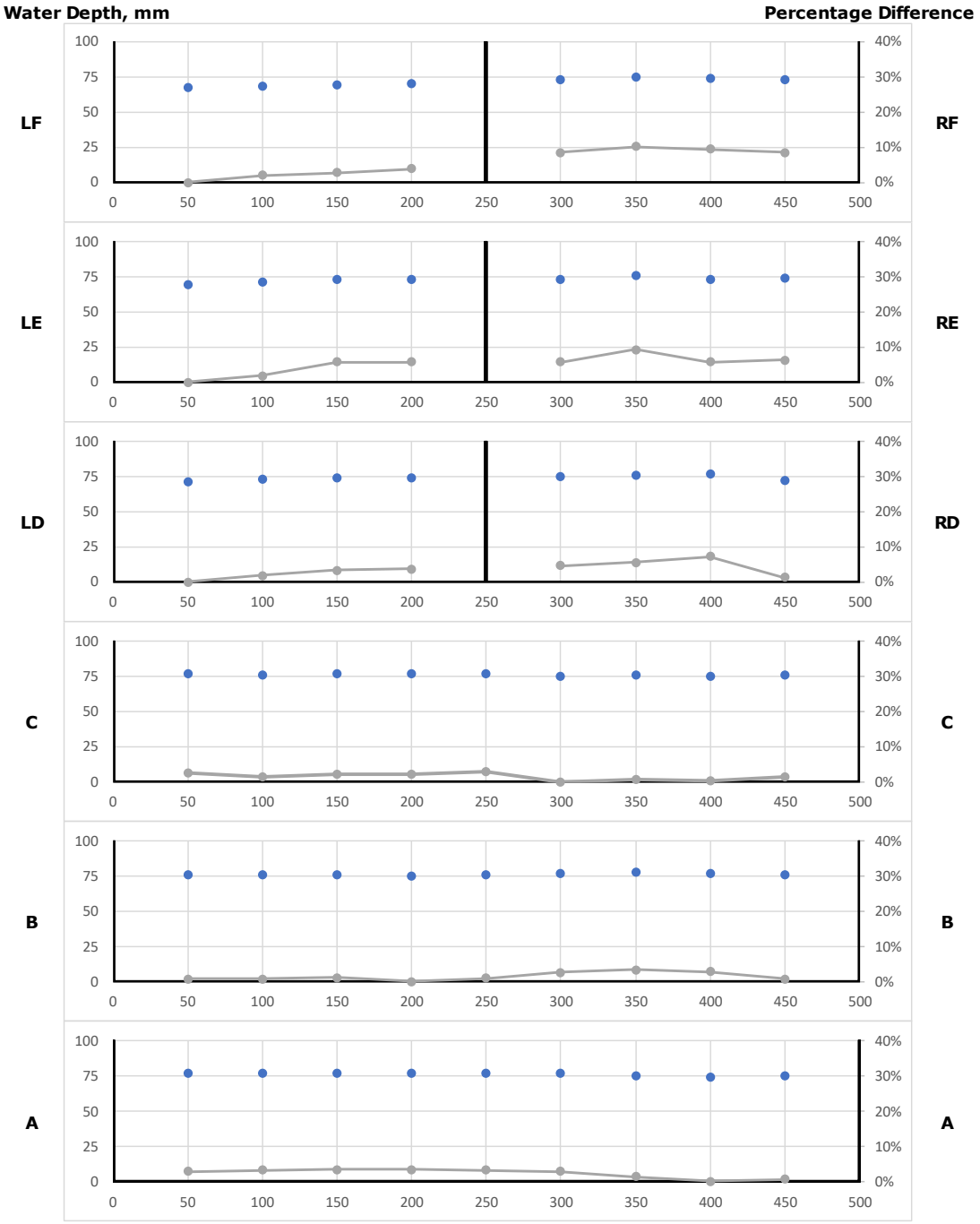
Appendix A2 Water Depth and Percentage Difference (Section)

Bifurcation Angle, °	Slope, %	Left Weir Height, mm	Right Weir Height, mm	Name of Run	Page Number
30	0.3	50	50	30_03_5050	A-30
		55	60	30_03_5560	A-31
		50	55	30_03_5055	A-32
	0.5	50	50	30_05_5050	A-33
		55	60	30_05_5560	A-34
		50	55	30_05_5055	A-35
	0.7	50	50	30_07_5050	A-36
		55	60	30_07_5560	A-37
		50	55	30_07_5055	A-38
40	0.3	50	50	40_03_5050	A-39
		55	60	40_03_5560	A-40
		50	55	40_03_5055	A-41
	0.5	50	50	40_05_5050	A-42
		55	60	40_05_5560	A-43
		50	55	40_05_5055	A-44
	0.7	50	50	40_07_5050	A-45
		55	60	40_07_5560	A-46
		50	55	40_07_5055	A-47
50	0.3	50	50	50_03_5050	A-48
		55	60	50_03_5560	A-49
		50	55	50_03_5055	A-50
	0.5	50	50	50_05_5050	A-51
		55	60	50_05_5560	A-52
		50	55	50_05_5055	A-53
	0.7	50	50	50_07_5050	A-54
		55	60	50_07_5560	A-55
		50	55	50_07_5055	A-56

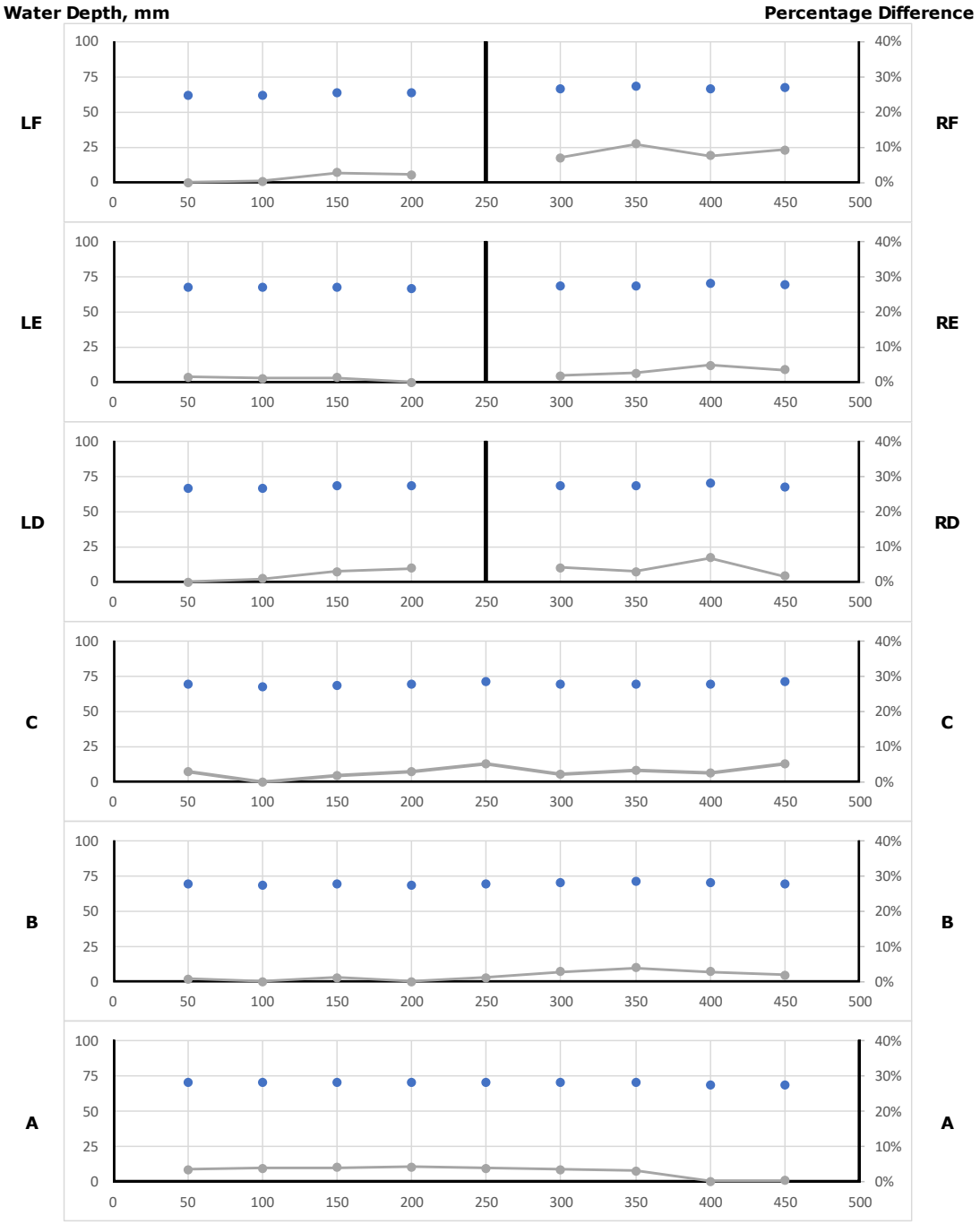
Water Depth and Percentage Difference: 30_03_5050



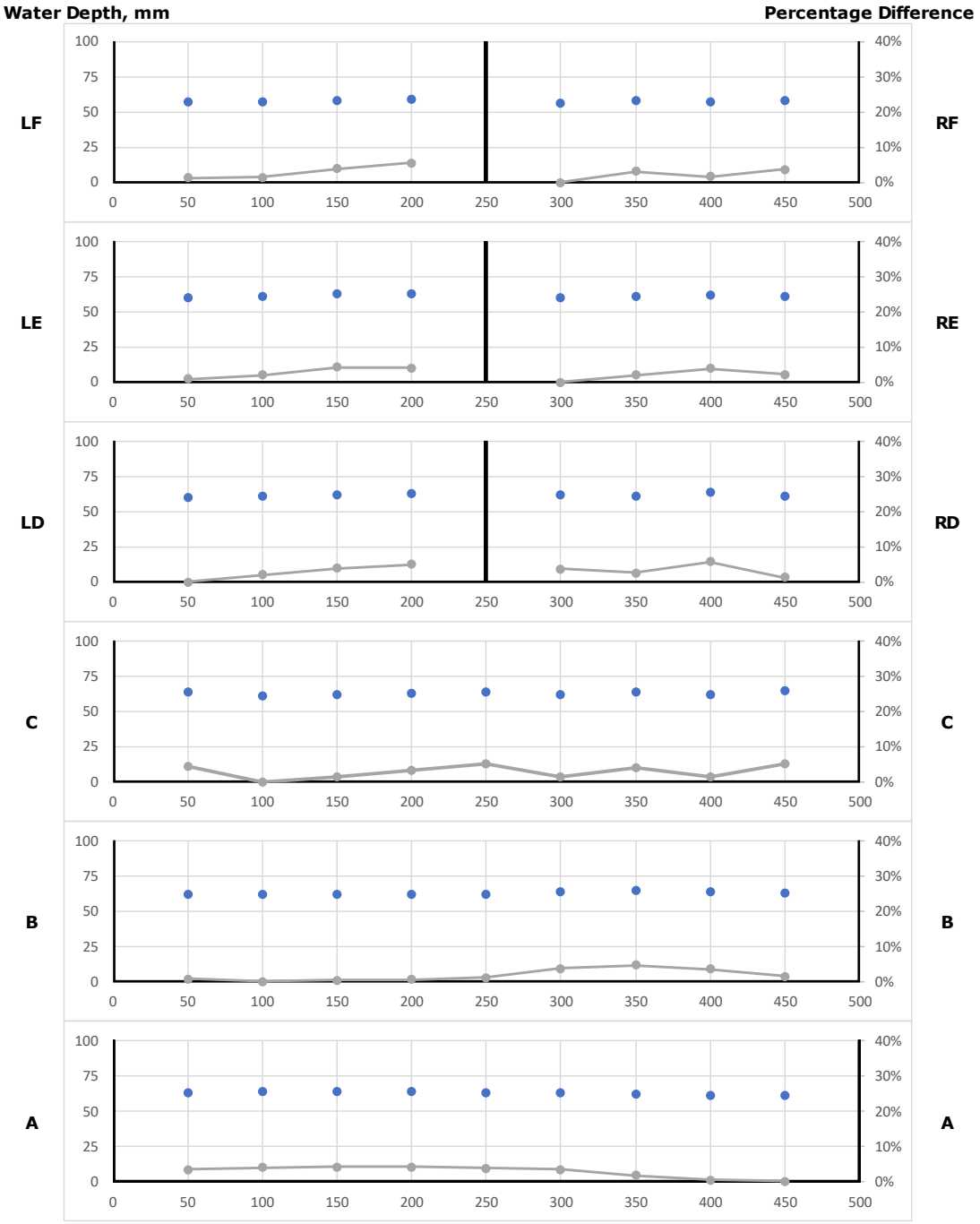
Water Depth and Percentage Difference: 30_03_5560



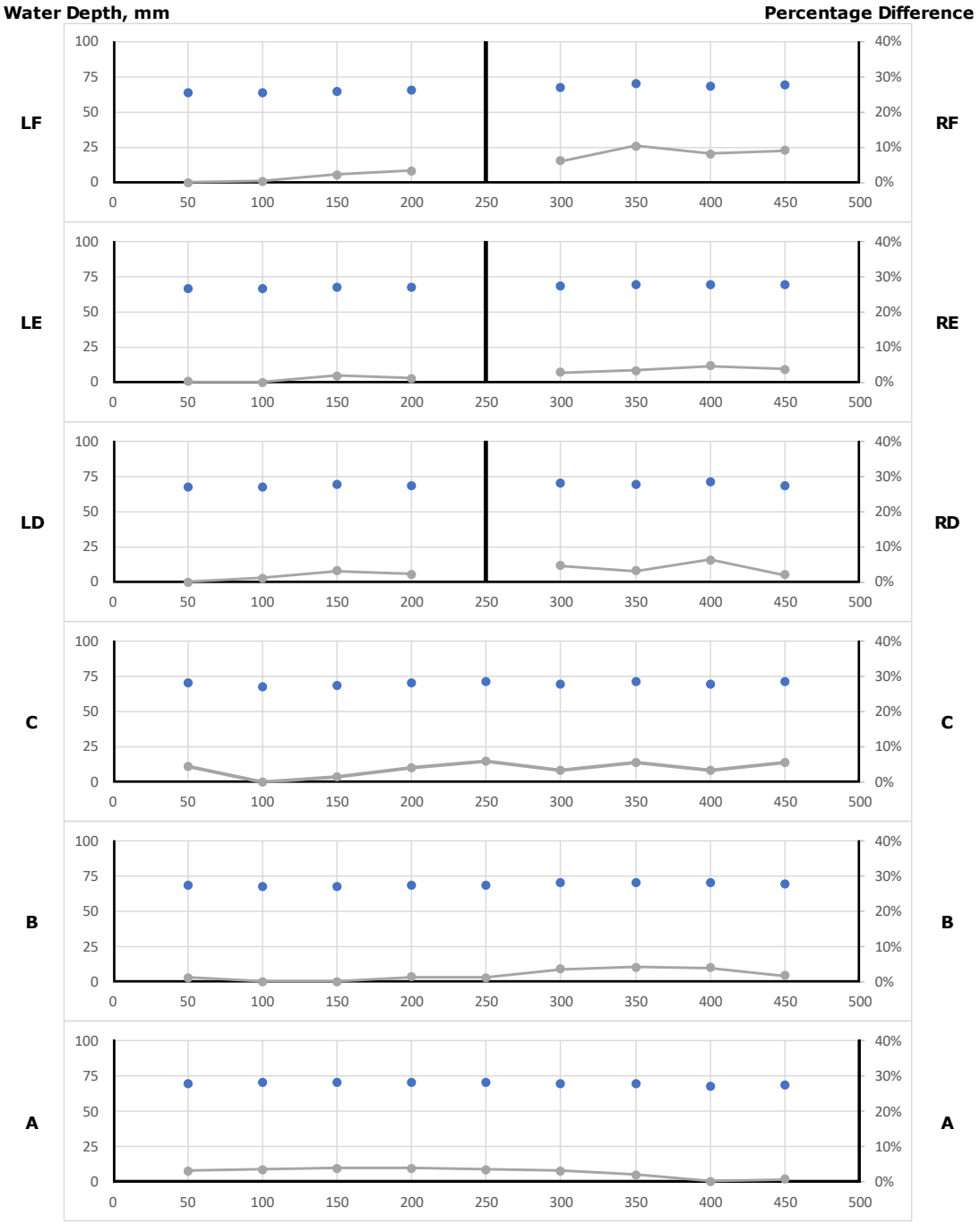
Water Depth and Percentage Difference: 30_03_5055



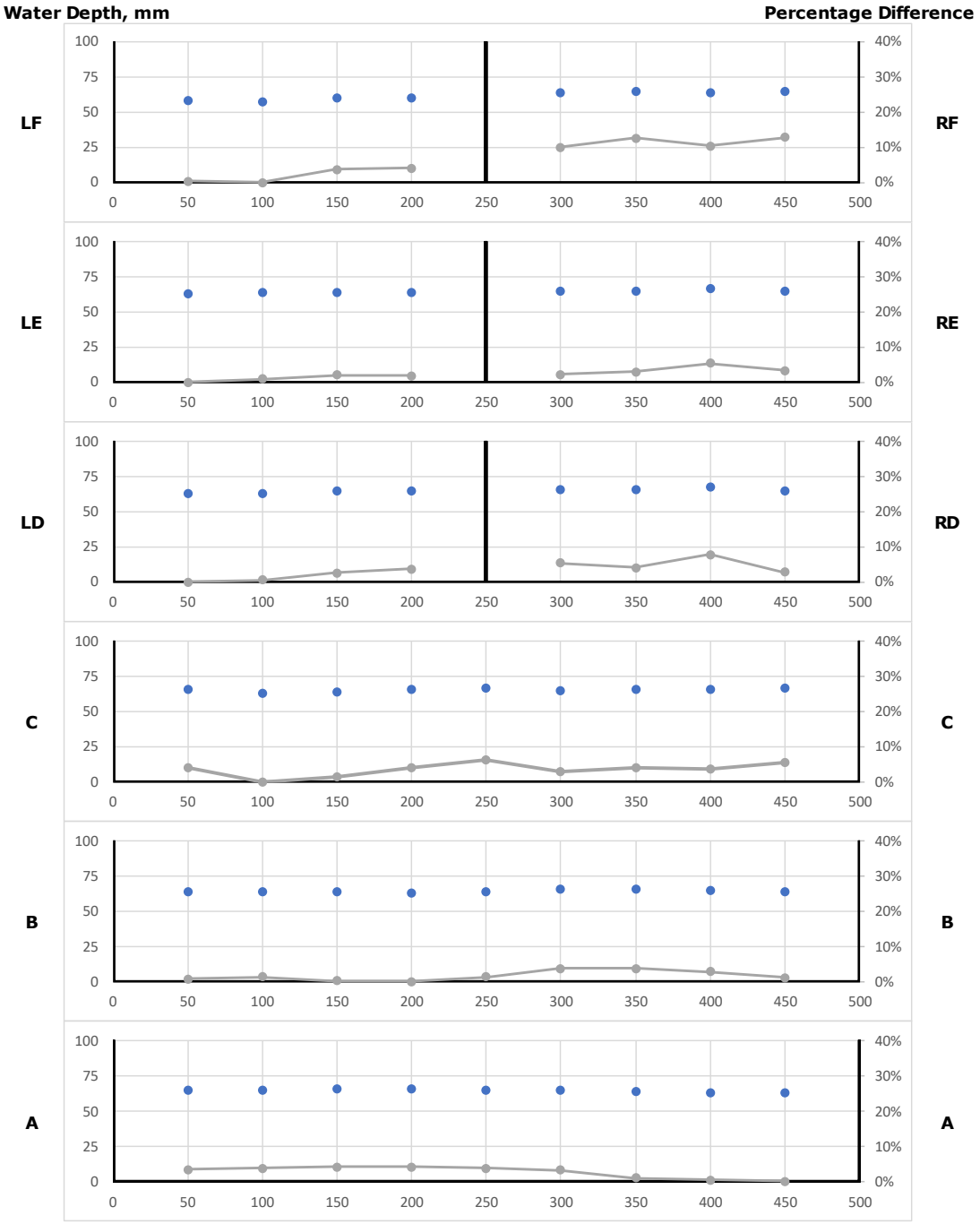
Water Depth and Percentage Difference: 30_05_5050



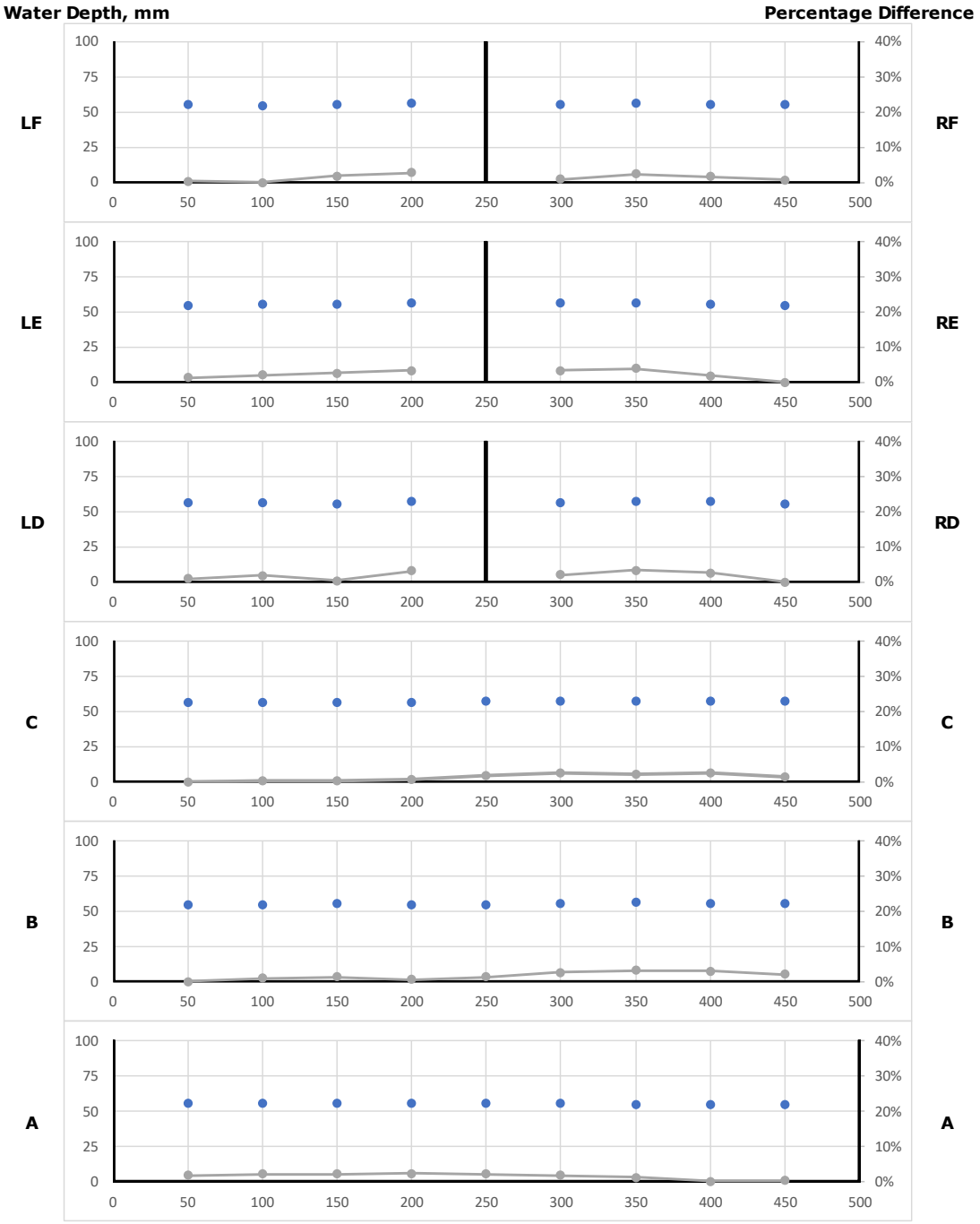
Water Depth and Percentage Difference: 30_05_5560



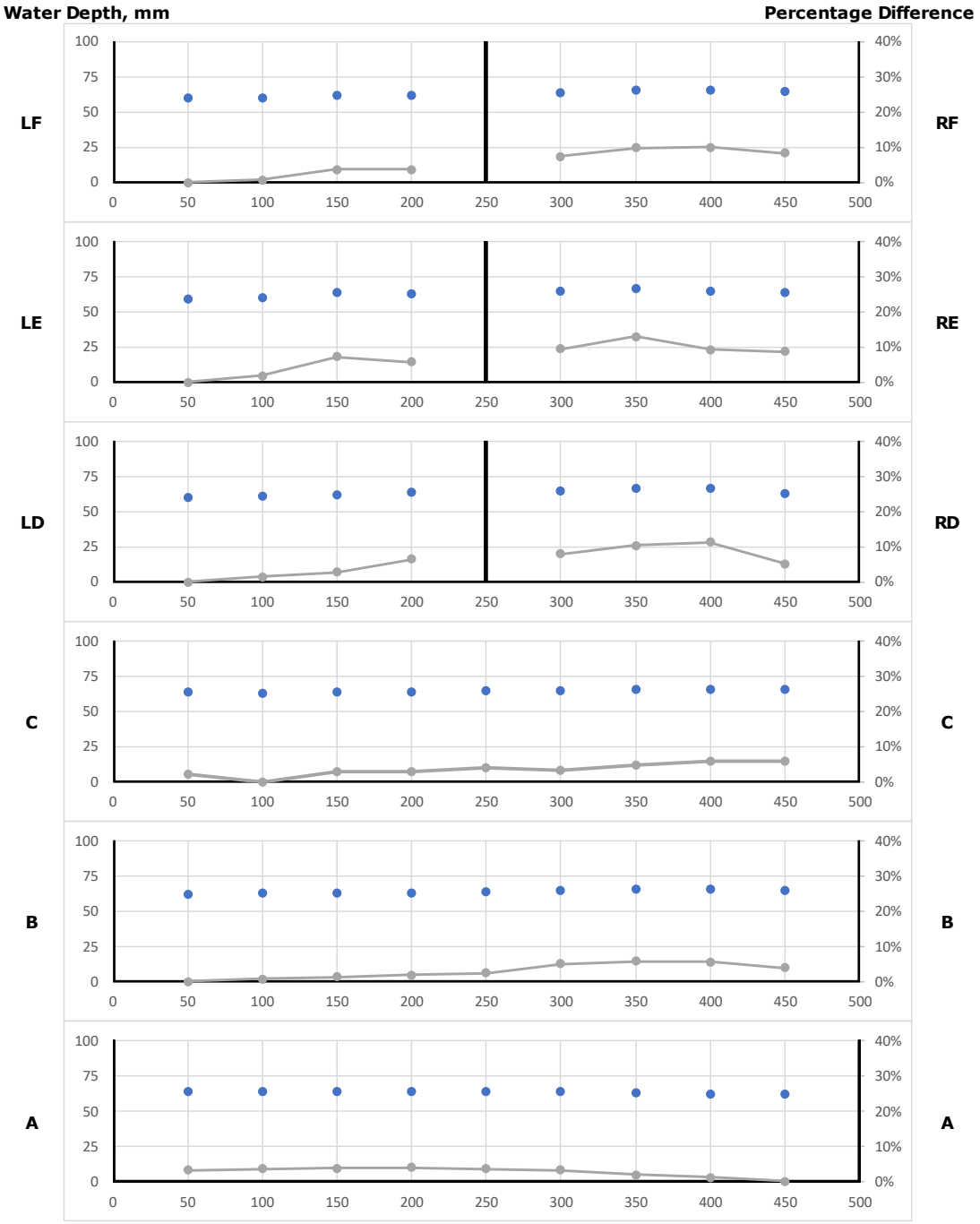
Water Depth and Percentage Difference: 30_05_5055



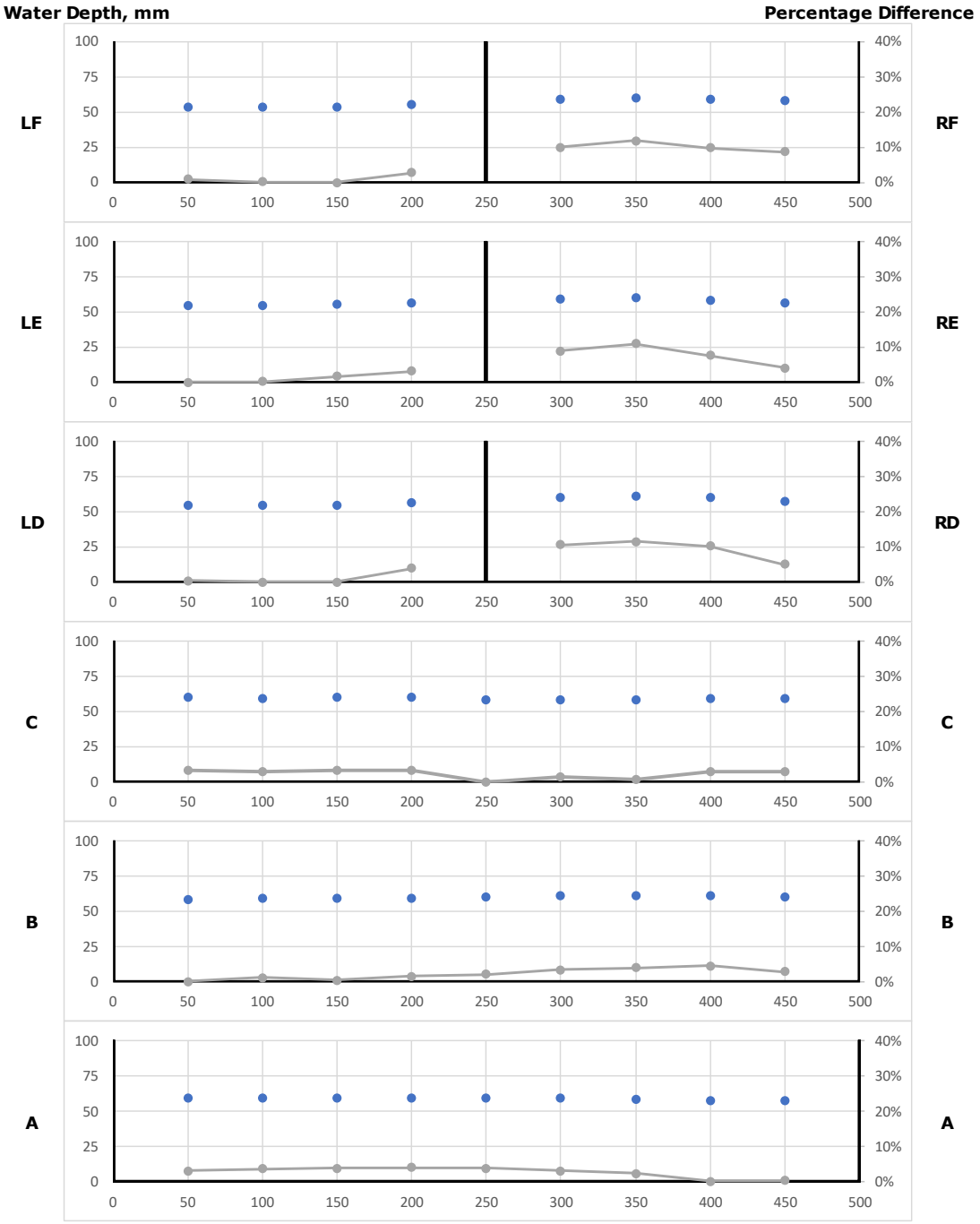
Water Depth and Percentage Difference: 30_07_5050



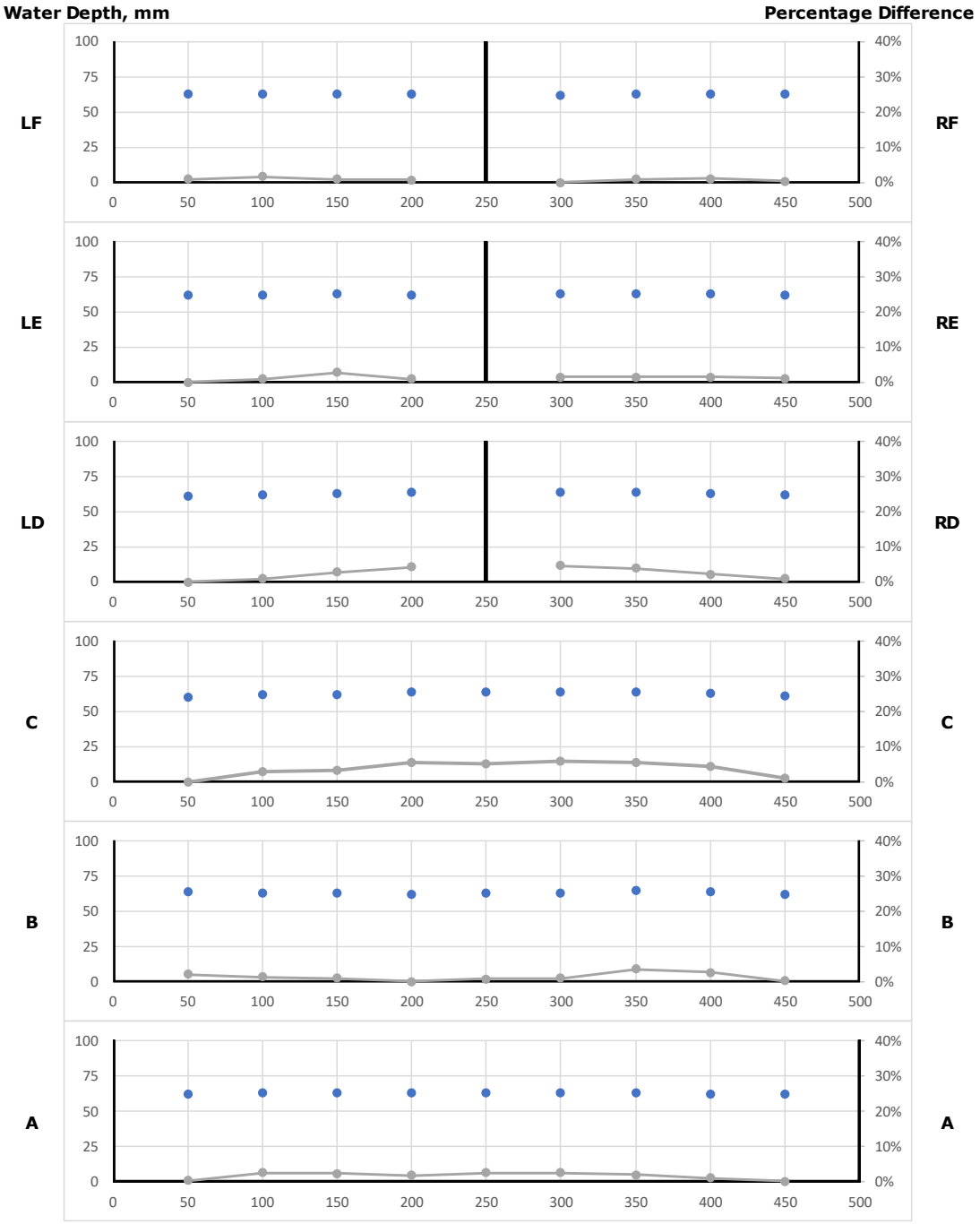
Water Depth and Percentage Difference: 30_07_5560



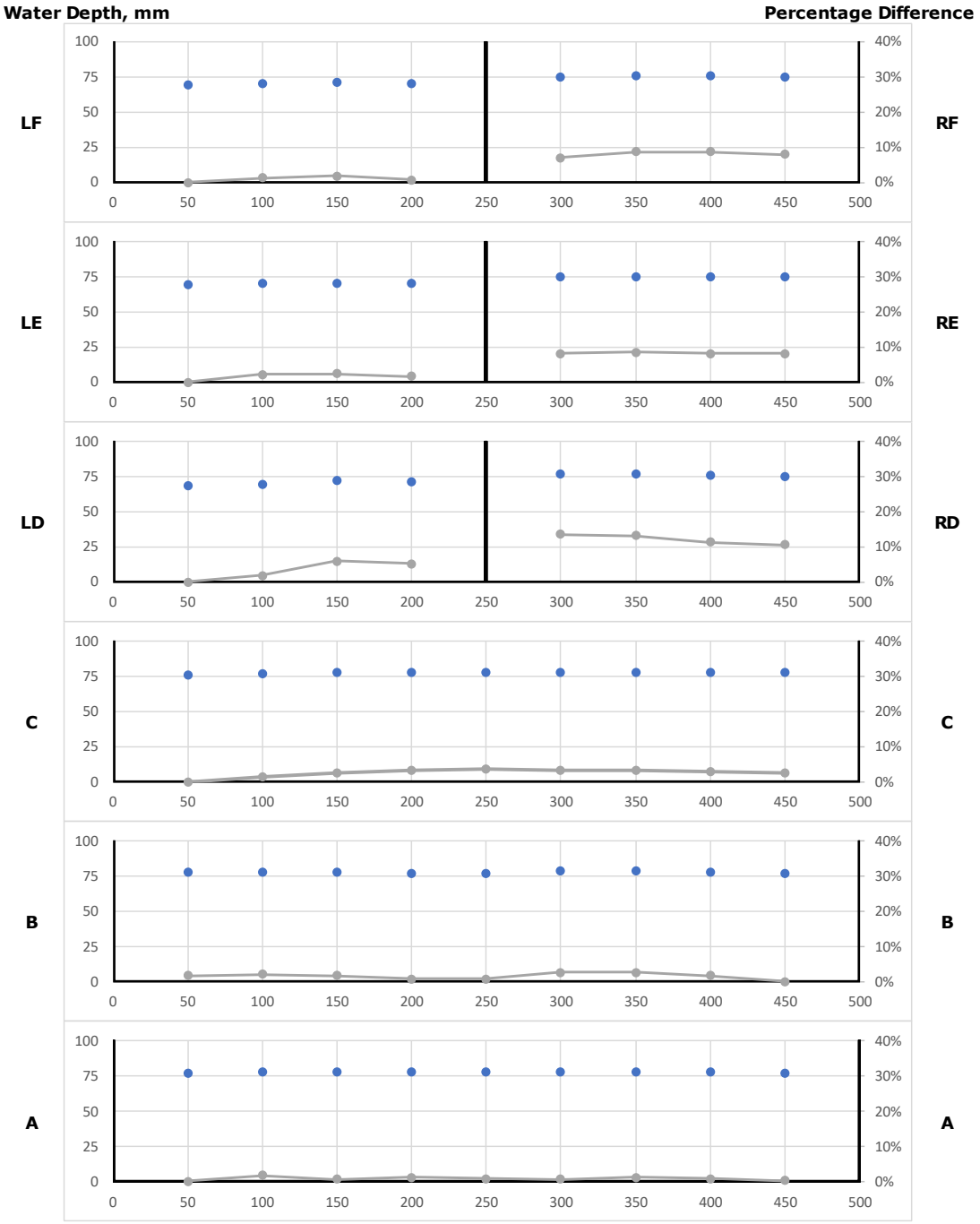
Water Depth and Percentage Difference: 30_07_5055



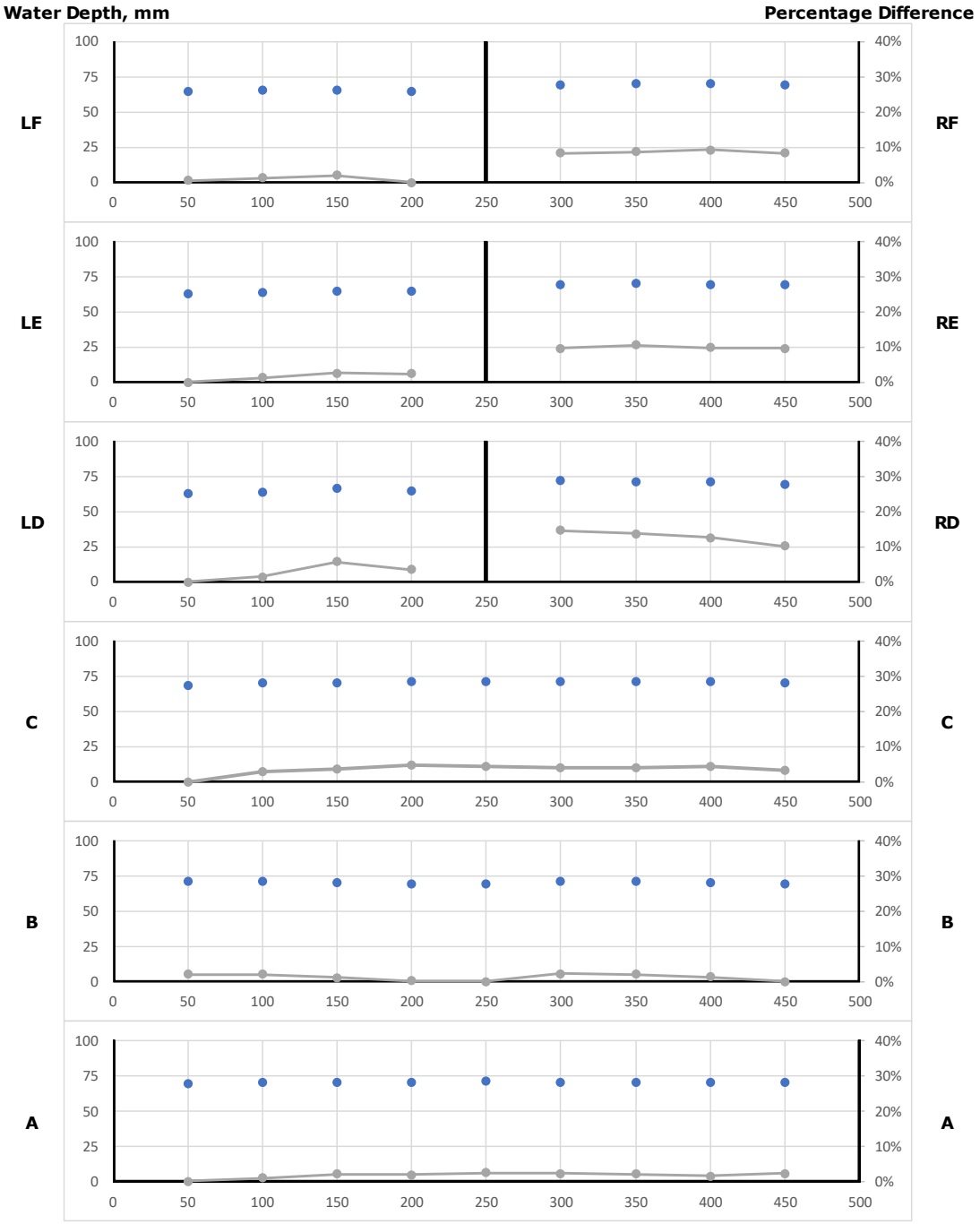
Water Depth and Percentage Difference: 40_03_5050



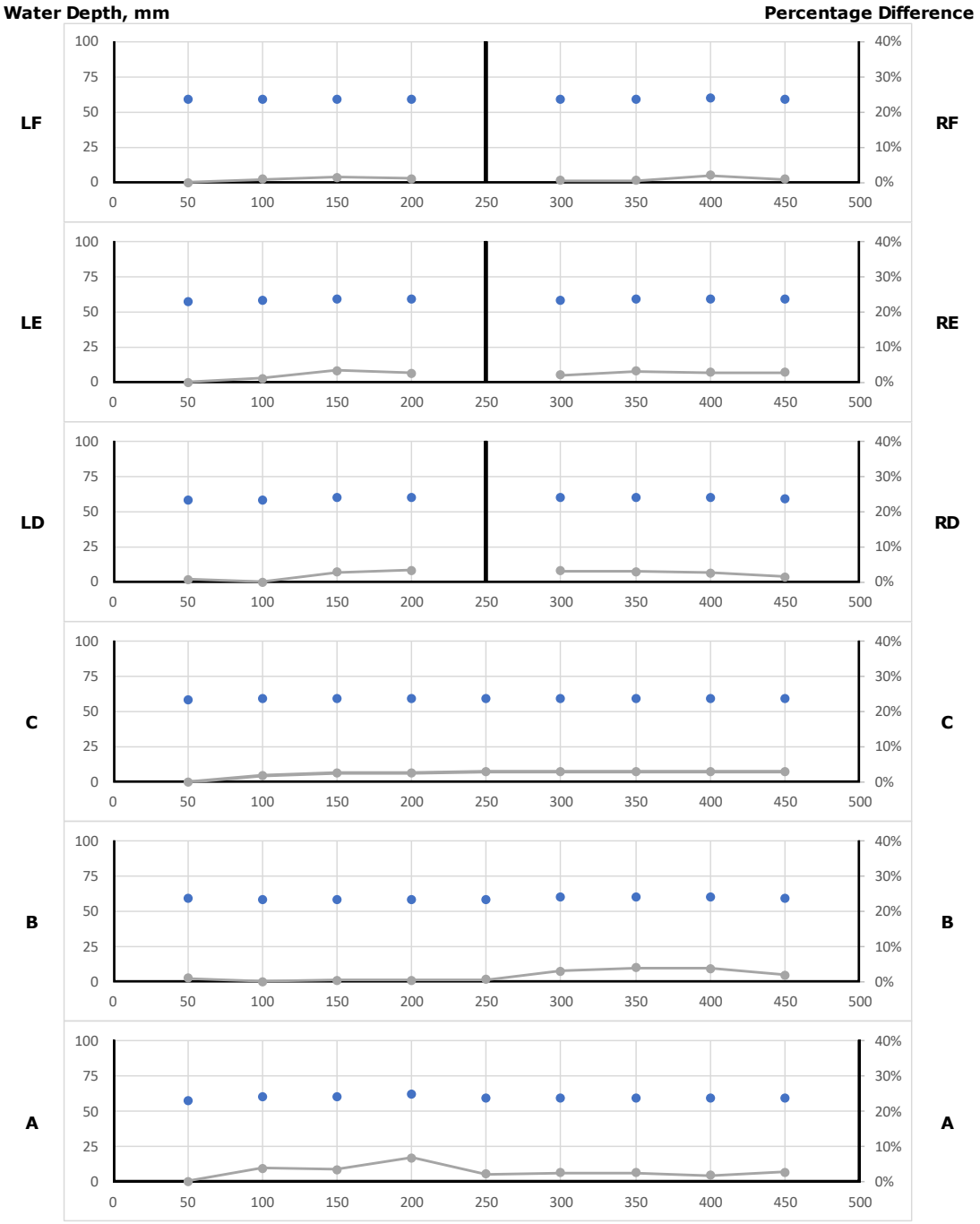
Water Depth and Percentage Difference: 40_03_5560



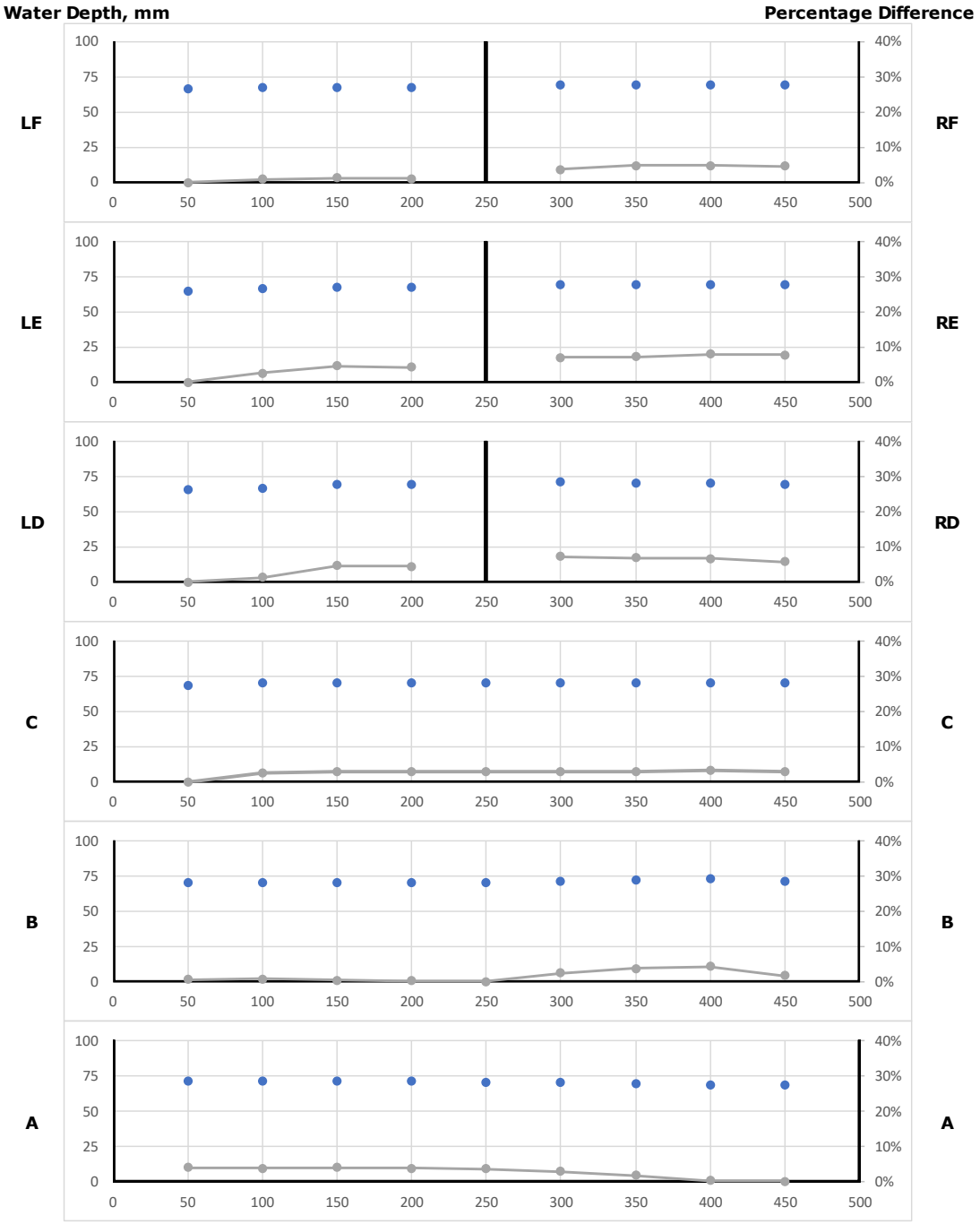
Water Depth and Percentage Difference: 40_03_5055



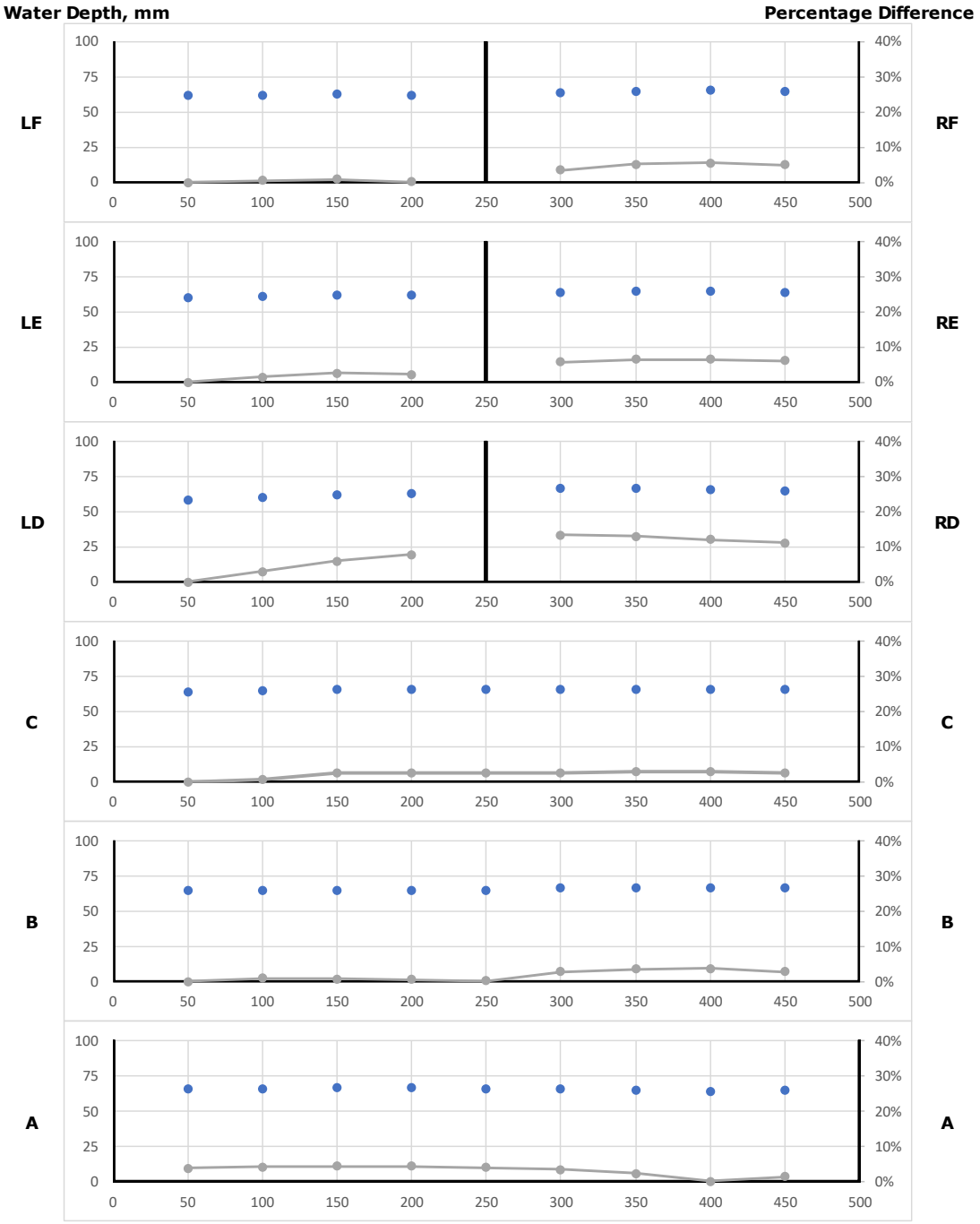
Water Depth and Percentage Difference: 40_05_5050



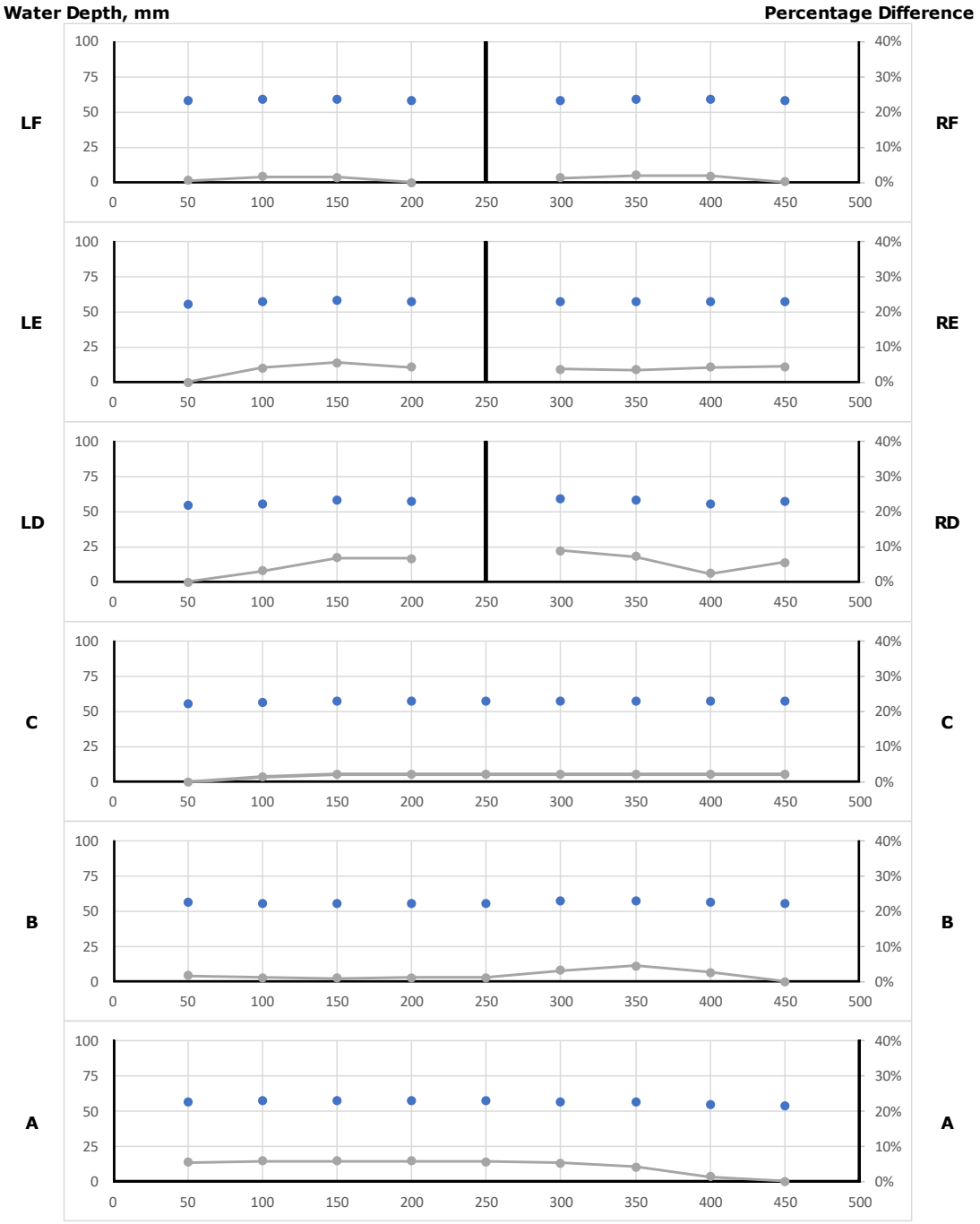
Water Depth and Percentage Difference: 40_05_5560



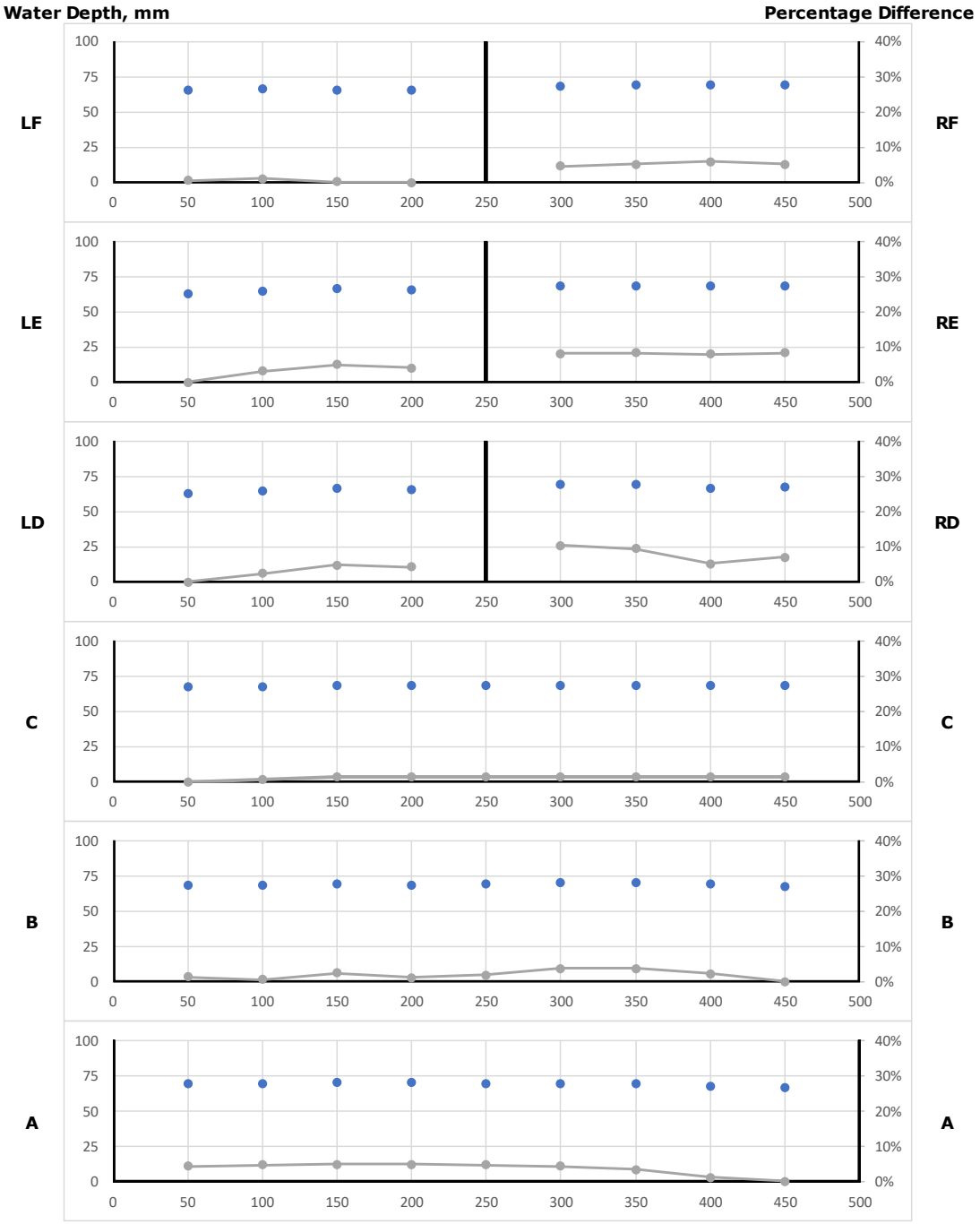
Water Depth and Percentage Difference: 40_05_5055



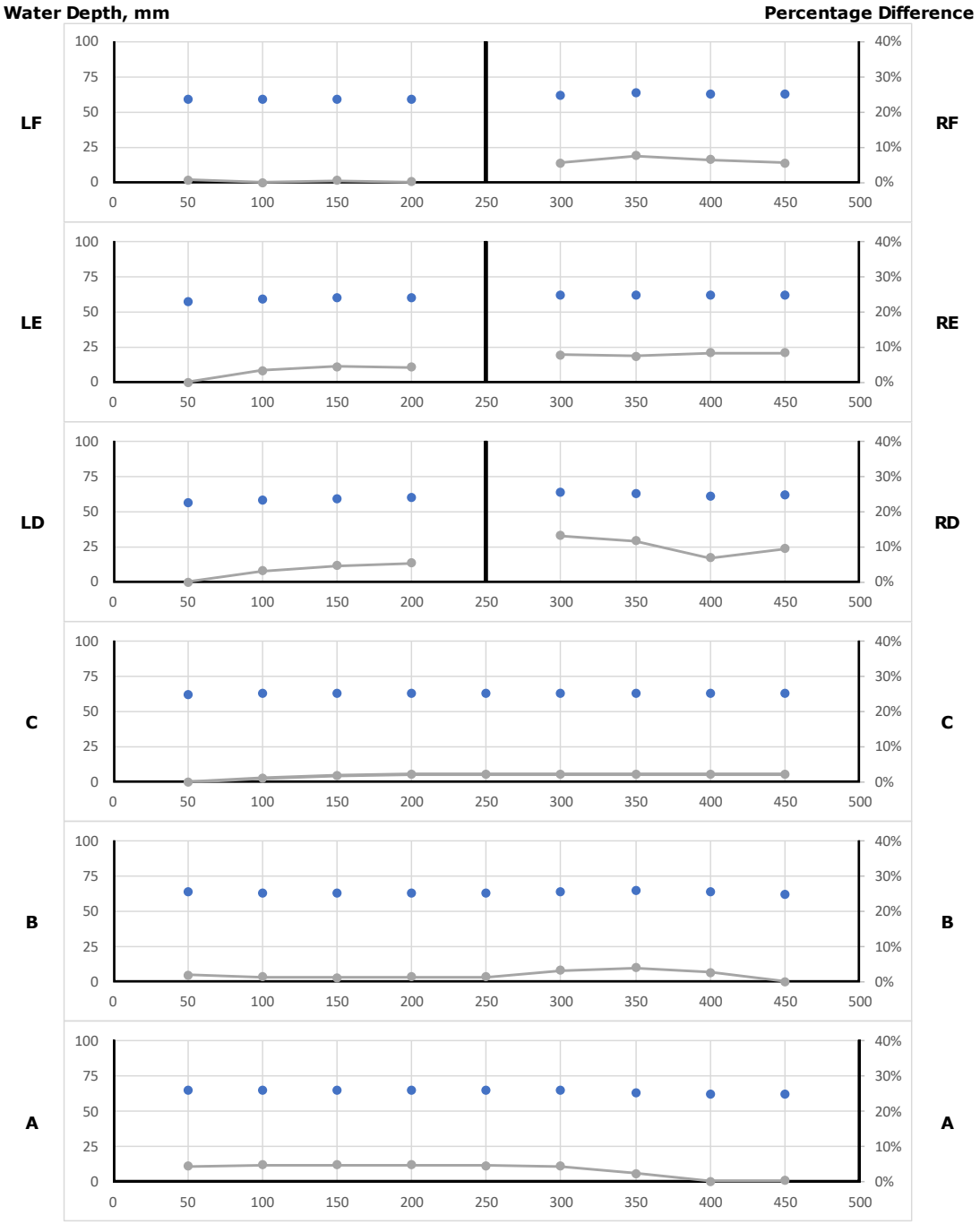
Water Depth and Percentage Difference: 40_07_5050



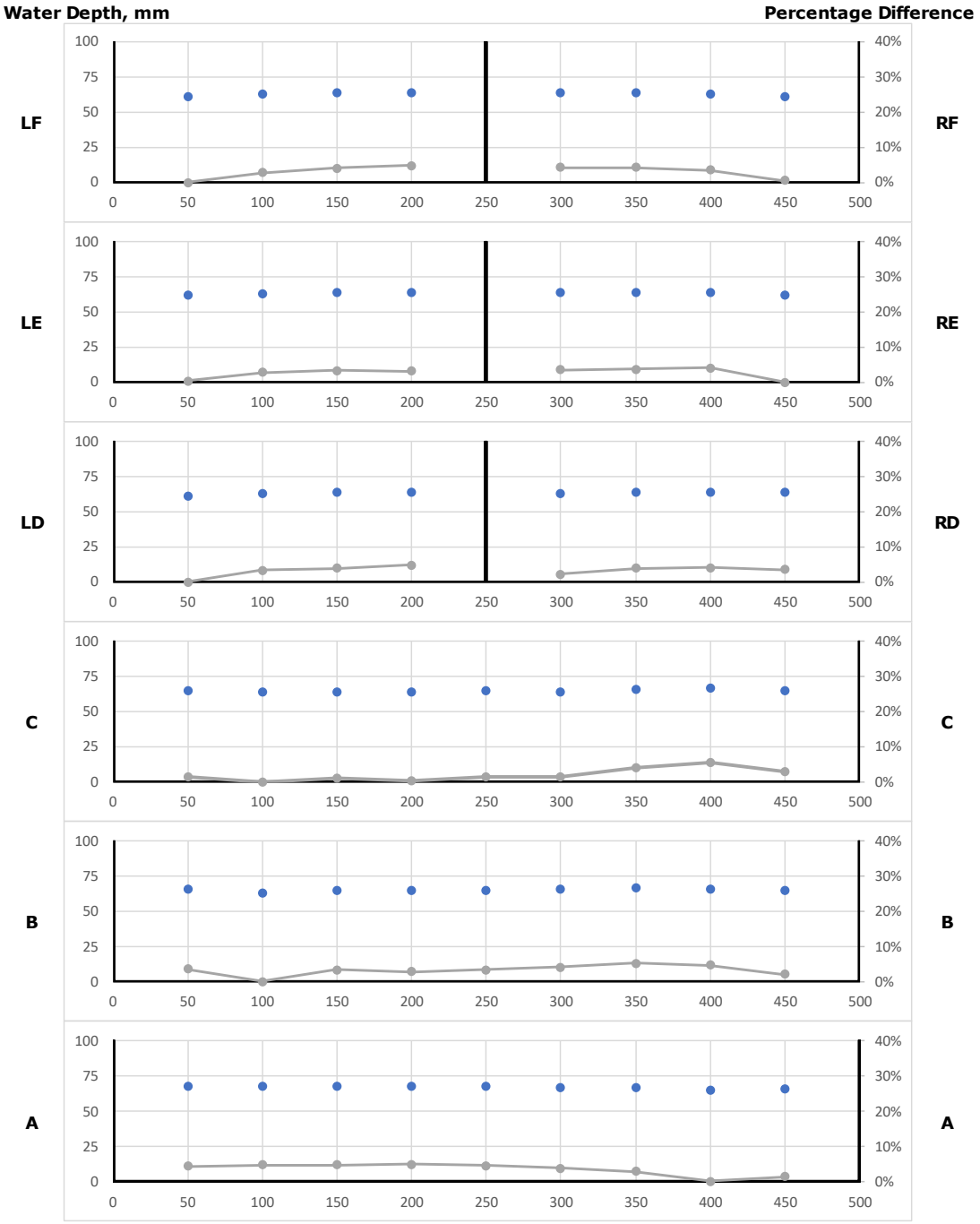
Water Depth and Percentage Difference: 40_07_5560



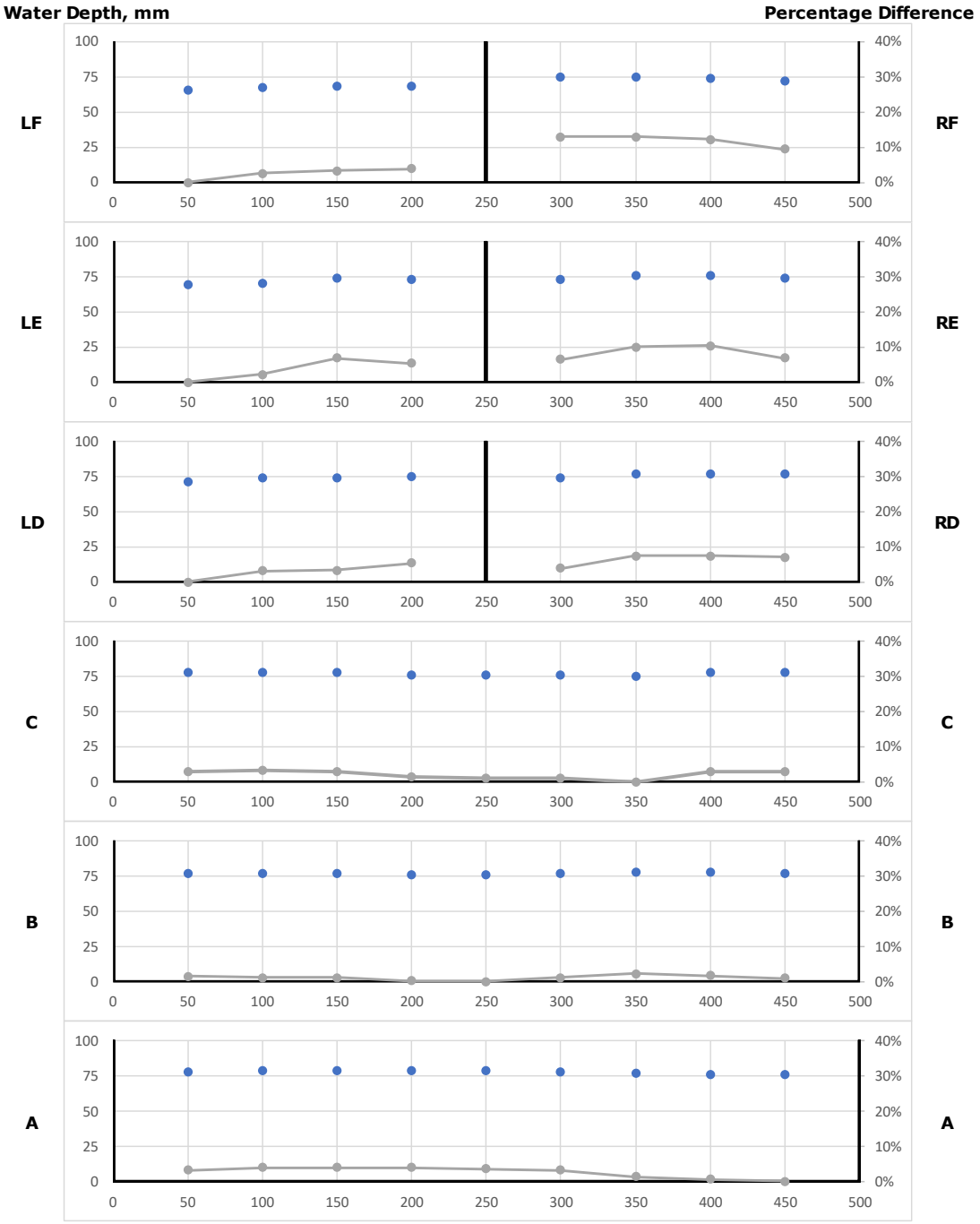
Water Depth and Percentage Difference: 40_07_5055



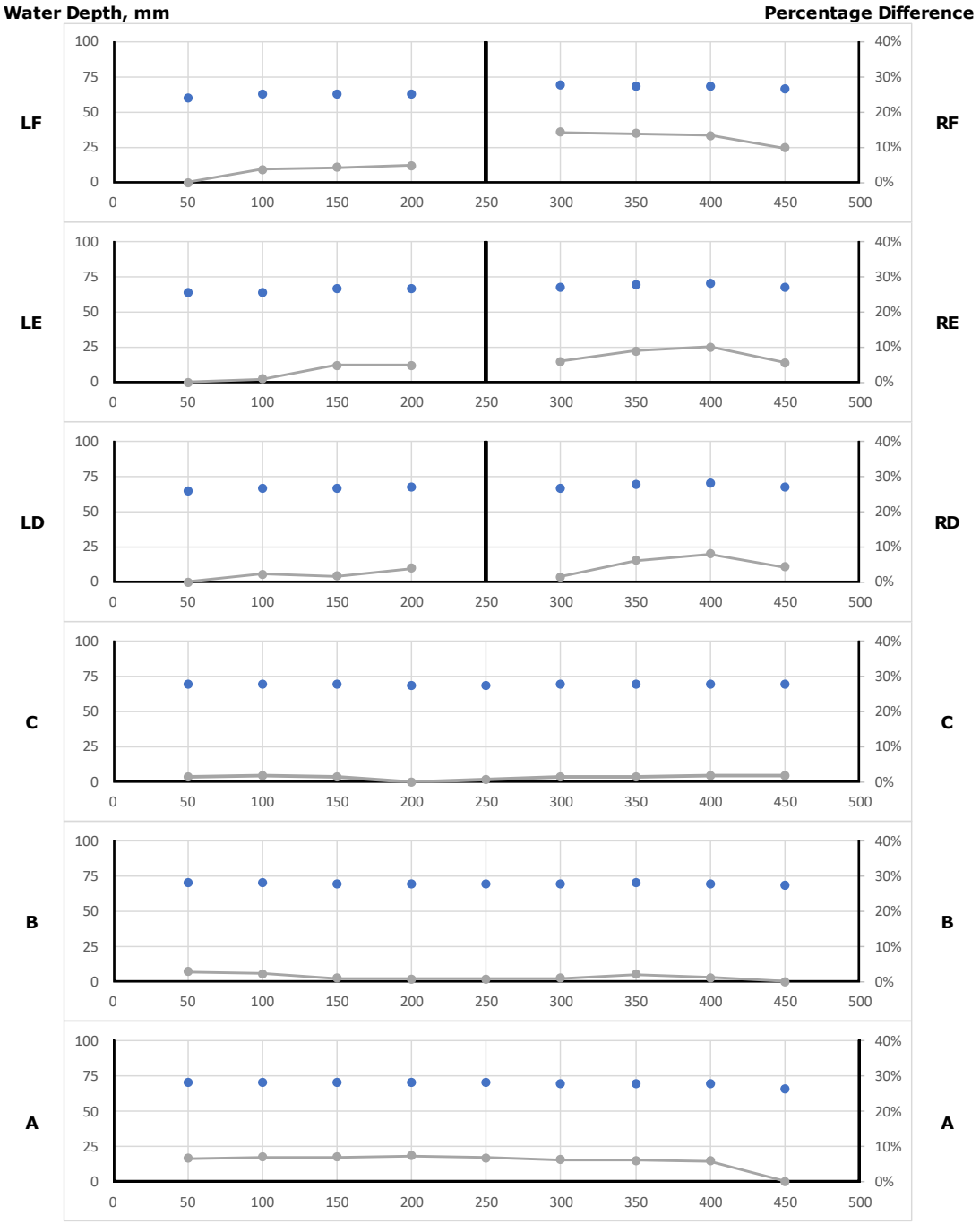
Water Depth and Percentage Difference: 50_03_5050



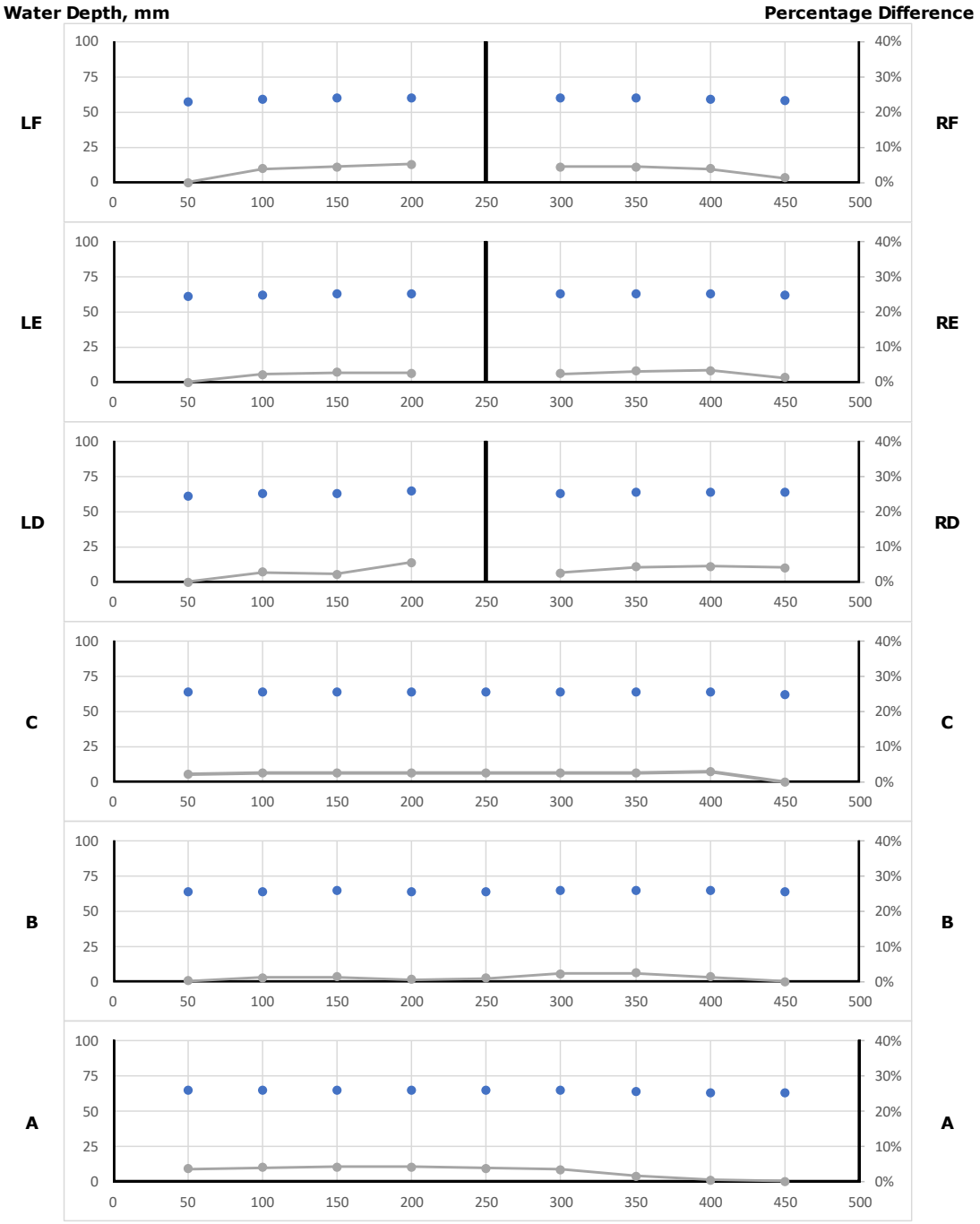
Water Depth and Percentage Difference: 50_03_5560



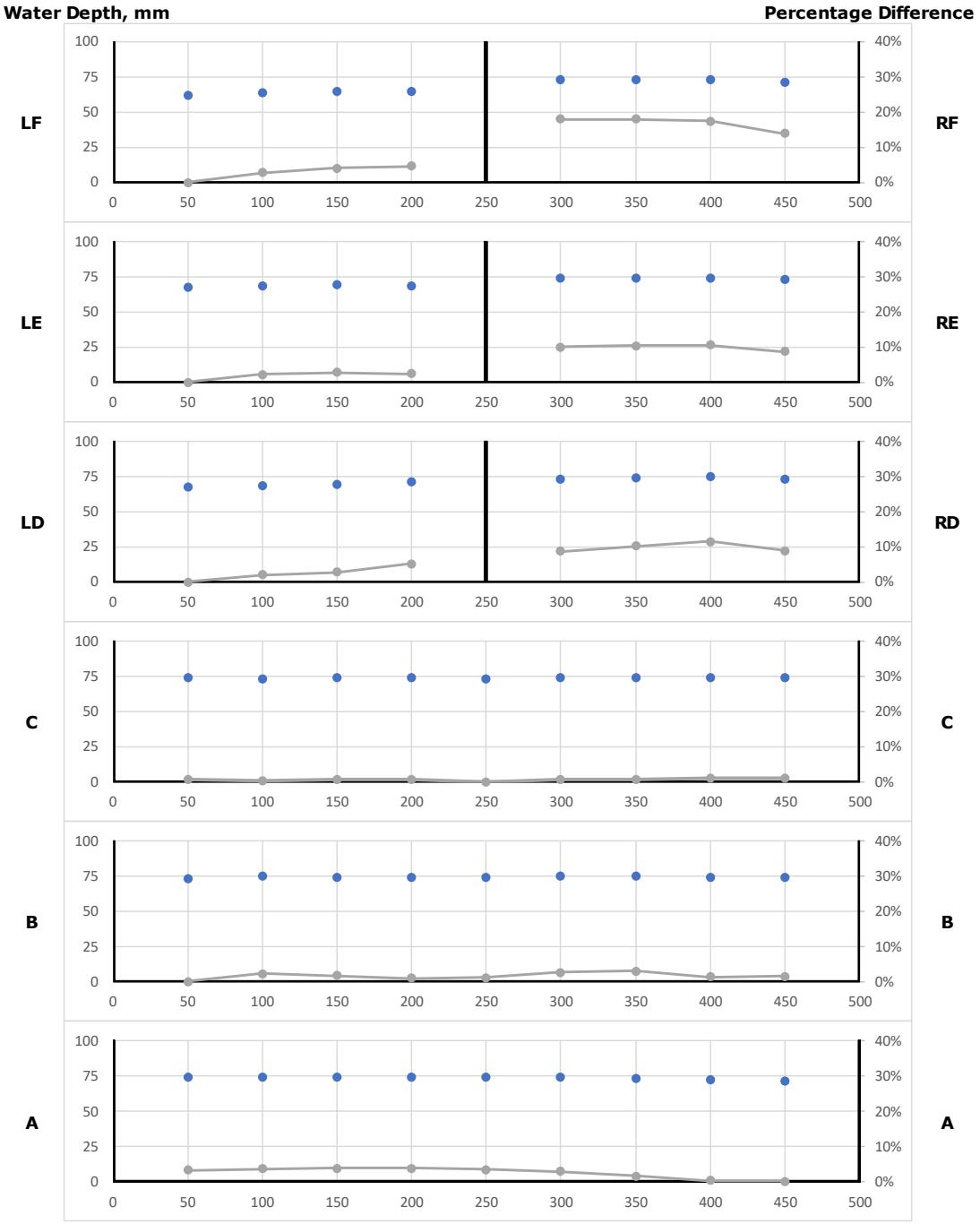
Water Depth and Percentage Difference: 50_03_5055



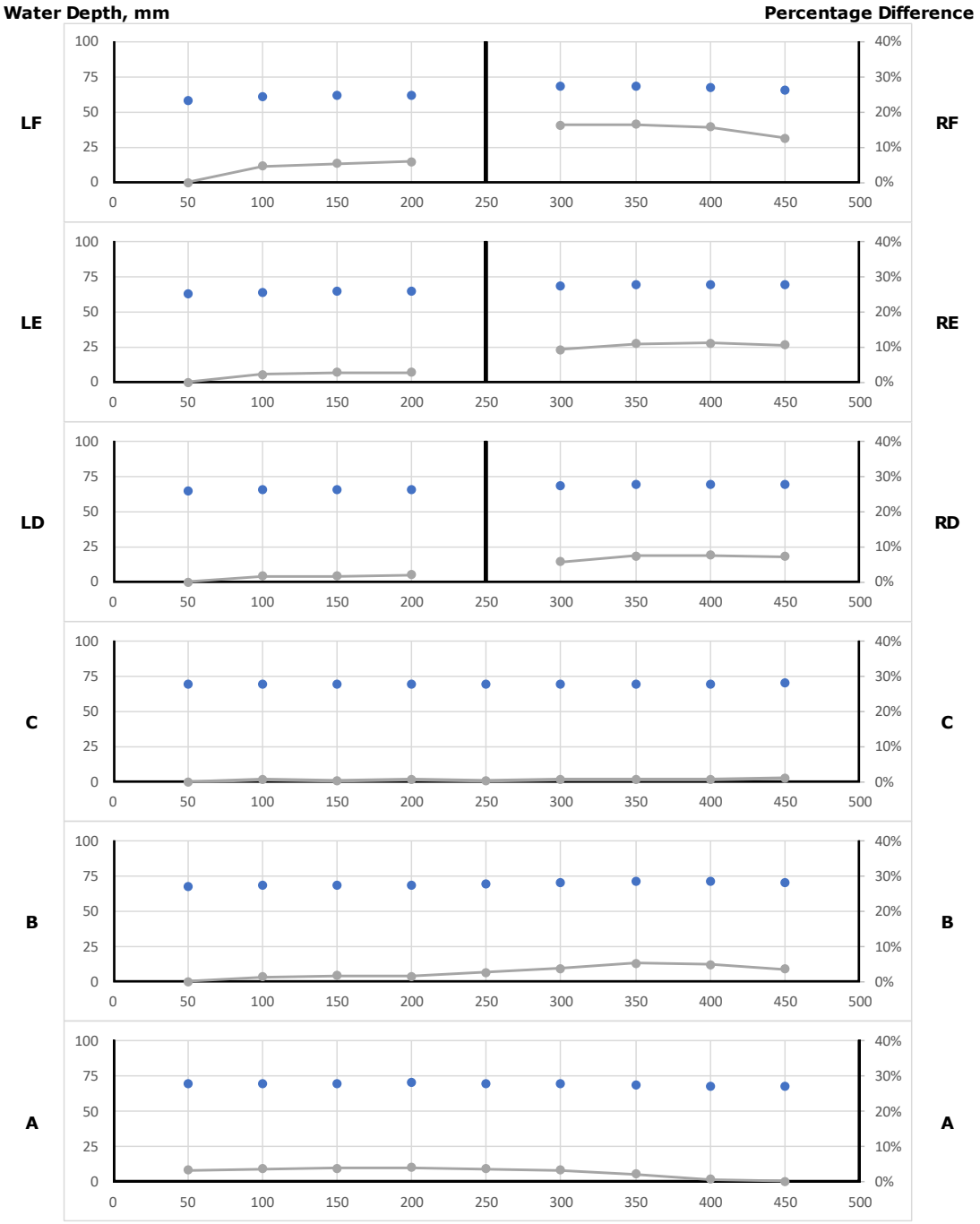
Water Depth and Percentage Difference: 50_05_5050



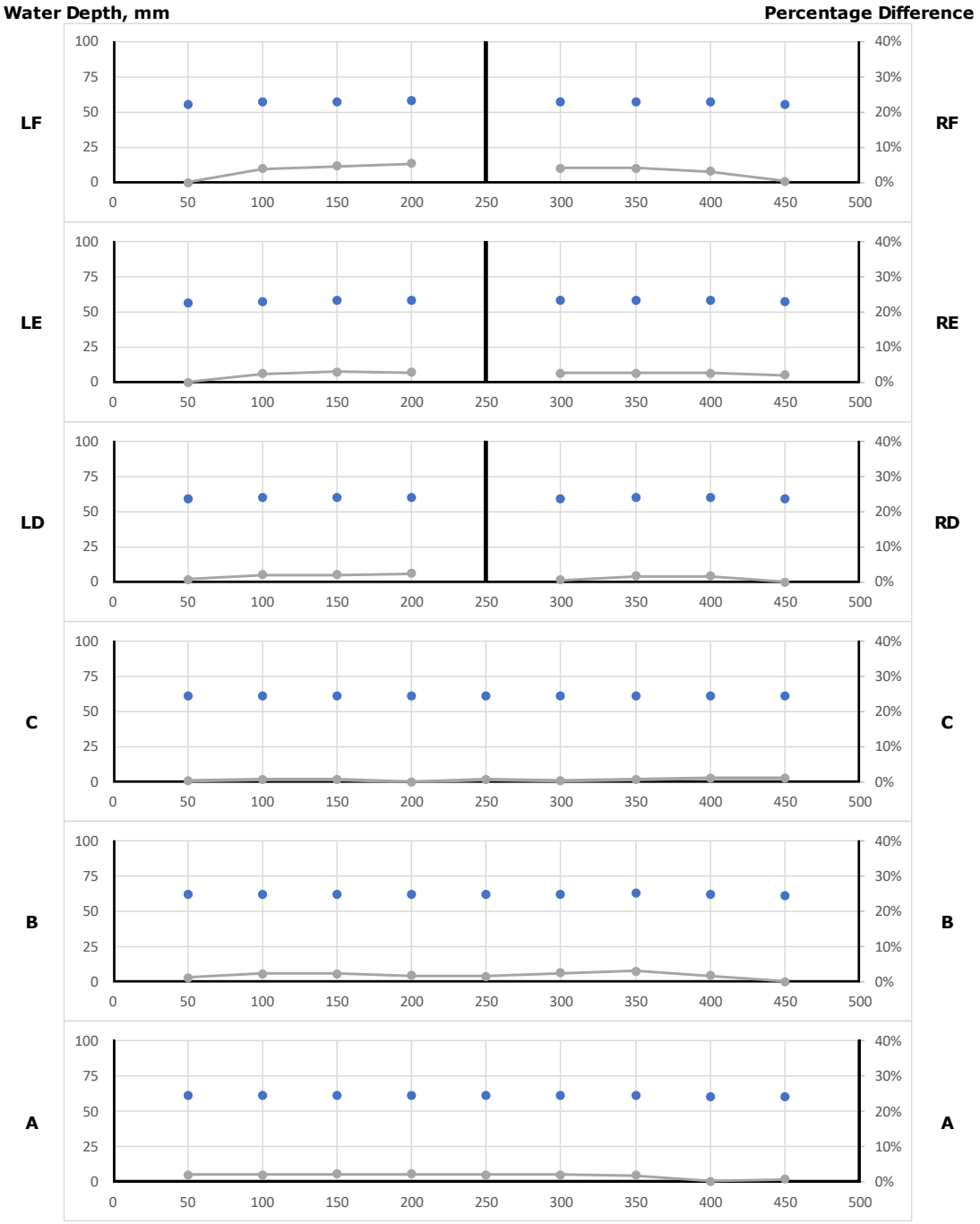
Water Depth and Percentage Difference: 50_05_5560



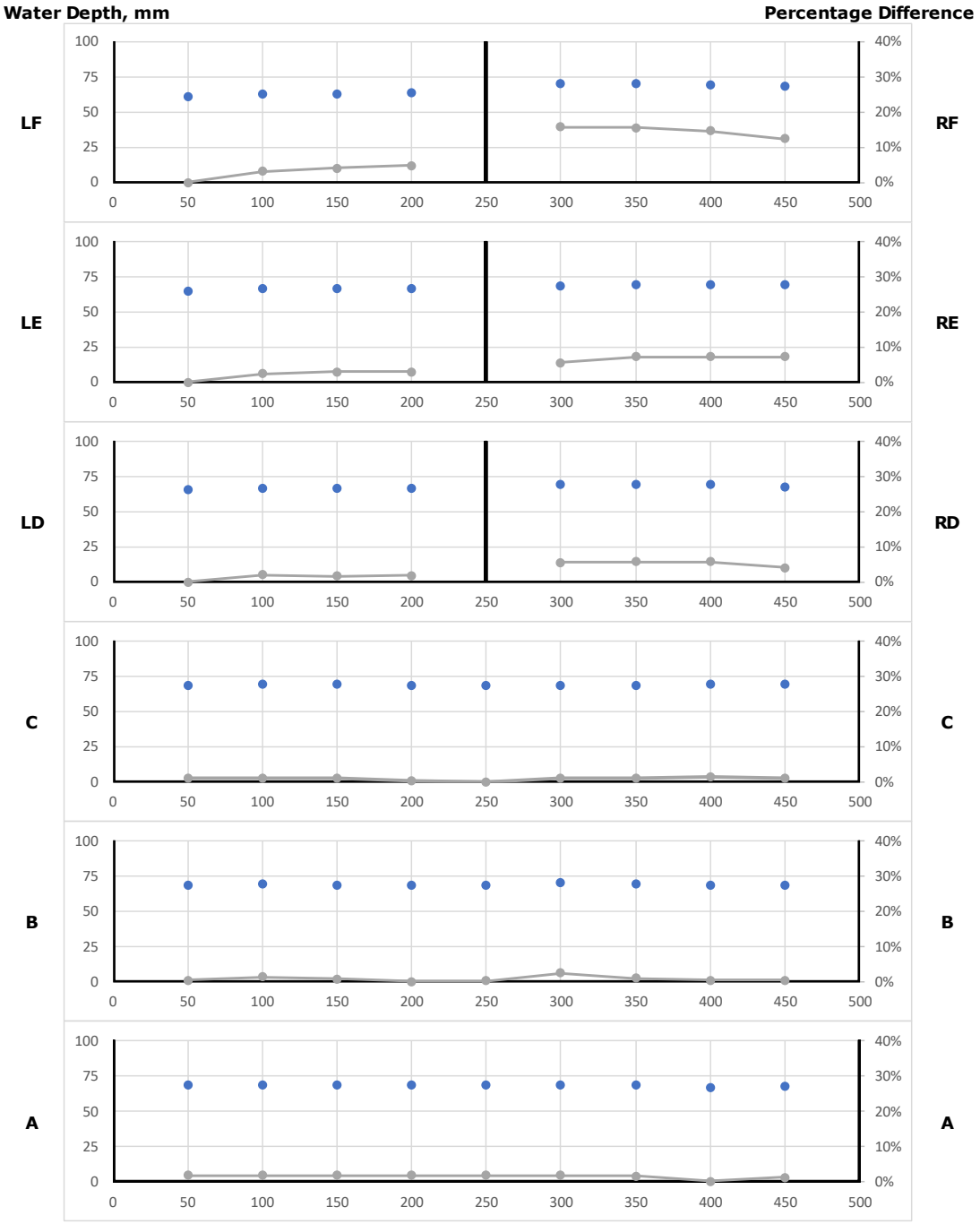
Water Depth and Percentage Difference: 50_05_5055



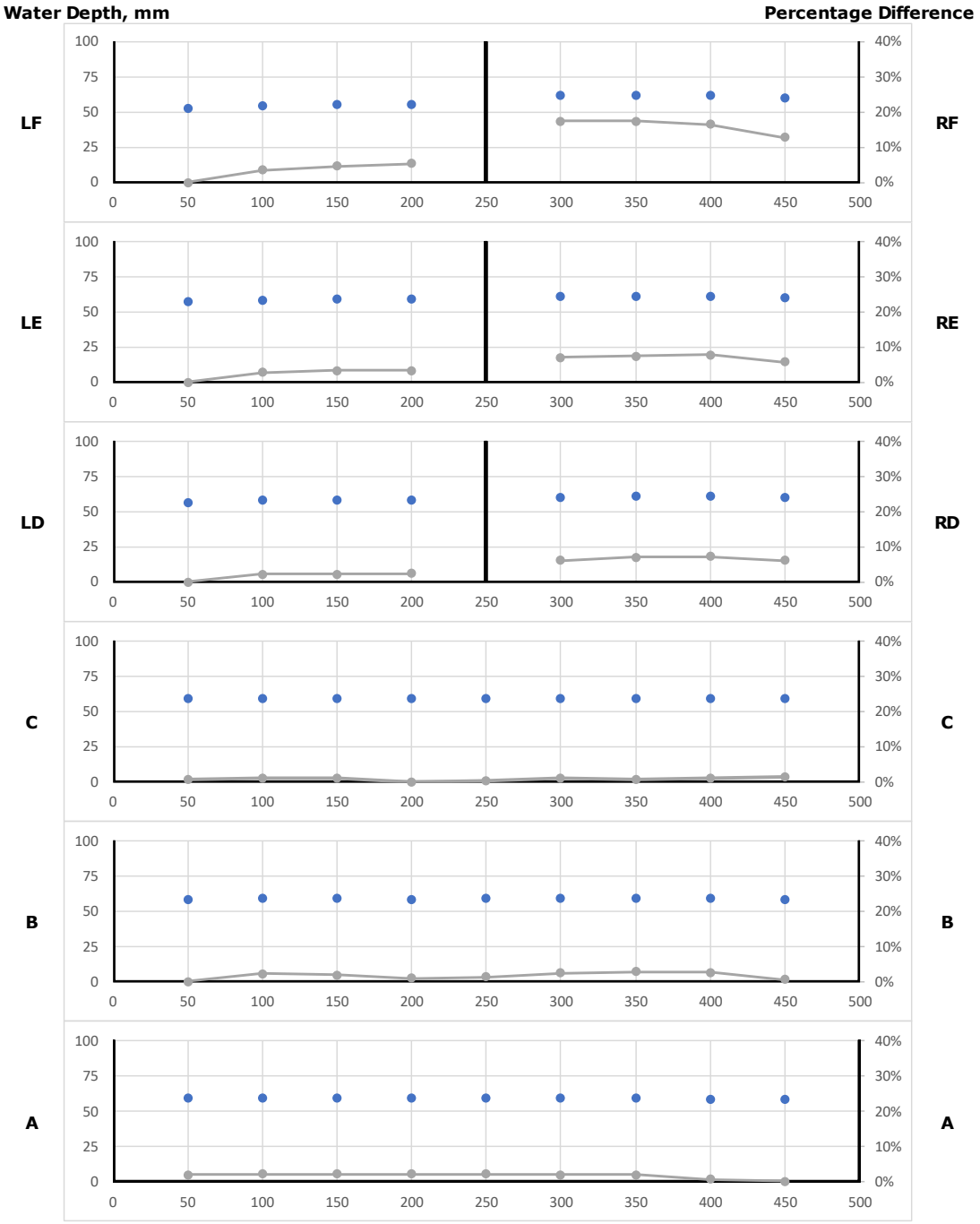
Water Depth and Percentage Difference: 50_07_5050



Water Depth and Percentage Difference: 50_07_5560



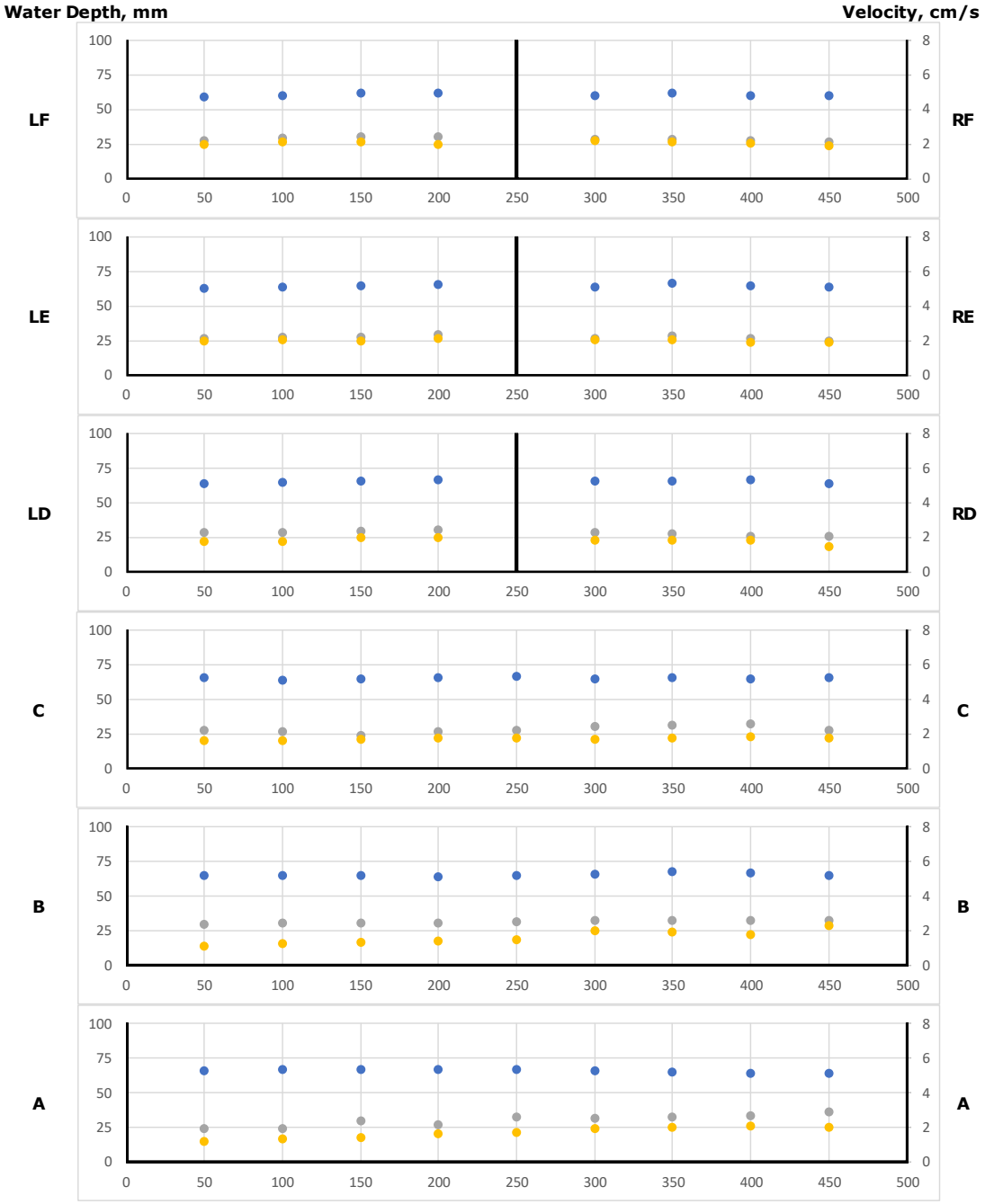
Water Depth and Percentage Difference: 50_07_5055



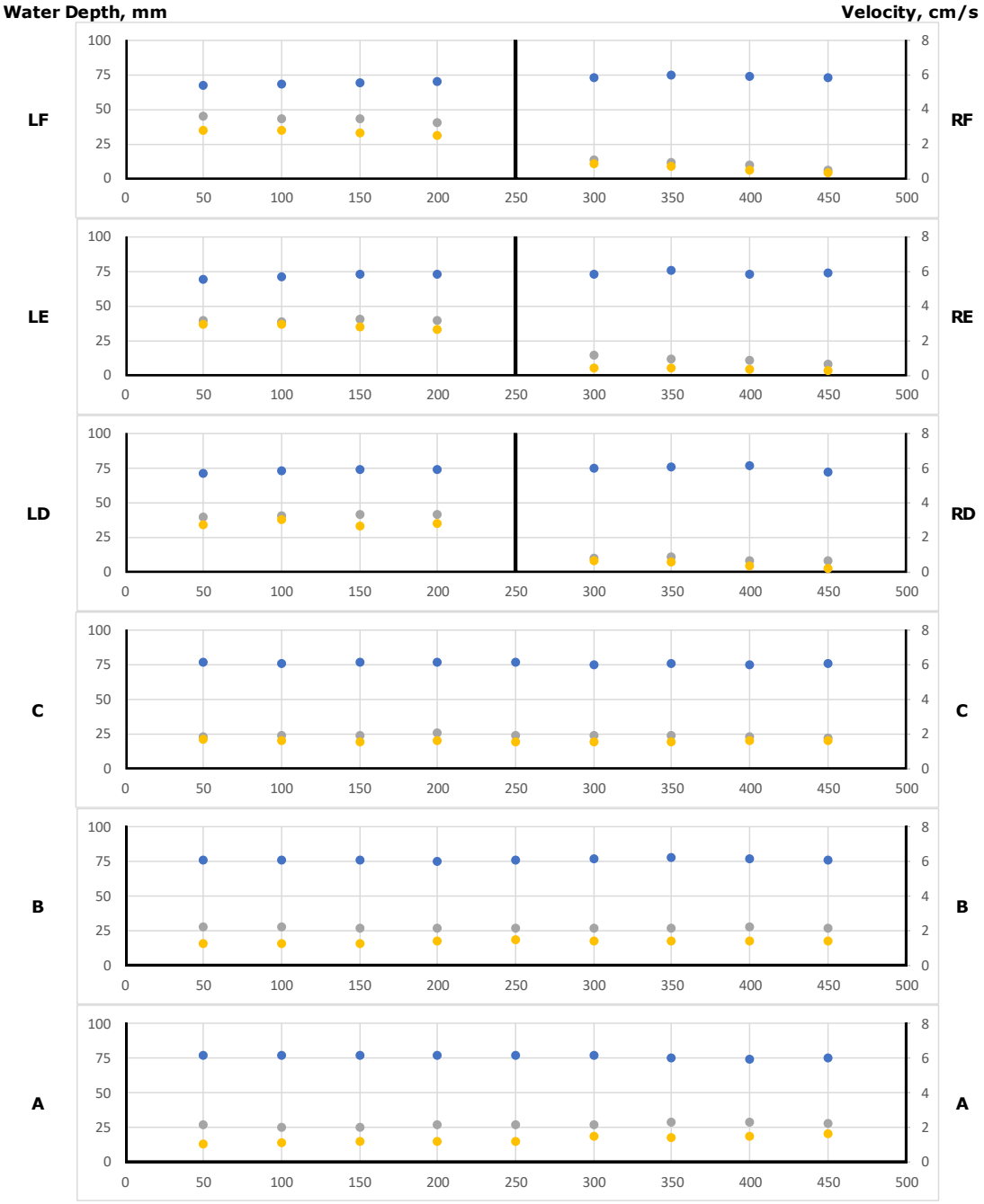
Appendix A3 Water Depth and Flow Velocity (Section)

Bifurcation Angle, °	Slope, %	Left Weir Height, mm	Right Weir Height, mm	Name of Run	Page Number
30	0.3	50	50	30_03_5050	A-58
		55	60	30_03_5560	A-59
		50	55	30_03_5055	A-60
	0.5	50	50	30_05_5050	A-61
		55	60	30_05_5560	A-62
		50	55	30_05_5055	A-63
	0.7	50	50	30_07_5050	A-64
		55	60	30_07_5560	A-65
		50	55	30_07_5055	A-66
40	0.3	50	50	40_03_5050	A-67
		55	60	40_03_5560	A-68
		50	55	40_03_5055	A-69
	0.5	50	50	40_05_5050	A-70
		55	60	40_05_5560	A-71
		50	55	40_05_5055	A-72
	0.7	50	50	40_07_5050	A-73
		55	60	40_07_5560	A-74
		50	55	40_07_5055	A-75
50	0.3	50	50	50_03_5050	A-76
		55	60	50_03_5560	A-77
		50	55	50_03_5055	A-78
	0.5	50	50	50_05_5050	A-79
		55	60	50_05_5560	A-80
		50	55	50_05_5055	A-81
	0.7	50	50	50_07_5050	A-82
		55	60	50_07_5560	A-83
		50	55	50_07_5055	A-84

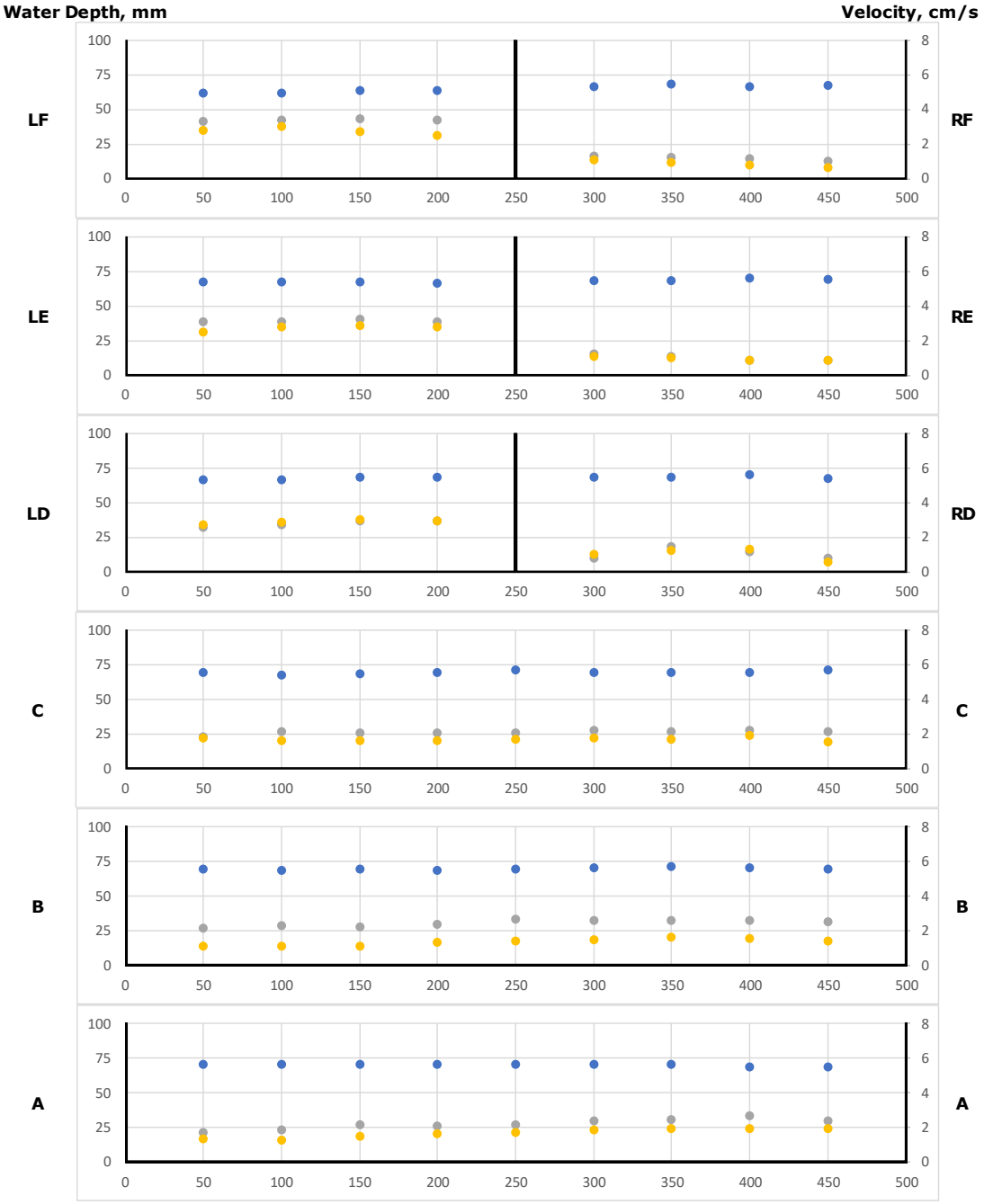
Water Depth and Flow Velocity: 30_03_5050



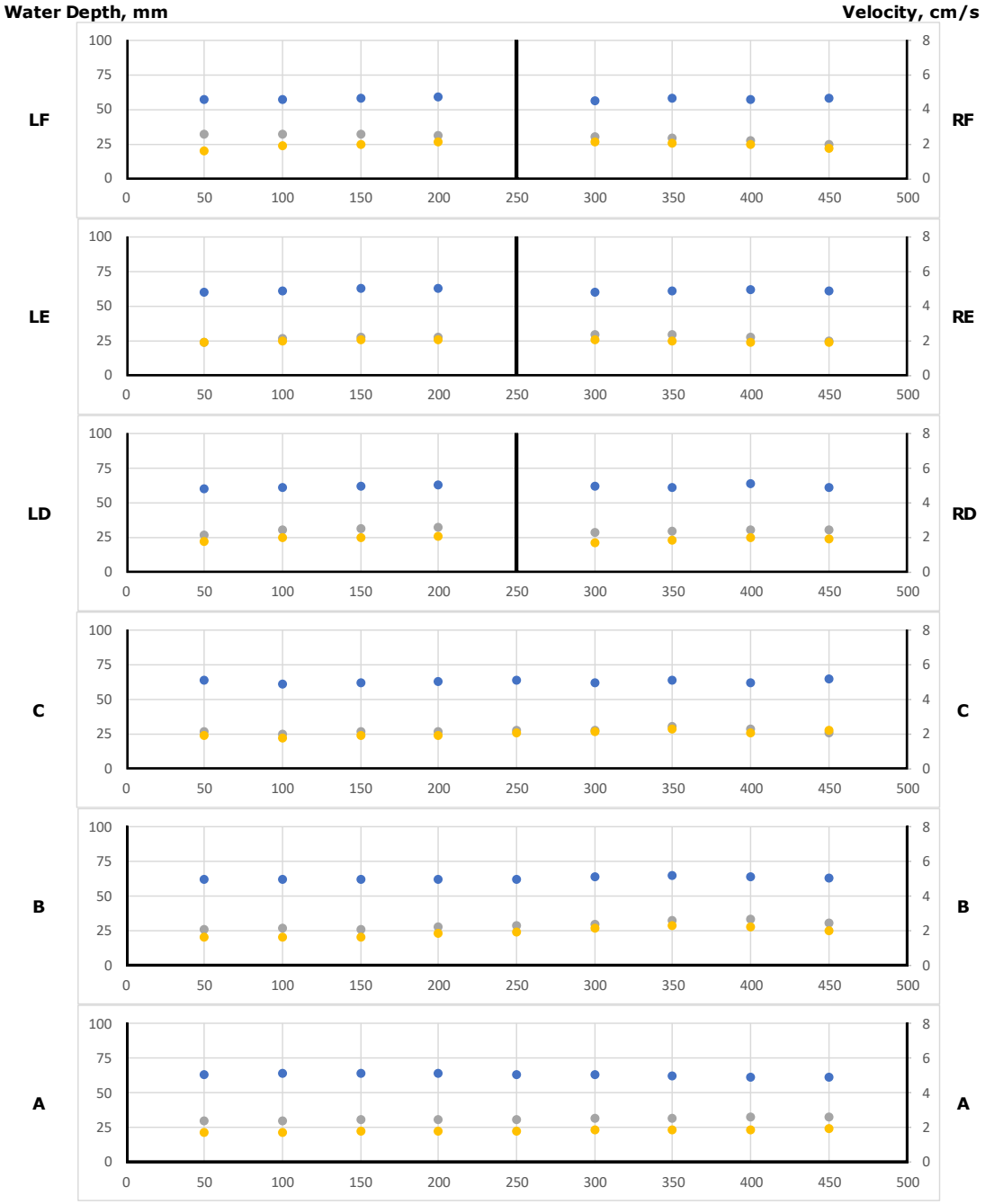
Water Depth and Flow Velocity: 30_03_5560



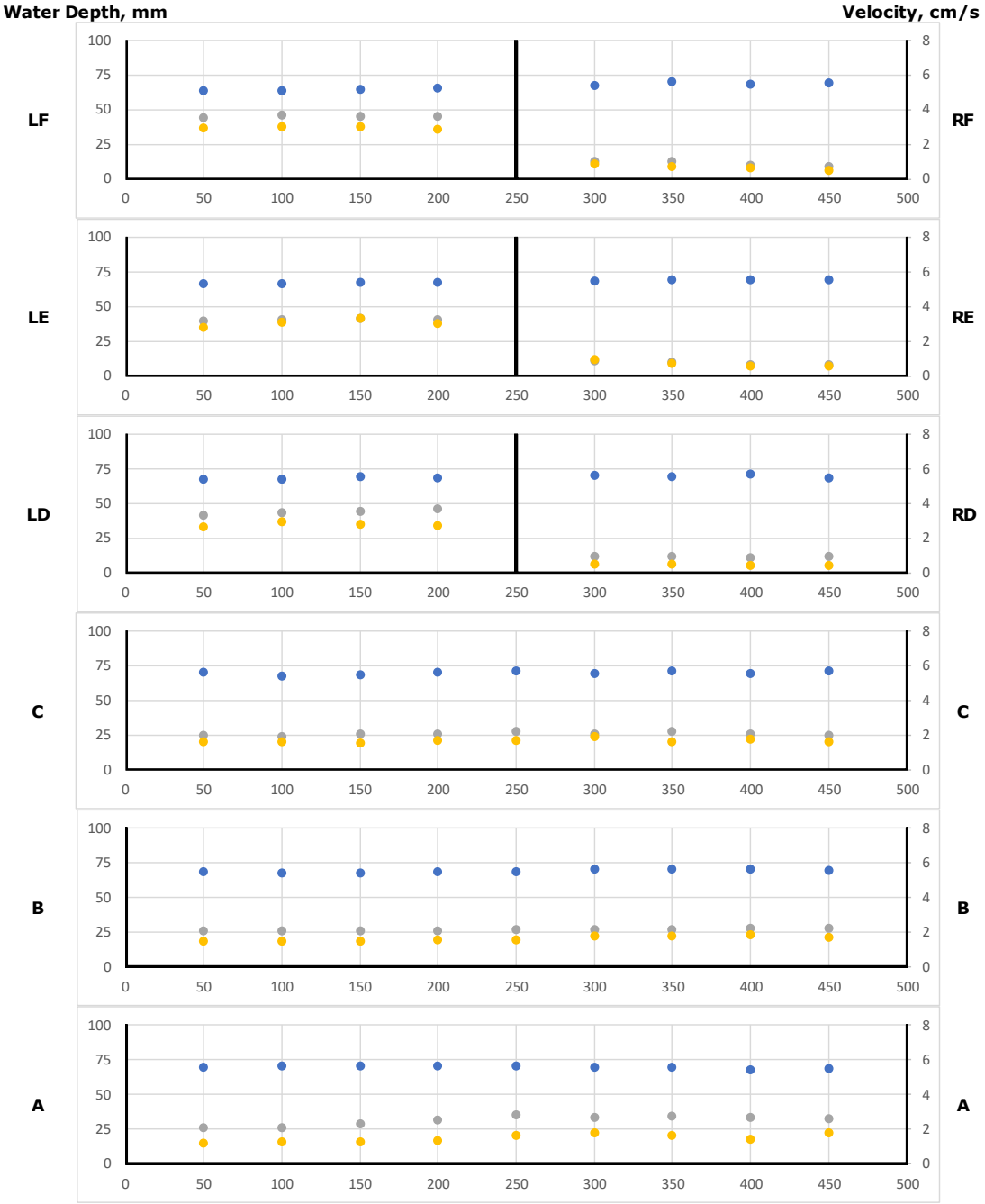
Water Depth and Flow Velocity: 30_03_5055



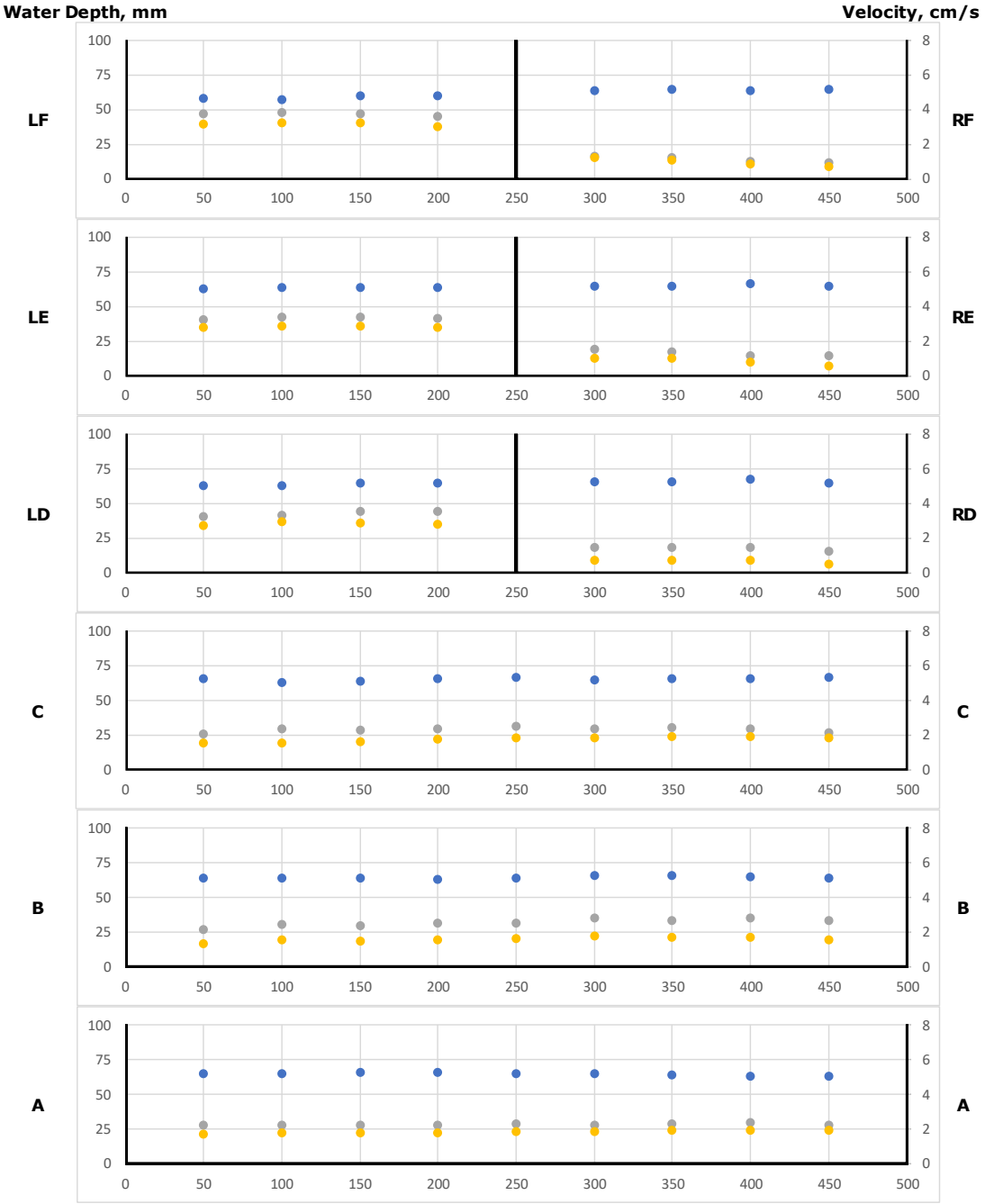
Water Depth and Flow Velocity: 30_05_5050



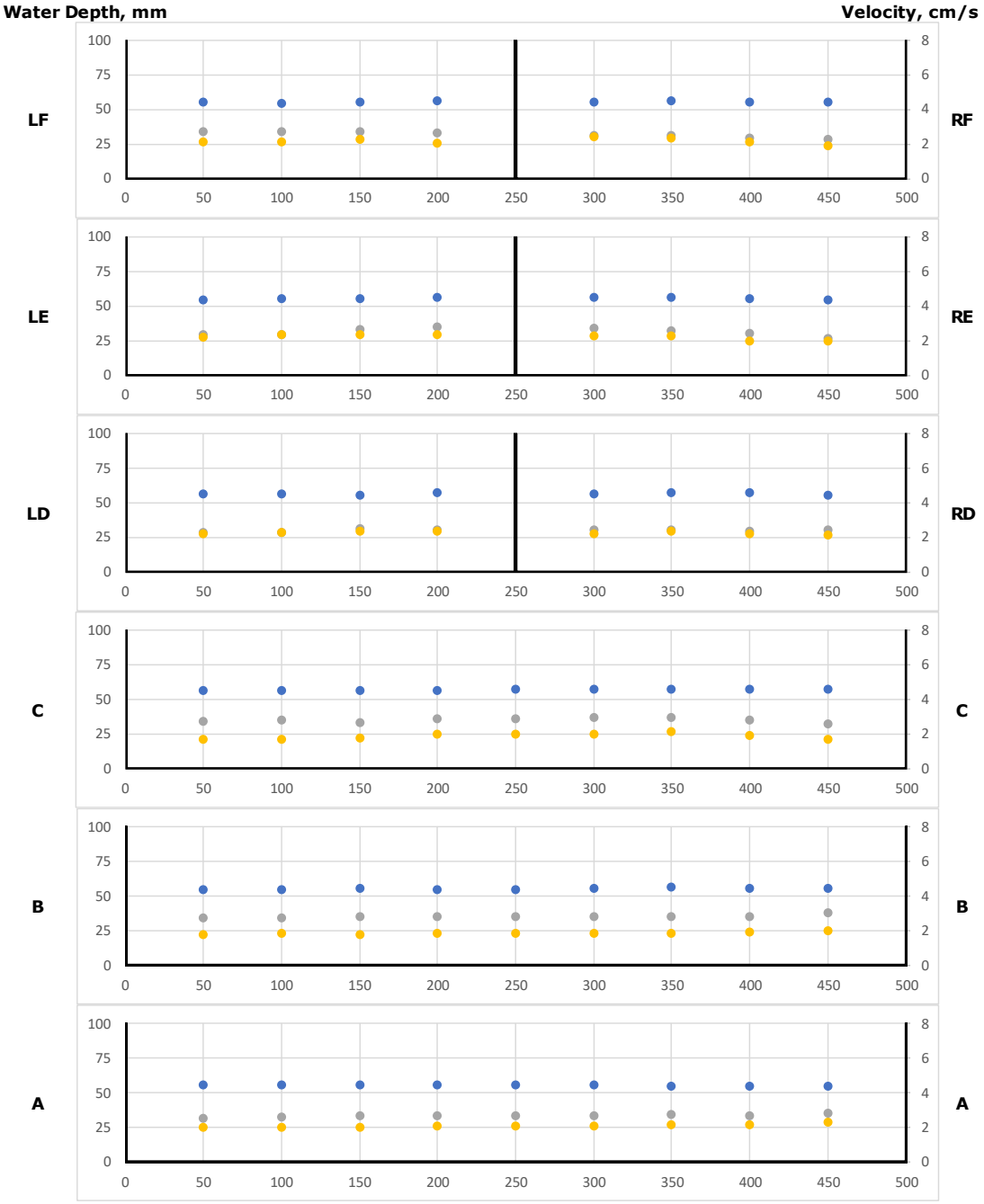
Water Depth and Flow Velocity: 30_05_5560



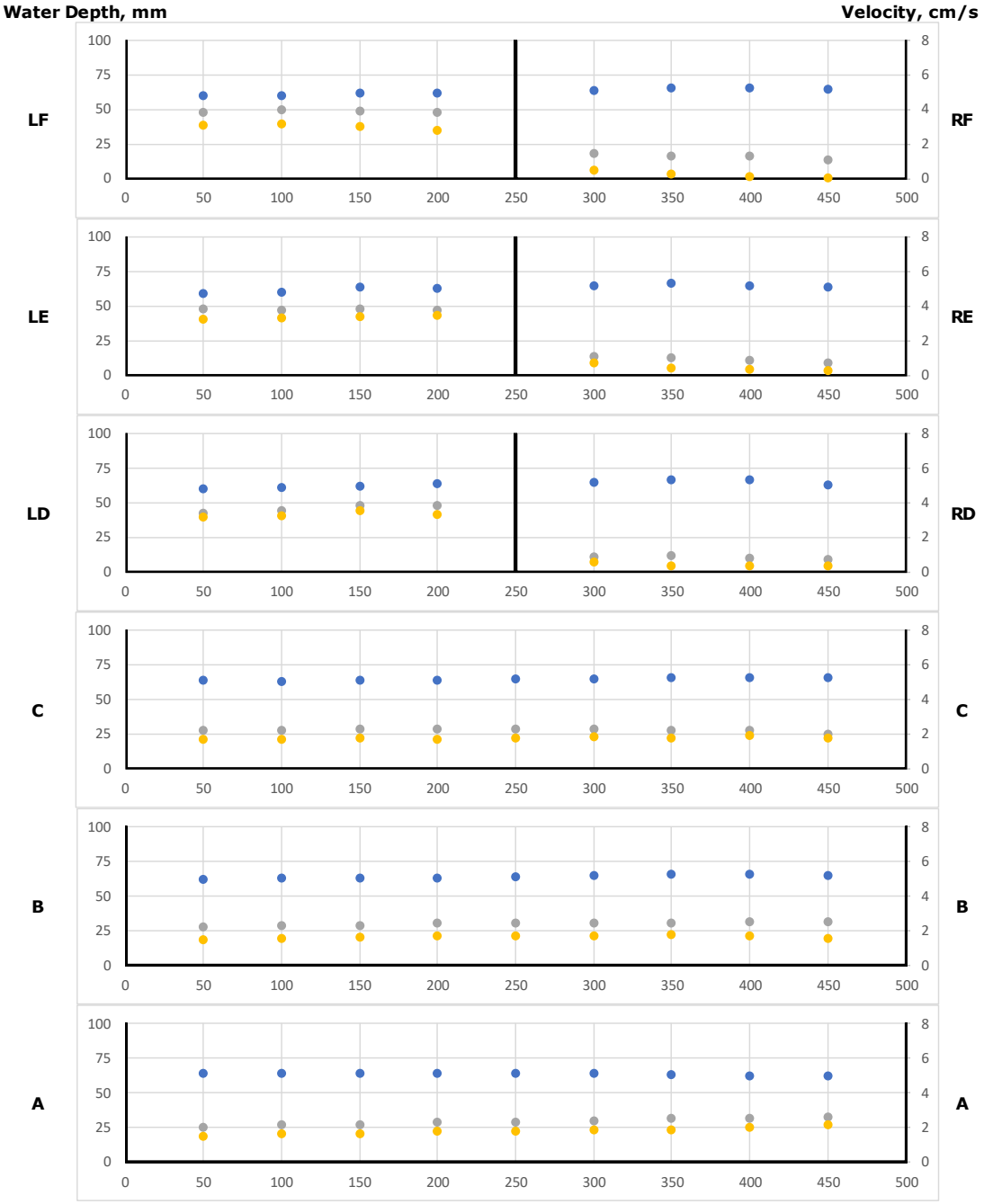
Water Depth and Flow Velocity: 30_05_5055



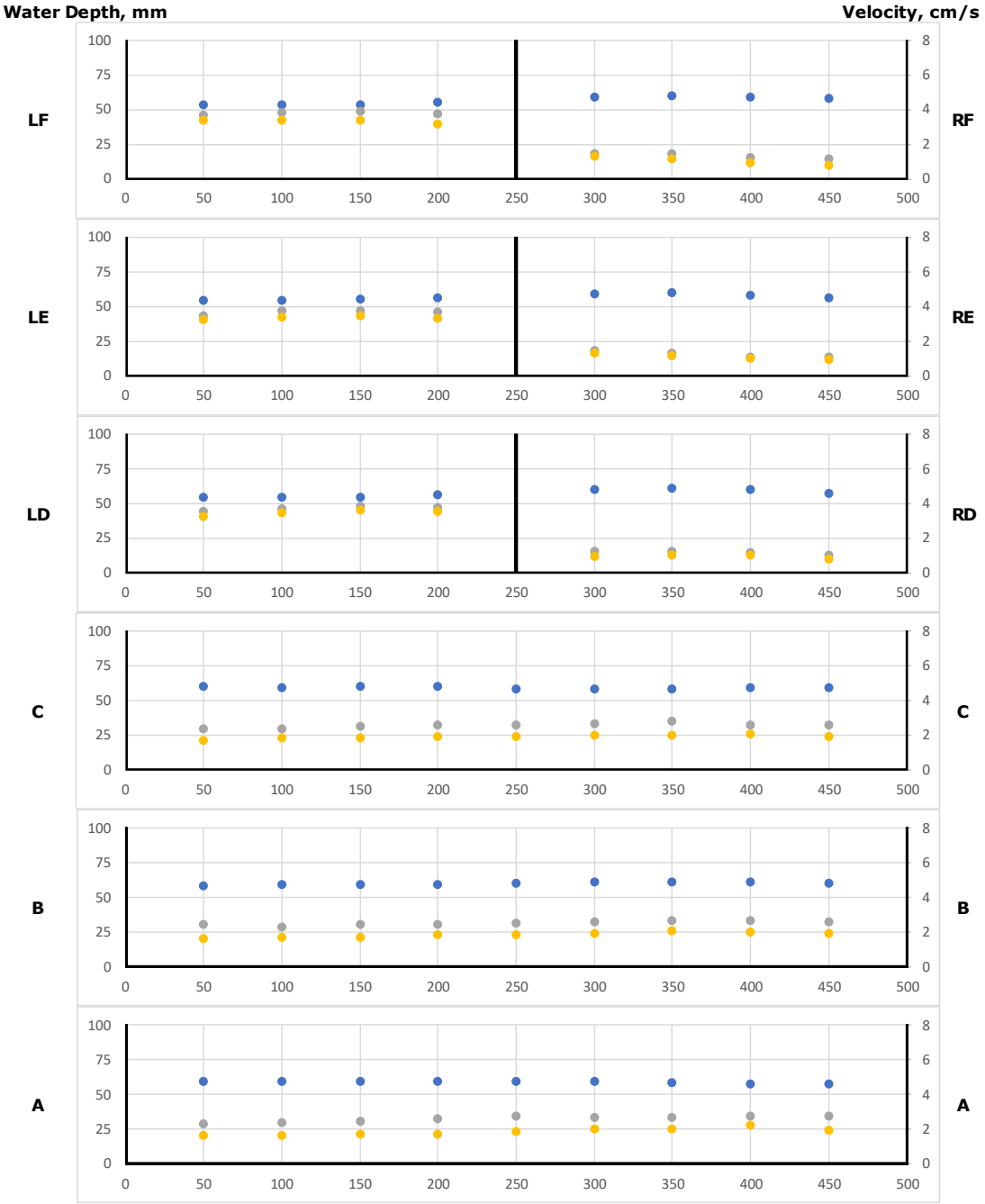
Water Depth and Flow Velocity: 30_07_5050



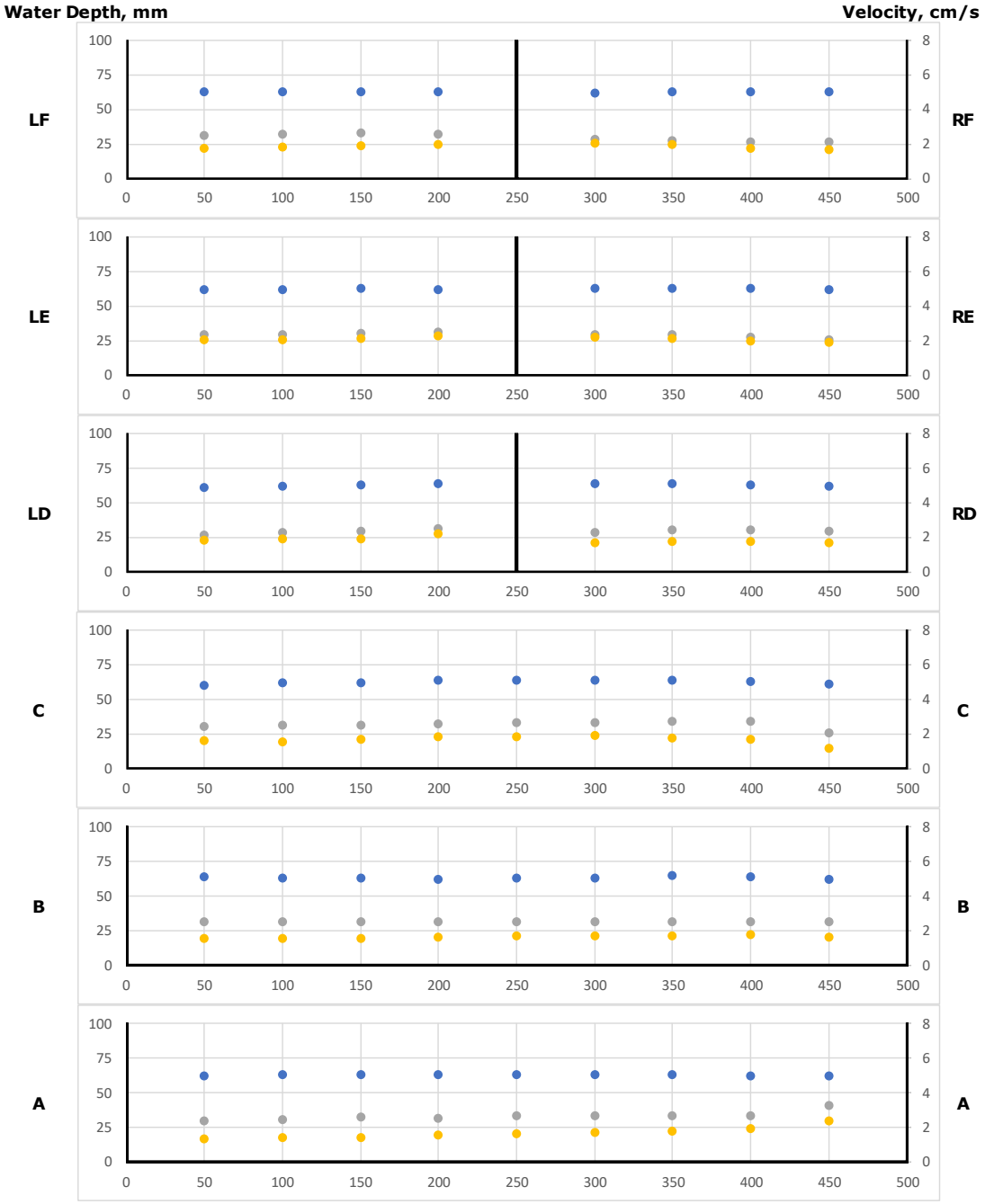
Water Depth and Flow Velocity: 30_07_5560



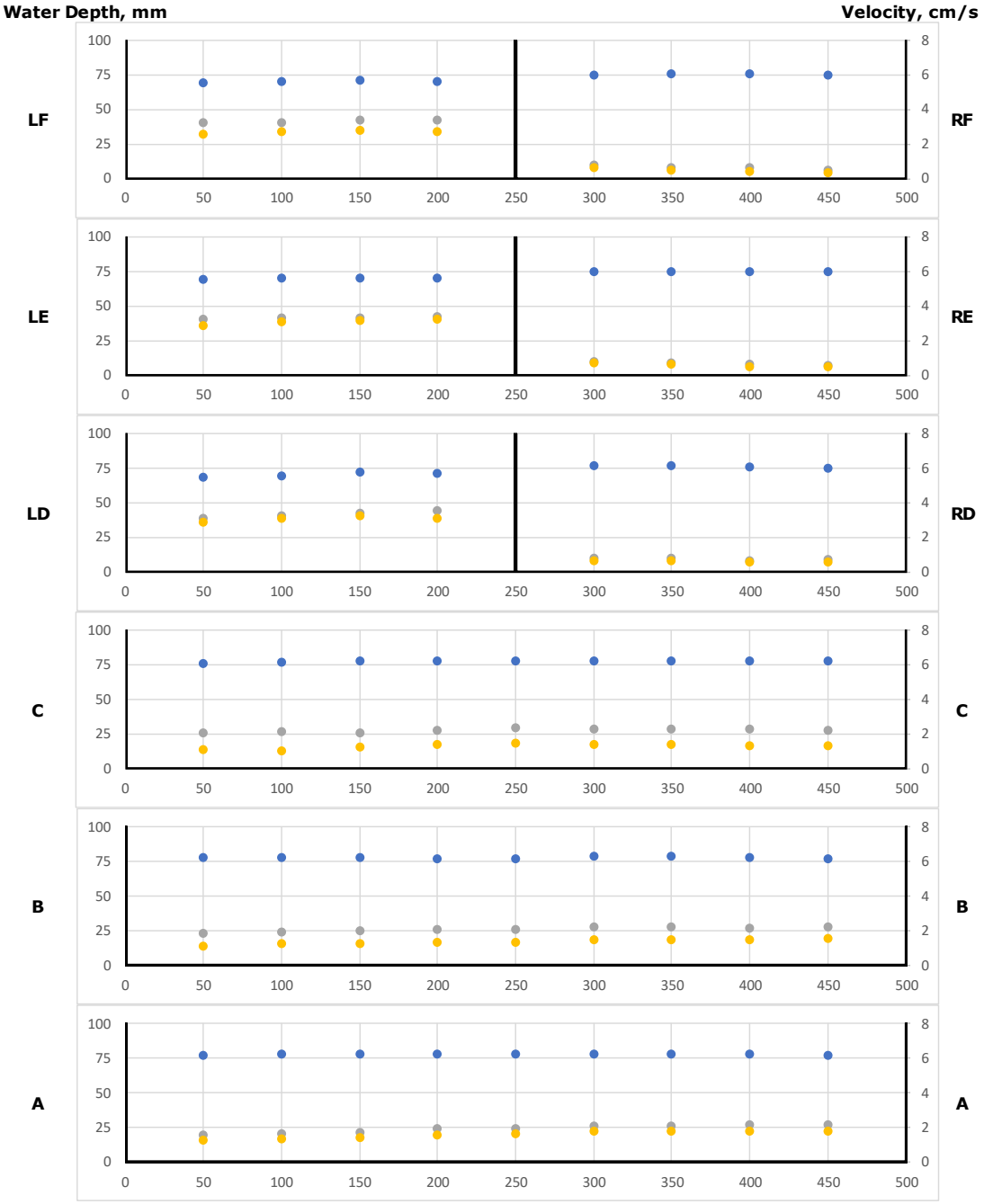
Water Depth and Flow Velocity: 30_07_5055



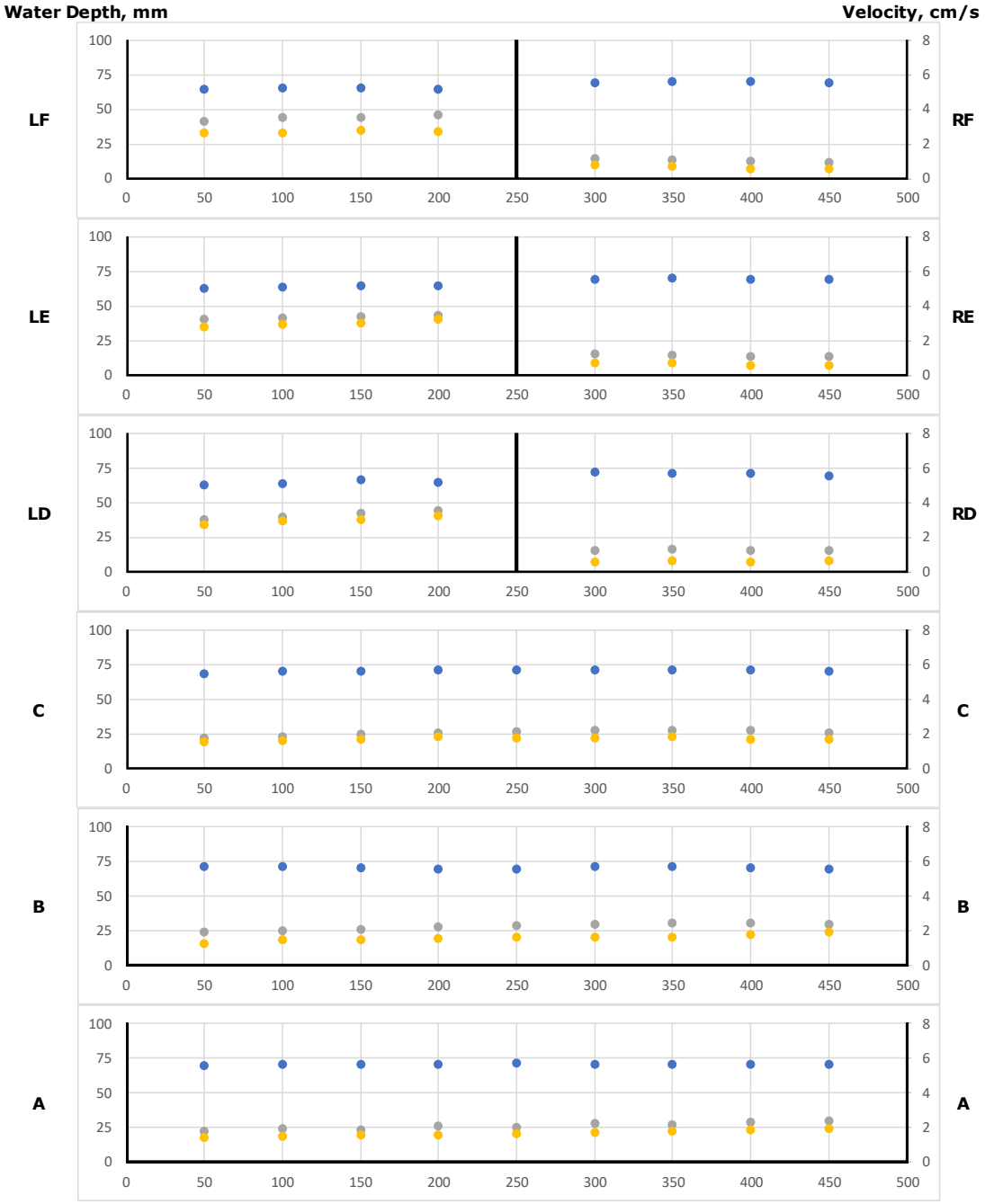
Water Depth and Flow Velocity: 40_03_5050



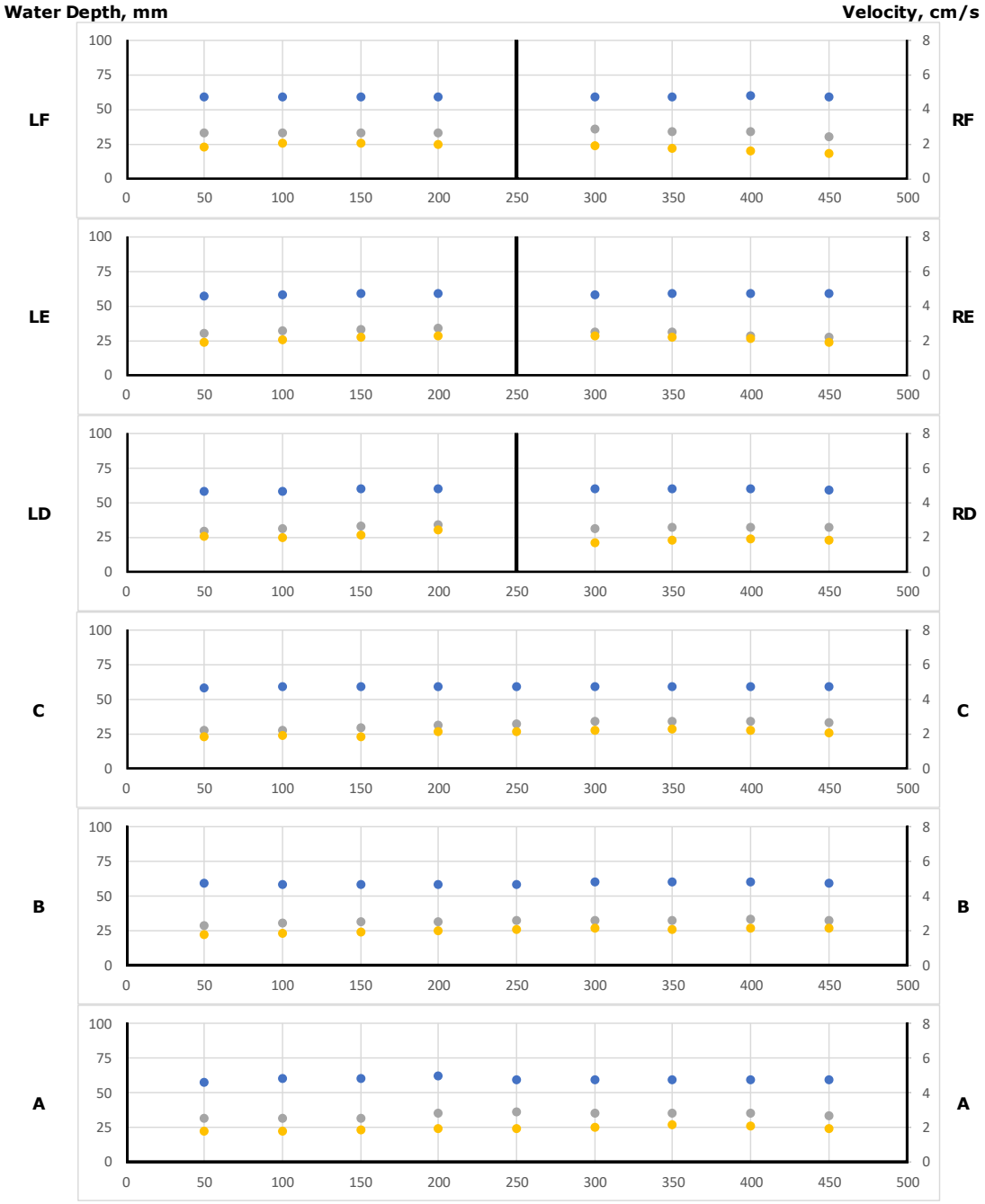
Water Depth and Flow Velocity: 40_03_5560



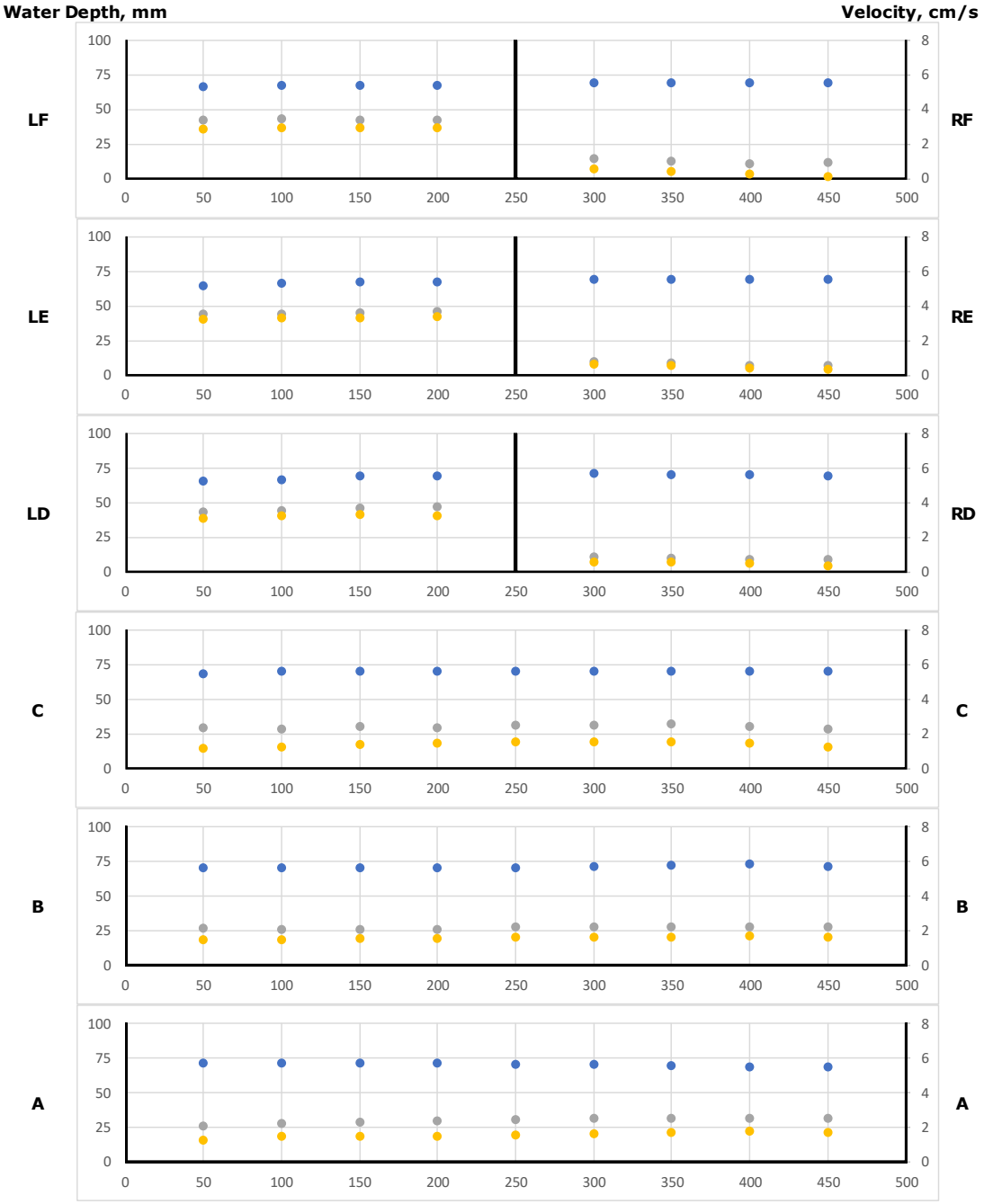
Water Depth and Flow Velocity: 40_03_5055



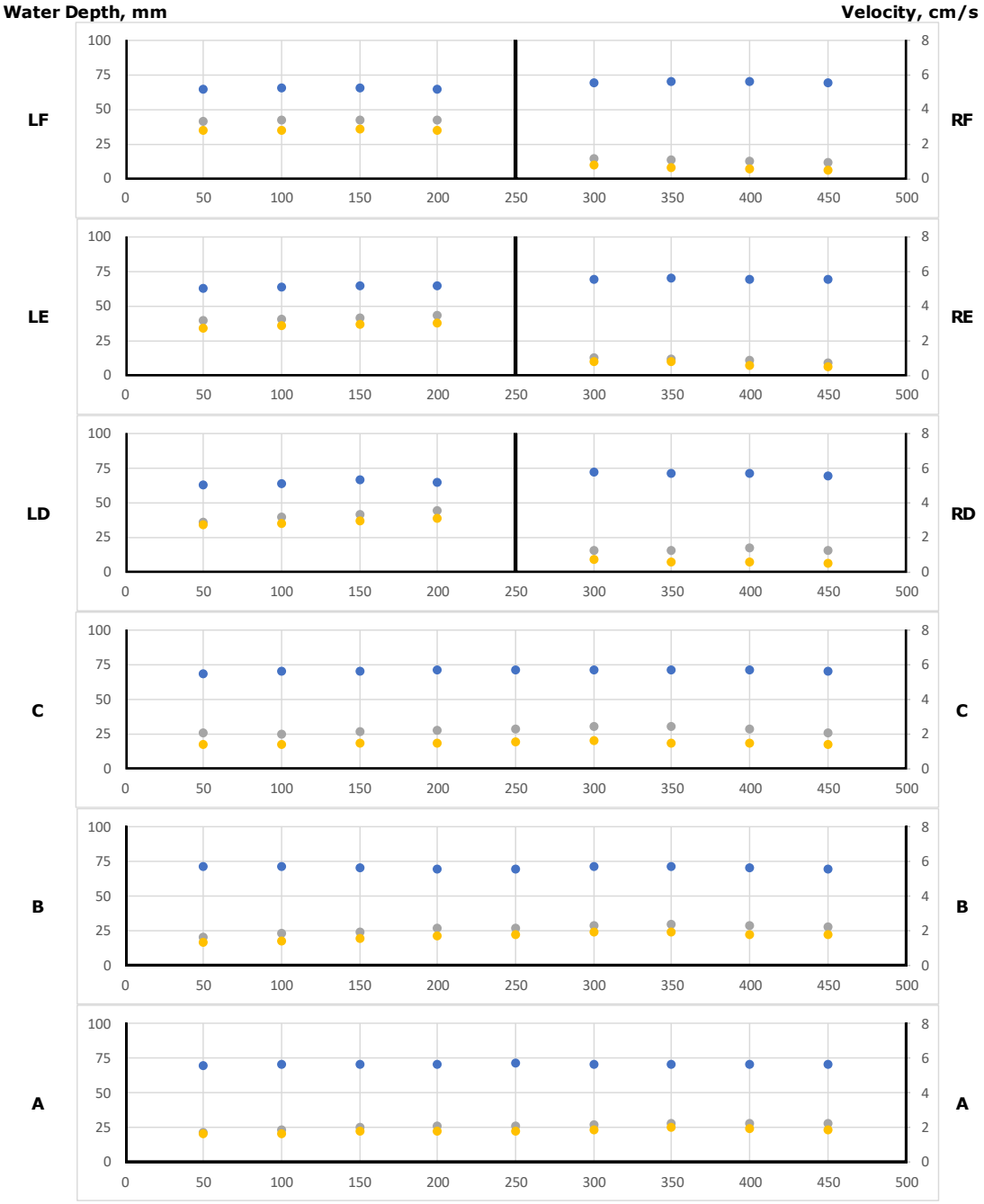
Water Depth and Flow Velocity: 40_05_5050



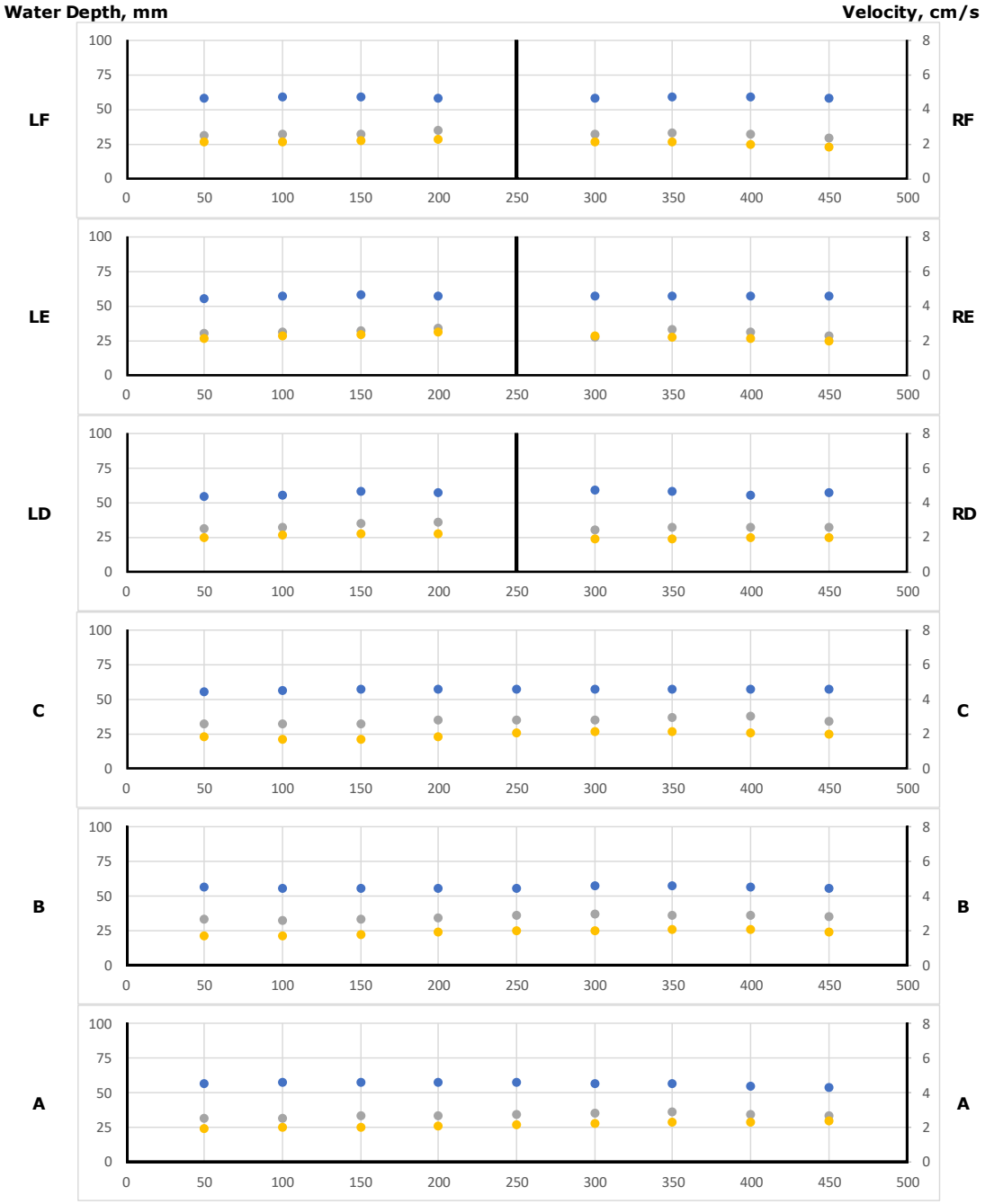
Water Depth and Flow Velocity: 40_05_5560



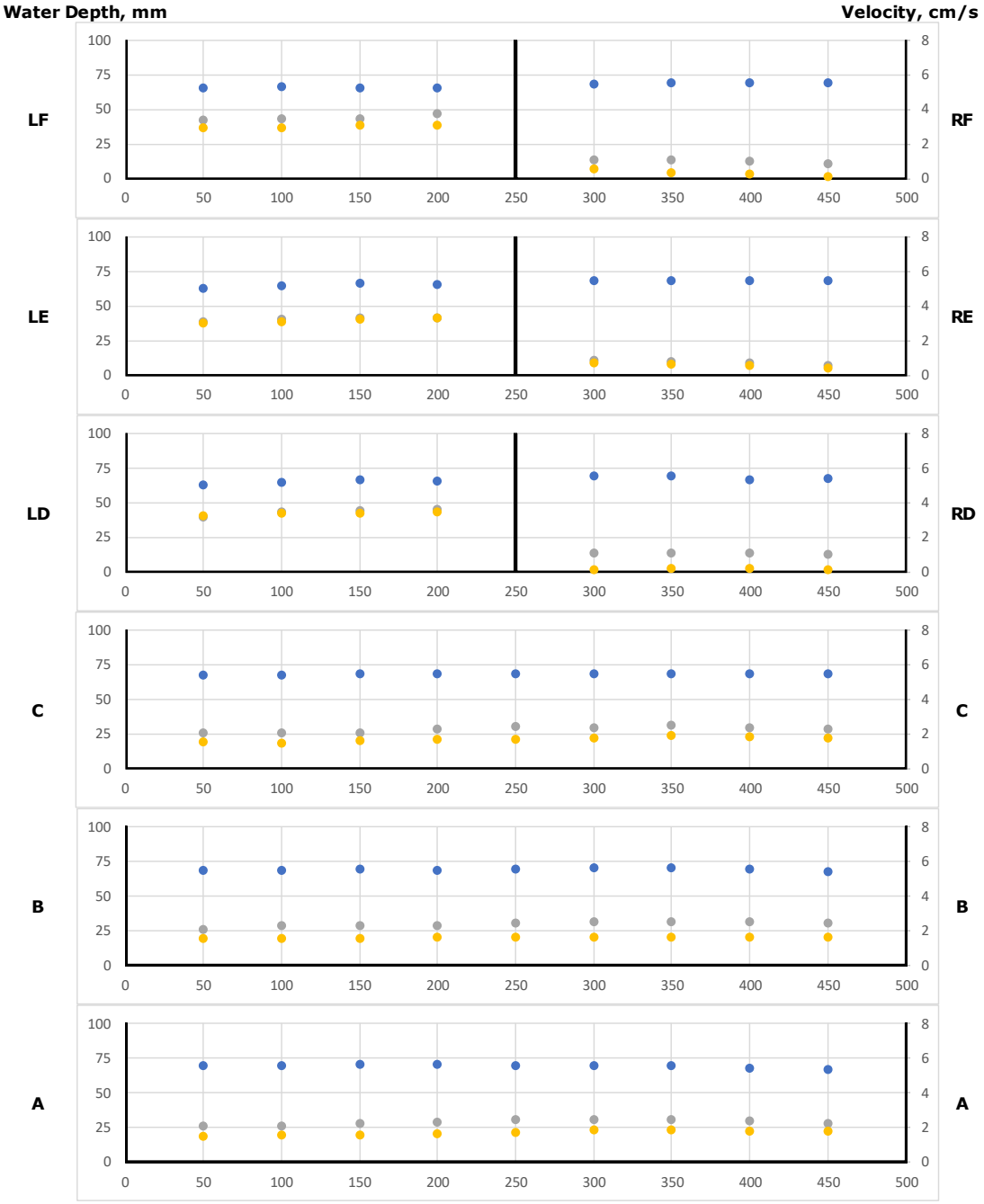
Water Depth and Flow Velocity: 40_05_5055



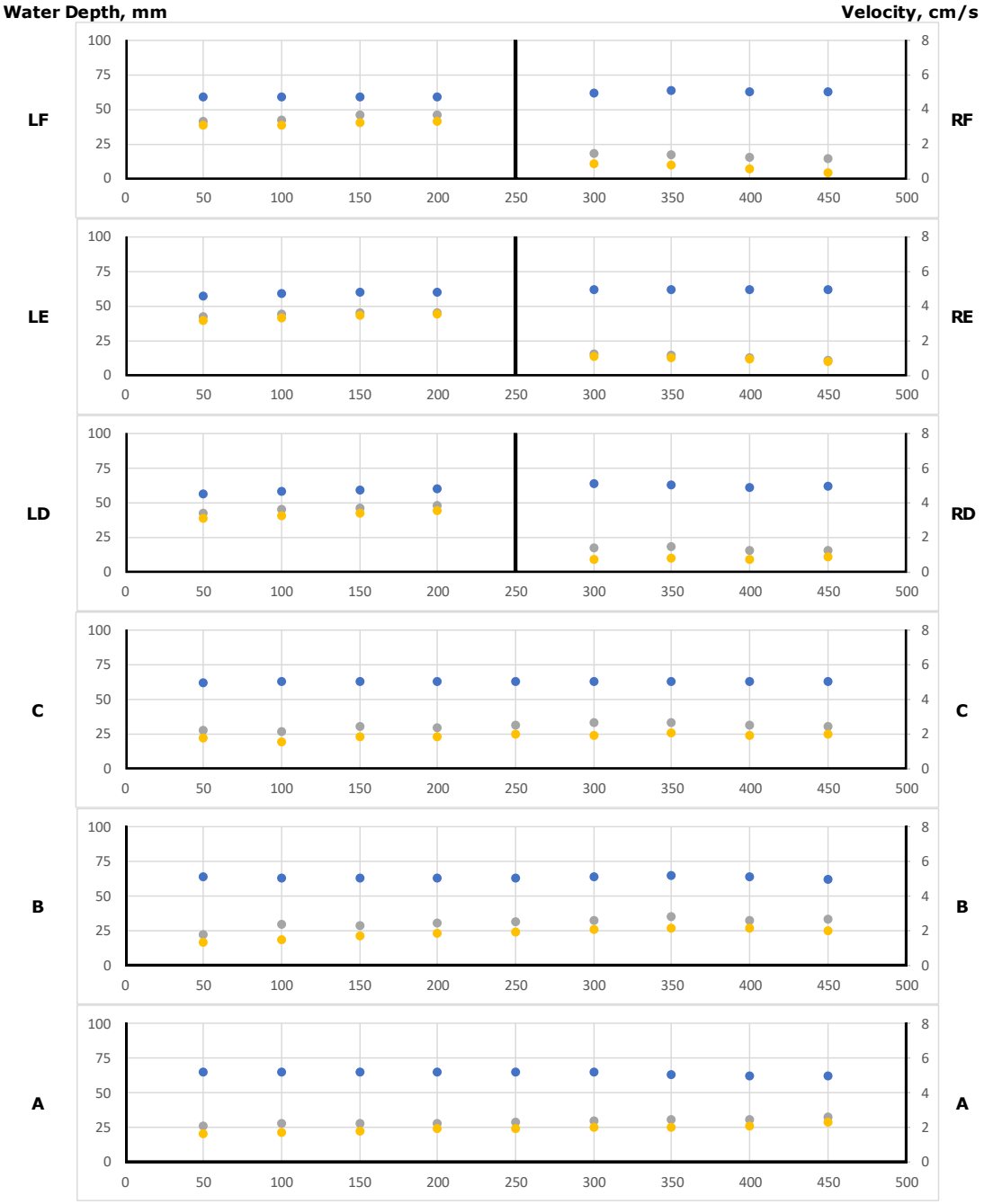
Water Depth and Flow Velocity: 40_07_5050



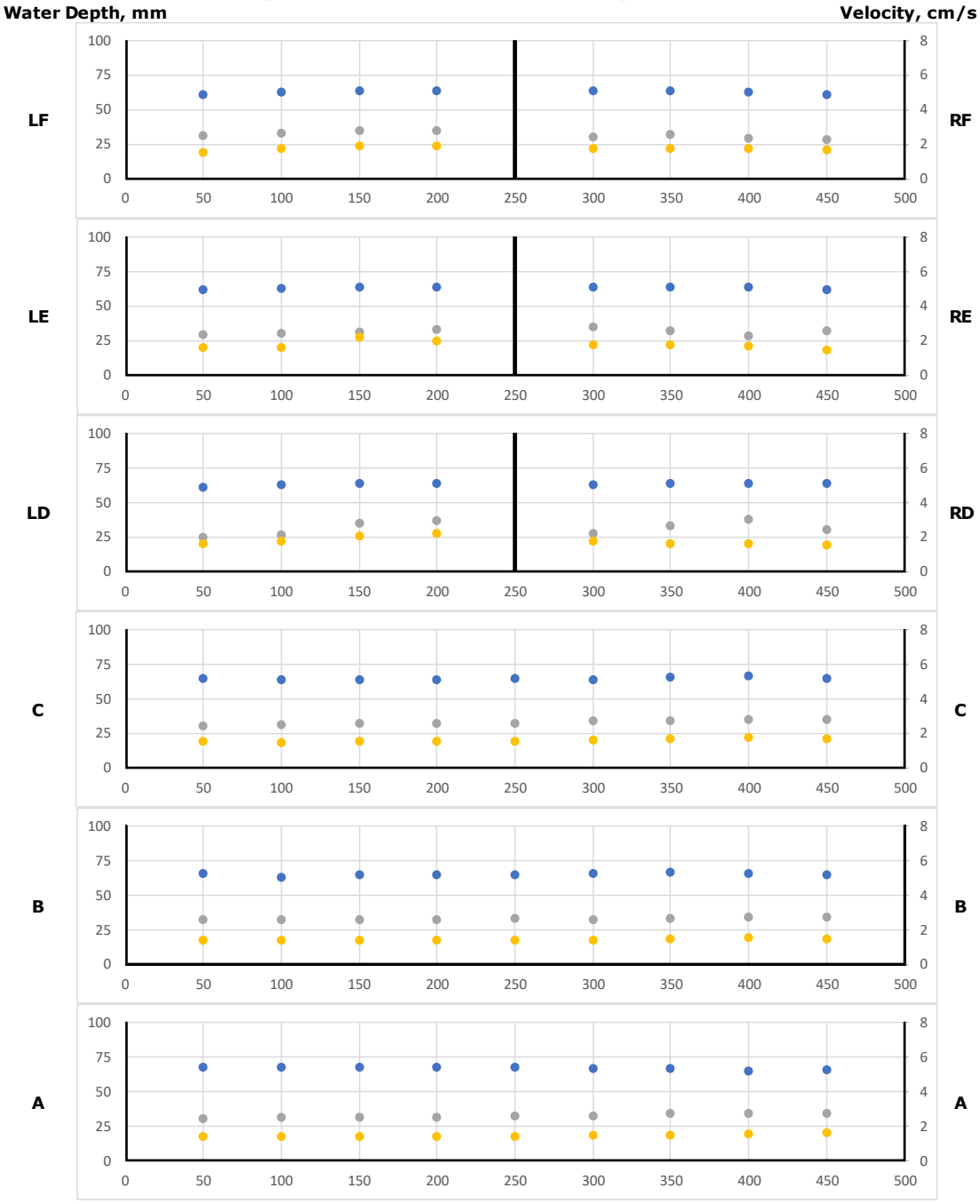
Water Depth and Flow Velocity: 40_07_5560



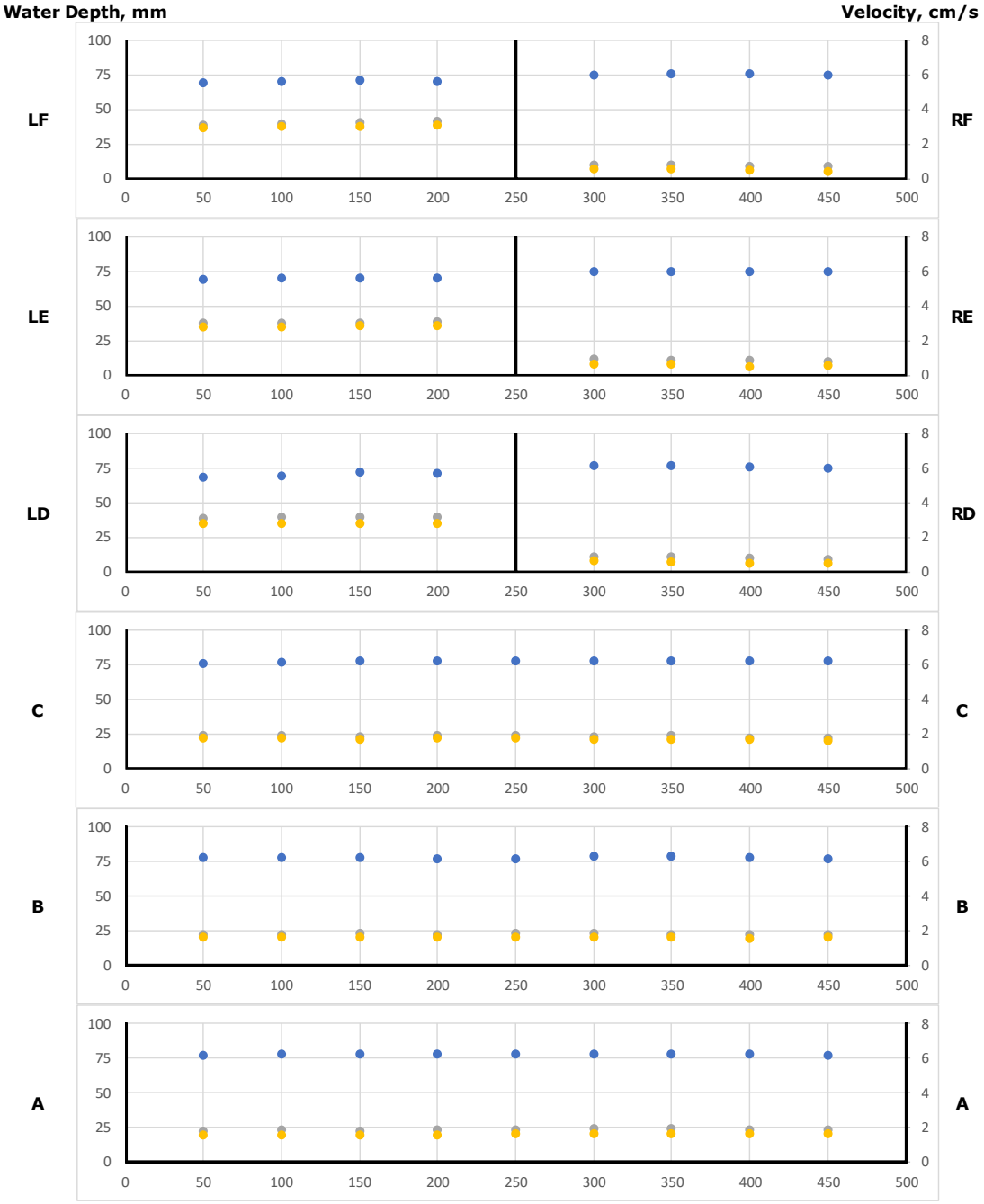
Water Depth and Flow Velocity: 40_05_5055



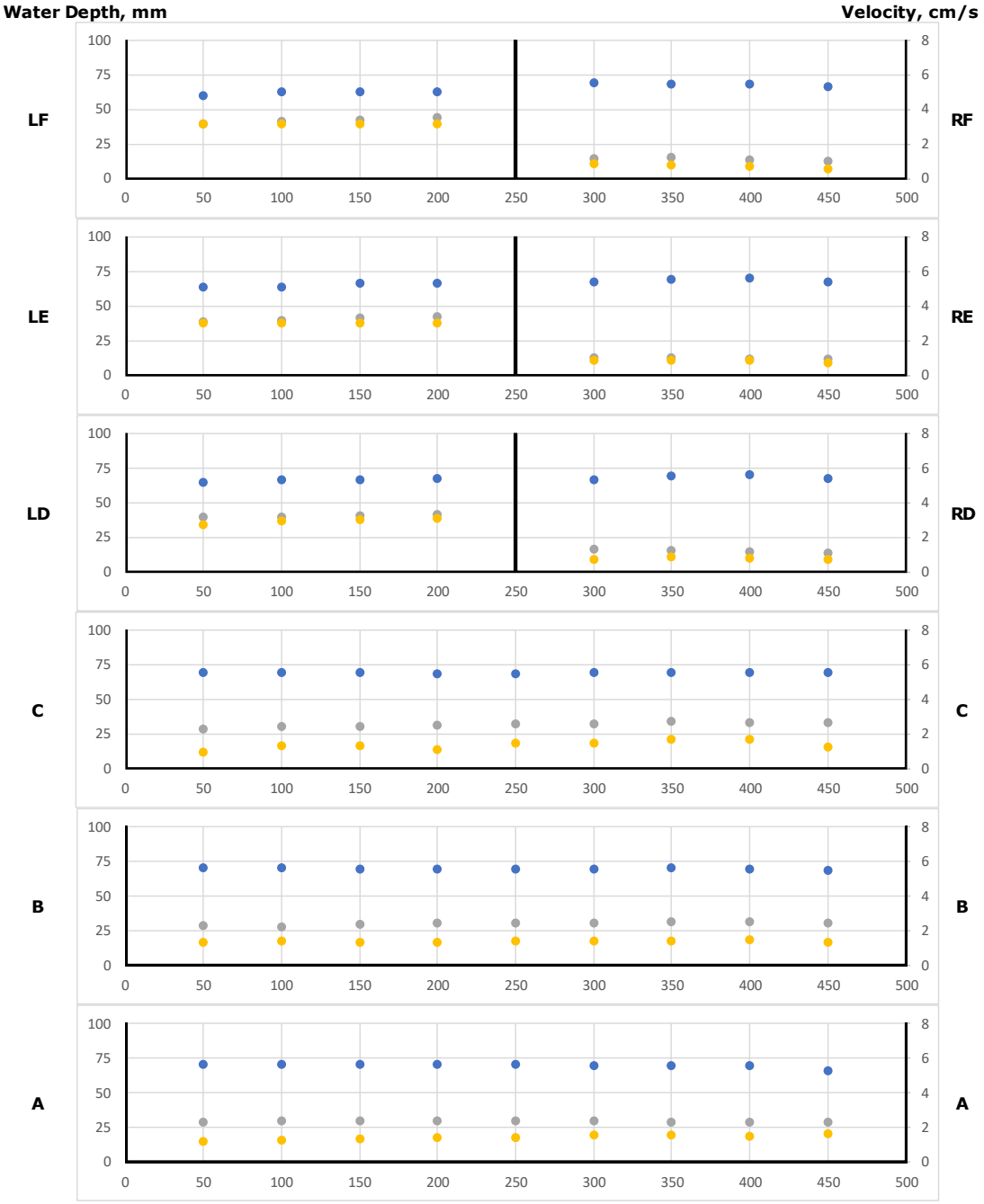
Water Depth and Flow Velocity: 50_03_5050



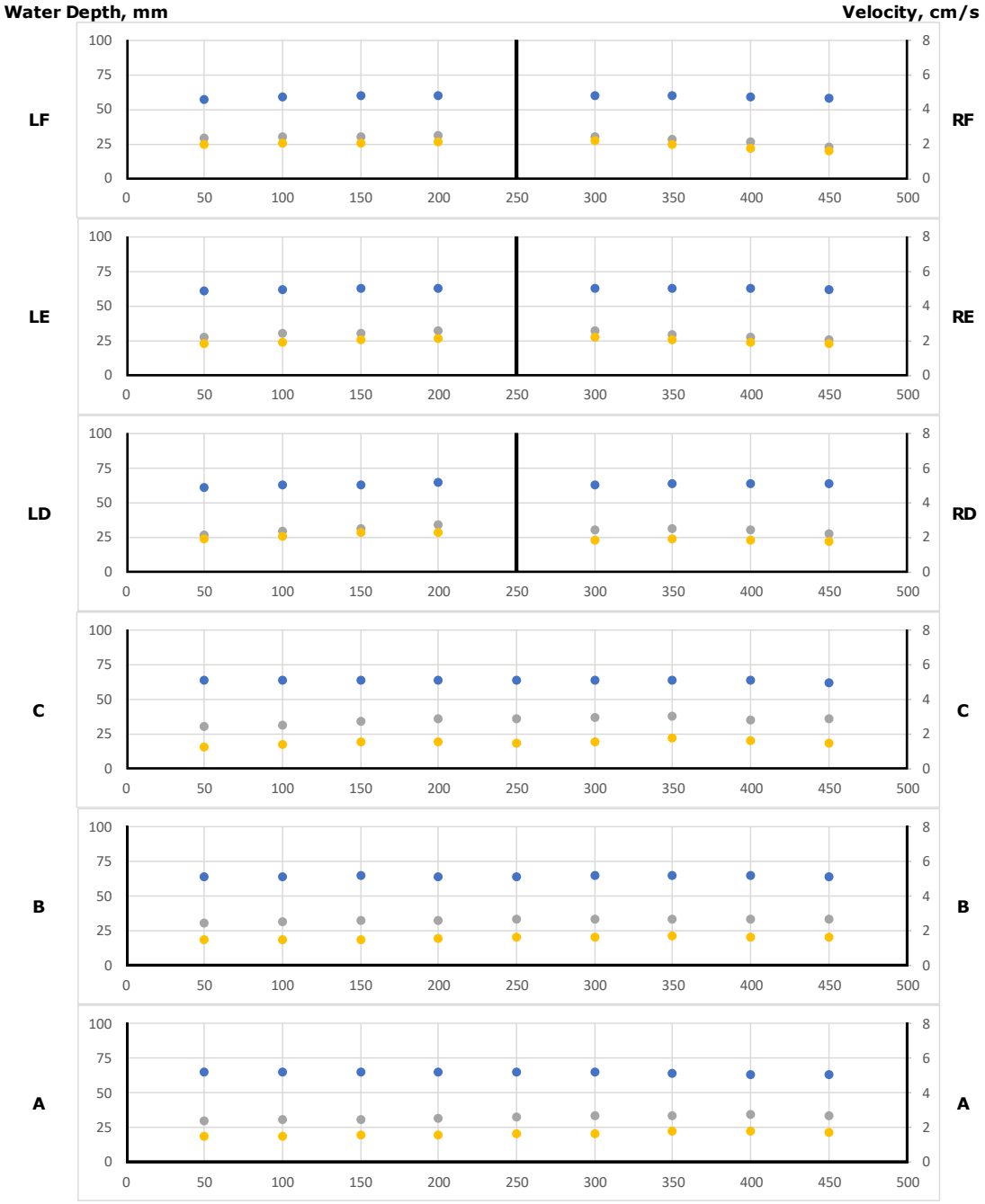
Water Depth and Flow Velocity: 50_03_5560



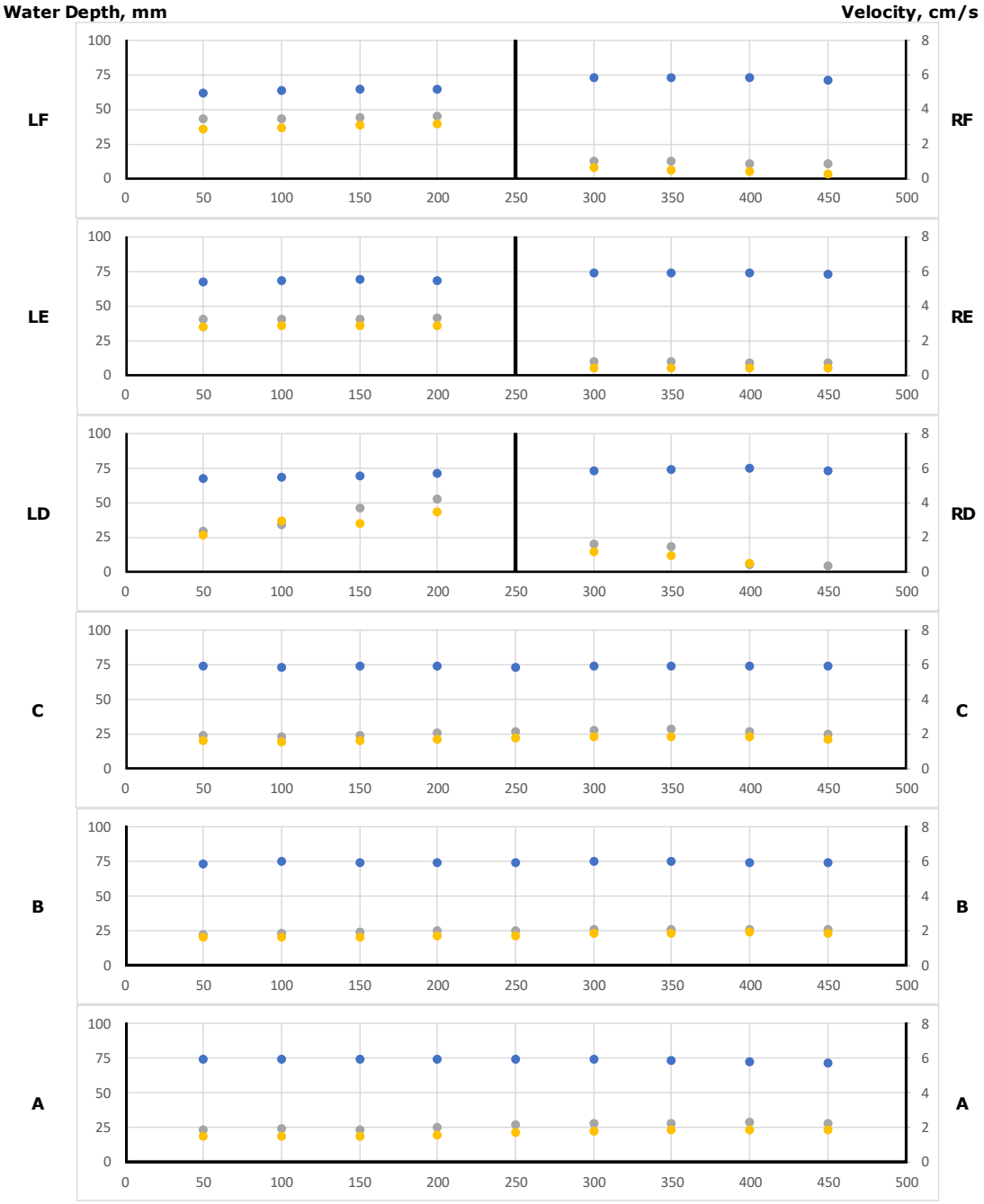
Water Depth and Flow Velocity: 50_03_5055



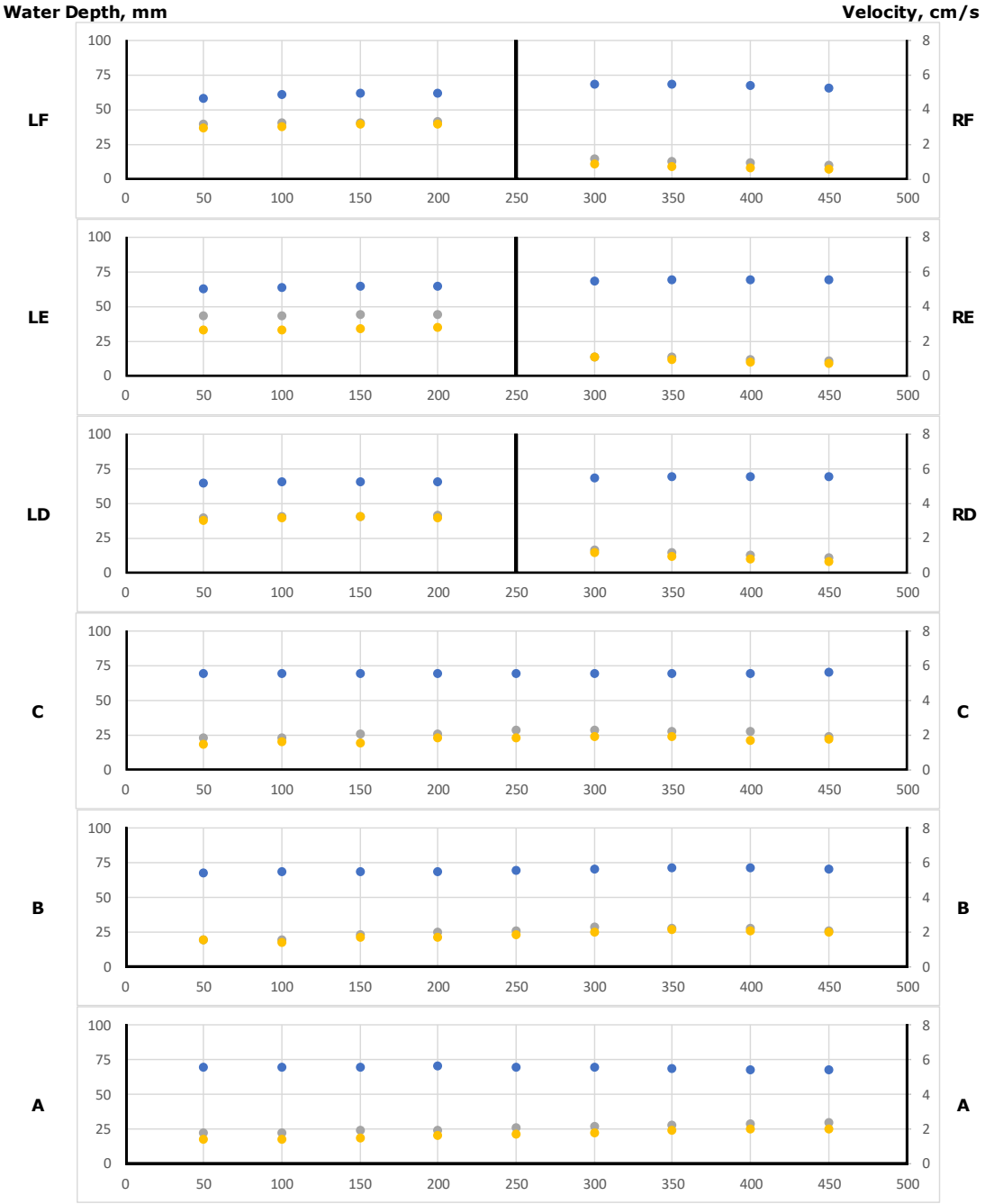
Water Depth and Flow Velocity: 50_05_5050



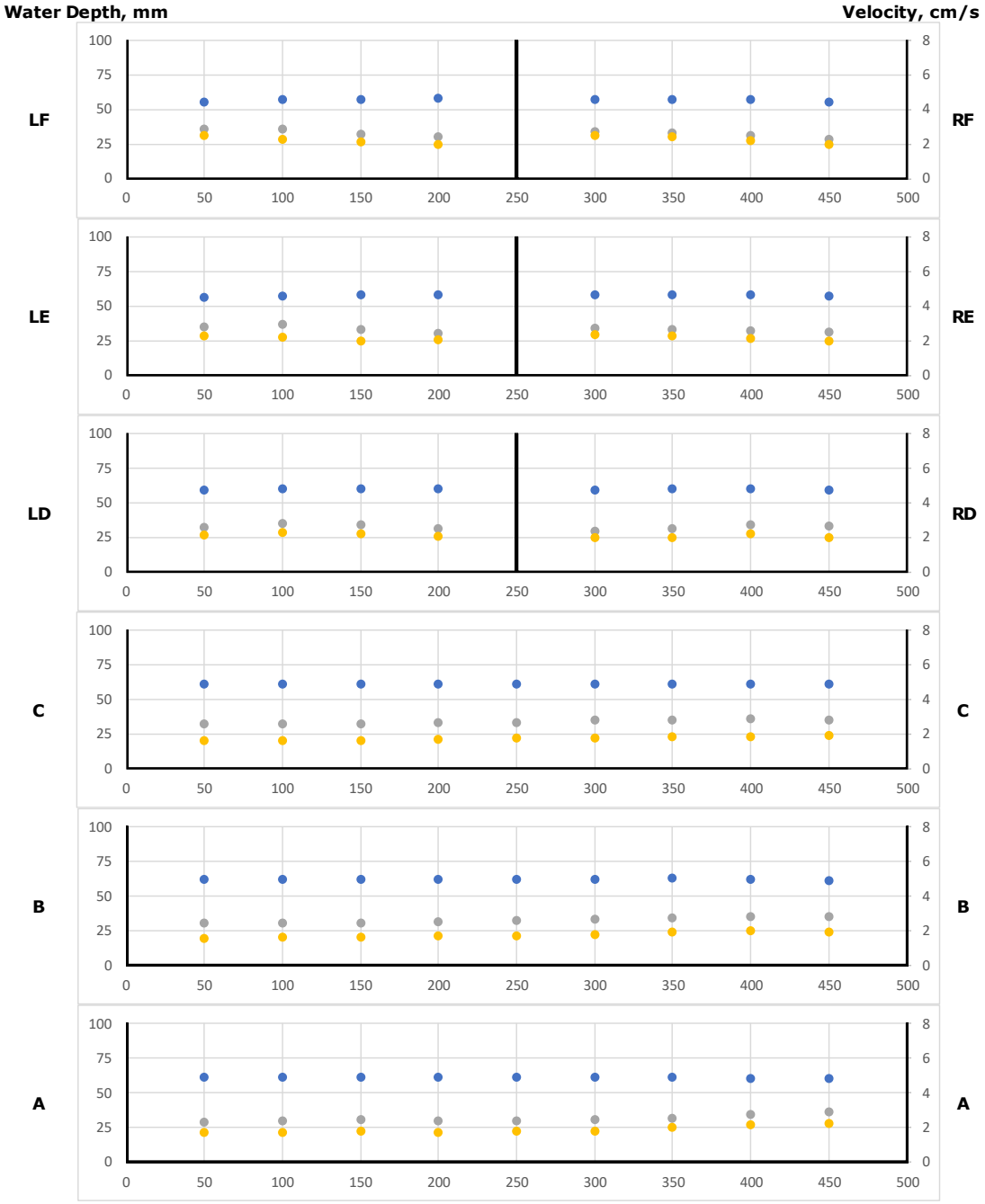
Water Depth and Flow Velocity: 50_05_5560



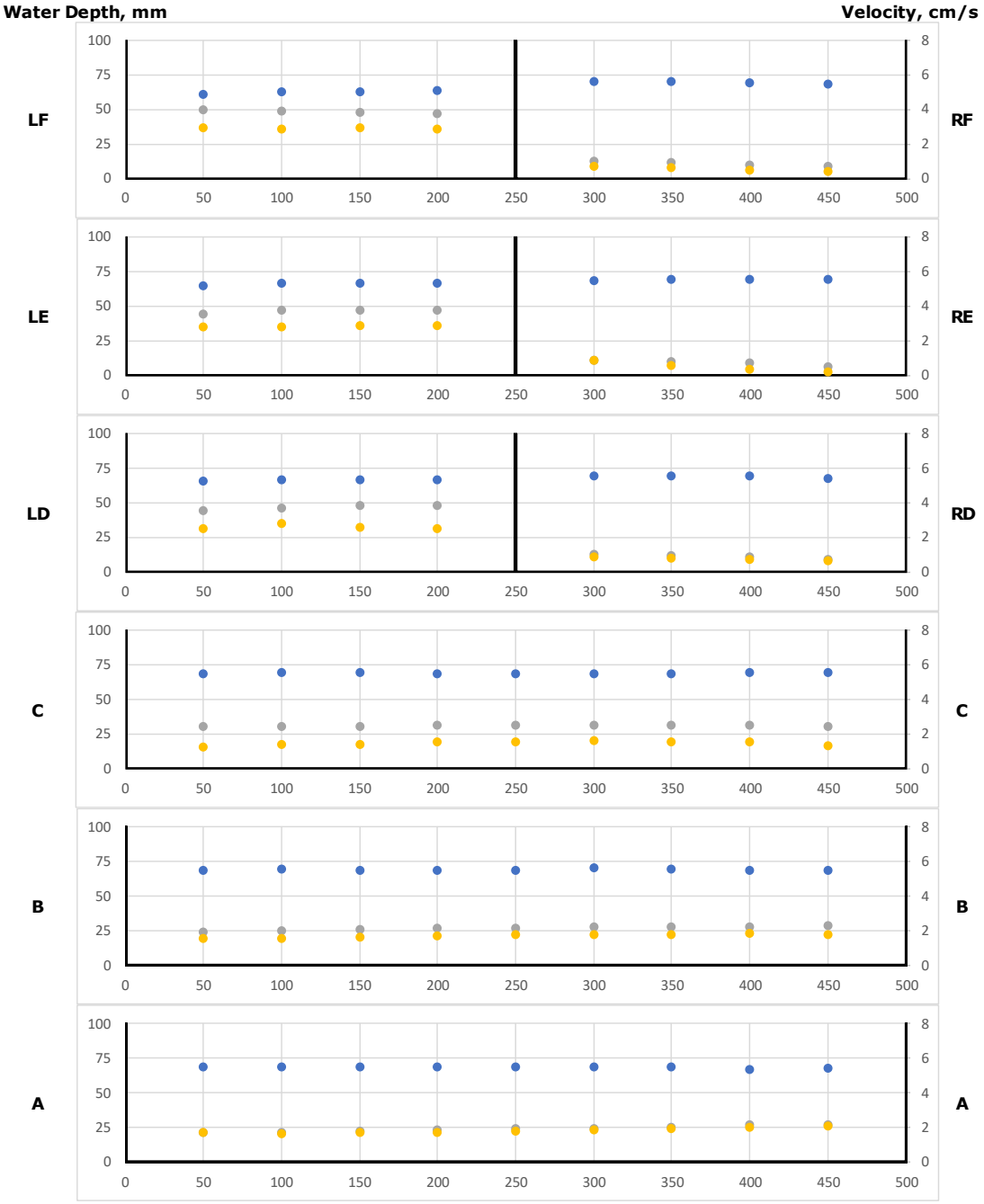
Water Depth and Flow Velocity: 50_05_5055



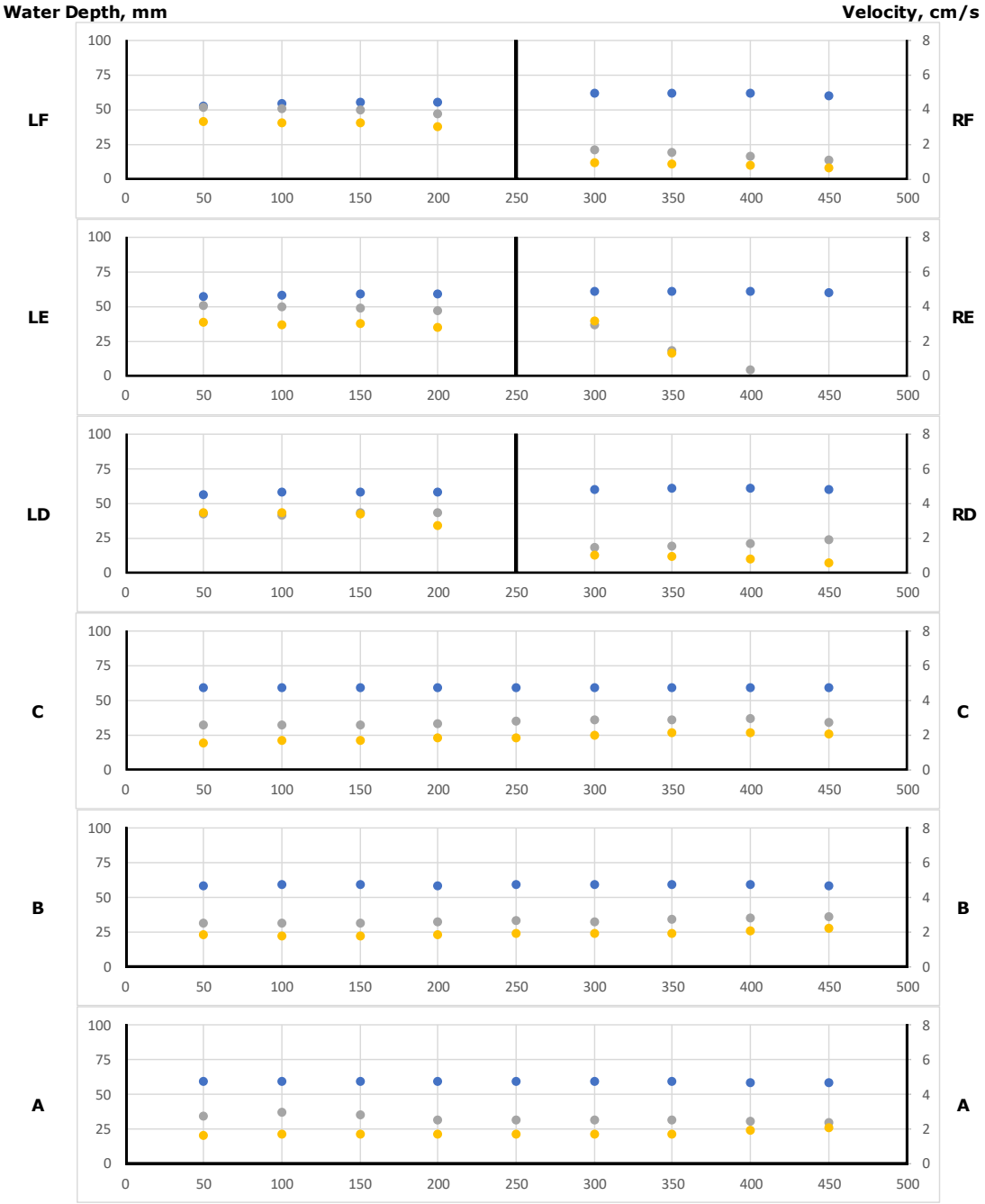
Water Depth and Flow Velocity: 50_07_5050



Water Depth and Flow Velocity: 50_07_5560



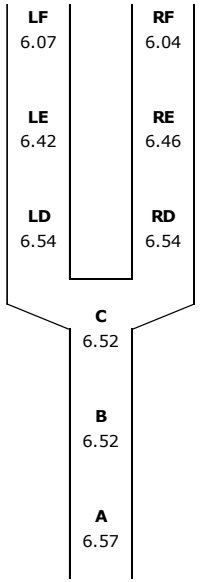
Water Depth and Flow Velocity: 50_07_5055

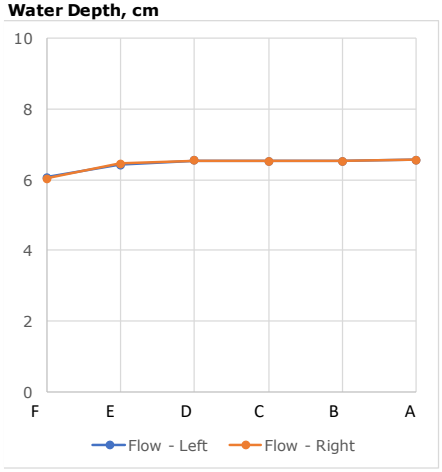


Appendix A4 Average Water Depth (Plan and Profile)

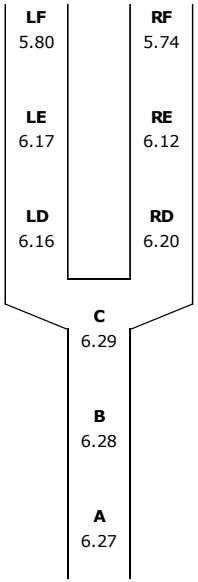
Left Weir Height, mm	Right Weir Height, mm	Bifurcation Angle, °	Slope, %	Name of Run	Page Number
50	50	30	0.3	30_03_5050	A-86
			0.5	30_05_5050	
			0.7	30_07_5050	
		40	0.3	40_03_5050	A-87
			0.5	40_05_5050	
			0.7	40_07_5050	
		50	0.3	50_03_5050	A-88
			0.5	50_05_5050	
			0.7	50_07_5050	
55	60	30	0.3	30_03_5560	A-89
			0.5	30_05_5560	
			0.7	30_07_5560	
		40	0.3	40_03_5560	A-90
			0.5	40_05_5560	
			0.7	40_07_5560	
		50	0.3	50_03_5560	A-91
			0.5	50_05_5560	
			0.7	50_07_5560	
50	55	30	0.3	30_03_5055	A-92
			0.5	30_05_5055	
			0.7	30_07_5055	
		40	0.3	40_03_5055	A-93
			0.5	40_05_5055	
			0.7	40_07_5055	
		50	0.3	50_03_5055	A-94
			0.5	50_05_5055	
			0.7	50_07_5055	

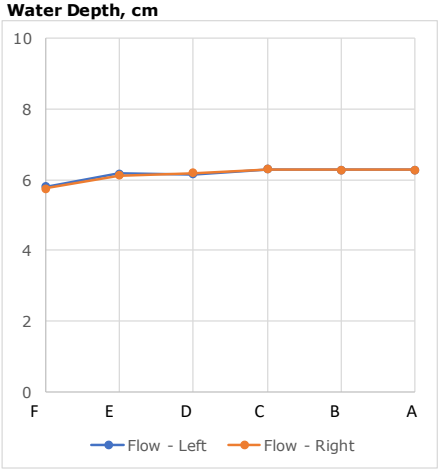
Water Depth: 30_03_5050



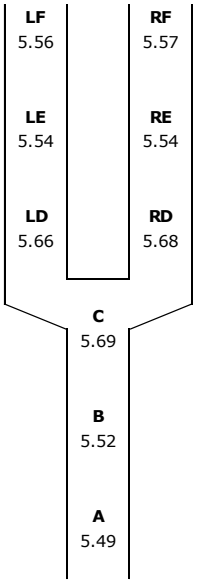


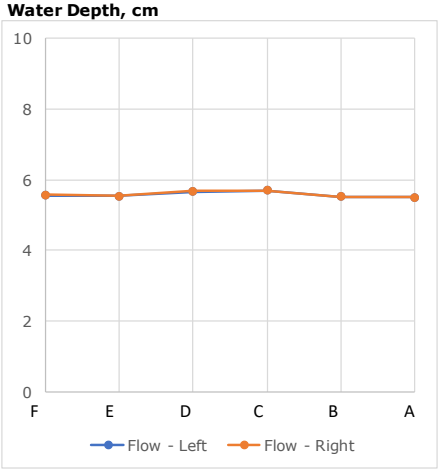
Water Depth: 30_05_5050



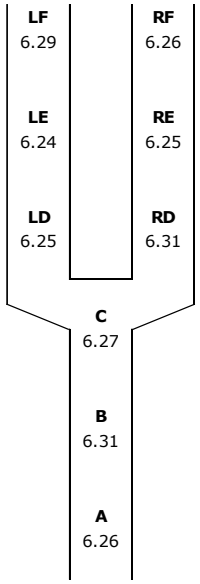


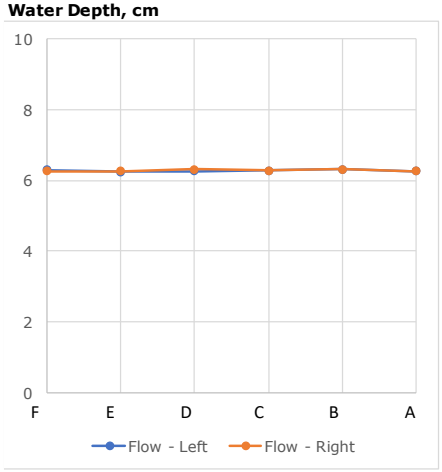
Water Depth: 30_07_5050



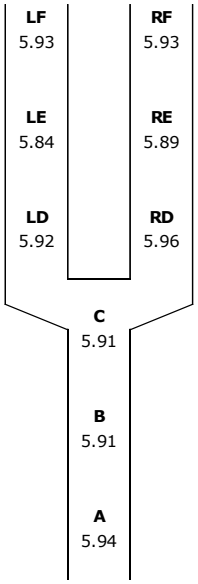


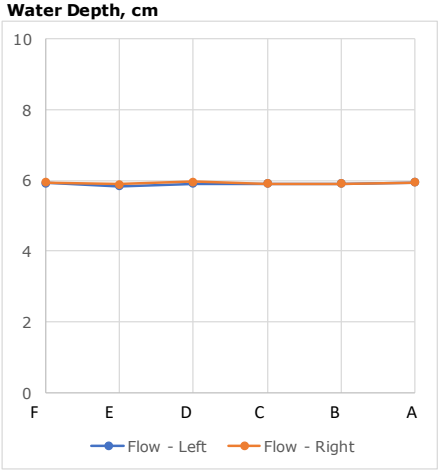
Water Depth: 40_03_5050



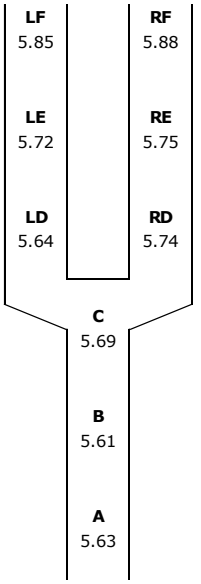


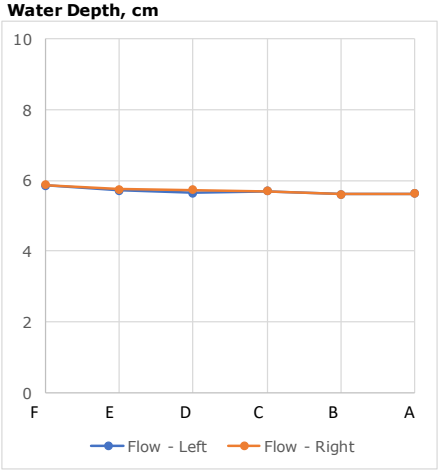
Water Depth: 40_05_5050



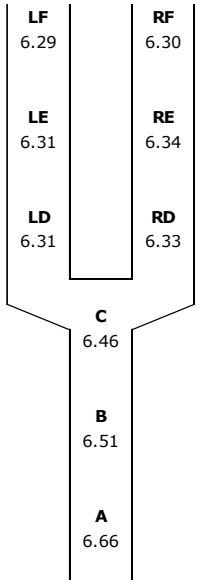


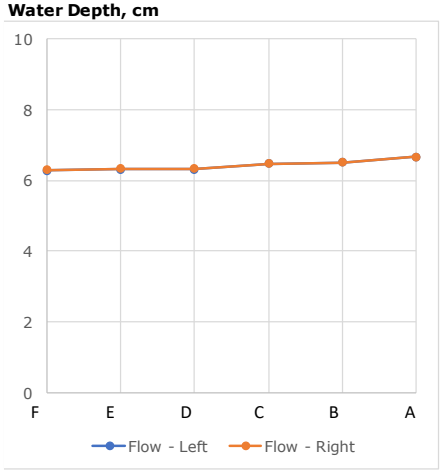
Water Depth: 40_07_5050



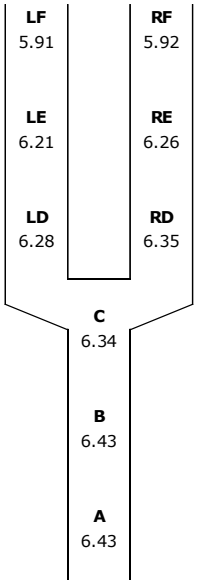


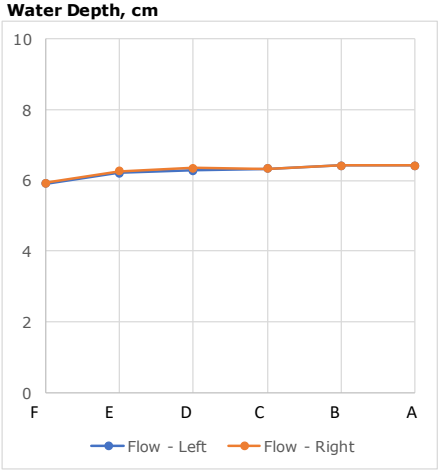
Water Depth: 50_03_5050



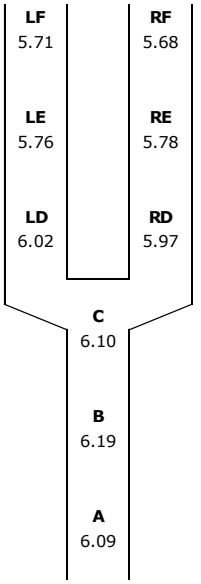


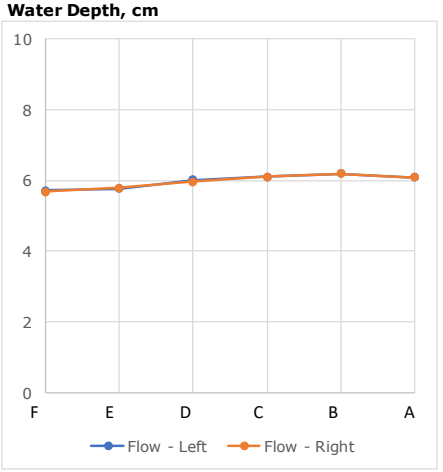
Water Depth: 50_05_5050



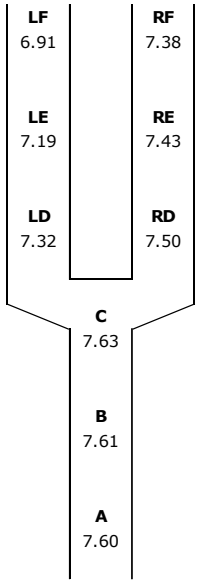


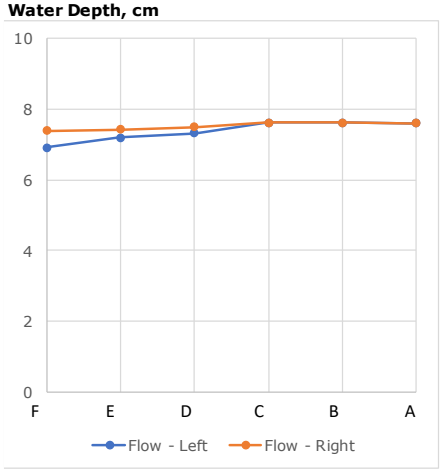
Water Depth: 50_07_5050



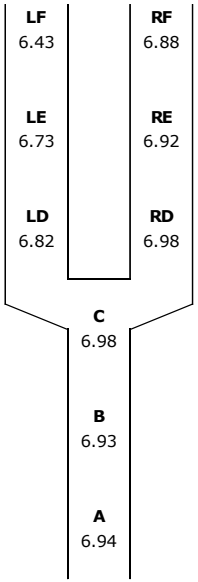


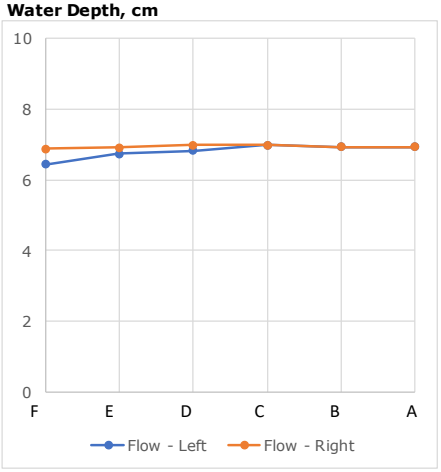
Water Depth: 30_03_5560



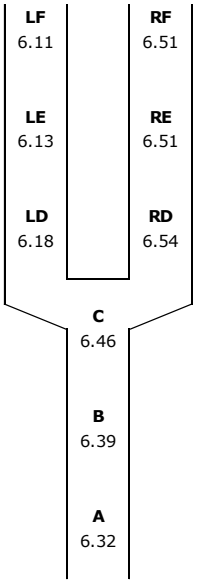


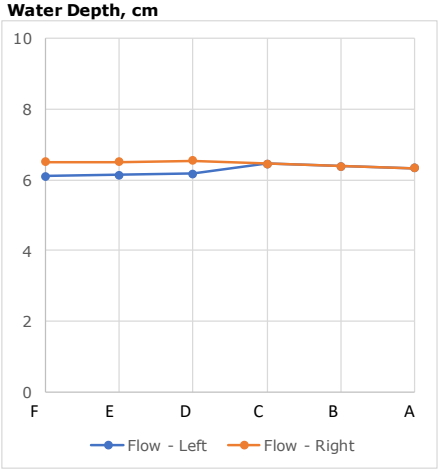
Water Depth: 30_05_5560



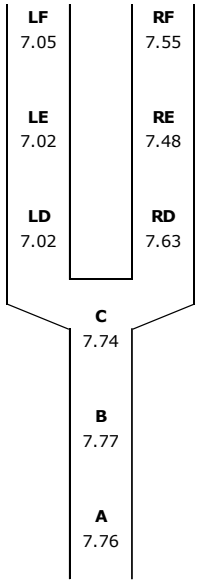


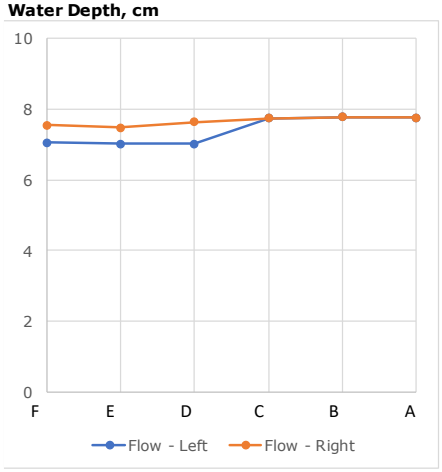
Water Depth: 30_07_5560



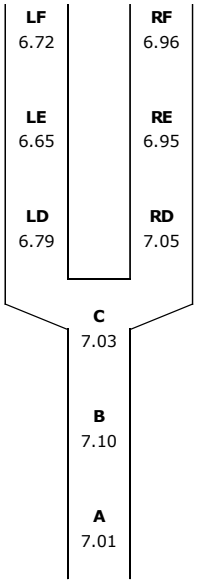


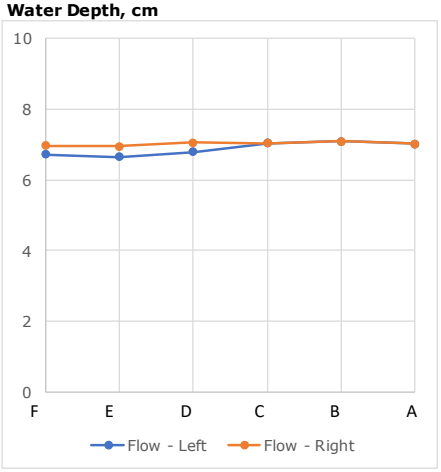
Water Depth: 40_03_5560



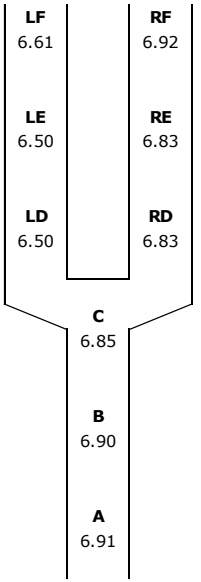


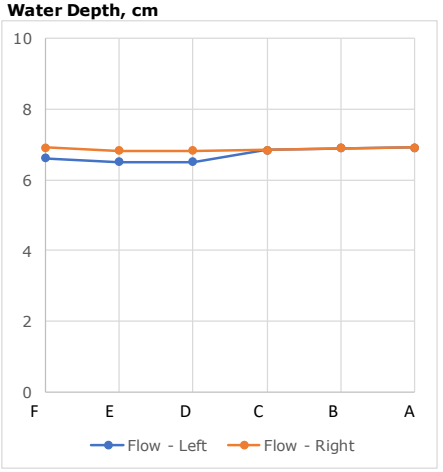
Water Depth: 40_05_5560



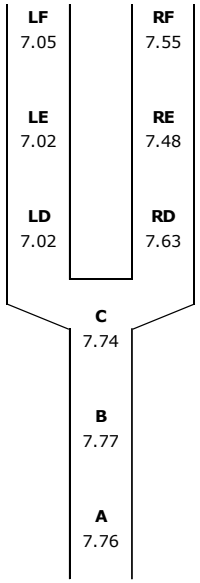


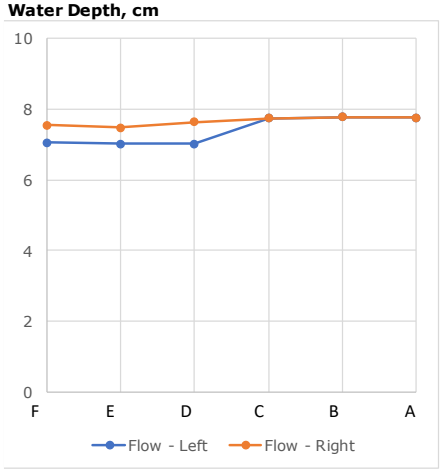
Water Depth: 40_07_5560



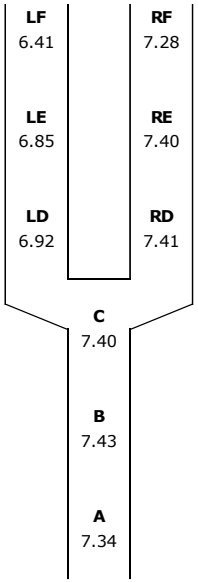


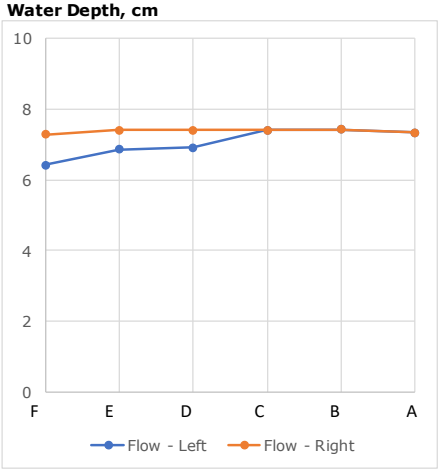
Water Depth: 50_03_5560



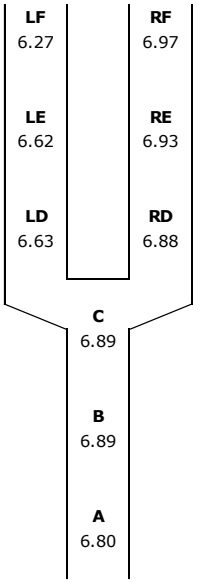


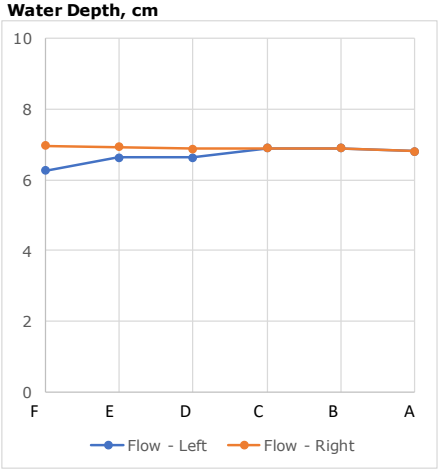
Water Depth: 50_05_5560



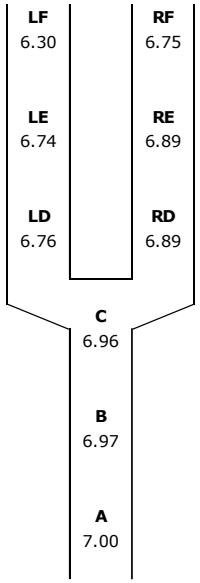


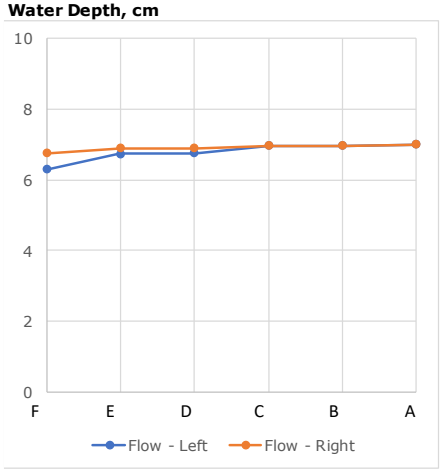
Water Depth: 50_07_5560



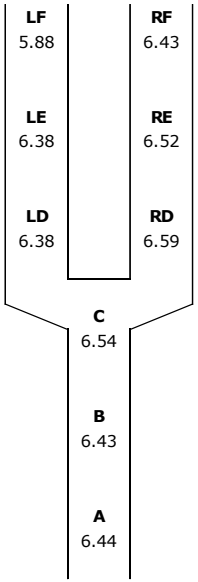


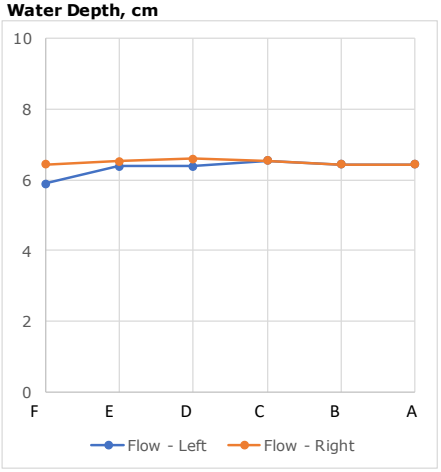
Water Depth: 30_03_5055



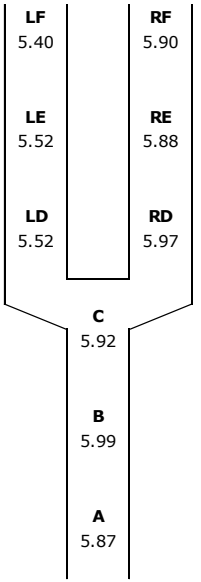


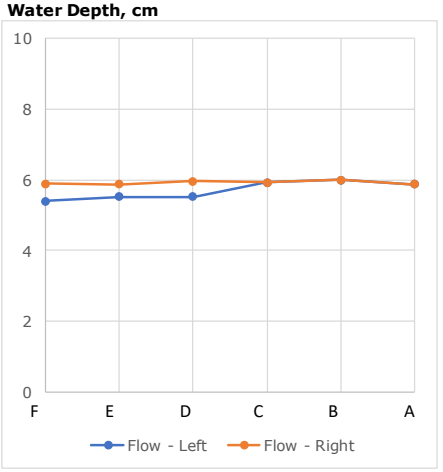
Water Depth: 30_05_5055



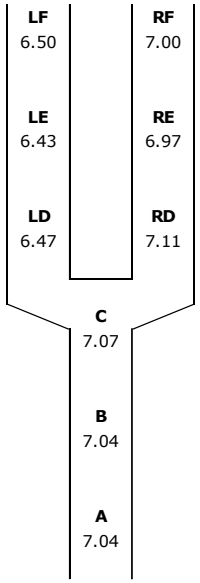


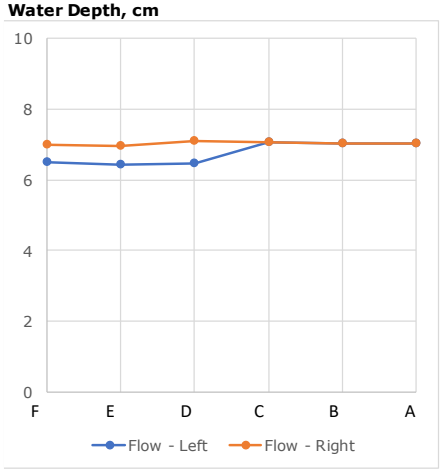
Water Depth: 30_07_5055



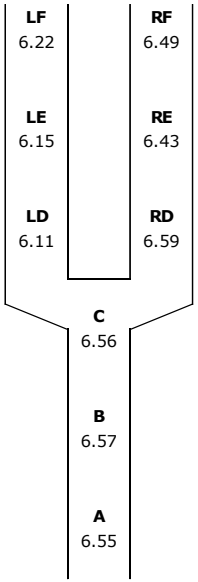


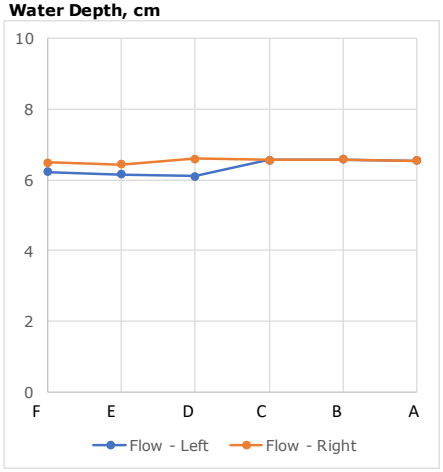
Water Depth: 40_03_5055



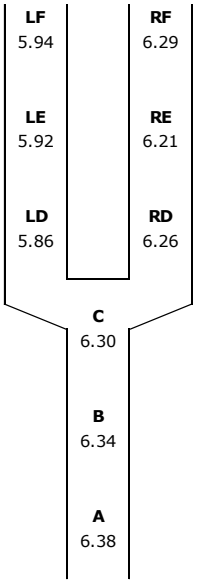


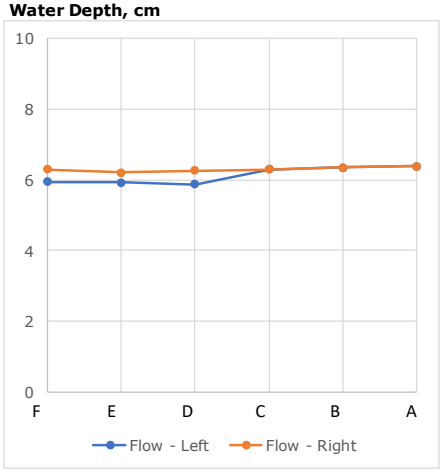
Water Depth: 40_05_5055



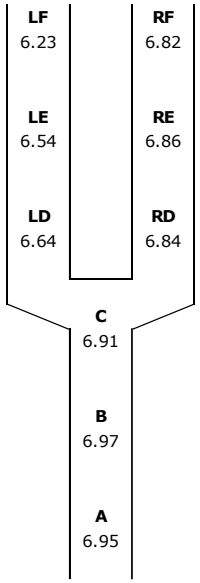


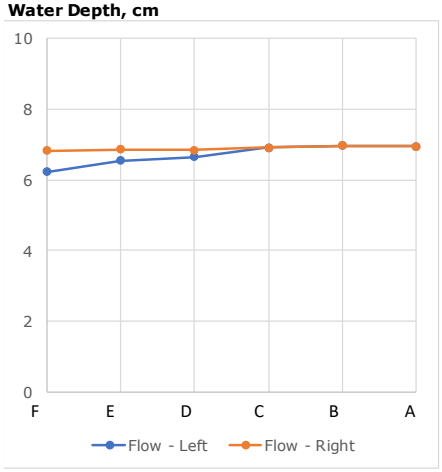
Water Depth: 40_07_5055



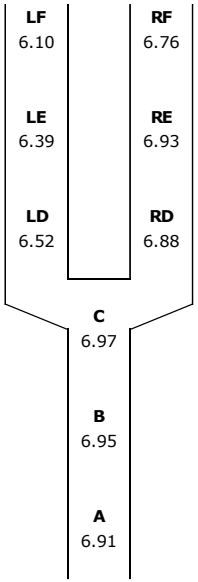


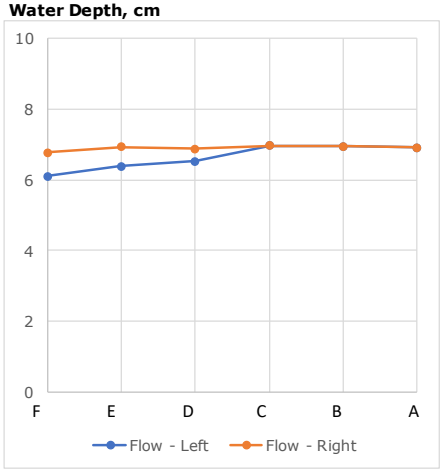
Water Depth: 50_03_5055



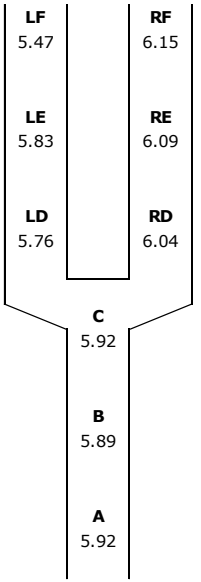


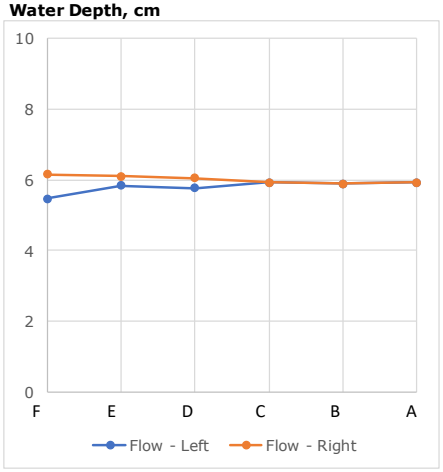
Water Depth: 50_05_5055





Water Depth: 50_07_5055

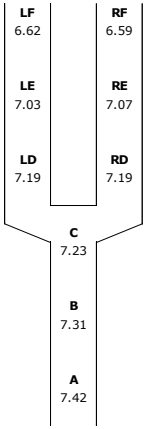


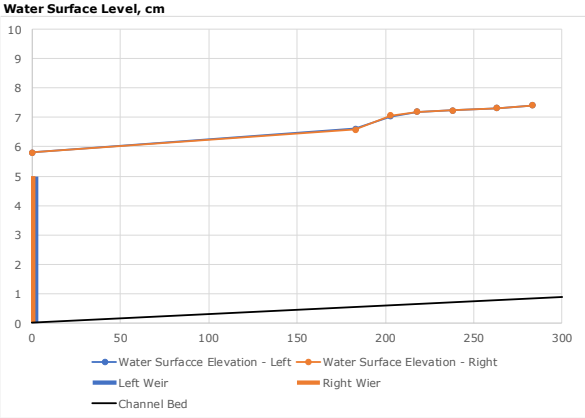


Appendix A5 Water Surface Level (Plan and Profile)

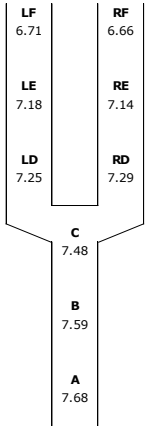
Left Weir Height, mm	Right Weir Height, mm	Bifurcation Angle, °	Slope, %	Name of Run	Page Number
50	50	30	0.3	30_03_5050	A-96
			0.5	30_05_5050	
			0.7	30_07_5050	
		40	0.3	40_03_5050	A-97
			0.5	40_05_5050	
			0.7	40_07_5050	
		50	0.3	50_03_5050	A-98
			0.5	50_05_5050	
			0.7	50_07_5050	
55	60	30	0.3	30_03_5560	A-99
			0.5	30_05_5560	
			0.7	30_07_5560	
		40	0.3	40_03_5560	A-100
			0.5	40_05_5560	
			0.7	40_07_5560	
		50	0.3	50_03_5560	A-101
			0.5	50_05_5560	
			0.7	50_07_5560	
50	55	30	0.3	30_03_5055	A-102
			0.5	30_05_5055	
			0.7	30_07_5055	
		40	0.3	40_03_5055	A-103
			0.5	40_05_5055	
			0.7	40_07_5055	
		50	0.3	50_03_5055	A-104
			0.5	50_05_5055	
			0.7	50_07_5055	

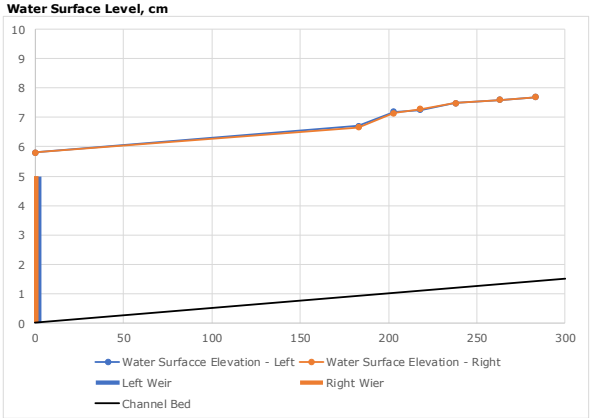
Water Surface Level: 30_03_5050



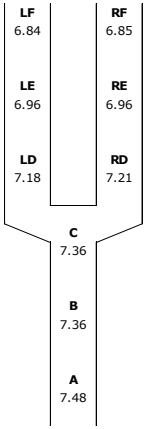


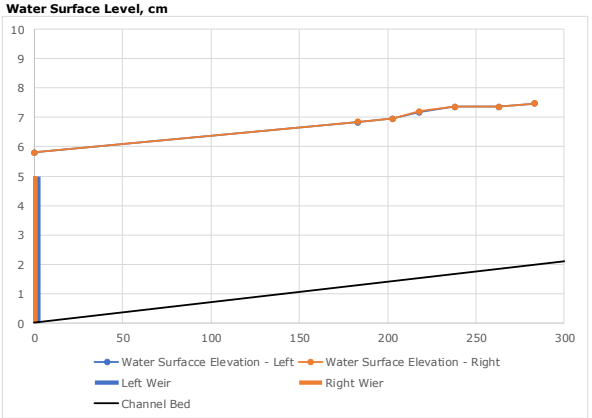
Water Surface Level: 30_05_5050



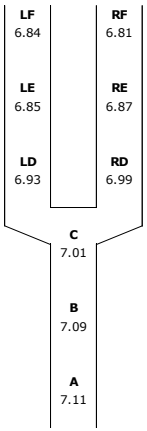


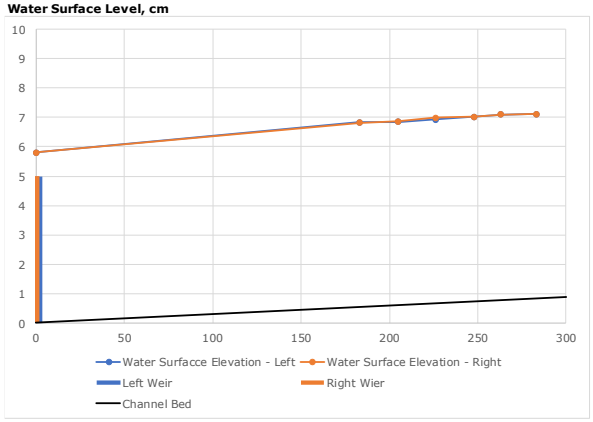
Water Surface Level: 30_07_5050



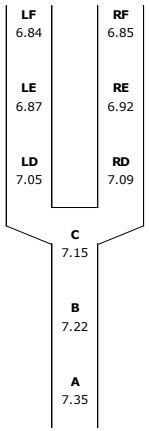


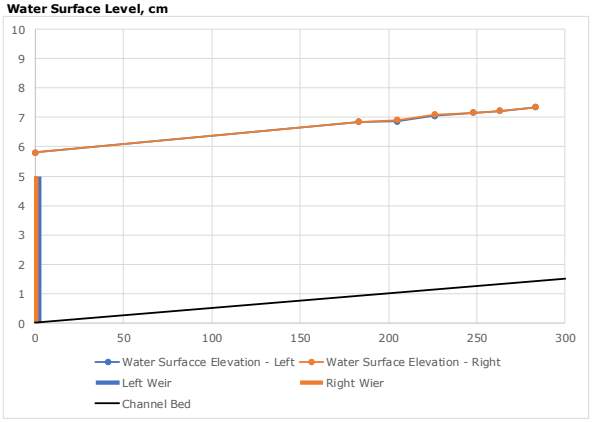
Water Surface Level: 40_03_5050



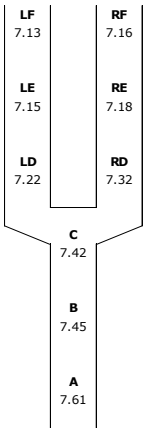


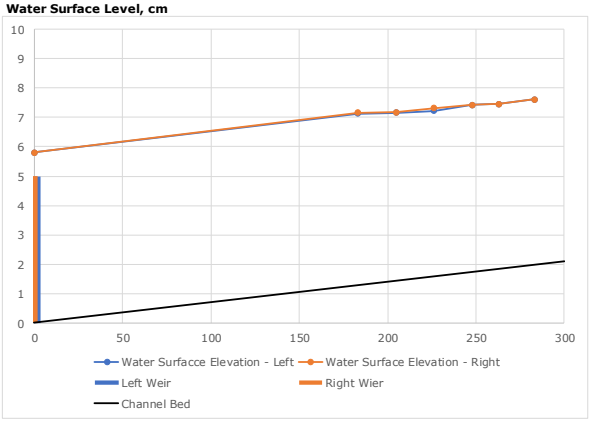
Water Surface Level: 40_05_5050



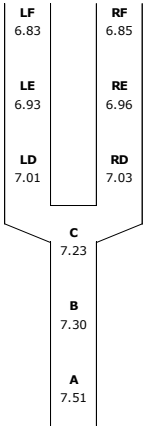


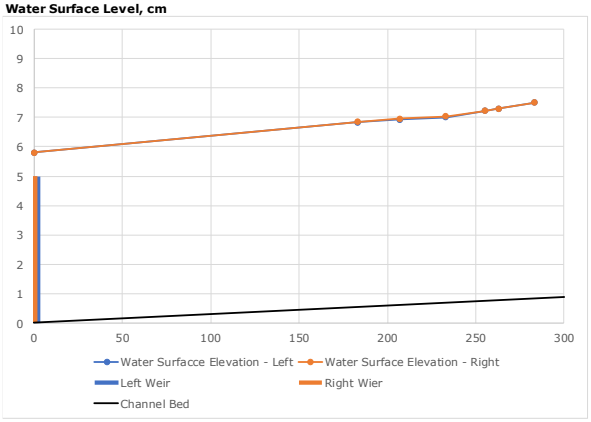
Water Surface Level: 40_07_5050



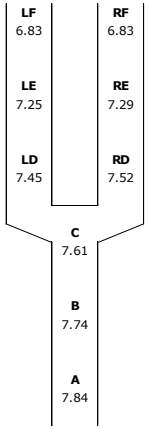


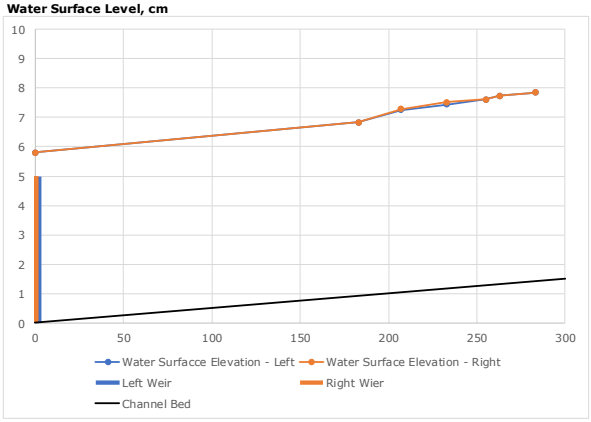
Water Surface Level: 50_03_5050



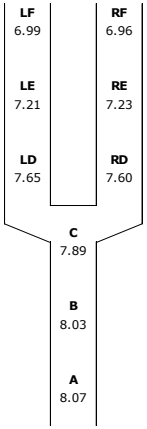


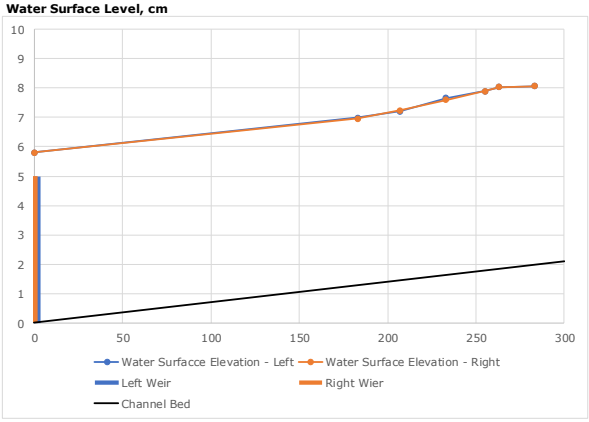
Water Surface Level: 50_05_5050



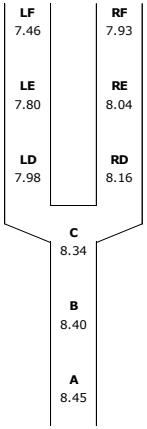


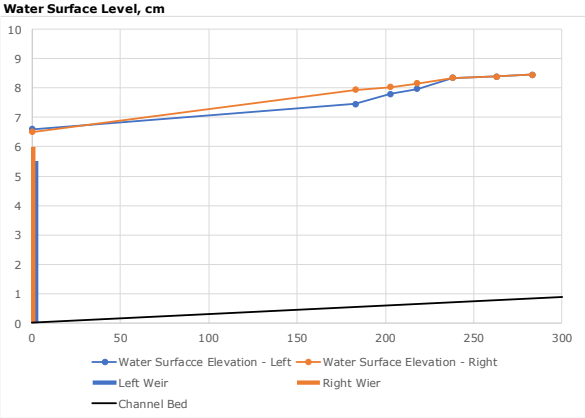
Water Surface Level: 50_07_5050



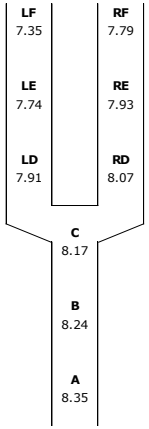


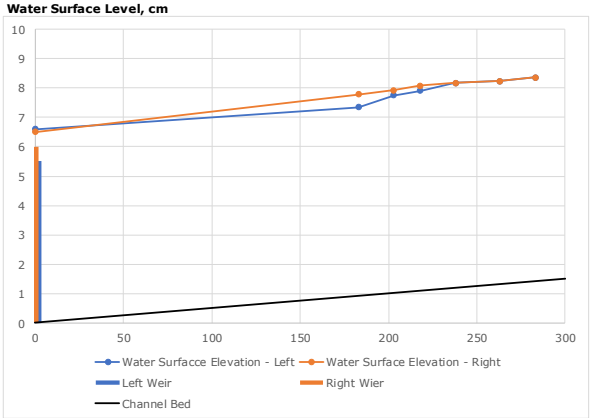
Water Surface Level: 30_03_5560



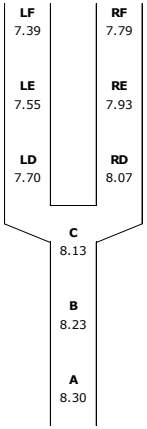


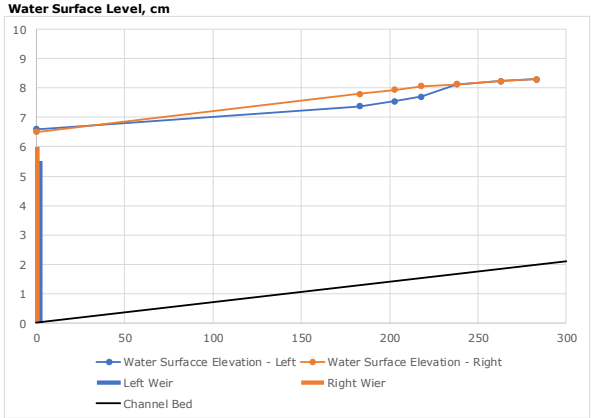
Water Surface Level: 30_05_5560



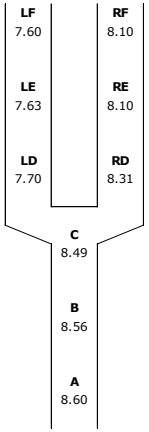


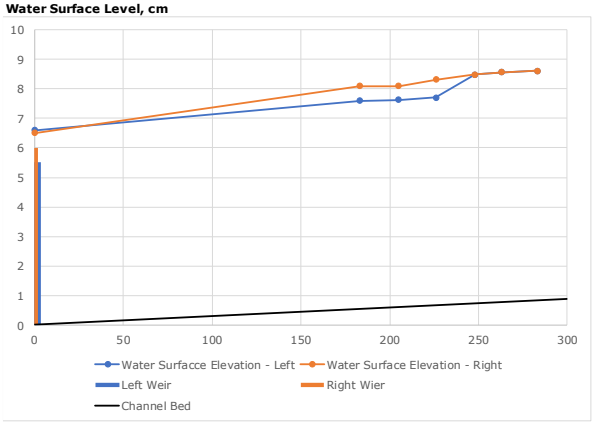
Water Surface Level: 30_07_5560



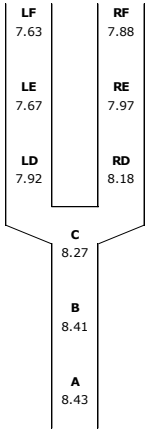


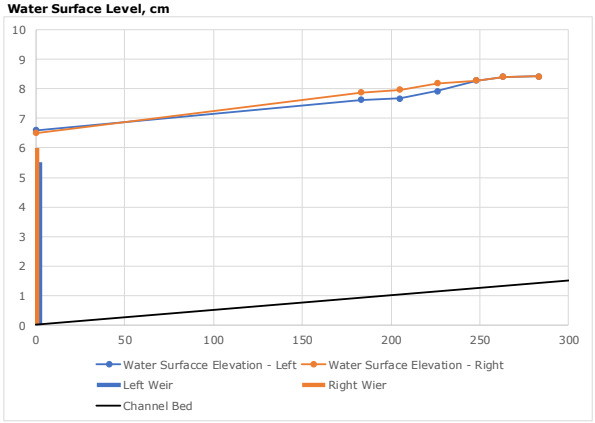
Water Surface Level: 40_03_5560



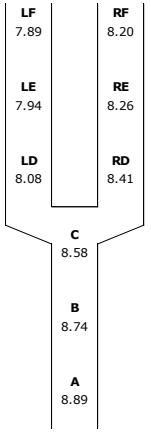


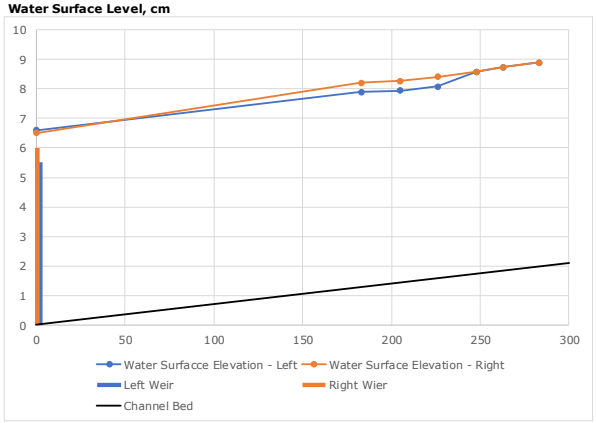
Water Surface Level: 40_05_5560



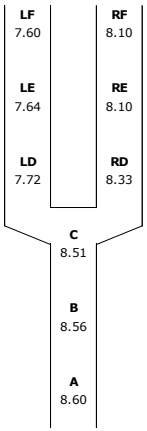


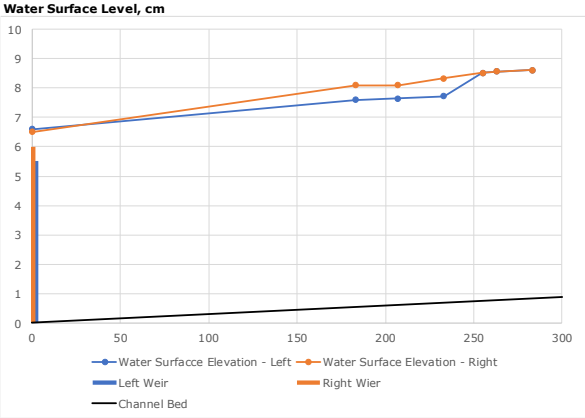
Water Surface Level: 40_07_5560



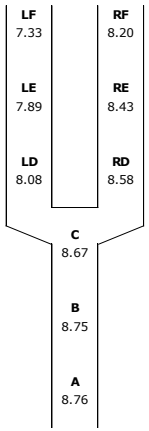


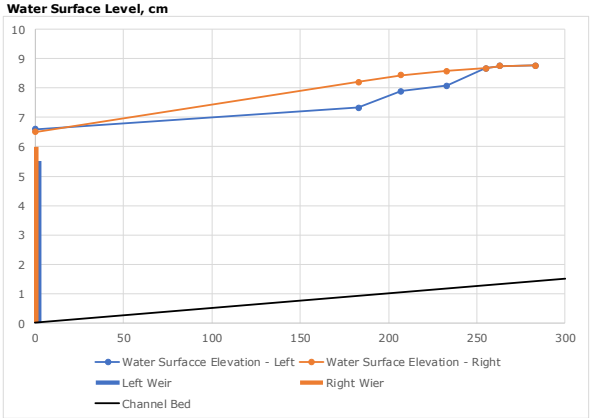
Water Surface Level: 50_03_5560



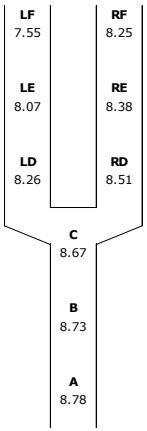


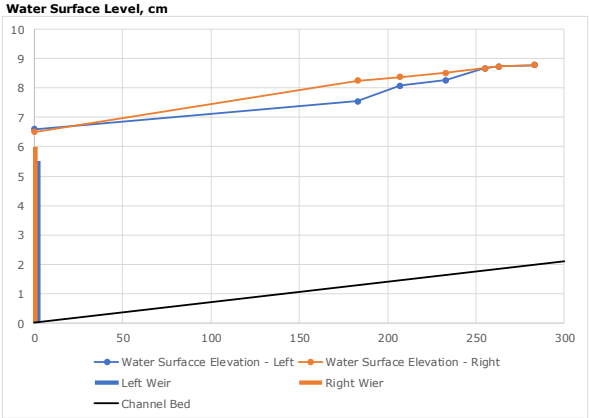
Water Surface Level: 50_05_5560



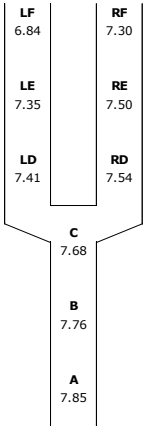


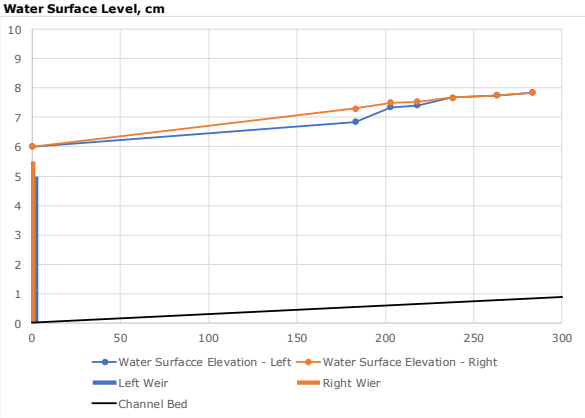
Water Surface Level: 50_07_5560



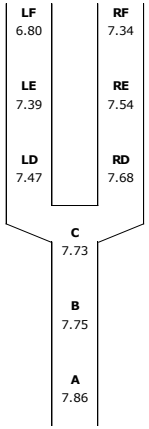


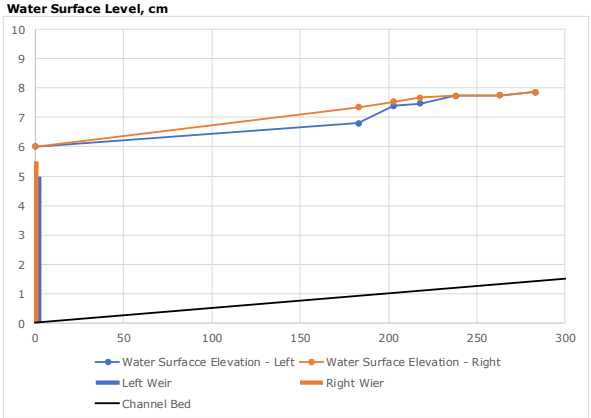
Water Surface Level: 30_03_5055



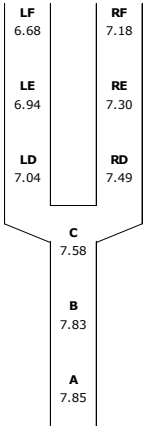


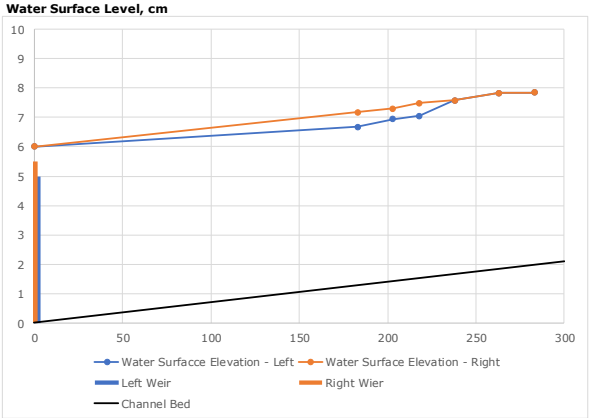
Water Surface Level: 30_05_5055



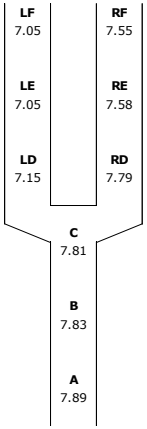


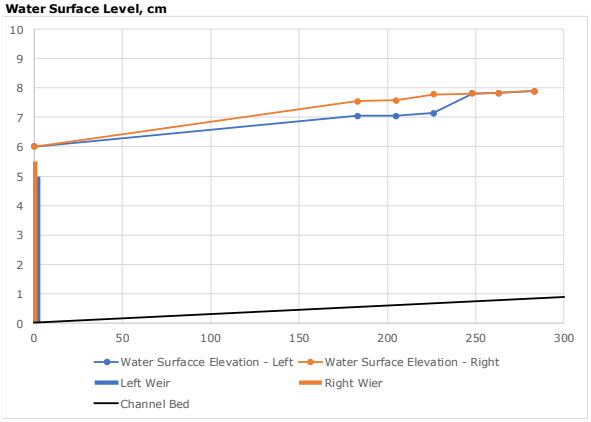
Water Surface Level: 30_07_5055



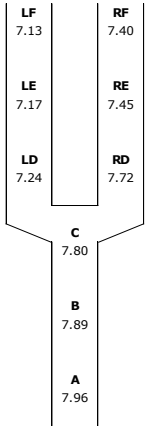


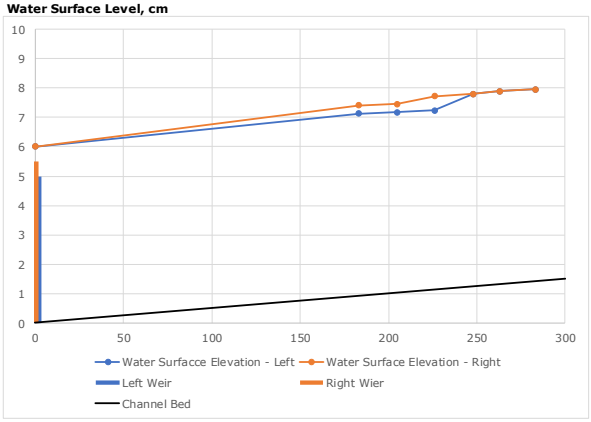
Water Surface Level: 40_03_5055



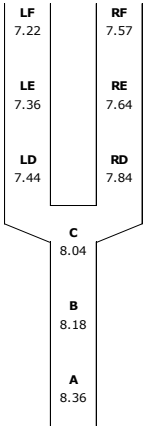


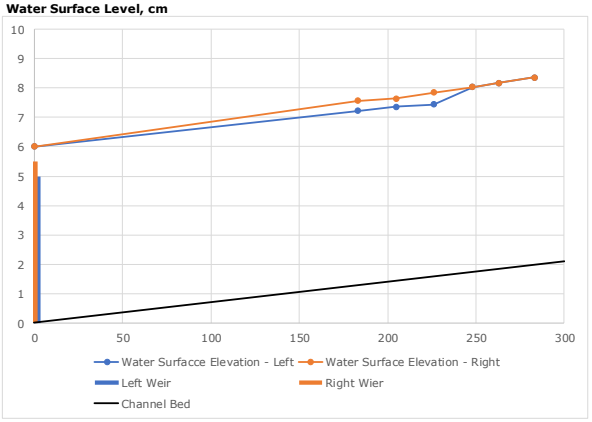
Water Surface Level: 40_05_5055



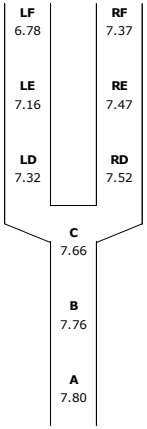


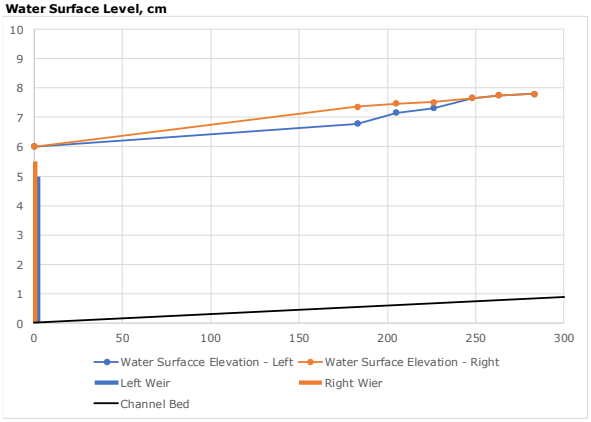
Water Surface Level: 40_07_5055



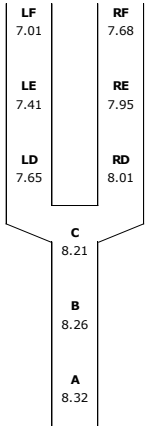


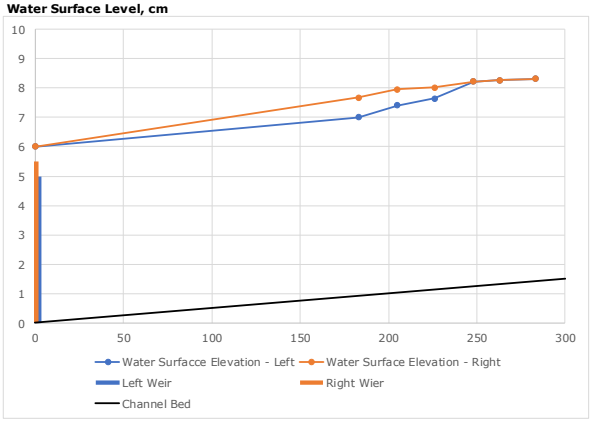
Water Surface Level: 50_03_5055



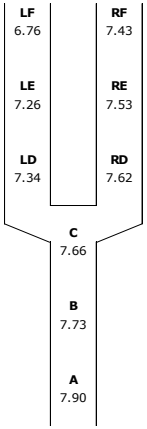


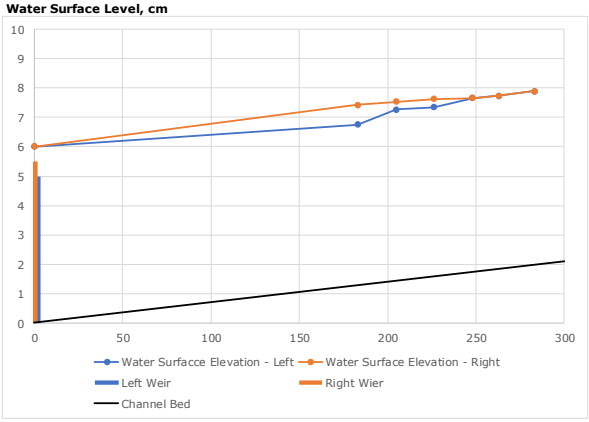
Water Surface Level: 50_05_5055





Water Surface Level: 50_07_5055

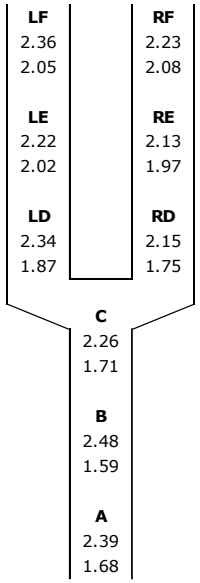


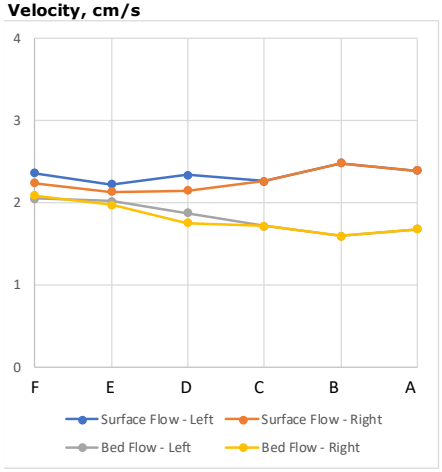


Appendix A6 Average Flow Velocity (Plan and Profile)

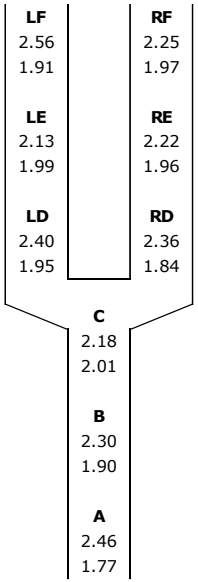
Left Weir Height, mm	Right Weir Height, mm	Bifurcation Angle, °	Slope, %	Name of Run	Page Number
50	50	30	0.3	30_03_5050	A-106
			0.5	30_05_5050	
			0.7	30_07_5050	
		40	0.3	40_03_5050	A-107
			0.5	40_05_5050	
			0.7	40_07_5050	
		50	0.3	50_03_5050	A-108
			0.5	50_05_5050	
			0.7	50_07_5050	
55	60	30	0.3	30_03_5560	A-109
			0.5	30_05_5560	
			0.7	30_07_5560	
		40	0.3	40_03_5560	A-110
			0.5	40_05_5560	
			0.7	40_07_5560	
		50	0.3	50_03_5560	A-111
			0.5	50_05_5560	
			0.7	50_07_5560	
50	55	30	0.3	30_03_5055	A-112
			0.5	30_05_5055	
			0.7	30_07_5055	
		40	0.3	40_03_5055	A-113
			0.5	40_05_5055	
			0.7	40_07_5055	
		50	0.3	50_03_5055	A-114
			0.5	50_05_5055	
			0.7	50_07_5055	

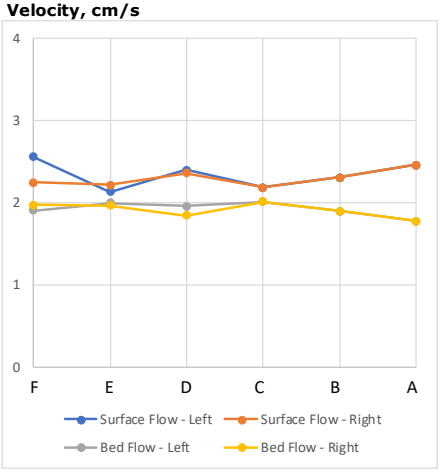
Average Flow Velocity: 30_03_5050



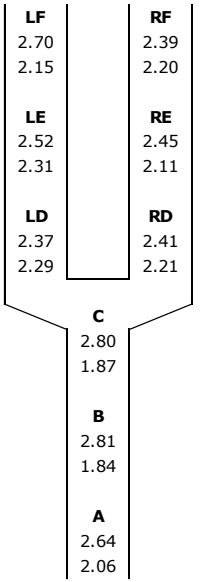


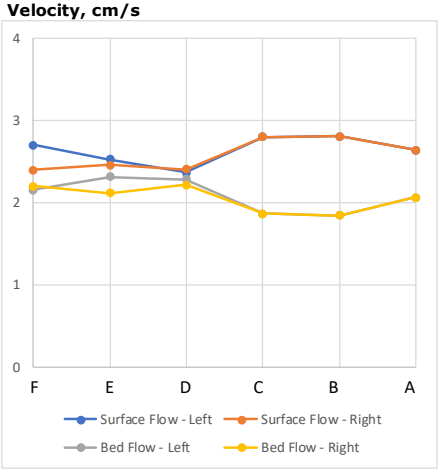
Average Flow Velocity: 30_05_5050



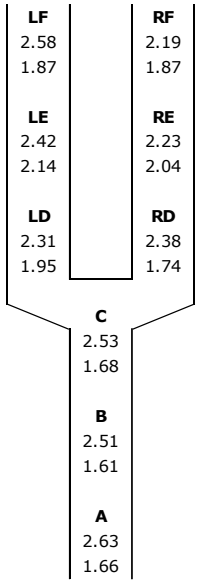


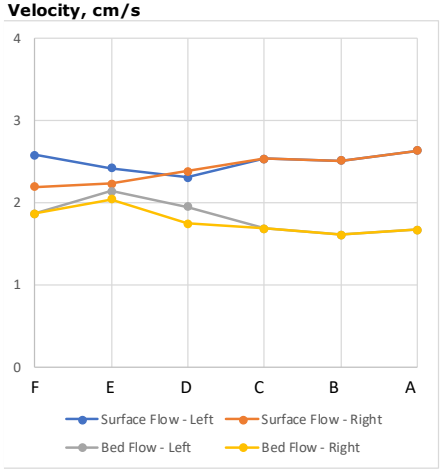
Average Flow Velocity: 30_07_5050



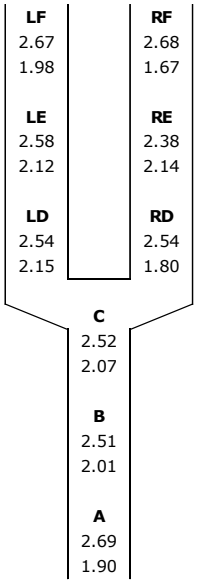


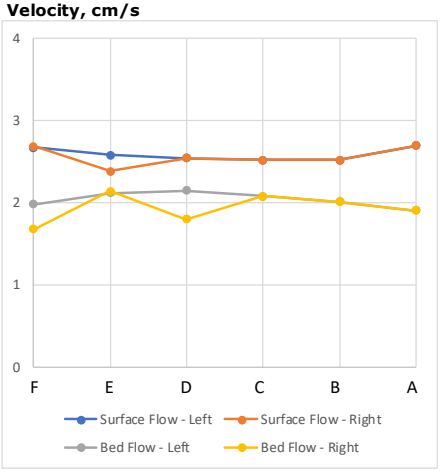
Average Flow Velocity: 40_03_5050



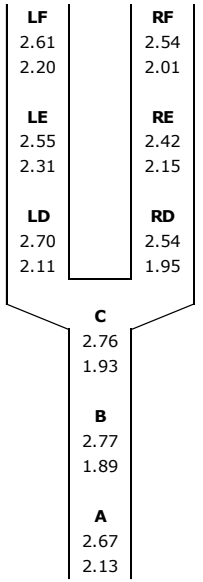


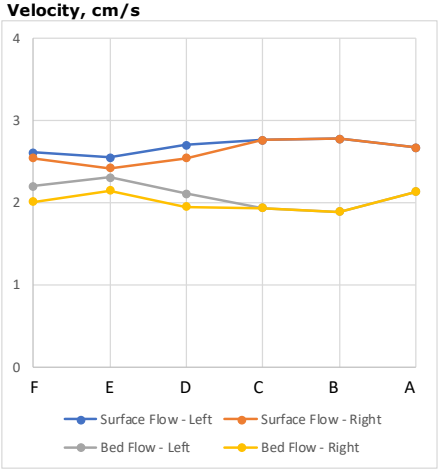
Average Flow Velocity: 40_05_5050



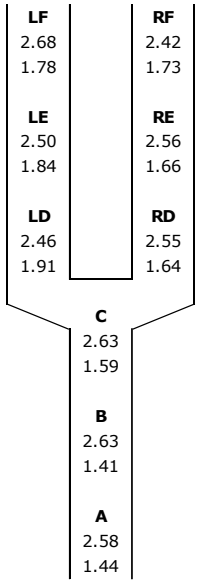


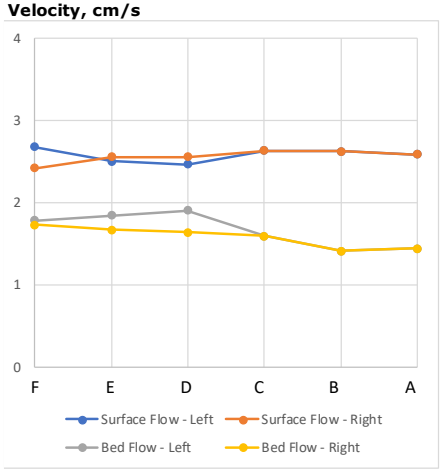
Average Flow Velocity: 40_07_5050



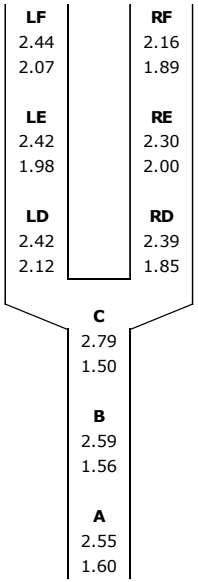


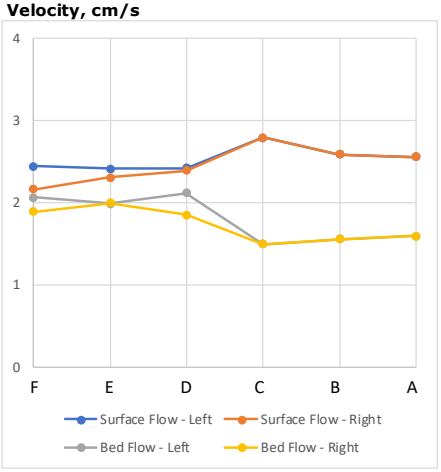
Average Flow Velocity: 50_03_5050



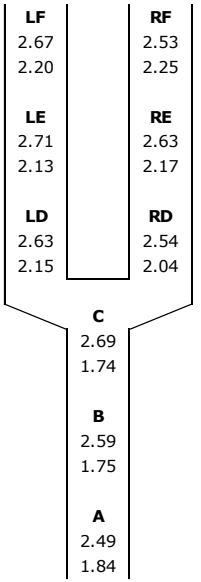


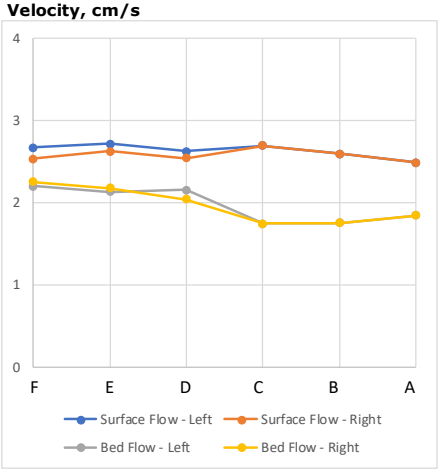
Average Flow Velocity: 50_05_5050





Average Flow Velocity: 50_07_5050

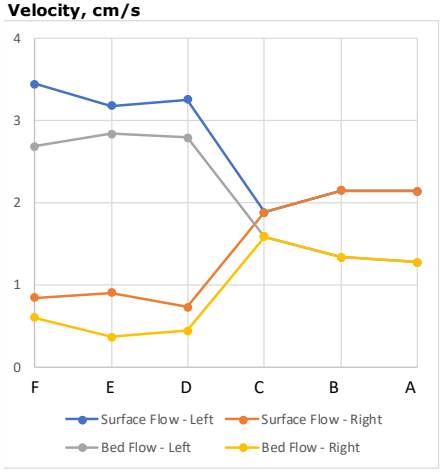




Average Flow Velocity: 30_03_5560

LF		RF
3.45		0.84
2.69		0.60
LE		**RE**
3.18		0.90
2.84		0.37
LD		**RD**
3.25		0.73
2.79		0.44
	C	
	1.88	
	1.58	
	B	
	2.15	
	1.34	
	A	
	2.14	
	1.27	

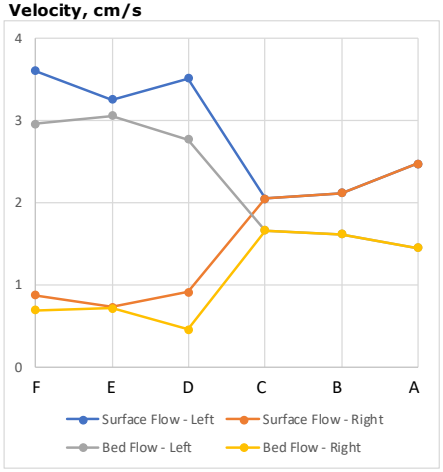
Velocity, cm/s



Average Flow Velocity: 30_05_5560

LF		RF
3.61		0.87
2.96		0.69
LE		**RE**
3.26		0.72
3.06		0.71
LD		**RD**
3.51		0.91
2.77		0.45
	C	
	2.05	
	1.66	
	B	
	2.11	
	1.62	
	A	
	2.48	
	1.45	

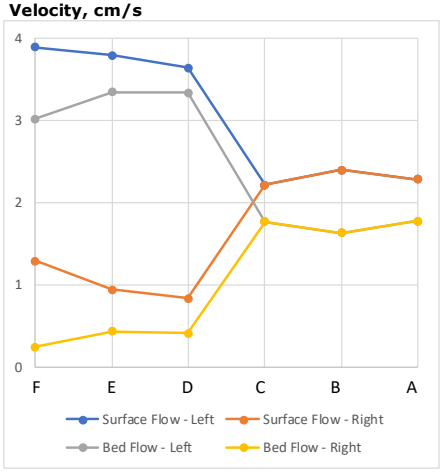
Velocity, cm/s



Average Flow Velocity: 30_07_5560

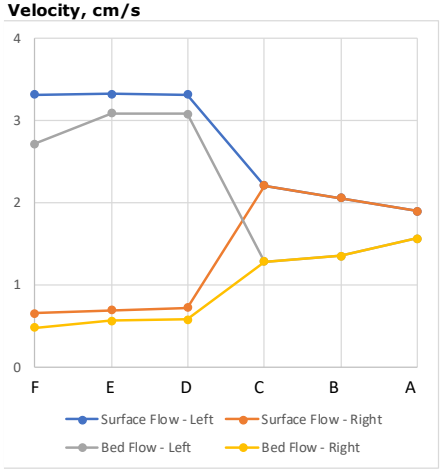
LF		RF
3.89		1.29
3.02		0.24
LE		**RE**
3.79		0.94
3.35		0.43
LD		**RD**
3.64		0.83
3.33		0.41
	C	
	2.21	
	1.77	
	B	
	2.39	
	1.63	
	A	
	2.28	
	1.78	

Velocity, cm/s



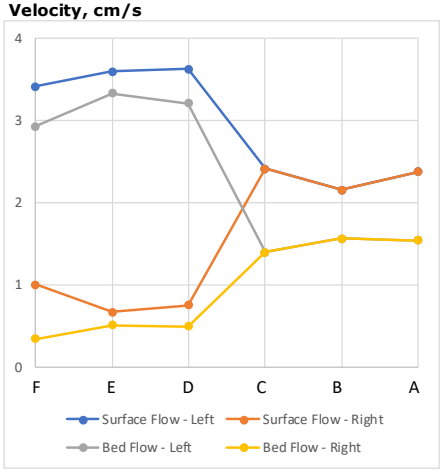
Average Flow Velocity: 40_03_5560

LF		RF
3.31		0.65
2.71		0.47
LE		**RE**
3.32		0.69
3.09		0.56
LD		**RD**
3.31		0.72
3.08		0.58
	C	
	2.20	
	1.28	
	B	
	2.05	
	1.35	
	A	
	1.90	
	1.56	



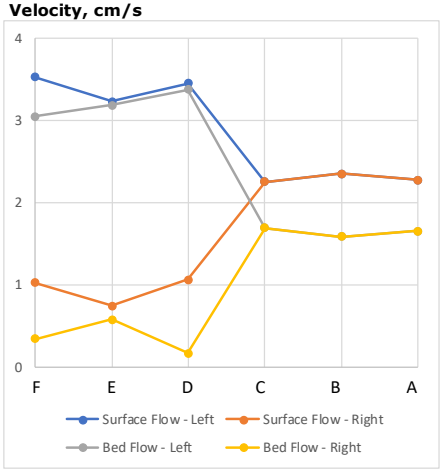
Average Flow Velocity: 40_05_5560

LF		RF
3.41		1.00
2.93		0.34
LE		**RE**
3.59		0.66
3.33		0.50
LD		**RD**
3.63		0.75
3.21		0.49
	C	
	2.41	
	1.40	
	B	
	2.16	
	1.56	
	A	
	2.37	
	1.54	



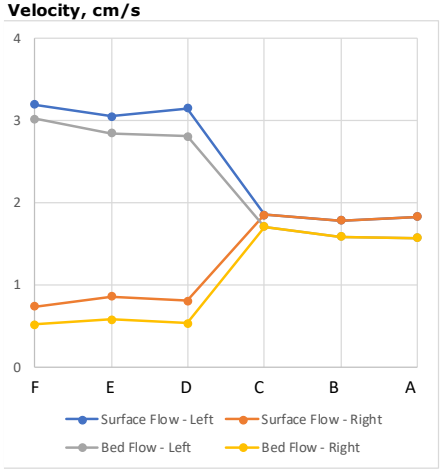
Average Flow Velocity: 40_07_5560

LF		RF
3.53		1.02
3.05		0.34
LE		**RE**
3.24		0.74
3.18		0.58
LD		**RD**
3.45		1.06
3.37		0.16
	C	
	2.25	
	1.69	
	B	
	2.35	
	1.59	
	A	
	2.27	
	1.65	



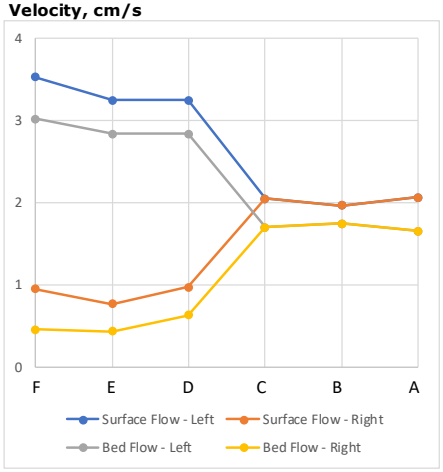
Average Flow Velocity: 50_03_5560

LF		RF
3.20		0.74
3.02		0.51
LE		**RE**
3.05		0.86
2.85		0.57
LD		**RD**
3.15		0.80
2.81		0.53
	C	
	1.85	
	1.70	
	B	
	1.78	
	1.59	
	A	
	1.82	
	1.57	



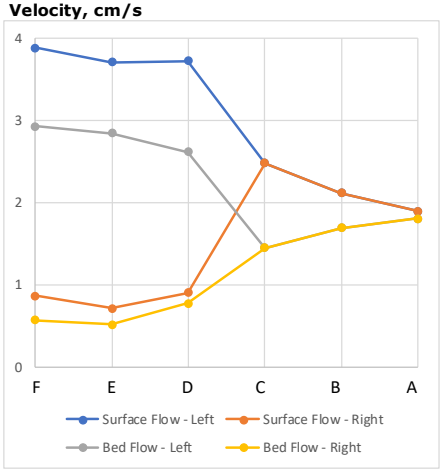
Average Flow Velocity: 50_05_5560

LF		RF
3.53		0.95
3.02		0.46
LE		**RE**
3.25		0.77
2.84		0.43
LD		**RD**
3.25		0.97
2.84		0.63
	C	
	2.05	
	1.69	
	B	
	1.96	
	1.74	
	A	
	2.06	
	1.65	



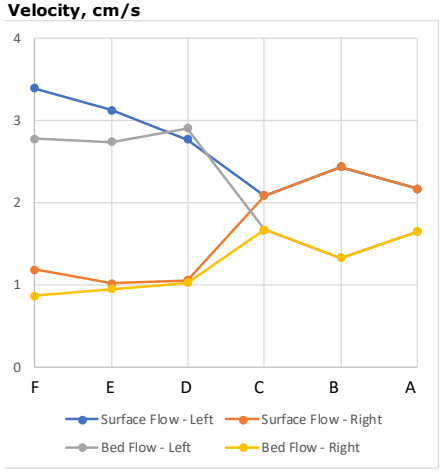
Average Flow Velocity: 50_07_5560

LF		RF
3.88		0.86
2.93		0.56
LE		**RE**
3.71		0.71
2.85		0.51
LD		**RD**
3.72		0.90
2.61		0.77
	C	
	2.48	
	1.44	
	B	
	2.12	
	1.69	
	A	
	1.90	
	1.81	



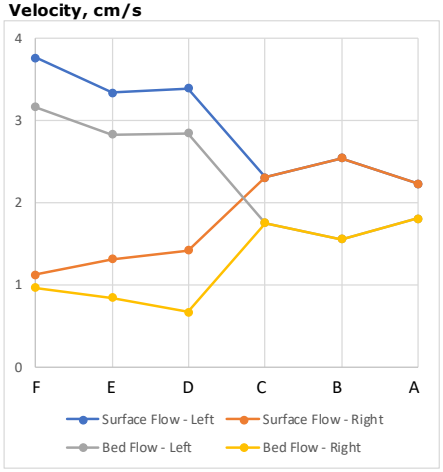
Average Flow Velocity: 30_03_5055

LF		RF
3.39		1.18
2.78		0.86
LE		**RE**
3.12		1.02
2.74		0.95
LD		**RD**
2.77		1.05
2.90		1.02
	C	
	2.09	
	1.66	
	B	
	2.43	
	1.33	
	A	
	2.17	
	1.64	



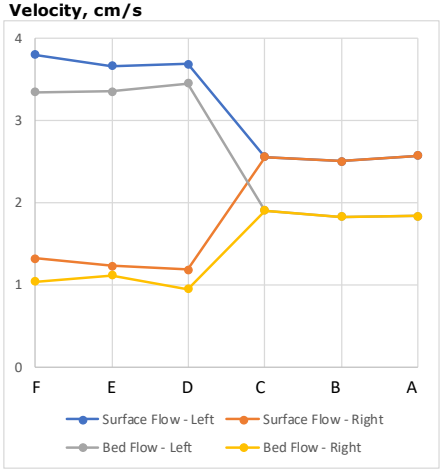
Average Flow Velocity: 30_05_5055

LF		RF
3.77		1.12
3.16		0.96
LE		**RE**
3.34		1.31
2.83		0.84
LD		**RD**
3.39		1.42
2.85		0.67
	C	
	2.31	
	1.75	
	B	
	2.54	
	1.55	
	A	
	2.23	
	1.80	



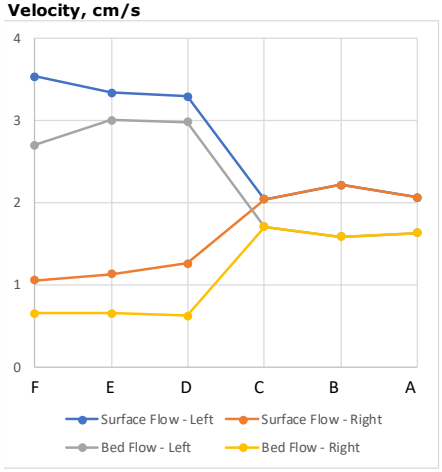
Average Flow Velocity: 30_07_5055

LF		RF
3.80		1.32
3.35		1.04
LE		**RE**
3.66		1.23
3.35		1.12
LD		**RD**
3.69		1.18
3.45		0.95
	C	
	2.56	
	1.90	
	B	
	2.50	
	1.83	
	A	
	2.57	
	1.83	



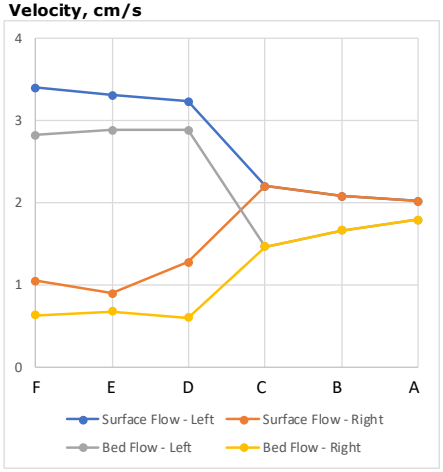
Average Flow Velocity: 40_03_5055

LF	RF
3.54	1.05
2.70	0.65
LE	**RE**
3.34	1.13
3.00	0.65
LD	**RD**
3.29	1.26
2.98	0.62
C	
2.04	
1.70	
B	
2.21	
1.58	
A	
2.06	
1.63	



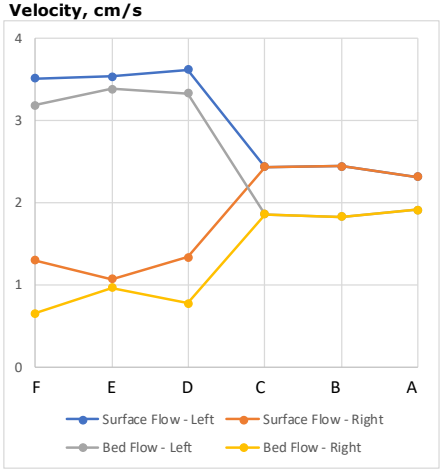
Average Flow Velocity: 40_05_5055

LF	RF
3.40	1.04
2.82	0.62
LE	**RE**
3.31	0.89
2.88	0.67
LD	**RD**
3.23	1.27
2.88	0.60
C	
2.20	
1.46	
B	
2.08	
1.66	
A	
2.02	
1.79	

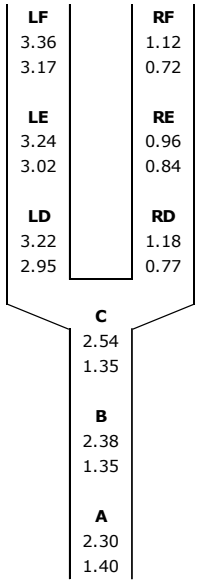


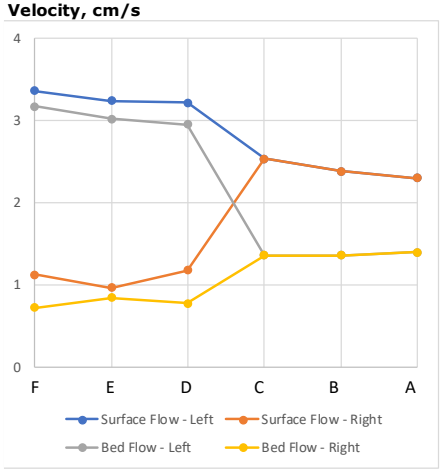
Average Flow Velocity: 40_07_5055

LF	RF
3.51	1.30
3.19	0.65
LE	**RE**
3.54	1.07
3.39	0.96
LD	**RD**
3.62	1.33
3.33	0.77
C	
2.43	
1.86	
B	
2.44	
1.83	
A	
2.31	
1.91	

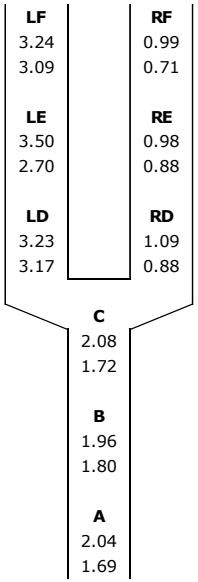


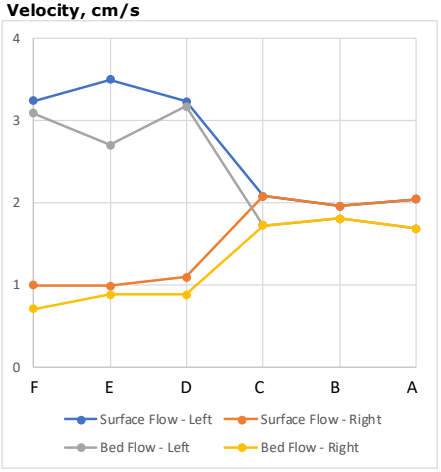
Average Flow Velocity: 50_03_5055



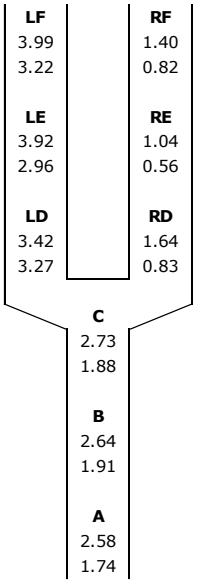


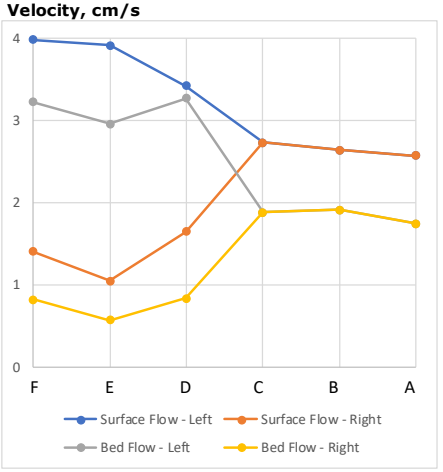
Average Flow Velocity: 50_05_5055





Average Flow Velocity: 50_07_5055

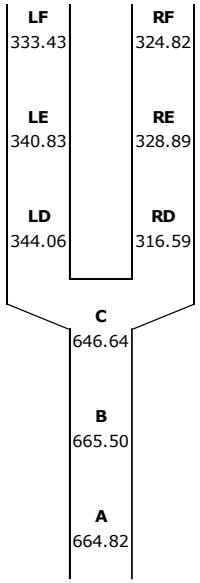


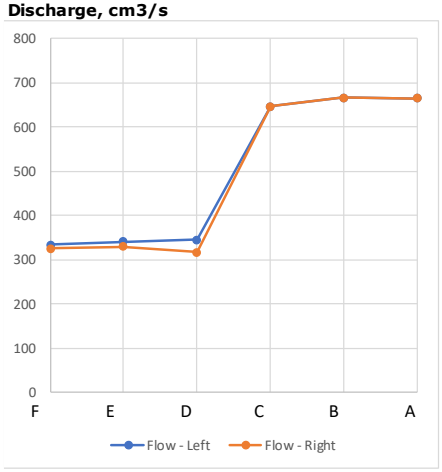


Appendix A7 Flow Discharge (Plan and Profile)

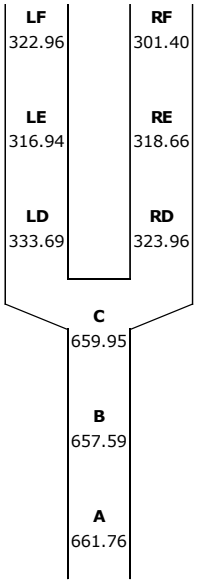
Left Weir Height, mm	Right Weir Height, mm	Bifurcation Angle, °	Slope, %	Name of Run	Page Number
50	50	30	0.3	30_03_5050	A-116
			0.5	30_05_5050	
			0.7	30_07_5050	
		40	0.3	40_03_5050	A-117
			0.5	40_05_5050	
			0.7	40_07_5050	
		50	0.3	50_03_5050	A-118
			0.5	50_05_5050	
			0.7	50_07_5050	
55	60	30	0.3	30_03_5560	A-119
			0.5	30_05_5560	
			0.7	30_07_5560	
		40	0.3	40_03_5560	A-120
			0.5	40_05_5560	
			0.7	40_07_5560	
		50	0.3	50_03_5560	A-121
			0.5	50_05_5560	
			0.7	50_07_5560	
50	55	30	0.3	30_03_5055	A-122
			0.5	30_05_5055	
			0.7	30_07_5055	
		40	0.3	40_03_5055	A-123
			0.5	40_05_5055	
			0.7	40_07_5055	
		50	0.3	50_03_5055	A-124
			0.5	50_05_5055	
			0.7	50_07_5055	

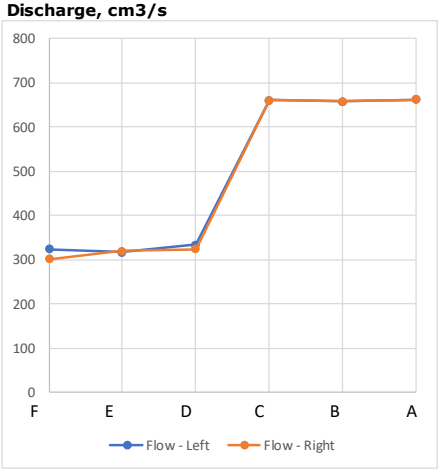
Discharge: 30_03_5050



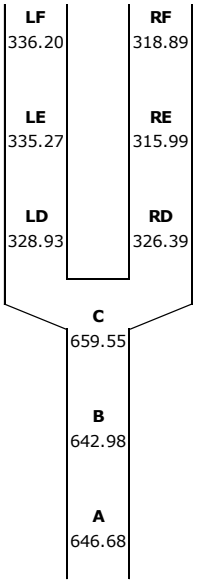


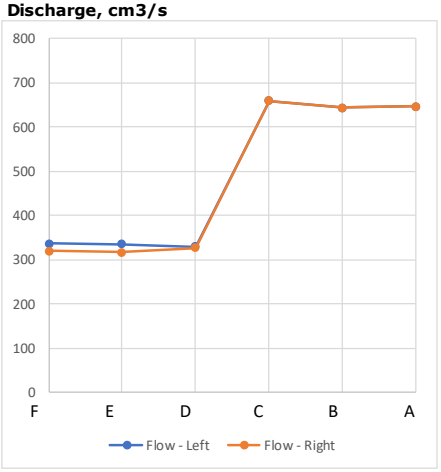
Discharge: 30_05_5050



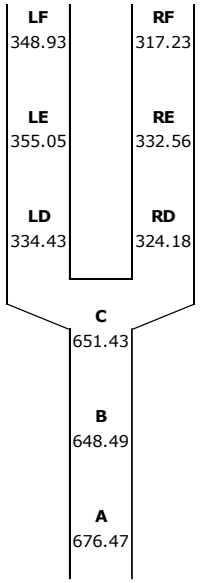


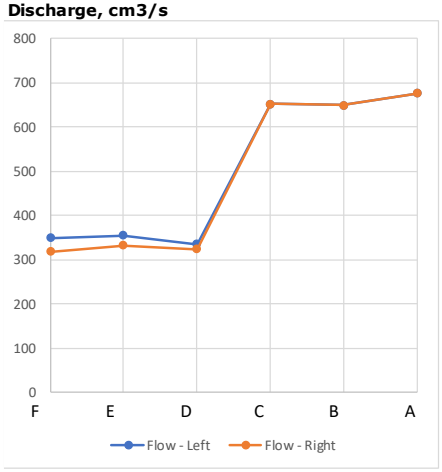
Discharge: 30_07_5050



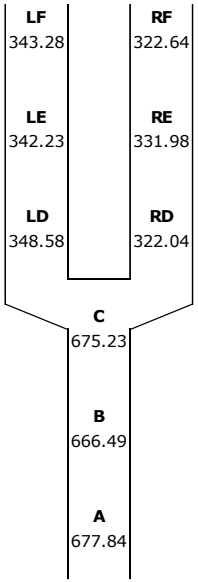


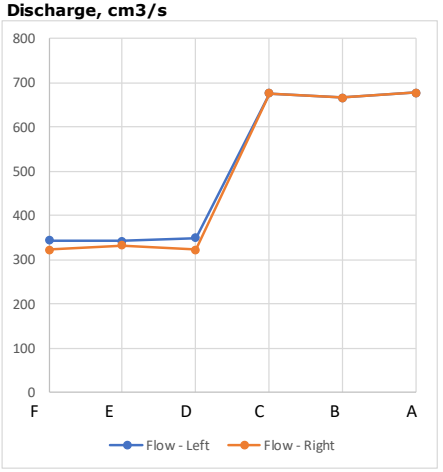
Discharge: 40_03_5050



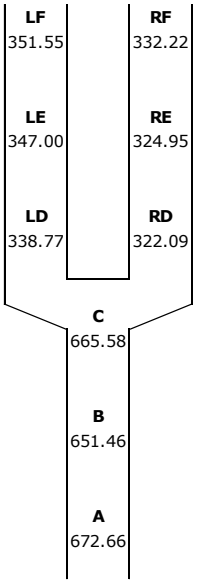


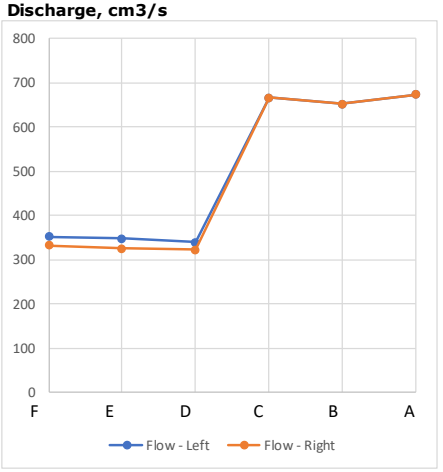
Discharge: 40_05_5050



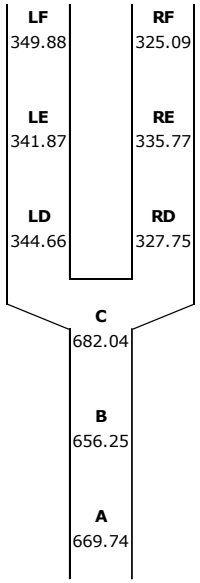


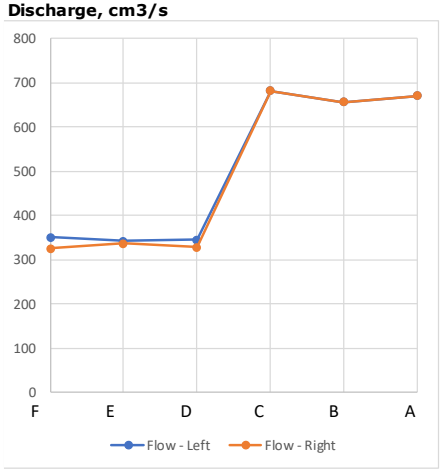
Discharge: 40_07_5050



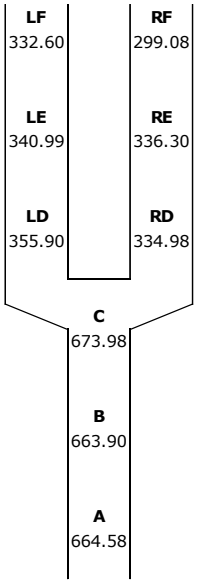


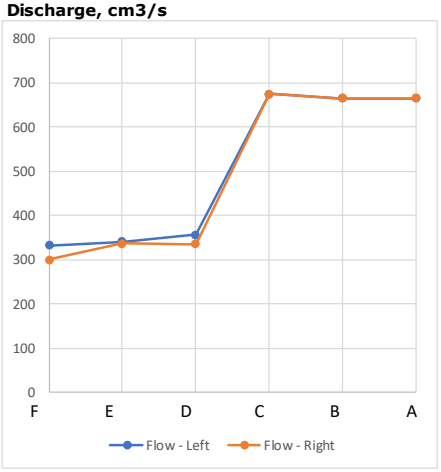
Discharge: 50_03_5050



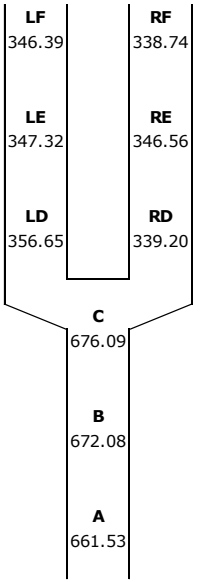


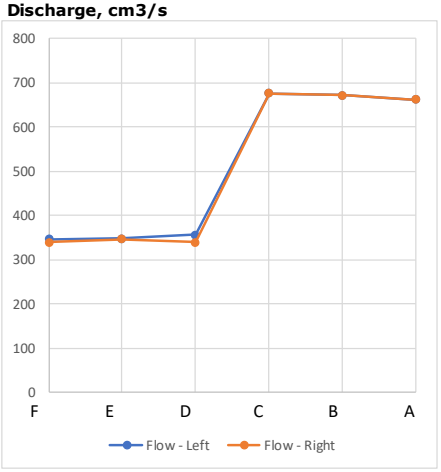
Discharge: 50_05_5050



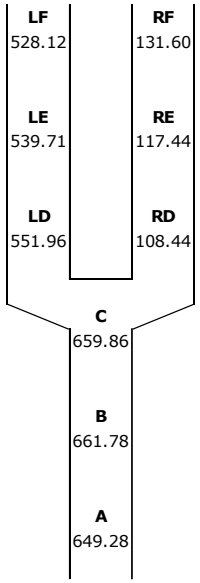


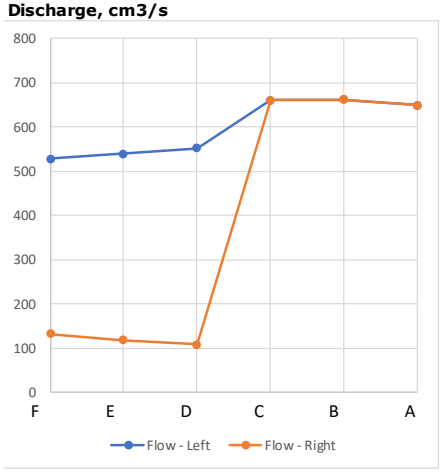
Discharge: 50_07_5050



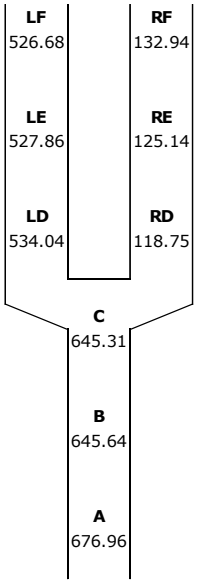


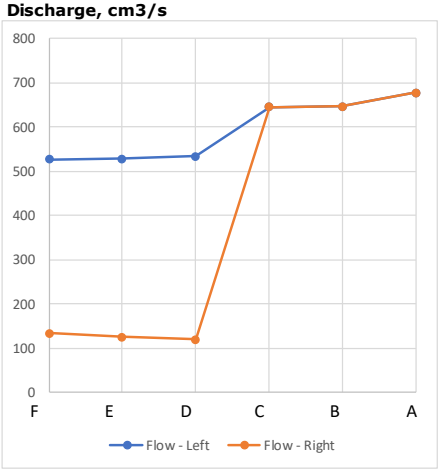
Discharge: 30_03_5560



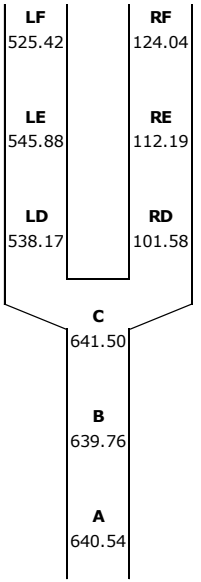


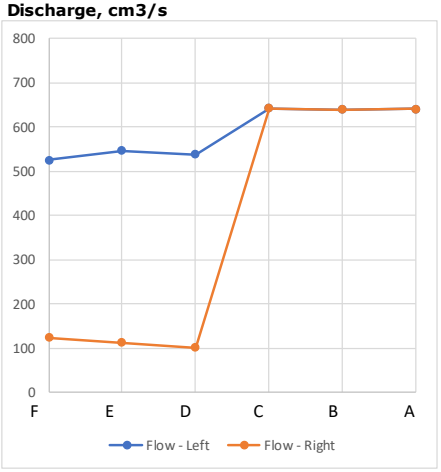
Discharge: 30_05_5560



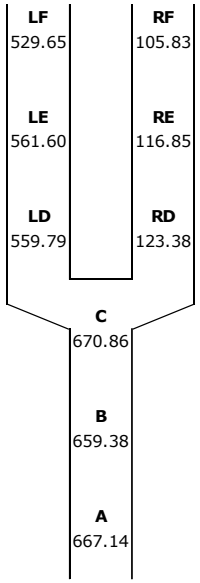


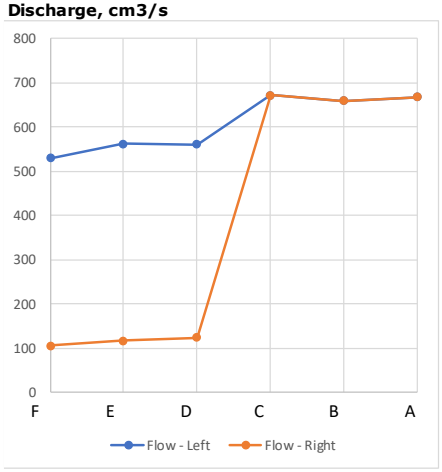
Discharge: 30_07_5560



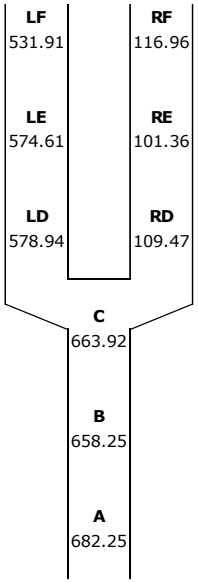


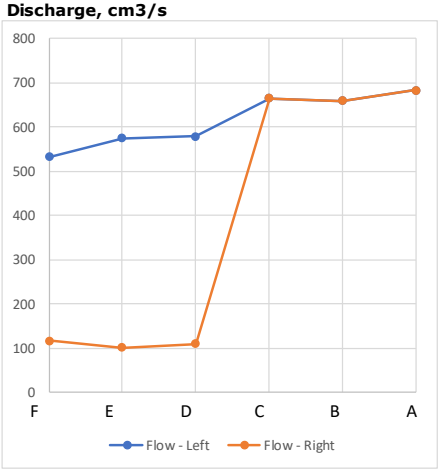
Discharge: 40_03_5560



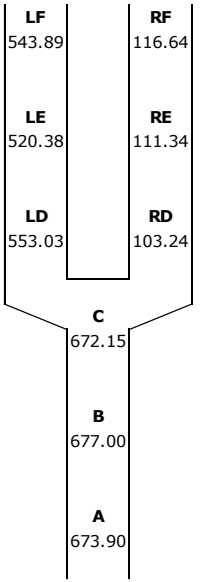


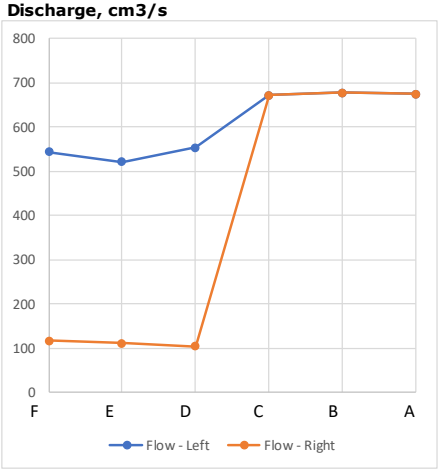
Discharge: 40_05_5560



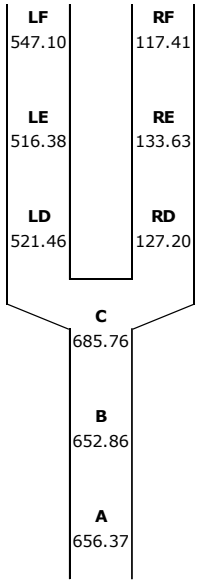


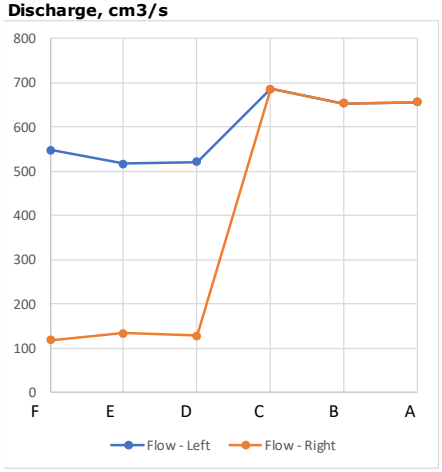
Discharge: 40_07_5560



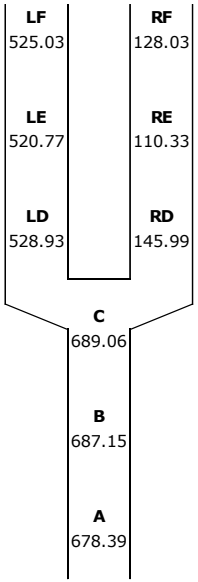


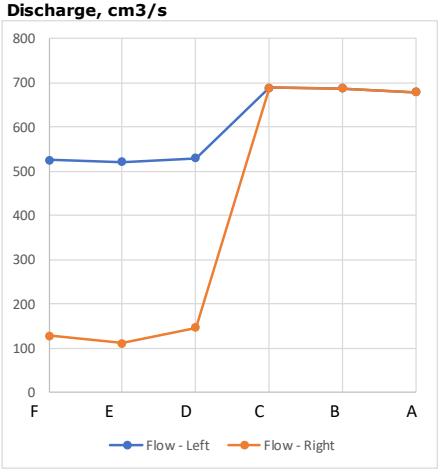
Discharge: 50_03_5560



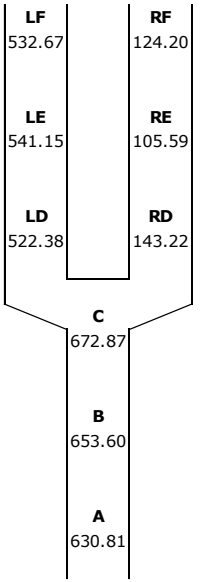


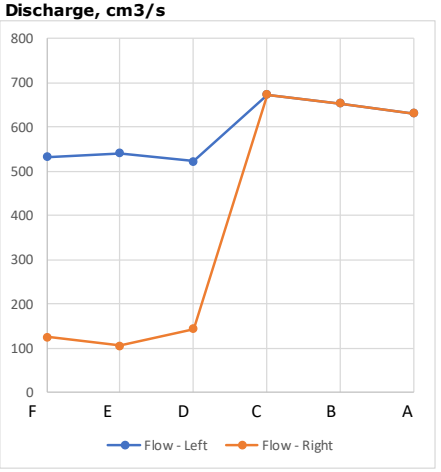
Discharge: 50_05_5560



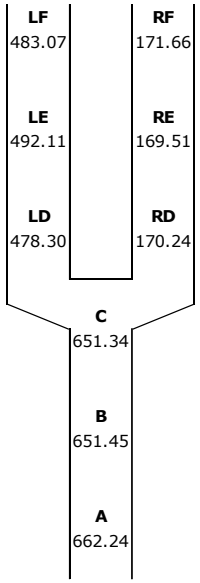


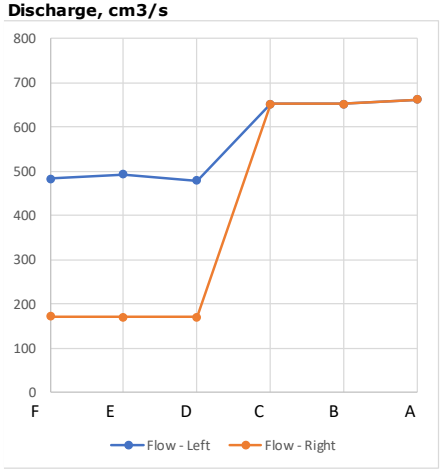
Discharge: 50_07_5560



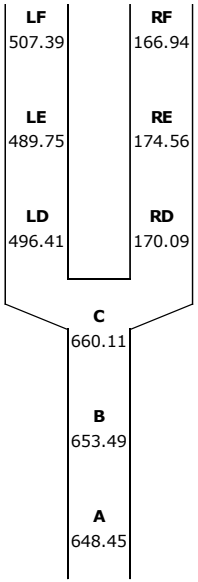


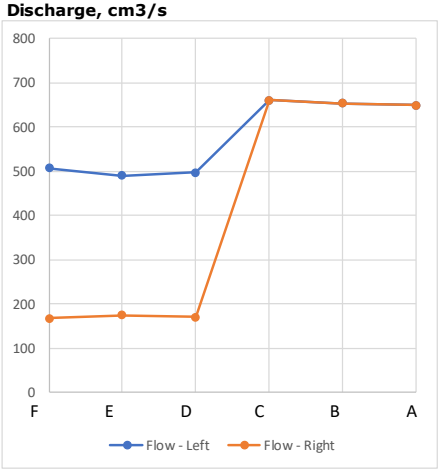
Discharge: 30_03_5055



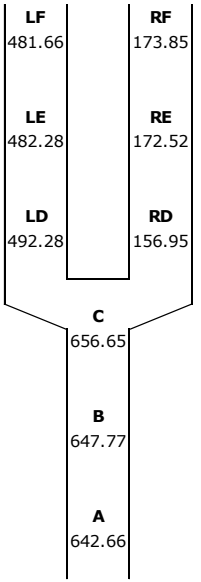


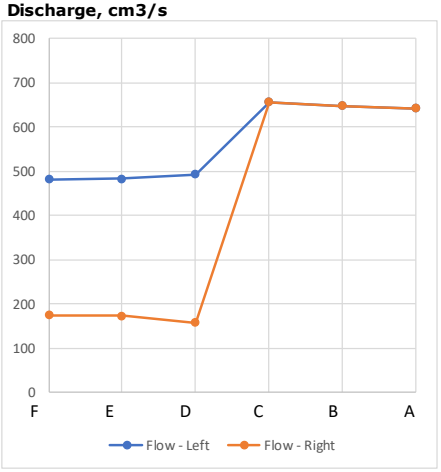
Discharge: 30_05_5055



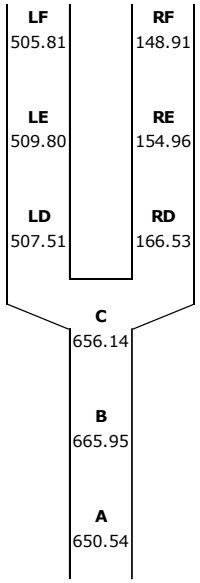


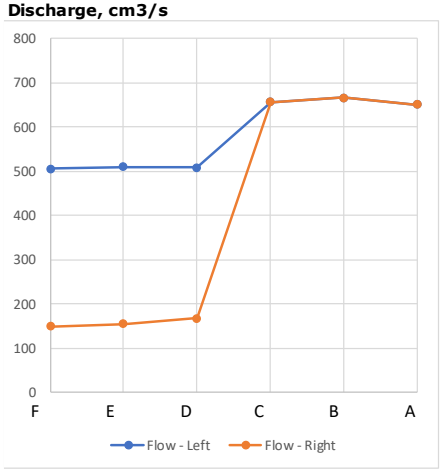
Discharge: 30_07_5055



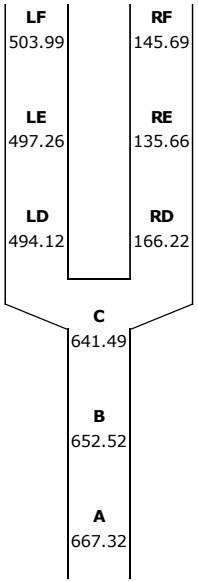


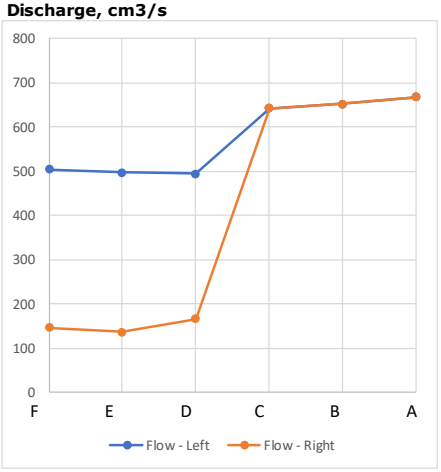
Discharge: 40_03_5055



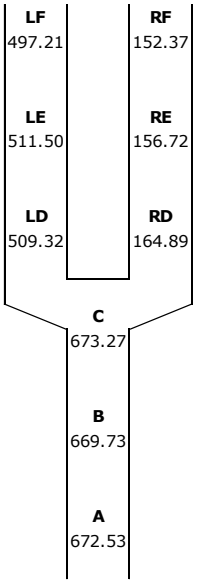


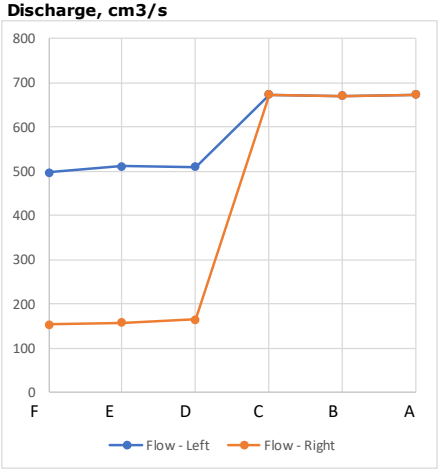
Discharge: 40_05_5055



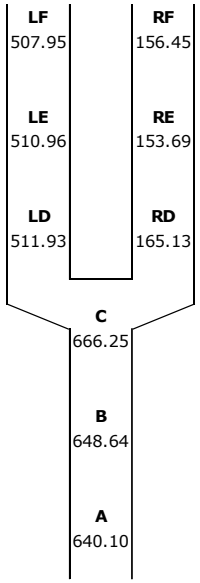


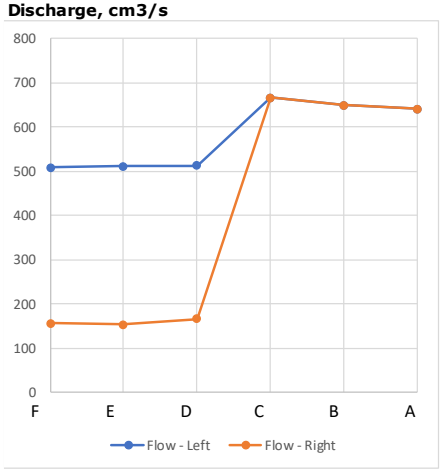
Discharge: 40_07_5055



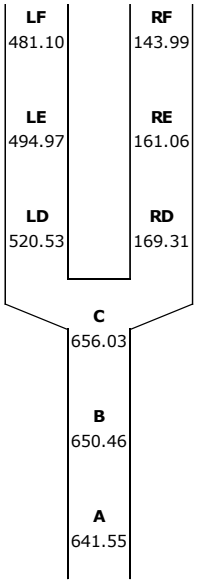


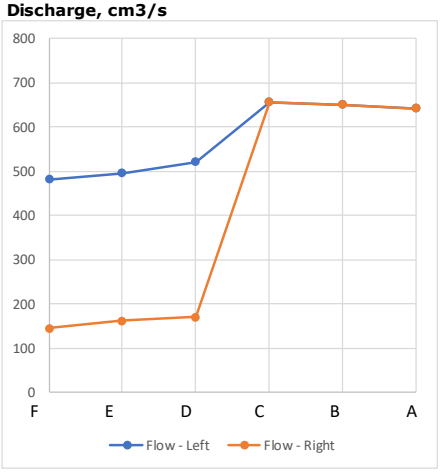
Discharge: 50_03_5055



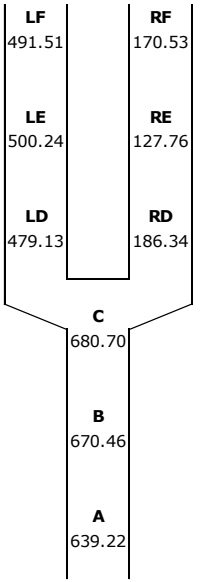


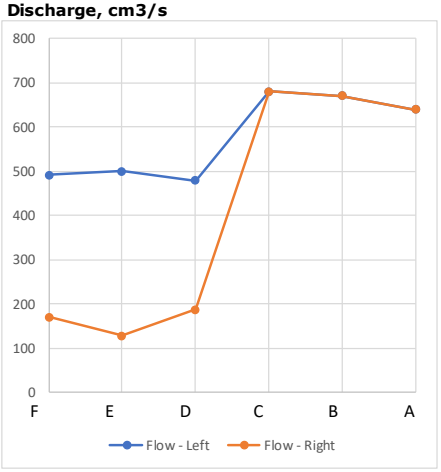
Discharge: 50_05_5055





Discharge: 50_07_5055

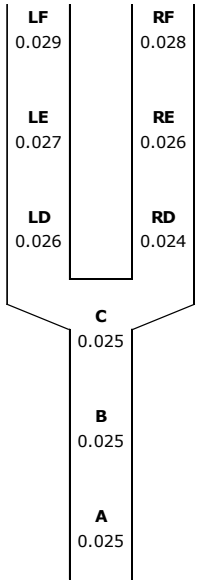


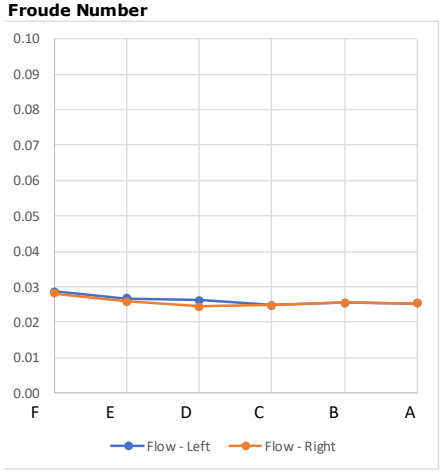


Appendix A8 Froude Number (Plan and Profile)

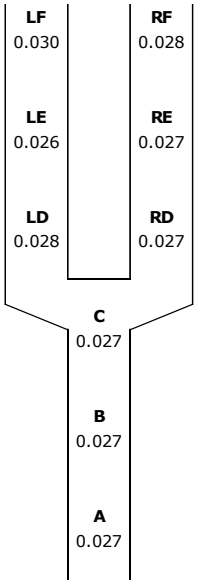
Left Weir Height, mm	Right Weir Height, mm	Bifurcation Angle, °	Slope, %	Name of Run	Page Number
50	50	30	0.3	30_03_5050	A-126
			0.5	30_05_5050	
			0.7	30_07_5050	
		40	0.3	40_03_5050	A-127
			0.5	40_05_5050	
			0.7	40_07_5050	
		50	0.3	50_03_5050	A-128
			0.5	50_05_5050	
			0.7	50_07_5050	
55	60	30	0.3	30_03_5560	A-129
			0.5	30_05_5560	
			0.7	30_07_5560	
		40	0.3	40_03_5560	A-130
			0.5	40_05_5560	
			0.7	40_07_5560	
		50	0.3	50_03_5560	A-131
			0.5	50_05_5560	
			0.7	50_07_5560	
50	55	30	0.3	30_03_5055	A-132
			0.5	30_05_5055	
			0.7	30_07_5055	
		40	0.3	40_03_5055	A-133
			0.5	40_05_5055	
			0.7	40_07_5055	
		50	0.3	50_03_5055	A-134
			0.5	50_05_5055	
			0.7	50_07_5055	

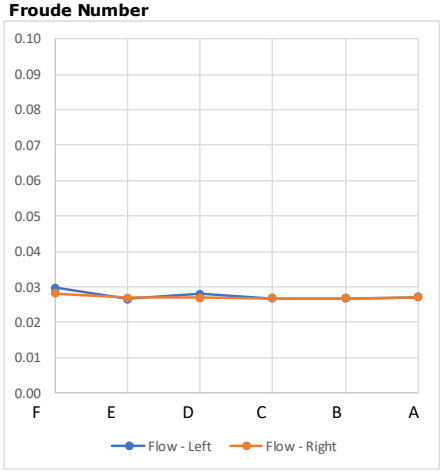
Froude: 30_03_5050



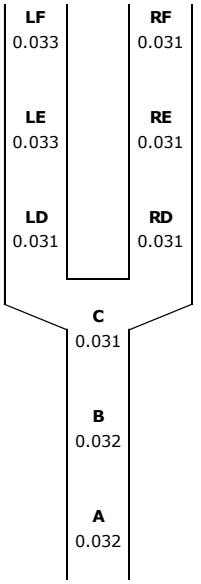


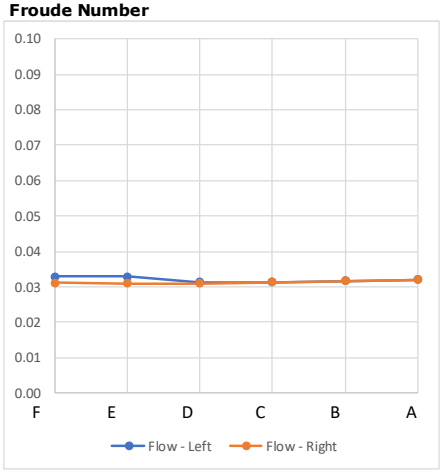
Froude: 30_05_5050



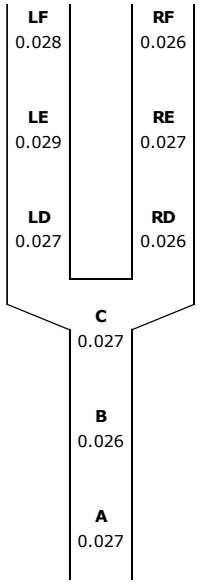


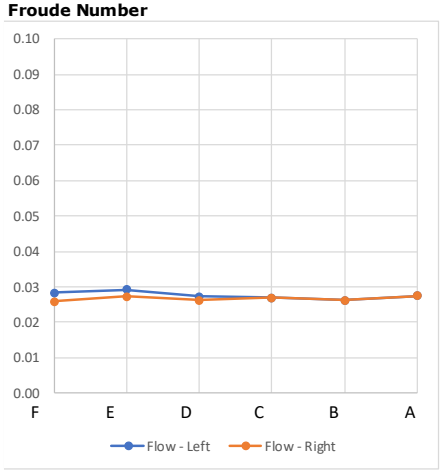
Froude: 30_07_5050



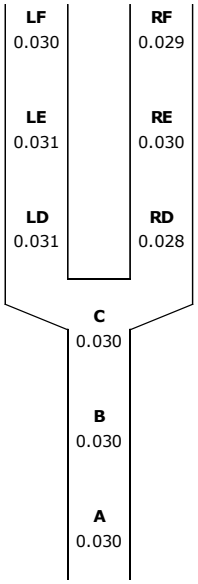


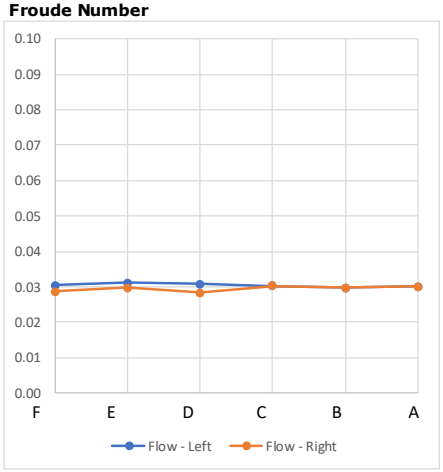
Froude: 40_03_5050



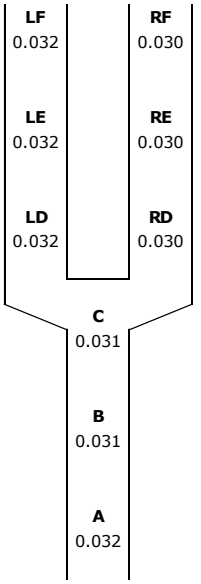


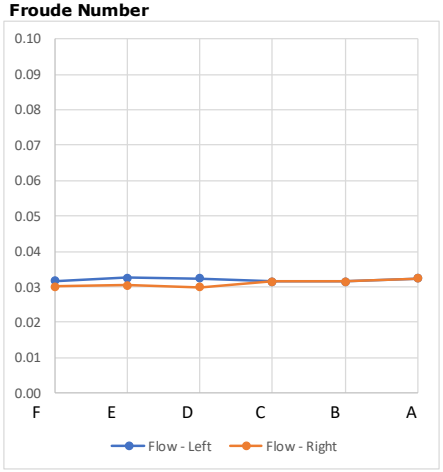
Froude: 40_05_5050



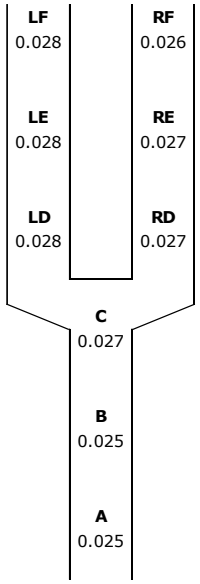


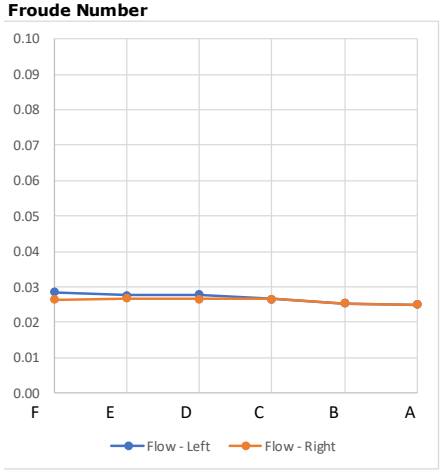
Froude: 40_07_5050



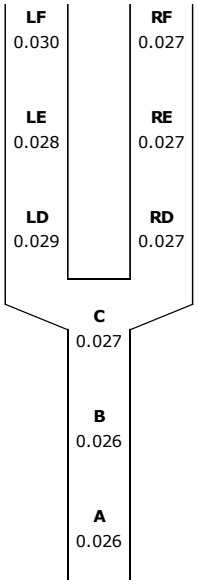


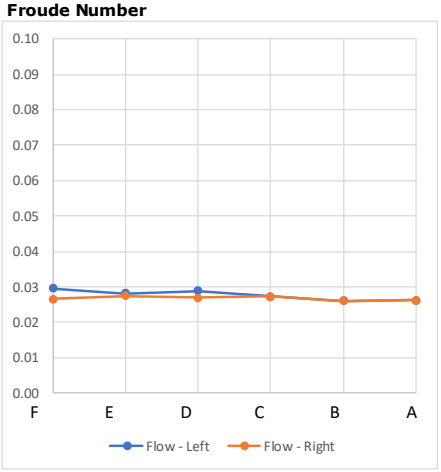
Froude: 50_03_5050



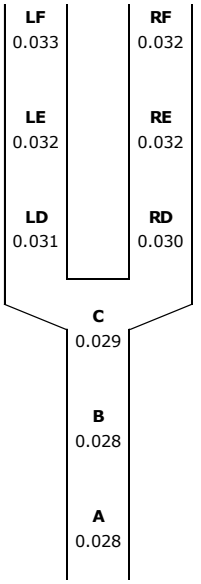


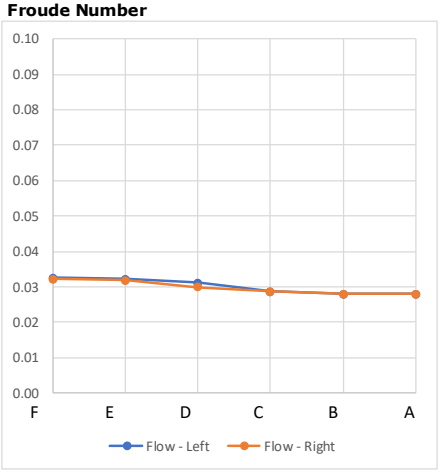
Froude: 50_05_5050



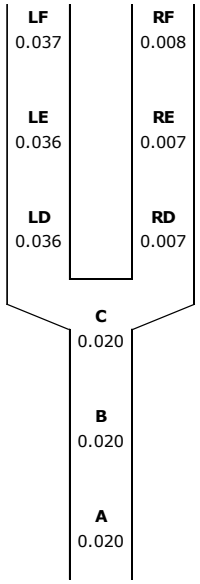


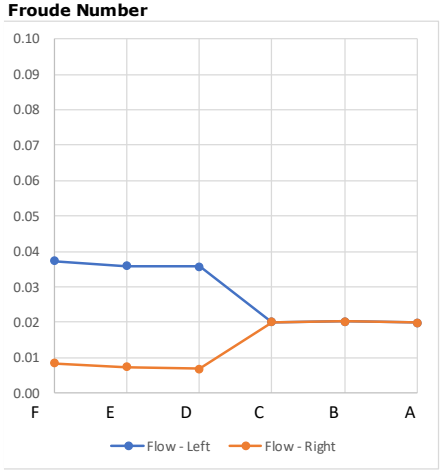
Froude: 50_07_5050



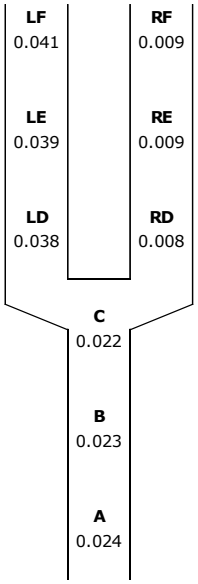


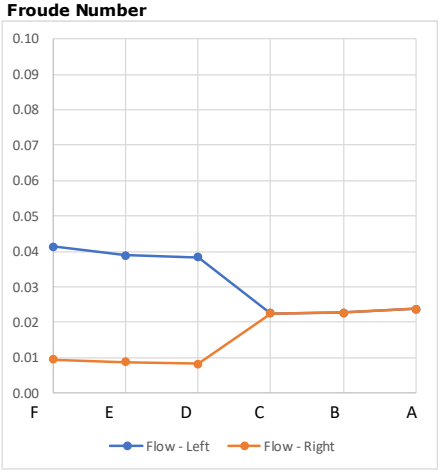
Froude: 30_03_5560



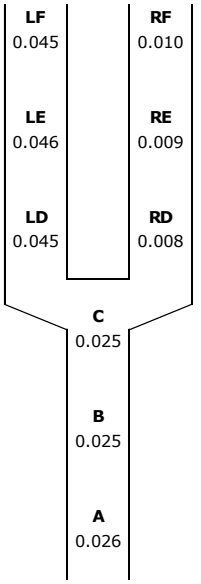


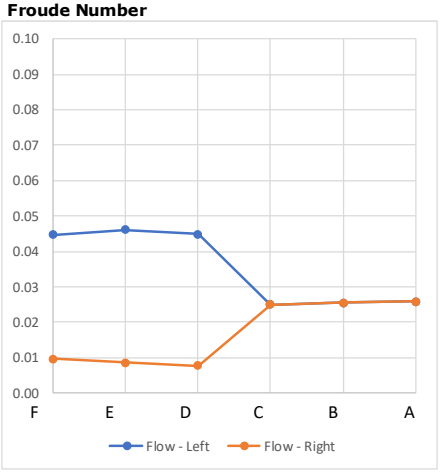
Froude: 30_05_5560



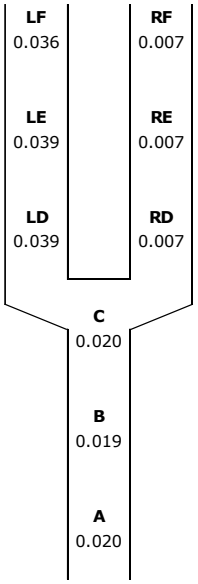


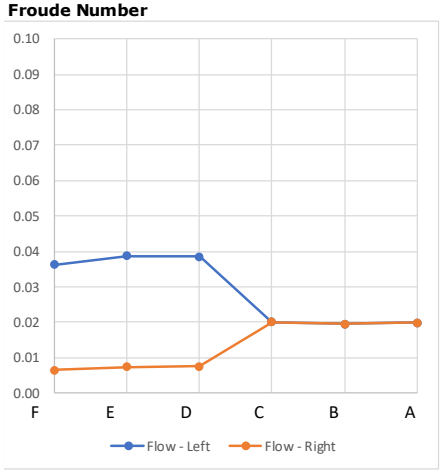
Froude: 30_07_5560



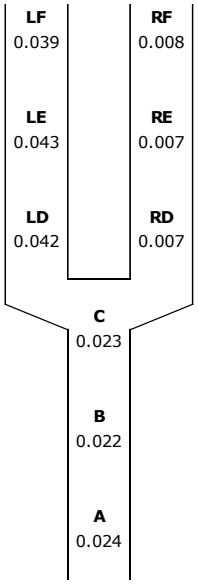


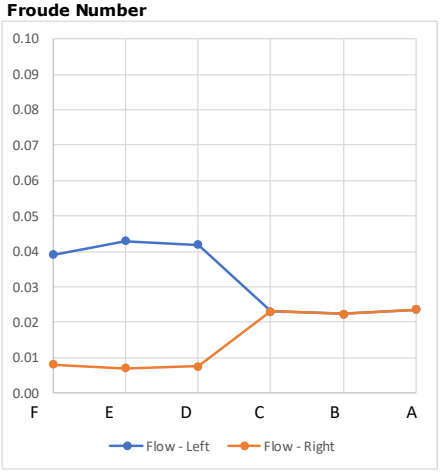
Froude: 40_03_5560



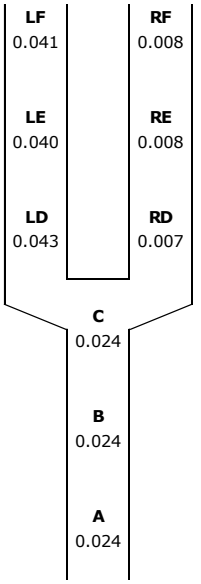


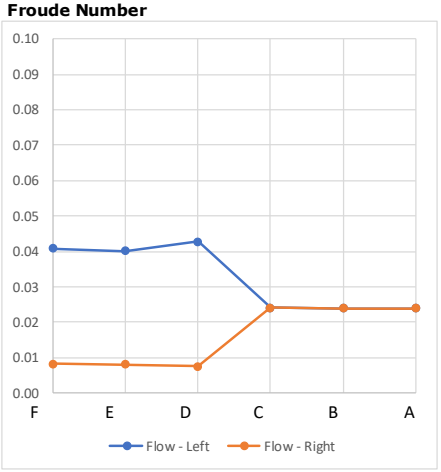
Froude: 40_05_5560



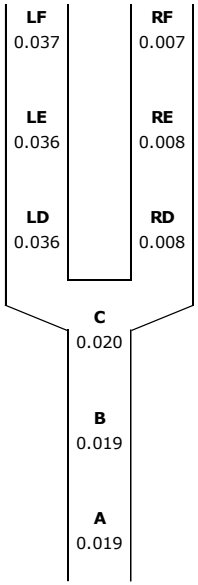


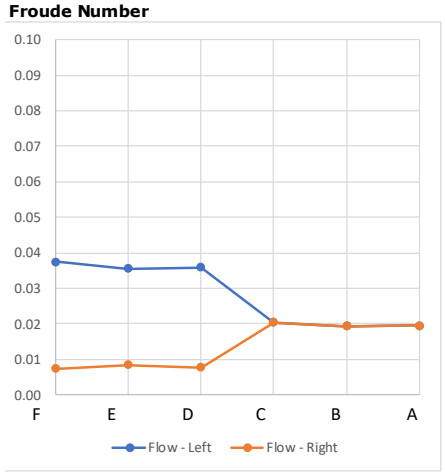
Froude: 40_07_5560



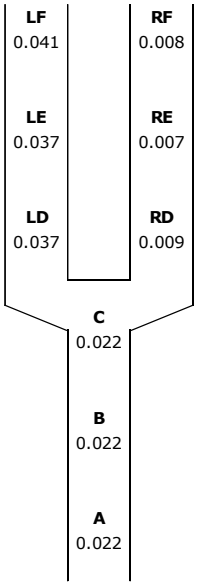


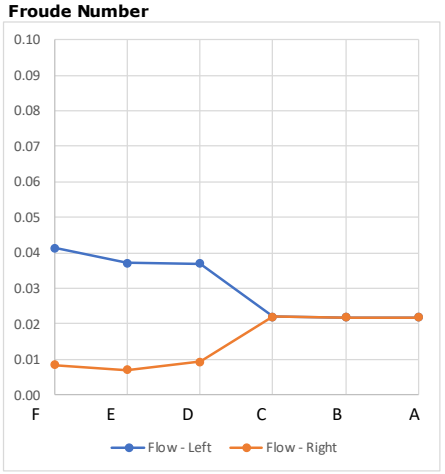
Froude: 50_03_5560



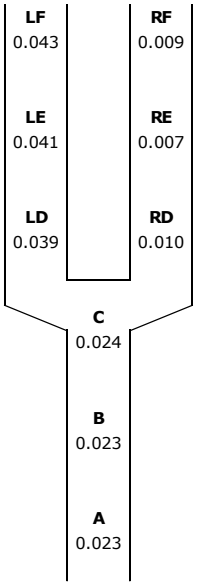


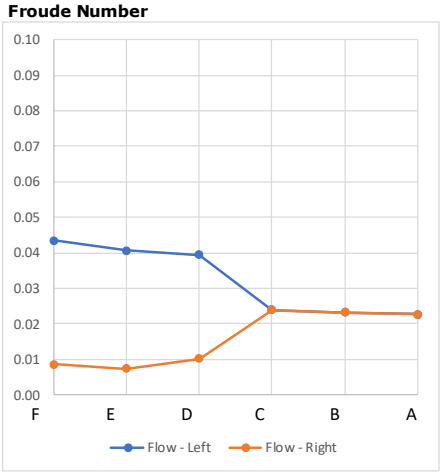
Froude: 50_05_5560



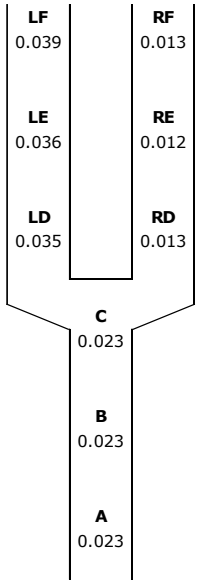


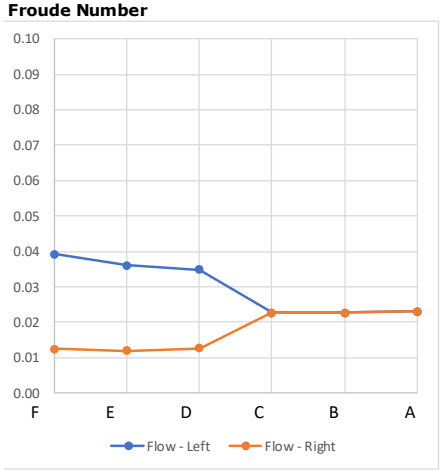
Froude: 50_07_5560



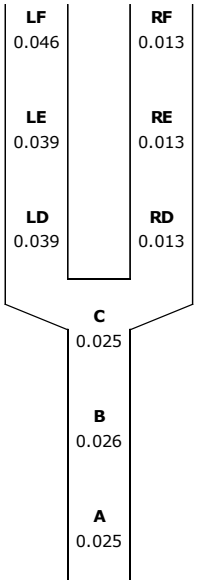


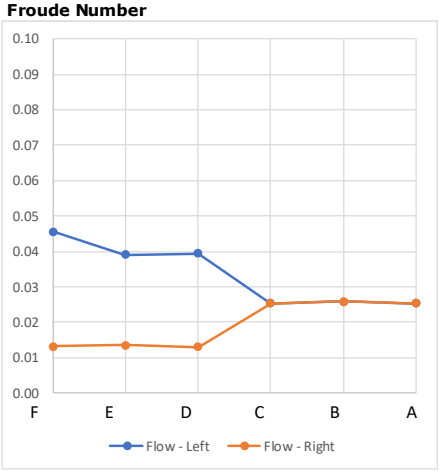
Froude: 30_03_5055



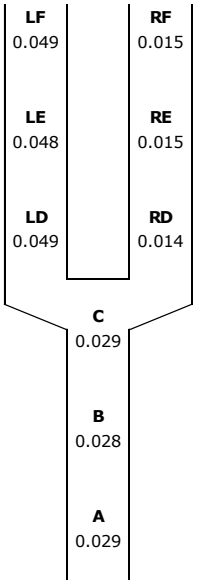


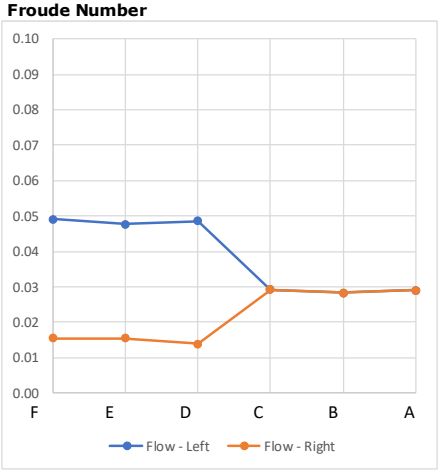
Froude: 30_05_5055



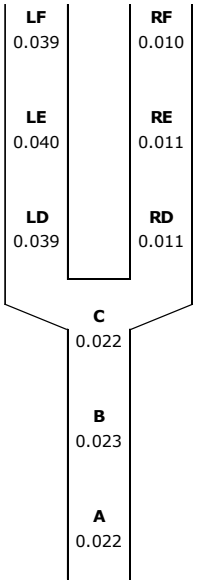


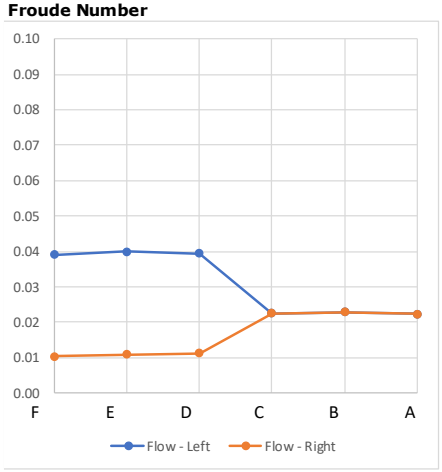
Froude: 30_07_5055



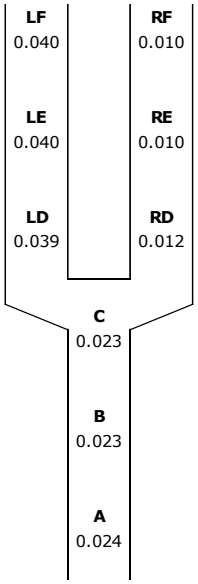


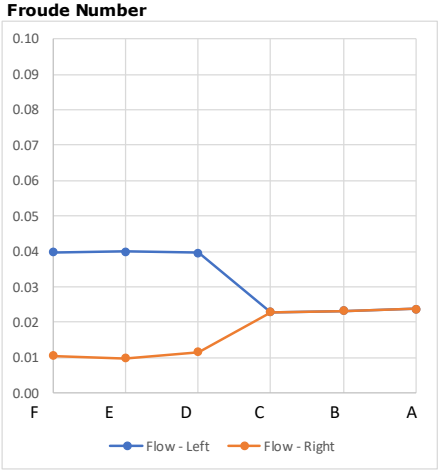
Froude: 40_03_5055



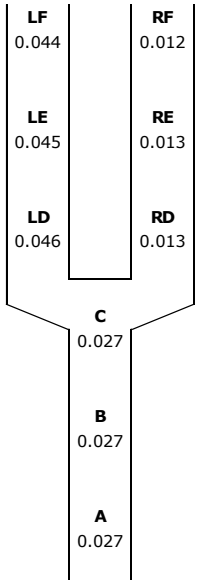


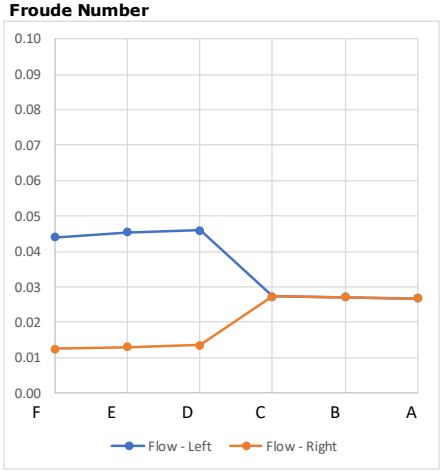
Froude: 40_05_5055



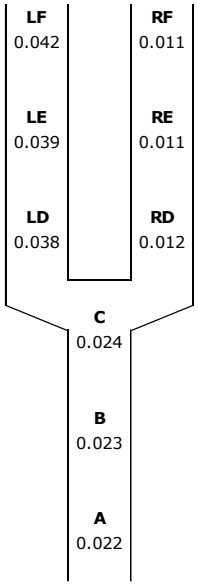


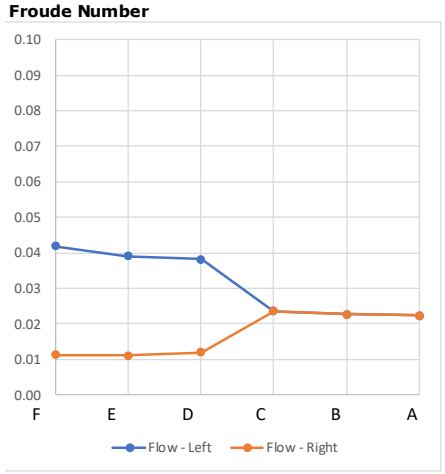
Froude: 40_07_5055



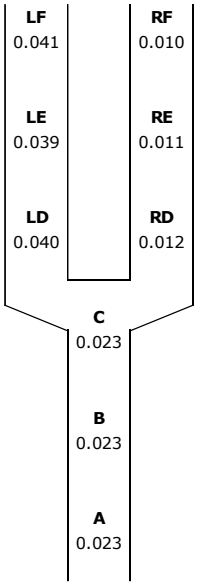


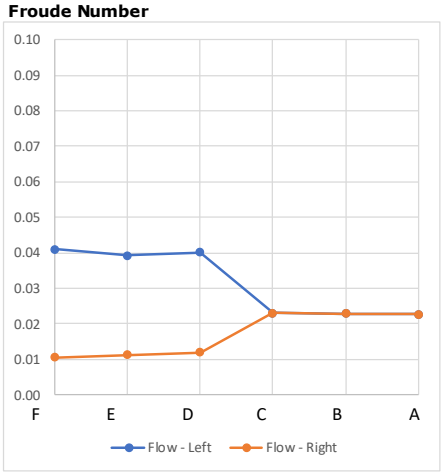
Froude: 50_03_5055



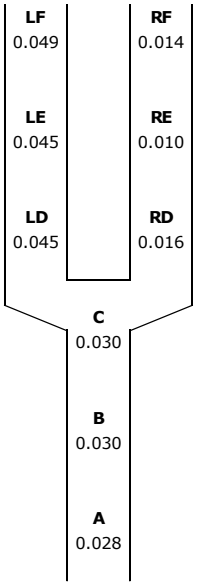


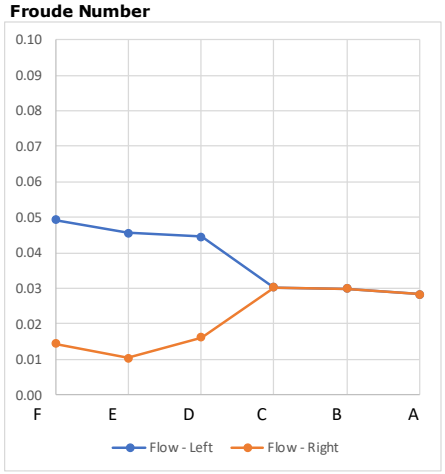
Froude: 50_05_5055





Froude: 50_07_5055

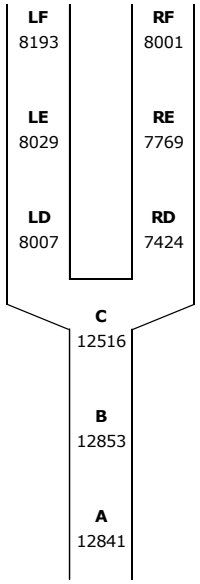


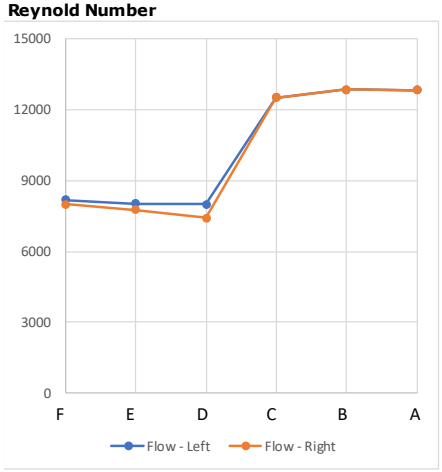


Appendix A9 Reynold Number (Plan and Profile)

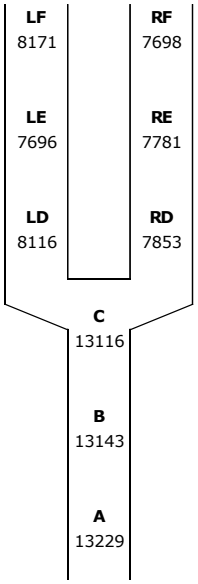
Left Weir Height, mm	Right Weir Height, mm	Bifurcation Angle, °	Slope, %	Name of Run	Page Number
50	50	30	0.3	30_03_5050	A-136
			0.5	30_05_5050	
			0.7	30_07_5050	
		40	0.3	40_03_5050	A-137
			0.5	40_05_5050	
			0.7	40_07_5050	
		50	0.3	50_03_5050	A-138
			0.5	50_05_5050	
			0.7	50_07_5050	
55	60	30	0.3	30_03_5560	A-139
			0.5	30_05_5560	
			0.7	30_07_5560	
		40	0.3	40_03_5560	A-140
			0.5	40_05_5560	
			0.7	40_07_5560	
		50	0.3	50_03_5560	A-141
			0.5	50_05_5560	
			0.7	50_07_5560	
50	55	30	0.3	30_03_5055	A-142
			0.5	30_05_5055	
			0.7	30_07_5055	
		40	0.3	40_03_5055	A-143
			0.5	40_05_5055	
			0.7	40_07_5055	
		50	0.3	50_03_5055	A-144
			0.5	50_05_5055	
			0.7	50_07_5055	

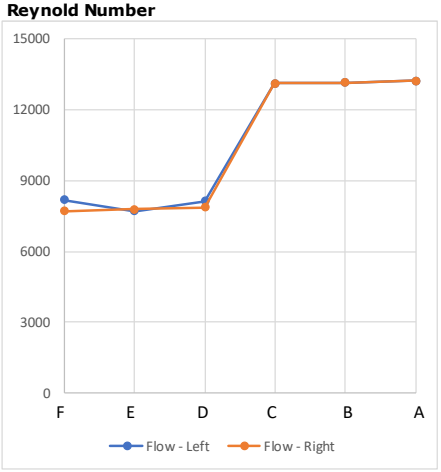
Reynold: 30_03_5050



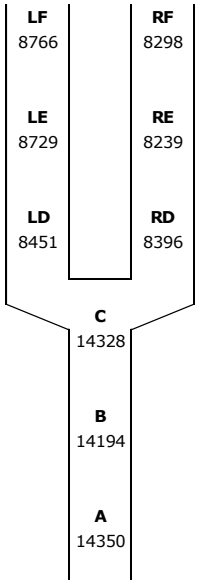


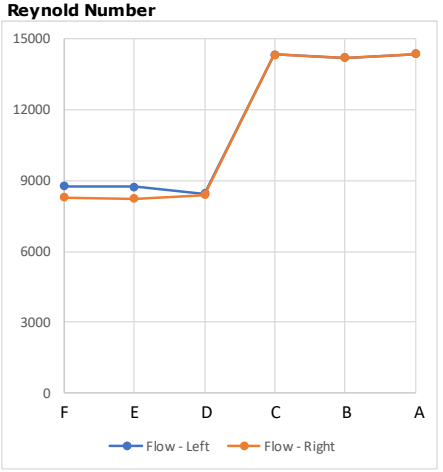
Reynold: 30_05_5050



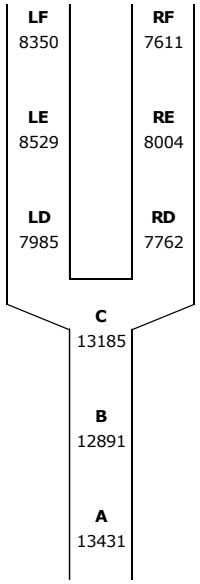


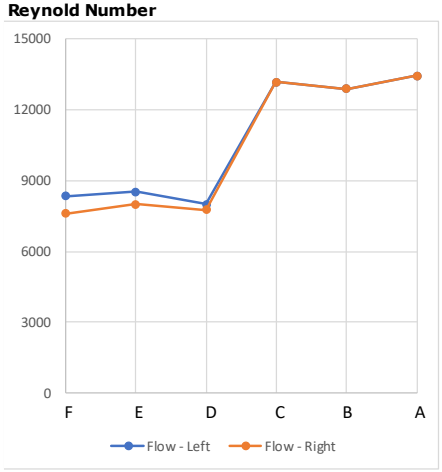
Reynold: 30_07_5050



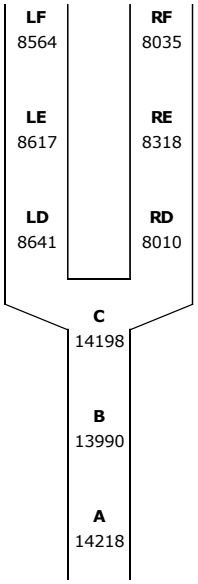


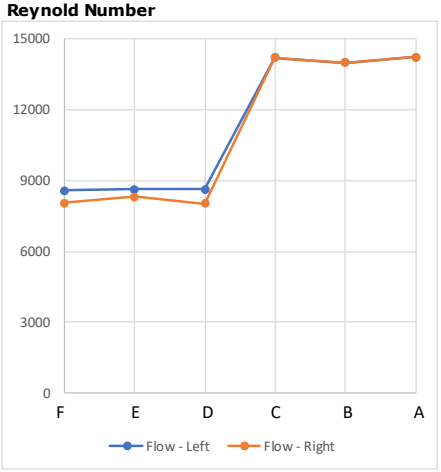
Reynold: 40_03_5050



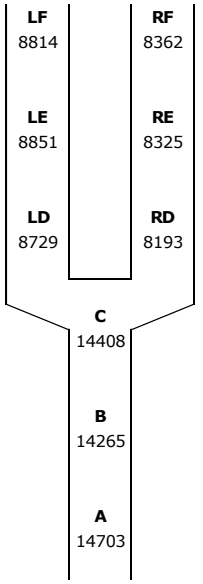


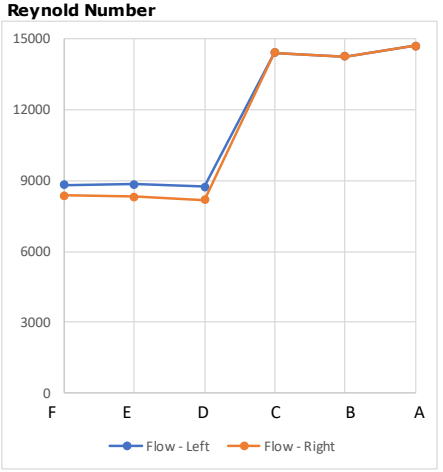
Reynold: 40_05_5050



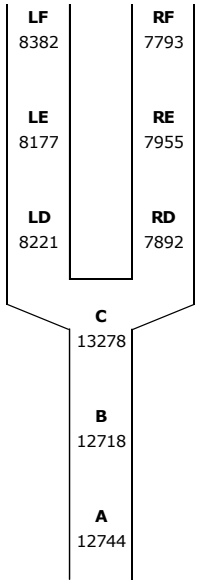


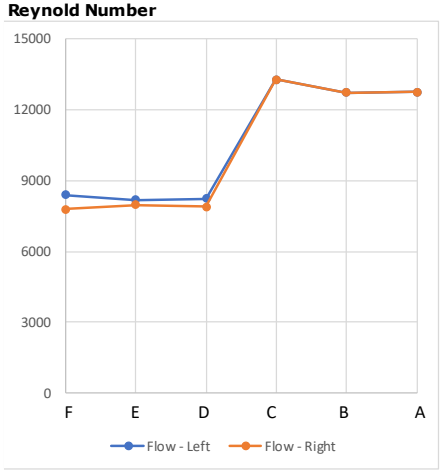
Reynold: 40_07_5050



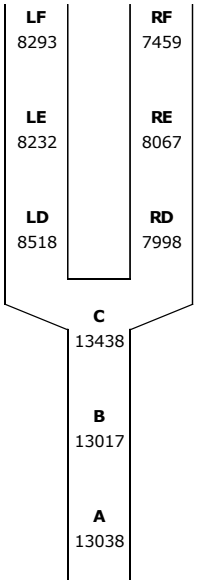


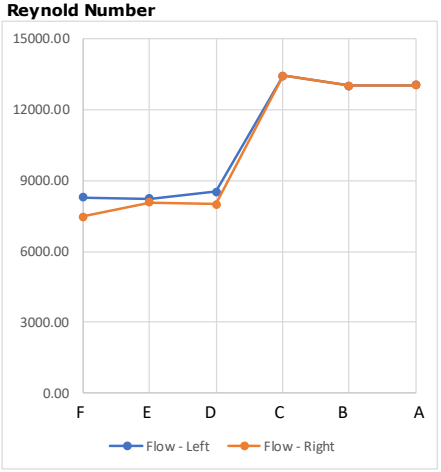
Reynold: 50_03_5050



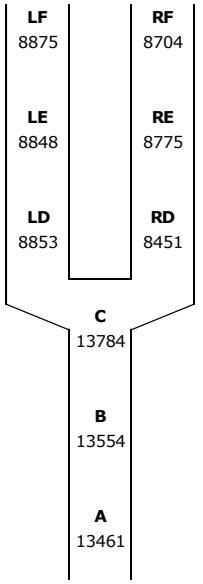


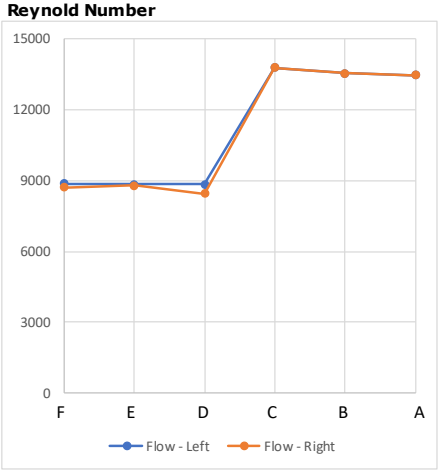
Reynold: 50_05_5050



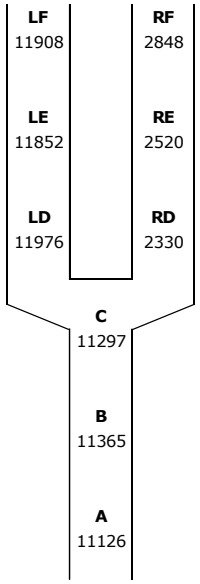


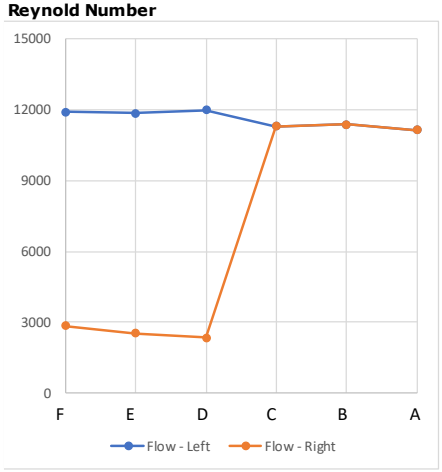
Reynold: 50_07_5050



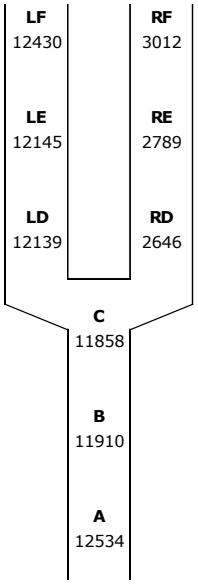


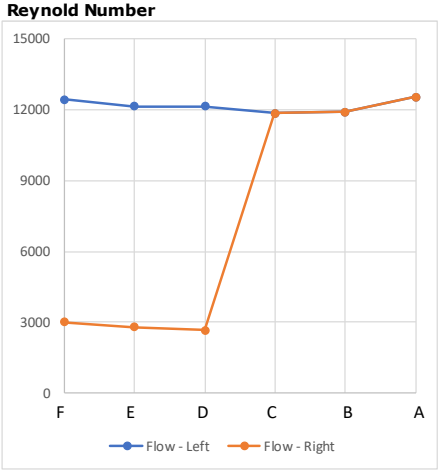
Reynold: 30_03_5560



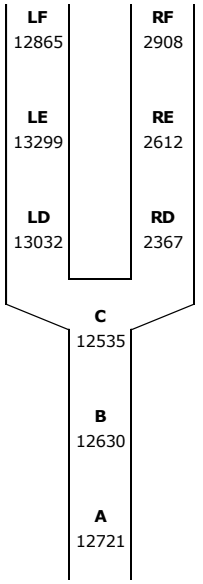


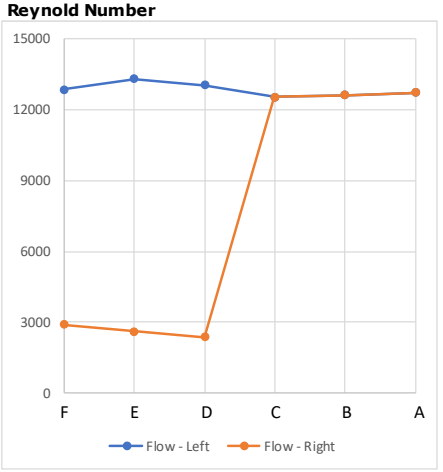
Reynold: 30_05_5560



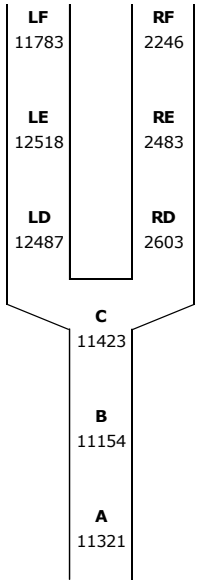


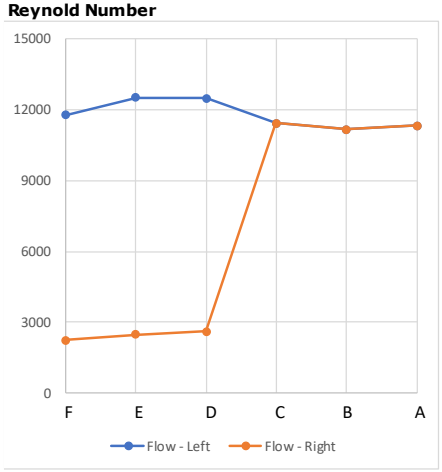
Reynold: 30_07_5560



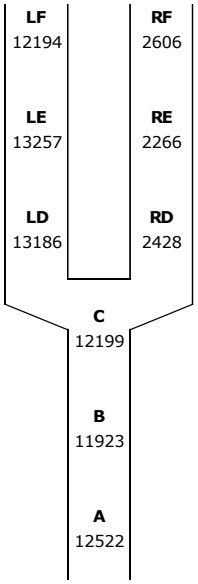


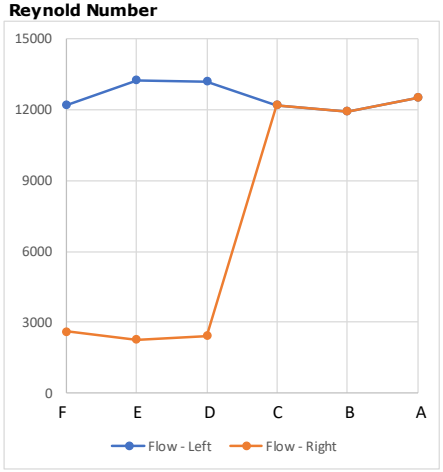
Reynold: 40_03_5560



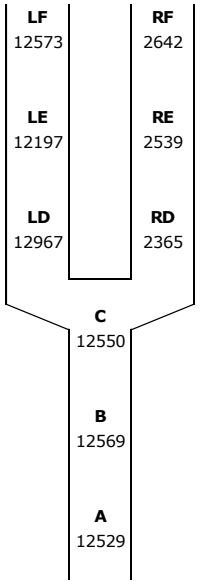


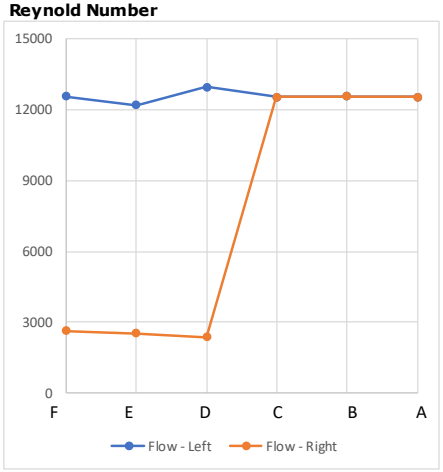
Reynold: 40_05_5560



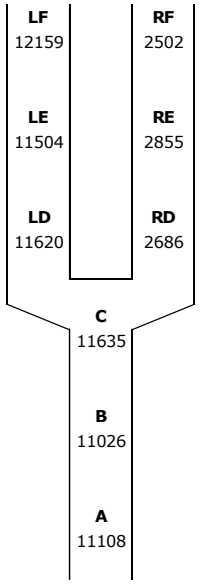


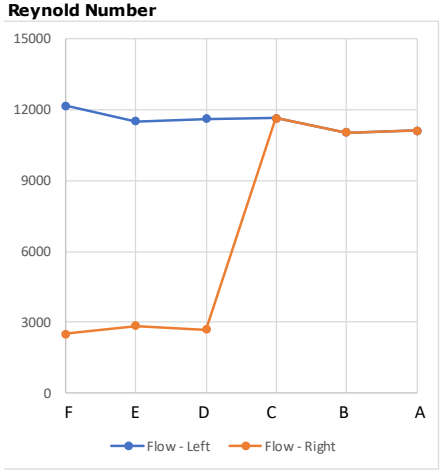
Reynold: 40_07_5560



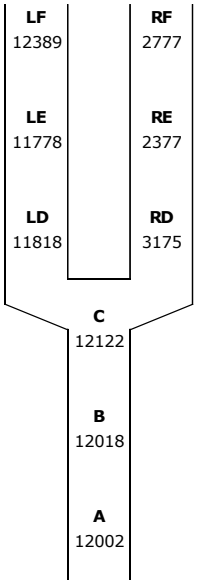


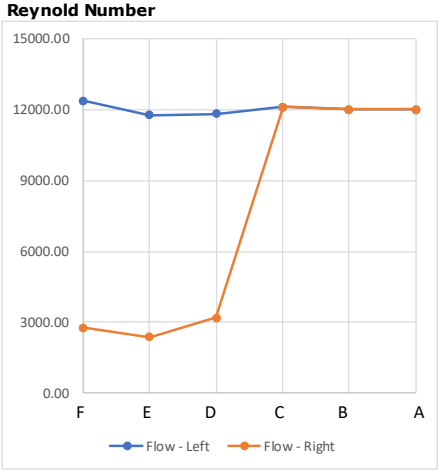
Reynold: 50_03_5560



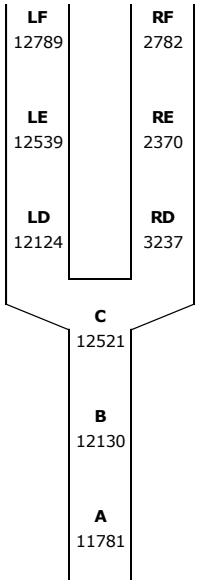


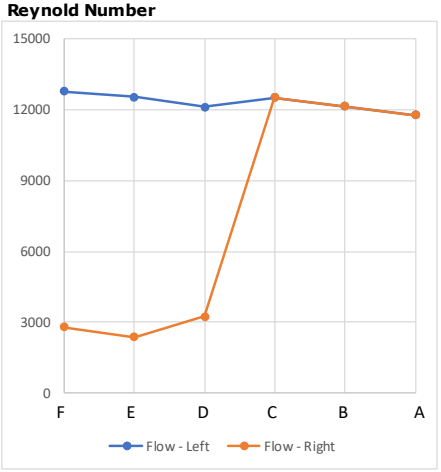
Reynold: 50_05_5560



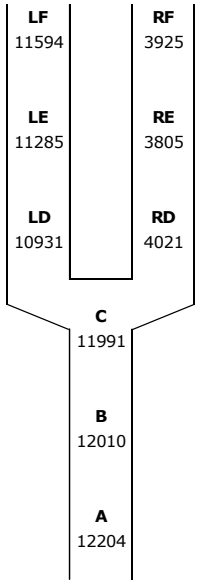


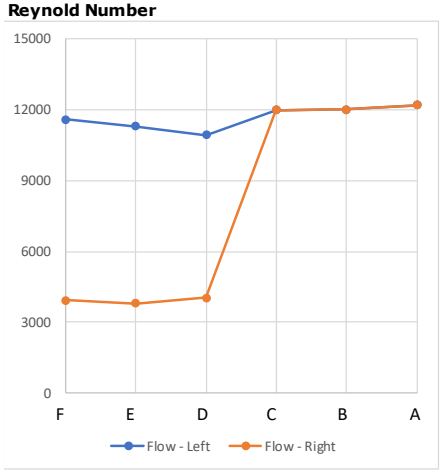
Reynold: 50_07_5560



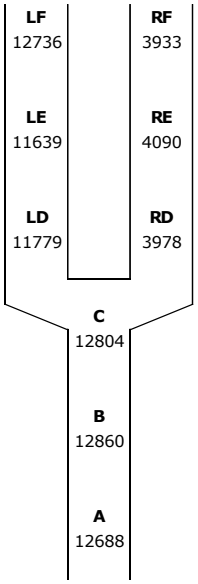


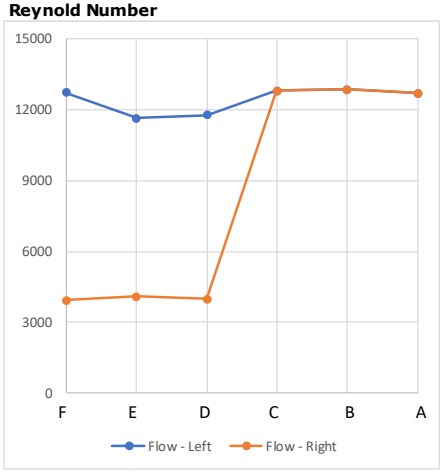
Reynold: 30_03_5055



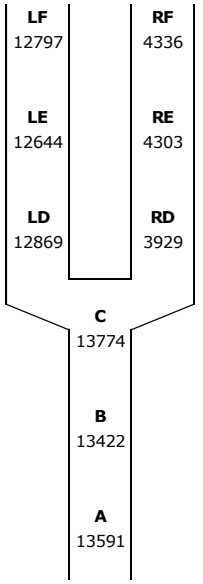


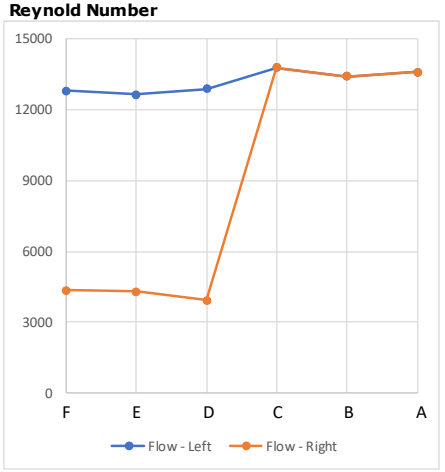
Reynold: 30_05_5055



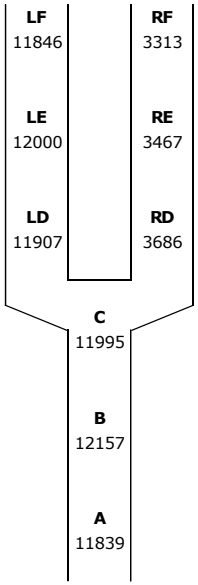


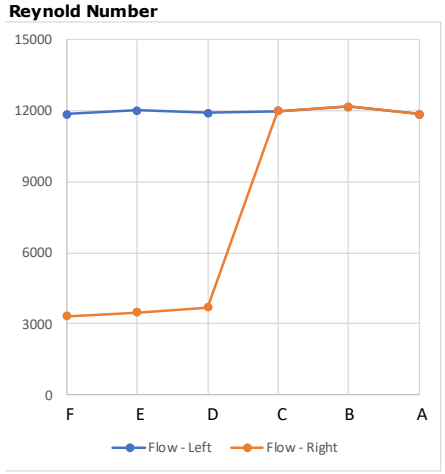
Reynold: 30_07_5055



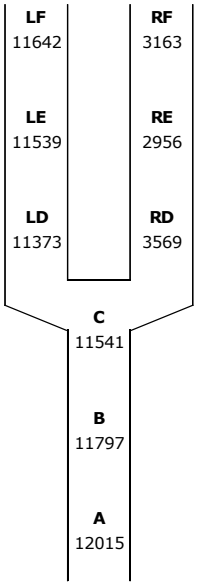


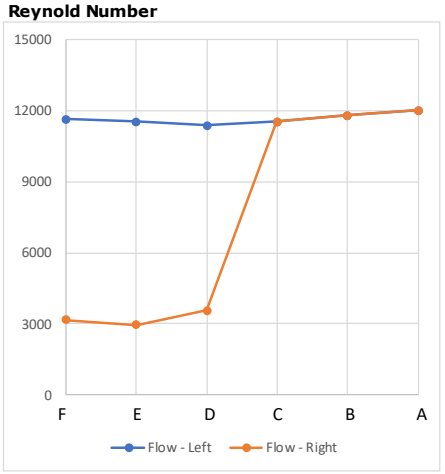
Reynold: 40_03_5055



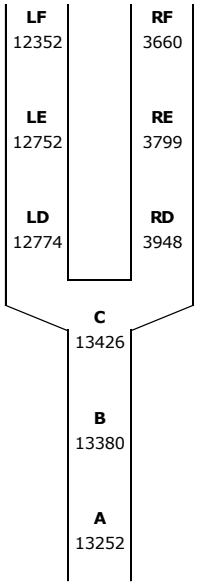


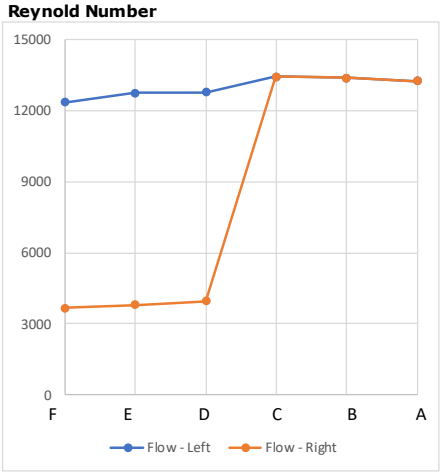
Reynold: 40_05_5055



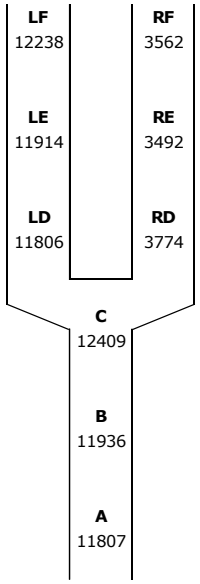


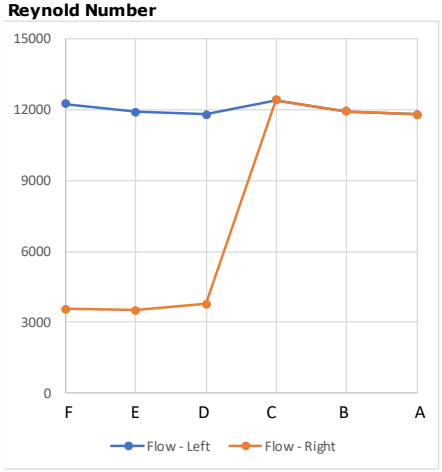
Reynold: 40_07_5055



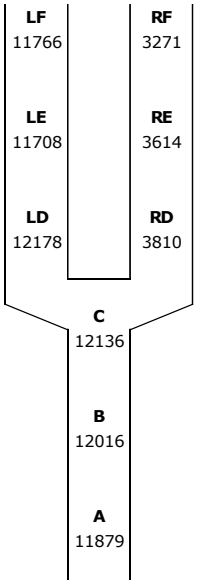


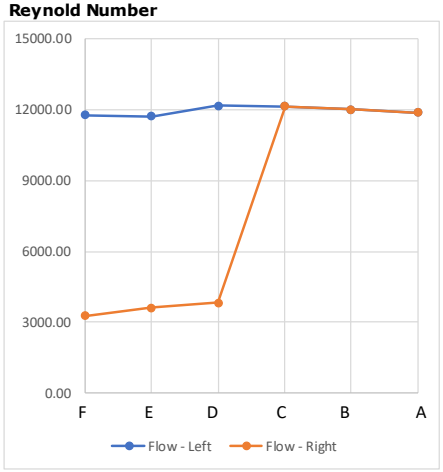
Reynold: 50_03_5055



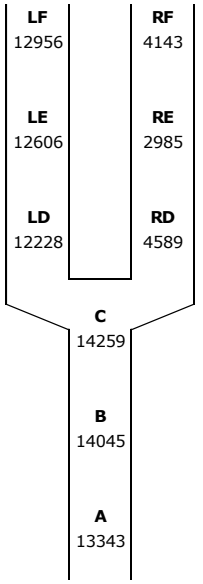


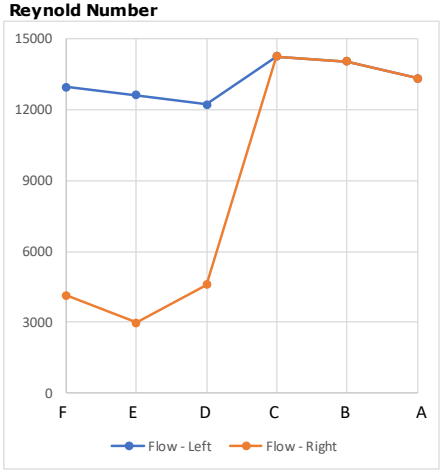
Reynold: 50_05_5055





Reynold: 50_07_5055





Appendix A10 Calculation Sheet

Bifurcation Angle, °	Slope, %	Left Weir Height, mm	Right Weir Height, mm	Name of Run	Page Number
30	0.3	50	50	30_03_5050	A-146
		55	60	30_03_5560	A-147
		50	55	30_03_5055	A-148
	0.5	50	50	30_05_5050	A-149
		55	60	30_05_5560	A-150
		50	55	30_05_5055	A-151
	0.7	50	50	30_07_5050	A-152
		55	60	30_07_5560	A-153
		50	55	30_07_5055	A-154
40	0.3	50	50	40_03_5050	A-155
		55	60	40_03_5560	A-156
		50	55	40_03_5055	A-157
	0.5	50	50	40_05_5050	A-158
		55	60	40_05_5560	A-159
		50	55	40_05_5055	A-160
	0.7	50	50	40_07_5050	A-161
		55	60	40_07_5560	A-162
		50	55	40_07_5055	A-163
50	0.3	50	50	50_03_5050	A-164
		55	60	50_03_5560	A-165
		50	55	50_03_5055	A-166
	0.5	50	50	50_05_5050	A-167
		55	60	50_05_5560	A-168
		50	55	50_05_5055	A-169
	0.7	50	50	50_07_5050	A-170
		55	60	50_07_5560	A-171
		50	55	50_07_5055	A-172

Calculation: 30_03_5050

Downstream

		Subsection Name		L50	L100	L150	L200	R50	R100	R150	R200
		Subsection Width	(mm)	75	50	50	75	75	50	50	75
Section F	A	Velocity	(cm/s)								
	A1	Near Surface Flow		2.22	2.38	2.43	2.42	2.29	2.28	2.23	2.14
	A2	Near Bed Flow		2.01	2.10	2.09	2.00	2.19	2.16	2.03	1.94
	B	Water Depth	(mm)	59.44	59.67	62.11	61.64	59.66	61.69	59.72	60.43
	C	Discharge	(cm3/s)								
	C1	Near Surface Flow		49.38	35.43	37.68	56.05	51.19	35.15	33.36	48.41
	C2	Near Bed Flow		44.85	31.29	32.51	46.23	49.03	33.38	30.31	43.99
	C3	Total Discharge		**94.23**	**66.73**	**70.19**	**102.29**	**100.22**	**68.53**	**63.68**	**92.40**
Section E	A	Velocity	(cm/s)								
	A1	Near Surface Flow		2.15	2.22	2.21	2.31	2.11	2.25	2.15	2.01
	A2	Near Bed Flow		1.95	2.02	2.00	2.11	2.06	2.03	1.91	1.88
	B	Water Depth	(mm)	62.59	64.24	64.74	65.35	64.02	66.23	64.59	63.41
	C	Discharge	(cm3/s)								
	C1	Near Surface Flow		50.53	35.64	35.70	56.71	50.55	37.22	34.67	47.85
	C2	Near Bed Flow		45.65	32.49	32.41	51.69	49.39	33.60	30.87	44.74
	C3	Total Discharge		**96.18**	**68.13**	**68.11**	**108.41**	**99.94**	**70.82**	**65.54**	**92.59**
Section D	A	Velocity	(cm/s)								
	A1	Near Surface Flow		2.26	2.28	2.38	2.42	2.25	2.23	2.07	2.03
	A2	Near Bed Flow		1.77	1.78	1.98	1.95	1.82	1.84	1.87	1.49
	B	Water Depth	(mm)	63.99	64.64	66.09	66.88	65.29	65.36	66.84	64.11
	C	Discharge	(cm3/s)								
	C1	Near Surface Flow		54.32	36.82	39.26	60.76	55.06	36.48	34.57	48.90
	C2	Near Bed Flow		42.55	28.74	32.70	48.90	44.64	30.01	31.17	35.77
	C3	Total Discharge		**96.87**	**65.56**	**71.96**	**109.67**	**99.70**	**66.49**	**65.74**	**84.66**

Upstream

		Subsection Name		U50	U100	U150	U200	U250	U300	U350	U400	U450
		Subsection Width	(mm)	75	50	50	50	50	50	50	50	75
Section C	A	Velocity	(cm/s)									
	A1	Near Surface Flow		2.21	2.16	1.87	2.12	2.22	2.44	2.48	2.57	2.23
	A2	Near Bed Flow		1.62	1.63	1.66	1.74	1.78	1.69	1.73	1.82	1.75
	B	Water Depth	(mm)	65.35	64.2	64.78	65.36	66.34	64.56	65.39	65.01	65.77
	C	Discharge	(cm3/s)									
	C1	Near Surface Flow		54.21	34.72	30.27	34.67	36.75	39.46	40.57	41.83	55.07
	C2	Near Bed Flow		39.67	26.09	26.88	28.38	29.52	27.33	28.30	29.65	43.28
	C3	Total Discharge		**93.88**	**60.81**	**57.15**	**63.05**	**66.27**	**66.79**	**68.86**	**71.47**	**98.35**
Section B	A	Velocity	(cm/s)									
	A1	Near Surface Flow		2.33	2.40	2.41	2.40	2.48	2.55	2.60	2.60	2.58
	A2	Near Bed Flow		1.06	1.26	1.32	1.38	1.48	1.95	1.91	1.73	2.26
	B	Water Depth	(mm)	64.77	64.86	64.59	64.12	64.71	66.04	67.11	66.21	64.63
	C	Discharge	(cm3/s)									
	C1	Near Surface Flow		56.67	38.94	38.88	38.43	40.10	42.03	43.70	42.96	62.46
	C2	Near Bed Flow		25.85	20.40	21.33	22.16	23.91	32.16	32.12	28.58	54.80
	C3	Total Discharge		**82.52**	**59.34**	**60.22**	**60.59**	**64.01**	**74.19**	**75.82**	**71.54**	**117.27**
Section A	A	Velocity	(cm/s)									
	A1	Near Surface Flow		1.89	1.90	2.38	2.15	2.54	2.51	2.60	2.66	2.90
	A2	Near Bed Flow		1.19	1.31	1.41	1.58	1.70	1.90	1.94	2.05	2.00
	B	Water Depth	(mm)	66.03	66.38	66.54	66.74	66.30	66.06	64.88	63.84	64.23
	C	Discharge	(cm3/s)									
	C1	Near Surface Flow		46.88	31.45	39.53	35.81	42.13	41.38	42.23	42.46	69.78
	C2	Near Bed Flow		29.54	21.70	23.52	26.32	28.12	31.44	31.52	32.77	48.25
	C3	Total Discharge		**76.42**	**53.16**	**63.05**	**62.13**	**70.25**	**72.82**	**73.74**	**75.23**	**118.03**

Water Depth

Average Water Depth, cm		Depth Ratio
LF	RF	RF/LF
6.07	6.04	0.99

Average Water Depth, cm		Depth Ratio
LE	RE	RE/LE
6.42	6.46	0.99

Average Water Depth, cm		Depth Ratio
LD	RD	RD/LD
6.54	6.54	1.00

Average Water Depth, cm
C
6.52

Average Water Depth, cm
B
6.52

Average Water Depth, cm
A
6.57

Velocity

Average Velocity, cm/s		Velocity Ratio
LF	RF	RF/LF
2.36	2.23	0.95
2.05	2.08	0.99

Average Velocity, cm/s		Velocity Ratio
LE	RE	RF/LF
2.22	2.13	0.96
2.02	1.97	0.98

Average Velocity, cm/s		Velocity Ratio
LD	RD	RF/LF
2.34	2.15	0.92
1.87	1.75	0.94

Average Velocity, cm/s
C
2.26
1.71

Average Velocity, cm/s
B
2.48
1.59

Average Velocity, cm/s
A
2.39
1.68

Discharge

Sum of Discharge, cm3/s			Discharge Ratio
LF	RF	LF+RF	RF/LF
333.4	324.8	658.3	0.97

Sum of Discharge, cm3/s			Discharge Ratio
LE	RE	LE+RE	RE/LE
340.8	328.9	669.7	0.96

Sum of Discharge, cm3/s			Discharge Ratio
LD	RD	LD+RD	RD/LD
344.1	316.6	660.6	0.92

Sum of Discharge, cm3/s
C
646.6

Sum of Discharge, cm3/s
B
665.5

Sum of Discharge, cm3/s
A
664.8

Froude

Froude Number	
LF	RF
0.0286	0.0280

Froude Number	
LE	RE
0.0267	0.0257

Froude Number	
LD	RD
0.0263	0.0243

Froude Number
C
0.0248

Froude Number
B
0.0255

Froude Number
A
0.0253

Reynold

Reynold Number	
LF	RF
8193	8001

Reynold Number	
LE	RE
8029	7769

Reynold Number	
LD	RD
8007	7424

Reynold Number
C
12516

Reynold Number
B
12853

Reynold Number
A
12841

Calculation: 30_03_5560

Downstream

		Subsection Name		L50	L100	L150	L200	R50	R100	R150	R200
		Subsection Width	(mm)	75	50	50	75	75	50	50	75
Section F	A	Velocity	(cm/s)								
	A1	Near Surface Flow		3.58	3.43	3.51	3.27	1.11	0.93	0.79	0.51
	A2	Near Bed Flow		2.81	2.77	2.68	2.49	0.88	0.69	0.50	0.31
	B	Water Depth	(mm)	67.64	68.92	69.50	70.19	73.43	74.58	73.97	73.34
	C	Discharge	(cm3/s)								
	C1	Near Surface Flow		90.82	59.16	60.91	86.09	30.58	17.37	14.70	14.01
	C2	Near Bed Flow		71.26	47.79	46.63	65.45	24.36	12.86	9.24	8.48
	C3	Total Discharge		**162.08**	**106.96**	**107.54**	**151.54**	**54.94**	**30.23**	**23.93**	**22.49**
Section E	A	Velocity	(cm/s)								
	A1	Near Surface Flow		3.18	3.13	3.21	3.20	1.15	0.91	0.86	0.67
	A2	Near Bed Flow		2.93	2.94	2.83	2.66	0.43	0.39	0.35	0.30
	B	Water Depth	(mm)	69.63	70.84	73.59	73.59	73.59	76.10	73.59	73.95
	C	Discharge	(cm3/s)								
	C1	Near Surface Flow		82.95	55.45	59.04	88.18	31.73	17.38	15.89	18.56
	C2	Near Bed Flow		76.58	52.14	52.04	73.33	11.82	7.33	6.35	8.38
	C3	Total Discharge		**159.53**	**107.59**	**111.08**	**161.52**	**43.55**	**24.72**	**22.24**	**26.94**
Section D	A	Velocity	(cm/s)								
	A1	Near Surface Flow		3.15	3.24	3.30	3.32	0.81	0.83	0.67	0.61
	A2	Near Bed Flow		2.72	3.00	2.62	2.83	0.62	0.53	0.37	0.23
	B	Water Depth	(mm)	71.67	72.95	74.00	74.24	74.93	75.68	76.82	72.61
	C	Discharge	(cm3/s)								
	C1	Near Surface Flow		84.56	59.13	61.04	92.34	22.63	15.69	12.86	16.49
	C2	Near Bed Flow		73.13	54.73	48.38	78.65	17.41	10.12	7.11	6.14
	C3	Total Discharge		**157.69**	**113.86**	**109.42**	**170.99**	**40.03**	**25.81**	**19.97**	**22.63**

Upstream

		Subsection Name		U50	U100	U150	U200	U250	U300	U350	U400	U450
		Subsection Width	(mm)	75	50	50	50	50	50	50	50	75
Section C	A	Velocity	(cm/s)									
	A1	Near Surface Flow		1.81	1.91	1.90	2.07	1.87	1.92	1.89	1.81	1.74
	A2	Near Bed Flow		1.68	1.63	1.56	1.58	1.57	1.49	1.52	1.60	1.63
	B	Water Depth	(mm)	77.01	76.11	76.68	76.72	77.28	75.21	75.73	75.23	76.33
	C	Discharge	(cm3/s)									
	C1	Near Surface Flow		52.17	36.31	36.40	39.72	36.17	36.03	35.69	33.96	49.92
	C2	Near Bed Flow		48.49	30.98	29.90	30.26	30.31	28.11	28.86	30.02	46.54
	C3	Total Discharge		**100.66**	**67.29**	**66.31**	**69.98**	**66.49**	**64.14**	**64.56**	**63.97**	**96.46**
Section B	A	Velocity	(cm/s)									
	A1	Near Surface Flow		2.17	2.17	2.14	2.16	2.12	2.11	2.12	2.18	2.16
	A2	Near Bed Flow		1.21	1.21	1.21	1.41	1.49	1.40	1.38	1.37	1.35
	B	Water Depth	(mm)	75.51	75.51	75.79	75.07	75.67	76.94	77.57	77.14	75.56
	C	Discharge	(cm3/s)									
	C1	Near Surface Flow		61.56	41.03	40.48	40.61	40.17	40.61	41.15	42.08	61.13
	C2	Near Bed Flow		34.33	22.75	22.86	26.43	28.17	27.02	26.77	26.40	38.22
	C3	Total Discharge		**95.89**	**63.78**	**63.34**	**67.04**	**68.34**	**67.64**	**67.92**	**68.48**	**99.35**
Section A	A	Velocity	(cm/s)									
	A1	Near Surface Flow		2.11	1.95	2.01	2.11	2.15	2.11	2.28	2.30	2.24
	A2	Near Bed Flow		1.00	1.05	1.14	1.18	1.20	1.42	1.37	1.45	1.64
	B	Water Depth	(mm)	76.42	76.71	76.84	76.80	76.68	76.41	75.35	74.40	74.80
	C	Discharge	(cm3/s)									
	C1	Near Surface Flow		60.43	37.48	38.69	40.48	41.25	40.31	42.93	42.76	62.71
	C2	Near Bed Flow		28.57	20.10	21.83	22.70	22.92	27.18	25.89	26.94	46.09
	C3	Total Discharge		**88.99**	**57.59**	**60.52**	**63.18**	**64.17**	**67.49**	**68.82**	**69.71**	**108.80**

Water Depth

Section F

Average Water Depth, cm		Depth Ratio
LF	RF	RF/LF
6.91	7.38	0.94

Section E

Average Water Depth, cm		Depth Ratio
LE	RE	RE/LE
7.19	7.43	0.97

Section D

Average Water Depth, cm		Depth Ratio
LD	RD	RD/LD
7.32	7.50	0.98

Section C

Average Water Depth, cm
C
7.63

Section B

Average Water Depth, cm
B
7.61

Section A

Average Water Depth, cm
A
7.60

Velocity

Section F

Average Velocity, cm/s		Velocity Ratio
LF	RF	RF/LF
3.45	0.84	0.24
2.69	0.60	0.22

Section E

Average Velocity, cm/s		Velocity Ratio
LE	RE	RF/LF
3.18	0.90	0.28
2.84	0.37	0.13

Section D

Average Velocity, cm/s		Velocity Ratio
LD	RD	RF/LF
3.25	0.73	0.22
2.79	0.44	0.16

Section C

Average Velocity, cm/s
C
1.88
1.58

Section B

Average Velocity, cm/s
B
2.15
1.34

Section A

Average Velocity, cm/s
A
2.14
1.27

Discharge

Section F

Sum of Discharge, cm3/s			Discharge Ratio
LF	RF	LF+RF	RF/LF
528.1	131.6	659.7	0.25

Section E

Sum of Discharge, cm3/s			Discharge Ratio
LE	RE	LE+RE	RE/LE
539.7	117.4	657.2	0.22

Section D

Sum of Discharge, cm3/s			Discharge Ratio
LD	RD	LD+RD	RD/LD
552.0	108.4	660.4	0.20

Section C

Sum of Discharge, cm3/s
C
659.9

Section B

Sum of Discharge, cm3/s
B
661.8

Section A

Sum of Discharge, cm3/s
A
649.3

Froude

Section F

Froude Number	
LF	RF
0.0373	0.0084

Section E

Froude Number	
LE	RE
0.0358	0.0074

Section D

Froude Number	
LD	RD
0.0356	0.0068

Section C

Froude Number
C
0.0200

Section B

Froude Number
B
0.0202

Section A

Froude Number
A
0.0198

Reynold

Section F

Reynold Number	
LF	RF
11908	2848

Section E

Reynold Number	
LE	RE
11852	2520

Section D

Reynold Number	
LD	RD
11976	2330

Section C

Reynold Number
C
11297

Section B

Reynold Number
B
11365

Section A

Reynold Number
A
11126

Calculation: 30_03_5055

Downstream

		Subsection Name		L50	L100	L150	L200	R50	R100	R150	R200
		Subsection Width	(mm)	75	50	50	75	75	50	50	75
Section F	A	Velocity	(cm/s)								
	A1	Near Surface Flow		3.32	3.36	3.47	3.41	1.33	1.21	1.14	1.02
	A2	Near Bed Flow		2.82	3.01	2.75	2.53	1.11	0.91	0.82	0.61
	B	Water Depth	(mm)	62.13	62.30	63.87	63.50	66.44	68.96	66.84	67.84
	C	Discharge	(cm3/s)								
	C1	Near Surface Flow		77.33	52.33	55.47	81.10	33.20	20.88	19.10	26.08
	C2	Near Bed Flow		65.63	46.91	43.93	60.35	27.57	15.75	13.66	15.41
	C3	Total Discharge		**142.97**	**99.24**	**99.41**	**141.45**	**60.77**	**36.63**	**32.76**	**41.49**
Section E	A	Velocity	(cm/s)								
	A1	Near Surface Flow		3.10	3.08	3.23	3.10	1.25	1.09	0.87	0.85
	A2	Near Bed Flow		2.52	2.77	2.89	2.78	1.07	0.99	0.88	0.85
	B	Water Depth	(mm)	67.77	67.53	67.63	66.80	68.05	68.46	70.00	69.15
	C	Discharge	(cm3/s)								
	C1	Near Surface Flow		78.79	51.93	54.58	77.54	31.83	18.58	15.28	22.16
	C2	Near Bed Flow		64.12	46.73	48.84	69.57	27.41	16.91	15.41	21.94
	C3	Total Discharge		**142.91**	**98.66**	**103.42**	**147.11**	**59.24**	**35.49**	**30.69**	**44.09**
Section D	A	Velocity	(cm/s)								
	A1	Near Surface Flow		2.54	2.72	2.92	2.91	0.78	1.43	1.18	0.82
	A2	Near Bed Flow		2.76	2.90	3.00	2.96	0.97	1.23	1.28	0.60
	B	Water Depth	(mm)	66.31	66.88	68.30	68.90	68.96	68.28	70.82	67.39
	C	Discharge	(cm3/s)								
	C1	Near Surface Flow		63.14	45.50	49.81	75.23	20.23	24.43	20.96	20.63
	C2	Near Bed Flow		68.54	48.44	51.30	76.35	25.17	21.04	22.61	15.15
	C3	Total Discharge		**131.68**	**93.93**	**101.11**	**151.58**	**45.41**	**45.47**	**43.58**	**35.79**

Upstream

		Subsection Name		U50	U100	U150	U200	U250	U300	U350	U400	U450
		Subsection Width	(mm)	75	50	50	50	50	50	50	50	75
Section C	A	Velocity	(cm/s)									
	A1	Near Surface Flow		1.82	2.15	2.04	2.03	2.09	2.19	2.15	2.18	2.13
	A2	Near Bed Flow		1.77	1.58	1.58	1.58	1.68	1.74	1.67	1.88	1.52
	B	Water Depth	(mm)	69.63	67.72	68.90	69.71	71.21	69.04	69.84	69.46	71.07
	C	Discharge	(cm3/s)									
	C1	Near Surface Flow		47.53	36.43	35.18	35.34	37.13	37.85	37.61	37.83	56.78
	C2	Near Bed Flow		46.21	26.71	27.17	27.45	29.93	29.98	29.12	32.58	40.52
	C3	Total Discharge		**93.74**	**63.13**	**62.35**	**62.79**	**67.06**	**67.83**	**66.73**	**70.42**	**97.30**
Section B	A	Velocity	(cm/s)									
	A1	Near Surface Flow		2.14	2.25	2.18	2.38	2.66	2.61	2.56	2.59	2.51
	A2	Near Bed Flow		1.08	1.09	1.11	1.33	1.35	1.46	1.58	1.53	1.40
	B	Water Depth	(mm)	69.04	68.63	69.31	68.62	69.40	70.54	71.31	70.47	69.81
	C	Discharge	(cm3/s)									
	C1	Near Surface Flow		55.52	38.62	37.71	40.80	46.14	45.95	45.71	45.70	65.70
	C2	Near Bed Flow		27.92	18.74	19.23	22.89	23.49	25.68	28.17	26.94	36.55
	C3	Total Discharge		**83.44**	**57.36**	**56.93**	**63.69**	**69.63**	**71.63**	**73.88**	**72.64**	**102.25**
Section A	A	Velocity	(cm/s)									
	A1	Near Surface Flow		1.66	1.80	2.13	2.08	2.16	2.33	2.39	2.61	2.37
	A2	Near Bed Flow		1.28	1.27	1.45	1.58	1.65	1.81	1.90	1.92	1.93
	B	Water Depth	(mm)	70.32	70.60	70.78	70.78	70.60	70.32	70.14	68.10	68.18
	C	Discharge	(cm3/s)									
	C1	Near Surface Flow		43.67	31.74	37.64	36.82	38.05	41.01	41.98	44.51	60.67
	C2	Near Bed Flow		33.66	22.44	25.65	28.01	29.14	31.86	33.29	32.73	49.38
	C3	Total Discharge		**77.33**	**54.18**	**63.29**	**64.82**	**67.18**	**72.88**	**75.27**	**77.23**	**110.05**

Water Depth

Average Water Depth, cm		Depth Ratio
LF	RF	RF/LF
6.30	6.75	0.93

Average Water Depth, cm		Depth Ratio
LE	RE	RE/LE
6.74	6.89	0.98

Average Water Depth, cm		Depth Ratio
LD	RD	RD/LD
6.76	6.89	0.98

Average Water Depth, cm
C
6.96

Average Water Depth, cm
B
6.97

Average Water Depth, cm
A
7.00

Velocity

Average Velocity, cm/s		Velocity Ratio
LF	RF	RF/LF
3.39	1.18	0.35
2.78	0.86	0.31

Average Velocity, cm/s		Velocity Ratio
LE	RE	RF/LF
3.12	1.02	0.32
2.74	0.95	0.35

Average Velocity, cm/s		Velocity Ratio
LD	RD	RF/LF
2.77	1.05	0.38
2.90	1.02	0.35

Average Velocity, cm/s
C
2.09
1.66

Average Velocity, cm/s
B
2.43
1.33

Average Velocity, cm/s
A
2.17
1.64

Discharge

Sum of Discharge, cm3/s			Discharge Ratio
LF	RF	LF+RF	RF/LF
483.1	171.7	654.7	0.36

Sum of Discharge, cm3/s			Discharge Ratio
LE	RE	LE+RE	RE/LE
492.1	169.5	661.6	0.34

Sum of Discharge, cm3/s			Discharge Ratio
LD	RD	LD+RD	RD/LD
478.3	170.2	648.5	0.36

Sum of Discharge, cm3/s
C
651.3

Sum of Discharge, cm3/s
B
651.5

Sum of Discharge, cm3/s
A
662.2

Froude

Froude Number	
LF	RF
0.0392	0.0125

Froude Number	
LE	RE
0.0361	0.0119

Froude Number	
LD	RD
0.0348	0.0126

Froude Number
C
0.0227

Froude Number
B
0.0227

Froude Number
A
0.0230

Reynold

Reynold Number	
LF	RF
11594	3925

Reynold Number	
LE	RE
11285	3805

Reynold Number	
LD	RD
10931	4021

Reynold Number
C
11991

Reynold Number
B
12010

Reynold Number
A
12204

Calculation: 30_05_5050

Downstream

	Subsection Name		L50	L100	L150	L200	R50	R100	R150	R200
	Subsection Width	(mm)	75	50	50	75	75	50	50	75
Section F	A Velocity	(cm/s)								
	A1 Near Surface Flow		2.54	2.60	2.58	2.52	2.45	2.38	2.20	1.94
	A2 Near Bed Flow		1.61	1.94	1.96	2.12	2.11	2.06	1.95	1.78
	B Water Depth	(mm)	56.94	57.11	58.41	59.37	56.27	57.97	57.17	58.3
	C Discharge	(cm3/s)								
	C1 Near Surface Flow		54.32	37.05	37.68	56.11	51.79	34.52	31.48	42.50
	C2 Near Bed Flow		34.35	27.69	28.62	47.15	44.45	29.79	27.88	38.99
	C3 Total Discharge		**88.67**	**64.74**	**66.29**	**103.26**	**96.24**	**64.31**	**59.36**	**81.49**
Section E	A Velocity	(cm/s)								
	A1 Near Surface Flow		1.93	2.15	2.20	2.24	2.38	2.34	2.18	1.97
	A2 Near Bed Flow		1.87	1.95	2.07	2.08	2.08	1.99	1.89	1.87
	B Water Depth	(mm)	60.56	61.17	62.55	62.48	60.02	61.25	62.38	61.29
	C Discharge	(cm3/s)								
	C1 Near Surface Flow		43.72	32.94	34.35	52.41	53.66	35.77	34.02	45.27
	C2 Near Bed Flow		42.44	29.88	32.36	48.83	46.88	30.48	29.55	43.03
	C3 Total Discharge		**86.17**	**62.82**	**66.71**	**101.24**	**100.53**	**66.26**	**63.57**	**88.30**
Section D	A Velocity	(cm/s)								
	A1 Near Surface Flow		2.13	2.40	2.51	2.54	2.24	2.35	2.41	2.42
	A2 Near Bed Flow		1.76	1.98	2.01	2.07	1.70	1.80	1.95	1.92
	B Water Depth	(mm)	59.98	61.14	62.26	62.99	62.22	61.48	63.39	60.76
	C Discharge	(cm3/s)								
	C1 Near Surface Flow		47.94	36.72	39.08	59.96	52.33	36.05	38.21	55.25
	C2 Near Bed Flow		39.58	30.19	31.27	48.95	39.68	27.69	30.92	43.84
	C3 Total Discharge		**87.52**	**66.91**	**70.34**	**108.91**	**92.01**	**63.73**	**69.13**	**99.08**

Upstream

	Subsection Name		U50	U100	U150	U200	U250	U300	U350	U400	U450
	Subsection Width	(mm)	75	50	50	50	50	50	50	50	75
Section C	A Velocity	(cm/s)									
	A1 Near Surface Flow		2.11	1.99	2.12	2.15	2.21	2.23	2.44	2.31	2.09
	A2 Near Bed Flow		1.88	1.73	1.87	1.91	2.05	2.09	2.31	2.03	2.20
	B Water Depth	(mm)	63.72	61.18	62.09	63.11	64.18	62.09	63.51	62.1	64.34
	C Discharge	(cm3/s)									
	C1 Near Surface Flow		50.33	30.49	32.84	33.85	35.39	34.67	38.69	35.92	50.42
	C2 Near Bed Flow		44.84	26.50	29.05	30.17	32.95	32.46	36.70	31.49	53.19
	C3 Total Discharge		**95.17**	**57.00**	**61.89**	**64.02**	**68.33**	**67.13**	**75.39**	**67.41**	**103.62**
Section B	A Velocity	(cm/s)									
	A1 Near Surface Flow		2.08	2.15	2.04	2.20	2.24	2.34	2.58	2.67	2.42
	A2 Near Bed Flow		1.58	1.59	1.57	1.82	1.88	2.13	2.31	2.19	1.99
	B Water Depth	(mm)	62.12	61.72	61.96	62.05	62.39	63.94	64.51	63.86	62.61
	C Discharge	(cm3/s)									
	C1 Near Surface Flow		48.39	33.21	31.66	34.07	35.01	37.48	41.61	42.65	56.87
	C2 Near Bed Flow		36.91	24.61	24.31	28.25	29.40	34.13	37.23	35.04	46.77
	C3 Total Discharge		**85.29**	**57.82**	**55.97**	**62.32**	**64.41**	**71.60**	**78.84**	**77.69**	**103.64**
Section A	A Velocity	(cm/s)									
	A1 Near Surface Flow		2.33	2.39	2.40	2.46	2.45	2.46	2.51	2.58	2.55
	A2 Near Bed Flow		1.65	1.70	1.75	1.77	1.79	1.81	1.80	1.80	1.88
	B Water Depth	(mm)	63.04	63.44	63.54	63.55	63.32	63.05	62.03	61.23	61.07
	C Discharge	(cm3/s)									
	C1 Near Surface Flow		54.99	37.85	38.09	39.03	38.82	38.84	38.92	39.44	58.50
	C2 Near Bed Flow		38.95	26.98	27.75	28.17	28.31	28.55	27.92	27.53	43.15
	C3 Total Discharge		**93.94**	**64.82**	**65.83**	**67.19**	**67.13**	**67.39**	**66.84**	**66.97**	**101.64**

Water Depth

Section F

Average Water Depth, cm		Depth Ratio
LF	RF	RF/LF
5.80	5.74	0.99

Section E

Average Water Depth, cm		Depth Ratio
LE	RE	RE/LE
6.17	6.12	0.99

Section D

Average Water Depth, cm		Depth Ratio
LD	RD	RD/LD
6.16	6.20	0.99

Section C

Average Water Depth, cm
C
6.29

Section B

Average Water Depth, cm
B
6.28

Section A

Average Water Depth, cm
A
6.27

Velocity

Section F

Average Velocity, cm/s		Velocity Ratio
LF	RF	RF/LF
2.56	2.25	0.88
1.91	1.97	0.97

Section E

Average Velocity, cm/s		Velocity Ratio
LE	RE	RF/LF
2.13	2.22	0.96
1.99	1.96	0.98

Section D

Average Velocity, cm/s		Velocity Ratio
LD	RD	RF/LF
2.40	2.36	0.98
1.95	1.84	0.94

Section C

Average Velocity, cm/s
C
2.18
2.01

Section B

Average Velocity, cm/s
B
2.30
1.90

Section A

Average Velocity, cm/s
A
2.46
1.77

Discharge

Section F

Sum of Discharge, cm3/s			Discharge Ratio
LF	RF	LF+RF	RF/LF
323.0	301.4	624.4	0.93

Section E

Sum of Discharge, cm3/s			Discharge Ratio
LE	RE	LE+RE	RE/LE
316.9	318.7	635.6	0.99

Section D

Sum of Discharge, cm3/s			Discharge Ratio
LD	RD	LD+RD	RD/LD
333.7	324.0	657.6	0.97

Section C

Sum of Discharge, cm3/s
C
659.9

Section B

Sum of Discharge, cm3/s
B
657.6

Section A

Sum of Discharge, cm3/s
A
661.8

Froude

Section F

Froude Number	
LF	RF
0.0296	0.0281

Section E

Froude Number	
LE	RE
0.0265	0.0270

Section D

Froude Number	
LD	RD
0.0280	0.0269

Section C

Froude Number
C
0.0267

Section B

Froude Number
B
0.0268

Section A

Froude Number
A
0.0270

Reynold

Section F

Reynold Number	
LF	RF
8171	7698

Section E

Reynold Number	
LE	RE
7696	7781

Section D

Reynold Number	
LD	RD
8116	7853

Section C

Reynold Number
C
13116

Section B

Reynold Number
B
13143

Section A

Reynold Number
A
13229

Calculation: 30_05_5560

Downstream

		Subsection Name		L50	L100	L150	L200	R50	R100	R150	R200
		Subsection Width	(mm)	75	50	50	75	75	50	50	75
Section F	A	Velocity	(cm/s)								
	A1	Near Surface Flow		3.51	3.68	3.62	3.62	0.97	1.01	0.76	0.74
	A2	Near Bed Flow		2.98	3.00	3.02	2.84	0.87	0.75	0.63	0.49
	B	Water Depth	(mm)	63.42	63.64	64.80	65.51	67.23	69.97	68.61	69.19
	C	Discharge	(cm3/s)								
	C1	Near Surface Flow		83.51	58.52	58.67	88.85	24.54	17.66	13.00	19.09
	C2	Near Bed Flow		70.76	47.66	48.86	69.86	21.95	13.06	10.81	12.82
	C3	Total Discharge		**154.27**	**106.18**	**107.53**	**158.71**	**46.50**	**30.72**	**23.81**	**31.91**
Section E	A	Velocity	(cm/s)								
	A1	Near Surface Flow		3.18	3.27	3.35	3.23	0.84	0.76	0.65	0.64
	A2	Near Bed Flow		2.81	3.09	3.33	3.01	0.93	0.73	0.60	0.59
	B	Water Depth	(mm)	66.89	66.80	67.94	67.56	68.59	69.02	69.82	69.23
	C	Discharge	(cm3/s)								
	C1	Near Surface Flow		79.81	54.60	56.90	81.85	21.68	13.09	11.32	16.72
	C2	Near Bed Flow		70.37	51.58	56.58	76.16	23.88	12.65	10.44	15.36
	C3	Total Discharge		**150.19**	**106.18**	**113.48**	**158.02**	**45.56**	**25.74**	**21.76**	**32.08**
Section D	A	Velocity	(cm/s)								
	A1	Near Surface Flow		3.34	3.47	3.55	3.69	0.95	0.90	0.87	0.91
	A2	Near Bed Flow		2.68	2.91	2.77	2.73	0.47	0.50	0.41	0.42
	B	Water Depth	(mm)	67.15	67.84	69.23	68.56	70.26	69.26	71.38	68.48
	C	Discharge	(cm3/s)								
	C1	Near Surface Flow		84.08	58.84	61.44	94.88	24.97	15.58	15.53	23.49
	C2	Near Bed Flow		67.39	49.40	47.94	70.07	12.46	8.62	7.23	10.86
	C3	Total Discharge		**151.47**	**108.25**	**109.37**	**164.95**	**37.43**	**24.20**	**22.76**	**34.35**

Upstream

		Subsection Name		U50	U100	U150	U200	U250	U300	U350	U400	U450
		Subsection Width	(mm)	75	50	50	50	50	50	50	50	75
Section C	A	Velocity	(cm/s)									
	A1	Near Surface Flow		1.98	1.91	2.09	2.02	2.19	2.05	2.17	2.07	1.94
	A2	Near Bed Flow		1.62	1.58	1.54	1.70	1.71	1.87	1.62	1.73	1.58
	B	Water Depth	(mm)	70.32	67.34	68.30	69.96	71.13	69.59	70.87	69.52	71.02
	C	Discharge	(cm3/s)									
	C1	Near Surface Flow		52.09	32.08	35.61	35.32	39.01	35.70	38.45	35.97	51.80
	C2	Near Bed Flow		42.70	26.58	26.24	29.75	30.35	32.62	28.76	30.13	42.16
	C3	Total Discharge		**94.79**	**58.66**	**61.85**	**65.07**	**69.36**	**68.31**	**67.21**	**66.09**	**93.96**
Section B	A	Velocity	(cm/s)									
	A1	Near Surface Flow		2.05	2.06	2.06	2.08	2.10	2.15	2.16	2.17	2.18
	A2	Near Bed Flow		1.46	1.45	1.49	1.53	1.56	1.76	1.74	1.84	1.72
	B	Water Depth	(mm)	68.79	68.03	68.03	68.86	68.77	70.33	70.82	70.70	69.14
	C	Discharge	(cm3/s)									
	C1	Near Surface Flow		52.81	35.06	35.11	35.84	36.13	37.87	38.28	38.43	56.49
	C2	Near Bed Flow		37.69	24.59	25.41	26.27	26.81	30.96	30.88	32.53	44.49
	C3	Total Discharge		**90.49**	**59.65**	**60.52**	**62.11**	**62.94**	**68.84**	**69.16**	**70.97**	**100.97**
Section A	A	Velocity	(cm/s)									
	A1	Near Surface Flow		2.06	2.05	2.27	2.53	2.80	2.66	2.70	2.66	2.54
	A2	Near Bed Flow		1.16	1.25	1.24	1.29	1.57	1.73	1.63	1.40	1.76
	B	Water Depth	(mm)	69.72	70.01	70.14	70.15	69.95	69.68	68.97	67.72	68.07
	C	Discharge	(cm3/s)									
	C1	Near Surface Flow		53.90	35.95	39.77	44.39	49.04	46.37	46.50	45.07	64.96
	C2	Near Bed Flow		30.43	21.93	21.83	22.55	27.46	30.12	28.03	23.73	44.91
	C3	Total Discharge		**84.33**	**57.88**	**61.60**	**66.94**	**76.51**	**76.49**	**74.52**	**68.81**	**109.87**

Water Depth

Average Water Depth, cm		Depth Ratio
LF	RF	RF/LF
6.43	6.88	0.94

Average Water Depth, cm		Depth Ratio
LE	RE	RE/LE
6.73	6.92	0.97

Average Water Depth, cm		Depth Ratio
LD	RD	RD/LD
6.82	6.98	0.98

Average Water Depth, cm
C
6.98

Average Water Depth, cm
B
6.93

Average Water Depth, cm
A
6.94

Velocity

Average Velocity, cm/s		Velocity Ratio
LF	RF	RF/LF
3.61	0.87	0.24
2.96	0.69	0.23

Average Velocity, cm/s		Velocity Ratio
LE	RE	RF/LF
3.26	0.72	0.22
3.06	0.71	0.23

Average Velocity, cm/s		Velocity Ratio
LD	RD	RF/LF
3.51	0.91	0.26
2.77	0.45	0.16

Average Velocity, cm/s
C
2.05
1.66

Average Velocity, cm/s
B
2.11
1.62

Average Velocity, cm/s
A
2.48
1.45

Discharge

Sum of Discharge, cm3/s			Discharge Ratio
LF	RF	LF+RF	RF/LF
526.7	132.9	659.6	0.25

Sum of Discharge, cm3/s			Discharge Ratio
LE	RE	LE+RE	RE/LE
527.9	125.1	653.0	0.24

Sum of Discharge, cm3/s			Discharge Ratio
LD	RD	LD+RD	RD/LD
534.0	118.7	652.8	0.22

Sum of Discharge, cm3/s
C
645.3

Sum of Discharge, cm3/s
B
645.6

Sum of Discharge, cm3/s
A
677.0

Froude

Froude Number	
LF	RF
0.0413	0.0095

Froude Number	
LE	RE
0.0389	0.0087

Froude Number	
LD	RD
0.0384	0.0082

Froude Number
C
0.0224

Froude Number
B
0.0226

Froude Number
A
0.0238

Reynold

Reynold Number	
LF	RF
12430	3012

Reynold Number	
LE	RE
12145	2789

Reynold Number	
LD	RD
12139	2646

Reynold Number
C
11858

Reynold Number
B
11910

Reynold Number
A
12534

Calculation: 30_05_5055

Downstream

		Subsection Name		L50	L100	L150	L200	R50	R100	R150	R200
		Subsection Width	(mm)	75	50	50	75	75	50	50	75
Section F	A	Velocity	(cm/s)								
	A1	Near Surface Flow		3.77	3.85	3.79	3.65	1.35	1.22	1.00	0.90
	A2	Near Bed Flow		3.15	3.23	3.25	3.01	1.24	1.05	0.85	0.69
	B	Water Depth	(mm)	57.83	57.67	59.75	59.99	63.48	64.98	63.60	65.04
	C	Discharge	(cm3/s)								
	C1	Near Surface Flow		81.69	55.56	56.64	82.21	32.02	19.81	15.96	22.02
	C2	Near Bed Flow		68.37	46.61	48.56	67.75	29.58	17.06	13.57	16.92
	C3	Total Discharge		**150.06**	**102.17**	**105.20**	**149.97**	**61.60**	**36.87**	**29.53**	**38.94**
Section E	A	Velocity	(cm/s)								
	A1	Near Surface Flow		3.27	3.38	3.39	3.29	1.51	1.41	1.17	1.15
	A2	Near Bed Flow		2.78	2.86	2.89	2.79	1.04	1.00	0.75	0.57
	B	Water Depth	(mm)	63.04	63.61	64.26	64.19	64.41	64.90	66.45	65.12
	C	Discharge	(cm3/s)								
	C1	Near Surface Flow		77.30	53.81	54.50	79.28	36.43	22.93	19.35	28.09
	C2	Near Bed Flow		65.72	45.49	46.42	67.22	25.10	16.29	12.46	13.92
	C3	Total Discharge		**143.02**	**99.30**	**100.93**	**146.50**	**61.53**	**39.22**	**31.82**	**42.01**
Section D	A	Velocity	(cm/s)								
	A1	Near Surface Flow		3.22	3.31	3.52	3.52	1.48	1.46	1.47	1.26
	A2	Near Bed Flow		2.74	2.96	2.88	2.80	0.74	0.69	0.71	0.51
	B	Water Depth	(mm)	62.76	63.01	64.38	65.11	66.10	65.28	67.63	64.47
	C	Discharge	(cm3/s)								
	C1	Near Surface Flow		75.83	52.08	56.69	85.85	36.65	23.84	24.89	30.58
	C2	Near Bed Flow		64.57	46.64	46.38	68.37	18.28	11.33	12.09	12.45
	C3	Total Discharge		**140.40**	**98.71**	**103.07**	**154.22**	**54.92**	**35.17**	**36.97**	**43.02**

Upstream

		Subsection Name		U50	U100	U150	U200	U250	U300	U350	U400	U450
		Subsection Width	(mm)	75	50	50	50	50	50	50	50	75
Section C	A	Velocity	(cm/s)									
	A1	Near Surface Flow		2.02	2.35	2.25	2.37	2.48	2.39	2.40	2.37	2.12
	A2	Near Bed Flow		1.56	1.54	1.62	1.78	1.85	1.82	1.90	1.89	1.83
	B	Water Depth	(mm)	65.76	63.21	64.09	65.69	67.10	65.08	65.74	65.40	66.69
	C	Discharge	(cm3/s)									
	C1	Near Surface Flow		49.88	37.06	36.05	38.97	41.58	38.81	39.43	38.73	53.09
	C2	Near Bed Flow		38.45	24.36	25.92	29.29	31.05	29.61	31.16	30.95	45.73
	C3	Total Discharge		**88.32**	**61.41**	**61.97**	**68.26**	**72.63**	**68.42**	**70.59**	**69.68**	**98.82**
Section B	A	Velocity	(cm/s)									
	A1	Near Surface Flow		2.12	2.45	2.38	2.49	2.48	2.79	2.69	2.78	2.68
	A2	Near Bed Flow		1.34	1.50	1.43	1.55	1.61	1.72	1.66	1.65	1.52
	B	Water Depth	(mm)	63.75	64.09	63.40	63.29	64.05	65.62	65.58	64.97	63.97
	C	Discharge	(cm3/s)									
	C1	Near Surface Flow		50.64	39.22	37.78	39.48	39.68	45.84	44.04	45.12	64.18
	C2	Near Bed Flow		31.99	23.96	22.71	24.46	25.83	28.24	27.15	26.83	36.36
	C3	Total Discharge		**82.63**	**63.19**	**60.48**	**63.93**	**65.50**	**74.08**	**71.18**	**71.95**	**100.54**
Section A	A	Velocity	(cm/s)									
	A1	Near Surface Flow		2.18	2.18	2.18	2.21	2.26	2.22	2.30	2.32	2.24
	A2	Near Bed Flow		1.66	1.73	1.72	1.78	1.82	1.84	1.90	1.88	1.91
	B	Water Depth	(mm)	64.87	65.19	65.32	65.34	65.12	64.79	63.39	63.03	62.84
	C	Discharge	(cm3/s)									
	C1	Near Surface Flow		52.99	35.56	35.55	36.03	36.85	35.94	36.50	36.58	52.78
	C2	Near Bed Flow		40.42	28.12	28.09	29.09	29.64	29.80	30.04	29.58	44.90
	C3	Total Discharge		**93.41**	**63.68**	**63.64**	**65.12**	**66.49**	**65.74**	**66.54**	**66.16**	**97.68**

Water Depth

Section F

Average Water Depth, cm		Depth Ratio
LF	RF	RF/LF
5.88	6.43	0.91

Section E

Average Water Depth, cm		Depth Ratio
LE	RE	RE/LE
6.38	6.52	0.98

Section D

Average Water Depth, cm		Depth Ratio
LD	RD	RD/LD
6.38	6.59	0.97

Section C

Average Water Depth, cm
C
6.54

Section B

Average Water Depth, cm
B
6.43

Section A

Average Water Depth, cm
A
6.44

Velocity

Section F

Average Velocity, cm/s		Velocity Ratio
LF	RF	RF/LF
3.77	1.12	0.30
3.16	0.96	0.30

Section E

Average Velocity, cm/s		Velocity Ratio
LE	RE	RF/LF
3.34	1.31	0.39
2.83	0.84	0.30

Section D

Average Velocity, cm/s		Velocity Ratio
LD	RD	RF/LF
3.39	1.42	0.42
2.85	0.67	0.23

Section C

Average Velocity, cm/s
C
2.31
1.75

Section B

Average Velocity, cm/s
B
2.54
1.55

Section A

Average Velocity, cm/s
A
2.23
1.80

Discharge

Section F

Sum of Discharge, cm3/s			Discharge Ratio
LF	RF	LF+RF	RF/LF
507.4	166.9	674.3	0.33

Section E

Sum of Discharge, cm3/s			Discharge Ratio
LE	RE	LE+RE	RE/LE
489.7	174.6	664.3	0.36

Section D

Sum of Discharge, cm3/s			Discharge Ratio
LD	RD	LD+RD	RD/LD
496.4	170.1	666.5	0.34

Section C

Sum of Discharge, cm3/s
C
660.1

Section B

Sum of Discharge, cm3/s
B
653.5

Section A

Sum of Discharge, cm3/s
A
648.5

Froude

Section F

Froude Number	
LF	RF
0.0456	0.0131

Section E

Froude Number	
LE	RE
0.0390	0.0134

Section D

Froude Number	
LD	RD
0.0394	0.0130

Section C

Froude Number
C
0.0253

Section B

Froude Number
B
0.0258

Section A

Froude Number
A
0.0254

Reynold

Section F

Reynold Number	
LF	RF
12736	3933

Section E

Reynold Number	
LE	RE
11639	4090

Section D

Reynold Number	
LD	RD
11779	3978

Section C

Reynold Number
C
12804

Section B

Reynold Number
B
12860

Section A

Reynold Number
A
12688

Calculation: 30_07_5050

Downstream

	Subsection Name		L50	L100	L150	L200	R50	R100	R150	R200
	Subsection Width	(mm)	75	50	50	75	75	50	50	75
Section F	A Velocity	(cm/s)								
	A1 Near Surface Flow		2.69	2.75	2.72	2.63	2.51	2.49	2.33	2.25
	A2 Near Bed Flow		2.15	2.16	2.25	2.06	2.44	2.33	2.10	1.93
	B Water Depth	(mm)	55.11	54.91	55.86	56.4	55.37	56.16	55.83	55.33
	C Discharge	(cm3/s)								
	C1 Near Surface Flow		55.65	37.78	37.99	55.73	52.18	34.90	32.55	46.67
	C2 Near Bed Flow		44.38	29.60	31.42	43.66	50.56	32.65	29.32	40.06
	C3 Total Discharge		**100.03**	**67.37**	**69.41**	**99.38**	**102.74**	**67.55**	**61.87**	**86.73**
Section E	A Velocity	(cm/s)								
	A1 Near Surface Flow		2.33	2.31	2.68	2.77	2.71	2.55	2.39	2.16
	A2 Near Bed Flow		2.21	2.32	2.36	2.37	2.26	2.25	2.00	1.95
	B Water Depth	(mm)	54.87	55.29	55.63	55.95	56.01	56.29	55.19	54.21
	C Discharge	(cm3/s)								
	C1 Near Surface Flow		47.86	31.99	37.34	58.04	56.93	35.90	33.01	43.93
	C2 Near Bed Flow		45.42	32.10	32.85	49.67	47.41	31.65	27.57	39.60
	C3 Total Discharge		**93.29**	**64.09**	**70.19**	**107.71**	**104.34**	**67.55**	**60.58**	**83.53**
Section D	A Velocity	(cm/s)								
	A1 Near Surface Flow		2.26	2.31	2.50	2.40	2.40	2.42	2.38	2.42
	A2 Near Bed Flow		2.19	2.26	2.32	2.37	2.17	2.34	2.23	2.10
	B Water Depth	(mm)	56.23	56.76	55.87	57.43	56.83	57.6	57.16	55.72
	C Discharge	(cm3/s)								
	C1 Near Surface Flow		47.73	32.80	34.87	51.76	51.10	34.91	34.07	50.56
	C2 Near Bed Flow		46.28	32.06	32.34	51.10	46.26	33.74	31.86	43.90
	C3 Total Discharge		**94.00**	**64.86**	**67.21**	**102.86**	**97.36**	**68.65**	**65.93**	**94.45**

Upstream

	Subsection Name		U50	U100	U150	U200	U250	U300	U350	U400	U450
	Subsection Width	(mm)	75	50	50	50	50	50	50	50	75
Section C	A Velocity	(cm/s)									
	A1 Near Surface Flow		2.72	2.80	2.67	2.85	2.88	2.96	2.95	2.81	2.57
	A2 Near Bed Flow		1.67	1.70	1.75	1.95	1.98	2.00	2.16	1.88	1.71
	B Water Depth	(mm)	56.22	56.37	56.37	56.59	57.19	57.56	57.48	57.55	57.02
	C Discharge	(cm3/s)									
	C1 Near Surface Flow		57.41	39.47	37.61	40.26	41.24	42.55	42.45	40.42	54.86
	C2 Near Bed Flow		35.28	23.95	24.61	27.60	28.36	28.75	31.02	27.09	36.61
	C3 Total Discharge		**92.69**	**63.42**	**62.22**	**67.86**	**69.60**	**71.30**	**73.47**	**67.52**	**91.47**
Section B	A Velocity	(cm/s)									
	A1 Near Surface Flow		2.70	2.72	2.81	2.82	2.80	2.81	2.81	2.81	3.01
	A2 Near Bed Flow		1.77	1.80	1.78	1.81	1.83	1.85	1.85	1.88	2.00
	B Water Depth	(mm)	54.36	54.87	55	54.58	54.99	55.74	56.01	55.91	55.47
	C Discharge	(cm3/s)									
	C1 Near Surface Flow		55.10	37.26	38.69	38.45	38.53	39.13	39.28	39.21	62.56
	C2 Near Bed Flow		36.09	24.69	24.52	24.68	25.17	25.75	25.97	26.23	41.66
	C3 Total Discharge		**91.19**	**61.95**	**63.21**	**63.13**	**63.70**	**64.88**	**65.25**	**65.44**	**104.22**
Section A	A Velocity	(cm/s)									
	A1 Near Surface Flow		2.53	2.57	2.62	2.64	2.66	2.65	2.69	2.66	2.77
	A2 Near Bed Flow		1.94	1.95	1.99	2.05	2.06	2.09	2.11	2.11	2.27
	B Water Depth	(mm)	55.10	55.25	55.31	55.32	55.25	55.06	54.78	54.19	54.25
	C Discharge	(cm3/s)									
	C1 Near Surface Flow		52.29	35.49	36.21	36.50	36.68	36.44	36.81	35.99	56.45
	C2 Near Bed Flow		40.18	26.92	27.50	28.31	28.40	28.72	28.96	28.63	46.20
	C3 Total Discharge		**92.47**	**62.41**	**63.71**	**64.81**	**65.08**	**65.16**	**65.77**	**64.62**	**102.65**

Water Depth

Section F

Average Water Depth, cm		Depth Ratio
LF	RF	RF/LF
5.56	5.57	1.00

Section E

Average Water Depth, cm		Depth Ratio
LE	RE	RE/LE
5.54	5.54	1.00

Section D

Average Water Depth, cm		Depth Ratio
LD	RD	RD/LD
5.66	5.68	1.00

Section C

Average Water Depth, cm
C
5.69

Section B

Average Water Depth, cm
B
5.52

Section A

Average Water Depth, cm
A
5.49

Velocity

Section F

Average Velocity, cm/s		Velocity Ratio
LF	RF	RF/LF
2.70	2.39	0.89
2.15	2.20	0.98

Section E

Average Velocity, cm/s		Velocity Ratio
LE	RE	RF/LF
2.52	2.45	0.97
2.31	2.11	0.91

Section D

Average Velocity, cm/s		Velocity Ratio
LD	RD	RF/LF
2.37	2.41	0.98
2.29	2.21	0.97

Section C

Average Velocity, cm/s
C
2.80
1.87

Section B

Average Velocity, cm/s
B
2.81
1.84

Section A

Average Velocity, cm/s
A
2.64
2.06

Discharge

Section F

Sum of Discharge, cm3/s			Discharge Ratio
LF	RF	LF+RF	RF/LF
336.2	318.9	655.1	0.95

Section E

Sum of Discharge, cm3/s			Discharge Ratio
LE	RE	LE+RE	RE/LE
335.3	316.0	651.3	0.94

Section D

Sum of Discharge, cm3/s			Discharge Ratio
LD	RD	LD+RD	RD/LD
328.9	326.4	655.3	0.99

Section C

Sum of Discharge, cm3/s
C
659.6

Section B

Sum of Discharge, cm3/s
B
643.0

Section A

Sum of Discharge, cm3/s
A
646.7

Froude

Section F

Froude Number	
LF	RF
0.0329	0.0311

Section E

Froude Number	
LE	RE
0.0328	0.0310

Section D

Froude Number	
LD	RD
0.0312	0.0309

Section C

Froude Number
C
0.0312

Section B

Froude Number
B
0.0316

Section A

Froude Number
A
0.0320

Reynold

Section F

Reynold Number	
LF	RF
8766	8298

Section E

Reynold Number	
LE	RE
8729	8239

Section D

Reynold Number	
LD	RD
8451	8396

Section C

Reynold Number
C
14328

Section B

Reynold Number
B
14194

Section A

Reynold Number
A
14350

Calculation: 30_07_5560

Downstream

		Subsection Name		L50	L100	L150	L200	R50	R100	R150	R200
		Subsection Width	(mm)	75	50	50	75	75	50	50	75
Section F	A	Velocity	(cm/s)								
	A1	Near Surface Flow		3.86	3.96	3.92	3.84	1.46	1.33	1.33	1.05
	A2	Near Bed Flow		3.11	3.19	3.02	2.77	0.49	0.29	0.14	0.03
	B	Water Depth	(mm)	59.84	60.29	62.00	62.07	64.21	65.76	65.79	64.79
	C	Discharge	(cm3/s)								
	C1	Near Surface Flow		86.67	59.64	60.70	89.29	35.16	21.79	21.80	25.58
	C2	Near Bed Flow		69.70	48.08	46.78	64.57	11.89	4.71	2.37	0.74
	C3	Total Discharge		**156.37**	**107.71**	**107.48**	**153.86**	**47.05**	**26.50**	**24.17**	**26.32**
Section E	A	Velocity	(cm/s)								
	A1	Near Surface Flow		3.81	3.77	3.85	3.73	1.12	1.03	0.88	0.74
	A2	Near Bed Flow		3.21	3.34	3.37	3.46	0.70	0.44	0.34	0.24
	B	Water Depth	(mm)	59.15	60.17	63.44	62.49	64.78	66.83	64.63	64.25
	C	Discharge	(cm3/s)								
	C1	Near Surface Flow		84.56	56.78	61.03	87.52	27.09	17.24	14.24	17.74
	C2	Near Bed Flow		71.20	50.31	53.44	81.03	17.09	7.40	5.51	5.87
	C3	Total Discharge		**155.76**	**107.09**	**114.47**	**168.55**	**44.18**	**24.65**	**19.74**	**23.62**
Section D	A	Velocity	(cm/s)								
	A1	Near Surface Flow		3.38	3.56	3.81	3.83	0.89	0.95	0.79	0.70
	A2	Near Bed Flow		3.17	3.27	3.54	3.36	0.59	0.37	0.34	0.34
	B	Water Depth	(mm)	60.18	60.99	61.86	64.05	64.95	66.44	67.00	63.31
	C	Discharge	(cm3/s)								
	C1	Near Surface Flow		76.30	54.22	58.86	91.98	21.59	15.77	13.25	16.63
	C2	Near Bed Flow		71.57	49.81	54.80	80.63	14.39	6.22	5.70	8.04
	C3	Total Discharge		**147.87**	**104.03**	**113.66**	**172.61**	**35.98**	**21.99**	**18.95**	**24.66**

Upstream

		Subsection Name		U50	U100	U150	U200	U250	U300	U350	U400	U450
		Subsection Width	(mm)	75	50	50	50	50	50	50	50	75
Section C	A	Velocity	(cm/s)									
	A1	Near Surface Flow		2.22	2.21	2.25	2.27	2.30	2.27	2.23	2.21	1.97
	A2	Near Bed Flow		1.70	1.72	1.75	1.72	1.75	1.86	1.73	1.91	1.79
	B	Water Depth	(mm)	63.67	62.49	64.15	64.18	64.95	64.57	65.48	66.00	66.07
	C	Discharge	(cm3/s)									
	C1	Near Surface Flow		52.97	34.55	36.16	36.42	37.27	36.62	36.52	36.46	48.85
	C2	Near Bed Flow		40.55	26.82	28.12	27.57	28.49	30.02	28.30	31.51	44.28
	C3	Total Discharge		**93.52**	**61.37**	**64.28**	**63.99**	**65.77**	**66.64**	**64.82**	**67.98**	**93.13**
Section B	A	Velocity	(cm/s)									
	A1	Near Surface Flow		2.20	2.31	2.27	2.40	2.46	2.46	2.45	2.54	2.47
	A2	Near Bed Flow		1.49	1.51	1.60	1.67	1.69	1.69	1.78	1.71	1.52
	B	Water Depth	(mm)	62.11	62.50	62.88	63.18	63.57	65.15	65.62	65.59	64.48
	C	Discharge	(cm3/s)									
	C1	Near Surface Flow		51.31	36.15	35.72	37.85	39.06	40.04	40.13	41.58	59.79
	C2	Near Bed Flow		34.69	23.62	25.15	26.39	26.80	27.57	29.23	28.03	36.66
	C3	Total Discharge		**86.00**	**59.76**	**60.87**	**64.24**	**65.86**	**67.61**	**69.35**	**69.61**	**96.45**
Section A	A	Velocity	(cm/s)									
	A1	Near Surface Flow		1.97	2.13	2.09	2.25	2.25	2.35	2.47	2.50	2.54
	A2	Near Bed Flow		1.48	1.59	1.62	1.77	1.77	1.80	1.85	2.00	2.12
	B	Water Depth	(mm)	63.47	63.77	63.91	63.96	63.76	63.53	62.75	62.27	61.61
	C	Discharge	(cm3/s)									
	C1	Near Surface Flow		46.84	33.90	33.44	36.02	35.93	37.37	38.73	38.85	58.71
	C2	Near Bed Flow		35.35	25.28	25.89	28.34	28.13	28.58	29.04	31.06	49.06
	C3	Total Discharge		**82.19**	**59.18**	**59.33**	**64.37**	**64.07**	**65.95**	**67.77**	**69.91**	**107.77**

Water Depth

Section F

Average Water Depth, cm		Depth Ratio
LF	RF	RF/LF
6.11	6.51	0.94

Section E

Average Water Depth, cm		Depth Ratio
LE	RE	RE/LE
6.13	6.51	0.94

Section D

Average Water Depth, cm		Depth Ratio
LD	RD	RD/LD
6.18	6.54	0.94

Section C

Average Water Depth, cm
C
6.46

Section B

Average Water Depth, cm
B
6.39

Section A

Average Water Depth, cm
A
6.32

Velocity

Section F

Average Velocity, cm/s		Velocity Ratio
LF	RF	RF/LF
3.89	1.29	0.33
3.02	0.24	0.08

Section E

Average Velocity, cm/s		Velocity Ratio
LE	RE	RF/LF
3.79	0.94	0.25
3.35	0.43	0.13

Section D

Average Velocity, cm/s		Velocity Ratio
LD	RD	RF/LF
3.64	0.83	0.23
3.33	0.41	0.12

Section C

Average Velocity, cm/s
C
2.21
1.77

Section B

Average Velocity, cm/s
B
2.39
1.63

Section A

Average Velocity, cm/s
A
2.28
1.78

Discharge

Section F

Sum of Discharge, cm3/s			Discharge Ratio
LF	RF	LF+RF	RF/LF
525.4	124.0	649.5	0.24

Section E

Sum of Discharge, cm3/s			Discharge Ratio
LE	RE	LE+RE	RE/LE
545.9	112.2	658.1	0.21

Section D

Sum of Discharge, cm3/s			Discharge Ratio
LD	RD	LD+RD	RD/LD
538.2	101.6	639.8	0.19

Section C

Sum of Discharge, cm3/s
C
641.5

Section B

Sum of Discharge, cm3/s
B
639.8

Section A

Sum of Discharge, cm3/s
A
640.5

Froude

Section F

Froude Number	
LF	RF
0.0447	0.0096

Section E

Froude Number	
LE	RE
0.0460	0.0086

Section D

Froude Number	
LD	RD
0.0448	0.0078

Section C

Froude Number
C
0.0250

Section B

Froude Number
B
0.0254

Section A

Froude Number
A
0.0258

Reynold

Section F

Reynold Number	
LF	RF
12865	2908

Section E

Reynold Number	
LE	RE
13299	2612

Section D

Reynold Number	
LD	RD
13032	2367

Section C

Reynold Number
C
12535

Section B

Reynold Number
B
12630

Section A

Reynold Number
A
12721

Calculation: 30_07_5055

Downstream

		Subsection Name		L50	L100	L150	L200	R50	R100	R150	R200
		Subsection Width	(mm)	75	50	50	75	75	50	50	75
Section F	A	Velocity	(cm/s)								
	A1	Near Surface Flow		3.71	3.85	3.90	3.74	1.47	1.44	1.21	1.16
	A2	Near Bed Flow		3.41	3.41	3.40	3.17	1.29	1.12	0.91	0.82
	B	Water Depth	(mm)	53.99	53.55	53.53	55.02	58.92	59.91	58.80	58.22
	C	Discharge	(cm3/s)								
	C1	Near Surface Flow		75.18	51.59	52.17	77.17	32.52	21.53	17.81	25.34
	C2	Near Bed Flow		69.08	45.68	45.44	65.36	28.44	16.85	13.44	17.93
	C3	Total Discharge		**144.26**	**97.27**	**97.61**	**142.53**	**60.96**	**38.37**	**31.25**	**43.27**
Section E	A	Velocity	(cm/s)								
	A1	Near Surface Flow		3.48	3.77	3.75	3.66	1.43	1.30	1.12	1.06
	A2	Near Bed Flow		3.25	3.39	3.46	3.32	1.31	1.16	1.04	0.96
	B	Water Depth	(mm)	54.54	54.60	55.43	56.26	59.40	60.46	58.62	56.70
	C	Discharge	(cm3/s)								
	C1	Near Surface Flow		71.09	51.44	51.97	77.15	31.79	19.59	16.42	22.48
	C2	Near Bed Flow		66.46	46.22	47.92	70.04	29.12	17.61	15.17	20.34
	C3	Total Discharge		**137.55**	**97.66**	**99.89**	**147.19**	**60.92**	**37.20**	**31.59**	**42.82**
Section D	A	Velocity	(cm/s)								
	A1	Near Surface Flow		3.51	3.66	3.82	3.78	1.26	1.26	1.18	1.03
	A2	Near Bed Flow		3.21	3.44	3.59	3.57	0.93	0.99	1.04	0.82
	B	Water Depth	(mm)	54.75	54.62	54.62	56.73	60.37	60.85	60.21	57.30
	C	Discharge	(cm3/s)								
	C1	Near Surface Flow		72.02	49.95	52.14	80.32	28.48	19.14	17.74	22.15
	C2	Near Bed Flow		65.98	47.02	48.99	75.86	21.02	15.11	15.66	17.64
	C3	Total Discharge		**138.00**	**96.97**	**101.12**	**156.19**	**49.51**	**34.25**	**33.40**	**39.79**

Upstream

		Subsection Name		U50	U100	U150	U200	U250	U300	U350	U400	U450
		Subsection Width	(mm)	75	50	50	50	50	50	50	50	75
Section C	A	Velocity	(cm/s)									
	A1	Near Surface Flow		2.34	2.38	2.46	2.59	2.59	2.66	2.79	2.61	2.57
	A2	Near Bed Flow		1.70	1.81	1.82	1.91	1.93	2.01	1.97	2.04	1.91
	B	Water Depth	(mm)	59.76	59.62	59.74	59.78	57.88	58.65	58.15	59.55	59.56
	C	Discharge	(cm3/s)									
	C1	Near Surface Flow		52.53	35.41	36.80	38.71	37.51	38.98	40.56	38.89	57.37
	C2	Near Bed Flow		38.16	26.91	27.21	28.49	27.98	29.42	28.67	30.38	42.67
	C3	Total Discharge		**90.69**	**62.32**	**64.00**	**67.20**	**65.49**	**68.40**	**69.24**	**69.27**	**100.04**
Section B	A	Velocity	(cm/s)									
	A1	Near Surface Flow		2.40	2.27	2.39	2.44	2.53	2.61	2.63	2.65	2.60
	A2	Near Bed Flow		1.59	1.66	1.71	1.82	1.85	1.89	2.04	1.96	1.92
	B	Water Depth	(mm)	58.67	59.26	58.89	59.45	59.87	60.63	60.97	61.29	60.27
	C	Discharge	(cm3/s)									
	C1	Near Surface Flow		52.86	33.60	35.22	36.31	37.90	39.54	40.14	40.55	58.87
	C2	Near Bed Flow		35.09	24.66	25.15	27.05	27.76	28.61	31.07	29.98	43.41
	C3	Total Discharge		**87.94**	**58.25**	**60.37**	**63.36**	**65.66**	**68.15**	**71.22**	**70.54**	**102.28**
Section A	A	Velocity	(cm/s)									
	A1	Near Surface Flow		2.26	2.38	2.44	2.54	2.74	2.65	2.66	2.74	2.71
	A2	Near Bed Flow		1.60	1.62	1.67	1.71	1.84	2.00	2.01	2.17	1.90
	B	Water Depth	(mm)	58.98	59.24	59.40	59.43	59.32	58.96	58.53	57.27	57.31
	C	Discharge	(cm3/s)									
	C1	Near Surface Flow		50.05	35.21	36.17	37.79	40.69	39.03	38.90	39.27	58.14
	C2	Near Bed Flow		35.48	23.93	24.75	25.39	27.23	29.53	29.34	31.02	40.73
	C3	Total Discharge		**85.53**	**59.14**	**60.92**	**63.18**	**67.91**	**68.56**	**68.25**	**70.29**	**98.87**

Water Depth

Average Water Depth, cm		Depth Ratio
LF	RF	RF/LF
5.40	5.90	0.92

Average Water Depth, cm		Depth Ratio
LE	RE	RE/LE
5.52	5.88	0.94

Average Water Depth, cm		Depth Ratio
LD	RD	RD/LD
5.52	5.97	0.92

Average Water Depth, cm
C
5.92

Average Water Depth, cm
B
5.99

Average Water Depth, cm
A
5.87

Velocity

Average Velocity, cm/s		Velocity Ratio
LF	RF	RF/LF
3.80	1.32	0.35
3.35	1.04	0.31

Average Velocity, cm/s		Velocity Ratio
LE	RE	RF/LF
3.66	1.23	0.33
3.35	1.12	0.33

Average Velocity, cm/s		Velocity Ratio
LD	RD	RF/LF
3.69	1.18	0.32
3.45	0.95	0.27

Average Velocity, cm/s
C
2.56
1.90

Average Velocity, cm/s
B
2.50
1.83

Average Velocity, cm/s
A
2.57
1.83

Discharge

Sum of Discharge, cm3/s			Discharge Ratio
LF	RF	LF+RF	RF/LF
481.7	173.9	655.5	0.36

Sum of Discharge, cm3/s			Discharge Ratio
LE	RE	LE+RE	RE/LE
482.3	172.5	654.8	0.36

Sum of Discharge, cm3/s			Discharge Ratio
LD	RD	LD+RD	RD/LD
492.3	156.9	649.2	0.32

Sum of Discharge, cm3/s
C
656.6

Sum of Discharge, cm3/s
B
647.8

Sum of Discharge, cm3/s
A
642.7

Froude

Froude Number	
LF	RF
0.0491	0.0155

Froude Number	
LE	RE
0.0477	0.0154

Froude Number	
LD	RD
0.0485	0.0139

Froude Number
C
0.0292

Froude Number
B
0.0282

Froude Number
A
0.0290

Reynold

Reynold Number	
LF	RF
12797	4336

Reynold Number	
LE	RE
12644	4303

Reynold Number	
LD	RD
12869	3929

Reynold Number
C
13774

Reynold Number
B
13422

Reynold Number
A
13591

Calculation: 40_03_5050

Downstream

		Subsection Name		L50	L100	L150	L200	R50	R100	R150	R200
		Subsection Width	(mm)	75	50	50	75	75	50	50	75
Section F	A	Velocity	(cm/s)								
	A1	Near Surface Flow		2.51	2.54	2.67	2.59	2.28	2.20	2.16	2.13
	A2	Near Bed Flow		1.78	1.82	1.90	1.96	2.03	1.99	1.78	1.67
	B	Water Depth	(mm)	62.85	63.32	62.76	62.71	62.28	62.77	62.94	62.52
	C	Discharge	(cm3/s)								
	C1	Near Surface Flow		59.11	40.22	41.94	60.93	53.24	34.48	33.98	49.92
	C2	Near Bed Flow		41.98	28.84	29.75	46.17	47.31	31.16	28.02	39.12
	C3	Total Discharge		**101.09**	**69.06**	**71.68**	**107.10**	**100.55**	**65.64**	**62.00**	**89.04**
Section E	A	Velocity	(cm/s)								
	A1	Near Surface Flow		2.33	2.38	2.44	2.52	2.35	2.34	2.21	2.02
	A2	Near Bed Flow		2.03	2.07	2.15	2.29	2.17	2.10	2.01	1.88
	B	Water Depth	(mm)	61.68	62.25	63.31	62.27	62.54	62.55	62.59	62.38
	C	Discharge	(cm3/s)								
	C1	Near Surface Flow		53.92	36.97	38.55	58.87	55.02	36.55	34.63	47.19
	C2	Near Bed Flow		47.06	32.24	34.05	53.39	50.97	32.85	31.39	43.96
	C3	Total Discharge		**100.99**	**69.22**	**72.59**	**112.26**	**105.99**	**69.41**	**66.01**	**91.15**
Section D	A	Velocity	(cm/s)								
	A1	Near Surface Flow		2.14	2.25	2.34	2.51	2.31	2.41	2.46	2.35
	A2	Near Bed Flow		1.82	1.90	1.90	2.18	1.71	1.77	1.78	1.71
	B	Water Depth	(mm)	61.36	61.87	62.98	63.97	64.21	63.73	62.67	61.94
	C	Discharge	(cm3/s)								
	C1	Near Surface Flow		49.30	34.75	36.86	60.12	55.59	38.40	38.50	54.56
	C2	Near Bed Flow		41.88	29.36	29.86	52.30	41.16	28.20	27.96	39.81
	C3	Total Discharge		**91.18**	**64.11**	**66.72**	**112.41**	**96.75**	**66.60**	**66.47**	**94.37**

Upstream

		Subsection Name		U50	U100	U150	U200	U250	U300	U350	U400	U450
		Subsection Width	(mm)	75	50	50	50	50	50	50	50	75
Section C	A	Velocity	(cm/s)									
	A1	Near Surface Flow		2.45	2.47	2.53	2.56	2.66	2.67	2.69	2.70	2.07
	A2	Near Bed Flow		1.64	1.56	1.71	1.81	1.85	1.88	1.79	1.70	1.19
	B	Water Depth	(mm)	60.49	62.2	62.44	63.69	63.64	63.94	63.69	63	61.15
	C	Discharge	(cm3/s)									
	C1	Near Surface Flow		55.64	38.44	39.49	40.70	42.37	42.69	42.85	42.55	47.53
	C2	Near Bed Flow		37.26	24.31	26.75	28.83	29.46	30.01	28.49	26.81	27.26
	C3	Total Discharge		**92.90**	**62.75**	**66.24**	**69.52**	**71.83**	**72.69**	**71.34**	**69.36**	**74.79**
Section B	A	Velocity	(cm/s)									
	A1	Near Surface Flow		2.52	2.49	2.51	2.48	2.52	2.52	2.52	2.51	2.50
	A2	Near Bed Flow		1.56	1.50	1.50	1.57	1.65	1.66	1.70	1.72	1.59
	B	Water Depth	(mm)	63.45	63.05	62.83	62.24	62.71	62.73	64.36	63.8	62.28
	C	Discharge	(cm3/s)									
	C1	Near Surface Flow		59.98	39.32	39.50	38.64	39.53	39.58	40.63	40.03	58.50
	C2	Near Bed Flow		37.11	23.68	23.58	24.50	25.84	26.09	27.33	27.43	37.25
	C3	Total Discharge		**97.09**	**63.00**	**63.08**	**63.14**	**65.36**	**65.67**	**67.95**	**67.45**	**95.74**
Section A	A	Velocity	(cm/s)									
	A1	Near Surface Flow		2.38	2.40	2.55	2.54	2.64	2.63	2.63	2.68	3.24
	A2	Near Bed Flow		1.32	1.41	1.41	1.57	1.61	1.68	1.73	1.88	2.36
	B	Water Depth	(mm)	61.74	63.08	62.97	62.63	63.10	63.05	62.80	62.15	61.65
	C	Discharge	(cm3/s)									
	C1	Near Surface Flow		55.20	37.86	40.19	39.70	41.59	41.53	41.34	41.58	74.96
	C2	Near Bed Flow		30.54	22.28	22.27	24.55	25.45	26.54	27.10	29.15	54.66
	C3	Total Discharge		**85.73**	**60.14**	**62.45**	**64.25**	**67.04**	**68.07**	**68.44**	**70.73**	**129.63**

Water Depth

Average Water Depth, cm		Depth Ratio
LF	RF	RF/LF
6.29	6.26	1.00

Average Water Depth, cm		Depth Ratio
LE	RE	RE/LE
6.24	6.25	1.00

Average Water Depth, cm		Depth Ratio
LD	RD	RD/LD
6.25	6.31	0.99

Average Water Depth, cm
C
6.27

Average Water Depth, cm
B
6.31

Average Water Depth, cm
A
6.26

Velocity

Average Velocity, cm/s		Velocity Ratio
LF	RF	RF/LF
2.58	2.19	0.85
1.87	1.87	1.00

Average Velocity, cm/s		Velocity Ratio
LE	RE	RF/LF
2.42	2.23	0.92
2.14	2.04	0.95

Average Velocity, cm/s		Velocity Ratio
LD	RD	RF/LF
2.31	2.38	0.97
1.95	1.74	0.90

Average Velocity, cm/s
C
2.53
1.68

Average Velocity, cm/s
B
2.51
1.61

Average Velocity, cm/s
A
2.63
1.66

Discharge

Sum of Discharge, cm3/s			Discharge Ratio
LF	RF	LF+RF	RF/LF
348.9	317.2	666.2	0.91

Sum of Discharge, cm3/s			Discharge Ratio
LE	RE	LE+RE	RE/LE
355.1	332.6	687.6	0.94

Sum of Discharge, cm3/s			Discharge Ratio
LD	RD	LD+RD	RD/LD
334.4	324.2	658.6	0.97

Sum of Discharge, cm3/s
C
651.4

Sum of Discharge, cm3/s
B
648.5

Sum of Discharge, cm3/s
A
676.5

Froude

Froude Number	
LF	RF
0.0283	0.0259

Froude Number	
LE	RE
0.0291	0.0273

Froude Number	
LD	RD
0.0272	0.0262

Froude Number
C
0.0269

Froude Number
B
0.0262

Froude Number
A
0.0274

Reynold

Reynold Number	
LF	RF
8350	7611

Reynold Number	
LE	RE
8529	8004

Reynold Number	
LD	RD
7985	7762

Reynold Number
C
13185

Reynold Number
B
12891

Reynold Number
A
13431

Calculation: 40_03_5560

Downstream

		Subsection Name		L50	L100	L150	L200	R50	R100	R150	R200
		Subsection Width	(mm)	75	50	50	75	75	50	50	75
Section F	A	Velocity	(cm/s)								
	A1	Near Surface Flow		3.26	3.27	3.36	3.36	0.81	0.67	0.61	0.50
	A2	Near Bed Flow		2.59	2.74	2.77	2.76	0.62	0.53	0.40	0.34
	B	Water Depth	(mm)	69.85	70.66	71.04	70.32	74.78	75.89	75.89	75.38
	C	Discharge	(cm3/s)								
	C1	Near Surface Flow		85.33	57.84	59.74	88.62	22.78	12.72	11.55	14.08
	C2	Near Bed Flow		67.84	48.45	49.17	72.67	17.45	9.99	7.61	9.64
	C3	Total Discharge		**153.17**	**106.29**	**108.91**	**161.29**	**40.23**	**22.71**	**19.16**	**23.73**
Section E	A	Velocity	(cm/s)								
	A1	Near Surface Flow		3.26	3.30	3.35	3.39	0.80	0.69	0.65	0.59
	A2	Near Bed Flow		2.88	3.09	3.13	3.25	0.69	0.62	0.45	0.46
	B	Water Depth	(mm)	69.13	70.58	70.71	70.29	74.80	74.97	74.75	74.74
	C	Discharge	(cm3/s)								
	C1	Near Surface Flow		84.45	58.16	59.14	89.38	22.49	13.01	12.23	16.67
	C2	Near Bed Flow		74.77	54.60	55.40	85.70	19.45	11.54	8.49	12.98
	C3	Total Discharge		**159.22**	**112.76**	**114.55**	**175.08**	**41.93**	**24.54**	**20.72**	**29.65**
Section D	A	Velocity	(cm/s)								
	A1	Near Surface Flow		3.07	3.23	3.43	3.53	0.76	0.76	0.67	0.68
	A2	Near Bed Flow		2.89	3.07	3.26	3.12	0.62	0.62	0.55	0.53
	B	Water Depth	(mm)	68.06	69.25	72.01	71.58	77.27	76.96	75.72	75.28
	C	Discharge	(cm3/s)								
	C1	Near Surface Flow		78.35	55.90	61.68	94.69	22.02	14.57	12.60	19.18
	C2	Near Bed Flow		73.75	53.09	58.70	83.63	17.83	11.90	10.41	14.87
	C3	Total Discharge		**152.10**	**108.99**	**120.38**	**178.32**	**39.85**	**26.47**	**23.01**	**34.05**

Upstream

		Subsection Name		U50	U100	U150	U200	U250	U300	U350	U400	U450
		Subsection Width	(mm)	75	50	50	50	50	50	50	50	75
Section C	A	Velocity	(cm/s)									
	A1	Near Surface Flow		2.02	2.10	2.09	2.22	2.33	2.31	2.31	2.30	2.17
	A2	Near Bed Flow		1.06	1.04	1.24	1.38	1.49	1.37	1.39	1.30	1.30
	B	Water Depth	(mm)	75.63	76.60	77.41	78.00	78.19	78.05	77.97	77.74	77.42
	C	Discharge	(cm3/s)									
	C1	Near Surface Flow		57.21	40.21	40.44	43.24	45.57	45.13	45.01	44.69	62.92
	C2	Near Bed Flow		29.99	19.85	23.93	26.98	29.09	26.68	27.02	25.25	37.64
	C3	Total Discharge		**87.20**	**60.06**	**64.37**	**70.21**	**74.67**	**71.81**	**72.03**	**69.94**	**100.57**
Section B	A	Velocity	(cm/s)									
	A1	Near Surface Flow		1.87	1.89	1.96	2.04	2.05	2.17	2.18	2.16	2.17
	A2	Near Bed Flow		1.12	1.20	1.27	1.30	1.34	1.44	1.49	1.48	1.51
	B	Water Depth	(mm)	77.77	78.09	77.81	77.14	77.14	78.54	78.48	77.85	76.56
	C	Discharge	(cm3/s)									
	C1	Near Surface Flow		54.46	36.87	38.05	39.42	39.53	42.68	42.81	41.98	62.44
	C2	Near Bed Flow		32.56	23.39	24.62	25.16	25.81	28.19	29.21	28.81	43.39
	C3	Total Discharge		**87.02**	**60.26**	**62.67**	**64.58**	**65.34**	**70.87**	**72.02**	**70.79**	**105.83**
Section A	A	Velocity	(cm/s)									
	A1	Near Surface Flow		1.55	1.63	1.69	1.94	1.94	2.03	2.07	2.14	2.10
	A2	Near Bed Flow		1.22	1.27	1.41	1.51	1.61	1.72	1.76	1.76	1.77
	B	Water Depth	(mm)	77.04	78.25	77.37	77.79	77.61	77.48	77.78	77.50	77.17
	C	Discharge	(cm3/s)									
	C1	Near Surface Flow		44.88	31.79	32.62	37.76	37.61	39.27	40.23	41.37	60.75
	C2	Near Bed Flow		35.14	24.94	27.26	29.40	31.19	33.32	34.21	34.07	51.34
	C3	Total Discharge		**80.02**	**56.73**	**59.88**	**67.16**	**68.80**	**72.59**	**74.44**	**75.44**	**112.09**

Water Depth

Average Water Depth, cm		Depth Ratio
LF	RF	RF/LF
7.05	7.55	0.93

Average Water Depth, cm		Depth Ratio
LE	RE	RE/LE
7.02	7.48	0.94

Average Water Depth, cm		Depth Ratio
LD	RD	RD/LD
7.02	7.63	0.92

Average Water Depth, cm
C
7.74

Average Water Depth, cm
B
7.77

Average Water Depth, cm
A
7.76

Velocity

Average Velocity, cm/s		Velocity Ratio
LF	RF	RF/LF
3.31	0.65	0.20
2.71	0.47	0.17

Average Velocity, cm/s		Velocity Ratio
LE	RE	RF/LF
3.32	0.69	0.21
3.09	0.56	0.18

Average Velocity, cm/s		Velocity Ratio
LD	RD	RF/LF
3.31	0.72	0.22
3.08	0.58	0.19

Average Velocity, cm/s
C
2.20
1.28

Average Velocity, cm/s
B
2.05
1.35

Average Velocity, cm/s
A
1.90
1.56

Discharge

Sum of Discharge, cm3/s			Discharge Ratio
LF	RF	LF+RF	RF/LF
529.7	105.8	635.5	0.20

Sum of Discharge, cm3/s			Discharge Ratio
LE	RE	LE+RE	RE/LE
561.6	116.9	678.5	0.21

Sum of Discharge, cm3/s			Discharge Ratio
LD	RD	LD+RD	RD/LD
559.8	123.4	683.2	0.22

Sum of Discharge, cm3/s
C
670.9

Sum of Discharge, cm3/s
B
659.4

Sum of Discharge, cm3/s
A
667.1

Froude

Froude Number	
LF	RF
0.0363	0.0065

Froude Number	
LE	RE
0.0386	0.0073

Froude Number	
LD	RD
0.0385	0.0075

Froude Number
C
0.0200

Froude Number
B
0.0195

Froude Number
A
0.0198

Reynold

Reynold Number	
LF	RF
11783	2246

Reynold Number	
LE	RE
12518	2483

Reynold Number	
LD	RD
12487	2603

Reynold Number
C
11423

Reynold Number
B
11154

Reynold Number
A
11321

Calculation: 40_03_5055

Downstream

	Subsection Name		L50	L100	L150	L200	R50	R100	R150	R200
	Subsection Width	(mm)	75	50	50	75	75	50	50	75
Section F	A Velocity	(cm/s)								
	A1 Near Surface Flow		3.36	3.52	3.57	3.70	1.16	1.09	0.98	0.97
	A2 Near Bed Flow		2.63	2.63	2.77	2.75	0.78	0.72	0.56	0.54
	B Water Depth	(mm)	64.72	65.25	65.73	64.41	69.74	69.99	70.33	69.80
	C Discharge	(cm3/s)								
	C1 Near Surface Flow		81.47	57.38	58.61	89.40	30.21	19.00	17.28	25.43
	C2 Near Bed Flow		63.90	42.97	45.54	66.54	20.28	12.62	9.86	14.22
	C3 Total Discharge		**145.37**	**100.35**	**104.15**	**155.95**	**50.49**	**31.62**	**27.14**	**39.65**
Section E	A Velocity	(cm/s)								
	A1 Near Surface Flow		3.24	3.29	3.37	3.45	1.21	1.15	1.10	1.06
	A2 Near Bed Flow		2.81	2.92	3.06	3.21	0.73	0.75	0.57	0.56
	B Water Depth	(mm)	63.37	64.17	64.94	64.84	69.43	70.10	69.64	69.43
	C Discharge	(cm3/s)								
	C1 Near Surface Flow		76.94	52.72	54.72	83.97	31.54	20.13	19.14	27.66
	C2 Near Bed Flow		66.76	46.88	49.66	78.15	18.93	13.09	9.92	14.55
	C3 Total Discharge		**143.71**	**99.59**	**104.38**	**162.13**	**50.47**	**33.22**	**29.06**	**42.21**
Section D	A Velocity	(cm/s)								
	A1 Near Surface Flow		3.04	3.17	3.40	3.57	1.25	1.31	1.24	1.25
	A2 Near Bed Flow		2.74	2.91	3.03	3.25	0.60	0.67	0.60	0.61
	B Water Depth	(mm)	63.04	63.88	66.64	65.20	72.31	71.64	71.01	69.51
	C Discharge	(cm3/s)								
	C1 Near Surface Flow		71.82	50.60	56.66	87.17	33.84	23.40	21.98	32.66
	C2 Near Bed Flow		64.79	46.48	50.56	79.43	16.20	11.99	10.58	15.87
	C3 Total Discharge		**136.61**	**97.08**	**107.22**	**166.60**	**50.05**	**35.39**	**32.56**	**48.53**

Upstream

	Subsection Name		U50	U100	U150	U200	U250	U300	U350	U400	U450
	Subsection Width	(mm)	75	50	50	50	50	50	50	50	75
Section C	A Velocity	(cm/s)									
	A1 Near Surface Flow		1.73	1.82	1.98	2.04	2.15	2.20	2.20	2.18	2.04
	A2 Near Bed Flow		1.53	1.57	1.68	1.79	1.77	1.72	1.86	1.70	1.69
	B Water Depth	(mm)	68.36	70.21	70.70	71.47	71.40	71.08	71.01	71.37	70.56
	C Discharge	(cm3/s)									
	C1 Near Surface Flow		44.44	32.02	34.95	36.51	38.31	39.02	39.06	38.87	54.07
	C2 Near Bed Flow		39.24	27.63	29.73	32.06	31.51	30.56	33.01	30.40	44.73
	C3 Total Discharge		**83.68**	**59.65**	**64.68**	**68.57**	**69.82**	**69.58**	**72.07**	**69.27**	**98.80**
Section B	A Velocity	(cm/s)									
	A1 Near Surface Flow		1.93	1.95	2.03	2.21	2.25	2.37	2.39	2.42	2.37
	A2 Near Bed Flow		1.24	1.43	1.43	1.57	1.63	1.63	1.63	1.79	1.88
	B Water Depth	(mm)	71.00	70.96	70.29	69.66	69.59	71.10	70.94	70.51	69.60
	C Discharge	(cm3/s)									
	C1 Near Surface Flow		51.37	34.56	35.69	38.48	39.19	42.07	42.47	42.73	61.81
	C2 Near Bed Flow		32.89	25.42	25.16	27.32	28.31	29.04	28.95	31.47	49.03
	C3 Total Discharge		**84.26**	**59.97**	**60.84**	**65.80**	**67.50**	**71.11**	**71.42**	**74.20**	**110.84**
Section A	A Velocity	(cm/s)									
	A1 Near Surface Flow		1.78	1.91	1.85	2.08	2.01	2.18	2.14	2.29	2.35
	A2 Near Bed Flow		1.39	1.44	1.51	1.52	1.63	1.69	1.75	1.86	1.89
	B Water Depth	(mm)	69.27	69.90	70.62	70.50	70.96	70.80	70.58	70.20	70.81
	C Discharge	(cm3/s)									
	C1 Near Surface Flow		46.14	33.40	32.60	36.67	35.65	38.51	37.81	40.13	62.33
	C2 Near Bed Flow		36.19	25.15	26.73	26.74	28.85	29.91	30.82	32.64	50.27
	C3 Total Discharge		**82.33**	**58.55**	**59.33**	**63.40**	**64.50**	**68.42**	**68.64**	**72.77**	**112.60**

Water Depth

Section F: Average Water Depth, cm		Depth Ratio
LF	RF	RF/LF
6.50	7.00	0.93

Section E: Average Water Depth, cm		Depth Ratio
LE	RE	RE/LE
6.43	6.97	0.92

Section D: Average Water Depth, cm		Depth Ratio
LD	RD	RD/LD
6.47	7.11	0.91

Section C: Average Water Depth, cm
C
7.07

Section B: Average Water Depth, cm
B
7.04

Section A: Average Water Depth, cm
A
7.04

Velocity

Section F: Average Velocity, cm/s		Velocity Ratio
LF	RF	RF/LF
3.54	1.05	0.30
2.70	0.65	0.24

Section E: Average Velocity, cm/s		Velocity Ratio
LE	RE	RF/LF
3.34	1.13	0.34
3.00	0.65	0.22

Section D: Average Velocity, cm/s		Velocity Ratio
LD	RD	RF/LF
3.29	1.26	0.38
2.98	0.62	0.21

Section C: Average Velocity, cm/s
C
2.04
1.70

Section B: Average Velocity, cm/s
B
2.21
1.58

Section A: Average Velocity, cm/s
A
2.06
1.63

Discharge

Section F: Sum of Discharge, cm3/s			Discharge Ratio
LF	RF	LF+RF	RF/LF
505.8	148.9	654.7	0.29

Section E: Sum of Discharge, cm3/s			Discharge Ratio
LE	RE	LE+RE	RE/LE
509.8	155.0	664.8	0.30

Section D: Sum of Discharge, cm3/s			Discharge Ratio
LD	RD	LD+RD	RD/LD
507.5	166.5	674.0	0.33

Section C: Sum of Discharge, cm3/s
C
656.1

Section B: Sum of Discharge, cm3/s
B
665.9

Section A: Sum of Discharge, cm3/s
A
650.5

Froude

Section F: Froude Number	
LF	RF
0.0390	0.0103

Section E: Froude Number	
LE	RE
0.0399	0.0108

Section D: Froude Number	
LD	RD
0.0394	0.0113

Section C: Froude Number
C
0.0225

Section B: Froude Number
B
0.0228

Section A: Froude Number
A
0.0222

Reynold

Section F: Reynold Number	
LF	RF
11846	3313

Section E: Reynold Number	
LE	RE
12000	3467

Section D: Reynold Number	
LD	RD
11907	3686

Section C: Reynold Number
C
11995

Section B: Reynold Number
B
12157

Section A: Reynold Number
A
11839

Calculation: 40_05_5050

Downstream

		Subsection Name		L50	L100	L150	L200	R50	R100	R150	R200
		Subsection Width	(mm)	75	50	50	75	75	50	50	75
Section F	A	Velocity	(cm/s)								
	A1	Near Surface Flow		2.64	2.67	2.68	2.68	2.84	2.73	2.73	2.44
	A2	Near Bed Flow		1.83	2.03	2.04	2.01	1.90	1.74	1.58	1.47
	B	Water Depth	(mm)	58.79	59.32	59.60	59.40	59.09	59.03	59.94	59.31
	C	Discharge	(cm3/s)								
	C1	Near Surface Flow		58.31	39.61	39.94	59.78	62.94	40.28	40.92	54.19
	C2	Near Bed Flow		40.44	30.11	30.38	44.71	42.07	25.68	23.75	32.81
	C3	Total Discharge		**98.75**	**69.72**	**70.31**	**104.49**	**105.01**	**65.96**	**64.67**	**87.00**
Section E	A	Velocity	(cm/s)								
	A1	Near Surface Flow		2.39	2.57	2.63	2.72	2.51	2.53	2.31	2.18
	A2	Near Bed Flow		1.90	2.08	2.21	2.28	2.29	2.23	2.11	1.93
	B	Water Depth	(mm)	57.42	58.04	59.34	58.87	58.58	59.19	58.94	59.02
	C	Discharge	(cm3/s)								
	C1	Near Surface Flow		51.53	37.26	39.06	60.08	55.19	37.48	34.01	48.27
	C2	Near Bed Flow		40.92	30.18	32.85	50.34	50.27	32.94	31.12	42.69
	C3	Total Discharge		**92.44**	**67.45**	**71.92**	**110.42**	**105.47**	**70.42**	**65.12**	**90.97**
Section D	A	Velocity	(cm/s)								
	A1	Near Surface Flow		2.34	2.47	2.68	2.69	2.48	2.55	2.59	2.55
	A2	Near Bed Flow		2.06	1.98	2.11	2.45	1.67	1.82	1.87	1.83
	B	Water Depth	(mm)	58.61	58.18	59.76	60.05	59.94	59.88	59.71	58.97
	C	Discharge	(cm3/s)								
	C1	Near Surface Flow		51.46	35.90	40.05	60.54	55.72	38.17	38.61	56.46
	C2	Near Bed Flow		45.37	28.74	31.45	55.07	37.44	27.21	27.89	40.53
	C3	Total Discharge		**96.83**	**64.64**	**71.50**	**115.61**	**93.16**	**65.38**	**66.51**	**96.99**

Upstream

		Subsection Name		U50	U100	U150	U200	U250	U300	U350	U400	U450
		Subsection Width	(mm)	75	50	50	50	50	50	50	50	75
Section C	A	Velocity	(cm/s)									
	A1	Near Surface Flow		2.18	2.23	2.39	2.49	2.61	2.71	2.70	2.74	2.62
	A2	Near Bed Flow		1.84	1.91	1.86	2.11	2.14	2.21	2.31	2.24	2.06
	B	Water Depth	(mm)	57.82	58.79	59.22	59.31	59.38	59.40	59.42	59.47	59.45
	C	Discharge	(cm3/s)									
	C1	Near Surface Flow		47.26	32.74	35.34	36.88	38.71	40.27	40.14	40.71	58.40
	C2	Near Bed Flow		39.81	28.01	27.50	31.32	31.79	32.86	34.33	33.29	45.86
	C3	Total Discharge		**87.07**	**60.75**	**62.84**	**68.20**	**70.51**	**73.14**	**74.47**	**74.00**	**104.26**
Section B	A	Velocity	(cm/s)									
	A1	Near Surface Flow		2.27	2.43	2.47	2.49	2.59	2.58	2.60	2.62	2.58
	A2	Near Bed Flow		1.75	1.86	1.94	1.98	2.05	2.15	2.08	2.16	2.13
	B	Water Depth	(mm)	58.73	58.18	58.37	58.34	58.42	59.84	60.42	60.33	59.20
	C	Discharge	(cm3/s)									
	C1	Near Surface Flow		50.06	35.38	36.02	36.30	37.78	38.66	39.20	39.52	57.31
	C2	Near Bed Flow		38.56	27.12	28.28	28.87	29.90	32.22	31.42	32.56	47.34
	C3	Total Discharge		**88.62**	**62.49**	**64.30**	**65.17**	**67.68**	**70.87**	**70.62**	**72.08**	**104.65**
Section A	A	Velocity	(cm/s)									
	A1	Near Surface Flow		2.48	2.48	2.53	2.81	2.90	2.82	2.80	2.81	2.62
	A2	Near Bed Flow		1.75	1.75	1.83	1.87	1.92	1.96	2.11	2.02	1.90
	B	Water Depth	(mm)	57.79	59.91	59.68	61.59	58.89	59.14	59.17	58.75	59.25
	C	Discharge	(cm3/s)									
	C1	Near Surface Flow		53.67	37.15	37.77	43.19	42.63	41.67	41.38	41.26	58.31
	C2	Near Bed Flow		37.93	26.27	27.32	28.79	28.24	29.04	31.24	29.71	42.27
	C3	Total Discharge		**91.60**	**63.42**	**65.09**	**71.99**	**70.87**	**70.71**	**72.62**	**70.98**	**100.58**

Water Depth

Average Water Depth, cm		Depth Ratio
LF	RF	RF/LF
5.93	5.93	1.00

Average Water Depth, cm		Depth Ratio
LE	RE	RE/LE
5.84	5.89	0.99

Average Water Depth, cm		Depth Ratio
LD	RD	RD/LD
5.92	5.96	0.99

Average Water Depth, cm
C
5.91

Average Water Depth, cm
B
5.91

Average Water Depth, cm
A
5.94

Velocity

Average Velocity, cm/s		Velocity Ratio
LF	RF	RF/LF
2.67	2.68	0.99
1.98	1.67	0.85

Average Velocity, cm/s		Velocity Ratio
LE	RE	RF/LF
2.58	2.38	0.92
2.12	2.14	0.99

Average Velocity, cm/s		Velocity Ratio
LD	RD	RF/LF
2.54	2.54	1.00
2.15	1.80	0.84

Average Velocity, cm/s
C
2.52
2.07

Average Velocity, cm/s
B
2.51
2.01

Average Velocity, cm/s
A
2.69
1.90

Discharge

Sum of Discharge, cm3/s			Discharge Ratio
LF	RF	LF+RF	RF/LF
343.3	322.6	665.9	0.94

Sum of Discharge, cm3/s			Discharge Ratio
LE	RE	LE+RE	RE/LE
342.2	332.0	674.2	0.97

Sum of Discharge, cm3/s			Discharge Ratio
LD	RD	LD+RD	RD/LD
348.6	322.0	670.6	0.92

Sum of Discharge, cm3/s
C
675.2

Sum of Discharge, cm3/s
B
666.5

Sum of Discharge, cm3/s
A
677.8

Froude

Froude Number	
LF	RF
0.0305	0.0286

Froude Number	
LE	RE
0.0310	0.0297

Froude Number	
LD	RD
0.0308	0.0284

Froude Number
C
0.0301

Froude Number
B
0.0297

Froude Number
A
0.0301

Reynold

Reynold Number	
LF	RF
8564	8035

Reynold Number	
LE	RE
8617	8318

Reynold Number	
LD	RD
8641	8010

Reynold Number
C
14198

Reynold Number
B
13990

Reynold Number
A
14218

Calculation: 40_05_5560

Downstream

		Subsection Name		L50	L100	L150	L200	R50	R100	R150	R200
		Subsection Width	(mm)	75	50	50	75	75	50	50	75
Section F	A	Velocity	(cm/s)								
	A1	Near Surface Flow		3.39	3.44	3.41	3.42	1.15	1.03	0.90	0.93
	A2	Near Bed Flow		2.89	2.96	2.94	2.93	0.57	0.42	0.26	0.11
	B	Water Depth	(mm)	66.65	67.26	67.46	67.29	69.04	69.79	69.85	69.75
	C	Discharge	(cm3/s)								
	C1	Near Surface Flow		84.70	57.82	57.54	86.18	29.80	18.06	15.66	24.26
	C2	Near Bed Flow		72.29	49.85	49.55	73.98	14.64	7.30	4.49	2.76
	C3	Total Discharge		**156.99**	**107.67**	**107.10**	**160.16**	**44.44**	**25.36**	**20.15**	**27.01**
Section E	A	Velocity	(cm/s)								
	A1	Near Surface Flow		3.53	3.58	3.61	3.66	0.79	0.71	0.60	0.55
	A2	Near Bed Flow		3.27	3.31	3.35	3.38	0.66	0.60	0.40	0.35
	B	Water Depth	(mm)	64.65	66.29	67.60	67.37	69.20	69.36	69.73	69.69
	C	Discharge	(cm3/s)								
	C1	Near Surface Flow		85.62	59.26	60.94	92.55	20.46	12.33	10.40	14.44
	C2	Near Bed Flow		79.39	54.89	56.70	85.28	17.18	10.35	6.93	9.27
	C3	Total Discharge		**165.01**	**114.14**	**117.64**	**177.83**	**37.64**	**22.68**	**17.33**	**23.71**
Section D	A	Velocity	(cm/s)								
	A1	Near Surface Flow		3.47	3.58	3.70	3.76	0.89	0.75	0.68	0.68
	A2	Near Bed Flow		3.11	3.21	3.30	3.22	0.56	0.58	0.47	0.35
	B	Water Depth	(mm)	66.16	67.02	69.20	69.07	70.98	70.63	70.61	69.88
	C	Discharge	(cm3/s)								
	C1	Near Surface Flow		86.17	59.91	63.99	97.51	23.61	13.24	12.09	17.76
	C2	Near Bed Flow		77.20	53.78	57.04	83.33	14.90	10.28	8.30	9.29
	C3	Total Discharge		**163.37**	**113.69**	**121.03**	**180.85**	**38.51**	**23.53**	**20.38**	**27.05**

Upstream

		Subsection Name		U50	U100	U150	U200	U250	U300	U350	U400	U450
		Subsection Width	(mm)	75	50	50	50	50	50	50	50	75
Section C	A	Velocity	(cm/s)									
	A1	Near Surface Flow		2.34	2.28	2.42	2.38	2.51	2.50	2.55	2.44	2.28
	A2	Near Bed Flow		1.19	1.23	1.37	1.48	1.56	1.57	1.51	1.47	1.20
	B	Water Depth	(mm)	68.62	70.32	70.43	70.55	70.56	70.62	70.65	70.71	70.67
	C	Discharge	(cm3/s)									
	C1	Near Surface Flow		60.14	40.00	42.68	42.00	44.34	44.19	45.03	43.14	60.43
	C2	Near Bed Flow		30.63	21.61	24.11	26.14	27.45	27.63	26.60	26.01	31.82
	C3	Total Discharge		**90.77**	**61.60**	**66.78**	**68.14**	**71.79**	**71.82**	**71.62**	**69.15**	**92.25**
Section B	A	Velocity	(cm/s)									
	A1	Near Surface Flow		2.12	2.09	2.09	2.08	2.18	2.23	2.22	2.21	2.20
	A2	Near Bed Flow		1.46	1.47	1.50	1.53	1.58	1.64	1.58	1.68	1.58
	B	Water Depth	(mm)	70.20	70.45	70.11	69.95	69.92	71.58	72.47	72.81	71.09
	C	Discharge	(cm3/s)									
	C1	Near Surface Flow		55.78	36.75	36.58	36.40	38.10	39.95	40.20	40.31	58.52
	C2	Near Bed Flow		38.44	25.87	26.21	26.82	27.67	29.31	28.64	30.57	42.11
	C3	Total Discharge		**94.22**	**62.63**	**62.80**	**63.22**	**65.77**	**69.26**	**68.83**	**70.88**	**100.63**
Section A	A	Velocity	(cm/s)									
	A1	Near Surface Flow		2.08	2.23	2.25	2.33	2.40	2.49	2.51	2.54	2.53
	A2	Near Bed Flow		1.23	1.43	1.46	1.49	1.51	1.61	1.67	1.74	1.69
	B	Water Depth	(mm)	71.02	70.90	71.01	70.96	70.73	70.25	69.45	68.51	68.41
	C	Discharge	(cm3/s)									
	C1	Near Surface Flow		55.52	39.53	39.91	41.37	42.46	43.65	43.54	43.44	64.99
	C2	Near Bed Flow		32.73	25.37	25.87	26.47	26.79	28.34	28.99	29.87	43.44
	C3	Total Discharge		**88.24**	**64.89**	**65.78**	**67.84**	**69.25**	**71.99**	**72.53**	**73.31**	**108.43**

Water Depth

Section F

Average Water Depth, cm		Depth Ratio
LF	RF	RF/LF
6.72	6.96	0.96

Section E

Average Water Depth, cm		Depth Ratio
LE	RE	RE/LE
6.65	6.95	0.96

Section D

Average Water Depth, cm		Depth Ratio
LD	RD	RD/LD
6.79	7.05	0.96

Section C

Average Water Depth, cm
C
7.03

Section B

Average Water Depth, cm
B
7.10

Section A

Average Water Depth, cm
A
7.01

Velocity

Section F

Average Velocity, cm/s		Velocity Ratio
LF	RF	RF/LF
3.41	1.00	0.29
2.93	0.34	0.11

Section E

Average Velocity, cm/s		Velocity Ratio
LE	RE	RF/LF
3.59	0.66	0.18
3.33	0.50	0.15

Section D

Average Velocity, cm/s		Velocity Ratio
LD	RD	RF/LF
3.63	0.75	0.21
3.21	0.49	0.15

Section C

Average Velocity, cm/s
C
2.41
1.40

Section B

Average Velocity, cm/s
B
2.16
1.56

Section A

Average Velocity, cm/s
A
2.37
1.54

Discharge

Section F

Sum of Discharge, cm3/s			Discharge Ratio
LF	RF	LF+RF	RF/LF
531.9	117.0	648.9	0.22

Section E

Sum of Discharge, cm3/s			Discharge Ratio
LE	RE	LE+RE	RE/LE
574.6	101.4	676.0	0.18

Section D

Sum of Discharge, cm3/s			Discharge Ratio
LD	RD	LD+RD	RD/LD
578.9	109.5	688.4	0.19

Section C

Sum of Discharge, cm3/s
C
663.9

Section B

Sum of Discharge, cm3/s
B
658.3

Section A

Sum of Discharge, cm3/s
A
682.3

Froude

Section F

Froude Number	
LF	RF
0.0391	0.0081

Section E

Froude Number	
LE	RE
0.0429	0.0071

Section D

Froude Number	
LD	RD
0.0419	0.0075

Section C

Froude Number
C
0.0229

Section B

Froude Number
B
0.0223

Section A

Froude Number
A
0.0236

Reynold

Section F

Reynold Number	
LF	RF
12194	2606

Section E

Reynold Number	
LE	RE
13257	2266

Section D

Reynold Number	
LD	RD
13186	2428

Section C

Reynold Number
C
12199

Section B

Reynold Number
B
11923

Section A

Reynold Number
A
12522

Calculation: 40_05_5055

Downstream

		Subsection Name		L50	L100	L150	L200	R50	R100	R150	R200
		Subsection Width	(mm)	75	50	50	75	75	50	50	75
Section F	A	Velocity	(cm/s)								
	A1	Near Surface Flow		3.33	3.43	3.40	3.43	1.14	1.08	1.02	0.92
	A2	Near Bed Flow		2.76	2.83	2.89	2.81	0.79	0.65	0.57	0.49
	B	Water Depth	(mm)	61.92	62.22	62.51	62.05	64.08	65.08	65.32	65.01
	C	Discharge	(cm3/s)								
	C1	Near Surface Flow		77.35	53.29	53.15	79.72	27.38	17.57	16.68	22.54
	C2	Near Bed Flow		64.13	44.04	45.18	65.41	18.97	10.56	9.31	11.92
	C3	Total Discharge		**141.48**	**97.33**	**98.33**	**145.13**	**46.35**	**28.14**	**25.99**	**34.47**
Section E	A	Velocity	(cm/s)								
	A1	Near Surface Flow		3.19	3.25	3.34	3.45	1.02	0.95	0.85	0.73
	A2	Near Bed Flow		2.72	2.84	2.96	3.00	0.82	0.77	0.57	0.52
	B	Water Depth	(mm)	60.56	61.42	62.13	61.85	64.04	64.49	64.43	64.22
	C	Discharge	(cm3/s)								
	C1	Near Surface Flow		72.48	49.91	51.81	79.99	24.47	15.38	13.76	17.62
	C2	Near Bed Flow		61.86	43.68	45.99	69.47	19.77	12.45	9.17	12.58
	C3	Total Discharge		**134.34**	**93.59**	**97.80**	**149.45**	**44.25**	**27.83**	**22.93**	**30.20**
Section D	A	Velocity	(cm/s)								
	A1	Near Surface Flow		2.90	3.16	3.31	3.55	1.27	1.24	1.35	1.24
	A2	Near Bed Flow		2.75	2.81	2.91	3.06	0.71	0.59	0.56	0.52
	B	Water Depth	(mm)	58.62	60.32	62.12	63.19	66.43	66.25	65.70	65.12
	C	Discharge	(cm3/s)								
	C1	Near Surface Flow		63.64	47.72	51.34	84.24	31.52	20.50	22.25	30.19
	C2	Near Bed Flow		60.38	42.34	45.24	72.53	17.75	9.85	9.13	12.76
	C3	Total Discharge		**124.03**	**90.06**	**96.58**	**156.77**	**49.27**	**30.35**	**31.38**	**42.95**

Upstream

		Subsection Name		U50	U100	U150	U200	U250	U300	U350	U400	U450
		Subsection Width	(mm)	75	50	50	50	50	50	50	50	75
Section C	A	Velocity	(cm/s)									
	A1	Near Surface Flow		2.03	2.00	2.09	2.22	2.26	2.44	2.39	2.26	2.09
	A2	Near Bed Flow		1.36	1.42	1.42	1.49	1.51	1.58	1.49	1.48	1.38
	B	Water Depth	(mm)	64.25	64.73	65.70	65.80	65.89	65.90	65.95	65.95	65.92
	C	Discharge	(cm3/s)									
	C1	Near Surface Flow		48.82	32.35	34.39	36.58	37.18	40.12	39.48	37.27	51.56
	C2	Near Bed Flow		32.84	22.96	23.40	24.43	24.82	26.03	24.59	24.47	34.23
	C3	Total Discharge		**81.65**	**55.31**	**57.79**	**61.01**	**62.00**	**66.15**	**64.07**	**61.74**	**85.79**
Section B	A	Velocity	(cm/s)									
	A1	Near Surface Flow		1.63	1.81	1.94	2.11	2.13	2.25	2.36	2.28	2.19
	A2	Near Bed Flow		1.31	1.38	1.55	1.65	1.75	1.89	1.91	1.72	1.79
	B	Water Depth	(mm)	64.66	65.21	65.06	64.94	64.77	66.42	66.85	67.06	66.37
	C	Discharge	(cm3/s)									
	C1	Near Surface Flow		39.47	29.44	31.50	34.19	34.43	37.34	39.44	38.27	54.46
	C2	Near Bed Flow		31.83	22.44	25.26	26.71	28.34	31.32	31.96	28.84	44.58
	C3	Total Discharge		**71.29**	**51.88**	**56.75**	**60.90**	**62.77**	**68.66**	**71.40**	**67.11**	**99.05**
Section A	A	Velocity	(cm/s)									
	A1	Near Surface Flow		1.69	1.82	1.94	2.05	2.03	2.10	2.18	2.17	2.18
	A2	Near Bed Flow		1.59	1.64	1.77	1.75	1.78	1.85	1.98	1.93	1.81
	B	Water Depth	(mm)	65.89	66.17	66.26	66.31	66.00	65.68	64.95	63.57	64.35
	C	Discharge	(cm3/s)									
	C1	Near Surface Flow		41.64	30.13	32.21	34.05	33.49	34.49	35.41	34.56	52.67
	C2	Near Bed Flow		39.34	27.13	29.30	29.06	29.39	30.39	32.14	30.67	43.71
	C3	Total Discharge		**80.98**	**57.26**	**61.50**	**63.10**	**62.88**	**64.88**	**67.54**	**65.23**	**96.38**

Water Depth

Section F

Average Water Depth, cm		Depth Ratio
LF	RF	RF/LF
6.22	6.49	0.96

Section E

Average Water Depth, cm		Depth Ratio
LE	RE	RE/LE
6.15	6.43	0.96

Section D

Average Water Depth, cm		Depth Ratio
LD	RD	RD/LD
6.11	6.59	0.93

Section C

Average Water Depth, cm
C
6.56

Section B

Average Water Depth, cm
B
6.57

Section A

Average Water Depth, cm
A
6.55

Velocity

Section F

Average Velocity, cm/s		Velocity Ratio
LF	RF	RF/LF
3.40	1.04	0.31
2.82	0.62	0.22

Section E

Average Velocity, cm/s		Velocity Ratio
LE	RE	RF/LF
3.31	0.89	0.27
2.88	0.67	0.23

Section D

Average Velocity, cm/s		Velocity Ratio
LD	RD	RF/LF
3.23	1.27	0.39
2.88	0.60	0.21

Section C

Average Velocity, cm/s
C
2.20
1.46

Section B

Average Velocity, cm/s
B
2.08
1.66

Section A

Average Velocity, cm/s
A
2.02
1.79

Discharge

Section F

Sum of Discharge, cm3/s			Discharge Ratio
LF	RF	LF+RF	RF/LF
482.3	134.9	617.2	0.28

Section E

Sum of Discharge, cm3/s			Discharge Ratio
LE	RE	LE+RE	RE/LE
475.2	125.2	600.4	0.26

Section D

Sum of Discharge, cm3/s			Discharge Ratio
LD	RD	LD+RD	RD/LD
467.4	154.0	621.4	0.33

Section C

Sum of Discharge, cm3/s
C
595.5

Section B

Sum of Discharge, cm3/s
B
609.8

Section A

Sum of Discharge, cm3/s
A
619.8

Froude

Section F

Froude Number	
LF	RF
0.0398	0.0104

Section E

Froude Number	
LE	RE
0.0398	0.0098

Section D

Froude Number	
LD	RD
0.0395	0.0116

Section C

Froude Number
C
0.0228

Section B

Froude Number
B
0.0233

Section A

Froude Number
A
0.0238

Reynold

Section F

Reynold Number	
LF	RF
11642	3163

Section E

Reynold Number	
LE	RE
11539	2956

Section D

Reynold Number	
LD	RD
11373	3569

Section C

Reynold Number
C
11541

Section B

Reynold Number
B
11797

Section A

Reynold Number
A
12015

Calculation: 40_07_5050

Downstream

	Subsection Name		L50	L100	L150	L200	R50	R100	R150	R200
	Subsection Width	(mm)	75	50	50	75	75	50	50	75
Section F	A Velocity	(cm/s)								
	A1 Near Surface Flow		2.51	2.56	2.58	2.77	2.60	2.62	2.59	2.33
	A2 Near Bed Flow		2.13	2.13	2.24	2.29	2.10	2.12	2.01	1.83
	B Water Depth	(mm)	58.26	58.96	58.85	58.01	58.70	59.20	59.02	58.12
	C Discharge	(cm3/s)								
	C1 Near Surface Flow		54.94	37.69	38.03	60.34	57.29	38.85	38.23	50.89
	C2 Near Bed Flow		46.45	31.35	32.92	49.85	46.17	31.36	29.60	39.85
	C3 Total Discharge		**101.38**	**69.03**	**70.94**	**110.19**	**103.46**	**70.20**	**67.83**	**90.73**
Section E	A Velocity	(cm/s)								
	A1 Near Surface Flow		2.45	2.48	2.58	2.69	2.21	2.65	2.51	2.30
	A2 Near Bed Flow		2.11	2.25	2.35	2.52	2.27	2.22	2.12	1.97
	B Water Depth	(mm)	55.27	57.48	58.37	57.6	57.28	57.23	57.64	57.68
	C Discharge	(cm3/s)								
	C1 Near Surface Flow		50.87	35.64	37.69	58.04	47.53	37.97	36.10	49.69
	C2 Near Bed Flow		43.66	32.35	34.30	54.45	48.68	31.79	30.62	42.57
	C3 Total Discharge		**94.53**	**67.99**	**71.99**	**112.50**	**96.21**	**69.76**	**66.72**	**92.25**
Section D	A Velocity	(cm/s)								
	A1 Near Surface Flow		2.51	2.61	2.78	2.91	2.46	2.60	2.56	2.55
	A2 Near Bed Flow		1.94	2.09	2.18	2.23	1.88	1.94	1.97	2.01
	B Water Depth	(mm)	54.13	55.79	57.8	57.69	58.93	57.99	55.37	57.12
	C Discharge	(cm3/s)								
	C1 Near Surface Flow		50.86	36.43	40.19	62.95	54.27	37.71	35.48	54.69
	C2 Near Bed Flow		39.42	29.20	31.52	48.21	41.56	28.09	27.33	42.97
	C3 Total Discharge		**90.28**	**65.63**	**71.71**	**111.16**	**95.83**	**65.79**	**62.81**	**97.66**

Upstream

	Subsection Name		U50	U100	U150	U200	U250	U300	U350	U400	U450
	Subsection Width	(mm)	75	50	50	50	50	50	50	50	75
Section C	A Velocity	(cm/s)									
	A1 Near Surface Flow		2.58	2.55	2.56	2.82	2.83	2.80	2.95	3.00	2.76
	A2 Near Bed Flow		1.86	1.72	1.69	1.85	2.04	2.11	2.12	2.06	1.95
	B Water Depth	(mm)	55.89	56.61	56.99	57.08	57.07	57.08	57.04	57.08	57.04
	C Discharge	(cm3/s)									
	C1 Near Surface Flow		54.08	36.14	36.41	40.29	40.33	40.00	42.02	42.87	59.04
	C2 Near Bed Flow		38.99	24.29	24.14	26.36	29.11	30.10	30.21	29.43	41.78
	C3 Total Discharge		**93.07**	**60.43**	**60.55**	**66.65**	**69.45**	**70.10**	**72.23**	**72.30**	**100.81**
Section B	A Velocity	(cm/s)									
	A1 Near Surface Flow		2.68	2.58	2.66	2.74	2.84	2.94	2.88	2.86	2.79
	A2 Near Bed Flow		1.65	1.71	1.78	1.88	1.96	2.01	2.03	2.03	1.93
	B Water Depth	(mm)	56.00	55.72	55.68	55.70	55.79	56.89	57.57	56.59	55.16
	C Discharge	(cm3/s)									
	C1 Near Surface Flow		56.19	35.93	37.05	38.16	39.67	41.79	41.41	40.43	57.69
	C2 Near Bed Flow		34.66	23.84	24.71	26.25	27.31	28.57	29.17	28.74	39.88
	C3 Total Discharge		**90.85**	**59.77**	**61.76**	**64.41**	**66.98**	**70.36**	**70.58**	**69.18**	**97.57**
Section A	A Velocity	(cm/s)									
	A1 Near Surface Flow		2.47	2.48	2.62	2.69	2.75	2.78	2.84	2.72	2.67
	A2 Near Bed Flow		1.94	1.97	1.98	2.05	2.13	2.21	2.29	2.28	2.35
	B Water Depth	(mm)	56.85	57.02	57.09	57.07	56.99	56.79	56.14	54.61	53.97
	C Discharge	(cm3/s)									
	C1 Near Surface Flow		52.58	35.40	37.44	38.32	39.17	39.53	39.82	37.16	53.99
	C2 Near Bed Flow		41.32	28.02	28.28	29.25	30.33	31.32	32.11	31.13	47.51
	C3 Total Discharge		**93.90**	**63.41**	**65.72**	**67.57**	**69.50**	**70.84**	**71.93**	**68.29**	**101.50**

Water Depth

Average Water Depth, cm		Depth Ratio
LF	RF	RF/LF
5.85	5.88	1.00

Average Water Depth, cm		Depth Ratio
LE	RE	RE/LE
5.72	5.75	1.00

Average Water Depth, cm		Depth Ratio
LD	RD	RD/LD
5.64	5.74	0.98

Average Water Depth, cm
C
5.69

Average Water Depth, cm
B
5.61

Average Water Depth, cm
A
5.63

Velocity

Average Velocity, cm/s		Velocity Ratio
LF	RF	RF/LF
2.61	2.54	0.97
2.20	2.01	0.92

Average Velocity, cm/s		Velocity Ratio
LE	RE	RF/LF
2.55	2.42	0.95
2.31	2.15	0.93

Average Velocity, cm/s		Velocity Ratio
LD	RD	RF/LF
2.70	2.54	0.94
2.11	1.95	0.92

Average Velocity, cm/s
C
2.76
1.93

Average Velocity, cm/s
B
2.77
1.89

Average Velocity, cm/s
A
2.67
2.13

Discharge

Sum of Discharge, cm3/s			Discharge Ratio
LF	RF	LF+RF	RF/LF
351.6	332.2	683.8	0.95

Sum of Discharge, cm3/s			Discharge Ratio
LE	RE	LE+RE	RE/LE
347.0	324.9	671.9	0.94

Sum of Discharge, cm3/s			Discharge Ratio
LD	RD	LD+RD	RD/LD
338.8	322.1	660.9	0.95

Sum of Discharge, cm3/s
C
665.6

Sum of Discharge, cm3/s
B
651.5

Sum of Discharge, cm3/s
A
672.7

Froude

Froude Number	
LF	RF
0.0317	0.0300

Froude Number	
LE	RE
0.0324	0.0304

Froude Number	
LD	RD
0.0324	0.0299

Froude Number
C
0.0314

Froude Number
B
0.0314

Froude Number
A
0.0323

Reynold

Reynold Number	
LF	RF
8814	8362

Reynold Number	
LE	RE
8851	8325

Reynold Number	
LD	RD
8729	8193

Reynold Number
C
14408

Reynold Number
B
14265

Reynold Number
A
14703

Calculation: 40_07_5560

Downstream

		Subsection Name		L50	L100	L150	L200	R50	R100	R150	R200
		Subsection Width	(mm)	75	50	50	75	75	50	50	75
Section F	A	Velocity	(cm/s)								
	A1	Near Surface Flow		3.38	3.50	3.49	3.74	1.11	1.12	1.04	0.82
	A2	Near Bed Flow		2.98	2.98	3.11	3.13	0.56	0.37	0.29	0.13
	B	Water Depth	(mm)	66.13	66.54	65.85	65.79	68.75	69.15	69.66	69.13
	C	Discharge	(cm3/s)								
	C1	Near Surface Flow		83.83	58.30	57.42	92.39	28.50	19.35	18.11	21.38
	C2	Near Bed Flow		73.90	49.58	51.22	77.25	14.42	6.44	5.08	3.35
	C3	Total Discharge		**157.73**	**107.88**	**108.65**	**169.63**	**42.93**	**25.79**	**23.19**	**24.73**
Section E	A	Velocity	(cm/s)								
	A1	Near Surface Flow		3.11	3.22	3.31	3.31	0.85	0.82	0.72	0.57
	A2	Near Bed Flow		3.04	3.13	3.26	3.30	0.70	0.65	0.53	0.42
	B	Water Depth	(mm)	63.15	65.07	66.25	65.67	68.24	68.35	68.21	68.35
	C	Discharge	(cm3/s)								
	C1	Near Surface Flow		73.59	52.31	54.81	81.48	21.64	13.94	12.28	14.65
	C2	Near Bed Flow		71.96	50.95	53.98	81.29	18.01	11.06	9.10	10.67
	C3	Total Discharge		**145.56**	**103.26**	**108.79**	**162.77**	**39.65**	**24.99**	**21.38**	**25.32**
Section D	A	Velocity	(cm/s)								
	A1	Near Surface Flow		3.17	3.47	3.54	3.62	1.05	1.12	1.09	0.98
	A2	Near Bed Flow		3.25	3.36	3.42	3.46	0.13	0.19	0.19	0.13
	B	Water Depth	(mm)	63.23	64.70	66.30	65.84	69.73	69.17	66.53	67.63
	C	Discharge	(cm3/s)								
	C1	Near Surface Flow		75.21	56.19	58.71	89.31	27.52	19.39	18.16	24.83
	C2	Near Bed Flow		77.11	54.34	56.61	85.54	3.51	3.32	3.21	3.31
	C3	Total Discharge		**152.32**	**110.53**	**115.32**	**174.86**	**31.02**	**22.71**	**21.37**	**28.14**

Upstream

		Subsection Name		U50	U100	U150	U200	U250	U300	U350	U400	U450
		Subsection Width	(mm)	75	50	50	50	50	50	50	50	75
Section C	A	Velocity	(cm/s)									
	A1	Near Surface Flow		2.03	2.02	2.08	2.28	2.40	2.33	2.50	2.35	2.29
	A2	Near Bed Flow		1.56	1.44	1.59	1.68	1.66	1.75	1.91	1.85	1.74
	B	Water Depth	(mm)	67.71	68.00	68.55	68.62	68.64	68.70	68.63	68.67	68.64
	C	Discharge	(cm3/s)									
	C1	Near Surface Flow		51.50	34.31	35.73	39.17	41.19	39.98	42.83	40.43	58.83
	C2	Near Bed Flow		39.69	24.48	27.24	28.85	28.47	30.07	32.81	31.78	44.80
	C3	Total Discharge		**91.18**	**58.79**	**62.97**	**68.02**	**69.66**	**70.05**	**75.64**	**72.21**	**103.63**
Section B	A	Velocity	(cm/s)									
	A1	Near Surface Flow		2.07	2.24	2.28	2.29	2.41	2.52	2.48	2.46	2.42
	A2	Near Bed Flow		1.56	1.54	1.57	1.59	1.58	1.60	1.63	1.62	1.60
	B	Water Depth	(mm)	68.65	68.09	69.39	68.40	69.01	70.21	70.23	69.26	67.75
	C	Discharge	(cm3/s)									
	C1	Near Surface Flow		53.22	38.18	39.47	39.19	41.66	44.20	43.59	42.66	61.41
	C2	Near Bed Flow		40.23	26.18	27.20	27.13	27.29	28.09	28.66	28.05	40.60
	C3	Total Discharge		**93.45**	**64.36**	**66.67**	**66.31**	**68.95**	**72.29**	**72.25**	**70.72**	**102.01**
Section A	A	Velocity	(cm/s)									
	A1	Near Surface Flow		2.03	2.08	2.23	2.28	2.41	2.45	2.42	2.36	2.20
	A2	Near Bed Flow		1.48	1.51	1.54	1.60	1.66	1.80	1.81	1.73	1.73
	B	Water Depth	(mm)	69.66	69.86	69.95	69.96	69.83	69.64	68.99	67.54	66.81
	C	Discharge	(cm3/s)									
	C1	Near Surface Flow		52.93	36.34	39.08	39.79	42.08	42.66	41.81	39.92	55.23
	C2	Near Bed Flow		38.59	26.41	27.01	28.06	28.93	31.26	31.27	29.17	43.35
	C3	Total Discharge		**91.52**	**62.75**	**66.09**	**67.85**	**71.01**	**73.92**	**73.08**	**69.08**	**98.58**

Water Depth

Average Water Depth, cm		Depth Ratio
LF	RF	RF/LF
6.61	6.92	0.96

Average Water Depth, cm		Depth Ratio
LE	RE	RE/LE
6.50	6.83	0.95

Average Water Depth, cm		Depth Ratio
LD	RD	RD/LD
6.50	6.83	0.95

Average Water Depth, cm
C
6.85

Average Water Depth, cm
B
6.90

Average Water Depth, cm
A
6.91

Velocity

Average Velocity, cm/s		Velocity Ratio
LF	RF	RF/LF
3.53	1.02	0.29
3.05	0.34	0.11

Average Velocity, cm/s		Velocity Ratio
LE	RE	RF/LF
3.24	0.74	0.23
3.18	0.58	0.18

Average Velocity, cm/s		Velocity Ratio
LD	RD	RF/LF
3.45	1.06	0.31
3.37	0.16	0.05

Average Velocity, cm/s
C
2.25
1.69

Average Velocity, cm/s
B
2.35
1.59

Average Velocity, cm/s
A
2.27
1.65

Discharge

Sum of Discharge, cm3/s			Discharge Ratio
LF	RF	LF+RF	RF/LF
543.9	116.6	660.5	0.21

Sum of Discharge, cm3/s			Discharge Ratio
LE	RE	LE+RE	RE/LE
520.4	111.3	631.7	0.21

Sum of Discharge, cm3/s			Discharge Ratio
LD	RD	LD+RD	RD/LD
553.0	103.2	656.3	0.19

Sum of Discharge, cm3/s
C
672.1

Sum of Discharge, cm3/s
B
677.0

Sum of Discharge, cm3/s
A
673.9

Froude

Froude Number	
LF	RF
0.0409	0.0083

Froude Number	
LE	RE
0.0402	0.0080

Froude Number	
LD	RD
0.0427	0.0075

Froude Number
C
0.0240

Froude Number
B
0.0239

Froude Number
A
0.0238

Reynold

Reynold Number	
LF	RF
12573	2642

Reynold Number	
LE	RE
12197	2539

Reynold Number	
LD	RD
12967	2365

Reynold Number
C
12550

Reynold Number
B
12569

Reynold Number
A
12529

Calculation: 40_05_5055

Downstream

		Subsection Name		L50	L100	L150	L200	R50	R100	R150	R200
		Subsection Width	(mm)	75	50	50	75	75	50	50	75
Section F	A	Velocity	(cm/s)								
	A1	Near Surface Flow		3.33	3.39	3.66	3.67	1.47	1.35	1.24	1.13
	A2	Near Bed Flow		3.10	3.11	3.23	3.32	0.89	0.80	0.58	0.34
	B	Water Depth	(mm)	59.57	59.15	59.49	59.19	62.44	63.61	62.93	62.46
	C	Discharge	(cm3/s)								
	C1	Near Surface Flow		74.32	50.13	54.49	81.47	34.53	21.49	19.53	26.42
	C2	Near Bed Flow		69.14	45.92	48.03	73.71	20.75	12.71	9.07	7.88
	C3	Total Discharge		**143.47**	**96.05**	**102.51**	**155.18**	**55.28**	**34.19**	**28.60**	**34.30**
Section E	A	Velocity	(cm/s)								
	A1	Near Surface Flow		3.40	3.51	3.63	3.61	1.21	1.17	1.03	0.86
	A2	Near Bed Flow		3.19	3.30	3.47	3.58	1.07	1.04	0.94	0.81
	B	Water Depth	(mm)	57.51	59.41	60.06	59.97	61.98	61.75	62.28	62.33
	C	Discharge	(cm3/s)								
	C1	Near Surface Flow		73.27	52.12	54.46	81.19	28.21	18.00	16.02	20.07
	C2	Near Bed Flow		68.86	49.06	52.04	80.51	24.81	16.01	14.64	18.97
	C3	Total Discharge		**142.13**	**101.18**	**106.49**	**161.70**	**53.01**	**34.01**	**30.66**	**39.03**
Section D	A	Velocity	(cm/s)								
	A1	Near Surface Flow		3.37	3.61	3.70	3.81	1.38	1.45	1.26	1.23
	A2	Near Bed Flow		3.12	3.27	3.41	3.54	0.73	0.80	0.73	0.83
	B	Water Depth	(mm)	56.79	58.50	59.35	59.87	64.25	63.37	60.67	62.19
	C	Discharge	(cm3/s)								
	C1	Near Surface Flow		71.83	52.81	54.83	85.54	33.36	22.98	19.07	28.71
	C2	Near Bed Flow		66.45	47.83	50.54	79.47	17.59	12.73	11.02	19.42
	C3	Total Discharge		**138.28**	**100.64**	**105.38**	**165.02**	**50.95**	**35.71**	**30.09**	**48.13**

Upstream

		Subsection Name		U50	U100	U150	U200	U250	U300	U350	U400	U450
		Subsection Width	(mm)	75	50	50	50	50	50	50	50	75
Section C	A	Velocity	(cm/s)									
	A1	Near Surface Flow		2.18	2.10	2.43	2.36	2.51	2.66	2.68	2.53	2.42
	A2	Near Bed Flow		1.73	1.57	1.80	1.80	1.94	1.91	2.05	1.94	1.97
	B	Water Depth	(mm)	62.00	62.69	63.10	63.22	63.21	63.20	63.20	63.23	63.20
	C	Discharge	(cm3/s)									
	C1	Near Surface Flow		50.75	32.93	38.33	37.36	39.70	42.09	42.39	40.05	57.44
	C2	Near Bed Flow		40.23	24.55	28.46	28.40	30.71	30.24	32.37	30.69	46.58
	C3	Total Discharge		**90.98**	**57.49**	**66.78**	**65.76**	**70.41**	**72.33**	**74.76**	**70.74**	**104.02**
Section B	A	Velocity	(cm/s)									
	A1	Near Surface Flow		1.77	2.38	2.29	2.45	2.51	2.61	2.76	2.58	2.61
	A2	Near Bed Flow		1.33	1.44	1.70	1.81	1.94	2.04	2.11	2.10	2.00
	B	Water Depth	(mm)	63.39	63.07	62.96	63.06	63.09	64.24	64.65	63.82	62.29
	C	Discharge	(cm3/s)									
	C1	Near Surface Flow		42.02	37.46	36.04	38.57	39.62	41.94	44.68	41.11	61.08
	C2	Near Bed Flow		31.68	22.66	26.82	28.55	30.55	32.77	34.07	33.45	46.66
	C3	Total Discharge		**73.69**	**60.12**	**62.86**	**67.12**	**70.16**	**74.71**	**78.76**	**74.56**	**107.73**
Section A	A	Velocity	(cm/s)									
	A1	Near Surface Flow		2.03	2.22	2.21	2.23	2.28	2.33	2.45	2.44	2.59
	A2	Near Bed Flow		1.64	1.66	1.75	1.87	1.91	2.01	2.00	2.08	2.29
	B	Water Depth	(mm)	64.41	64.59	64.65	64.66	64.55	64.35	63.12	61.79	61.82
	C	Discharge	(cm3/s)									
	C1	Near Surface Flow		49.11	35.80	35.73	36.04	36.82	37.55	38.72	37.71	59.96
	C2	Near Bed Flow		39.65	26.78	28.33	30.30	30.90	32.32	31.62	32.19	53.00
	C3	Total Discharge		**88.76**	**62.58**	**64.06**	**66.34**	**67.72**	**69.87**	**70.34**	**69.90**	**112.96**

Water Depth

Average Water Depth, cm		Depth Ratio
LF	RF	RF/LF
5.94	6.29	0.94

Average Water Depth, cm		Depth Ratio
LE	RE	RE/LE
5.92	6.21	0.95

Average Water Depth, cm		Depth Ratio
LD	RD	RD/LD
5.86	6.26	0.94

Average Water Depth, cm
C
6.30

Average Water Depth, cm
B
6.34

Average Water Depth, cm
A
6.38

Velocity

Average Velocity, cm/s		Velocity Ratio
LF	RF	RF/LF
3.51	1.30	0.37
3.19	0.65	0.20

Average Velocity, cm/s		Velocity Ratio
LE	RE	RF/LF
3.54	1.07	0.30
3.39	0.96	0.28

Average Velocity, cm/s		Velocity Ratio
LD	RD	RF/LF
3.62	1.33	0.37
3.33	0.77	0.23

Average Velocity, cm/s
C
2.43
1.86

Average Velocity, cm/s
B
2.44
1.83

Average Velocity, cm/s
A
2.31
1.91

Discharge

Sum of Discharge, cm3/s			Discharge Ratio
LF	RF	LF+RF	RF/LF
497.2	152.4	649.6	0.31

Sum of Discharge, cm3/s			Discharge Ratio
LE	RE	LE+RE	RE/LE
511.5	156.7	668.2	0.31

Sum of Discharge, cm3/s			Discharge Ratio
LD	RD	LD+RD	RD/LD
509.3	164.9	674.2	0.32

Sum of Discharge, cm3/s
C
673.3

Sum of Discharge, cm3/s
B
669.7

Sum of Discharge, cm3/s
A
672.5

Froude

Froude Number	
LF	RF
0.0439	0.0124

Froude Number	
LE	RE
0.0454	0.0130

Froude Number	
LD	RD
0.0459	0.0134

Froude Number
C
0.0273

Froude Number
B
0.0271

Froude Number
A
0.0267

Reynold

Reynold Number	
LF	RF
12352	3660

Reynold Number	
LE	RE
12752	3799

Reynold Number	
LD	RD
12774	3948

Reynold Number
C
13426

Reynold Number
B
13380

Reynold Number
A
13252

Calculation: 50_03_5050

Downstream

		Subsection Name		L50	L100	L150	L200	R50	R100	R150	R200
		Subsection Width	(mm)	75	50	50	75	75	50	50	75
Section F	A	Velocity	(cm/s)								
	A1	Near Surface Flow		2.51	2.63	2.76	2.82	2.44	2.56	2.37	2.30
	A2	Near Bed Flow		1.56	1.76	1.87	1.94	1.77	1.76	1.74	1.65
	B	Water Depth	(mm)	61.09	62.79	63.53	64.01	63.71	63.67	63.23	61.43
	C	Discharge	(cm3/s)								
	C1	Near Surface Flow		57.46	41.31	43.90	67.65	58.23	40.81	37.54	52.91
	C2	Near Bed Flow		35.82	27.56	29.68	46.50	42.29	27.95	27.43	37.93
	C3	Total Discharge		**93.29**	**68.87**	**73.58**	**114.14**	**100.52**	**68.76**	**64.97**	**90.84**
Section E	A	Velocity	(cm/s)								
	A1	Near Surface Flow		2.39	2.46	2.52	2.65	2.81	2.54	2.27	2.61
	A2	Near Bed Flow		1.61	1.62	2.19	1.96	1.79	1.75	1.65	1.47
	B	Water Depth	(mm)	61.85	63.29	63.65	63.52	63.80	63.93	64.14	61.65
	C	Discharge	(cm3/s)								
	C1	Near Surface Flow		55.39	38.89	40.14	63.00	67.13	40.66	36.47	60.34
	C2	Near Bed Flow		37.33	25.70	34.79	46.62	42.76	28.00	26.46	33.95
	C3	Total Discharge		**92.73**	**64.58**	**74.93**	**109.63**	**109.89**	**68.66**	**62.94**	**94.28**
Section D	A	Velocity	(cm/s)								
	A1	Near Surface Flow		1.96	2.15	2.79	2.95	2.19	2.62	3.00	2.41
	A2	Near Bed Flow		1.57	1.79	2.08	2.18	1.76	1.62	1.60	1.56
	B	Water Depth	(mm)	61.24	63.30	63.60	64.21	62.54	63.56	63.66	63.42
	C	Discharge	(cm3/s)								
	C1	Near Surface Flow		45.06	34.09	44.39	71.07	51.43	41.69	47.71	57.21
	C2	Near Bed Flow		36.09	28.27	33.07	52.61	41.31	25.67	25.53	37.20
	C3	Total Discharge		**81.16**	**62.36**	**77.47**	**123.67**	**92.75**	**67.35**	**73.24**	**94.41**

Upstream

		Subsection Name		U50	U100	U150	U200	U250	U300	U350	U400	U450
		Subsection Width	(mm)	75	50	50	50	50	50	50	50	75
Section C	A	Velocity	(cm/s)									
	A1	Near Surface Flow		2.41	2.49	2.54	2.56	2.58	2.75	2.74	2.81	2.78
	A2	Near Bed Flow		1.51	1.49	1.51	1.52	1.56	1.61	1.67	1.74	1.68
	B	Water Depth	(mm)	64.35	63.41	64.06	63.43	64.32	64.28	65.89	66.84	65.12
	C	Discharge	(cm3/s)									
	C1	Near Surface Flow		58.27	39.53	40.76	40.66	41.47	44.26	45.14	46.94	67.86
	C2	Near Bed Flow		36.48	23.65	24.23	24.12	25.12	25.84	27.58	29.09	41.05
	C3	Total Discharge		**94.75**	**63.18**	**64.99**	**64.78**	**66.59**	**70.10**	**72.72**	**76.03**	**108.91**
Section B	A	Velocity	(cm/s)									
	A1	Near Surface Flow		2.57	2.56	2.59	2.60	2.64	2.61	2.65	2.70	2.70
	A2	Near Bed Flow		1.35	1.35	1.39	1.41	1.36	1.42	1.48	1.52	1.43
	B	Water Depth	(mm)	65.30	63.06	65.18	64.78	65.15	65.56	66.29	65.92	64.33
	C	Discharge	(cm3/s)									
	C1	Near Surface Flow		63.01	40.43	42.14	42.05	42.95	42.78	44.00	44.56	65.19
	C2	Near Bed Flow		33.01	21.27	22.66	22.87	22.18	23.23	24.51	24.98	34.43
	C3	Total Discharge		**96.02**	**61.69**	**64.80**	**64.92**	**65.13**	**66.01**	**68.51**	**69.55**	**99.62**
Section A	A	Velocity	(cm/s)									
	A1	Near Surface Flow		2.41	2.52	2.52	2.54	2.58	2.57	2.69	2.70	2.73
	A2	Near Bed Flow		1.37	1.38	1.38	1.38	1.40	1.49	1.44	1.53	1.59
	B	Water Depth	(mm)	67.18	67.42	67.33	67.52	67.22	66.82	66.18	64.43	65.25
	C	Discharge	(cm3/s)									
	C1	Near Surface Flow		60.65	42.42	42.49	42.82	43.36	43.00	44.56	43.51	66.74
	C2	Near Bed Flow		34.53	23.24	23.21	23.27	23.56	24.89	23.88	24.68	38.93
	C3	Total Discharge		**95.17**	**65.66**	**65.69**	**66.09**	**66.92**	**67.90**	**68.44**	**68.19**	**105.67**

Water Depth

Average Water Depth, cm		Depth Ratio
LF	RF	RF/LF
6.29	6.30	1.00

Average Water Depth, cm		Depth Ratio
LE	RE	RE/LE
6.31	6.34	1.00

Average Water Depth, cm		Depth Ratio
LD	RD	RD/LD
6.31	6.33	1.00

Average Water Depth, cm
C
6.46

Average Water Depth, cm
B
6.51

Average Water Depth, cm
A
6.66

Velocity

Average Velocity, cm/s		Velocity Ratio
LF	RF	RF/LF
2.68	2.42	0.90
1.78	1.73	0.97

Average Velocity, cm/s		Velocity Ratio
LE	RE	RF/LF
2.50	2.56	0.98
1.84	1.66	0.90

Average Velocity, cm/s		Velocity Ratio
LD	RD	RF/LF
2.46	2.55	0.96
1.91	1.64	0.86

Average Velocity, cm/s
C
2.63
1.59

Average Velocity, cm/s
B
2.63
1.41

Average Velocity, cm/s
A
2.58
1.44

Discharge

Sum of Discharge, cm3/s			Discharge Ratio
LF	RF	LF+RF	RF/LF
349.9	325.1	675.0	0.93

Sum of Discharge, cm3/s			Discharge Ratio
LE	RE	LE+RE	RE/LE
341.9	335.8	677.6	0.98

Sum of Discharge, cm3/s			Discharge Ratio
LD	RD	LD+RD	RD/LD
344.7	327.7	672.4	0.95

Sum of Discharge, cm3/s
C
682.0

Sum of Discharge, cm3/s
B
656.2

Sum of Discharge, cm3/s
A
669.7

Froude

Froude Number	
LF	RF
0.0284	0.0264

Froude Number	
LE	RE
0.0276	0.0268

Froude Number	
LD	RD
0.0278	0.0266

Froude Number
C
0.0265

Froude Number
B
0.0253

Froude Number
A
0.0249

Reynold

Reynold Number	
LF	RF
8382	7793

Reynold Number	
LE	RE
8177	7955

Reynold Number	
LD	RD
8221	7892

Reynold Number
C
13278

Reynold Number
B
12718

Reynold Number
A
12744

Calculation: 50_03_5560

Downstream

		Subsection Name		L50	L100	L150	L200	R50	R100	R150	R200
		Subsection Width	(mm)	75	50	50	75	75	50	50	75
Section F	A	Velocity	(cm/s)								
	A1	Near Surface Flow		3.09	3.19	3.23	3.28	0.78	0.76	0.73	0.68
	A2	Near Bed Flow		2.95	3.01	3.05	3.08	0.57	0.55	0.49	0.44
	B	Water Depth	(mm)	69.85	70.66	71.04	70.32	74.78	75.89	75.89	75.38
	C	Discharge	(cm3/s)								
	C1	Near Surface Flow		80.99	56.31	57.31	86.60	21.96	14.33	13.80	19.27
	C2	Near Bed Flow		77.32	53.15	54.13	81.30	16.09	10.35	9.28	12.33
	C3	Total Discharge		**158.31**	**109.46**	**111.44**	**167.89**	**38.06**	**24.68**	**23.08**	**31.60**
Section E	A	Velocity	(cm/s)								
	A1	Near Surface Flow		3.00	3.03	3.06	3.10	0.92	0.88	0.84	0.78
	A2	Near Bed Flow		2.79	2.82	2.88	2.90	0.62	0.61	0.52	0.54
	B	Water Depth	(mm)	69.13	70.58	70.71	70.29	74.80	74.97	74.75	74.74
	C	Discharge	(cm3/s)								
	C1	Near Surface Flow		77.83	53.50	54.07	81.63	25.76	16.56	15.65	21.89
	C2	Near Bed Flow		72.29	49.80	50.91	76.34	17.42	11.43	9.78	15.14
	C3	Total Discharge		**150.13**	**103.30**	**104.98**	**157.97**	**43.19**	**27.99**	**25.42**	**37.03**
Section D	A	Velocity	(cm/s)								
	A1	Near Surface Flow		3.12	3.17	3.14	3.16	0.85	0.86	0.76	0.74
	A2	Near Bed Flow		2.79	2.82	2.83	2.79	0.60	0.55	0.51	0.46
	B	Water Depth	(mm)	68.06	69.25	72.01	71.58	77.27	76.96	75.72	75.28
	C	Discharge	(cm3/s)								
	C1	Near Surface Flow		79.51	54.92	56.50	84.87	24.57	16.48	14.45	20.91
	C2	Near Bed Flow		71.09	48.85	50.86	74.85	17.51	10.64	9.71	12.94
	C3	Total Discharge		**150.61**	**103.77**	**107.36**	**159.72**	**42.08**	**27.12**	**24.15**	**33.85**

Upstream

		Subsection Name		U50	U100	U150	U200	U250	U300	U350	U400	U450
		Subsection Width	(mm)	75	50	50	50	50	50	50	50	75
Section C	A	Velocity	(cm/s)									
	A1	Near Surface Flow		1.89	1.87	1.85	1.90	1.91	1.84	1.87	1.79	1.74
	A2	Near Bed Flow		1.75	1.76	1.71	1.74	1.73	1.70	1.64	1.68	1.59
	B	Water Depth	(mm)	75.63	76.60	77.41	78.00	78.19	78.05	77.97	77.74	77.42
	C	Discharge	(cm3/s)									
	C1	Near Surface Flow		53.49	35.90	35.85	37.01	37.32	35.90	36.44	34.81	50.53
	C2	Near Bed Flow		49.62	33.71	33.18	33.89	33.84	33.26	32.05	32.70	46.26
	C3	Total Discharge		**103.11**	**69.61**	**69.03**	**70.90**	**71.15**	**69.16**	**68.49**	**67.51**	**96.79**
Section B	A	Velocity	(cm/s)									
	A1	Near Surface Flow		1.75	1.75	1.80	1.79	1.81	1.79	1.79	1.75	1.77
	A2	Near Bed Flow		1.58	1.59	1.57	1.60	1.60	1.60	1.58	1.56	1.59
	B	Water Depth	(mm)	77.77	78.09	77.81	77.14	77.14	78.54	78.48	77.85	76.56
	C	Discharge	(cm3/s)									
	C1	Near Surface Flow		51.07	34.10	35.01	34.52	34.86	35.23	35.08	34.11	50.88
	C2	Near Bed Flow		46.22	31.11	30.62	30.79	30.88	31.37	31.02	30.41	45.58
	C3	Total Discharge		**97.29**	**65.21**	**65.64**	**65.31**	**65.73**	**66.60**	**66.10**	**64.52**	**96.46**
Section A	A	Velocity	(cm/s)									
	A1	Near Surface Flow		1.79	1.81	1.79	1.81	1.85	1.88	1.87	1.81	1.82
	A2	Near Bed Flow		1.51	1.55	1.54	1.57	1.58	1.58	1.60	1.59	1.59
	B	Water Depth	(mm)	77.04	78.25	77.37	77.79	77.61	77.48	77.78	77.50	77.17
	C	Discharge	(cm3/s)									
	C1	Near Surface Flow		51.62	35.34	34.64	35.25	35.96	36.39	36.35	35.01	52.62
	C2	Near Bed Flow		43.56	30.29	29.70	30.46	30.57	30.68	31.16	30.76	46.02
	C3	Total Discharge		**95.18**	**65.63**	**64.34**	**65.71**	**66.52**	**67.07**	**67.50**	**65.77**	**98.64**

Water Depth

Section F

Average Water Depth, cm		Depth Ratio
LF	RF	RF/LF
7.05	7.55	0.93

Section E

Average Water Depth, cm		Depth Ratio
LE	RE	RE/LE
7.02	7.48	0.94

Section D

Average Water Depth, cm		Depth Ratio
LD	RD	RD/LD
7.02	7.63	0.92

Section C

Average Water Depth, cm
C
7.74

Section B

Average Water Depth, cm
B
7.77

Section A

Average Water Depth, cm
A
7.76

Velocity

Section F

Average Velocity, cm/s		Velocity Ratio
LF	RF	RF/LF
3.20	0.74	0.23
3.02	0.51	0.17

Section E

Average Velocity, cm/s		Velocity Ratio
LE	RE	RF/LF
3.05	0.86	0.28
2.85	0.57	0.20

Section D

Average Velocity, cm/s		Velocity Ratio
LD	RD	RF/LF
3.15	0.80	0.25
2.81	0.53	0.19

Section C

Average Velocity, cm/s
C
1.85
1.70

Section B

Average Velocity, cm/s
B
1.78
1.59

Section A

Average Velocity, cm/s
A
1.82
1.57

Discharge

Section F

Sum of Discharge, cm3/s			Discharge Ratio
LF	RF	LF+RF	RF/LF
547.1	117.4	664.5	0.21

Section E

Sum of Discharge, cm3/s			Discharge Ratio
LE	RE	LE+RE	RE/LE
516.4	133.6	650.0	0.26

Section D

Sum of Discharge, cm3/s			Discharge Ratio
LD	RD	LD+RD	RD/LD
521.5	127.2	648.7	0.24

Section C

Sum of Discharge, cm3/s
C
685.8

Section B

Sum of Discharge, cm3/s
B
652.9

Section A

Sum of Discharge, cm3/s
A
656.4

Froude

Section F

Froude Number	
LF	RF
0.0374	0.0073

Section E

Froude Number	
LE	RE
0.0355	0.0083

Section D

Froude Number	
LD	RD
0.0359	0.0077

Section C

Froude Number
C
0.0204

Section B

Froude Number
B
0.0193

Section A

Froude Number
A
0.0194

Reynold

Section F

Reynold Number	
LF	RF
12159	2502

Section E

Reynold Number	
LE	RE
11504	2855

Section D

Reynold Number	
LD	RD
11620	2686

Section C

Reynold Number
C
11635

Section B

Reynold Number
B
11026

Section A

Reynold Number
A
11108

Calculation: 50_03_5055

Downstream

		Subsection Name		L50	L100	L150	L200	R50	R100	R150	R200
		Subsection Width	(mm)	75	50	50	75	75	50	50	75
Section F	A	Velocity	(cm/s)								
	A1	Near Surface Flow		3.18	3.33	3.42	3.51	1.18	1.20	1.10	1.02
	A2	Near Bed Flow		3.14	3.20	3.18	3.18	0.86	0.79	0.68	0.55
	B	Water Depth	(mm)	60.41	62.56	62.96	63.33	69.08	68.83	68.49	66.28
	C	Discharge	(cm3/s)								
	C1	Near Surface Flow		71.95	52.03	53.83	83.39	30.48	20.62	18.90	25.23
	C2	Near Bed Flow		71.06	50.07	50.04	75.58	22.38	13.54	11.70	13.60
	C3	Total Discharge		**143.01**	**102.10**	**103.88**	**158.96**	**52.86**	**34.15**	**30.60**	**38.84**
Section E	A	Velocity	(cm/s)								
	A1	Near Surface Flow		3.07	3.20	3.32	3.36	1.03	1.00	0.93	0.90
	A2	Near Bed Flow		3.00	3.02	3.06	3.00	0.89	0.86	0.87	0.74
	B	Water Depth	(mm)	63.75	64.30	66.83	66.77	67.55	69.37	70.11	67.23
	C	Discharge	(cm3/s)								
	C1	Near Surface Flow		73.38	51.38	55.47	84.23	26.07	17.28	16.22	22.71
	C2	Near Bed Flow		71.82	48.49	51.09	75.09	22.60	14.96	15.30	18.54
	C3	Total Discharge		**145.20**	**99.88**	**106.56**	**159.32**	**48.67**	**32.25**	**31.52**	**41.25**
Section D	A	Velocity	(cm/s)								
	A1	Near Surface Flow		3.13	3.20	3.25	3.29	1.28	1.21	1.15	1.07
	A2	Near Bed Flow		2.73	2.93	3.02	3.12	0.73	0.85	0.82	0.70
	B	Water Depth	(mm)	65.21	66.61	66.21	67.74	66.18	69.22	70.33	67.94
	C	Discharge	(cm3/s)								
	C1	Near Surface Flow		76.66	53.23	53.85	83.52	31.86	20.89	20.24	27.16
	C2	Near Bed Flow		66.72	48.86	49.91	79.18	18.08	14.63	14.49	17.79
	C3	Total Discharge		**143.38**	**102.09**	**103.77**	**162.70**	**49.93**	**35.52**	**34.73**	**44.95**

Upstream

		Subsection Name		U50	U100	U150	U200	U250	U300	U350	U400	U450
		Subsection Width	(mm)	75	50	50	50	50	50	50	50	75
Section C	A	Velocity	(cm/s)									
	A1	Near Surface Flow		2.26	2.44	2.44	2.50	2.56	2.61	2.70	2.66	2.65
	A2	Near Bed Flow		0.96	1.33	1.29	1.09	1.42	1.49	1.67	1.71	1.21
	B	Water Depth	(mm)	69.24	69.38	69.24	68.29	68.78	69.21	69.30	69.43	69.39
	C	Discharge	(cm3/s)									
	C1	Near Surface Flow		58.66	42.25	42.21	42.62	44.11	45.19	46.77	46.21	68.88
	C2	Near Bed Flow		24.90	23.11	22.39	18.64	24.45	25.79	28.86	29.75	31.45
	C3	Total Discharge		**83.56**	**65.37**	**64.60**	**61.26**	**68.56**	**70.97**	**75.63**	**75.97**	**100.34**
Section B	A	Velocity	(cm/s)									
	A1	Near Surface Flow		2.26	2.23	2.37	2.39	2.40	2.42	2.47	2.48	2.40
	A2	Near Bed Flow		1.27	1.35	1.34	1.30	1.37	1.38	1.42	1.43	1.32
	B	Water Depth	(mm)	70.64	70.36	69.44	69.35	69.34	69.46	70.21	69.51	68.82
	C	Discharge	(cm3/s)									
	C1	Near Surface Flow		59.98	39.27	41.08	41.45	41.57	42.01	43.33	43.15	62.02
	C2	Near Bed Flow		33.75	23.73	23.28	22.55	23.69	23.97	24.85	24.77	34.18
	C3	Total Discharge		**93.74**	**63.00**	**64.36**	**64.00**	**65.27**	**65.98**	**68.18**	**67.92**	**96.20**
Section A	A	Velocity	(cm/s)									
	A1	Near Surface Flow		2.29	2.32	2.32	2.33	2.32	2.32	2.26	2.26	2.26
	A2	Near Bed Flow		1.18	1.23	1.31	1.35	1.36	1.51	1.53	1.49	1.61
	B	Water Depth	(mm)	69.97	70.25	70.27	70.45	70.11	69.79	69.66	69.54	65.76
	C	Discharge	(cm3/s)									
	C1	Near Surface Flow		60.14	40.80	40.82	40.96	40.67	40.50	39.35	39.37	55.77
	C2	Near Bed Flow		30.99	21.65	22.93	23.71	23.82	26.28	26.69	25.82	39.81
	C3	Total Discharge		**91.13**	**62.45**	**63.75**	**64.67**	**64.49**	**66.78**	**66.05**	**65.19**	**95.58**

Water Depth

Section F

Average Water Depth, cm		Depth Ratio
LF	RF	RF/LF
6.23	6.82	0.91

Section E

Average Water Depth, cm		Depth Ratio
LE	RE	RE/LE
6.54	6.86	0.95

Section D

Average Water Depth, cm		Depth Ratio
LD	RD	RD/LD
6.64	6.84	0.97

Section C

Average Water Depth, cm
C
6.91

Section B

Average Water Depth, cm
B
6.97

Section A

Average Water Depth, cm
A
6.95

Velocity

Section F

Average Velocity, cm/s		Velocity Ratio
LF	RF	RF/LF
3.36	1.12	0.33
3.17	0.72	0.23

Section E

Average Velocity, cm/s		Velocity Ratio
LE	RE	RF/LF
3.24	0.96	0.30
3.02	0.84	0.28

Section D

Average Velocity, cm/s		Velocity Ratio
LD	RD	RF/LF
3.22	1.18	0.37
2.95	0.77	0.26

Section C

Average Velocity, cm/s
C
2.54
1.35

Section B

Average Velocity, cm/s
B
2.38
1.35

Section A

Average Velocity, cm/s
A
2.30
1.40

Discharge

Section F

Sum of Discharge, cm3/s			Discharge Ratio
LF	RF	LF+RF	RF/LF
507.9	156.5	664.4	0.31

Section E

Sum of Discharge, cm3/s			Discharge Ratio
LE	RE	LE+RE	RE/LE
511.0	153.7	664.6	0.30

Section D

Sum of Discharge, cm3/s			Discharge Ratio
LD	RD	LD+RD	RD/LD
511.9	165.1	677.1	0.32

Section C

Sum of Discharge, cm3/s
C
666.3

Section B

Sum of Discharge, cm3/s
B
648.6

Section A

Sum of Discharge, cm3/s
A
640.1

Froude

Section F

Froude Number	
LF	RF
0.0418	0.0113

Section E

Froude Number	
LE	RE
0.0391	0.0110

Section D

Froude Number	
LD	RD
0.0382	0.0119

Section C

Froude Number
C
0.0236

Section B

Froude Number
B
0.0226

Section A

Froude Number
A
0.0224

Reynold

Section F

Reynold Number	
LF	RF
12238	3562

Section E

Reynold Number	
LE	RE
11914	3492

Section D

Reynold Number	
LD	RD
11806	3774

Section C

Reynold Number
C
12409

Section B

Reynold Number
B
11936

Section A

Reynold Number
A
11807

Calculation: 50_05_5050

Downstream

		Subsection Name		L50	L100	L150	L200	R50	R100	R150	R200
		Subsection Width	(mm)	75	50	50	75	75	50	50	75
Section F	A	Velocity	(cm/s)								
	A1	Near Surface Flow		2.39	2.42	2.43	2.52	2.42	2.27	2.11	1.85
	A2	Near Bed Flow		2.02	2.06	2.08	2.10	2.17	2.01	1.79	1.59
	B	Water Depth	(mm)	57.20	59.37	59.73	60.17	59.68	59.77	59.35	57.91
	C	Discharge	(cm3/s)								
	C1	Near Surface Flow		51.16	35.89	36.25	56.92	54.11	33.85	31.26	40.22
	C2	Near Bed Flow		43.23	30.59	31.11	47.42	48.52	30.05	26.54	34.53
	C3	Total Discharge		**94.40**	**66.48**	**67.37**	**104.35**	**102.63**	**63.90**	**57.81**	**74.75**
Section E	A	Velocity	(cm/s)								
	A1	Near Surface Flow		2.23	2.43	2.45	2.55	2.54	2.38	2.21	2.08
	A2	Near Bed Flow		1.80	1.91	2.07	2.15	2.22	2.05	1.92	1.80
	B	Water Depth	(mm)	61.04	62.33	62.65	62.54	62.48	62.88	63.02	61.83
	C	Discharge	(cm3/s)								
	C1	Near Surface Flow		50.99	37.94	38.35	59.83	59.48	37.47	34.84	48.28
	C2	Near Bed Flow		41.22	29.80	32.37	50.50	52.11	32.16	30.23	41.73
	C3	Total Discharge		**92.21**	**67.73**	**70.72**	**110.33**	**111.59**	**69.63**	**65.07**	**90.01**
Section D	A	Velocity	(cm/s)								
	A1	Near Surface Flow		2.12	2.34	2.52	2.69	2.39	2.49	2.43	2.24
	A2	Near Bed Flow		1.88	2.06	2.26	2.28	1.86	1.90	1.87	1.79
	B	Water Depth	(mm)	61.21	62.92	62.49	64.58	62.72	63.82	63.93	63.72
	C	Discharge	(cm3/s)								
	C1	Near Surface Flow		48.57	36.80	39.43	65.12	56.27	39.78	38.89	53.42
	C2	Near Bed Flow		43.17	32.38	35.24	55.20	43.73	30.26	29.82	42.81
	C3	Total Discharge		**91.73**	**69.18**	**74.67**	**120.31**	**100.00**	**70.04**	**68.71**	**96.23**

Upstream

		Subsection Name		U50	U100	U150	U200	U250	U300	U350	U400	U450
		Subsection Width	(mm)	75	50	50	50	50	50	50	50	75
Section C	A	Velocity	(cm/s)									
	A1	Near Surface Flow		2.45	2.50	2.71	2.89	2.88	2.98	3.02	2.82	2.89
	A2	Near Bed Flow		1.21	1.37	1.55	1.51	1.48	1.57	1.75	1.58	1.42
	B	Water Depth	(mm)	63.40	63.48	63.56	63.51	63.51	63.46	63.62	63.78	62.02
	C	Discharge	(cm3/s)									
	C1	Near Surface Flow		58.34	39.73	43.00	45.85	45.65	47.27	47.96	44.99	67.30
	C2	Near Bed Flow		28.76	21.80	24.67	23.99	23.54	24.84	27.91	25.27	33.10
	C3	Total Discharge		**87.10**	**61.53**	**67.66**	**69.84**	**69.20**	**72.11**	**75.87**	**70.26**	**100.40**
Section B	A	Velocity	(cm/s)									
	A1	Near Surface Flow		2.46	2.49	2.56	2.56	2.64	2.65	2.63	2.67	2.62
	A2	Near Bed Flow		1.46	1.44	1.49	1.54	1.57	1.59	1.65	1.64	1.63
	B	Water Depth	(mm)	63.69	64.25	64.41	63.84	64.12	64.92	65.07	64.42	63.58
	C	Discharge	(cm3/s)									
	C1	Near Surface Flow		58.71	39.99	41.22	40.87	42.30	42.96	42.72	43.00	62.56
	C2	Near Bed Flow		34.85	23.21	23.98	24.54	25.23	25.84	26.79	26.35	38.79
	C3	Total Discharge		**93.56**	**63.19**	**65.20**	**65.41**	**67.53**	**68.80**	**69.51**	**69.35**	**101.35**
Section A	A	Velocity	(cm/s)									
	A1	Near Surface Flow		2.37	2.42	2.46	2.52	2.58	2.63	2.62	2.70	2.68
	A2	Near Bed Flow		1.43	1.46	1.51	1.54	1.61	1.64	1.73	1.73	1.71
	B	Water Depth	(mm)	64.79	65.04	65.11	65.07	64.90	64.59	63.43	62.77	62.59
	C	Discharge	(cm3/s)									
	C1	Near Surface Flow		57.66	39.30	39.97	41.03	41.92	42.44	41.56	42.32	62.98
	C2	Near Bed Flow		34.78	23.73	24.57	25.13	26.16	26.47	27.36	27.11	40.09
	C3	Total Discharge		**92.45**	**63.02**	**64.54**	**66.16**	**68.08**	**68.91**	**68.92**	**69.43**	**103.07**

Water Depth

Average Water Depth, cm		Depth Ratio
LF	RF	RF/LF
5.91	5.92	1.00

Average Water Depth, cm		Depth Ratio
LE	RE	RE/LE
6.21	6.26	0.99

Average Water Depth, cm		Depth Ratio
LD	RD	RD/LD
6.28	6.35	0.99

Average Water Depth, cm
C
6.34

Average Water Depth, cm
B
6.43

Average Water Depth, cm
A
6.43

Velocity

Average Velocity, cm/s		Velocity Ratio
LF	RF	RF/LF
2.44	2.16	0.89
2.07	1.89	0.91

Average Velocity, cm/s		Velocity Ratio
LE	RE	RF/LF
2.42	2.30	0.95
1.98	2.00	0.99

Average Velocity, cm/s		Velocity Ratio
LD	RD	RF/LF
2.42	2.39	0.99
2.12	1.85	0.87

Average Velocity, cm/s
C
2.79
1.50

Average Velocity, cm/s
B
2.59
1.56

Average Velocity, cm/s
A
2.55
1.60

Discharge

Sum of Discharge, cm3/s			Discharge Ratio
LF	RF	LF+RF	RF/LF
332.6	299.1	631.7	0.90

Sum of Discharge, cm3/s			Discharge Ratio
LE	RE	LE+RE	RE/LE
341.0	336.3	677.3	0.99

Sum of Discharge, cm3/s			Discharge Ratio
LD	RD	LD+RD	RD/LD
355.9	335.0	690.9	0.94

Sum of Discharge, cm3/s
C
674.0

Sum of Discharge, cm3/s
B
663.9

Sum of Discharge, cm3/s
A
664.6

Froude

Froude Number	
LF	RF
0.0296	0.0266

Froude Number	
LE	RE
0.0282	0.0275

Froude Number	
LD	RD
0.0289	0.0269

Froude Number
C
0.0272

Froude Number
B
0.0261

Froude Number
A
0.0261

Reynold

Reynold Number	
LF	RF
8293	7459

Reynold Number	
LE	RE
8232	8067

Reynold Number	
LD	RD
8518	7998

Reynold Number
C
13438

Reynold Number
B
13017

Reynold Number
A
13038

Calculation: 50_05_5560

Downstream

		Subsection Name		L50	L100	L150	L200	R50	R100	R150	R200
		Subsection Width	(mm)	75	50	50	75	75	50	50	75
Section F	A	Velocity	(cm/s)								
	A1	Near Surface Flow		3.47	3.49	3.55	3.61	1.05	1.00	0.88	0.87
	A2	Near Bed Flow		2.91	2.97	3.06	3.14	0.62	0.51	0.40	0.29
	B	Water Depth	(mm)	62.37	64.09	64.90	65.23	73.57	73.56	73.19	71.06
	C	Discharge	(cm3/s)								
	C1	Near Surface Flow		81.07	55.89	57.64	88.21	28.85	18.38	16.02	23.17
	C2	Near Bed Flow		68.00	47.67	49.66	76.88	17.18	9.42	7.36	7.64
	C3	Total Discharge		**149.08**	**103.56**	**107.31**	**165.09**	**46.03**	**27.81**	**23.39**	**30.81**
Section E	A	Velocity	(cm/s)								
	A1	Near Surface Flow		3.21	3.23	3.27	3.29	0.79	0.79	0.75	0.74
	A2	Near Bed Flow		2.81	2.84	2.84	2.86	0.45	0.44	0.42	0.40
	B	Water Depth	(mm)	67.32	68.77	69.12	68.91	74.10	74.31	74.40	73.14
	C	Discharge	(cm3/s)								
	C1	Near Surface Flow		81.10	55.48	56.45	84.95	22.00	14.60	13.86	20.35
	C2	Near Bed Flow		70.95	48.85	49.00	73.98	12.46	8.20	7.86	11.00
	C3	Total Discharge		**152.05**	**104.32**	**105.46**	**158.93**	**34.46**	**22.80**	**21.72**	**31.35**
Section D	A	Velocity	(cm/s)								
	A1	Near Surface Flow		2.35	2.70	3.71	4.23	1.61	1.46	0.44	0.36
	A2	Near Bed Flow		2.16	2.92	2.79	3.47	1.13	0.95	0.48	-0.05
	B	Water Depth	(mm)	67.53	68.84	69.33	71.03	73.34	74.46	75.23	73.47
	C	Discharge	(cm3/s)								
	C1	Near Surface Flow		59.52	46.55	64.36	112.55	44.19	27.16	8.23	9.96
	C2	Near Bed Flow		54.79	50.28	48.43	92.46	31.10	17.78	9.05	-1.47
	C3	Total Discharge		**114.31**	**96.82**	**112.79**	**205.01**	**75.29**	**44.94**	**17.28**	**8.49**

Upstream

		Subsection Name		U50	U100	U150	U200	U250	U300	U350	U400	U450
		Subsection Width	(mm)	75	50	50	50	50	50	50	50	75
Section C	A	Velocity	(cm/s)									
	A1	Near Surface Flow		1.92	1.86	1.94	2.05	2.10	2.18	2.24	2.13	2.00
	A2	Near Bed Flow		1.59	1.51	1.62	1.66	1.72	1.81	1.84	1.85	1.65
	B	Water Depth	(mm)	73.87	73.60	74.07	74.06	73.54	74.03	74.06	74.34	74.24
	C	Discharge	(cm3/s)									
	C1	Near Surface Flow		53.16	34.13	35.95	37.89	38.64	40.42	41.53	39.67	55.60
	C2	Near Bed Flow		43.91	27.81	30.05	30.73	31.64	33.50	34.05	34.37	46.03
	C3	Total Discharge		**97.07**	**61.94**	**65.99**	**68.62**	**70.28**	**73.92**	**75.58**	**74.03**	**101.63**
Section B	A	Velocity	(cm/s)									
	A1	Near Surface Flow		1.77	1.82	1.88	1.96	1.98	2.07	2.07	2.03	2.07
	A2	Near Bed Flow		1.63	1.59	1.61	1.70	1.72	1.85	1.84	1.90	1.85
	B	Water Depth	(mm)	73.17	74.79	74.36	73.83	74.00	74.98	75.31	74.06	74.25
	C	Discharge	(cm3/s)									
	C1	Near Surface Flow		48.61	34.10	34.95	36.26	36.71	38.80	38.94	37.60	57.67
	C2	Near Bed Flow		44.63	29.73	29.97	31.41	31.75	34.65	34.71	35.23	51.44
	C3	Total Discharge		**93.24**	**63.84**	**64.92**	**67.66**	**68.46**	**73.45**	**73.65**	**72.83**	**109.11**
Section A	A	Velocity	(cm/s)									
	A1	Near Surface Flow		1.81	1.92	1.85	1.99	2.10	2.17	2.24	2.25	2.20
	A2	Near Bed Flow		1.43	1.48	1.49	1.56	1.67	1.75	1.84	1.84	1.81
	B	Water Depth	(mm)	73.99	74.19	74.34	74.32	74.10	73.72	72.70	71.82	71.71
	C	Discharge	(cm3/s)									
	C1	Near Surface Flow		50.20	35.69	34.45	36.99	38.89	40.01	40.64	40.41	59.03
	C2	Near Bed Flow		39.63	27.54	27.76	28.97	30.94	32.17	33.40	33.02	48.65
	C3	Total Discharge		**89.82**	**63.23**	**62.21**	**65.96**	**69.83**	**72.18**	**74.05**	**73.43**	**107.68**

Water Depth

Section F

Average Water Depth, cm		Depth Ratio
LF	RF	RF/LF
6.41	7.28	0.88

Section E

Average Water Depth, cm		Depth Ratio
LE	RE	RE/LE
6.85	7.40	0.93

Section D

Average Water Depth, cm		Depth Ratio
LD	RD	RD/LD
6.92	7.41	0.93

Section C

Average Water Depth, cm
C
7.40

Section B

Average Water Depth, cm
B
7.43

Section A

Average Water Depth, cm
A
7.34

Velocity

Section F

Average Velocity, cm/s		Velocity Ratio
LF	RF	RF/LF
3.53	0.95	0.27
3.02	0.46	0.15

Section E

Average Velocity, cm/s		Velocity Ratio
LE	RE	RF/LF
3.25	0.77	0.24
2.84	0.43	0.15

Section D

Average Velocity, cm/s		Velocity Ratio
LD	RD	RF/LF
3.25	0.97	0.30
2.84	0.63	0.22

Section C

Average Velocity, cm/s
C
2.05
1.69

Section B

Average Velocity, cm/s
B
1.96
1.74

Section A

Average Velocity, cm/s
A
2.06
1.65

Discharge

Section F

Sum of Discharge, cm3/s			Discharge Ratio
LF	RF	LF+RF	RF/LF
525.0	128.0	653.1	0.24

Section E

Sum of Discharge, cm3/s			Discharge Ratio
LE	RE	LE+RE	RE/LE
520.8	110.3	631.1	0.21

Section D

Sum of Discharge, cm3/s			Discharge Ratio
LD	RD	LD+RD	RD/LD
528.9	146.0	674.9	0.28

Section C

Sum of Discharge, cm3/s
C
689.1

Section B

Sum of Discharge, cm3/s
B
687.2

Section A

Sum of Discharge, cm3/s
A
678.4

Froude

Section F

Froude Number	
LF	RF
0.0413	0.0083

Section E

Froude Number	
LE	RE
0.0371	0.0070

Section D

Froude Number	
LD	RD
0.0369	0.0093

Section C

Froude Number
C
0.0220

Section B

Froude Number
B
0.0217

Section A

Froude Number
A
0.0219

Reynold

Section F

Reynold Number	
LF	RF
12389	2777

Section E

Reynold Number	
LE	RE
11778	2377

Section D

Reynold Number	
LD	RD
11818	3175

Section C

Reynold Number
C
12122

Section B

Reynold Number
B
12018

Section A

Reynold Number
A
12002

Calculation: 50_05_5055

Downstream

		Subsection Name		L50	L100	L150	L200	R50	R100	R150	R200
		Subsection Width	(mm)	75	50	50	75	75	50	50	75
Section F	A	Velocity	(cm/s)								
	A1	Near Surface Flow		3.17	3.22	3.28	3.28	1.17	1.04	0.93	0.82
	A2	Near Bed Flow		2.98	3.05	3.15	3.17	0.89	0.75	0.63	0.55
	B	Water Depth	(mm)	58.65	61.34	61.74	62.14	68.28	68.35	67.93	66.03
	C	Discharge	(cm3/s)								
	C1	Near Surface Flow		69.75	49.45	50.61	76.54	29.91	17.83	15.87	20.40
	C2	Near Bed Flow		65.46	46.70	48.67	73.91	22.91	12.77	10.67	13.63
	C3	Total Discharge		**135.22**	**96.14**	**99.28**	**150.46**	**52.82**	**30.60**	**26.54**	**34.03**
Section E	A	Velocity	(cm/s)								
	A1	Near Surface Flow		3.49	3.47	3.51	3.52	1.10	1.05	0.93	0.86
	A2	Near Bed Flow		2.64	2.63	2.72	2.81	1.07	0.94	0.77	0.72
	B	Water Depth	(mm)	62.70	64.07	64.37	64.37	68.50	69.58	69.69	69.37
	C	Discharge	(cm3/s)								
	C1	Near Surface Flow		82.13	55.62	56.45	85.05	28.20	18.35	16.17	22.29
	C2	Near Bed Flow		62.01	42.20	43.80	67.73	27.53	16.41	13.40	18.72
	C3	Total Discharge		**144.13**	**97.81**	**100.24**	**152.78**	**55.73**	**34.76**	**29.56**	**41.00**
Section D	A	Velocity	(cm/s)								
	A1	Near Surface Flow		3.16	3.21	3.28	3.29	1.29	1.18	1.01	0.87
	A2	Near Bed Flow		3.03	3.20	3.23	3.21	1.16	0.92	0.76	0.67
	B	Water Depth	(mm)	64.35	65.41	65.38	65.62	68.06	69.13	69.16	68.98
	C	Discharge	(cm3/s)								
	C1	Near Surface Flow		76.19	52.54	53.59	80.89	32.96	20.33	17.45	22.55
	C2	Near Bed Flow		73.19	52.40	52.84	78.88	29.51	15.94	13.16	17.40
	C3	Total Discharge		**149.38**	**104.94**	**106.43**	**159.77**	**62.48**	**36.28**	**30.61**	**39.95**

Upstream

		Subsection Name		U50	U100	U150	U200	U250	U300	U350	U400	U450
		Subsection Width	(mm)	75	50	50	50	50	50	50	50	75
Section C	A	Velocity	(cm/s)									
	A1	Near Surface Flow		1.81	1.86	2.04	2.08	2.28	2.27	2.18	2.23	1.92
	A2	Near Bed Flow		1.46	1.59	1.56	1.79	1.83	1.87	1.91	1.71	1.75
	B	Water Depth	(mm)	69.36	69.71	69.53	69.85	69.39	69.81	69.86	69.89	70.14
	C	Discharge	(cm3/s)									
	C1	Near Surface Flow		47.10	32.50	35.51	36.40	39.48	39.61	38.13	38.95	50.39
	C2	Near Bed Flow		38.04	27.76	27.04	31.34	31.83	32.72	33.40	29.94	45.90
	C3	Total Discharge		**85.14**	**60.26**	**62.55**	**67.74**	**71.31**	**72.33**	**71.53**	**68.88**	**96.30**
Section B	A	Velocity	(cm/s)									
	A1	Near Surface Flow		1.54	1.52	1.82	1.97	2.04	2.25	2.22	2.17	2.08
	A2	Near Bed Flow		1.52	1.40	1.68	1.65	1.85	1.96	2.12	2.07	1.98
	B	Water Depth	(mm)	67.67	68.56	68.79	68.63	69.34	70.11	71.15	70.84	70.07
	C	Discharge	(cm3/s)									
	C1	Near Surface Flow		39.01	25.99	31.26	33.80	35.43	39.49	39.47	38.44	54.73
	C2	Near Bed Flow		38.58	24.06	28.91	28.32	32.15	34.43	37.66	36.59	52.14
	C3	Total Discharge		**77.58**	**50.05**	**60.18**	**62.12**	**67.58**	**73.92**	**77.13**	**75.04**	**106.86**
Section A	A	Velocity	(cm/s)									
	A1	Near Surface Flow		1.73	1.77	1.87	1.93	2.02	2.16	2.22	2.26	2.38
	A2	Near Bed Flow		1.42	1.40	1.49	1.60	1.66	1.75	1.89	2.00	1.96
	B	Water Depth	(mm)	69.44	69.67	69.80	69.90	69.65	69.40	68.61	67.70	67.31
	C	Discharge	(cm3/s)									
	C1	Near Surface Flow		44.92	30.86	32.64	33.73	35.19	37.54	38.11	38.24	59.97
	C2	Near Bed Flow		36.97	24.30	26.00	28.01	28.89	30.44	32.35	33.83	49.57
	C3	Total Discharge		**81.89**	**55.16**	**58.64**	**61.74**	**64.07**	**67.98**	**70.46**	**72.07**	**109.54**

Water Depth

Average Water Depth, cm		Depth Ratio
LF	RF	RF/LF
6.10	6.76	0.90

Average Water Depth, cm		Depth Ratio
LE	RE	RE/LE
6.39	6.93	0.92

Average Water Depth, cm		Depth Ratio
LD	RD	RD/LD
6.52	6.88	0.95

Average Water Depth, cm
C
6.97

Average Water Depth, cm
B
6.95

Average Water Depth, cm
A
6.91

Velocity

Average Velocity, cm/s		Velocity Ratio
LF	RF	RF/LF
3.24	0.99	0.31
3.09	0.71	0.23

Average Velocity, cm/s		Velocity Ratio
LE	RE	RF/LF
3.50	0.98	0.28
2.70	0.88	0.32

Average Velocity, cm/s		Velocity Ratio
LD	RD	RF/LF
3.23	1.09	0.34
3.17	0.88	0.28

Average Velocity, cm/s
C
2.08
1.72

Average Velocity, cm/s
B
1.96
1.80

Average Velocity, cm/s
A
2.04
1.69

Discharge

Sum of Discharge, cm3/s			Discharge Ratio
LF	RF	LF+RF	RF/LF
481.1	144.0	625.1	0.30

Sum of Discharge, cm3/s			Discharge Ratio
LE	RE	LE+RE	RE/LE
495.0	161.1	656.0	0.33

Sum of Discharge, cm3/s			Discharge Ratio
LD	RD	LD+RD	RD/LD
520.5	169.3	689.8	0.33

Sum of Discharge, cm3/s
C
656.0

Sum of Discharge, cm3/s
B
650.5

Sum of Discharge, cm3/s
A
641.5

Froude

Froude Number	
LF	RF
0.0409	0.0104

Froude Number	
LE	RE
0.0392	0.0113

Froude Number	
LD	RD
0.0400	0.0120

Froude Number
C
0.0229

Froude Number
B
0.0228

Froude Number
A
0.0226

Reynold

Reynold Number	
LF	RF
11766	3271

Reynold Number	
LE	RE
11708	3614

Reynold Number	
LD	RD
12178	3810

Reynold Number
C
12136

Reynold Number
B
12016

Reynold Number
A
11879

Calculation: 50_07_5050

Downstream

	Subsection Name		L50	L100	L150	L200	R50	R100	R150	R200
	Subsection Width	(mm)	75	50	50	75	75	50	50	75
Section F	A Velocity	(cm/s)								
	A1 Near Surface Flow		2.88	2.84	2.57	2.40	2.74	2.64	2.49	2.28
	A2 Near Bed Flow		2.48	2.28	2.10	1.94	2.47	2.42	2.17	1.95
	B Water Depth	(mm)	55.19	57.30	57.73	58.12	57.36	57.42	56.88	55.36
	C Discharge	(cm3/s)								
	C1 Near Surface Flow		59.65	40.68	37.05	52.23	58.87	37.83	35.34	47.38
	C2 Near Bed Flow		51.36	32.70	30.34	42.37	53.12	34.79	30.84	40.56
	C3 Total Discharge		**111.01**	**73.39**	**67.39**	**94.60**	**111.99**	**72.62**	**66.19**	**87.95**
Section E	A Velocity	(cm/s)								
	A1 Near Surface Flow		2.81	2.94	2.64	2.46	2.73	2.68	2.60	2.50
	A2 Near Bed Flow		2.25	2.23	2.01	2.05	2.36	2.27	2.10	1.97
	B Water Depth	(mm)	56.45	57.74	58.07	58.03	57.92	57.85	57.90	57.60
	C Discharge	(cm3/s)								
	C1 Near Surface Flow		59.51	42.40	38.38	53.45	59.20	38.69	37.64	54.05
	C2 Near Bed Flow		47.61	32.12	29.18	44.65	51.29	32.80	30.41	42.48
	C3 Total Discharge		**107.13**	**74.53**	**67.56**	**98.11**	**110.49**	**71.49**	**68.05**	**96.54**
Section D	A Velocity	(cm/s)								
	A1 Near Surface Flow		2.56	2.76	2.71	2.47	2.33	2.51	2.69	2.62
	A2 Near Bed Flow		2.11	2.26	2.22	2.02	1.97	2.02	2.18	1.99
	B Water Depth	(mm)	59.60	60.32	60.35	60.57	59.45	60.07	60.06	59.15
	C Discharge	(cm3/s)								
	C1 Near Surface Flow		57.32	41.67	40.89	56.19	51.90	37.76	40.34	58.20
	C2 Near Bed Flow		47.23	34.01	33.54	45.81	43.85	30.26	32.69	44.19
	C3 Total Discharge		**104.54**	**75.67**	**74.43**	**102.00**	**95.75**	**68.02**	**73.03**	**102.39**

Upstream

	Subsection Name		U50	U100	U150	U200	U250	U300	U350	U400	U450
	Subsection Width	(mm)	75	50	50	50	50	50	50	50	75
Section C	A Velocity	(cm/s)									
	A1 Near Surface Flow		2.54	2.59	2.56	2.64	2.66	2.78	2.79	2.85	2.80
	A2 Near Bed Flow		1.63	1.60	1.63	1.69	1.76	1.77	1.84	1.87	1.88
	B Water Depth	(mm)	60.75	61.08	61.15	60.69	60.96	60.92	61.13	61.29	61.28
	C Discharge	(cm3/s)									
	C1 Near Surface Flow		57.84	39.53	39.11	40.06	40.59	42.38	42.66	43.67	64.46
	C2 Near Bed Flow		37.05	24.44	24.98	25.67	26.81	26.95	28.12	28.59	43.18
	C3 Total Discharge		**94.89**	**63.97**	**64.09**	**65.73**	**67.40**	**69.33**	**70.78**	**72.26**	**107.63**
Section B	A Velocity	(cm/s)									
	A1 Near Surface Flow		2.39	2.46	2.43	2.53	2.57	2.63	2.72	2.79	2.83
	A2 Near Bed Flow		1.57	1.61	1.63	1.65	1.72	1.73	1.91	2.01	1.94
	B Water Depth	(mm)	61.56	62.17	62.20	61.87	61.75	62.30	62.68	61.91	60.89
	C Discharge	(cm3/s)									
	C1 Near Surface Flow		55.27	38.17	37.81	39.06	39.68	41.04	42.57	43.12	64.51
	C2 Near Bed Flow		36.13	24.96	25.33	25.55	26.50	27.02	29.98	31.16	44.21
	C3 Total Discharge		**91.41**	**63.13**	**63.15**	**64.61**	**66.17**	**68.06**	**72.55**	**74.28**	**108.72**
Section A	A Velocity	(cm/s)									
	A1 Near Surface Flow		2.31	2.36	2.42	2.35	2.37	2.43	2.51	2.73	2.91
	A2 Near Bed Flow		1.67	1.68	1.75	1.72	1.76	1.78	1.94	2.13	2.17
	B Water Depth	(mm)	61.11	61.14	61.16	61.15	61.13	61.10	61.03	60.01	60.26
	C Discharge	(cm3/s)									
	C1 Near Surface Flow		52.83	36.09	36.94	35.91	36.28	37.16	38.26	40.96	65.73
	C2 Near Bed Flow		38.17	25.71	26.68	26.23	26.89	27.15	29.66	31.90	48.98
	C3 Total Discharge		**91.00**	**61.80**	**63.62**	**62.13**	**63.17**	**64.30**	**67.92**	**72.87**	**114.71**

Water Depth

Average Water Depth, cm		Depth Ratio
LF	RF	RF/LF
5.71	5.68	0.99

Average Water Depth, cm		Depth Ratio
LE	RE	RE/LE
5.76	5.78	1.00

Average Water Depth, cm		Depth Ratio
LD	RD	RD/LD
6.02	5.97	0.99

Average Water Depth, cm
C
6.10

Average Water Depth, cm
B
6.19

Average Water Depth, cm
A
6.09

Velocity

Average Velocity, cm/s		Velocity Ratio
LF	RF	RF/LF
2.67	2.53	0.95
2.20	2.25	0.98

Average Velocity, cm/s		Velocity Ratio
LE	RE	RF/LF
2.71	2.63	0.97
2.13	2.17	0.98

Average Velocity, cm/s		Velocity Ratio
LD	RD	RF/LF
2.63	2.54	0.97
2.15	2.04	0.95

Average Velocity, cm/s
C
2.69
1.74

Average Velocity, cm/s
B
2.59
1.75

Average Velocity, cm/s
A
2.49
1.84

Discharge

Sum of Discharge, cm3/s			Discharge Ratio
LF	RF	LF+RF	RF/LF
346.4	338.7	685.1	0.98

Sum of Discharge, cm3/s			Discharge Ratio
LE	RE	LE+RE	RE/LE
347.3	346.6	693.9	1.00

Sum of Discharge, cm3/s			Discharge Ratio
LD	RD	LD+RD	RD/LD
356.7	339.2	695.8	0.95

Sum of Discharge, cm3/s
C
676.1

Sum of Discharge, cm3/s
B
672.1

Sum of Discharge, cm3/s
A
661.5

Froude

Froude Number	
LF	RF
0.0326	0.0321

Froude Number	
LE	RE
0.0322	0.0319

Froude Number	
LD	RD
0.0311	0.0299

Froude Number
C
0.0286

Froude Number
B
0.0279

Froude Number
A
0.0280

Reynold

Reynold Number	
LF	RF
8875	8704

Reynold Number	
LE	RE
8848	8775

Reynold Number	
LD	RD
8853	8451

Reynold Number
C
13784

Reynold Number
B
13554

Reynold Number
A
13461

Calculation: 50_07_5560

Downstream

		Subsection Name		L50	L100	L150	L200	R50	R100	R150	R200
		Subsection Width	(mm)	75	50	50	75	75	50	50	75
Section F	A	Velocity	(cm/s)								
	A1	Near Surface Flow		3.97	3.94	3.86	3.77	1.00	0.94	0.82	0.70
	A2	Near Bed Flow		2.94	2.91	2.97	2.90	0.70	0.63	0.52	0.40
	B	Water Depth	(mm)	60.85	62.75	63.32	63.71	70.42	70.28	69.81	68.40
	C	Discharge	(cm3/s)								
	C1	Near Surface Flow		90.64	61.80	61.02	90.14	26.47	16.46	14.30	17.86
	C2	Near Bed Flow		67.08	45.63	47.01	69.35	18.57	11.15	9.01	10.37
	C3	Total Discharge		**157.72**	**107.44**	**108.03**	**159.48**	**45.05**	**27.61**	**23.31**	**28.23**
Section E	A	Velocity	(cm/s)								
	A1	Near Surface Flow		3.55	3.77	3.77	3.76	0.89	0.76	0.71	0.48
	A2	Near Bed Flow		2.81	2.83	2.89	2.85	0.89	0.59	0.35	0.21
	B	Water Depth	(mm)	64.90	66.48	66.81	66.80	68.47	69.51	69.59	69.55
	C	Discharge	(cm3/s)								
	C1	Near Surface Flow		86.30	62.69	62.99	94.07	22.93	13.22	12.34	12.39
	C2	Near Bed Flow		68.31	47.08	48.25	71.46	22.94	10.32	6.03	5.42
	C3	Total Discharge		**154.61**	**109.77**	**111.24**	**165.53**	**45.87**	**23.54**	**18.37**	**17.81**
Section D	A	Velocity	(cm/s)								
	A1	Near Surface Flow		3.51	3.71	3.82	3.85	1.04	0.97	0.89	0.70
	A2	Near Bed Flow		2.51	2.82	2.61	2.51	0.90	0.82	0.70	0.66
	B	Water Depth	(mm)	65.39	66.72	66.47	66.56	68.99	69.12	69.13	68.01
	C	Discharge	(cm3/s)								
	C1	Near Surface Flow		86.10	61.90	63.52	96.09	26.91	16.75	15.46	17.79
	C2	Near Bed Flow		61.57	47.09	43.38	62.73	23.20	14.15	12.18	16.78
	C3	Total Discharge		**147.67**	**108.99**	**106.90**	**158.82**	**50.11**	**30.90**	**27.64**	**34.56**

Upstream

		Subsection Name		U50	U100	U150	U200	U250	U300	U350	U400	U450
		Subsection Width	(mm)	75	50	50	50	50	50	50	50	75
Section C	A	Velocity	(cm/s)									
	A1	Near Surface Flow		2.42	2.43	2.46	2.49	2.53	2.53	2.53	2.49	2.46
	A2	Near Bed Flow		1.26	1.36	1.35	1.50	1.55	1.58	1.52	1.53	1.34
	B	Water Depth	(mm)	68.91	69.01	68.98	68.43	68.33	68.91	68.95	69.15	69.09
	C	Discharge	(cm3/s)									
	C1	Near Surface Flow		62.56	41.87	42.47	42.67	43.17	43.51	43.62	43.10	63.69
	C2	Near Bed Flow		32.60	23.52	23.31	25.59	26.55	27.26	26.25	26.53	34.60
	C3	Total Discharge		**95.16**	**65.38**	**65.79**	**68.26**	**69.72**	**70.77**	**69.86**	**69.63**	**98.29**
Section B	A	Velocity	(cm/s)									
	A1	Near Surface Flow		1.93	1.97	2.04	2.10	2.13	2.21	2.23	2.19	2.24
	A2	Near Bed Flow		1.53	1.55	1.62	1.66	1.72	1.74	1.79	1.81	1.77
	B	Water Depth	(mm)	68.57	69.26	68.82	68.42	68.48	70.04	69.00	68.68	68.63
	C	Discharge	(cm3/s)									
	C1	Near Surface Flow		49.63	34.13	35.08	36.00	36.39	38.69	38.45	37.59	57.71
	C2	Near Bed Flow		39.31	26.90	27.85	28.34	29.52	30.48	30.88	31.11	45.55
	C3	Total Discharge		**88.94**	**61.04**	**62.93**	**64.34**	**65.91**	**69.17**	**69.33**	**68.70**	**103.25**
Section A	A	Velocity	(cm/s)									
	A1	Near Surface Flow		1.68	1.68	1.76	1.83	1.93	1.93	1.99	2.12	2.15
	A2	Near Bed Flow		1.69	1.61	1.67	1.71	1.78	1.86	1.94	1.99	2.03
	B	Water Depth	(mm)	68.18	68.20	68.21	68.21	68.19	68.16	68.09	67.10	67.79
	C	Discharge	(cm3/s)									
	C1	Near Surface Flow		42.91	28.66	30.04	31.12	32.89	32.91	33.86	35.60	54.63
	C2	Near Bed Flow		43.18	27.53	28.50	29.08	30.28	31.77	32.99	33.34	51.51
	C3	Total Discharge		**86.10**	**56.19**	**58.55**	**60.20**	**63.17**	**64.67**	**66.85**	**68.94**	**106.15**

Water Depth

Average Water Depth, cm		Depth Ratio
LF	RF	RF/LF
6.27	6.97	0.90

Average Water Depth, cm		Depth Ratio
LE	RE	RE/LE
6.62	6.93	0.96

Average Water Depth, cm		Depth Ratio
LD	RD	RD/LD
6.63	6.88	0.96

Average Water Depth, cm
C
6.89

Average Water Depth, cm
B
6.89

Average Water Depth, cm
A
6.80

Velocity

Average Velocity, cm/s		Velocity Ratio
LF	RF	RF/LF
3.88	0.86	0.22
2.93	0.56	0.19

Average Velocity, cm/s		Velocity Ratio
LE	RE	RF/LF
3.71	0.71	0.19
2.85	0.51	0.18

Average Velocity, cm/s		Velocity Ratio
LD	RD	RF/LF
3.72	0.90	0.24
2.61	0.77	0.29

Average Velocity, cm/s
C
2.48
1.44

Average Velocity, cm/s
B
2.12
1.69

Average Velocity, cm/s
A
1.90
1.81

Discharge

Sum of Discharge, cm3/s			Discharge Ratio
LF	RF	LF+RF	RF/LF
532.7	124.2	656.9	0.23

Sum of Discharge, cm3/s			Discharge Ratio
LE	RE	LE+RE	RE/LE
541.2	105.6	646.7	0.20

Sum of Discharge, cm3/s			Discharge Ratio
LD	RD	LD+RD	RD/LD
522.4	143.2	665.6	0.27

Sum of Discharge, cm3/s
C
672.9

Sum of Discharge, cm3/s
B
653.6

Sum of Discharge, cm3/s
A
630.8

Froude

Froude Number	
LF	RF
0.0435	0.0086

Froude Number	
LE	RE
0.0407	0.0074

Froude Number	
LD	RD
0.0393	0.0102

Froude Number
C
0.0239

Froude Number
B
0.0231

Froude Number
A
0.0227

Reynold

Reynold Number	
LF	RF
12789	2782

Reynold Number	
LE	RE
12539	2370

Reynold Number	
LD	RD
12124	3237

Reynold Number
C
12521

Reynold Number
B
12130

Reynold Number
A
11781

Calculation: 50_07_5055

Downstream

		Subsection Name		L50	L100	L150	L200	R50	R100	R150	R200
		Subsection Width	(mm)	75	50	50	75	75	50	50	75
Section F	A	Velocity	(cm/s)								
	A1	Near Surface Flow		4.15	4.05	3.96	3.79	1.71	1.52	1.31	1.06
	A2	Near Bed Flow		3.33	3.27	3.24	3.04	0.97	0.89	0.77	0.65
	B	Water Depth	(mm)	52.95	54.83	55.43	55.76	62.23	62.16	61.68	59.74
	C	Discharge	(cm3/s)								
	C1	Near Surface Flow		82.42	55.54	54.80	79.17	39.86	23.69	20.20	23.83
	C2	Near Bed Flow		66.19	44.81	44.93	63.64	22.65	13.80	11.88	14.62
	C3	Total Discharge		**148.61**	**100.35**	**99.73**	**142.82**	**62.51**	**37.50**	**32.08**	**38.45**
Section E	A	Velocity	(cm/s)								
	A1	Near Surface Flow		4.06	3.96	3.88	3.76	2.92	1.48	0.34	-0.57
	A2	Near Bed Flow		3.11	2.92	2.99	2.83	3.19	1.34	-0.56	-1.71
	B	Water Depth	(mm)	56.96	58.47	58.84	58.86	60.95	61.15	61.41	60.20
	C	Discharge	(cm3/s)								
	C1	Near Surface Flow		86.74	57.92	57.14	82.90	66.81	22.66	5.17	-12.94
	C2	Near Bed Flow		66.42	42.66	43.91	62.55	72.90	20.53	-8.66	-38.71
	C3	Total Discharge		**153.16**	**100.58**	**101.05**	**145.45**	**139.71**	**43.19**	**-3.49**	**-51.65**
Section D	A	Velocity	(cm/s)								
	A1	Near Surface Flow		3.43	3.34	3.49	3.44	1.47	1.52	1.70	1.88
	A2	Near Bed Flow		3.44	3.50	3.41	2.74	0.99	0.97	0.81	0.56
	B	Water Depth	(mm)	56.65	57.93	57.92	58.00	60.08	60.63	60.77	60.10
	C	Discharge	(cm3/s)								
	C1	Near Surface Flow		72.79	48.37	50.50	74.77	33.08	22.97	25.86	42.46
	C2	Near Bed Flow		73.08	50.71	49.41	59.50	22.37	14.64	12.36	12.60
	C3	Total Discharge		**145.87**	**99.08**	**99.91**	**134.28**	**55.45**	**37.61**	**38.22**	**55.06**

Upstream

		Subsection Name		U50	U100	U150	U200	U250	U300	U350	U400	U450
		Subsection Width	(mm)	75	50	50	50	50	50	50	50	75
Section C	A	Velocity	(cm/s)									
	A1	Near Surface Flow		2.55	2.58	2.59	2.63	2.80	2.85	2.84	2.97	2.76
	A2	Near Bed Flow		1.57	1.71	1.69	1.84	1.82	1.98	2.13	2.14	2.04
	B	Water Depth	(mm)	59.26	59.28	59.31	58.81	58.88	59.29	59.15	59.48	59.49
	C	Discharge	(cm3/s)									
	C1	Near Surface Flow		56.78	38.29	38.40	38.68	41.27	42.23	42.00	44.22	61.52
	C2	Near Bed Flow		34.81	25.33	25.05	27.07	26.82	29.34	31.46	31.80	45.62
	C3	Total Discharge		**91.59**	**63.62**	**63.45**	**65.76**	**68.09**	**71.57**	**73.47**	**76.02**	**107.14**
Section B	A	Velocity	(cm/s)									
	A1	Near Surface Flow		2.50	2.49	2.52	2.56	2.64	2.61	2.73	2.82	2.86
	A2	Near Bed Flow		1.81	1.78	1.79	1.83	1.92	1.93	1.90	2.05	2.17
	B	Water Depth	(mm)	57.99	59.24	58.99	58.45	58.73	59.38	59.56	59.42	58.25
	C	Discharge	(cm3/s)									
	C1	Near Surface Flow		54.36	36.83	37.11	37.37	38.82	38.70	40.69	41.89	62.56
	C2	Near Bed Flow		39.40	26.35	26.35	26.71	28.23	28.70	28.36	30.52	47.48
	C3	Total Discharge		**93.77**	**63.19**	**63.46**	**64.08**	**67.05**	**67.41**	**69.05**	**72.41**	**110.04**
Section A	A	Velocity	(cm/s)									
	A1	Near Surface Flow		2.70	2.91	2.78	2.47	2.51	2.52	2.49	2.41	2.38
	A2	Near Bed Flow		1.64	1.68	1.68	1.65	1.69	1.68	1.67	1.88	2.09
	B	Water Depth	(mm)	59.36	59.38	59.39	59.39	59.38	59.35	59.30	58.60	58.28
	C	Discharge	(cm3/s)									
	C1	Near Surface Flow		60.09	43.24	41.29	36.70	37.22	37.40	36.91	35.31	52.08
	C2	Near Bed Flow		36.54	24.88	24.93	24.56	25.09	24.94	24.81	27.60	45.62
	C3	Total Discharge		**96.63**	**68.12**	**66.22**	**61.26**	**62.32**	**62.34**	**61.72**	**62.91**	**97.70**

Water Depth

Section F — Average Water Depth, cm		Depth Ratio
LF	RF	RF/LF
5.47	6.15	0.89

Section E — Average Water Depth, cm		Depth Ratio
LE	RE	RE/LE
5.83	6.09	0.96

Section D — Average Water Depth, cm		Depth Ratio
LD	RD	RD/LD
5.76	6.04	0.95

Section C — Average Water Depth, cm
C
5.92

Section B — Average Water Depth, cm
B
5.89

Section A — Average Water Depth, cm
A
5.92

Velocity

Section F — Average Velocity, cm/s		Velocity Ratio
LF	RF	RF/LF
3.99	1.40	0.35
3.22	0.82	0.25

Section E — Average Velocity, cm/s		Velocity Ratio
LE	RE	RF/LF
3.92	1.04	0.27
2.96	0.56	0.19

Section D — Average Velocity, cm/s		Velocity Ratio
LD	RD	RF/LF
3.42	1.64	0.48
3.27	0.83	0.25

Section C — Average Velocity, cm/s
C
2.73
1.88

Section B — Average Velocity, cm/s
B
2.64
1.91

Section A — Average Velocity, cm/s
A
2.58
1.74

Discharge

Section F — Sum of Discharge, cm3/s			Discharge Ratio
LF	RF	LF+RF	RF/LF
491.5	170.5	662.0	0.35

Section E — Sum of Discharge, cm3/s			Discharge Ratio
LE	RE	LE+RE	RE/LE
500.2	127.8	628.0	0.26

Section D — Sum of Discharge, cm3/s			Discharge Ratio
LD	RD	LD+RD	RD/LD
479.1	186.3	665.5	0.39

Section C — Sum of Discharge, cm3/s
C
680.7

Section B — Sum of Discharge, cm3/s
B
670.5

Section A — Sum of Discharge, cm3/s
A
639.2

Froude

Section F — Froude Number	
LF	RF
0.0492	0.0143

Section E — Froude Number	
LE	RE
0.0455	0.0104

Section D — Froude Number	
LD	RD
0.0445	0.0161

Section C — Froude Number
C
0.0303

Section B — Froude Number
B
0.0299

Section A — Froude Number
A
0.0283

Reynold

Section F — Reynold Number	
LF	RF
12956	4143

Section E — Reynold Number	
LE	RE
12606	2985

Section D — Reynold Number	
LD	RD
12228	4589

Section C — Reynold Number
C
14259

Section B — Reynold Number
B
14045

Section A — Reynold Number
A
13343

Appendix B1 Discharge Result and Calculation

Bifurcation Angle (°)	Slope (%)	Left Weir Height (mm)	Right Weir Height (mm)	Name of Run	Page Number
30	0.3	50	50	30_03_5050	B-5
			53	30_03_5053	B-6
			55	30_03_5055	B-7
			57	30_03_5057	B-8
			60	30_03_5060	B-9
		55	60	30_03_5560	B-10
			62	30_03_5562	B-11
			65	30_03_5565	B-12
	0.5	50	50	30_05_5050	B-13
			53	30_05_5053	B-14
			55	30_05_5055	B-15
			57	30_05_5057	B-16
			60	30_05_5060	B-17
		55	60	30_05_5560	B-18
			62	30_05_5562	B-19
			65	30_05_5565	B-20
	0.7	50	50	30_07_5050	B-21
			53	30_07_5053	B-22
			55	30_07_5055	B-23
			57	30_07_5057	B-24
			60	30_07_5060	B-25
		55	60	30_07_5560	B-26
			62	30_07_5562	B-27
			65	30_07_5565	B-28
	0.9	50	50	30_09_5050	B-29
			53	30_09_5053	B-30
			55	30_09_5055	B-31
			57	30_09_5057	B-32
			60	30_09_5060	B-33
		55	60	30_09_5560	B-34
			62	30_09_5562	B-35
			65	30_09_5565	B-36

Bifurcation Angle (°)	Slope (%)	Left Weir Height (mm)	Right Weir Height (mm)	Name of Run	Page Number
40	0.3	50	50	40_03_5050	B-37
			53	40_03_5053	B-38
			55	40_03_5055	B-39
			57	40_03_5057	B-40
			60	40_03_5060	B-41
		55	60	40_03_5560	B-42
			62	40_03_5562	B-43
			65	40_03_5565	B-44
	0.5	50	50	40_05_5050	B-45
			53	40_05_5053	B-46
			55	40_05_5055	B-47
			57	40_05_5057	B-48
			60	40_05_5060	B-49
		55	60	40_05_5560	B-50
			62	40_05_5562	B-51
			65	40_05_5565	B-52
	0.7	50	50	40_07_5050	B-53
			53	40_07_5053	B-54
			55	40_07_5055	B-55
			57	40_07_5057	B-56
			60	40_07_5060	B-57
		55	60	40_07_5560	B-58
			62	40_07_5562	B-59
			65	40_07_5565	B-60
	0.9	50	50	40_09_5050	B-61
			53	40_09_5053	B-62
			55	40_09_5055	B-63
			57	40_09_5057	B-64
			60	40_09_5060	B-65
		55	60	40_09_5560	B-66
			62	40_09_5562	B-67
			65	40_09_5565	B-68

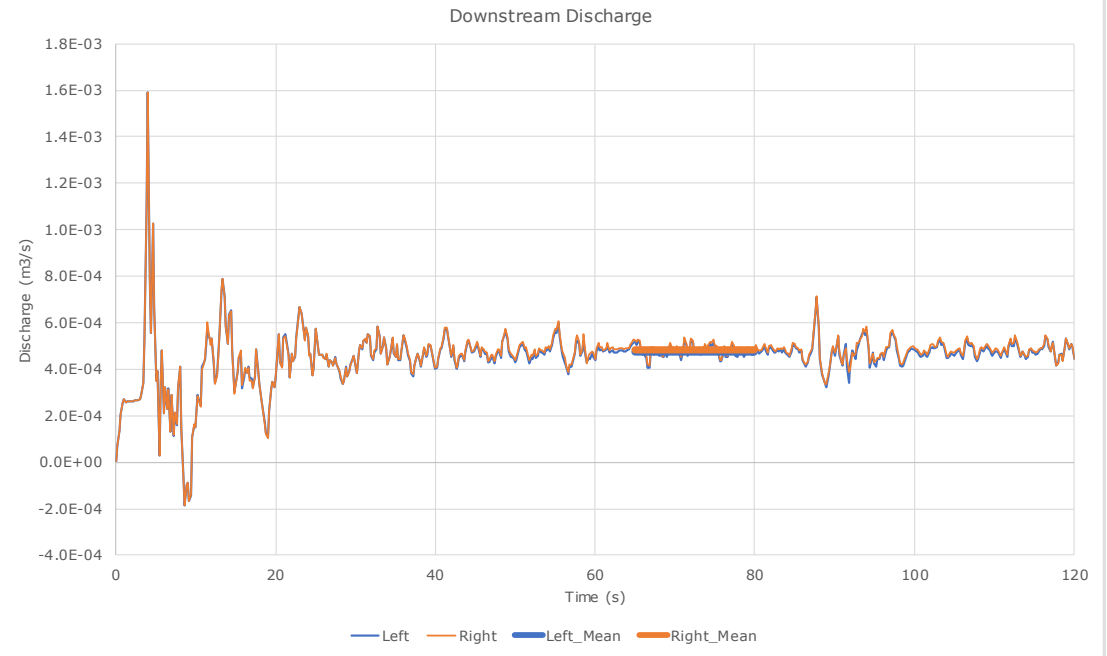
Bifurcation Angle (°)	Slope (%)	Left Weir Height (mm)	Right Weir Height (mm)	Name of Run	Page Number
50	0.3	50	50	50_03_5050	B-69
			53	50_03_5053	B-70
			55	50_03_5055	B-71
			57	50_03_5057	B-72
			60	50_03_5060	B-73
		55	60	50_03_5560	B-74
			62	50_03_5562	B-75
			65	50_03_5565	B-76
	0.5	50	50	50_05_5050	B-77
			53	50_05_5053	B-78
			55	50_05_5055	B-79
			57	50_05_5057	B-80
			60	50_05_5060	B-81
		55	60	50_05_5560	B-82
			62	50_05_5562	B-83
			65	50_05_5565	B-84
	0.7	50	50	50_07_5050	B-85
			53	50_07_5053	B-86
			55	50_07_5055	B-87
			57	50_07_5057	B-88
			60	50_07_5060	B-89
		55	60	50_07_5560	B-90
			62	50_07_5562	B-91
			65	50_07_5565	B-92
	0.9	50	50	50_09_5050	B-93
			53	50_09_5053	B-94
			55	50_09_5055	B-95
			57	50_09_5057	B-96
			60	50_09_5060	B-97
		55	60	50_09_5560	B-98
			62	50_09_5562	B-99
			65	50_09_5565	B-100

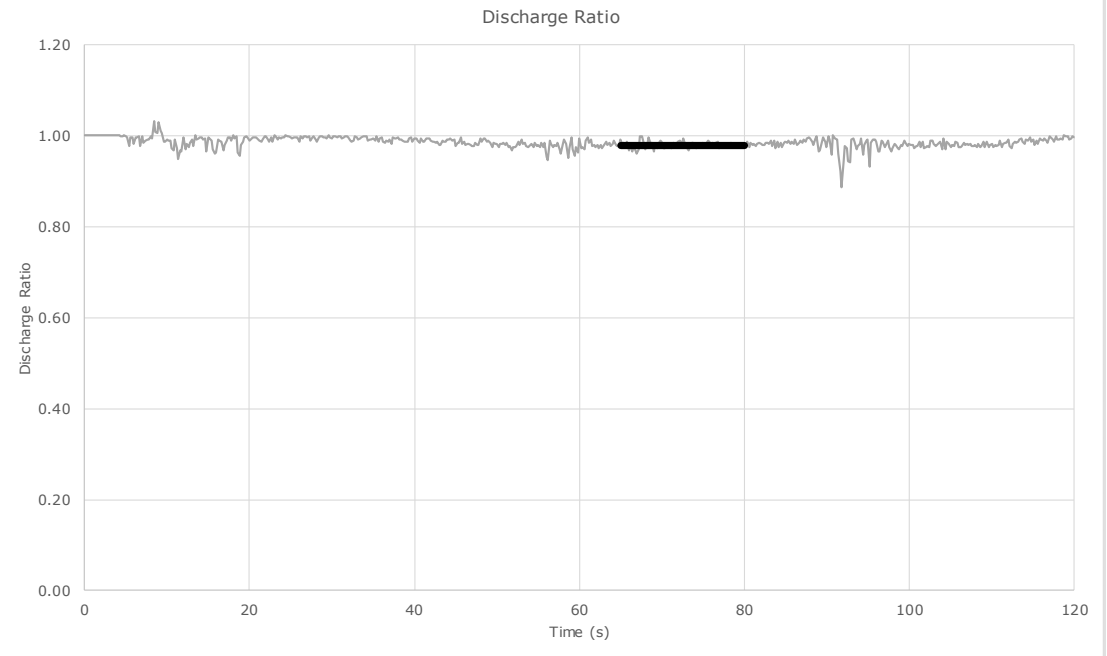
Bifurcation Angle (°)	Slope (%)	Left Weir Height (mm)	Right Weir Height (mm)	Name of Run	Page Number
60	0.3	50	50	60_03_5050	B-101
			53	60_03_5053	B-102
			55	60_03_5055	B-103
			57	60_03_5057	B-104
			60	60_03_5060	B-105
		55	60	60_03_5560	B-106
			62	60_03_5562	B-107
			65	60_03_5565	B-108
	0.5	50	50	60_05_5050	B-109
			53	60_05_5053	B-110
			55	60_05_5055	B-111
			57	60_05_5057	B-112
			60	60_05_5060	B-113
		55	60	60_05_5560	B-114
			62	60_05_5562	B-115
			65	60_05_5565	B-116
	0.7	50	50	60_07_5050	B-117
			53	60_07_5053	B-118
			55	60_07_5055	B-119
			57	60_07_5057	B-120
			60	60_07_5060	B-121
		55	60	60_07_5560	B-122
			62	60_07_5562	B-123
			65	60_07_5565	B-124
	0.9	50	50	60_09_5050	B-125
			53	60_09_5053	B-126
			55	60_09_5055	B-127
			57	60_09_5057	B-128
			60	60_09_5060	B-129
		55	60	60_09_5560	B-130
			62	60_09_5562	B-131
			65	60_09_5565	B-132

30_03_5050

Name	Symbol	Left	Right	Unit
Weir Height	WH	50	50	mm
Initial Time	Ti	65	65	s
End Time	Te	80	80	s
Initial Number	Ni	325	325	unitless
End Number	Ne	400	400	unitless
Average Discharge	$\bar{Q}$	4.752E-04	4.854E-04	m3/s

Name	Symbol	Equation	Result	Unit
Weir Height Ratio	WHr	WHL/WHR	1.000	dimensionless
Discharge Ratio	Qr	$\bar{Q}$_L/$\bar{Q}$_R	0.979	dimensionless
Time Step Discharge Ratio	Qr,t	Average[Q_(r,t=n)···Q_(r,t=n+N)]	0.979	dimensionless

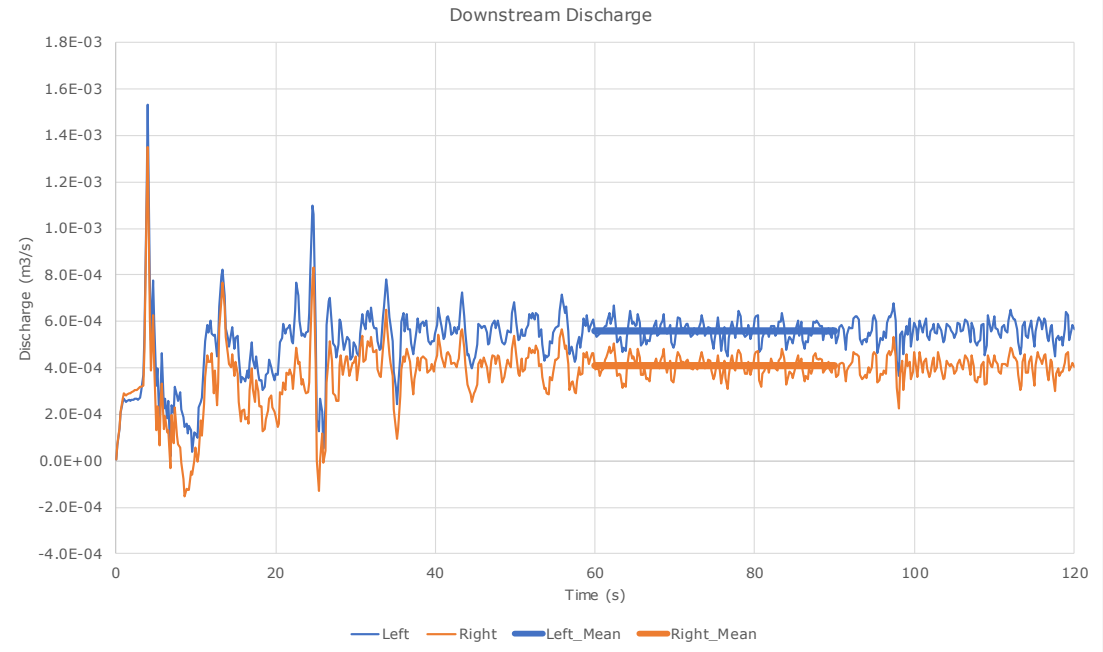


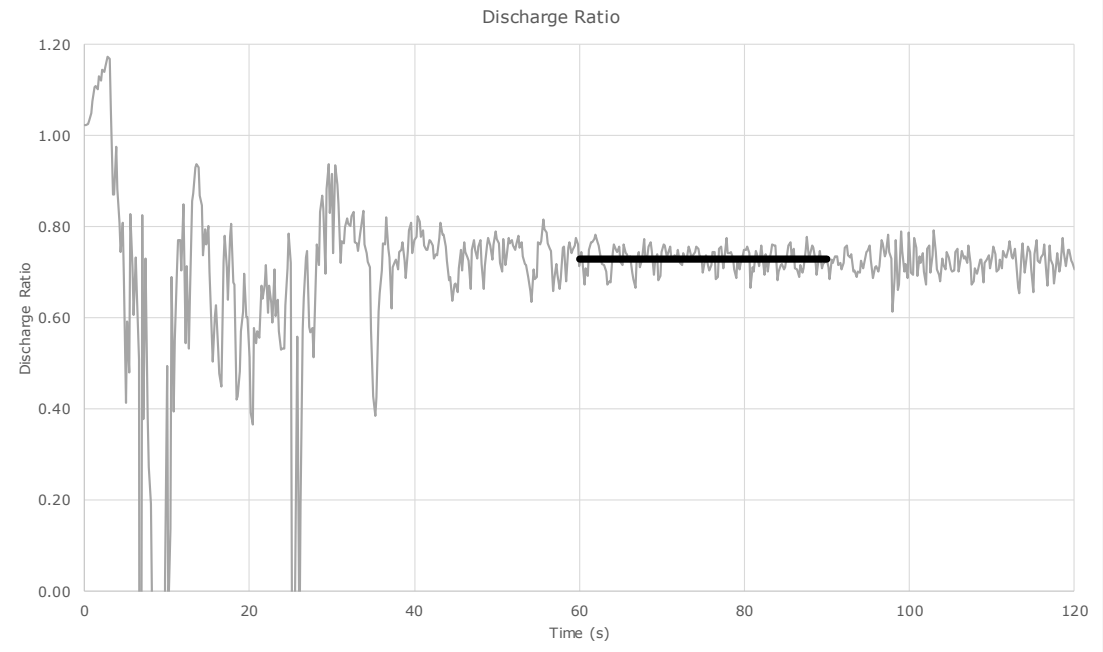


30_03_5053

Name	Symbol	Left	Right	Unit
Weir Height	WH	50	53	mm
Initial Time	Ti	60	60	s
End Time	Te	90	90	s
Initial Number	Ni	300	300	unitless
End Number	Ne	450	450	unitless
Average Discharge	$\bar{Q}$	5.588E-04	4.083E-04	m3/s

Name	Symbol	Equation	Result	Unit
Weir Height Ratio	WHr	WHL/WHR	0.943	dimensionless
Discharge Ratio	Qr	$\bar{Q}$_L/$\bar{Q}$_R	0.731	dimensionless
Time Step Discharge Ratio	Qr,t	Average[Q_(r,t=n)···Q_(r,t=n+N)]	0.730	dimensionless

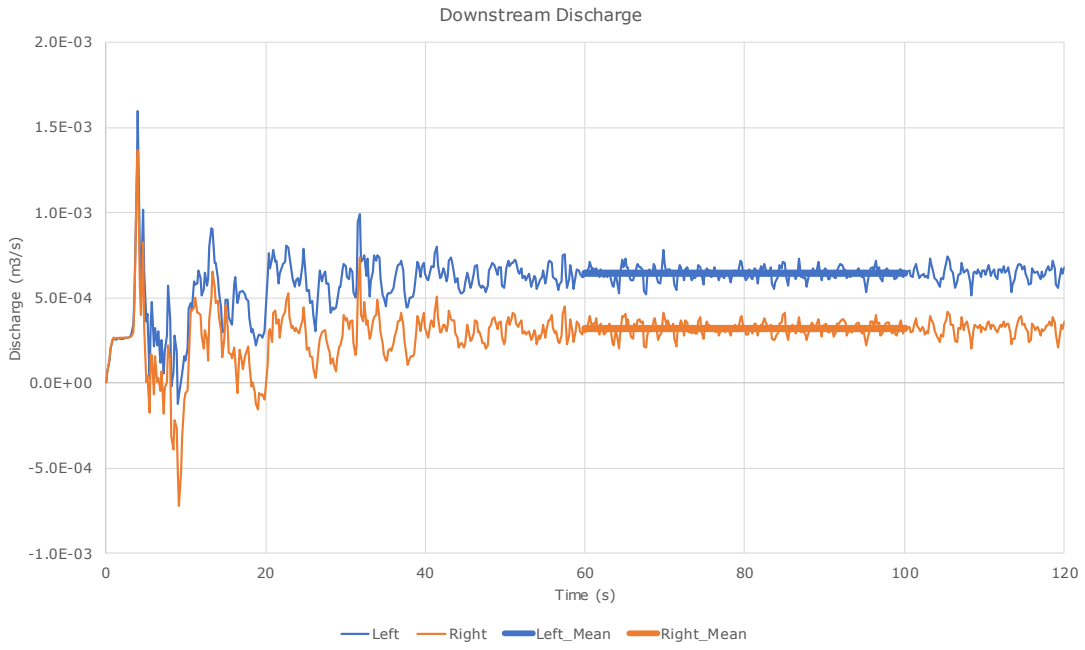


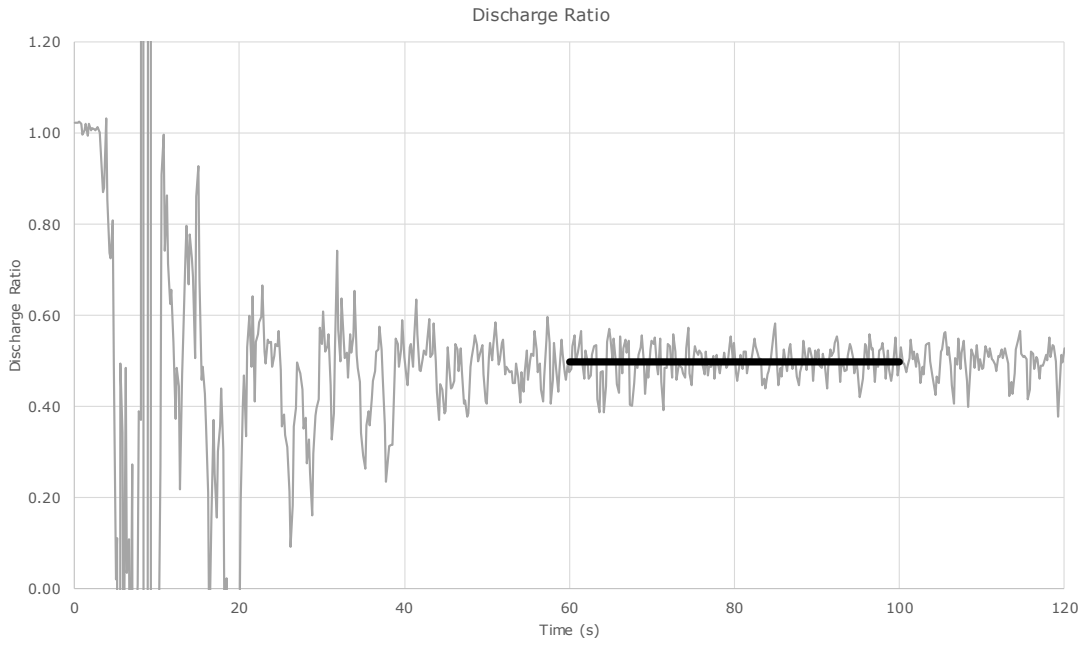


30_03_5055

Name	Symbol	Left	Right	Unit
Weir Height	WH	50	55	mm
Initial Time	Ti	60	60	s
End Time	Te	100	100	s
nitial Number	Ni	300	300	unitless
End Number	Ne	500	500	unitless
:rage Discharge	$\bar{Q}$	6.435E-04	3.217E-04	m3/s

Name	Symbol	Equation	Result	Unit
:ir Height Ratio	WHr	WHL/WHR	0.909	dimensionless
scharge Ratio	Qr	$\bar{Q}$_L/$\bar{Q}$_R	0.500	dimensionless
:ep Discharge Ratio	Qr,t	Average[Q_(r,t=n)···Q_(r,t=n+N)]	0.498	dimensionless

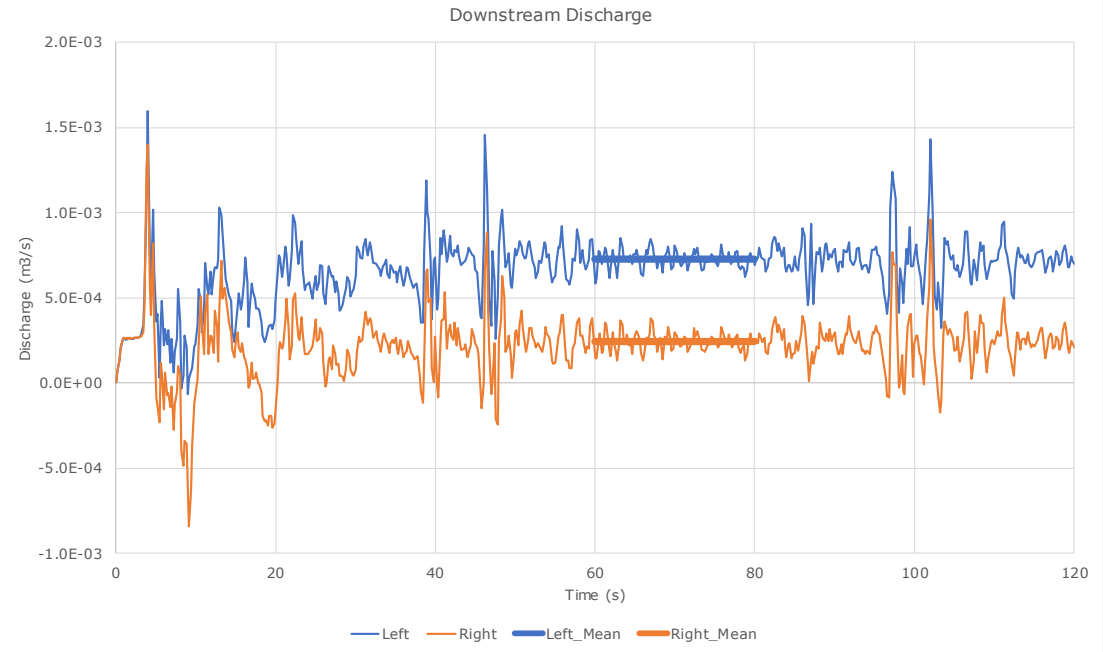


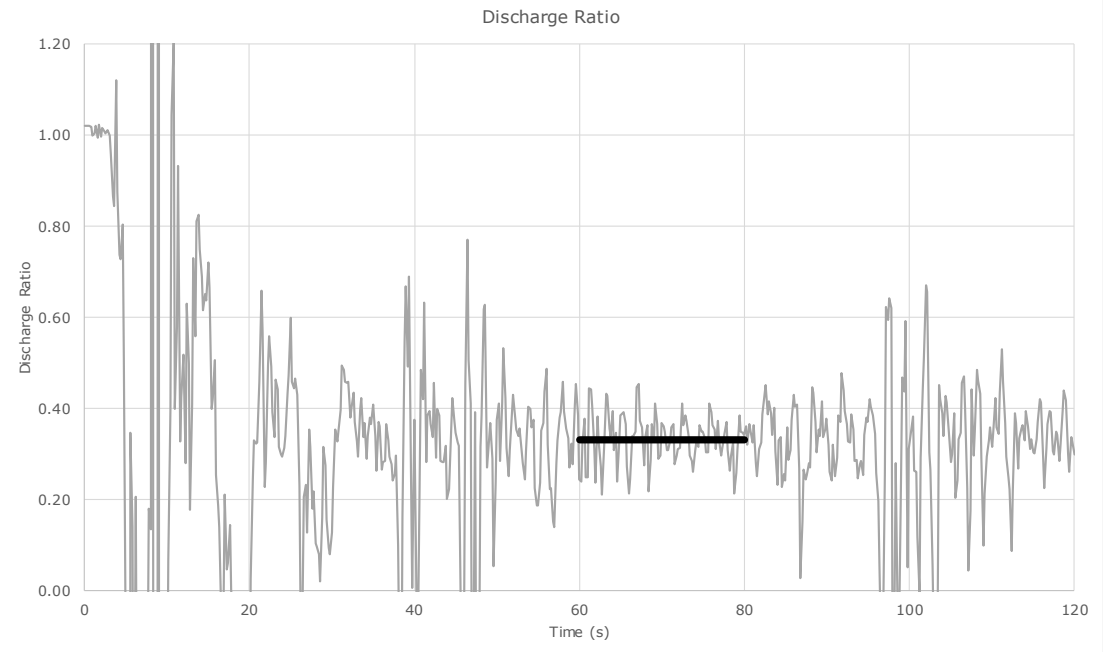


30_03_5057

Name	Symbol	Left	Right	Unit
Weir Height	WH	50	57	mm
Initial Time	Ti	60	60	s
End Time	Te	80	80	s
Initial Number	Ni	300	300	unitless
End Number	Ne	400	400	unitless
Average Discharge	$\bar{Q}$	7.267E-04	2.435E-04	m3/s

Name	Symbol	Equation	Result	Unit
Weir Height Ratio	WHr	WHL/WHR	0.877	dimensionless
Discharge Ratio	Qr	$\bar{Q}$_L/$\bar{Q}$_R	0.335	dimensionless
Time Step Discharge Ratio	Qr,t	Average[Q_(r,t=n)···Q_(r,t=n+N)]	0.332	dimensionless

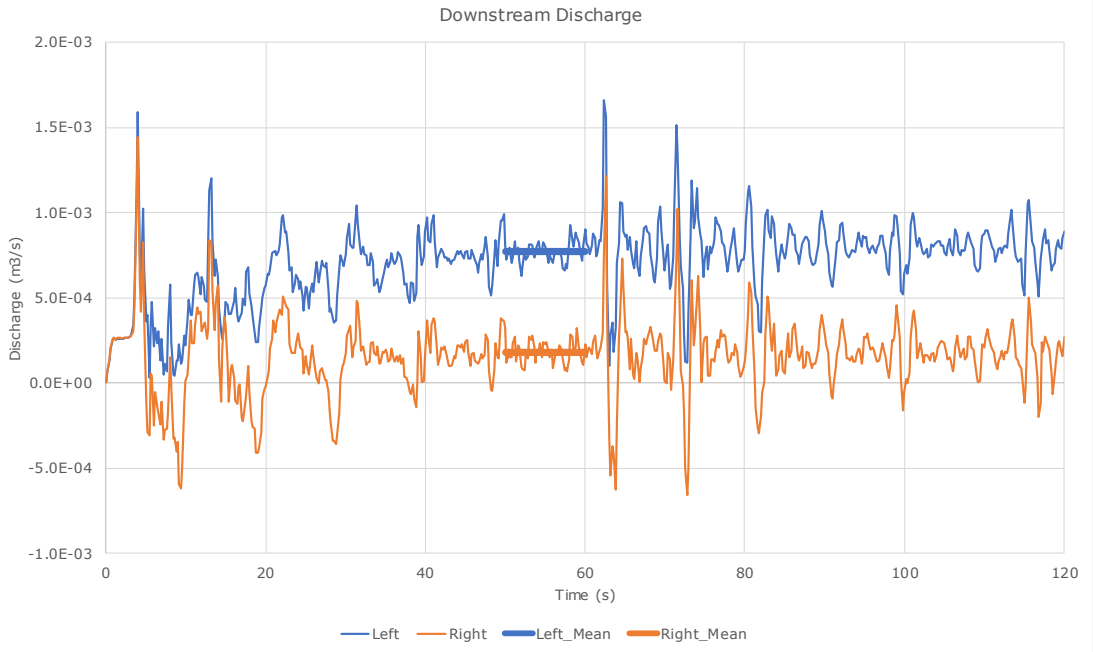


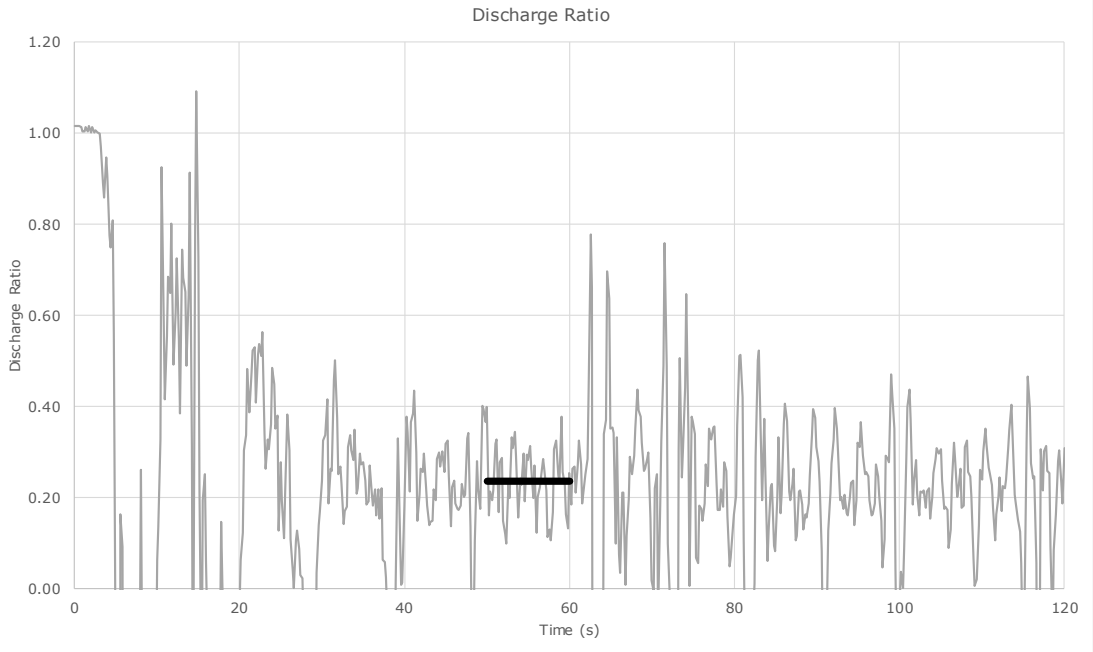


30_03_5060

Name	Symbol	Left	Right	Unit
Weir Height	WH	50	60	mm
Initial Time	Ti	50	50	s
End Time	Te	60	60	s
Initial Number	Ni	250	250	dimensionless
End Number	Ne	300	300	dimensionless
Average Discharge	$\bar{Q}$	7.722E-04	1.835E-04	m3/s

Name	Symbol	Equation	Result	Unit
Weir Height Ratio	WHr	WHL/WHR	0.833	dimensionless
Discharge Ratio	Qr	$\bar{Q}$_L/$\bar{Q}$_R	0.238	dimensionless
me Step Discharge Ratio	Qr,t	Average[Q_(r,t=n)···Q_(r,t=n+N)]	0.235	dimensionless

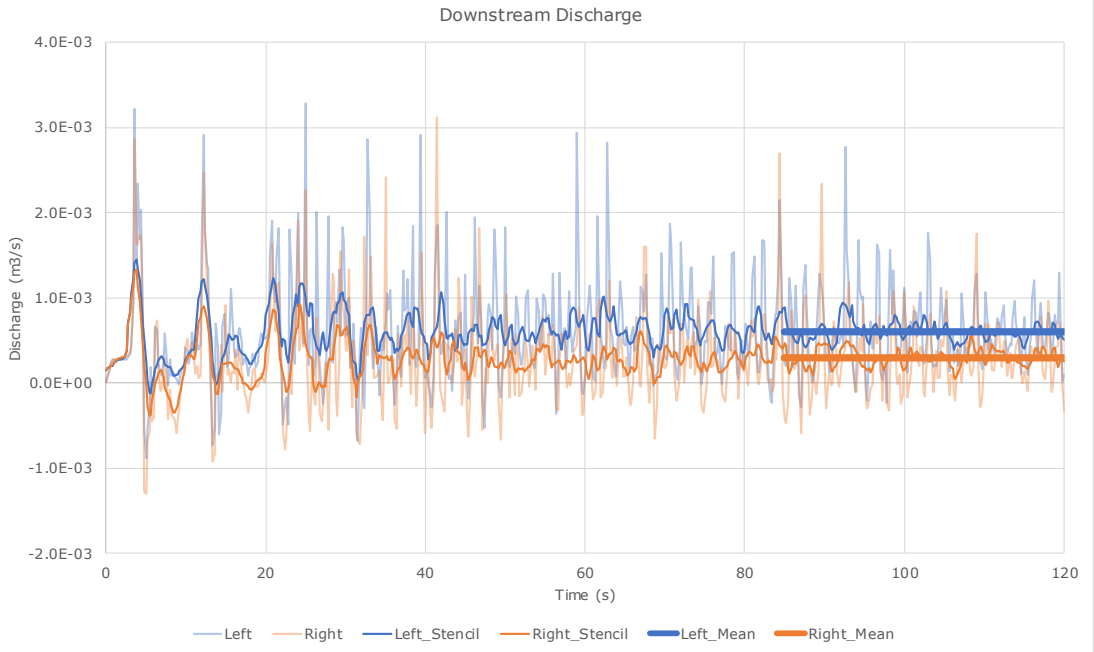


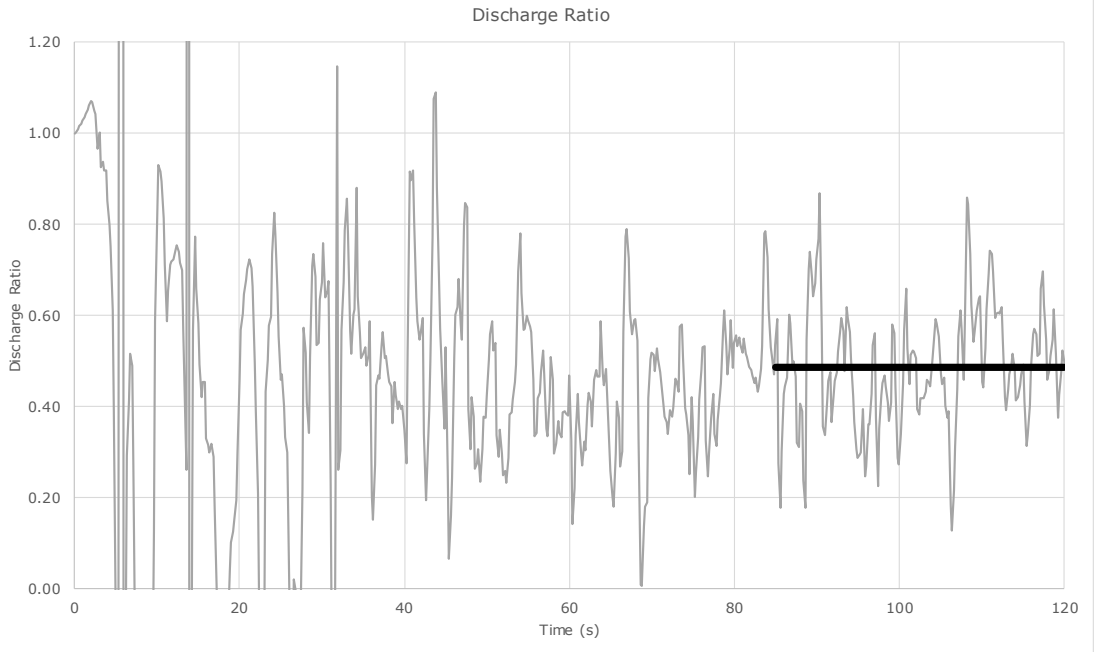


30_03_5560

Name	Symbol	Left	Right	Unit
Weir Height	WH	55	60	mm
Initial Time	Ti	85	85	s
End Time	Te	120	120	s
Initial Number	Ni	425	425	dimensionless
End Number	Ne	600	600	dimensionless
Average Discharge	$\bar{Q}$	6.063E-04	2.972E-04	m3/s

Name	Symbol	Equation	Result	Unit
Weir Height Ratio	WHr	WHL/WHR	0.917	dimensionless
Discharge Ratio	Qr	$\bar{Q}_L/\bar{Q}_R$	0.490	dimensionless
Time Step Discharge Ratio	Qr,t	Average[Q_(r,t=n)···Q_(r,t=n+N)]	0.485	dimensionless

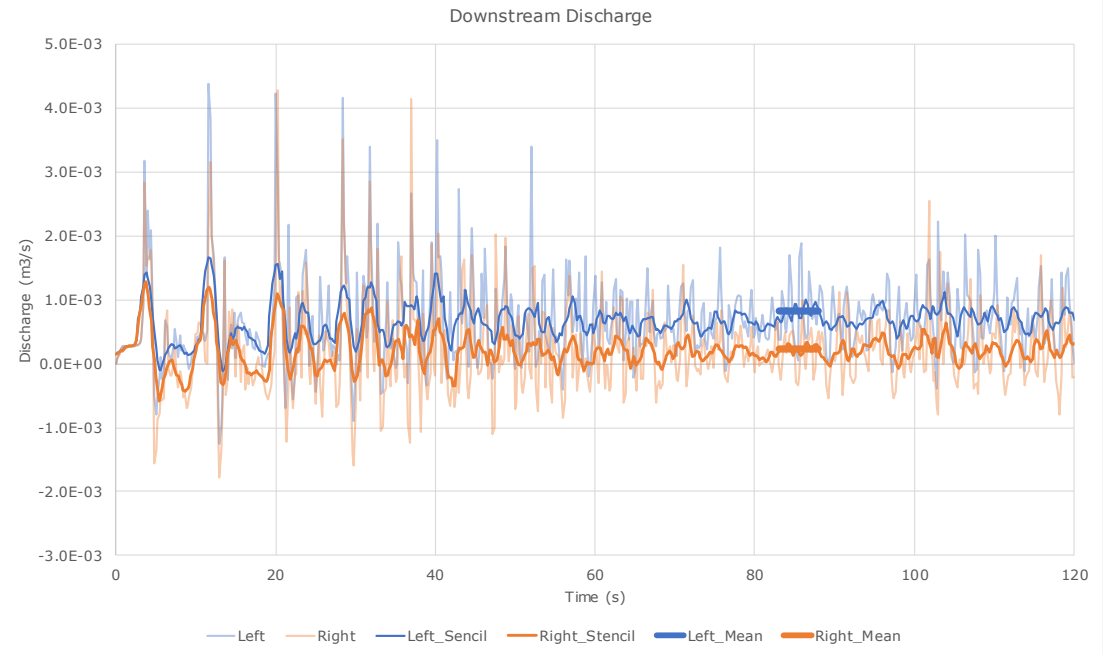


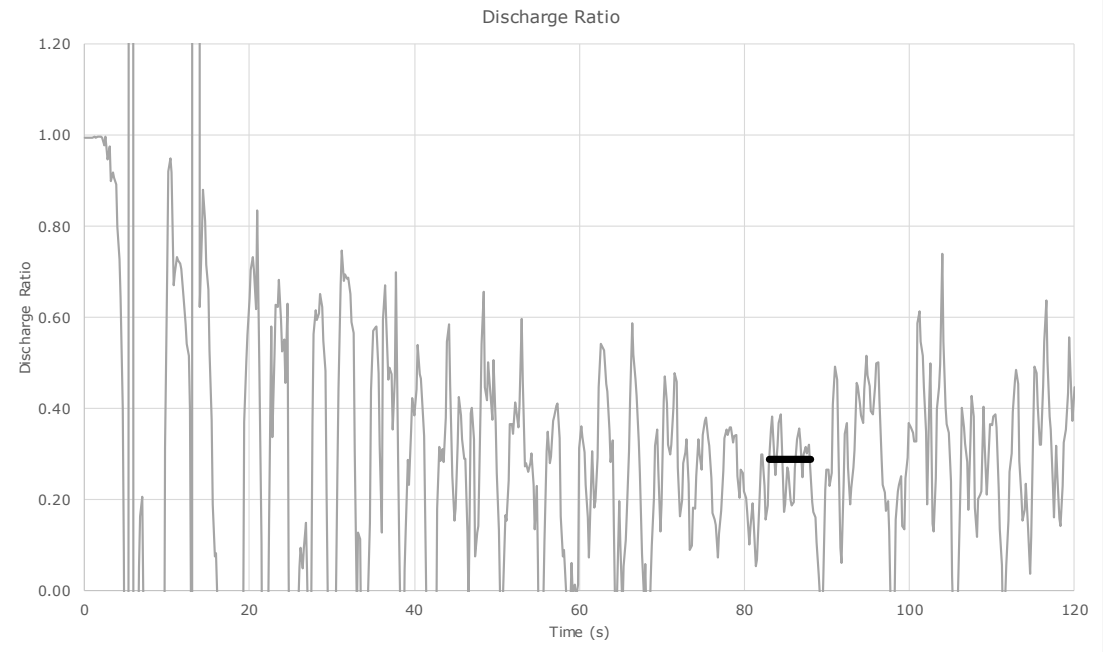


30_03_5562

Name	Symbol	Left	Right	Unit
Weir Height	WH	55	62	mm
Initial Time	Ti	83	83	s
End Time	Te	88	88	s
Initial Number	Ni	415	415	dimensionless
End Number	Ne	440	440	dimensionless
Average Discharge	$\bar{Q}$	8.188E-04	2.354E-04	m3/s

Name	Symbol	Equation	Result	Unit
Weir Height Ratio	WHr	WHL/WHR	0.887	dimensionless
Discharge Ratio	Qr	$\bar{Q}_L/\bar{Q}_R$	0.287	dimensionless
Time Step Discharge Ratio	Qr,t	Average[Q_(r,t=n)···Q_(r,t=n+N)]	0.288	dimensionless

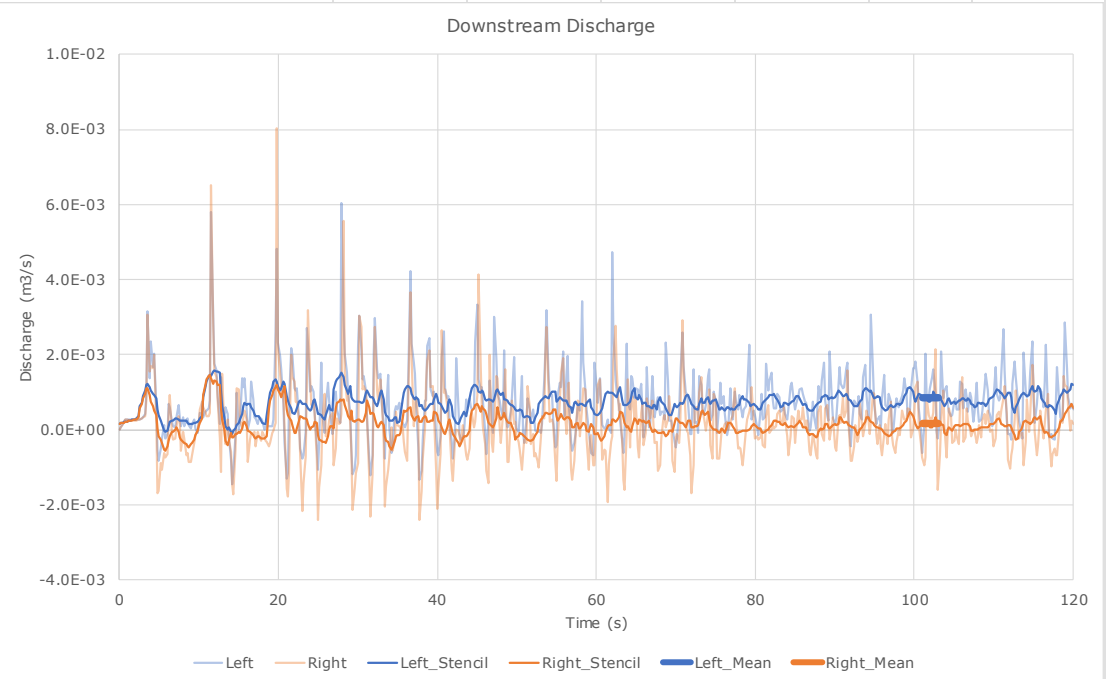


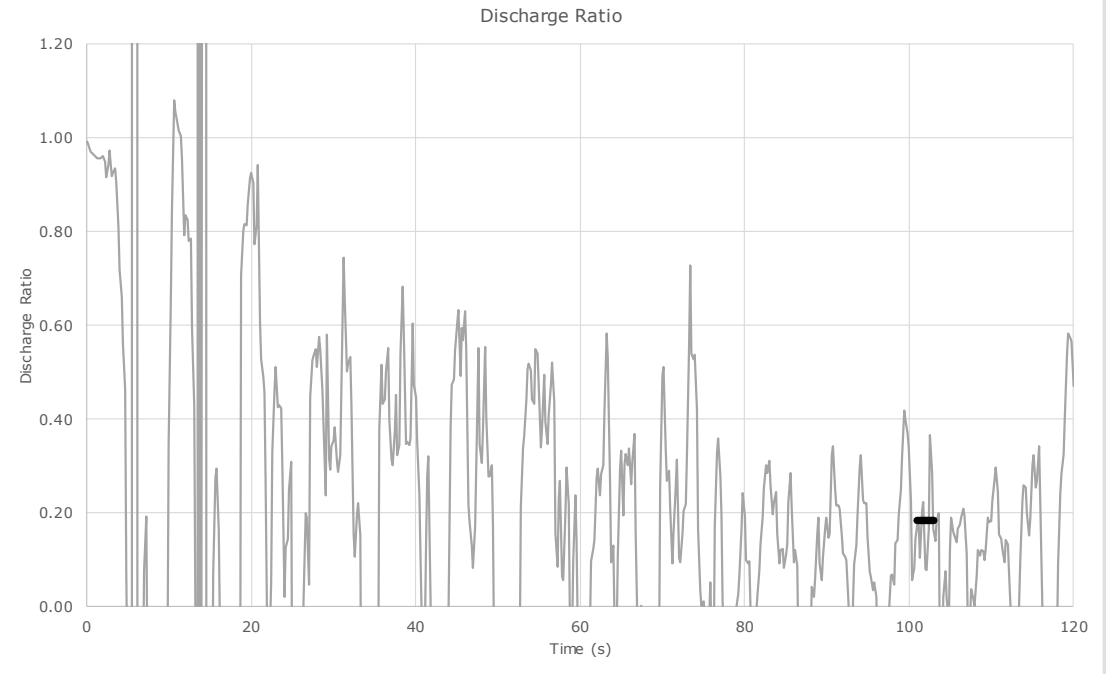


30_03_5565

Name	Symbol	Left	Right	Unit
Weir Height	WH	55	65	mm
Initial Time	Ti	101	101	s
End Time	Te	103	103	s
Initial Number	Ni	505	505	dimensionless
End Number	Ne	515	515	dimensionless
Average Discharge	$\bar{Q}$	8.651E-04	1.603E-04	m3/s

Name	Symbol	Equation	Result	Unit
Weir Height Ratio	WHr	WHL/WHR	0.846	dimensionless
Discharge Ratio	Qr	$\bar{Q}_L/\bar{Q}_R$	0.185	dimensionless
Time Step Discharge Ratio	Qr,t	Average[Q_(r,t=n)···Q_(r,t=n+N)]	0.183	dimensionless

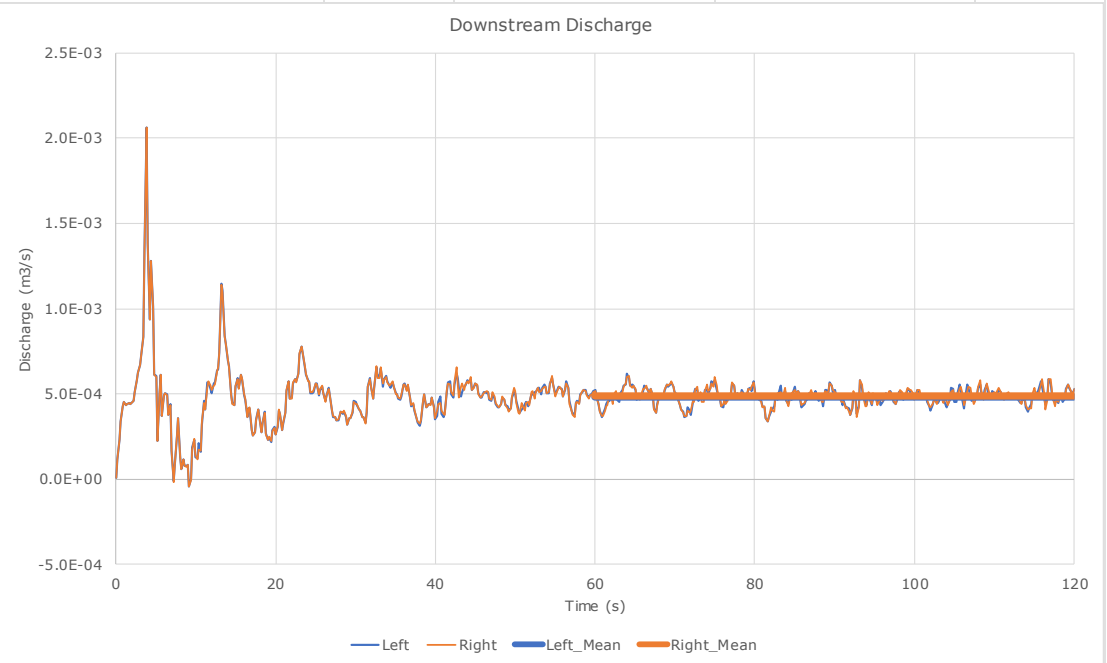


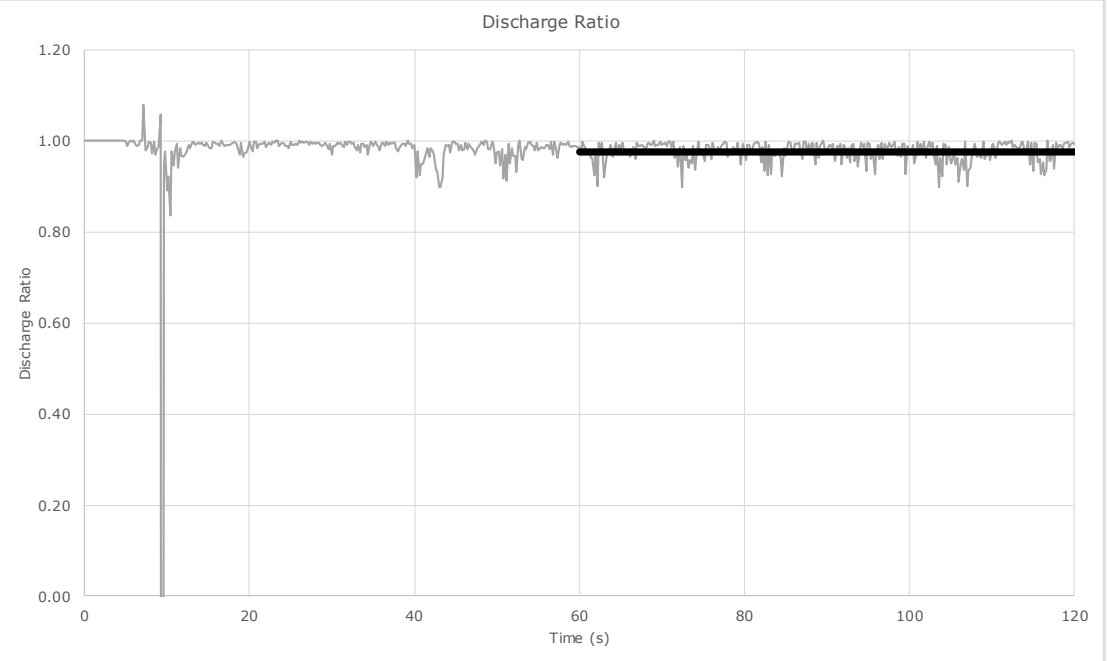


30_05_5050

Name	Symbol	Left	Right	Unit
Weir Height	WH	50	50	mm
Initial Time	Ti	60	60	s
End Time	Te	120	120	s
Initial Number	Ni	300	300	unitless
End Number	Ne	600	600	unitless
Average Discharge	$\bar{Q}$	4.839E-04	4.855E-04	m3/s

Name	Symbol	Equation	Result	Unit
Weir Height Ratio	WHr	WHL/WHR	1.000	dimensionless
Discharge Ratio	Qr	$\bar{Q}$_L/$\bar{Q}$_R	0.997	dimensionless
Time Step Discharge Ratio	Qr,t	Average[Q_(r,t=n)···Q_(r,t=n+N)]	0.976	dimensionless

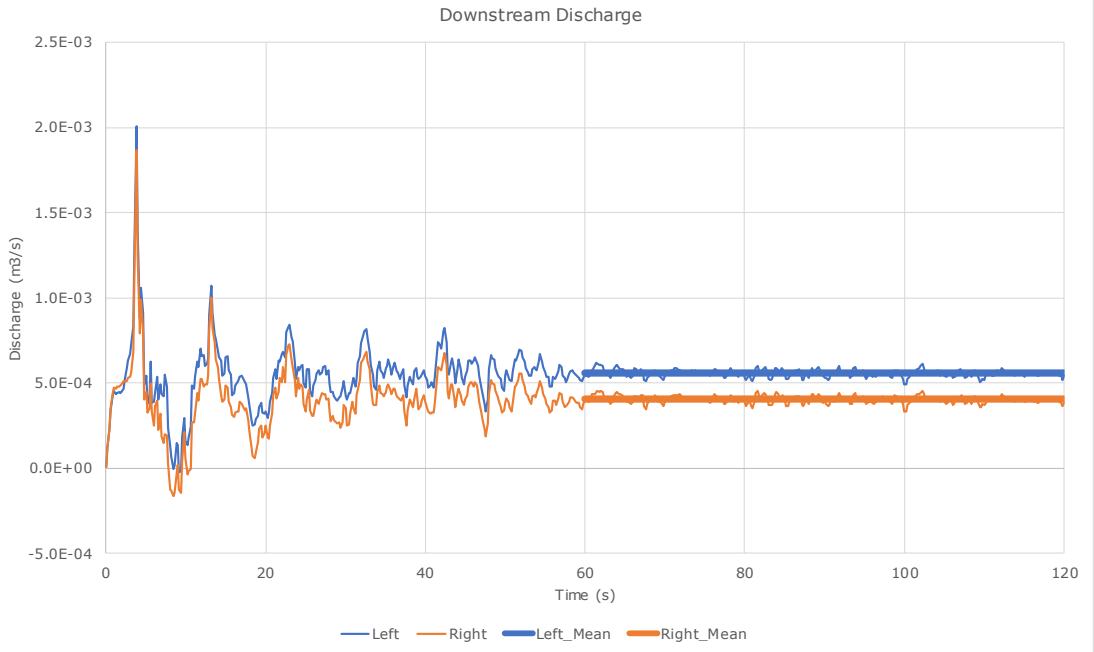


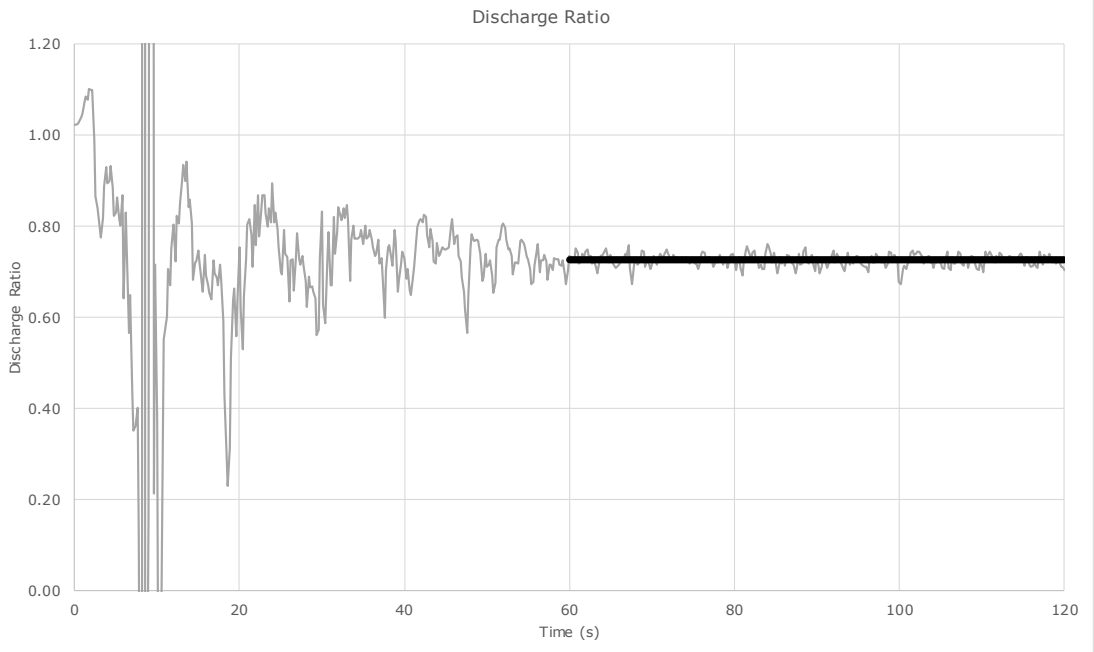


30_05_5053

	Symbol	Left	Right	Unit
	WH	50	53	mm
	Ti	60	60	s
	Te	120	120	s
-	Ni	300	300	unitless
	Ne	600	600	unitless
rge	$\bar{Q}$	5.581E-04	4.051E-04	m3/s

	Symbol	Equation	Result	Unit
tio	WHr	WHL/WHR	0.943	dimensionless
o	Qr	$\bar{Q}$_L/$\bar{Q}$_R	0.726	dimensionless
e Ratio	Qr,t	Average[Q_(r,t=n)···Q_(r,t=n+N)]	0.725	dimensionless

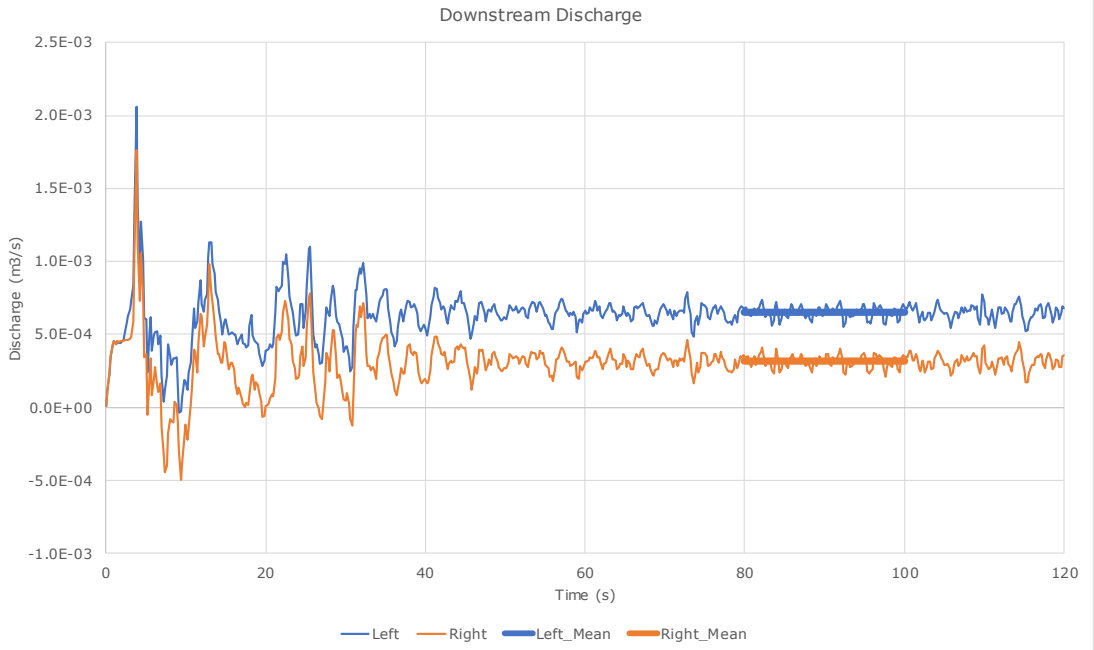


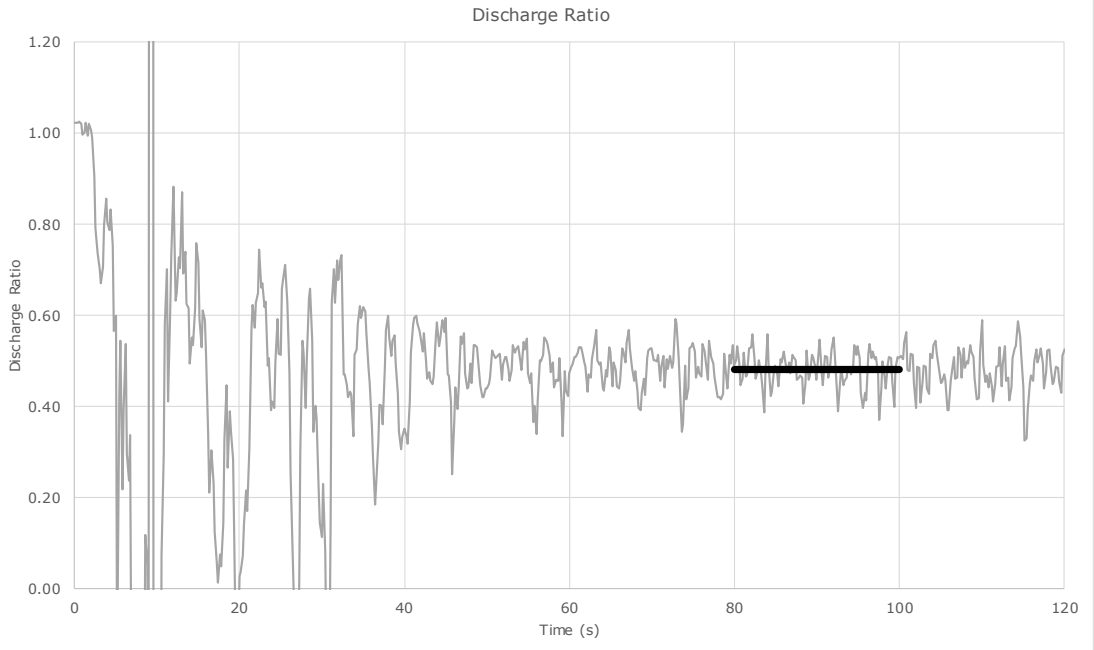


30_05_5055

Name	Symbol	Left	Right	Unit
Weir Height	WH	50	55	mm
Initial Time	Ti	80	80	s
End Time	Te	100	100	s
Initial Number	Ni	400	400	unitless
End Number	Ne	500	500	unitless
Average Discharge	$\bar{Q}$	6.510E-04	3.147E-04	m3/s

Name	Symbol	Equation	Result	Unit
Weir Height Ratio	WHr	WHL/WHR	0.909	dimensionless
Discharge Ratio	Qr	$\bar{Q}$_L/$\bar{Q}$_R	0.483	dimensionless
Time Step Discharge Ratio	Qr,t	Average[Q_(r,t=n)···Q_(r,t=n+N)]	0.481	dimensionless

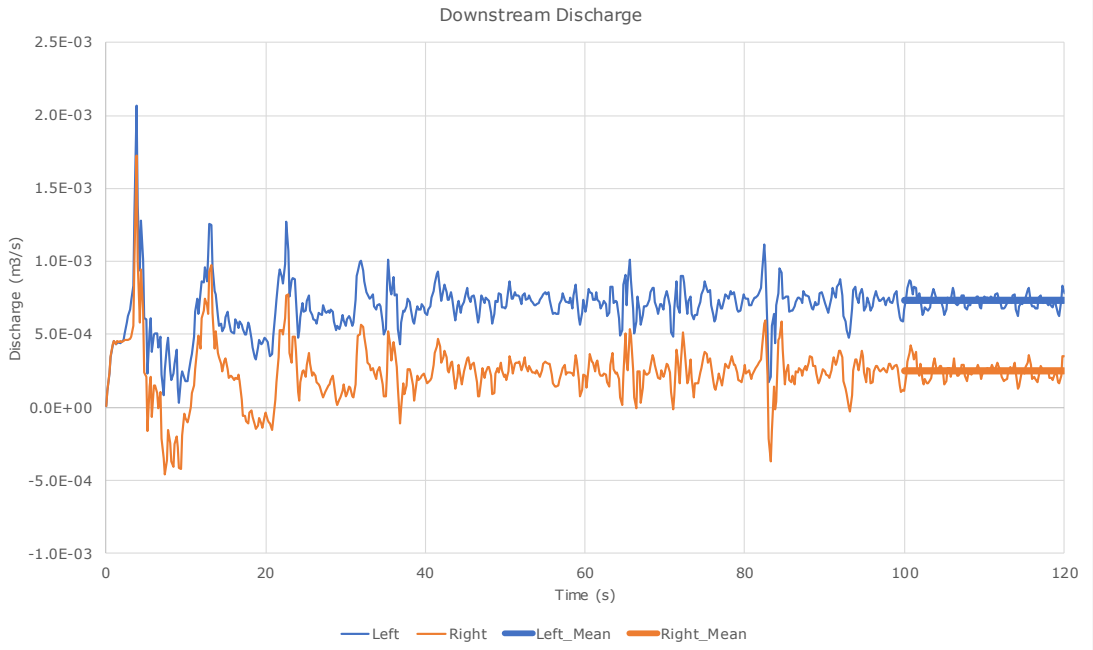


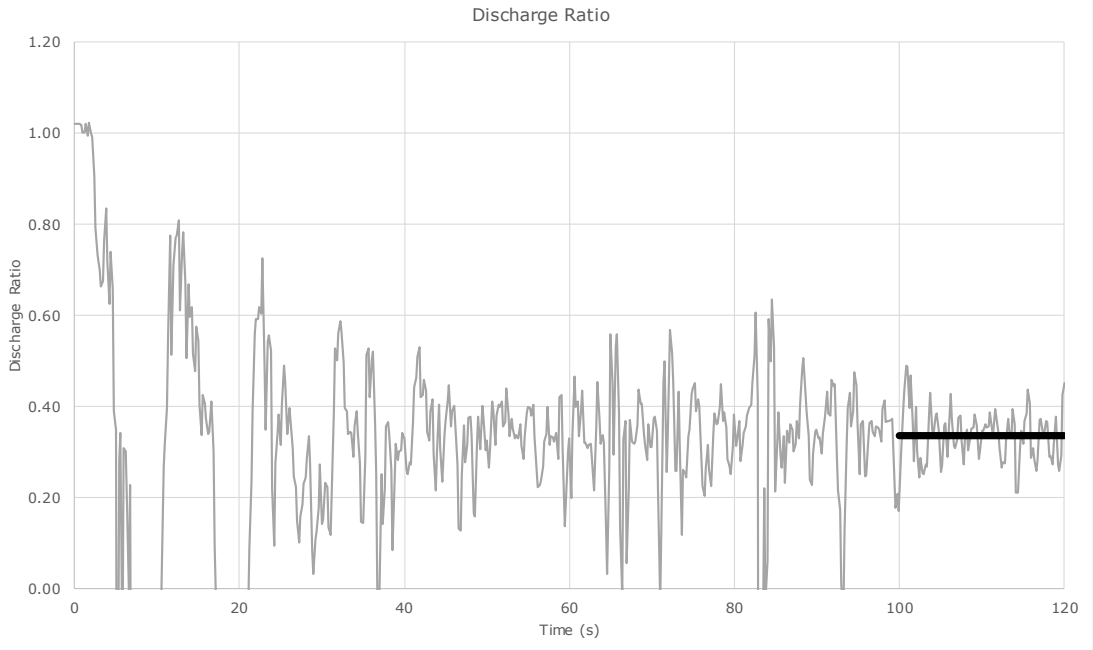


30_05_5057

Name	Symbol	Left	Right	Unit
Weir Height	WH	50	57	mm
Initial Time	Ti	100	100	s
End Time	Te	120	120	s
Initial Number	Ni	500	500	unitless
End Number	Ne	600	600	unitless
Average Discharge	$\bar{Q}$	7.305E-04	2.479E-04	m3/s

Name	Symbol	Equation	Result	Unit
Weir Height Ratio	WHr	WHL/WHR	0.877	dimensionless
Discharge Ratio	Qr	$\bar{Q}$_L/$\bar{Q}$_R	0.339	dimensionless
Time Step Discharge Ratio	Qr,t	Average[Q_(r,t=n)···Q_(r,t=n+N)]	0.336	dimensionless

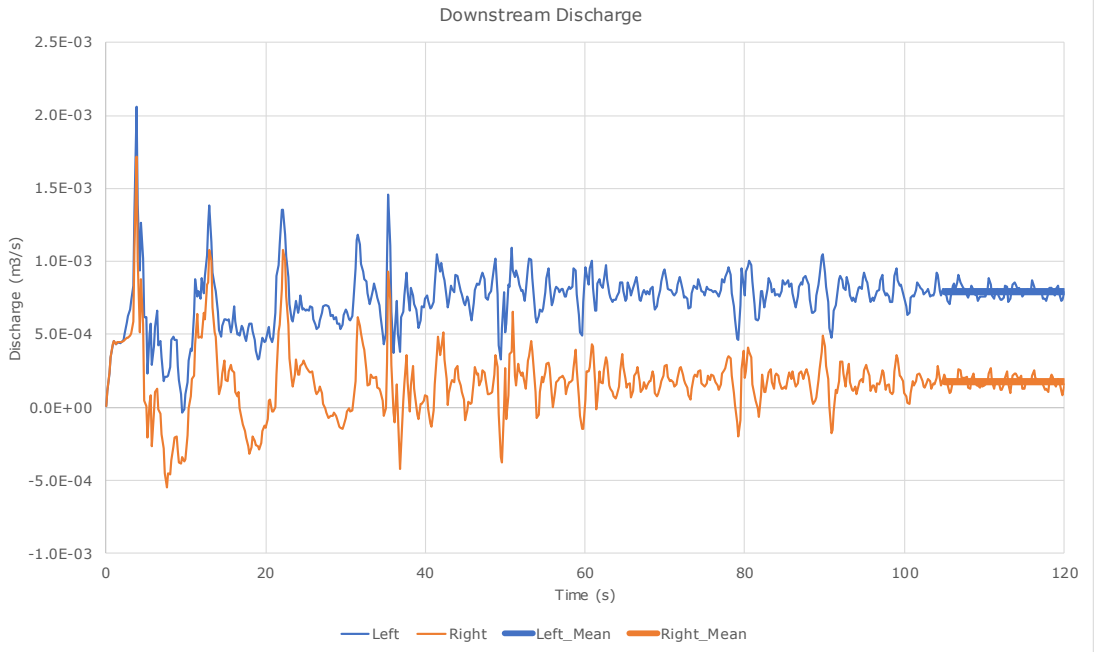


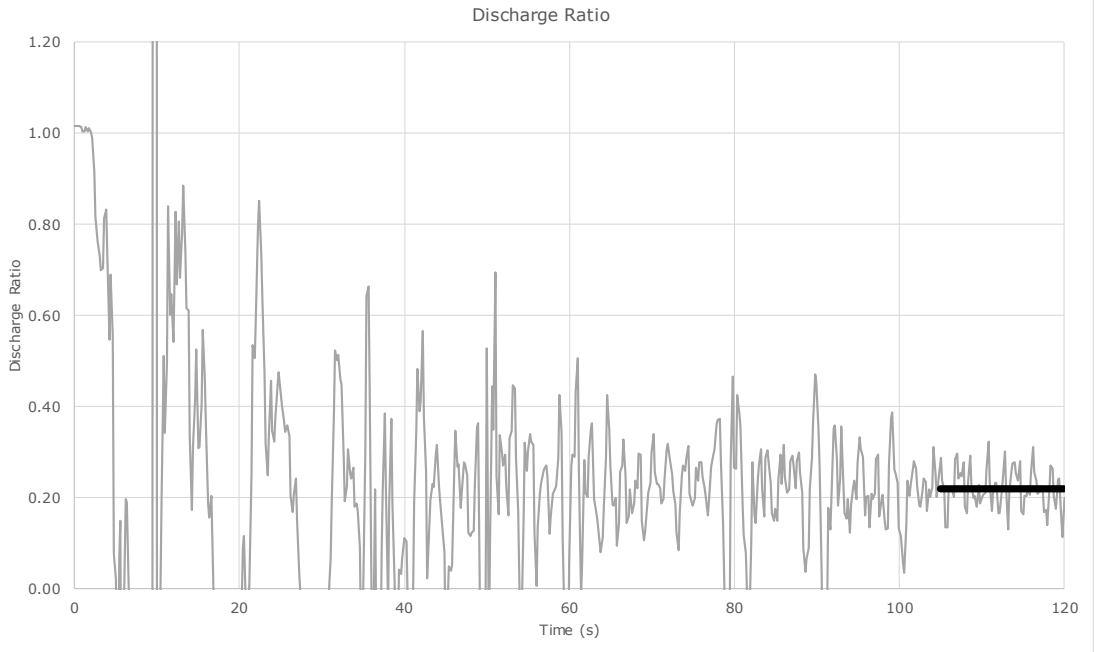


30_05_5060

Name	Symbol	Left	Right	Unit
eir Height	WH	50	60	mm
itial Time	Ti	105	105	s
End Time	Te	120	120	s
ial Number	Ni	525	525	dimensionless
d Number	Ne	600	600	dimensionless
ge Discharge	$\bar{Q}$	7.915E-04	1.752E-04	m3/s

Name	Symbol	Equation	Result	Unit
Height Ratio	WHr	WHL/WHR	0.833	dimensionless
harge Ratio	Qr	$\bar{Q}$_L/$\bar{Q}$_R	0.221	dimensionless
p Discharge Ratio	Qr,t	Average[Q_(r,t=n)···Q_(r,t=n+N)]	0.220	dimensionless

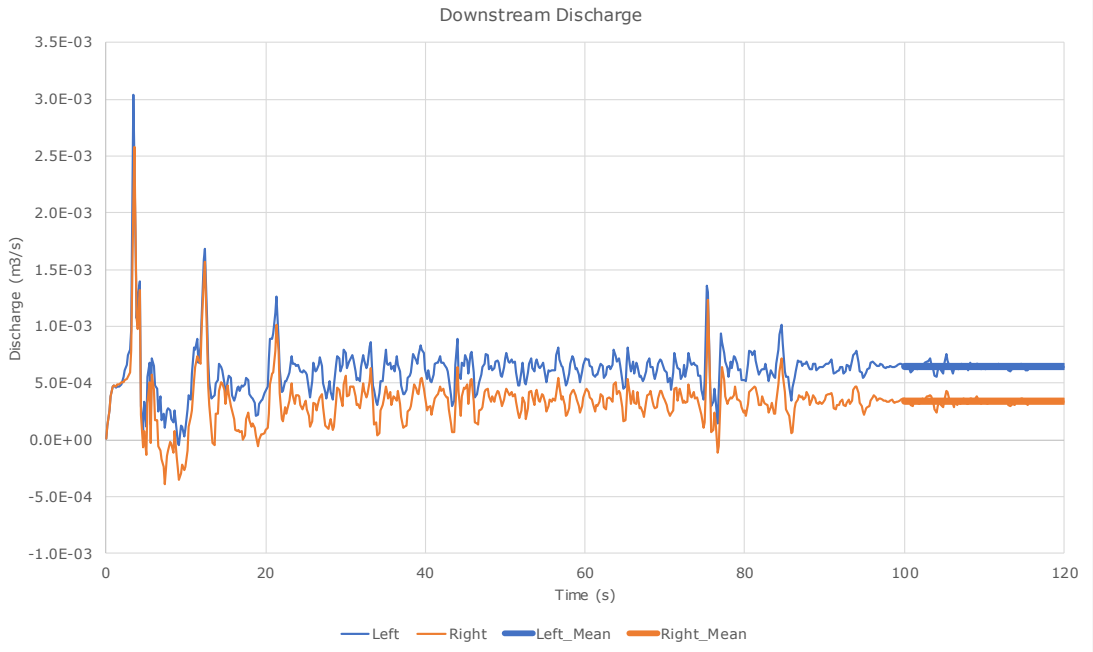


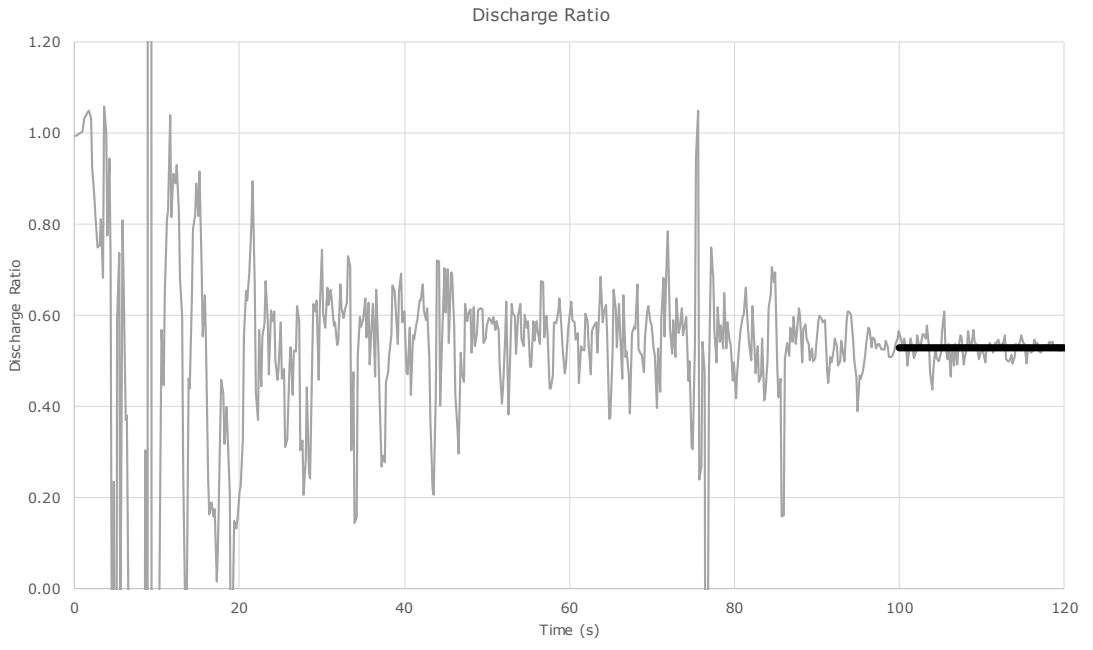


30_05_5560

Name	Symbol	Left	Right	Unit
Weir Height	WH	55	60	mm
Initial Time	Ti	100	100	s
End Time	Te	120	120	s
Initial Number	Ni	500	500	dimensionless
End Number	Ne	600	600	dimensionless
Average Discharge	$\bar{Q}$	6.434E-04	3.400E-04	m3/s

Name	Symbol	Equation	Result	Unit
Weir Height Ratio	WHr	WHL/WHR	0.917	dimensionless
Discharge Ratio	Qr	$\bar{Q}$_L/$\bar{Q}$_R	0.529	dimensionless
Time Step Discharge Ratio	Qr,t	Average[Q_(r,t=n)···Q_(r,t=n+N)]	0.528	dimensionless

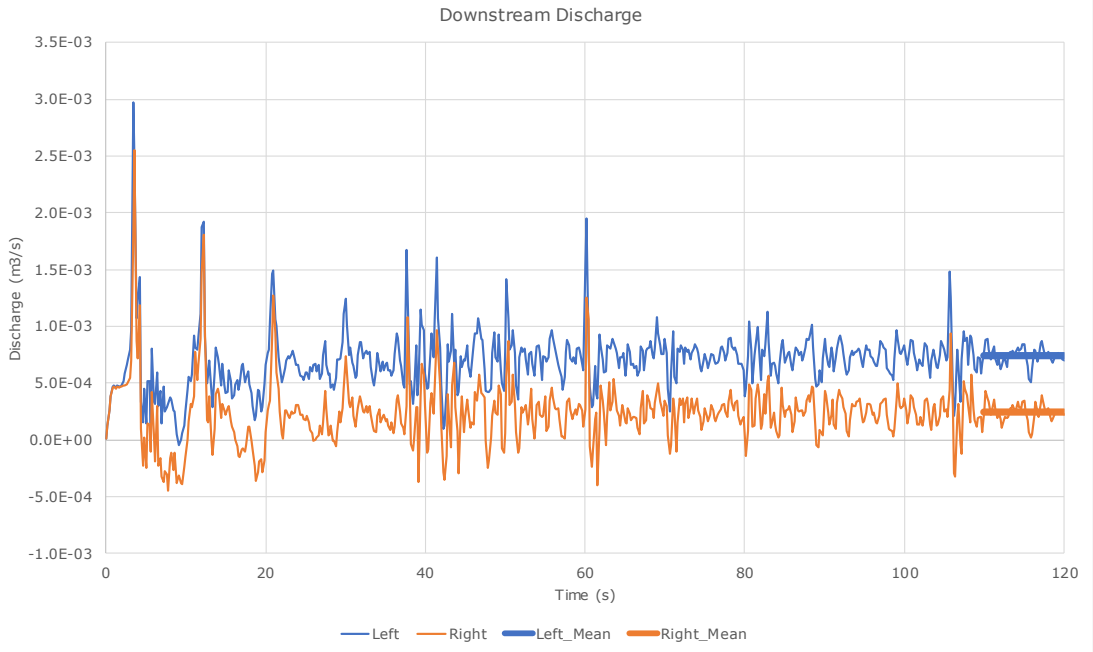


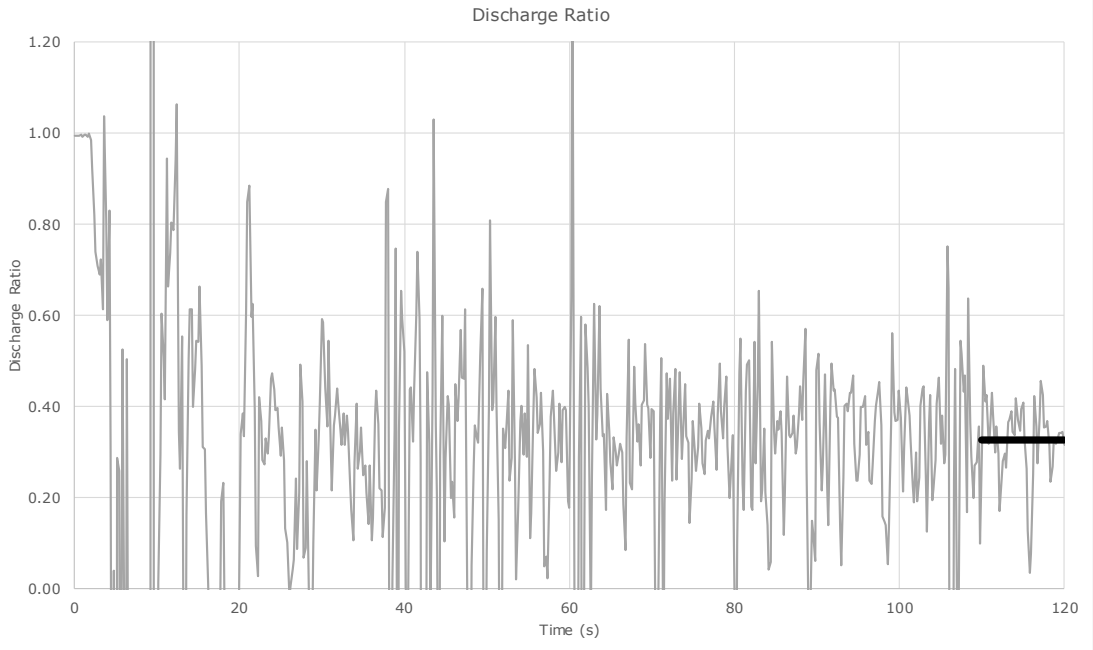


30_05_5562

Name	Symbol	Left	Right	Unit
Weir Height	WH	55	62	mm
Initial Time	Ti	110	110	s
End Time	Te	120	120	s
Initial Number	Ni	550	550	dimensionless
End Number	Ne	600	600	dimensionless
Average Discharge	$\bar{Q}$	7.435E-04	2.486E-04	m3/s

Name	Symbol	Equation	Result	Unit
Weir Height Ratio	WHr	WHL/WHR	0.887	dimensionless
Discharge Ratio	Qr	$\bar{Q}$_L/$\bar{Q}$_R	0.334	dimensionless
Time Step Discharge Ratio	Qr,t	Average[Q_(r,t=n)···Q_(r,t=n+N)]	0.327	dimensionless

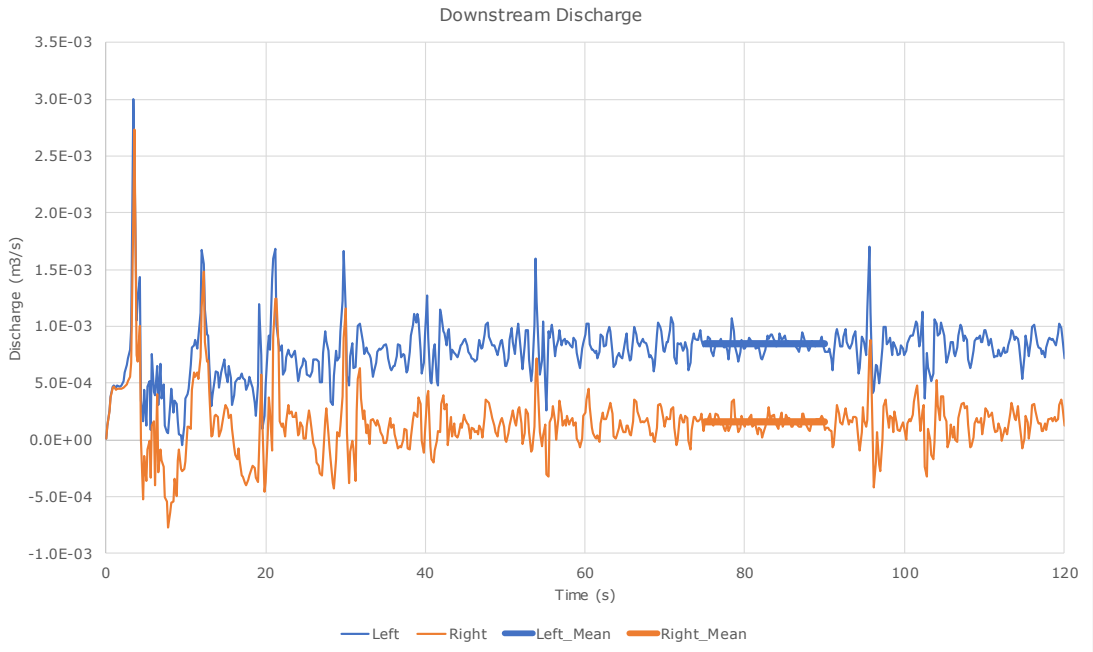


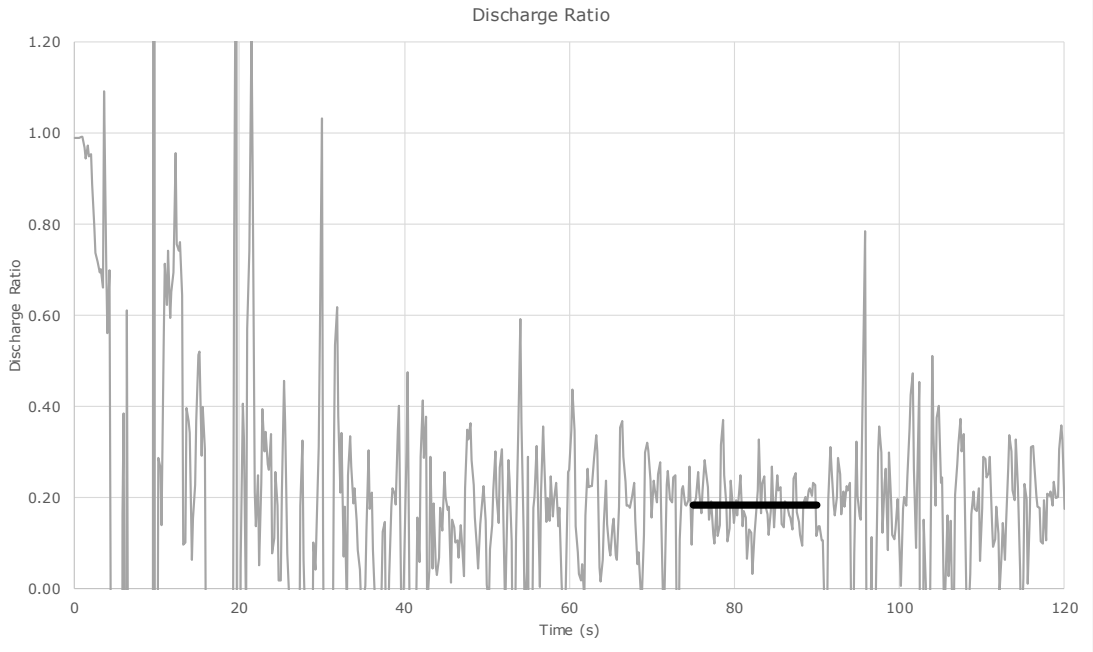


30_05_5565

Name	Symbol	Left	Right	Unit
Weir Height	WH	55	65	mm
Initial Time	Ti	75	75	s
End Time	Te	90	90	s
Initial Number	Ni	375	375	dimensionless
End Number	Ne	450	450	dimensionless
Average Discharge	$\bar{Q}$	8.439E-04	1.574E-04	m3/s

Name	Symbol	Equation	Result	Unit
Weir Height Ratio	WHr	WHL/WHR	0.846	dimensionless
Discharge Ratio	Qr	$\bar{Q}$_L/$\bar{Q}$_R	0.187	dimensionless
Time Step Discharge Ratio	Qr,t	Average[Q_(r,t=n)···Q_(r,t=n+N)]	0.184	dimensionless

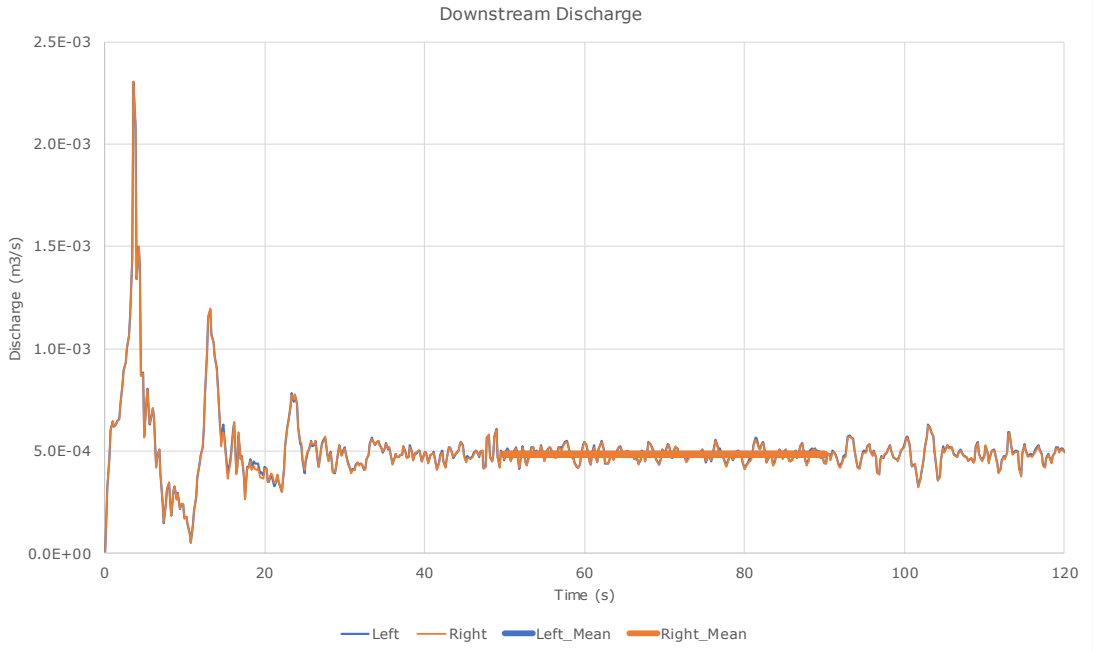


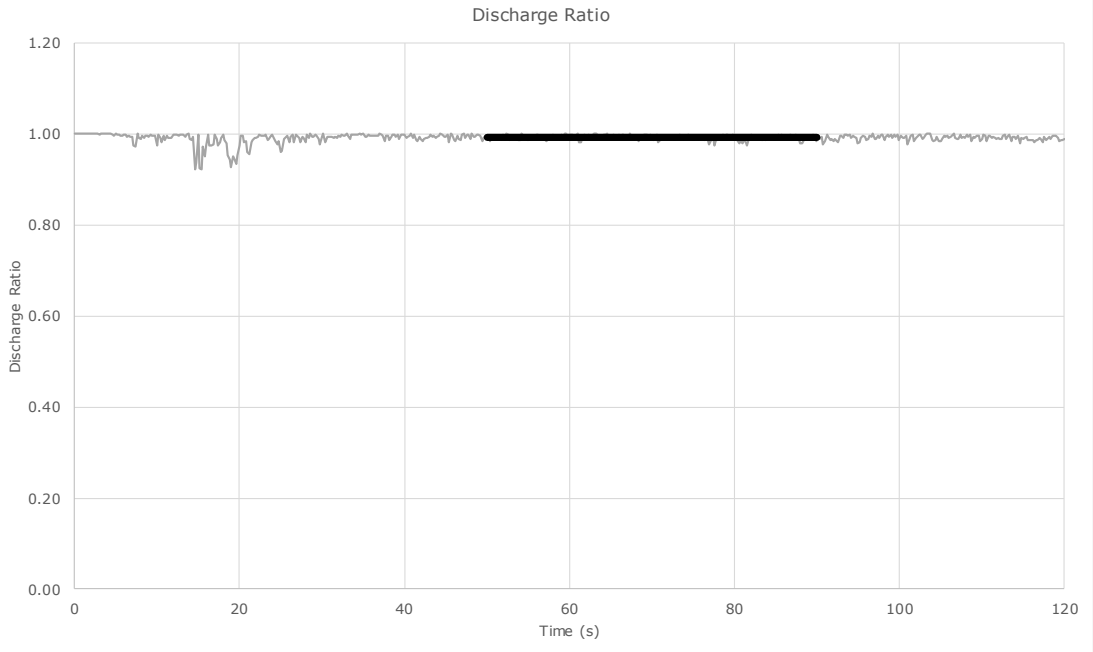


30_07_5050

Name	Symbol	Left	Right	Unit
Weir Height	WH	50	50	mm
Initial Time	Ti	50	50	s
End Time	Te	90	90	s
Initial Number	Ni	250	250	unitless
End Number	Ne	450	450	unitless
Average Discharge	$\bar{Q}$	4.863E-04	4.835E-04	m3/s

Name	Symbol	Equation	Result	Unit
Weir Height Ratio	WHr	WHL/WHR	1.000	dimensionless
Discharge Ratio	Qr	$\bar{Q}$_L/$\bar{Q}$_R	0.994	dimensionless
Time Step Discharge Ratio	Qr,t	Average[Q_(r,t=n)···Q_(r,t=n+N)]	0.992	dimensionless

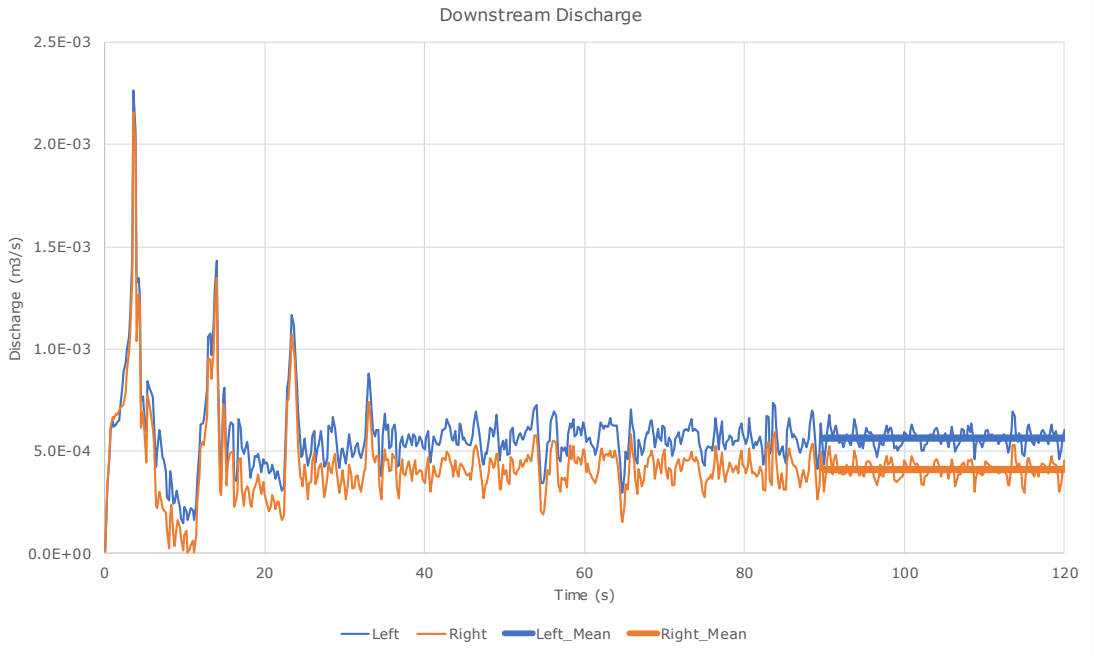


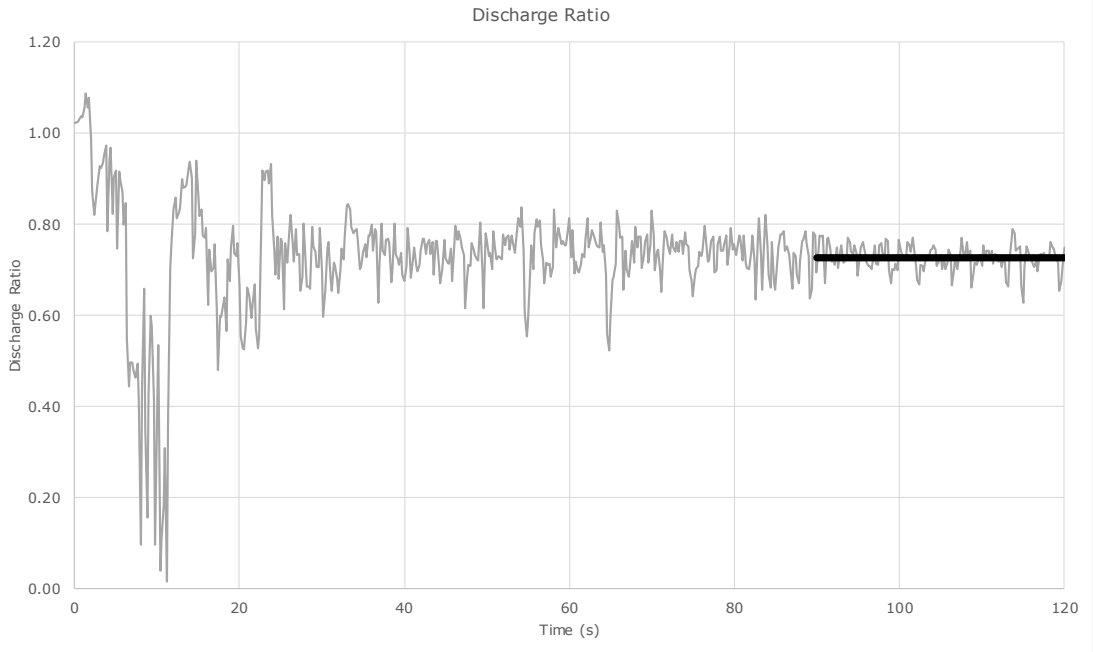


30_07_5053

Name	Symbol	Left	Right	Unit
Weir Height	WH	50	53	mm
Initial Time	Ti	90	90	s
End Time	Te	120	120	s
Initial Number	Ni	450	450	unitless
End Number	Ne	600	600	unitless
Average Discharge	$\bar{Q}$	5.653E-04	4.115E-04	m3/s

Name	Symbol	Equation	Result	Unit
Weir Height Ratio	WHr	WHL/WHR	0.943	dimensionless
Discharge Ratio	Qr	$\bar{Q}$_L/$\bar{Q}$_R	0.728	dimensionless
Time Step Discharge Ratio	Qr,t	Average[Q_(r,t=n)···Q_(r,t=n+N)]	0.726	dimensionless

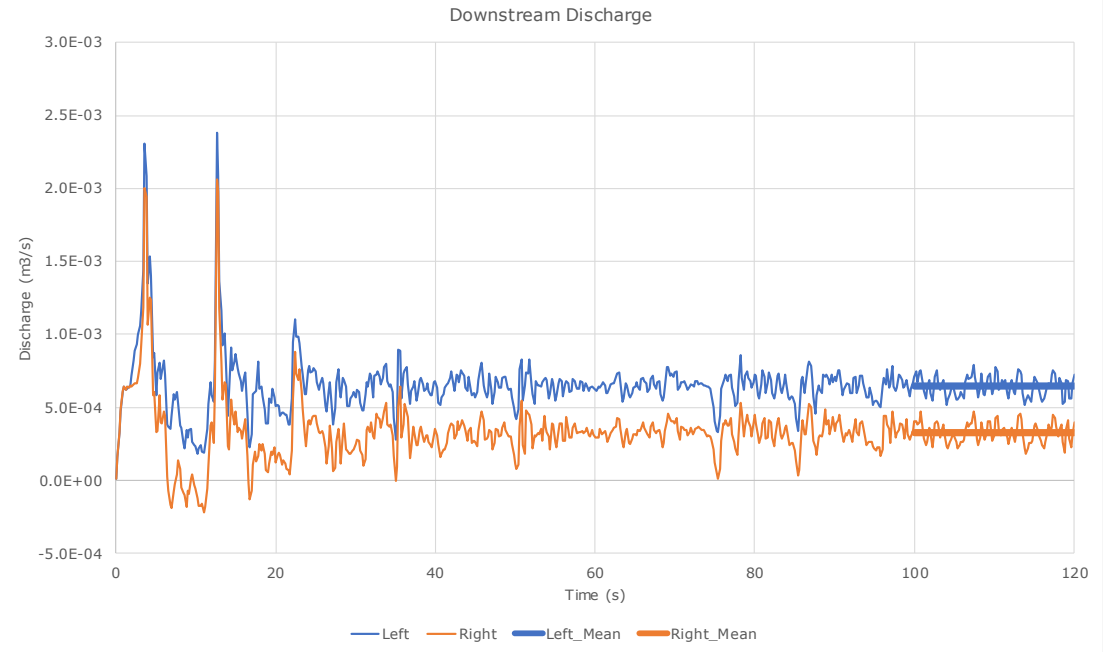


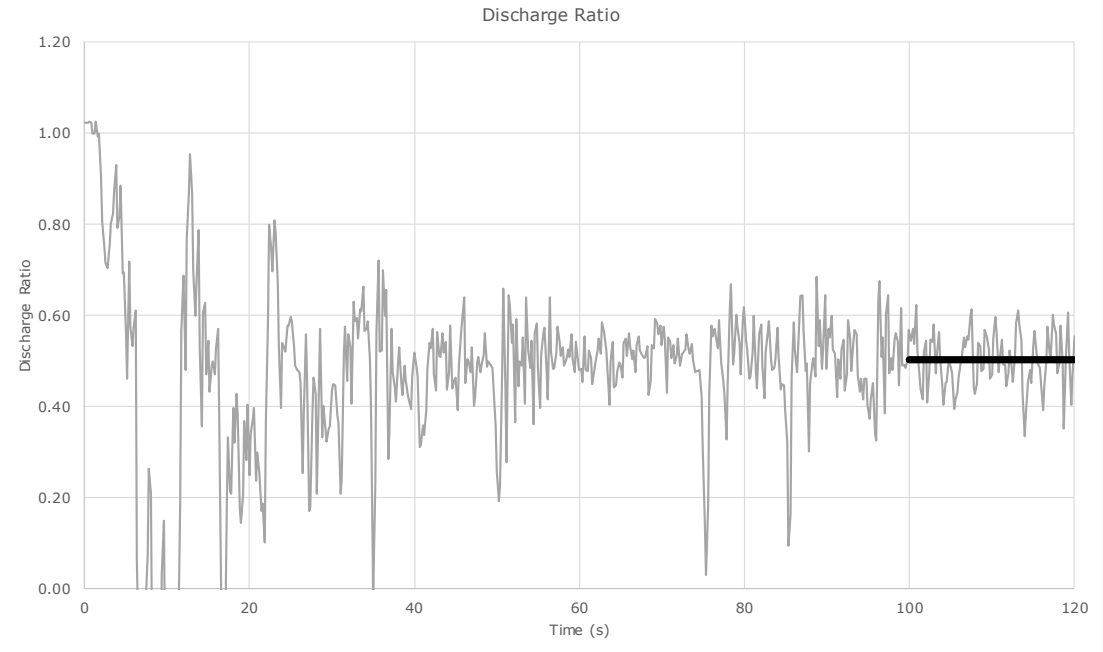


30_07_5055

Name	Symbol	Left	Right	Unit
Weir Height	WH	50	55	mm
Initial Time	Ti	100	100	s
End Time	Te	120	120	s
Initial Number	Ni	500	500	unitless
End Number	Ne	600	600	unitless
Average Discharge	$\bar{Q}$	6.461E-04	3.277E-04	m3/s

Name	Symbol	Equation	Result	Unit
Weir Height Ratio	WHr	WHL/WHR	0.909	dimensionless
Discharge Ratio	Qr	$\bar{Q}$_L/$\bar{Q}$_R	0.507	dimensionless
Time Step Discharge Ratio	Qr,t	Average[Q_(r,t=n)···Q_(r,t=n+N)]	0.502	dimensionless

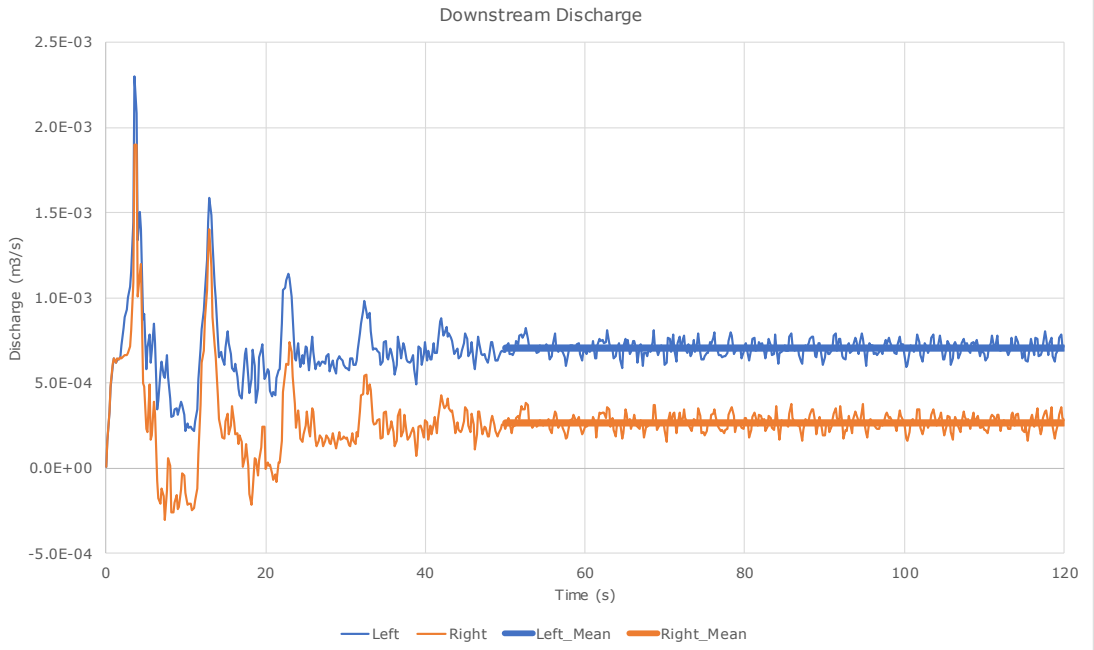


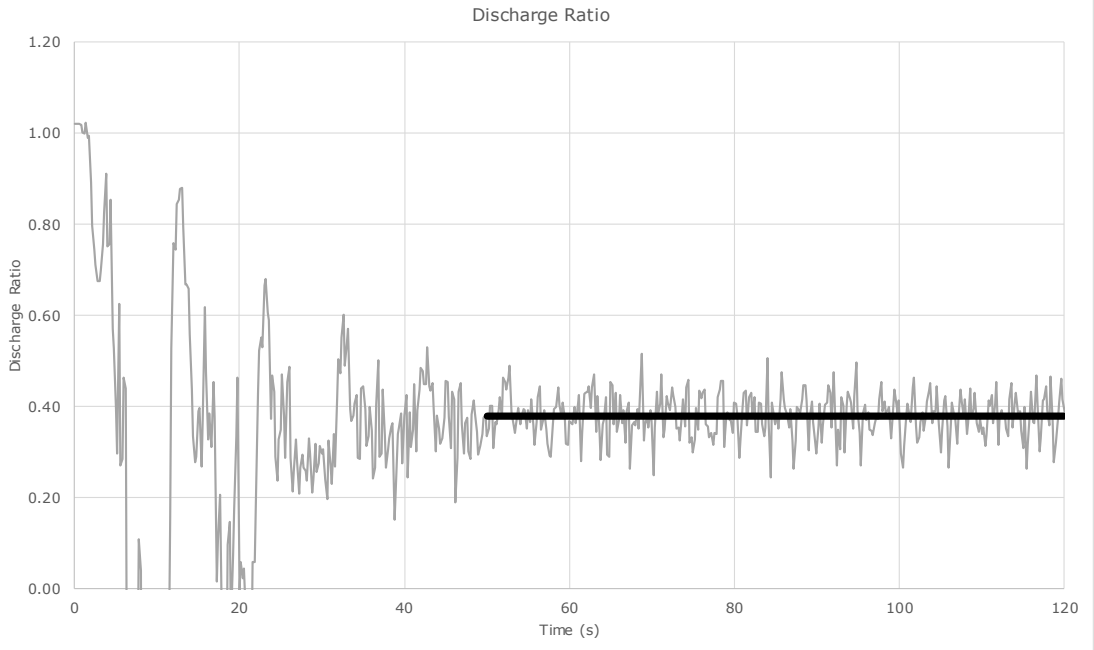


30_07_5057

ne	Symbol	Left	Right	Unit
eight	WH	50	57	mm
Time	Ti	50	50	s
ime	Te	120	120	s
mber	Ni	250	250	unitless
mber	Ne	600	600	unitless
ischarge	$\bar{Q}$	7.059E-04	2.695E-04	m3/s

ne	Symbol	Equation	Result	Unit
ht Ratio	WHr	WHL/WHR	0.877	dimensionless
e Ratio	Qr	$\bar{Q}$_L/$\bar{Q}$_R	0.382	dimensionless
charge Ratio	Qr,t	Average[Q_(r,t=n)···Q_(r,t=n+N)]	0.380	dimensionless

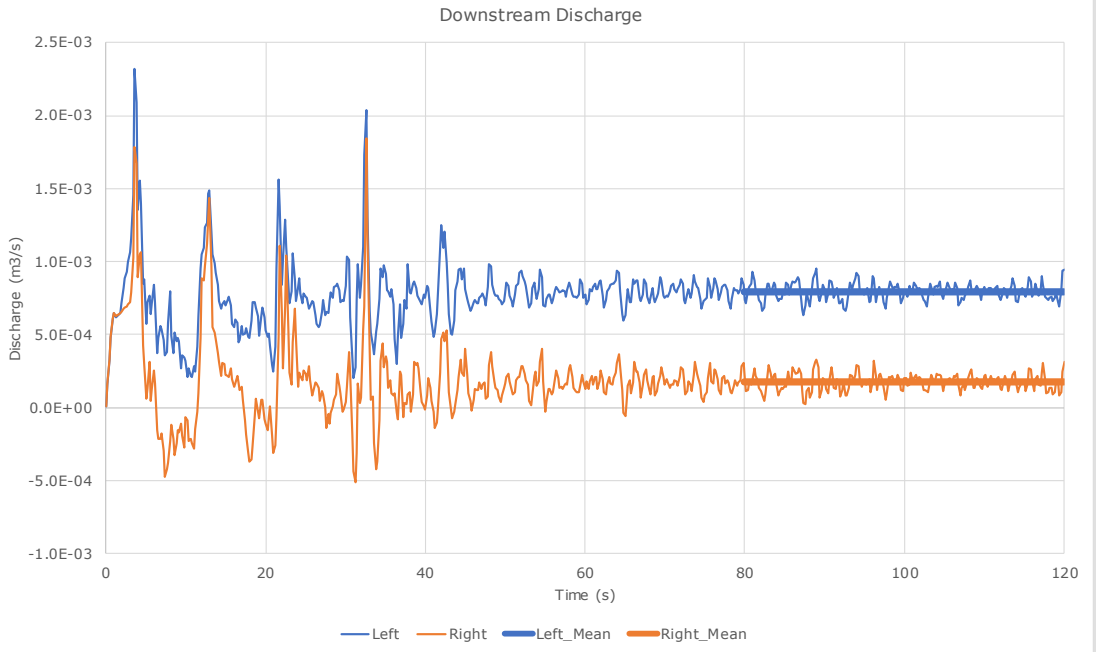


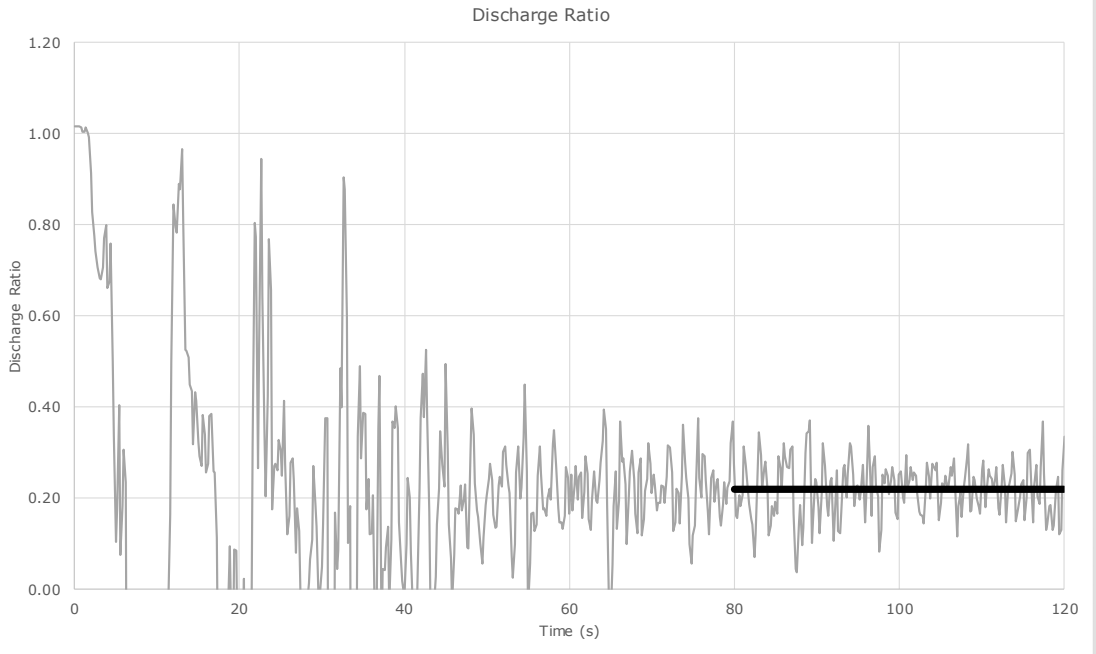


30_07_5060

Name	Symbol	Left	Right	Unit
Weir Height	WH	50	60	mm
Initial Time	Ti	80	80	s
End Time	Te	120	120	s
Initial Number	Ni	400	400	dimensionless
End Number	Ne	600	600	dimensionless
Average Discharge	$\bar{Q}$	7.960E-04	1.768E-04	m3/s

Name	Symbol	Equation	Result	Unit
Weir Height Ratio	WHr	WHL/WHR	0.833	dimensionless
Discharge Ratio	Qr	$\bar{Q}$_L/$\bar{Q}$_R	0.222	dimensionless
ne Step Discharge Ratio	Qr,t	Average[Q_(r,t=n)···Q_(r,t=n+N)]	0.219	dimensionless

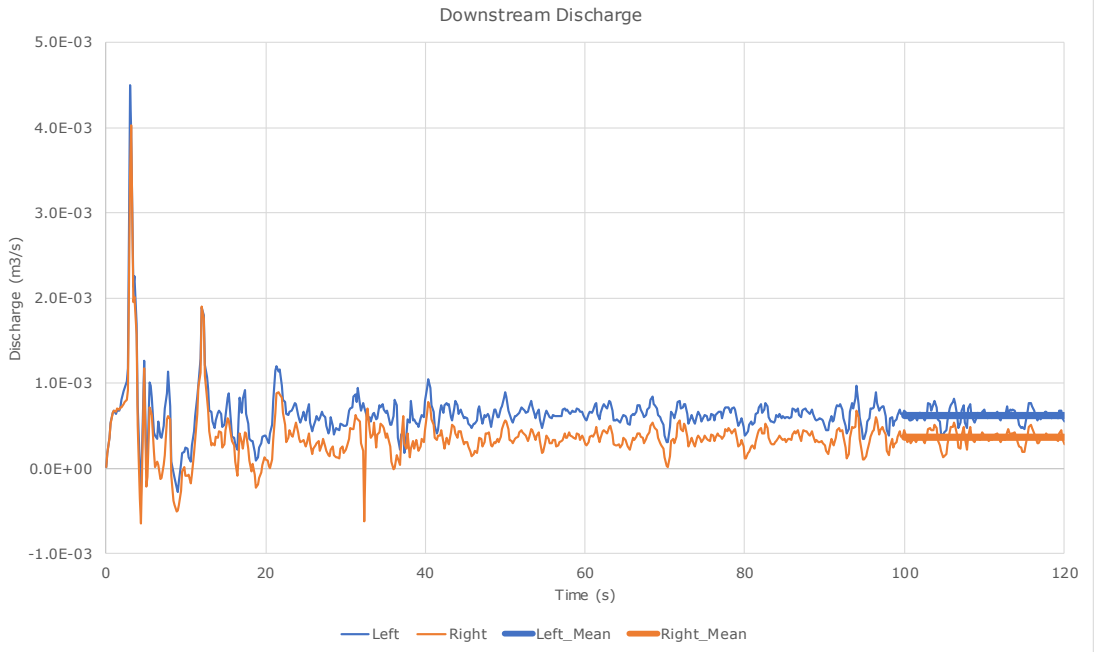


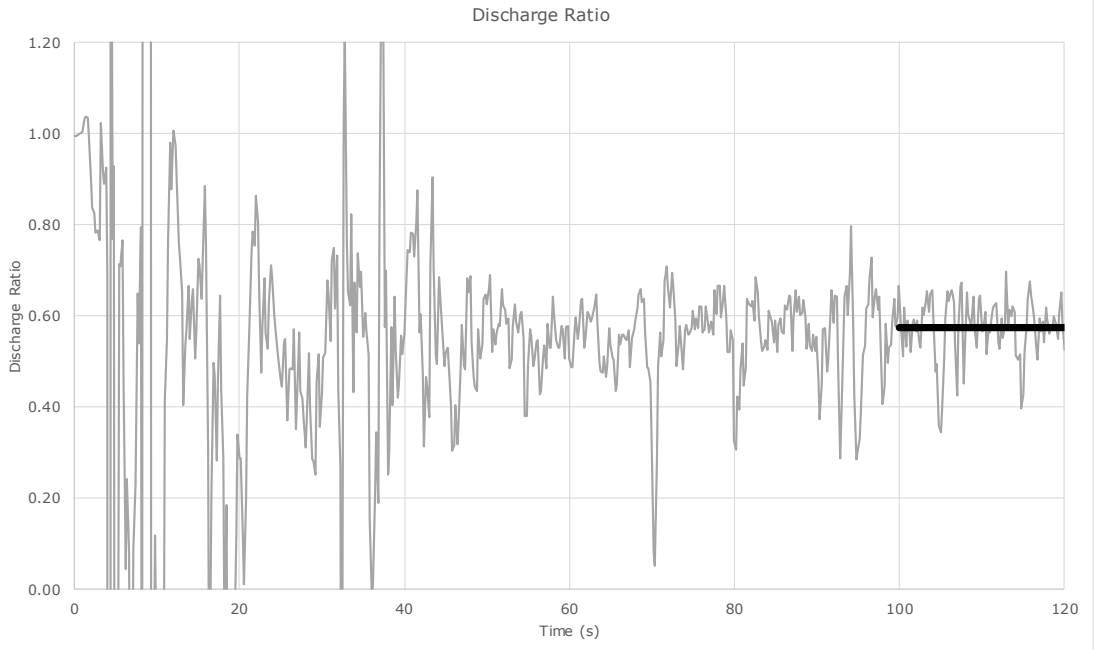


30_07_5560

ne	Symbol	Left	Right	Unit
leight	WH	55	60	mm
Time	Ti	100	100	s
ime	Te	120	120	s
lumber	Ni	500	500	dimensionless
umber	Ne	600	600	dimensionless
Discharge	Q¯	6.254E-04	3.634E-04	m3/s

ne	Symbol	Equation	Result	Unit
ht Ratio	WHr	WHL/WHR	0.917	dimensionless
e Ratio	Qr	Q¯_L/Q¯_R	0.581	dimensionless
charge Ratio	Qr,t	Average[Q_(r,t=n)···Q_(r,t=n+N)]	0.574	dimensionless

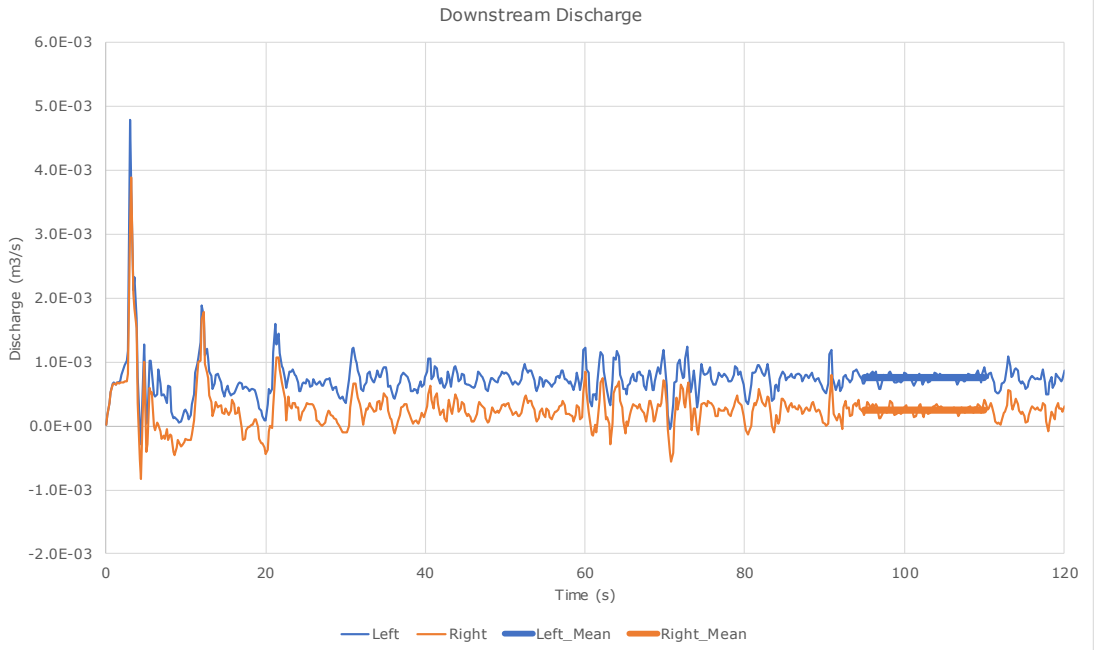


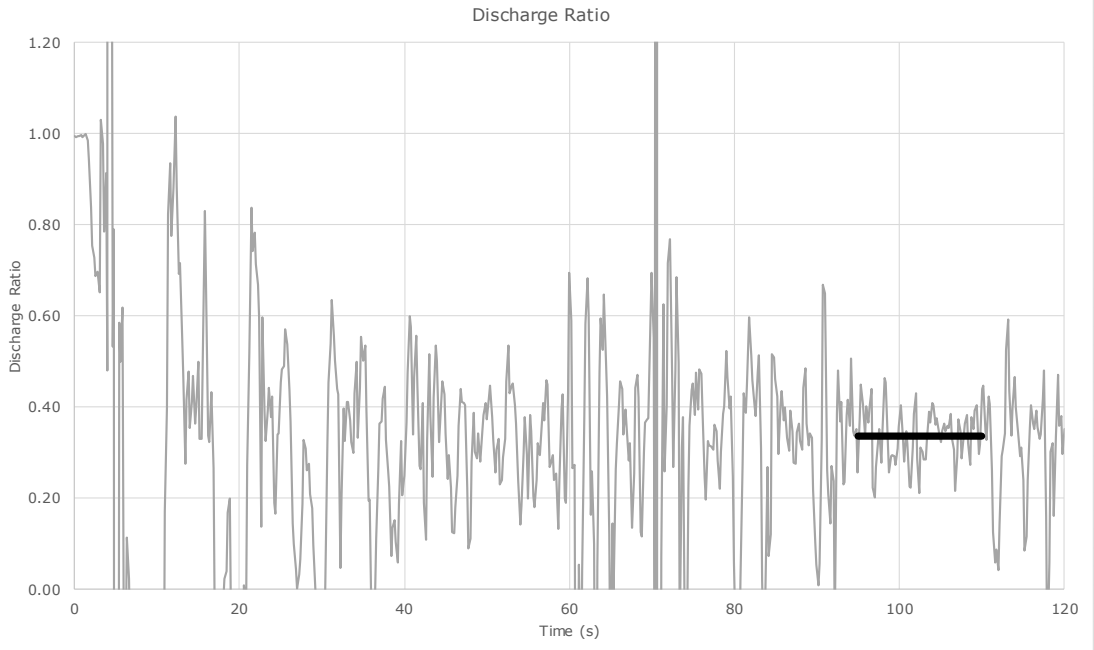


30_07_5562

Name	Symbol	Left	Right	Unit
/eir Height	WH	55	62	mm
nitial Time	Ti	95	95	s
End Time	Te	110	110	s
tial Number	Ni	475	475	dimensionless
nd Number	Ne	550	550	dimensionless
age Discharge	$\bar{Q}$	7.523E-04	2.553E-04	m3/s

Name	Symbol	Equation	Result	Unit
· Height Ratio	WHr	WHL/WHR	0.887	dimensionless
:harge Ratio	Qr	$\bar{Q}$_L/$\bar{Q}$_R	0.339	dimensionless
p Discharge Ratio	Qr,t	Average[Q_(r,t=n)···Q_(r,t=n+N)]	0.336	dimensionless

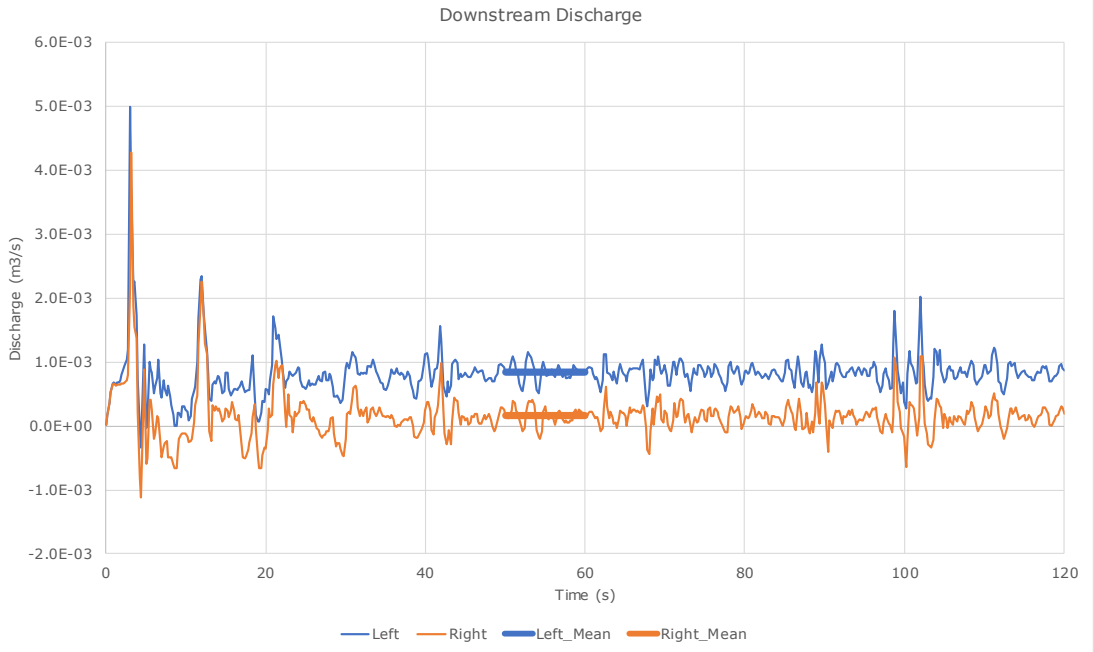


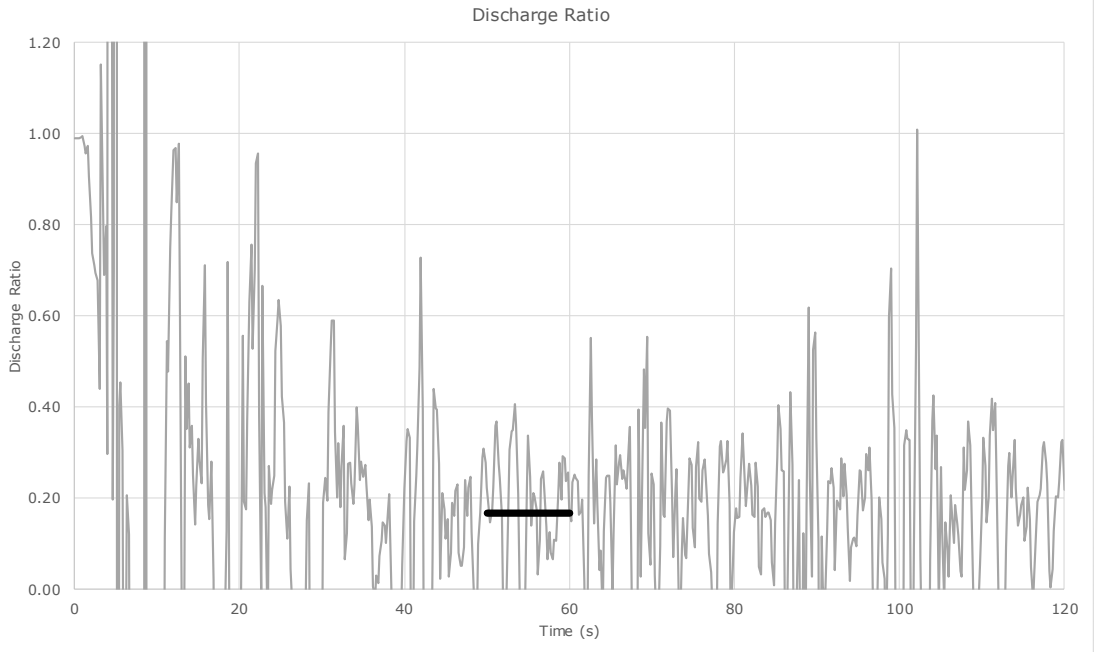


30_07_5565

Name	Symbol	Left	Right	Unit
Weir Height	WH	55	65	mm
Initial Time	Ti	50	50	s
End Time	Te	60	60	s
Initial Number	Ni	250	250	dimensionless
End Number	Ne	300	300	dimensionless
verage Discharge	$\bar{Q}$	8.457E-04	1.565E-04	m3/s

Name	Symbol	Equation	Result	Unit
Weir Height Ratio	WHr	WHL/WHR	0.846	dimensionless
Discharge Ratio	Qr	$\bar{Q}$_L/$\bar{Q}$_R	0.185	dimensionless
Step Discharge Ratio	Qr,t	Average[Q_(r,t=n)···Q_(r,t=n+N)]	0.166	dimensionless

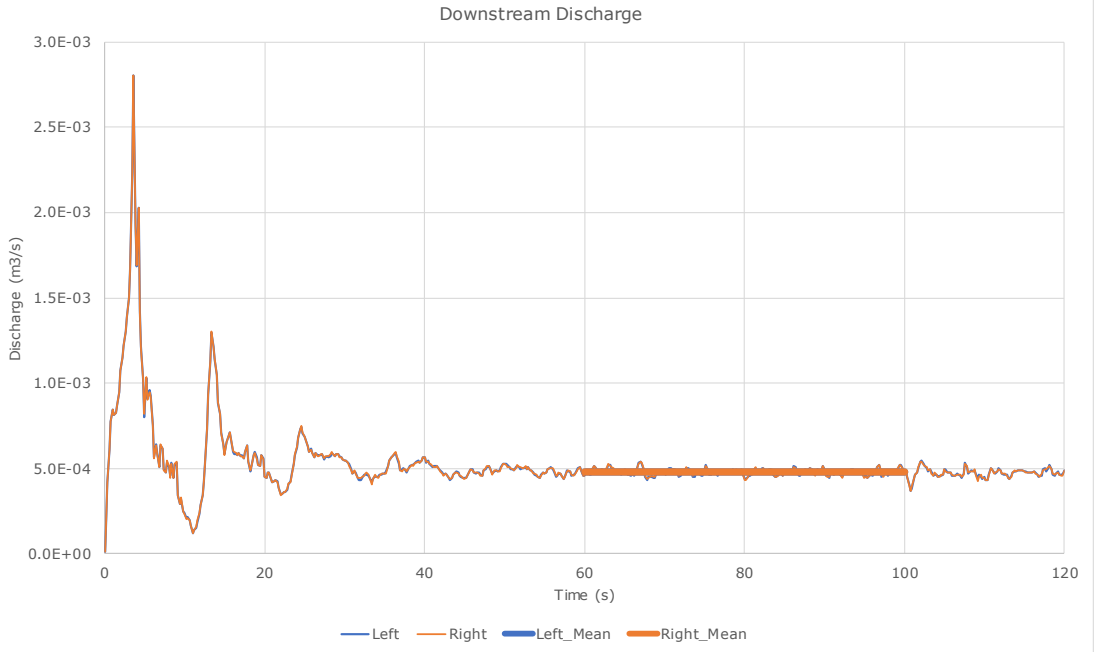


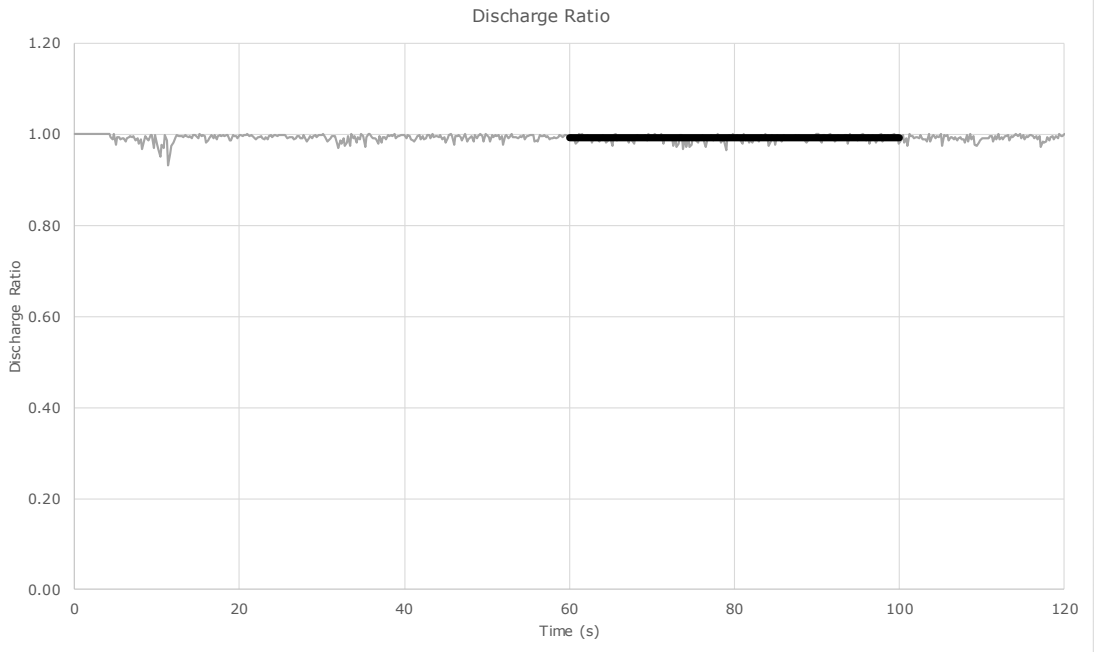


30_09_5050

Name	Symbol	Left	Right	Unit
Weir Height	WH	50	50	mm
Initial Time	Ti	60	60	s
End Time	Te	100	100	s
Initial Number	Ni	300	300	unitless
End Number	Ne	500	500	unitless
Average Discharge	$\bar{Q}$	4.793E-04	4.803E-04	m3/s

Name	Symbol	Equation	Result	Unit
Weir Height Ratio	WHr	WHL/WHR	1.000	dimensionless
Discharge Ratio	Qr	$\bar{Q}$_L/$\bar{Q}$_R	0.998	dimensionless
Time Step Discharge Ratio	Qr,t	Average[Q_(r,t=n)···Q_(r,t=n+N)]	0.991	dimensionless

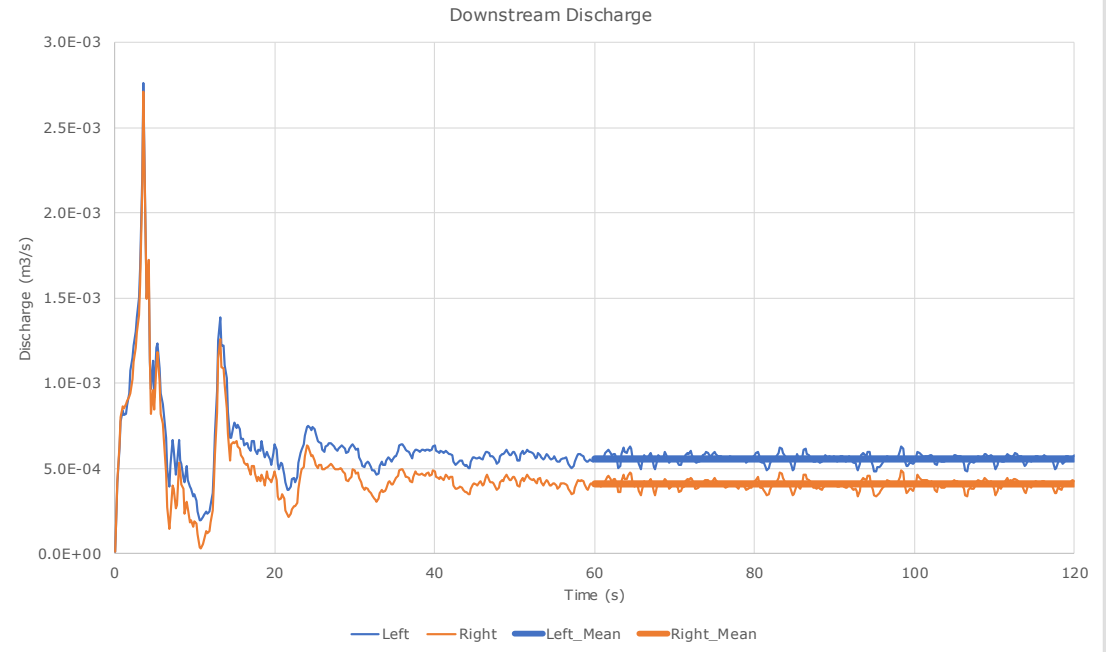


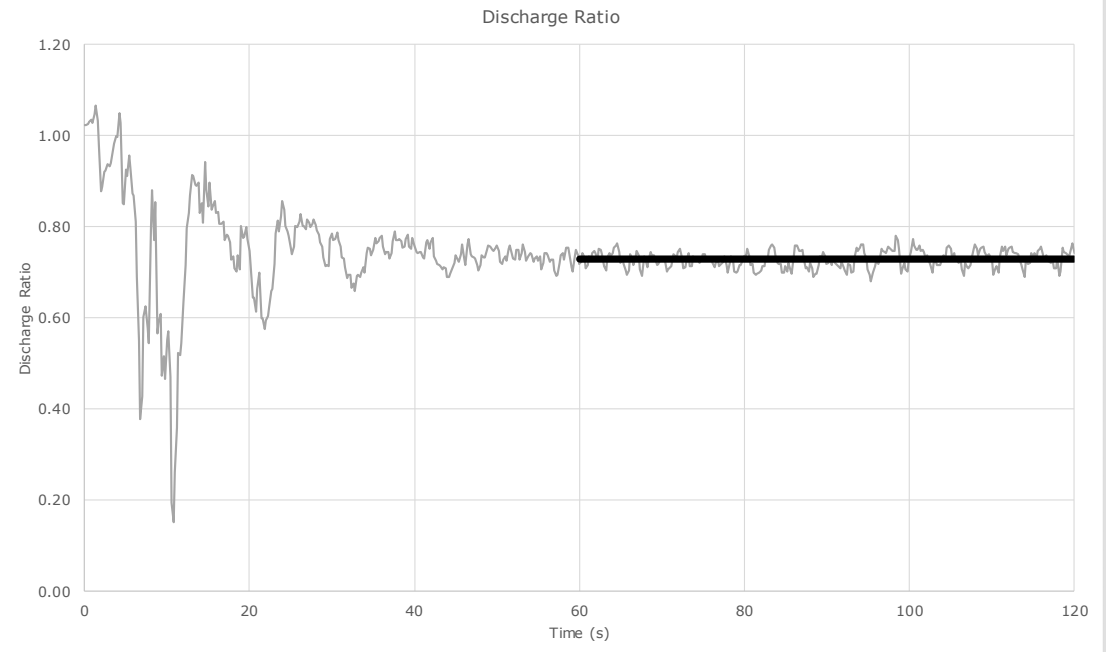


30_09_5053

	Symbol	Left	Right	Unit
ıt	WH	50	53	mm
ıe	Ti	60	60	s
ı	Te	120	120	s
ɔer	Ni	300	300	unitless
er	Ne	600	600	unitless
ıarge	Q¯	5.590E-04	4.073E-04	m3/s

	Symbol	Equation	Result	Unit
Ratio	WHr	WHL/WHR	0.943	dimensionless
atio	Qr	Q¯L/Q¯R	0.729	dimensionless
rge Ratio	Qr,t	Average[Q_(r,t=n)···Q_(r,t=n+N)]	0.728	dimensionless

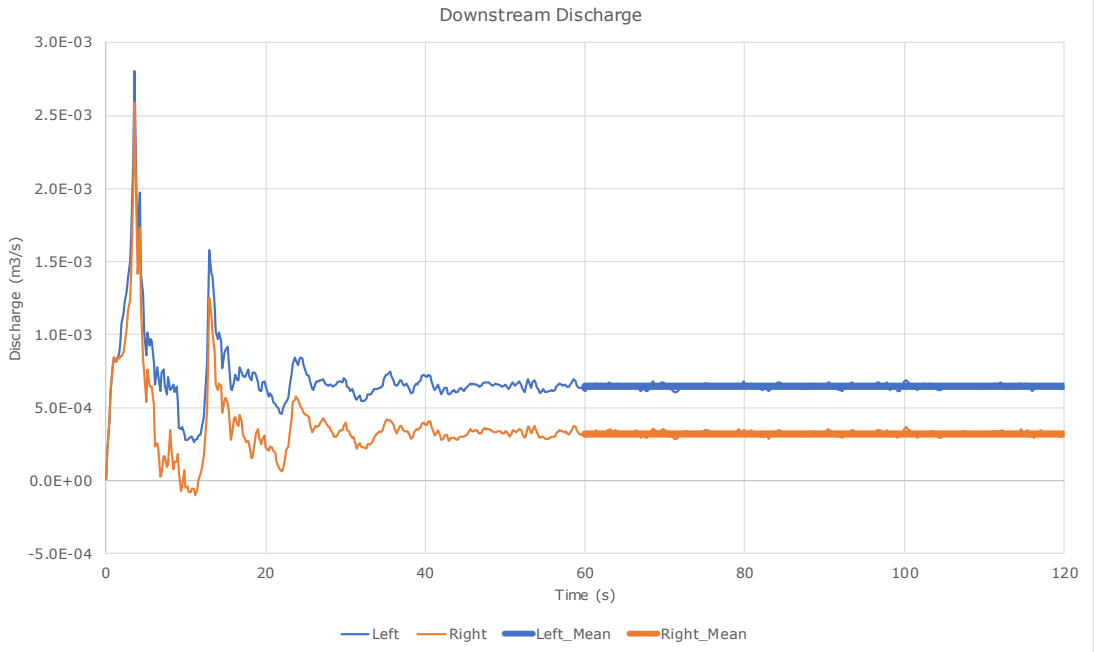


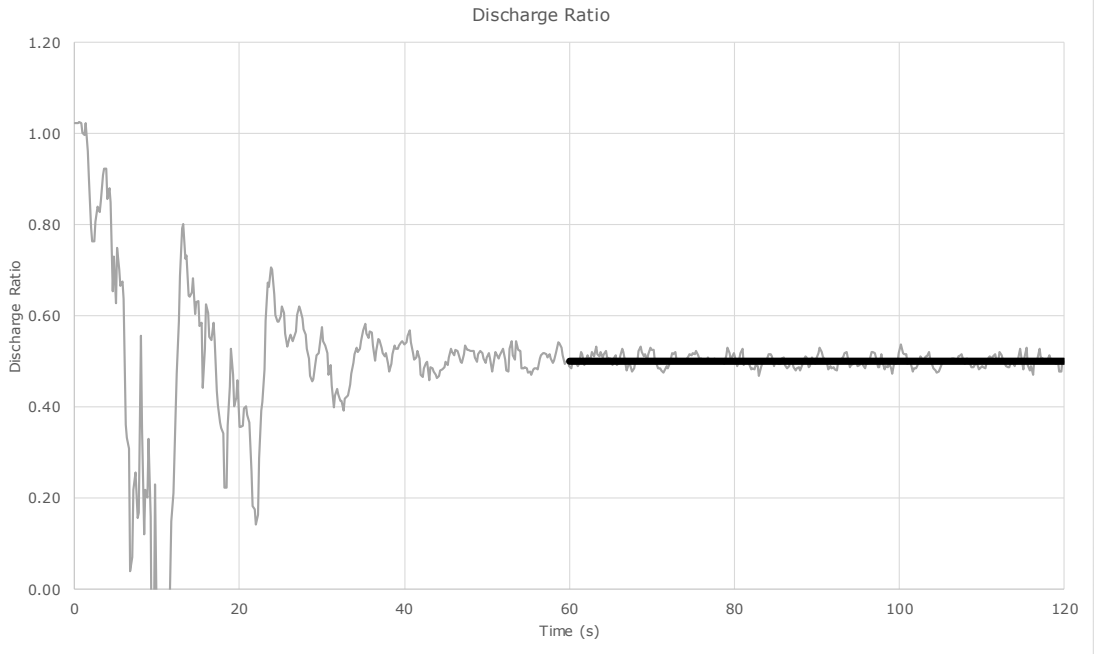


30_09_5055

Name	Symbol	Left	Right	Unit
Weir Height	WH	50	55	mm
Initial Time	Ti	60	60	s
End Time	Te	120	120	s
Initial Number	Ni	300	300	unitless
End Number	Ne	600	600	unitless
Average Discharge	$\bar{Q}$	6.458E-04	3.236E-04	m3/s

Name	Symbol	Equation	Result	Unit
Weir Height Ratio	WHr	WHL/WHR	0.909	dimensionless
Discharge Ratio	Qr	$\bar{Q}$_L/$\bar{Q}$_R	0.501	dimensionless
Time Step Discharge Ratio	Qr,t	Average[Q_(r,t=n)···Q_(r,t=n+N)]	0.501	dimensionless

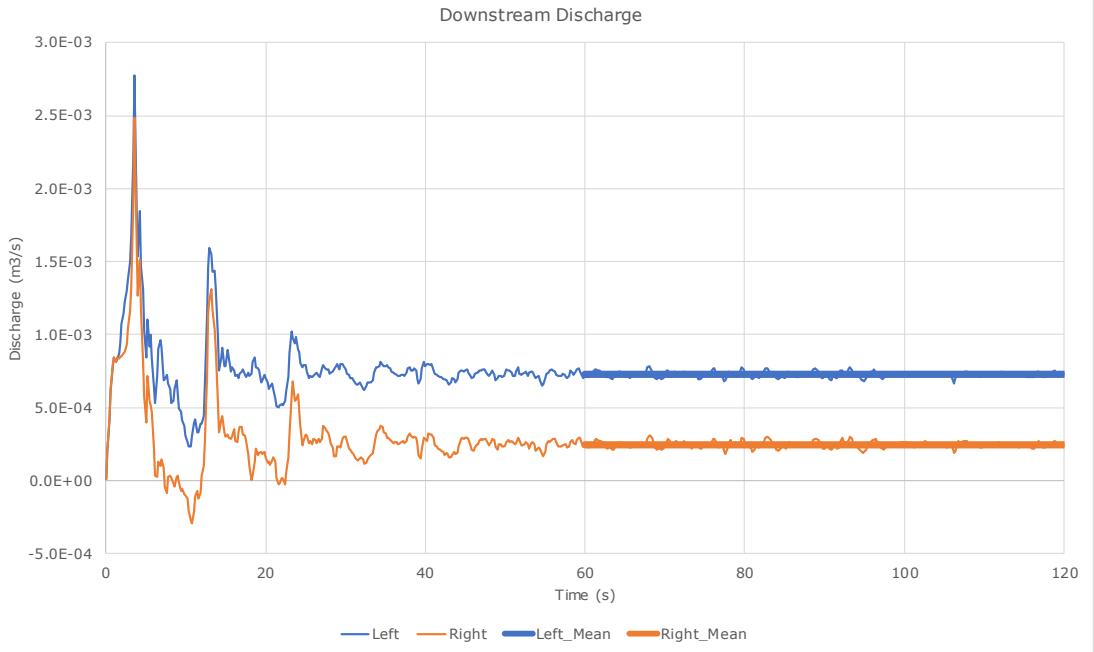


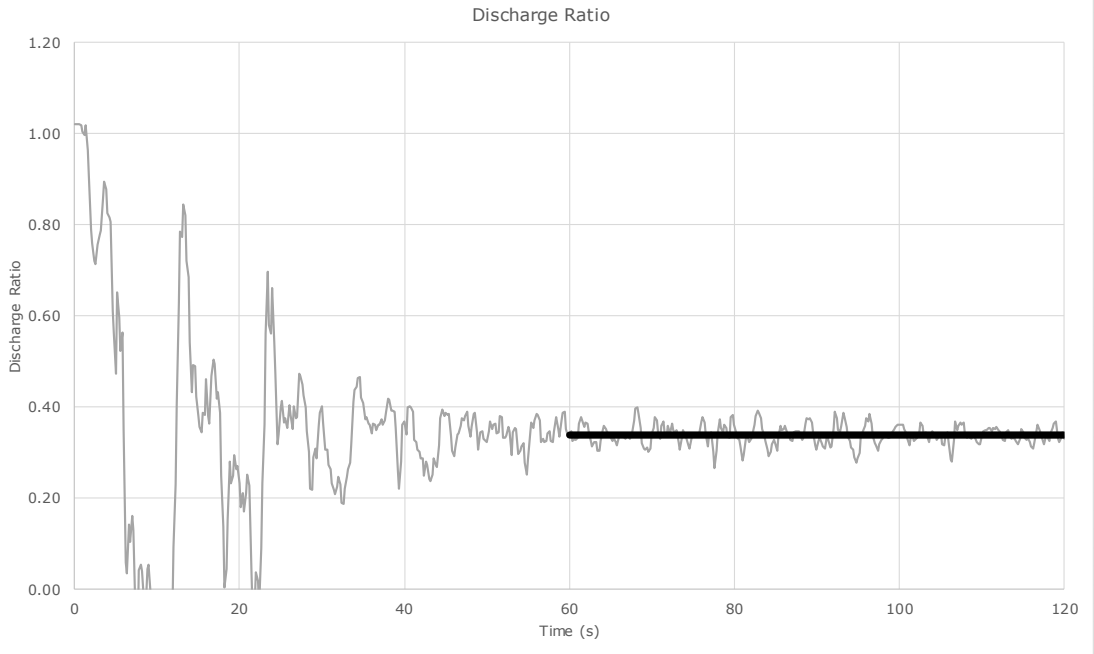


30_09_5057

Name	Symbol	Left	Right	Unit
Weir Height	WH	50	57	mm
Initial Time	Ti	60	60	s
End Time	Te	120	120	s
Initial Number	Ni	300	300	unitless
End Number	Ne	600	600	unitless
Average Discharge	$\bar{Q}$	7.267E-04	2.464E-04	m3/s

Name	Symbol	Equation	Result	Unit
Weir Height Ratio	WHr	WHL/WHR	0.877	dimensionless
Discharge Ratio	Qr	$\bar{Q}$_L/$\bar{Q}$_R	0.339	dimensionless
Time Step Discharge Ratio	Qr,t	Average[Q_(r,t=n)···Q_(r,t=n+N)]	0.339	dimensionless

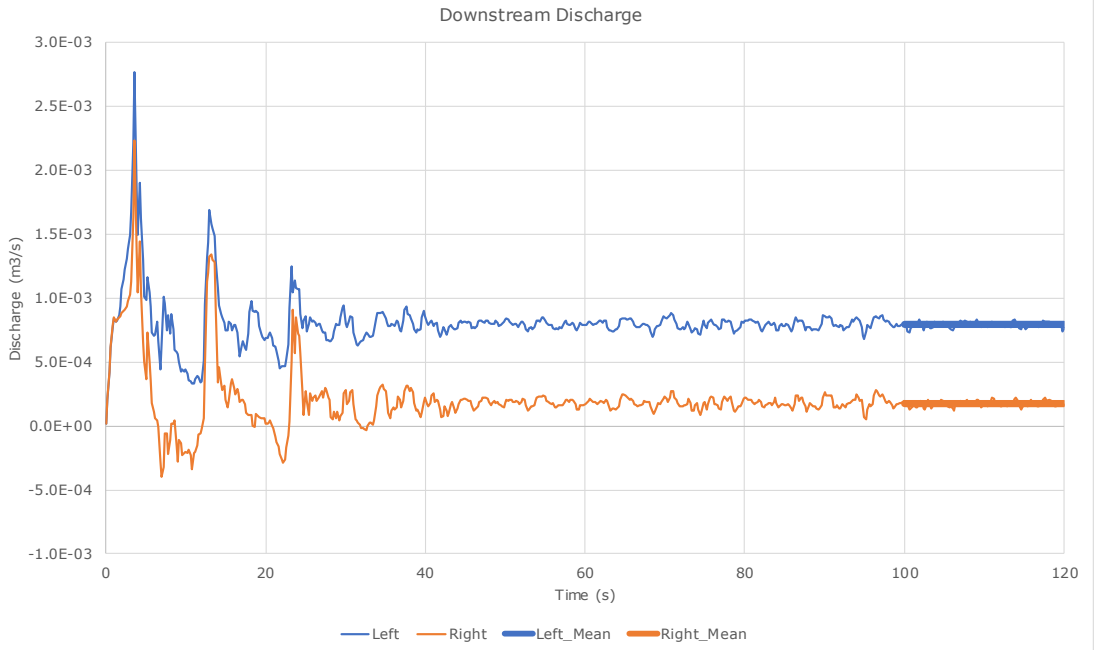


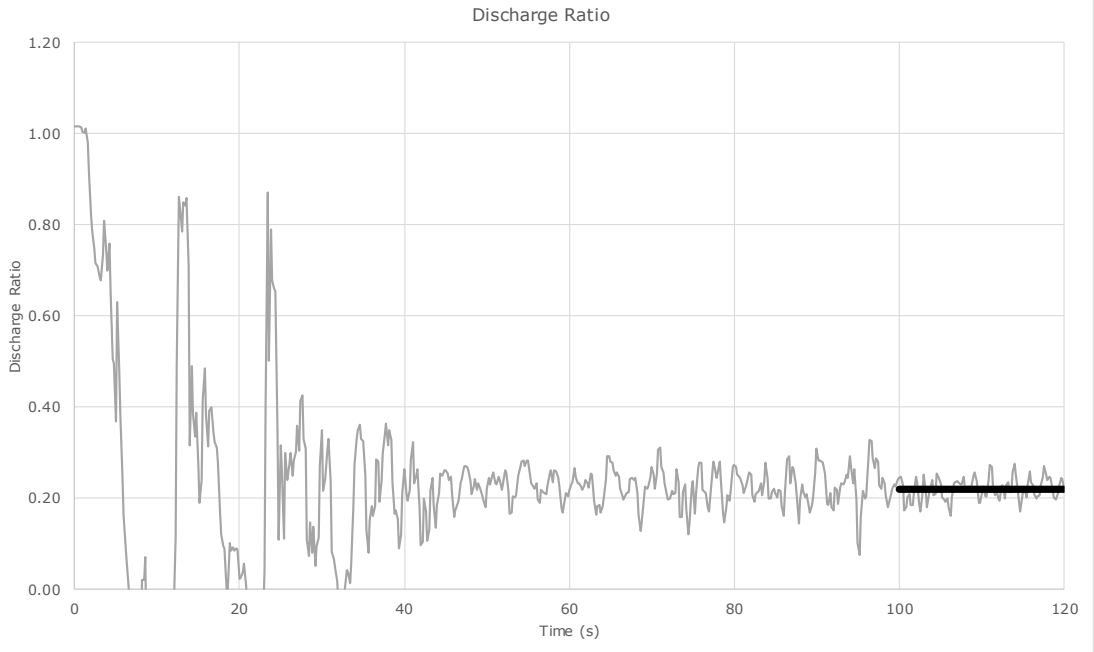


30_09_5060

Name	Symbol	Left	Right	Unit
Weir Height	WH	50	60	mm
Initial Time	Ti	100	100	s
End Time	Te	120	120	s
Initial Number	Ni	500	500	dimensionless
End Number	Ne	600	600	dimensionless
Average Discharge	$\bar{Q}$	7.914E-04	1.743E-04	m3/s

Name	Symbol	Equation	Result	Unit
Weir Height Ratio	WHr	WHL/WHR	0.833	dimensionless
Discharge Ratio	Qr	$\bar{Q}$_L/$\bar{Q}$_R	0.220	dimensionless
Step Discharge Ratio	Qr,t	Average[Q_(r,t=n)···Q_(r,t=n+N)]	0.220	dimensionless

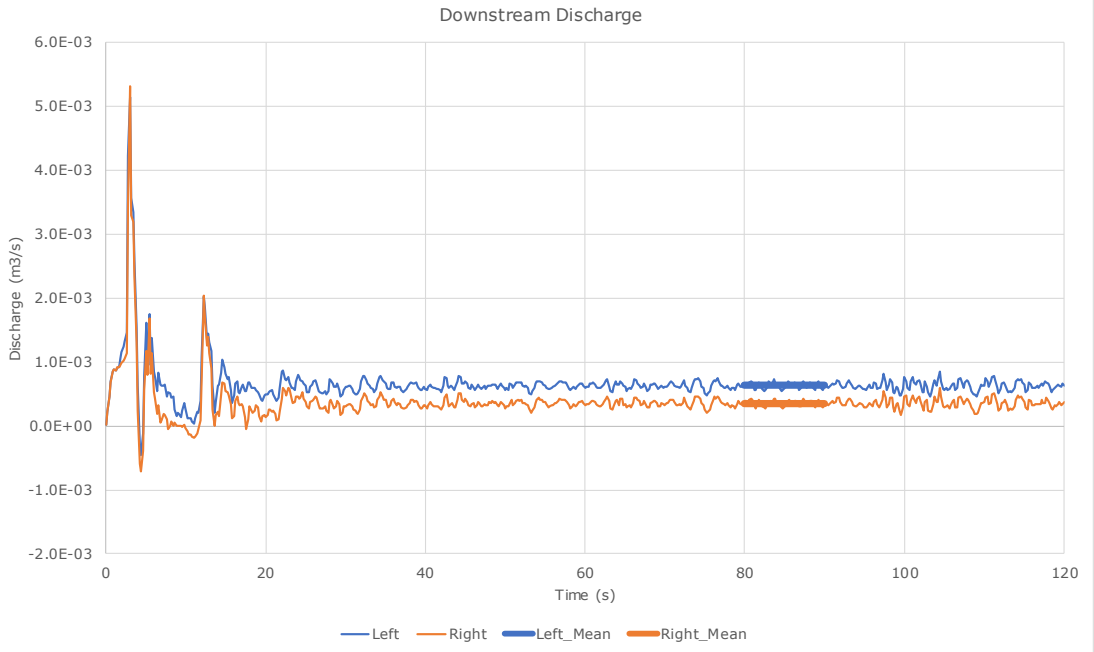


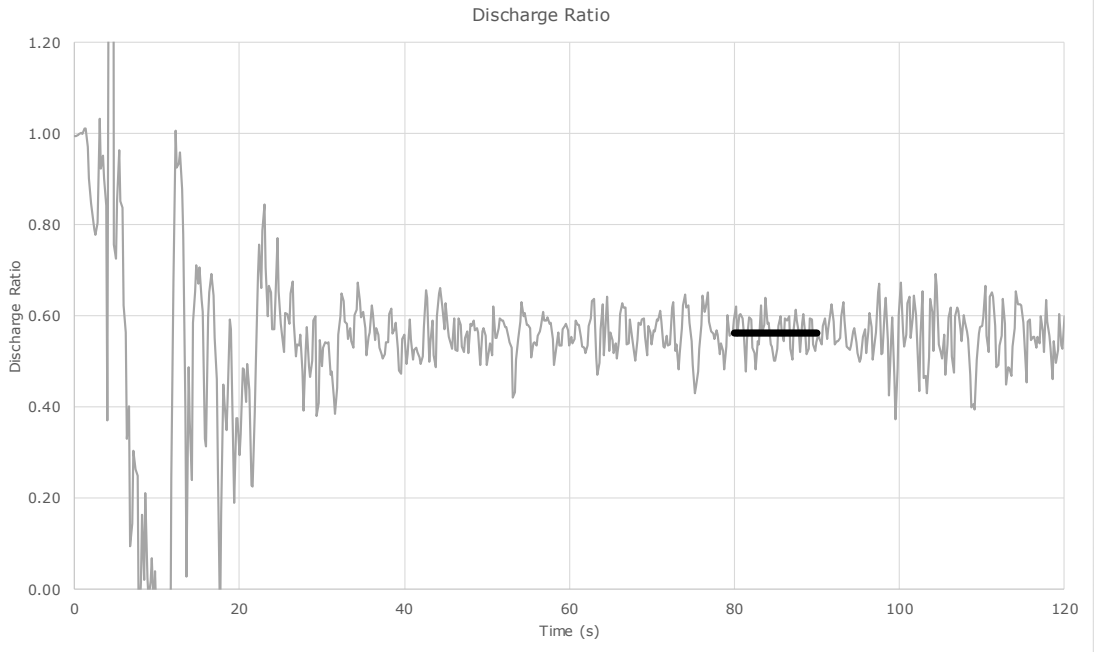


30_09_5560

Name	Symbol	Left	Right	Unit
/eir Height	WH	55	60	mm
ıitial Time	Ti	80	80	s
End Time	Te	90	90	s
tial Number	Ni	400	400	dimensionless
ıd Number	Ne	450	450	dimensionless
ıge Discharge	$\bar{Q}$	6.325E-04	3.566E-04	m3/s

Name	Symbol	Equation	Result	Unit
· Height Ratio	WHr	WHL/WHR	0.917	dimensionless
:harge Ratio	Qr	$\bar{Q}$_L/$\bar{Q}$_R	0.564	dimensionless
p Discharge Ratio	Qr,t	Average[Q_(r,t=n)···Q_(r,t=n+N)]	0.562	dimensionless

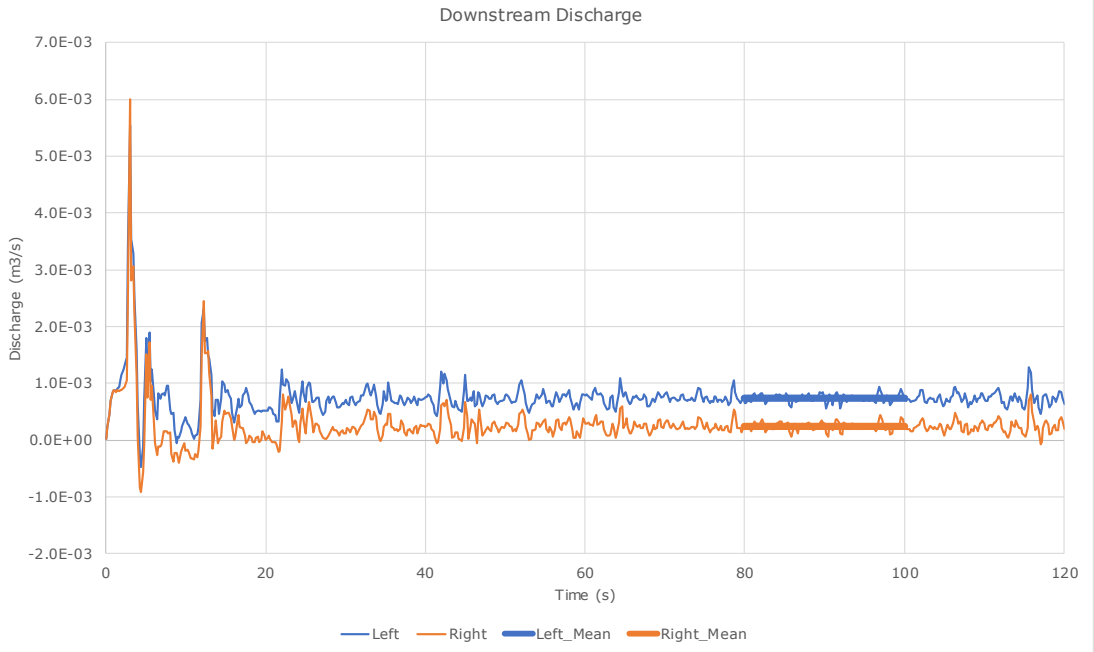


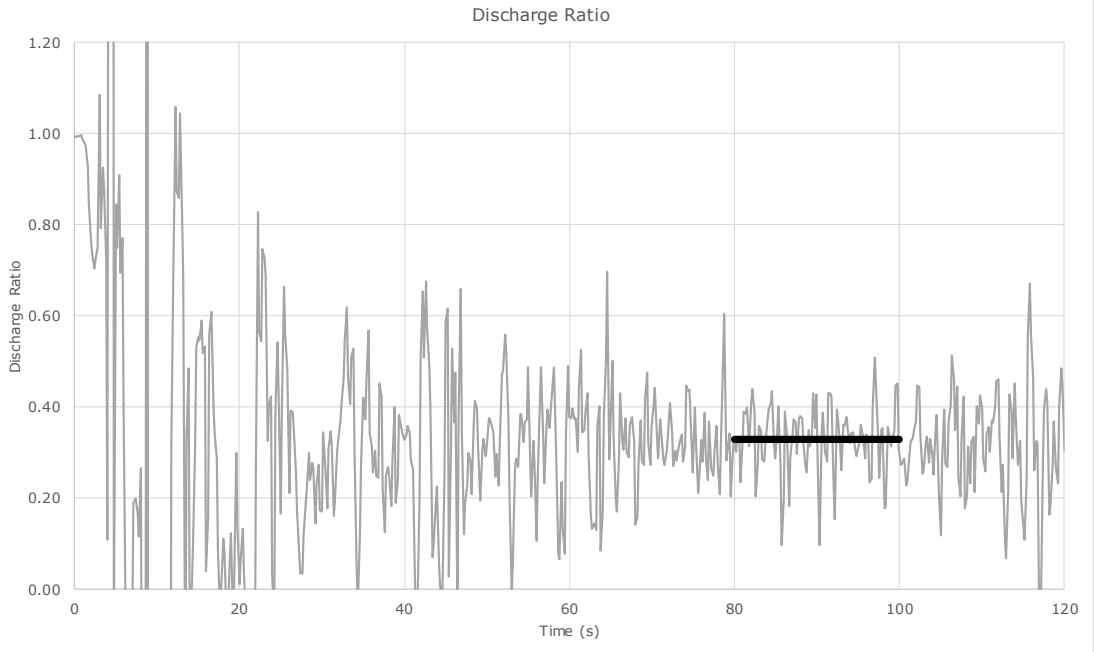


30_09_5562

Name	Symbol	Left	Right	Unit
Weir Height	WH	55	62	mm
Initial Time	Ti	80	80	s
End Time	Te	100	100	s
Initial Number	Ni	400	400	dimensionless
End Number	Ne	500	500	dimensionless
Average Discharge	$\bar{Q}$	7.403E-04	2.471E-04	m3/s

Name	Symbol	Equation	Result	Unit
Weir Height Ratio	WHr	WHL/WHR	0.887	dimensionless
Discharge Ratio	Qr	$\bar{Q}$_L/$\bar{Q}$_R	0.334	dimensionless
Time Step Discharge Ratio	Qr,t	Average[Q_(r,t=n)···Q_(r,t=n+N)]	0.329	dimensionless

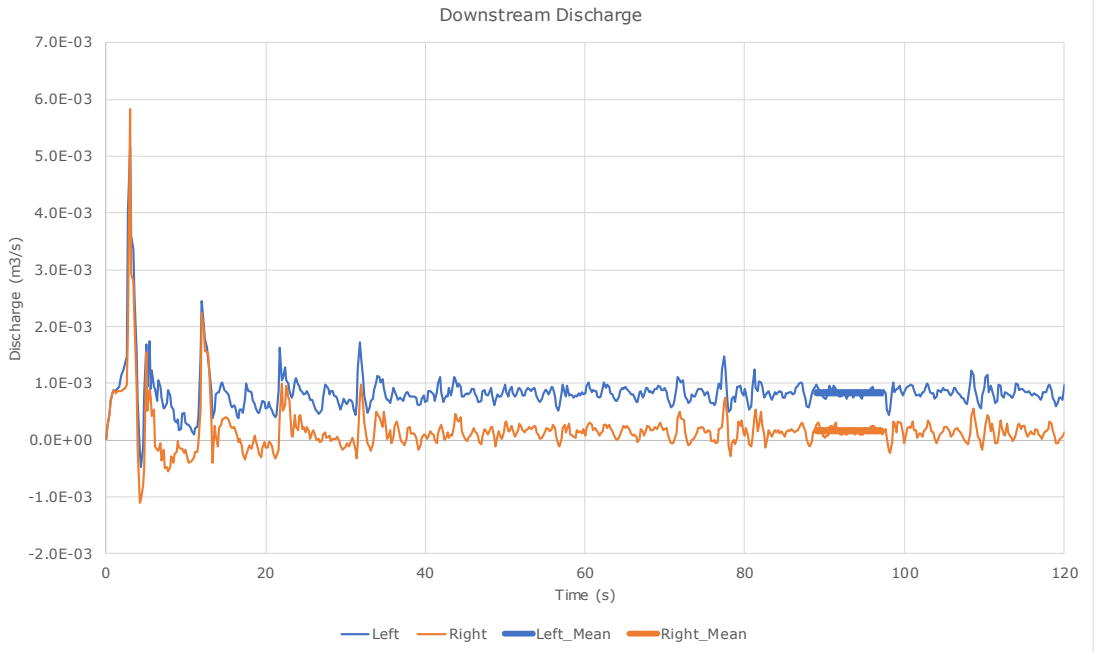


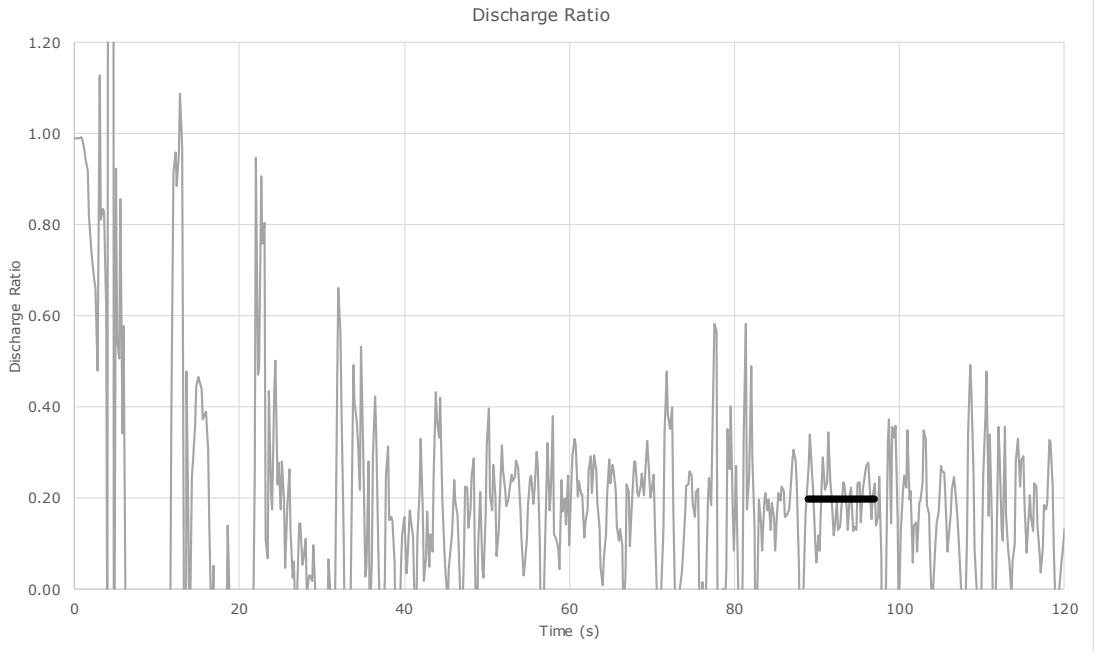


30_09_5565

Name	Symbol	Left	Right	Unit
Weir Height	WH	55	65	mm
Initial Time	Ti	89	89	s
End Time	Te	97	97	s
Initial Number	Ni	445	445	dimensionless
End Number	Ne	485	485	dimensionless
verage Discharge	$\bar{Q}$	8.349E-04	1.689E-04	m3/s

Name	Symbol	Equation	Result	Unit
Weir Height Ratio	WHr	WHL/WHR	0.846	dimensionless
Discharge Ratio	Qr	$\bar{Q}$_L/$\bar{Q}$_R	0.202	dimensionless
Step Discharge Ratio	Qr,t	Average[Q_(r,t=n)···Q_(r,t=n+N)]	0.199	dimensionless

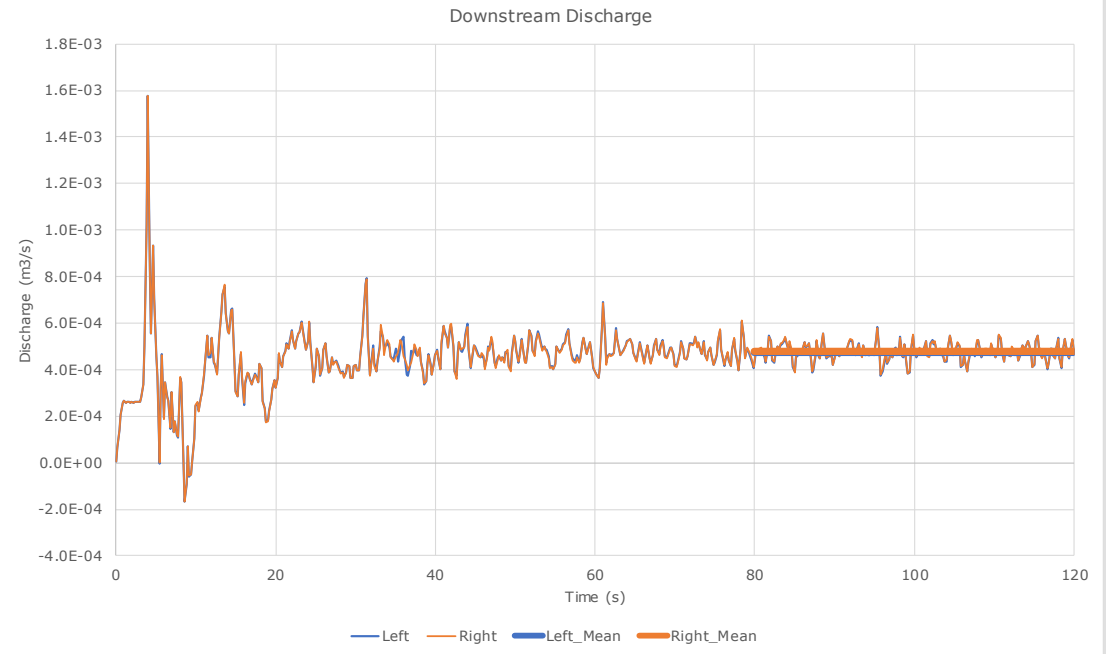


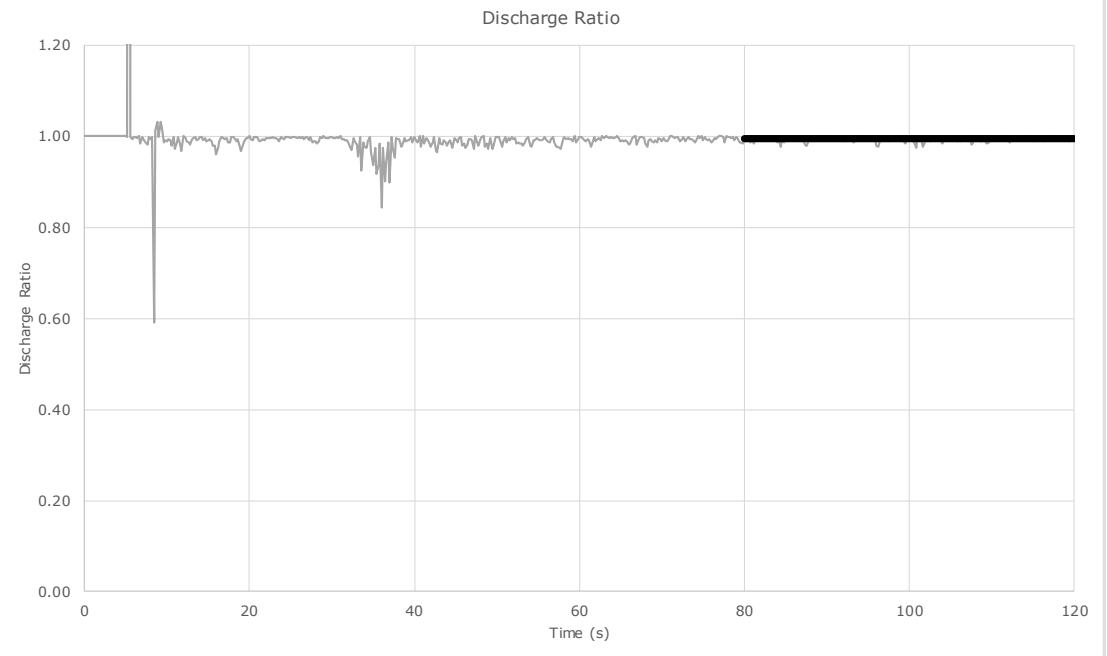


40_03_5050

Name	Symbol	Left	Right	Unit
Weir Height	WH	50	50	mm
Initial Time	Ti	80	80	s
End Time	Te	120	120	s
Initial Number	Ni	400	400	unitless
End Number	Ne	600	600	unitless
Average Discharge	$\bar{Q}$	4.761E-04	4.777E-04	m3/s

Name	Symbol	Equation	Result	Unit
Weir Height Ratio	WHr	WHL/WHR	1.000	dimensionless
Discharge Ratio	Qr	$\bar{Q}$_L/$\bar{Q}$_R	0.997	dimensionless
Time Step Discharge Ratio	Qr,t	Average[Q_(r,t=n)···Q_(r,t=n+N)]	0.993	dimensionless

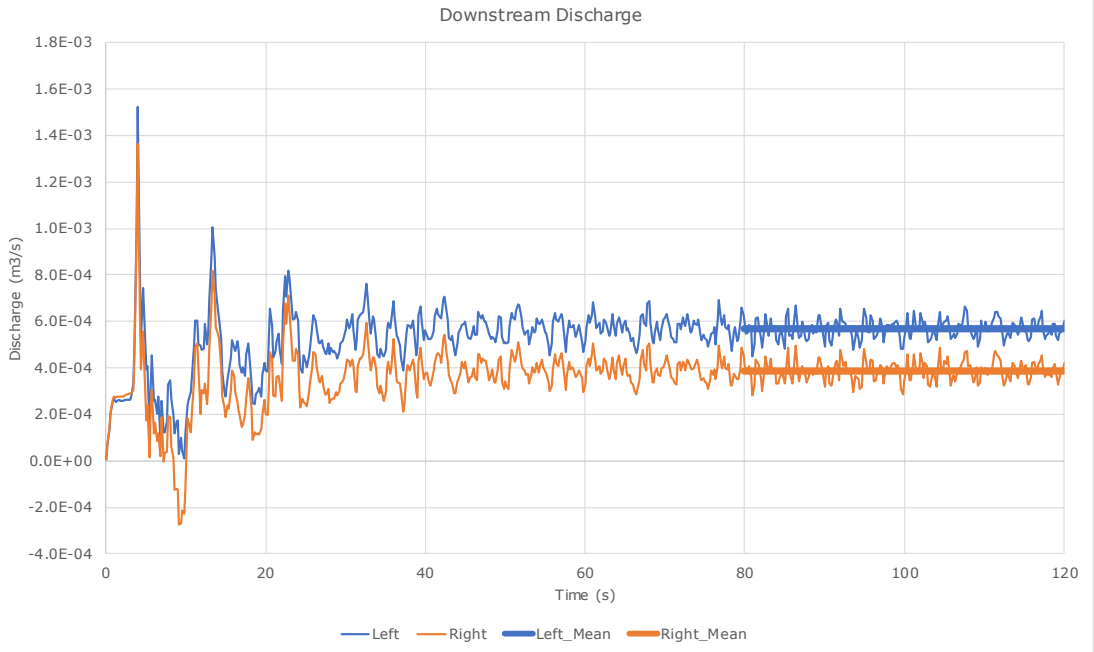


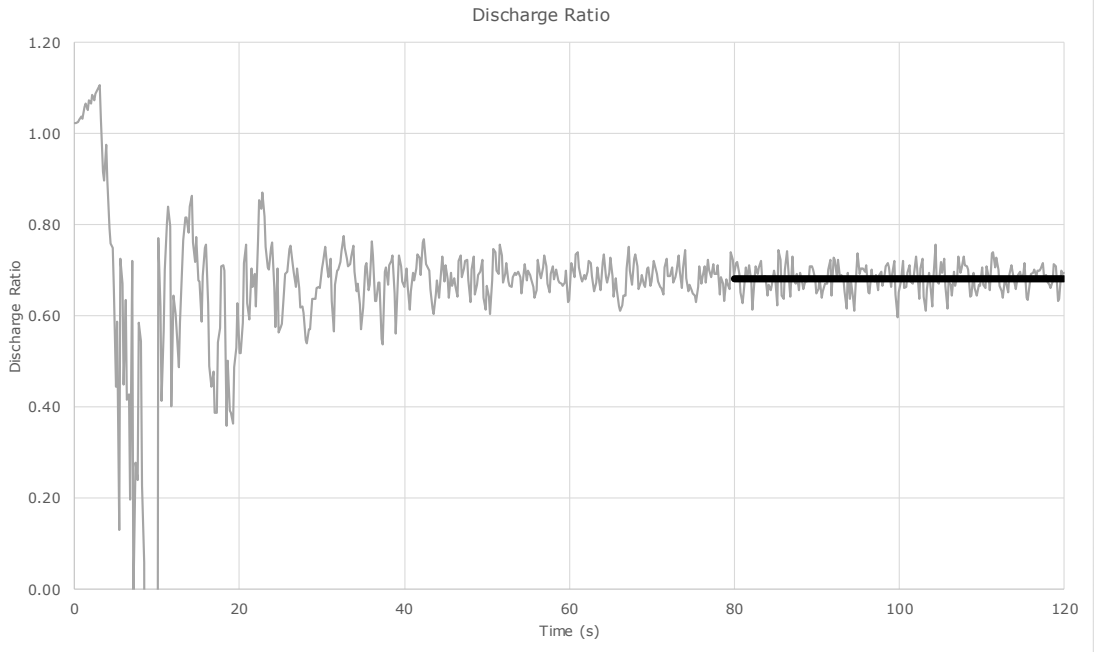


40_03_5053

Name	Symbol	Left	Right	Unit
Weir Height	WH	50	53	mm
Initial Time	Ti	80	80	s
End Time	Te	120	120	s
Initial Number	Ni	400	400	unitless
End Number	Ne	600	600	unitless
Average Discharge	$\bar{Q}$	5.674E-04	3.878E-04	m3/s

Name	Symbol	Equation	Result	Unit
Weir Height Ratio	WHr	WHL/WHR	0.943	dimensionless
Discharge Ratio	Qr	$\bar{Q}$_L/$\bar{Q}$_R	0.683	dimensionless
Time Step Discharge Ratio	Qr,t	Average[Q_(r,t=n)···Q_(r,t=n+N)]	0.682	dimensionless

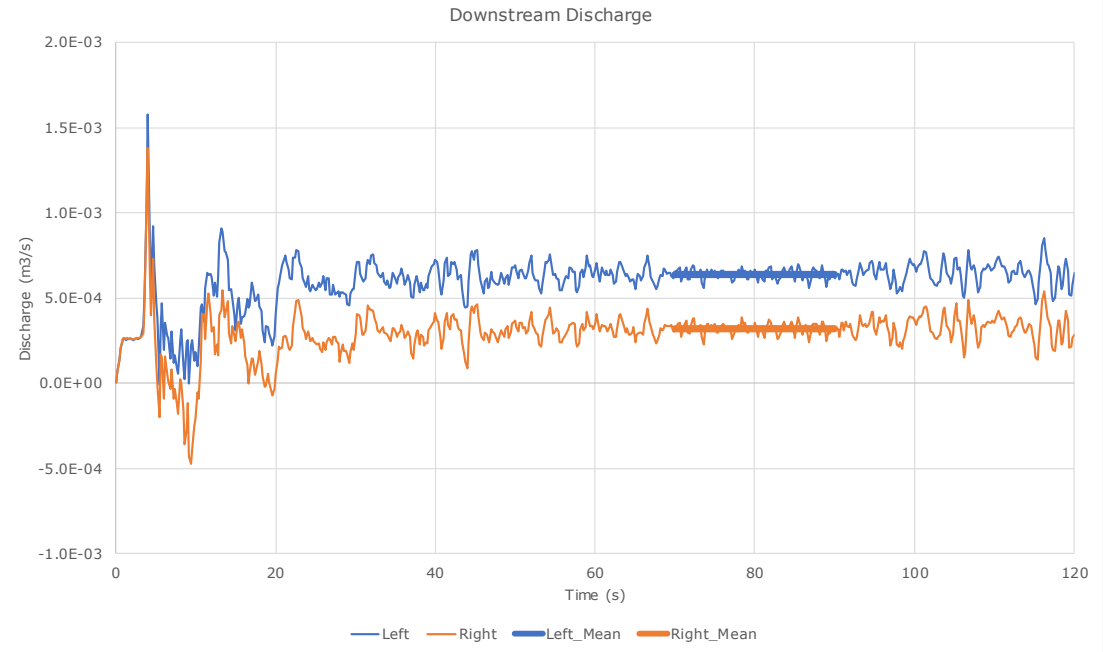


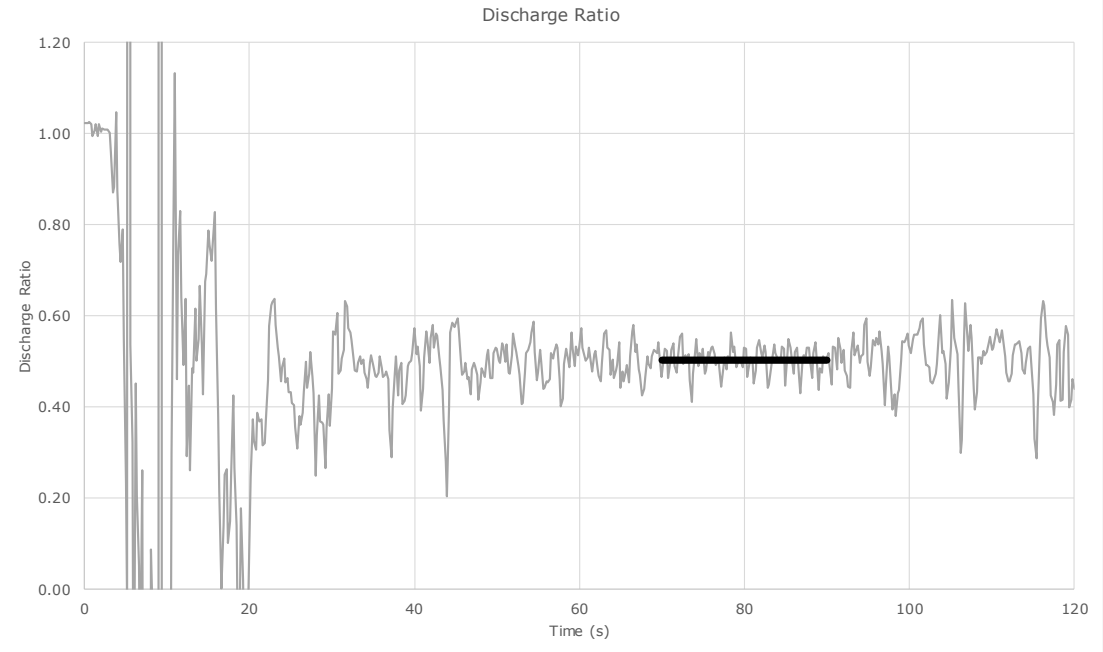


40_03_5055

ne	Symbol	Left	Right	Unit
eight	WH	50	55	mm
Time	Ti	70	70	s
ime	Te	90	90	s
umber	Ni	350	350	unitless
mber	Ne	450	450	unitless
ischarge	$\bar{Q}$	6.394E-04	3.223E-04	m3/s

ne	Symbol	Equation	Result	Unit
ht Ratio	WHr	WHL/WHR	0.909	dimensionless
e Ratio	Qr	$\bar{Q}$_L/$\bar{Q}$_R	0.504	dimensionless
charge Ratio	Qr,t	Average[Q_(r,t=n)···Q_(r,t=n+N)]	0.503	dimensionless

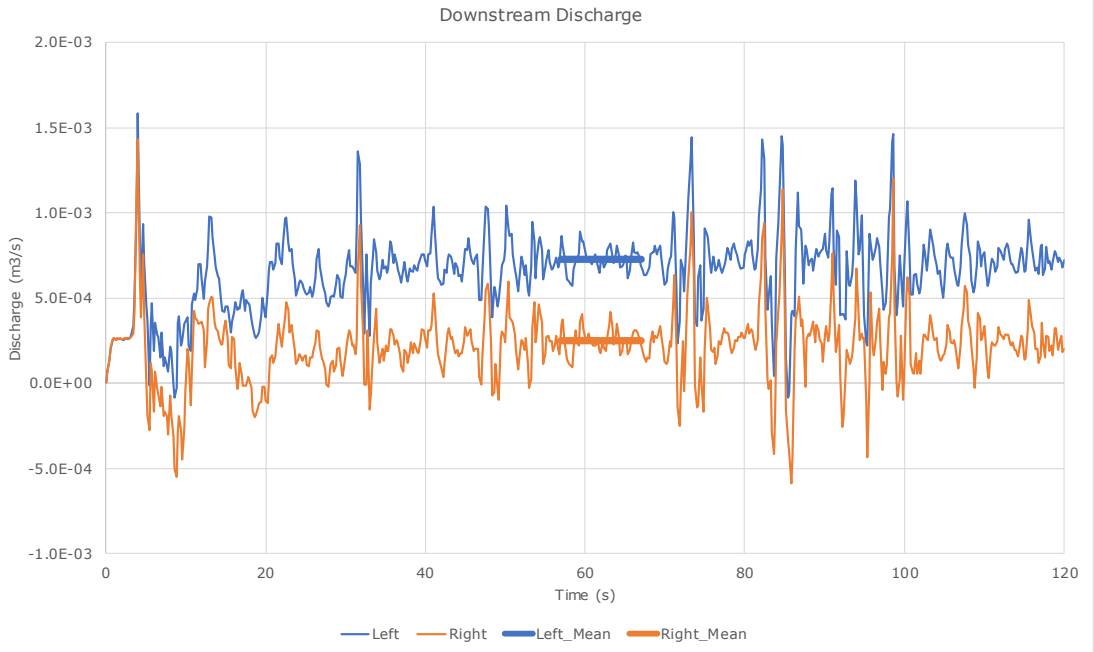


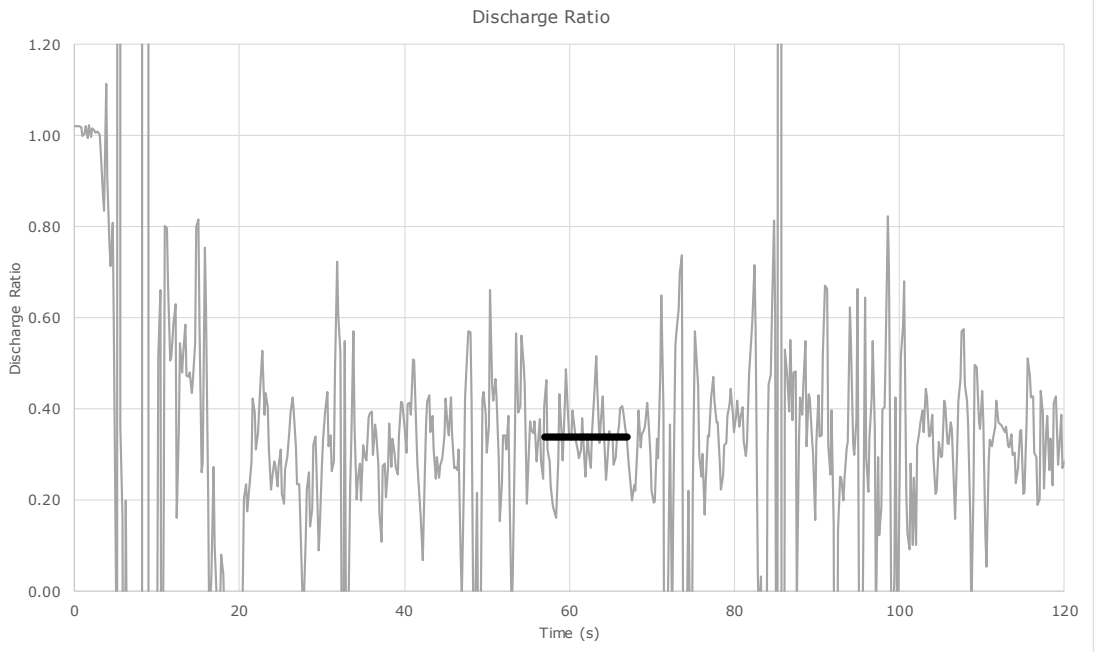


40_03_5057

Name	Symbol	Left	Right	Unit
ir Height	WH	50	57	mm
tial Time	Ti	57	57	s
ıd Time	Te	67	67	s
al Number	Ni	285	285	unitless
l Number	Ne	335	335	unitless
ge Discharge	$\bar{Q}$	7.290E-04	2.509E-04	m3/s

Name	Symbol	Equation	Result	Unit
eight Ratio	WHr	WHL/WHR	0.877	dimensionless
ıarge Ratio	Qr	$\bar{Q}$_L/$\bar{Q}$_R	0.344	dimensionless
Discharge Ratio	Qr,t	Average[Q_(r,t=n)···Q_(r,t=n+N)]	0.339	dimensionless

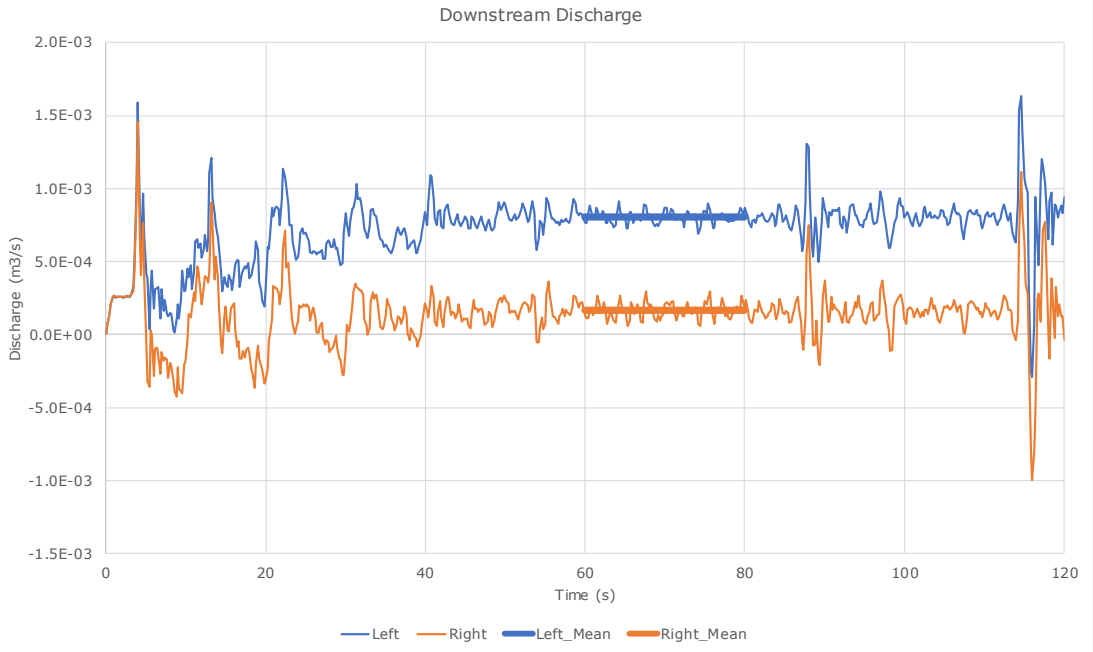


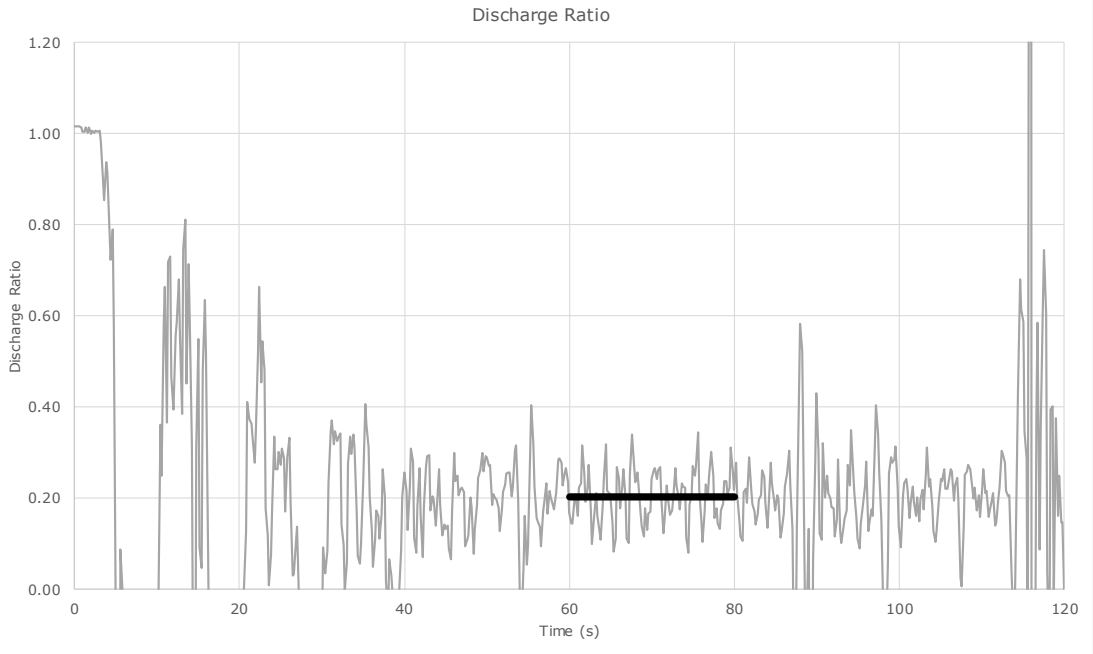


40_03_5060

Name	Symbol	Left	Right	Unit
/eir Height	WH	50	60	mm
nitial Time	Ti	60	60	s
End Time	Te	80	80	s
tial Number	Ni	300	300	dimensionless
nd Number	Ne	400	400	dimensionless
age Discharge	$\bar{Q}$	8.045E-04	1.648E-04	m3/s

Name	Symbol	Equation	Result	Unit
· Height Ratio	WHr	WHL/WHR	0.833	dimensionless
:harge Ratio	Qr	$\bar{Q}$_L/$\bar{Q}$_R	0.205	dimensionless
p Discharge Ratio	Qr,t	Average[Q_(r,t=n)···Q_(r,t=n+N)]	0.203	dimensionless

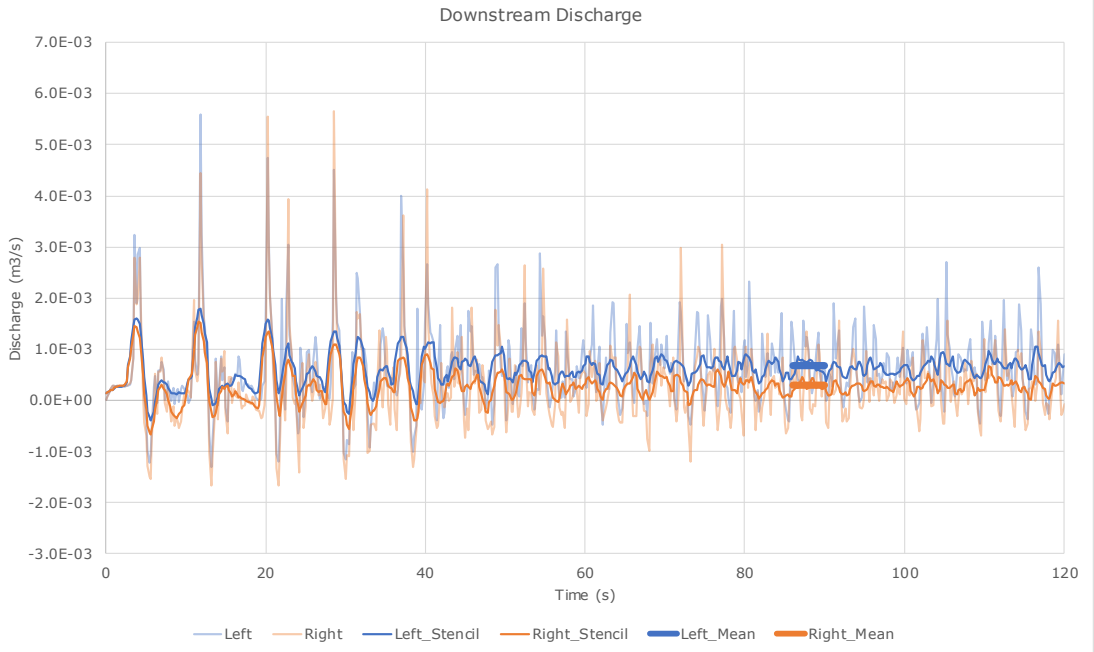


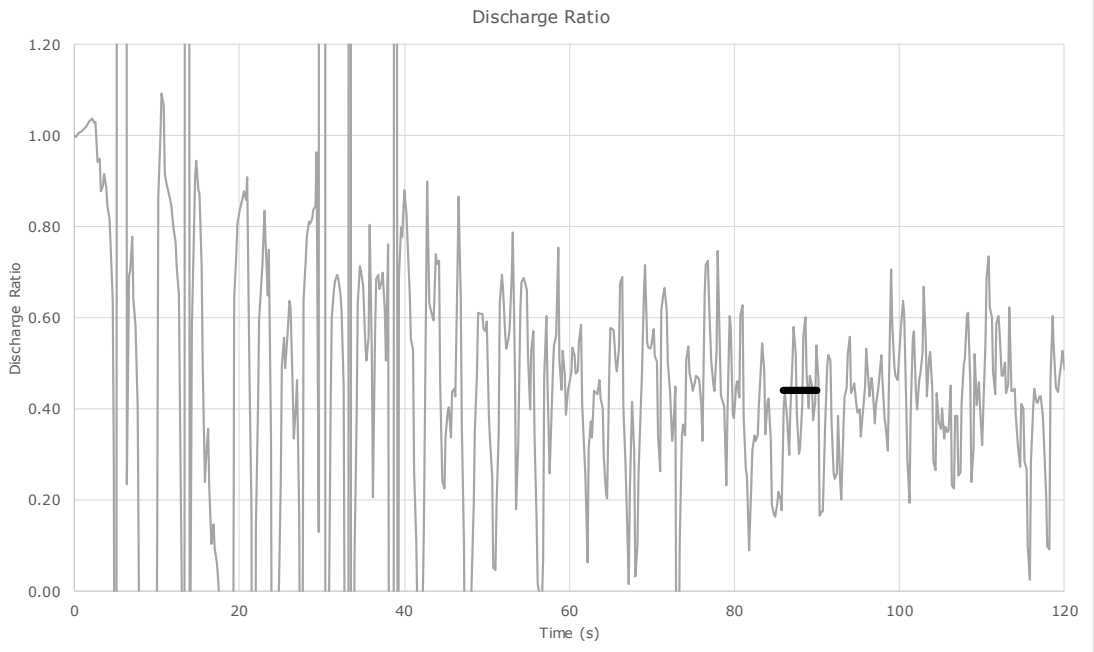


40_03_5560

Name	Symbol	Left	Right	Unit
Weir Height	WH	55	60	mm
Initial Time	Ti	86	86	s
End Time	Te	90	90	s
Initial Number	Ni	430	430	dimensionless
End Number	Ne	450	450	dimensionless
Average Discharge	$\bar{Q}$	6.783E-04	2.977E-04	m3/s

Name	Symbol	Equation	Result	Unit
Weir Height Ratio	WHr	WHL/WHR	0.917	dimensionless
Discharge Ratio	Qr	$\bar{Q}$_L/$\bar{Q}$_R	0.439	dimensionless
Step Discharge Ratio	Qr,t	Average[Q_(r,t=n)···Q_(r,t=n+N)]	0.439	dimensionless

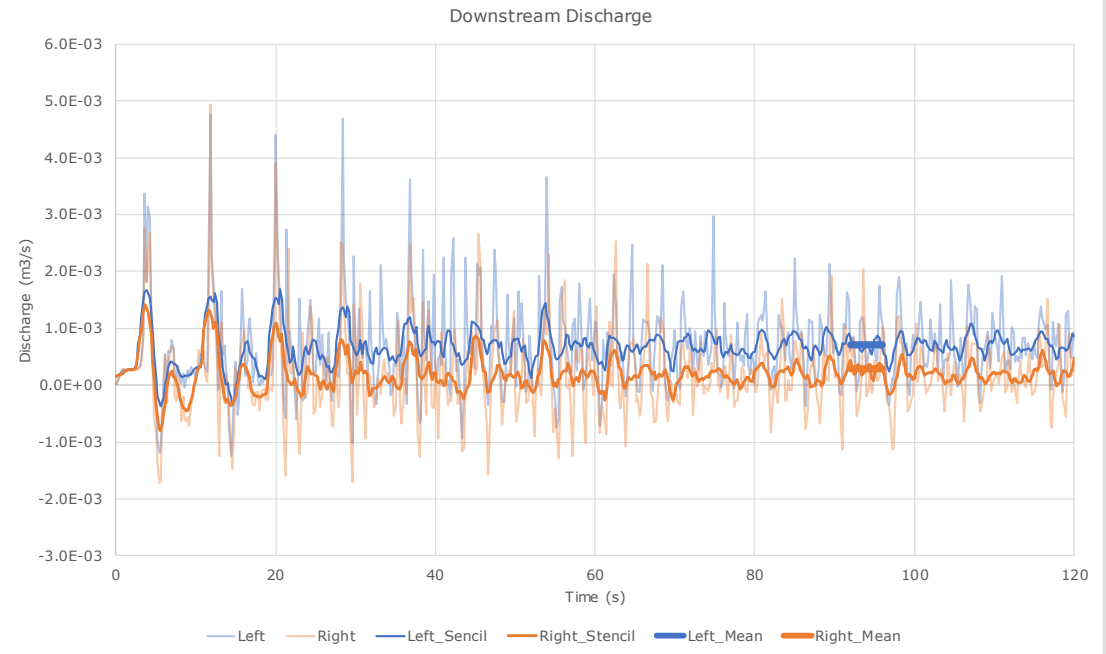


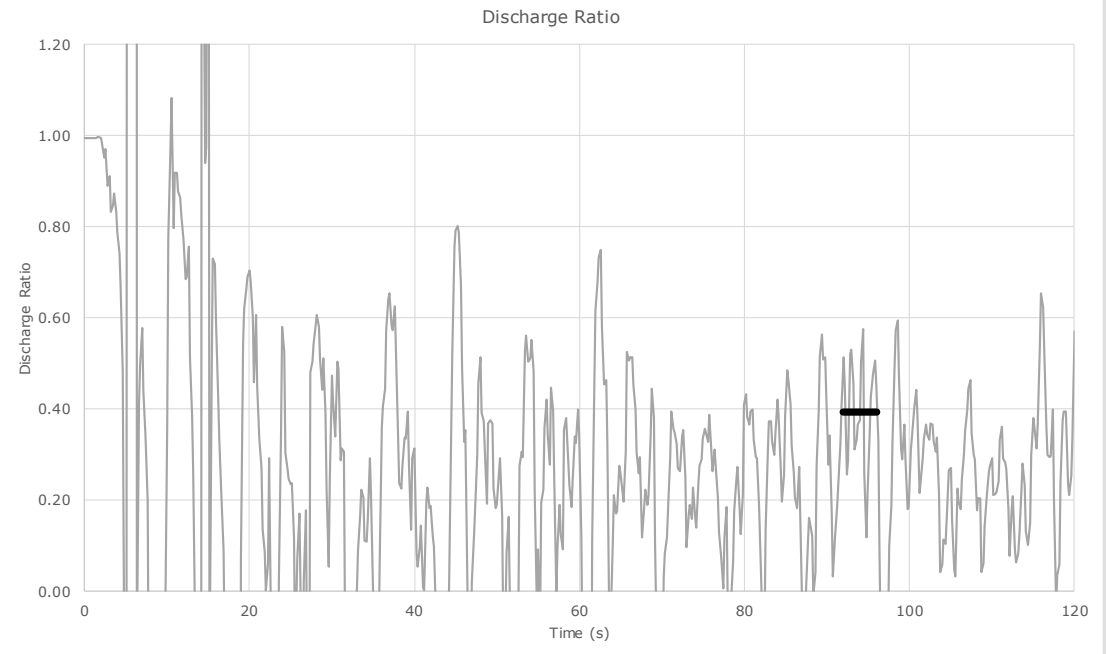


40_03_5562

Name	Symbol	Left	Right	Unit
Weir Height	WH	55	62	mm
Initial Time	Ti	92	92	s
End Time	Te	96	96	s
Initial Number	Ni	460	460	dimensionless
End Number	Ne	480	480	dimensionless
Average Discharge	$\bar{Q}$	7.104E-04	2.808E-04	m3/s

Name	Symbol	Equation	Result	Unit
Weir Height Ratio	WHr	WHL/WHR	0.887	dimensionless
Discharge Ratio	Qr	$\bar{Q}$_L/$\bar{Q}$_R	0.395	dimensionless
Time Step Discharge Ratio	Qr,t	Average[Q_(r,t=n)···Q_(r,t=n+N)]	0.394	dimensionless

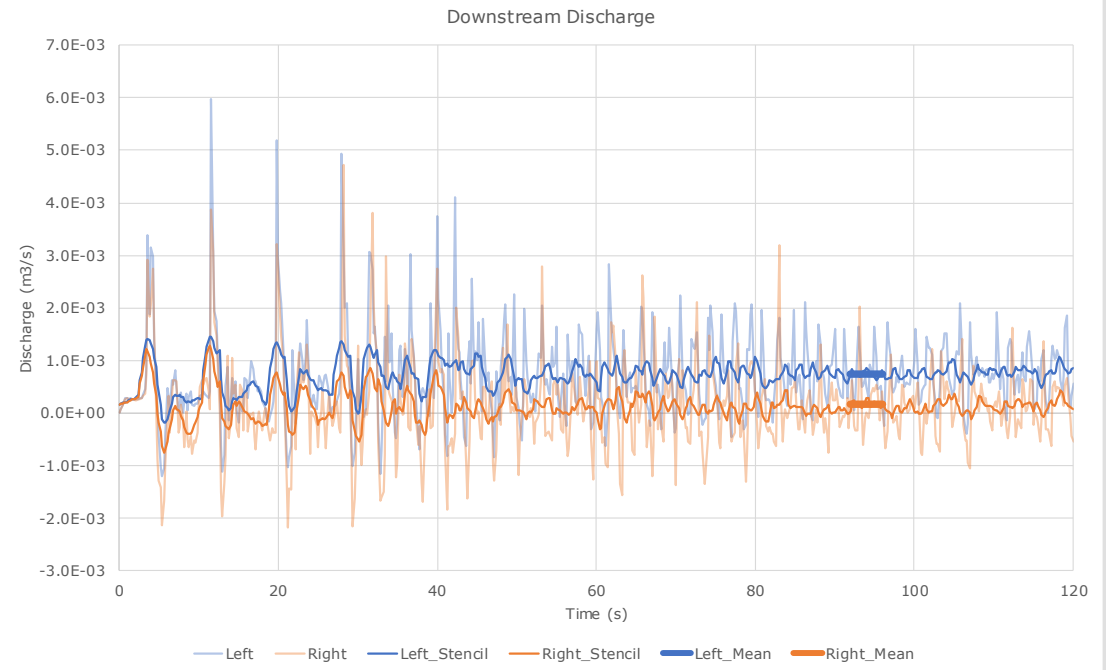


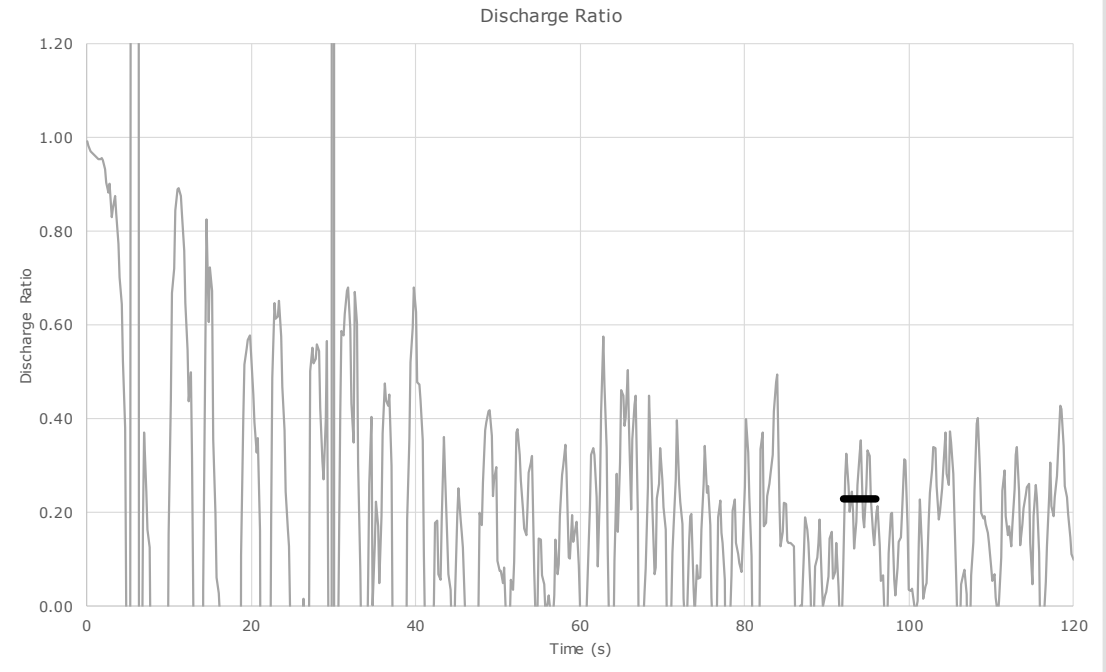


40_03_5565

Name	Symbol	Left	Right	Unit
Weir Height	WH	55	65	mm
Initial Time	Ti	92	92	s
End Time	Te	96	96	s
Initial Number	Ni	460	460	dimensionless
End Number	Ne	480	480	dimensionless
Average Discharge	$\bar{Q}$	7.519E-04	1.716E-04	m3/s

Name	Symbol	Equation	Result	Unit
Weir Height Ratio	WHr	WHL/WHR	0.846	dimensionless
Discharge Ratio	Qr	$\bar{Q}_L/\bar{Q}_R$	0.228	dimensionless
Time Step Discharge Ratio	Qr,t	Average[Q_(r,t=n)···Q_(r,t=n+N)]	0.228	dimensionless

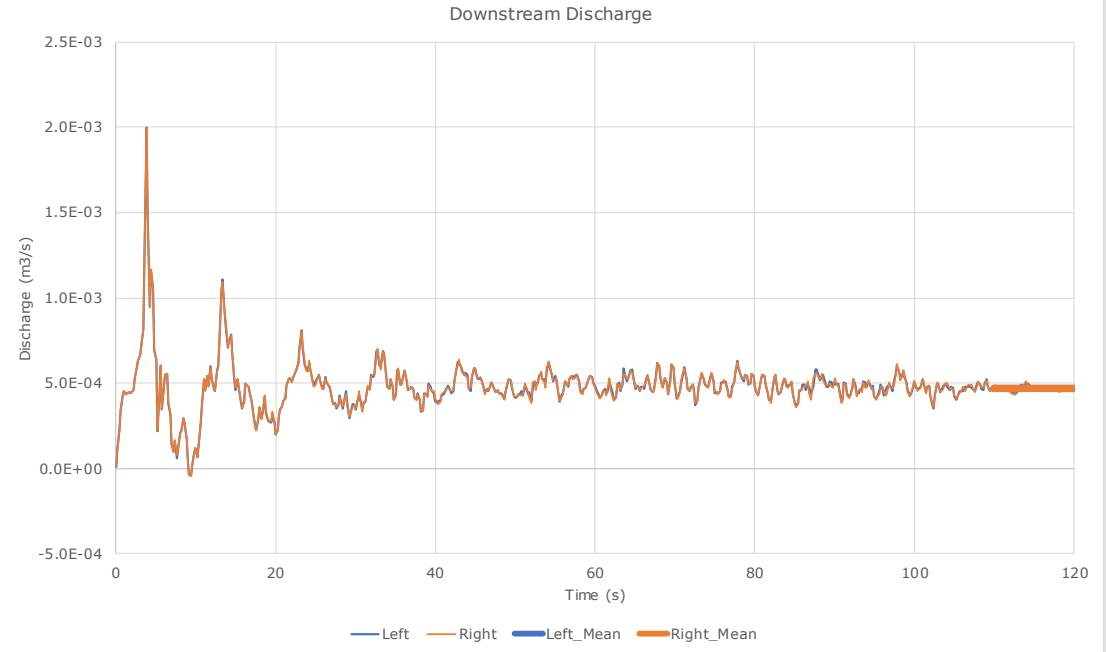


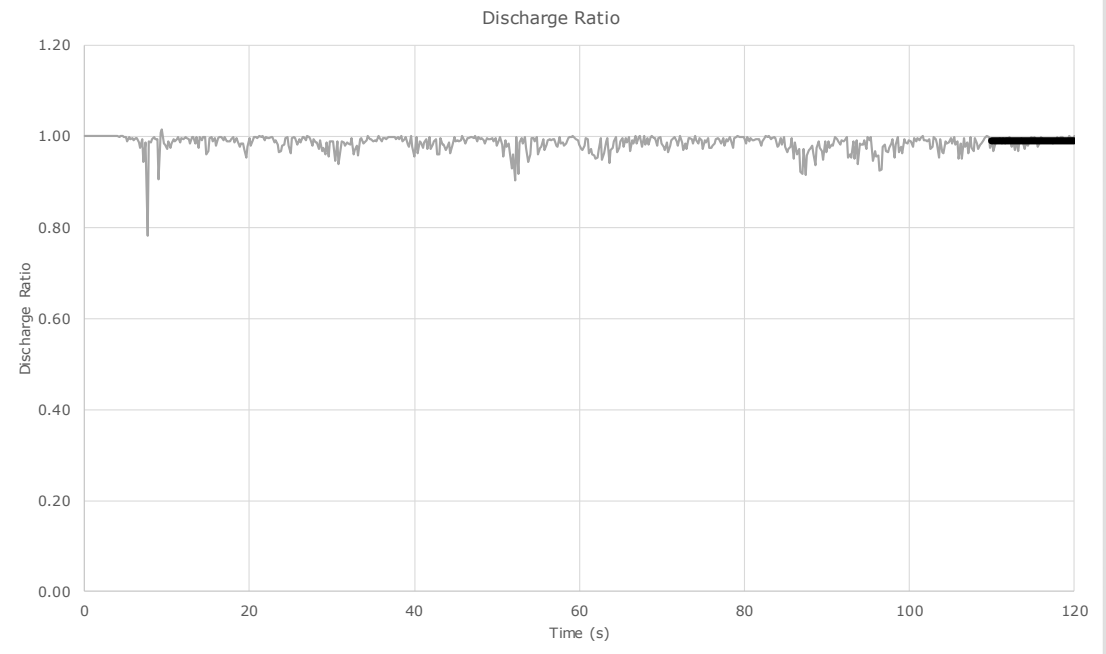


40_05_5050

Name	Symbol	Left	Right	Unit
Weir Height	WH	50	50	mm
Initial Time	Ti	110	110	s
End Time	Te	120	120	s
Initial Number	Ni	550	550	unitless
End Number	Ne	600	600	unitless
Average Discharge	$\bar{Q}$	4.677E-04	4.668E-04	m3/s

Name	Symbol	Equation	Result	Unit
Weir Height Ratio	WHr	WHL/WHR	1.000	dimensionless
Discharge Ratio	Qr	$\bar{Q}$_L/$\bar{Q}$_R	0.998	dimensionless
Time Step Discharge Ratio	Qr,t	Average[Q_(r,t=n)···Q_(r,t=n+N)]	0.989	dimensionless

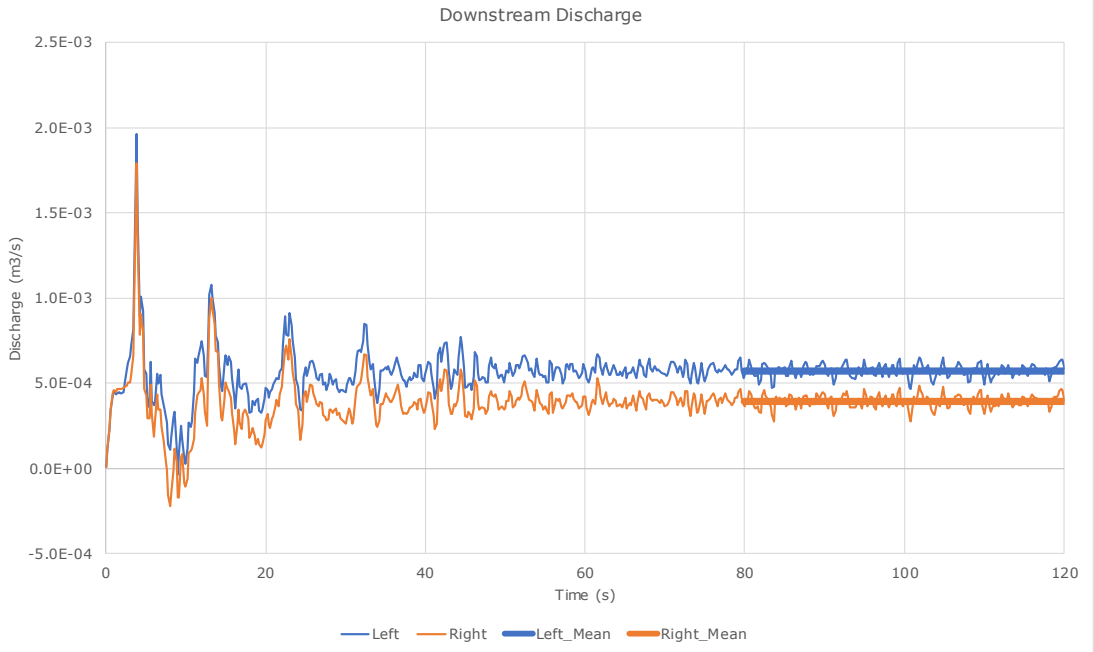


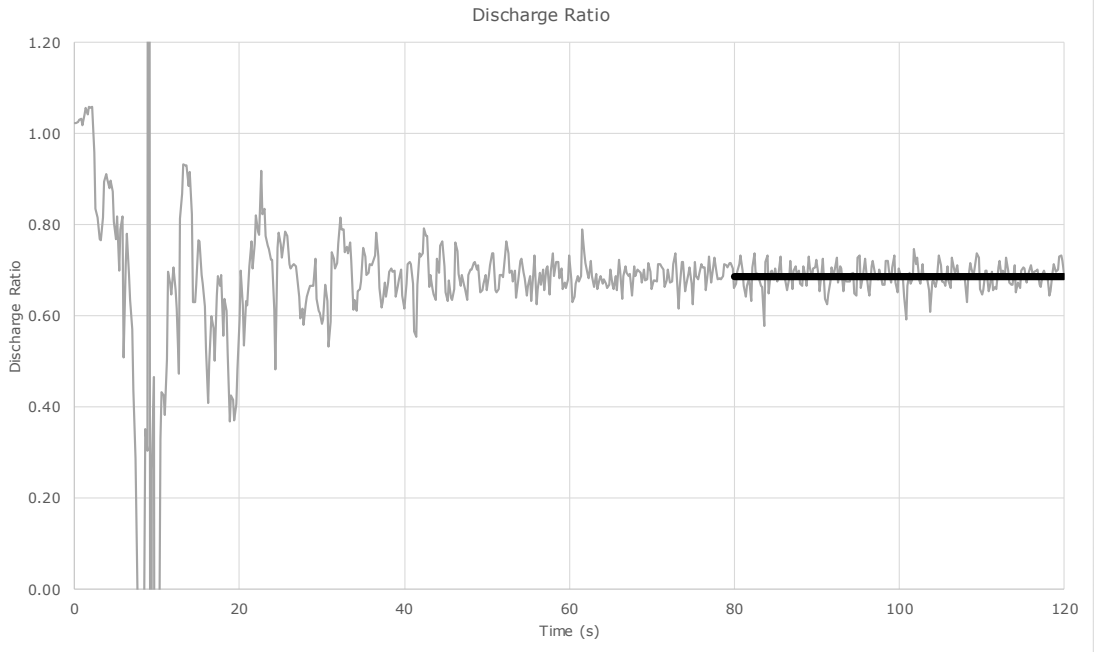


40_05_5053

Name	Symbol	Left	Right	Unit
Weir Height	WH	50	53	mm
Initial Time	Ti	80	80	s
End Time	Te	120	120	s
Initial Number	Ni	400	400	unitless
End Number	Ne	600	600	unitless
Average Discharge	$\bar{Q}$	5.746E-04	3.953E-04	m3/s

Name	Symbol	Equation	Result	Unit
Weir Height Ratio	WHr	WHL/WHR	0.943	dimensionless
Discharge Ratio	Qr	$\bar{Q}$_L/$\bar{Q}$_R	0.688	dimensionless
Time Step Discharge Ratio	Qr,t	Average[Q_(r,t=n)···Q_(r,t=n+N)]	0.687	dimensionless

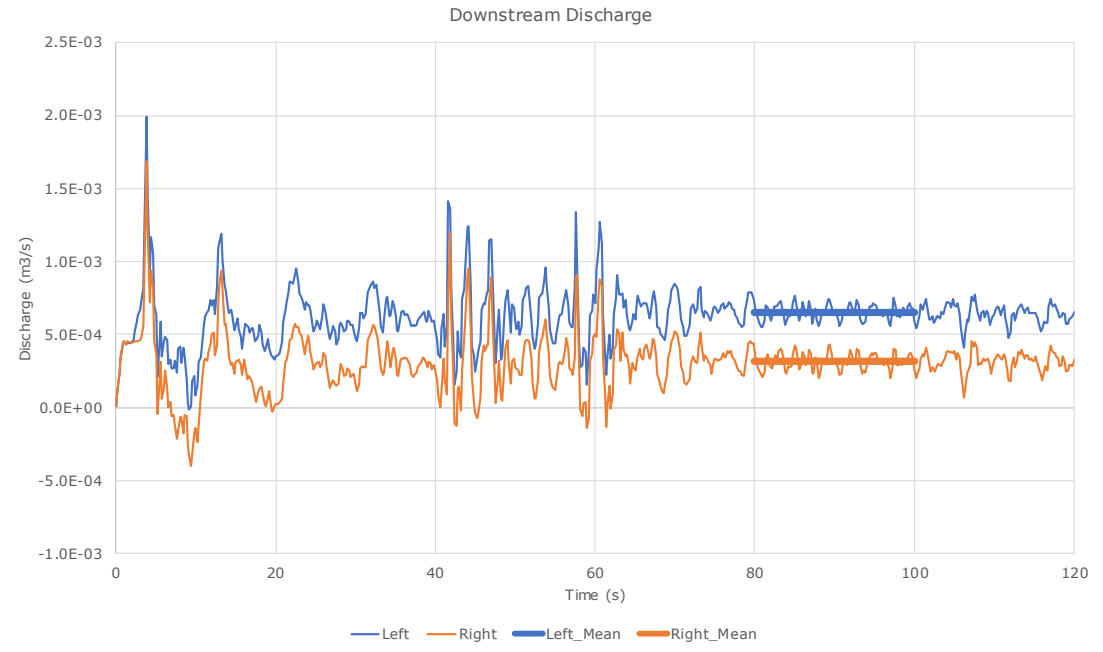


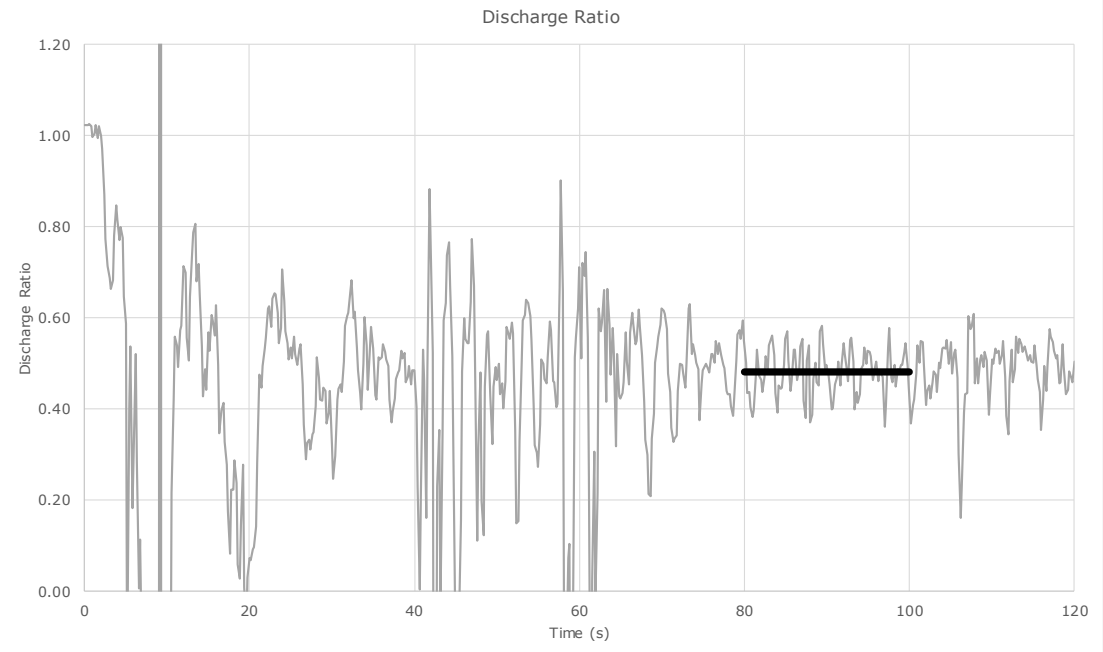


40_05_5055

Name	Symbol	Left	Right	Unit
Weir Height	WH	50	55	mm
Initial Time	Ti	80	80	s
End Time	Te	100	100	s
Initial Number	Ni	400	400	unitless
End Number	Ne	500	500	unitless
Average Discharge	$\bar{Q}$	6.534E-04	3.167E-04	m3/s

Name	Symbol	Equation	Result	Unit
Weir Height Ratio	WHr	WHL/WHR	0.909	dimensionless
Discharge Ratio	Qr	$\bar{Q}$_L/$\bar{Q}$_R	0.485	dimensionless
Time Step Discharge Ratio	Qr,t	Average[Q_(r,t=n)···Q_(r,t=n+N)]	0.482	dimensionless

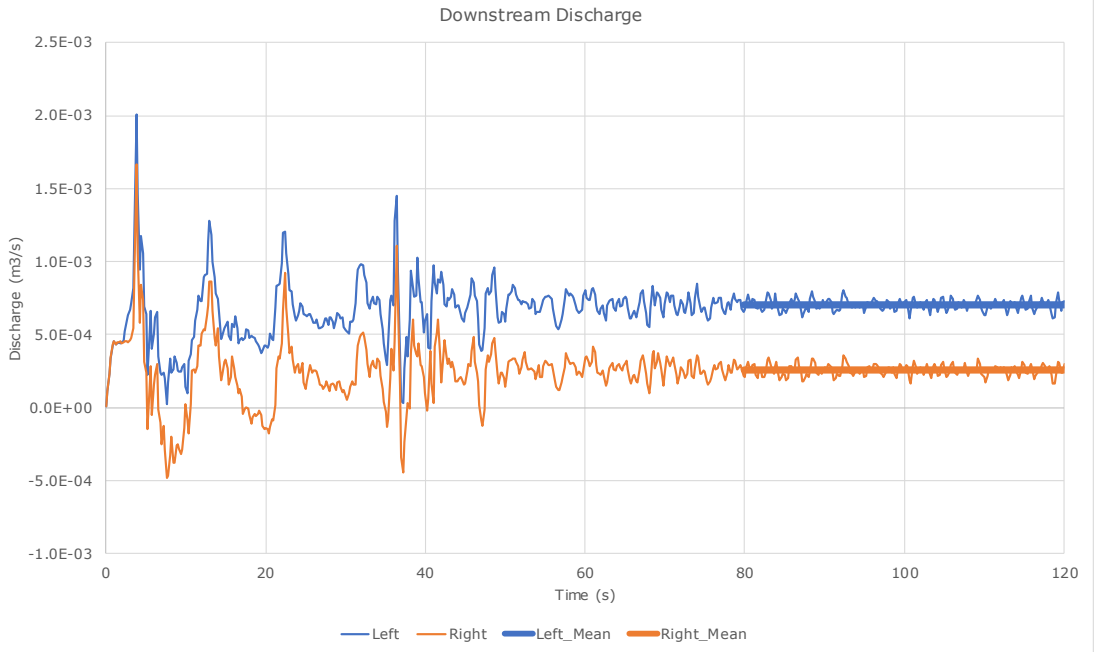


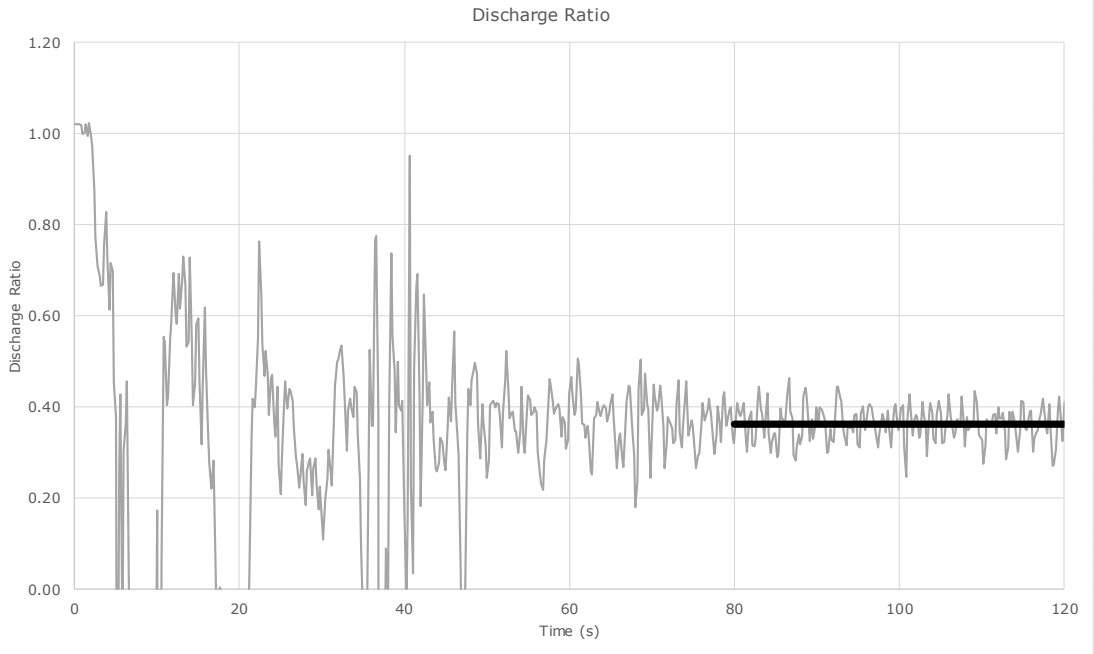


40_05_5057

Name	Symbol	Left	Right	Unit
Weir Height	WH	50	57	mm
Initial Time	Ti	80	80	s
End Time	Te	120	120	s
Initial Number	Ni	400	400	unitless
End Number	Ne	600	600	unitless
Average Discharge	$\bar{Q}$	7.044E-04	2.564E-04	m3/s

Name	Symbol	Equation	Result	Unit
Weir Height Ratio	WHr	WHL/WHR	0.877	dimensionless
Discharge Ratio	Qr	$\bar{Q}$_L/$\bar{Q}$_R	0.364	dimensionless
Step Discharge Ratio	Qr,t	Average[Q_(r,t=n)···Q_(r,t=n+N)]	0.362	dimensionless

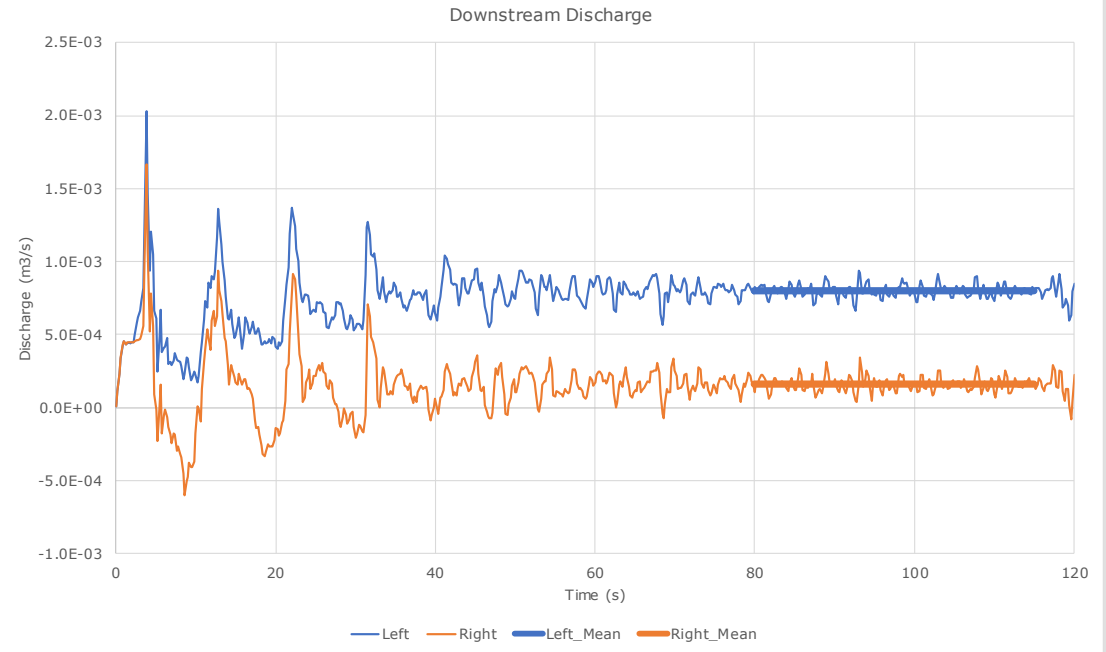


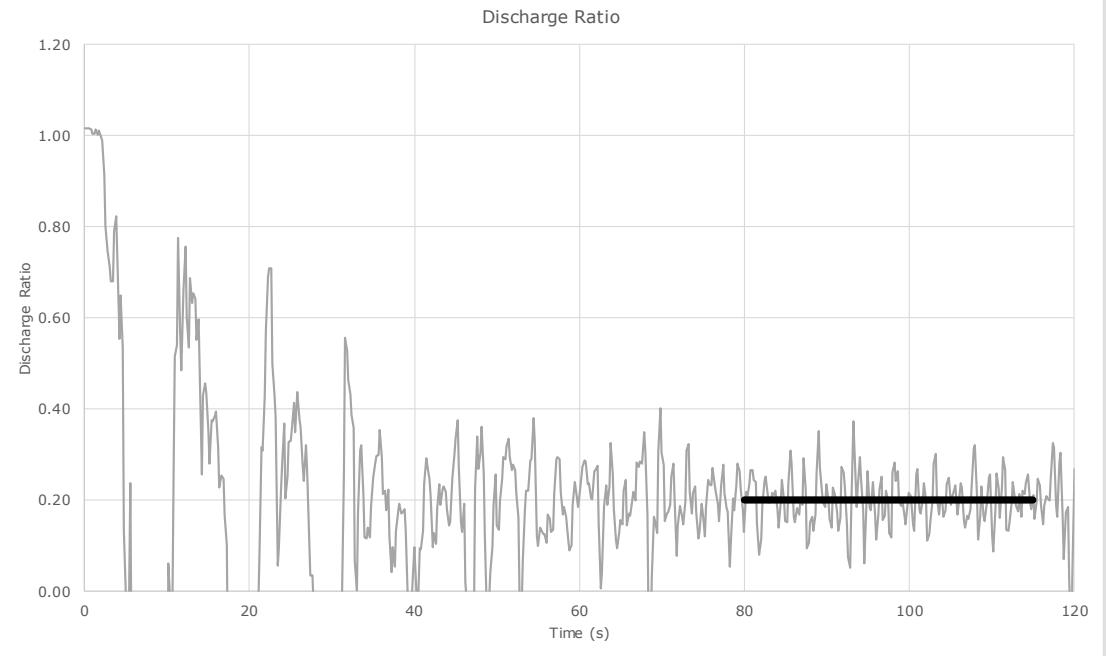


40_05_5060

Name	Symbol	Left	Right	Unit
Weir Height	WH	50	60	mm
Initial Time	Ti	80	80	s
End Time	Te	115	115	s
Initial Number	Ni	400	400	dimensionless
End Number	Ne	575	575	dimensionless
Average Discharge	$\bar{Q}$	8.002E-04	1.605E-04	m3/s

Name	Symbol	Equation	Result	Unit
Weir Height Ratio	WHr	WHL/WHR	0.833	dimensionless
Discharge Ratio	Qr	$\bar{Q}$_L/$\bar{Q}$_R	0.201	dimensionless
ıe Step Discharge Ratio	Qr,t	Average[Q_(r,t=n)···Q_(r,t=n+N)]	0.199	dimensionless

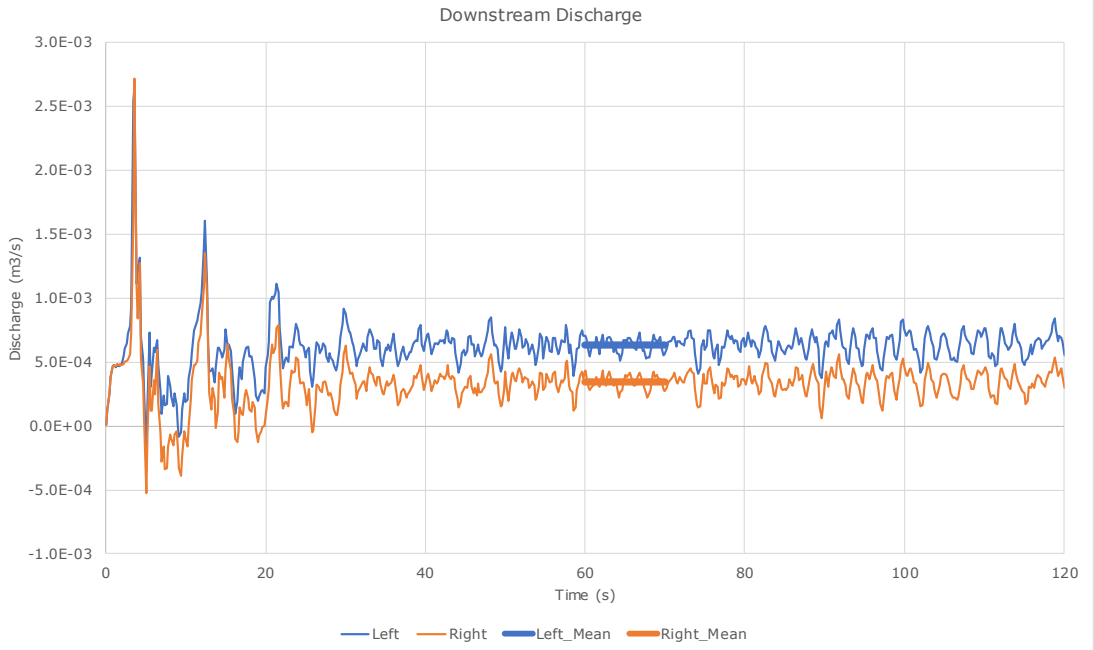


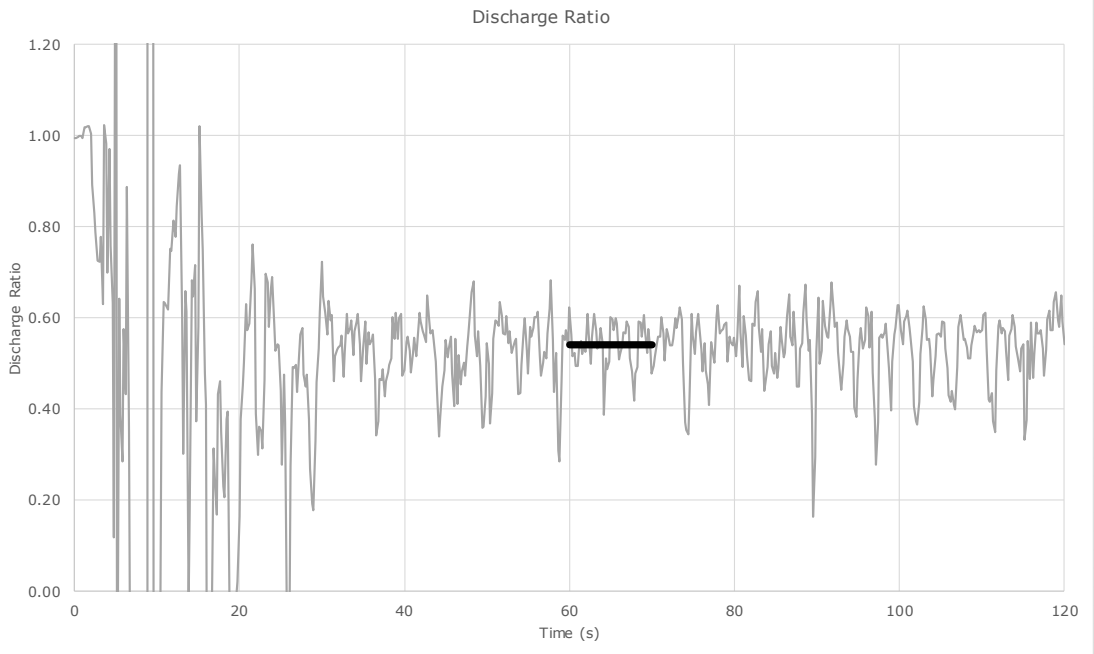


40_05_5560

Name	Symbol	Left	Right	Unit
Weir Height	WH	55	60	mm
Initial Time	Ti	60	60	s
End Time	Te	70	70	s
nitial Number	Ni	300	300	dimensionless
End Number	Ne	350	350	dimensionless
erage Discharge	$\bar{Q}$	6.316E-04	3.437E-04	m3/s

Name	Symbol	Equation	Result	Unit
eir Height Ratio	WHr	WHL/WHR	0.917	dimensionless
ischarge Ratio	Qr	$\bar{Q}$_L/$\bar{Q}$_R	0.544	dimensionless
tep Discharge Ratio	Qr,t	Average[Q_(r,t=n)···Q_(r,t=n+N)]	0.541	dimensionless

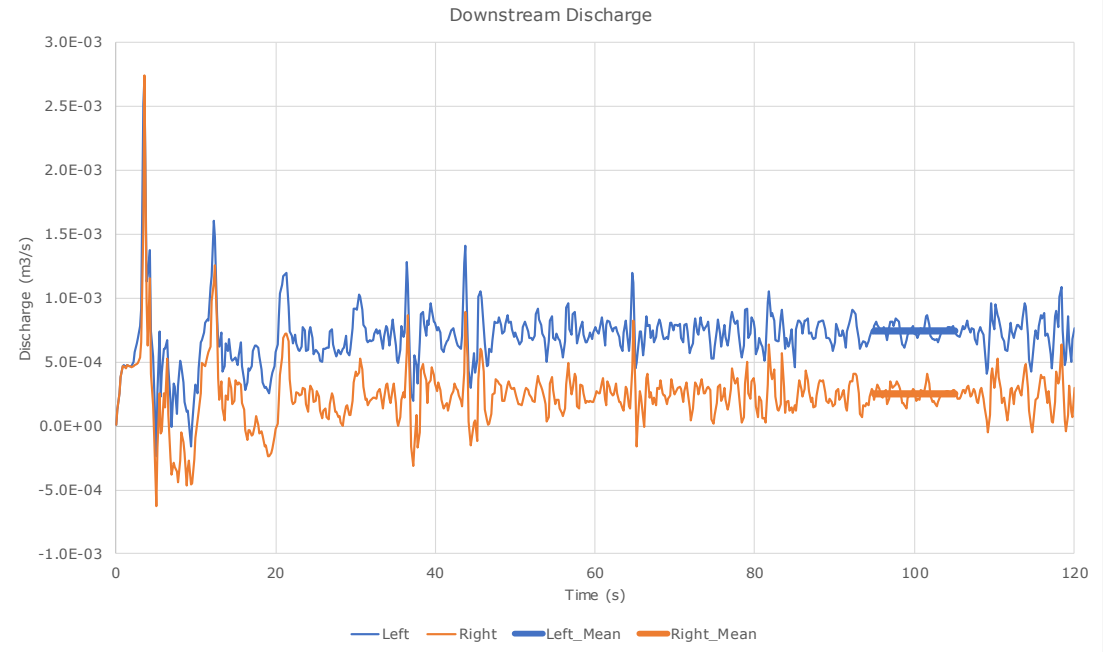


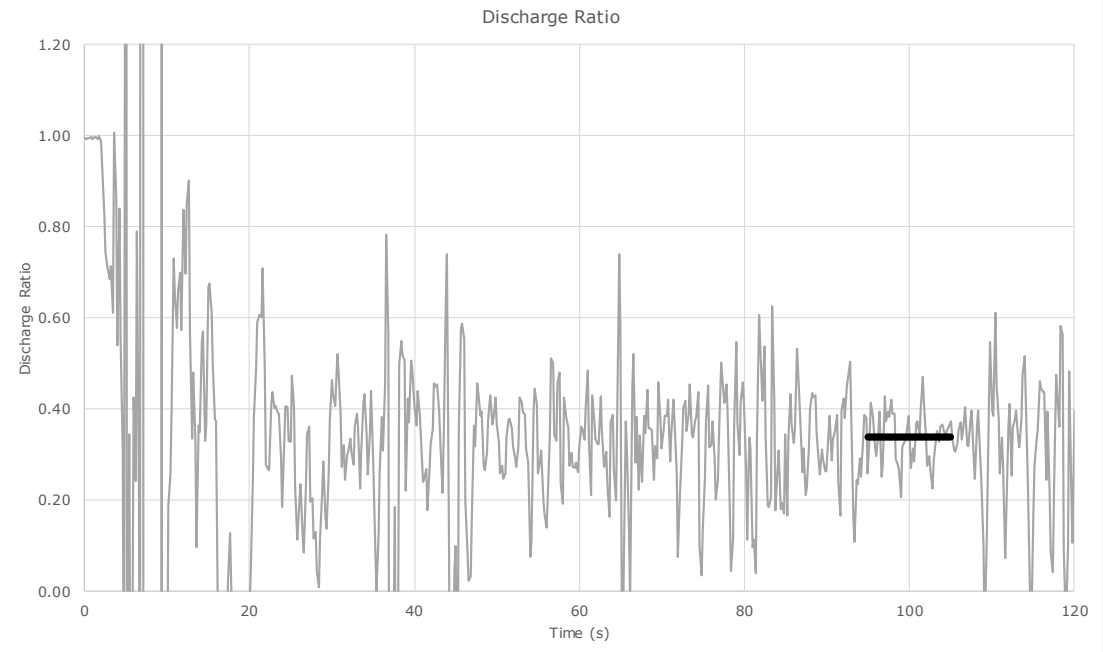


40_05_5562

Name	Symbol	Left	Right	Unit
Weir Height	WH	55	62	mm
Initial Time	Ti	95	95	s
End Time	Te	105	105	s
Initial Number	Ni	475	475	dimensionless
End Number	Ne	525	525	dimensionless
Average Discharge	$\bar{Q}$	7.434E-04	2.537E-04	m3/s

Name	Symbol	Equation	Result	Unit
Weir Height Ratio	WHr	WHL/WHR	0.887	dimensionless
Discharge Ratio	Qr	$\bar{Q}$_L/$\bar{Q}$_R	0.341	dimensionless
ime Step Discharge Ratio	Qr,t	Average[Q_(r,t=n)···Q_(r,t=n+N)]	0.338	dimensionless

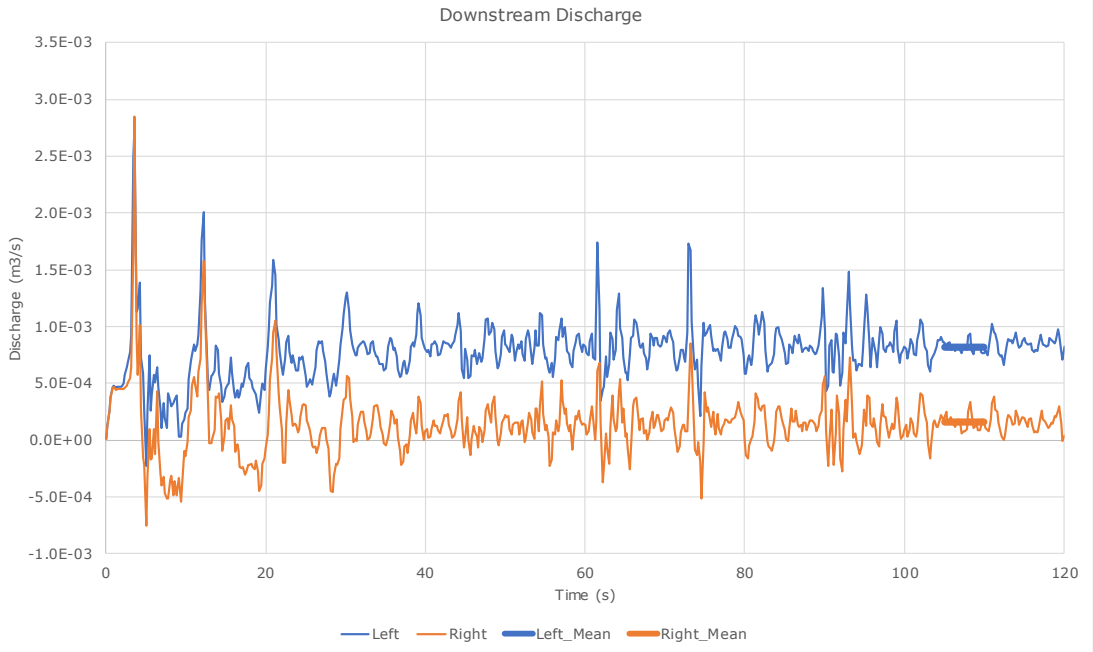


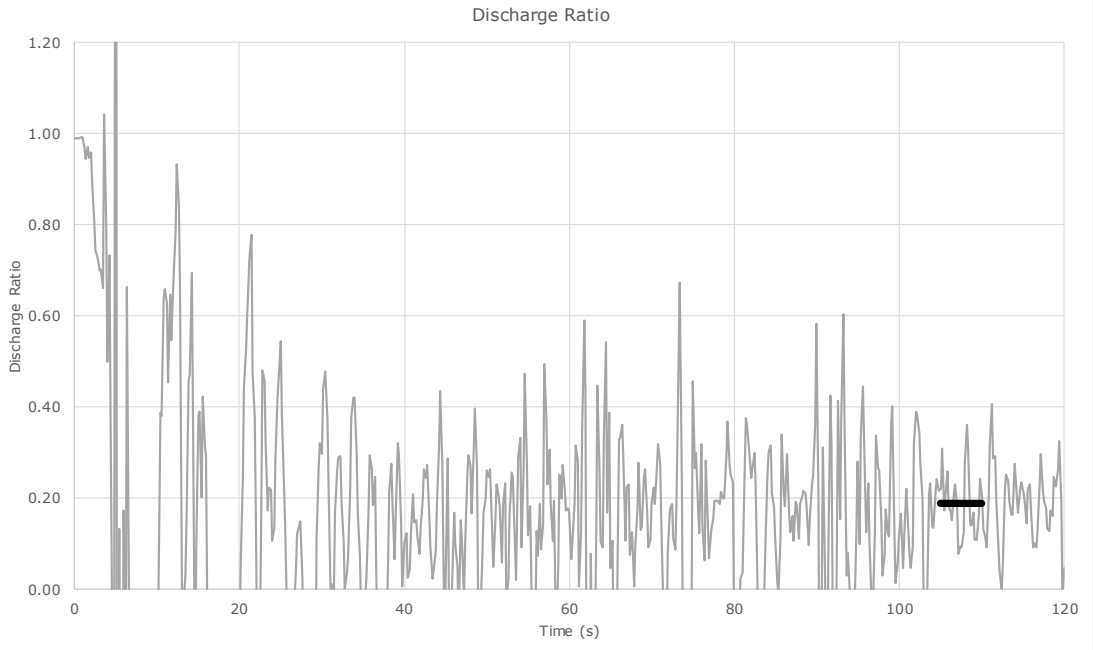


40_05_5565

Name	Symbol	Left	Right	Unit
Weir Height	WH	55	65	mm
Initial Time	Ti	105	105	s
End Time	Te	110	110	s
Initial Number	Ni	525	525	dimensionless
End Number	Ne	550	550	dimensionless
Average Discharge	$\bar{Q}$	8.158E-04	1.550E-04	m3/s

Name	Symbol	Equation	Result	Unit
Weir Height Ratio	WHr	WHL/WHR	0.846	dimensionless
Discharge Ratio	Qr	$\bar{Q}$_L/$\bar{Q}$_R	0.190	dimensionless
Time Step Discharge Ratio	Qr,t	Average[Q_(r,t=n)···Q_(r,t=n+N)]	0.188	dimensionless

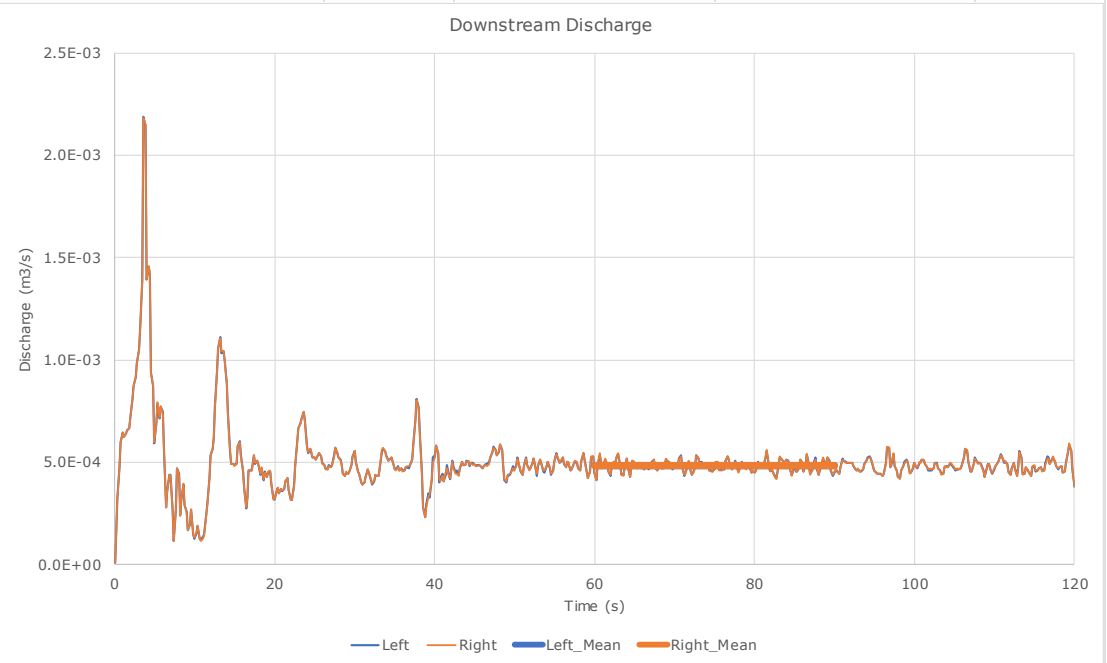


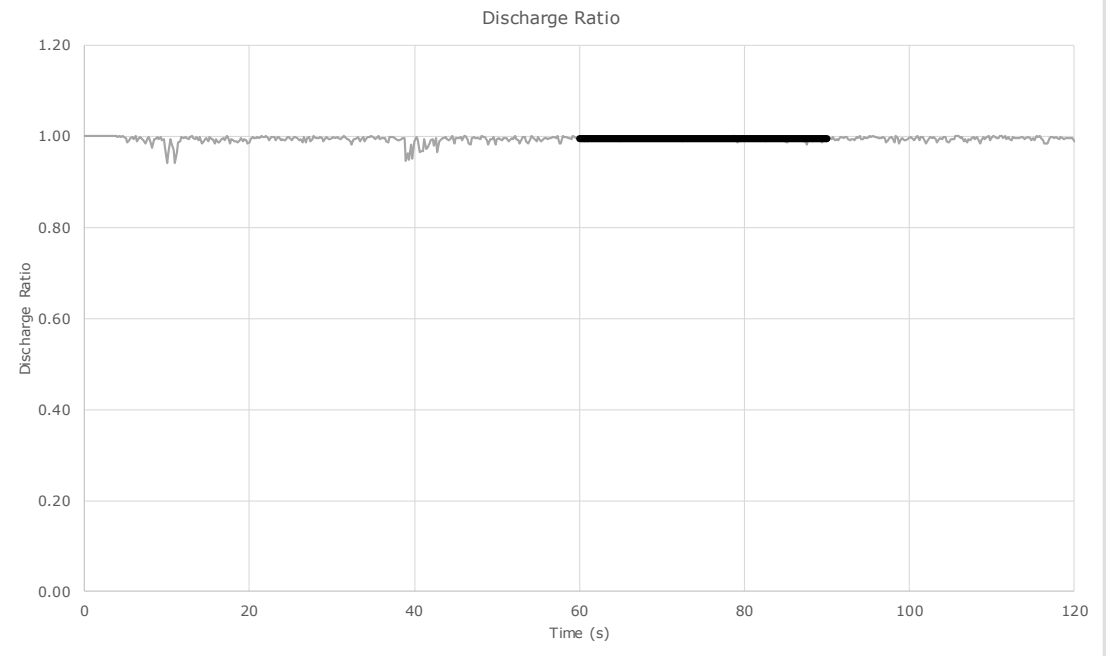


40_07_5050

Name	Symbol	Left	Right	Unit
Weir Height	WH	50	50	mm
Initial Time	Ti	60	60	s
End Time	Te	90	90	s
Initial Number	Ni	300	300	unitless
End Number	Ne	450	450	unitless
Average Discharge	$\bar{Q}$	4.823E-04	4.824E-04	m3/s

Name	Symbol	Equation	Result	Unit
Weir Height Ratio	WHr	WHL/WHR	1.000	dimensionless
Discharge Ratio	Qr	$\bar{Q}$_L/$\bar{Q}$_R	1.000	dimensionless
Time Step Discharge Ratio	Qr,t	Average[Q_(r,t=n)···Q_(r,t=n+N)]	0.995	dimensionless

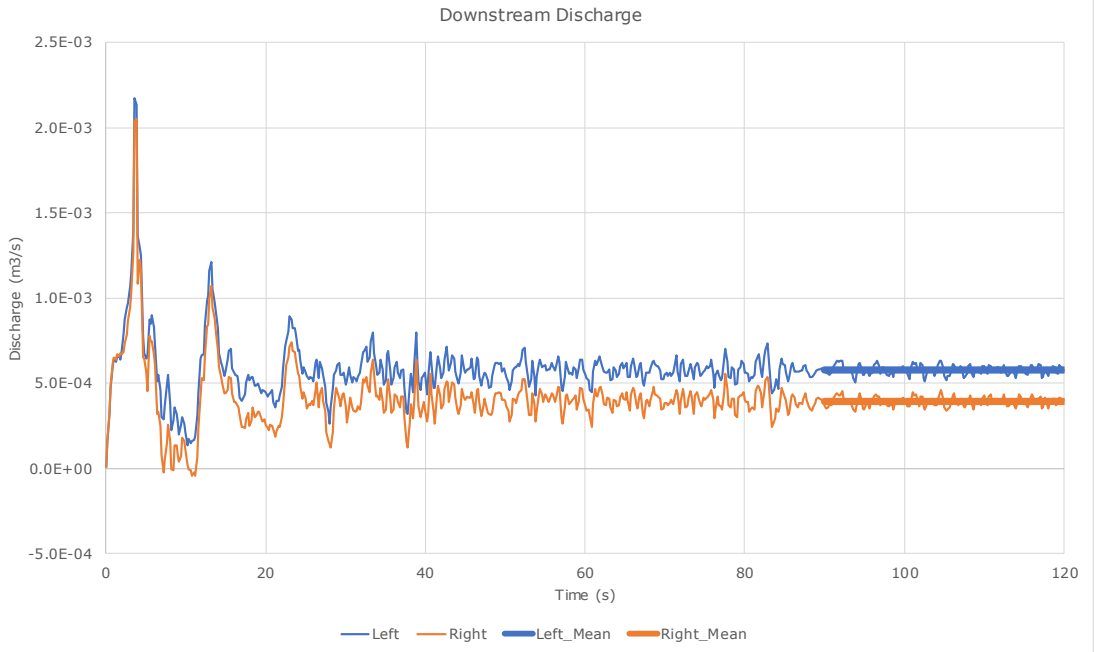


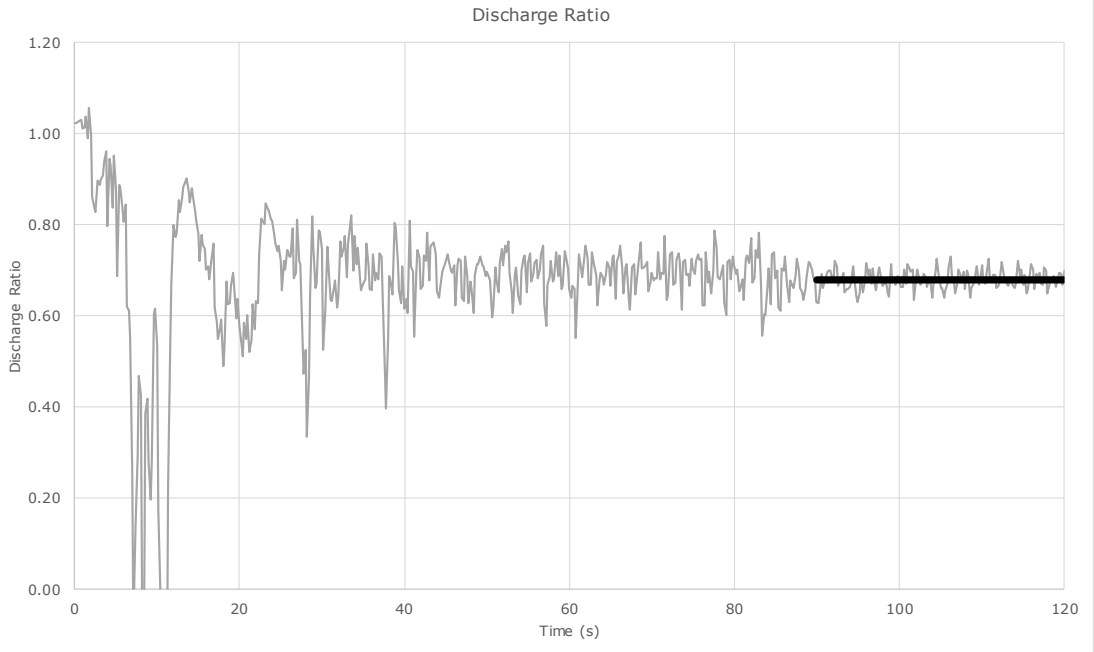


40_07_5053

Name	Symbol	Left	Right	Unit
Weir Height	WH	50	53	mm
Initial Time	Ti	90	90	s
End Time	Te	120	120	s
nitial Number	Ni	450	450	unitless
End Number	Ne	600	600	unitless
erage Discharge	$\bar{Q}$	5.784E-04	3.932E-04	m3/s

Name	Symbol	Equation	Result	Unit
eir Height Ratio	WHr	WHL/WHR	0.943	dimensionless
ischarge Ratio	Qr	$\bar{Q}$_L/$\bar{Q}$_R	0.680	dimensionless
tep Discharge Ratio	Qr,t	Average[Q_(r,t=n)···Q_(r,t=n+N)]	0.679	dimensionless

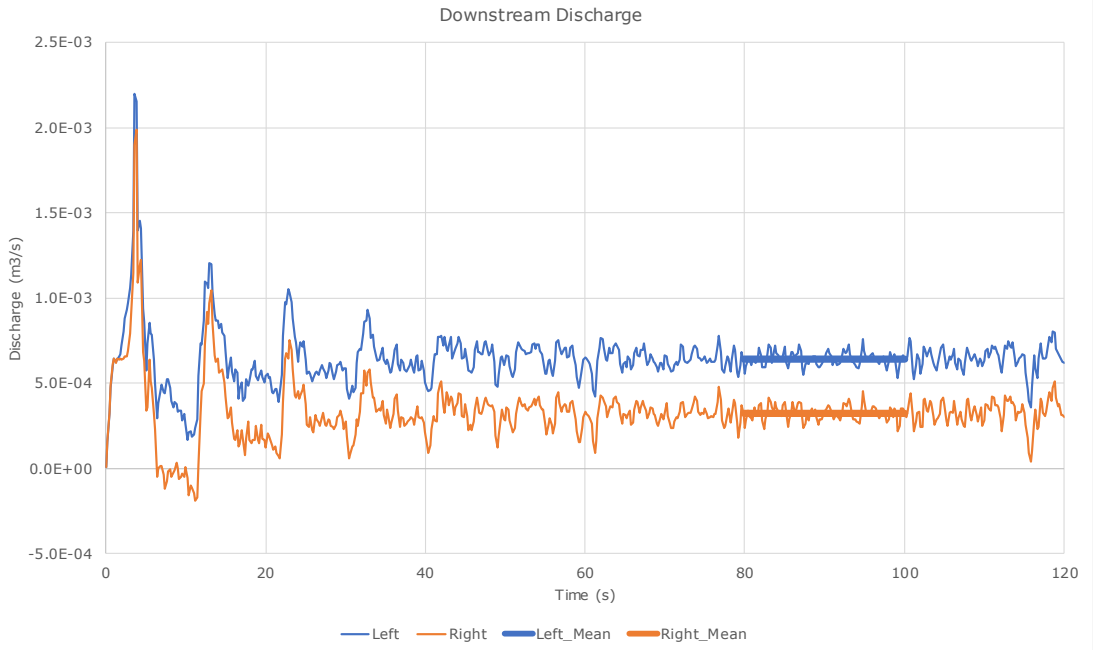


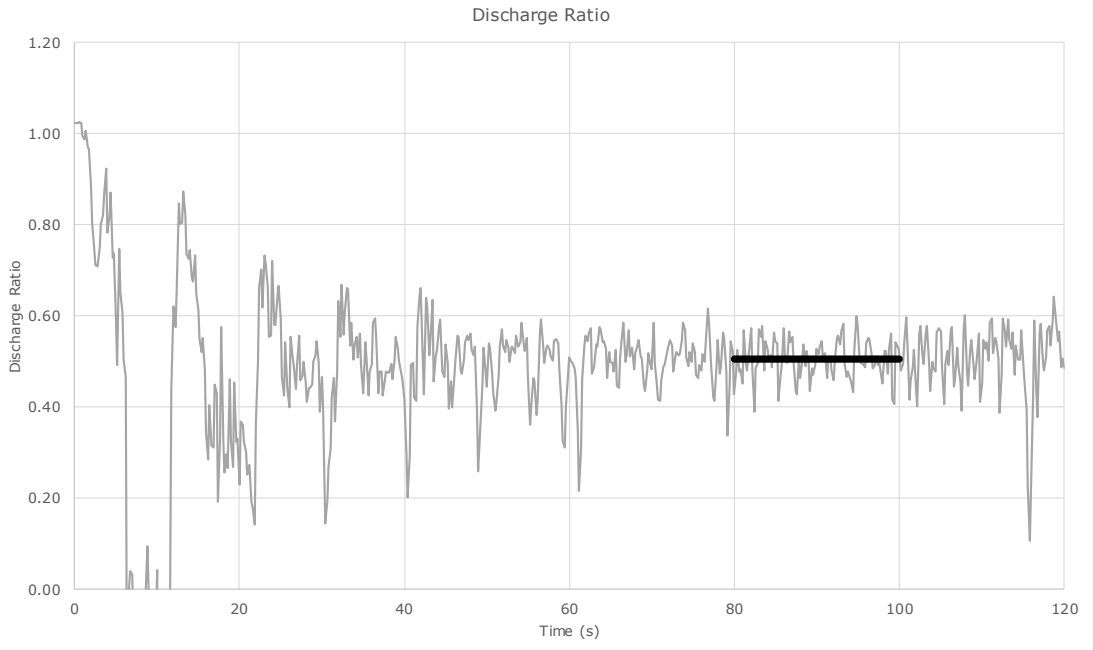


40_07_5055

lame	Symbol	Left	Right	Unit
· Height	WH	50	55	mm
al Time	Ti	80	80	s
l Time	Te	100	100	s
Number	Ni	400	400	unitless
Number	Ne	500	500	unitless
ᵢ Discharge	$\bar{Q}$	6.443E-04	3.266E-04	m3/s

lame	Symbol	Equation	Result	Unit
ₑight Ratio	WHr	WHL/WHR	0.909	dimensionless
ırge Ratio	Qr	$\bar{Q}$_L/$\bar{Q}$_R	0.507	dimensionless
Discharge Ratio	Qr,t	Average[Q_(r,t=n)···Q_(r,t=n+N)]	0.505	dimensionless

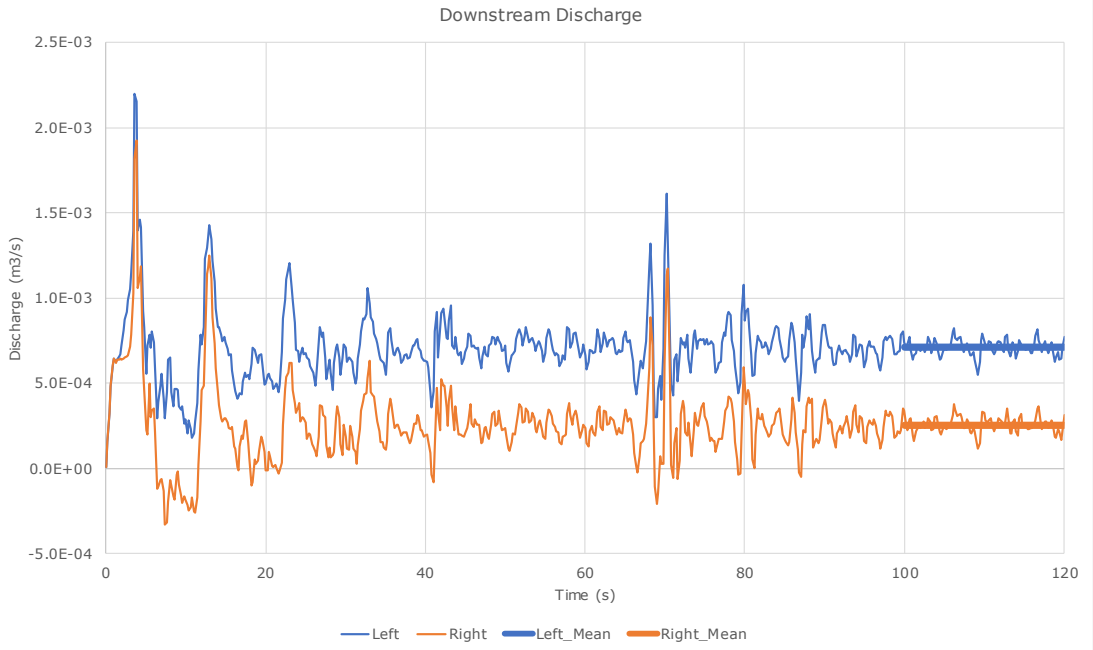


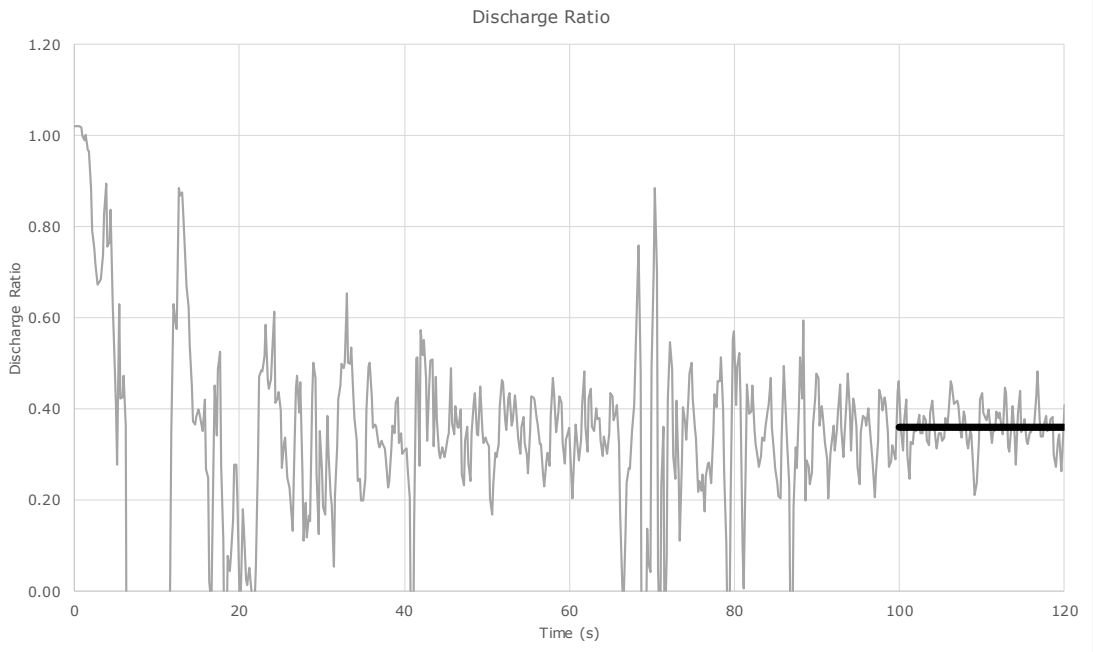


40_07_5057

	Symbol	Left	Right	Unit
	WH	50	57	mm
	Ti	100	100	s
	Te	120	120	s
ır	Ni	500	500	unitless
·	Ne	600	600	unitless
ırge	Q¯	7.098E-04	2.572E-04	m3/s

	Symbol	Equation	Result	Unit
ıtio	WHr	WHL/WHR	0.877	dimensionless
io	Qr	Q¯_L/Q¯_R	0.362	dimensionless
ıe Ratio	Qr,t	Average[Q_(r,t=n)···Q_(r,t=n+N)]	0.360	dimensionless

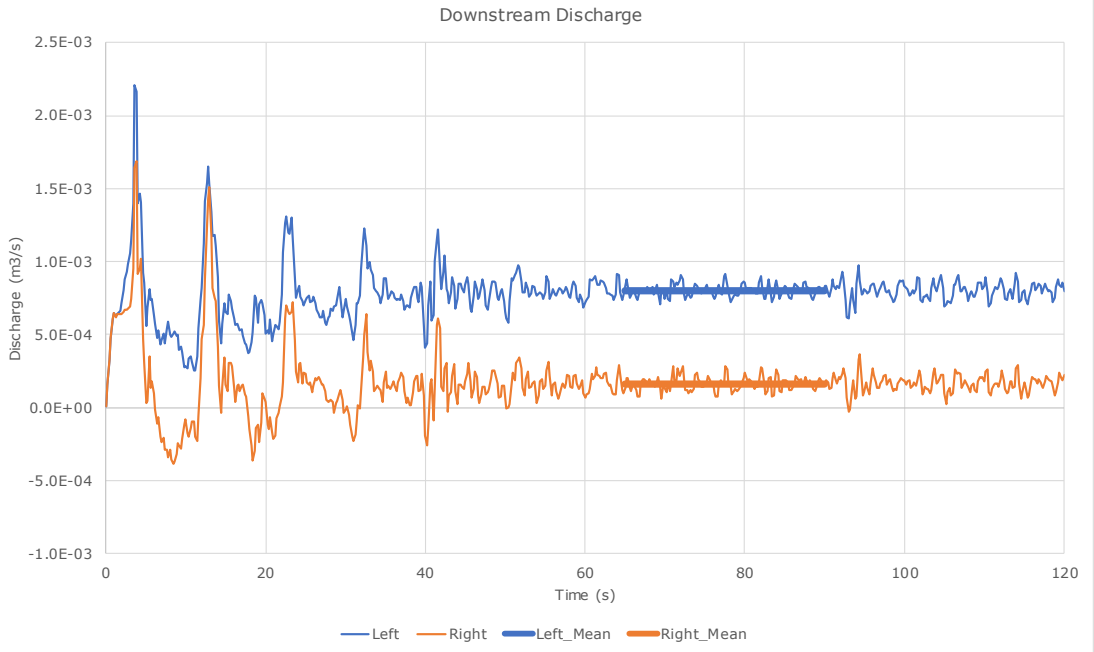


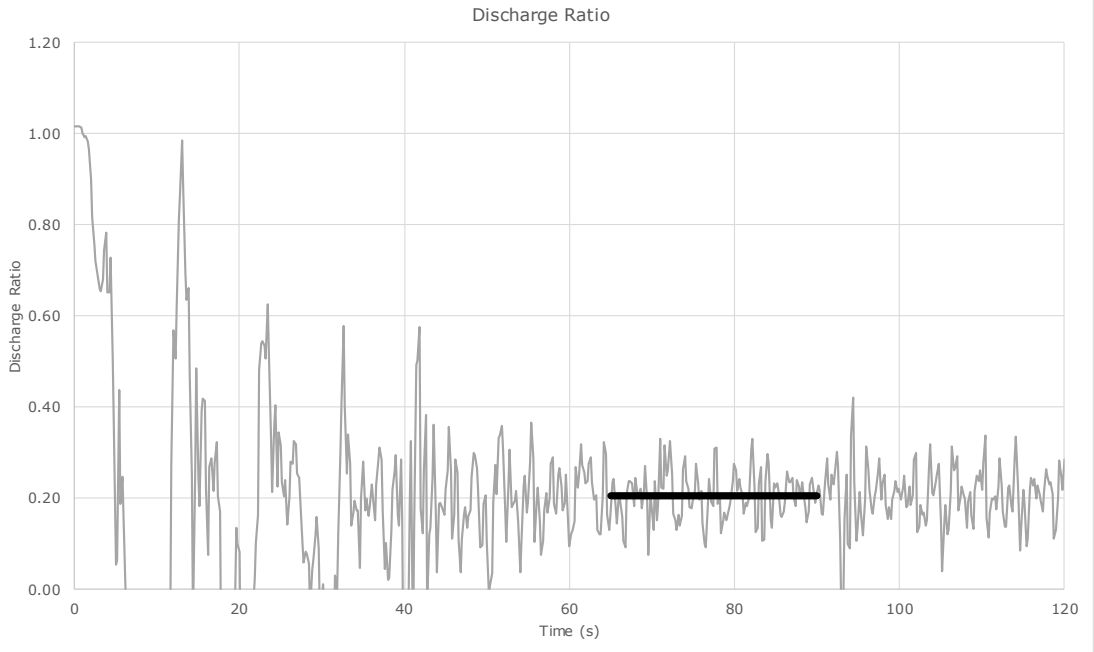


40_07_5060

Name	Symbol	Left	Right	Unit
Weir Height	WH	50	60	mm
Initial Time	Ti	65	65	s
End Time	Te	90	90	s
Initial Number	Ni	325	325	dimensionless
End Number	Ne	450	450	dimensionless
Average Discharge	$\bar{Q}$	8.044E-04	1.656E-04	m3/s

Name	Symbol	Equation	Result	Unit
Weir Height Ratio	WHr	WHL/WHR	0.833	dimensionless
Discharge Ratio	Qr	$\bar{Q}$_L/$\bar{Q}$_R	0.206	dimensionless
Time Step Discharge Ratio	Qr,t	Average[Q_(r,t=n)···Q_(r,t=n+N)]	0.204	dimensionless

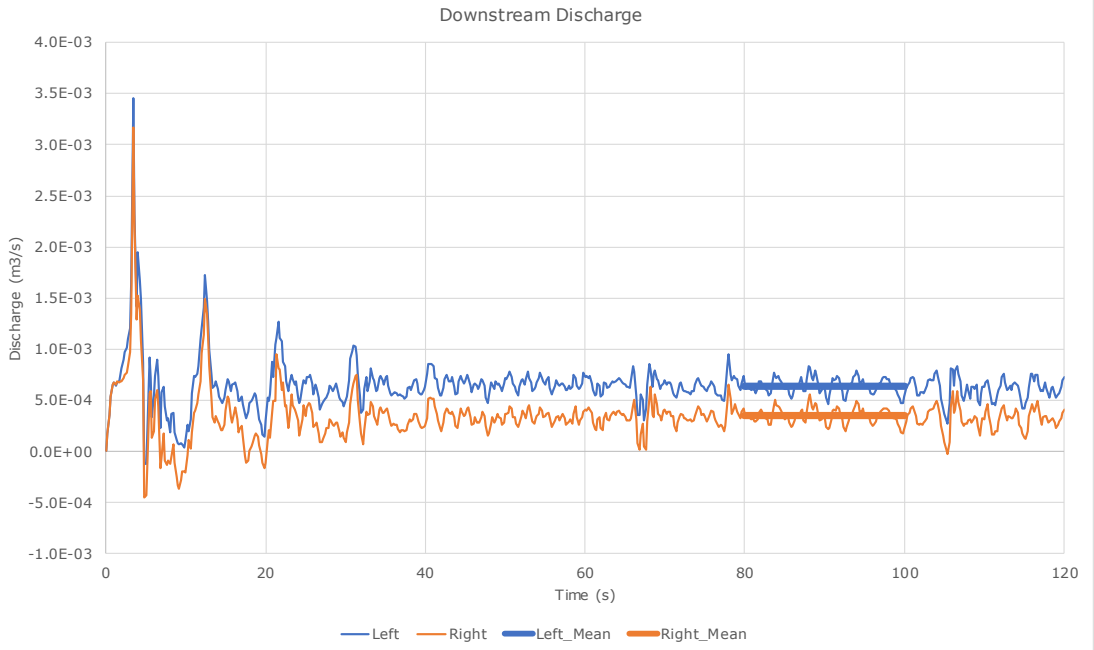


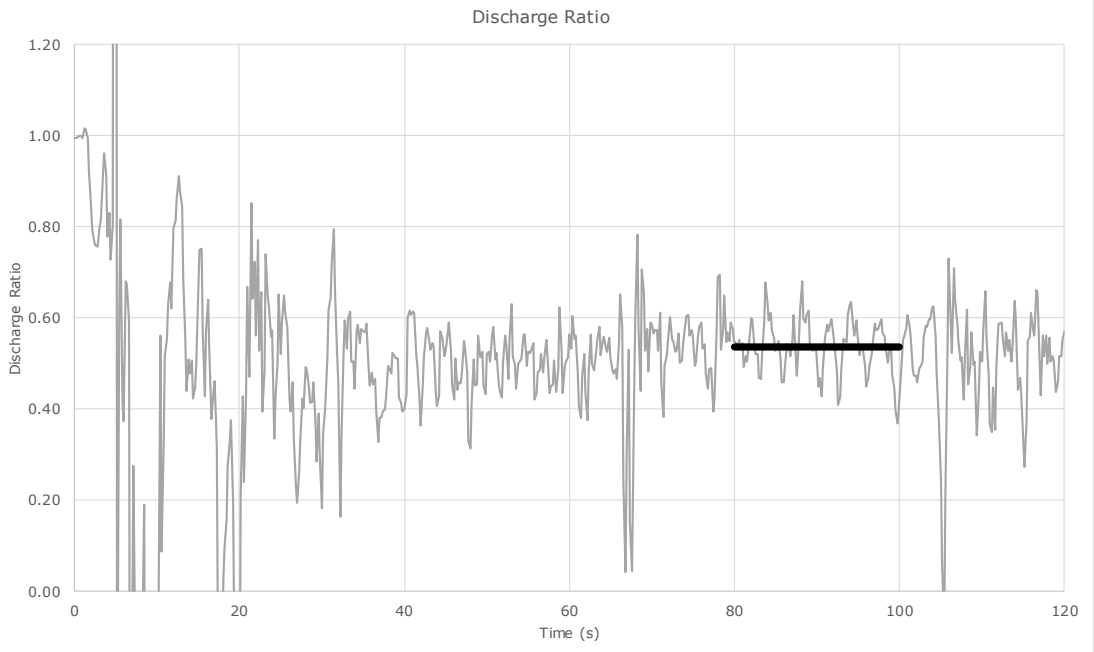


40_07_5560

Name	Symbol	Left	Right	Unit
Weir Height	WH	55	60	mm
Initial Time	Ti	80	80	s
End Time	Te	100	100	s
Initial Number	Ni	400	400	dimensionless
End Number	Ne	500	500	dimensionless
verage Discharge	$\bar{Q}$	6.427E-04	3.486E-04	m3/s

Name	Symbol	Equation	Result	Unit
Weir Height Ratio	WHr	WHL/WHR	0.917	dimensionless
Discharge Ratio	Qr	$\bar{Q}$_L/$\bar{Q}$_R	0.542	dimensionless
Step Discharge Ratio	Qr,t	Average[Q_(r,t=n)···Q_(r,t=n+N)]	0.536	dimensionless

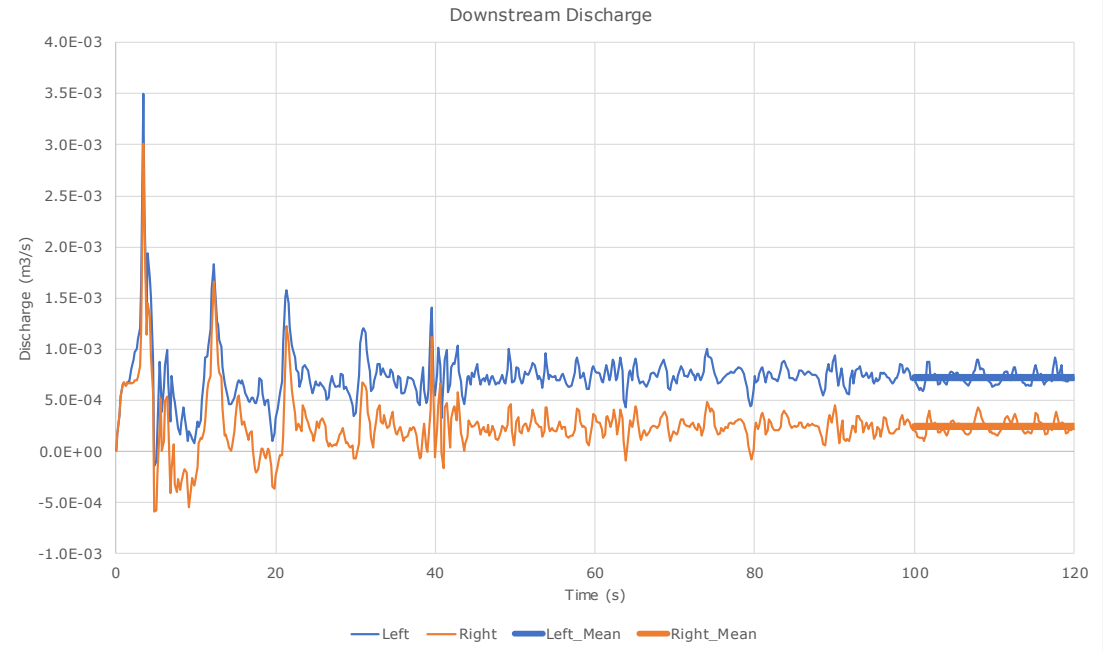


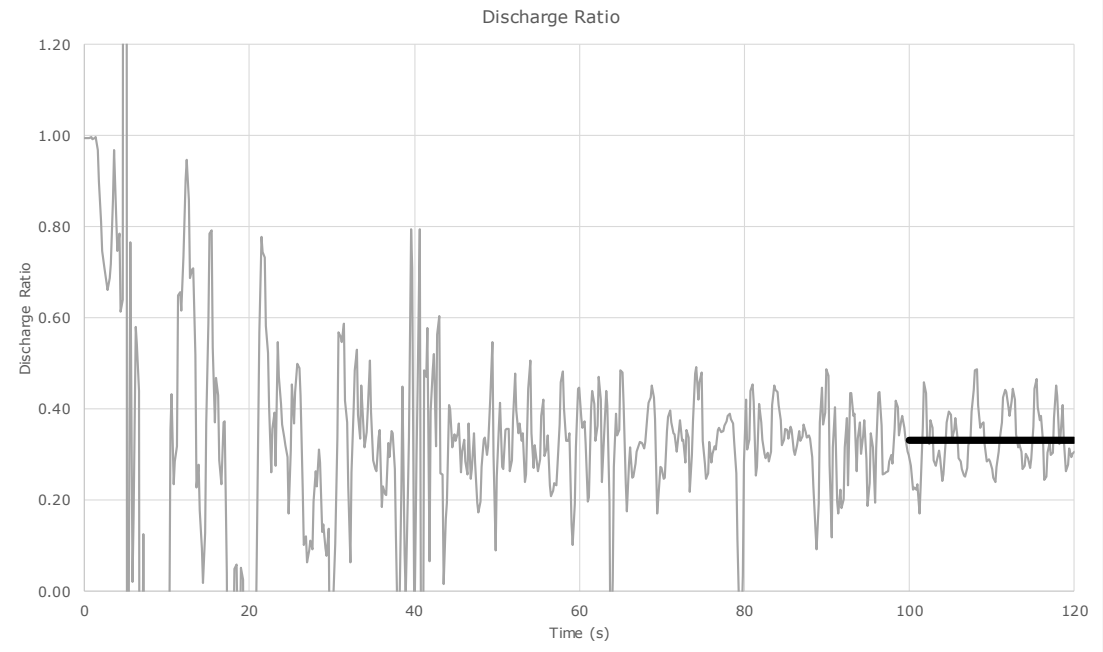


40_07_5562

ne	Symbol	Left	Right	Unit
eight	WH	55	62	mm
Time	Ti	100	100	s
ime	Te	120	120	s
umber	Ni	500	500	dimensionless
mber	Ne	600	600	dimensionless
ischarge	$\bar{Q}$	7.250E-04	2.433E-04	m3/s

ne	Symbol	Equation	Result	Unit
ht Ratio	WHr	WHL/WHR	0.887	dimensionless
e Ratio	Qr	$\bar{Q}$_L/$\bar{Q}$_R	0.336	dimensionless
charge Ratio	Qr,t	Average[Q_(r,t=n)···Q_(r,t=n+N)]	0.331	dimensionless

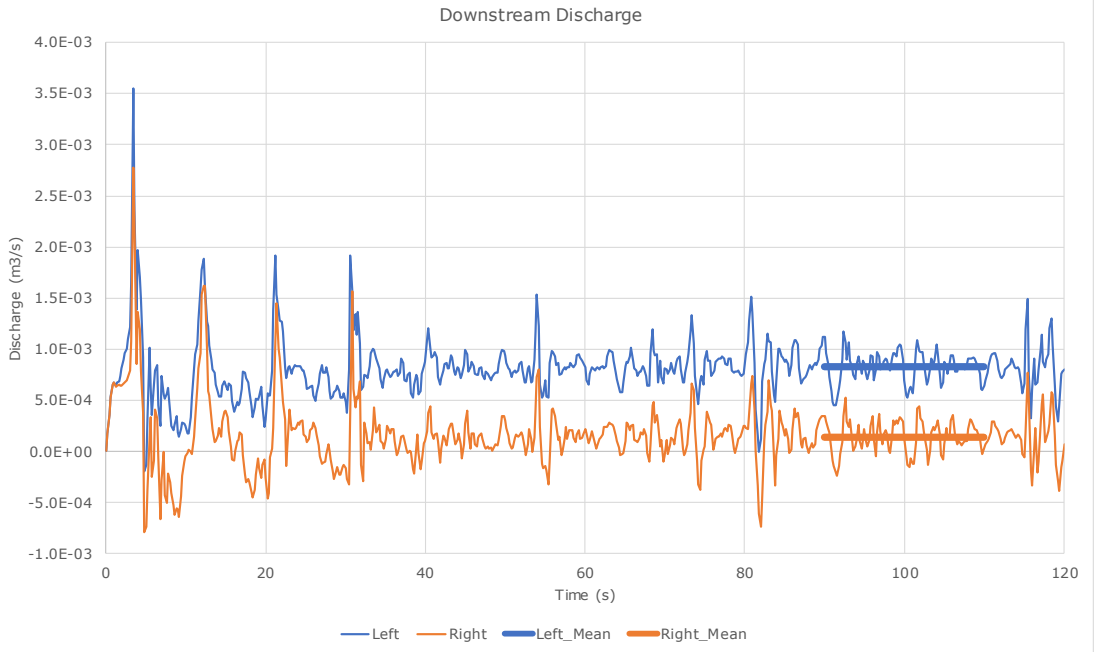


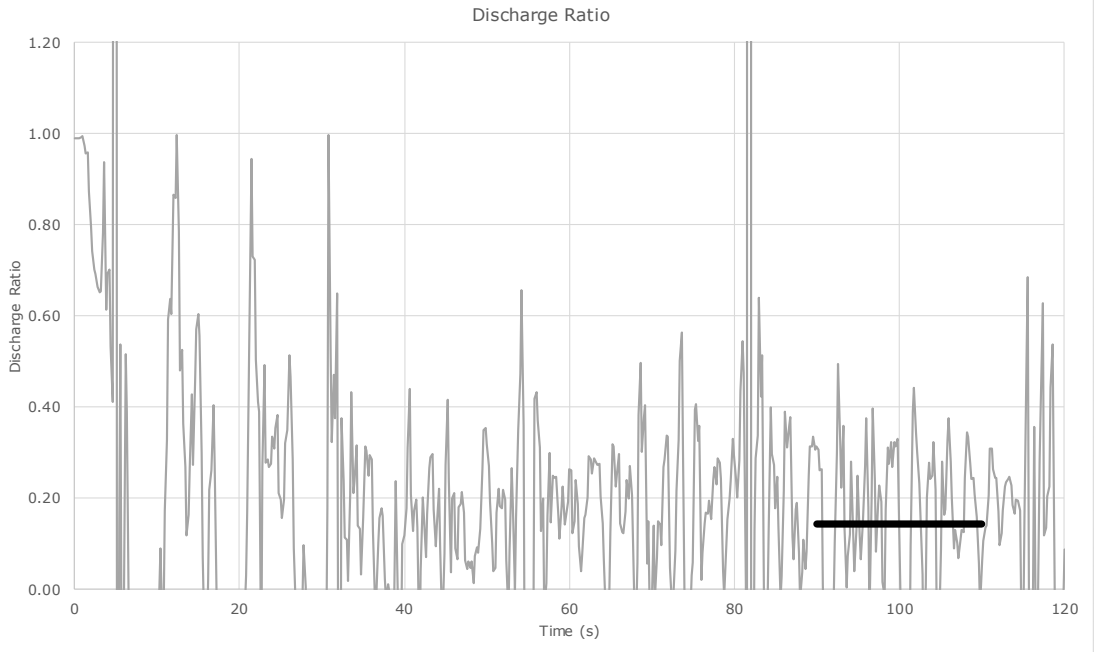


40_07_5565

Name	Symbol	Left	Right	Unit
Weir Height	WH	55	65	mm
Initial Time	Ti	90	90	s
End Time	Te	110	110	s
Initial Number	Ni	450	450	dimensionless
End Number	Ne	550	550	dimensionless
Average Discharge	$\bar{Q}$	8.267E-04	1.417E-04	m3/s

Name	Symbol	Equation	Result	Unit
Weir Height Ratio	WHr	WHL/WHR	0.846	dimensionless
Discharge Ratio	Qr	$\bar{Q}$_L/$\bar{Q}$_R	0.171	dimensionless
Time Step Discharge Ratio	Qr,t	Average[Q_(r,t=n)···Q_(r,t=n+N)]	0.143	dimensionless

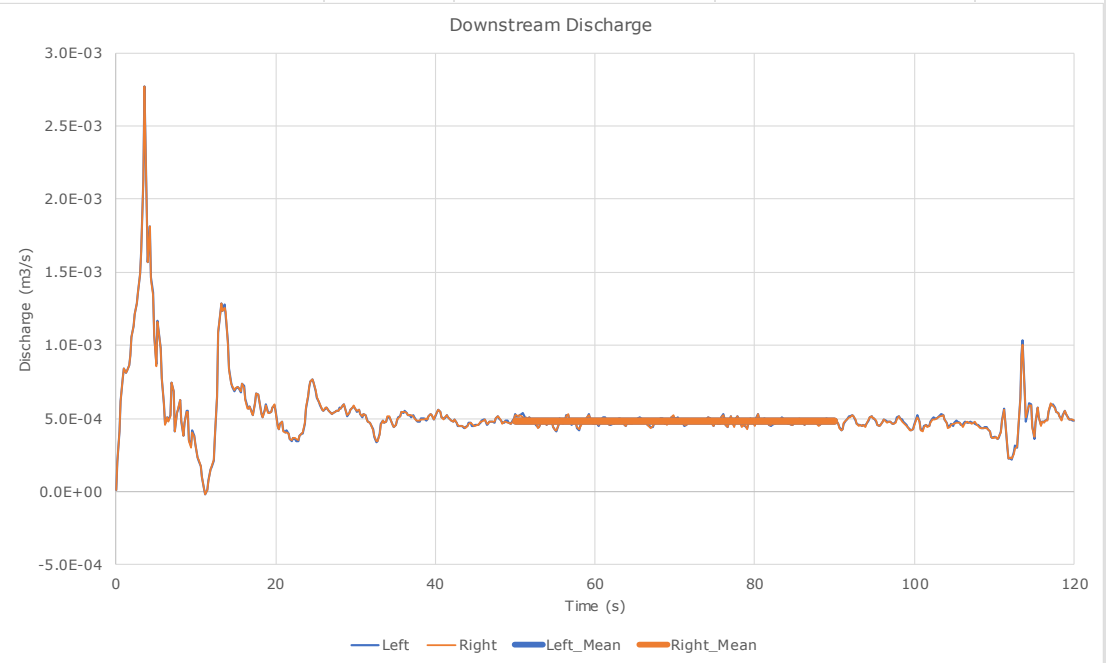


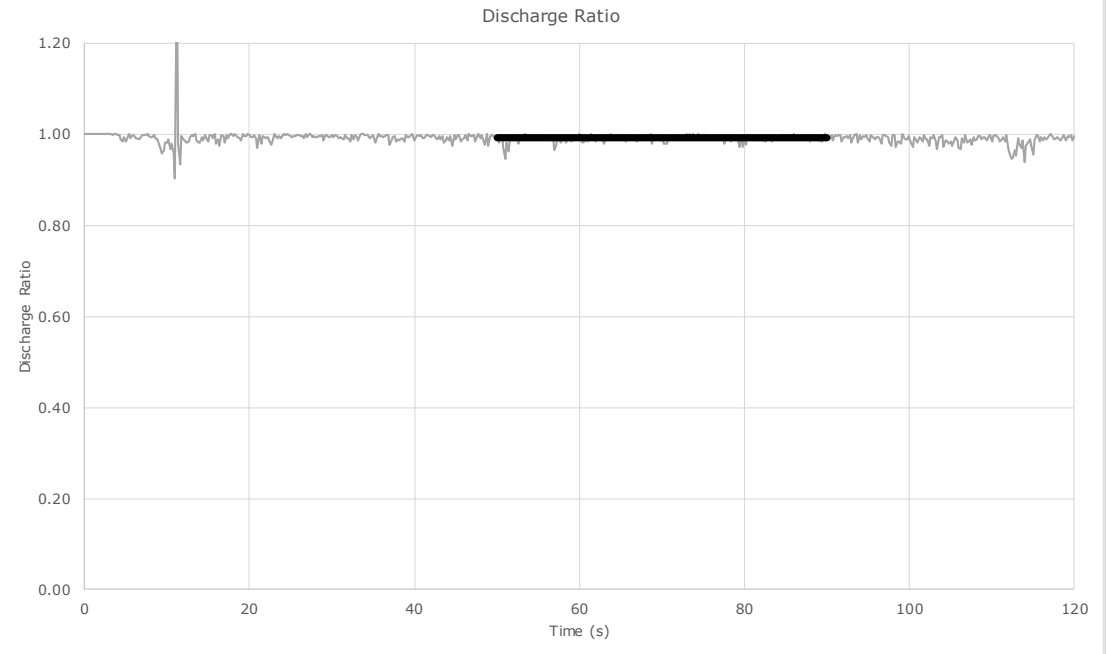


40_09_5050

Name	Symbol	Left	Right	Unit
Weir Height	WH	50	50	mm
Initial Time	Ti	50	50	s
End Time	Te	90	90	s
Initial Number	Ni	250	250	unitless
End Number	Ne	450	450	unitless
Average Discharge	$\bar{Q}$	4.795E-04	4.790E-04	m3/s

Name	Symbol	Equation	Result	Unit
Weir Height Ratio	WHr	WHL/WHR	1.000	dimensionless
Discharge Ratio	Qr	$\bar{Q}$_L/$\bar{Q}$_R	0.999	dimensionless
Time Step Discharge Ratio	Qr,t	Average[Q_(r,t=n)···Q_(r,t=n+N)]	0.991	dimensionless

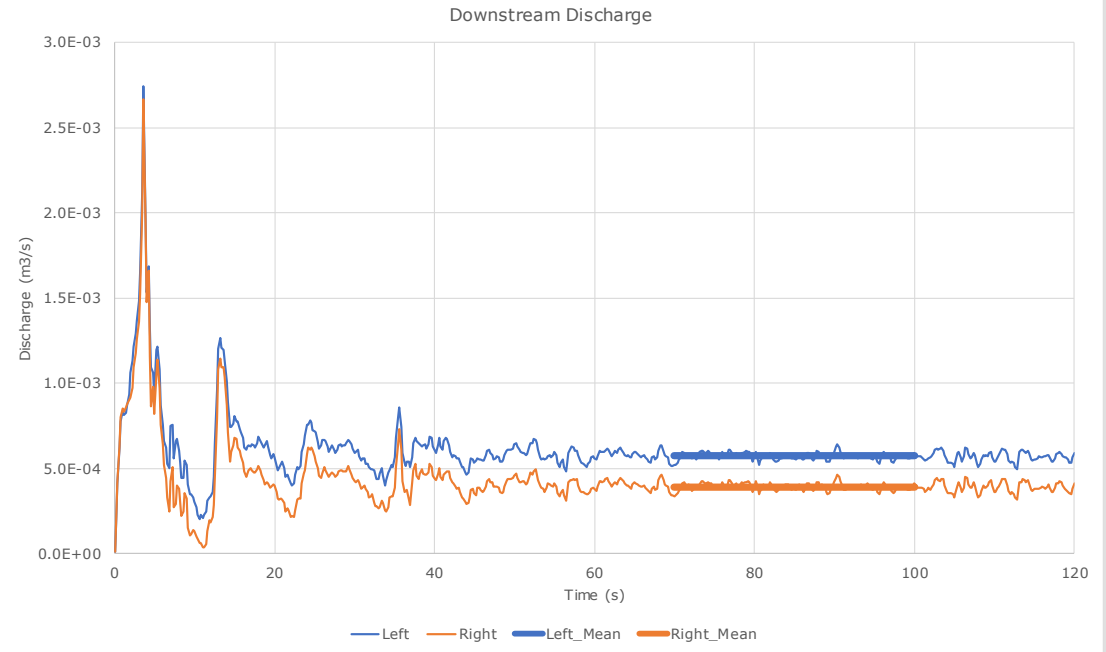


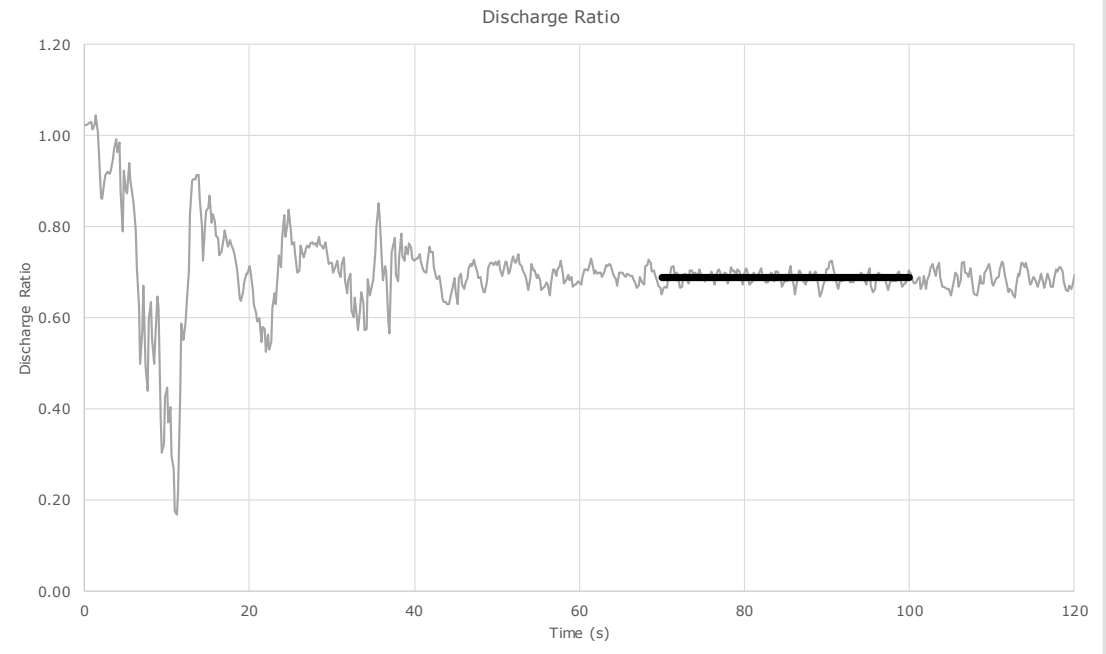


40_09_5053

ame	Symbol	Left	Right	Unit
Height	WH	50	53	mm
ıl Time	Ti	70	70	s
Time	Te	100	100	s
Number	Ni	350	350	unitless
Number	Ne	500	500	unitless
Discharge	$\bar{Q}$	5.727E-04	3.943E-04	m3/s

ame	Symbol	Equation	Result	Unit
ight Ratio	WHr	WHL/WHR	0.943	dimensionless
rge Ratio	Qr	$\bar{Q}$_L/$\bar{Q}$_R	0.688	dimensionless
ischarge Ratio	Qr,t	Average[Q_(r,t=n)···Q_(r,t=n+N)]	0.688	dimensionless

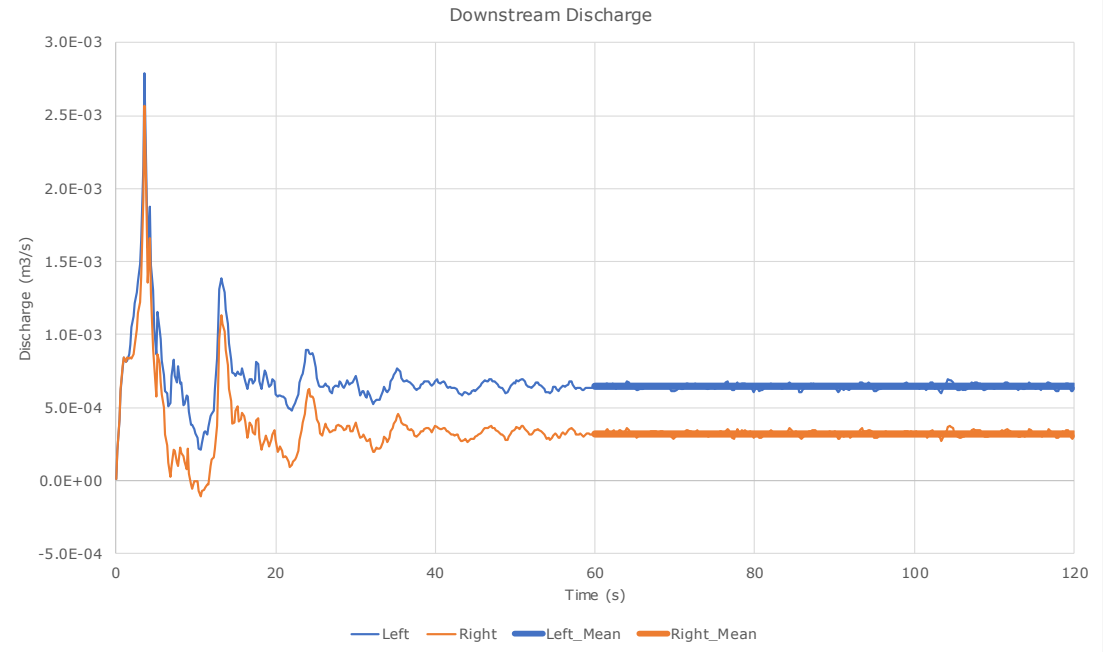


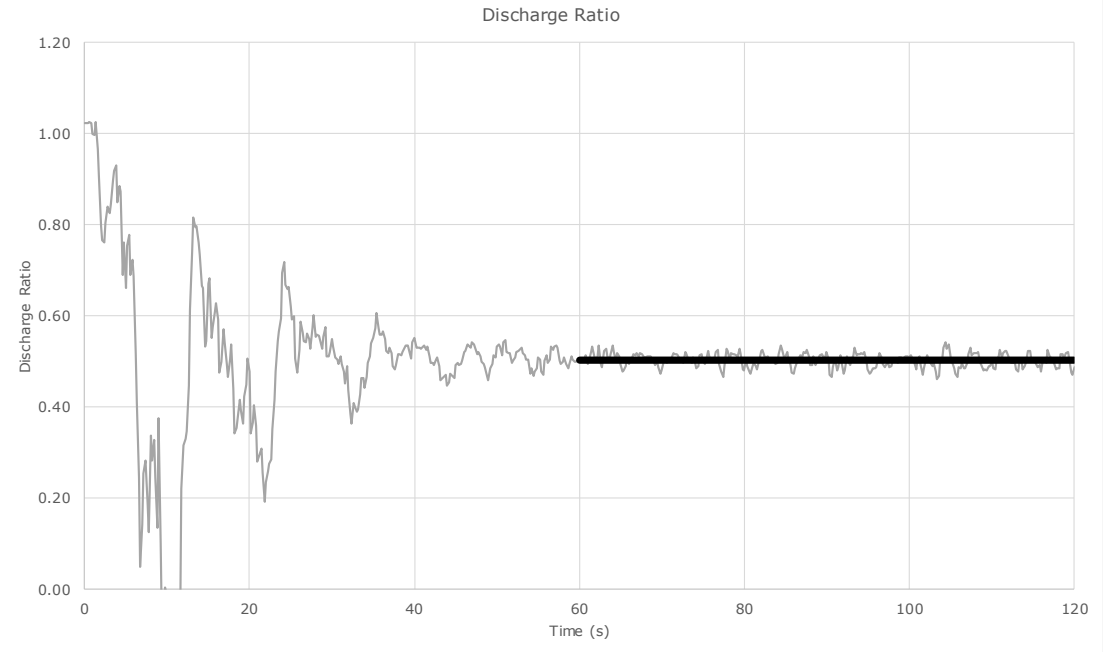


40_09_5055

ne	Symbol	Left	Right	Unit
eight	WH	50	55	mm
Time	Ti	60	60	s
ime	Te	120	120	s
umber	Ni	300	300	unitless
mber	Ne	600	600	unitless
ischarge	$\bar{Q}$	6.450E-04	3.240E-04	m3/s

ne	Symbol	Equation	Result	Unit
ht Ratio	WHr	WHL/WHR	0.909	dimensionless
e Ratio	Qr	$\bar{Q}$_L/$\bar{Q}$_R	0.502	dimensionless
charge Ratio	Qr,t	Average[Q_(r,t=n)···Q_(r,t=n+N)]	0.502	dimensionless

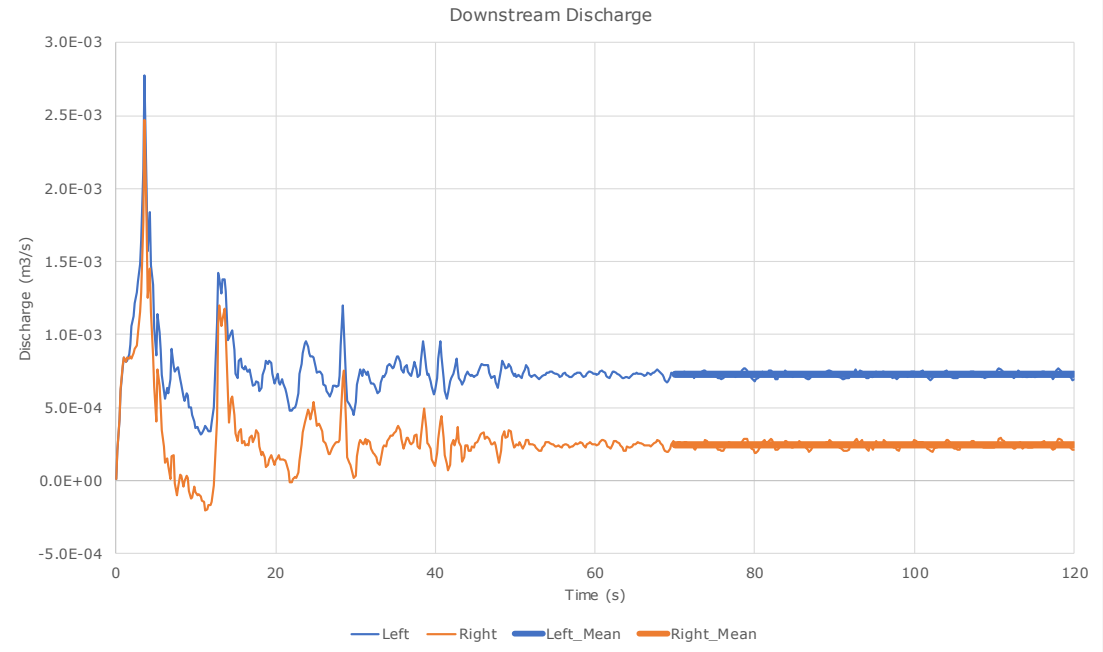


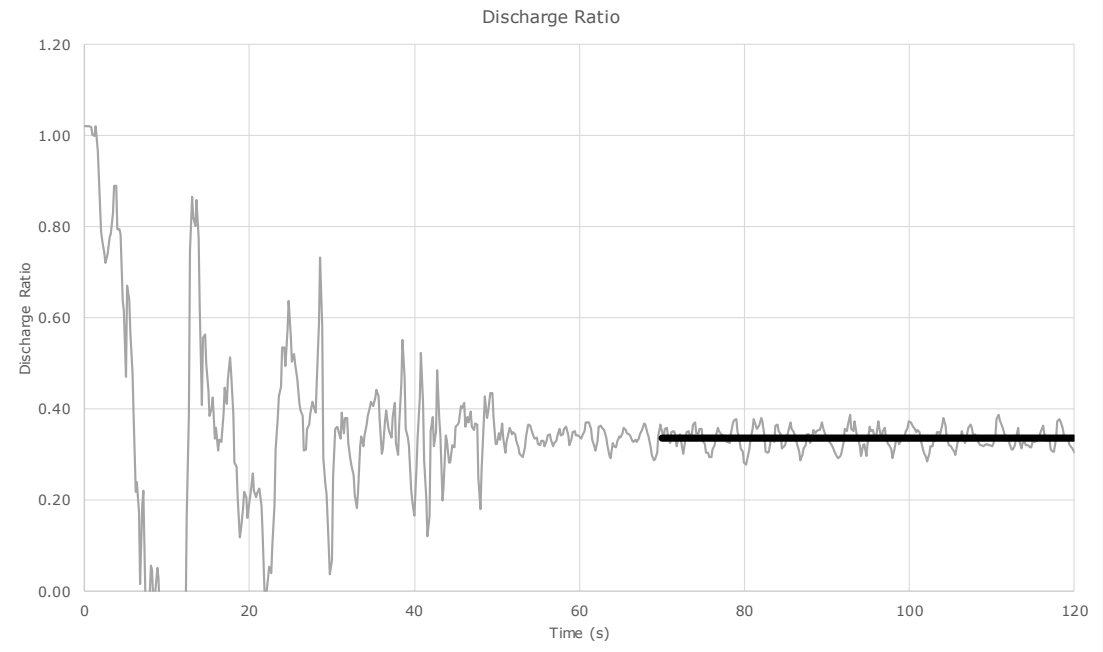


40_09_5057

Name	Symbol	Left	Right	Unit
Weir Height	WH	50	57	mm
Initial Time	Ti	70	70	s
End Time	Te	120	120	s
Initial Number	Ni	350	350	unitless
End Number	Ne	600	600	unitless
Average Discharge	$\bar{Q}$	7.259E-04	2.438E-04	m3/s

Name	Symbol	Equation	Result	Unit
Weir Height Ratio	WHr	WHL/WHR	0.877	dimensionless
Discharge Ratio	Qr	$\bar{Q}$_L/$\bar{Q}$_R	0.336	dimensionless
Mean Discharge Ratio	Qr,t	Average[Q_(r,t=n)···Q_(r,t=n+N)]	0.335	dimensionless

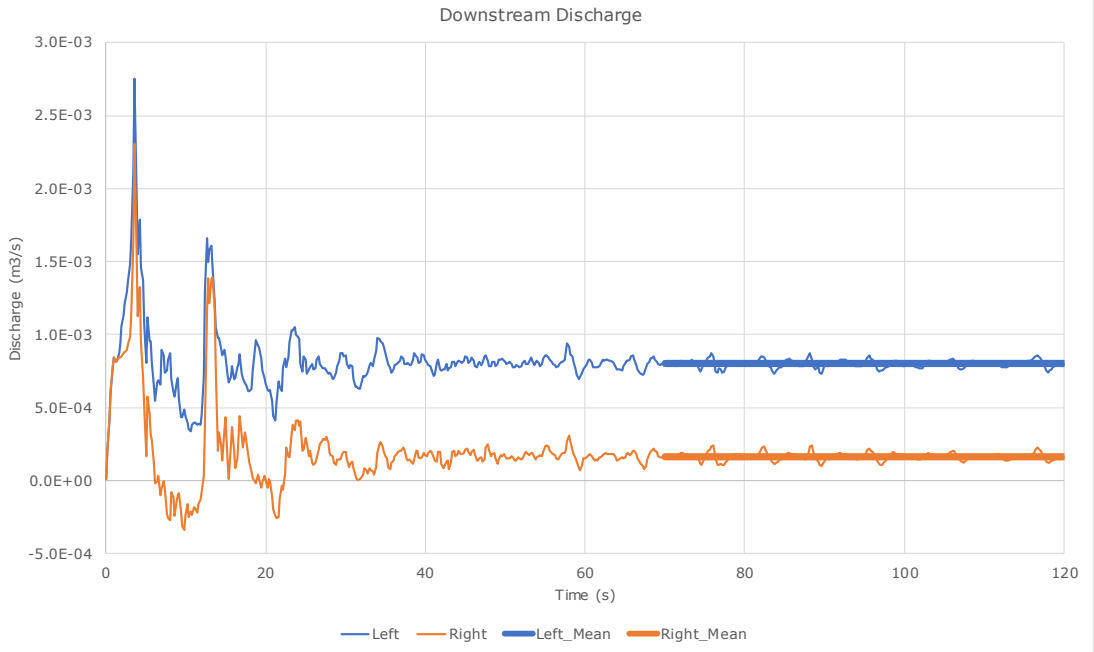


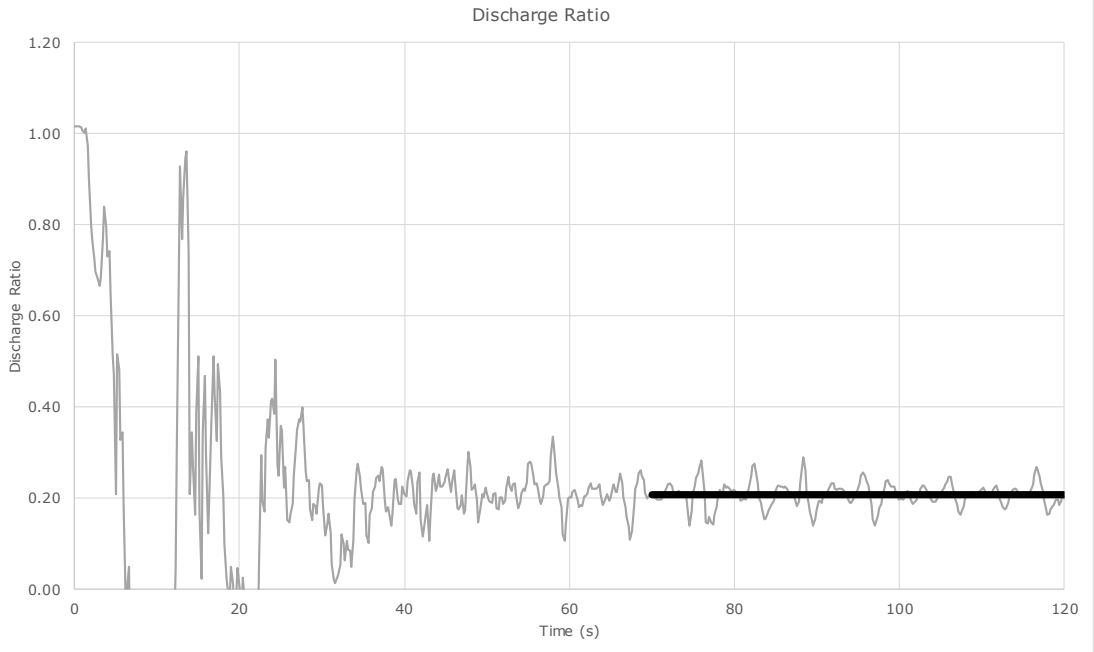


40_09_5060

Name	Symbol	Left	Right	Unit
ːir Height	WH	50	60	mm
tial Time	Ti	70	70	s
ɲd Time	Te	120	120	s
al Number	Ni	350	350	dimensionless
ɨ Number	Ne	600	600	dimensionless
ɟe Discharge	$\bar{Q}$	8.008E-04	1.664E-04	m3/s

Name	Symbol	Equation	Result	Unit
⁺eight Ratio	WHr	WHL/WHR	0.833	dimensionless
ɹarge Ratio	Qr	$\bar{Q}$_L/$\bar{Q}$_R	0.208	dimensionless
Discharge Ratio	Qr,t	Average[Q_(r,t=n)···Q_(r,t=n+N)]	0.207	dimensionless

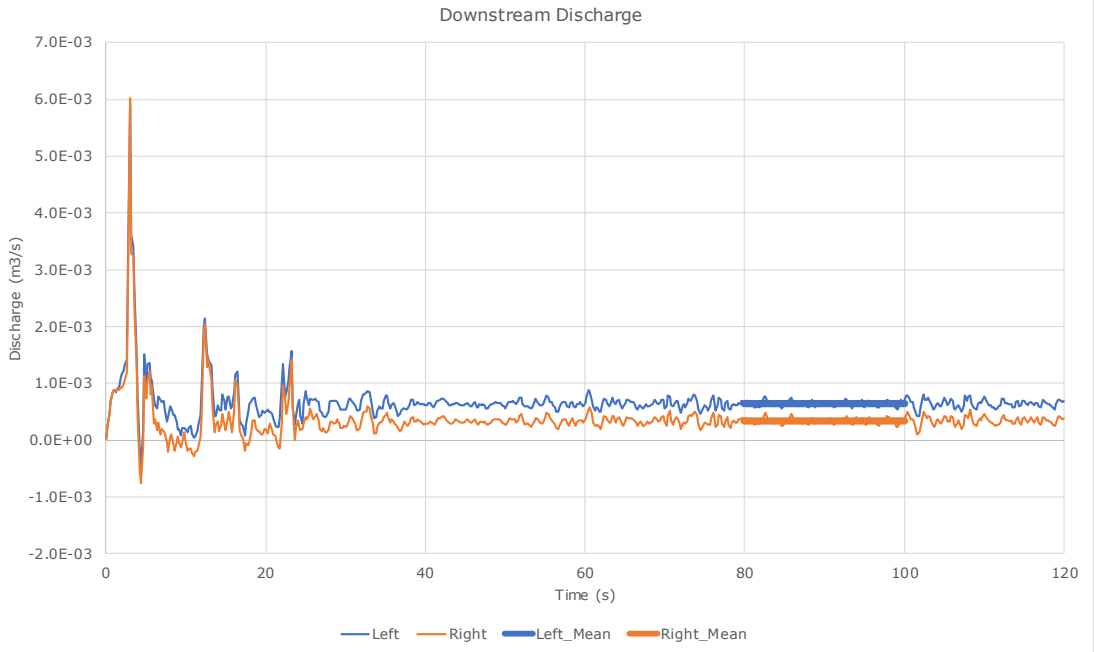


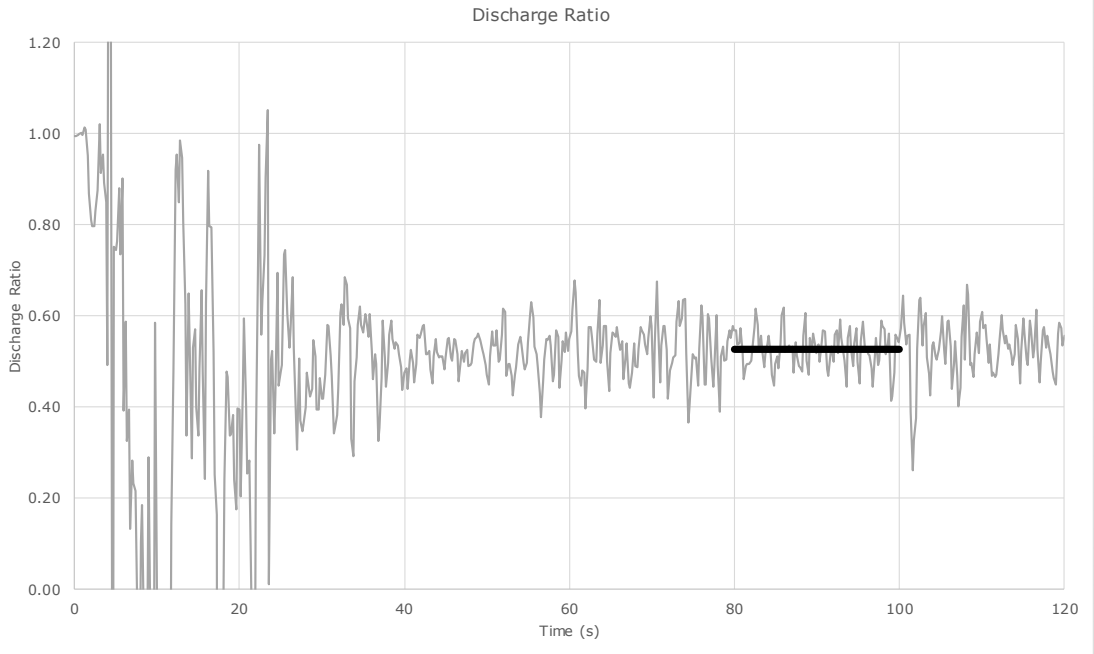


40_09_5560

ame	Symbol	Left	Right	Unit
Height	WH	55	60	mm
il Time	Ti	80	80	s
Time	Te	100	100	s
Number	Ni	400	400	dimensionless
lumber	Ne	500	500	dimensionless
Discharge	$\bar{Q}$	6.414E-04	3.383E-04	m3/s

ame	Symbol	Equation	Result	Unit
ight Ratio	WHr	WHL/WHR	0.917	dimensionless
ge Ratio	Qr	$\bar{Q}$_L/$\bar{Q}$_R	0.527	dimensionless
ischarge Ratio	Qr,t	Average[Q_(r,t=n)···Q_(r,t=n+N)]	0.525	dimensionless

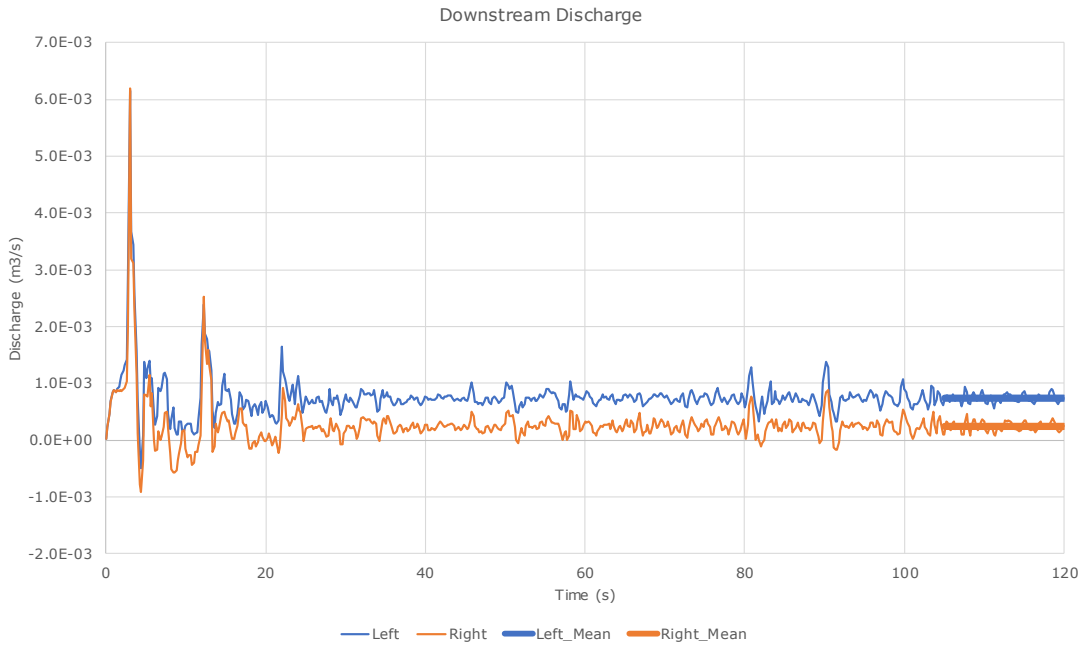


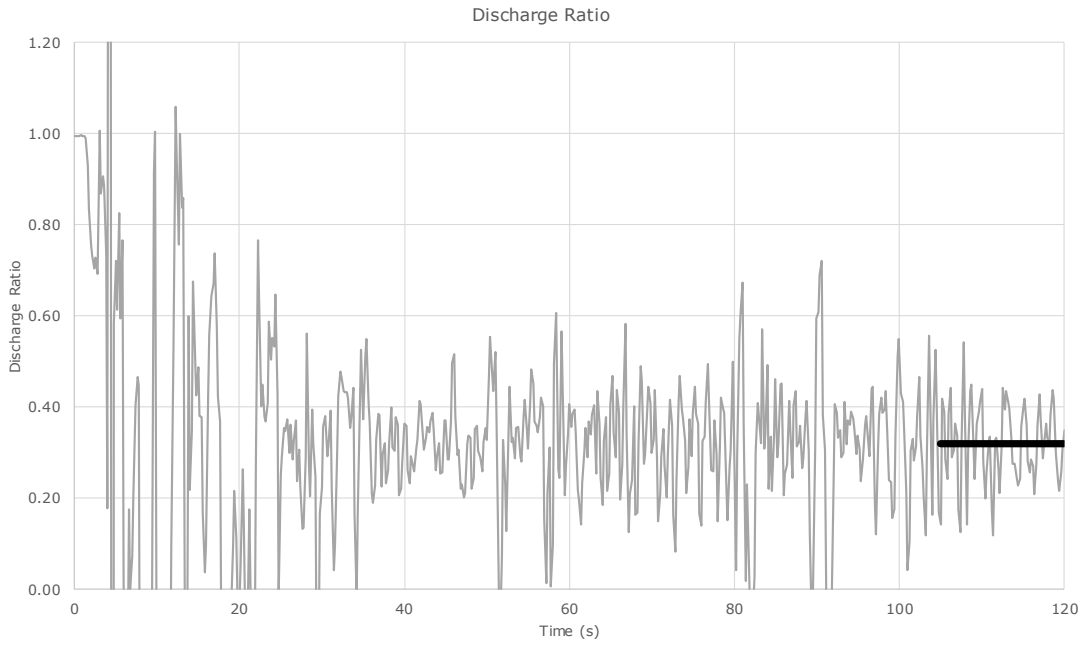


40_09_5562

Name	Symbol	Left	Right	Unit
Weir Height	WH	55	62	mm
Initial Time	Ti	105	105	s
End Time	Te	120	120	s
Initial Number	Ni	525	525	dimensionless
End Number	Ne	600	600	dimensionless
erage Discharge	$\bar{Q}$	7.407E-04	2.405E-04	m3/s

Name	Symbol	Equation	Result	Unit
'eir Height Ratio	WHr	WHL/WHR	0.887	dimensionless
)ischarge Ratio	Qr	$\bar{Q}$_L/$\bar{Q}$_R	0.325	dimensionless
;tep Discharge Ratio	Qr,t	Average[Q_(r,t=n)···Q_(r,t=n+N)]	0.319	dimensionless

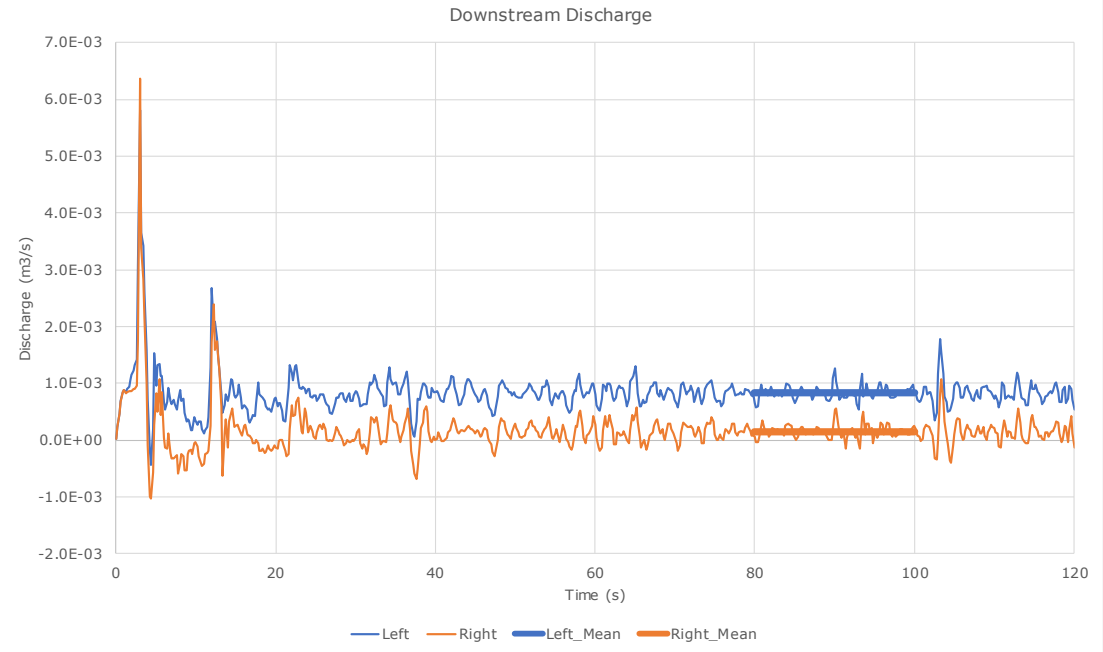


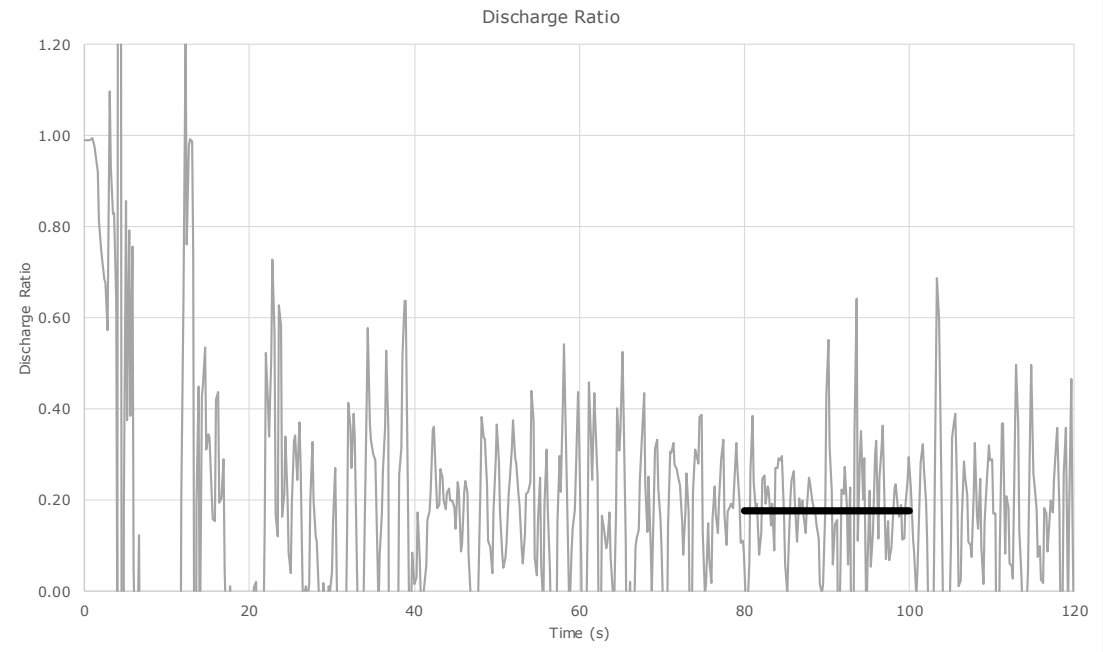


40_09_5565

ne	Symbol	Left	Right	Unit
leight	WH	55	65	mm
Time	Ti	80	80	s
ime	Te	100	100	s
lumber	Ni	400	400	dimensionless
umber	Ne	500	500	dimensionless
Discharge	Q¯	8.347E-04	1.552E-04	m3/s

ne	Symbol	Equation	Result	Unit
ht Ratio	WHr	WHL/WHR	0.846	dimensionless
e Ratio	Qr	Q¯_L/Q¯_R	0.186	dimensionless
charge Ratio	Qr,t	Average[Q_(r,t=n)···Q_(r,t=n+N)]	0.177	dimensionless

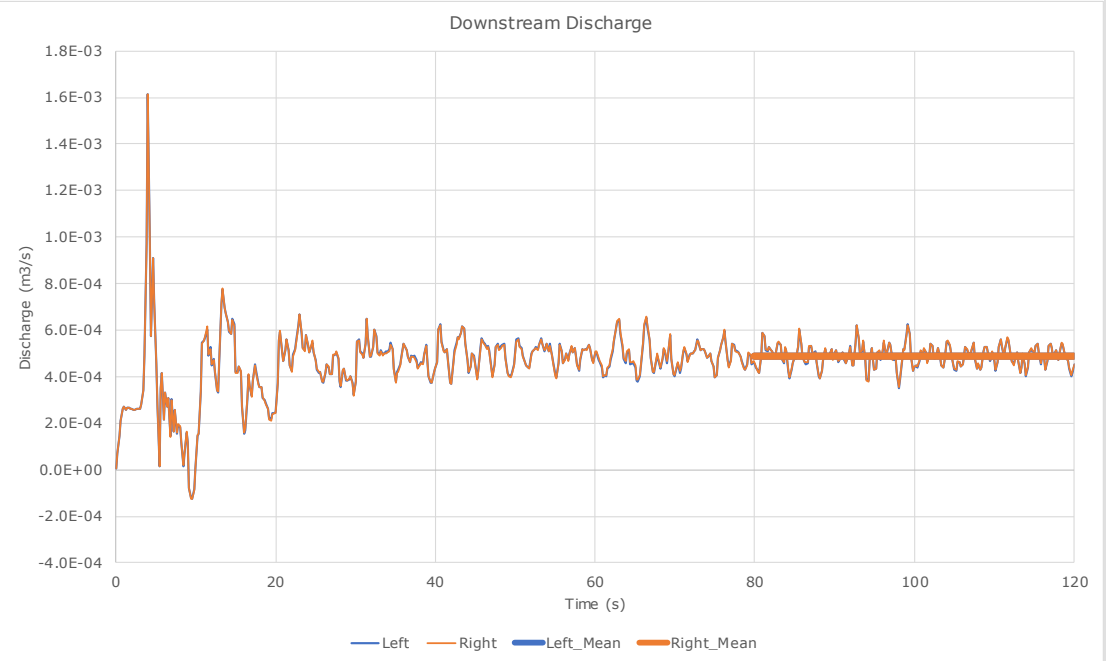


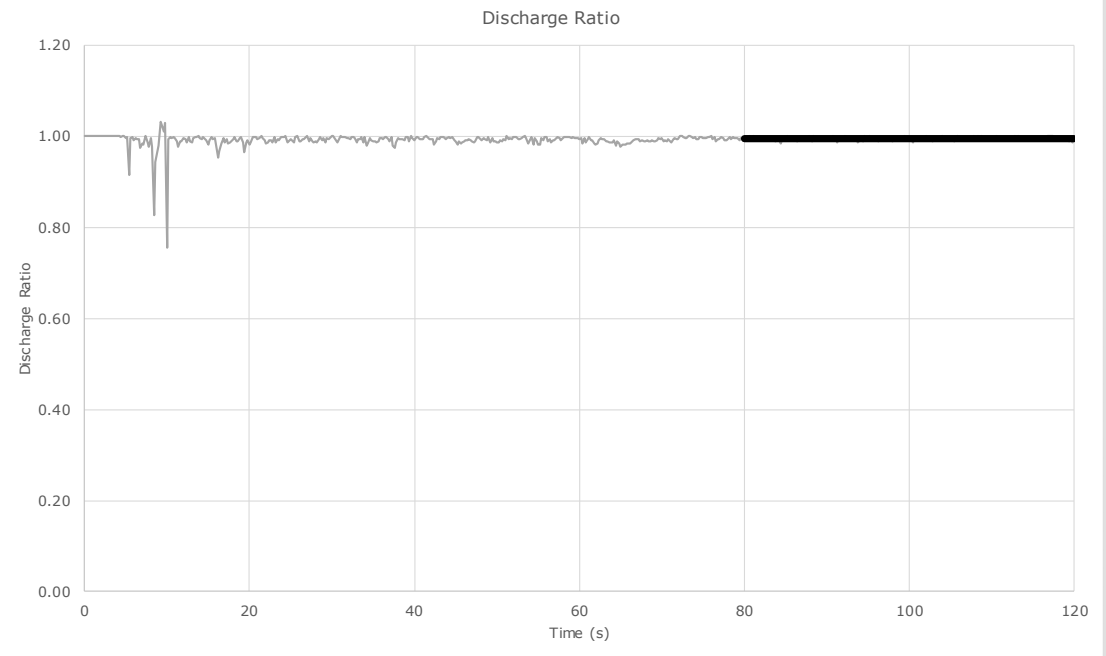


50_03_5050

Name	Symbol	Left	Right	Unit
Weir Height	WH	50	50	mm
Initial Time	Ti	80	80	s
End Time	Te	120	120	s
Initial Number	Ni	400	400	unitless
End Number	Ne	600	600	unitless
Average Discharge	$\bar{Q}$	4.880E-04	4.897E-04	m3/s

Name	Symbol	Equation	Result	Unit
Weir Height Ratio	WHr	WHL/WHR	1.000	dimensionless
Discharge Ratio	Qr	$\bar{Q}$_L/$\bar{Q}$_R	0.996	dimensionless
Time Step Discharge Ratio	Qr,t	Average[Q_(r,t=n)···Q_(r,t=n+N)]	0.995	dimensionless

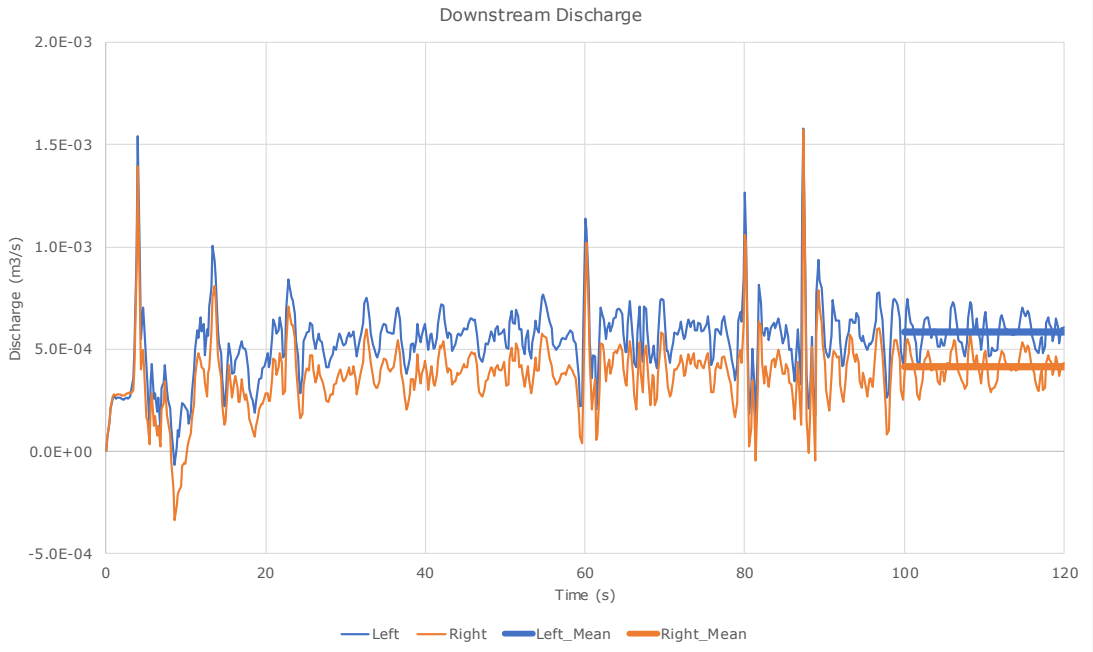


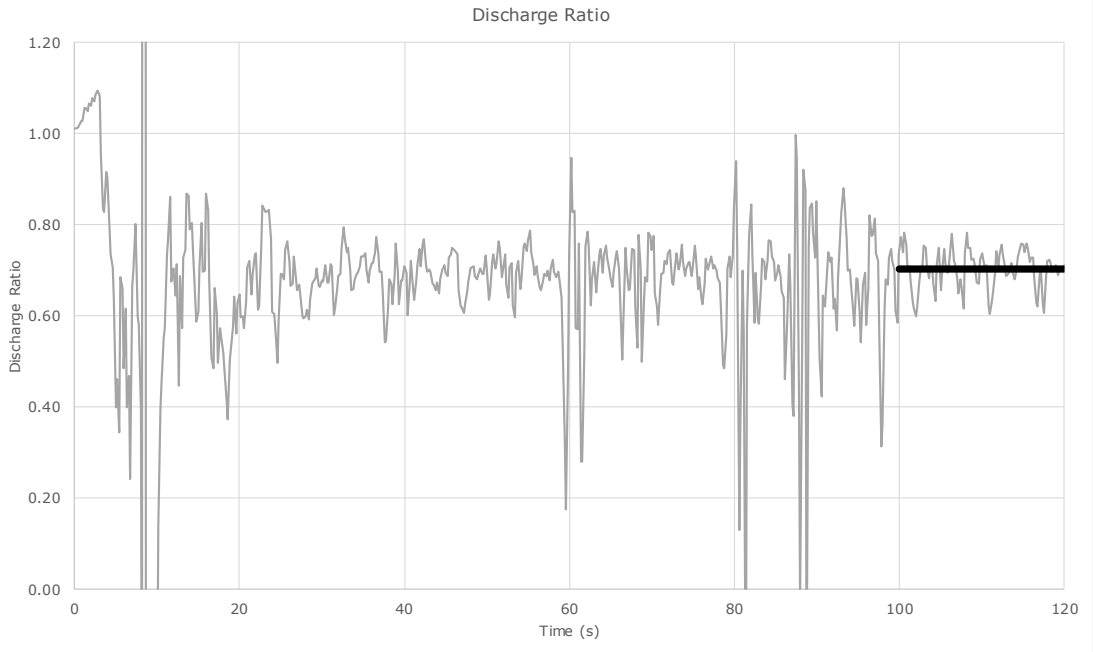


50_03_5053

Name	Symbol	Left	Right	Unit
Weir Height	WH	50	53	mm
Initial Time	Ti	100	100	s
End Time	Te	120	120	s
Initial Number	Ni	500	500	unitless
End Number	Ne	600	600	unitless
Average Discharge	$\bar{Q}$	5.857E-04	4.138E-04	m3/s

Name	Symbol	Equation	Result	Unit
Weir Height Ratio	WHr	WHL/WHR	0.943	dimensionless
Discharge Ratio	Qr	$\bar{Q}$_L/$\bar{Q}$_R	0.706	dimensionless
Time Step Discharge Ratio	Qr,t	Average[Q_(r,t=n)···Q_(r,t=n+N)]	0.703	dimensionless

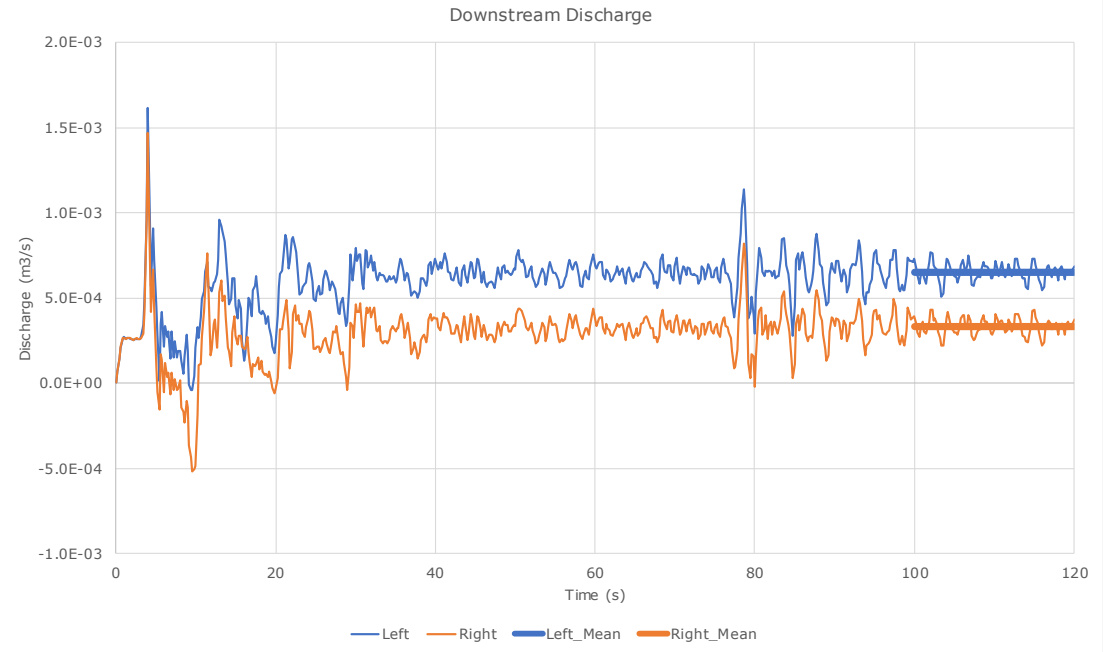


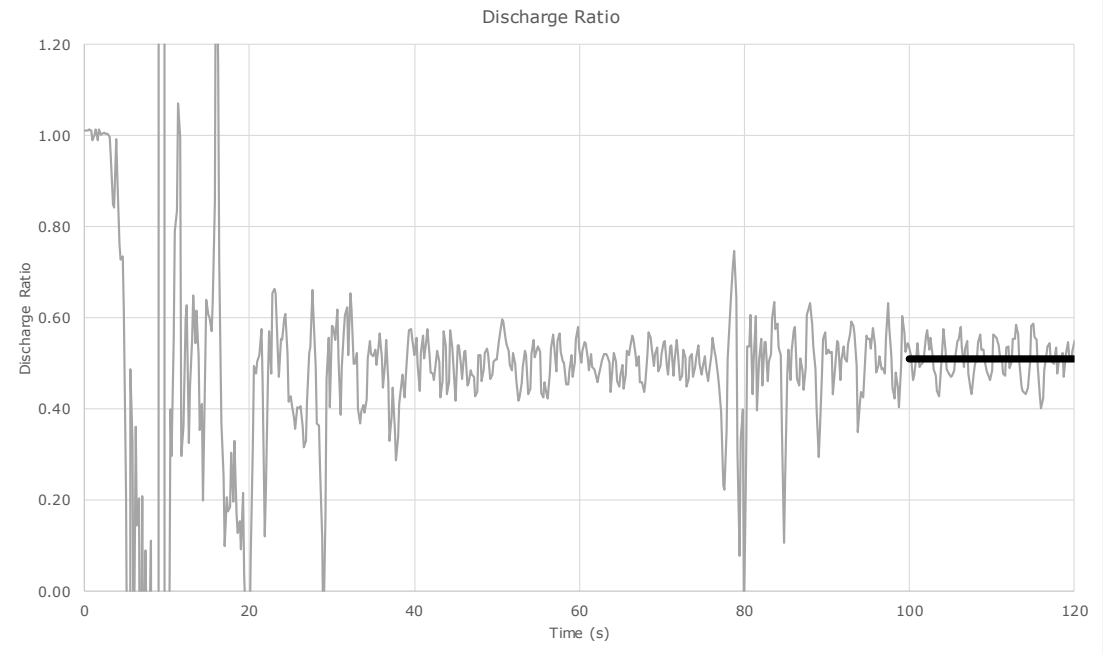


50_03_5055

Name	Symbol	Left	Right	Unit
Weir Height	WH	50	55	mm
Initial Time	Ti	100	100	s
End Time	Te	120	120	s
Initial Number	Ni	500	500	unitless
End Number	Ne	600	600	unitless
Average Discharge	$\bar{Q}$	6.537E-04	3.342E-04	m3/s

Name	Symbol	Equation	Result	Unit
Weir Height Ratio	WHr	WHL/WHR	0.909	dimensionless
Discharge Ratio	Qr	$\bar{Q}$_L/$\bar{Q}$_R	0.511	dimensionless
Time Step Discharge Ratio	Qr,t	Average[Q_(r,t=n)···Q_(r,t=n+N)]	0.509	dimensionless

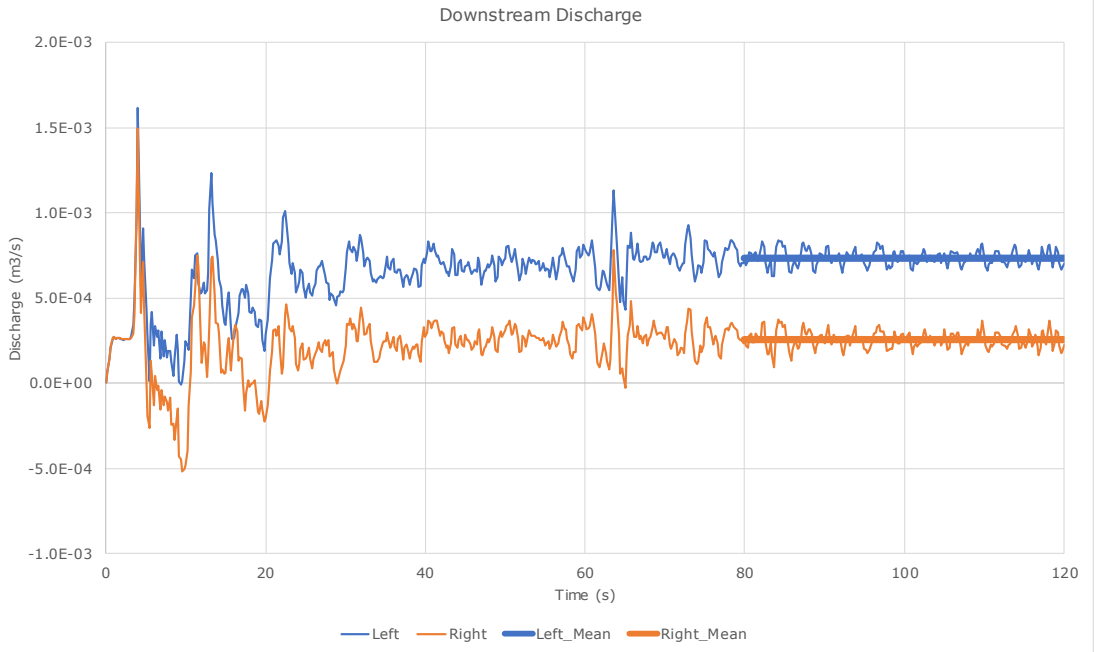


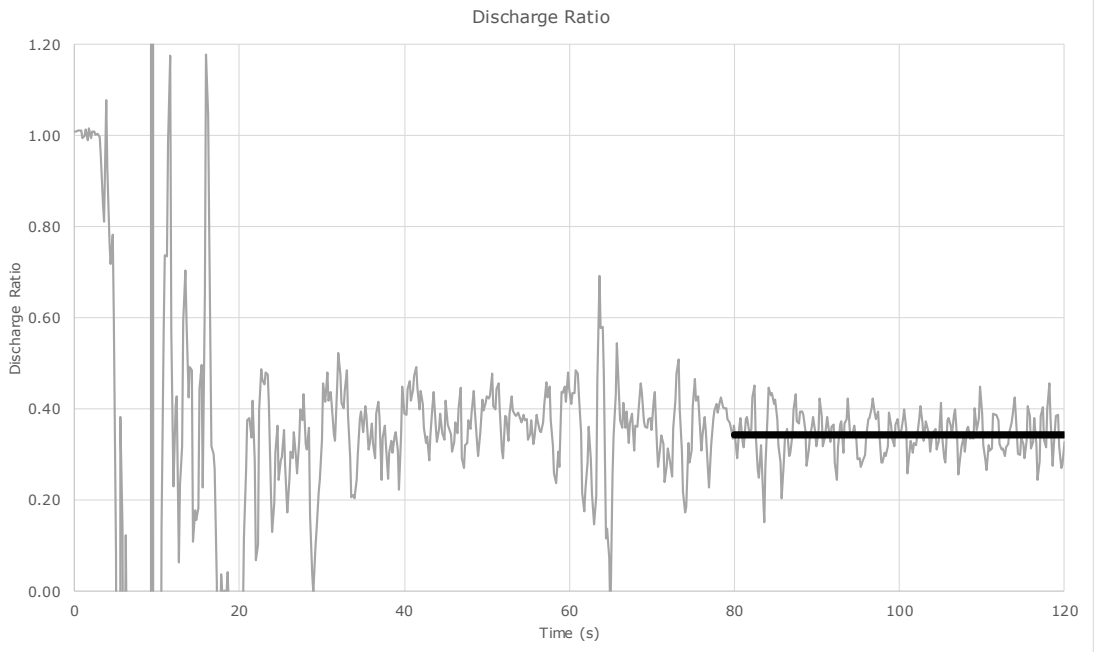


50_03_5057

Name	Symbol	Left	Right	Unit
Weir Height	WH	50	57	mm
Initial Time	Ti	80	80	s
End Time	Te	120	120	s
Initial Number	Ni	400	400	unitless
End Number	Ne	600	600	unitless
Average Discharge	$\bar{Q}$	7.376E-04	2.555E-04	m3/s

Name	Symbol	Equation	Result	Unit
Weir Height Ratio	WHr	WHL/WHR	0.877	dimensionless
Discharge Ratio	Qr	$\bar{Q}$_L/$\bar{Q}$_R	0.346	dimensionless
Time Step Discharge Ratio	Qr,t	Average[Q_(r,t=n)···Q_(r,t=n+N)]	0.344	dimensionless

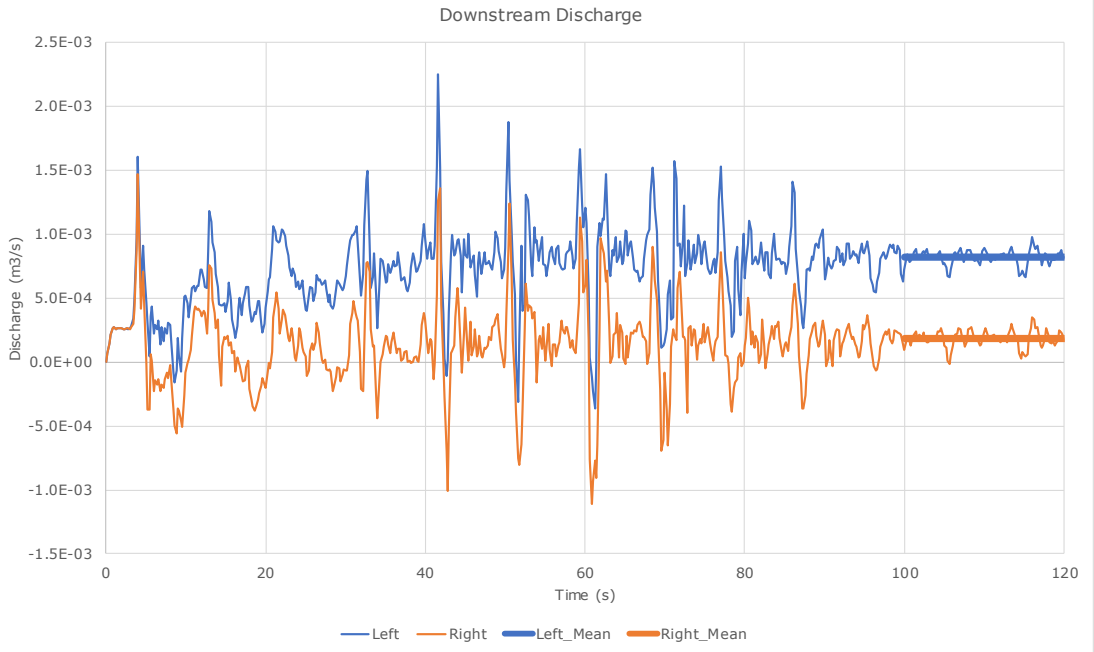


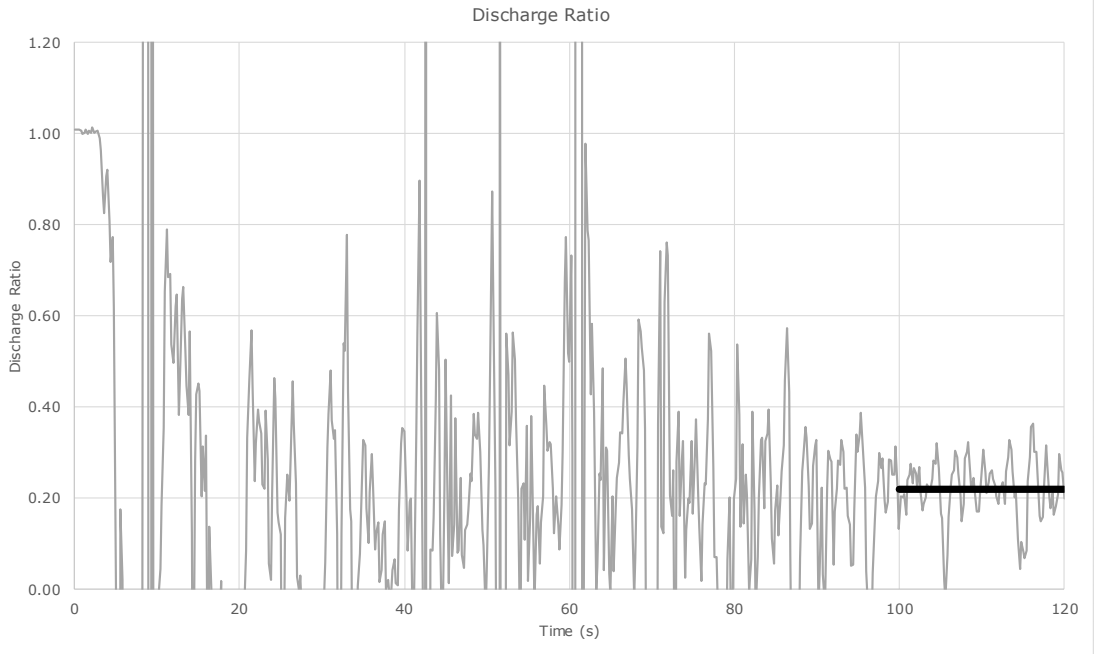


50_03_5060

Name	Symbol	Left	Right	Unit
/eir Height	WH	50	60	mm
nitial Time	Ti	100	100	s
End Time	Te	120	120	s
tial Number	Ni	500	500	dimensionless
nd Number	Ne	600	600	dimensionless
age Discharge	$\bar{Q}$	8.198E-04	1.836E-04	m3/s

Name	Symbol	Equation	Result	Unit
· Height Ratio	WHr	WHL/WHR	0.833	dimensionless
:harge Ratio	Qr	$\bar{Q}$_L/$\bar{Q}$_R	0.224	dimensionless
p Discharge Ratio	Qr,t	Average[Q_(r,t=n)···Q_(r,t=n+N)]	0.220	dimensionless

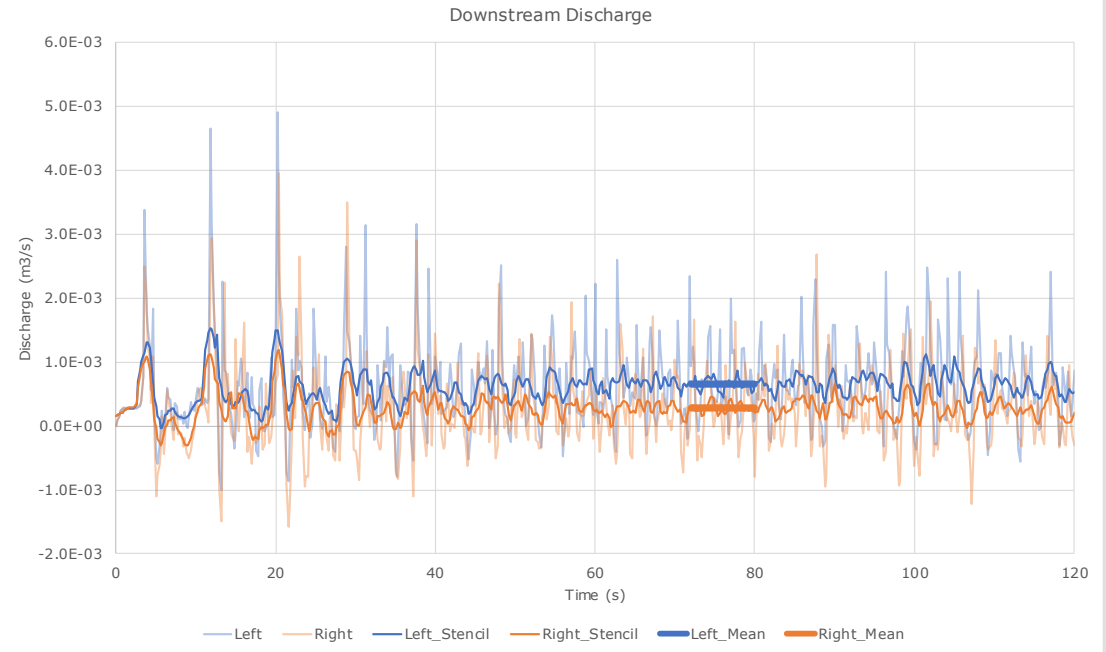


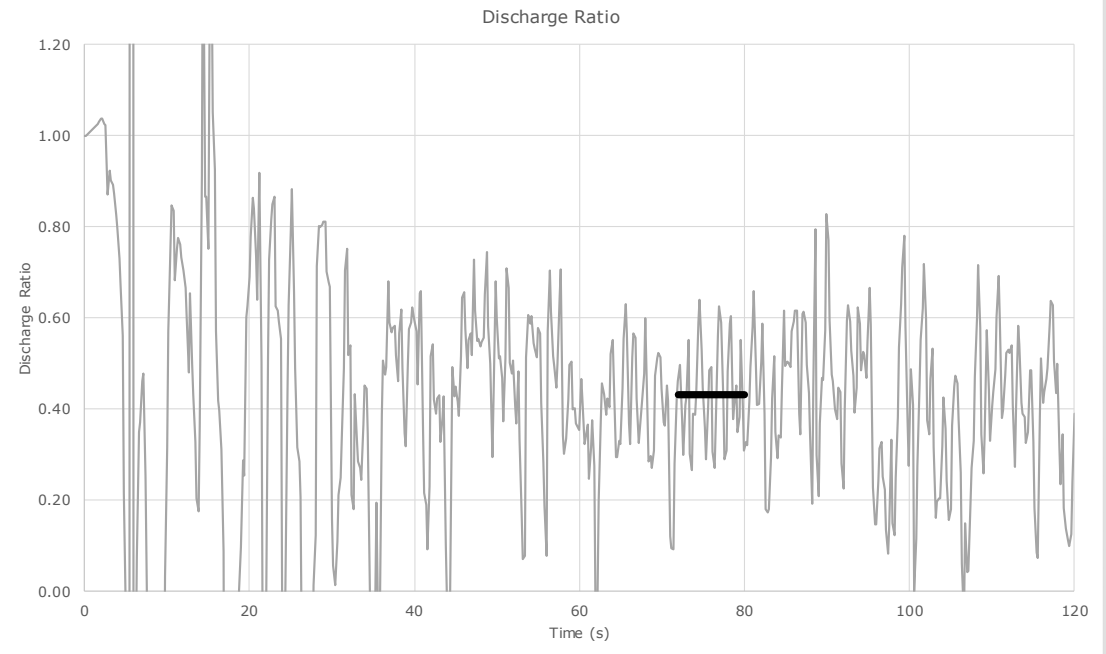


50_03_5560

Name	Symbol	Left	Right	Unit
Weir Height	WH	55	60	mm
Initial Time	Ti	72	72	s
End Time	Te	80	80	s
Initial Number	Ni	360	360	dimensionless
End Number	Ne	400	400	dimensionless
Average Discharge	$\bar{Q}$	6.561E-04	2.821E-04	m3/s

Name	Symbol	Equation	Result	Unit
Weir Height Ratio	WHr	WHL/WHR	0.917	dimensionless
Discharge Ratio	Qr	$\bar{Q}$_L/$\bar{Q}$_R	0.430	dimensionless
Step Discharge Ratio	Qr,t	Average[Q_(r,t=n)···Q_(r,t=n+N)]	0.431	dimensionless

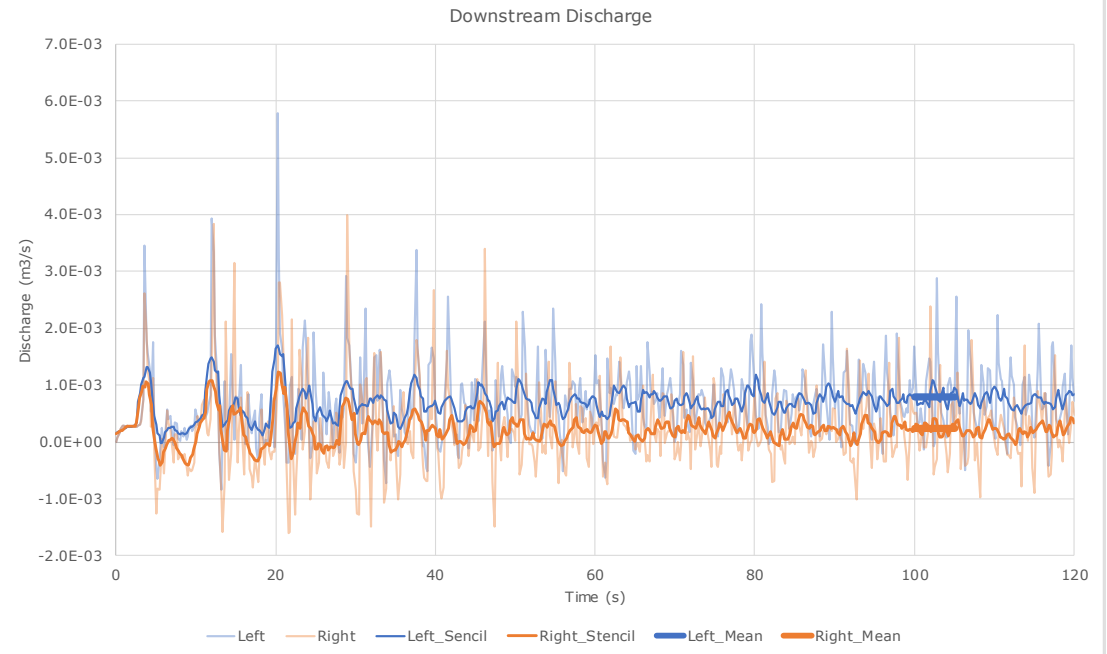


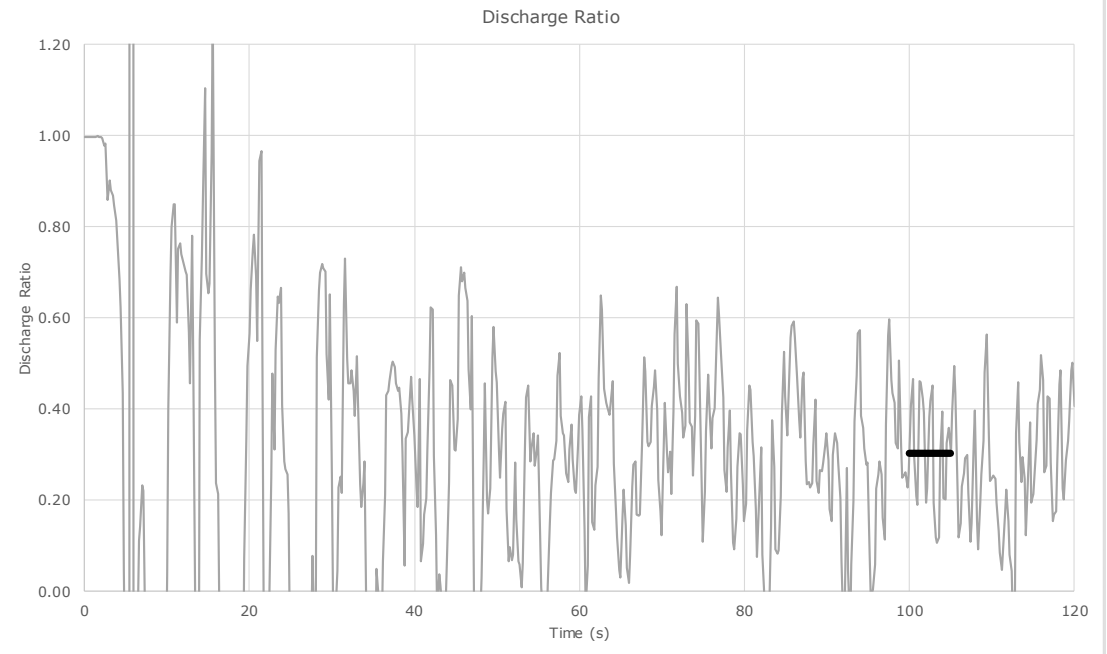


50_03_5562

Name	Symbol	Left	Right	Unit
Weir Height	WH	55	62	mm
Initial Time	Ti	100	100	s
End Time	Te	105	105	s
Initial Number	Ni	500	500	dimensionless
End Number	Ne	525	525	dimensionless
Average Discharge	$\bar{Q}$	7.928E-04	2.378E-04	m3/s

Name	Symbol	Equation	Result	Unit
Weir Height Ratio	WHr	WHL/WHR	0.887	dimensionless
Discharge Ratio	Qr	$\bar{Q}$_L/$\bar{Q}$_R	0.300	dimensionless
Time Step Discharge Ratio	Qr,t	Average[Q_(r,t=n)···Q_(r,t=n+N)]	0.302	dimensionless

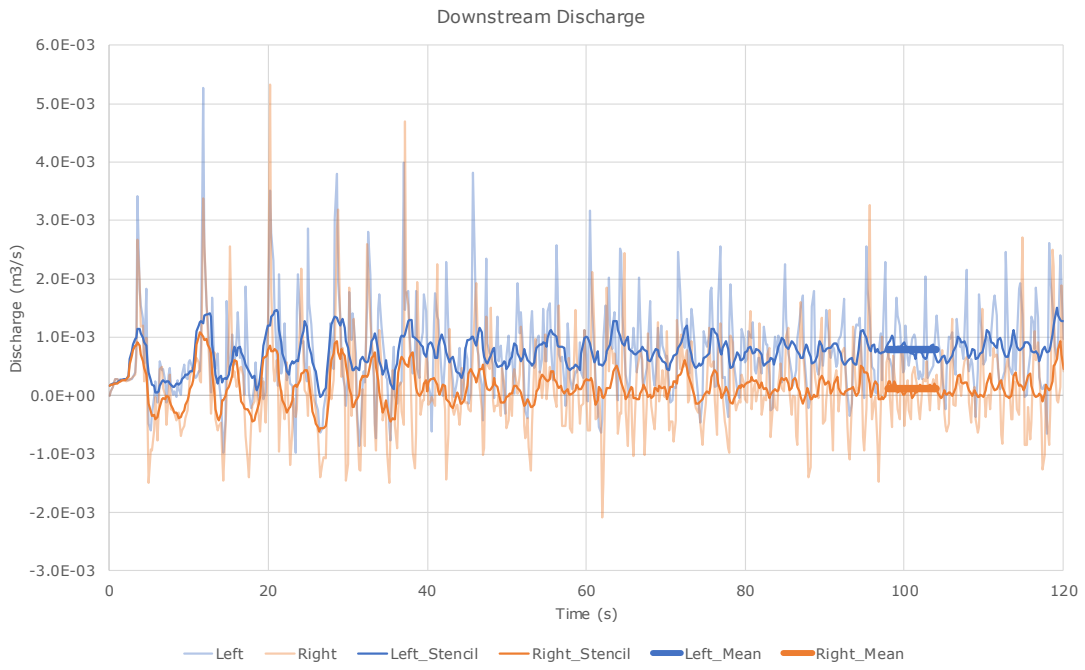


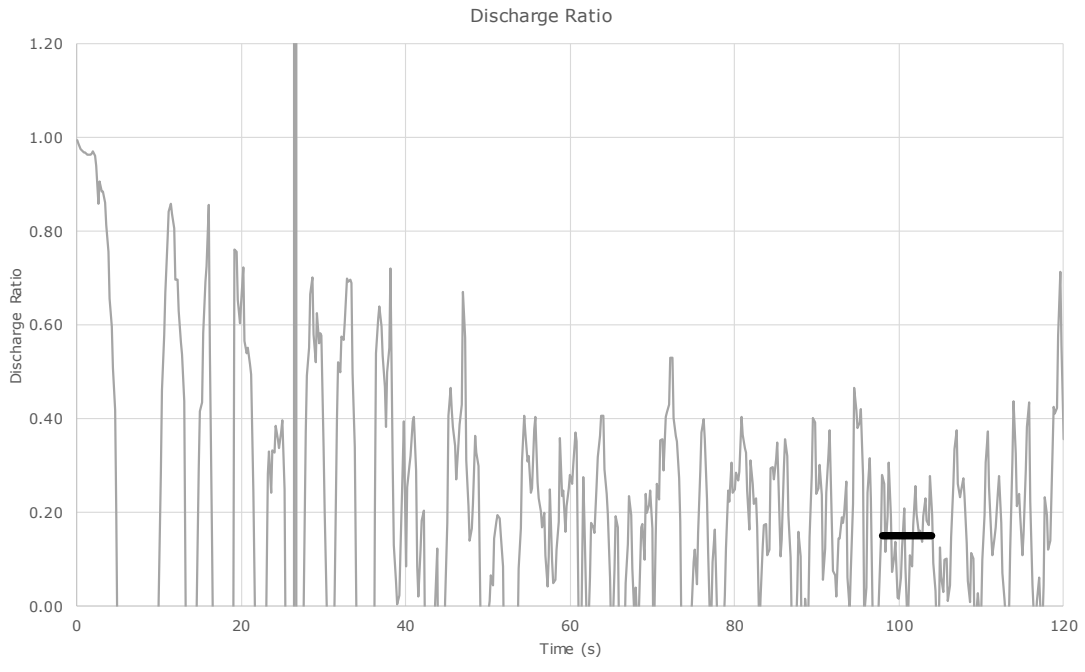


50_03_5565

Name	Symbol	Left	Right	Unit
Weir Height	WH	55	65	mm
Initial Time	Ti	98	98	s
End Time	Te	104	104	s
Initial Number	Ni	490	490	dimensionless
End Number	Ne	520	520	dimensionless
ıverage Discharge	$\bar{Q}$	7.955E-04	1.201E-04	m3/s

Name	Symbol	Equation	Result	Unit
Weir Height Ratio	WHr	WHL/WHR	0.846	dimensionless
Discharge Ratio	Qr	$\bar{Q}$_L/$\bar{Q}$_R	0.151	dimensionless
Step Discharge Ratio	Qr,t	Average[Q_(r,t=n)···Q_(r,t=n+N)]	0.151	dimensionless

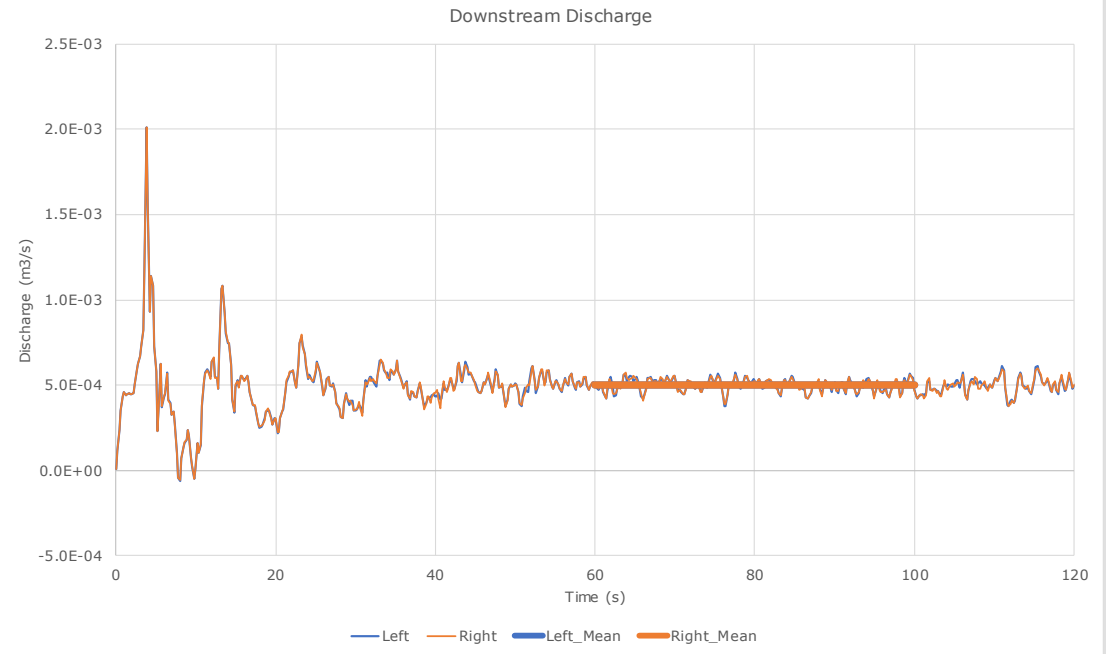


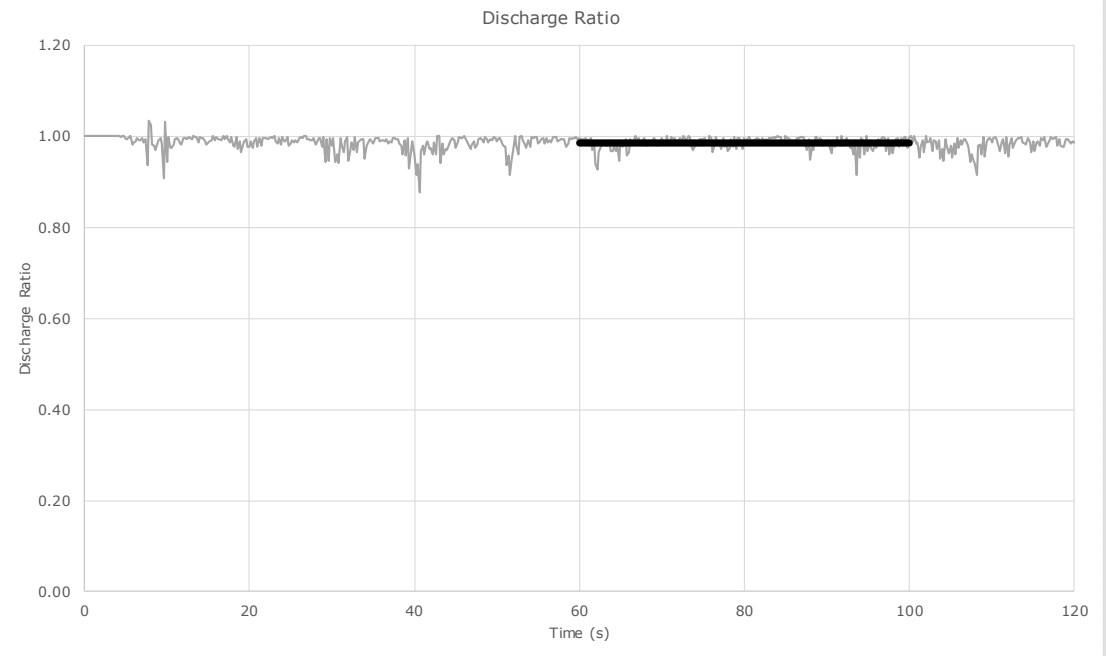


50_05_5050

Name	Symbol	Left	Right	Unit
Weir Height	WH	50	50	mm
Initial Time	Ti	60	60	s
End Time	Te	100	100	s
Initial Number	Ni	300	300	unitless
End Number	Ne	500	500	unitless
Average Discharge	$\bar{Q}$	4.992E-04	4.992E-04	m3/s

Name	Symbol	Equation	Result	Unit
Weir Height Ratio	WHr	WHL/WHR	1.000	dimensionless
Discharge Ratio	Qr	$\bar{Q}$_L/$\bar{Q}$_R	1.000	dimensionless
Time Step Discharge Ratio	Qr,t	Average[Q_(r,t=n)···Q_(r,t=n+N)]	0.985	dimensionless

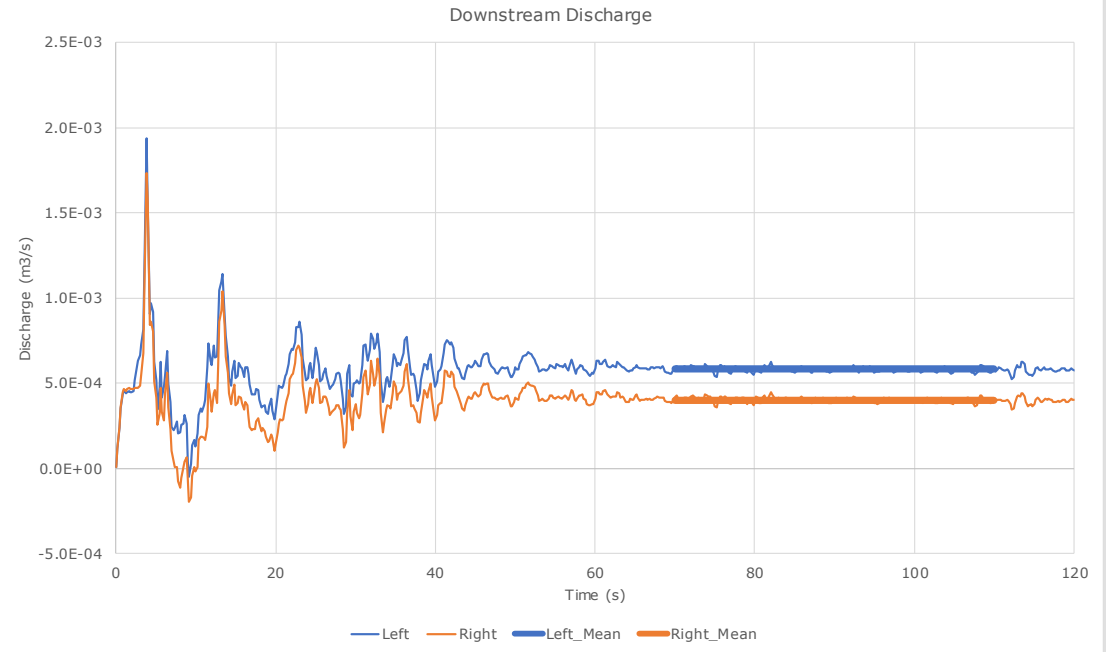


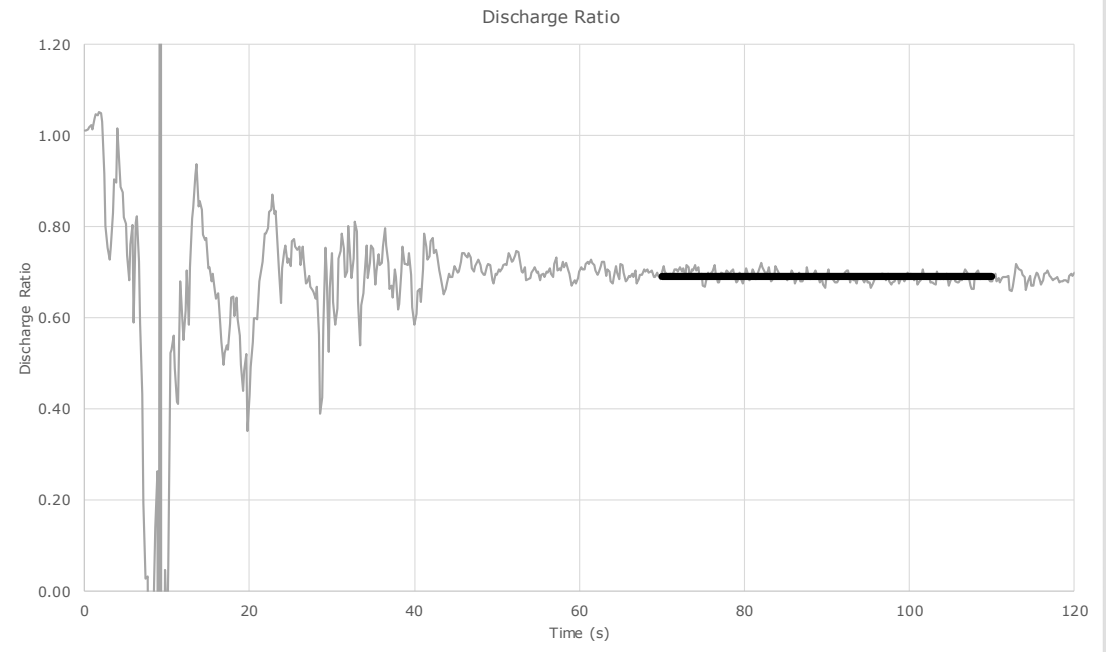


50_05_5053

ame	Symbol	Left	Right	Unit
Height	WH	50	53	mm
ıl Time	Ti	70	70	s
Time	Te	110	110	s
Number	Ni	350	350	unitless
Number	Ne	550	550	unitless
Discharge	$\bar{Q}$	5.827E-04	4.026E-04	m3/s

ame	Symbol	Equation	Result	Unit
ight Ratio	WHr	WHL/WHR	0.943	dimensionless
rge Ratio	Qr	$\bar{Q}$_L/$\bar{Q}$_R	0.691	dimensionless
ischarge Ratio	Qr,t	Average[Q_(r,t=n)···Q_(r,t=n+N)]	0.691	dimensionless

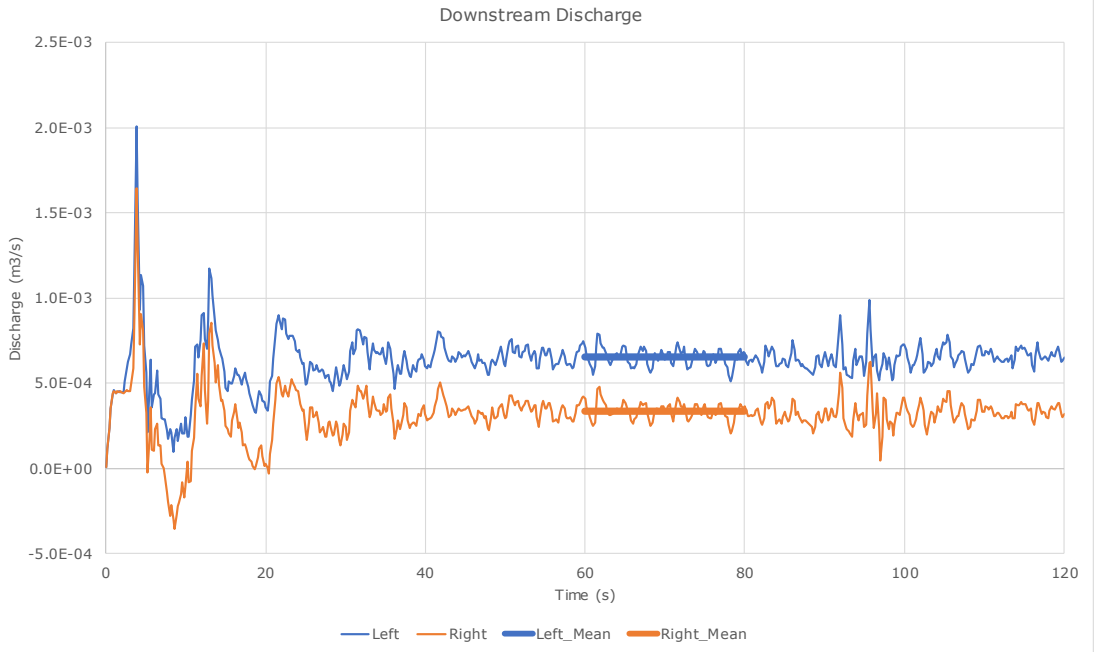


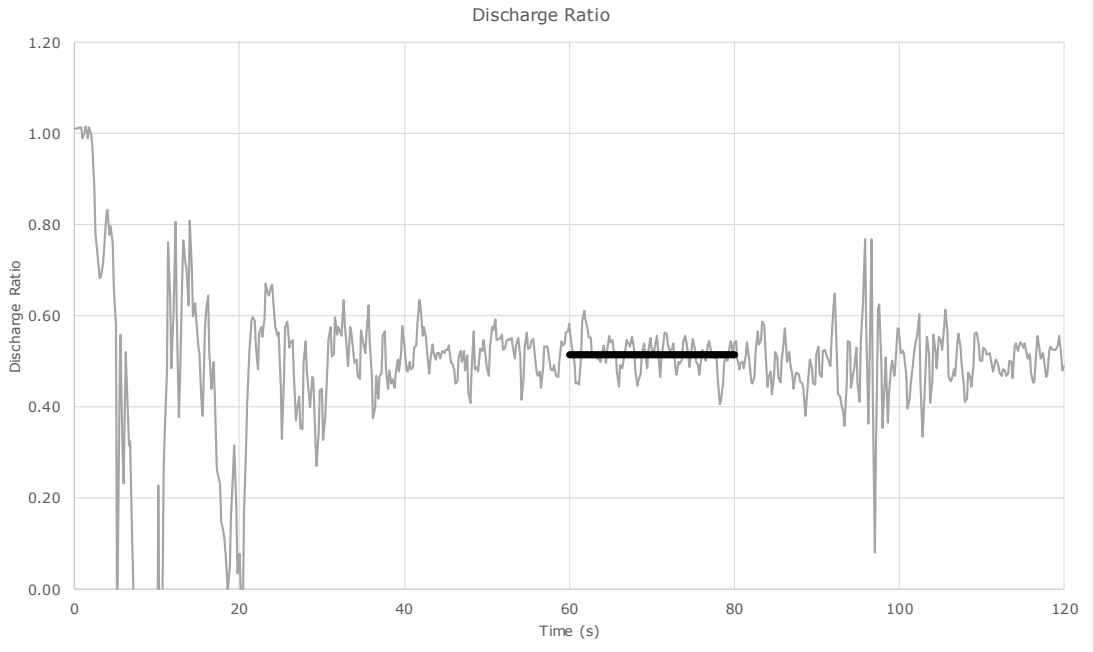


50_05_5055

Name	Symbol	Left	Right	Unit
Weir Height	WH	50	55	mm
Initial Time	Ti	60	60	s
End Time	Te	80	80	s
Initial Number	Ni	300	300	unitless
End Number	Ne	400	400	unitless
Average Discharge	$\bar{Q}$	6.530E-04	3.377E-04	m3/s

Name	Symbol	Equation	Result	Unit
Weir Height Ratio	WHr	WHL/WHR	0.909	dimensionless
Discharge Ratio	Qr	$\bar{Q}$_L/$\bar{Q}$_R	0.517	dimensionless
Time Step Discharge Ratio	Qr,t	Average[Q_(r,t=n)···Q_(r,t=n+N)]	0.515	dimensionless

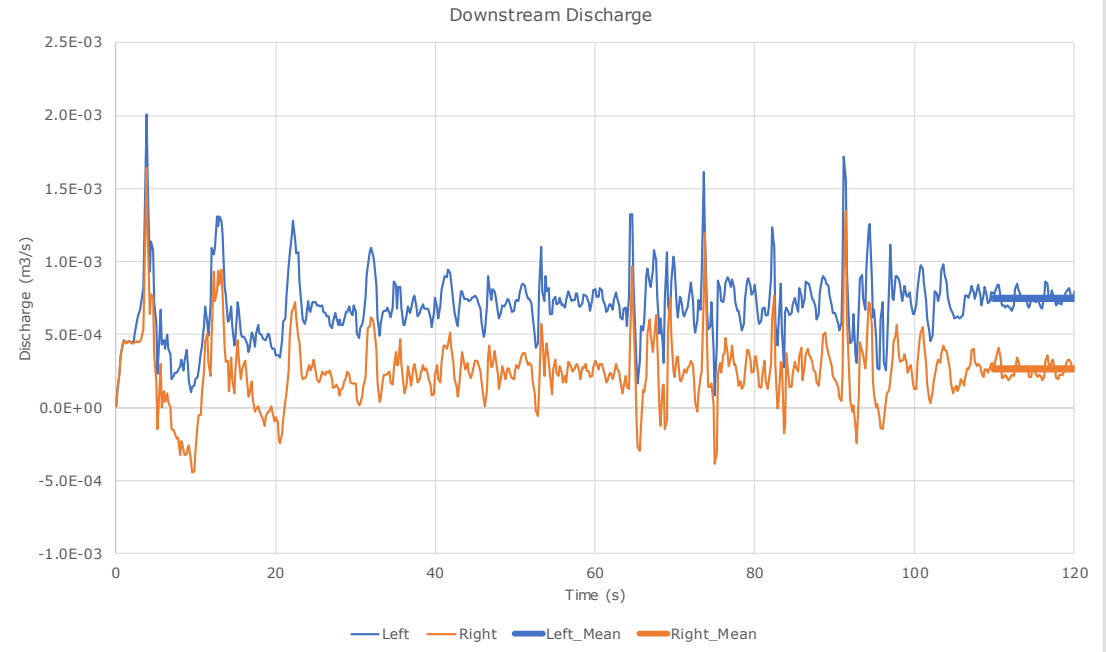


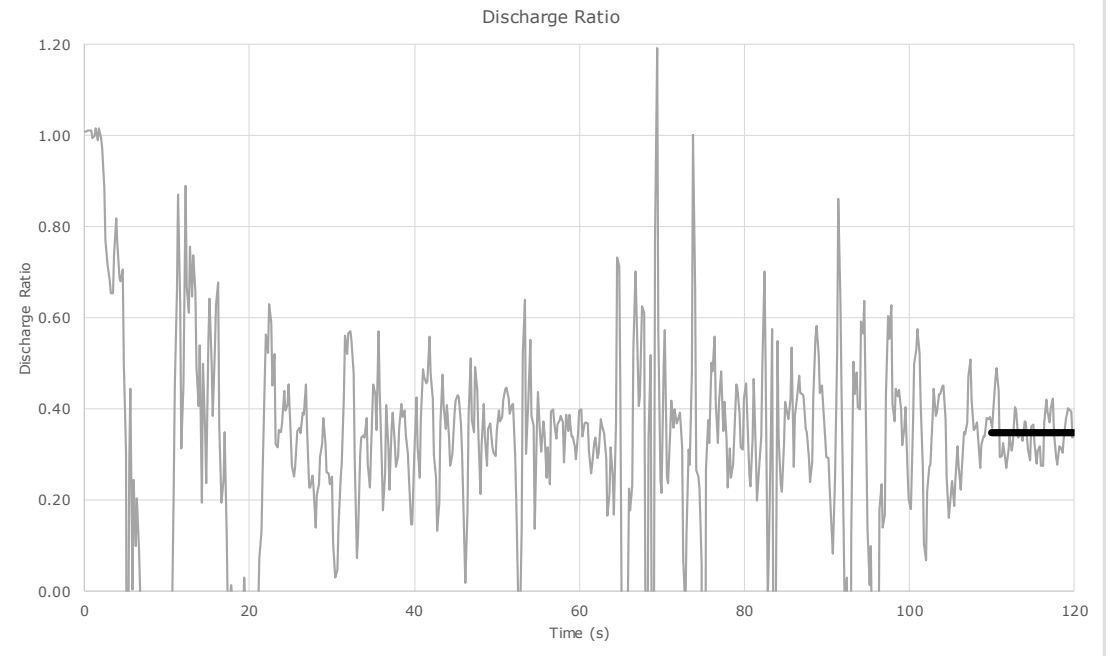


50_05_5057

	Symbol	Left	Right	Unit
ght	WH	50	57	mm
me	Ti	110	110	s
ie	Te	120	120	s
nber	Ni	550	550	unitless
ber	Ne	600	600	unitless
charge	$\bar{Q}$	7.513E-04	2.631E-04	m3/s

	Symbol	Equation	Result	Unit
Ratio	WHr	WHL/WHR	0.877	dimensionless
Ratio	Qr	$\bar{Q}$_L/$\bar{Q}$_R	0.350	dimensionless
arge Ratio	Qr,t	Average[Q_(r,t=n)···Q_(r,t=n+N)]	0.348	dimensionless

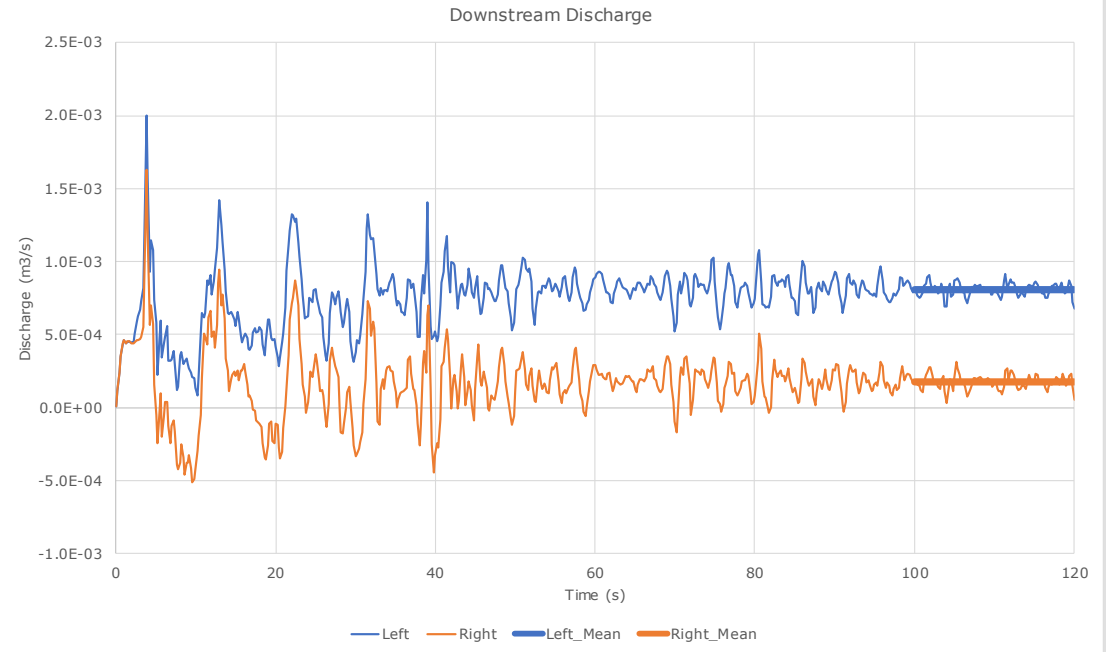


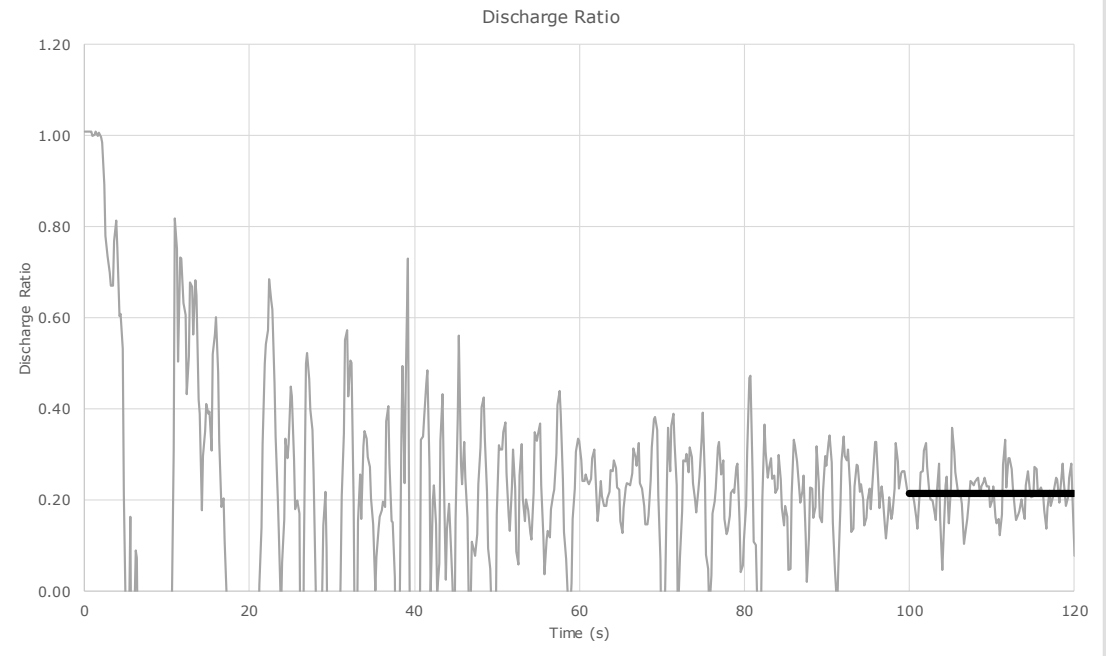


50_05_5060

Name	Symbol	Left	Right	Unit
Weir Height	WH	50	60	mm
Initial Time	Ti	100	100	s
End Time	Te	120	120	s
Initial Number	Ni	500	500	dimensionless
End Number	Ne	600	600	dimensionless
Average Discharge	$\bar{Q}$	8.097E-04	1.749E-04	m3/s

Name	Symbol	Equation	Result	Unit
Weir Height Ratio	WHr	WHL/WHR	0.833	dimensionless
Discharge Ratio	Qr	$\bar{Q}$_L/$\bar{Q}$_R	0.216	dimensionless
me Step Discharge Ratio	Qr,t	Average[Q_(r,t=n)···Q_(r,t=n+N)]	0.214	dimensionless

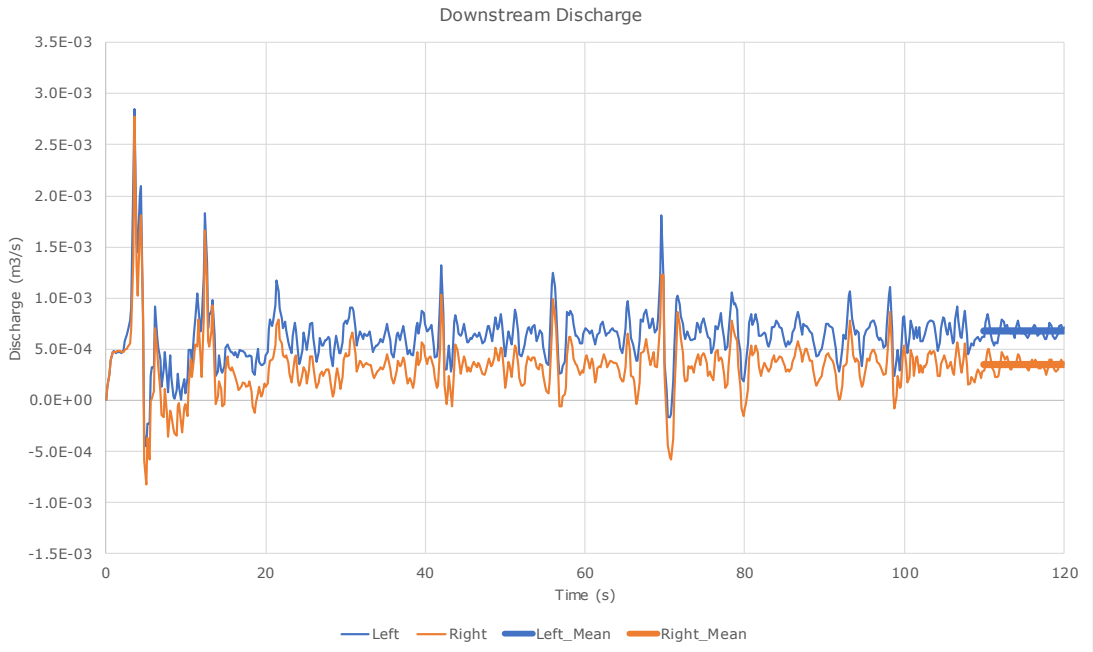


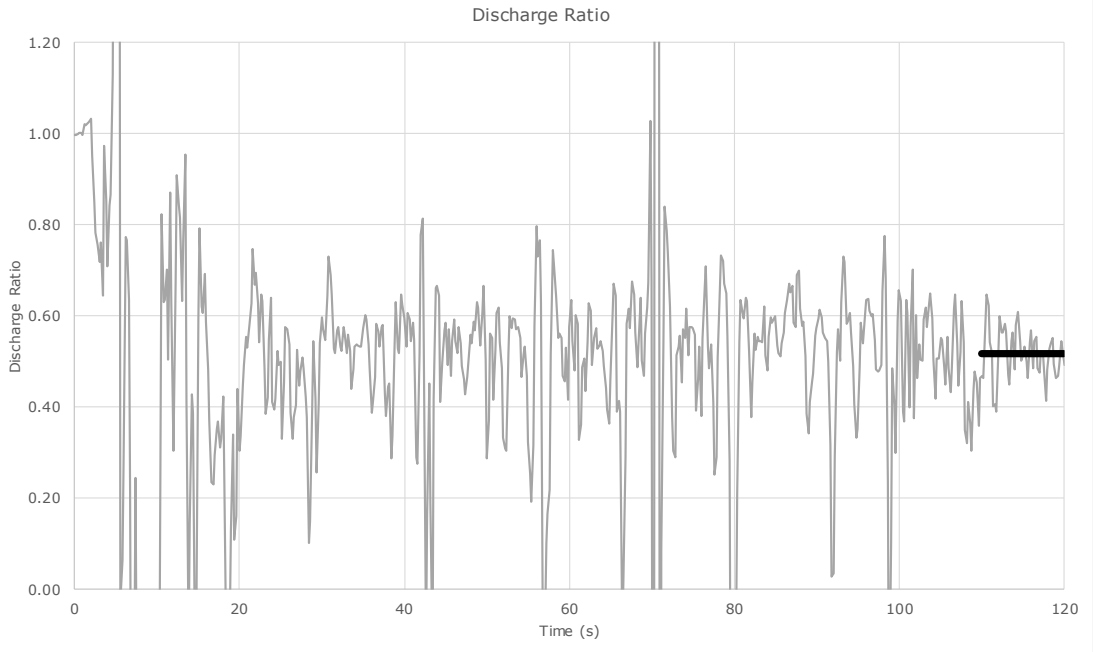


50_05_5560

Name	Symbol	Left	Right	Unit
Weir Height	WH	55	60	mm
Initial Time	Ti	110	110	s
End Time	Te	120	120	s
Initial Number	Ni	550	550	dimensionless
End Number	Ne	600	600	dimensionless
Average Discharge	$\bar{Q}$	6.771E-04	3.518E-04	m3/s

Name	Symbol	Equation	Result	Unit
Weir Height Ratio	WHr	WHL/WHR	0.917	dimensionless
Discharge Ratio	Qr	$\bar{Q}$_L/$\bar{Q}$_R	0.520	dimensionless
Time Step Discharge Ratio	Qr,t	Average[Q_(r,t=n)···Q_(r,t=n+N)]	0.517	dimensionless

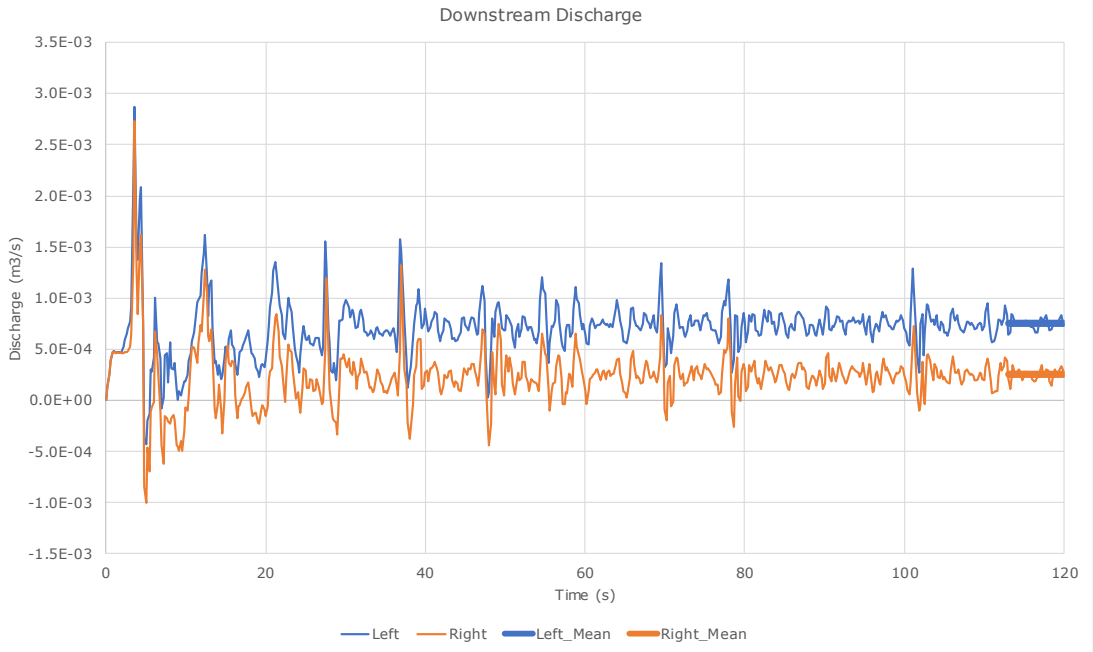


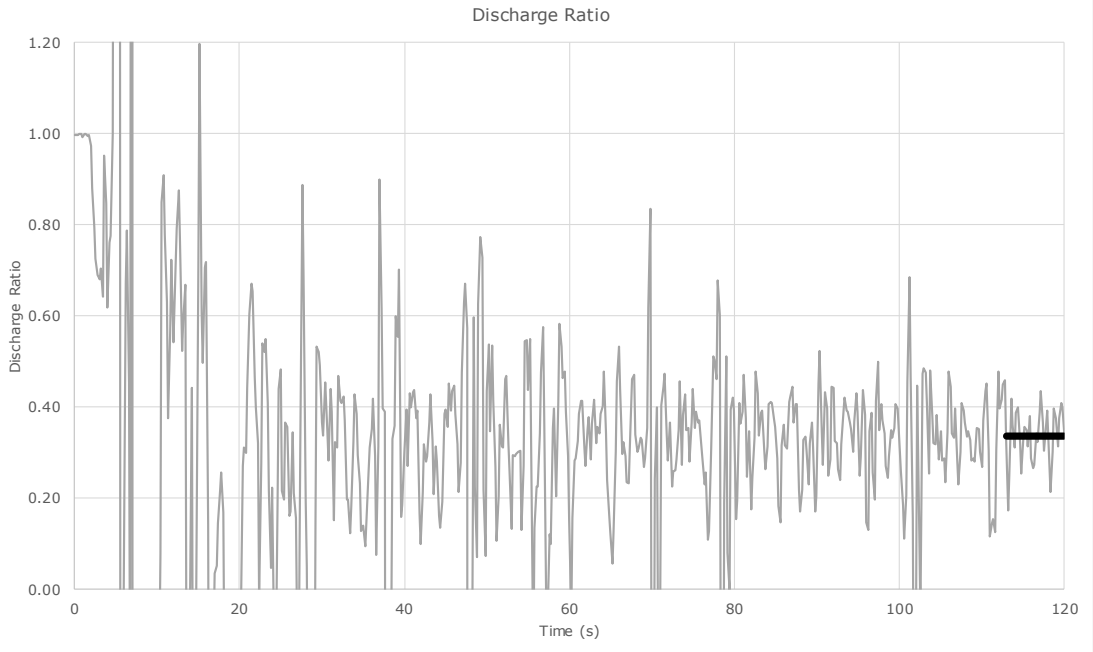


50_05_5562

Name	Symbol	Left	Right	Unit
Weir Height	WH	55	62	mm
Initial Time	Ti	113	113	s
End Time	Te	120	120	s
Initial Number	Ni	565	565	dimensionless
End Number	Ne	600	600	dimensionless
Average Discharge	$\bar{Q}$	7.521E-04	2.533E-04	m3/s

Name	Symbol	Equation	Result	Unit
Weir Height Ratio	WHr	WHL/WHR	0.887	dimensionless
Discharge Ratio	Qr	$\bar{Q}$_L/$\bar{Q}$_R	0.337	dimensionless
Time Step Discharge Ratio	Qr,t	Average[Q_(r,t=n)···Q_(r,t=n+N)]	0.335	dimensionless

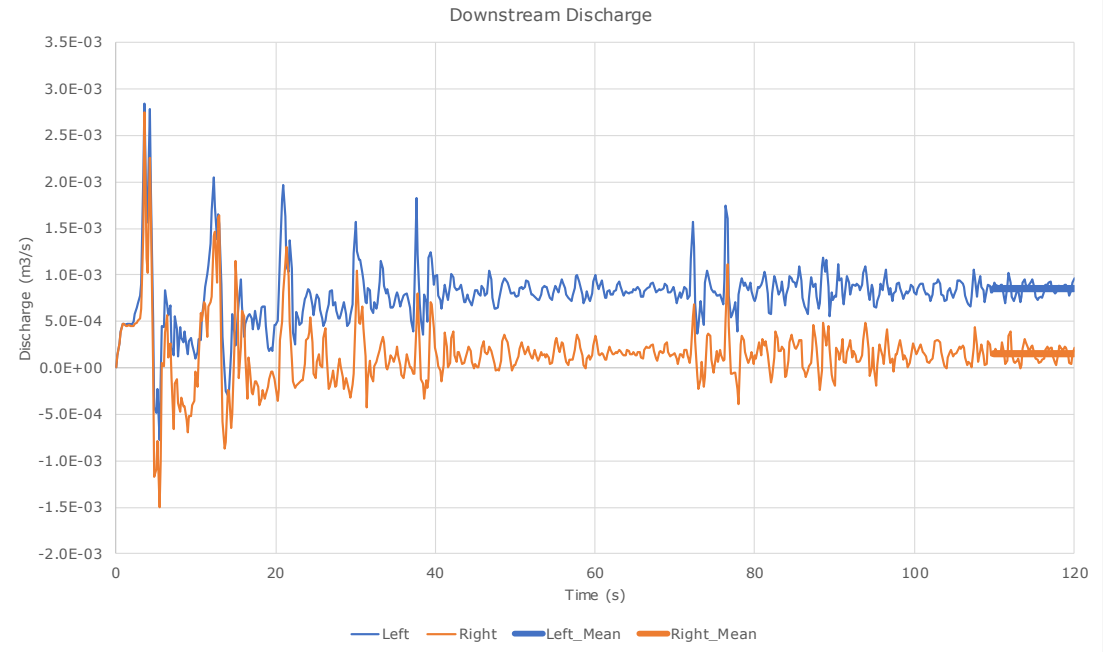


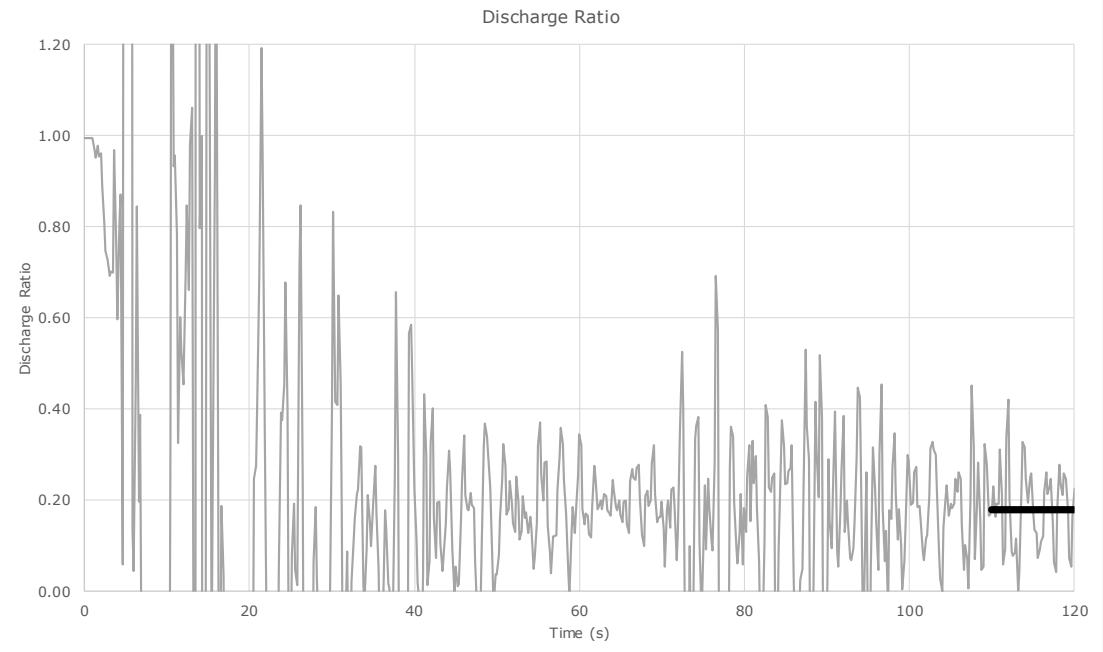


50_05_5565

Name	Symbol	Left	Right	Unit
Weir Height	WH	55	65	mm
Initial Time	Ti	110	110	s
End Time	Te	120	120	s
Initial Number	Ni	550	550	dimensionless
End Number	Ne	600	600	dimensionless
Average Discharge	$\bar{Q}$	8.512E-04	1.576E-04	m3/s

Name	Symbol	Equation	Result	Unit
Weir Height Ratio	WHr	WHL/WHR	0.846	dimensionless
Discharge Ratio	Qr	$\bar{Q}$_L/$\bar{Q}$_R	0.185	dimensionless
Time Step Discharge Ratio	Qr,t	Average[Q_(r,t=n)···Q_(r,t=n+N)]	0.179	dimensionless

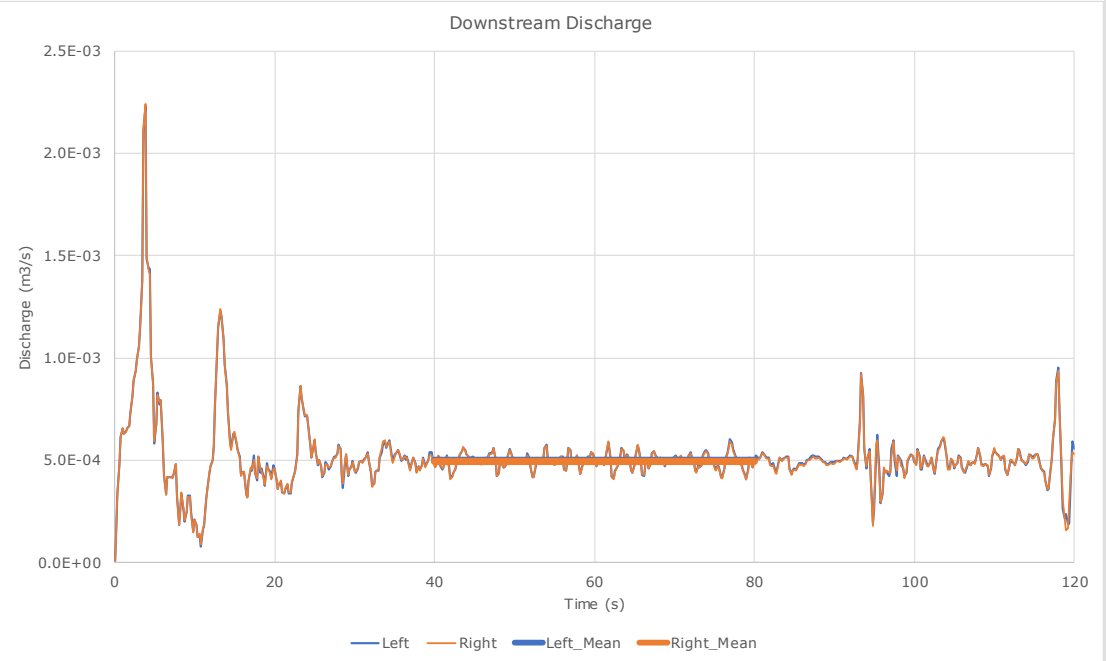


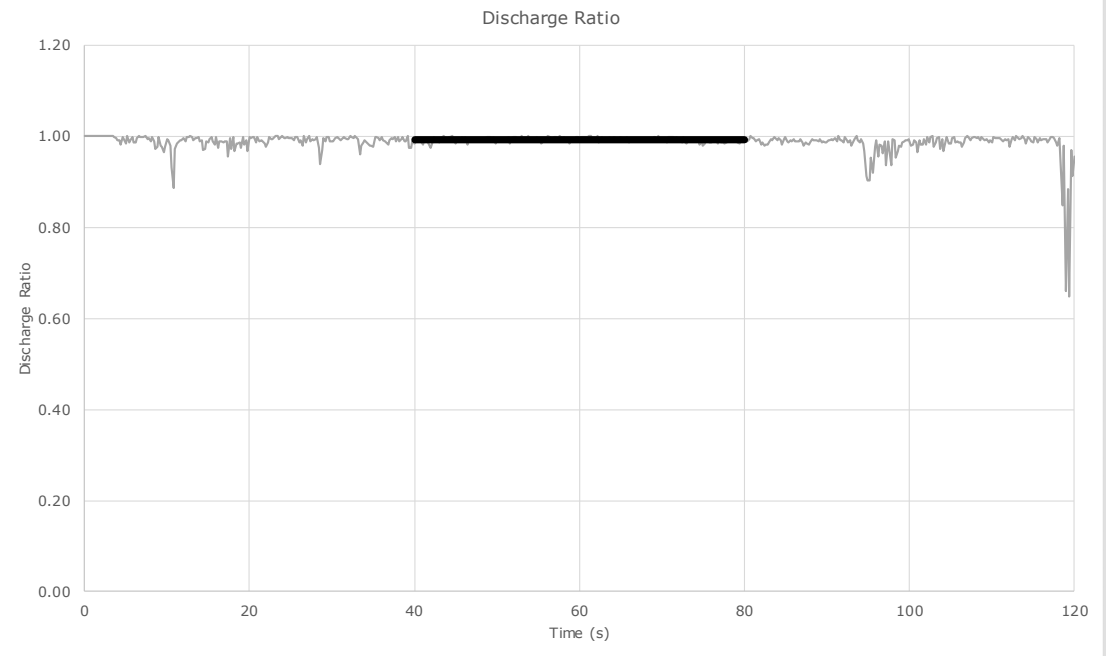


50_07_5050

Name	Symbol	Left	Right	Unit
Weir Height	WH	50	50	mm
Initial Time	Ti	40	40	s
End Time	Te	80	80	s
Initial Number	Ni	200	200	unitless
End Number	Ne	400	400	unitless
Average Discharge	$\bar{Q}$	4.983E-04	4.962E-04	m3/s

Name	Symbol	Equation	Result	Unit
Weir Height Ratio	WHr	WHL/WHR	1.000	dimensionless
Discharge Ratio	Qr	$\bar{Q}$_L/$\bar{Q}$_R	0.996	dimensionless
Time Step Discharge Ratio	Qr,t	Average[Q_(r,t=n)···Q_(r,t=n+N)]	0.993	dimensionless

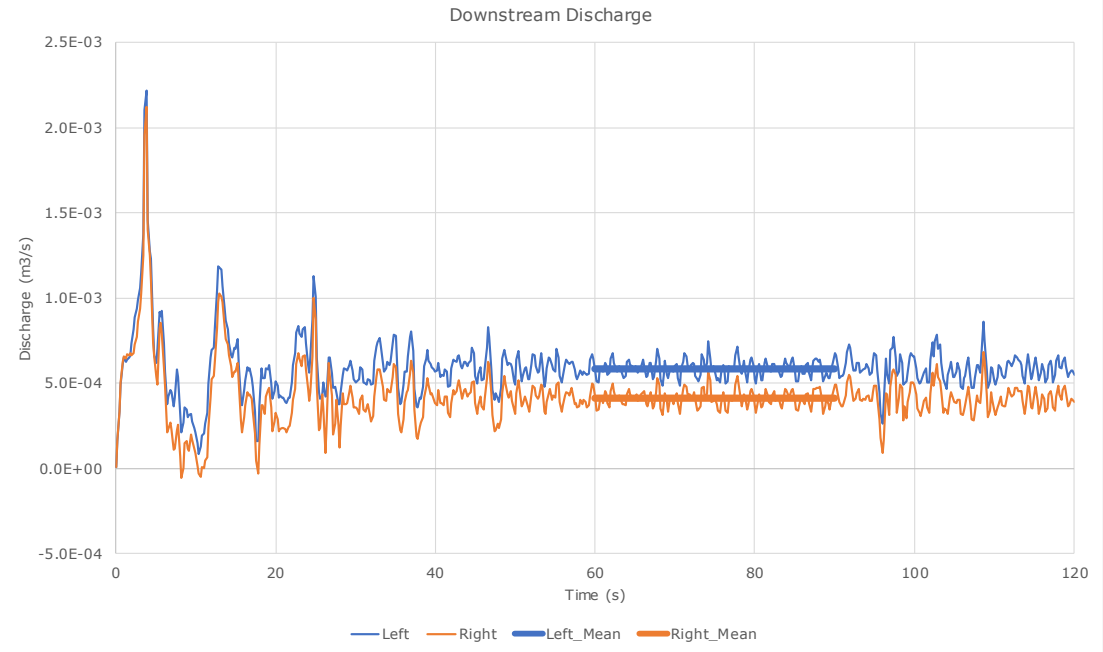


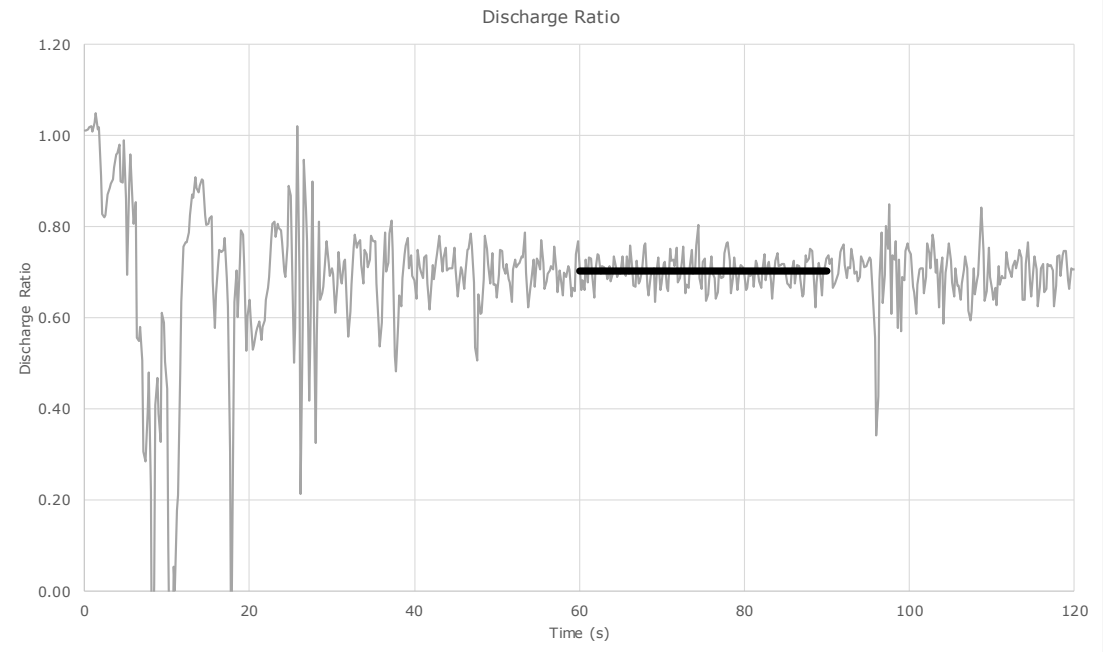


50_07_5053

Name	Symbol	Left	Right	Unit
Weir Height	WH	50	53	mm
Initial Time	Ti	60	60	s
End Time	Te	90	90	s
Initial Number	Ni	300	300	unitless
End Number	Ne	450	450	unitless
Average Discharge	$\bar{Q}$	5.866E-04	4.125E-04	m3/s

Name	Symbol	Equation	Result	Unit
Weir Height Ratio	WHr	WHL/WHR	0.943	dimensionless
Discharge Ratio	Qr	$\bar{Q}$_L/$\bar{Q}$_R	0.703	dimensionless
Time Step Discharge Ratio	Qr,t	Average[Q_(r,t=n)···Q_(r,t=n+N)]	0.701	dimensionless

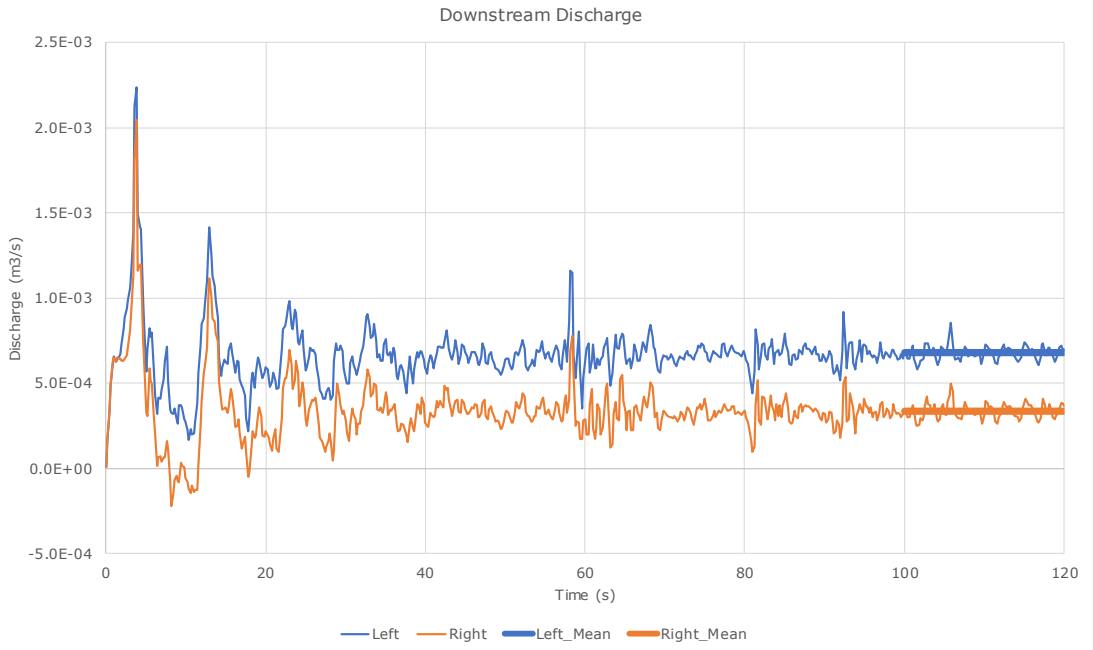


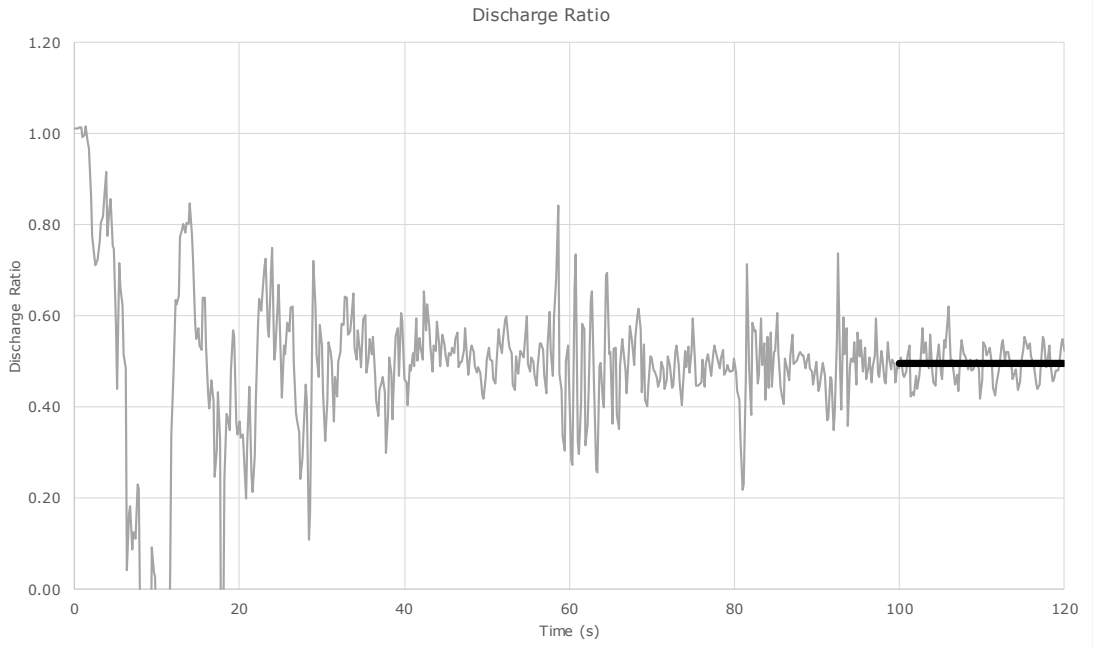


50_07_5055

Name	Symbol	Left	Right	Unit
Weir Height	WH	50	55	mm
Initial Time	Ti	100	100	s
End Time	Te	120	120	s
Initial Number	Ni	500	500	unitless
End Number	Ne	600	600	unitless
Average Discharge	$\bar{Q}$	6.784E-04	3.375E-04	m3/s

Name	Symbol	Equation	Result	Unit
Weir Height Ratio	WHr	WHL/WHR	0.909	dimensionless
Discharge Ratio	Qr	$\bar{Q}$_L/$\bar{Q}$_R	0.498	dimensionless
Time Step Discharge Ratio	Qr,t	Average[Q_(r,t=n)···Q_(r,t=n+N)]	0.496	dimensionless

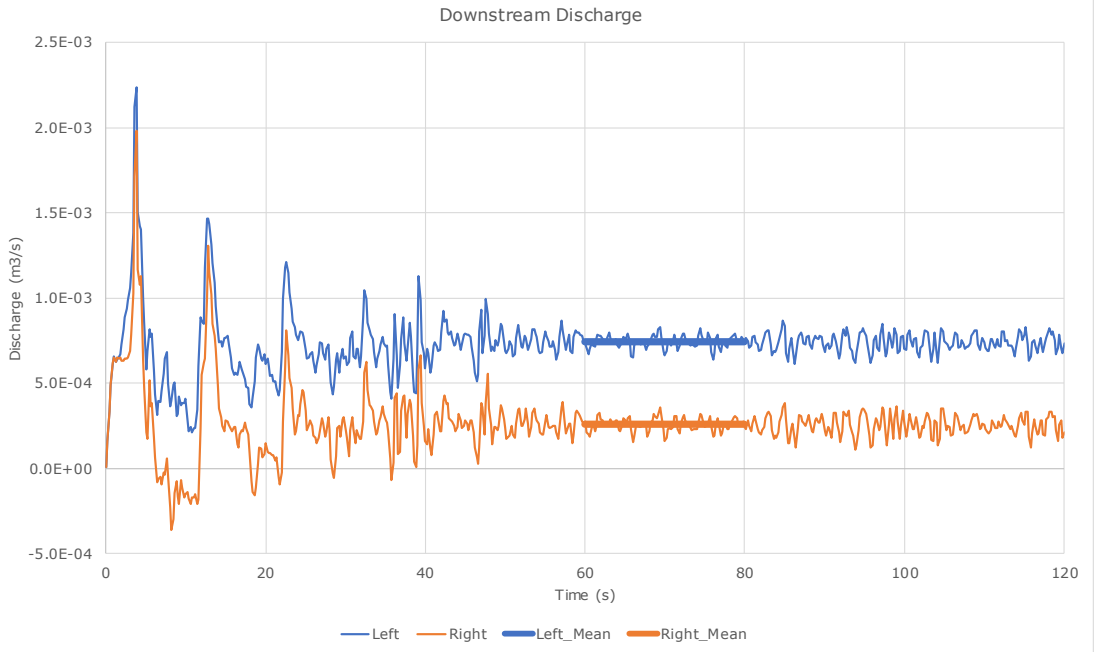


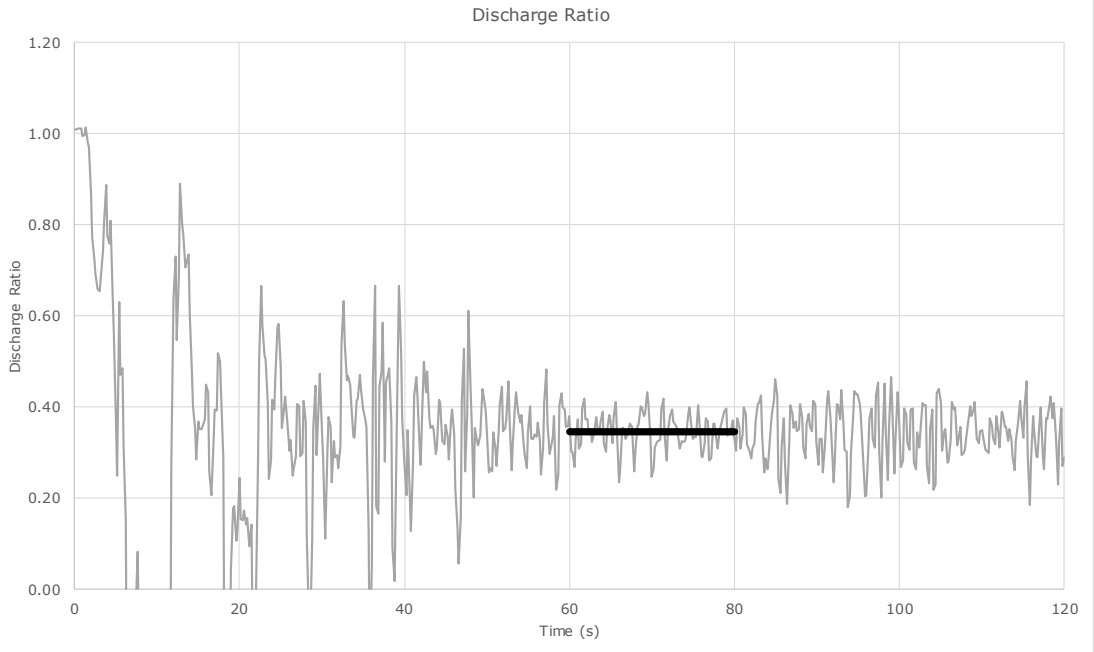


50_07_5057

Name	Symbol	Left	Right	Unit
r Height	WH	50	57	mm
ial Time	Ti	60	60	s
d Time	Te	80	80	s
ıl Number	Ni	300	300	unitless
Number	Ne	400	400	unitless
e Discharge	$\bar{Q}$	7.434E-04	2.581E-04	m3/s

Name	Symbol	Equation	Result	Unit
leight Ratio	WHr	WHL/WHR	0.877	dimensionless
arge Ratio	Qr	$\bar{Q}$_L/$\bar{Q}$_R	0.347	dimensionless
Discharge Ratio	Qr,t	Average[Q_(r,t=n)···Q_(r,t=n+N)]	0.346	dimensionless

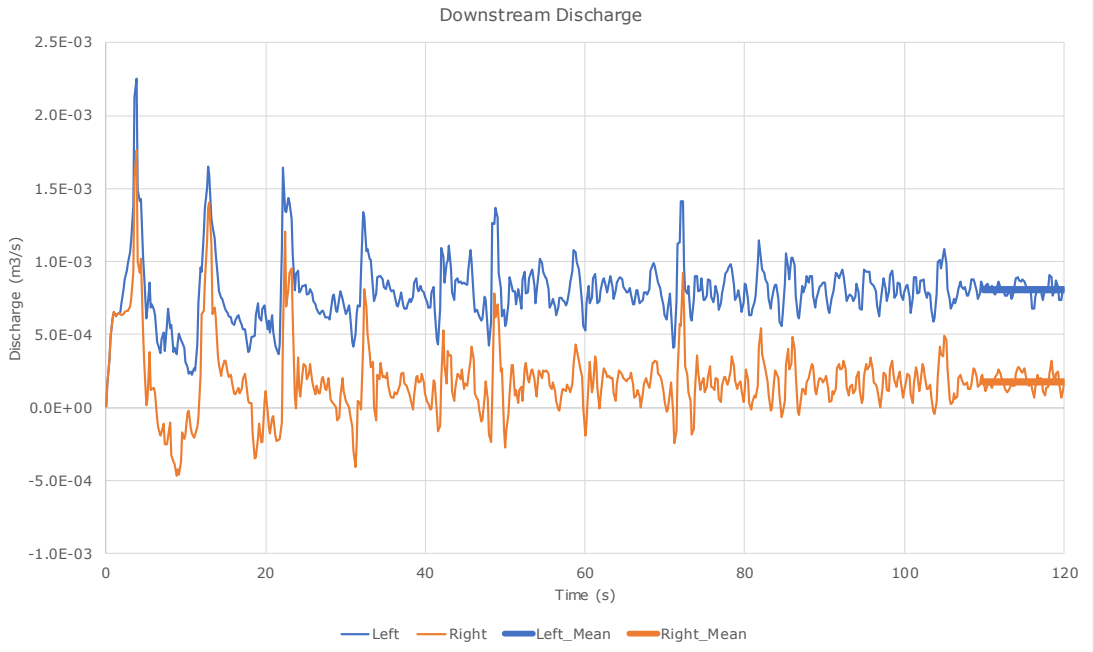


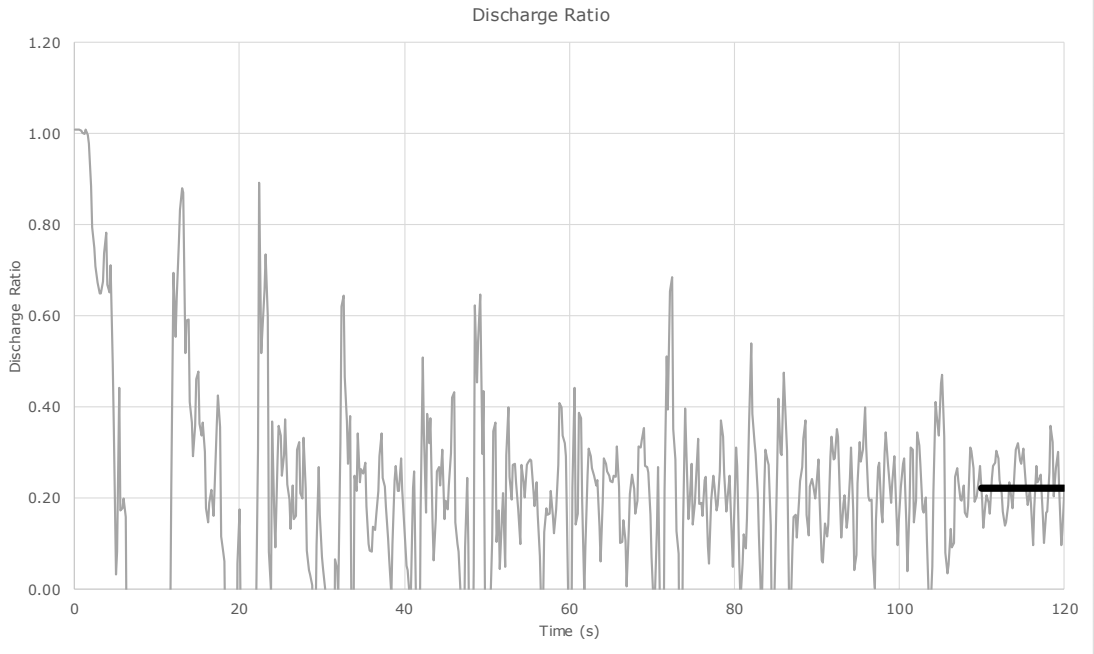


50_07_5060

Name	Symbol	Left	Right	Unit
Weir Height	WH	50	60	mm
Initial Time	Ti	110	110	s
End Time	Te	120	120	s
Initial Number	Ni	550	550	dimensionless
End Number	Ne	600	600	dimensionless
ıverage Discharge	$\bar{Q}$	8.098E-04	1.801E-04	m3/s

Name	Symbol	Equation	Result	Unit
Weir Height Ratio	WHr	WHL/WHR	0.833	dimensionless
Discharge Ratio	Qr	$\bar{Q}$_L/$\bar{Q}$_R	0.222	dimensionless
Step Discharge Ratio	Qr,t	Average[Q_(r,t=n)···Q_(r,t=n+N)]	0.220	dimensionless

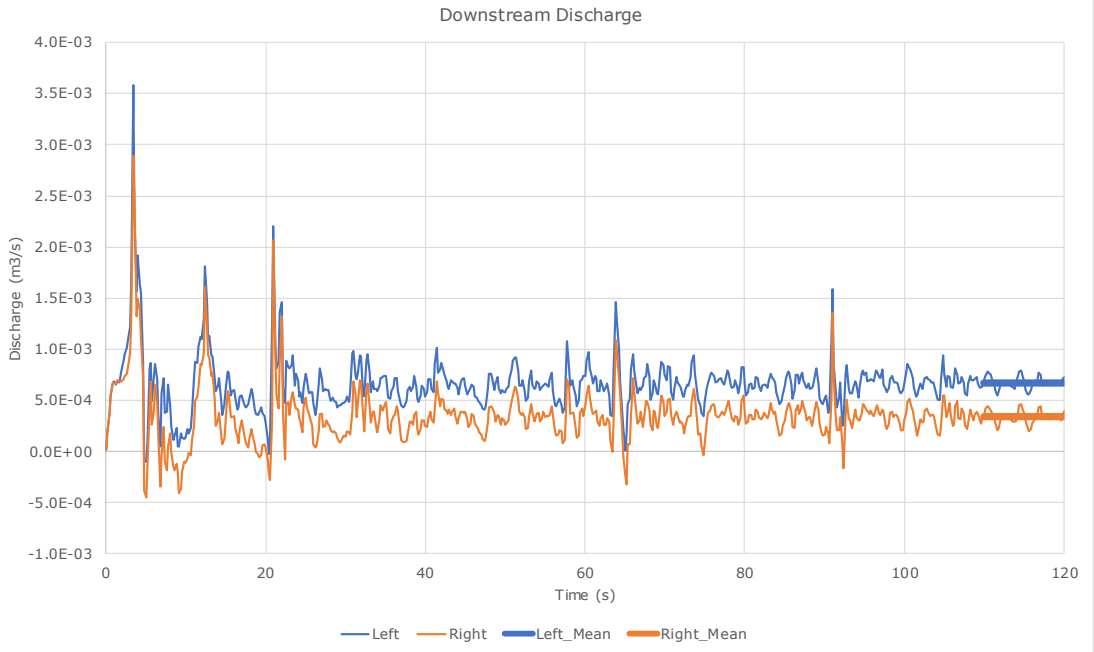


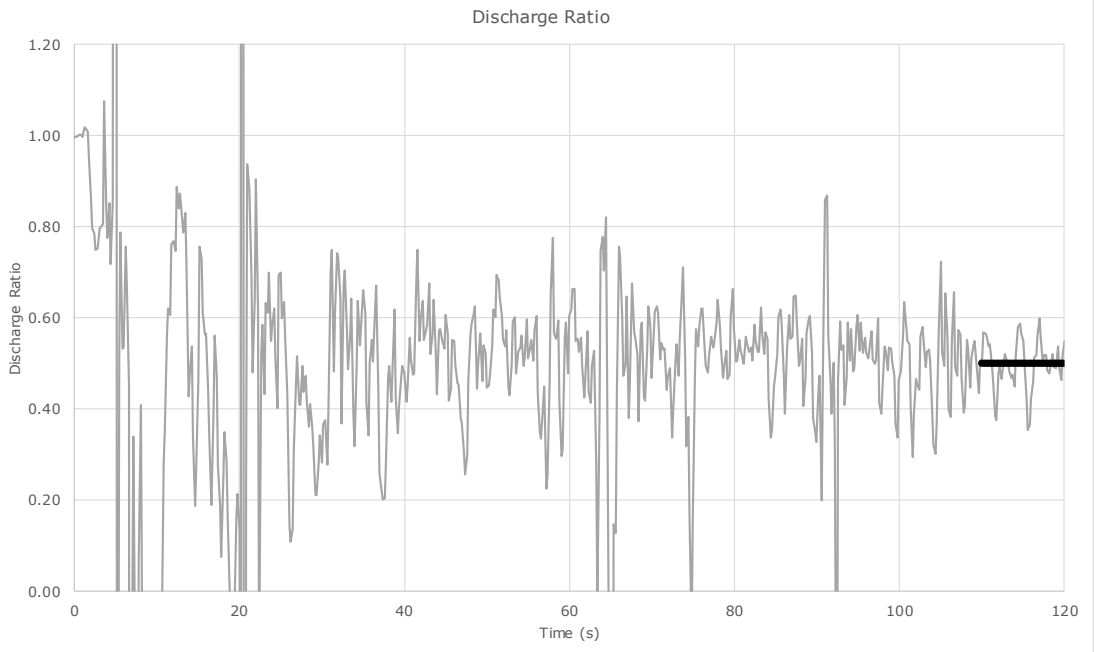


50_07_5560

ame	Symbol	Left	Right	Unit
Height	WH	55	60	mm
il Time	Ti	110	110	s
Time	Te	120	120	s
Number	Ni	550	550	dimensionless
lumber	Ne	600	600	dimensionless
Discharge	$\bar{Q}$	6.747E-04	3.393E-04	m3/s

ame	Symbol	Equation	Result	Unit
ight Ratio	WHr	WHL/WHR	0.917	dimensionless
ge Ratio	Qr	$\bar{Q}$_L/$\bar{Q}$_R	0.503	dimensionless
ischarge Ratio	Qr,t	Average[Q_(r,t=n)···Q_(r,t=n+N)]	0.499	dimensionless

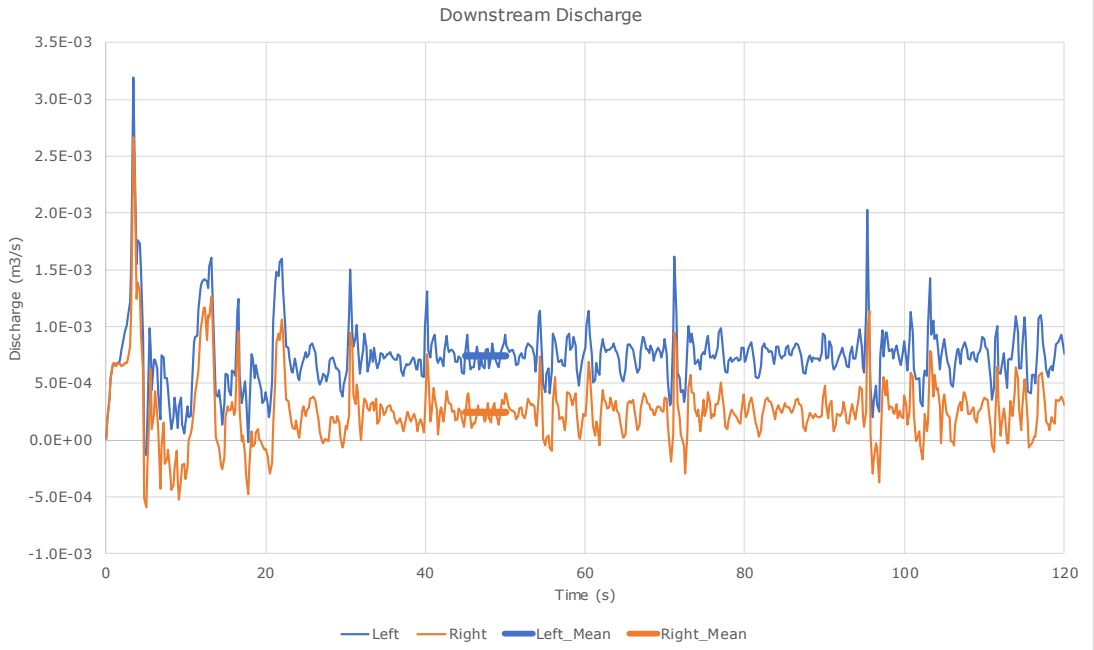


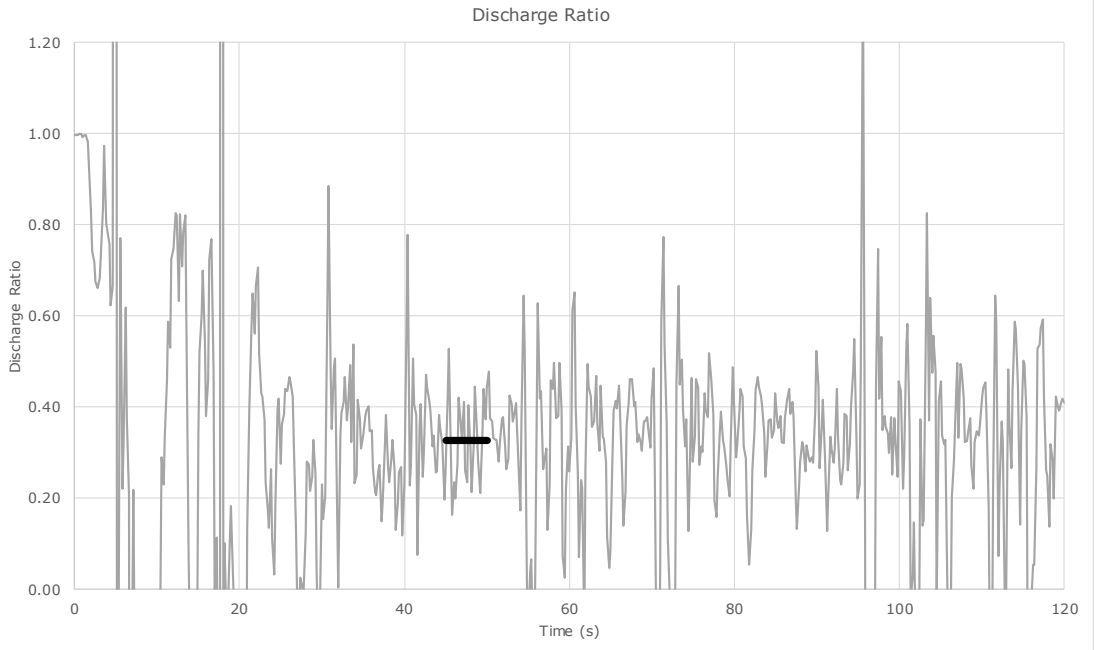


50_07_5562

Name	Symbol	Left	Right	Unit
Weir Height	WH	55	62	mm
Initial Time	Ti	45	45	s
End Time	Te	50	50	s
Initial Number	Ni	225	225	dimensionless
End Number	Ne	250	250	dimensionless
Average Discharge	$\bar{Q}$	7.396E-04	2.461E-04	m3/s

Name	Symbol	Equation	Result	Unit
Weir Height Ratio	WHr	WHL/WHR	0.887	dimensionless
Discharge Ratio	Qr	$\bar{Q}$_L/$\bar{Q}$_R	0.333	dimensionless
Time Step Discharge Ratio	Qr,t	Average[Q_(r,t=n)···Q_(r,t=n+N)]	0.327	dimensionless

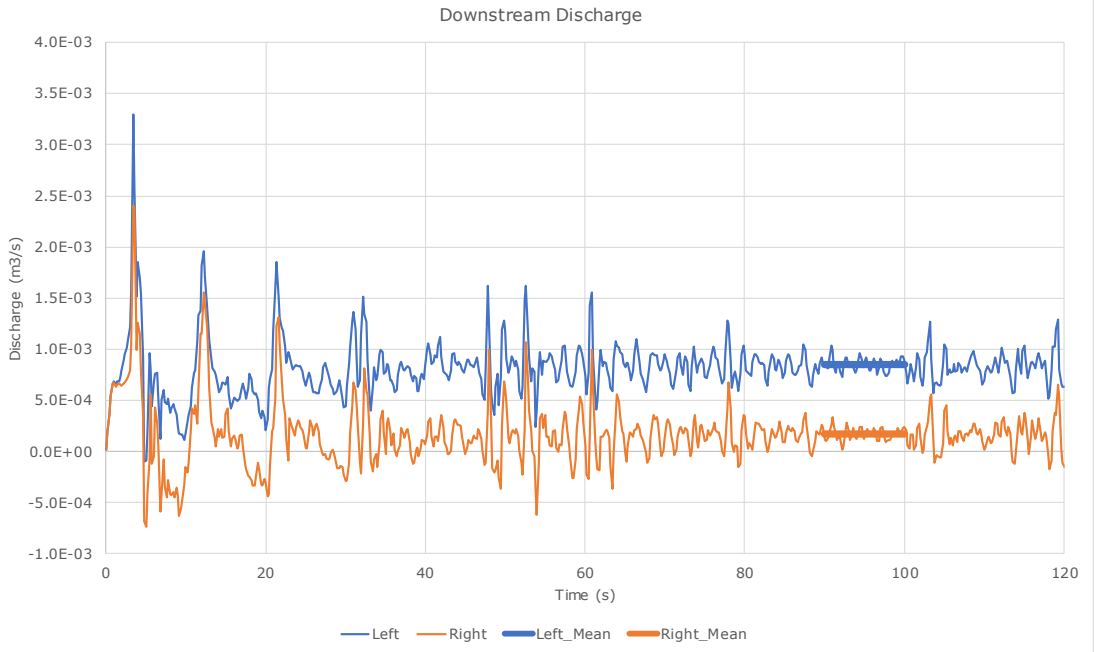


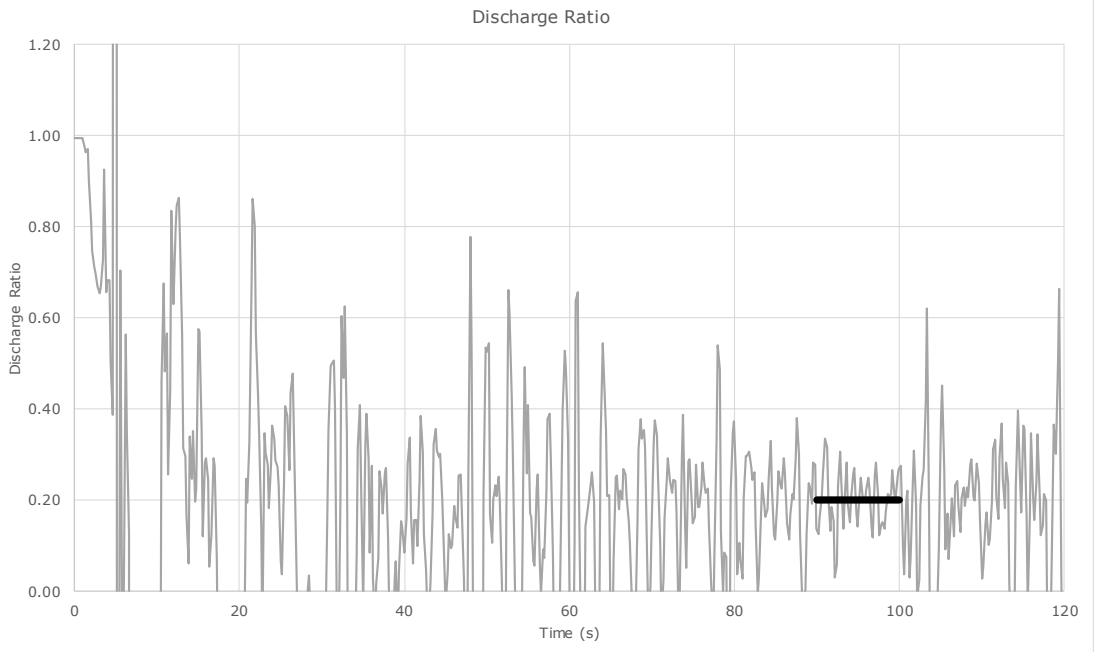


50_07_5565

Name	Symbol	Left	Right	Unit
Weir Height	WH	55	65	mm
Initial Time	Ti	90	90	s
End Time	Te	100	100	s
Initial Number	Ni	450	450	dimensionless
End Number	Ne	500	500	dimensionless
Average Discharge	$\bar{Q}$	8.530E-04	1.729E-04	m3/s

Name	Symbol	Equation	Result	Unit
Weir Height Ratio	WHr	WHL/WHR	0.846	dimensionless
Discharge Ratio	Qr	$\bar{Q}$_L/$\bar{Q}$_R	0.203	dimensionless
Step Discharge Ratio	Qr,t	Average[Q_(r,t=n)···Q_(r,t=n+N)]	0.200	dimensionless

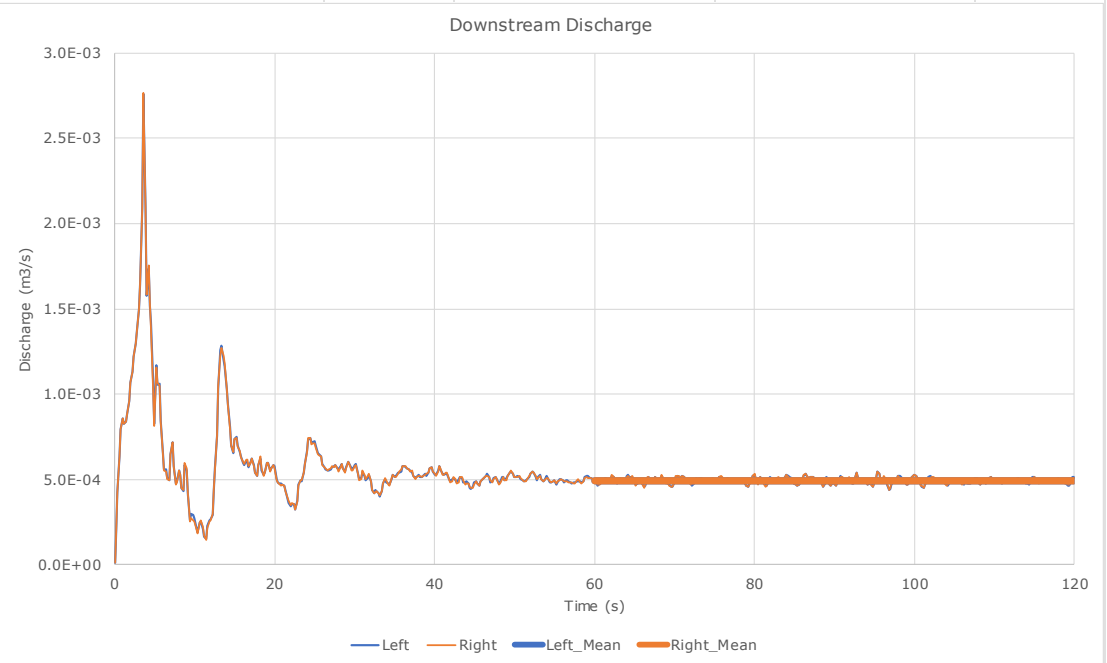


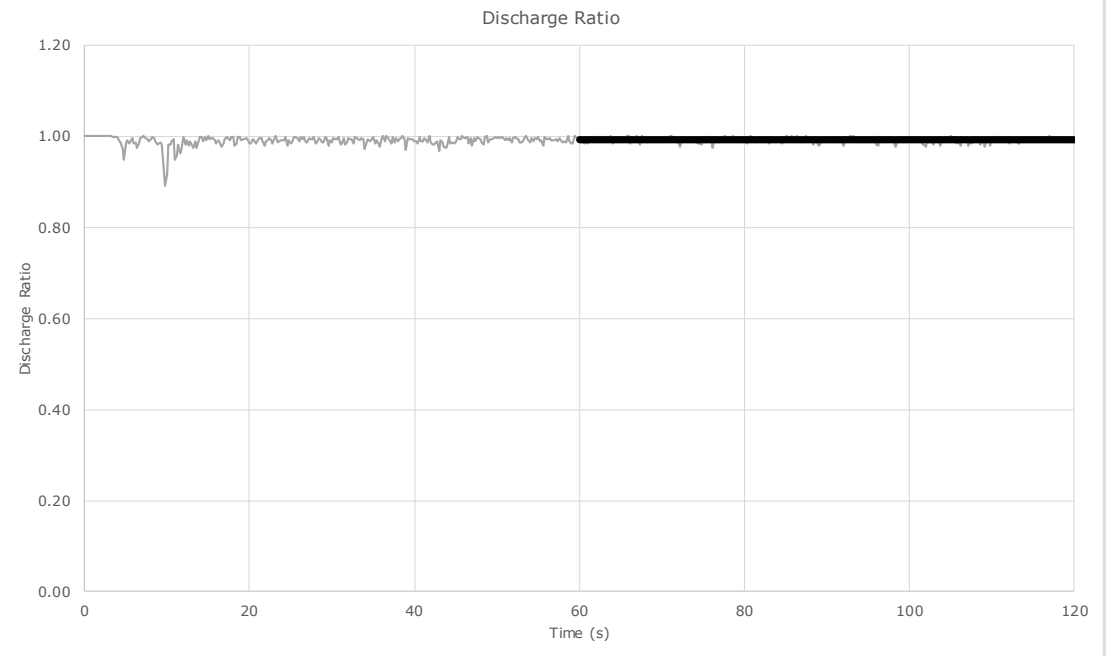


50_09_5050

Name	Symbol	Left	Right	Unit
Weir Height	WH	50	50	mm
Initial Time	Ti	60	60	s
End Time	Te	120	120	s
Initial Number	Ni	300	300	unitless
End Number	Ne	600	600	unitless
Average Discharge	$\bar{Q}$	4.933E-04	4.929E-04	m3/s

Name	Symbol	Equation	Result	Unit
Weir Height Ratio	WHr	WHL/WHR	1.000	dimensionless
Discharge Ratio	Qr	$\bar{Q}$_L/$\bar{Q}$_R	0.999	dimensionless
Time Step Discharge Ratio	Qr,t	Average[Q_(r,t=n)···Q_(r,t=n+N)]	0.993	dimensionless

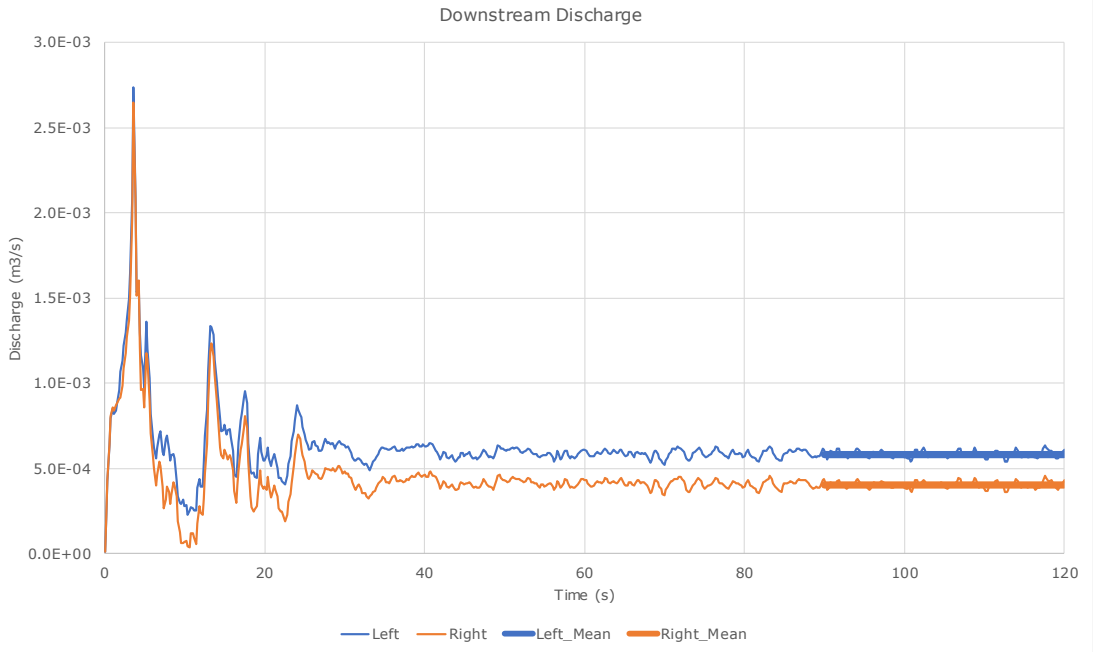


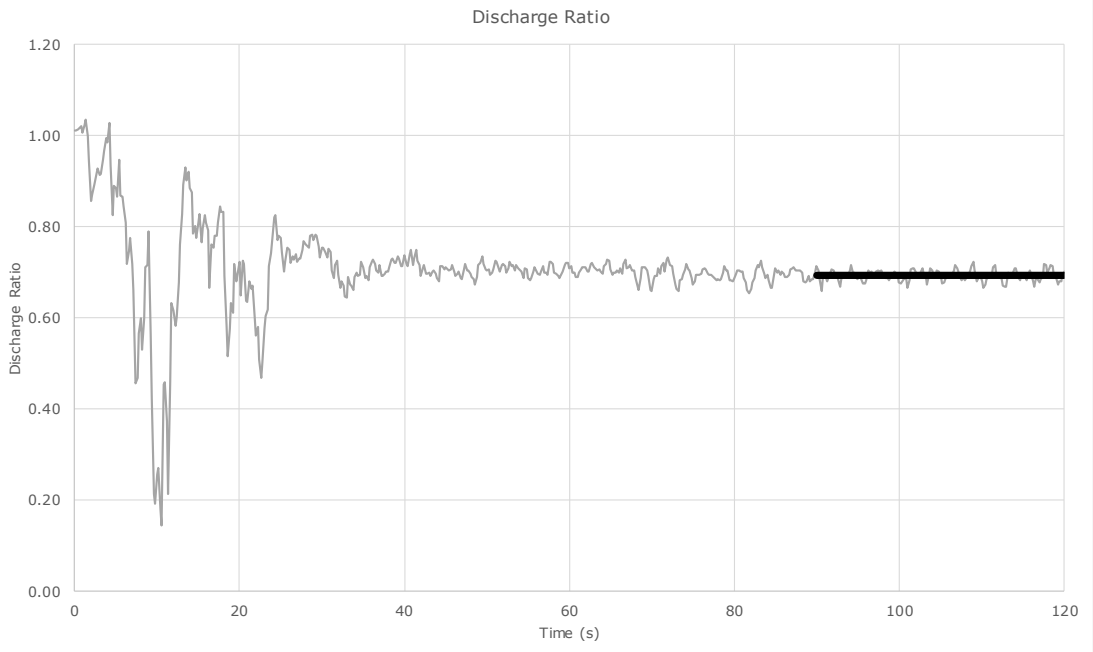


50_09_5053

Name	Symbol	Left	Right	Unit
Weir Height	WH	50	53	mm
Initial Time	Ti	90	90	s
End Time	Te	120	120	s
Initial Number	Ni	450	450	unitless
End Number	Ne	600	600	unitless
Average Discharge	$\bar{Q}$	5.846E-04	4.052E-04	m3/s

Name	Symbol	Equation	Result	Unit
Weir Height Ratio	WHr	WHL/WHR	0.943	dimensionless
Discharge Ratio	Qr	$\bar{Q}$_L/$\bar{Q}$_R	0.693	dimensionless
₃ Step Discharge Ratio	Qr,t	Average[Q_(r,t=n)···Q_(r,t=n+N)]	0.693	dimensionless

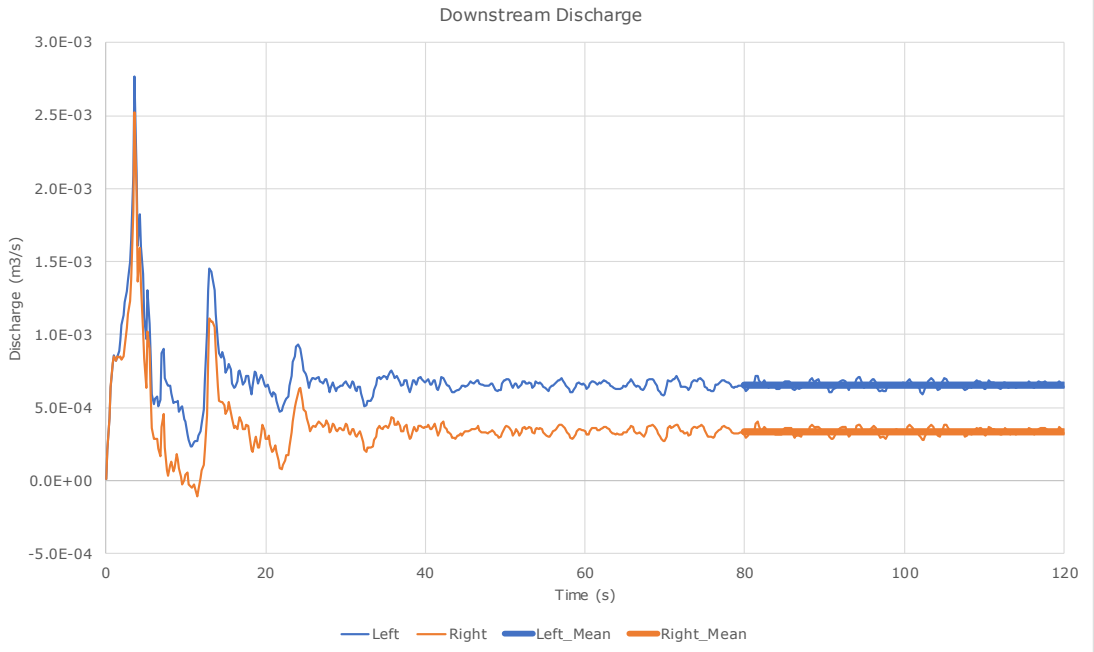


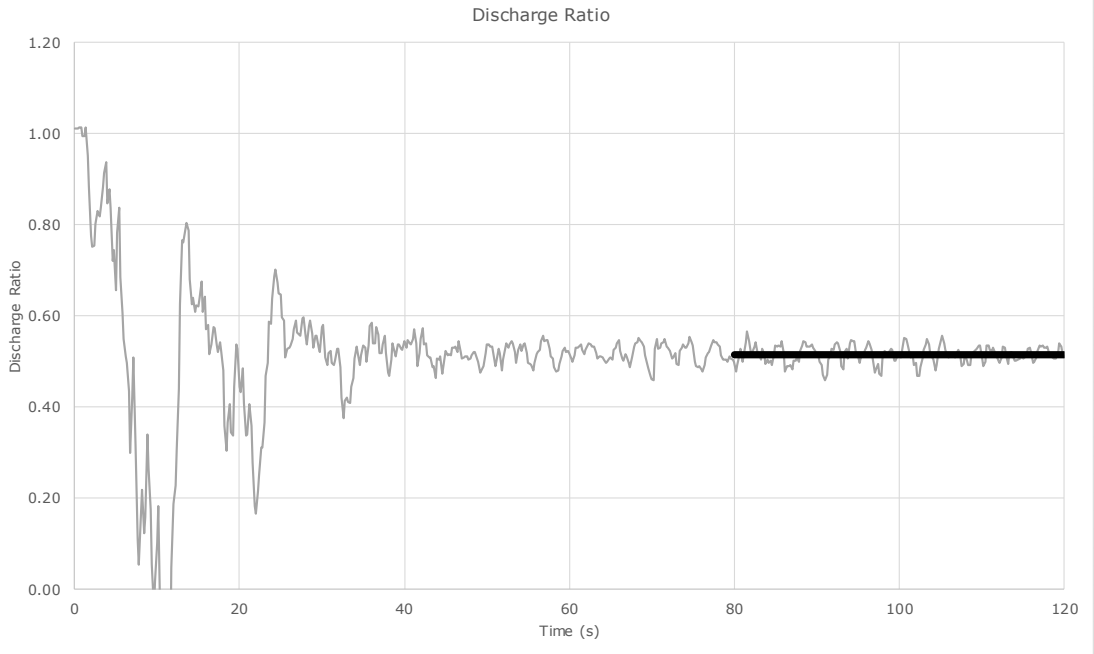


50_09_5055

Name	Symbol	Left	Right	Unit
Weir Height	WH	50	55	mm
Initial Time	Ti	80	80	s
End Time	Te	120	120	s
Initial Number	Ni	400	400	unitless
End Number	Ne	600	600	unitless
Average Discharge	$\bar{Q}$	6.568E-04	3.385E-04	m3/s

Name	Symbol	Equation	Result	Unit
Weir Height Ratio	WHr	WHL/WHR	0.909	dimensionless
Discharge Ratio	Qr	$\bar{Q}$_L/$\bar{Q}$_R	0.515	dimensionless
Time Step Discharge Ratio	Qr,t	Average[Q_(r,t=n)···Q_(r,t=n+N)]	0.515	dimensionless

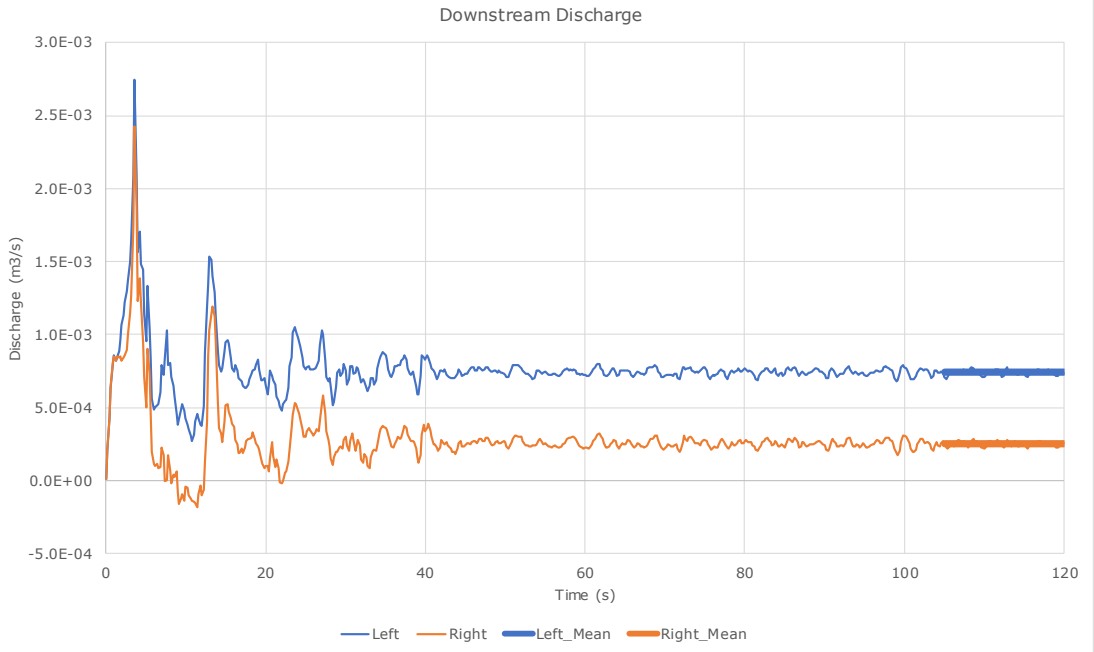


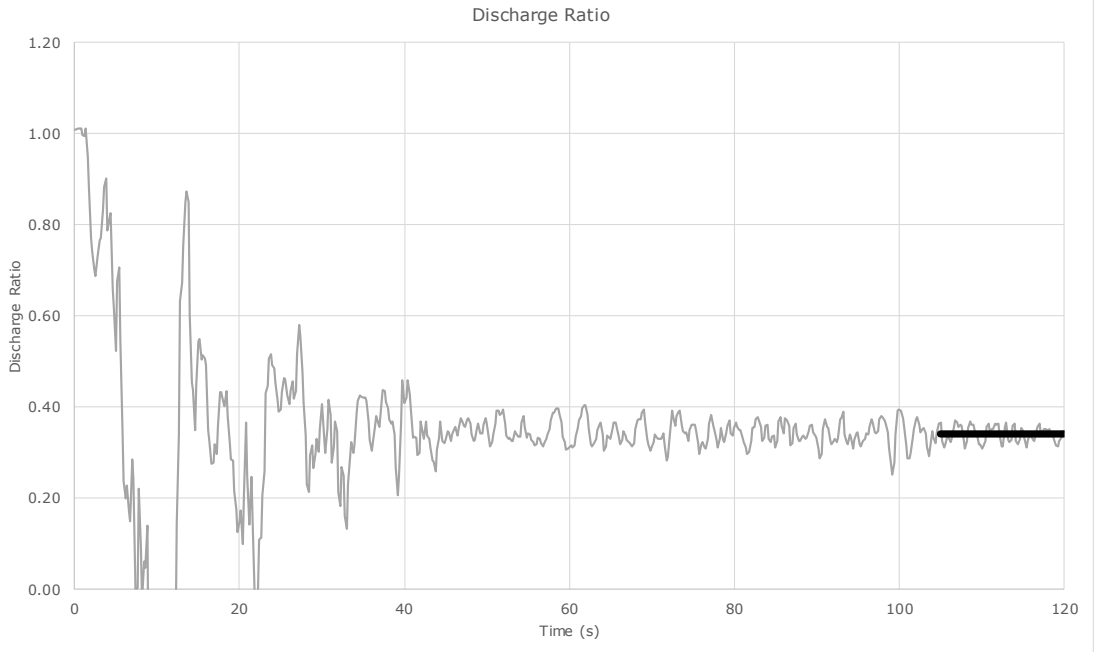


50_09_5057

Name	Symbol	Left	Right	Unit
Weir Height	WH	50	57	mm
Initial Time	Ti	105	105	s
End Time	Te	120	120	s
Initial Number	Ni	525	525	unitless
End Number	Ne	600	600	unitless
Average Discharge	$\bar{Q}$	7.410E-04	2.522E-04	m3/s

Name	Symbol	Equation	Result	Unit
Weir Height Ratio	WHr	WHL/WHR	0.877	dimensionless
Discharge Ratio	Qr	$\bar{Q}$_L/$\bar{Q}$_R	0.340	dimensionless
Mean Discharge Ratio	Qr,t	Average[Q_(r,t=n)···Q_(r,t=n+N)]	0.340	dimensionless

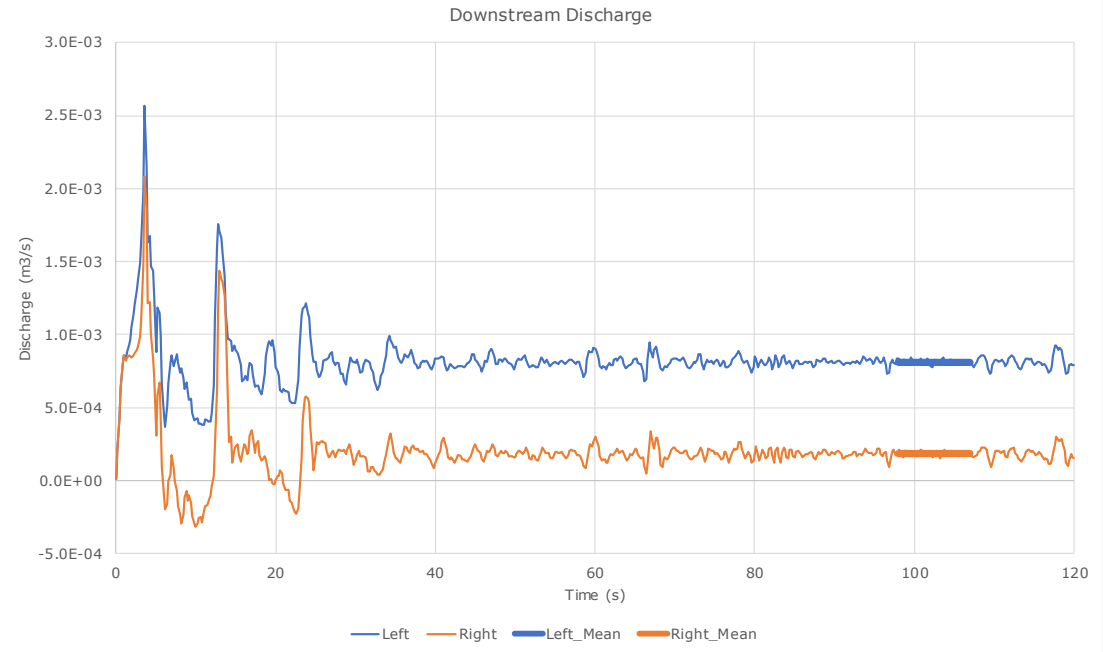


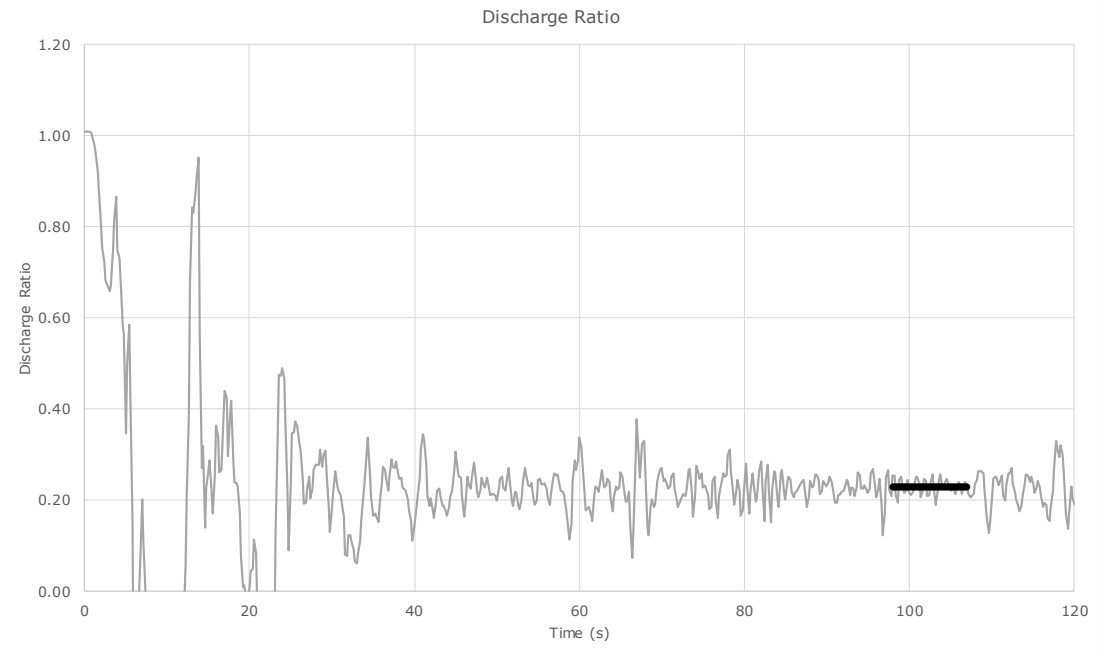


50_09_5060

Name	Symbol	Left	Right	Unit
Weir Height	WH	50	60	mm
Initial Time	Ti	98	98	s
End Time	Te	107	107	s
Initial Number	Ni	490	490	dimensionless
End Number	Ne	535	535	dimensionless
Average Discharge	$\bar{Q}$	8.142E-04	1.869E-04	m3/s

Name	Symbol	Equation	Result	Unit
Weir Height Ratio	WHr	WHL/WHR	0.833	dimensionless
Discharge Ratio	Qr	$\bar{Q}$_L/$\bar{Q}$_R	0.230	dimensionless
Time Step Discharge Ratio	Qr,t	Average[Q_(r,t=n)···Q_(r,t=n+N)]	0.229	dimensionless

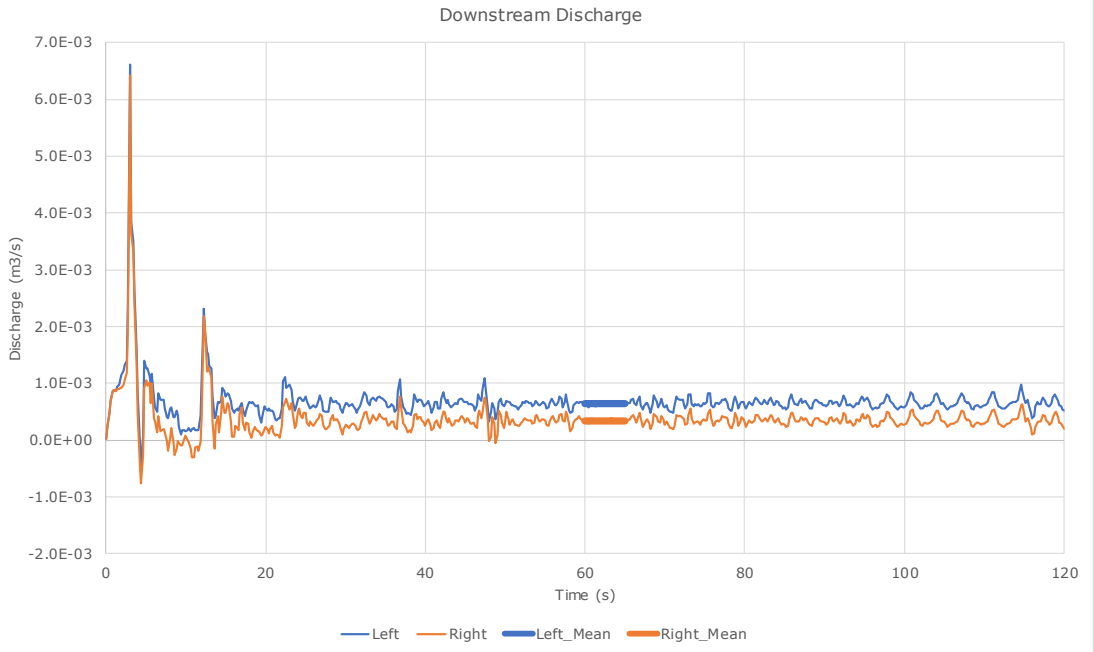


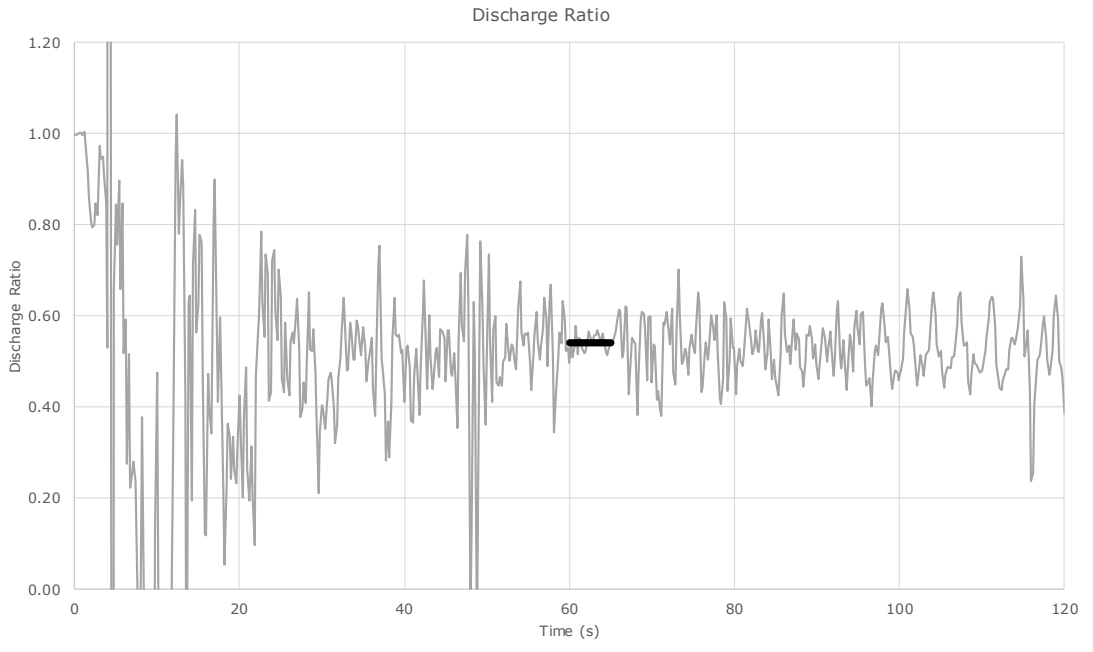


50_09_5560

Name	Symbol	Left	Right	Unit
Weir Height	WH	55	60	mm
Initial Time	Ti	60	60	s
End Time	Te	65	65	s
Initial Number	Ni	300	300	dimensionless
End Number	Ne	325	325	dimensionless
Average Discharge	$\bar{Q}$	6.428E-04	3.469E-04	m3/s

Name	Symbol	Equation	Result	Unit
Weir Height Ratio	WHr	WHL/WHR	0.917	dimensionless
Discharge Ratio	Qr	$\bar{Q}$_L/$\bar{Q}$_R	0.540	dimensionless
ime Step Discharge Ratio	Qr,t	Average[Q_(r,t=n)···Q_(r,t=n+N)]	0.539	dimensionless

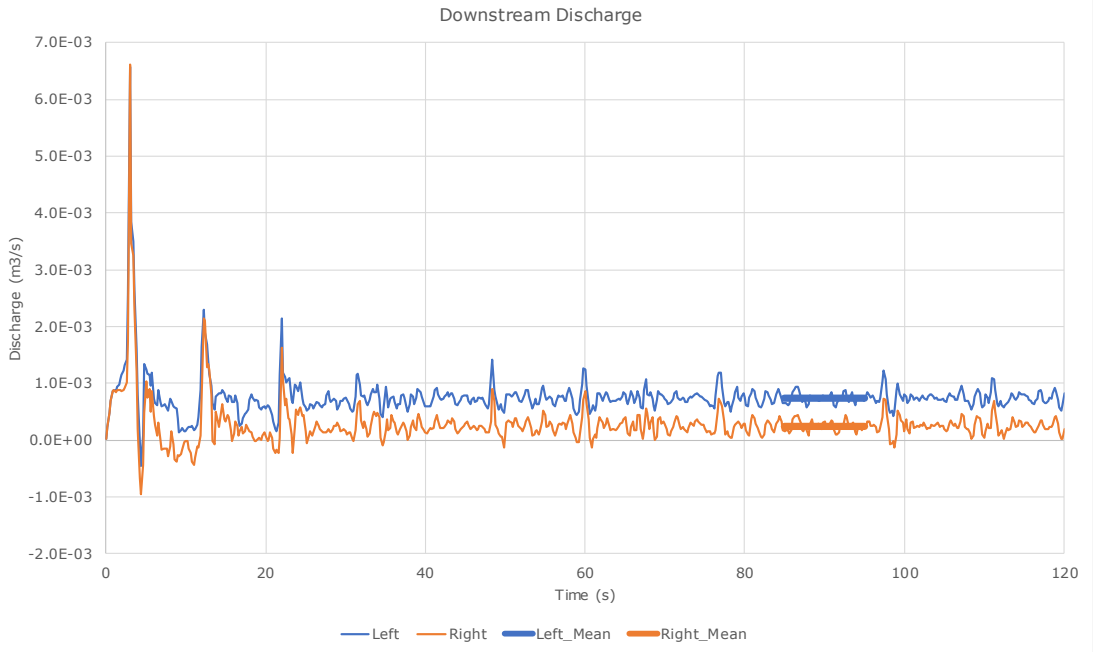


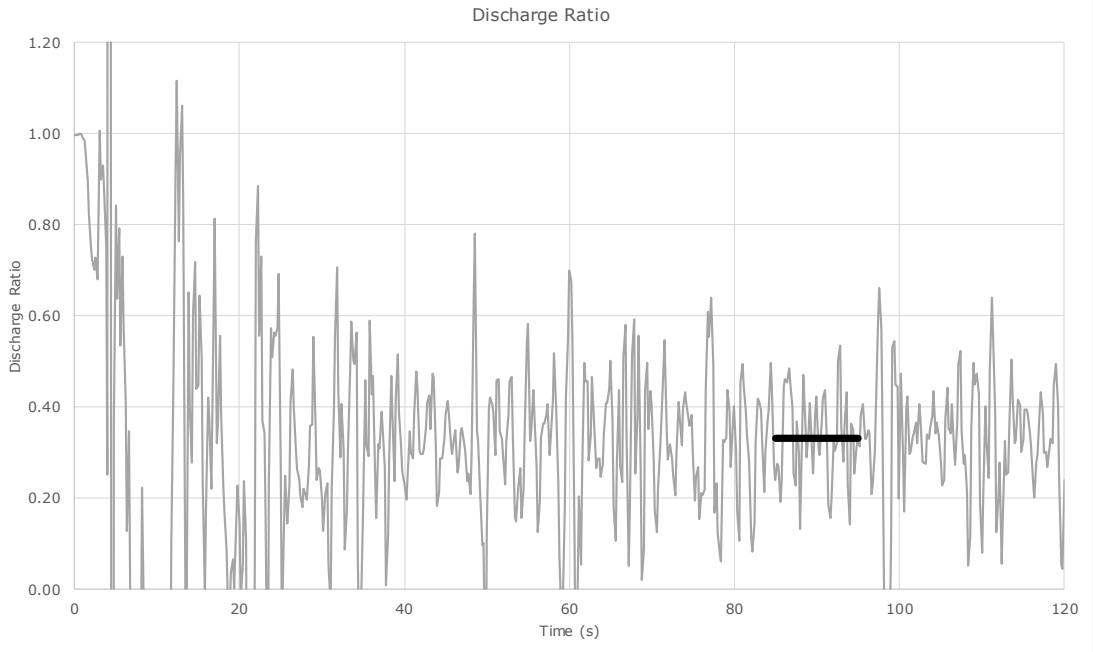


50_09_5562

Name	Symbol	Left	Right	Unit
Weir Height	WH	55	62	mm
Initial Time	Ti	85	85	s
End Time	Te	95	95	s
Initial Number	Ni	425	425	dimensionless
End Number	Ne	475	475	dimensionless
erage Discharge	$\bar{Q}$	7.373E-04	2.489E-04	m3/s

Name	Symbol	Equation	Result	Unit
'eir Height Ratio	WHr	WHL/WHR	0.887	dimensionless
)ischarge Ratio	Qr	$\bar{Q}$_L/$\bar{Q}$_R	0.338	dimensionless
;tep Discharge Ratio	Qr,t	Average[Q_(r,t=n)···Q_(r,t=n+N)]	0.330	dimensionless

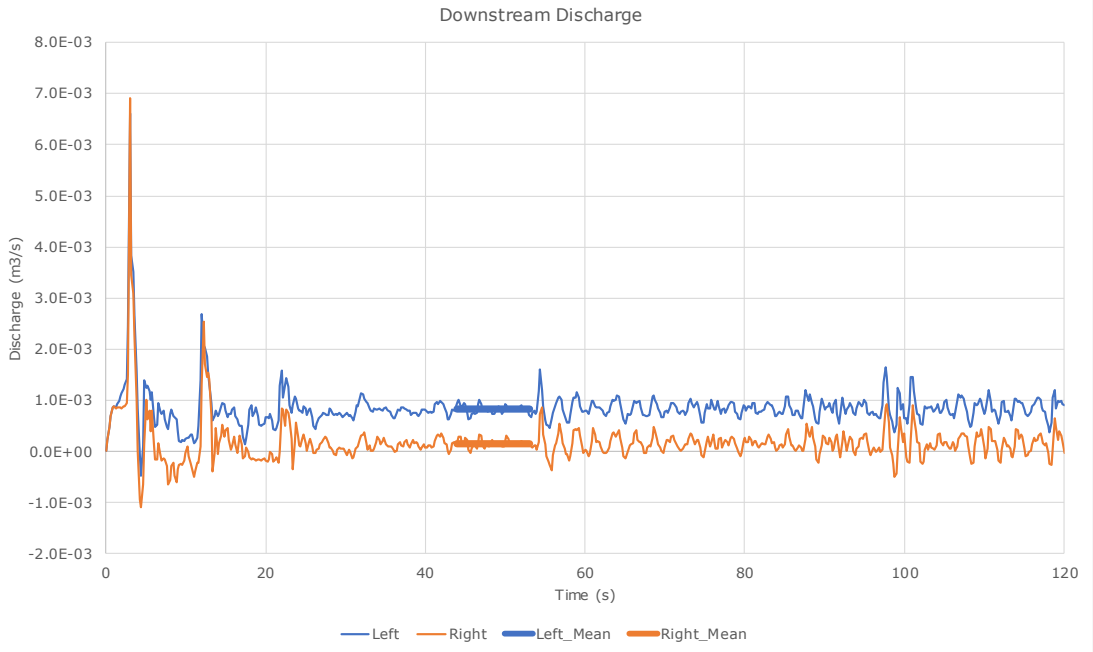


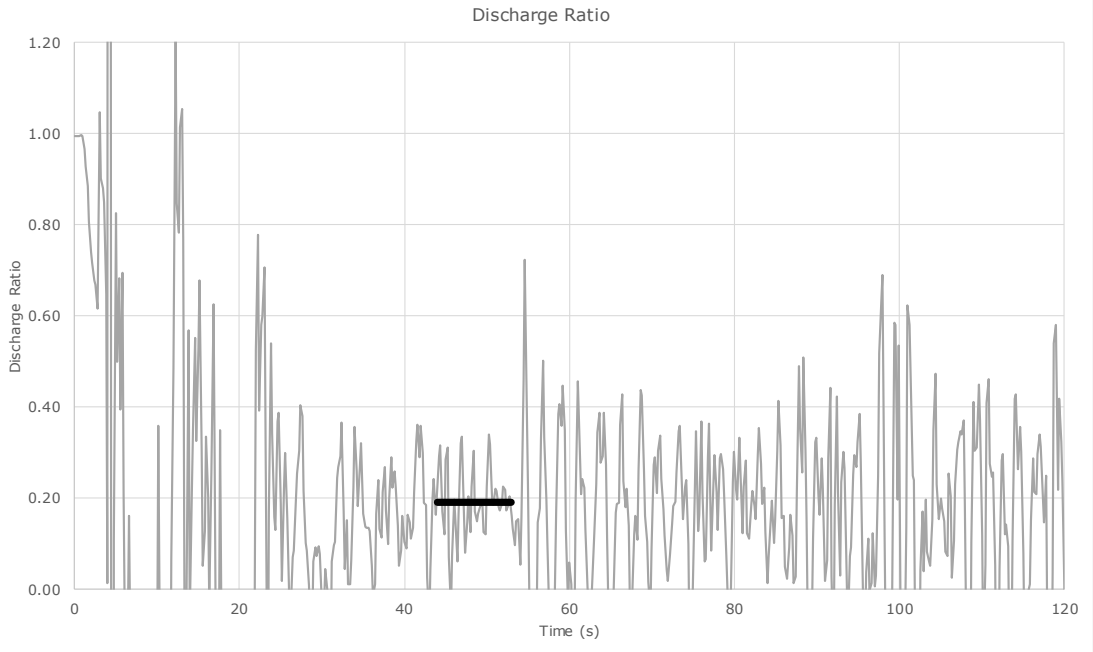


50_09_5565

Name	Symbol	Left	Right	Unit
Weir Height	WH	55	65	mm
Initial Time	Ti	44	44	s
End Time	Te	53	53	s
Initial Number	Ni	220	220	dimensionless
End Number	Ne	265	265	dimensionless
Average Discharge	$\bar{Q}$	8.292E-04	1.617E-04	m3/s

Name	Symbol	Equation	Result	Unit
Weir Height Ratio	WHr	WHL/WHR	0.846	dimensionless
Discharge Ratio	Qr	$\bar{Q}$_L/$\bar{Q}$_R	0.195	dimensionless
Step Discharge Ratio	Qr,t	Average[Q_(r,t=n)···Q_(r,t=n+N)]	0.191	dimensionless

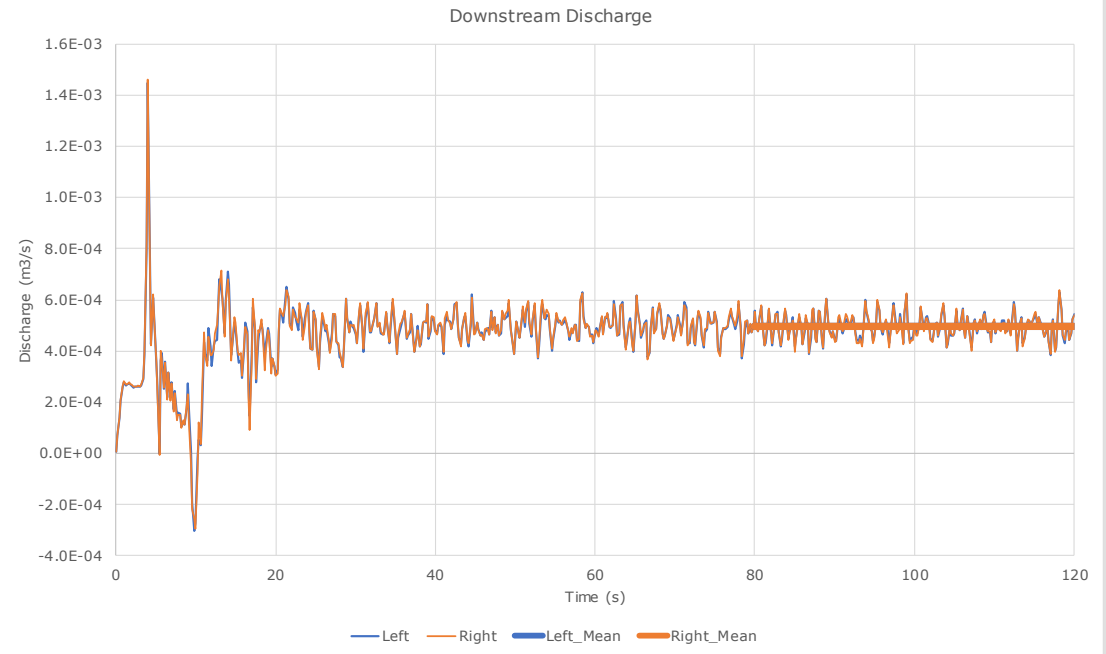


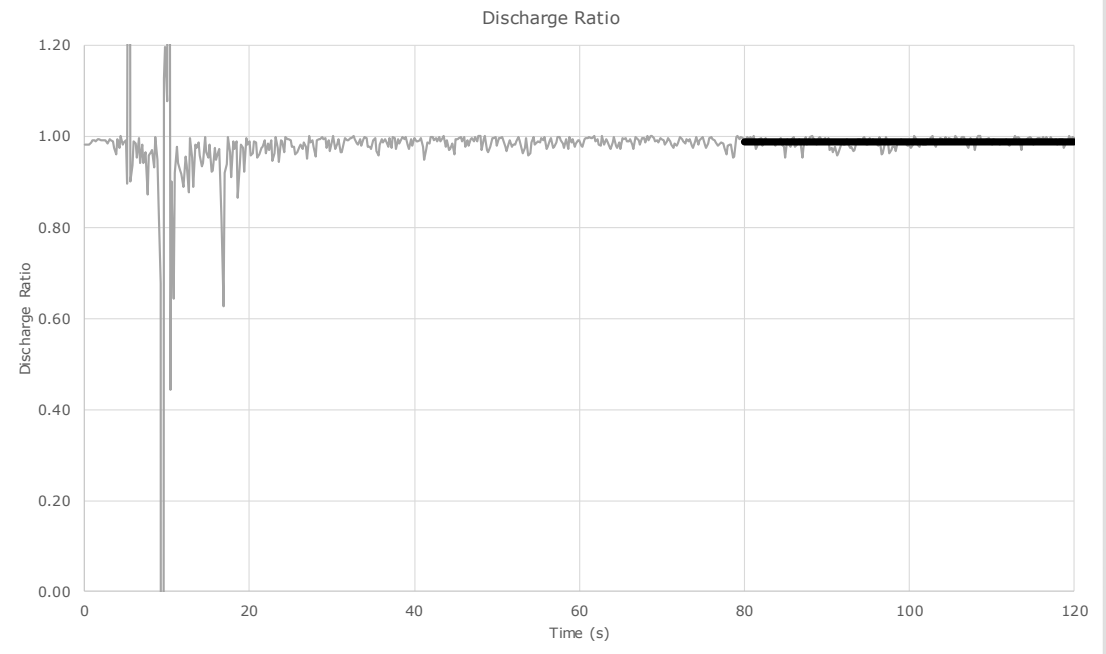


60_03_5050

Name	Symbol	Left	Right	Unit
Weir Height	WH	50	50	mm
Initial Time	Ti	80	80	s
End Time	Te	120	120	s
Initial Number	Ni	400	400	unitless
End Number	Ne	600	600	unitless
Average Discharge	$\bar{Q}$	4.951E-04	4.947E-04	m3/s

Name	Symbol	Equation	Result	Unit
Weir Height Ratio	WHr	WHL/WHR	1.000	dimensionless
Discharge Ratio	Qr	$\bar{Q}$_L/$\bar{Q}$_R	0.999	dimensionless
Time Step Discharge Ratio	Qr,t	Average[Q_(r,t=n)···Q_(r,t=n+N)]	0.987	dimensionless

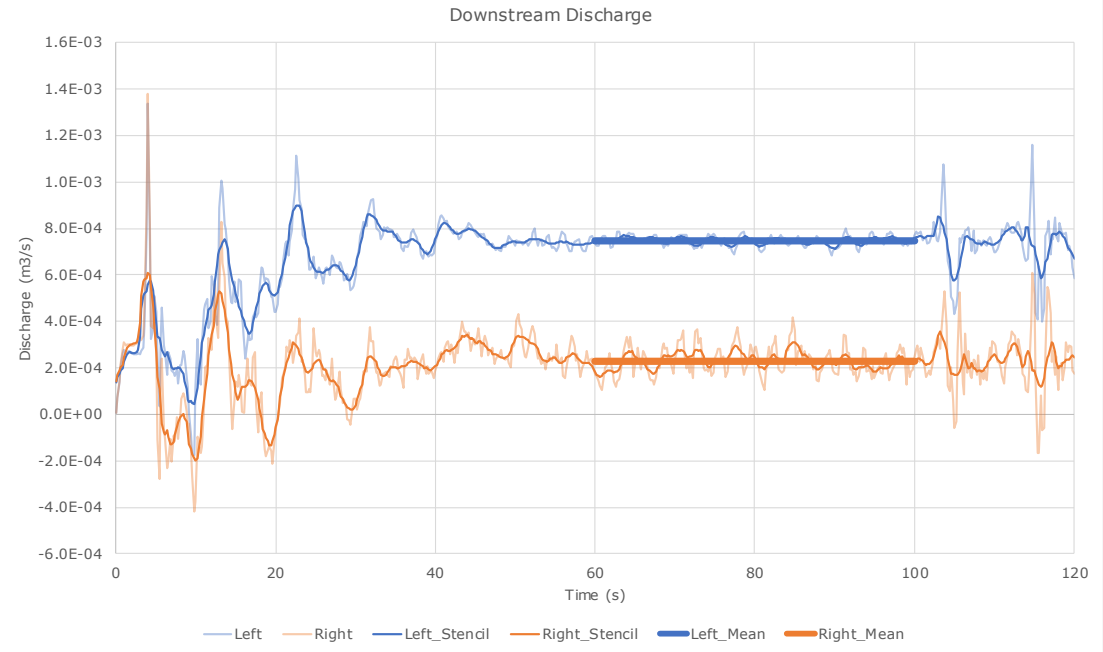


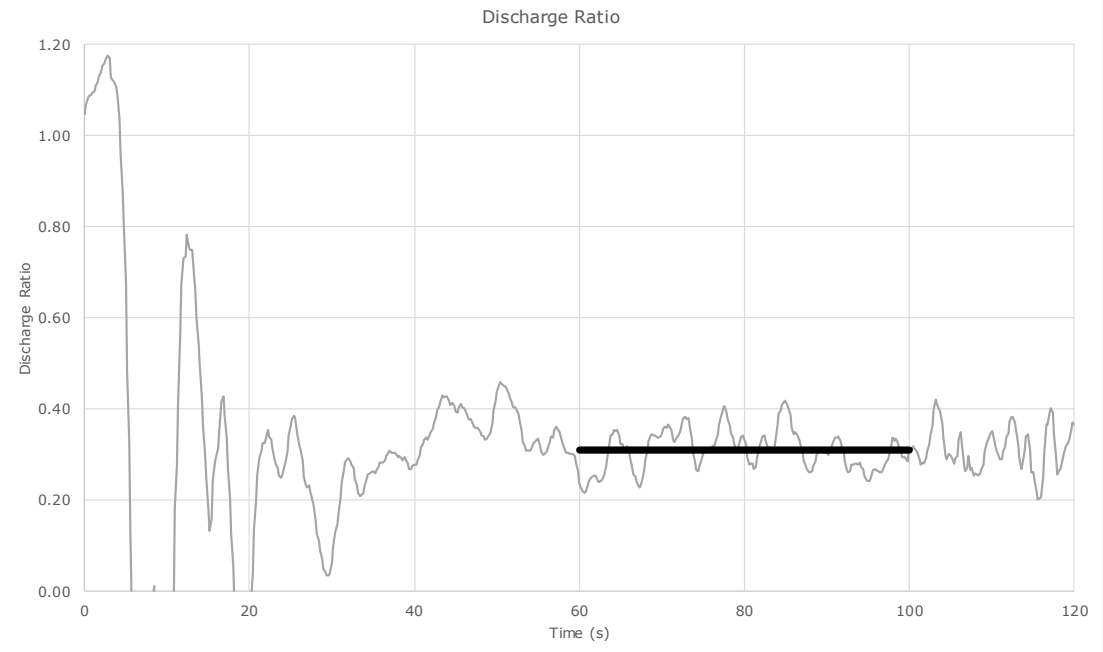


60_03_5053

	Symbol	Left	Right	Unit
	WH	50	53	mm
	Ti	60	60	s
	Te	100	100	s
	Ni	300	300	unitless
	Ne	500	500	unitless
ıe	$\bar{Q}$	7.472E-04	2.308E-04	m3/s

	Symbol	Equation	Result	Unit
o	WHr	WHL/WHR	0.943	dimensionless
	Qr	$\bar{Q}$_L/$\bar{Q}$_R	0.309	dimensionless
Ratio	Qr,t	Average[Q_(r,t=n)···Q_(r,t=n+N)]	0.309	dimensionless

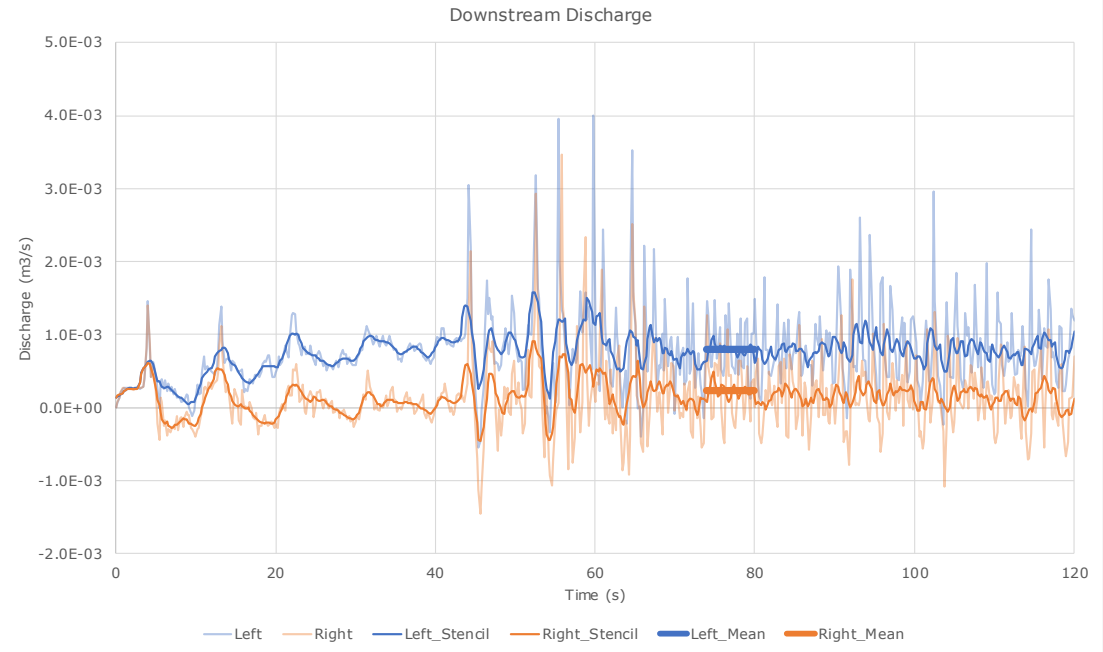


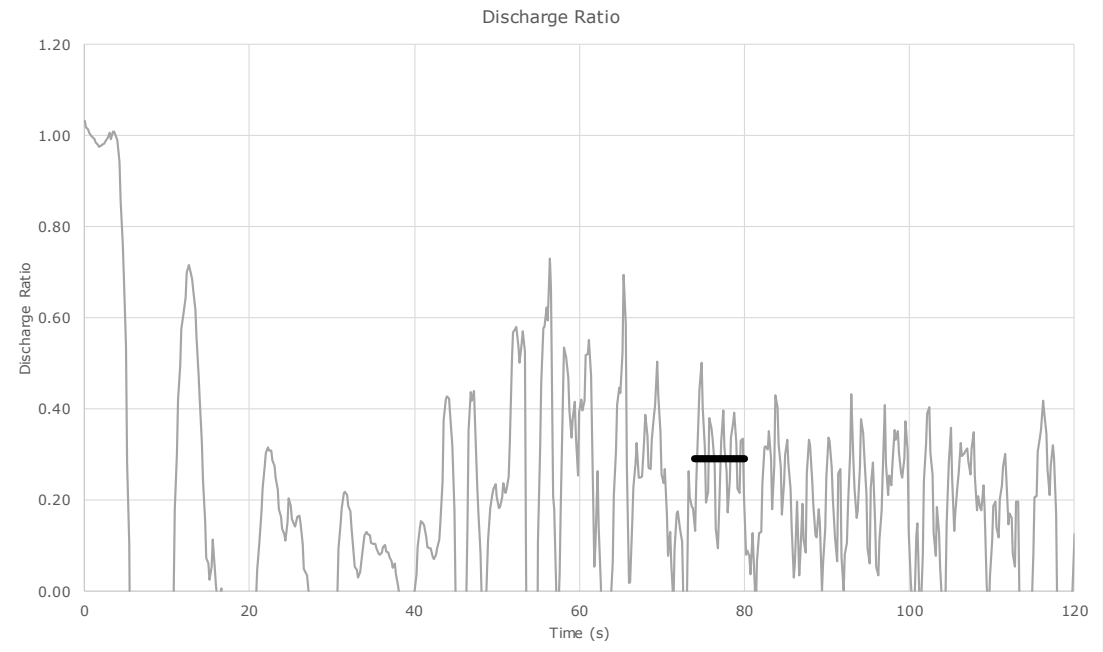


60_03_5055

Name	Symbol	Left	Right	Unit
Weir Height	WH	50	55	mm
Initial Time	Ti	74	74	s
End Time	Te	80	80	s
Initial Number	Ni	370	370	unitless
End Number	Ne	400	400	unitless
Average Discharge	$\bar{Q}$	7.937E-04	2.347E-04	m3/s

Name	Symbol	Equation	Result	Unit
Weir Height Ratio	WHr	WHL/WHR	0.909	dimensionless
Discharge Ratio	Qr	$\bar{Q}$_L/$\bar{Q}$_R	0.296	dimensionless
Time Step Discharge Ratio	Qr,t	Average[Q_(r,t=n)···Q_(r,t=n+N)]	0.291	dimensionless

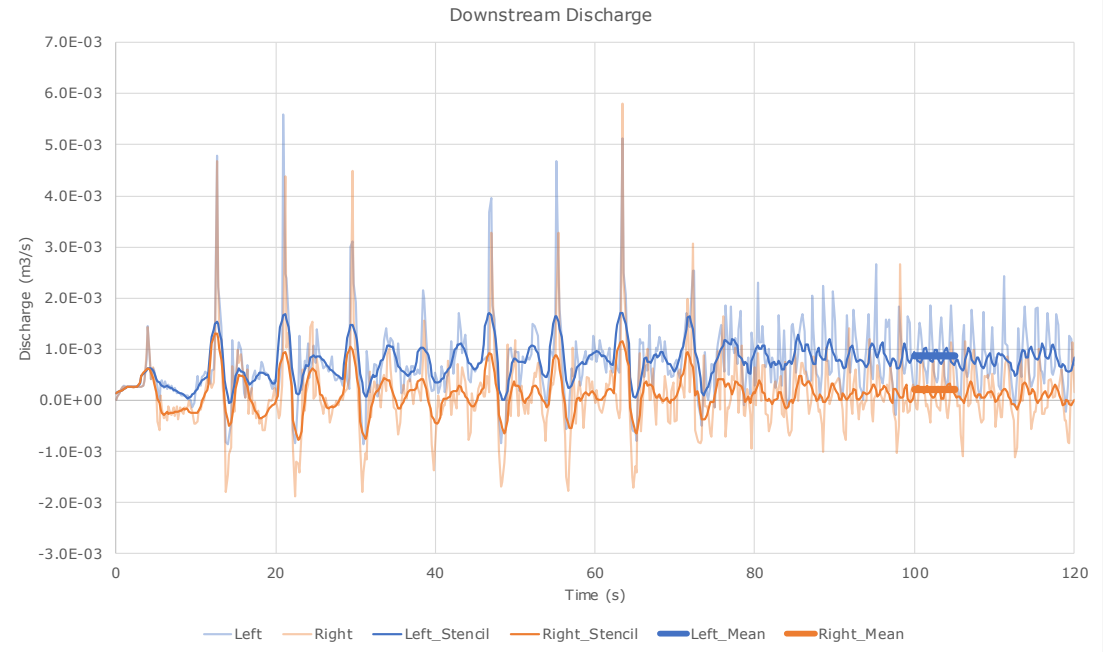


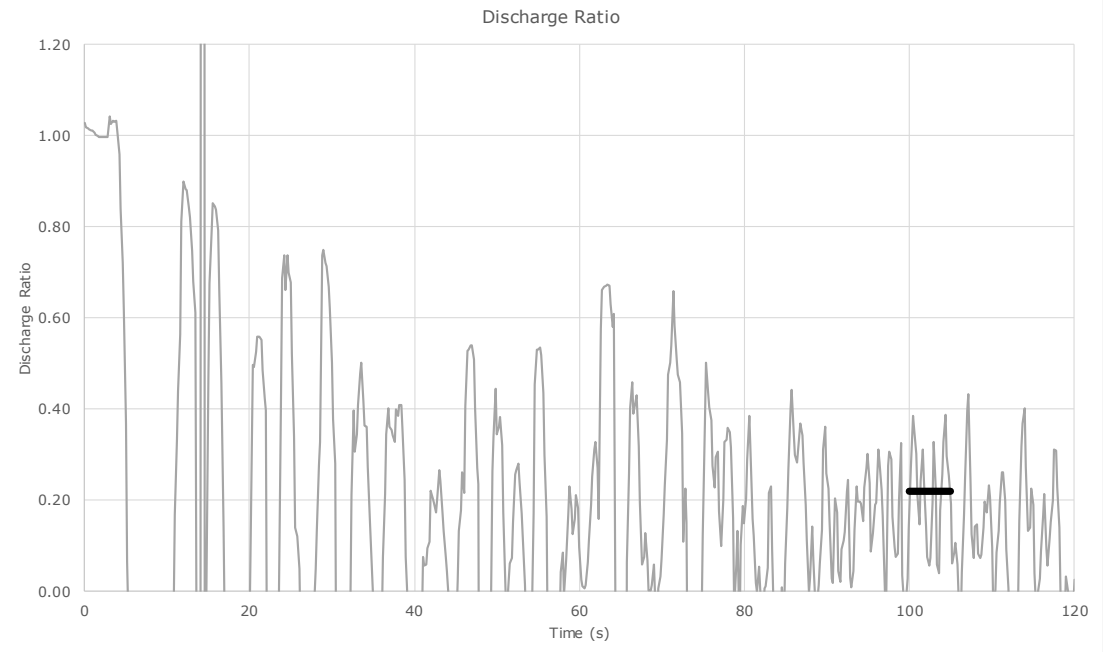


60_03_5057

Name	Symbol	Left	Right	Unit
Weir Height	WH	50	57	mm
Initial Time	Ti	100	100	s
End Time	Te	105	105	s
Initial Number	Ni	500	500	unitless
End Number	Ne	525	525	unitless
Average Discharge	$\bar{Q}$	8.657E-04	2.050E-04	m3/s

Name	Symbol	Equation	Result	Unit
Weir Height Ratio	WHr	WHL/WHR	0.877	dimensionless
Discharge Ratio	Qr	$\bar{Q}_L/\bar{Q}_R$	0.237	dimensionless
Time Step Discharge Ratio	Qr,t	Average[Q_(r,t=n)···Q_(r,t=n+N)]	0.219	dimensionless

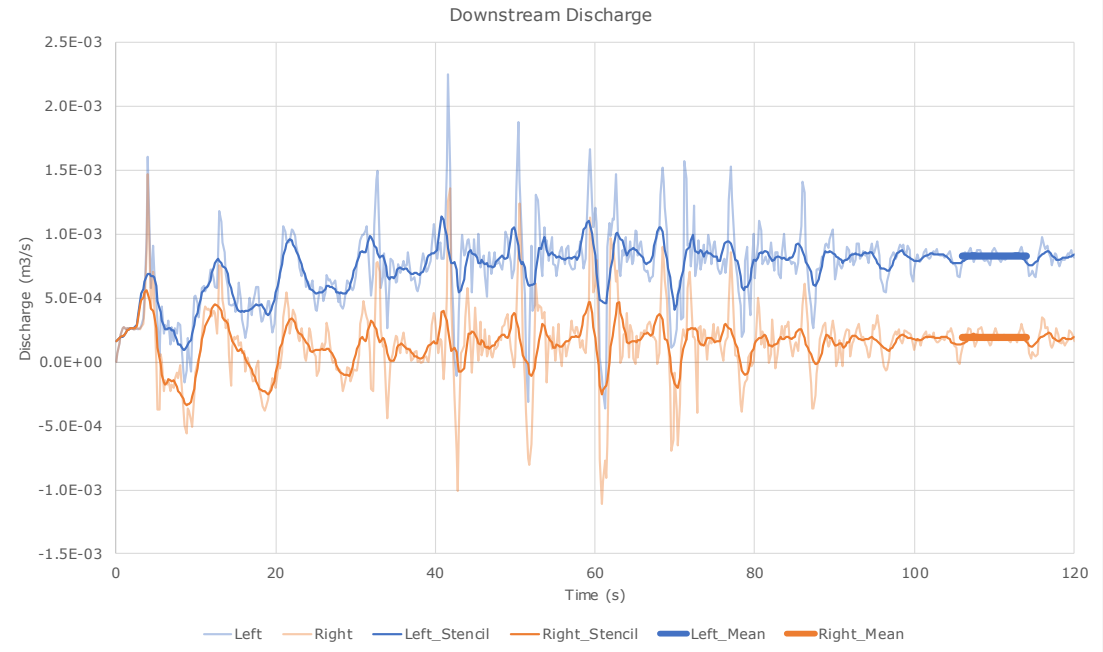


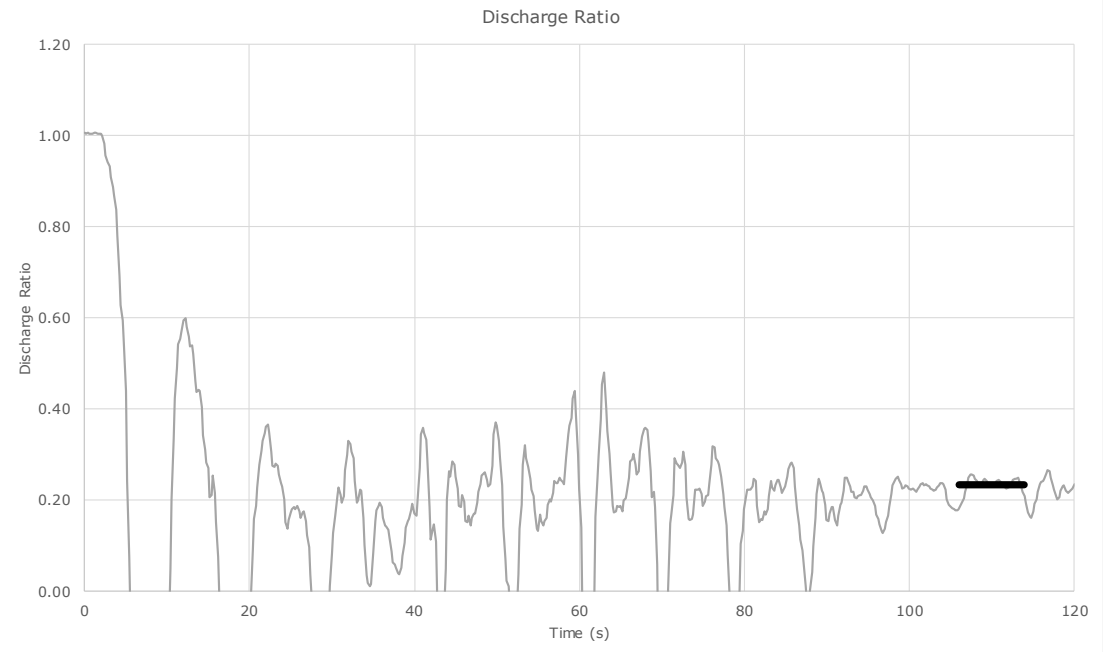


60_03_5060

Name	Symbol	Left	Right	Unit
Weir Height	WH	50	60	mm
Initial Time	Ti	106	106	s
End Time	Te	114	114	s
Initial Number	Ni	530	530	dimensionless
End Number	Ne	570	570	dimensionless
Average Discharge	$\bar{Q}$	8.258E-04	1.922E-04	m3/s

Name	Symbol	Equation	Result	Unit
Weir Height Ratio	WHr	WHL/WHR	0.833	dimensionless
Discharge Ratio	Qr	$\bar{Q}$_L/$\bar{Q}$_R	0.233	dimensionless
Time Step Discharge Ratio	Qr,t	Average[Q_(r,t=n)···Q_(r,t=n+N)]	0.232	dimensionless

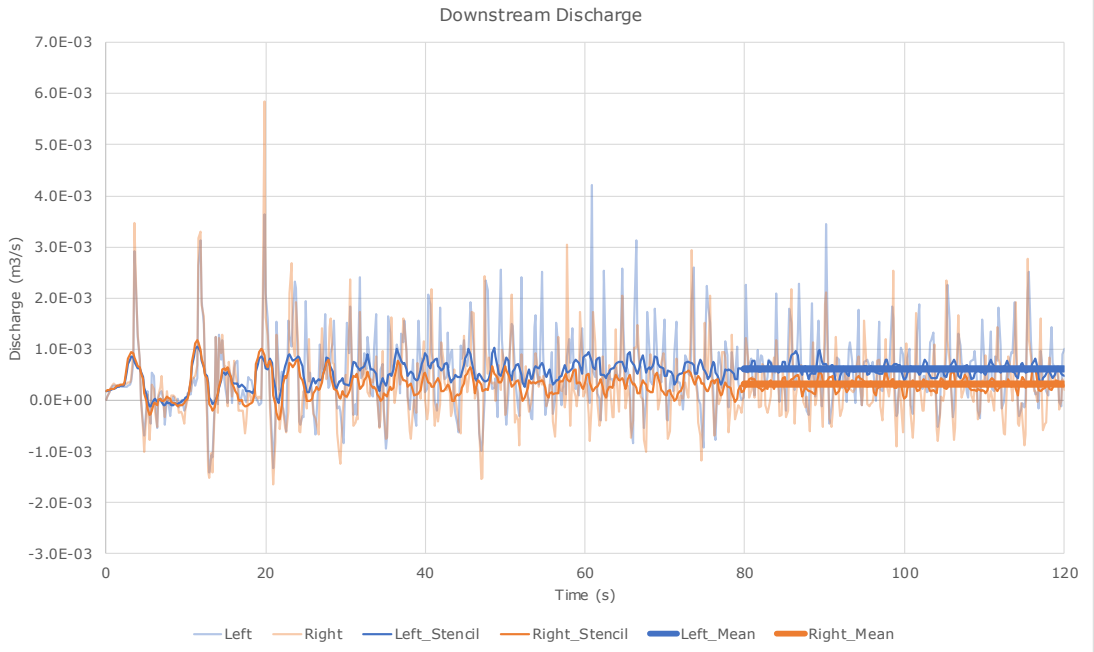


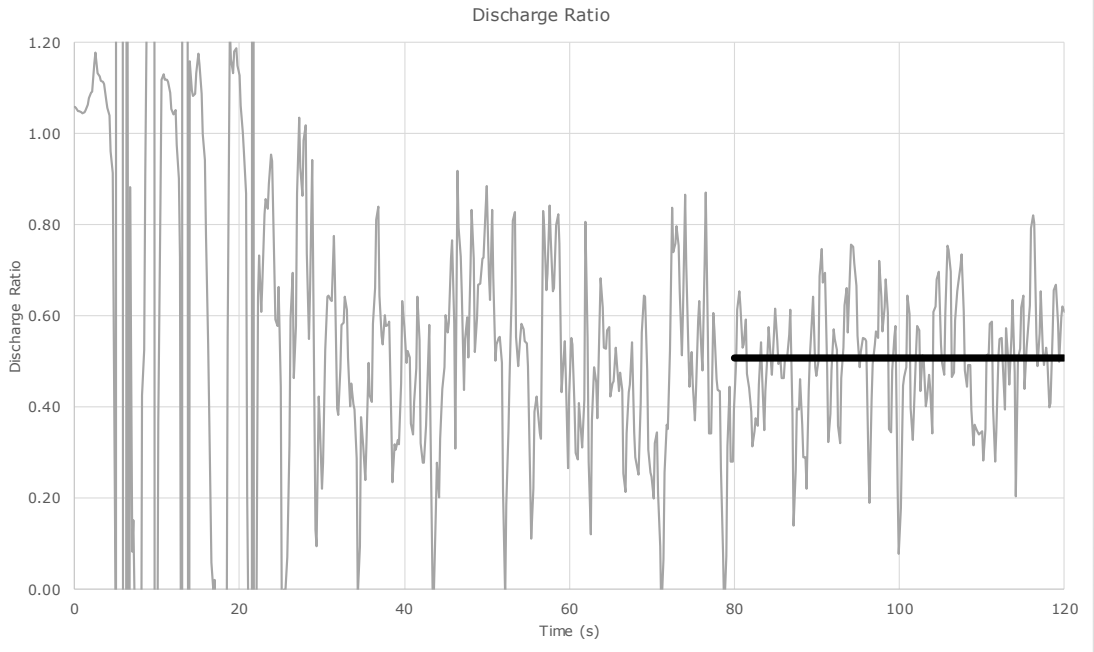


60_03_5560

Name	Symbol	Left	Right	Unit
Weir Height	WH	55	60	mm
Initial Time	Ti	80	80	s
End Time	Te	120	120	s
Initial Number	Ni	400	400	dimensionless
End Number	Ne	600	600	dimensionless
Average Discharge	$\bar{Q}$	6.069E-04	3.119E-04	m3/s

Name	Symbol	Equation	Result	Unit
Weir Height Ratio	WHr	WHL/WHR	0.917	dimensionless
Discharge Ratio	Qr	$\bar{Q}$_L/$\bar{Q}$_R	0.514	dimensionless
Time Step Discharge Ratio	Qr,t	Average[Q_(r,t=n)···Q_(r,t=n+N)]	0.507	dimensionless

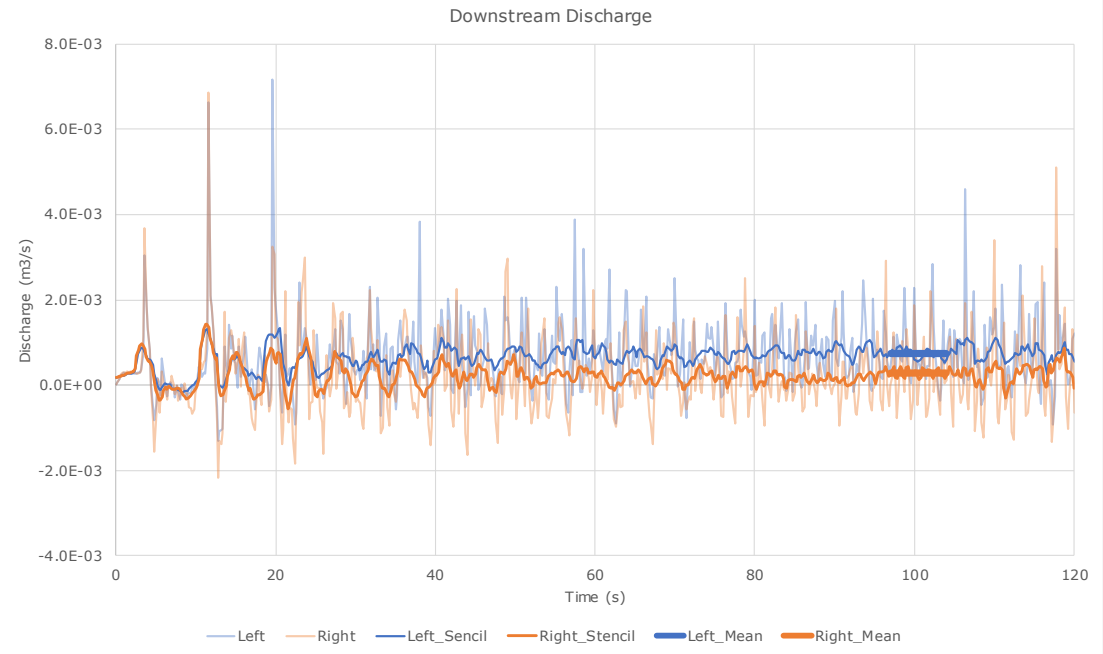


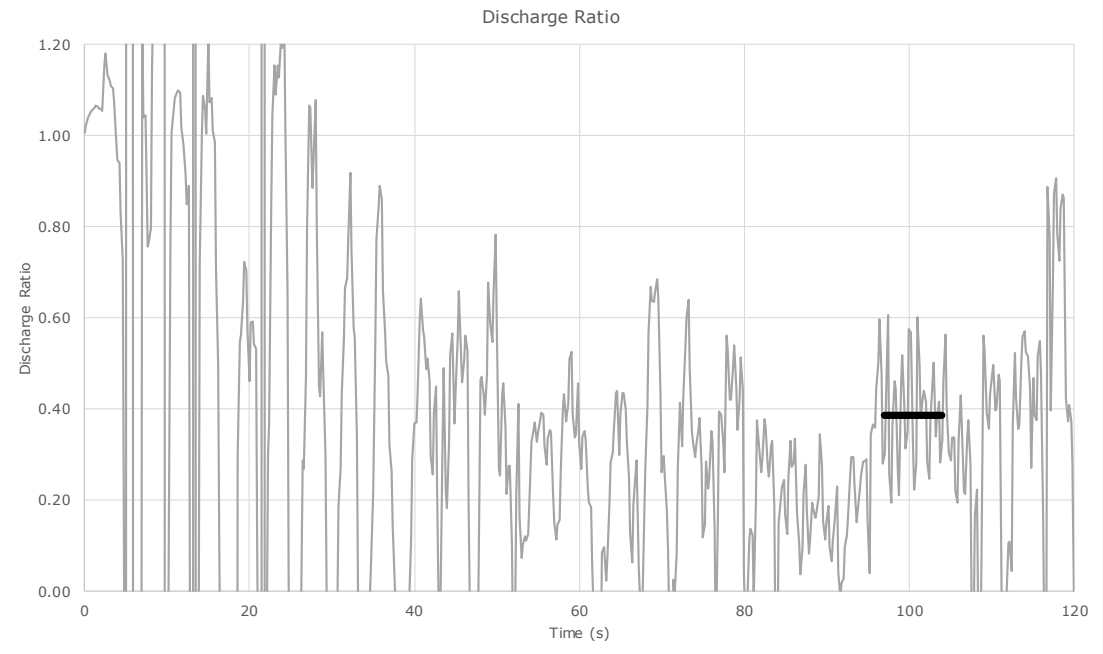


60_03_5562

Name	Symbol	Left	Right	Unit
Weir Height	WH	55	62	mm
Initial Time	Ti	97	97	s
End Time	Te	104	104	s
Initial Number	Ni	485	485	dimensionless
End Number	Ne	520	520	dimensionless
Average Discharge	$\bar{Q}$	7.460E-04	2.887E-04	m3/s

Name	Symbol	Equation	Result	Unit
Weir Height Ratio	WHr	WHL/WHR	0.887	dimensionless
Discharge Ratio	Qr	$\bar{Q}_L/\bar{Q}_R$	0.387	dimensionless
Time Step Discharge Ratio	Qr,t	Average[Q_(r,t=n)···Q_(r,t=n+N)]	0.386	dimensionless

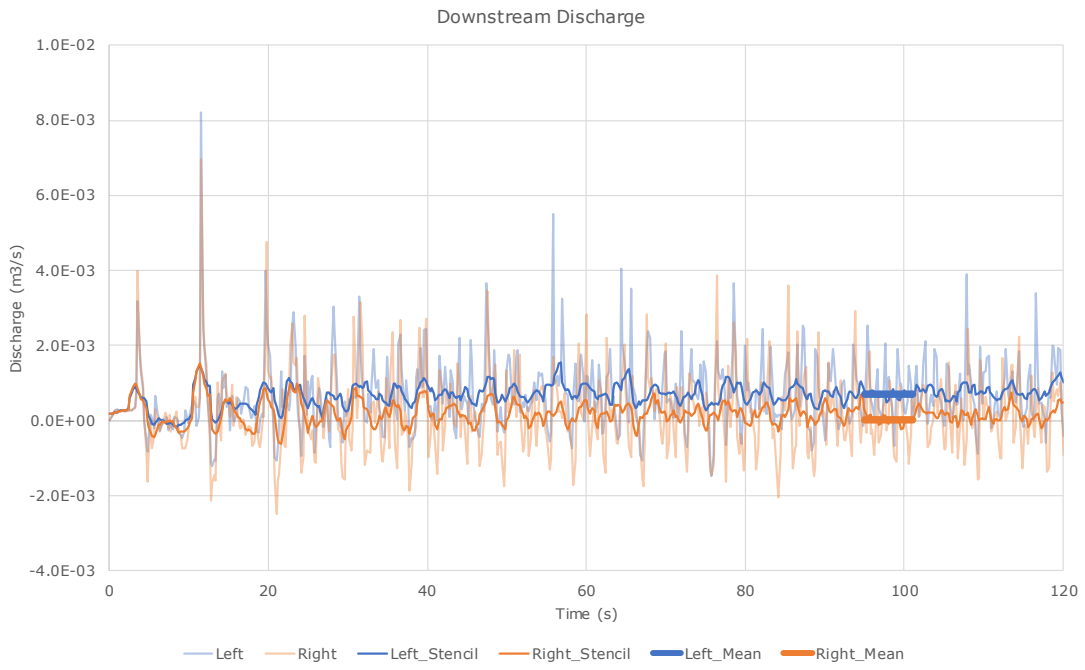


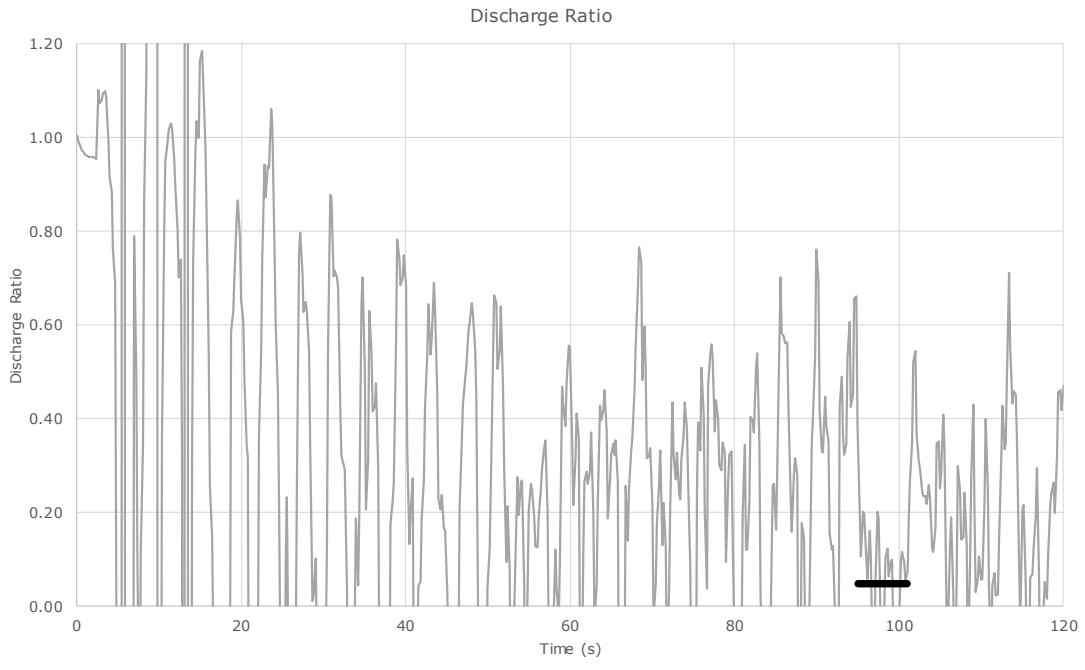


60_03_5565

Name	Symbol	Left	Right	Unit
Weir Height	WH	55	65	mm
Initial Time	Ti	95	95	s
End Time	Te	101	101	s
Initial Number	Ni	475	475	dimensionless
End Number	Ne	505	505	dimensionless
Average Discharge	$\bar{Q}$	6.941E-04	3.889E-05	m3/s

Name	Symbol	Equation	Result	Unit
Weir Height Ratio	WHr	WHL/WHR	0.846	dimensionless
Discharge Ratio	Qr	$\bar{Q}_L/\bar{Q}_R$	0.056	dimensionless
Time Step Discharge Ratio	Qr,t	Average[Q_(r,t=n)···Q_(r,t=n+N)]	0.047	dimensionless

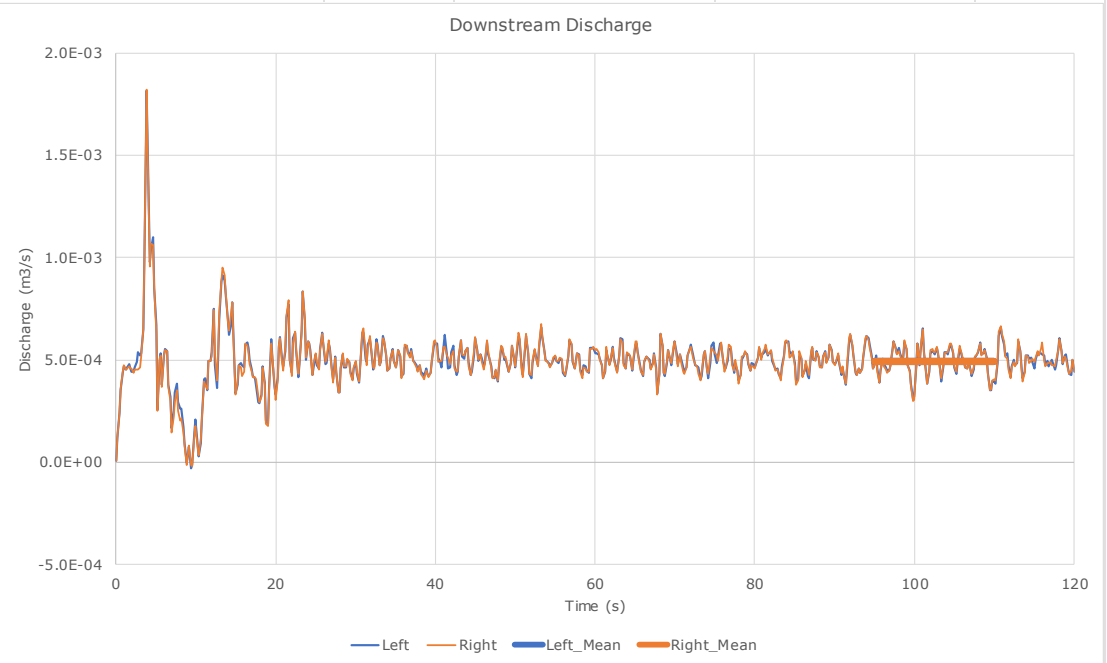


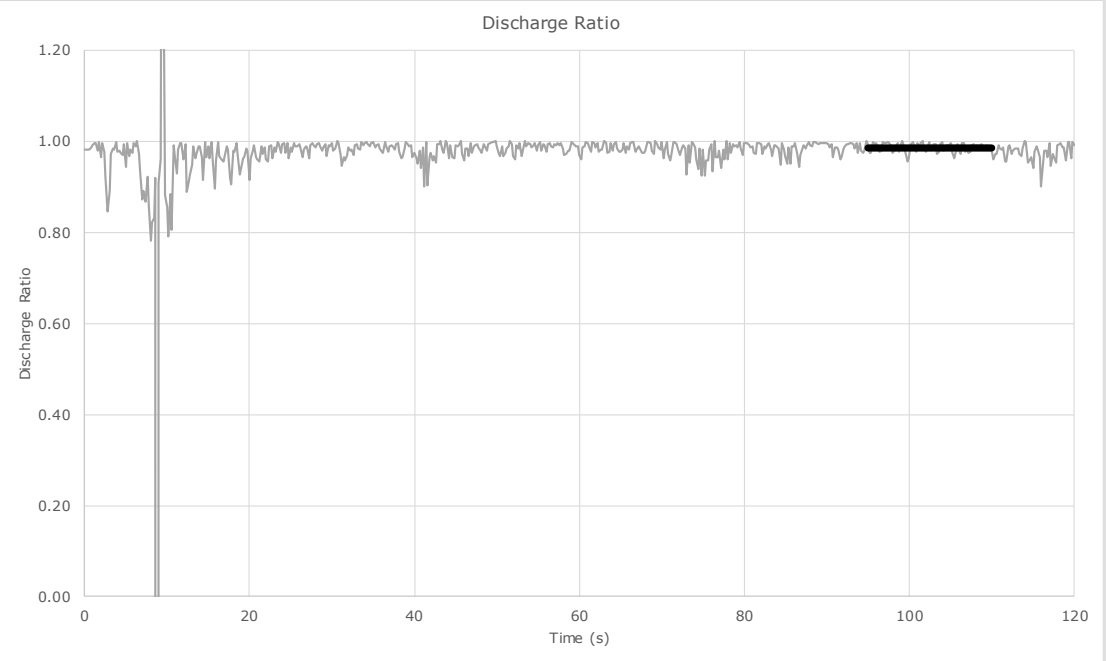


60_05_5050

Name	Symbol	Left	Right	Unit
Weir Height	WH	50	50	mm
Initial Time	Ti	95	95	s
End Time	Te	110	110	s
Initial Number	Ni	475	475	unitless
End Number	Ne	550	550	unitless
Average Discharge	$\bar{Q}$	4.913E-04	4.922E-04	m3/s

Name	Symbol	Equation	Result	Unit
Weir Height Ratio	WHr	WHL/WHR	1.000	dimensionless
Discharge Ratio	Qr	$\bar{Q}$_L/$\bar{Q}$_R	0.998	dimensionless
Time Step Discharge Ratio	Qr,t	Average[Q_(r,t=n)···Q_(r,t=n+N)]	0.986	dimensionless

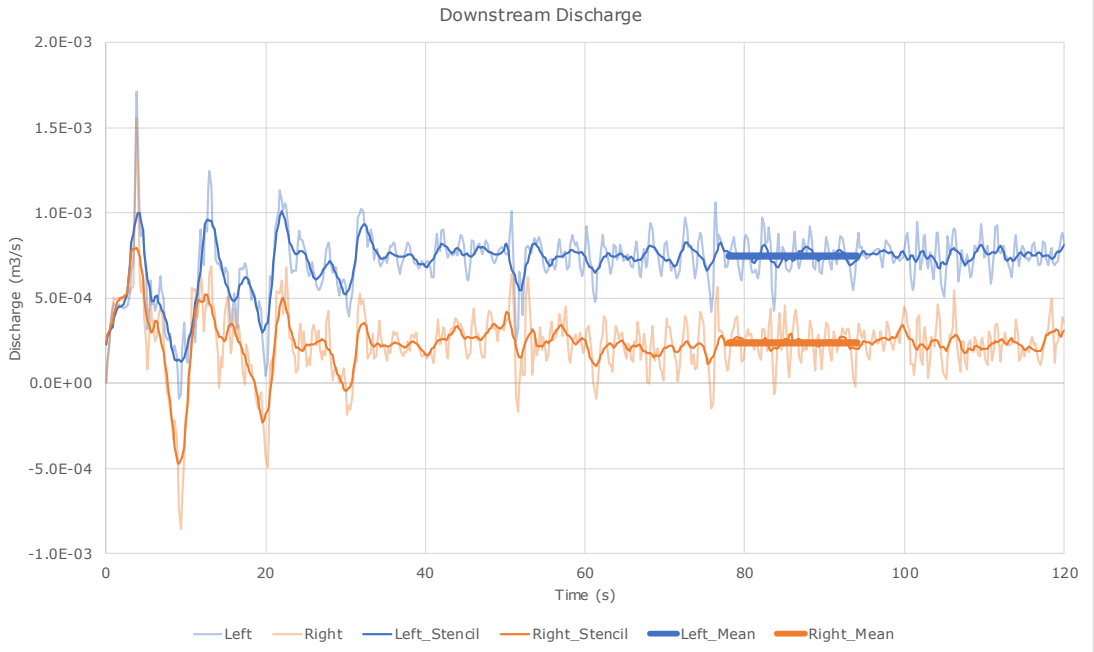


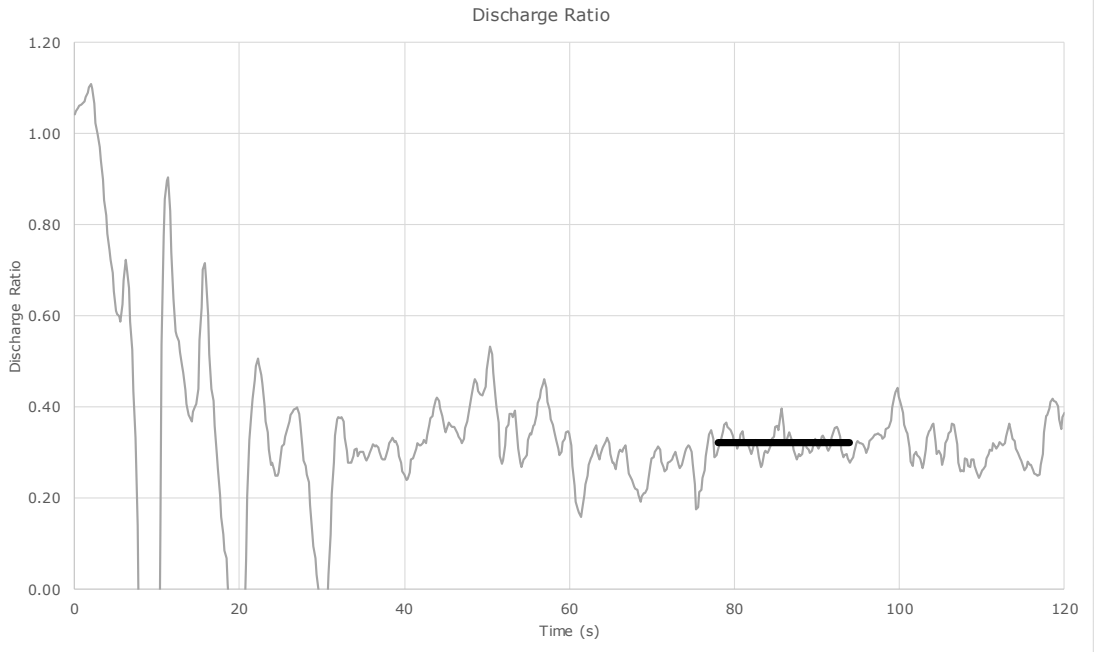


60_05_5053

	Symbol	Left	Right	Unit
ght	WH	50	53	mm
me	Ti	78	78	s
ne	Te	94	94	s
nber	Ni	390	390	unitless
ber	Ne	470	470	unitless
charge	$\bar{Q}$	7.457E-04	2.397E-04	m3/s

	Symbol	Equation	Result	Unit
Ratio	WHr	WHL/WHR	0.943	dimensionless
Ratio	Qr	$\bar{Q}_L/\bar{Q}_R$	0.322	dimensionless
arge Ratio	Qr,t	Average[Q_(r,t=n)···Q_(r,t=n+N)]	0.321	dimensionless

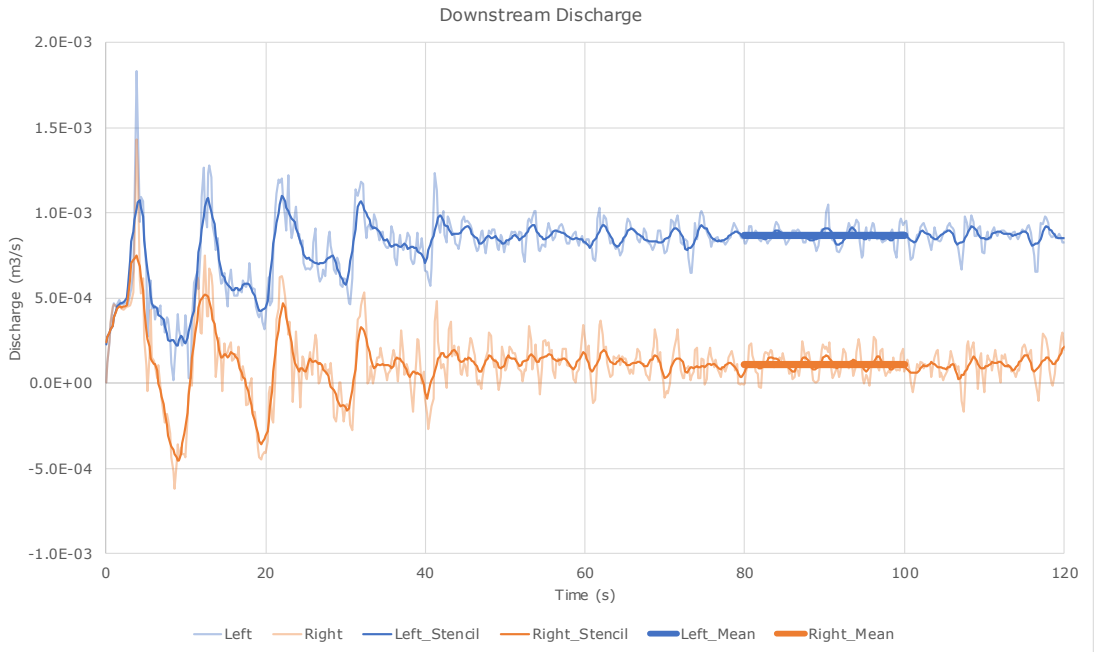


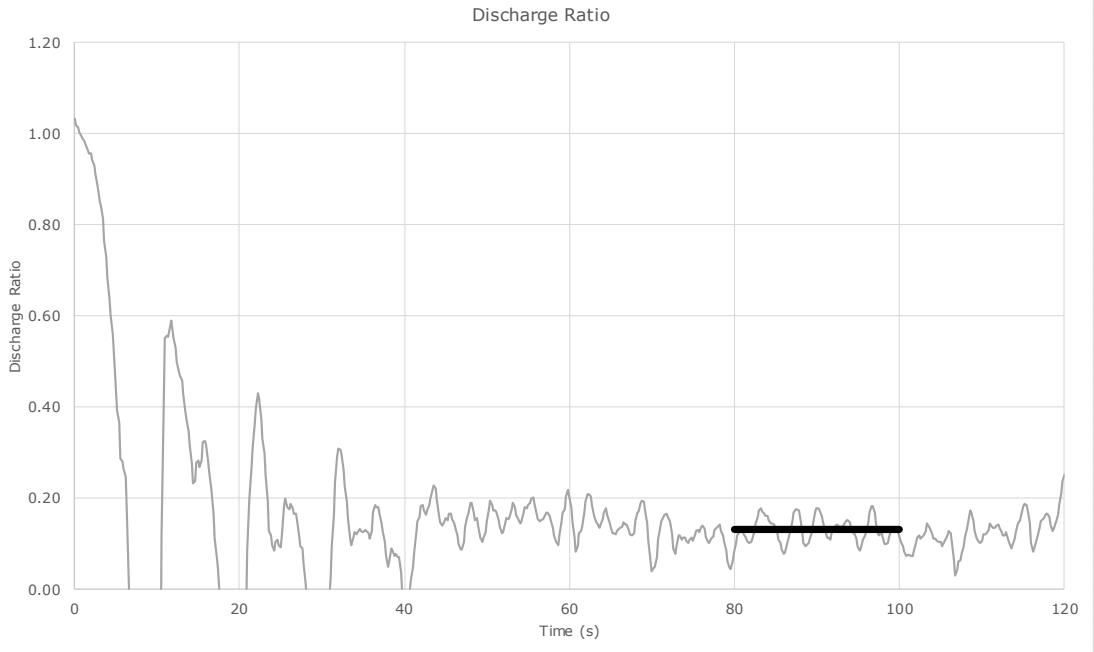


60_05_5055

Name	Symbol	Left	Right	Unit
Weir Height	WH	50	55	mm
Initial Time	Ti	80	80	s
End Time	Te	100	100	s
Initial Number	Ni	400	400	unitless
End Number	Ne	500	500	unitless
Average Discharge	$\bar{Q}$	8.672E-04	1.138E-04	m3/s

Name	Symbol	Equation	Result	Unit
Weir Height Ratio	WHr	WHL/WHR	0.909	dimensionless
Discharge Ratio	Qr	$\bar{Q}$_L/$\bar{Q}$_R	0.131	dimensionless
Time Step Discharge Ratio	Qr,t	Average[Q_(r,t=n)···Q_(r,t=n+N)]	0.131	dimensionless

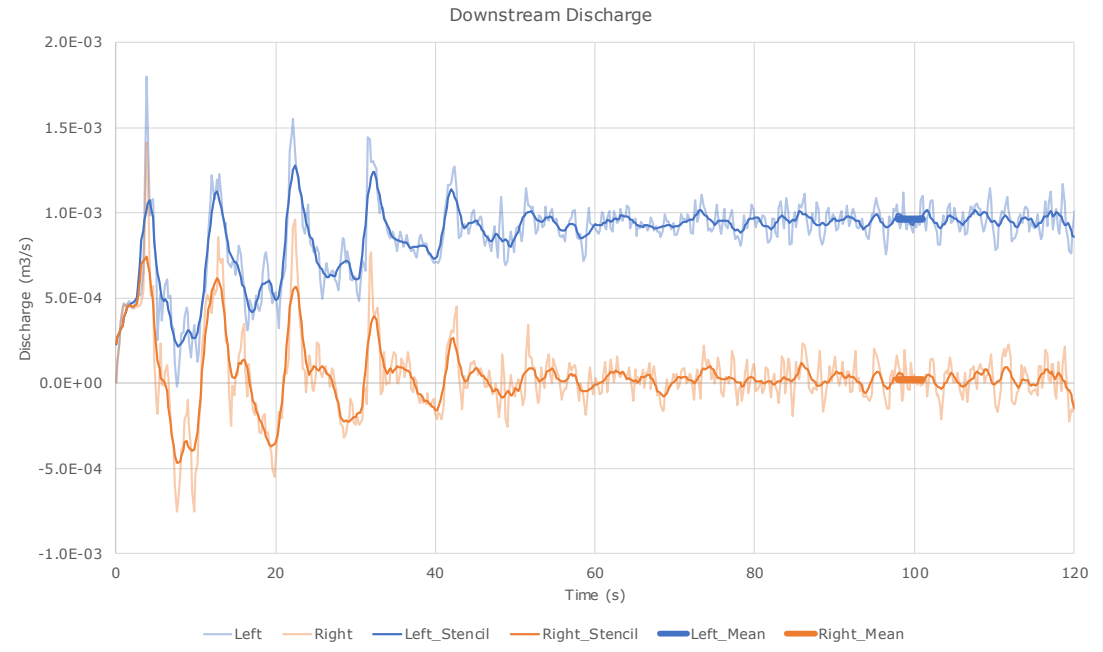


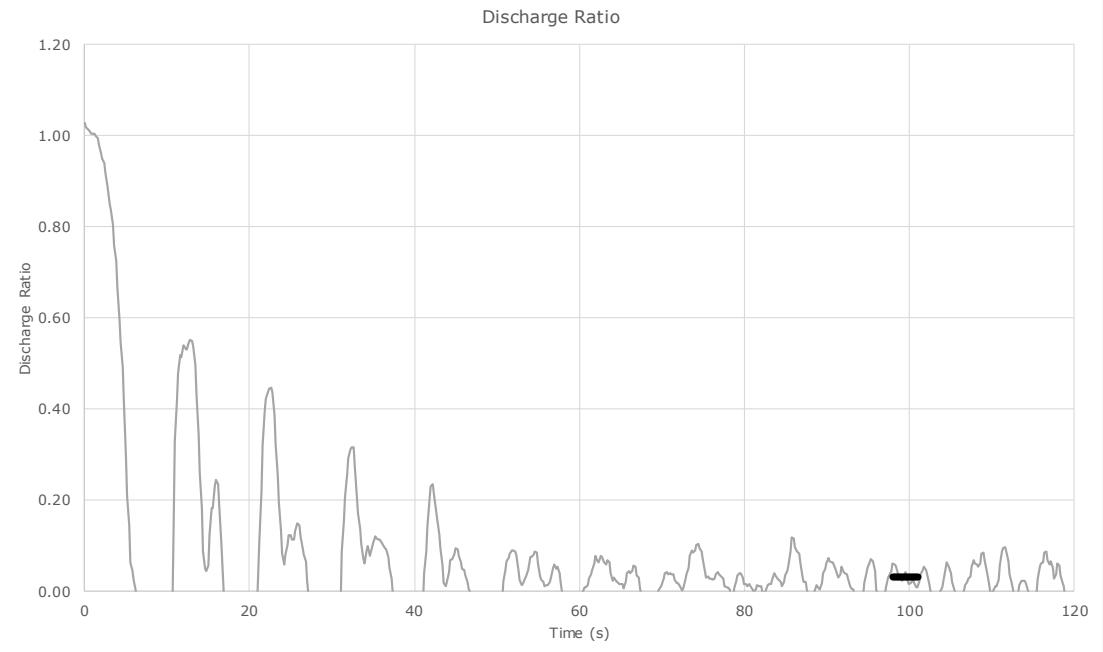


60_05_5057

Name	Symbol	Left	Right	Unit
Weir Height	WH	50	57	mm
Initial Time	Ti	98	98	s
End Time	Te	101	101	s
Initial Number	Ni	490	490	unitless
End Number	Ne	505	505	unitless
Average Discharge	$\bar{Q}$	9.659E-04	2.301E-05	m3/s

Name	Symbol	Equation	Result	Unit
Weir Height Ratio	WHr	WHL/WHR	0.877	dimensionless
Discharge Ratio	Qr	$\bar{Q}_L/\bar{Q}_R$	0.024	dimensionless
Time Step Discharge Ratio	Qr,t	Average[Q_(r,t=n)···Q_(r,t=n+N)]	0.030	dimensionless

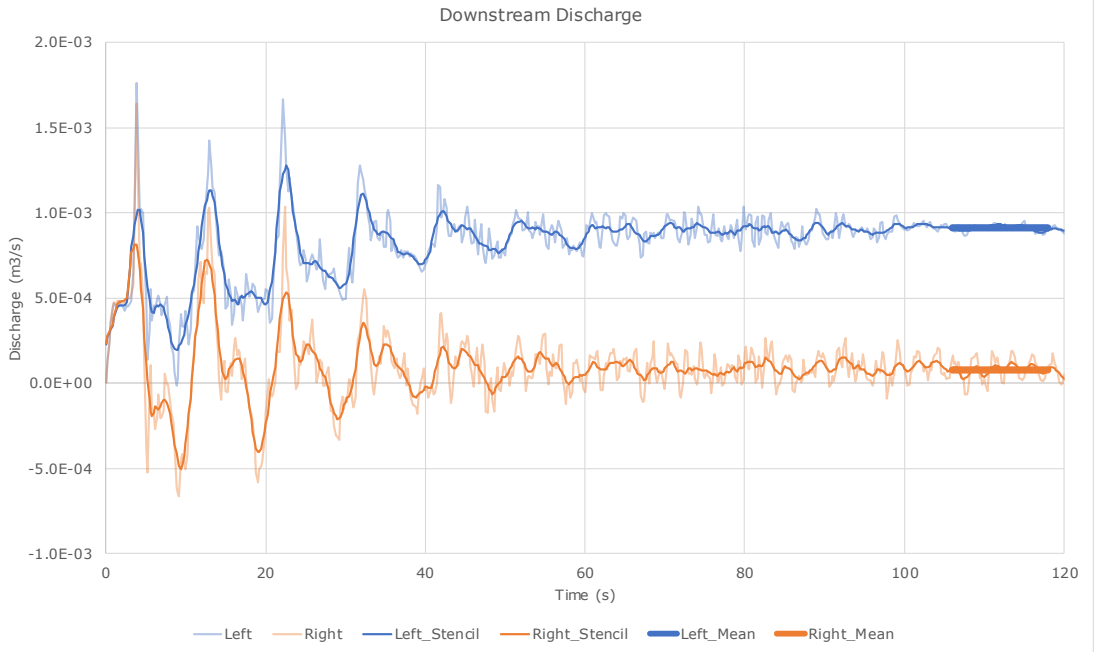


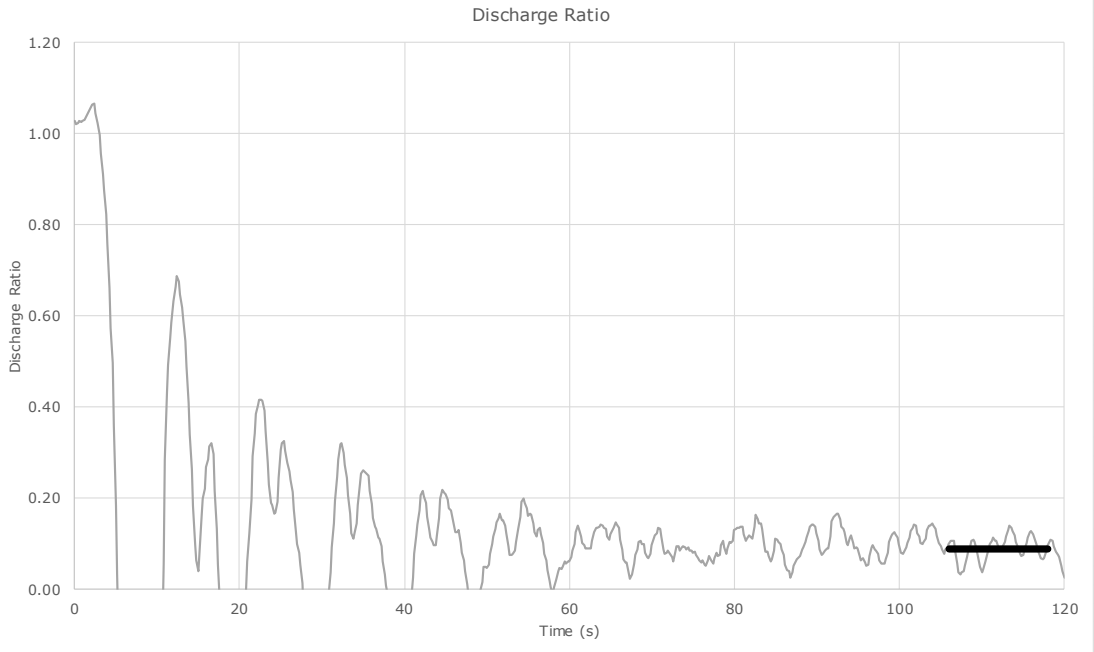


60_05_5060

Name	Symbol	Left	Right	Unit
Weir Height	WH	50	60	mm
Initial Time	Ti	106	106	s
End Time	Te	118	118	s
Initial Number	Ni	530	530	dimensionless
End Number	Ne	590	590	dimensionless
Average Discharge	$\bar{Q}$	9.120E-04	8.098E-05	m3/s

Name	Symbol	Equation	Result	Unit
Weir Height Ratio	WHr	WHL/WHR	0.833	dimensionless
Discharge Ratio	Qr	$\bar{Q}$_L/$\bar{Q}$_R	0.089	dimensionless
Time Step Discharge Ratio	Qr,t	Average[Q_(r,t=n)···Q_(r,t=n+N)]	0.089	dimensionless

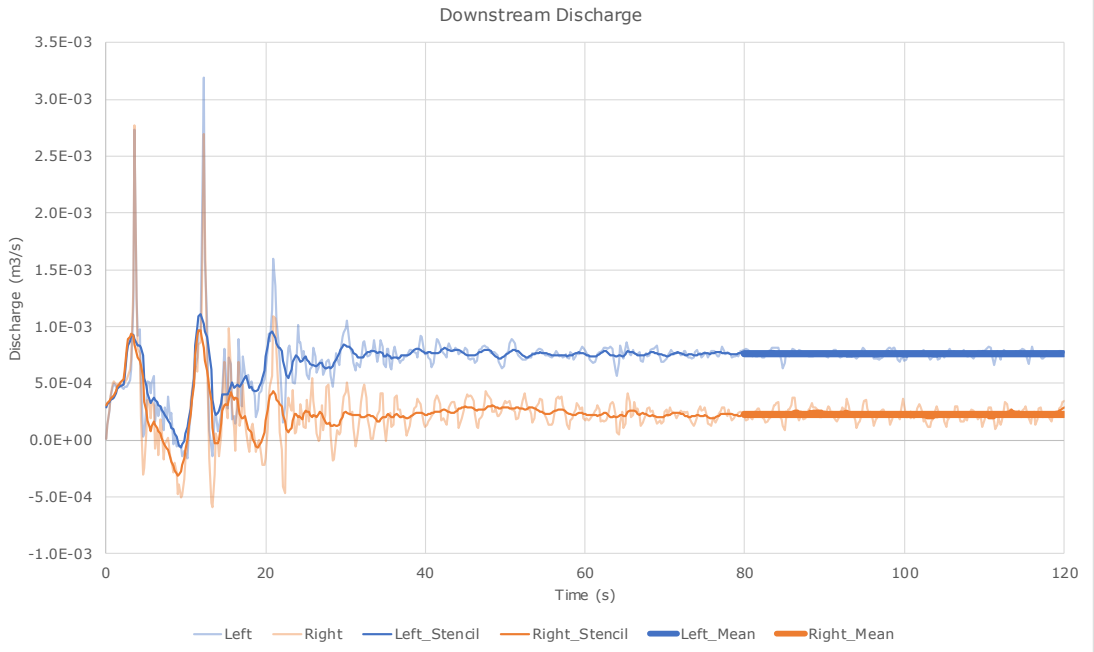


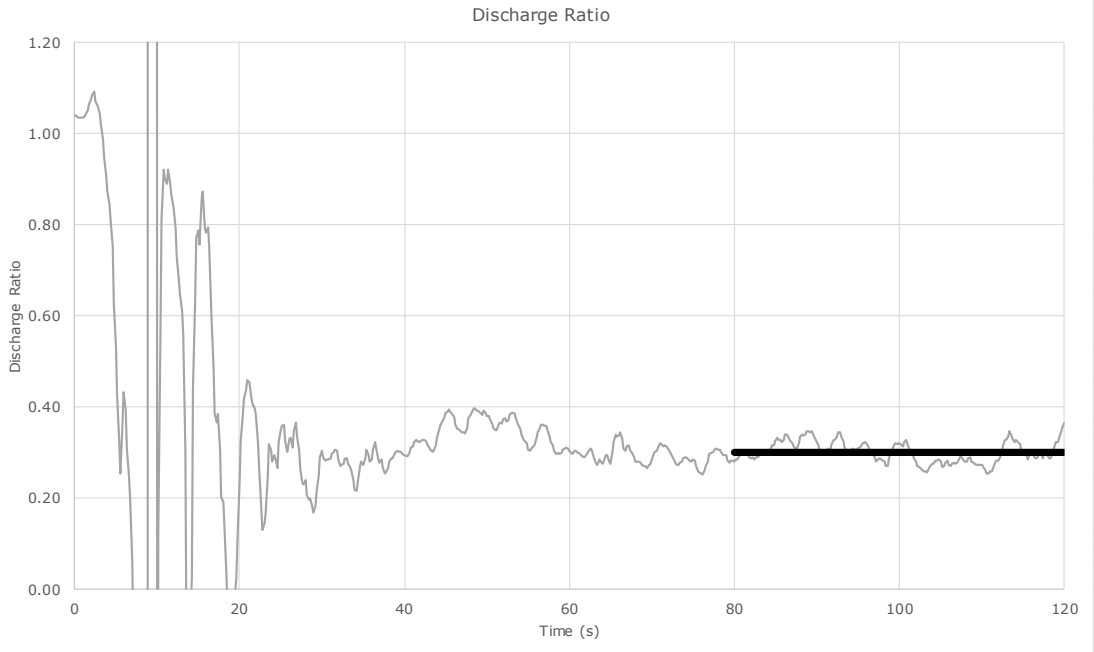


60_05_5560

Name	Symbol	Left	Right	Unit
Weir Height	WH	55	60	mm
Initial Time	Ti	80	80	s
End Time	Te	120	120	s
Initial Number	Ni	400	400	dimensionless
End Number	Ne	600	600	dimensionless
Average Discharge	$\bar{Q}$	7.606E-04	2.289E-04	m3/s

Name	Symbol	Equation	Result	Unit
Weir Height Ratio	WHr	WHL/WHR	0.917	dimensionless
Discharge Ratio	Qr	$\bar{Q}$_L/$\bar{Q}$_R	0.301	dimensionless
Time Step Discharge Ratio	Qr,t	Average[Q_(r,t=n)···Q_(r,t=n+N)]	0.301	dimensionless

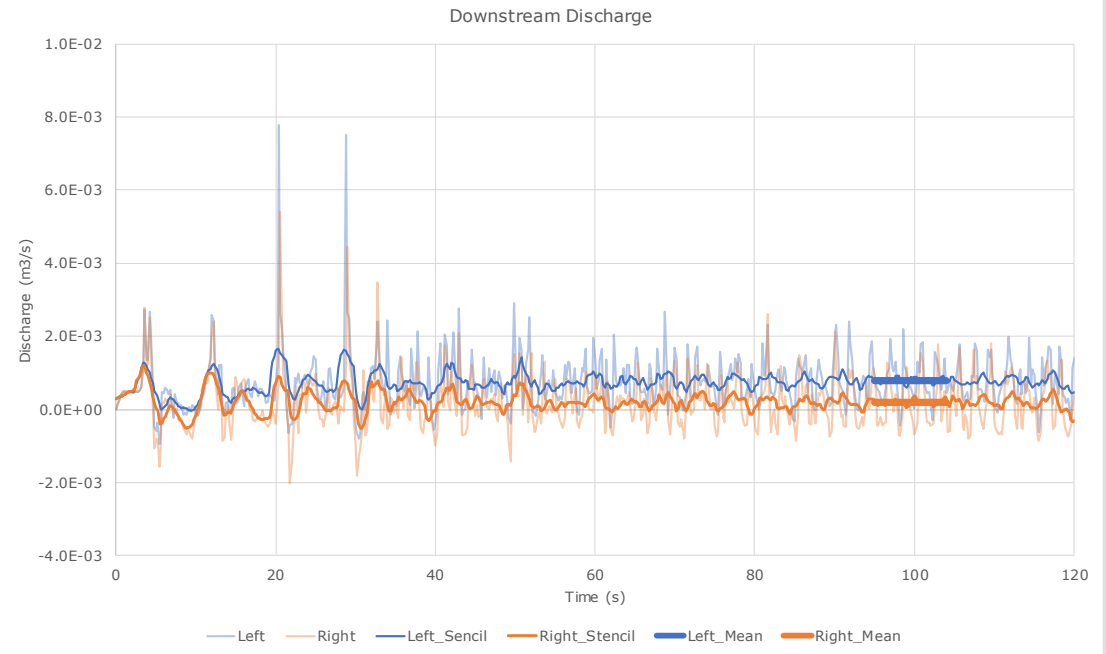


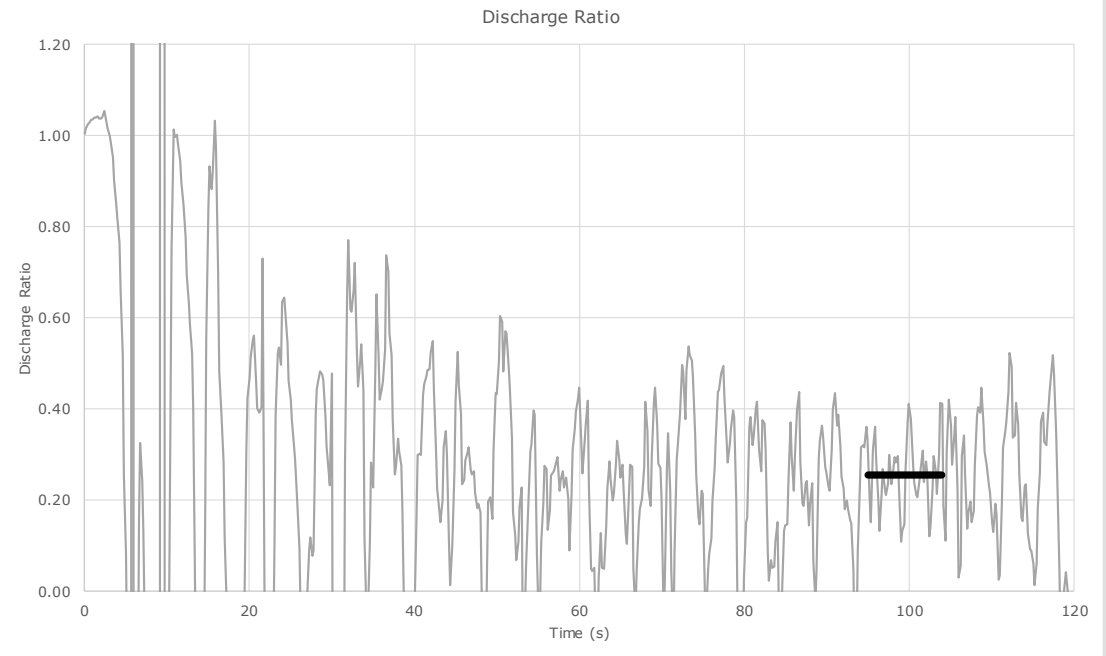


60_05_5562

Name	Symbol	Left	Right	Unit
Weir Height	WH	55	62	mm
Initial Time	Ti	95	95	s
End Time	Te	104	104	s
Initial Number	Ni	475	475	dimensionless
End Number	Ne	520	520	dimensionless
Average Discharge	$\bar{Q}$	7.945E-04	2.049E-04	m3/s

Name	Symbol	Equation	Result	Unit
Weir Height Ratio	WHr	WHL/WHR	0.887	dimensionless
Discharge Ratio	Qr	$\bar{Q}_L/\bar{Q}_R$	0.258	dimensionless
Time Step Discharge Ratio	Qr,t	Average[Q_(r,t=n)···Q_(r,t=n+N)]	0.255	dimensionless

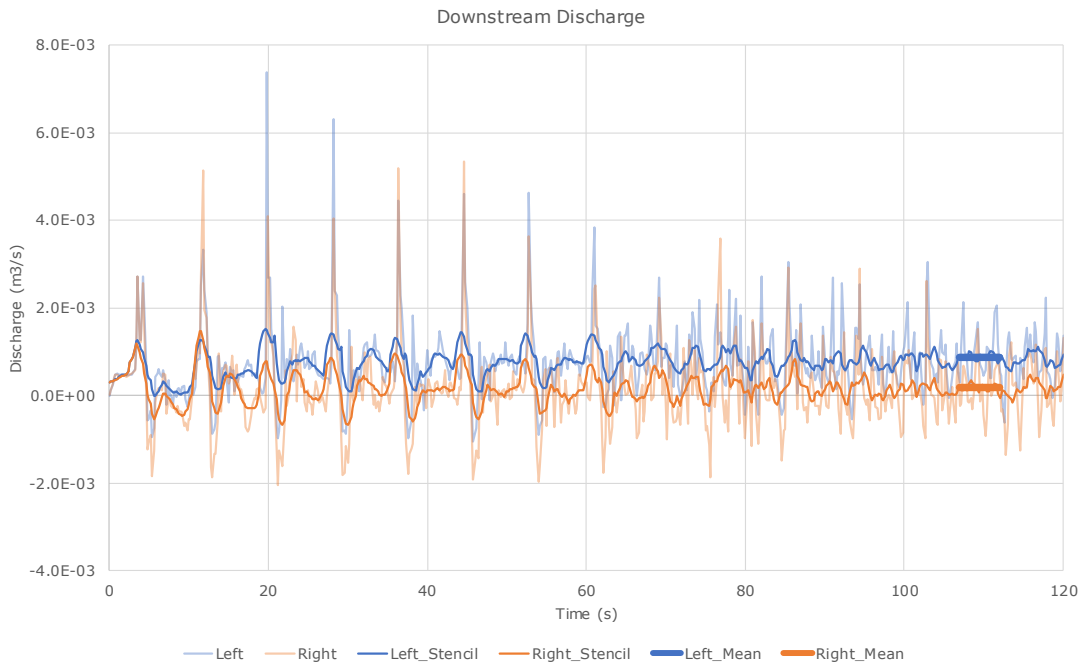


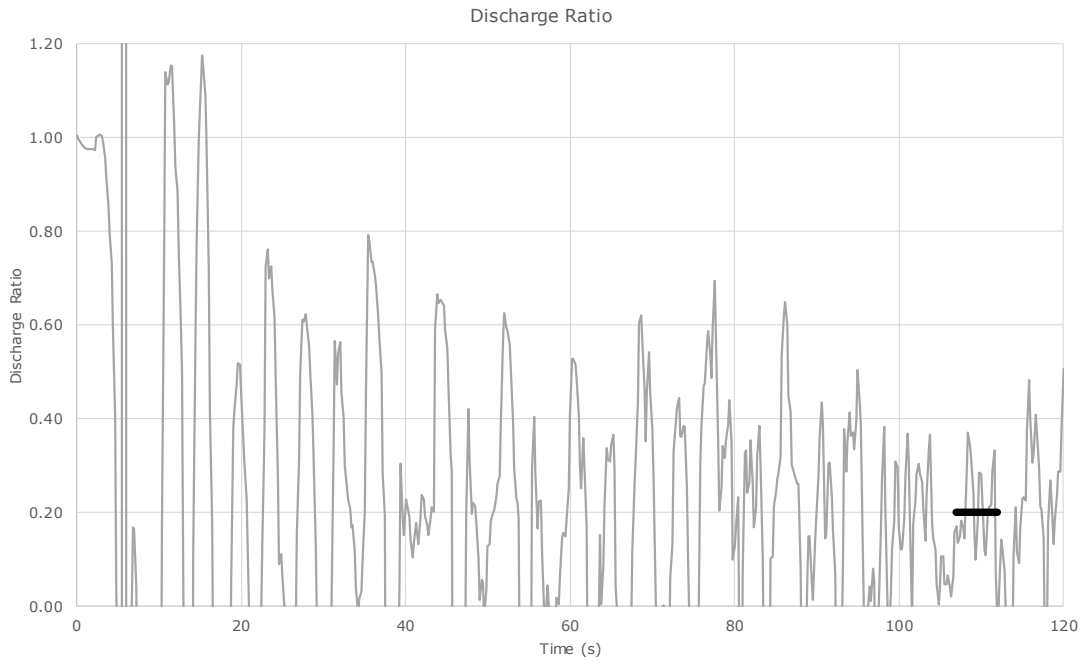


60_05_5565

Name	Symbol	Left	Right	Unit
Weir Height	WH	55	65	mm
Initial Time	Ti	107	107	s
End Time	Te	112	112	s
Initial Number	Ni	535	535	dimensionless
End Number	Ne	560	560	dimensionless
Average Discharge	$\bar{Q}$	8.750E-04	1.766E-04	m3/s

Name	Symbol	Equation	Result	Unit
Weir Height Ratio	WHr	WHL/WHR	0.846	dimensionless
Discharge Ratio	Qr	$\bar{Q}$_L/$\bar{Q}$_R	0.202	dimensionless
Time Step Discharge Ratio	Qr,t	Average[Q_(r,t=n)···Q_(r,t=n+N)]	0.200	dimensionless

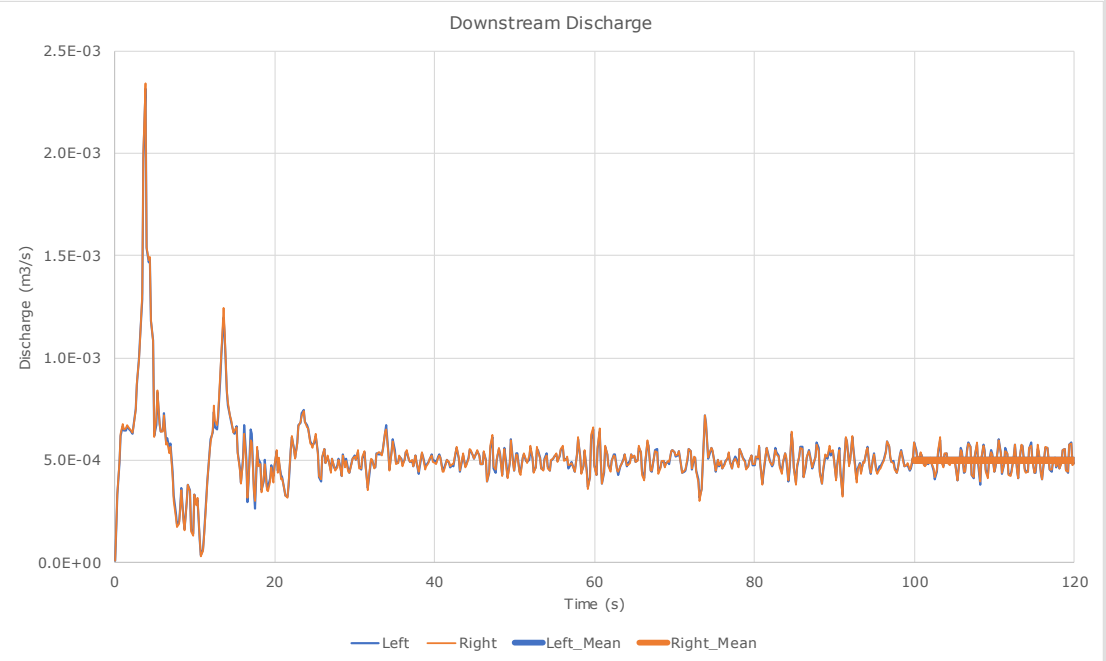


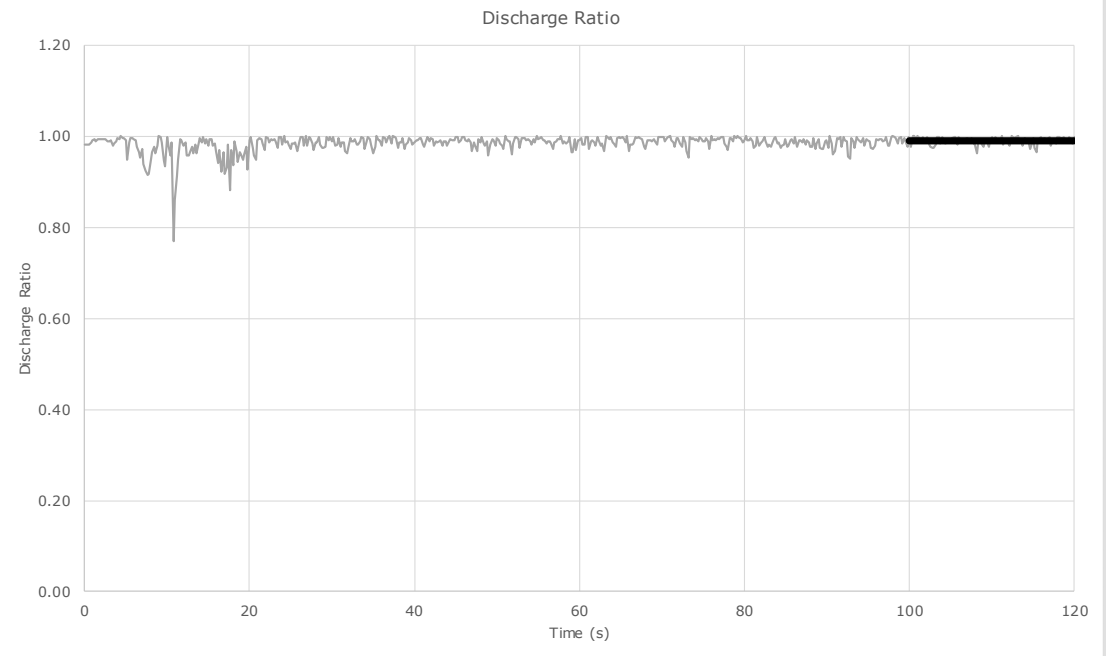


60_07_5050

Name	Symbol	Left	Right	Unit
Weir Height	WH	50	50	mm
Initial Time	Ti	100	100	s
End Time	Te	120	120	s
Initial Number	Ni	500	500	unitless
End Number	Ne	600	600	unitless
Average Discharge	$\bar{Q}$	4.994E-04	4.993E-04	m3/s

Name	Symbol	Equation	Result	Unit
Weir Height Ratio	WHr	WHL/WHR	1.000	dimensionless
Discharge Ratio	Qr	$\bar{Q}$_L/$\bar{Q}$_R	1.000	dimensionless
Time Step Discharge Ratio	Qr,t	Average[Q_(r,t=n)···Q_(r,t=n+N)]	0.990	dimensionless

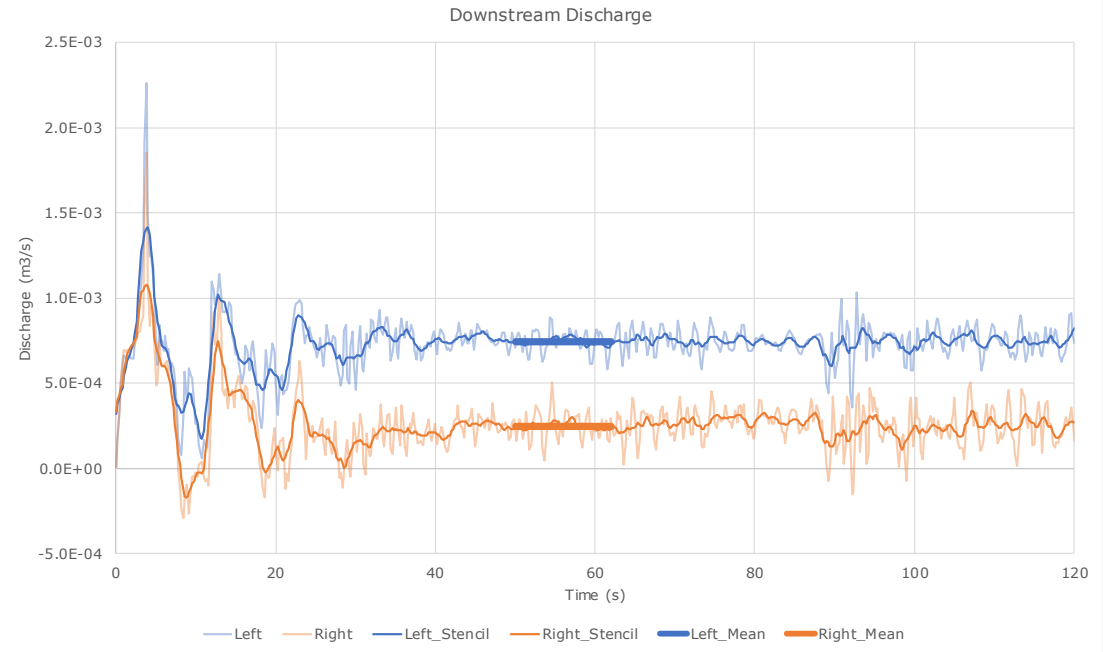


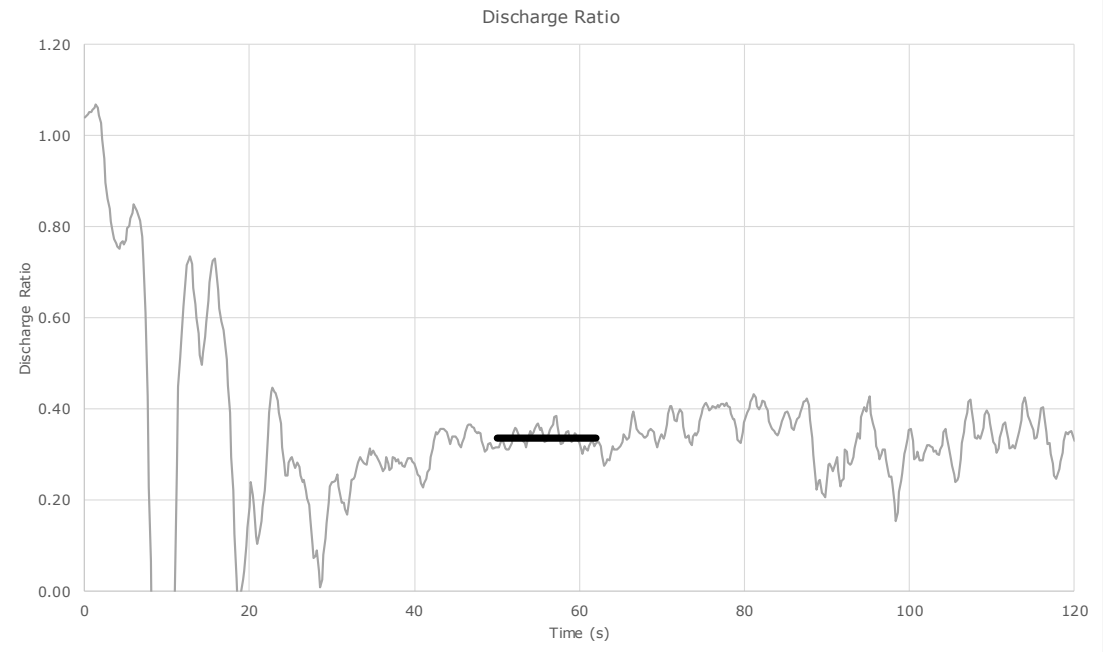


60_07_5053

	Symbol	Left	Right	Unit
ght	WH	50	53	mm
me	Ti	50	50	s
ne	Te	62	62	s
nber	Ni	250	250	unitless
ber	Ne	310	310	unitless
charge	$\bar{Q}$	7.461E-04	2.508E-04	m3/s

	Symbol	Equation	Result	Unit
Ratio	WHr	WHL/WHR	0.943	dimensionless
Ratio	Qr	$\bar{Q}_L/\bar{Q}_R$	0.336	dimensionless
arge Ratio	Qr,t	Average[Q_(r,t=n)···Q_(r,t=n+N)]	0.336	dimensionless

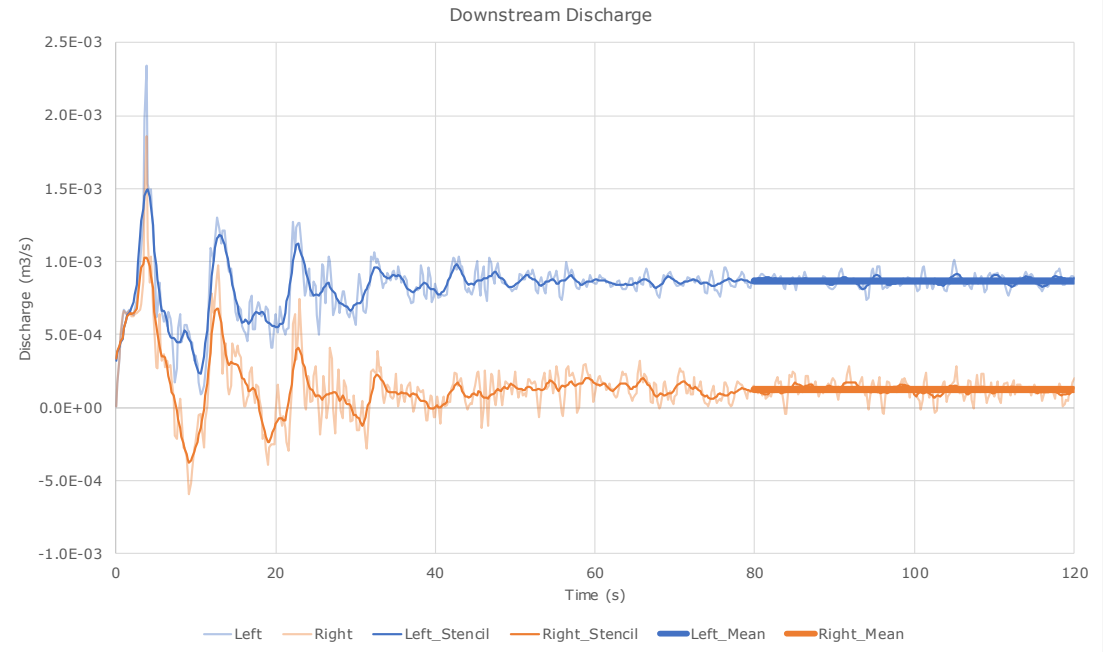


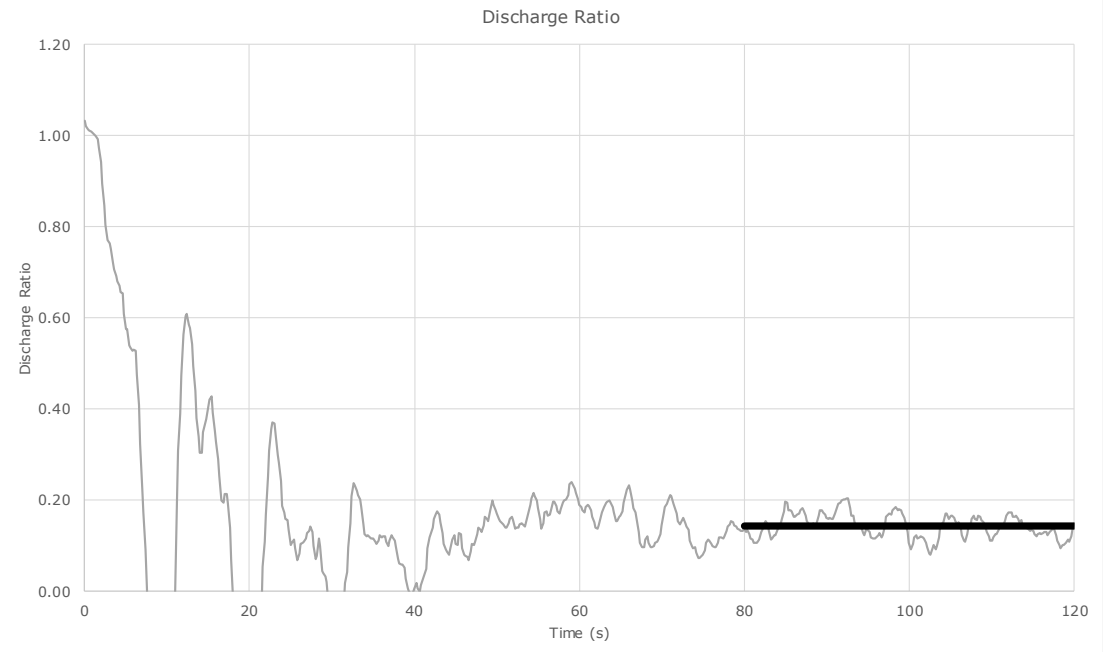


60_07_5055

Name	Symbol	Left	Right	Unit
Weir Height	WH	50	55	mm
Initial Time	Ti	80	80	s
End Time	Te	120	120	s
Initial Number	Ni	400	400	unitless
End Number	Ne	600	600	unitless
Average Discharge	$\bar{Q}$	8.688E-04	1.241E-04	m3/s

Name	Symbol	Equation	Result	Unit
Weir Height Ratio	WHr	WHL/WHR	0.909	dimensionless
Discharge Ratio	Qr	$\bar{Q}_L/\bar{Q}_R$	0.143	dimensionless
Time Step Discharge Ratio	Qr,t	Average[Q_(r,t=n)···Q_(r,t=n+N)]	0.143	dimensionless

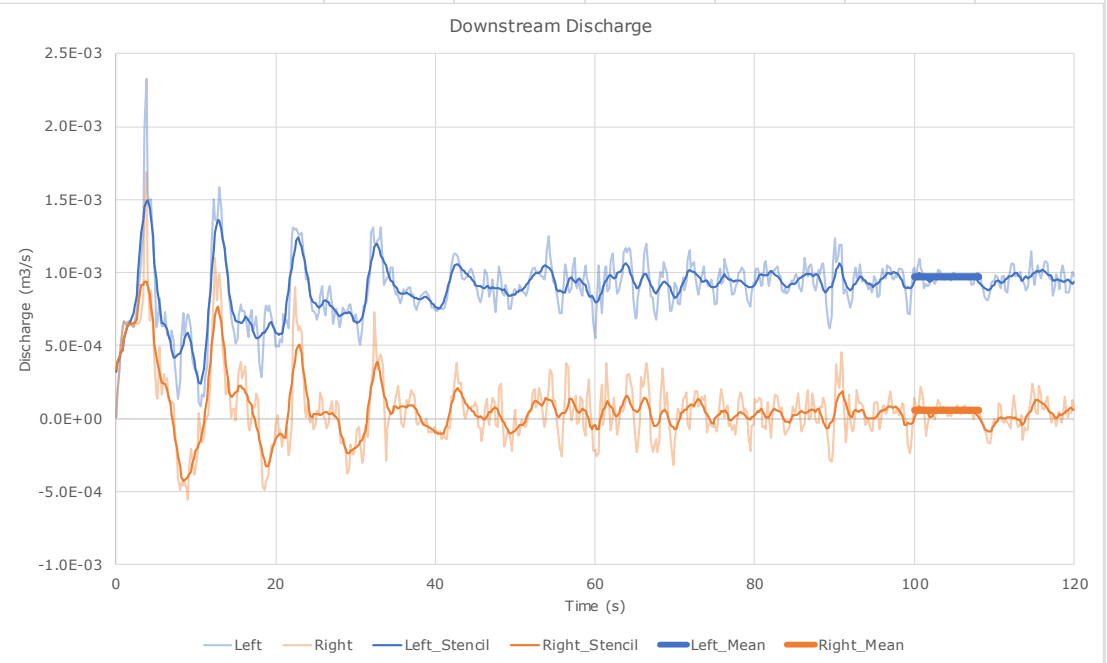


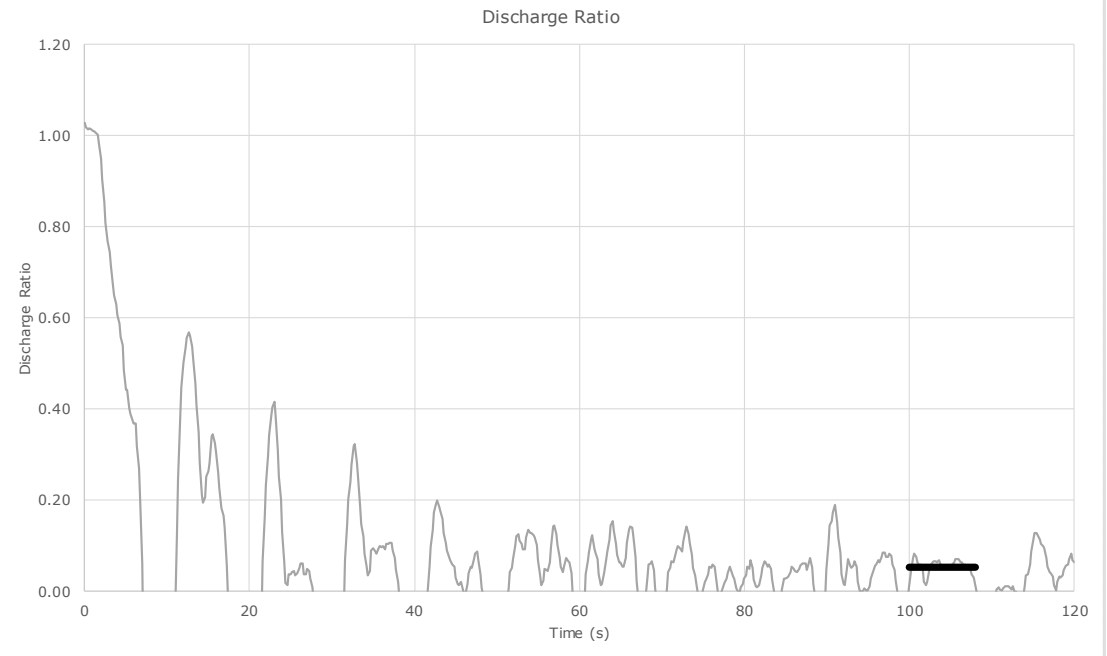


60_07_5057

Name	Symbol	Left	Right	Unit
Weir Height	WH	50	57	mm
Initial Time	Ti	100	100	s
End Time	Te	108	108	s
Initial Number	Ni	500	500	unitless
End Number	Ne	540	540	unitless
Average Discharge	$\bar{Q}$	9.727E-04	5.868E-05	m3/s

Name	Symbol	Equation	Result	Unit
Weir Height Ratio	WHr	WHL/WHR	0.877	dimensionless
Discharge Ratio	Qr	$\bar{Q}$_L/$\bar{Q}$_R	0.060	dimensionless
ıe Step Discharge Ratio	Qr,t	Average[Q_(r,t=n)···Q_(r,t=n+N)]	0.053	dimensionless

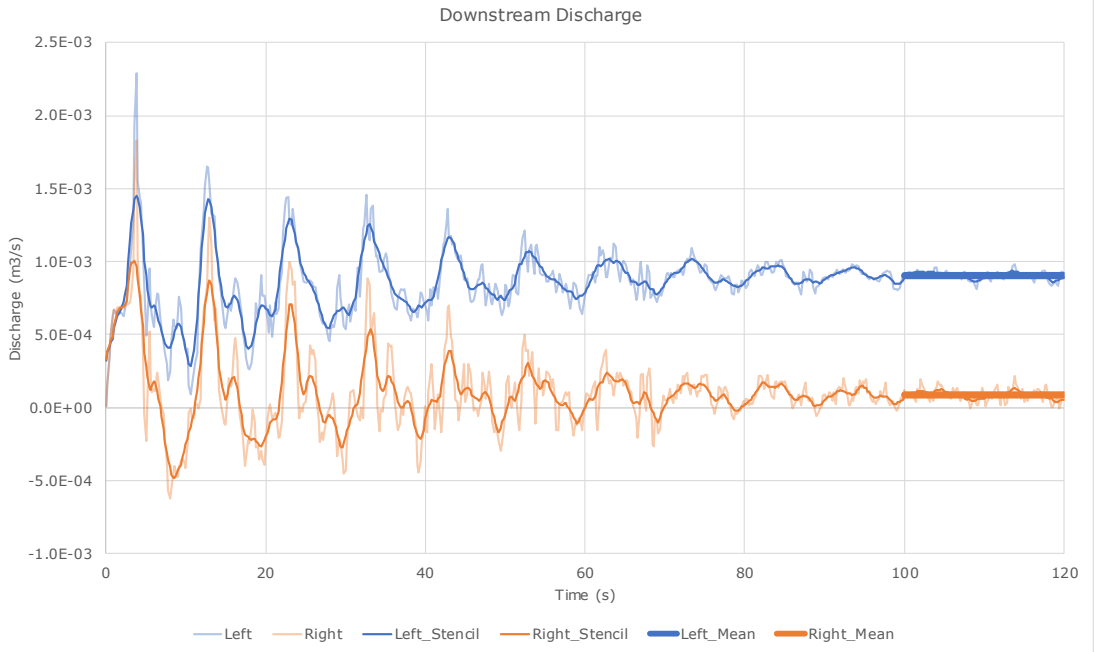


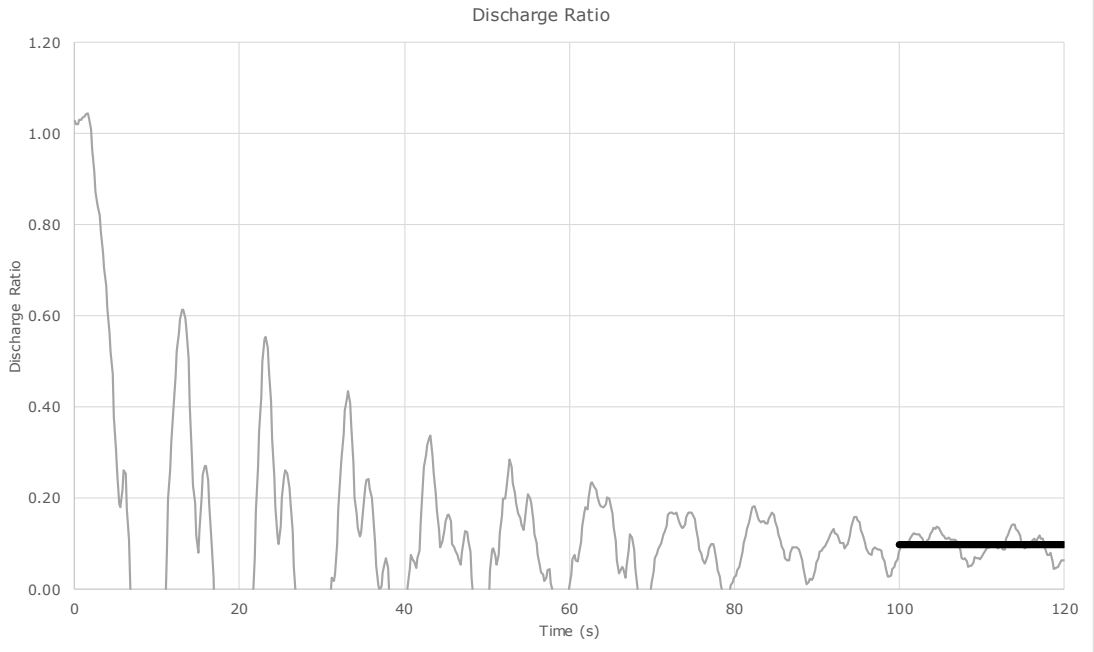


60_07_5060

Name	Symbol	Left	Right	Unit
Weir Height	WH	50	60	mm
Initial Time	Ti	100	100	s
End Time	Te	120	120	s
Initial Number	Ni	500	500	dimensionless
End Number	Ne	600	600	dimensionless
Average Discharge	$\bar{Q}$	9.051E-04	8.776E-05	m3/s

Name	Symbol	Equation	Result	Unit
Weir Height Ratio	WHr	WHL/WHR	0.833	dimensionless
Discharge Ratio	Qr	$\bar{Q}$_L/$\bar{Q}$_R	0.097	dimensionless
ime Step Discharge Ratio	Qr,t	Average[Q_(r,t=n)···Q_(r,t=n+N)]	0.096	dimensionless

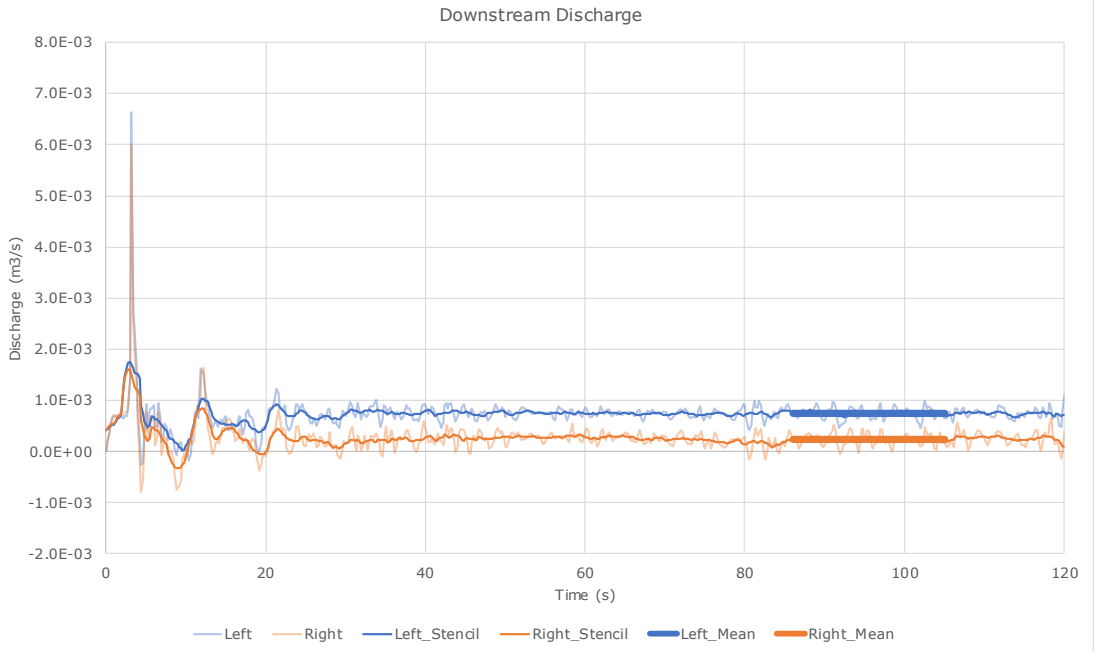


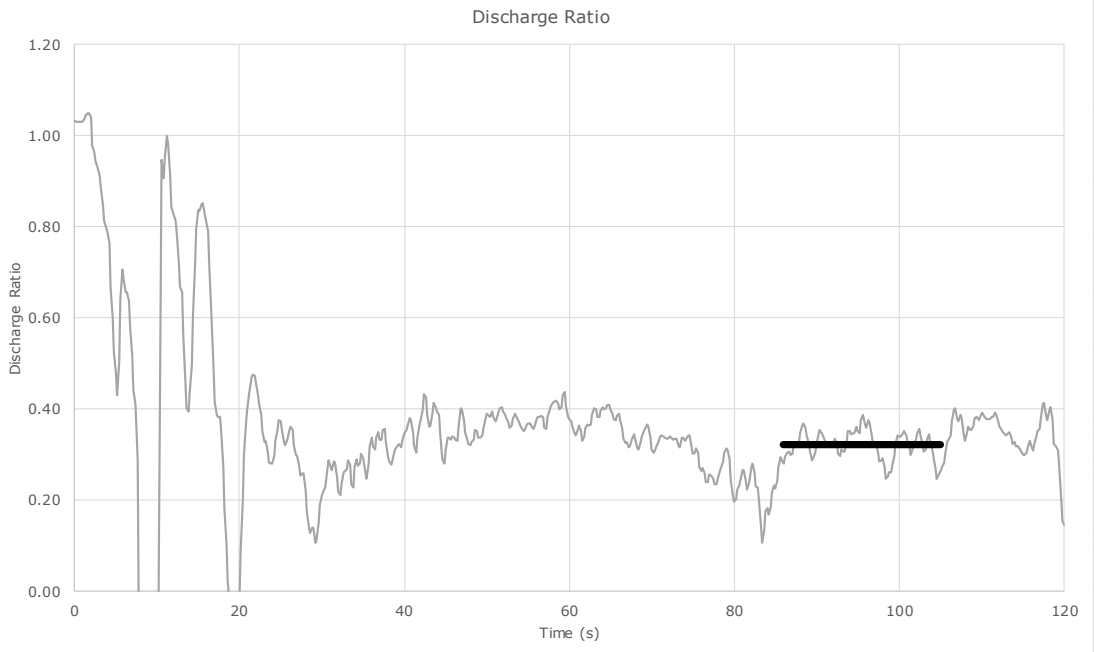


60_07_5560

Name	Symbol	Left	Right	Unit
Weir Height	WH	55	60	mm
Initial Time	Ti	86	86	s
End Time	Te	105	105	s
Initial Number	Ni	430	430	dimensionless
End Number	Ne	525	525	dimensionless
Average Discharge	$\bar{Q}$	7.480E-04	2.402E-04	m3/s

Name	Symbol	Equation	Result	Unit
Weir Height Ratio	WHr	WHL/WHR	0.917	dimensionless
Discharge Ratio	Qr	$\bar{Q}$_L/$\bar{Q}$_R	0.321	dimensionless
ime Step Discharge Ratio	Qr,t	Average[Q_(r,t=n)···Q_(r,t=n+N)]	0.321	dimensionless

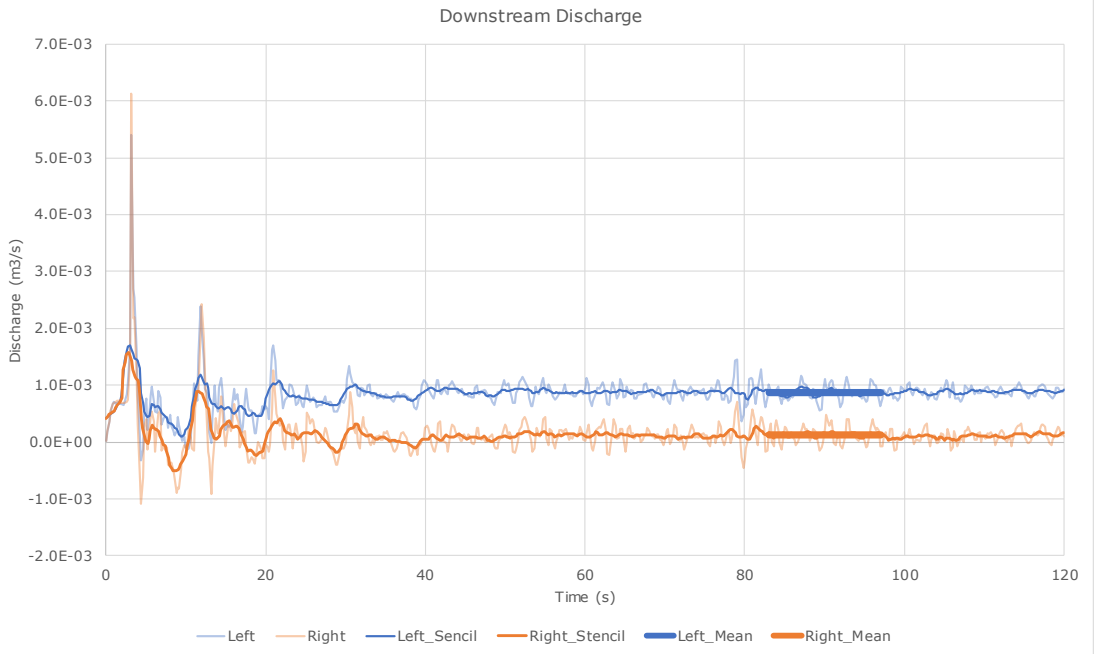


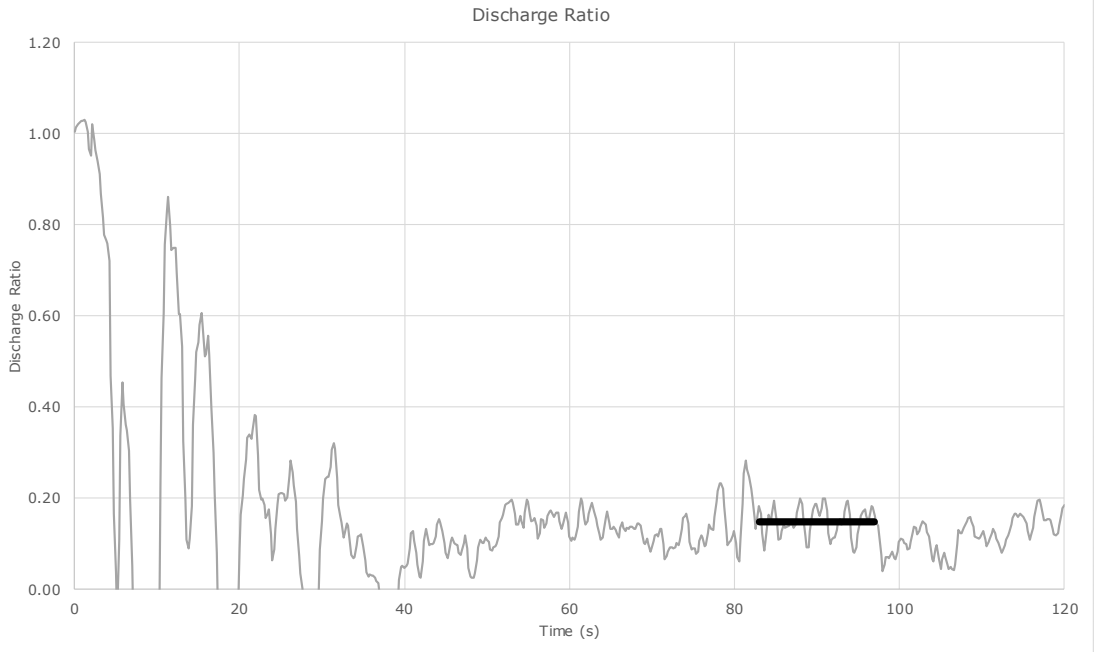


60_07_5562

Name	Symbol	Left	Right	Unit
Weir Height	WH	55	62	mm
Initial Time	Ti	83	83	s
End Time	Te	97	97	s
Initial Number	Ni	415	415	dimensionless
End Number	Ne	485	485	dimensionless
Average Discharge	$\bar{Q}$	8.723E-04	1.294E-04	m3/s

Name	Symbol	Equation	Result	Unit
Weir Height Ratio	WHr	WHL/WHR	0.887	dimensionless
Discharge Ratio	Qr	$\bar{Q}$_L/$\bar{Q}$_R	0.148	dimensionless
Step Discharge Ratio	Qr,t	Average[Q_(r,t=n)···Q_(r,t=n+N)]	0.148	dimensionless

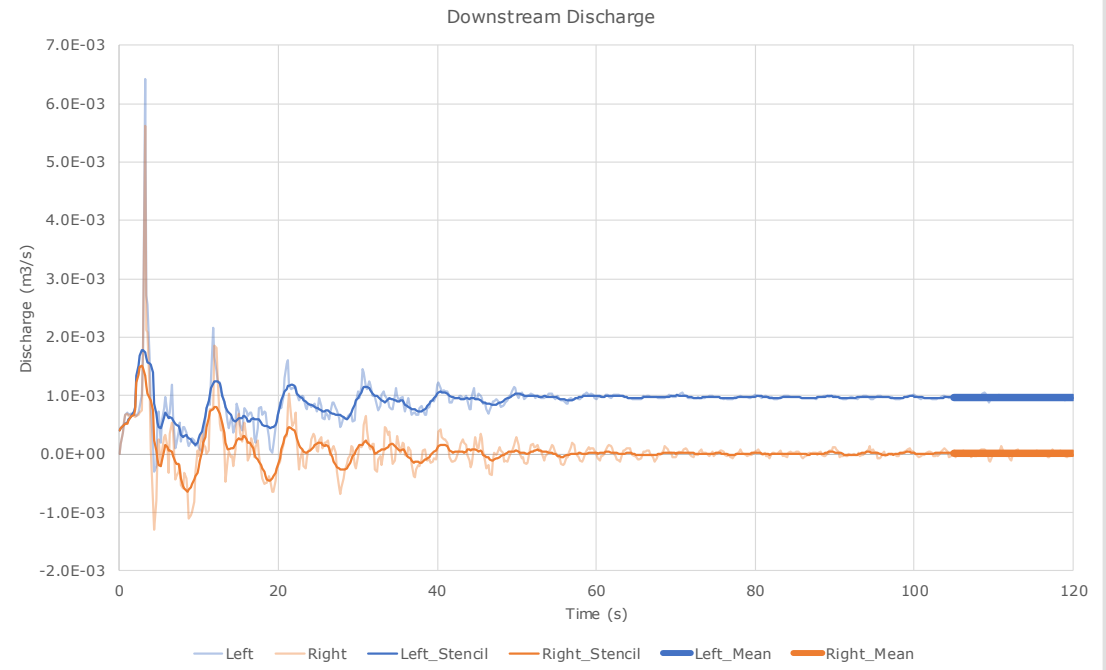


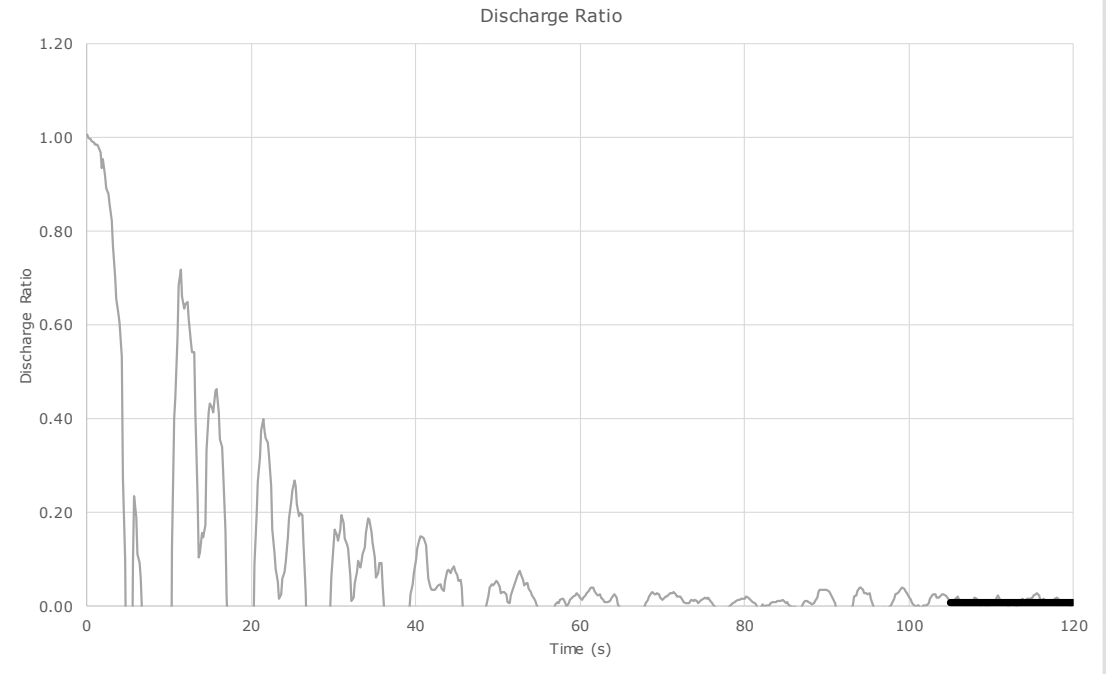


60_07_5565

Name	Symbol	Left	Right	Unit
Weir Height	WH	55	65	mm
Initial Time	Ti	105	105	s
End Time	Te	120	120	s
Initial Number	Ni	525	525	dimensionless
End Number	Ne	600	600	dimensionless
Average Discharge	$\bar{Q}$	9.678E-04	7.812E-06	m3/s

Name	Symbol	Equation	Result	Unit
Weir Height Ratio	WHr	WHL/WHR	0.846	dimensionless
Discharge Ratio	Qr	$\bar{Q}$_L/$\bar{Q}$_R	0.008	dimensionless
Time Step Discharge Ratio	Qr,t	Average[Q_(r,t=n)···Q_(r,t=n+N)]	0.008	dimensionless

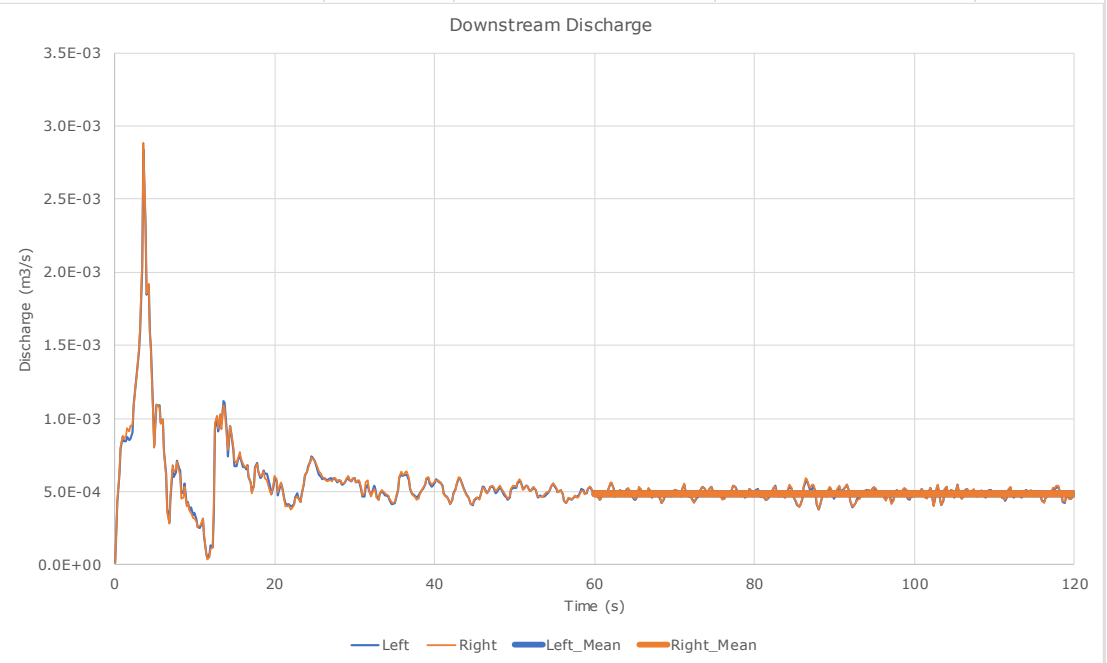


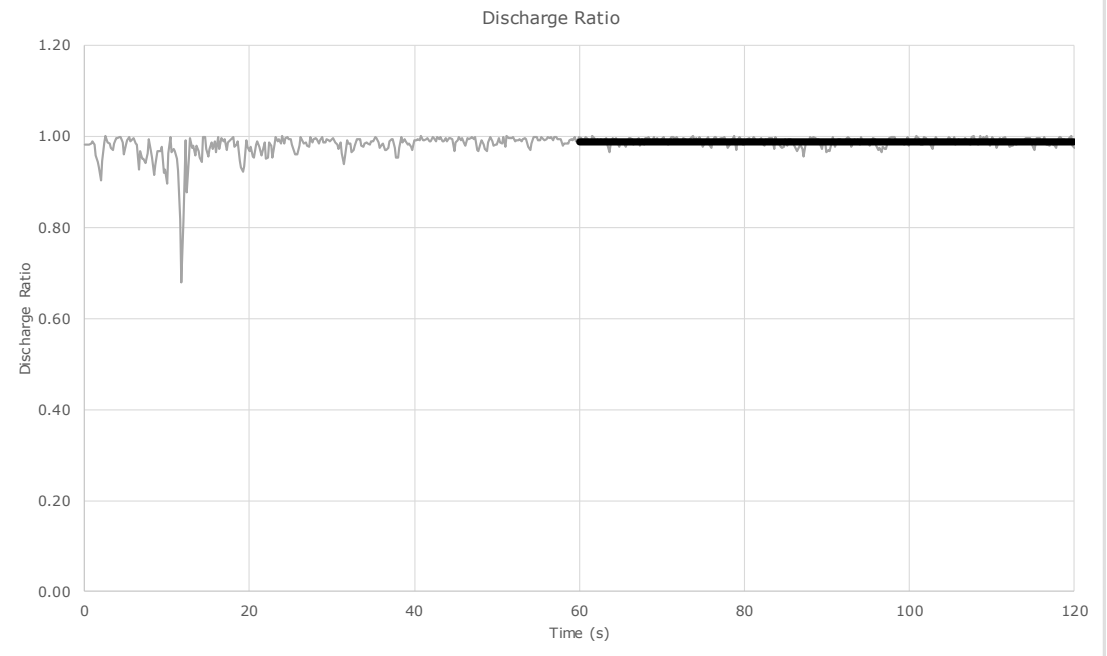


60_09_5050

Name	Symbol	Left	Right	Unit
Weir Height	WH	50	50	mm
Initial Time	Ti	60	60	s
End Time	Te	120	120	s
Initial Number	Ni	300	300	unitless
End Number	Ne	600	600	unitless
Average Discharge	$\bar{Q}$	4.853E-04	4.865E-04	m3/s

Name	Symbol	Equation	Result	Unit
Weir Height Ratio	WHr	WHL/WHR	1.000	dimensionless
Discharge Ratio	Qr	$\bar{Q}$_L/$\bar{Q}$_R	0.998	dimensionless
Time Step Discharge Ratio	Qr,t	Average[Q_(r,t=n)···Q_(r,t=n+N)]	0.988	dimensionless

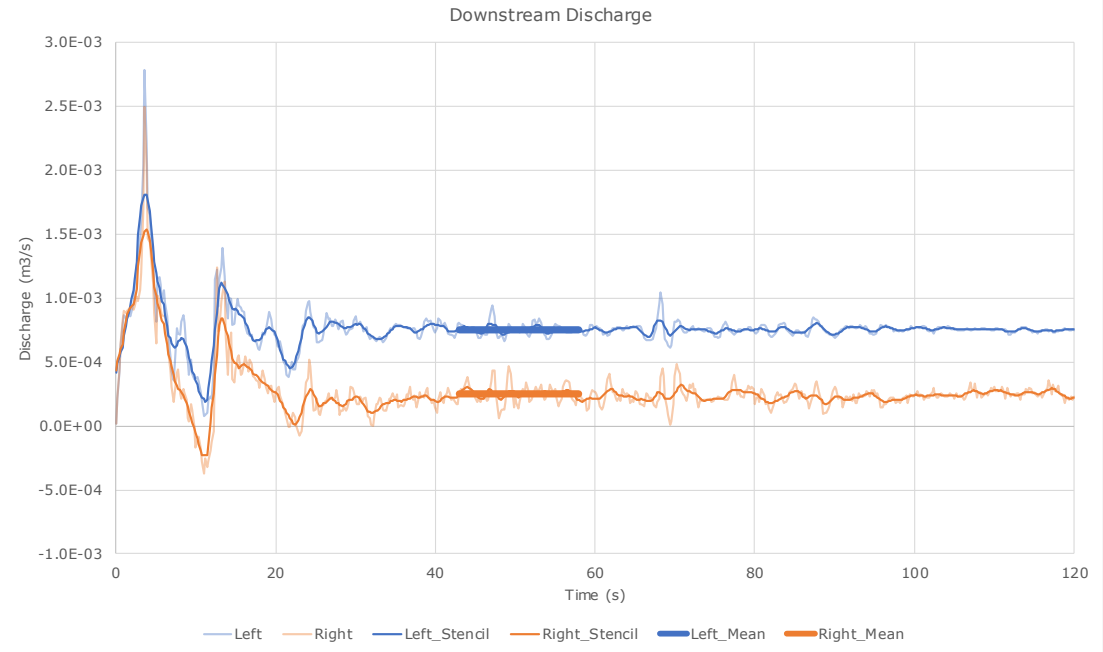


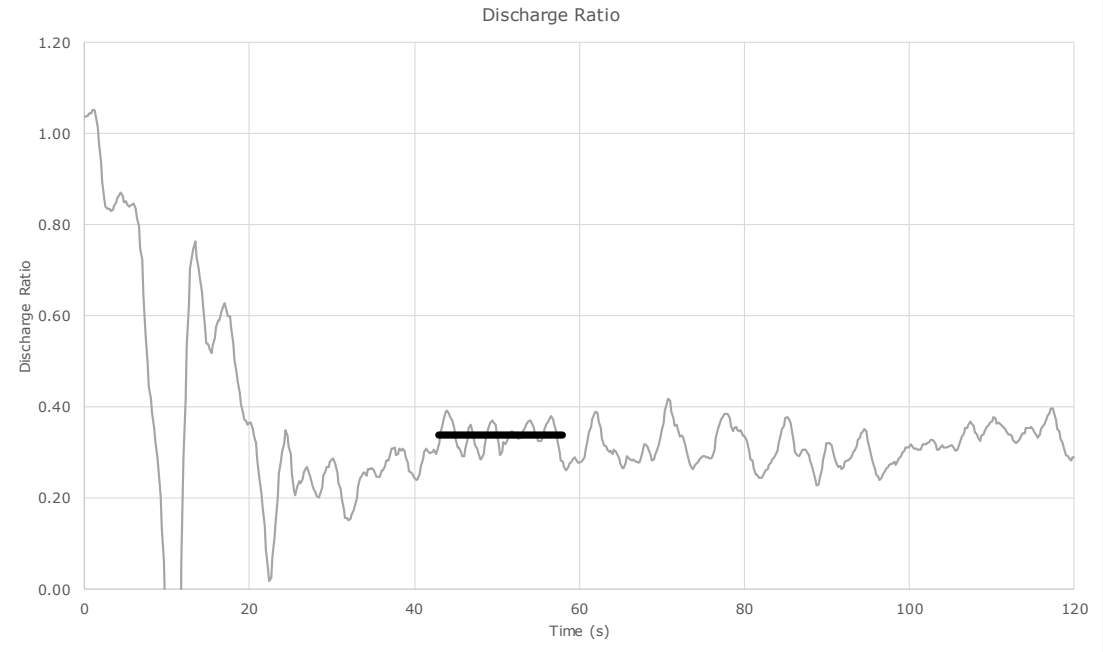


60_09_5053

	Symbol	Left	Right	Unit
	WH	50	53	mm
	Ti	43	43	s
	Te	58	58	s
	Ni	215	215	unitless
	Ne	290	290	unitless
ge	$\bar{Q}$	7.545E-04	2.547E-04	m3/s

	Symbol	Equation	Result	Unit
io	WHr	WHL/WHR	0.943	dimensionless
	Qr	$\bar{Q}$_L/$\bar{Q}$_R	0.338	dimensionless
Ratio	Qr,t	Average[Q_(r,t=n)···Q_(r,t=n+N)]	0.337	dimensionless

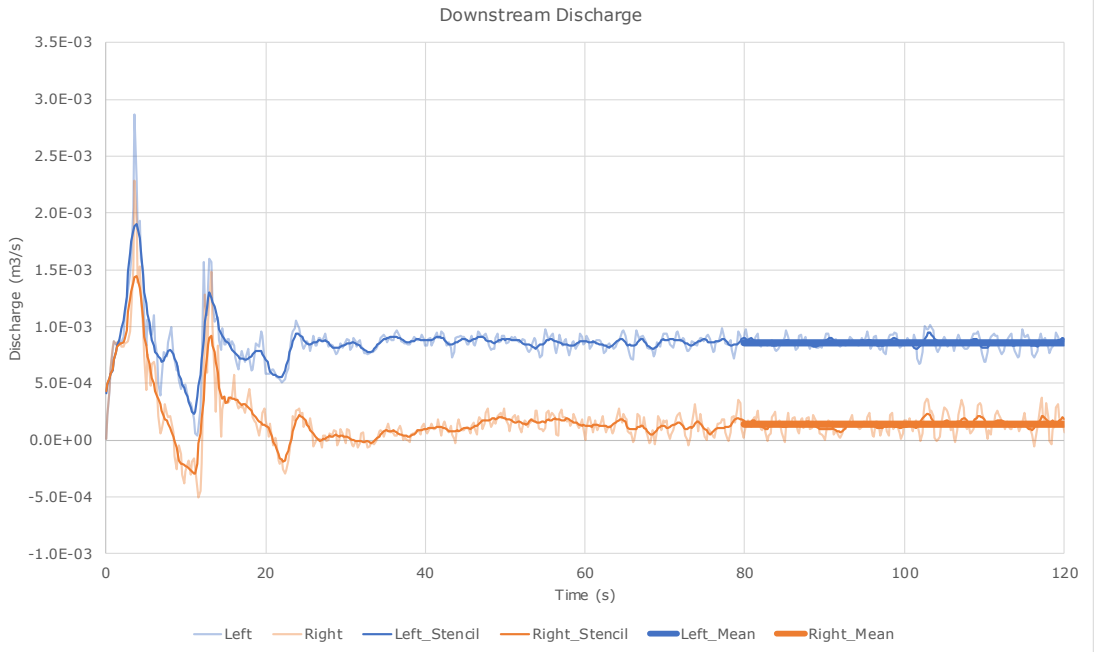


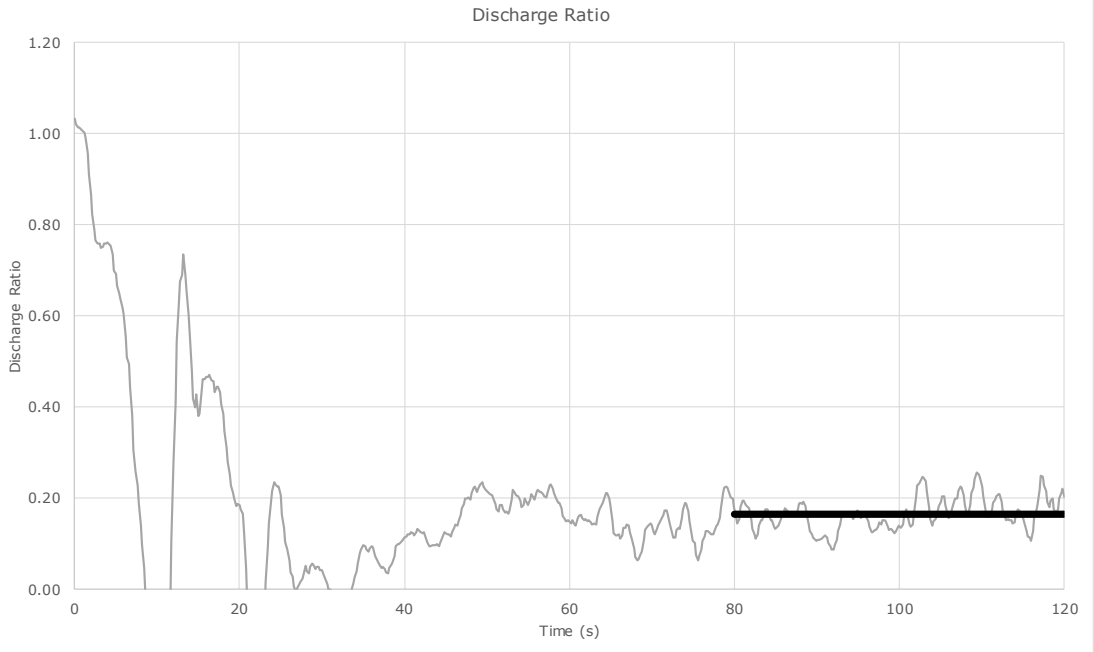


60_09_5055

Name	Symbol	Left	Right	Unit
Weir Height	WH	50	55	mm
Initial Time	Ti	80	80	s
End Time	Te	120	120	s
Initial Number	Ni	400	400	unitless
End Number	Ne	600	600	unitless
Average Discharge	$\bar{Q}$	8.598E-04	1.421E-04	m3/s

Name	Symbol	Equation	Result	Unit
Weir Height Ratio	WHr	WHL/WHR	0.909	dimensionless
Discharge Ratio	Qr	$\bar{Q}$_L/$\bar{Q}$_R	0.165	dimensionless
Time Step Discharge Ratio	Qr,t	Average[Q_(r,t=n)···Q_(r,t=n+N)]	0.165	dimensionless

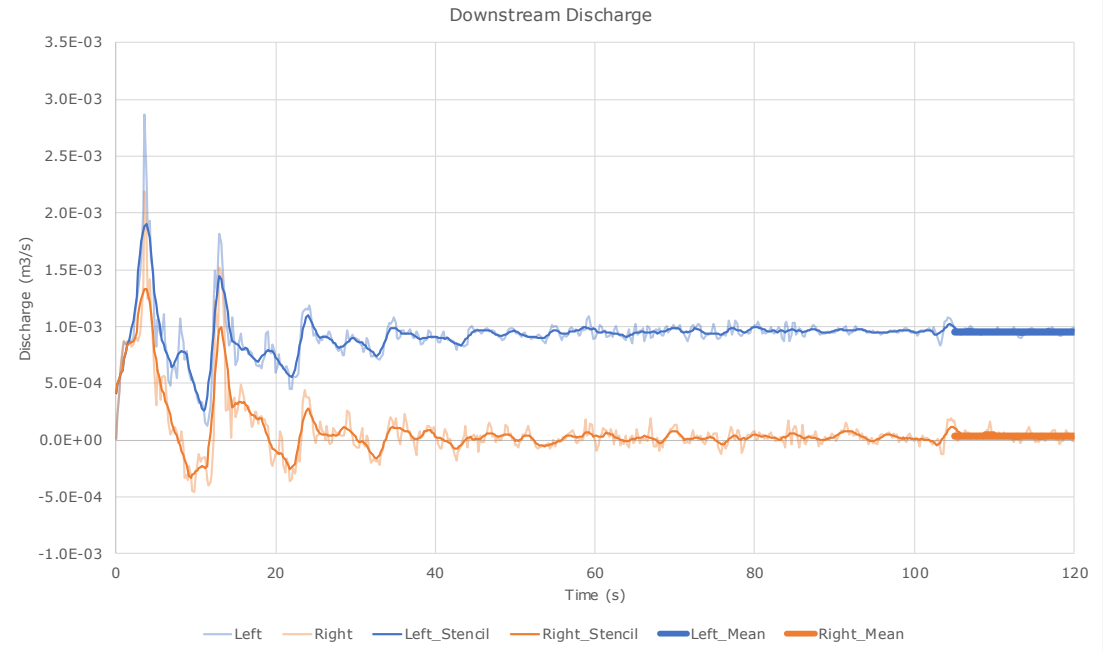


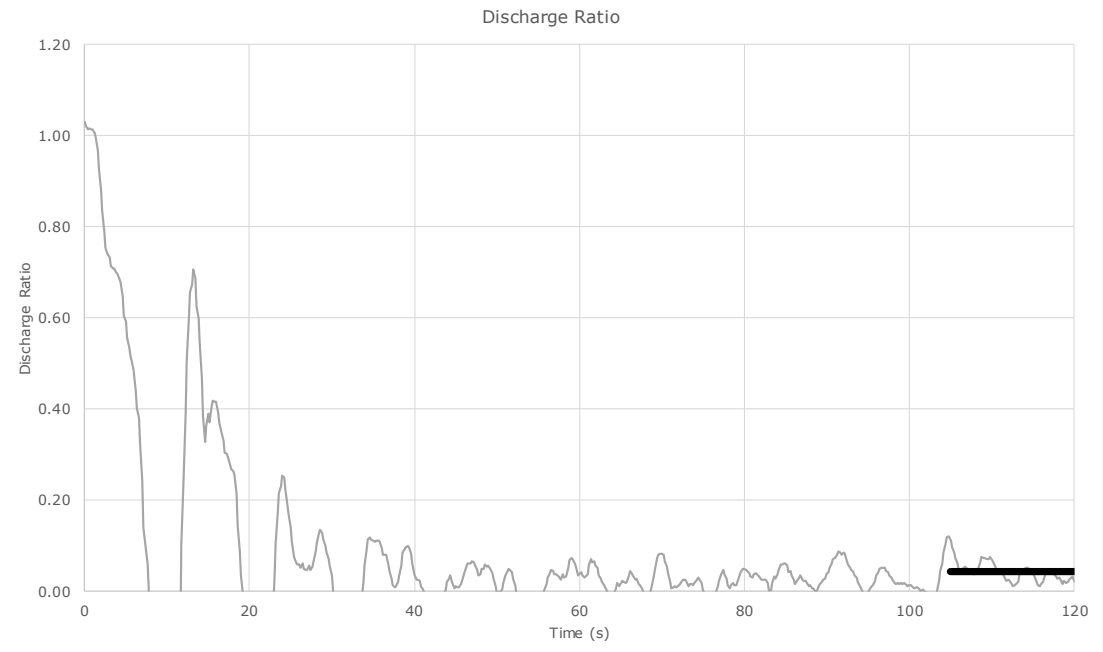


60_09_5057

Name	Symbol	Left	Right	Unit
Weir Height	WH	50	57	mm
Initial Time	Ti	105	105	s
End Time	Te	120	120	s
Initial Number	Ni	525	525	unitless
End Number	Ne	600	600	unitless
Average Discharge	$\bar{Q}$	9.555E-04	3.873E-05	m3/s

Name	Symbol	Equation	Result	Unit
Weir Height Ratio	WHr	WHL/WHR	0.877	dimensionless
Discharge Ratio	Qr	$\bar{Q}$_L/$\bar{Q}$_R	0.041	dimensionless
Time Step Discharge Ratio	Qr,t	Average[Q_(r,t=n)···Q_(r,t=n+N)]	0.042	dimensionless

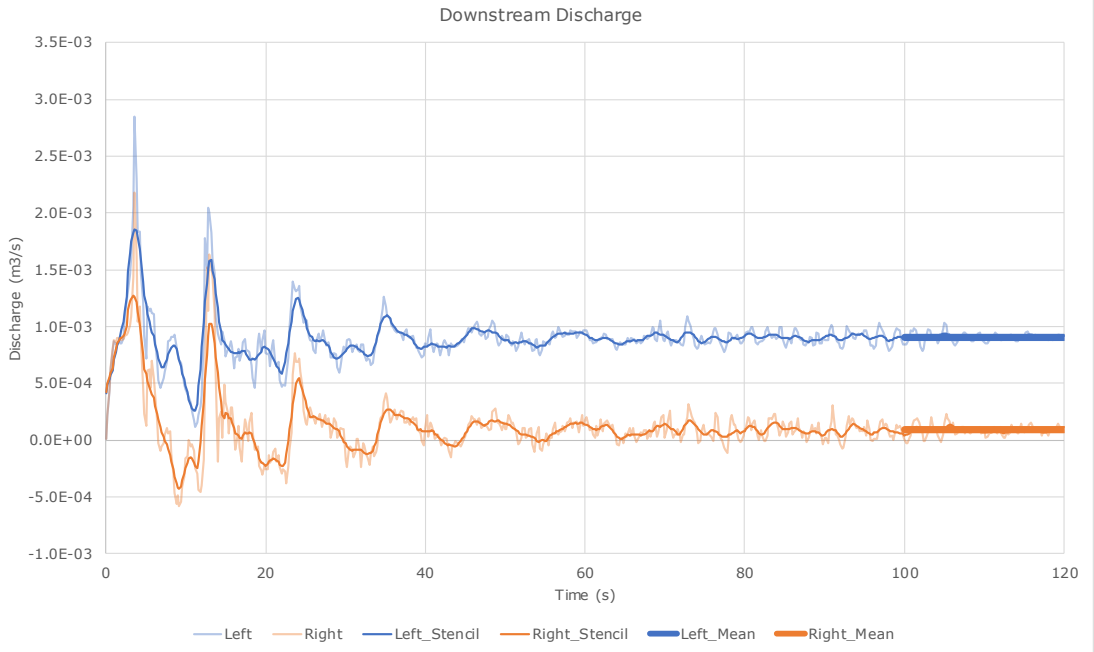


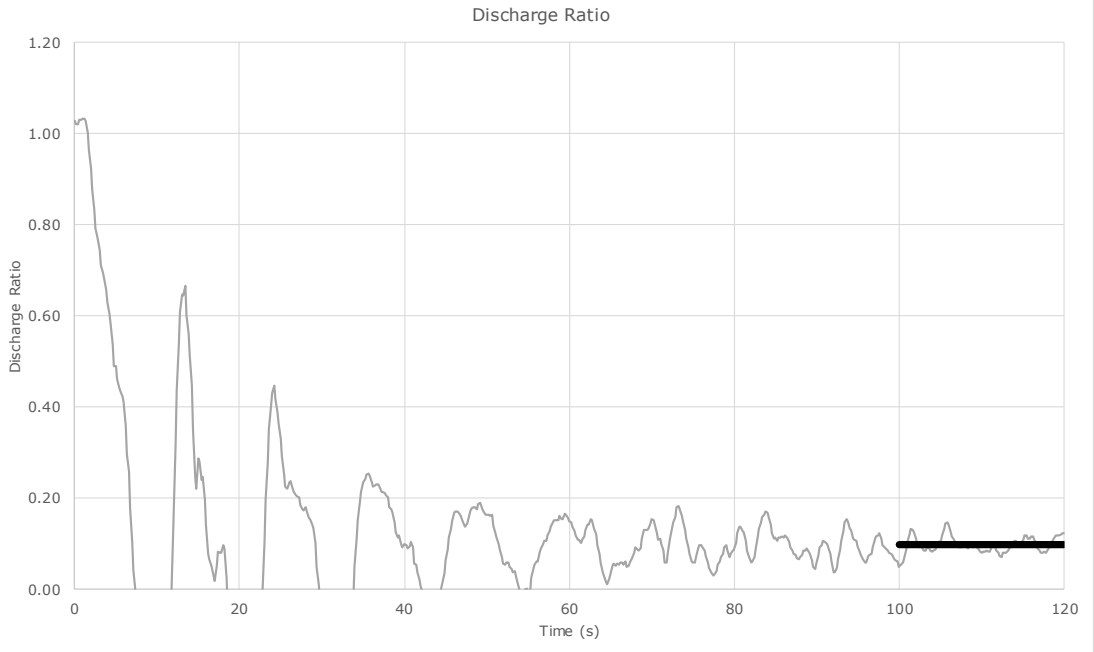


60_09_5060

Name	Symbol	Left	Right	Unit
Weir Height	WH	50	60	mm
Initial Time	Ti	100	100	s
End Time	Te	120	120	s
Initial Number	Ni	500	500	dimensionless
End Number	Ne	600	600	dimensionless
Average Discharge	$\bar{Q}$	9.058E-04	8.816E-05	m3/s

Name	Symbol	Equation	Result	Unit
Weir Height Ratio	WHr	WHL/WHR	0.833	dimensionless
Discharge Ratio	Qr	$\bar{Q}_L/\bar{Q}_R$	0.097	dimensionless
Time Step Discharge Ratio	Qr,t	Average[Q_(r,t=n)···Q_(r,t=n+N)]	0.097	dimensionless

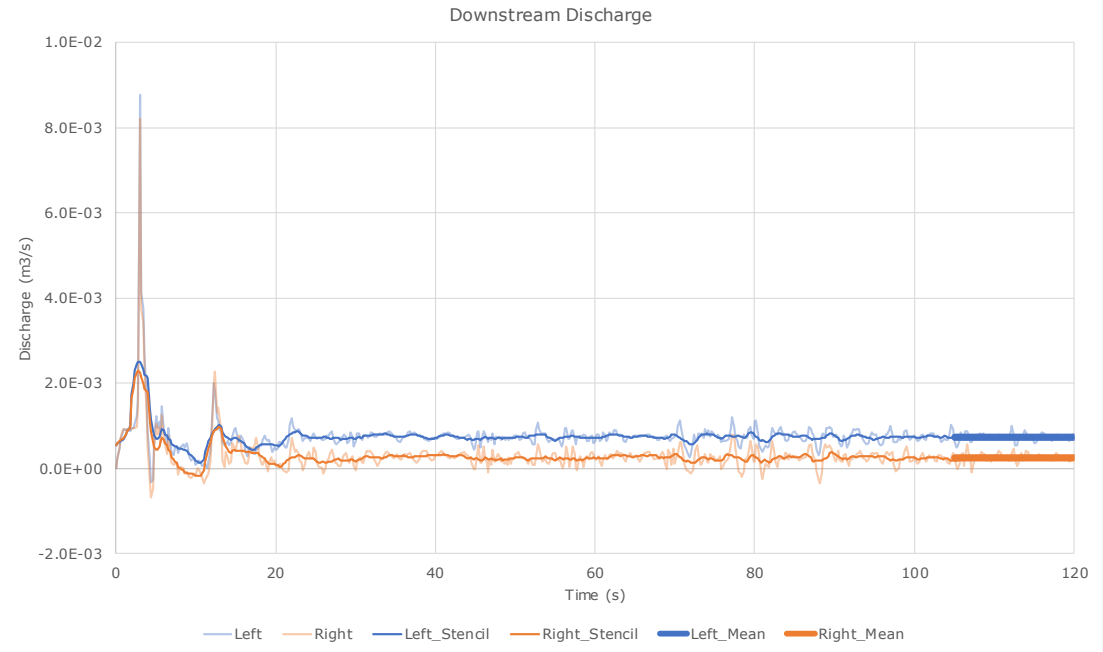


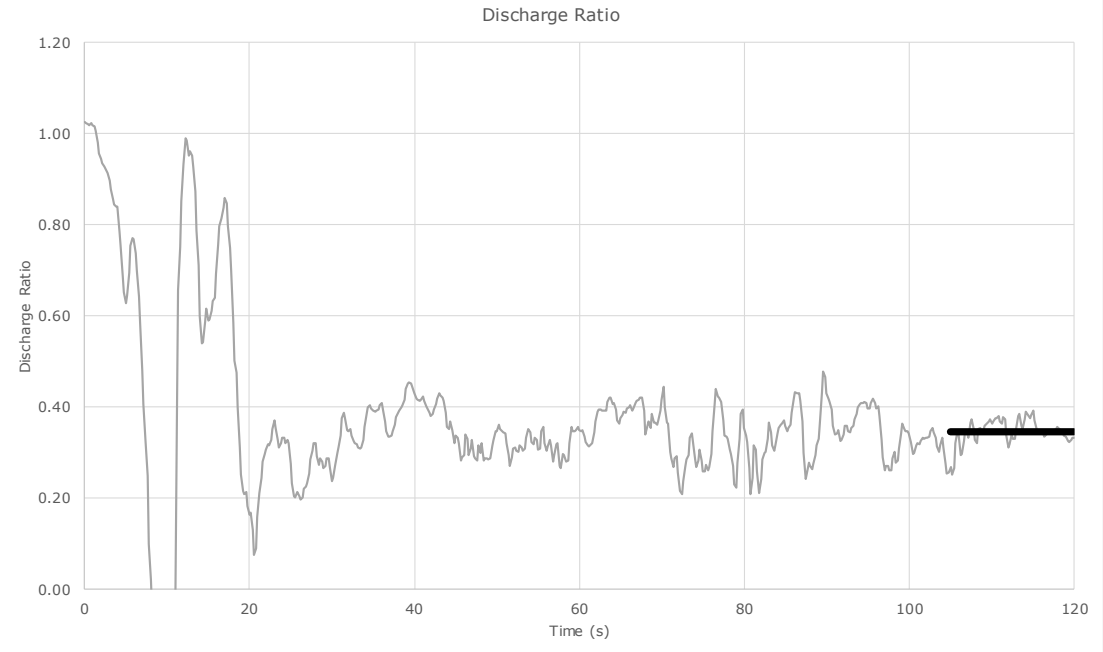


60_09_5560

Name	Symbol	Left	Right	Unit
Weir Height	WH	55	60	mm
Initial Time	Ti	105	105	s
End Time	Te	120	120	s
Initial Number	Ni	525	525	dimensionless
End Number	Ne	600	600	dimensionless
Average Discharge	$\bar{Q}$	7.455E-04	2.582E-04	m3/s

Name	Symbol	Equation	Result	Unit
Weir Height Ratio	WHr	WHL/WHR	0.917	dimensionless
Discharge Ratio	Qr	$\bar{Q}$_L/$\bar{Q}$_R	0.346	dimensionless
Time Step Discharge Ratio	Qr,t	Average[Q_(r,t=n)···Q_(r,t=n+N)]	0.346	dimensionless

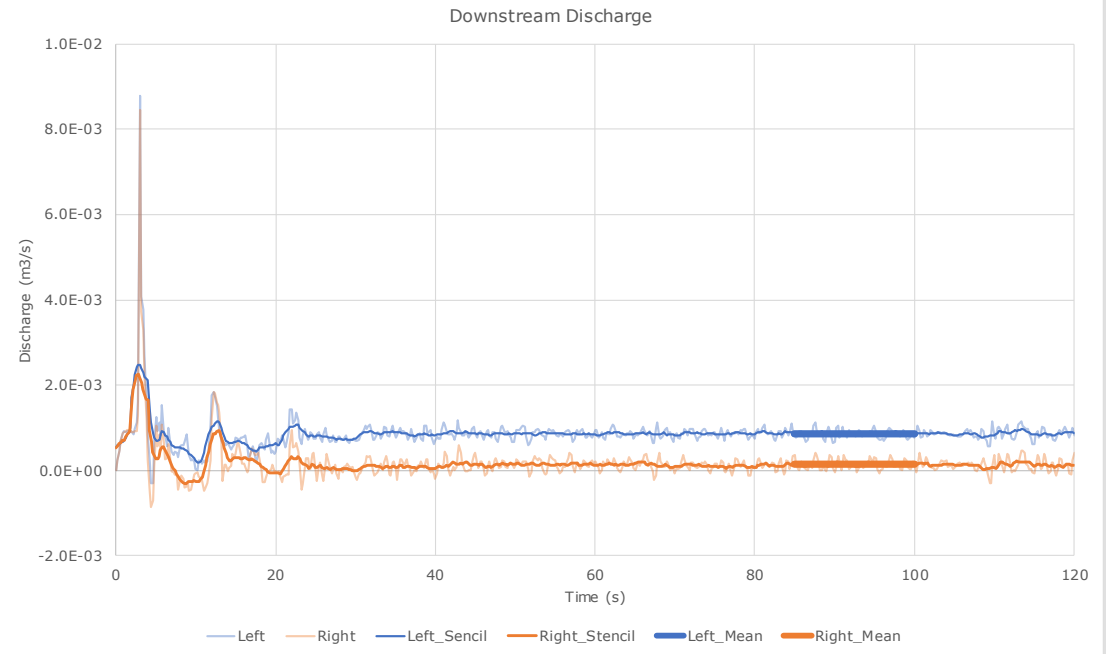


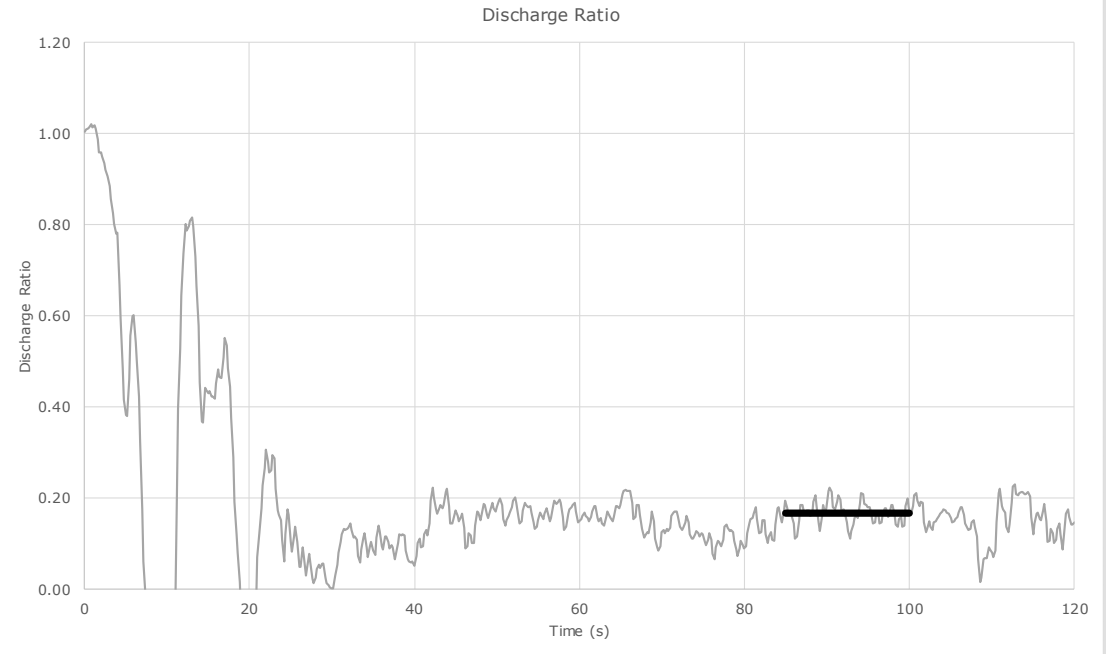


60_09_5562

Name	Symbol	Left	Right	Unit
Weir Height	WH	55	62	mm
Initial Time	Ti	85	85	s
End Time	Te	100	100	s
Initial Number	Ni	425	425	dimensionless
End Number	Ne	500	500	dimensionless
Average Discharge	$\bar{Q}$	8.647E-04	1.453E-04	m3/s

Name	Symbol	Equation	Result	Unit
Weir Height Ratio	WHr	WHL/WHR	0.887	dimensionless
Discharge Ratio	Qr	$\bar{Q}_L/\bar{Q}_R$	0.168	dimensionless
Time Step Discharge Ratio	Qr,t	Average[Q_(r,t=n)···Q_(r,t=n+N)]	0.168	dimensionless

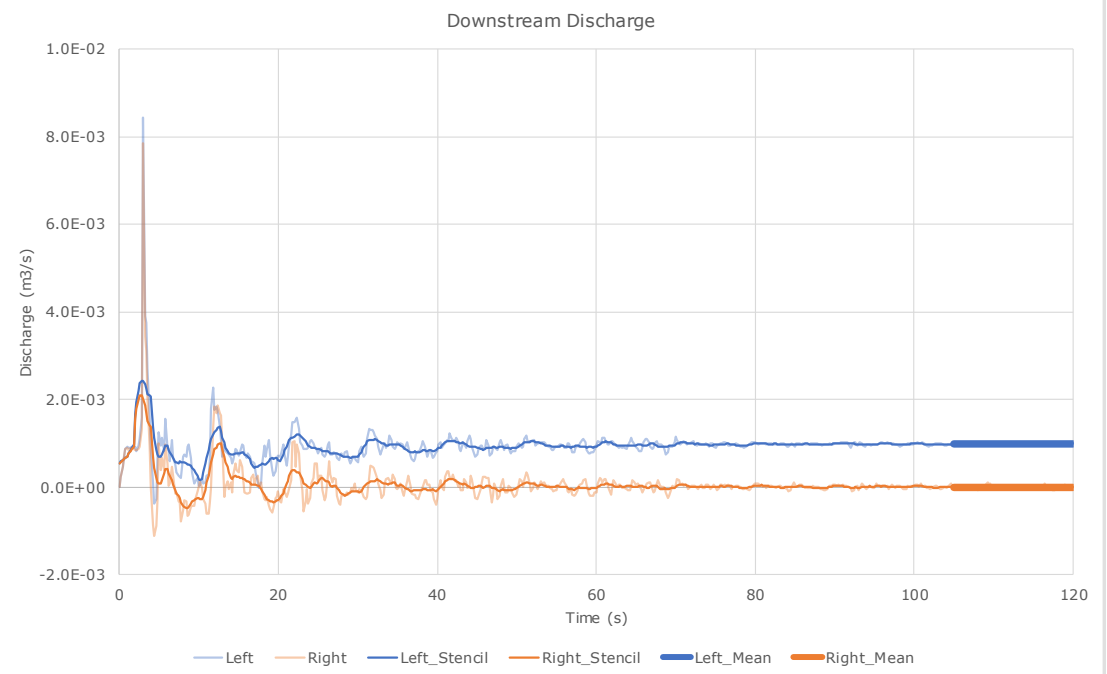


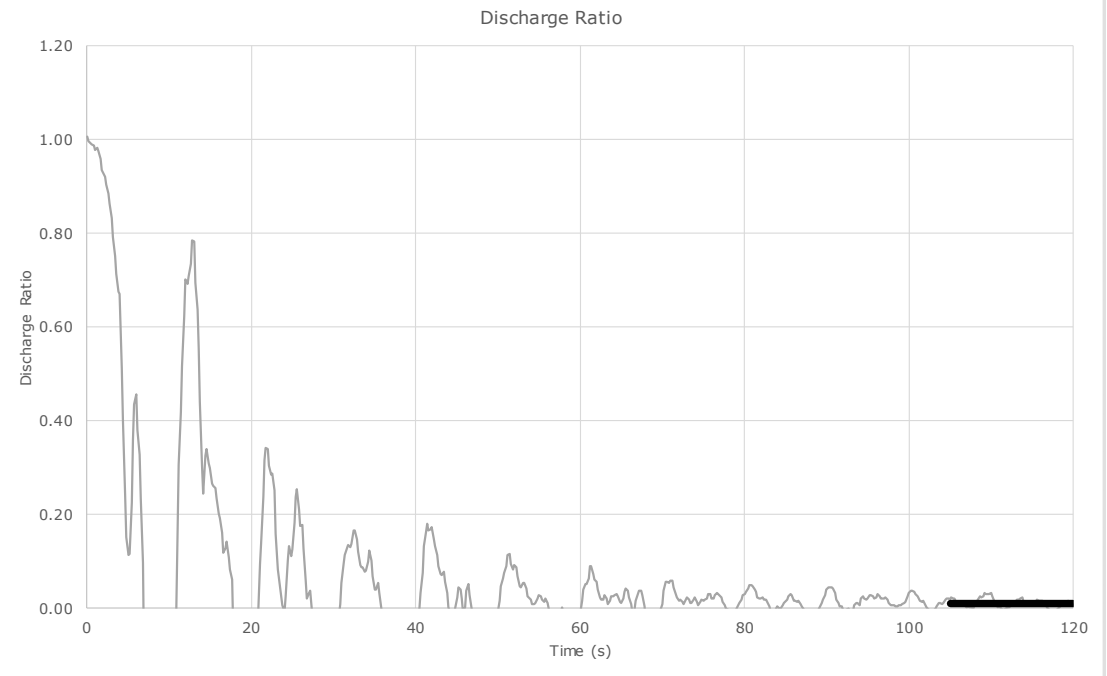


60_09_5565

Name	Symbol	Left	Right	Unit
Weir Height	WH	55	65	mm
Initial Time	Ti	105	105	s
End Time	Te	120	120	s
Initial Number	Ni	525	525	dimensionless
End Number	Ne	600	600	dimensionless
Average Discharge	$\bar{Q}$	9.897E-04	9.694E-06	m3/s

Name	Symbol	Equation	Result	Unit
Weir Height Ratio	WHr	WHL/WHR	0.846	dimensionless
Discharge Ratio	Qr	$\bar{Q}_L/\bar{Q}_R$	0.010	dimensionless
Time Step Discharge Ratio	Qr,t	Average[Q_(r,t=n)···Q_(r,t=n+N)]	0.010	dimensionless





Appendix C1 Data for Machine Learning Model Training

Source	Name	Discharge (cm3/s)	Bifurcation Angle (°)	Slope	Left Weir Height (mm)	Right Weir Height (mm)	Weir Height Ratio	Discharge Ratio
Physical Model Result	30_03_5050	660.932	30	0.003	50	50	1.000	0.953
	30_05_5050	649.483	30	0.005	50	50	1.000	0.966
	30_07_5050	651.812	30	0.007	50	50	1.000	0.961
	40_03_5050	664.797	40	0.003	50	50	1.000	0.938
	40_05_5050	671.717	40	0.005	50	50	1.000	0.945
	40_07_5050	667.714	40	0.007	50	50	1.000	0.944
	50_03_5050	672.175	50	0.003	50	50	1.000	0.954
	50_05_5050	667.051	50	0.005	50	50	1.000	0.942
	50_07_5050	680.759	50	0.007	50	50	1.000	0.976
	30_03_5560	658.031	30	0.003	55	60	0.917	0.221
	30_05_5560	655.552	30	0.005	55	60	0.917	0.237
	30_07_5560	644.845	30	0.007	55	60	0.917	0.210
	40_03_5560	665.747	40	0.003	55	60	0.917	0.209
	40_05_5560	669.616	40	0.005	55	60	0.917	0.195
	40_07_5560	661.929	40	0.007	55	60	0.917	0.205
	50_03_5560	659.697	50	0.003	55	60	0.917	0.239
	50_05_5560	668.949	50	0.005	55	60	0.917	0.244
	50_07_5560	654.417	50	0.007	55	60	0.917	0.234
	30_03_5055	654.986	30	0.003	50	55	0.909	0.352
	30_05_5055	661.200	30	0.005	50	55	0.909	0.343
	30_07_5055	651.104	30	0.007	50	55	0.909	0.346
	40_03_5055	661.026	40	0.003	50	55	0.909	0.309
	40_05_5055	610.680	40	0.005	50	55	0.909	0.291
	40_07_5055	667.922	40	0.007	50	55	0.909	0.312
	50_03_5055	660.183	50	0.003	50	55	0.909	0.310
	50_05_5055	653.165	50	0.005	50	55	0.909	0.317
	50_07_5055	657.650	50	0.007	50	55	0.909	0.330

Source	Name	Discharge (cm3/s)	Bifurcation Angle (°)	Slope	Left Weir Height (mm)	Right Weir Height (mm)	Weir Height Ratio	Discharge Ratio
Numerical Model Result	NB30_03_5050	1000	30	0.003	50	50	1.000	0.979
	NB30_03_5053	1000	30	0.003	50	53	0.943	0.731
	NB30_03_5055	1000	30	0.003	50	55	0.909	0.500
	NB30_03_5057	1000	30	0.003	50	57	0.877	0.335
	NB30_03_5060	1000	30	0.003	50	60	0.833	0.238
	NB30_03_5560	1000	30	0.003	55	60	0.917	0.490
	NB30_03_5562	1000	30	0.003	55	62	0.887	0.287
	NB30_03_5565	1000	30	0.003	55	65	0.846	0.185
	NB30_05_5050	1000	30	0.005	50	50	1.000	0.997
	NB30_05_5053	1000	30	0.005	50	53	0.943	0.726
	NB30_05_5055	1000	30	0.005	50	55	0.909	0.483
	NB30_05_5057	1000	30	0.005	50	57	0.877	0.339
	NB30_05_5060	1000	30	0.005	50	60	0.833	0.221
	NB30_05_5560	1000	30	0.005	55	60	0.917	0.529
	NB30_05_5562	1000	30	0.005	55	52	1.058	0.334
	NB30_05_5565	1000	30	0.005	55	65	0.846	0.187
	NB30_07_5050	1000	30	0.007	50	50	1.000	0.994
	NB30_07_5053	1000	30	0.007	50	53	0.943	0.728
	NB30_07_5055	1000	30	0.007	50	55	0.909	0.507
	NB30_07_5057	1000	30	0.007	50	57	0.877	0.382
	NB30_07_5060	1000	30	0.007	50	60	0.833	0.222
	NB30_07_5560	1000	30	0.007	55	60	0.917	0.581
	NB30_07_5562	1000	30	0.007	55	52	1.058	0.339
	NB30_07_5565	1000	30	0.007	55	65	0.846	0.185
	NB30_09_5050	1000	30	0.009	50	50	1.000	0.998
	NB30_09_5053	1000	30	0.009	50	53	0.943	0.729
	NB30_09_5055	1000	30	0.009	50	55	0.909	0.501
	NB30_09_5057	1000	30	0.009	50	57	0.877	0.339
	NB30_09_5060	1000	30	0.009	50	60	0.833	0.220
	NB30_09_5560	1000	30	0.009	55	60	0.917	0.564
	NB30_09_5562	1000	30	0.009	55	52	1.058	0.334
	NB30_09_5565	1000	30	0.009	55	65	0.846	0.202

Source	Name	Discharge (cm3/s)	Bifurcation Angle (°)	Slope	Left Weir Height (mm)	Right Weir Height (mm)	Weir Height Ratio	Discharge Ratio
Numerical Model Result	NB40_03_5050	1000	40	0.003	50	50	1.000	0.997
	NB40_03_5053	1000	40	0.003	50	53	0.943	0.683
	NB40_03_5055	1000	40	0.003	50	55	0.909	0.504
	NB40_03_5057	1000	40	0.003	50	57	0.877	0.344
	NB40_03_5060	1000	40	0.003	50	60	0.833	0.205
	NB40_03_5560	1000	40	0.003	55	60	0.917	0.439
	NB40_03_5562	1000	40	0.003	55	52	1.058	0.395
	NB40_03_5565	1000	40	0.003	55	65	0.846	0.228
	NB40_05_5050	1000	40	0.005	50	50	1.000	0.998
	NB40_05_5053	1000	40	0.005	50	53	0.943	0.688
	NB40_05_5055	1000	40	0.005	50	55	0.909	0.485
	NB40_05_5057	1000	40	0.005	50	57	0.877	0.364
	NB40_05_5060	1000	40	0.005	50	60	0.833	0.201
	NB40_05_5560	1000	40	0.005	55	60	0.917	0.544
	NB40_05_5562	1000	40	0.005	55	52	1.058	0.341
	NB40_05_5565	1000	40	0.005	55	65	0.846	0.190
	NB40_07_5050	1000	40	0.007	50	50	1.000	1.000
	NB40_07_5053	1000	40	0.007	50	53	0.943	0.680
	NB40_07_5055	1000	40	0.007	50	55	0.909	0.507
	NB40_07_5057	1000	40	0.007	50	57	0.877	0.362
	NB40_07_5060	1000	40	0.007	50	60	0.833	0.206
	NB40_07_5560	1000	40	0.007	55	60	0.917	0.542
	NB40_07_5562	1000	40	0.007	55	52	1.058	0.336
	NB40_07_5565	1000	40	0.007	55	65	0.846	0.171
	NB40_09_5050	1000	40	0.009	50	50	1.000	0.999
	NB40_09_5053	1000	40	0.009	50	53	0.943	0.688
	NB40_09_5055	1000	40	0.009	50	55	0.909	0.502
	NB40_09_5057	1000	40	0.009	50	57	0.877	0.336
	NB40_09_5060	1000	40	0.009	50	60	0.833	0.208
	NB40_09_5560	1000	40	0.009	55	60	0.917	0.527
	NB40_09_5562	1000	40	0.009	55	52	1.058	0.325
	NB40_09_5565	1000	40	0.009	55	65	0.846	0.186

Source	Name	Discharge (cm3/s)	Bifurcation Angle (°)	Slope	Left Weir Height (mm)	Right Weir Height (mm)	Weir Height Ratio	Discharge Ratio
Numerical Model Result	NB50_03_5050	1000	50	0.003	50	50	1.000	0.996
	NB50_03_5053	1000	50	0.003	50	53	0.943	0.706
	NB50_03_5055	1000	50	0.003	50	55	0.909	0.511
	NB50_03_5057	1000	50	0.003	50	57	0.877	0.346
	NB50_03_5060	1000	50	0.003	50	60	0.833	0.224
	NB50_03_5560	1000	50	0.003	55	60	0.917	0.430
	NB50_03_5562	1000	50	0.003	55	52	1.058	0.300
	NB50_03_5565	1000	50	0.003	55	65	0.846	0.151
	NB50_05_5050	1000	50	0.005	50	50	1.000	1.000
	NB50_05_5053	1000	50	0.005	50	53	0.943	0.691
	NB50_05_5055	1000	50	0.005	50	55	0.909	0.517
	NB50_05_5057	1000	50	0.005	50	57	0.877	0.350
	NB50_05_5060	1000	50	0.005	50	60	0.833	0.216
	NB50_05_5560	1000	50	0.005	55	60	0.917	0.520
	NB50_05_5562	1000	50	0.005	55	52	1.058	0.337
	NB50_05_5565	1000	50	0.005	55	65	0.846	0.185
	NB50_07_5050	1000	50	0.007	50	50	1.000	0.996
	NB50_07_5053	1000	50	0.007	50	53	0.943	0.703
	NB50_07_5055	1000	50	0.007	50	55	0.909	0.498
	NB50_07_5057	1000	50	0.007	50	57	0.877	0.347
	NB50_07_5060	1000	50	0.007	50	60	0.833	0.222
	NB50_07_5560	1000	50	0.007	55	60	0.917	0.503
	NB50_07_5562	1000	50	0.007	55	52	1.058	0.333
	NB50_07_5565	1000	50	0.007	55	65	0.846	0.203
	NB50_09_5050	1000	50	0.009	50	50	1.000	0.999
	NB50_09_5053	1000	50	0.009	50	53	0.943	0.693
	NB50_09_5055	1000	50	0.009	50	55	0.909	0.515
	NB50_09_5057	1000	50	0.009	50	57	0.877	0.340
	NB50_09_5060	1000	50	0.009	50	60	0.833	0.230
	NB50_09_5560	1000	50	0.009	55	60	0.917	0.540
	NB50_09_5562	1000	50	0.009	55	52	1.058	0.338
	NB50_09_5565	1000	50	0.009	55	65	0.846	0.195

Source	Name	Discharge (cm3/s)	Bifurcation Angle (°)	Slope	Left Weir Height (mm)	Right Weir Height (mm)	Weir Height Ratio	Discharge Ratio
Numerical Model Result	NB60_03_5050	1000	60	0.003	50	50	1.000	0.999
	NB60_03_5053	1000	60	0.003	50	53	0.943	0.309
	NB60_03_5055	1000	60	0.003	50	55	0.909	0.296
	NB60_03_5057	1000	60	0.003	50	57	0.877	0.237
	NB60_03_5060	1000	60	0.003	50	60	0.833	0.233
	NB60_03_5560	1000	60	0.003	55	60	0.917	0.514
	NB60_03_5562	1000	60	0.003	55	52	1.058	0.387
	NB60_03_5565	1000	60	0.003	55	65	0.846	0.056
	NB60_05_5050	1000	60	0.005	50	50	1.000	0.998
	NB60_05_5053	1000	60	0.005	50	53	0.943	0.322
	NB60_05_5055	1000	60	0.005	50	55	0.909	0.131
	NB60_05_5057	1000	60	0.005	50	57	0.877	0.024
	NB60_05_5060	1000	60	0.005	50	60	0.833	0.089
	NB60_05_5560	1000	60	0.005	55	60	0.917	0.301
	NB60_05_5562	1000	60	0.005	55	52	1.058	0.258
	NB60_05_5565	1000	60	0.005	55	65	0.846	0.202
	NB60_07_5050	1000	60	0.007	50	50	1.000	1.000
	NB60_07_5053	1000	60	0.007	50	53	0.943	0.336
	NB60_07_5055	1000	60	0.007	50	55	0.909	0.143
	NB60_07_5057	1000	60	0.007	50	57	0.877	0.060
	NB60_07_5060	1000	60	0.007	50	60	0.833	0.097
	NB60_07_5560	1000	60	0.007	55	60	0.917	0.321
	NB60_07_5562	1000	60	0.007	55	52	1.058	0.148
	NB60_07_5565	1000	60	0.007	55	65	0.846	0.008
	NB60_09_5050	1000	60	0.009	50	50	1.000	0.998
	NB60_09_5053	1000	60	0.009	50	53	0.943	0.338
	NB60_09_5055	1000	60	0.009	50	55	0.909	0.165
	NB60_09_5057	1000	60	0.009	50	57	0.877	0.041
	NB60_09_5060	1000	60	0.009	50	60	0.833	0.097
	NB60_09_5560	1000	60	0.009	55	60	0.917	0.346
	NB60_09_5562	1000	60	0.009	55	52	1.058	0.168
	NB60_09_5565	1000	60	0.009	55	65	0.846	0.010

Source	Name	Discharge (cm3/s)	Bifurcation Angle (°)	Slope	Left Weir Height (mm)	Right Weir Height (mm)	Weir Height Ratio	Discharge Ratio
Thomas et al. (2011)	A-L35R45	6936.667	54	0.001	35	45	0.778	0.790
	A-L35R55	6666.667	54	0.001	35	55	0.636	0.520
	A-L40R45	7136.667	54	0.001	40	45	0.889	0.810
	A-L40R50	6876.667	54	0.001	40	50	0.800	0.680
	A-L45R45	6796.667	54	0.001	45	45	1.000	1.000
	A-L45R50	6613.333	54	0.001	45	50	0.900	0.830
	A-L45R55	7023.333	54	0.001	45	55	0.818	0.690
	B-L35R45	6760.000	54	0.001	35	45	0.778	0.730
	B-L35R55	6936.667	54	0.001	35	55	0.636	0.520
	B-L45R45	6803.333	54	0.001	45	45	1.000	0.990
	B-L45R55	6526.667	54	0.001	45	55	0.818	0.720

Appendix C2 Data for Machine Learning Model Prediction

Discharge (cm3/s)	Bifurcation Angle (°)	Slope	Left Weir Height (mm)	Right Weir Height (mm)	Weir Height Ratio
200	30	0.003	50	50	1.000
300	30	0.003	50	50	1.000
400	30	0.003	50	50	1.000
500	30	0.003	50	50	1.000
600	30	0.003	50	50	1.000
700	30	0.003	50	50	1.000
800	30	0.003	50	50	1.000
900	30	0.003	50	50	1.000
1000	30	0.003	50	50	1.000
1200	30	0.003	50	50	1.000
1400	30	0.003	50	50	1.000
1600	30	0.003	50	50	1.000
1800	30	0.003	50	50	1.000
2000	30	0.003	50	50	1.000
2200	30	0.003	50	50	1.000
2400	30	0.003	50	50	1.000
2600	30	0.003	50	50	1.000
2800	30	0.003	50	50	1.000
3000	30	0.003	50	50	1.000
3200	30	0.003	50	50	1.000
3400	30	0.003	50	50	1.000
3600	30	0.003	50	50	1.000
3800	30	0.003	50	50	1.000
4000	30	0.003	50	50	1.000
4200	30	0.003	50	50	1.000
4400	30	0.003	50	50	1.000
4600	30	0.003	50	50	1.000
4800	30	0.003	50	50	1.000
5000	30	0.003	50	50	1.000
5200	30	0.003	50	50	1.000
5400	30	0.003	50	50	1.000
5600	30	0.003	50	50	1.000
5800	30	0.003	50	50	1.000
6000	30	0.003	50	50	1.000
6200	30	0.003	50	50	1.000
6400	30	0.003	50	50	1.000
6600	30	0.003	50	50	1.000
6800	30	0.003	50	50	1.000

7000	30	0.003	50	50	1.000
7200	30	0.003	50	50	1.000
7400	30	0.003	50	50	1.000
7600	30	0.003	50	50	1.000
7800	30	0.003	50	50	1.000
8000	30	0.003	50	50	1.000
8200	30	0.003	50	50	1.000
8400	30	0.003	50	50	1.000
8600	30	0.003	50	50	1.000
8800	30	0.003	50	50	1.000
9000	30	0.003	50	50	1.000
9200	30	0.003	50	50	1.000
9400	30	0.003	50	50	1.000
9600	30	0.003	50	50	1.000
9800	30	0.003	50	50	1.000
10000	30	0.003	50	50	1.000
10200	30	0.003	50	50	1.000
10400	30	0.003	50	50	1.000
10600	30	0.003	50	50	1.000
10800	30	0.003	50	50	1.000
11000	30	0.003	50	50	1.000
11200	30	0.003	50	50	1.000
11400	30	0.003	50	50	1.000
11600	30	0.003	50	50	1.000
11800	30	0.003	50	50	1.000
12000	30	0.003	50	50	1.000
200	30	0.003	50	55	0.909
300	30	0.003	50	55	0.909
400	30	0.003	50	55	0.909
500	30	0.003	50	55	0.909
600	30	0.003	50	55	0.909
700	30	0.003	50	55	0.909
800	30	0.003	50	55	0.909
900	30	0.003	50	55	0.909
1000	30	0.003	50	55	0.909
1200	30	0.003	50	55	0.909
1400	30	0.003	50	55	0.909
1600	30	0.003	50	55	0.909
1800	30	0.003	50	55	0.909
2000	30	0.003	50	55	0.909
2200	30	0.003	50	55	0.909
2400	30	0.003	50	55	0.909
2600	30	0.003	50	55	0.909
2800	30	0.003	50	55	0.909
3000	30	0.003	50	55	0.909

3200	30	0.003	50	55	0.909
3400	30	0.003	50	55	0.909
3600	30	0.003	50	55	0.909
3800	30	0.003	50	55	0.909
4000	30	0.003	50	55	0.909
4200	30	0.003	50	55	0.909
4400	30	0.003	50	55	0.909
4600	30	0.003	50	55	0.909
4800	30	0.003	50	55	0.909
5000	30	0.003	50	55	0.909
5200	30	0.003	50	55	0.909
5400	30	0.003	50	55	0.909
5600	30	0.003	50	55	0.909
5800	30	0.003	50	55	0.909
6000	30	0.003	50	55	0.909
6200	30	0.003	50	55	0.909
6400	30	0.003	50	55	0.909
6600	30	0.003	50	55	0.909
6800	30	0.003	50	55	0.909
7000	30	0.003	50	55	0.909
7200	30	0.003	50	55	0.909
7400	30	0.003	50	55	0.909
7600	30	0.003	50	55	0.909
7800	30	0.003	50	55	0.909
8000	30	0.003	50	55	0.909
8200	30	0.003	50	55	0.909
8400	30	0.003	50	55	0.909
8600	30	0.003	50	55	0.909
8800	30	0.003	50	55	0.909
9000	30	0.003	50	55	0.909
9200	30	0.003	50	55	0.909
9400	30	0.003	50	55	0.909
9600	30	0.003	50	55	0.909
9800	30	0.003	50	55	0.909
10000	30	0.003	50	55	0.909
10200	30	0.003	50	55	0.909
10400	30	0.003	50	55	0.909
10600	30	0.003	50	55	0.909
10800	30	0.003	50	55	0.909
11000	30	0.003	50	55	0.909
11200	30	0.003	50	55	0.909
11400	30	0.003	50	55	0.909
11600	30	0.003	50	55	0.909
11800	30	0.003	50	55	0.909
12000	30	0.003	50	55	0.909

200	30	0.003	50	60	0.833
300	30	0.003	50	60	0.833
400	30	0.003	50	60	0.833
500	30	0.003	50	60	0.833
600	30	0.003	50	60	0.833
700	30	0.003	50	60	0.833
800	30	0.003	50	60	0.833
900	30	0.003	50	60	0.833
1000	30	0.003	50	60	0.833
1200	30	0.003	50	60	0.833
1400	30	0.003	50	60	0.833
1600	30	0.003	50	60	0.833
1800	30	0.003	50	60	0.833
2000	30	0.003	50	60	0.833
2200	30	0.003	50	60	0.833
2400	30	0.003	50	60	0.833
2600	30	0.003	50	60	0.833
2800	30	0.003	50	60	0.833
3000	30	0.003	50	60	0.833
3200	30	0.003	50	60	0.833
3400	30	0.003	50	60	0.833
3600	30	0.003	50	60	0.833
3800	30	0.003	50	60	0.833
4000	30	0.003	50	60	0.833
4200	30	0.003	50	60	0.833
4400	30	0.003	50	60	0.833
4600	30	0.003	50	60	0.833
4800	30	0.003	50	60	0.833
5000	30	0.003	50	60	0.833
5200	30	0.003	50	60	0.833
5400	30	0.003	50	60	0.833
5600	30	0.003	50	60	0.833
5800	30	0.003	50	60	0.833
6000	30	0.003	50	60	0.833
6200	30	0.003	50	60	0.833
6400	30	0.003	50	60	0.833
6600	30	0.003	50	60	0.833
6800	30	0.003	50	60	0.833
7000	30	0.003	50	60	0.833
7200	30	0.003	50	60	0.833
7400	30	0.003	50	60	0.833
7600	30	0.003	50	60	0.833
7800	30	0.003	50	60	0.833
8000	30	0.003	50	60	0.833
8200	30	0.003	50	60	0.833

8400	30	0.003	50	60	0.833
8600	30	0.003	50	60	0.833
8800	30	0.003	50	60	0.833
9000	30	0.003	50	60	0.833
9200	30	0.003	50	60	0.833
9400	30	0.003	50	60	0.833
9600	30	0.003	50	60	0.833
9800	30	0.003	50	60	0.833
10000	30	0.003	50	60	0.833
10200	30	0.003	50	60	0.833
10400	30	0.003	50	60	0.833
10600	30	0.003	50	60	0.833
10800	30	0.003	50	60	0.833
11000	30	0.003	50	60	0.833
11200	30	0.003	50	60	0.833
11400	30	0.003	50	60	0.833
11600	30	0.003	50	60	0.833
11800	30	0.003	50	60	0.833
12000	30	0.003	50	60	0.833
200	30	0.003	50	65	0.769
300	30	0.003	50	65	0.769
400	30	0.003	50	65	0.769
500	30	0.003	50	65	0.769
600	30	0.003	50	65	0.769
700	30	0.003	50	65	0.769
800	30	0.003	50	65	0.769
900	30	0.003	50	65	0.769
1000	30	0.003	50	65	0.769
1200	30	0.003	50	65	0.769
1400	30	0.003	50	65	0.769
1600	30	0.003	50	65	0.769
1800	30	0.003	50	65	0.769
2000	30	0.003	50	65	0.769
2200	30	0.003	50	65	0.769
2400	30	0.003	50	65	0.769
2600	30	0.003	50	65	0.769
2800	30	0.003	50	65	0.769
3000	30	0.003	50	65	0.769
3200	30	0.003	50	65	0.769
3400	30	0.003	50	65	0.769
3600	30	0.003	50	65	0.769
3800	30	0.003	50	65	0.769
4000	30	0.003	50	65	0.769
4200	30	0.003	50	65	0.769
4400	30	0.003	50	65	0.769

4600	30	0.003	50	65	0.769
4800	30	0.003	50	65	0.769
5000	30	0.003	50	65	0.769
5200	30	0.003	50	65	0.769
5400	30	0.003	50	65	0.769
5600	30	0.003	50	65	0.769
5800	30	0.003	50	65	0.769
6000	30	0.003	50	65	0.769
6200	30	0.003	50	65	0.769
6400	30	0.003	50	65	0.769
6600	30	0.003	50	65	0.769
6800	30	0.003	50	65	0.769
7000	30	0.003	50	65	0.769
7200	30	0.003	50	65	0.769
7400	30	0.003	50	65	0.769
7600	30	0.003	50	65	0.769
7800	30	0.003	50	65	0.769
8000	30	0.003	50	65	0.769
8200	30	0.003	50	65	0.769
8400	30	0.003	50	65	0.769
8600	30	0.003	50	65	0.769
8800	30	0.003	50	65	0.769
9000	30	0.003	50	65	0.769
9200	30	0.003	50	65	0.769
9400	30	0.003	50	65	0.769
9600	30	0.003	50	65	0.769
9800	30	0.003	50	65	0.769
10000	30	0.003	50	65	0.769
10200	30	0.003	50	65	0.769
10400	30	0.003	50	65	0.769
10600	30	0.003	50	65	0.769
10800	30	0.003	50	65	0.769
11000	30	0.003	50	65	0.769
11200	30	0.003	50	65	0.769
11400	30	0.003	50	65	0.769
11600	30	0.003	50	65	0.769
11800	30	0.003	50	65	0.769
12000	30	0.003	50	65	0.769
200	30	0.003	50	70	0.714
300	30	0.003	50	70	0.714
400	30	0.003	50	70	0.714
500	30	0.003	50	70	0.714
600	30	0.003	50	70	0.714
700	30	0.003	50	70	0.714
800	30	0.003	50	70	0.714

900	30	0.003	50	70	0.714
1000	30	0.003	50	70	0.714
1200	30	0.003	50	70	0.714
1400	30	0.003	50	70	0.714
1600	30	0.003	50	70	0.714
1800	30	0.003	50	70	0.714
2000	30	0.003	50	70	0.714
2200	30	0.003	50	70	0.714
2400	30	0.003	50	70	0.714
2600	30	0.003	50	70	0.714
2800	30	0.003	50	70	0.714
3000	30	0.003	50	70	0.714
3200	30	0.003	50	70	0.714
3400	30	0.003	50	70	0.714
3600	30	0.003	50	70	0.714
3800	30	0.003	50	70	0.714
4000	30	0.003	50	70	0.714
4200	30	0.003	50	70	0.714
4400	30	0.003	50	70	0.714
4600	30	0.003	50	70	0.714
4800	30	0.003	50	70	0.714
5000	30	0.003	50	70	0.714
5200	30	0.003	50	70	0.714
5400	30	0.003	50	70	0.714
5600	30	0.003	50	70	0.714
5800	30	0.003	50	70	0.714
6000	30	0.003	50	70	0.714
6200	30	0.003	50	70	0.714
6400	30	0.003	50	70	0.714
6600	30	0.003	50	70	0.714
6800	30	0.003	50	70	0.714
7000	30	0.003	50	70	0.714
7200	30	0.003	50	70	0.714
7400	30	0.003	50	70	0.714
7600	30	0.003	50	70	0.714
7800	30	0.003	50	70	0.714
8000	30	0.003	50	70	0.714
8200	30	0.003	50	70	0.714
8400	30	0.003	50	70	0.714
8600	30	0.003	50	70	0.714
8800	30	0.003	50	70	0.714
9000	30	0.003	50	70	0.714
9200	30	0.003	50	70	0.714
9400	30	0.003	50	70	0.714
9600	30	0.003	50	70	0.714

9800	30	0.003	50	70	0.714
10000	30	0.003	50	70	0.714
10200	30	0.003	50	70	0.714
10400	30	0.003	50	70	0.714
10600	30	0.003	50	70	0.714
10800	30	0.003	50	70	0.714
11000	30	0.003	50	70	0.714
11200	30	0.003	50	70	0.714
11400	30	0.003	50	70	0.714
11600	30	0.003	50	70	0.714
11800	30	0.003	50	70	0.714
12000	30	0.003	50	70	0.714
1000	20	0.003	50	50	1.000
1000	25	0.003	50	50	1.000
1000	30	0.003	50	50	1.000
1000	35	0.003	50	50	1.000
1000	40	0.003	50	50	1.000
1000	45	0.003	50	50	1.000
1000	50	0.003	50	50	1.000
1000	55	0.003	50	50	1.000
1000	60	0.003	50	50	1.000
1000	65	0.003	50	50	1.000
1000	70	0.003	50	50	1.000
1000	75	0.003	50	50	1.000
1000	80	0.003	50	50	1.000
1000	85	0.003	50	50	1.000
1000	90	0.003	50	50	1.000
1000	20	0.003	50	55	0.909
1000	25	0.003	50	55	0.909
1000	30	0.003	50	55	0.909
1000	35	0.003	50	55	0.909
1000	40	0.003	50	55	0.909
1000	45	0.003	50	55	0.909
1000	50	0.003	50	55	0.909
1000	55	0.003	50	55	0.909
1000	60	0.003	50	55	0.909
1000	65	0.003	50	55	0.909
1000	70	0.003	50	55	0.909
1000	75	0.003	50	55	0.909
1000	80	0.003	50	55	0.909
1000	85	0.003	50	55	0.909
1000	90	0.003	50	55	0.909
1000	20	0.003	50	60	0.833
1000	25	0.003	50	60	0.833
1000	30	0.003	50	60	0.833

1000	35	0.003	50	60	0.833
1000	40	0.003	50	60	0.833
1000	45	0.003	50	60	0.833
1000	50	0.003	50	60	0.833
1000	55	0.003	50	60	0.833
1000	60	0.003	50	60	0.833
1000	65	0.003	50	60	0.833
1000	70	0.003	50	60	0.833
1000	75	0.003	50	60	0.833
1000	80	0.003	50	60	0.833
1000	85	0.003	50	60	0.833
1000	90	0.003	50	60	0.833
1000	20	0.003	50	65	0.769
1000	25	0.003	50	65	0.769
1000	30	0.003	50	65	0.769
1000	35	0.003	50	65	0.769
1000	40	0.003	50	65	0.769
1000	45	0.003	50	65	0.769
1000	50	0.003	50	65	0.769
1000	55	0.003	50	65	0.769
1000	60	0.003	50	65	0.769
1000	65	0.003	50	65	0.769
1000	70	0.003	50	65	0.769
1000	75	0.003	50	65	0.769
1000	80	0.003	50	65	0.769
1000	85	0.003	50	65	0.769
1000	90	0.003	50	65	0.769
1000	20	0.003	50	70	0.714
1000	25	0.003	50	70	0.714
1000	30	0.003	50	70	0.714
1000	35	0.003	50	70	0.714
1000	40	0.003	50	70	0.714
1000	45	0.003	50	70	0.714
1000	50	0.003	50	70	0.714
1000	55	0.003	50	70	0.714
1000	60	0.003	50	70	0.714
1000	65	0.003	50	70	0.714
1000	70	0.003	50	70	0.714
1000	75	0.003	50	70	0.714
1000	80	0.003	50	70	0.714
1000	85	0.003	50	70	0.714
1000	90	0.003	50	70	0.714
1000	40	0.003	50	50	1.000
1000	40	0.005	50	50	1.000
1000	40	0.007	50	50	1.000

1000	40	0.009	50	50	1.000
1000	40	0.011	50	50	1.000
1000	40	0.015	50	50	1.000
1000	40	0.017	50	50	1.000
1000	40	0.019	50	50	1.000
1000	40	0.021	50	50	1.000
1000	40	0.023	50	50	1.000
1000	40	0.025	50	50	1.000
1000	40	0.027	50	50	1.000
1000	40	0.029	50	50	1.000
1000	40	0.031	50	50	1.000
1000	40	0.033	50	50	1.000
1000	40	0.003	50	55	0.909
1000	40	0.005	50	55	0.909
1000	40	0.007	50	55	0.909
1000	40	0.009	50	55	0.909
1000	40	0.011	50	55	0.909
1000	40	0.015	50	55	0.909
1000	40	0.017	50	55	0.909
1000	40	0.019	50	55	0.909
1000	40	0.021	50	55	0.909
1000	40	0.023	50	55	0.909
1000	40	0.025	50	55	0.909
1000	40	0.027	50	55	0.909
1000	40	0.029	50	55	0.909
1000	40	0.031	50	55	0.909
1000	40	0.033	50	55	0.909
1000	40	0.003	50	60	0.833
1000	40	0.005	50	60	0.833
1000	40	0.007	50	60	0.833
1000	40	0.009	50	60	0.833
1000	40	0.011	50	60	0.833
1000	40	0.015	50	60	0.833
1000	40	0.017	50	60	0.833
1000	40	0.019	50	60	0.833
1000	40	0.021	50	60	0.833
1000	40	0.023	50	60	0.833
1000	40	0.025	50	60	0.833
1000	40	0.027	50	60	0.833
1000	40	0.029	50	60	0.833
1000	40	0.031	50	60	0.833
1000	40	0.033	50	60	0.833
1000	40	0.003	50	65	0.769
1000	40	0.005	50	65	0.769
1000	40	0.007	50	65	0.769

1000	40	0.009	50	65	0.769
1000	40	0.011	50	65	0.769
1000	40	0.015	50	65	0.769
1000	40	0.017	50	65	0.769
1000	40	0.019	50	65	0.769
1000	40	0.021	50	65	0.769
1000	40	0.023	50	65	0.769
1000	40	0.025	50	65	0.769
1000	40	0.027	50	65	0.769
1000	40	0.029	50	65	0.769
1000	40	0.031	50	65	0.769
1000	40	0.033	50	65	0.769
1000	40	0.003	50	70	0.714
1000	40	0.005	50	70	0.714
1000	40	0.007	50	70	0.714
1000	40	0.009	50	70	0.714
1000	40	0.011	50	70	0.714
1000	40	0.015	50	70	0.714
1000	40	0.017	50	70	0.714
1000	40	0.019	50	70	0.714
1000	40	0.021	50	70	0.714
1000	40	0.023	50	70	0.714
1000	40	0.025	50	70	0.714
1000	40	0.027	50	70	0.714
1000	40	0.029	50	70	0.714
1000	40	0.031	50	70	0.714
1000	40	0.033	50	70	0.714
1000	40	0.005	24	30	0.800
1000	40	0.005	25.6	32	0.800
1000	40	0.005	27.2	34	0.800
1000	40	0.005	28.8	36	0.800
1000	40	0.005	30.4	38	0.800
1000	40	0.005	32	40	0.800
1000	40	0.005	33.6	42	0.800
1000	40	0.005	35.2	44	0.800
1000	40	0.005	36.8	46	0.800
1000	40	0.005	38.4	48	0.800
1000	40	0.005	40	50	0.800
1000	40	0.005	41.6	52	0.800
1000	40	0.005	43.2	54	0.800
1000	40	0.005	44.8	56	0.800
1000	40	0.005	46.4	58	0.800
1000	40	0.005	48	60	0.800
1000	40	0.005	49.6	62	0.800
1000	40	0.005	51.2	64	0.800

1000	40	0.005	52.8	66	0.800
1000	40	0.005	54.4	68	0.800
1000	40	0.005	56	70	0.800
1000	40	0.005	57.6	72	0.800
1000	40	0.005	59.2	74	0.800
1000	40	0.005	60.8	76	0.800
1000	40	0.005	62.4	78	0.800
1000	40	0.005	64	80	0.800
1000	40	0.005	65.6	82	0.800
1000	40	0.005	67.2	84	0.800
1000	40	0.005	68.8	86	0.800
1000	40	0.005	70.4	88	0.800
1000	40	0.005	72	90	0.800
1000	40	0.005	73.6	92	0.800
1000	40	0.005	75.2	94	0.800
1000	40	0.005	76.8	96	0.800
1000	40	0.005	78.4	98	0.800
1000	40	0.005	80	100	0.800
1000	40	0.005	81.6	102	0.800
1000	40	0.005	83.2	104	0.800
1000	40	0.005	84.8	106	0.800
1000	40	0.005	86.4	108	0.800
1000	40	0.005	88	110	0.800
1000	40	0.005	89.6	112	0.800
1000	40	0.005	91.2	114	0.800
1000	40	0.005	92.8	116	0.800
1000	40	0.005	94.4	118	0.800
1000	40	0.005	96	120	0.800
1000	40	0.005	97.6	122	0.800
1000	40	0.005	99.2	124	0.800
1000	40	0.005	100.8	126	0.800
1000	40	0.005	102.4	128	0.800
1000	40	0.005	104	130	0.800
1000	40	0.005	105.6	132	0.800
1000	40	0.005	107.2	134	0.800
1000	40	0.005	108.8	136	0.800
1000	40	0.005	110.4	138	0.800
1000	40	0.005	112	140	0.800
1000	40	0.005	113.6	142	0.800
1000	40	0.005	115.2	144	0.800
1000	40	0.005	116.8	146	0.800
1000	40	0.005	118.4	148	0.800
1000	40	0.005	120	150	0.800
1000	40	0.005	121.6	152	0.800
1000	40	0.005	123.2	154	0.800

1000	40	0.005	124.8	156	0.800
1000	40	0.005	126.4	158	0.800
1000	40	0.005	128	160	0.800
1000	40	0.005	129.6	162	0.800
1000	40	0.005	131.2	164	0.800
1000	40	0.005	132.8	166	0.800
1000	40	0.005	134.4	168	0.800
1000	40	0.005	136	170	0.800
1000	40	0.005	137.6	172	0.800
1000	40	0.005	139.2	174	0.800
1000	40	0.005	140.8	176	0.800
1000	40	0.005	142.4	178	0.800